PERIODICAL Calif. Univ. S.I.O.
Contributions

58

1958

UNIVERSITY OF CALIFORNIA

SCRIPPS INSTITUTION OF OCEANOGRAPHY

LIBRARY
DEC 17 1959
FISH & WILDLIFE SERVICE

CONTRIBUTIONS

1958

THE LIBRARY
UNIVERSITY OF CALIFORNIA
SCRIPPS INSTITUTION OF OCEANOGRAPHY
LA JOLLA, CALIFORNIA

PERIODICAL

Calif. (Univ.), Scripps
Instit. of
Oceanog.
Contributions.

1958

DATE	ISSUED TO
DEC 2 1960	K. Sherman
7/14/67	Manar

PERIODICAL

Calif. (Univ.),Scripps
Instit. of Oceanog.
Contributions.

1958

LIBRARY
BUR. OF COMM. FISH.
HON. BIOL. LAB.

UNIVERSITY OF CALIFORNIA

SCRIPPS INSTITUTION OF OCEANOGRAPHY

LIBRARY
DEC 17 1959
FISH & WILDLIFE SERVICE

CONTRIBUTIONS

1958

This volume contains contributions from the Scripps Institution of Oceanography which appeared during 1958 in publications other than *Bulletins of the Scripps Institution of Oceanography.*

THE LIBRARY
UNIVERSITY OF CALIFORNIA
SCRIPPS INSTITUTION OF OCEANOGRAPHY
LA JOLLA, CALIFORNIA

November 1959

Periodical
Calif. Univ. S.I.O.
Contributions 1958

2344 60

PHOTOLITHOPRINTED BY CUSHING - MALLOY, INC.
ANN ARBOR, MICHIGAN, UNITED STATES OF AMERICA
1959

UNIVERSITY OF CALIFORNIA
SCRIPPS INSTITUTION OF OCEANOGRAPHY
CONTRIBUTIONS, NEW SERIES
1958

NUMERICAL INDEX

Contrib. Number		Page Number
967	MILNE, LORUS J. and MARGERY. "Photosensitivity in invertebrates." Handbook of Physiology. Neurophysiology volumes.	*
968	MILNE, LORUS J. and MARGERY. "Foresight and hindsight on a punchcard bibliography." Punched Cards: their application to science and industry. 2nd ed.	*
969	HUBBS, CARL L. Position of anal fin and length of body cavity in catostomid and cyprinid fishes. Copeia, no. 1, February 21, 1958. p.56	1
970	RECHNITZER, ANDREAS B. and JAMES BÖHLKE. *Ichthyococcus irregularis*, a new gonostomatine fish from the eastern Pacific. Copeia, no.1, February 21, 1958. pp.10-15	849
971	REX, ROBERT and EDWARD GOLDBERG. Quartz contents of pelagic sediments of the Pacific Ocean. Tellus, no.1, 1958. pp.153-159	15
972	GHELARDI, RAYMOND and WHEELER NORTH. A possible ecological effect of upwelling in a submarine canyon. Nature, v.181, no.4603, January 18, 1958. pp.207-208	23
973	RICHARDS, ADRIAN F. Transpacific distribution of floating pumice from Isla San Benedicto, Mexico. Deep-Sea Research, v.5, no.1, May 1958. pp.29-35	25
974	HASTINGS, J. WOODLAND and BEATRICE M. SWEENEY. The luminescent reaction in extracts of the marine dinoflagellate, *Gonyaulax polyedra*. Journal of Cellular and Comparative Physiology, v.49, no.2, April 1957. pp.209-225	37
975	TOKIOKA, TAKASI and LEO BERNER. Two new doliolids from the eastern Pacific Ocean. Pacific Science, v.12, no.2, April 1958. pp.135-138	55
976	GROVES, GORDON. Tides. Encyclopedia Britannica, 1958 ed.	59
977	SNODGRASS, FRANK E. Shore-based recorder of low frequency ocean waves. American Geophysical Union, Transactions, v.39, no.1, February 1958. pp.109-113	73

* Not available for exchange.

Contrib. Number		Page Number
978	SNODGRASS, FRANK, WALTER MUNK and M. J. TUCKER. Offshore recording of low-frequency ocean waves. American Geophysical Union, Transactions, v.39, no.1, February 1958. pp.114-120	80
979	RAKESTRAW, NORRIS W. Training in chemical oceanography. Journal of Chemical Education, v.35, no.3, March 1958. pp.123-124	87
980	ECKART, CARL. Properties of water, Part II. The equation of state of water and sea water at low temperatures and pressures. American Journal of Science, v.256, no.4, 1958. pp.225-240	89
981	GOLDBERG, EDWARD D. The processes regulating the composition of sea water. Journal of Chemical Education, v.35, no.3, 1958. pp.116-119	105
982	AHLSTROM, E. H., JOHN D. ISAACS, JAMES R. THRAILKILL and LEWIS W. KIDD. A high-speed plankton sampler. United States Department of the Interior, Fish and Wildlife Service, Fishery Bulletin, v.58, no.132, 1958. pp.187-214	109
983	UREY, HAROLD C. and HANS E. SUESS. Die Haufigkeit der Elemente in Planeten und Meteoriten. Astrophysik. Berlin, Springer-Verlag, v.2, Sternaufbau, 1958. pp.296-324. (Handbuch der Physik, v.51)	*
984	SHOR, GEORGE G., JR. and ELLIS ROBERTS. San Miguel, Baja California Norte, Earthquakes of February, 1956: a field report. Seismological Society of America, Bulletin, v.48, no.2, April 1958. pp.101-116	143
985	FISHER, ROBERT, ALFRED CARSOLA and GEORGE SHUMWAY. Deep-sea bathymetry north of Point Barrow, Alaska. Deep-Sea Research, v.5, no.1, 1958. pp.1-6	159
986	BIEN, GEORGE S., DAVID E. CONTOIS and WILLIAM H. THOMAS. The removal of soluble silica from fresh water entering the sea. Geochimica et Cosmochimica Acta, v.14, no.1 & 2, 1958. pp.35-54	165
987	BODEN, BRIAN P. and ELIZABETH KAMPA. Lumiére, bioluminescence et migrations de la couche diffusante profonde en Méditerranée Occidentale. Vie et Milieu, Bulletin du Laboratoire Arago, v.9, no.1, 1958. pp.1-10	185
988	FOX, DENIS L. and EUGENE CORCORAN. Thermal and osmotic countermeasures against some typical marine fouling organisms. Corrosion, v.14, 1958. pp.31-32	197
989	GROVES, GORDON and TOWNSEND CROMWELL. Experimental investigation of the effect of "secondary instability" on mixing processes. Journal of Marine Research, v.16, no.1, November 30, 1957. pp.8-11	199

* Not available for exchange.

Contrib. Number — Page Number

990 JOHNSON, MARTIN W. *Bathycalanus sverdrupi* N. Sp., a copepod crustacean from great depths in the Pacific Ocean. California Academy of Sciences, Proceedings. 4th Series, v.29, no.6, July 10, 1958. pp.257-265 205

991 POOLE, DAVID M. Heavy mineral variation in San Antonio and Mesquite Bays of the central Texas coast. Journal of Sedimentary Petrology, v.28, no.1, March 1958. pp.65-74 215

992 HAXO, FRANCIS T. and C. OHEOCHA. Chromoproteins of algae. Handb. d. Pflanzenphysiologie, Bd.V . . . . . *

993 REID, JOSEPH L., JR. A comparison of drogue and GEK measurements in deep water. Limnology and Oceanography, v.3, no.2, April 1958. pp.160-165 226

994 VAN ANDEL, TJEERD. Origin and classification of Cretaceous, Paleocene, and Eocene sandstones of western Venezuela. American Association of Petroleum Geologists, Bulletin, v.42, no.4, April 1958. pp.734-763 233

995 MAZIA, DANIEL. The production of twin embryos in *Dendraster* by means of mercaptoethanol (monothioethylene glycol). Biological Bulletin, v.114, no.2, 1958. pp.247-254 265

996 WOOSTER, WARREN S. and TOWNSEND CROMWELL. An oceanographic description of the eastern tropical Pacific. Bulletin of the Scripps Institution of Oceanography, University of California, La Jolla, California, v.7, no.3, 1958. pp.169-282 . . . . . *

997 SHEPARD, FRANCIS P. Sedimentation in the northwestern Gulf of Mexico. Geologischen Rundschau, v.47, no.1, 1958. pp.150-167 273

998 REID, JOSEPH L., JR., GUNNAR RODEN and JOHN WYLLIE. Studies of the California current system. California Cooperative Oceanic Fisheries Investigations. Progress Report, 1 July 1956 to 1 January 1958. pp.27-57 293

999 FISHER, FRED H. Effect of high pressure on sound absorption and chemical equilibrium. Acoustical Society of America, Journal, v.30, no.5, May 1958. pp.442-448 325

1000 DUNTLEY, SEIBERT Q. Atmospheric limitations on missile photography. Society of Motion Picture and Television Engineers, Journal, v.67, April 1958. pp.231-233 333

1001 HUBBS, CARL L. and KARL LAGLER. List of fishes of the Great Lakes and tributary waters. University of Michigan, "Michigan Fisheries," no.1, October 31, 1957 337

1002 PREISENDORFER, RUDOLPH W. Invariant imbedding relation for the principles of invariance. National Academy of Sciences, Proceedings, v.44, no.4, April 1958. pp.320-323 343

* Not available for exchange.

Contrib. Number		Page Number
1003	PREISENDORFER, RUDOLPH W. Functional relations for the R and T operators on plane-parallel media. National Academy of Sciences, Proceedings, v.44, no.4, April 1958. pp.323-327.	347
1004	PREISENDORFER, RUDOLPH W. Time-dependent principles of invariance. National Academy of Sciences, Proceedings, v.44, no.4, April 1958. pp.328-332	353
1005	ZoBELL, CLAUDE E. Ecology of sulfate reducing bacteria. Producers Monthly, v.22, no.7, May 1958. pp.12-29	359
1006	REVELLE, ROGER. Sun, sea, and air: IGY studies of the heat and water budget of the earth. Geophysics and the IGY, Geophysical Monograph no.2, American Geophysical Union, Washington, D. C., July 1958. NAS-NRC Publication no.590.	371
1007	MUNK, WALTER H. The seasonal budget of water. Geophysics and the IGY, Geophysical Monograph no.2, American Geophysical Union, Washington, D. C., July 1958. pp.175-176	379
1008	SACKETT, WILLIAM M., HERBERT A. POTRATZ and EDWARD GOLDBERG. Thorium content of ocean water. Science, v.128, no.3317, July 25, 1958. pp.204-205.	381
√ 1009	ANDERSON, VICTOR C. Arrays for the investigation of ambient noise in the ocean. Acoustical Society of America, Journal, v.30, no.5, May 1958. pp.470-477	383
1010	VAN ANDEL, TJEERD H. A defense of the term alterite. Journal of Sedimentary Petrology, v.28, no.2, June 1958. pp.234-235	391
1011	MUNK, WALTER and RICHARD HAUBRICH. The annual pole tide. Nature, v.182, no.4627, July 5, 1958. p.42	393
1012	RIEDEL, WILLIAM R. Radiolaria in Antarctic sediments. B.A.N.Z. Antarctic Research 1929-1931 Expedition. Reports. Series B (Zoology and Botany), v.6, pt.10, April 1958. pp.219-247	395
√ 1013	HOLMES, ROBERT W. Surface chlorophyll "A", surface primary production, and zooplankton volumes in the eastern Pacific Ocean. International Council for the Exploration of the Sea. Rapports et procès-verbaux des réunions, v.144, 1958. pp.109-116	435
√ 1014	MENARD, HENRY W. and ROBERT L. FISHER. Clipperton fracture zone in the northeastern equatorial Pacific. Journal of Geology, v.66, no.3, May 1958. pp.239-253	443
1015	MENARD, HENRY W. and VICTOR VACQUIER. Magnetic survey of part of the deep sea floor off the coast of California. Research Reviews, June 1958. pp.1-5	465
1016	SNODGRASS, FRANK E. and ROBERT R. PUTZ. A wave height and frequency meter. 6th International Conference on Coastal Engineering, Proceedings. pp.209-224	471

Contrib. Number | Page Number

1017 **HOLTEDAHL, HANS.** Some remarks on geomorphology of continental shelves off Norway, Labrador, and southeast Alaska. Journal of Geology, v.66, no.4, July 1958. pp.461-471. 487

1018 **BIEN, GEORGE S.** Salt effect correction in determining soluble silica in sea water by the silicomolybdic acid method. Analytical Chemistry, v.30, no.9, September 1958. pp.1525-1526. 502

1019 **CRAIG, HARMON.** Critical evaluation of radiocarbon techniques for determining mixing rates in the oceans and the atmosphere. Proceedings, 2nd Geneva Conference on the Peaceful Uses of Atomic Energy, June 1958. A/CONF.15/P/1979 503

1020 **GOLDBERG, EDWARD, C. PATTERSON and T. CHOW.** Ionium-thorium and lead isotope ratios as indicators of oceanic water masses. Proceedings, 2nd Geneva Conference on the Peaceful Uses of Atomic Energy. June 1958. A/CONF.15/P/1980 U.S.A. 519

1021 **INMAN, DOUGLAS L. and THEODORE K. CHAMBERLAIN.** Experiments with radioactive sand as a tracer of beach sand movement. Proceedings, 2nd International Conference on the Peaceful Uses of Atomic Energy. June 1958. A/CONF.15/P/2357 U.S.A. 527

1022 **SCHAEFER, MILNER and YVONNE M. BISHOP.** Particulate iron in offshore waters of the Panama Bight and in the Gulf of Panama. Limnology and Oceanography, v.3, no.2, April 1958. pp.137-149 541

1023 **KNAUSS, JOHN A. and JOSEPH E. KING.** Observations of the Pacific Equatorial undercurrent. Nature, v.182, no.4655, August 30, 1958. pp.601-602 555

1024 **ECKART, CARL.** Disturbances in an idealized atmosphere on a flat planet without rotation. Journal of Geophysical Research, v.63, no.3, September 1958. pp.599-604 557

1025 **MENARD, HENRY W.** Development of median elevations in ocean basins. Geological Society of America, Bulletin, v.69, no.9, September 1958. pp.1179-1186 563

1026 **LIMBAUGH, CONRAD.** Marine outfall studies by qualified diving investigators. 12th Industrial Waste Conference. Proceedings, May 13, 14 and 15, 1957. pp.210-216 . . . . *

1027 **HOURSTON, ALAN S.** Population studies on juvenile herring in Barkley Sound, British Columbia. Journal of the Fisheries Research Board of Canada, (Nanaimo Station Anniversary Issue, September 1958), v.15, no.5, 1958. pp.909-960. 571

1028 **SWEENEY, BEATRICE and WOODLAND J. HASTINGS.** Rhythmic cell division in populations of *Gonaulax polyedra*. Journal of Protozoology, v.5, no.3, 1958. pp.217-224 623

1029 **TYLER, JOHN E. and W. H. RICHARDSON.** Nephelometer for the measurement of volume scattering function *in situ*. Optical Society of America, Journal, v.48, no.5, May 1958. pp.354-357. . . . 631

* Not available for exchange.

Contrib. Number | Page Number

1030 GOLDBERG, EDWARD D. and MINORU KOIDE. Ionium-thorium chronology in deep-sea sediments of the Pacific. Science, v.128, no.3330, October 24, 1958. p.1003. 635

1031 MENARD, HENRY W. and CARL J. SHIPEK. Surface concentrations of manganese nodules. Nature (letter to editors), v.182, no.4643, October 25, 1958. pp.1156-1158 637

1032 TOKIOKA, TAKASI and LEO BERNER. On certain Thaliacea (Tunicata) from the Pacific Ocean, with descriptions of two new species of doliolids. Pacific Science, v.12, no.4, October 1958. pp.317-326 641

1033 BUZZATI-TRAVERSO, ADRIANO A., EDITOR. Perspectives in marine biology. (Symposium, March 24-April 2, 1956. Scripps Institution of Oceanography, La Jolla, California.) Berkeley, University of California Press, 1958. 651

1034 LEWIN, RALPH A. Genetics and marine algae. Perspectives in Marine Biology. March 24-April 2, 1956. pp.547-557 661

1035 BELSER, WILLIAM L. Marine microörganisms: Some generalizations concerning their importance to marine life. Perspectives in Marine Biology. March 24-April 2, 1956. pp.405-408 673

1036 JAFFE, LIONEL. Tropistic responses of Zygotes of the fucaceae to polarized light. Experimental Cell Research, v.15, no.2, October 1958. pp.282-299 678

1037 SNODGRASS, JAMES M. and JOHN H. CAWLEY, JR. Bathythermometer telemeters ocean data. Electronics, v.30, no.5, May 1, 1957. pp.142-145 697

1038 SILAS, ERIC GODWIN. The Ceylonese cyprinid genus *Eustira* Gunther considered a synonym of *Danio* Hamilton. Copeia, no.1, April 5, 1957. pp.61-62 703

1039 ORTON, GRACE L. Embryology and evolution of the pelagic fish egg. Copeia, no.1, April 5, 1957. pp.56-58 708

1040 MASON, RONALD G. A magnetic survey off the West Coast of the United States between latitudes 32° and 36° N, and longitudes 121° and 128° W. Geophysical Journal. Royal Astronomical Society, v.1, no.4, December 1958. pp.320-329 709

1041 SUESS, HANS E. The radioactivity of the atmosphere and hydrosphere. Annual Review of Nuclear Science, v.8, 1958. pp.243-256 723

1042 STEWART, HARRIS B., JR. Sedimentary reflections of depositional environment in San Miguel Lagoon, Baja California, Mexico. American Association Petroleum Geologists, Bulletin, v.42, no.11, November 1958. pp.2567-2618 737

1043 HUBBS, CARL L. *Dikellorhynchus* and *Kanazawaichthys:* nominal fish genera interpreted as based on prejuveniles of *Malacanthus* and *Antennarius*, respectively. Copeia, no.4, December 22, 1958. pp.282-285 790

Contrib. Number		Page Number
1044	HUBBS, CARL and CLARK HUBBS. *Notropis saladonis* a new cyprinid fish endemic in the Rio Salado of northeastern Mexico. Copeia, no.4, December 22, 1958. pp.297-307	795
1045	HUBBS, CARL. *Ogcocephalus darwini*, a new batfish endemic at the Galapagos Islands. Copeia, no.3, August 28, 1958. pp.161-170	807
1046	STEWART, JAMES R. Black Swan in kelp off Southern California. The Condor, v.59, no.6, November-December 1957. pp.400-401	828
1047	BRANDHORST, WILHELM. Thermocline topography, zooplankton standing crop and mechanisms of fertilization in the eastern tropical Pacific. Journal du Conseil, International Conseil pour l'Exploration de la Mer, v.24, no.1, 1958. pp.16-31	832
1048	HUBBS, CARL L. and ANDREAS B. RECHNITZER. A new fish, *Chaetodon falcifer*, from Guadalupe Island, Baja California, with notes on related species. California Academy of Sciences. Proceedings. 4th Series, v.29, no.8, July 10, 1958. pp.273-313	849
1049	JENSEN, DAVID. Some observations on cardiac automatism in certain animals. Journal of General Physiology, v.42, no.2, November 20, 1958. pp.289-302	891
1050	HUBBS, CARL L., EDITOR. "Zoogeography - General conclusions." American Association for the Advancement of Science. Washington, D. C., 1958	905
1051	JANNASCH, HOLGER W. Schwellenkonzentrationen verschiedener Stickstoffquellen für die Vermehrung einiger Bakterien aus narstoffarmen Gewassern. Mit 3 Texabbildungen. Archiv für Mikrobiologie, v.31, no.1, April 24, 1958. pp.114-124	*
1052	BERGER, LESLIE RALPH. Some effects of pressure on a phenylglycosidase. Biochimica et Biophysica Acta, v.30, no.3, December 1958. pp.522-528	921
1053	HUBBS, CARL L. Natural history of the gray whale. 15th International Congress of Zoology. Section 3, paper 46. pp.1-3	929
1054	MUNK, WALTER H. Remarks concerning the present position of the pole. Geophysica (Palmen-volume), v.6, no.3, University of Helsinki, Institute of Meteorology. pp.335-355	933
1055	TOKIOKA, TAKASI. Further notes on some appendicularians from the eastern Pacific. Publications Seto Marine Biological Laboratory, v.7, no.1, December 1958. pp.1-17	955
1056	BUZZATI-TRAVERSO, ADRIANO A. Genetische probleme der marinen biologie. Revue Suisse de Zoologie, v.65, no.33, July 1958. pp.461-484	973

* Not available for exchange.

Contrib. Number — Page Number

1057 GROVES, GORDON W. and JOSEPH L. REID, JR. Estudios Oceanograficos sobre las Aguas de Baja California. PRIMER CONGRESO DE HISTORIA REGIONAL. Memoria Mexicali, 1958. pp. 89-121. 997

1058 SWEENEY, BEATRICE M. and WOODLAND J. HASTINGS. A persistent diurnal rhythm of luminescence in *Gonyaulax polyedra*. Biological Bulletin, v.115, no.3, December 1958. pp.440-458 1033

1059 MANWELL, CLYDE. On the evolution of hemoglobin. Respiratory properties of the hemoglobin of the California hagfish, *Polistotrema stouti*. Biological bulletin, v.115, no.2, October 1958. pp.227-238 1053

1060 ECKART, CARL. The surface wake of a submerged sphere. Physics of Fluids, v.1, no.6, November/December 1958. pp.457-461 1065

1061 RODEN, GUNNAR I. Spectral analysis of a sea-surface temperature and atmospheric pressure record off southern California. Journal of Marine Research, v.16, no.2, August 31, 1958. pp.90-96 1072

1062 TYLER, JOHN E. Comparison of light distribution above and below water. Journal of Marine Research, v.16, no.2, August 31, 1958. pp.96-100. 1080

UNIVERSITY OF CALIFORNIA
SCRIPPS INSTITUTION OF OCEANOGRAPHY
CONTRIBUTIONS, NEW SERIES
1958

AUTHOR INDEX

	Contrib. Number	Page Number
AHLSTROM, E. H.		
(with John D. Isaacs, James R. Thrailkill, and Lewis W. Kidd) A high-speed plankton sampler	982	109
ANDERSON, VICTOR C.		
Arrays for the investigation of ambient noise in the ocean	1009	383
BELSER, WILLIAM L.		
Marine microörganisms: Some generalizations concerning their importance to marine life	1035	673
BERGER, LESLIE RALPH		
Some effects of pressure on a phenylglycosidase	1052	921
BERNER, LEO		
(with Takasi Tokioka) On certain Thaliacea (Tunicata) from the Pacific Ocean, with descriptions of two new species of doliolids	1032	641
(with Takasi Tokioka) Two new doliolids from the eastern Pacific Ocean	975	55
BIEN, GEORGE S.		
Salt effect correction in determining soluble silica in sea water by the silicomolybdic acid method	1018	501
(with David E. Contois, and William H. Thomas) The removal of soluble silica from fresh water entering the sea	986	165
BISHOP, YVONNE M.		
(with Milner Schaefer) Particulate iron in offshore waters of the Panama Bight and in the Gulf of Panama	1022	541
BODEN, BRIAN P.		
(with Elizabeth Kampa) Lumiére, bioluminescence et migrations de la couche diffusante profonde en Méditerranée Occidentale	987	185
BÖHLKE, JAMES		
(with Andreas B. Rechnitzer) *Ichthyococcus irregularis*, a new gonostomatine fish from the eastern Pacific	970	849
BRANDHORST, WILHELM		
Thermocline topography, zooplankton standing crop and mechanisms of fertilization in the eastern tropical Pacific	1047	832
BUZZATI-TRAVERSO, ADRIANO A.		
Genetische probleme der marinen biologie	1056	973
Perspectives in marine biology, (summary)	1033	651

	Contrib. Number	Page Number
CARSOLA, ALFRED		
(with Robert Fisher and George Shumway) Deep-sea bathymetry north of Point Barrow, Alaska.	985	159
CAWLEY, JOHN H., JR.		
(with James M. Snodgrass) Bathythermometer telemeters ocean data	1037	697
CHAMBERLAIN, THEODORE K.		
(with Douglas L. Inman) Experiments with radioactive sand as a tracer of beach sand movement.	1021	527
CHOW, T.		
(with Edward Goldberg and C. Patterson) Ionium-thorium and lead isotope ratios as indicators of oceanic water masses	1020	519
CONTOIS, DAVID E.		
(with George S. Bien and William H. Thomas) The removal of soluble silica from fresh water entering the sea.	986	165
CORCORAN F., EUGENE		
(with Denis L. Fox) Thermal and osmotic countermeasures against some typical marine fouling organisms	988	197
CRAIG, HARMON		
Critical evaluation of radiocarbon techniques for determining mixing rates in the oceans and the atmosphere	1019	503
CROMWELL, TOWNSEND		
(with Gordon Groves) Experimental investigation of the effect of "secondary instability" on mixing processes	989	199
(with Warren S. Wooster) An oceanographic description of the eastern tropical Pacific	996	*
DUNTLEY, SEIBERT Q.		
Atmospheric limitations on missile photography	1000	333
ECKART, CARL		
Disturbances in an idealized atmosphere on a flat planet without rotation.	1024	557
Properties of water, Part II. The equation of state of water and sea water at low temperatures and pressures	980	89
The surface wake of a submerged sphere	1060	1065
FISHER, FRED H.		
Effect of high pressure on sound absorption and chemical equilibrium	999	325
FISHER, ROBERT L.		
(with Henry W. Menard) Clipperton fracture zone in the northeastern Equatorial Pacific	1014	443
(with Alfred Carsola and George Shumway) Deep-sea bathymetry north of Point Barrow, Alaska.	985	159
FOX, DENIS L.		
(with Eugene Corcoran) Thermal and osmotic countermeasures against some typical marine fouling organisms	988	197

* Not available for exchange.

	Contrib. Number	Page Number
GHELARDI, RAYMOND		
(with Wheeler North) A possible ecological effect of upwelling in a submarine canyon	972	23
GOLDBERG, EDWARD		
(with Robert Rex) Quartz contents of pelagic sediments of the Pacific Ocean	971	15
(with William M. Sackett and Herbert A. Potratz) Thorium content of ocean water	1008	381
(with C. Patterson and T. Chow) Ionium-thorium and lead isotope ratios as indicators of oceanic water masses	1020	519
(with Minoru Koide) Ionium-thorium chronology in deep-sea sediments of the Pacific	1030	635
The processes regulating the composition of sea water	981	105
GROVES, GORDON W.		
(with Joseph L. Reid, Jr.) Estudios Oceanograficos sobre las Aguas de Baja California	1057	997
(with Townsend Cromwell) Experimental investigation of the effect of "secondary instability" on mixing processes	989	199
Tides	976	59
HASTINGS, J. WOODLAND		
(with Beatrice Sweeney) Rhythmic cell division in populations of *Gonyaulax polyedra*	1028	623
(with Beatrice Sweeney) The luminescent reaction in extracts of the marine dinoflagellate, *Gonyaulax polyedra*	974	37
(with Beatrice Sweeney) A persistent diurnal rhythm of luminescence in *Gonyaulax polyedra*	1058	1033
HAUBRICH, RICHARD		
(with Walter Munk) The annual pole tide	1011	393
HAXO, FRANCIS T.		
(with C. Oheocha) Chromoproteins of algae	992	*
HOLMES, ROBERT W.		
Surface chlorophyll "A", surface primary production, and zooplankton volumes in the eastern Pacific Ocean	1013	435
HOLTEDAHL, HANS		
Some remarks on geomorphology of continental shelves off Norway, Labrador, and southeast Alaska	1017	487
HOURSTON, ALAN S.		
Population studies on juvenile herring in Barkley Sound, British Columbia	1027	571
HUBBS, CARL L.		
Dikellorhynchus and *Kanazawaichthys:* nominal fish genera interpreted as based on prejuveniles of *Malacanthus* and *Antennarius*, respectively	1043	790
(with Karl Lagler) List of fishes of the Great Lakes and tributary waters	1001	337
Natural history of the gray whale	1053	929

* Not available for exchange.

	Contrib. Number	Page Number
HUBBS, CARL L. (continued)		
(with Andreas B. Rechnitzer) A new fish, *Chaetodon falcifer*, from Guadalupe Island, Baja California, with notes on related species.	1048	849
(with Clark Hubbs) *Notropis saladonis*, a new cyprinid fish endemic in the Rió Salado of northeastern México	1044	795
Ogcocephalus darwini, a new batfish endemic at the Galapagos Islands	1045	807
Position of anal fin and length of body cavity in catostomid and cyprinid fishes.	969	1
Zoogeography — General conclusions	1050	905
HUBBS, CLARK		
(with Carl L. Hubbs) *Notropis saladonis*, a new cyprinid fish endemic in the Rió Salado of northeastern México	1044	795
INMAN, DOUGLAS L.		
(with Theodore K. Chamberlain) Experiments with radioactive sand as a tracer of beach sand movement	1021	527
ISAACS, JOHN D.		
(with E. H. Ahlstrom, James R. Thrailkill and Lewis W. Kidd) A high-speed plankton sampler	982	109
JAFFE, LIONEL		
Tropistic responses of Zygotes of the fucaceae to polarized light	1036	678
JANNASCH, HOLGER W.		
Schwellenkonzentrationen verschiedener Stickstoffquellen für die Vermehrung einiger Baktierien aus narstoffarmen Gewassern. Mit 3 Texabbildugen.	1051	*
JENSEN, DAVID		
Some observations on cardiac automatism in certain animals	1049	891
JOHNSON, MARTIN W.		
Bathycalanus sverdrupi N. Sp., a copepod crustacean from great depths in the Pacific Ocean	990	205
KAMPA, ELIZABETH		
(with Brian P. Boden) Lumiere, bioluminescence et migrations de la couche diffusante profonde en Méditerranée Occidentale	987	185
KIDD, LEWIS W.		
(with E. H. Ahlstrom, John D. Isaacs and James R. Thrailkill) A high-speed plankton sampler	982	109
KING, JOSEPH E.		
(with John A. Knauss) Observations of the Pacific Equatorial undercurrent	1023	555
KNAUSS, JOHN A.		
(with Joseph E. King) Observations of the Pacific Equatorial undercurrent	1023	555

---

* Not available for exchange.

	Contrib. Number	Page Number
KOIDE, MINORU		
(with Edward D. Goldberg) Ionium-thorium chronology in deep-sea sediments of the Pacific.	1030	635
LAGLER, KARL		
(with Carl L. Hubbs) List of fishes of the Great Lakes and tributary waters	1001	337
LEWIN, RALPH A.		
Genetics and marine algae	1034	661
LIMBAUGH, CONRAD		
Marine outfall studies by qualified diving investigators	1026	*
MANWELL, CLYDE		
On the evolution of hemoglobin. Respiratory properties of the hemoglobin of the California hagfish, *Polistotrema stouti*	1059	1053
MASON, RONALD G.		
A magnetic survey off the West Coast of the United States between latitudes 32° and 36° N, and longitudes 121° and 128° W	1040	709
MAZIA, DANIEL		
The production of twin embryos in *Dendraster* by means of mercaptoethanol (monothioethylene glycol)	995	265
MENARD, HENRY W.		
(with Robert L. Fisher) Clipperton fracture zone in the northeastern Equatorial Pacific	1014	443
Development of median elevations in ocean basins.	1025	563
(with Victor Vacquier) Magnetic survey of part of the deep sea floor off the coast of California.	1015	465
(with Carl J. Shipek) Surface concentrations of manganese nodules.	1031	637
MILNE, LORUS J.		
(with Margery) Foresight and hindsight on a punch-card bibliography	968	*
(with Margery) Photosensitivity in invertebrates	967	*
MUNK, WALTER H.		
(with Frank Snodgrass and M. J. Tucker) Off-shore recording of low-frequency ocean waves	978	80
(with Richard Haubrich) The annual pole tide.	1011	393
Remarks concerning the present position of the pole	1054	933
The seasonal budget of water	1007	379
NORTH, WHEELER		
(with Raymond Ghelardi) A possible ecological effect of upwelling in a submarine canyon	972	23
OHEOCHA, C.		
(with Francis T. Haxo) Chromoproteins of algae	992	*
ORTON, GRACE L.		
Embryology and evolution of the pelagic fish egg	1039	708

---

* Not available for exchange.

	Contrib. Number	Page Number
PATTERSON, C.		
(with Edward Goldberg and T. Chow) Ionium-thorium and lead isotope ratios as indicators of oceanic water masses.	1020	519
POOLE, DAVID M.		
Heavy mineral variation in San Antonio and Mesquite Bays of the central Texas coast	991	215
POTRATZ, HERBERT A.		
(with William M. Sackett and Edward Goldberg) Thorium content of ocean water	1008	381
PREISENDORFER, RUDOLPH W.		
Functional relations for the R and T operators on plane-parallel media	1003	347
Invariant imbedding relation for the principles of invariance	1002	343
Time-dependent principles of invariance	1004	353
PUTZ, ROBERT R.		
(with Frank E. Snodgrass) A wave height and frequency meter. . . .	1016	471
RAKESTRAW, NORRIS W.		
Training in chemical oceanography	979	87
RECHNITZER, ANDREAS B.		
(with Carl L. Hubbs) A new fish, *Chaetodon falcifer*, from Guadalupe Island, Baja California, with notes on related species	1048	849
(with James Böhlke) *Ichthyococcus irregularis*, a new gonostomatine fish from the eastern Pacific.	970	849
REID, JOSEPH L., JR.		
(with Gordon W. Groves) Estudios Oceanograficos sobre las Aguas de Baja California.	1057	997
A comparison of drogue and GEK measurements in deep water. . . .	993	226
(with Gunnar Roden and John Wyllie) Studies of the California current system	998	293
REVELLE, ROGER		
Sun, sea, and air: IGY studies of the heat and water budget of the earth	1006	371
REX, ROBERT		
(with Edward Goldberg) Quartz contents of pelagic sediments of the Pacific Ocean	971	15
RICHARDS, ADRIAN F.		
Transpacific distribution of floating pumice from Isla San Benedicte, Mexico	973	25
RICHARDSON, W. H.		
(with John E. Tyler) Nephelometer for the measurement of volume scattering function *in situ*	1029	631
RIEDEL, WILLIAM R.		
Radiolaria in Antarctic sediments	1012	395

	Contrib. Number	Page Number
ROBERTS, ELLIS		
(with George G. Shor, Jr.) San Miguel, Baja California Norte, Earthquakes of February, 1956: a field report	984	143
RODEN, GUNNAR I.		
(with Joseph L. Reid, Jr. and John Wyllie) Studies of the California current system	998	293
Spectral analysis of a sea-surface temperature and atmospheric pressure record off southern California	1061	1072
SACKETT, WILLIAM M.		
(with Herbert A. Potratz and Edward Goldberg) Thorium content of ocean water	1008	381
SCHAEFER, MILNER		
(with Yvonne M. Bishop) Particulate iron in offshore waters of the Panama Bight and in the Gulf of Panama	1022	541
SHEPARD, FRANCIS P.		
Sedimentation in the northwestern Gulf of Mexico	997	273
SHIPEK, CARL J.		
(with Henry W. Menard) Surface concentrations of manganese nodules	1031	637
SHOR, GEORGE G., JR.		
(with Ellis Roberts) San Miguel, Baja California Norte, Earthquakes of February, 1956: a field report	984	143
SHUMWAY, GEORGE		
(with Robert L. Fisher and Alfred Carsola) Deep-sea bathymetry north of Point Barrow, Alaska	985	159
SILAS, ERIC GODWIN		
The Ceylonese cyprinid genus *Eustira* Gunther considered a synonym of *Danio* Hamilton	1038	703
SNODGRASS, FRANK E.		
(with Walter Munk and M. J. Tucker) Off-shore recording of low-frequency ocean waves	978	73
Shore-based recorder of low frequency ocean waves	977	73
(with Robert R. Putz) A wave height and frequency meter	1016	471
SNODGRASS, JAMES M.		
(with John H. Cawley, Jr.) Bathythermometer telemeters ocean data	1037	697
STEWART, HARRIS B., JR.		
Sedimentary reflections of depositional environment in San Miguel Lagoon, Baja California, Mexico	1042	737
STEWART, JAMES R.		
Black Swan in kelp off Southern California	1046	828
SUESS, HANS E.		
(with Harold C. Urey) Die Haufigkeit der Elemente in Planeten und Meteoriten	983	*

---

* Not available for exchange.

	Contrib. Number	Page Number
SUESS, HANS E. (continued)		
The radioactivity of the atmosphere and hydrosphere	1041	723
SWEENEY, BEATRICE M.		
(with Woodland J. Hastings) The luminescent reaction in extracts of the marine dinoflagellate, *Gonyaulax polyedra*	974	37
(with Woodland J. Hastings) A persistent diurnal rhythm of luminescence in *Gonyaulax polyedra*	1058	1033
(with Woodland J. Hastings) Rhythmic cell division in populations of *Gonyaulax polyedra*	1028	623
THOMAS, WILLIAM H.		
(with George S. Bien and David E. Contois) The removal of soluble silica from fresh water entering the sea	986	165
THRAILKILL, JAMES R.		
(with E. H. Ahlstrom, John D. Isaacs and Lewis W. Kidd) A high-speed plankton sampler	982	109
TOKIOKA, TAKASI		
(with Leo Berner) On Certain Thaliacea (Tunicata) from the Pacific Ocean, with descriptions of two new species of doliolids	1032	641
(with Leo Berner) Two new doliolids from the eastern Pacific Ocean	975	55
Further notes on some appendicularians from the eastern Pacific	1055	955
TUCKER, M. J.		
(with Frank E. Snodgrass and Walter Munk) Off-shore recording of low-frequency ocean waves	978	80
TYLER, JOHN E.		
(with W. H. Richardson) Nephelometer for the measurement of volume scattering function *in situ*	1029	631
Comparison of light distribution above and below water	1062	1080
UREY, HAROLD C.		
(with Hans E. Suess) Die Haufigkeit der Elemente in Planeten und Meteoriten	983	*
VACQUIER, VICTOR		
(with Henry W. Menard) Magnetic survey of part of the deep sea floor off the coast of California	1015	465
VAN ANDEL, TJEERD H.		
A defense of the term alterite	1010	391
Origin and classification of Cretaceous, Paleocene, and Eocene sandstones of western Venezuela	994	233
WOOSTER, WARREN S.		
(with Townsend Cromwell) An oceanographic description of the eastern tropical Pacific	996	*
WYLLIE, JOHN		
(with Joseph L. Reid, Jr. and Gunnar Roden) Studies of the California current system	998	293
ZoBELL, CLAUDE E.		
Ecology of sulfate reducing bacteria	1005	359

* Not available for exchange.

POSITION OF ANAL FIN AND LENGTH OF BODY CAVITY IN CATOSTOMID AND CYPRINID FISHES.—In "Fishes of the Great Lakes Region" (1949, Cranbrook Inst. Sci., Bull. 26: 24 and 45) Hubbs and Lagler pointed out that members of the sucker family (Catostomidae) may be distinguished readily from the minnows (Cyprinidae) by a superficial character, namely the more posterior anal fin: the distance from the origin of that fin to the caudal base is contained more, instead of less, than 2.5 times in the preanal length. It was further indicated, however, that in this respect the introduced carp, *Cyprinus carpio,* is like a catostomid. We were fully aware that many other extralimital cyprinids have the anal fin far back. The family key was obviously artificial and carries the reservation that it "will not apply to regions distant from the Great Lakes." The same warning was further stressed on page 2.

Overlooking this reservation and warning, Kafuku (1957, Jap. Jour. Ichth., 5: 163–73, figs. 1–3) dignified our family-separating character for Great Lakes Ostariophysi as the "morphological law on anal fin" and showed (as we were aware) that it did not apply consistently to Japanese cyprinids. Specifically, he indicated that the sucker-like Gobioninae have the anal fin far back and that they further agree with the catostomids in having the mouths inferior and more or less modified as a sucking organ, and in being bottom dwellers. He further expressed the opinion that the quoted distinction drawn by Hubbs and Lagler is "based on general relation between the mode of living and proportional length of body parts," that the Gobioninae have occupied in Asia the niche appropriated by Catostomidae in North America, and that the strong resemblances between the two groups is an example of parallelism in evolution.

I quite agree. The posterior location of the anal fin, where the ventral contour rises toward the caudal fin, brings the anal fin out of contact with the bottom or allows its lower and often thickened, morphologically anterior border to rest on the bottom in line with the long flattish ventral surface. Furthermore, the longer abdomen in the more or less vegetarian or ooze-eating bottom fishes makes room for a lengthening of the intestine that is associated with such diet, even without recourse to increased coiling.—CARL L. HUBBS, *Scripps Institution of Oceanography, University of California, La Jolla, California* (Contributions, New Series, No. 969).

(1)

Reproduced by Permission

(2)

Reprinted from COPEIA, 1958, No. 1, pp. 10–15, February 21
Printed in U. S. A.

Ichthyococcus irregularis, a New Gonostomatine Fish from the Eastern Pacific[1]

ANDREAS B. RECHNITZER AND JAMES BÖHLKE[2]

FOR approximately a century the genus *Ichthyococcus* Bonaparte (1840), of the family Sternoptychidae, subfamily Gonostomatinae, was known only from the type species *Ichthyococcus ovatus* (Cocco). In 1941

---

[1] Contributions from Scripps Institution of Oceanography, New Series, No. 970.

[2] The authorship is collaborative, the paper a combination of studies begun separately.

Reproduced by Permission

(4)

Imai described *Ichthyococcus elongatus* on the basis of a single specimen from Sagami Sea, Japan. Three adults of this species were captured by the Research Vessel "Horizon", during the Northern Holiday Expedition of the Scripps Institution of Oceanography, in collection H51-359 (field no. NH9), at 41°42′ N. Lat., 150°00′ W. Long.; depth of water recorded at 2,700 fathoms (4,938 m.); calculated depth of haul (10-foot Isaacs-Kidd midwater beam trawl) 600–850 m.; GCT 5:52–8:30 p.m., 11 August 1951.

Recently 13 specimens of a form described herein as new have been taken in the tropical and temperate eastern Pacific by vessels from the same institution and three additional examples were taken earlier (1925) by the *Arcturus* Oceanographic Expedition of the New York Zoological Society. A large number of larvae of *Ichthyococcus,* thought to be the young of this species, have been taken off California and Baja California (Fig. 3).

Ichthyococcus irregularis, *sp. nov.*
Pl. I, Figs. 1–3

Holotype—U. S. National Museum (USNM) 169735, an adult 76 mm. in standard length, taken by the Research Vessel "Paolina-T" off Baja California, Mexico, in collection H51-90, between 25°44′ N. Lat., 114°52′ W. Long. and 25°52′ N. Lat., 114°40′ W. Long.; depth of water "to 2,000 fathoms" (3,658 m.); calculated depth of haul (10-foot Isaacs-Kidd midwater beam trawl) 2,213 m.; 11:42 p.m. to 9:30 a.m., 21–22 March 1951.

Following are the data on the additional specimens that we have examined: Stanford University = SU 46348 (New York Zoological Society = NYZS 5975), 1 specimen (in poor condition), 34.2 mm. long, taken by the *Arcturus* Oceanographic Expedition of the New York Zoological Society at Sta. 74-OT3, 60 mi. south of Cocos Island; 4°50′ N. Lat., 87°00′ W. Long.; "nearest sounding 514–900 fathoms"; duration 1 hr., 29 min.; calculated depth of otter trawl 833 fathoms (1,524 m.); 2:11 p.m., 29 May 1925.

SU 46346 (NYZS 6276), 1 paratype, 33.0 mm. in standard length, taken on the same expedition at Sta. 84-T21, at the Galápagos Islands (Archipiélago de Colón) 1 mile north of Narborough Island (Isla Fernandina); 00°17′ S. Lat., 91°34′ W. Long.; nearest sounding 672 fathoms (1,229 m.); calculated depth of tow net 600 fathoms (1,097 m.); duration 1 hr., 32 min.; 2:06 p.m., 11 June 1925.

SU 46349 (NYZS 6313), 1 specimen (in bad condition), about 24.5 mm. long, taken on the same expedition at Sta. 86-PT1, 16 miles southwest of Narborough Island; 00°42′ N. Lat., 91°47′ W. Long.; nearest sounding 1,900 fathoms (3,475 m.); calculated depth of Petersen trawl 1,000 fathoms (1,829 m.); duration 51 min.; 9:39 a.m., 12 June 1925.

1 paratype, 34.3 mm. long, taken by the Research Vessel "Horizon" on Cruise 32, off central Baja California, in collection H51-406 (field no. H-32-1) between 27°17.6′ N. Lat., 117°04.9′ W. Long. and 26°56.8′ N. Lat., 117°00.9′ W. Long.; depth of water 3,292–3,658 m.; calculated depth of haul (10-foot Isaacs-Kidd midwater beam trawl) 2,926 m.; 7:10 p.m. to 7:50 p.m., 29–30 November 1951.

1 paratype, 47.5 mm. long, taken by the Research Vessel "Horizon" on the Shellback Expedition of Scripps Institution of Oceanography off Central America, in collection H52-390, between 08°09′ and 08°16′ N. Lat., along 84°58′ W. Long.; depth of water 1,230 fathoms (2,250 m.); calculated depth of haul (10-foot Isaacs-Kidd midwater beam trawl) 450 m., 1:22 p.m. to 4:10 p.m., 31 July 1952.

2 paratypes, 27.5 and 38.6 mm. long, taken by Dr. Gordon Tucker on the Research Vessel "E. W. Scripps," in collection T319, at 32°47.4′ N. Lat., 117°35.7′ W. Long.; in a 6 × 6-foot beam tow net hauled obliquely to the surface from a depth of about 360 m. at a rate of 10 m. per min.; 9:55 to 10:35 a.m., 1 August 1952.

2 specimens about 21 to 33 mm. long, collected by the Research Vessel "Horizon" on the Eastropic Expedition of Scripps Institution in collection SIO 55-232 (field no. ET(B)-H-31); between 10°52′ N. Lat., 88°02′ W. Long. and 10°59′ N. Lat., 88°05′ W. Long.; depth of water 2,771–2,780 m.; calculated depth of haul (10-foot Isaacs-Kidd midwater beam trawl) 450 mm.; 7:55 to 10:15 p.m., 4 November 1955.

1 paratype, 31.5 mm. long, taken on same expedition between 02°00′ S. Lat., 90°33′ W. Long. and 02°03′ N. Lat., 90°54′ W. Long.; in collection SIO 55-258 (field no. ET(B)-H-58); depth of water 3,192–3,237 m.; depth of haul (10-foot Isaacs-Kidd midwater beam trawl) 1,509–1,692 m.; 8:20 p.m. to 1:45 a.m., 28–29 November 1955.

4 paratypes, 14.8 to 32.7 mm. long (in poor condition), taken on the same expedition in the eastern Pacific in collection SIO 55-265 (field no. ET(B)-H-65); 00°02′ N. Lat., 100°23′ W. Long.; depth of water 3,283–3,457 m.; calculated depth of haul (10-foot Isaacs-

Kidd midwater beam trawl) between 1,107 and 1,335 m.; 12:35 to 4:45 a.m., 6 December 1955.

2 specimens, about 28 mm. long (badly damaged), taken on the Eastropic Expedition between 10°52′ N. Lat., 88°02′ W. Long. and 10°59′ N. Lat., 88°02′ W. Long. in collection SIO 55-232; water depth 3,000 m.; depth of haul (10-foot Isaacs-Kidd midwater beam trawl) 445–326 m.; 7:55 p.m. to 10:15 p.m., 4 November 1955.

Since no closing device was used on these midwater trawl hauls, the specimens were subject to capture during the lowering and raising of the net.

All specimens other than the holotype and those bearing Stanford University identification numbers are deposited at the Scripps Institution of Oceanography.

The following key is based primarily on an examination of the specimens of *I. elongatus* and *I. irregularis* just recorded and on three of *I. ovatus*. One of the *I. ovatus* specimens, SU 9502, taken at Messina, Italy, came from the Royal Zoological Museum at Florence. Two others (H52-199 in Scripps Institution of Oceanography) 39.5 and 41.0 mm. long, were taken at Sta. 1370 I, at 36°36′ N. Lat., 26°14′ W. Long., with 1,000 m. of wire out, at 2:30 a.m., 13 June 1922; "Redskat; E 300"; they were sent from the Carlsberg Laboratorium by Å. Vedel Tåning. The study of these specimens has been supplemented by an examination of the accounts of the species of the genus by Brauer (1906: 94), Jespersen and Tåning (1926: 38), Imai (1941: 234), Borodin (1931: 69), Sanzo (1931: 49), and Norman (1939: 20).

KEY TO THE SPECIES OF *Ichthyococcus*

A. Dorsal rays 10–13; gillrakers 15–19 on lower limb of first arch; photophores in upper series totaling 23–26; greatest depth of body 2.3–3.1 in standard length; scales in a lateral series 32–39; vertebrae 38–39.

B. I–P series of ventral photophores in a straight line when viewed from below, with No. 8 only displaced laterally; A–C series continuous; interorbital region extremely narrow, with a median longitudinal ridge (Mediterranean Sea, eastern Atlantic Ocean, and, reportedly, Indian Ocean)....*I. ovatus*

BB. I–P series of photophores highly irregular (Fig. 1 and Pl. I); No. 8 displaced far outward; No. 9 displaced inward (and reduced in size); No. 10 displaced moderately outward, and Nos. 10 to 14 of each side converging posteriorly; A–C series interrupted; interorbital region comparatively broad, without a median ridge, but with lateral longitudinal ridges or flanges on either side (eastern Pacific)...............*I. irregularis*

AA. Dorsal rays 15; gillrakers 24–26; photophores in upper series 31; greatest depth of body 4.6; scales 42–44; vertebrae 47. Photophores arranged as in *ovatus*; interorbital rather broad and flat, approaching that of *irregularis* (northeastern Pacific and North Pacific Drift)........................*I. elongatus*

DESCRIPTION

D. 11 or 12; A. 13 (13–15); P 8/8; P_2 7/7; lateral scales 35 (34–36); gillrakers of first arch usually 8 + 17–19. Depth of body averageing 2.8 (range 2.6–3.0); length of head 2.8 (2.6–3.1); snout to dorsal 2.0 (1.9–2.1); snout to adipose 1.3 (1.3–1.4); snout to pectoral 3.0 (2.8–3.2); snout to pelvic 1.7; snout to anal 1.3, and least depth of caudal peduncle 9.3 (8.2–10.1), all in standard length. Diameter of eye 3.0, length of snout 3.7, width of bony interorbital 8.4, snout to end of maxillary 2.1, length of pectoral 1.5, length of pelvic

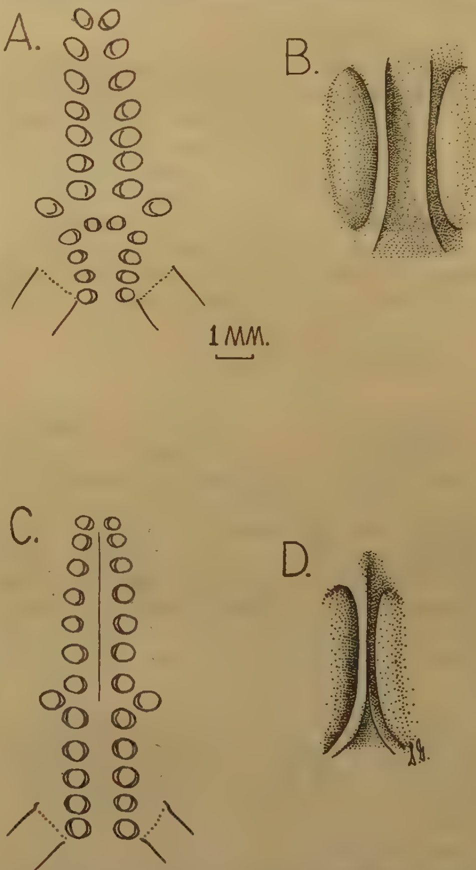

Fig. 1. Pattern of prepectoral photophores and form of interorbital in *Ichthyococcus irregularis* (A and B) and in *I. ovatus* (C and D), drawn from specimens SU 46346 and 9502, respectively.

(6)

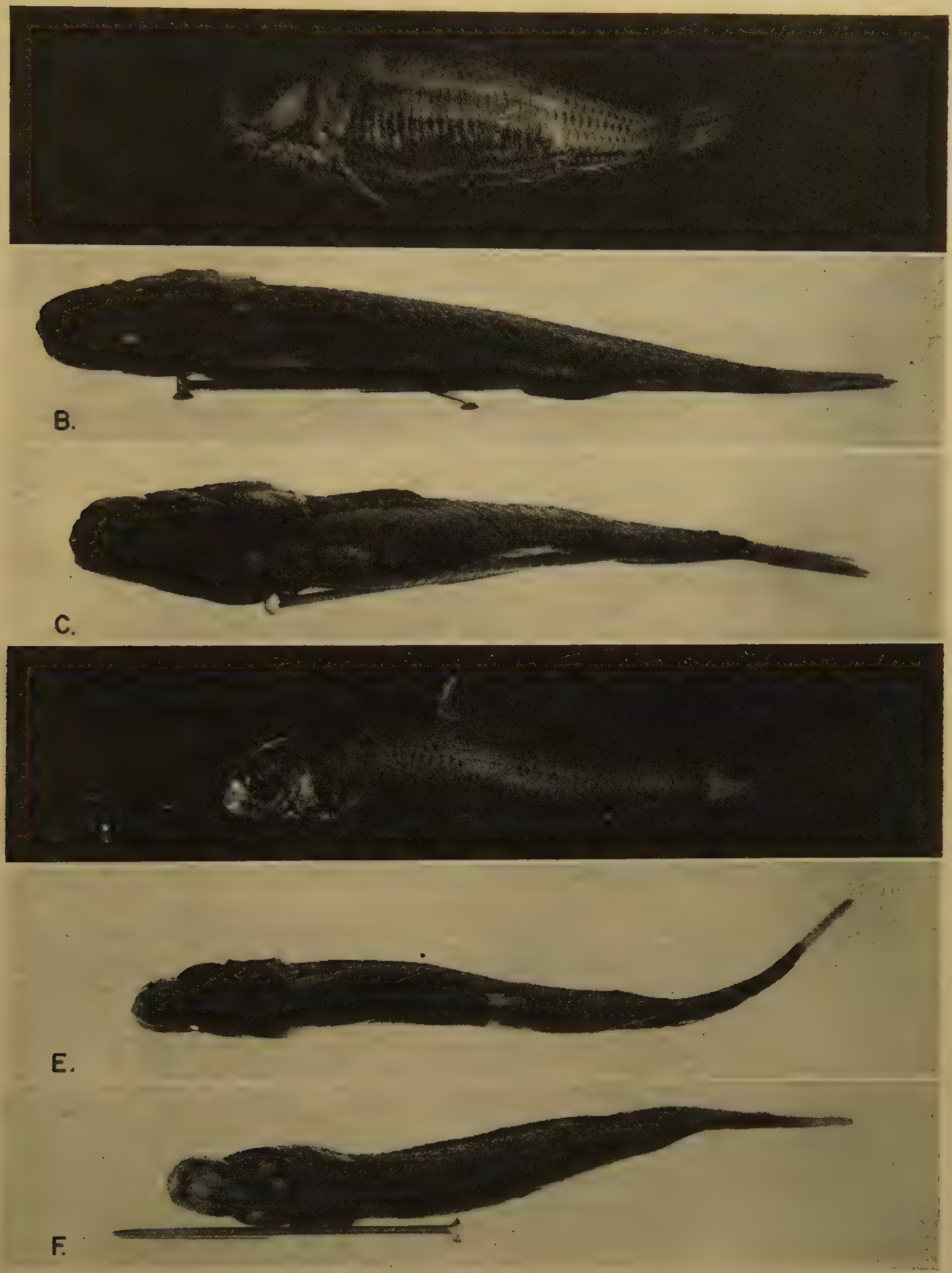

Plate I

A–C. *Ichthyococcus irregularis:* lateral, ventral, and dorsal views of holotype (76 mm. standard length); collected at 25°44′N. Lat., 114°52′W. Long.; USNM 169735.

D–F. *Ichthyococcus elongatus:* lateral, ventral, and dorsal views of specimen (H51-359) from eastern Pacific 41°42′N. Lat., 150°00′W. Long., 78 mm. long.

2.2, length of dorsal base 1.7, length of adipose base 2.2, and length of anal base 2.5, all in head length.

Body shape same as that of *Ichthyococcus ovatus* (Fig. 23, one of Jespersen and Tåning, 1926). Greatest body depth at origin of dorsal, which is equidistant from tip of snout and base of caudal fin. Pelvic fins inserted below the interspace between the seventh and eighth dorsal rays. Anal originating behind a vertical through origin of adipose dorsal. Pectorals not nearly reaching pelvics; pelvics failing to reach to anus.

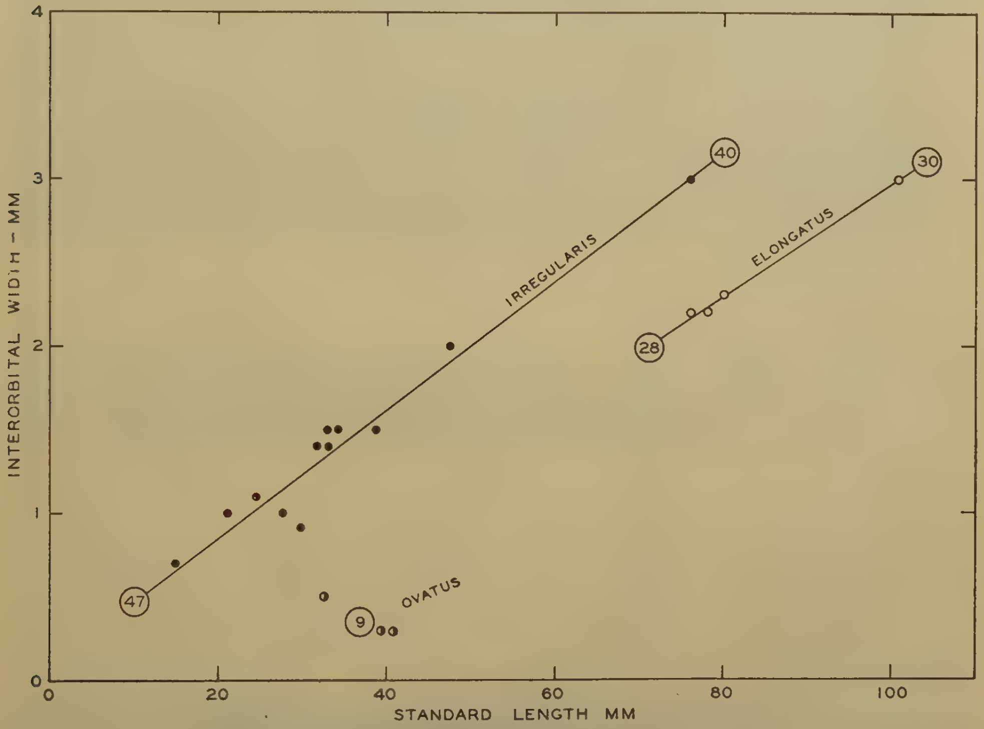

Fig. 2. Relation between least bony interorbital width and standard length in the three species of *Ichthyococcus*. The ringed figures indicate proportions, at indicated points, as thousandths of standard length.

Five photophores on either side of head: one before eye, one below eye, one at angle of preopercle, one on lower portion of opercle, and one at upper end of opercle. Branchiostegal series 12. In the upper lateral series P–V 13, V–A 10. In the lower lateral series: I–P 11 (plus an additional organ lateral and adjacent to the interspace between photophores 7 and 8 of the main series), P–V 13, V–A 9, A–C 12–13 (usually 7 + 5). It is in the I–P photophores of the ventral series that most of the modifications have occurred which distinguish this species. In *ovatus* the only photophore that is out of line is No. 8, which is displaced about its full width outward. A similar displacement occurs in the other species. In *irregularis,* in addition, photophore 9 is displaced inward so that the pair of the two sides lie close together, and this organ is somewhat reduced in size; No. 10 is displaced outward a little, and Nos. 10 to 14 of each side converge posteriorly. From back to front, the two ventral series diverge evenly (beginning below the pectoral base) to photophore 10 mentioned above; in fact, the photophore 8 of the I–V series might be considered the anterior member of this series, which has flared out laterally, were it not for the simpler pattern displayed by the other species. It is certainly in line with them (Pls. IB and E, IIB).

Scales cycloid, thin, very deciduous. The counts in the accompanying table are made from scale pockets and the vertical pigment streaks, each of which appears to correspond to one scale.

Interorbital space broad, flat in the middle, rising on either side to a longitudinal ridge (Fig. 1 and Pl. IC). This condition contrasts sharply with that in *I. ovatus,* in which the interorbital is narrow, with a median ridge (Fig. 1 and Pl. IIC). Differences in the relation between interorbital width and standard length are trenchant (Fig. 2).

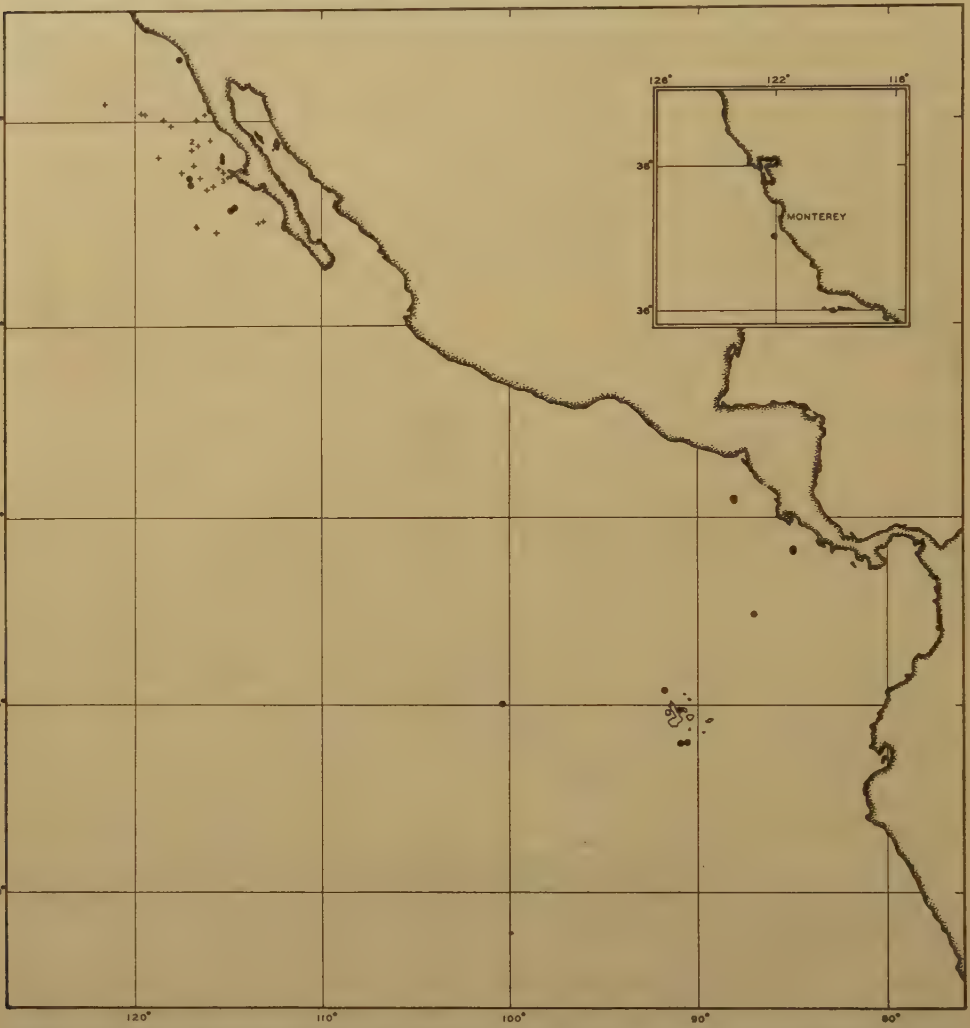

Fig. 3. Known distribution in the Pacific Ocean of *Ichthyococcus irregularis.* (solid circles) Known distribution in the Pacific Ocean of larvae of *Ichthyococcus* presumed to represent *irregularis.* (crosses) Most specimens were collected off Baja California due to extensive collecting in this area. Presumably additional larvae and adults will be collected in other areas, particularly in more tropical waters.

DERIVATION OF NAME

The name *irregularis* refers to the irregular arrangement of the ventral photophores before the pectoral fin.

DISTRIBUTION

So far as known, the three species of *Ichthyococcus* are allopatric. *I. ovatus* is definitely known from the Mediterranean Sea and the eastern Atlantic Ocean, and has been reported (Brauer, 1906: 96; Norman, 1939: 20), from the Indian Ocean. On the basis of two young specimens that may represent *I. irregularis,* Brauer counted 12 branchiostegal photophores, as we do in *irregularis,* and he figured the anal series as interrupted—as it is in *irregularis.* Our material of *irregularis* all

(10)

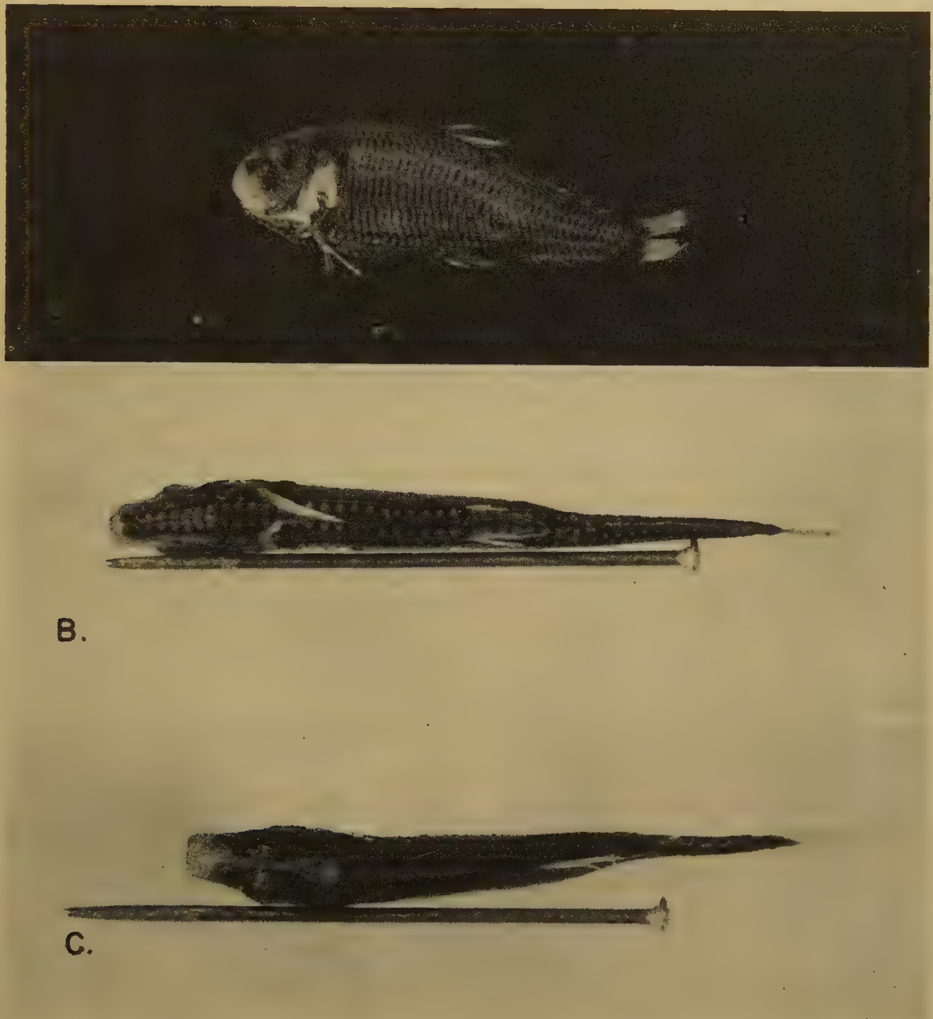

Plate II

A–C. *Ichthyococcus ovatus:* lateral, ventral, and dorsal views of specimen H52-199 from Atlantic Ocean, 36°36′N. Lat., 26°14′W. Long., 39.5 mm. long.

comes from the eastern Pacific, from tropical waters to off southern California. One of the collections of larvae, presumed to be of this species, is from off central California, to which region it might have been carried by the Davidson Countercurrent. *I. elongatus* appears to be one of the species of the northwestern Pacific that ranges into the northeastern Pacific along the North Pacific Drift.

RELATIONSHIPS

Ichthyococcus irregularis is most similar, and presumably most closely related, to *I. ovatus,* contrasting in several respects sharply with *I. elongatus* (as is indicated in the key). *I. irregularis* and *I. ovatus* have the same general body form and are very similar in meristic counts. Both contrast with *elongatus* in their relatively short and deep bodies and in the reduced numbers of vertebrae, scales, dorsal rays, photophores, and gillrakers. *I. irregularis* contrasts with *I. ovatus* (and also with *elongatus*) in the odd arrangement of the ventral photophores before the pectoral fin (Fig. 1 and Pl. I) and in the interruption of the anal series of photophores; it also has a much wider interorbital (Figs. 1–2) with raised rims and no median ridge (in which respect *elongatus* is more like *irregularis* than *ovatus*). Less trenchant differences between *irregularis* and *ovatus* are the somewhat lower counts of anal rays, caudal vertebrae, P–V photophores both lateral and ventral, and A–C photophores; and the slightly more numerous gillrakers.

These three well-differentiated species form a series that parallels within limits the striking evolutionary sequence (Gonostomatinae—Maurolicinae—Sternoptychinae) that led Hubbs (1953) to refer all these diverse types to one family (Sternoptychidae). The sequence in *Ichthyococcus* is *elongatus—ovatus—irregularis. I. elongatus* most nearly approaches the generalized attenuate gonostomatines, such as *Vinciguerria,* and is presumably the most primitive form. In the evolutionary sequence the body becomes deep and foreshortened, with an enlarged head region, and with a reduced number of segmental structures. The interruption of the anal photophores is in the same line of evolution, and the out-of-line arrangement of the anterior ventral photophores is an obvious specialization. An enlargement of the photophores, especially in the vertical axis, marks both the species sequence and the subfamily sequence.

ACKNOWLEDGMENTS

We wish to thank Dr. George S. Myers and Miss Margaret Storey of the Natural History Museum of Stanford University for the loan of material of *I. ovatus* and of the new species; Dr. Å. Vedel Tåning of the Carlsberg Laboratorium for two specimens of *I. ovatus,* which are now a part of the Scripps Institution of Oceanography collection; Dr. Gordon H. Tucker of San Diego State College for two specimens of the new species; Dr. Elbert H. Ahlstrom for identifications and distribution data on the larvae presumed to represent *I. irregularis;* and Dr. Carl L. Hubbs of the Scripps Institution of Oceanography, who originally participated in the identification of the new species, for numerous helpful suggestions and for a critical examination of the manuscript.

Our thanks to Dr. Denys Tucker of the British Museum (Natural History), for reexamining a single, 13 mm., nearly broken specimen reported by Norman (1939: 20) to most likely be *I. ovatas.* Using our key he confirms the identification, but retains some reservation for change because of its poor condition.

LITERATURE CITED

BORODIN, N. A. 1931. Atlantic deep-sea fishes. *Bull. Mus. Comp. Zool. Harvard Coll., 72: 55–89, 5 pls.*

BRAUER, AUGUST. 1906. Die Tiefsee-Fische. I. Systematischer Teil. *Wissenschaftlichen Ergebnisse der deutschen Tiefsee-Expedition auf dem Dampfer "Valdivia" 1898–1899, 15: 1–432, figs. 1–176, pls. 1–18.*

HUBBS, CARL L. 1953. Synonymy of the bathypelagic fish genus *Rhynchohyalus,* referred to the expanded family Argentinidae. COPEIA, 1953 (2): 96–97.

IMAI, SADAHIKO. 1941. Seven new deep-sea fishes obtained in Sagami Sea and Suruga Bay. *Japanese Jour. Zool., 9: 235–250, figs. 1–17.*

JESPERSEN, P., AND Å. VEDEL TÅNING. 1926. Mediterranean Sternoptychidae. *Report on the Danish Oceanographical Expeditions 1908–10 to the Mediterranean and adjacent seas, 2, Biology, A. 12: 1–59, figs. 1–30.*

NORMAN, J. R. 1939. The John Murray Expedition 1933–34. *Scientific Reports,* 7 (1): 20.

———. 1930. Oceanic fishes and flatfishes collected in 1925–1927. *Discovery Reports, 2: 261–370, figs. 1–47, pl. 2.*

SANZO, L. 1931. Uova, larve e stadî giovanilli di teleostei. *Fauna ē Flora del Gulfo di Napoli: 49–55.*

U. S. NAVY ELECTRONICS LABORATORY, SAN DIEGO 52, CALIFORNIA, AND ACADEMY OF NATURAL SCIENCES, PHILADELPHIA 3, PENNSYLVANIA.

(14)

Särtryck ur Tellus nr 1, 1958

Quartz Contents of Pelagic Sediments of the Pacific Ocean[1]

ROBERT W. REX and EDWARD D. GOLDBERG
Scripps Institution of Oceanography, University of California, La Jolla, California

(Manuscript received July 30, 1957)

Abstract

The quartz contents of pelagic clays from the Eastern Pacific Ocean show a marked latitudinal dependence with a maximum around 30° N. Present evidence indicates that the quartz is mainly transported to the deposits through the atmosphere and that the observed distribution is probably related to the latitudinal values of the atmospheric wind fluxes and exposed arid land areas. A number of sediments display a distinct change in quartz content with depth. In all cases there is a marked decrease going from the recent to the older strata. It is suggested that the changes indicate a major climatic change that occured sometime during the Late Tertiary.

Quartz is one of the major minerals in igneous rocks (12 – 20% on the average) and is one of the most resistant substances to chemical and mechanical weathering (PETTIJOHN, 1957), yet its role in the major sedimentary cycle is poorly understood. Few determinations of its concentration in recent marine sediments have been made. CORRENS (1937), REVELLE (1944), KUENEN and NEEB (1943), and GRIM ET AL. (1949) give semi-quantitative estimates in their studies, while REVELLE ET AL. (1955) present figures of 2 – 5% in Pacific buff clays. Inasmuch as the total amounts of quartz in sediments may serve as an indicator both of the lithogenous contribution as well as of the mechanics of deposition, it appeared worthwhile to make an intensive quantitative study of its space and time distribution in the Pacific Ocean deposits.

The determinations were made by x-ray diffractometry and the results are reproducible to ±3% of the absolute values obtained with a minimum sensitivity of 0.3% quartz. The details of the method will be published elsewhere.

The quartz particles in the sediments are found as chips and shards and are well sorted with maximum concentrations between 1 and 20 microns (Figure 1). There is no microscopic evidence for crystal overgrowth. Quartz bipyramids, characteristic of volcanic beta quartz, have not been observed in any of the samples. There is no evidence for the authigenic formation of quartz in the marine environment. INGERSON (1955) points out that there is no known example of the crystallization of quartz from aqueous solutions below 100° C. and no conversion of biogenous silica to quartz has been observed in unmetamorphosed sediments dating back to the Miocene (BRAMLETTE, 1946). Inspection of biogenous silica in sediments as old as Paleocene showed no significant conversion of opal to quartz. In this presentation almost all of the samples are apparently of Miocene age or younger.

---

[1] This paper represents in part results of research carried out by the University of California under contract with the Office of Naval Research.

Contribution from the Scripps Institution of Oceanography, New Series No. 971.

Reproduced by Permission

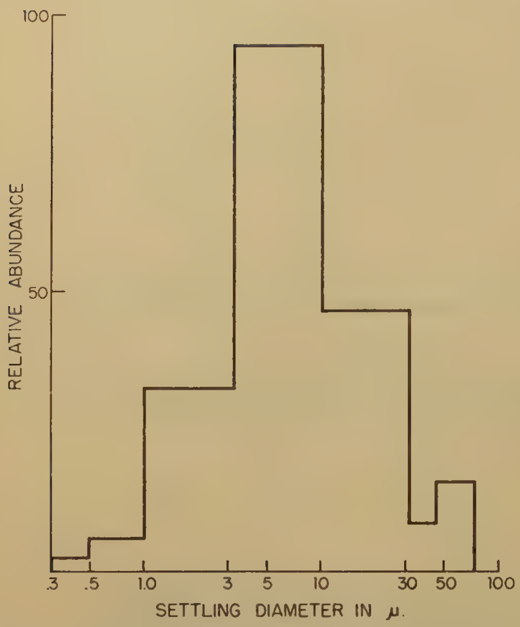

Fig. 1. The size distribution of quartz in pelagic clay sample PAS 19121 (Lat. 19°49«N; Long. 121°43.5«W; and depth 4,350 meters).

Space and Time Distribution of Quartz

The two principle results of the study are the space and the time distribution of quartz in the pelagic sediments. The major feature of the surface distribution in the Eastern Pacific is a marked latitudinal dependence of the quartz concentration with a maximum at around 30° North and decreasing in both the north and south directions (Figure 2). The values are for the calcium carbonate free fraction of the sample. Perturbations of this general pattern can be effected in the following ways. The introduction to the deposits of biogenous silica or carbonates reduces the observed quartz values. This is evident in the highly diatomaceous samples from the Bering Sea and from the area to the immediate south of the Aleutian trench and in the siliceous and carbonaceous deposits of the equatorial belt.

A second type of dilution is found in the quartz distribution in the sediments surrounding the Hawaiian Islands (Figure 3). These islands belong to a basaltic province and the magmas are strikingly deficient in quartz compared to the average abundance in igneous rocks. The deposits are diluted to a distance of 150 miles north by the weathering products from the erosion of the islands. The Hawaiian Arch appears to form the outer margin of transport of materials. Again, volcanic ash layers in cores from the Gulf of Alaska show smaller values of quartz than adjacent strata.

The latitudinal pattern can also be disturbed by turbidity current deposits which occur on abyssal plains, walls and bottom of deep trenches and archipelagic aprons. For example, on the shoreward side of the Acapulco trench area, where turbidity flows are thought to occur, the quartz ranges between 12 and 24%, while in the seaward deposits of the trench, free of such flow from the coastal area, the values are of the order of 8%. Further evidence of the influence of turbidity currents upon the quartz contents of sediments will be discussed below.

A number of red clay cores display a distinct change in the characteristics of the sediment type with depth. Such variations exist either as discrete discontinuities or gradual changes. In all such cases, there is a marked decrease in the quartz concentration in the lower levels of the cores (Table 1). The quartz values above and below the zones of change are remarkably uniform (Figure 4). In most cases the upper sediment contained a Quarternary radiolarian fauna. Three of the cores contained Middle Tertiary radiolarian fauna in the lower quartz poor strata (Riedel, W., personal communication). The remaining cores contained no age-indicating fossils below the discontinuity.

Sources of the Quartz

Two significant problems relative to these results are the sources and modes of transport of the quartz. Since we have ruled out an authigenic origin, there remains the consideration of the relative contributions of continental detritus and marine volcanic ejecta. The quartz contents of sediments containing large amounts of pyroclastics are notably low. The presence of quartz as chips and shards and the absence in the sediments of quartz phenocrysts, typical of volcanic lava, support the argument of a continental source.

The consistent appearance of the same broad band (3.18 – 3.24Å°) in the x-ray diffraction spectra of pelagic clays in the Pacific represents a composite of feldspar peaks. This indicates contributions from many sources with sub-

TABLE 1

Depth Distribution of Quartz in North Pacific Sediments

Core	Zonation (cm.)		Contact	Quartz Content		Samples Run	Notes
	Upper	Lower		Upper	Lower		
Chubasco 10 10° 21.4′ N 124° 26.3′ W 4,645 meters	0—86	86—120	Discontinuous	8%	3%	Upper: 0—4; Lower: 116—120	Upper zone contains Quaternary radiolaria with admixed Tertiary. No age-indicating fossils in lower zone.
Chubasco 9 10° 18.5′ N 125° 27.2′ W 4,545 meters	0—32	32—100	»	8%	3%	Upper: 0—4, 16—20; Lower: 44—48, 96—100	Upper zone contains Quat. rads. with admixed Tertiary. Lower zone contains Middle Tert. rads.
Mid-Pac 14 9° 57.7′ N 145° 12.7′ W 5,232 meters	0—4½	4½—79	»	8%	2%	Upper: 3—4; Lower: 74—76	Upper zone contains Quat. rads. with much admixed Tert. Lower zone contains Middle and Early Tert.
Capricorn 49 BP 9° 17′ N 124° 09′ W 4,410 meters	0—124	228—832	Gradational from 124 to 228 cm.	8%	3%	Upper: 0—4; Lower: 300—304	Upper zone to at least 40 cm. probably Quat. with Tert. admixture. Lower zone Middle Tert.
Capricorn 50 BP 14° 55′ N 124° 12′ W 4,270 meters	0—302	302—812	Discontinuous	9.8 ± 0.9%	2.8 ± 0.5%	Upper: 0—302 (72 samples); Lower: 302—812 one sample every 20 cm. (18 samples)	Upper zone perhaps Quat. Lower zone no age-indicating fossils.
Chinook 2 35° 09′ N 157° 17.5′ W 5,610 meters	0—21	21—54	»	16%	6%	Upper: 0—4; Lower: 51—54	No age-indicating fossils in core.
Chinook 4 42°29.9 N 162°8.2′W 5,400 meters	0—126	126—157	»	15%	12%	Upper: 0—5, 10—12, 12—16; Lower: 128—132, 140—144, 144—148, 154—157	Upper zone Quat. rads. Lower zone no age indicating fossils.

sequent mixing. The continents provide the necessary variety of feldspars to produce such a composite peak. Further, in samples from areas where pyroclastics are abundant in the deposits, the composite feldspar band is overshadowed by sharp peaks characteristic of the feldspars from local sources of volcanic activity.

Transport Mechanics

It is difficult to conceive of the water transport of quartz particles with their observed size distributions from the continental boundaries to pelagic areas, which are inaccessible to turbidity flow or ice rafting. For example, the area of abundant quartz, north of Hawaii, is approximately 2,000 miles from the nearest continental area. The Stoke's settling times for quartz particles of 10 micra diameter, which are near the mean of those in the sediments, is approximately 2 years for 4,000 meters. (In suggesting these Stoke's Law settling times we have not included any enhancements attributable to the aggregation of particles by filter feeding organisms and a subsequent excretion in larger, more rapidly settling masses). These data demand an *average horizontal westerly* com-

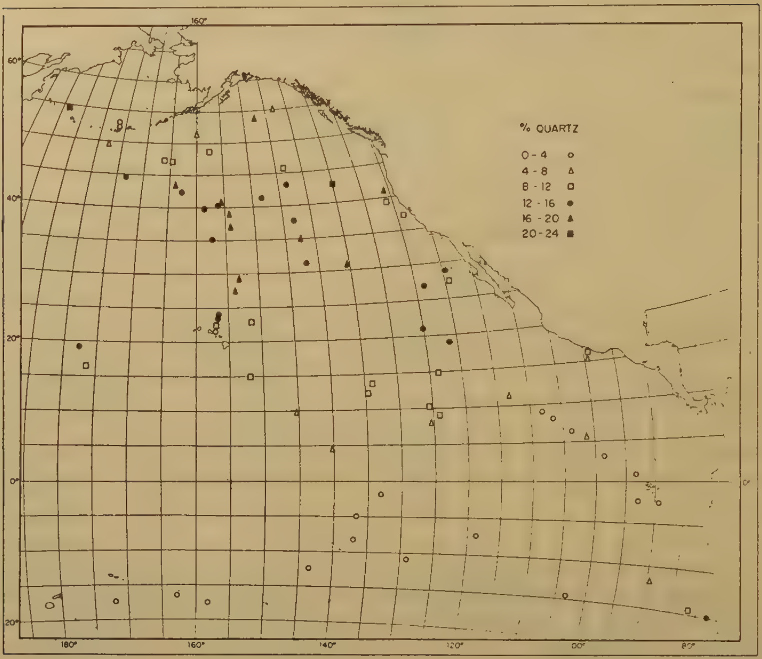

Fig. 2. The concentration of quartz in surface sediment samples from the Eastern Pacific Ocean.

ponent of ocean currents from the North American coast to the deposition site of 0.1 to 0.2 knots for that part of the water column containing the quartz. Such currents have not yet been observed in the descriptive oceanographic studies of this region. Further, the latitudinal variation in the quartz contents is inconsistent with the observed circulation of the North Pacific. Finally, it is difficult to explain the maximum in the quartz concentration in pelagic sediments that are furthest from land by a water transport mechanism. Any water fractionation mechanism that will sort quartz from the more slowly settling, small clay particles would result in a distribution in which quartz would be present in decreasing concentrations with increasing distance from land.

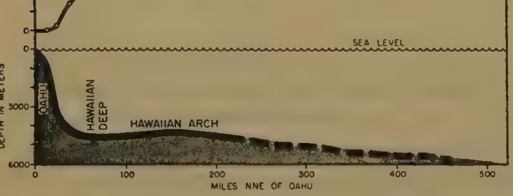

Fig. 3. The dilution of quartz contents in pelagic sediments by weathering products from Oahu Island.

The abyssal plain deposits of the Gulf of Alaska, provide examples of two possible mechanisms for the water transport of quartz: turbidity flow and ice rafting. Two samples, Cusp 5P (Lat. 43°00′N; Long. 134°27′W) and Cusp 11G (Lat. 45°34′N; Long. 143°11′W) situated at approximately 500 and 1,000 miles respectively from the continents, have high quartz contents in the sand and silt sizes and are accompanied by abundant mica which is low or absent from the nearby red clay deposits on topographic highs. The nearshore sample Cusp 5P, contained 22% quartz whereas the more distant deposits contained 10%. The values can most satisfactorily be explained by the sorting action of turbidity currents as described by KUENEN (1950) where the coarser particles are dropped out near the source of flow. The neighboring pelagic clays have values of 15% quartz

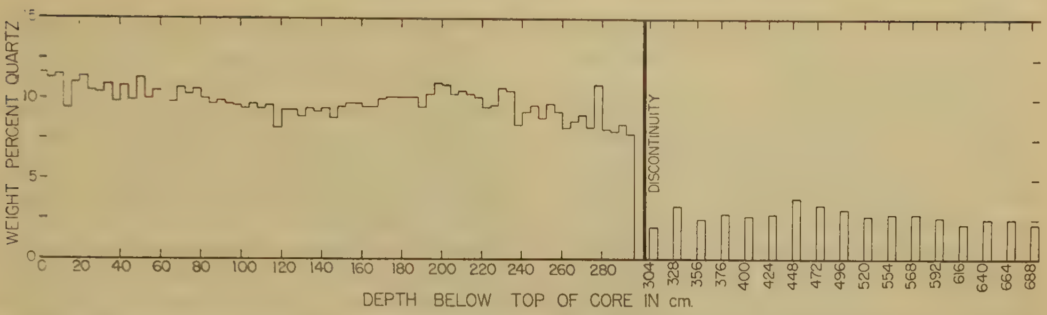

Fig. 4. The quartz concentrations as a function of depth in Capricorn 50 BP (Lat. 14°55«N; Long. 124°12« W). The depth scale is discontinuous after the discontinuity.

and this suggests that the turbidity flow at its extremeties is low in quartz and serves to dilute the quartz contents of the normal pelagic clays. Ice rafting in the Northern Gulf of Alaska, as described by MENARD (1953), introduces a wide variety of poorly sorted materials which give erratic values to the quartz contents in the sediments. For example, Northern Holiday 3, (Lat. 53°22.6′N; Long. 147°13.6′W) contains 17% quartz while nearby NH2 (Lat. 51°34′N; Long. 149°58′W) and NH5 (Lat. 55°7.8′N; Long. 142°55′W) contain 7 and 3% respectively. All of these cores show miscellaneous assemblages of continental pebbles and grit.

Transport of particles by marine organisms appears to be relatively unimportant. The ingestion and subsequent excretion of inorganic particles probably takes place over relatively short periods of time and hence of space. Further, algal transport of significant amounts of sedimentary components appears to be negligible.

In the past not much more than general statements could be made concerning the importance of atmospheric transport of particles to the marine environment, yet there has been a general recognition of the importance of eolian particles in sediments (TWENHOFEL, 1939; CORRENS, 1953). Quantitative estimates of the contribution of such transported particles are lacking, however, a number of lines of evidence from this work converge upon the significance of eolian components in some marine deposits:

(1) The latitudinal variation of quartz corresponds to (a) the intensity of atmospheric fluxes in the troposphere and (b) the amounts of exposed arid regions of the northern hemisphere (Figure 5). The wind movements in the troposphere are dominantly zonal. Both of these parameters would directly influence the amount of dust transported, yet the relative importance of each has not yet been ascertained. As yet there is a paucity of samples from the Southern Hemisphere to complement these observations, and possibly to suggest which of these two parameters is the more significant.

(2) Quartz and other detrital minerals, including feldspars, amphiboles and pyroxenes

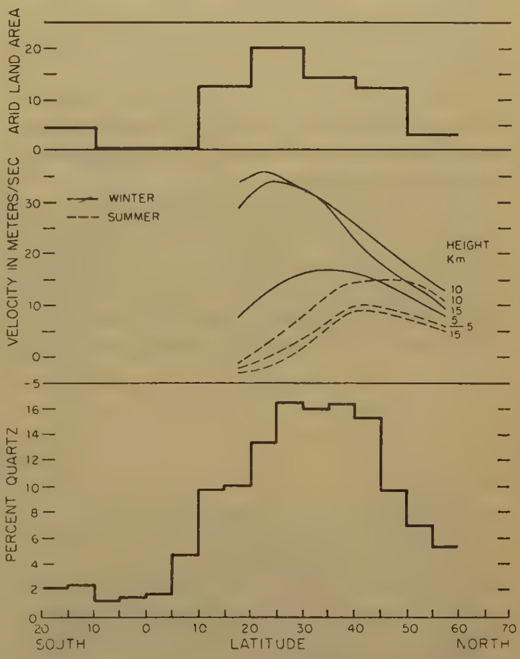

Fig. 5. Lower: The quartz distribution as a function of latitude in sediments from the Eastern Pacific; middle: Mean zonal component of the geostrophic wind. Taken from BYERS (1954); upper: the area of steppe and desert regions in arbitrary units (KÖPPEN and GEIGER, 1936).

have been observed in the guts of filter-feeding pelagic organisms living in the surface waters of the mid-Pacific ocean.

(3) The size distribution of quartz (Figure 1) is similar to observed atmospheric fallout distant from its point of origin. Glawion (1938) reports a grain size maximum between 3 and 5 micra for Sahara dust collected high in the Swiss Alps. Correns (1953) has emphasized the similarity of grain size distribution of marine sediments with atmospheric deposits by matching curves from both sources. His maxima ranged between approximately 10 and 50 micra.

(4) Quartz is consistently reported as a constituent of atmospheric dusts whose mineral compositions are ascertained. Kampe, Weickmann and Kedesdy (1952) detected quartz in addition to clays, lampblack and organic substances in snowcrystal nuclei in New Jersey. Leroux and Trillat (1954) find as common constituents of atmospheric dusts quartz, gypsum, anhydrite, calcite, feldspar, magnetite and hematite. Further, in our laboratories, quartz has been observed in snows from the high coastal mountains of Southern California, and from the Arctic ocean area, in Anarctica and in radioactive rain water from Japan.

Certain deductions can be made from the above evidences that the quartz in most pelagic sediments is atmospherically transported from the continental areas.

Pelagic sediments, deposited below the area of the jet stream in the Northern Hemisphere, are composed to a significant extent of materials that were atmospherically transported. Quartz is not the only mineral found in atmospheric dusts that is refractory to marine weathering processes. Such weathering resistant minerals as feldspar, magnetite and certain clays are *in toto* quantitatively as important as the quartz, in the atmospheric dust, according to the work previously cited. Hence, in pelagic sediments containing 20 % quartz, it is reasonable to assume that around one half of the solid phases are of eolian origin.

Studies of quartz concentrations in areas of turbidity flow can be used to describe the hydraulic flow pattern. For example, the turbidity flows on the Hawaiian archipelagic apron (Menard, 1956) are apparently limited by the Hawaiian arch with a relief of 600 meters. This not only establishes an upper limit to the extent of the flow, but also establishes that such flows are confined to near bottom waters.

The decrease in quartz content with depth in the North Pacific sediments provides clear evidence for a major climatic change that occurred sometime during the Late Tertiary. These changes are accompanied by changes in the gross chemical composition (Revelle et al, 1955) which have been interpreted by Goldberg and Arrhenius (Geochim. Cosmochim. Acta, in press), as reflecting differences in rates of accumulation of solid phases. Thus, quartz concentrations, coupled with chemical compositions, may provide useful stratigraphic indicators for fossilfree clays.

Finally, this pattern of *natural fallout* may be of some use in studies of *radioactive fallout*. The particles in the normal atmospheric dusts may act as scavangers for the radioactive atoms and molecules and hence the distribution of such guest materials will be influenced both by paths of the host dust particles and subsequent chemical interactions with the environment.

LITERATURE

Bramlette, M. N., 1946: The Monterey formation of California and the origin of its siliceous rocks. *U. S. Geol. Survey Prof. Paper* **212** 55 pp.

Byers, H. R., 1954: In *The Earth as a Planet* (G. Kuiper, ed.). Chicago: University of Chicago Press, Chapter 7.

Correns, C. W., 1937: Die Sedimente des äquatorialen Atlantischen Ozeans. *Deutsche Atlantische Exped. Meteor* **1925—27 3**, 298 pp.

—, 1953: Der Anteil des Staubes an der Bildung der Sedimentgesteine. *Z. Ver. deut. Ing.* **95**, pp. 294—6.

Glawion, H., 1938: Staub und Staubfalle in Arosa. *Beitr. physik. freien Atmos.* **23**, pp. 1—43.

Grim, R. E., Dietz, R. S., and Bradley, W. F., 1949: Clay mineral composition of some sediments from the Pacific Ocean off the California coast and the Gulf of California. *Bull. Geol. Soc. Amer.* **60**, pp. 1785—1808.

Ingerson, E., 1955: Geologic thermometry. *Geol. Soc. Amer. Special Paper* **62** pp. 465—88.

Kampe, H. J., Weickmann, H. K., and Kedesdy, H. H., 1952: Remarks on "electron microscope study" of snow-crystal nuclei. *J. Meteor.* **9**, pp. 374—5.

Köppen, W. and Geiger, R., 1936: *Handbuch der Klimatologie I* Berlin: Gebrüder Borntraeger, Chapter C.

KUENEN, PH. H., 1950: *Marine Geology* New York: John Wiley and Sons, 568 pp.

—, and NEEB, G. A. 1943: *Bottom Samples, The Snellius Expedition* **5**, 268 pp.

LEROUX, J. and JACQUES-TRILLAT, J., 1954: Etude comparativ des poussieres atmospheriques minerales des quelques villes. *Compt. rend.* **238**, 1748—50.

MENARD, H. W., 1953: Pleistocene and recent sediment from the floor of the Northeastern Pacific Ocean. *Bull. Geol. Soc. Amer.* **64**, pp. 1279—94.

—, 1956: Archipelagic aprons. *Bull. Amer. Assoc. Petrol. Geol.* **40**, pp. 2195—2210.

PETTIJOHN, F. J., 1957: *Sedimentary Rocks* New York: Harper and Brothers, 718 pp.

REVELLE, R. R., 1944: Marine bottom samples collected in the Pacific Ocean by the Carnegie on its last cruise. *Carnegie Inst. Wash. Publ.* **556** Pt. **1**, 180 pp.

—, BRAMLETTE, M., ARRHENIUS, G., and GOLDBERG, E. D., 1955: Pelagic sediments of the Pacific. *Geol. Soc. Amer. Special Paper* **62** pp. 221—36.

TWENHOFEL, W. H., 1939: *Principles of Sedimentation* New York: McGraw-Hill, 610 pp.

PRINTED IN SWEDEN
ESSELTE, STHLM 58

(21)

(*Reprinted from Nature, Vol.* 181, *pp.* 207–208, *January* 18, 1958)
Reproduced by Permission

A Possible Ecologial Effect of Upwelling in a Submarine Canyon*

DURING July–November 1956, an exploratory ecological survey along the south-west edge of the La Jolla submarine canyon was conducted over a sandy bottom using self-contained underwater breathing apparatus[1] diving techniques (for a chart of the region see Shepard and Emery[2]), and the following preliminary information may be of general interest.

There are sharp changes in the dominant species of animals as one swims toward the north-west along the canyon axis between the 27- to 37-m. contours. In the shoreward regions (area 1) abundant populations of the sea-pen, *Stylatula elongata*, and the sea-star, *Astropecten californicus*, exist. Abruptly the community changes and is almost entirely *Astropecten* for about 50 m. (area 2). Continuing farther (area 3), brittle stars, *Ophiura lütkeni*, are found almost exclusively. On the broad, sandy continental shelf to the north *Ophiura* are not found until a depth of 47–50 m. is reached; *Astropecten* here occurs at 40–23 m. and *Stylatula* at 23–10 m. Boundaries between communities on the shelf appear to run parallel to the depth contours; at the canyon they run across the contours.

100–150 m. traverses were swum near the 30-m. contour along the edge of the canyon through the regions mentioned above. Centrally within these regions counts of animals were made in areas chosen at random by quadrats cast down blindly. Table 1 presents the marked differences which were found.

The areas on the canyon rim are not characterized by any large differences in substrate, depth and

Table 1

Animal	Size of quadrat (m.^{2})	No. of individuals in each sample	Individuals (per m.^{2})
Area 1			
Astropecten	1	0, 0, 0, 0, 0, 0, 0, 2, 0, 3, 3	1
Stylatula	1	2, 1, 2, 1, 0, 0, 3, 5, 7, 6, 0	2
Ophiura	1	0, 0, 0, 0, 0, 0, 0, 0, 0, 0, 0,	0
Area 2			
Astropecten	1	1, 6, 4, 10, 2, 1	4
Stylatula	1	0, 0 0, 0, 0, 0	0
Ophiura	1	0, 0, 0, 0, 0, 0	0
Area 3			
Astropecten	1	0, 0, 0, ½, 0, 0, 0, 0, 0, 0	0
Stylatula	(three observed during a 50-m. swim)		0
Ophiura	0·05	4, 5, 4, 3, 2, 0, 3, 0, 5, 3, 0, 4	60

---

* Contributions from the Scripps Institution of Oceanography, New Series, No. 972.

Reproduced by Permission

temperature. We have, however, while on the bottom in area 3, observed water currents coming from the direction of the canyon travelling up slopes as steep as 26°. Current velocities are variable both in magnitude and direction ; but this is characteristic of near-shore currents in southern California. Velocity measurements, determined by timing the progress of a cloud of permanganate solution for 1 m., yielded vertical components as great as 45 cm./min. upwards. Studies of area 1 have as yet failed to give evidence of upwelling ; this difference may be an important factor influencing the distributions discussed above. The commercially harvested kelp beds of *Macrocystis pyrifera* just south of area 3 may also be affected by the upwelling.

Tides, internal waves, and northerly currents could contribute to the upwelling ; the biological data suggest that northerly currents may play an important part. Ophiuran populations occurring at 50 m. depth on the shelf and at 30 m. in the canyon allow the possibility of a water mass common to both places. Currents from the north at the 50 m. depth would run into the south wall of the canyon below area 3 and may upwell and flow across this region. Area 1 and possibly area 2, however, below 27 m. are protected from northerly currents by the shoal opposite wall of the canyon.

We are grateful for criticism and assistance to Prof. D. L. Fox and to Dr. E. W. Fager. The work was supported by the George A. Bisbee Donation and a Rockefeller Foundation donation for research in marine biology.

RAYMOND J. GHELARDI
WHEELER J. NORTH

Division of Marine Biochemistry,
University of California,
Scripps Institution of Oceanography,
La Jolla, California.

Oct. 29.

---

[1] North, W. J., *Yale Sci. Mag.*, **31** (1956).

[2] Shepard, F. P., and Emery, K. O., Geol. Soc. Amer. Spec. Paper No. 31 (1941).

Printed in Great Britain by Fisher, Knight & Co., Ltd., St. Albans.

(24)

Deep-Sea Research, 1958, Vol. 5, pp. 29 to 35. Pergamon Press Ltd., London

Transpacific distribution of floating pumice from Isla San Benedicto, Mexico

ADRIAN F. RICHARDS

Abstract—A probable transpacific drift of floating trachytic pumice originating from the 1952 erruption of Volcán Bárcena on Isla San Benedicto off the west coast of Mexico is reported. Pumice from San Benedicto was collected in the Islas Revillagigedo and on Hawaii, Johnston, Wake and the Marshall Islands. It may have reached the Palau Islands 12,000 km from Isla San Benedicto. Identification was based primarily on the index of refraction of glass and phenocrysts. A comparative study of pumices collected from widely different geographic localities in the north Pacific between 1951 and 1956 indicates that San Benedicto pumice is sufficiently distinctive, compared to pumices from other sources, to be identified with certainty. The following mean drift rates in the North Equatorial Current were determined : to Hawaii 22 cm/sec (264 days – 4800 km) ; to Johnston Island 33 cm/sec (225 days – 6100 km); to Wake Island and Ailinginae Atoll in the Marshall Islands 18 cm/sec (about 560 days – 8700 km). A comparison between the actual drift and a computed drift from surface current charts is made and discussed. An average figure of 22 cm/sec also has been calculated for the rate of a trans-Indian Ocean drift of pumice, in the South Equatorial Current, originating from the 1883 volcanic eruptions of Krakatoa.

INTRODUCTION

ALTHOUGH exotic pumice is not uncommon on islands in the Pacific Ocean (SACHET 1955), a few attempts have been made to determine its origin (HEDLEY, 1905 ; LACROIX, 1939a, 1939b ; MACDONALD, 1954, p. 123) and apparently none to compute rate of drift over an extended distance.

Concurrent with the August 1, 1952, eruption of Volcán Bárcena (RICHARDS and DIETZ, 1956) on Isla San Benedicto off the west coast of Mexico an extensive " drift bottle experiment " began which furnished an ideal opportunity to determine not only the extent of drift but also the mean rate. Fortuitously San Benedicto is located in the general region where the North Equatorial Current begins (Fig. 1).

DISTRIBUTION

The first report of drifting pumice from Isla San Benedicto was made when the *Horizon* of the Scripps Institution of Oceanograph passed through a large area of drifting pumice on August 24, 1952. At stations located 55 and 104 nautical miles approximately north of Isla San Benedicto (A and B, Fig. 1) specimens of pumice (Fig. 2), wood, barnacles (*Lepas anatifera**), gastropods (*Litiopa melanostoma*†), and *Halobates* eggs and larvae* were dip-netted by Mr. GEORGE SHUMWAY.

On September 13 the S.S. *Hawaiian Citizen* passed through a 64-mile area of discoloured water about 320 miles west-southwest of San Benedicto (C, Fig. 1). M. G. MICHAELEDES, Second Officer, noted that the pumice was aligned in southwest-northeast streaks, and that as the ship proceeded west the streaks became more

---

*Identification by Dr. LEO BERNER of the Scripps Institution.
†Identification by Mr. ROBERT PARKER of the Scripps Institution.

Reproduced by Permission

numerous and appeared to stretch to the horizon (U.S. Navy Hydrographic Office, 1952). Some of the floating blocks were observed to be about 3 ft sq. A sample was collected and submitted to the U.S. Navy Hydrographic Office whence it was forwarded to the Scripps Institution.

In September the S.S. *Virginia Lykes* steamed through a field of pumice that was about 345 nautical miles long (D-E, Fig. 1) with the densest concentration about 230 miles south-west of San Benedicto (F, Fig. 1). In December a copy of the following report from the Second Officer to the Hydrographic Office was sent to the Scripps Institution :

> " On the morning of Sept. 20, 1952, bound from Panama to Yokohama, in lat. 15° 30′ [N], long. 110° 30′ [W], at 10 a.m. local time and 1730 G.M.T., we began passing through numerous patches of what appeared to be lava or volcanic ash. It was of various sizes, some as large as a man's head, but mostly the size of rough gravel. It was light grey in colour. We passed through it all that day and at 8 p.m. local time of Sept. 20, 0330 G.M.T. of Sept. 21, in lat. 16°00′, long. 113° 02′, it had increased to huge patches surrounding the ship. After this time it began to decrease until at 6 a.m. local time of Sept. 21 and 1330 G.M.T., in lat. 16° 34′, long. 115° 37′, it had decreased to only occasional very small patches. By 8 a.m. local time and 1530 G.M.T. of Sept. 21 in lat. 16° 40′, long. 116° 09′, it had disappeared and no more was seen."

Pumice originating from Isla San Benedicto was collected on Isla Socorro and Isla Clarión, in the Islas Revillagigedo, on the island of Hawaii, and on Johnston Island during 1953. Only a little pumice was deposited on Hawaii (C. K. WENTWORTH, personal communication). According to EMERY (1956, p. 1516), beginning in March 1953 several hundred pounds of well rounded pieces of pumice, up to 7·5 cm in diameter, landed on Johnston Island and the nearby Sand Island. The greatest quantity arrived in September and October and filled screens and pipes of the water evaporators on Johnston.

By mid-February 1954 San Benedicto pumice had reached Wake Island and the Marshall Islands. Mr. FRED LIBBY collected a specimen 19 cm in length (Fig. 3) from the east side of Wake Island in the middle of February. Mrs. INA MOORE (personal communication) reported that such large pieces were rare on Wake ; it was mostly walnut to potato size and sparsely scattered on the beach. A moderate amount of pumice was present on Ailinginae Atoll, Marshall Islands, on February 10 and similar material was seen on Bikini Atoll a few weeks before, (JOHN ISAACS, personal communication).

In 1956 Dr. F. R. FOSBERG sent the writer pumice from five atolls in the Marshall Islands. On the east beach of Rongelap Islet pumice pebbles lay on both the upper part of the beach and on the flat back of the top of the beach. Small, rounded, fine-grained pebbles were most common and in places covered the sand. Some of the larger pieces (San Benedicto pumice) were much fresher-looking than presumably older, non-San Benedicto material. Small corals were attached to certain specimens (F. R. FOSBERG, from field notes). San Benedicto pumice was not present in a number of samples examined by the writer which were collected in the Marshall Islands by FOSBERG in 1951 and 1952.

Attempts to identify San Benedicto pumice west of the Marshalls have been unsuccessful. Mr. A. B. BRONSON (personal communication) wrote that the drift apparently missed Guam. However, he reported the interesting observation that :

> " During 1954 and early 55 a great amount of pumice washed up on the beaches in the Palau group of the Western Carolines. It was not unusual to pass through rather dense formations floating

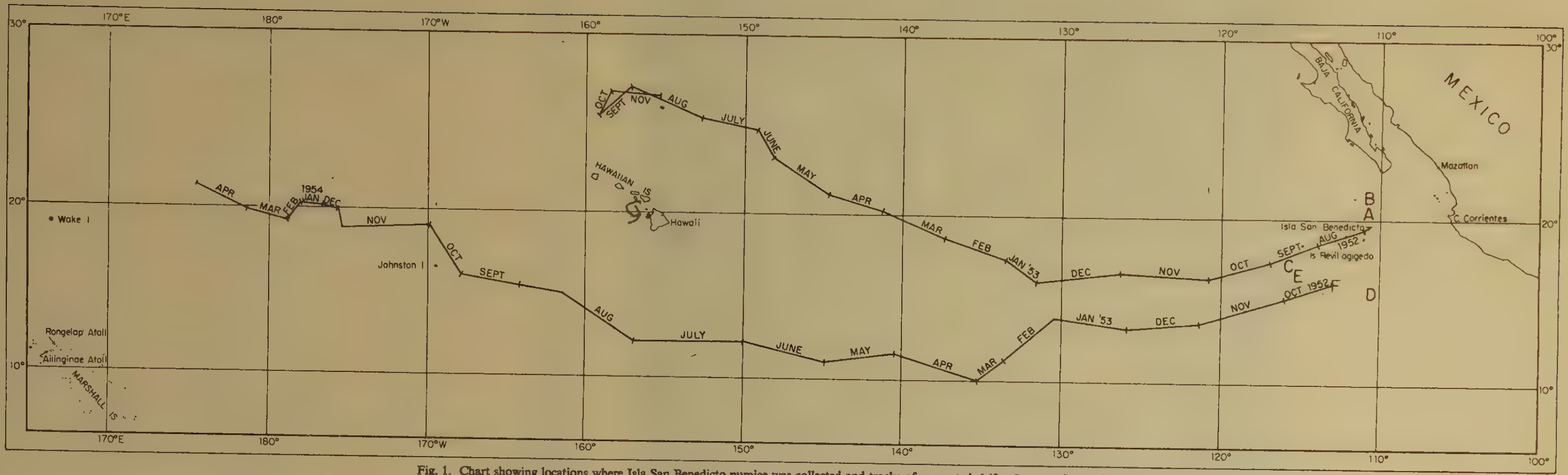
MEXICO
BAJA CALIFORNIA
Mazatlan
C. Corrientes
Isla San Benedicto
Is Revil agigedo
A
B
C
D
E
F
AUG 1952
SEPT
OCT
NOV
DEC
JAN '53
FEB
MAR
APR
MAY
JUNE
JULY
AUG
SEPT
OCT
NOV
OCT 1952
NOV
DEC
JAN '53
FEB
MAR
APR
MAY
JUNE
JULY
AUG
SEPT
OCT
NOV
DEC
1954 JAN
FEB
MAR
APR
HAWAIIAN IS
Hawaii
Johnston I
Wake I
Rongelap Atoll
Ailinginae Atoll
MARSHALL IS
30°
20°
10°
170°E
180°
170°W
160°
150°
140°
130°
120°
110°
100°

Fig. 1. Chart showing locations where Isla San Benedicto pumice was collected and tracks of computed drift. See text for explanation.

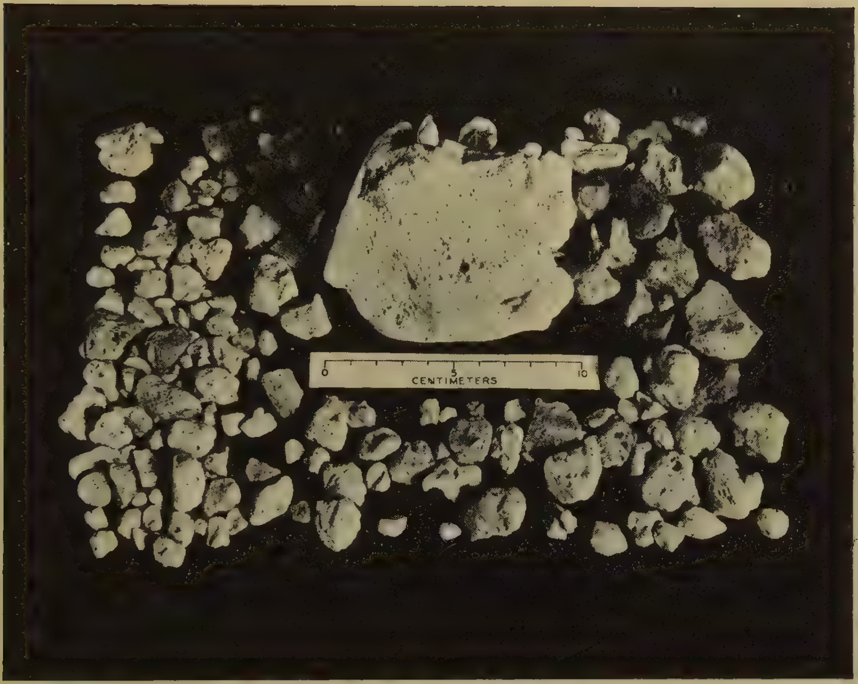

Fig. 2. Pumice collected floating in the Pacific Ocean about 104 miles north of Isla San Benedicto. A barnacle is attached to the top of the largest piece. U.S. Navy Official photograph.

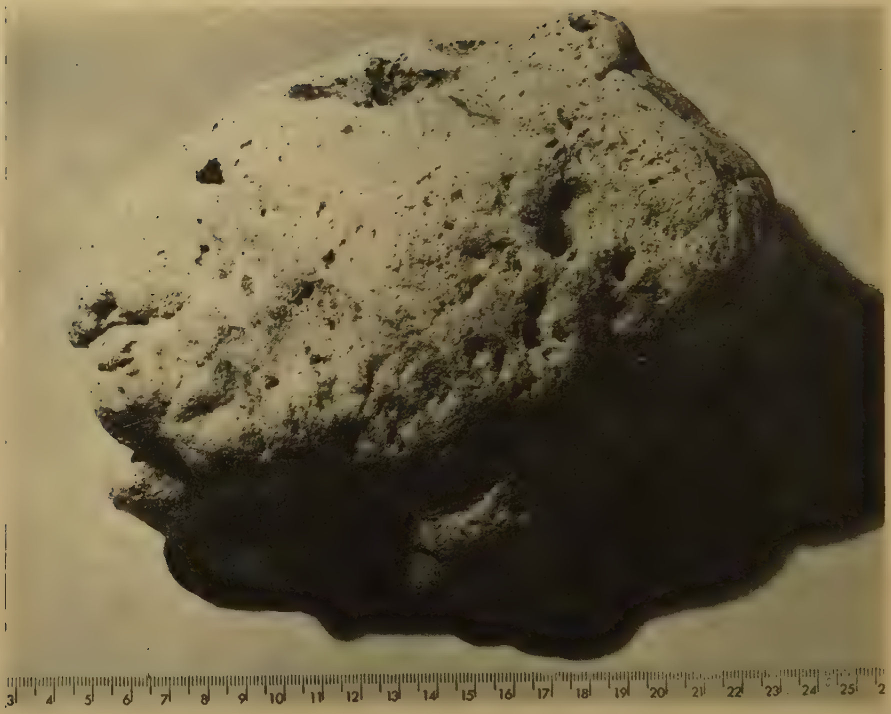
3 4 5 6 7 8 9 10 11 12 13 14 15 16 17 18 19 20 21 22 23 24 25 2

Fig. 3. Piece of San Benedicto pumice 19 cm long collected on the beach of Wake Island. Scale in centimetres. Scripps Institution of Oceanography photograph.

in the open sea near that group. All this material, or nearly all, bore a growth of barnacles and appeared to have been a long time at sea."

In February 1956 BRONSON noticed small blocks of pumice floating at sea between Palau and north-west New Guinea and wrote to the writer that :

> " On the islands of Biak and Japen and in some of the adjacent atolls there were pieces of pumice washing back and forth on the beaches with the tide. There was not as much as there had been previously in Palau, but it still seemed to be drifting in that area."

Unfortunately no samples were collected.

IDENTIFICATION

The trachytic pumice from Isla San Benedicto was identified primarily by microscopical determination of the index of refraction of glass and indices of refraction of phenocrysts (Table 1). Colour and vesicular texture of the pumice were also used as an aid to identification. Phenocrysts were separated from the glassy matrix by hand picking and by ingestion of glass by hydrofluosilicic acid (see KNOPF, 1933). Index of refraction measurements were made using white light and liquids in 0·002 intervals for glass and feldspars and 0·01 intervals for pyroxene. The temperature correction of the high index liquids, composed of methylene iodide and sulphur, was not stated by the manufacturer ; 0·0007 — *dn*/*dt* was assumed in making adjustments for temperature. Orientation of mineral grains was determined from interference figures. Index of refraction measurements of the phenocrysts listed in Table 1 indicate a weight percentage of about Or_{55} $(Ab + An)_{45}$ for sanidine (TUTTLE, 1952, p. 559) and a molecular composition of about Ac_{30} Di_{70} for aegerine-augite (TROGER, 1952, p. 64), except from the Bárcena sample, which has a composition of about Ac_{20} Di_{80} ; the values of plagioclase weight percentage are obtained from CHAYES (1952, p. 51).

Phenocrysts of sanidine and aegerine-augite in the drifted pumice were comparatively abundant and plagioclase was rare. Plagioclase phenocrysts were not seen in samples from 320 miles west-southwest of San Benedicto, Socorro, Clarión, Hawaii, Johnston, Wake, and Ailinginae Atoll in the Marshall Islands. However, most of these samples were small ; had there been more material, plagioclase probably would have been found. The Rongelap Atoll sample was large and plagioclase was present.

A number of drift samples collected in the east, central, and west Pacific Ocean also were examined in order to determine and compare mineralogical variation. None of the samples from other sources resembles pumice from Isla San Benedicto, except for somewhat similar values obtained for the index of refraction of glass (1·491-1·510). Pumice from the 1952 eruption of Myojin Reef (NIINO, *et al.*, 1953 ; MORIMOTO and OSSAKA, 1955), which is located about 200 miles south of Tokyo, is particularly dissimilar. A sample examined by the writer contains quartz and the glass has an index of refraction of 1·491 ± 0·003.

ORIGIN OF PUMICE ON ISLA SAN BENEDICTO

There are only two possible sources on San Benedicto from which pumice could have been erupted : Volcán Bárcena and the eroded pyroclastic cone Montículo Cinerítico, which is located under and to the south of Bárcena. Bárcena is predominantly composed of volcanic dust or ash ; pumice from breadcrust bombs is not abundant and is darker, heavier, and poorly vesiculated compared to Montículo

Cinerítico pumice. Only pumice from Montículo Cinerítico resembles the drift pumice in appearance. The phenocrysts in pumice from both sources are nearly identical ; however, the index of refraction of glass differs slightly, ranging from 1·510 to approximately 1·523 in Bárcena pumice and comparatively constant at about 1·503 in Montículo Cinerítico pumice. It appears probable that little or none of the drift pumice originated from Volcán Bárcena ; apparently most if not all came from the part of Montículo Cinerítico blown up at the birth of Bárcena.

Table 1. Determinative mineralogy of Isla San Benedicto pumice

Location where collected	*Index of refraction of glass (± 0·002)*	*Index of refraction of sanidine (± 0·002)*	*Index of refraction of plagioclase (± 0·002)*	*Plagioclase composition*	*Index of refraction of aegerine-augite (± 0·006)*
Isla San Benedicto, Volcán Bárcena Pumice	1·516	N_x 1·522 N_y 1·527 N_z 1·528	N_x 1·530 N_y 1.534 N_z 1·538	An_{2-3}	N_x 1·713 N_y 1·724 N_z 1·743
Isla San Benedicto, Montículo Cinerítico pumice	1·503	1·521 1·527 1·528	1·532 1.536 1·541	An_{6-8}	1·726 1.734 1·761
Isla San Benedicto, drift pumice from Volteadura Beach	1·505	1·522 1·527 1·528	1·530 1·534 1·537	An_{2-3}	1·726 1·735 1·756
104 miles north of Isla San Benedicto 21° 02′N, 110° 34′W	1·502	1·521 1·527 1·528	1·535 1·540 1·546	An_{15-17}	1·727 1·734 1·762
320 miles west-southwest of Isla San Benedicto, 16° 54′N, 116° 20′W	1·504	1·521 1·527 1·528	see text		1·729 1·734 1·762
Hawaii Island, northwest coast	1·505	1·521 1·527 1·528	see text		1·727 1·738 1·755
Johnston Island	1·502	1·521 1·527 1·528	see text		1·725 1·737 1·756
Wake Island	1·502	1·521 1·527 1·528	see text		1·727 1·737 1·756
Marshall Islands, Ailinginae Atoll	1·505	1·521 1·527 1·528	see text		1·727 1·735 1·754
Marshall Islands, Rongelap Atoll	1.503	1.521 1·527 1·528	1·529 1·534 1·538	An_{2-3}	1·727 1·734 1·756

It is difficult to estimate how much pumice originated from Montículo Cinerítico. The magnitude of the craters of Bárcena and Montículo Cinerítico – the latter shown in photographs taken before the birth of Bárcena – indicates that about 3,000,000 m^3 of pumice and ash may have been blown up and deposited in the sea.

RATE OF DRIFT

Isla San Benedicto pumice – Distances, travel time in days, and calculated drift rates are tabulated in Table 2. Distances are based on straight-line travel from a Mercator projection. Travel time was computed on the assumption that pumice entered the water at San Benedicto on August 2, 1952, the second day of the eruption. Time of arrival at Hawaii, Johnston and Wake is believed to be correct within about one week. The mean drift rates are probably conservative.

If the large patches of floating pumice seen in the vicinity of the Palau Islands in late 1954 originated from Isla San Benedicto the computed drift rate would be about 18 cm/sec, based on a 12,000 km drift in approximately 790 days (to October 1, 1954). An earlier or later arrival of two months would only change this figure by about 10 per cent.

Table 2. Drift rates of pumice from Isla San Benedicto

Location of drift pumice	*Collector*	*Date collected*	*Travel time in days*	*Distance from San Benedicto*		*Travel per day*		*Calculated drift rate*	
				naut. miles	*km*	*naut. miles*	*km*	*knots*	*cm/sec*
104 miles north of Isla San Benedicto, 21° 02′N, 110° 34′W	G. Shumway	24/8/52	22	104	193	4·7	8·7	0·2	10·1
320 miles west-southwest of Isla San Benedicto, 16° 54′N, 116° 20′W	M. G. Michaeledes	13/9/52	42	320	593	7·6	14·1	0·32	16·3
Hawaii Island, north-west coast	C. K. Wentworth‡	10/4/53	264	2600	4820	10·4	19·2	0·43	22·2
Johnston Island	K. O. Emery	15/3/53	225	3300	6120	14·7	27·2	0·61	33·4
Wake Island	F. Libby	15/2/54	562	4700	8710	8·4	15·5	0·35	18·0
Marshall Islands, Ailinginae Atoll	J. Isaacs	10/2/54	556	4700	8710	8·5	15·7	0·35	18·2

‡Forwarded by G. A. Macdonald.

All specimens of pumice collected from the sea or beaches that have been examined by the writer were rounded by abrasion (Figs. 2 and 3). Drift probably was induced predominantly by oceanic currents rather than wind, because floating San Benedicto pumice has little freeboard and the emergent part is streamlined.

Krakatoa pumice – A rate of drift similar to that of pumice from San Benedicto is obtained from calculations of the drift of floating pumice, presumably originating from the 1883 volcanic eruptions of Krakatoa in the Strait of Sunda between Sumatra and Java, across the Indian Ocean. Activity of Krakatoa that ejected pumice appears to have started about May 20, 1883, and culminated with the violent eruptions of

August 26-27 (JUDD, 1888). Charts published by MELDRUM (1885) show the drift of this pumice across the Indian Ocean as it was observed by ship captains. According to SCOTT (1888) the pumice reached the coast of Natal, south-east Africa, September 27-28, 1884. Assuming an eruption of the pumice in May, 1883, the rate of drift in the South Equatorial Current over a distance of about 8500 km would be approximately 20 cm/sec ; erupting in August, 1883, it would be about 24 cm/sec. An average of these two figures, or 22 cm/sec, appears to be a not improbable rate of drift. It is probably coincidental that this average is nearly identical to the 23 cm/sec average of four central Pacific drift rates of San Benedicto pumice in the North Equatorial Current.

In comparison with San Benedicto pumice it is noteworthy that JUDD (1888, p. 38) stated that Krakatoa pumice floated with a large portion of its mass above the water and he believed that the prevailing winds might have influenced the drift.

Computed drift – A comparison with the actual drift of San Benedicto pumice was made with the computed current drift from published surface current charts (U.S. Navy Hydrographic Office, 1947, 1950). Current roses, which show the frequency of direction and average current speed within the directions for quadrangles about five degrees square, were resolved for resultant vectors of the direction and speed of current drift. It was assumed that San Benedicto pumice travelled in the resultant direction of current drift, the distance depending on the resultant speed and the number of days during which the drift was applicable.

Using this method, beginning at Isla San Benedicto on August 1, 1952, a drifting object would not approach Hawaii until August 1953, when it would tend to gyral about 300 nautical miles north of Oahu (Fig. 1). Assuming a departure from lat. 16° N and long. 113° W on October 1, 1952, about the time when large quantities of pumice were observed in this area, a drifting object would travel approximately 360 miles south of Oahu by mid-August 1953 and would be 60 miles east of Johnston Island in early October, but over 500 miles east of Wake Island by the end of April 1954 (Fig. 1).

The drift track of this theoretical object would pass well north of the Marshall Islands and would arrive late at each of the islands on which San Benedicto pumice was collected. This is not too surprising considering the averaging processes used in the compilation of the charts and in making the computations given above. In conclusion, it is noteworthy that the range of current direction and velocity shown on the charts can easily account for the rate and direction of the actual pumice drift.

Radioactive tracer – WOOSTER and KETCHUM (in press) determined that the rate of drift of radioactive dissolved substances over a distance of about 7,000 km west of Bikini Atoll in the Marshall Islands was approximately 20 cm/sec. This figure approximates the 23 cm/sec average obtained from the rate of drifting San Benedicto pumice.

Acknowledgments—I am greatly indebted to all of the numerous people who donated samples of drift pumice and provided information on distribution. In particular, I am grateful to Dr. F. R. FOSBERG who made available field notes and his extensive collection of pumice from the Marshall Islands. At the Scripps Institution of Oceanography Prof. R. S. Arthur suggested the method of computing surface currents, and Profs. M. N. Bramlette and D. L. Inman kindly provided index of refraction liquids. I also wish to thank Dr. E. L. Hamilton of the U.S. Navy Electronics Laboratory who lent the petrographic microscope used in this study. Profs. K. O. EMERY, University of

Southern California, R. S. ARTHUR, Scripps Institution and Dr. J. LYMAN** of the U.S. Navy Hydrographic Office read the manuscript and offered helpful suggestions.

*University of California***
Scripps Institution of Oceanography,
La Jolla, California.

Contribution from the Scripps Institution of Oceanography, New Series, No. 973. *This paper represents results of research carried out by the University of California under contract with the Office of Naval Research. Reproduction in whole or in part is permitted for any purpose of the United States Government.*

***Present address. Oceanography Division, U.S. Navy Hydrographic Office, Washingston* 25, *D.C.*

REFERENCES

CHAYES F. (1952) Relations between composition and indices of refraction in natural plagioclase. *Amer. Jour. Sci. Bowen vol.* 85-105.

EMERY K. O. (1956) Marine geology of Johnston Island and its surrounding shallows, central Pacific Ocean. *Bull. Geol. Soc. Amer.* **67**, 1505-1519.

HEDLEY C. (1905) Notes and exhibits. *Proc. Linn. Soc. N.S.W.* **30**, pt. 2, p. 351.

JUDD J. W. (1888) On the volcanic phenomena of the eruption, and on the nature and distribution of the ejected materials. IN: SYMONS G. J. (Ed.) *The eruption of Krakatoa, and subsequent phenomena.* Rep. Krakotoa Comm. Royal Soc., London, Trübner and Co., 1-46.

KNOPF A. (1933) The quantitative determinations of quartz (" free silica ") in dusts. *U.S. Treas. Dept., Public Health Rep.* **48**, 183-190.

LACROIX A. (1939a) Remarques sur les volcans sous-marins, à propos de ponces rhyolitiques recueillies sur l'atoll Marutea du Sud (Archipel des Tuamotu). *C. R. Acad. Sci. Paris* **208**, 609-611.

LACROIX (1939b) Les ponces dacitiques flottant sur l'océan, entre des Fiji, les Nouvelles-Hébrides et la Nouvelle-Caldédonie. *C. R. Acad. Sci. Paris* **208**, 853-857.

MACDONALD G. A. (1954) Igneous rocks. IN : EMERY K. O. *et al.* Geology of Bikini and nearby atolls. *U.S. Geol. Survey Prof. Paper* **260-A**, 120-124.

MELDRUM C. (1885) A tabular statement of the dates at which, and the localities where, pumice or volcanic dust was seen in the Indian Ocean in 1883-84. *Rep. 55th meet. British Assoc. Adv. Sci.*, 773-776.

MORIMOTO R. and OSSAKA J. (1955) The 1952-1953 submarine eruption of the Myojin Reef near the Bayonnaise Rocks, Japan. *Bull. Earthq. Res. Inst.* **33**, 221-250.

NIINO H., *et al.* (1953) Report on the submarine eruption of Myojin-sho. *Jour. Tokyo Univ. of Fisheries.* **40** (special no. 2), 1-43.

RICHARDS A. F. and DIETZ R. S. (1956) Eruption of Bárcena Volcano, San Benedicto Island, Mexico. *Proc. 8th Pac. Sci. Congr.* **2**, 157-176.

SACHET M.-H. (1955) Pumice and other extraneous volcanic materials on coral reefs. *Atoll Res. Bull.* **37**, 1-27.

SCOTT R. H. (1888) Memorandum. IN : SYMONS G. J. (Ed.) *The eruption of Krakatoa and subsequent phenomena.* Rep. Krakatoa Comm. Roy. Soc., London, Trübner and Co., p. 47.

TRÖGER W. E. (1952) *Tabellen zur optischen Bestimmung der gesteinsbildenden Minerale.* Stuttgart, Erwin Nägele, 1-147.

TUTTLE O. F. (1952) Optical studies on alkali feldspars. *Amer. Jour. Sci. Bowen vol.* 553-567.

U.S. Navy Hydrographic Office (1947) Atlas of surface currents northeastern Pacific Ocean. *H.O. Publ.* **570**, 1-12.

U.S. Navy Hydrographic Office (1950) Atlas of surface currents northwestern Pacific Ocean. *H.O. Publ.* **569**, 1-12.

U.S. Navy Hydrographic Office (1952) Discolored water of volcanic origin. *Hydrog. Bull.* **41**, Oct. 11.

WOOSTER W. and KETCHUM B. H. (In press) Transport and disposal of radioactive elements in the sea. Report of a study on the biological effects of atomic radiation, *Nat. Acad. Sci.*

Printed in Great Britain by The Salisbury Press Ltd., Publicity House, Wilton Road, Salisbury, Wilts. (9593)

Reprinted from the JOURNAL OF CELLULAR AND COMPARATIVE PHYSIOLOGY
Vol. 49, No. 2, April 1957

THE LUMINESCENT REACTION IN EXTRACTS OF THE MARINE DINOFLAGELLATE, GONYAULAX POLYEDRA[1]

J. WOODLAND HASTINGS AND BEATRICE M. SWEENEY
Department of Biological Sciences, Northwestern University, Evanston, Illinois, and Department of Marine Botany, Scripps Institution of Oceanography, La Jolla, California

NINE FIGURES

INTRODUCTION

Bioluminescence, or the production of light by living organisms, occurs in a great variety of unrelated and diverse animals and plants (Harvey, '52). The nature of the luminescent display may vary, but the reaction in all cases is evidently an enzymatic chemiluminescence, usually an oxidation. The bioluminescent reaction has been carefully studied in only three groups of organisms, namely *Cypridina,* fireflies and bacteria. The light emitting reaction of each differs markedly in requirements (Tsuji, Chase and Harvey, '55; McElroy and Hastings, '55; Strehler, '55; Hastings and McElroy, '55). The present paper, which describes characteristics of the reaction in *Gonyaulax,* indicates that this reaction differs from the three previously described.

Gonyaulax polyedra is a marine armored dinoflagellate which is both photosynthetic and luminescent. The so-called phosphorescence or, more properly, luminescence of the ocean at night is generally believed to be due principally to the luminescence of dinoflagellates (Harvey, '52). *Gonyaulax* has recently been isolated and grown in pure culture by one

---

[1] This research has been supported in part by grants from The National Science Foundation and the Graduate School of Northwestern University. Contribution from the Scripps Institution of Oceanography, University of California, New Series No. 974

Reproduced by Permission

(37)

of the authors (B.M.S.), making possible a study of its physiology and biochemistry. The characteristic luminescence of *Gonyaulax* occurs upon stimulation as a brilliant flash, having a duration of about 0.1 sec. (fig. 9). Maximum luminescent responses occur in darkness and are about 40 to 60 times as bright as the responses in daylight. A preliminary account of the luminescence of living *Gonyaulax* has been given by Haxo and Sweeney ('55) and more detailed studies along these lines are published elsewhere (Sweeney and Hastings, '57).

MATERIALS AND METHODS

Cells were grown in Fernbach flasks, each containing 1500 ml of medium, placed on shelves in windows (north exposure) at room temperature (23°–26°C.). The culture medium was composed of 75% filtered sea water, 2% soil extract (Pringsheim, '46), 2×10^{-3} M KNO_3, 2×10^{-4} M K_2HPO_4, 6×10^{-6} M $FeCl_3$, and 2.7×10^{-5} M ethylenediaminetetraacetic acid (EDTA) at pH 8.0–8.2. All distilled water used in these experiments was distilled a second time in a glass still.

Cells were inoculated at a cell density of about 800 cells per milliliter and harvested 6 days later at a density of about 6000 cells per milliliter. In preliminary studies it was found that extracts from cells harvested at midnight were about 10 times more active than those from cells harvested at noon, so the procedure was carried out thereafter at midnight. The cells were harvested with a Buchner funnel on Wratten no. 4 filter paper, washed several times with distilled water to remove residual salts and plunged into cold acetone at —25°C., removing a considerable amount of the pigment. The acetone was removed by filtration and the resultant powder dried *in vacuo* over calcium chloride and paraffin. A yield of about 45 mg of dry powder per liter of culture was generally obtained. Light intensity was measured with highly sensitive apparatus, utilizing a photomultiplier tube as described previously (Hastings, McElroy and Coulombre, '53), and recorded on an Esterline-Angus graphic meter.

EXPERIMENTAL RESULTS

Crude extracts

When initial preparations of the dry powder were mixed with distilled water a very faint, slowly decaying luminescence was observed. However, when distilled water was replaced with sea water, the intensity was increased several fold, suggesting a salt requirement in the reaction. In subsequent preparations care was taken to remove residual salt by washing the cells with distilled water, as described above. Such salt free powders then gave essentially no light when mixed with distilled water, but when optimum salt was added, a dim, but readily visible, luminescence occurred. The salt-free powder therefore was routinely extracted with distilled water (20 mg/ml) in the cold with a Potter homogenizer and centrifuged for 10 min. at 20,000 RPM in a Spinco preparative centrifuge (head no. 40) for 10 minutes at 0°C. The clear yellow-green supernatant contained the activity.

It was found that NaCl would completely replace sea water in stimulating luminescence. As shown in figure 1, unusually high concentrations of salt, about 1.2 M, are required for maximum activity. It was found that KCl, $(NH_4)_2SO_4$, and sodium and potassium phosphates (pH 6.6) were equally effective at the same concentration in replacing NaCl for the stimulation of luminescence. Versene (EDTA) was not inhibitory in a final concentration of 10^{-3} M when added secondarily. The salt requirement was also found in partially purified preparations of the enzyme (see below). The role of salt in this reaction is not clear and has not been studied in any detail. Salt in lower concentrations is known to affect light production in other luminescent reactions however (Anderson, '37; McElroy, Hastings, Sonnenfeld and Coulombre, '54).

The reaction is markedly dependent upon pH, as shown in figure 2, with an optimum at about pH 6.6. Similar results have been obtained using sodium phosphate and potassium phosphate buffers, including the sharp drop in activity above

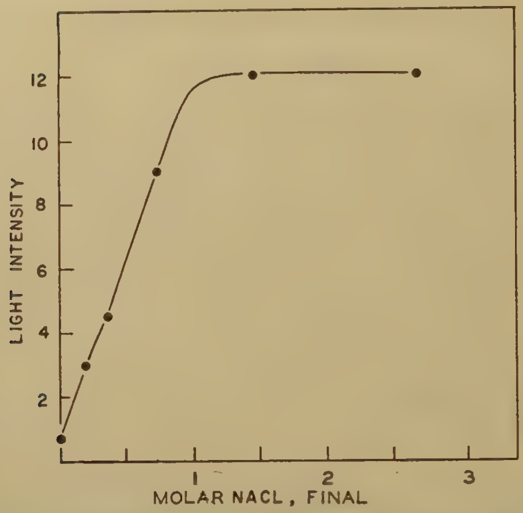

Fig. 1 Relationship between NaCl concentration and light intensity. Reaction mixture contained 1.0 ml crude extract, 0.4 ml 0.05 M tris-maleate buffer pH 6.4, water and NaCl to a total volume of 2.5 ml.

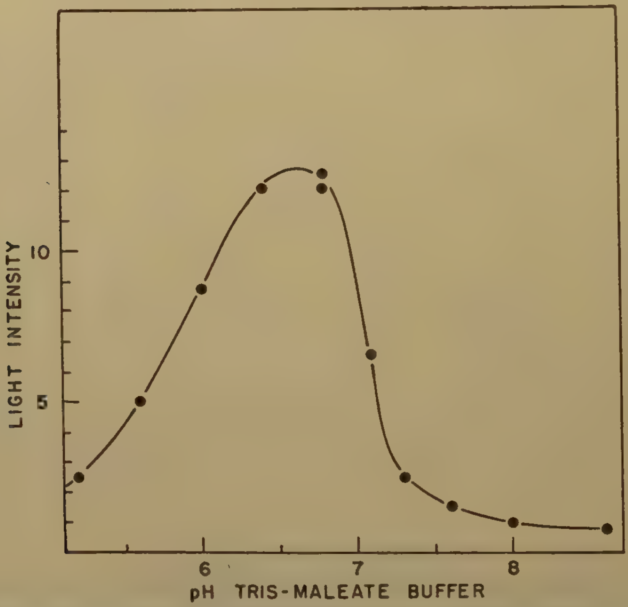

Fig. 2 Relationship between pH and light intensity. Reaction mixture contained 1.0 ml crude extract, 0.4 ml 0.05 M tris-maleate buffer, 0.6 ml 6.1 M NaCl, and 0.5 ml H_2O.

pH 7. There was little difference betwen different buffers in the maximum luminescence obtained, and tris-maleic acid buffer (trihydroxyamino-methane and maleic acid adjusted to pH with NaOH) was used routinely in all experiments.

The light emitted by the living cells is blue to blue-green. Utilizing concentrated extracts, it has been possible to determine the emission spectrum of the *in vitro* reaction. As shown in figure 3, the emission peak is at about 478 mμ. Since ammonium sulfate in place of NaCl had been found to result in a much slower decay of luminescence, it was used in these experiments. The reaction mixture was placed at the entrance slit of a Bausch and Lomb grating monochromator, and the photomultiplier tube at the exit slit. Both slits were set at 5 mm and the light intensity was recorded at various wave length settings. The values obtained were corrected both for

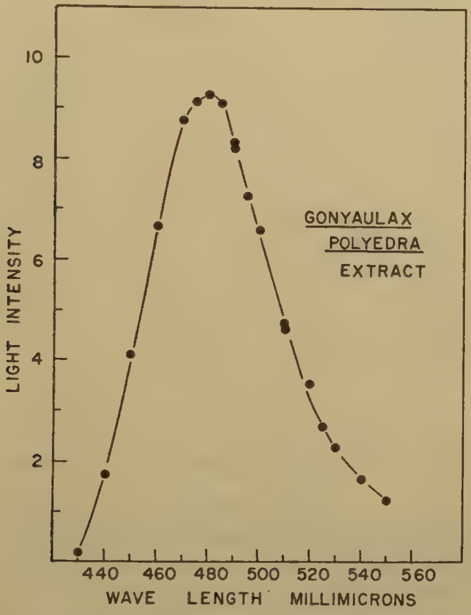

Fig. 3 Emission spectrum of *Gonyaulax* extracts. Reaction mixture contained 1.6 ml crude extract, 0.2 ml 0.1 M tris-maleate buffer pH 6.6, and 0.2 ml 6 M $(NH_4)_2SO_4$. Time during determinations, 6 min.

the decay of the reaction and for the color sensitivity of the phototube.[2] A second determination gave identical results.

The effect of temperature upon the reaction was determined both with the crude extract and with the purified enzyme (see below). In both cases the optimum was found to be at about 24°C., and a curve for the purified enzyme is shown in figure 4. The reaction mixture without enzyme was adjusted to the desired temperature and placed in front of the phototube. Enzyme was rapidly added to initiate the reaction and the initial light intensity recorded as the reaction rate. An Arrhenius plot of the data indicates an activation energy of about 9000 calories, and a similar plot for the rate of enzyme inactivation by heat gives an activation energy of about 60,000 calories.

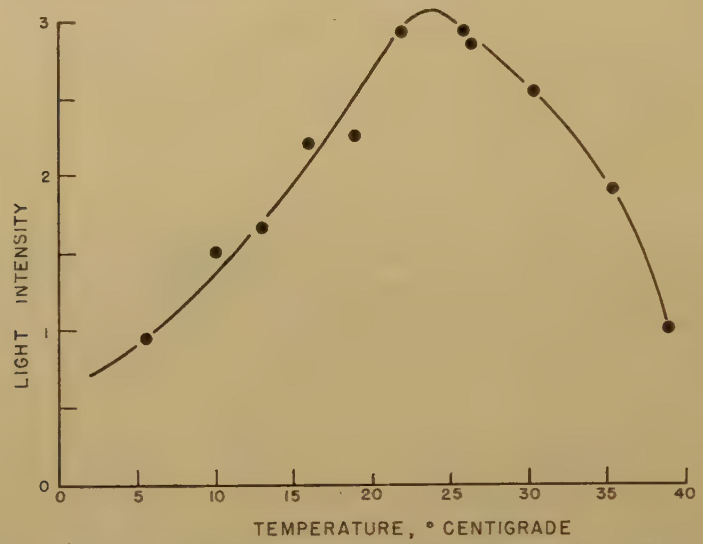

Fig. 4 Effect of temperature upon luminescence. Reaction mixture contained 0.2 ml purified enzyme, 1.0 ml boiled crude extract, 1.2 ml 6.1 M NaCl, 0.4 ml 0.1 M tris-maleate buffer pH 6.6, and 1.2 ml H_2O.

Enzymatic activity was completely destroyed at 100°C. for one minute, but the loss of activity of purified enzyme was less than 5% after two hours at 22°C. However, the crude extract is quite unstable and loses activity relatively rapidly, as shown in figure 5. In this experiment the crude extract was kept in an ice bath at about 4°C. and at the times indicated was assayed for activity. Varying the temperature of the extract from 4° to 30°C. during this period had only a relatively small effect upon the rate of decay. This suggests that the decrease is not due to enzyme destruction since denaturation is generally characterized by a large temperature coefficient. Additional evidence for this is presented in a later section. The possibility that a slow auto-oxidation of substrate was taking place was tested by bubbling aliquots with pure oxygen and pure nitrogen. In each of three trials oxygen not only failed to accelerate the decay of the extract but actually resulted in a slight increase in activity. It is considered possible that the decay is due to the production of potent in-

---

[2] We are grateful to Mr. John Tyler for determining the color sensitivity of our phototube.

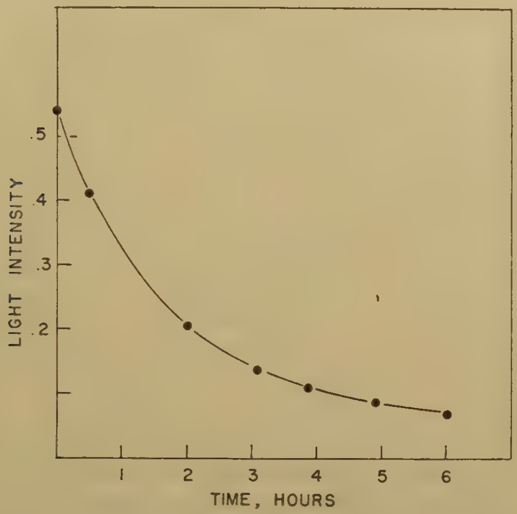

Fig. 5 Spontaneous decay in activity of crude extract kept at 4°C. Aliquots were taken at time intervals indicated and assayed for luminescence. Reaction mixture contained 0.5 ml crude extract, 0.4 ml 0.05 M tris-maleate buffer pH 6.6, 0.6 ml 6.1 M NaCl, and 0.5 ml H_2O.

hibitors since old extracts which have decayed are highly inhibitory to fresh extracts.

The effect of concentration of crude extract is shown in figure 6. The shape of the curve indicates that a second factor, presumably substrate, is limiting in the reaction at low concentrations.

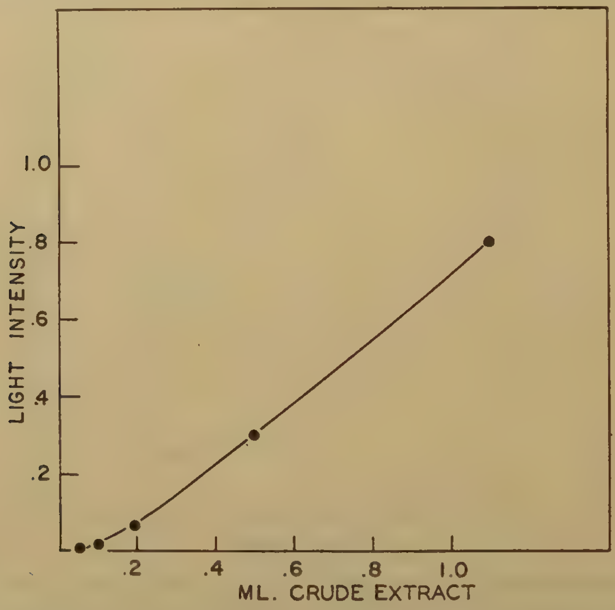

Fig. 6 Relationship between the concentration of crude extract and light intensity. Reaction mixture consisted of 0.5 ml 6.1 M NaCl, 0.4 ml 0.05 M tris-maleate buffer pH 6.6, and water and enzyme to a volume of 2.0 ml.

The intensity of luminescence of the crude extract is dependent upon oxygen concentration. When hydrogen is bubbled through a luminescing reaction mixture, the intensity decreases to a low level. When air is subsequently readmitted, the intensity is increased. No excess flash of luminescence, such as has been reported in the case of extracts of *Cypridina*, (Chance, Harvey, Johnson and Millikan, '40), the firefly (Hastings, McElroy and Coulombre, '53) and the luminous bacteria (Hastings, '55), was observed. It may be concluded

(44)

however that the *Gonyaulax* reaction is an oxidative one similar, in this respect, to other bioluminescent reactions.

Purified enzyme

Preliminary purification procedures have resulted in the separation of the enzyme from the heat stable substrate or substrates. Ammonium sulfate was added to the crude extract to 35% saturation, and allowed to stand for 15 minutes at 5°C., and centrifuged at 25,000 RPM (Spinco, Head no. 40) for 12 minutes. A green precipitate resulted, which was inactive, insoluble in water, methanol soluble, and showed absorption suggesting a mixture of chlorophyll and carotenoid pigments. Ammonium sulfate was added to the supernatant to 75% saturation and the resulting precipitate was clear and readily soluble in water. By itself this fraction was completely inactive, but when added together with a boiled crude extract, excellent activity resulted. Figure 7 shows the effect of purified

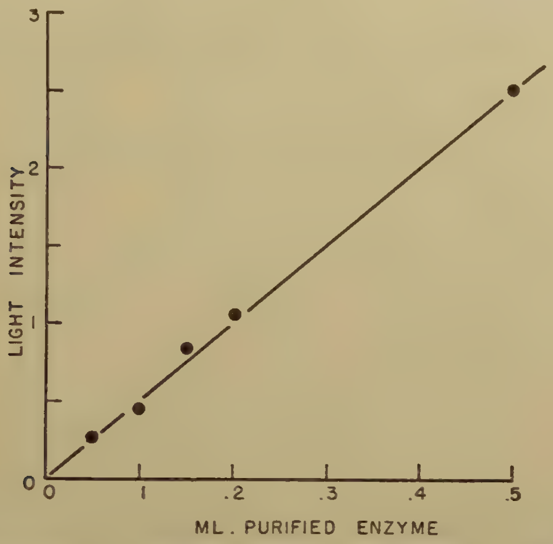

Fig. 7 Relationship of purified enzyme concentration to light intensity. Reaction mixture contained 0.6 ml 6.1 M NaCl, 0.5 ml heated crude, 0.2 ml 0.1 M tris-maleate buffer pH 6.6, and water and enzyme to a volume of 2.0 ml.

(45)

enzyme concentration upon initial light intensity with boiled crude extract (non-saturating concentration) added, indicating that no other factor was carried along in the enzyme fraction. The reaction with the purified enzyme appears to have the same characteristics as the crude extract insofar as the salt requirement, pH optimum and temperature coefficient are concerned.

Figure 8 shows the effect of different added amounts of a boiled crude extract upon the initial light intensity. The boiled crude extract appears to be relatively stable, but different preparations have given different values for maximum light intensity at saturation. This again suggests that inhibitors in crude extracts may influence the reaction, and that in such experiments they may have been present in greater or lesser concentrations.

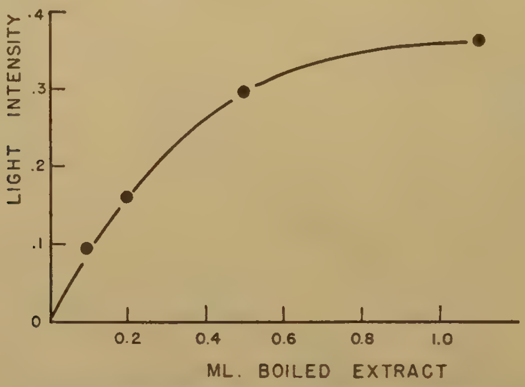

Fig. 8 Effect of the concentration of boiled crude extract upon luminescence of purified enzyme. Reaction mixture was composed of 0.6 ml 6.1 M NaCl, 0.2 ml 0.1 M tris-maleate buffer pH 6.6, 0.1 ml purified enzyme, and boiled crude extract and water to a volume of 2.0 ml.

Since it was thought that the decrease in activity of the crude extract (fig. 5) was not due to enzyme destruction, it was of interest to check this by determining the activity of an ammonium sulfate fraction from freshly prepared crude extract together with the activity of a similar fraction prepared from crude extract in which the activity had decayed

(46)

The activities before fractionation were in the ratio of 7.0 to 1.3 for fresh extracts and decayed extracts respectively, while the purified fractions had relative activities of 3.5 and 2.0 respectively, indicating that a major portion of the enzyme is recoverable after the decay of the crude extract.

The nature of the factor in the heat stable fraction has not been determined. In preliminary dialysis experiments it has not been possible to demonstrate any activity in the dialysate. A variety of cofactors, intermediates and other compounds have been tested with regard to their effect upon the reaction, and for their ability to replace this factor. None have been found to be active. Those tested include adenosine triphosphate, oxidized and reduced diphosphopyridine nucleotide, triphosphopyridine nucleotide, dodecyl aldehyde, oxidized and reduced flavins (riboflavin, riboflavin-5-phosphate, and flavin mononucleotide), thiamine pyrophosphate, coenzyme A, vitamin B_{12}, choline, acetylcholine, lipoic acid, liver and yeast concentrates, glucose, and glucose-6-phosphate. Crude homogenates of various organs of the rat and of the Pacific mussel were also tested and found to be either inactive or inhibitory. Irradiation with ultraviolet light, which has been shown to be effective in increasing enzyme activity in extracts of luminous bacteria, was found to have no similar effect upon the *Gonyaulax* enzyme. Cross tests between *Cypridina* luciferin and luciferase and similar *Gonyaulax* preparations did not give luminescence.

As mentioned previously, luminescence of the living organism is from 40 to 60 times greater at night than by day. Similarly, crude extracts prepared at night were found to be more active than those prepared in the daylight, but only by a factor of from 5 to 15 times. By ammonium sulfate fractionation it has been found that at least part of this difference in activity can be ascribed to enzyme concentration, and part to the activity of the heat stable fraction. In one experiment the crude extract from the night harvest was 8 times as active as the one from the daytime harvest. The purified enzymes from these fractions differed in activity roughly by a factor of 4 and the activities of the boiled crude extracts differed by a factor of about two, the fraction from the night harvest being more active in each case. Presumably therefore, both enzyme and substrate vary in concentration during the course of the day.

The decrease in luminescence with time in the reaction mixture is approximately logarithmic, suggesting that the reaction is first order in nature. In crude extracts the decay during the first two or three minutes is more rapid than during the later logarithmic period. In the purified extracts this phenomenon is much less marked. When $(NH_4)_2SO_4$ is used in place of NaCl in the reaction, the velocity constant is decreased by a factor of approximately 3/5.

It is of interest to mention that the classical luciferin-luciferase test does not give a positive reaction with *Gonyaulax* extracts. The test involves restoring luminescence to a reaction mixture which is dark following luminescence by adding an extract which was boiled before the decay of luminescence (see Harvey, '52). This is interpreted as a demonstration of the oxidation or utilization of a heat stable substrate, usually called luciferin, by the enzyme luciferase. The dark mixture contains only luciferase (the luciferin having been utilized in the luminescent reaction), and the boiled extract unoxidized luciferin. In the case of *Gonyaulax,* when boiled crude extract is added to a reaction mixture which is dim following luminescence a very slight (up to 10%) stimulation sometimes occurs, and at other times none at all. From the experiments with the purified enzyme it is clear that both an enzyme and a heat stable factor are involved in the reaction in a classical type luciferin-luciferase mechanism. It is not clear why the usual luciferin-luciferase test is negative, but the possibility that a product of the luminescent reaction itself is highly inhibitory is an attractive one. Extracts which have decayed spontaneously or those which have decayed with luminescence are inhibitory to the luminescent reaction, and the inhibition may be such that little or no response is obtained in the luciferin-luciferase test. It is

(48)

also of interest that the living cell, which emits a flash upon stimulation, is rapidly (within 10–20 sec.) and almost completely fatigued with continuous stimulation. It is possible that this decrease in luminescence is due not to the exhaustion of the substrate but to the intracellular accumulation of the inhibitory products of the reaction.

DISCUSSION

A rhythmic expression of a variety of activities has been observed in a large number of organisms (Welsh, '38; Kleitman, '49). The present studies however, have provided evidence for the nature of the biochemical changes which may be correlated with the physiological rhythmicity of the organism. Although the variations in enzyme and substrate concentrations found in *Gonyaulax* occurred in phase with the diurnal changes in light intensity, there is good evidence from studies with living cells (Sweeney and Hastings, '57) that similar changes occur when the organisms are kept in the dark. Cells kept in continuous darkness show persistent fluctuations in light intensity. In preliminary studies it has been found that these fluctuations are correlated with similar changes in the activities of the extracts. The rhythmicity is therefore evidently at least partially the result of changes in concentration of the luminescent system. Further studies should provide information relevant to the general problem of the mechanisms controlling enzyme synthesis and destruction.

Certain properties of *Gonyaulax* extracts suggest that the reaction is a relatively simple oxidation such as occurs in *Cypridina,* where the reaction is often written as

$$\begin{aligned} LH_2 + \tfrac{1}{2}O_2 &\xrightarrow{\text{luciferase}} L^* + H_2O \\ L^* &\longrightarrow L + \text{light} \end{aligned} \tag{1}$$

where LH_2 is the reduced substrate, luciferin, present as such in the extracts. When luciferin is oxidized in the presence of the enzyme (luciferase) an excited molecule results (L^*) which subsequently falls to the ground state with the emission of a quantum of light. All three bioluminescent reactions which have been studied are known to involve such a terminal oxidative reaction, which is characteristically very rapid (Hastings, McElroy and Coulombre, '53; Chance, Harvey, Johnson and Millikan, '40; Strehler and Cormier, '54; Hastings, '55). In both the firefly and bacterial extracts however, there are dark reactions preliminary to the oxidative step which are relatively slow, resulting in high overall

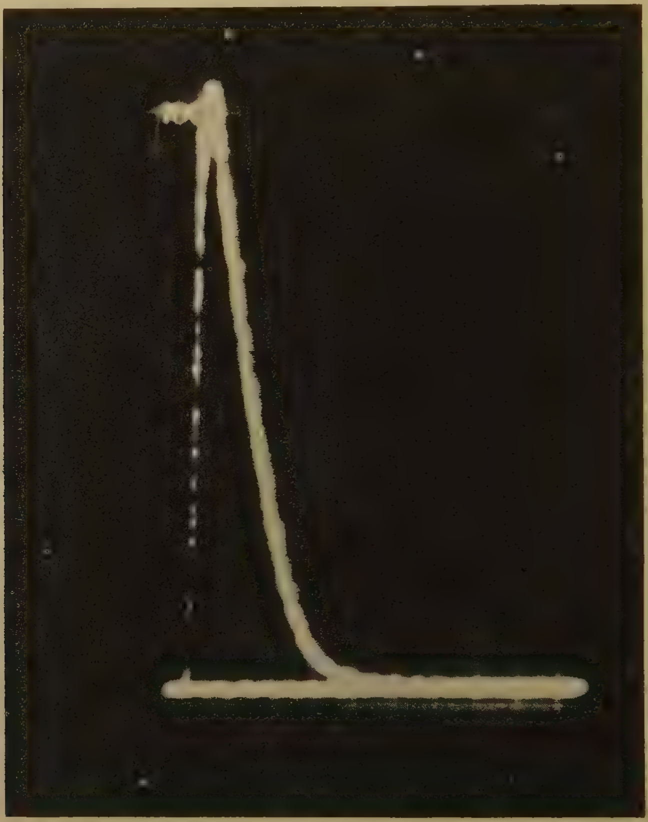

Fig. 9 Luminescent flash of *Gonyaulax* in response to mechanical stimulation, as photographed from the oscilloscope screen. Ordinate light intensity, abscissa time. Sweep time, 0.25 sec. One small division equals 0.025 sec. A test tube containing 5 ml of culture (about 1000 cells/ml.) was placed in front of the phototube and tapped very lightly. The flash is presumably the response of a single cell or of several cells flashing simultaneously.

activation energies (Strehler, '55; McElroy and Strehler, '49). Since the activation energy of *Gonyaulax* luminescence is lower (somewhat higher than *Cypridina),* it suggests that only a terminal rapid oxidation is involved in the luminescence of the extracts. If, as is possible, additional reactions preceding the oxidation are involved, they must be very rapid. The logarithmic decay is also in agreement with such a mechanism.

The blue color of the light is very similar to that of *Cypridina.* Since no light was obtained when *Cypridina* luciferin was added to crude or purified *Gonyaulax* enzyme, it must be concluded that the luciferins are different, even though it is possible that the mechanisms may be similar. It also seems certain that neither bacterial nor firefly components are involved in the reaction. It seems that not only has luminescence evolved independently in a great variety of unrelated organisms, but also, as Harvey ('53) has pointed out, that a considerable number of different luminescent systems have arisen independently.

The very rapid flash of *Gonyaulax* (fig. 9) is an excellent example of a precisely controlled biological reaction, and it is most logical to consider it as a type of cellular excitation. The mechanism by which an enzymatic reaction may be so regulated constitutes a major problem in modern physiology and biochemistry. As pointed out by Harvey ('52), the unicellular luminescent forms may be of great value in the study of these fundamental cellular processes.

SUMMARY

The extraction, partial purification and properties of the luminescent system in the marine dinoflagellate *Gonyaulax polyedra* are described. Crude cell-free water extracts of acetone powders emit light in the presence of salts, such as NaCl. The reaction also requires oxygen, and shows an optimum activity at pH 6.6 and 24°C. The light is blue-green with the emission peak at 478 mμ. The enzyme, purified by ammonium sulfate fractionation, requires for luminescence a

factor present in boiled crude extracts. It is suggested that this factor may be designated as *Gonyaulax* luciferin. The reaction appears to involve an oxidation of the luciferin. The intensity of luminescence of living cells shows a type of diurnal rhythmicity. The amount of both luciferin and luciferase which can be extracted from cells is correlated with these rhythmic intensity fluctuations. This phenomenon, as well as the mechanism of the reaction, is discussed.

LITERATURE CITED

ANDERSON, R. S. 1937 Chemical studies on bioluminescence. IV. Salt effects on the total light emitted by a chemiluminescent reaction. J. Amer. Chem. Soc., *59:* 2115–2117.

CHANCE, B., E. N. HARVEY, F. H. JOHNSON AND G. MILLIKAN 1940 The kinetics of bioluminescent flashes. A study in consecutive reactions. J. Cell. and Comp. Physiol., *15:* 195–215.

HARVEY, E. N. 1952 Bioluminescence. Academic Press, New York, N. Y.

——— 1953 Bioluminescence: Evolution and comparative biochemistry. Federation Proc., *12:* 597–600.

HASTINGS, J. W. 1955 The effect of oxygen upon the luminescence of bacterial extracts. Anat. Rec., *122:* 458.

HASTINGS, J. W., W. D. MCELROY AND J. COULOMBRE 1953 The effect of oxygen upon the immobilization reaction in firefly luminescence. J. Cell. and Comp. Physiol., *42*· 137–150.

HASTINGS, J. W., AND W. D. MCELROY 1955 Purification and properties of bacterial luciferase, in The Luminescence of Biological Systems (F.H. Johnson, ed.) pp. 257–264. A.A.A.S. Press, Washington, D.C.

HAXO, F. T., AND B. M. SWEENEY 1955 Bioluminescence in *Gonyaulax polyedra*, in The Luminescence of Biological Systems (F. H. Johnson, ed.) pp. 415–420. A.A.A.S. Press, Washington, D.C.

KLEITMAN, N. 1949 Biological rhythms and cycles. Physiol. Rev., *29:* 1–30.

MCELROY, W. D., J. W. HASTINGS, V. SONNENFELD AND J. COULOMBRE 1954 Partial purification and properties of bacterial luciferin and luciferase. J. Bacteriol., *67:* 402–408.

MCELROY, W. D., AND J. W. HASTINGS 1955 Biochemistry of firefly luminescence, in The Luminescence of Biological Systems (F. H. Johnson, ed.) pp. 160–198. A.A.A.S. Press, Washington, D.C.

MCELROY, W. D., AND B. L. STREHLER 1949 Factors influencing the response of the bioluminescent reaction to adenosine triphosphate. Arch. Biochem., *22:* 420–433.

PRINGSHEIM, E. G. 1946 Pure Cultures of the Algae. pp. 41–42. Cambridge Univ. Press., 119 pages.

STREHLER, B. L. 1955 Factors and biochemistry of bacterial luminescence. in The Luminescence of Biological Systems (F. H. Johnson, ed.) pp. 209–255. A.A.A.S. Press, Washington, D. C.

(52)

STREHLER, B. L., AND M. J. CORMIER 1954 Kinetic aspects of the bacterial luciferin-luciferase reaction *in vitro.* Arch. Biochem. and Biophys., *53:* 138–156.

SWEENEY, B. M., AND J. W. HASTINGS 1957 Characteristics of the diurnal rhythm of luminescence in *Gonyaulax polyedra.* J. Cell. and Comp. Physiol., *49:* 115–128.

TSUJI, F. I., A. M. CHASE AND E. N. HARVEY 1955 Recent studies on the chemistry of *Cypridina* luciferin, in The Luminescence of Biological Systems (F. H. Johnson, ed.) pp. 127–159. A.A.A.S. Press, Washington, D.C.

WELSH, J. H. 1938 Diurnal rhythms. Quart. Rev. Biol., *13:* 123–139.

Reprinted from PACIFIC SCIENCE, *vol. XII, no. 2, April, 1958*

Two New Doliolids from the Eastern Pacific Ocean[1]

TAKASI TOKIOKA[2] and LOE BERNER[3]

THE MATERIAL upon which this report is based was collected during the Shellback Expedition carried out by Scripps Institution of Oceanography in 1952. This expedition conducted its work in the east central Pacific Ocean off Central America and northern South America. While the authors were examining the many plankton samples they found two unusual doliolids. These specimens were from samples taken in the waters off Peru. The specimens are all gonozooids; and although they are not in a good state of preservation, the arrangements of muscles, alimentary organs, and gonads have been determined by close examination, after staining with Rose Bengal. One of the two forms belongs to the genus *Doliopsoides* established by Krüger (1939: 138–139). This genus, in the appearance of the musculature, shows an intermediate state between the Cylomyaria and the Desmomyaria. The other form belongs to the genus *Doliolina*. Both forms differ from any previously described species known to us and we consider them to be new species.

This is the first reported occurrence of the genus *Doliopsoides* from the Pacific Ocean and, indeed, is the first report of the genus since it was described by Krüger. At present the known distributions of *D. horizoni* and of *D. undulatum* are limited to only two stations.

Doliopsoides horizoni new species

Fig. 1

Three gonozooids are dealt with here. All were found in the sample from station SB-115 located at 8° 16′ S., 83° 42′ W. They are 3.9 mm., 4.6 mm., and 5.2 mm. in length. One additional specimen was taken at station SB-118 located at 9° 49′ S., 83° 02.5′ W. The body is roughly barrel-shaped with the oral aperture at the anterior end and the atrial aperture at the posterior end of the body. Both apertures are rather wide and fringed with a narrow margin which is, apparently, without lappets. The test is of moderate thickness, very soft, and easily stripped from the body. The mantle is extremely thin and delicate. The muscles are rather narrow, especially I, VII, and VIII. Muscles I through IV and VIII form complete hoops. The first and seventh intermuscular zones are narrow while the second is quite wide. Muscle V runs obliquely from the posteroventral to the anterodorsal side and is widely interrupted at the middorsal line. Each dorsal end of muscle V turns backwards for a short distance and then runs obliquely to the posteroventral side. These parts represent muscle VI and are arranged parallel to muscle V. They are not continuous across the mid-ventral line. There is a short section on each of the ventral ends of muscle VI which turns slightly forward. Each of the ventral ends of muscle VII passes external to muscle VI on the side of the body. Muscle VII ends slightly below the mid-ventral line, just after crossing muscle VI. In addition to these muscles there are two narrow, short connecting muscles (lateral longitudinal muscle, l.l.m.) between muscles IV

---

[1] Contribution from Scripps Institution of Oceanography, New Series No. 975. This work was supported in part by grants from the Rockefeller Foundation and the Office of Naval Research. Manuscript received October 23, 1956.

[2] Present address: Seto Marine Biological Laboratory, Japan.

[3] Scripps Institution of Oceanography, University of California, La Jolla, California.

Reproduced by Permission

(55)

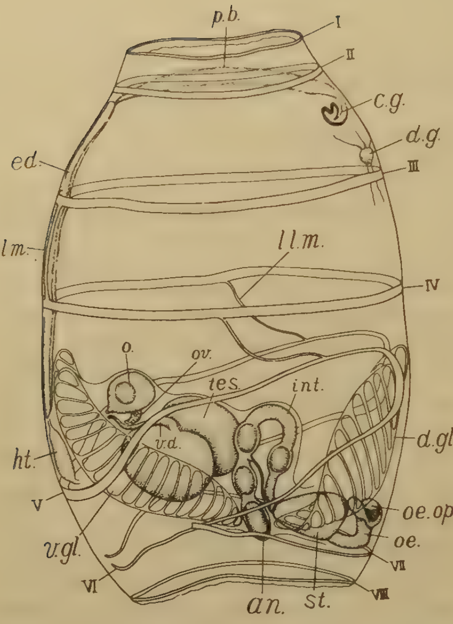

FIG. 1. *Doliopsoides horizoni* n. sp., gonozooid from left side. I–VIII, circular body muscles; *an.*, anus; *c.g.*, ciliated groove; *d.g.*, dorsal ganglion; *d.gl.*, dorsal gill; *ed.*, endostyle; *ht.*, heart; *int.*, intestine; *l.l.m.*, lateral longitudinal muscle; *o.*, mature ovum; *oe.*, oesophagus; *oe.op.*, oesophageal opening; *ov.*, ovary; *p.b.*, peripharyngeal band; *st.*, stomach; *tes.*, testis; *v. d.*, vas deferens; *v.gl.*, ventral gill; *v.l.m.*, ventral longitudinal muscle.

and V, one on each side of the body. These muscles extend from just below the midlateral portion of muscle IV obliquely upward, joining muscle V just above the midlateral line. Another narrow longitudinal muscle (ventral longitudinal muscle, v.l.m.) connects muscles III and IV along the midventral line.

The endostyle (ed.) is long and rather thick although its consistency does not seem to be compact. Anteriorly it begins just behind muscle II and extends posteriorly to slightly beyond the middle of the fourth intermuscular zone. The anterior margins of the peripharyngeal bands (p.b.) project slightly in front of muscle II. The ciliated groove (c.g.) is located near the middle of the second intermuscular zone, the dorsal ganglion (d.g.) is in the same zone near muscle III. The gill consists of a dorsal (d.gl.) and a ventral pair (v.gl.) of lamellae. It extends dorsally to the level of the ends of muscle V and ventrally to the middle of the fourth intermuscular zone or slightly anterior to it. The dorsal and ventral lamellae approach just above the juncture of muscle VI and VII. The gill bears in all 30 to 40 elongate stigmata.

The oesophageal opening (oe.op.) is located on the dorsomedian line near muscle VII, the oesophagus (oe.) itself is strongly curved. The stomach (st.) is situated vertically and in outline roughly forms an elongate triangle with the pyloric portion the narrowest. The intestine (int.) forms a U-shaped loop in the saggital plane of the body which ends with the anus (an.) near the pyloric end of the stomach. The proximal portion of the loop is somewhat thinner than the other portions and it is not certain whether this represents a hind stomach. The formation of fecal pellets was observed in all three specimens. Krüger in his description of *D. meteori* mentioned the formation of "Kotballen" in the intestine. There is a thin but distinct vessel connecting the pyloric portion of the stomach with the middle of the ventral branch of the intestinal loop. The ovary (ov.) is situated just dorsal to the posterior end of the endostyle and slightly to the right of the median line. In one specimen the ovary contains a large mature ovum (o.). The oviduct is so short as to be practically absent. The testis (tes.) is located between the ovary and the intestinal loop. It consists of two spherical lobes. The vas deferens (v.d.) is short but distinct, and extends from the testicular lobes to near the ovary, probably in the region of the female genital pore. The heart (ht.) lies between the posterior end of the endostyle and muscle V.

REMARKS

This form is evidentally very closely related to *Doliopsoides meteori* (Krüger, 1939). Krüger's genus and species were described from a plankton sample taken at Meteor station 267, in the layer between 400 and 200 meters, in the Atlantic Ocean off Cape Verde. Our specimens differ distinctly from Krüger's species in the following points: (1) The ventral longitudinal muscle connects muscles III and IV rather than muscles II and III as in *D. meteori.* (2) The oesophageal opening is situated on the middorsal line just anterior to muscle VII while in *D. meteori* it is located centrally on the level with muscle VI (see Krüger's fig. 87). (3) Muscle VI is interrupted at the midventral line in *D. horizoni* while it is continuous in *D. meteori.* In one part of Krüger's text figure the ventral ends of muscle VII are shown as if they passed internally to muscle VI, in another as if they passed externally to muscle VI. This apparent error may have been due to the poor condition of his specimens, but makes it impossible to compare the two species on this point. The specific name *horizoni* refers to the vessel which carried the Shellback Expedition; this follows Krüger's lead in naming his species after the ship from which it was taken. Comparing the structures of *D. meteori* and *D. horizoni* we have come to the conclusion that the genus *Doliopsoides* may be defined as follows:

Doliopsoides Krüger 1939: oozooid, trophozooid, and phorozooid unknown.

Gonozooid: The gonozooid is barrel-shaped with eight nearly hooplike muscles. Muscles I through IV and VIII form complete hoops while V, VI, and VII are interrupted. In addition to the circular muscles there are some longitudinal muscles, which are variously placed on the body. Both the ciliated groove and the dorsal ganglion are situated in the second intermuscular zone. The gill consists of a dorsal and a ventral pair of lamellae. The gonads are located anteroventrally to the alimentary organs. Although there are some rather marked differences between our specimens and Krüger's description we do not feel they warrant more than specific treatment. The type species is *Doliopsoides meteori* Krüger 1939.

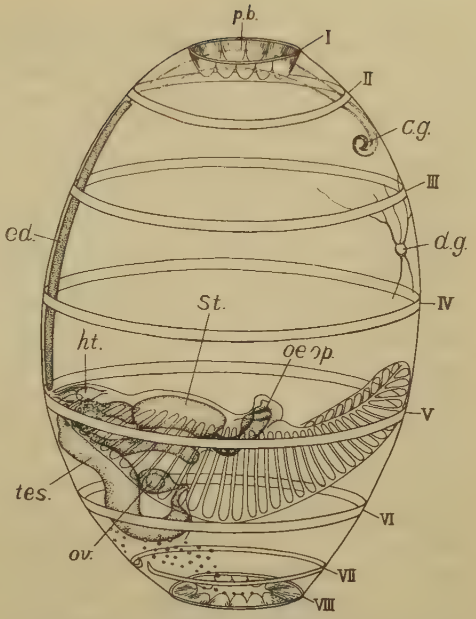

FIG. 2. *Doliolina undulatum* n. sp., gonozooid from left side. For abbreviations see Figure 1.

Doliolina undulatum new species
Fig. 2

This species is represented by five gonozooids from station SB-115 and four gonozooids from station SB-94. The location of SB-115 is given above, SB-94 was located at 9° 58.5′ S. and 95° 01′ W. These latter specimens are in a very poor state of preservation and we will deal here only with those from SB-115. They range from 3.3 to 4.6 mm. in length. The test is of moderate thickness but very soft and easily stripped from the body. The general appearance of the body and the arrangement of the eight circular muscles is quite similar to *D. intermedium* (Neumann, 1906), which occurs frequently in the Shellback area. A most striking difference is the interruption of muscle VII at the mid-ventral line in this new species. The mantle is thin. The muscles are narrow, especially I and VIII. Muscle VII is also somewhat narrower than the rest.

The endostyle (ed.) is very long, extending anteriorly nearly to muscle II and posteriorly to the anterior margin of muscle V. The anterior margin of the peripharyngeal band (p.b.) extends forward almost to muscle I. The ciliated groove (c.g.) is situated near the middle of the second intermuscular zone. The dorsal ganglion is situated in the third intermuscular zone, its posterior edge is at the middle of the zone. The gill septum extends from the middle of the fourth intermuscular zone dorsally, obliquely back to the level of muscle VI and then obliquely forward to the level of muscle V ventrally. It bears 30–40 pairs of elongate stigmata.

The oesophageal opening (oe.op.) is located approximately on the longitudinal axis near the posterior margin of muscle V. The stomach (st.) is located vertically at the same level; it is roughly rectangular in outline, slightly curved with the convex side forward. The intestine forms a simple loop and ends with the anal opening near the cardiac portion of the stomach and on a level with the middle of the fifth intermuscular zone. The hind stomach and mid-intestine are rather distinctly marked. There appears to be a thin short vessel connecting the pyloric end of the stomach with the middle of the posterior branch of the intestinal loop.

The ovary (ov.) is situated on a level with muscle VI, slightly to the right of the mid-ventral line. The testis (tes.) is somewhat sausage-shaped. It extends, with an undulating course, along the left side of the body between muscle V and the genital pore. There are a number of small cell groups scattered over the ventral half of the sixth intermuscular zone and on a small portion of the seventh intermuscular zone.

REMARKS

The oozooid, trophozooid, and the phorozooid of this species are unknown.

Gonozooid: At a glance the present new species may be confused with *D. intermedium* (Neumann, 1905: 211). The longer endostyle in *D. undulatum* can be used as a good indicator to distinguish it from *D. intermedium*. In most of the specimens of *D. intermedium* collected in the Shellback area the endostyle reaches only slightly beyond the middle of the second intermuscular zone and its posterior end is located near the middle of the fourth intermuscular zone. The mid-ventral interruption of muscle VII is also unique in *D. undulatum*. *Dolioletta mirabilis* is the only doliolid, outside the genus *Doliopsoides*, which has an interrupted muscle band. In this case there is a mid-ventral interruption of muscle VI below the gut. The characteristic appearance of the testis, from which the specific name of the new species has come, is also unique and serves to separate the species from all others in the genus.

The following material, upon which part of the descriptions herein are based, has been deposited in the U. S. National Museum:

1. *Doliopsoides horizoni*, gonozooids, SYNTYPES, 3 specimens USNM Cat. No. 11368. These specimens were poorly preserved and it was felt impossible to designate a type from among them. They are all from station SB-115.
2. *Doliolina undulatum*, gonozooid, HOLOTYPE, 1 specimen USNM Cat. No. 11369.
3. *Doliolina undulatum*, gonozooids, PARATYPES, 4 specimens USNM Cat. No. 11370.

REFERENCES

GARSTANG, W. 1933. Report on the Tunicata. Part I. Doliolida. *British Antarctic (Terra Nova) Exped. of 1910, Zool.* 4: 195–251.

KRÜGER, H. 1939. Die Thaliaceen der "Meteor" Expedition. *Wiss. Ergeb. Deut. Atlantische Exped. "Meteor" of 1925–1927* 13(2): 111–152.

NEUMANN, G. 1906. *Ergeb. Deut. Tiefsee-Exped. (Valdivia)*. XII, *Doliolum*, pp. 93–243.

SEWELL, R. B. S. 1953. The pelagic Tunicata. *Sci. Rpt. John Murray Exped.* X(1): 1–90.

TIDES

by

GORDON W. GROVES

Reprinted from Encyclopaedia Britannica
Copyright 1958

Printed in U. S. A.

TIDES. The word tide refers to those alternating relative motions of the matter of a planet, satellite or star, which are attributed to the gravitational actions of external bodies. Such motions are known to occur in all three principal divisions of the earth. The

Contributions from the Scripps Institution of Oceanography, New Series, no. 976
Reproduced by Permission

alternating slight changes of shape of the solid body or lithosphere of the earth attributed to the gravitational action of the moon and sun are known as bodily tides. Similarly, there are the atmospheric tides in the atmosphere, and the familiar ordinary ocean tides in the hydrosphere. A still wider use of the word is based on descriptive instead of on causal and astronomical ideas, and takes for its criterion that the motions in question have certain features in common with ocean tides. This extension includes those long waves of the sea, or tsunamis, which are sometimes caused by earthquakes, as well as effects on the sea of variable atmospheric pressure and wind, known as meteorological tides. In this article tides will be considered under these sections:

I. Ordinary Tides
II. History of the Study of Tides
III. Tide-Generating Forces
IV. Dynamics of Ocean Tides
V. Actual Tides in the Ocean
VI. Tidal Analysis and Prediction
VII. Nonastronomical Variations of Sea Level
VIII. Miscellaneous Tidal Problems
IX. Atmospheric Tides
X. Bodily Tides

I. ORDINARY TIDES

General Description of Phenomena.—At most seaside places the water reaches its highest level approximately twice a day, the average interval between two successive high waters being 12 hr. 25 min., though this interval varies considerably during the course of a week. At certain places in the East Indian seas two successive high waters are separated by an interval of 12 hr., while at certain places in the China sea the interval is often more than 24 hr. At places on the shores of the oceans the time taken by the tide in rising is about equal to the time taken in falling on the same day, but in estuaries the tide usually rises more quickly than it falls. At certain places, such as Southampton, Eng., the high waters are often doubled; *i.e.*, the water reaches a maximum height, falls a little and then rises to a maximum again. At other places the low waters are often doubled. As one goes along any stretch of coast the time of high water generally becomes progressively earlier or later, while as one goes up an estuary from the sea the time of high water always becomes progressively later.

At most places, on the average, a high water is about as much above the mean level of the sea as the succeeding low water is below it. The difference in level between successive high and low waters is called the range of tide. The range of tide at any place may vary much from day to day. At most places it reaches a maximum once a fortnight, and a minimum at times midway between two successive maxima. At London bridge the greatest range of the fortnight has an average value of 21 ft. while the least range of the fortnight has an average value of 15 ft. At the head of the Bay of Fundy the range of tide reaches 50 ft. while at certain islands of the Pacific and over most of the Mediterranean the range never exceeds 2 ft. At many places outside the Atlantic the heights of two successive high or low waters are markedly different, a phenomenon known as the diurnal inequality.

At a place in a strait or narrow sea the tidal current usually flows for about 6 hr. 12 min. in one direction, and then for about the same time in the opposite direction. At the reversal of such a current there is the state of rest usually called slack water. In estuaries the current generally flows downstream for a greater length of time than it flows upstream. At a place in the open sea the direction of the current often takes all points of the compass, making the complete revolution in the tidal period. During this period there are usually two times of maximum current and two intermediate times of minimum current. The times of maximum current are separated by about half the tidal period and the directions of maximum current are nearly directly opposite; similarly for the two minimum currents. There is no fixed general relation between the time of high water and the time of maximum current. If the current flows directly in and out of a bay it will reach its inward maximum nearly a quarter period before high water at the head of the bay, so that slack water is simultaneous with high water. On the other hand, in an estuary the current continues to flow upstream for some considerable time after high water and to run downstream similarly after low water. When the current is directed toward land or up an estuary it is called the flood current; when it runs away from land or down an estuary it is called the ebb current. The speeds of tidal currents vary greatly from place to place; *e.g.*, in the Mersey at Liverpool, Eng., the maximum current reaches seven knots, while in the North sea it rarely exceeds one knot. At some distance up certain rivers—as, for example, the Severn—the rising water spreads over the flat sands in a roaring surf and travels up the river almost like a wall of water. This phenomenon is called a bore. Near a headland separating two bays there is sometimes a swift current termed a race.

Relation to Motions of Moon and Sun.—The times of high water bear an intimate relation to the positions of the moon and sun. The period of 12 hr. 25 min. is half that of the moon's apparent revolution around the earth. The length of time between the moon's crossing of the meridian of a place and the next high water at that place is known as the lunitidal interval, or the high-water interval, for the place. Similarly, the length of time between the moon's crossing of the meridian and the next low water is called the low-water interval. For London bridge the average value of the lunitidal interval is 1 hr. 31 min. In many cases, including those of British waters, the chief variation in the lunitidal interval is associated with the phase of the moon. The average value of the lunitidal interval on the days of new and full moon is known as the establishment of the port. For London bridge the establishment is 1 hr. 58 min.

The range of tide may be similarly correlated. In British waters it reaches its maximum a day or so after new and full moon and its minimum a day or so after the quarters. In these circumstances the maximum tides are known as spring tides and the minimum tides as neap tides. About the time of the equinoxes spring tides are generally larger and about the time of the solstices they are generally smaller than usual. The average interval between new or full moon and the next following spring tide is known as the age of the tide at the place in question. At certain places in Canadian waters the chief variation in the range of tide is associated with the varying distance of the moon from the earth, while at others it is associated with the varying declination of the moon. The diurnal inequality is always associated with the declination of the moon or sun. But the most complete correlation between the tides and astronomical variables is provided by the harmonic methods.

II. HISTORY OF THE STUDY OF TIDES

The writings of various Chinese, Arabic and Icelandic authors show that they paid some attention to the tides, but the theories advanced are fantastic. The writings of the classical authors of antiquity contain but a few references to the tides, for the Greeks and Romans lived on the shores of an almost tideless sea.

Johann Kepler in the early 17th century recognized the tendency of the water of the ocean to move toward the sun and moon, but Galileo's explanation referred the phenomenon to the rotation and orbital motions of the earth. It was Isaac Newton who, in his *Principia* of 1687, laid the foundation of the modern theory of the tides when he brought his generalization of universal gravitation to bear on the subject. He gave a geometrical construction for the tide-generating force, and calculated the magnitude of the solar equilibrium tide. He considered a canal encircling the earth and applied to each particle of water the laws which he had deduced for a satellite. He accounted for many of the general properties of the tides, such as the phenomenon of springs and neaps, priming and lagging, diurnal and elliptic inequalities. The only important factor which he did not mention is the dynamical effect of the earth's rotation. Newton's work was continued by D. Bernoulli, L. Euler and C. Maclaurin who adopted not only the theory of gravitation but also Newton's method of the superposition of two ellipsoids. In 1746 Jean le Rond d'Alembert wrote a paper on atmospheric tides, but this work, like Maclaurin's, is chiefly remarkable for the importance of collateral points.

The theory of the tidal movements of an ocean was almost untouched when in 1773 Pierre Laplace first undertook the subject. In his *Mécanique célèste* he formulated the equation of continuity and the dynamical equations, and applied them to the case of an ocean covering the whole earth. He also established the principle of forced oscillations, which forms the foundation of the harmonic methods.

The connection between the tides and the movements of the moon and sun is so obvious that tidal predictions founded on empirical methods were regularly made and published long before mathematicians had devoted their attention to them. The best example of this kind of tide table was afforded by Moses Holden's tables for Liverpool, based on 20 years of personal observation by a harbour master named William Hutchinson. The use of automatic tide gauges appears to have begun about 1830.

The work of J. Lubbock, Sr. and W. Whewell is chiefly remarkable for the co-ordination and analysis of data at various ports, and for the construction of tide tables. Sir George Airy in his *Tides and Waves* of 1842 studied profoundly the theory of tidal motions in canals, while in 1847 and 1857 F. W. Beechy published the results of a survey of tidal currents over the Irish sea, the English channel and the North sea.

About 1863 W. Thomson (afterward Lord Kelvin) became interested in the problems presented by earth tides. In 1866 he took up the analysis of ordinary tidal observations and established the harmonic methods, which quickly developed. He introduced the rotation of the earth into the tidal dynamics of small seas, and in 1872 he designed a tide-predicting machine.

In 1874 W. Ferrel, of the U.S. coast and geodetic survey, published his *Tidal Researches* which included a harmonic development of the generating potential, and from the same year A. W. Baird, of the survey of India, organized a service of observation and harmonic analysis for Indian tides. In 1882 G. H. Darwin took up harmonic analysis and produced memoirs which for a long time formed the standard manual on the subject, and about this time J. E. Pillsbury, of the U.S. coast survey, began the observations of currents by means of current meters. In 1885 C. Börgen introduced new ideas into the methods of harmonic analysis. Between 1870 and 1890 F. A. Forel made illuminating studies of the seiches of Lake Geneva, Switz., and about 1890 M. Margules investigated the dynamics of atmospheric tides.

From 1894 to 1907 R. A. Harris, of the U.S. coast survey, published his *Manual of Tides*. This work contained charts showing cotidal lines for the whole world, based on theories and hypotheses the leading feature of which was the principle of resonance. It was assumed that in each ocean there exists regions capable of free oscillation with a period near one of the principal tidal periods, and that the nature of these free oscillations may be calculated approximately, without allowing for the earth's rotation or the interaction with neighbouring regions.

After 1900 a number of Scandinavian oceanographers, notably V. W. Ekman, O. Pettersson and J. P. Jacobsen, invented current meters and L. Favé observed tidal elevations in the open sea by means of his self-registering instrument.

In 1912 A. Blondel applied the narrow sea theory, through the principle of least action, to the tides of the Red sea. From 1913 to 1920 R. Sterneck and A. Defant developed the narrow sea theory with special reference to the Adriatic sea. Defant applied this theory to the Red sea, the Persian gulf, the English channel and the Irish sea.

After about 1895 the dynamical theory of tides and seiches was much advanced by the mathematicians: H. Lamb, H. H. Hough, J. H. Poincaré, Lord Rayleigh, G. Chrystal, E. Fichot, G. R. Goldsbrough, G. I. Taylor, Harold Jeffreys, G. Bertrand, S. Goldstein and J. Proudman; while between 1920 and the latter 1950s much was done on the analysis of observations by A. T. Doodson, K. Hessen and H. Rauschelbach.

III. TIDE-GENERATING FORCES

Dynamics of Earth-Moon System.—The moon attracts every particle of the earth and ocean. By the law of gravitation the force acting on any particle is directed toward the moon's centre, and is jointly proportional to the masses of the particle and of the moon, and inversely proportional to the square of the distance between the particle and the moon's centre. If one can imagine the earth and ocean subdivided into a number of small particles of equal mass, then the average, both as to direction and intensity, of the forces acting on these particles, is equal to the force acting on that particle which is at the earth's centre. If every particle of the earth and ocean were being urged by equal and parallel forces there would be no cause for relative motion between the ocean and the earth. Hence it is the departure of the force acting on any particle from the average which constitutes the tide-generating force. Now it is obvious that on the side of the earth toward the moon the departure from the average is a small force directed toward the moon; and on the side of the earth away from the moon the departure is a small force directed away from the moon. All around the sides of the earth along a great circle perpendicular to the line joining the moon and earth the departure is a force directed inward toward the earth's centre. Thus it can be seen that the tidal forces tend to pull the water toward and away from the moon, and to depress the water at right angles to that direction. In fig. 1 this distribution of forces is illustrated graphically. The relative magnitudes of the forces are given by the numbers on the figure, *M* being in the direction of the moon. The separate attractions of the moon at the earth's centre and at a point on the earth's surface are each inversely proportional to the square of the moon's distance, so that the difference between the two, which gives the tide-generating force, is approximately inversely proportional to the cube of the moon's distance.

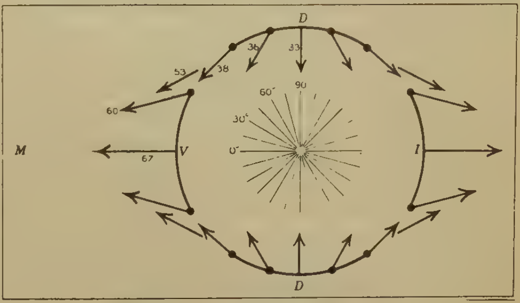

FIG. 1.—TIDE-GENERATING FORCE

The vertical component of the tide-generating force coincides in direction with the gravitational force of the earth itself, and thus acts as a slight modification of weight. This component does not tend to alter the position of equilibrium which the water would take up in the absence of any disturbance from an extraterrestrial body. The effective tide-generating forces, therefore, are the horizontal components of those indicated in fig. 1.

Equilibrium Form of the Tide.—For many purposes it is convenient to specify the distribution of the tide-generating forces at any instant by reference to a fictitious tide. If a completely rigid earth were completely covered by a layer of ocean, and if the tide-generating forces were to remain constant, there would be an invariable elevation of water at each point of the ocean surface and no tidal currents. If the distribution of forces were the same as that of the actual tide-generating forces at any instant, then the consequential elevation of water might be used as a specification of these forces. This distribution of fictitious tidal elevation is known as the equilibrium form of the tide. It is a real and accurate specification of the actual tide-generating forces throughout the earth's body as well as on its surface. When the equilibrium form is stated for every instant there is a complete specification of these forces, and henceforth the terms equilibrium tide and tide-generating force will be used interchangeably.

In this equilibrium form the inclination, to the horizontal, of the surface of the water would be always such that the consequential pressure gradient would everywhere balance the tide-generating force. It is therefore clear that the surface of the water would slope upward from *DD* toward the points *V* and *I*, the water being raised by a maximum amount at *V* and *I* and depressed by a maximum amount along the great circle through *DD*. The surface of the water would be nearly that of an ellipsoid of revolution. The volume of this ellipsoid would be the same as that enclosed by the surface of the undisturbed ocean. Owing to the motion of the moon relative to the earth, the tidal ellipsoid moves over the earth so that V is always directly under the moon and I always directly opposite, while owing to the varying distance of the moon the equilibrium ellipsoid changes slightly in shape.

The tide-generating forces attributable to the sun's gravitation may be similarly specified. The sun's mass is nearly 27,000,000 times the moon's mass and the sun's distance is about 390 times the moon's distance from the earth. Consequently the sun's tide-generating forces are to those of the moon in the ratio of 27,000,000 to 390^3; *i.e.*, .460 or $\frac{1}{2.17}$. This means that at corresponding points of the two ellipsoids representing the lunar and solar equilibrium forms the tidal elevations on the average will be in the ratio of 2.17 to 1.

Harmonic Constituents.—The study of tides on the earth has been greatly facilitated by the fact that the tidal motions, whether in the atmosphere, hydrosphere or lithosphere, are to a high degree of precision linear with respect to the tide-generating forces which cause them. This will be demonstrated later in the case of the dynamics of the ocean tide.

The significance of this linearity is that the tide-generating force can be considered as the sum of a number of constituents, the actual tide being the sum of the individual effects that each constituent would produce separately in the absence of all the others. As an example, the lunar and solar tides can be considered separately. The tide which would be produced under the combined action of moon and sun would be almost exactly what one would obtain by adding the separate contributions of moon and sun. In other words, there is little interaction between the lunar and solar tides.

The tide-generating forces can be expressed quite precisely by a finite series of harmonic terms, and in practice it has been found that about 30 terms generally give an adequate approximation. Furthermore, linear systems have the important property that their response is harmonic when they are acted upon by a force varying harmonically with time, the response having the same frequency as the force. The above two facts form the basis of the harmonic development of the tide, which has been in use since the time of Pierre S. Laplace.

Each term of the series representing the elevation of the equilibrium tide at some particular point on the earth's surface will be of the form $H \cos(nt-\epsilon)$, where t is time, H is the amplitude, n is the frequency or speed (commonly expressed in units of degrees per hour), and ϵ is the epoch. For any given constituent the speed is constant, while the amplitude and epoch are constant in time but may depend on geographical location. The harmonic terms representing actual tides will be of the same form. In the case of the ocean tides H may represent the amplitude of the elevation of the water surface relative to the ground, for bodily tides H may represent the amplitude of a component of particle displacement, and for atmospheric tides H may represent the amplitude of a pressure fluctuation.

Let us now consider the effect of only one tide-generating body, such as the moon. As demonstrated in the previous section, the tide-generating forces of the moon can be specified completely by the shape and geographic orientation of the tidal ellipsoid, whose major axis is oriented along the line joining the centres of earth and moon. Now for the moment, let us consider what would happen if the moon remained at a constant distance from the earth and revolved about the earth in the equatorial plane with constant speed. An observer located at any given geographical position would experience two maxima and two minima of the equilibrium tide each lunar day. The amplitude would be a maximum at the equator and would decrease with increasing northern or southern latitude to a value of zero at the poles. The rise and fall of the equilibrium tide would be approximately harmonic with speed $n = 2(\gamma-\sigma)$ where γ denotes the angular speed of the earth's rotation relative to the stars and σ the mean speed of revolution of the moon about the earth, and the equilibrium tide would be represented very closely by a single harmonic constituent. Since the moon's speed of revolution is small compared to the earth's speed of rotation, the period of this constituent is approximately semidiurnal. The moon's varying declination (angular distance from equatorial plane), varying apparent angular speed of revolution about the earth and varying distance from the earth cause many modifications in this simplified example.

If the moon revolved about the earth with constant angular speed at some constant declination not equal to zero, one of the two poles of the equilibrium tidal ellipsoid would be always in the northern hemisphere, and the other in the southern hemisphere. The two equilibrium high waters that a point on earth not on the equator would experience as the earth rotates would therefore not be equal, and the introduction of a new constituent of speed $n = \gamma-\sigma$, approximately diurnal, would be required. This effect is known as the diurnal inequality. The variable declination of the moon results from the moon's motion in an orbit whose plane intersects the earth's equatorial plane at an angle I. The lunar declination thus passes through a monthly cycle but since both north and south declinations have essentially the same effect; *i.e.*, that of decreasing the semidiurnal and increasing the diurnal contribution, the two constituents suffer a fortnightly modulation. Strictly speaking, such constituents cannot be considered harmonic, as there is implied in this term the invariability of amplitude, speed and epoch. These constituents can, however, be expressed precisely as the sum of a number of strictly harmonic terms, and more will be said about this point later.

The distance from earth to moon varies throughout a monthly cycle giving rise to a monthly modulation in the amplitude of the equilibrium tide. The maxima occur when the moon is at perigee, the point on the moon's orbit which is closest to the earth; the minima occur at apogee, when the moon is farthest from the earth. The time between successive lunar passages through perigee or apogee is the so-called anomalistic month, whose average length is 27.55 (mean solar) days. The speed of revolution of the moon about the earth varies inversely with the moon's distance according to Kepler's laws (*see* ORBIT). This causes the epoch of the equilibrium tide to vary according to the moon's position in its orbit, resulting in an apparent increase of period at apogee as compared to perigee. This monthly modulation of both amplitude and epoch of the equilibrium tide can again be expressed by a sum of purely harmonic constituents.

There are many other irregularities in the moon's motion, all of which can be expressed by the addition of more harmonic terms insofar as their effect on the equilibrium tide is concerned. The plane of the lunar orbit does not remain with constant orientation in space. Its movement is best described by the motion of the moon's nodes, which are the two points on the lunar orbit which lie on the plane of the ecliptic. Relative to the stars these nodes describe a westward motion known as the regression of the nodes, completing a cycle in about 19 years. Also, the major axis of the lunar orbit revolves eastward relative to the stars, completing a cycle in about nine years.

The solar effects are in every way analogous to the corresponding lunar effects.

Species.—In the above section it was seen that many cases arise where a constituent having a slow periodic variation of amplitude or epoch can be represented by the sum of two or more purely harmonic constituents. The speeds of these purely harmonic constituents will belong to the series, $n \pm \omega$, $n \pm 2\omega$, $n \pm 3\omega, \ldots,$ where n is the speed of the original constituent and ω is the speed corresponding to the fundamental period of variation of its amplitude or epoch. If ω is small as compared to n, the speeds of the purely harmonic constituents will cluster closely about the speed of the original constituent. In the case of the actual tide, most of the constituents are approximately semidiurnal, diurnal, or of a longer (fortnightly or longer) period of variation, and their amplitudes and epochs pass through a much longer period of variation than that of the actual constituent. As a result, the periods of purely harmonic constituents representing the equilibrium tide are clustered about 12 hr., 24 hr. and much longer periods, offering a logical basis for classification of the tidal constituents.

The scheme of classification shown in Table I was developed by

George Darwin in 1882 and has been adopted by most of the world's tidal authorities. Within any given species the coefficient is proportional to the equilibrium amplitude, and this proportionality holds roughly between constituents belonging to different species. The subscript on the symbol designating the constituent refers to the species to which it belongs. The long-period constituents have no subscript, the diurnal species have the subscript "one," the semidiurnal species the subscript "two." In addition to the constituents tabulated in Table I, there are terdiurnal, 4-diurnal, etc., constituents in the equilibrium tide, but these are of much lower amplitude and are not of much importance on earth.

TABLE I.—*Tidal Constituents*

Symbol	Name	Speed	Speed in °/hr.	Coefficient
Long-period species				
Mf	Lunar fortnightly	2σ	1.098	.078
Ssa	Solar semiannual	2η	.082	.036
—	Nineteen yearly	N	.002	.033
Diurnal species				
K_1	Lunisolar	γ	15.041	.265
O_1	Larger lunar	$\gamma-2\sigma$	13.943	.189
P_1	Larger solar	$\gamma-2\eta$	14.959	.088
Semidiurnal species				
M_2	Principal lunar	$2(\gamma-\sigma)$	28.984	.454
S_2	Principal solar	$2(\gamma-\eta)$	30.000	.211
N_2	Larger lunar elliptic	$2\gamma-3\sigma+w$	28.440	.088
K_2	Lunisolar	2γ	30.082	.058

The earth's speed of rotation γ is the largest of all the parameters contributing to the speeds of the tidal constituents, and its numerical multiplier in the expression for the speed determines to which species a given constituent belongs. The other quantities in Table I which determine the speeds of the constituents are the mean motion of the moon σ, the mean motion of the sun η, the speed of revolution of the moon's nodes N, and the mean motion of the lunar perigee w. These quantities have a smaller effect and merely determine the period of the constituent within its species. It can therefore be said that the fundamental reason that the tidal constituents clump conveniently into species is that the day is much shorter than either the month or the year.

The equilibrium constituents of any given species all have the same geographical form. The long-period constituents are characterized by a standing wave symmetrical about the earth's axis. The polar regions oscillate in phase with each other and are 180° out of phase with the equilibrium tide in low latitudes. The two nodal lines lie along latitudes 35.26° north and south. The diurnal constituents have the form of a progressive wave rotating relative to the earth about its axis from east to west. At any given instant there are two maxima at opposite extremes of the earth and two minima similarly situated, all lying at latitudes 45° north and south on a great circle passing through the earth's poles. The amplitude of the diurnal equilibrium tide vanishes at equator and poles. The semidiurnal constituents also have the form of a progressive wave rotating about the earth from east to west. There are two maxima on the equator at opposite extremes of the earth and two minima also on the equator 90° from the maxima. The amplitude of the semidiurnal equilibrium tide is maximum at the equator and dies off with increasing latitude, vanishing at the poles.

Description of the Constituents.—Let us consider first the semidiurnal constituents. As can be seen from the value of their coefficients tabulated in Table I, the principal lunar constituent M_2 is the most important. The other semidiurnal constituents "beat" against M_2 giving rise to a modulation, the speed of which is equal to the difference of speeds of the two constituents. That is, the period of the modulation is the synodic period of the two constituents. The next strongest semidiurnal constituent is the principal solar constituent S_2, which beats against M_2 causing the fortnightly spring-neap modulation. Next comes the larger lunar elliptic constituent N_2 which beats with M_2 causing a monthly modulation of the latter associated with the variable distance between earth and moon resulting from the ellipticity of the moon's orbit. The lunisolar constituent K_2 actually represents the sum of two constituents, one of lunar the other of solar origin, which cannot be separated from each other by analysis because their periods are equal. The lunar part of this constituent beats with M_2 giving rise to a fortnightly modulation associated with the variable declination of the moon. It will be recalled that the amplitude of the semidiurnal part of the tide is at a maximum when the tide-generating body has zero declination. In similar fashion the solar part of the K_2 constituent beats with S_2 causing a semiannual modulation of this principal solar constituent which is associated with the variable declination of the sun.

The lunisolar diurnal constituent K_1 is similarly composed of a lunar and a solar contribution. The lunar part of this constituent beats with the larger lunar constituent O_1 causing a fortnightly modulation associated with the variable declination of the moon. It will be recalled that the amplitude of the diurnal part of the equilibrium tide vanishes when the tide-generating body has zero declination. Similarly, the solar part of the constituent K_1 beats with the larger solar constituent P_1 causing a semiannual modulation associated with the variable declination of the sun.

The constituents Mf and Ssa result from the variable declination of the tide-generating body and are at a maximum when this body is at zero declination. The lunar fortnightly constituent Mf thus reflects the variable declination of the moon, and the solar semiannual constituent Ssa similarly reflects the variable declination of the sun. In addition there is a small 19-year constituent which arises from the 19-year cycle in the regression of the moon's nodes, as well as many other minor long-period constituents.

In Darwin's harmonic development the tide-generating forces (the equilibrium tide) are not analyzed into strictly harmonic constituents; that is, the amplitudes and epochs of Darwin's constituents are not truly constant. They exhibit the 19-year cycle of the regression of the moon's nodes. However, during any one year the amplitudes and epochs vary so slightly that the constituents can be considered as true harmonic terms without incurring appreciable error. The nodal variation in amplitude is accounted for by taking the constituent coefficients c (those values tabulated in Table I) to be constant in time while denoting the true amplitude of the equilibrium constituents by the quantity fc where f is called the node factor and is the quantity which varies. The mean value of f is taken to be unity, and its values have been tabulated for each year for all important constituents. The value of f changes so slowly that it is adequate to take its mean value during any given year in place of its true value at any instant during that year.

In 1921 Doodson developed the equilibrium tide into a series of harmonic constituents whose amplitudes and epochs do not exhibit this 19-year cycle, and therefore do not need the artifice of node factors. For this reason it may be said that Doodson's development is more nearly perfectly harmonic than is Darwin's. Even though Doodson's development does not attempt to take into account such long-term variations as secular changes in the distance between earth, moon and sun, and geologic changes in sea level, it is doubtful that a more elaborate development will ever be needed for tidal work.

IV. DYNAMICS OF OCEAN TIDES

Equations of Motion.—The dynamical theory of tides introduced by Laplace in the 18th century has given much insight into the problem of tides in the ocean. The following assumptions and approximations are commonly introduced:

(1) The water is assumed to be homogeneous; (2) vertical displacements and velocities of the water particles are assumed small in comparison to the horizontal displacements and velocities; (3) the water pressure at any point in the water is given adequately by the hydrostatic law; *i.e.*, it is equal to the head of water above the given point; (4) all dissipative forces are neglected; and (5) the ocean basins are assumed rigid (as if there were no bodily tide), and the gravitational potential of the tidally displaced masses is neglected.

If assumptions (1) and (3) are valid it can readily be shown that the tidal currents at any locality are uniform with depth.

Take a to denote the radius of the earth and g the acceleration of gravity at its surface. Position on the earth's surface will be designated by the longitude ϕ and the co-latitude (angular distance from the north pole to the point under consideration) θ. Let h denote the depth of the ocean at any point, so that h is a function of θ and ϕ. Also, let ζ denote the elevation of the free surface at any point of the ocean above its mean level, and u and v the southward and eastward components of the tidal current, so that these three quantities are functions of θ, ϕ as well as of the time t. Then the equation of continuity, which expresses the condition that the volume of any mass of water must remain constant, may be written in the form

$$\frac{1}{a \sin\theta}\left\{\frac{\partial}{\partial\theta}(hu \sin\theta)+\frac{\partial}{\partial\phi}(hv)\right\}+\frac{\partial\zeta}{\partial t}=0 \tag{1}$$

provided that the elevation of the sea surface is everywhere small compared to the depth of water. If this is not the case then h must be replaced by $h+\zeta$ in equation (1). This equation may be derived by expressing the condition that the net rate at which volume of water enters the sides of a vertical column is equal to the rate of increase of the volume at the top of this column by virtue of the time rate of increase of the elevation of the sea surface ζ. Along a coast line the condition that the tidal current have no component perpendicular to the coast must be satisfied.

The equations of motion are formed by equating the southward and eastward components of acceleration of the water particles to the sum of all the forces per unit mass acting on the water in the southward and eastward directions, respectively. The acceleration consists of three parts: the local acceleration; the field acceleration; and the Coriolis acceleration resulting from the earth's rotation. As an example, the southward component of acceleration is equal to

$$\frac{\partial u}{\partial t}+\frac{u}{a}\,\frac{\partial u}{\partial\theta}+\frac{v}{a \sin\theta}\,\frac{\partial u}{\partial\phi}-\frac{v^2}{a}\cot\theta-2\omega v\cos\theta$$

where the first term represents the local, the second, third and fourth terms combined represent the field, and the last term the Coriolis accelerations, respectively. Here ω represents the angular speed of the earth's rotation. At this point an additional assumption shown to be valid for tidal motion in true oceanic regions is introduced: that the field acceleration is negligible as compared to the local acceleration. In accordance with the foregoing approximations, the only forces acting on the water are the tide-generating forces and those attributable to the pressure gradient resulting from the slope of the sea surface. The southward and eastward components of the pressure gradient are given by

$$\frac{g\rho}{a}\,\frac{\partial\zeta}{\partial\theta},\quad \frac{g\rho}{a\sin\theta}\,\frac{\partial\zeta}{\partial\phi},$$

ρ being the water density, and the southward and eastward components of the tide-generating force are given by

$$\frac{g\rho}{a}\,\frac{\partial\bar{\zeta}}{\partial\theta},\quad \frac{g\rho}{a\sin\theta}\,\frac{\partial\bar{\zeta}}{\partial\phi},$$

where $\bar{\zeta}$ represents the elevation of the equilibrium tide. This quantity is a function of θ, ϕ and t and is assumed known as it can be deduced from knowledge of the relative movements of the earth, moon and sun. The equations of motion can then be written in the form

$$\begin{aligned}\frac{\partial u}{\partial t}-2\omega v\cos\theta&=-\frac{g}{a}\,\frac{\partial}{\partial\theta}(\zeta-\bar{\zeta})\\ \frac{\partial v}{\partial t}+2\omega u\cos\theta&=-\frac{g}{a\sin\theta}\,\frac{\partial}{\partial\phi}(\zeta-\bar{\zeta}).\end{aligned} \tag{2}$$

The equations (1) and (2) serve to determine completely, at least in theory, the tidal currents and elevation over the entire oceans and for all times, given a complete description of the tide-generating forces and the boundaries of the ocean basins. In practice, however, such a general solution has never been obtained owing to the complicated nature of the distribution of sea and land masses and the varying depth of water. For this reason tidal research has been based primarily on observations and general principles (such as linearity, etc.) derived from theory.

It may be noted that these equations are linear in u, v, ζ and $\bar{\zeta}$ with the result that the tide-generating forces may be separated into several constituents, the sum of whose effects are exactly equivalent to the effect produced by the sum total of all the tide-generating constituents. Indeed, as has already been pointed out, this is the basis of the harmonic development of the tide. Let us review under what conditions the ocean tide is truly linear and under what conditions this linearity breaks down. Unless the elevation of the sea surface above its mean position is always small as compared to the mean depth h, equation (1) becomes nonlinear. Similarly, if the field acceleration becomes so large it is no longer negligible as compared to the local acceleration equations (2) become nonlinear. This is most likely to occur in regions of large tidal currents with a large spatial rate of change (current shear). Nonlinear dissipative forces may be another source of nonlinearity. All these effects are quite small in the vast oceanic regions but tend to become larger in regions of shallow water and in the vicinity of the coast line, and consequently are referred to as shallow-water tides.

As to the other approximations, that of neglecting all dissipative mechanisms (4) is not a very good one, but more will be said about this point in the section on *Tidal Friction.* The bodily tides of the earth invalidate to a certain extent assumption (5) by virtue of a small variable movement of the sea floor and of the earth's own gravitational field. If ζ_e designates the variable elevation of the sea floor above its mean position, equation (1) will stand unaltered if we take ζ to denote the elevation of the sea surface relative to the sea floor, but in the formulas for pressure gradients ζ must be replaced by $\zeta+\zeta_e$. The disturbance in the gravitational forces brought about by the displacements of water and solid earth must be accounted for by adding a term $\bar{\zeta}_e$ to $\bar{\zeta}$. Inhomogeneities in the sea water have been neglected according to assumption (1), but may have a more important effect in tidal motions than has been anticipated. At any given time of the year a large part of the ocean is covered by a nearly homogeneous layer of light, warm water 50 to 200 m. thick. Such stratification of the sea water may influence the vertical structure of the tidal current with resulting deviations from their generally assumed uniformity with depth. Bottom friction will also introduce vertical shear in the tidal current.

Suppose now that we consider the ocean's response to one harmonic constituent of the equilibrium tide. If we take a long-period constituent, $\bar{\zeta}$ will have the form of a standing wave over the entire earth. A constituent of any other species will have the form of a progressive wave rotating relative to the earth about its axis in the westward direction. Such progressive waves can, however, be expressed as the sum of two standing waves separated in longitude by 90°, and separated in time also by 90°. In any case, therefore, it will suffice to express $\bar{\zeta}$ in the form

$$\bar{\zeta}=H_0\cos n(t-\tau_0)$$

where n and τ_0 are absolute constants and H is a function of geographic position but independent of time. The actual response of the ocean will then be the sum of a number of solutions to such inputs. The solutions for the tidal elevation ζ and current u, v from equations (1) and (2) will have the form

$$\zeta=H\cos n(t-\tau)$$
$$u=U\cos n(t-\tau_1),\qquad v=V\cos n(t-\tau_2),$$

where H, U, V, τ, τ_1, and τ_2 are all functions of geographical position only. While it is not feasible to actually determine these functions analytically, if their values are determined for a certain location on the earth by appropriate analysis of tidal observations, the response to the constituent under consideration could be predicted for all time. In the case of the tidal elevation, wherever H and τ have been determined for all important constituents, the tidal elevations there can be predicted for any time. It may be remarked that at a given place H_0 and H are generally quite different; *i.e.*, the true tide bears little resemblance to the equilibrium tide.

Nonlinear Distortion (Shallow-Water Tides).—At places where the tidal elevation becomes appreciable as compared to the water depth, or other nonlinear effects occur, the principle of superposition breaks down. One might think that under these circumstances the concept of harmonic constituents would be completely useless, but it has been found possible to retain this concept provided that additional constituents, the so-called shallow-water tides, be included. The regions where this phenomenon occurs are generally confined to rivers, estuaries and shallow gulfs. The shallow-water constituents are not produced by the direct action of the tide-generating forces, but by the distortion attributable to shoal water of already existing tidal constituents which have been formed in the ocean. In fact, if the region of distortion is small enough (as it usually is), the tide-generating forces have little or no direct effect on the shallow-water tide.

It is no longer correct to consider separately the reactions to individual equilibrium constituents, but let us take the simple example of only one equilibrium constituent in order to gain insight into the problem. The response of a nonlinear system to the harmonic forcing constituent will not be harmonic, but at least it will be periodic having the same period as the forcing or primary constituent. If $2\pi/\sigma$ is the period of the primary constituent, it is well known from the theory of Fourier series that a periodic function of this period can be expressed as the sum of purely harmonic terms having speeds σ, 2σ, 3σ, etc. Extending this idea to the actual situation one should expect to find shallow-water constituents having periods of one-half, one-third, etc., of those of the major tidal constituents. The shallow-water constituents obtained in this way are called overtides because of their analogy to overtones in acoustics. The same symbol is used to designate these overtides as is used to designate the equilibrium constituent which gives rise to them, and again the subscript designates the species (approximate number of periods in a day) to which the overtide belongs. For example the constituent M_2 gives rise to the series of overtides M_4, M_6, etc., and K_1 gives rise to the overtides K_2, K_3, etc. In some cases an overtide will have exactly the same period as another equilibrium constituent and it will be impossible to separate the two by harmonic analysis. For example, K_2 represents the lunisolar semidiurnal constituent, but an overtide of exactly the same period as K_2 is produced by nonlinear distortion of the lunisolar diurnal constituent K_1. In this and in similar cases the symbol K_2 (referring to the actual tide) represents the combined effect of both the linear reaction to the equilibrium constituent K_2 and to the overtide.

The theory of progressive shallow-water waves of finite height has been used to estimate the relationship between the amplitudes of the overtides and primary tide. The amplitude of the nth overtide is found to be proportional to the nth power of the amplitude of its primary at any given place, as the amplitude of the primary varies in time. For example, if the range of the semidiurnal tide is twice as great during the spring tides as during the neap tides, the range of the quarter-diurnal overtide resulting from distortion of the semidiurnal tide will be approximately four times as great during the spring tides as during the neaps. The range of the 6-diurnal overtides will be eight times as great during the spring tides, etc. As to the 19-year nodal variation in amplitude, the node factors f of the overtides bear a relation to those of the primary as illustrated in the following example in the case of the overtides of the constituent M_2:

$$f\,(M_4)=[f\,(M_2)]^2,\quad f\,(M_6)=[f\,(M_2)]^3,\ \text{etc.}$$

The above relations seem to be confirmed fairly well in most cases by tidal observations in spite of the fact that assumptions in the theory from which they have been derived are far from fulfilled. For example, in many regions where overtides are important, such as some rivers and estuaries, the tidal wave has more nearly the form of a standing wave than that of a progressive wave, but the theory for standing shallow-water waves of finite height has not been adequately developed. Also, the nonlinear effects caused by one constituent cannot, strictly speaking, be superimposed on those caused by another.

The nonlinear interaction between two or more primary constituents can be accounted for by the inclusion of compound constituents. In the case of two interacting primary constituents having speeds σ_1, and σ, a series of compound constituents will result, having speeds $\sigma_1 \pm \sigma_2$, $\sigma_1 \pm 2\sigma_2$, $2\sigma_1 \pm \sigma_2$, etc., including all possible combinations of the form $a\sigma_1 \pm b\sigma_2$, a and b being integers. The relationship of the amplitudes of the compound constituents to those of their primaries has been approximated by assuming that the system responds like a power-law filter; *i.e.*, like a system whose output is equal to a polynomial function of the input. In this way the relative importance of the compound constituents of any given species as well as the dependence of their node factors on those of the primary constituents can be evaluated. No general conclusions can be drawn concerning the relative importance of two compound constituents belonging to different species.

TABLE II.—*Shallow-Water Constituents*

Symbol	Speed	Speed in °/hr.	Node factor
$2SM_2$	$2\gamma+2\sigma-4\eta$	31.016	$[f(M_2)]^2$
MNS_2	$2\gamma-5\sigma+2\eta+\varpi$	27.424	$f(M_2)$
MK_3	$3\gamma-2\sigma$	44.025	$f(M_2)f(K_1)$
MK_3	$3\gamma-4\sigma$	42.927	$[f(M_2)]^2f(K_1)$
M_4	$4\gamma-4\sigma$	57.968	$[f(M_2)]^2$
MS_4	$4\gamma-2\sigma-2\eta$	58.984	$f(M_2)$

Table II includes the more important shallow-water constituents, both overtides and compound constituents. In the table, only two of each of the semidiurnal, terdiurnal and 4-diurnal shallow-water constituents are given for illustration, but there are ports for which many others would be needed to give an accurate representation of the tide. In fact for some ports the number of these constituents that would be needed is so high that the harmonic method becomes impractical. It may be noted that the two terdiurnal constituents listed in Table II are given the same symbol. Actually there is some confusion as to the designation of the compound constituents. The designations given in Table II are based on the nomenclature used by the United States coast and geodetic survey.

V. ACTUAL TIDES IN THE OCEAN

Progressive Tides in Canals.—Let us consider a long narrow canal, open at both ends, along which a tidal wave is progressing. In accordance with the well-known properties of progressive waves, the water particle velocity at the crests of the wave will be in the same direction as that of the propagation of the wave form, while the water particle velocity at the troughs will be in the opposite direction.

Now, the rotation of the earth tends to deflect any particle in motion to the right (in a horizontal plane in the northern hemisphere) relative to the earth with an acceleration proportional to the speed of the particle. This is the so-called Coriolis acceleration that was discussed above. In order to balance this Coriolis acceleration the water surface at the crest must slope upward to the right (in the northern hemisphere), if one is facing in the direction of propagation of the wave. Similarly, the water surface at the trough must slope upward toward the left. Therefore, the crests are higher and the troughs lower along the right coast of the canal, and at any point on the right coast of the canal there will be a higher range of the tide than for a point situated on the left coast.

The above considerations are substantiated by tidal observations in the English channel and Irish sea. The tidal wave progresses eastward through the English channel passing out through the Straits of Dover into the North sea. The tidal range is greater on the French coast (the right side) than on the English coast. In the Irish sea, the tidal wave progresses northward, and the tidal range is greater on the English and Welsh coasts (again the right side) than on the Irish coast.

Tides in Adjacent Seas.—If the region under consideration is small enough the tide within it is influenced predominately by the tide immediately outside the region and not appreciably by the direct action of the tide-generating forces. It is on the water of the great oceans that the gravitational forces of the moon and sun generate the greater part of the tide, while the tides in the small seas bordering the oceans can be considered as free waves.

A great deal of theoretical work has been done on the tides of adjacent seas, but invariably it is necessary to approximate the sea by some simple geometric shape. Nevertheless, many satisfactory explanations of the actual tide in small bodies of water have been obtained.

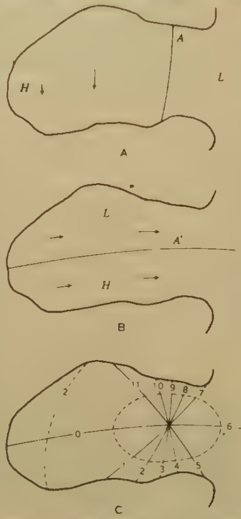

FIG. 2.—MOVEMENT OF THE TIDES IN A GULF. H INDICATES HIGH-WATER LEVEL. L LOW-WATER LEVEL. (SEE TEXT FOR FURTHER EXPLANATION.)

The theory of free long waves states that a tidal wave in a narrow canal of constant depth is propagated with a velocity of $\sqrt{gh}$, the wave length being given by the expression $T\sqrt{gh}$, where g is the acceleration of gravity, h is the water depth and T is the period of the wave (time interval between successive high waters). In the case of the tide, T will have approximately the value of 12 hr. for the semidiurnal tide, or 24 hr. for the diurnal tide.

Let us neglect, for the time being, the effect of the earth's rotation and consider a tidal basin of constant depth having rectangular shape with one end closed and the other end in communication with the ocean. Only motions parallel to the length of the basin will be considered. The tides within the basin are influenced by the boundary conditions (1) that the elevation at the mouth of the basin is at any instant the same as that in the ocean immediately exterior to the basin; and (2) that the horizontal orbital motion at the closed end vanishes. The situation is analogous to the acoustical problem of stationary oscillations within an organ pipe open at one end. The spatial distribution of amplitude of the oscillation is characterized by the positions of nodes, or places where there is no tidal oscillation of the water surface, or no pressure oscillation in the case of the organ pipe, and of antinodes or places where the oscillations attain their maximum amplitude. A standing wave in the pipe has an antinode at the closed end, while one quarter of a wave length away there is a node, and so forth, with nodes and antinodes alternating along the length of the pipe with a quarter of a wave length between them. If the open end is at or near a node the oscillation within the pipe attains a magnitude much greater than that outside the mouth of the pipe, and resonance is said to occur. Thus, in the case of the rectangular tidal basin, resonance would occur if the length L of the basin had any of the values

$$\tfrac{1}{4}T\sqrt{gh},\ \tfrac{3}{4}T\sqrt{gh},\ \tfrac{5}{4}T\sqrt{gh},\ \text{etc.}$$

Or, for a given length, resonance would occur if the period of oscillation had any of the values

$$\frac{4L}{\sqrt{gh}},\ \frac{4L}{3\sqrt{gh}},\ \frac{4L}{5\sqrt{gh}},\ \text{etc.}$$

but in actual practice the successive values have diminishing importance and usually only the first one, corresponding to a quarter wave-length basin, is considered. This is called the gravest free mode.

If the basin is less than a quarter of a wave length long, the entire basin oscillates with the same phase. If the length of the basin is between a quarter wave length and a half wave length, there is one nodal line and the oscillation at the head of the basin is 180° out of phase with that at the mouth. Every node line represents a phase change of 180°.

The Bay of Fundy on the east coast of North America has the greatest tidal range of any place on earth, and this fact is attributed to a resonance phenomenon based on the foregoing considerations. The shape of the Bay of Fundy is reasonably well approximated by a rectangular basin having a length of 170 mi. and a depth of 240 ft. The above relationships indicate that such a basin would have a resonance period of approximately 11½ hr., which is very close to that of the semidiurnal tide. It should therefore be expected that the semidiurnal tide would be greatly magnified relative to the diurnal, and this is found to be the case. At certain places at the head of the bay the spring tide attains a range of 50 ft.

Elongated seas of variable depth and cross-sectional area also can be studied mathematically provided these quantities vary slowly enough along the length of the sea. Good agreement between theory and observation has been obtained for tides in the Gulf of California, the Red sea and other adjacent seas. The Gulf of California is computed to have a resonance period of approximately 25 hr., roughly that of the diurnal tide. The tide at the head of the gulf near the mouth of the Colorado river has been observed to be predominantly diurnal in character with a maximum range of approximately 20 ft. The computed variation of amplitude and phase of the M_2 constituent in the Red sea is in good agreement with the observed variation, and both theory and observations indicate the presence of a nodal line close to Port Sudan, near the mid-point of the sea's length.

To consider geostrophic effects (*i.e.*, those resulting from the earth's rotation) it is necessary to take into account the Coriolis acceleration. Consider a standing oscillation in a gulf as shown in fig. 2A at the instant of high water at the head of the gulf. The curve A has been drawn through all points where the deviation of the water level from its mean is zero at this instant. One quarter period later the water is flowing out of the gulf. At this instant, in the absence of the Coriolis force, the elevation everywhere within the gulf would have its mean value (except for a small frictional effect), and the curve A would represent a nodal line. Actually, the elevation will be higher to the right of the outward flowing current, as is shown in fig. 2B, with the curve A' lying along points whose elevation is at the mean level. Continuity considerations show that there must have been currents flowing at the instant of high water within the gulf in order to produce the distribution of water level shown in fig. 2B. Possible directions for these currents are shown in fig. 2A.

At the intersection of the curves A and A' there will be no rise and fall of sea level, and such a point is known as an amphidromic point. Let it be assumed that the constituent under consideration is a semidiurnal one, and divide its period into 12 equal time intervals called constituent hours, and let the zero constituent hour

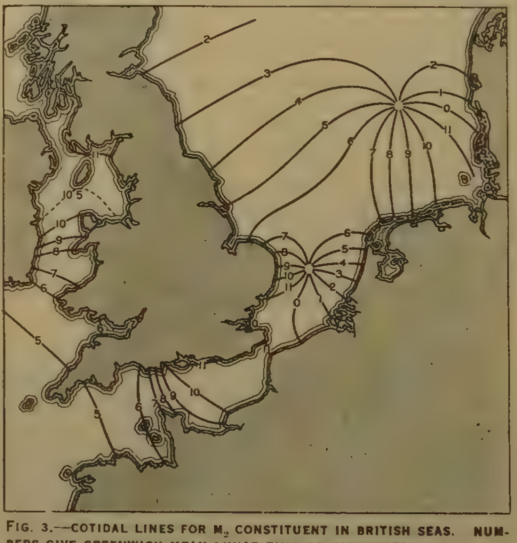

FIG. 3.—COTIDAL LINES FOR M_2 CONSTITUENT IN BRITISH SEAS. NUMBERS GIVE GREENWICH MEAN LUNAR TIME OF HIGH WATER

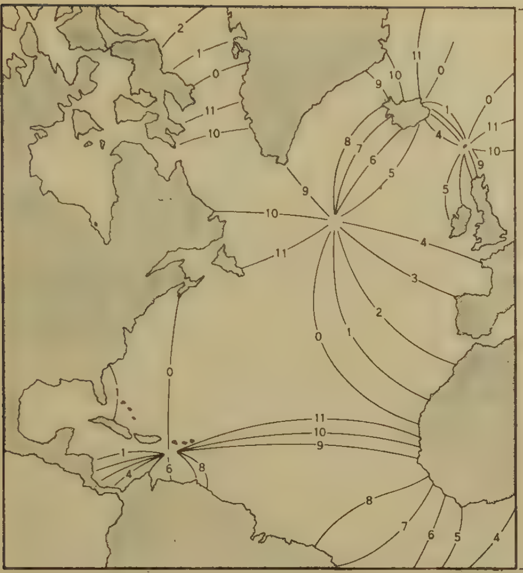

FROM A. T. DOODSON AND H. D. WARBURG. "ADMIRALTY MANUAL OF TIDES"; REPRODUCED BY PERMISSION OF THE CONTROLLER, HER BRITANNIC MAJESTY'S STATIONERY OFFICE

FIG. 4.—COTIDAL CHART OF THE ATLANTIC OCEAN

correspond to the instant of high water within the gulf as depicted by fig. 2A. Fig. 2C then gives the curves along which high water occurs for each of the 12 constituent hours. Such curves are called cotidal lines. The hypothetical distribution of range of tide is indicated by the dashed curves, called corange lines, each of which connects points having equal range of tide. The amphidromic point, at which the tidal range is zero, lies in the centre of the concentric family of corange lines. The cotidal lines indicate the position of the crest of the tidal wave at any instant, and it is seen that this crest rotates in counterclockwise fashion (in the northern hemisphere) about the amphidromic point. Such amphidromic systems with counterclockwise movement of the tidal crest are characteristic also of the oceans and adjacent (large) bodies of water.

Geographical Distribution of the Ocean Tide.—Cotidal maps, such as the one described above, are useful in illustrating the distribution of tidal elevation in a body of water, but it should be kept in mind that such charts are, strictly speaking, useful only in describing a single harmonic constituent. In theory it would be necessary to have one complete cotidal map of the world's oceans for each and every tidal constituent in order to characterize completely the form of the tidal wave, or the rise and fall of water at every point in the ocean. The only constituent for which such charts have been prepared, to any extent, has been the M_2 constituent, which is somewhat representative of the other semidiurnal constituents.

Except along the boundaries of the oceans the tidal elevations are extremely difficult to measure, and what meagre knowledge we have of the geographic distribution of the tide in the whole ocean has been deduced principally by extrapolating from coastal tide stations and, where possible, making use of tidal current measurements. The equations of motion connect the tidal currents with the elevation gradients and external forces, including those of friction, and so from a knowledge of the currents and a law for the frictional forces the elevation gradients can be calculated. When the elevation is also known at a particular point, the directions of the cotidal and corange lines and also the distance apart of neighbouring members of these families of lines can be calculated. Such conditions are fulfilled for many coasts. If the elevation gradients can be calculated along a line which passes through one or more points at which the elevation is known, it is clear that the elevation can be calculated all along the line. In this way the semidiurnal (M_2) tide over the North and Irish seas was determined by Proudman and Doodson in 1923 (*see* fig. 3).

Cotidal charts for the M_2 constituent have been prepared for the oceans but they are uncertain, however, especially at large distances from the coasts and islands where tide gauge observations have been made. Tidal current determinations are rarely made in the open ocean. Another difficulty is that tide gauges are frequently located in sheltered bays or atoll lagoons where the time of high water may be delayed by as much as several hours. The cotidal chart of the Atlantic ocean shown in fig. 4 was prepared by Sterneck in 1920.

Mathematical solutions for the tide in ocean basins of simplified shapes have been obtained. Laplace in 1776 studied the dynamical problem of the semidiurnal tide in an ocean covering the entire earth and having constant depth. His solution takes into account the inertia of the water and the rotation of the earth. Some interesting aspects of this solution are summarized in Table III.

TABLE III.—*Laplace's Solution of the Dynamical Problem of the Semidiurnal Tide*

Depth (fathoms)	Ratio of elevation to equilibrium elevation at equator	Depth (fathoms)	Ratio of elevation to equilibrium elevation at equator
1,210	−7.4	4,840	11.3
2,420	−1.8	9,680	1.9

Positive values in the second column indicate that the tide at the equator is direct—that is, that high water occurs simultaneously with high water of the equilibrium tide. Negative values indicate that the tide is inverted, or 180° out of phase with the equilibrium tide. For the diurnal tide Laplace obtained the curious result that there is no tidal oscillation of elevation on this worldwide ocean of constant depth, although there are tidal currents.

Several solutions have been obtained for the special case of an ocean of constant depth bounded by two meridians. The result of one of the solutions obtained by Proudman and Doodson is shown in fig. 5, which represents a cotidal chart of the K_2 tide in an ocean of depth 14,520 ft. bounded by meridians 70° apart. The K_2 tide was selected because of mathematical simplifications, but the M_2 tide should be quite similar. Comparison of fig. 5 representing a mathematical solution with fig. 4 derived from observations discloses no striking similarities except for the general occurrence of amphidromic systems.

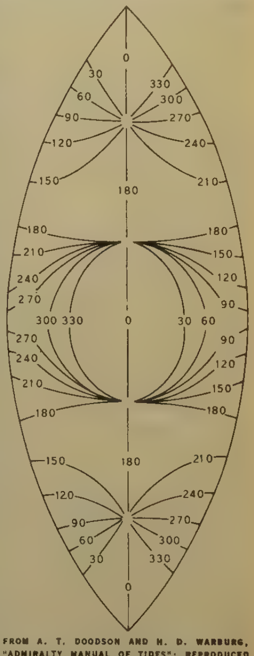

FROM A. T. DOODSON AND H. D. WARBURG, "ADMIRALTY MANUAL OF TIDES"; REPRODUCED BY PERMISSION OF THE CONTROLLER, HER BRITANNIC MAJESTY'S STATIONERY OFFICE

FIG. 5.—COTIDAL CHART OF A HYPOTHETICAL OCEAN OF CONSTANT DEPTH BOUNDED BY MERIDIANS SEPARATED BY 70°

Tides in Lakes.—If all natural periods of oscillation of a completely enclosed basin are short as compared to those of the tidal constituents, the tide should be approximately at equilibrium with the tide-generating forces at all times. According to the theory of long-standing waves in a rectangular basin of constant depth, the length of the basin is equal to one-half wave length of its gravest free mode. The period of the gravest mode is given by the expression $2L/\sqrt{gh}$ where L is the length of the basin. For example, the gravest mode of a lake 20 km. long having constant depth of 40 m. will have a period of approximately ½ hr. according to the above formula, and the tide in such a lake would therefore be determined with quite sufficient accuracy by static principles.

If the above condition is fulfilled the slope of the lake's surface is equal, at any instant, to the slope of the equilibrium tide at that location, and the actual tidal elevation at any point within the lake is determined by the condition that the total volume of water remain constant. The tide will usually differ considerably from the equilibrium tide according to these conditions, generally being considerably smaller in amplitude. For example, the maximum slope of the equilibrium tide is of the order of a metre in one-fourth the earth's circumference, 10,000 km., giving a value of 10^{-7}. For a lake whose length is 10 km. the maximum difference of elevation between its extremes will be of the order of 10 x 10^{-7} km. or 1 mm. The tide in small lakes is thus seen to be extremely small, and is usually overshadowed by other effects such as a variable amount of water volume related to variable runoff and evaporation, wind effects, seiches, etc.

There is no variation of tidal elevation at the centroid of the lake's surface area. If the gravest free oscillation of the lake approaches that of the semidiurnal tide, then of course the above concepts no longer are true, and a dynamical treatment of the problem is necessary. This elementary discussion has also omitted two other important effects: the yielding of the lake's bottom with the tidal deformation of the earth's body, and the potential of the tidally displaced matter of the earth (*see* section X).

VI. TIDAL ANALYSIS AND PREDICTION

Tidal Observations.—Probably the greatest achievement of tidal study is that it has been made possible to predict to a fair degree of accuracy what the sea level would be at any desired time for a great number of ports. The method used is essentially the following: The constants in the harmonic development of the tide at any place are determined by analysis of a long series of observations at that place. Knowing the values of these constants, it is possible to reconstruct or synthesize the tide for any past, present or future time. This is the harmonic method, and it can be applied to any observable tidal quantity which depends linearly on the tide-generating forces, such as the north or east components of the tidal current (not the speed or the direction of the current), the tidal variations of gravity or atmospheric pressure, etc.

The theoretical problem of the tide in the oceans has not been solved, and knowledge of the tide at any place depends on some observations having been made at the place. The prediction process may be loosely considered as one of extrapolation of the observations. It is possible that at some future time tidal theory will have been advanced sufficiently that full knowledge of the tide at a given place may be obtained theoretically without the need of previous observations at the place.

Observation of the variable elevation of the sea surface is carried out by means of an instrument called a tide gauge, which usually consists of a float and pulley system so arranged that the height of the float determines the position of a recording pen on a moving chart. The chart is made to move at constant speed by means of a clock mechanism, so that in the result one obtains a graph of the height of sea level as a function of time. Such a graph is called a marigram.

The float is usually suspended within a vertical pipe or well having a small orifice at the bottom in order that the float not be subjected to rapid erratic motions by the ocean waves. A pier piling is an ideal structure on which to fasten the tide well. The diameter of the orifice and the inner cross-sectional area of the tide well determine the frequency response of the gauge. The orifice must be small enough to insure that the ordinary high-frequency ocean waves have greatly reduced amplitude within the well, but large enough so that no appreciable lag be introduced in case of the tide. The frequency response of the tide gauge is usually arranged so that fluctuations of water level taking place over five minutes or longer are quite faithfully reproduced on the marigram, so that the gauge may be useful in recording tsunamis (seismic sea waves) and other such phenomena. The gauge is periodically levelled in with a series of bench marks located nearby on the land in order to compensate for any long-period changes in the height of the gauge as a whole that might be brought about by slow sinking of the pier on which it is fastened, etc. In this way the gauge is useful for studying extremely long-period phenomena such as the year to year variation of mean sea level.

After the marigram is obtained, the usual procedure is to read off at hourly intervals the height of sea level, and to correct these hourly tidal heights for any variation of datum that may have occurred. Vast quantities of these hourly tidal heights for many seaports are on file at the world's principal tidal agencies.

Analysis of Observations.—If a long enough series of observations has been obtained from a locality, it is possible to determine the harmonic constants for each important tidal constituent with good accuracy. The procedure for finding the harmonic constants for any one constituent will be illustrated in the case of the principal solar series, S_1, S_2, S_4, whose periods are exactly 24, 12 and 6 hr. At instants of time separated by 24 hr. each constituent of this series will have the same value. Let us assume that we have a whole year of data. If we take the average of the 365 hourly tidal heights corresponding to the zero hour of each day, the resulting value will be practically free from the effects of all the other constituents whose periods are not submultiples of 24 hr., because their phases will differ from the zero hour of one day to the zero hour of the next day. Such a constituent will sometimes have positive values on the zero hour, and another day it will have a negative value, and on the average its value will be close to zero. The constituents of the principal solar series, on the other hand, will have the same value, on the average of all the zero hours, as for the zero hour of any given day. This averaging is repeated for each of the 24 hr. of the day and in the result one obtains a complete daily cycle of the combined effect of the constituents S_1, S_2, S_4 practically free of the effects of the other constituents. The amplitudes and epochs of each of the constituents of this series can now be found by the well-known methods of harmonic analysis.

For constituents other than those of the principal solar series the averaging must be carried out in similar fashion but based on the fundamental period of the constituent under consideration instead of 24 hr. Here there is a slight complication if the data are tabulated in the form of hourly tidal heights, as the times for which the tidal values are needed do not coincide exactly with the times at which the values are tabulated. In this case it is customary to use the tabulated value in closest proximity to the time for which the value is actually needed, and it is seen that the error in time will never exceed 30 min. The small error incurred in this process can be corrected by applying an augmenting factor.

If the series of observations is short it is not possible to separate completely any given constituent from the disturbing effects of the others. However, the harmonic constants of all the constituents can be determined approximately, using the above technique, and a first order correction can then be applied. This process is called elimination.

Inference of Harmonic Constants.—It is impractical to use the method discussed above for a constituent whose amplitude is small as compared to possible errors arising from various sources. The harmonic constants of such a constituent are usually inferred from those of one of the major constituents having approximately the same period. Such inference is based on the supposition that the ocean's response to a periodic tide-generating force varies continuously and relatively slowly with the period of the force. Hence it is assumed that two equilibrium constituents whose periods are nearly equal will cause tidal constituents in the ocean at any given locality, whose amplitudes are proportional to those of the equilibrium constituents causing them.

It is best to infer harmonic constants of a given constituent X from those of one of the most important constituents whose period is as close as possible to that of X. Suppose that the constituent M_2 meets these requirements. If H represents the actual amplitude of the constituents and c their constituent coefficients (which are proportional to the amplitudes of the equilibrium constituents), the relationship

$$\frac{H\ (X)}{c\ (X)}=\frac{H\ (M_2)}{c\ (M_2)}$$

is used to relate the amplitudes of X and M_2. The epochs (intervals by which the oceanic constituents lag behind their equilibrium counterparts) can be set equal, to a first approximation, while a more refined method of estimating the epoch of constituent X is given in *Special Publication 98*, U.S. coast and geodetic survey. The constituent coefficients have been precisely determined from astronomic observations, and if the amplitude and epoch of M_2 have been determined from tidal observations, the amplitude and epoch of X can be calculated from the above relationships. The validity of the above relations can be checked by also evaluating the constants of X by conventional means, and it is usually found that the inference method gives fair results if the periods of the two constituents are nearly enough to being equal. It should be emphasized that the inference method can never be used to relate the constants of constituents belonging to different species.

Prediction: Tide Tables.—For many purposes it is of great importance to know in advance the times and heights of high water at a particular place on a particular day. Consequently governments and harbour authorities publish, a year or so in advance, tables giving such information for all the principal ports of the world. In a few cases tables are similarly published giving the height of water above some datum at every hour of the year, while for a certain number of navigable channels tables of the times of slack water are also issued.

The standard method of tidal prediction is the harmonic method based on the idea of harmonic constituents, and the necessary information for any particular place is provided by the process of analysis discussed above. The only theoretical results which are utilized in tidal prediction are (1) the decomposition of the entire tide-generating force as the sum of a number of harmonic equilibrium constituents; and (2) the linearity of the ocean tide. Thus, the periods of the constituents are obtained from the observed motions of earth, moon and sun, while their amplitudes and epochs are obtained from tidal observation: tidal prediction is largely an empirical science.

The process of harmonic prediction consists of the calculation of the value of each harmonic constituent for a given time, and then the addition of the values obtained for all the constituents. When this is done for every hour of a year, the computational task becomes enormous, and to obviate this special computing machines, called tide-predicting machines, have been constructed. Those in use at mid-20th century were of the analogue type and usually consisted of a series of gears or pulleys by which means the analogue addition of the constituents could be carried out. The amplitude and epoch of each constituent could be adjusted into the machine so that it could be used for any location and for any tidal quantity.

Of course, only that part of the rise and fall of the sea surface related to astronomical quantities can be predicted, and hence any individual prediction is liable to differ considerably from the actual occurrence, as will be seen below.

VII. NONASTRONOMICAL VARIATIONS OF SEA LEVEL

"Geologic" Tides.—Any change in shape of the ocean basins or in the total quantity of water in them can bring about changes of level at a given locality. Another effect, however, is to change the dynamical response of the oceans to the tide-generating forces, and we should consequently expect the tidal harmonic "constants" to change.

The geological change in sea level is quite slow as compared to that effected by the moon and sun, and is manifested by a small year to year variation in mean annual sea level. There is evidence that the average sea level over the entire earth rose by the order of 10 cm. from 1850 to 1950. This has been related to a shrinking of the ice caps of the world, particularly those over Antarctica and Greenland. About 1000 B.C., during the postglacial temperature maximum, sea level probably stood about 5 m. above its present level. At the present time there are localities where the average annual sea level is rising and others where it is falling, and this is attributed to a relative downward or upward motion of the land area in the vicinity. The horizontal extent over which these year to year sea level records appear similar gives a good indication as to the size of the portions of the earth's crust that are sinking and rising. Actually, the similarity extends over many hundreds of kilometres, indicating that masses somewhat smaller than continents are moving as a whole.

Variation of the tidal harmonic "constants" by the processes just described is probably a slow process, and it may be doubted that a detectable change would occur within tens of thousands of years. At locations where the tidal constants depend critically on the local, small-scale topography, however, this is not the case. For example, the tide up a river may depend critically on the conditions of the channel at the river's mouth. At many ports the tide has changed noticeably after the construction of port facilities, such as breakwaters, etc. In such cases the altered regime of sedimentation and erosion of sand usually plays an important part. Also, sand bars can form and disappear quite rapidly, and a semienclosed lagoon behind such a condition would experience variable tidal "constants."

Meteorologic Tides.—The principal meteorologic effects can be ascribed directly or indirectly to variations in atmospheric pressure on the sea surface, tangential stress on the sea surface exerted by the wind, heating and cooling of the sea water.

A varying atmospheric pressure acting on the oceans has the characteristic of a body force, as the pressure gradients are transmitted through the water practically simultaneously from the sea surface to the bottom. For this reason, the dynamical problem is formally equivalent to that concerned with the effect of the tide-generating forces on the oceans, and equations (1) and (2) are still valid provided that $\bar{\zeta}$ is replaced by $-p_a/\rho g$, p_a being the atmospheric pressure and ρ the water density.

Under certain circumstances the dynamical response of the ocean to the atmospheric pressure disturbance can become large. If a tidal basin is subjected to a variable atmospheric pressure disturbance acting periodically with a frequency near that of one of the free modes of oscillation of the basin, the amplitude of its response will tend to increase until it is ultimately limited by frictional dissipation. The same is true in the case of a pressure disturbance travelling across the sea surface with the that the depth of the open ocean is so great that storms seldom attain same velocity as that of a long free wave, or $\sqrt{gh}$. It may be noted this critical velocity, and so such magnifying effects are more often encountered in shallow seas.

For a longer-period fluctuation the dynamical effects are less important, and under these conditions the ocean's response is similar to that of an inverted barometer. The sea surface is depressed approximately a centimetre for each millibar of pressure increase, and vice versa, according to the hydrostatic law

$$\zeta = -\frac{p_a}{\rho g}.$$

Pressure changes of 20 millibars occurring in a few days are common at many ports, and so it may be seen that this effect could be one of the principal sources of error in tidal predictions.

Wind blowing across the water surface exerts a horizontal stress on the water directed downwind, largely by virtue of the difference in air pressure on the lee and windward sides of the water waves generated by the same wind. An exact law for this stress as a function of wind speed has not yet been discovered, but the semiempirical relationship

$$\tau = \gamma \rho_a v^2$$

gives a good approximation. Here τ is the wind stress, ρ_a the density of air, v the wind speed at an elevation of 15 m. above the water surface and γ is a numerical constant for which the value .0026 gives the best fit to the empirical data.

Wind stress on the sea surface directed toward the coast has the effect of piling up water against the coast, raising the sea level. Longshore winds blowing so that the land lies to the right relative to the wind direction also tend to raise the sea level against the shore (in the northern hemisphere), owing to the effect of the earth's rotation. There are dynamic effects to be considered in both these cases as the wind is seldom so steady that static equilibrium is reached, except in small basins whose period of free oscillation is quite short.

The effect of the wind stress is enhanced by shoal water for the following reason, based on static considerations. Let us consider the balance of forces in one dimension only, say, the east-west direction. The stress caused by a west wind (blowing eastward) must be balanced by a slope of the sea surface in which its elevation increases eastward. The horizontal pressure gradient associated with this surface slope is essentially constant with depth, so that the greater the water depth the greater is the total force exerted on a vertical water column. Therefore a given surface slope will require greater wind stress to balance it in deeper water than in the shallower water.

Meteorologic disturbances over shallow seas have given rise to disastrous storm surges, such as those that frequently inundate the coasts of the North sea and the Gulf of Mexico. These surges frequently have a roughly periodic character with periods of the order of hours, and under severe conditions their amplitude can attain several metres. The horizontal stress on the water surface due to the wind is usually more important in these surges than the normal force due to the atmospheric pressure disturbance. Such variations of sea level cannot be predicted by the same procedures used to predict the astronomic tide, but considerable success has been obtained in understanding the dynamics of these phenomena, and in a few cases fairly accurate predictions have been made, particularly in the North sea area by a method developed by R. H. Corkan and Proudman. In order to make such a prediction the wind and pressure fields must be known (or estimated with sufficient accuracy) over the water surface of the region and for all necessary instants of time preceding the hour to be predicted.

Variations of water density, caused either by local heating and cooling or by advection of water of different properties, give rise to variations in elevation of the sea surface. If the change in surface level is calculated on the basis that the total water mass in a vertical column remains constant, the hydrostatic law shows that the relative height of the surface is

$$\zeta_s = -\frac{1}{g}\int_{p_s}^{p_b} \alpha\, dp$$

where α is the specific volume of the water, and p_b is the bottom pressure. The quantity ζ_s has been called the steric height, and is quite closely related to the dynamic height used in dynamical oceanography. Changes of the order of 10 cm. taking place from one month to the next are common in the ocean. In the seasonal variation of sea level the changes of density of the water are much more important than the long-period tidal constituents.

VIII. MISCELLANEOUS TIDAL PROBLEMS

Tidal Friction.—The effect of dissipation of the ocean tide by friction has so far been left out of the discussion, but it is known to be an important factor. Harold Jeffreys has calculated that if the tide-generating forces of the moon and sun could be suddenly turned off, half the tidal energy in the earth's oceans would be dissipated in approximately a day. This dissipation is known to occur practically entirely by the friction of tidal currents against the bottom of a few shallow seas of the earth, and against the long shorelines of the continents and islands. It is a curious fact that probably half of the entire tidal dissipation of energy in the ocean takes place in the shallow Bering sea. This rapid rate of energy dissipation should have a considerable effect on the tides of the world.

The matter of tidal friction is of considerable importance in the motions of the planets and their satellites because it provides a mechanism whereby angular momentum is transferred from one type of motion to another. The tidal protuberance created on the primary by the tide-generating force of one of its satellites is not symmetrical with respect to the line joining their centres, and the satellite's own gravitational attraction on this protuberance exerts a torque on the primary. It can be shown in general that if there were no tidal dissipation, there would be no such torque, and that if the angular speed of the planet's rotation is faster than that of the revolution of its satellite about it, then this torque always tends to decelerate the planet's rotation. In such a case, the gravitational force of the primary on its satellite deviates slightly from the direction toward the primary's centre of gravity, and tends to accelerate the revolution of the satellite about its primary, provided this revolution has the same sense as the rotation of the primary about its axis. Then, the distance between the primary and its satellite will increase as the satellite's speed of revolution is increased, according to Kepler's laws. The above-stated conditions apply, of course, in the case of the earth-moon system.

The same deductions can be arrived at by an alternative point of view: the frictional force of the tidal currents on the sea bottom and coasts must itself exert a decelerating torque on the earth. If the tidal currents were known accurately enough over all critical regions where the bulk of the tidal dissipation takes place, the decelerating torque could be calculated, since it is known that by far the greater part of the tidal dissipation occurs in the oceans and only a negligible amount in the lithosphere. Actually, the form of the tide over the vast regions of the oceans is so poorly known that neither the gravitational torque method nor the frictional torque method can be applied quantitatively, and it is through records of ancient eclipses and modern observations on the moon's position that the average rate of lengthening of the day and lunar period of revolution has been estimated. It should be remarked that the lunar effect on the earth's rotation should be about three to five times as large as the solar effect.

There are four principal effects: (1) tides raised in the satellites by their primaries will tend to make each keep the same face toward its primary (as the moon presently faces the earth); (2) tides raised in the primaries by the satellites will alter the rates of rotation of the primaries; (3) tides raised in the primaries by the satellites will alter the distances between them; and (4) solar tides will affect all the rotations.

On the basis of the above considerations it has been deduced that during previous ages the earth had a much shorter day and much shorter month (period of lunar revolution), and that the moon was much closer to earth. The day has probably lengthened by a second in the last 120,000 years.

Internal Tides in the Ocean.—It has been shown that the tidal current would be uniform from top to bottom at any given locality and instant provided that the sea water had uniform density throughout the oceans. In the actual case, however, variations in the salinity and temperature lead to both time and space variations in the density, and it is possible that this condition would lead to a vertical shear in the tidal current. In any case, there is no reason to believe that there should not exist tidal variations in the water density at any given point in the ocean, and there is evidence on several occasions that such tidal variations may have been actually observed.

The outstanding feature of the density structure of the ocean is that the lighter water is found in the upper layers of the ocean, and in a large number of dynamical problems the ocean can be treated successfully as though the water were stratified; *i.e.*, as though the water in any horizontal plane were homogenous. In such a situation there can exist an important class of wave motions in which the maximum amplitude of the vertical displacement of the water particles occurs at some depth beneath the surface. These are called internal waves to contrast them with the more familiar surface waves, for which the vertical displacements of the water particles have their maximum amplitude at the surface. Internal waves are similar in many respects to surface waves, but have some important differences: their speed of propagation is much less than that of a surface wave having the same wave length; and the vertical movement of the water particles (at the level of maximum movement) is a great deal larger than in the case of a surface wave having the same energy. Such waves have been observed by making periodical determinations of the vertical density profile from an anchored ship, and the results of such observations indicate that such internal wave motion is common, and that amplitudes of the order of tens of metres are to be expected. The oscillations are irregular, but frequently there appear to be dominant waves of diurnal or semidiurnal period having all the characteristics of a tidal variation. In order to prove conclusively the tidal origin of such waves, a considerable series of observations would be necessary, and the difficulties and expense of having a ship remain at the same location for a protracted period of time have prevented this study from being carried out.

IX. ATMOSPHERIC TIDES

As air, like all other matter, is subject to gravitational influence, there will be tides in the atmosphere possessing many features of similarity with those in the ocean. One of the characteristics of these tides will be a very small oscillatory variation in the atmospheric pressure at any place, and this may be regarded as the superposition of harmonic constituents with the ordinary tidal periods. By the systematic analysis of long series of regular barometric records, the principal lunar semidiurnal constituent M_2 of the barometric variation has been determined for a number of places, and found to have an amplitude of the order of .001 in. The dynamical theory of these tides has been the subject of considerable study. The derivation of the equations is not so simple as for ocean tides, one difficulty being that of taking account of the physical conditions in the upper regions. The equations which have been proposed are of the same general form as those for ocean tides, but the theory is still imperfect. The results of analysis for the S_2 constituent show a much larger oscillation with an amplitude of barometric variation of the order of .03 in. For this constituent, however, it is certain that thermal factors play a larger part than gravitational factors, and the theory is far from complete.

X. BODILY TIDES

The solid body of the earth, or lithosphere, suffers periodic deformation because of the tide-generating forces just as do the oceans and atmosphere. These bodily tides manifest themselves in the following ways: (1) a variation of the vertical, or plumb line, with respect to any solid structure imbedded in the earth's crust; and (2) a variation in the acceleration of gravity at any point due to the potential of the displaced matter in the earth's body, quite aside from the variation of gravity directly associated with the tide-generating forces.

The gravest free elastic oscillations of the earth's body as a whole have periods of the order of an hour, which is much less than those of the principal tide-generating forces. Therefore, it is probably correct to assume that the bodily tides will approximate closely to their equilibrium forms, or in other words, that they may be calculated on the principles of statics. Owing to the earth's rigidity, the vertical rise and fall of the earth's solid surface at any position on it is somewhat less than that based on the equilibrium tide. The fractional height of the equilibrium tide attained by this surface vertical displacement is practically independent of geographical location, and is designated by the symbol h. The potential of the displaced matter is additive to the tide-generating potential, its fractional contribution to the latter at any point on the earth's surface being designated by the symbol k. As in the case of h, k also is practically independent of geographical location. The numbers h and k were introduced by the theoretician in the field of elasticity, A. E. H. Love, and henceforth have been called the Love numbers.

The values of h and k depend on the geographical form of the disturbing potential, but it is common usage to consider only those values corresponding to a disturbing potential having the form of a spherical harmonic of the second degree, of which the semidiurnal equilibrium form is an example.

Various types of geophysical observations have been used to evaluate the Love numbers. For instance, it can be shown that the acceleration of the earth's gravity at the surface is altered by the amount

$$-\frac{2g\bar{\zeta}}{a}\left(1-\frac{3}{2}k+h\right)$$

where $\bar{\zeta}$ is the equilibrium tidal height at the place under consideration and a is the radius of the earth. A body of water whose natural period is short compared with the tidal periods will set itself so that its free surface is one of constant potential. If ζ' is the elevation of the water surface at a given position relative to the bottom, it can be shown that

$$\zeta'-(1+k-h)\bar{\zeta}=\text{const.}$$

provided that the total volume of water in the basin remains constant. The yielding of the bottom tends to diminish the apparent tide while the additional potential of the displaced mass in the earth tends to increase it, hence the algebraic signs in the terms of h and k.

Thus it is seen that precise measurements of the acceleration of the earth's gravity at a point would give a determination of the quantity $1-\frac{3}{2}k+h$ while measurements of the water level in a long sheltered tube, free from winds and other disturbances would give a determination of the quantity $1+k-h$. This quantity also determines the position of the vertical as can be measured by a plumb line or a special instrument called the horizontal pendulum.

It should also be possible to determine the quantity $1+k-h$ by means of observations of the ordinary ocean tide, provided its dynamics were well understood. The long-period tides, especially the lunar fortnightly tide *Mf*, have usually been utilized for this purpose. It is generally assumed that the periods of these constituents are very much longer than those of all natural oscillations in the ocean basins, and that the equilibrium law would therefore hold. This assumption is certainly valid in the case of ordinary inertio-gravitational standing wave motion in the oceans, but serious objections have been raised on the basis of the possible existence of geostrophic or planetary wave modes characterized by steady or nearly steady ocean currents. There is a further serious difficulty in isolating the purely astronomical long-period constituents in analysis, and it may well be doubted whether reliable constants for the *Mf* constituent have ever yet been obtained from the records of observation. The values of h and k determined vary considerably depending on the type of observation used, and for this reason are subject to appreciable error. The value of h is somewhere in the vicinity of 0.6, that of k is near 0.3.

The above discussion of the bodily tide has omitted any reference to the complications introduced by the tides in the ocean. There are two effects: the warping of the earth's crust by the varying load on the ocean floor; and the contribution to the total gravitational potential by the displaced water mass. Generally, these effects are more serious closer to the coast and the greater the tidal range at the coast nearby. For this reason measurements of the bodily tide are usually attempted near the centre of large continents.

If the rigidity and density at all points in the earth's body were exactly known, it should be possible to calculate the Love numbers theoretically without need for recourse to observations. The internal constitution of the earth is not precisely known, but certain hypotheses concerning this internal constitution can be rejected on the basis of results of bodily tide observations. Lord Kelvin used the observed height of the fortnightly tide to show that the earth's rigidity, on the average, is greater than that of steel.

Bibliography.—P. Schureman, "A Manual of the Harmonic Analysis and Prediction of Tides," U.S. Coast and Geodetic Survey, *Special Publication 98* (Washington, D.C., 1941); A. T. Doodson and H. D. Warburg, *Admiralty Manual of Tides* (H.M.S.O., 1941); Sir Horace Lamb, *Hydrodynamics* (New York, London, 1945); Harald U. Sverdrup, *et al., The Oceans* (New York, 1942; London, 1944); Sir Harold Jeffreys, *The Earth* (London, New York, 1952); J. Proudman, *Dynamical Oceanography* (New York, London, 1953).

(J. Pr.; G. W. Gs.)

Shore-Based Recorder of Low-Frequency Ocean Waves*

FRANK E. SNODGRASS

Abstract—A pressure head on the sea bottom contains a hydraulic filter which attenuates high-frequency signals caused by ordinary gravity waves, and low-frequency signals caused by tides. Maximum response is for frequencies at about one cycle per 1000 sec. A strain-gage transducer converts the filtered pressure fluctuations into electrical signals, which are transmitted to shore through a cable.

Introduction—The instrument described in this paper was designed for the study of ocean waves whose frequency lies between those of the ordinary waves and those of the tides. Such low-frequency waves fall into two categories: (1) a low-frequency noise, which is always present and appears to be associated with meteorologic factors, and (2) tsunami waves, which arrive every year or two and are associated with earthquakes under the sea floor.

The existence of such low-frequency waves has long been known from ordinary tide-gage records, but these are not well adapted to record them, particularly the low-amplitude noise. In 1948 a pier-mounted gage with a three-stage hydraulic filter [*Munk*, *Iglesias* and *Folsom*, 1948] was installed at the end of Scripps Pier for the particular purpose of studying these waves. In 1952 a second instrument was installed at Oceanside Pier, 24 mi north of the Scripps instrument and connected to it by radio link. Subsequently a portable instrument for operation on remote islands was developed [*Van Dorn*, 1956] which employed a shore-based hydraulic filter connected to the sea by a tube or pipe. An instrument for offshore measurements from shipboard which employs a Vibrotron transducer and digital recording is discussed by *Snodgrass*, *Munk*, and *Tucker* [1958].

Description—Sea pressure is transmitted through a rubber bellows (Fig. 1 and 2). Two capillaries, R_1 and R_2, lead to two domes with metal bellows, C_1 and C_2. The rubber bellows, capillary tubing, and the compliant chambers between the dome and the outside of the metal bellows are filled with silicone fluid. The inside of the bellows and of the transducer chamber is filled with air maintained at atmospheric pressure. The total air reservoir is large relative to the bellows, and the variation in air pressure due to the deflection of the bellows is negligible compared to the changes in outside pressure. The transducer chamber and the inside of the bellows can be pressurized to extend the depth of installation, which is otherwise limited by the bellows to 10 m (one bar).

Two identical bellows are used in the compliant chambers, but the capillary tubes are adjusted so that their resistances to the flow of hydraulic fluid have a ratio of about four to one. A strain-gage pressure transducer is connected between the two compliant chambers to sense the differences in pressure. Because of the flow resistance of the capillary tubing, pressure fluctuations of very high frequency (ordinary waves) cause negligible pressure changes within the compliant chambers and between them. For pressure fluctuations of very low frequency (tides) the pressure in each chamber essentially equals the applied pressure, and the pressure difference between the chambers is again negligible. For intermediate frequencies the pressure in the two chambers is unequal owing to the difference in resistance of the capillary tubes, and an appreciable signal will be produced by the transducer.

Response characteristics—The equivalent electrical circuit of the pressure head is shown in Figure 2. Any arrangement of two resistors and two condensers to produce a band pass filter has a complex voltage attenuation of

$$e_0/e_i = A/(1 + jB) \tag{1}$$

For the particular arrangements shown in Figure 2, the constants have the values

$$A = (\beta - 1)/(\beta + 1) \tag{2}$$

$$B = \beta^{\frac{1}{2}}\ (k - 1/k)/(\beta + 1) \tag{3}$$

where

$$\beta = t_2/t_1 = R_2C_2/R_1C_1\,, \qquad t_2 > t_1 \tag{4}$$

$$k = f/f_0\,, \qquad f_0 = 1/2\pi\sqrt{t_1t_2} \tag{5}$$

t_1 and t_2 are the time constants associated with the circuit, f is the frequency of the applied signal, and

---

* Contribution from the Scripps Institution of Oceanography, New Series No. 977.

Reproduced by Permission

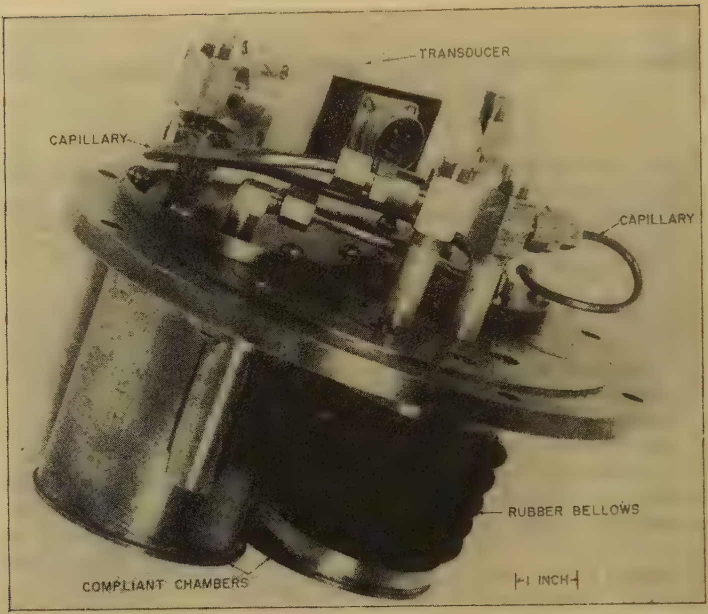

FIG. 1 – The pressure head assembly removed from its pressure case

f_0 is the center frequency of the filter. Thus the frequency response characteristics of this filter are described completely if the two time constants are known.

For a unit harmonic input, $\cos 2\pi ft$, the output can be written $r\cos(2\pi ft + \theta)$ where

$$r = \text{real part} \quad A/(1 + jB) = A\cos\theta,$$

$$\tan\theta = B \qquad (6)$$

At the center frequency $k = 1$, $r = A$ and $\theta = 0$ (the output is in phase with the input). The half power points of the filter are at a frequency such that

$$k = (1/2\delta)[\sqrt{1 + 4\delta^2} \pm 1], \qquad \delta = \beta^{\frac{1}{2}}/(\beta + 1) \qquad (7)$$

The asymptotic behaviors are

$$r = Ak/\delta, \qquad \theta = 90^\circ \qquad \text{for } k \ll 1 \qquad (8)$$

$$r = A/\delta k, \qquad \theta = -90^\circ \qquad \text{for } k \gg 1 \qquad (9)$$

The frequency response curves in Figure 3 indicate results obtained using values of $\beta = 3.5$ and $f_0 = 1.37$ cycles/kilosec (730 sec/cycle). These values centered the filter in the low frequency band being studied and provided good attenuation of the signal produced by ordinary gravity waves and tides.

Calibration of the pressure head—The response of the pressure head is completely and conveniently described in terms of the two time constants, and relatively simple tests can be made to calibrate the pressure head. A step pressure input at time $t = 0$ (by suddenly lowering the pressure head through several inches of water) results in a transient response

$$x(t) = e^{-t/t_2} - e^{-t/t_1} \qquad (10)$$

The time constants t_1 and t_2 can be determined from the measurements of the time t_m and the maximum amplitude x_m of the transient response

$$x_m = \frac{\beta - 1}{\beta}\beta^{-1/(\beta+1)}, \qquad t_m = t_2\frac{\ln\beta}{\beta - 1} \qquad (11)$$

with $\beta = t_2/t_1$. The initial slope of the transient response curve

$$[dx/dt]_{t=0} = 1/t_1 - 1/t_2 = \ln\beta/t_m \qquad (12)$$

can be used as a check.

Temperature effects—The principal temperature effect results from the linear dependence of the time constants, t_1 and t_2, on the viscosity of the oil. Results of calibrations at four temperatures are plotted in Figure 4. These data indicated that within the range of temperatures to which the instrument might be subjected, log t_1 and log t_2 decrease linearly with temperature; accordingly log f_0 increases linearly with temperature. Since both time constants are affected proportionally,

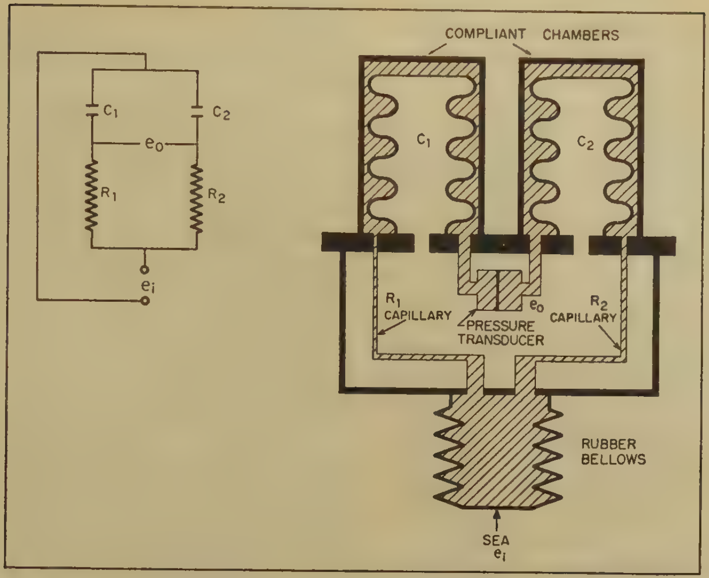

FIG. 2 – Schematic diagram of the hydraulic and equivalent electrical circuits of the pressure head; shaded region is oil-filled; remaining volume is filled with air

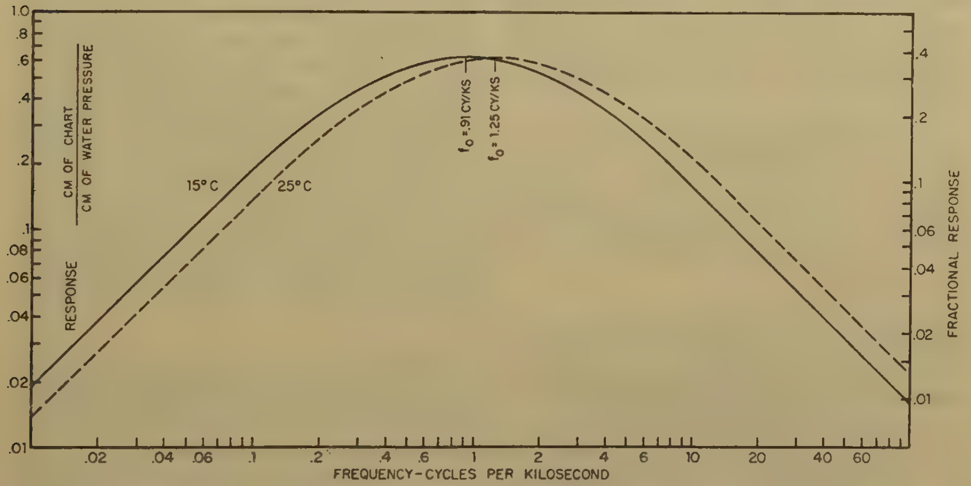

FIG. 3 – Amplitude response of the recorder; the right scale refers to the response r (Eq. 6) of the hydraulic filter; the left scale to the over-all response, including the electric components, which was used in obtaining the record shown on Fig. 5

the ratio of the time constants β is not affected. Thus the response curve (Fig. 3) is translated along the frequency axis. In our work it was necessary to allow for this effect in the interpretation of the instrument output, particularly at the high and low frequencies.

In addition to the problem involving the mean water temperature there are also output signals due to temperature transients. This effect arises on account of the differential expansion between the metal parts of the compliant chamber and the oil contained within these chambers, the oil expanding more rapidly than the metal container.

An estimate of the pressure change in the compliant chamber Δp due to a sudden temperature change ΔT is $\Delta p = \frac{\alpha V \Delta T}{C}$ where α is the coefficient of expansion of the oil, V the oil volume, and C the bellows spring constant. Setting $V = 100$ cm^3, $\alpha = 1.2 \cdot 10^{-3}/°C$, and $C = 0.036$ cm^3/(cm of water pressure) gives $p = 3.3$ (cm of water pressure)/°C. Laboratory tests indicate that the effect is somewhat smaller.

Since these changes occur simultaneously in both compliant chambers, an increase in water temperature by 1°C produces a signal which is indistinguishable from a corresponding decrease of water pressure of a few centimeters. The pressure head therefore is most sensitive to temperature fluctuations with frequencies near the center of the pressure response curve. In our work it was imperative that the instrument be shielded from temperature fluctuations in the frequency band of interest.

Temperature shielding was accomplished by burying the pressure head in the sand bottom to a depth of about one foot. If the test site did not have a suitable sand area, the pressure head was installed in a box filled with sand; the size of the box was such that a minimum of six inches of sand surrounded the instrument. This insulation assures that fluctuations with frequencies higher than one cycle/hr (0.28 cycles/kilosec) are reduced by at least a factor of 100.

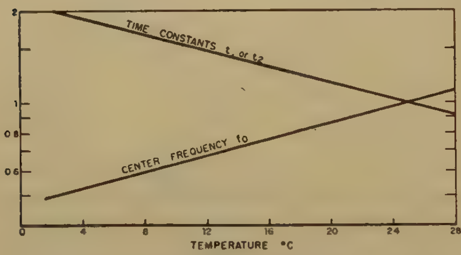

FIG. 4 – The effect of temperature on the time constants t_1, t_2, and on the center frequency f_0 all referred to their values at 25°C

Temperature measurements made with the instrument buried one foot in the sand bottom indicated fluctuations less than 0.01°C for frequencies greater than one cycle/hr, although daily variations of 0.5°C were recorded. The electric power dissipated in the transducer raised the temperature of the pressure head 0.5°C above that of the bottom water.

It follows that temperature signals are very small. Daily variations of temperature and heating by the transducer also have negligible effect on the response characteristics.

Mechanical features—In order that the pressure head can be buried in sand the unit is encased in a brass container and provided with a snorkel. The snorkel, a $\frac{1}{4}$-inch pipe, is shielded by an outer tube so that suspended material in water cannot settle into the instrument. Silicone oil was selected for the hydraulic fluid for the following reasons: (1) the oil is chemically inert and has excellent electrical properties which permit its use in the transducer, (2) the viscosity of the oil varies relatively little with temperature so that the temperature effects on calibration are small, (3) it is available at high viscosities (500 centistokes was used) which permit the use of large diameter capillary tubing and so minimize difficulties due to plugging.

Capillary tubes were made of copper tubing as follows: (1) 15-inch length, $\frac{3}{16}$-inch tubing with 0.125-inch ID, (2) $4\frac{3}{4}$-inch length, $\frac{1}{8}$-inch tubing, 0.062-inch ID. The metal bellows dimensions were: $2\frac{3}{8}$-inch OD, $2\frac{7}{8}$-inch live length, volume change, 2.25 in^3/bar; maximum allowable compression, one bar.

The space between the outside of the bellows and the dome is used as the compliant chamber. The bellows then remain in compression at all

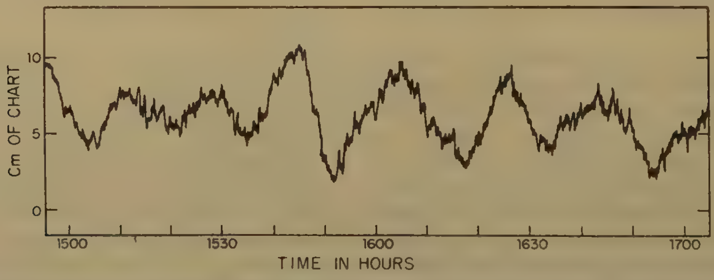

FIG. 5 – Sample wave record; vertical scale is in chart centimeters corresponding to the calibration curve, Fig. 3; the record, which is unusually active, was taken on Feb. 23, 1956, off Camp Pendleton, Oceanside, California

times and provide a nearly uniform spring constant. The arrangement permits the use of a small oil volume, and this in turn reduces temperature signals.

An important design consideration is that no air pockets should remain in the oil-filled portion of the instrument. The gage is filled with hydraulic fluid by removing the four pipe plugs in the hydraulic tubing (see Fig. 1) and connecting a reservoir of oil to these points. The unit then is installed in the brass housing and evacuated with a pump. Air contained in the complaint chamber, transducer, capillaries, etc., is drawn out. When atmospheric pressure is reapplied, the unit fills with oil. Any remaining air bubbles are absorbed by the fluid since most of the air normally in solution has been removed.

Electrical features—The pressure transducer must withstand many meters of water pressure during installation, yet be capable of sensing a millimeter of water pressure after reaching equilibrium on the bottom. A strain-gage transducer rated at 1.0 psi differential can withstand ±10 psi differential; the gage therefore can be lowered suddenly through 13.7 m of water without damage to the transducer. Equipped with a 2000-ohm, 31 v strain-gage element, it has a conversion factor of 0.9 mv/(cm water pressure) over its ±1 psi differential operating range. By connecting the gage output directly to a standard, self-balancing-potentiometer recorder, such as a Speedomax, overall recording sensitivities of the order of one centimeter of chart per centimeter of water pressure are readily obtained. Equivalent sensitivities were obtained without difficulty using d-c amplifiers and recording milliammeters, such as the Esterline-Angus.

Electrical power (30 v at 15 milliamp) was supplied to the gage from an electronically regulated power supply whenever 110-v a c power was available. At remote beach sites the gage was operated from wet cell batteries with a Speedomax recorder being driven by a 28-v d c to 110-v a c, 60-cycle converter. Thirty hours of operation could be obtained from four 6-v automobile batteries. Operating time can be greatly increased by using transistor amplifiers and spring-driven chart recorders.

Four-conductor cable is required for the bridge-type strain-gage transducer, while an additional two conductors are required if a thermistor circuit is used to indicate temperature of the pressure head. Cable lengths of several miles can be used providing leakage resistance between leads and between the cable and earth does not drop below about 0.1 megohm. Below these resistances the shunting effects or voltages generated due to sea water leakage may affect the readings.

Results—Several gages using the design described in this report have been used for three years with good results. Figure 5 shows an unusually active record. Ordinary gravity waves of 12-sec period (80 cycles/kilosec) are recorded with a response factor of 0.02 (chart cm)/(cm water pressure). These waves are responsible for the thickness of the trace. On the original record individual waves can barely be identified. For surf beat in the period band 1 to 4 minutes (4 to 16 cycles/kilosec) the response factor is between about 0.3 and 0.1. Twenty-minute-surges (0.83 cycles/kilosec) have a factor of 0.62. The tide, being reduced to 0.04 of its amplitude, is indicated as a slight drift in the record. The features here indicated can be resolved by a frequency analysis. A discussion will be given in a forthcoming paper.

Acknowledgments—The author wishes to thank Walter Munk for many helpful suggestions and Frank Peterson for his assistance in laboratory and field tests. This paper represents results of research carried out by the University of California under contract with the Office of Naval Research and the Bureau of Ships of the Navy Department.

REFERENCES

MUNK, W. H., H. V. IGLESIAS, AND T. R. FOLSOM, An instrument for recording low-frequency ocean waves, *Rev. Sci. Instr.*, **19**, 654–658, 1948.

SNODGRASS, F., W. MUNK, AND M. J. TUCKER, Offshore recording of low-frequency ocean waves, *Trans. Amer. Geophys. Union*, **39**, 114–120, 1958.

VAN DORN, W. G., A portable tsunami recorder, *Trans. Amer. Geophys. Union*, **37**, 27–30, 1956.

Scripps Institution of Oceanography, La Jolla, California.

(Communicated manuscript received May 27, 1957; open for formal discussion until July 1, 1958).

Offshore Recording of Low-Frequency Ocean Waves*

F. SNODGRASS, W. MUNK, AND M. J. TUCKER

Abstract—A Vibrotron transducer on the sea bottom converts pressure into frequency of a stretched wire. The oscillations are counted and recorded on shipboard in a form suitable for subsequent filtering and spectrum analysis by high speed digital computers. Oscillation by 1 mm of water pressure in the frequency range 0.2 to 100 cycles/kilosec (periods 5000 to 10 sec) have been recorded at depths exceeding 100 m.

Introduction—In the introduction to *Snodgrass* [1958] a brief account is given of the installation of pier-based tsunami recorders along the California Coast. In a sense these shore installations have been a disappointment. Tsunami waves appear to be so well reflected by the continental slope that relatively little wave energy reaches the shore installations. The result is that tsunamis are better recorded by the standard tide gage at Honolulu than by the special instruments along the California Coast.

The instruments did, however, provide interesting information about the day-by-day low-frequency noise, with the suggestion that this noise was in the form of edge waves traveling up and down the continental shelf and borderland. The principal characteristic of edge waves is that their amplitude diminishes rapidly seaward. To test this hypothesis the present instrument was built, and simultaneous measurements were made onshore [see *Snodgrass*, 1958] and offshore. The hypothesis was subsequently confirmed [*Munk*, *Snodgrass*, and *Carrier*, 1956]. By now more than 30 offshore stations have been occupied. The instrument promises to be useful also for the deep-sea recording of tides.

Our requirements are that the instrument should be capable of measuring waves with an amplitude of a few millimeters in the frequency range 0.1 to 10 cycles/kilosec, at depths exceeding 100 m. We first attempted to design a differential pressure gage, using air or springs as the compliant element. In the case of the air volume the instrument turned out to be a far better thermometer than a pressure transducer; the latter case called for special development of springs. A solution which easily met the above requirements turned out (perhaps surprisingly) to be an absolute pressure gage, using a Vibrotron pressure transducer, which converts pressure to frequency.

Pressure transducer—The Vibrotron pressure transducer [*Poindexter*, 1952; *Ohman*, 1955; *Prast* and others, 1955] was originally developed by the Southwest Research Institute, and is now being produced by B.-J. Electronics, Borg-Warner Corporation, Santa Ana, California. A pressure signal varies the frequency of a wire vibrating in a magnetic field. The induced voltage can be transmitted, recorded, or analyzed with all the advantages normally attributed to frequency modulated systems.

The vibrating wire is made of tungsten; the diameter is 0.025 mm and the length about 6 mm. It is stretched between the rigid structure and a small diaphragm exposed to pressure. The wire and its support is encased in an evacuated 2-cm dia cylinder 9 cm long, with electrical connections at one end, the diaphragm and pressure port at the other (Fig. 1). The wire is under tension of 15,000 to 20,000 bars. Increasing the pressure applied at the pressure port deflects the diaphragm inward, diminishes the tension, and decreases the natural frequency of the wire.

The wire vibrates in a magnetic field provided by Alnico V magnets with a field strength of 5,000 to 10,000 gauss and a gap of about 0.25 mm. This vibrating wire and a second, non-vibrating wire are connected in a bridge which is approximately balanced for d c. The output of the bridge, which is essentially the a c voltage induced in the vibrating wire, is amplified and fed back to the bridge in the sense required to maintain the wire in oscillation. The amplifier provides also for a sufficient power output (10 v across 100,000 ohms) to drive recorders or analyzers. Step-down transformers are used to match the output to low-impedance cables.

Transistor amplifiers—A thermionic amplifier matched to the Vibrotron transducer is available from the manufacturer, but this unit is not practical when power is supplied through long high-resistance cables. A transistorized amplifier was used which required only 4 ma at 20-v d c.

The amplifier circuit shown in Figure 2 (based

---

* Contribution from the Scripps Institution of Oceanography, New Series No. 978.

Reproduced by Permission

(80)

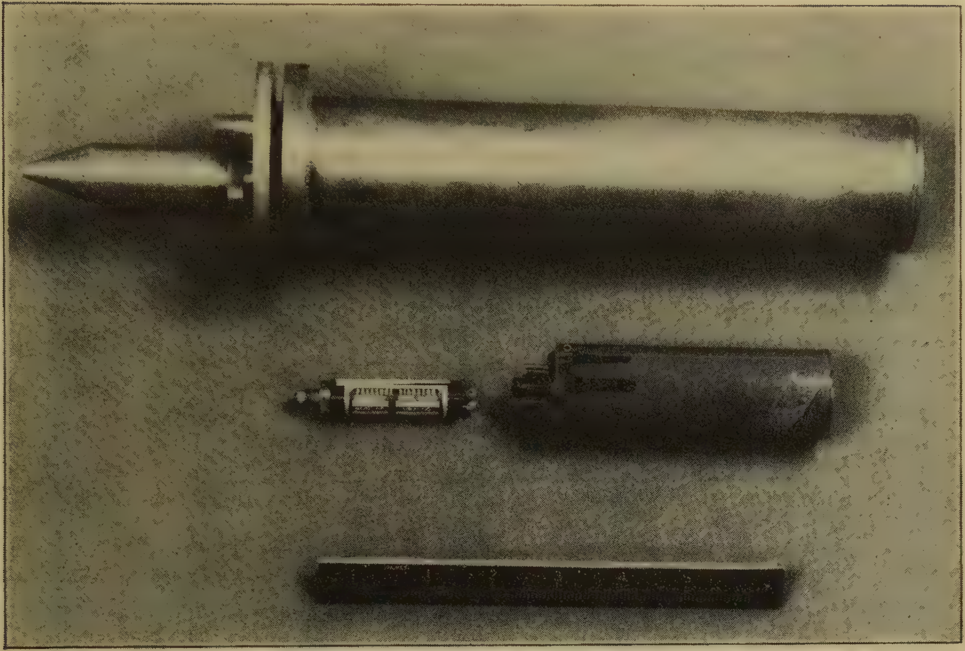

FIG. 1 – The Vibrotron transducer, transistor amplifier, and pressure case

on a development by *Snodgrass* and *Cawley* [1956]) has a gain of about 20,000 with an output of about 6 v. The resistance of the vibrating wire is low compared to the emitter load resistance, so that the Vibrotron can be connected directly to the first transistor amplifier. The second transistor acts as an impedance converter to reduce phase shifts resulting from the cut-off effect and the shunt input capacitance of the following transistor. The reduced phase shift of the amplifier, measured with the feedback condenser removed, is of the order of 60° and needs to be reduced still farther. The feedback condenser for each amplifier is adjusted by trial and error to produce zero phase shift at about 12 kc. The phase shift over the entire band 10 to 17 kc is then acceptable.

The complete system must have considerable frequency stability, since frequency is measured to one part in 10^6. This stability requires a constant amplitude of vibration of the wire. Effective amplitude control was accomplished by allowing the amplifier to overdrive in its last stage. The resulting distortion in the output wave form is not troublesome inasmuch as the recorded values depend only on zero axis crossings.

The amplifier was built as a potted plug-in unit with a diameter 3.8 cm and an overall length of 12.7 cm (Fig. 1).

Pressure sensitivity—We used two types of transducer, with the following characteristics:

Transducer	Pressure range		Frequency
	m	lb/in² abs	cycles/sec
Deep	0–750	0–1100	17,500–10,000
Shallow	0–180	0–250	17,500–10,000

A typical calibration for the shallow transducer is shown in Figure 3. The straight line is fitted to the equations $f^2 = -AP + B$ for $A = 1.26$ (kc/sec)²/(m of water pressure) and $B = 317$ (kc/sec)². The pressure sensitivity $df/dP = -A/2f$ varies from 0.36 (cycles/sec)/(cm of water pressure) at zero absolute pressure to 0.64 (cycles/sec)/(cm of water pressure) at absolute pressure of 180 m of water (depth = 170 m).

Temperature sensitivity—The mechanical structure of the vibrating wire element is designed to minimize differential thermal expansion between the vibrating wire and the support structure for the wire. The manufacturer guarantees a temperature sensitivity of not more than 0.05 pct of the band width per degree Fahrenheit. For a transducer with a frequency band of 10,000 to 17,500 cycles/sec, the maximum response to temperature change by 1°C is then $0.0005 \times 7500 \times 1.8 = 6.75$ cycles/sec, which is equivalent to $6.75/0.36 =$

(81)

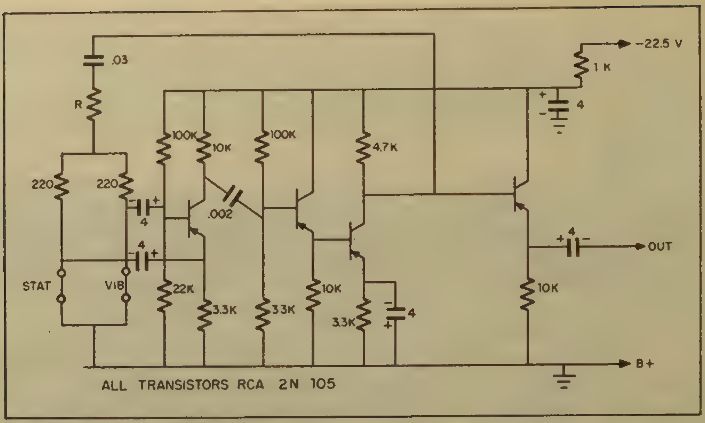

FIG. 2 – Schematic diagram of the Vibrotron transistorized amplifier

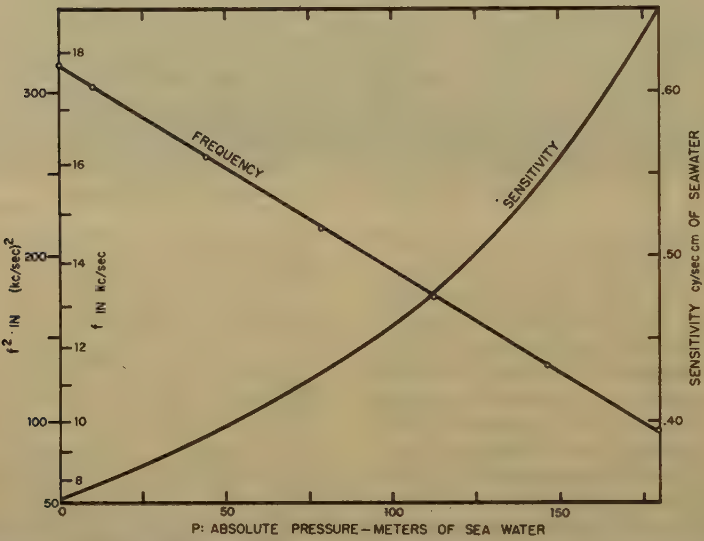

FIG. 3 – Frequency f and sensitivity df/dP of the Vibrotron plotted against pressure (not depth); the straight line is fitted to $f^2 = -1.26\ P + 317$ in the units indicated

18.7 cm of water pressure. Both pressure and temperature sensitivity increase with pressure in the same proportion; accordingly this value 18.7 cm/°C is independent of pressure.

The temperature of the bottom water at depths of several hundred meters may change rather suddenly by large fractions of a degree. In order for temperature 'noise' to be less than 1 mm of water pressure it is necessary that the temperature fluctuations of the Vibrotron transducer be less than that of the water by a factor of 100 for the frequency range of interest. This result was achieved by insulating the unit with moist sand. In water depths of less than 40 m the instrument was buried in the bottom by divers using self-contained underwater breathing apparatus. At greater depths the unit was lowered in the center of a wooden box filled with sand, measuring roughly 50 x 50 x 70 cm.

The theoretical response of a cylindrical box of compatible dimensions and filled with water (the role of the sand is to prevent convective heat transfer) indicates a reduction by a factor of 100 for a frequency of one cycle per hour (0.36 cycles/kilosec), by a larger factor at higher frequencies. The result was confirmed by comparing computed and measured response to a step change in temperature. In the laboratory the sand-insulated

Vibrotron was submerged in an ice bath, and at sea into the cold bottom water. Roughly 12 hr are required to reach equilibrium temperature (Fig. 4). In the case of tide measurement, the daily temperature variation of the Vibrotron had to be allowed for.

Stability—Various tests were performed with the Vibrotron and transistorized amplifier. A change of battery voltage from 22 v to 18 v altered the frequency by 0.1 cycles/sec. A change in the amplifier temperature from 25°C to 43°C decreased the frequency by 1.5 cycle/sec. Connecting a 1.0 mfd capacitor across the output transformer secondary (to simulate a long cable) decreased the frequency by 0.7 cycle/sec. A test of the over-all stability under ordinary working conditions is discussed under the heading *Noise spectrum*.

Digital recording—The pressure fluctuations of greatest interest in the present work have frequencies between 0.3 and 3 cycles/kilosec (periods between five minutes to one hour) and amplitudes of a few millimeters. Since the Vibrotron is an absolute pressure device, its output contains tides and ordinary waves, and these components are several hundred times the amplitude of the required signals. In the case of the shore-based recorder [see *Snodgrass*, 1958] the filtering of tides and ordinary waves is done pneumatically. Electronic filters were found to be unreliable at such low frequencies, but they were useful for monitoring the equipment during the tests. Our solution is to filter by numerical methods using high speed digital computers. Fortunately the output of the Vibrotron transducer is convenient for digital recording.

Commercial devices are available which count the number of cycles in a given time, using a quartz crystal clock to control the counting interval. This appears to be the most straight-forward and reliable means of recording. A Berkeley Scientific EPUT (events per unit time) meter equipped with a scanning and printing unit was used to tabulate the data on an adding machine tape. The timing interval can be selected as any multiple of one second up to 60 sec and is stable to one part in 10^6. A one-second time interval for the printing interval is also controlled by the crystal clock.

As an example, consider conditions summarized in the first line of Table 1. The shallow Vibrotron is very near the surface (absolute pressure about 10 m of sea water), and the oscillations are counted over a one-second interval. The sensitivity is 0.36 (cycles/sec)/cm water pressure, and hence a difference in count by one unit (say from 17,300 to 17,299) corresponds to 2.78 cm of water pressure. The last digit is in doubt, and hence this pressure equivalent of the EPUT least count is a measure of uncertainty.

The low precision is the result of dealing only with an integral number of cycles during a short time interval. There are two remedies. One is to deal with units smaller than entire cycles, such as half cycles, or third cycles, and this can be accomplished by multiplying Vibrotron frequency by

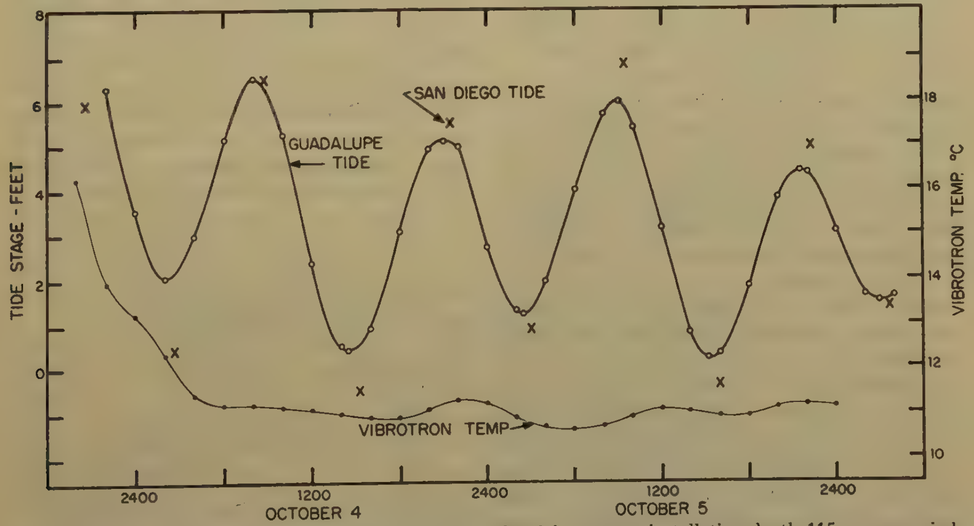

FIG. 4 – Tide and temperature data obtained at Isla de Guadalupe; gage installation depth 115 m; open circle points represent 5-min averages of uncorrected Vibrotron data; the measured Guadalupe tides were lower in amplitude and occurred earlier than predicted San Diego tides

TABLE 1 – *Digital recording least count*

Vibrotron range water pressure	Installed depth	Vibrotron		Multiplying factor	Counting interval	EPUT least count water pressure
		Frequency	Sensitivity[a]			
m	m	kc/sec			sec	cm
0–180	0	17.3	0.36	1	1	2.78
0–180	0	17.3	0.36	5	3	0.19
0–180	100	13.3	0.47	7	3	0.10
0–180	170	9.6	0.65	10	3	0.051
0–750	0	17.5	0.08	5	3	0.83
0–750	400	14.0	0.10	7	15	0.095
				1	59	0.17
0–750	740	9.9	0.14	9	15	0.053
				1	59	0.12

[a] Cycles per second per centimeter of water pressure

two or three, and counting the mutliplied frequency. The other remedy is to count over intervals of time longer than one second. It is advantageous to do both; that is, multiply the Vibrotron frequency and count for several seconds.

The frequency of modulation and its amplitude (again in units of frequency) are both exceedingly small compared to the carrier frequency. Under these circumstances the multiplying factor is limited by the electronic counters. The equipment used has a maximum counting rate of 100 kc/sec. The multiplying factors used vary from 5 at shallow depths (Vibrotron frequency 17.3 kc/sec; EPUT frequency $5 \times 17.3 = 86.5$ kc/sec) to 10 near maximum depth (Vibrotron frequency 9.6 kc/sec; EPUT frequency $10 \times 9.6 = 96$ kc/sec). These multiplication factors, in conjunction with a counting interval of 3 sec, reduced the EPUT least count to something like 1 mm (Table 1). Harmonics of the Vibrotron frequency were obtained by squaring the Vibrotron wave form and differentiating to produce pulses. Selective filtering of the appropriate harmonic was accomplished with a resonant L-C circuit that could be tuned within the band of 80 to 100 kc/sec. The ultimate limit of accuracy using multipliers and extending counting intervals depends upon the stability of the Vibrotron system.

Table 1 gives a summary of the multiplying factors and counting intervals that have been used. In much of our work a least count of about 1 mm was achieved. The usual arrangement was to count the multiplied frequency for three seconds with a repetition rate of four seconds, leaving one second for the printing operation. This permits one to compute spectra for periods in excess of eight seconds. For longer periods it is possible to use longer counting periods, but this introduces the aliasing problem; if there is an appreciable signal component near the sampling frequency, the difference frequency will appear as a spurious low-frequency component. In our work this is a serious problem, because the low-frequency waves are so much smaller than the ordinary waves present. The safest procedure is to maintain the sampling frequency sufficiently high so that the bottom pressure fluctuations induced by waves of that frequency are essentially eliminated at the depth of the instrument [for further details see *Munk*, *Snodgrass*, and *Tucker*, in press]. For measurements of tides, and of the mean absolute depth, very long counting times are entirely appropriate.

The noise spectrum—There is no single number expressing the stability of the instrument. It depends upon the frequency under consideration. A convenient presentation is the energy (or power) spectrum of noise level. This was obtained by analyzing the output of a Vibrotron with a capped pressure port using just the same methods as for the actual wave measurements [*Munk*, *Snodgrass*, and *Tucker*, in press]. For temperature protection the capped Vibrotron and transistor amplifier were buried 120 cm in the sand bottom at a water depth of 8 m.

The result of three spectra is summarized in Table 2. The noise record from the capped instrument is interpreted in terms of equivalent pressure fluctuations on an uncapped instrument. The first line states that the contribution to the mean square pressure deviation of the record from the frequency band 99.5 to 100.5 cycles/kilosec equals 1.3×10^{-4} (cm of water pressure)^2. The sensitivity was taken as (0.372 cycles/sec)/(cm of water pressure), equal to that of the uncapped instrument at the actual depth. Thus the energy density could be written as $1.3 \times 10^{-4} (0.372)^2 = 1.8 \times$

TABLE 2 – *Vibrotron noise spectrum; energy density in (cm of water pressure)^2/(cycles/kilosec)*

Frequency	Multiplying factor		
	4	4	1
	Counting interval (sec)		
	3	14	60
cycles/kilosec			
100	1.3×10^{-4}		
25	1.5×10^{-4}	1.5×10^{-5}	
5	2.5×10^{-4}	2.3×10^{-5}	5.0×10^{-5}
1		1.6×10^{-4}	4.0×10^{-5}
0.2			1.0×10^{-3}
Energy density from least count	0.9×10^{-4}	1.9×10^{-5}	6.0×10^{-5}

(84)

10^{-5} (cycles/sec)^2/(cycles/kilosec), or 0.018 (cycles/sec)^2/(cycles/sec).

The last line gives the energy density of a white noise generated by a random variation of $\pm\frac{1}{2}$ count of the last recorded digit. For each test the high-frequency noise was at roughly this level, and thus the accuracy was limited by the EPUT counting rate (10^5 cycles/sec) rather than by the Vibrotron. (At high frequencies better results are obtained by reading off values from a continuous line record; see next section.)

In each of the three spectra the values rise for low frequencies. There is some evidence that this is due to temperature effects on the EPUT crystal. Thus within the range of frequencies covered by the noise spectra (periods 10 to 5000 sec) the present limitations appear to be imposed by the recording equipment rather than the transducer. But it must be emphasized that the over-all stability of the system is well within the exacting limits required by our work.

In addition there is a steady drift of frequencies which cannot be attributed to the recording system. This drift does not contribute appreciably to the frequencies covered by the noise spectra. The Vibrotron frequency increased by 0.37 (cycles/sec)/day (−1 cm of equivalent water pressure per day) at the beginning of a continuous 25-day test period. This drift rate diminished gradually and at the end of the test period was about two-thirds the initial rate.

Continuous line recording—A graphical record is very useful for monitoring while the test is underway. The graphical records were not used for analysis except at frequencies above 125 cycles/kilosec (periods less than 8 sec). At these high frequencies the electrical equipment is relatively stable and the limitation of the least count is avoided. In fact, we have recorded actual energy levels as low as 10^{-6} cm^2/(cycles/kilosec) at a frequency of 200 cycles/kilosec (period 5 sec) with the Vibrotron at 115-m depth off Guadalupe, using values read off the continuous Speedomax record.

The arrangement is indicated by the block diagram (Fig. 5). The multiplied frequency of the Vibrotron was heterodyned with a crystal oscillator, and the difference frequency converted to a voltage by a Hewlett Packard frequency meter. The voltage was filtered through a series of RC-circuits of very long time constant, and recorded on a multichannel Speedomax recorder.

The crystal oscillator unit was designed to provide an output signal that could be adjusted throughout the band of 80 to 100 kc/sec. This adjustment was accomplished by heterodyning dual temperature-controlled crystal oscillators operating near 5 mc/sec to produce a difference frequency within this band. Each of the oscillators was provided with ten crystals. The crystals of the first oscillator were cut at 2000 cycles/sec intervals, the crystals of the second oscillator cut at 200 cycles/sec intervals. The 100 combinations provided frequencies spaced at 200 cycles/sec. By means of a small variable condenser connected across the crystal in one oscillator it was possible to tune the difference frequencies by about ±200 cycles/sec so that any desired frequency could be obtained within the frequency band of 80 to 100 kc/sec.

The Hewlett Packard frequency meter provided an output of 1 ma in a 1300-ohm load resistance, or 1.3 v, for full scale reading. Thus on a 0 to 500-cycle band the conversion factor would be 1.3 v/500 cycles/sec or 2.6 mv/(cycles/sec).

Consider a typical operating condition. The Vibrotron is installed in 115 m (125 m abs); the average frequency is 12.7 kc/sec, and the Vibrotron sensitivity 0.50 (cycles/sec)/(cm of water pressure). Using a multiplier of 7, the frequency becomes 88.9 kc/sec and the EPUT sensitivity 3.5 (cycles/sec)/(cm of water pressure). A crystal

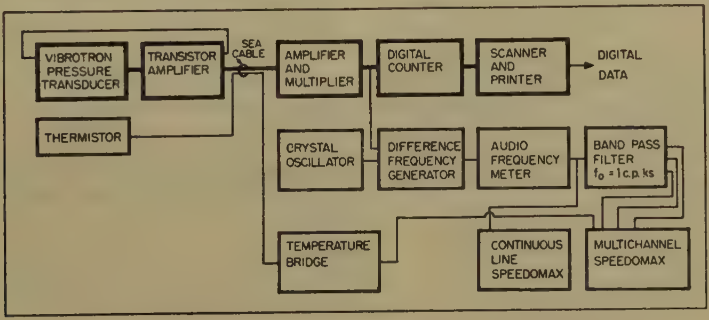

FIG. 5 – Block diagram of the low-frequency wave-recording system

oscillator frequency of 88.7 kc/sec provides a difference frequency of 200 cycles/sec. On a 0 to 500-cycles/sec band of the frequency meter, the average voltage is 200 × 2.6 = 520 mv, and the sensitivity 2.6 × 3.5 = 9.1 mv/(cm of water pressure). These values are reduced to 52 mv and 0.91 mv/cm respectively by using a 10/1 step-down attenuator. Now by recording on a 10-mv range Speedomax with a 0 to 100-mv biasing control, chart sensitivities 2.5 (chart cm)/(cm of water pressure) are obtained.

Rapid drifting due to tides and large fluctuations due to ordinary gravity waves are suppressed by means of band pass filters using biased electrolytic condensers. The condensers must be insulated against large temperature changes. Their leakage must be taken into account when evaluating the filter response. The condensers also exhibit a hysteresis effect (sometimes referred to as soaking). For the present purpose of obtaining qualitative results, the electrolytic condensers provide a simple and adequate means of obtaining the long-time constants.

Installations—The Vibrotron is placed on the sea bottom and connected with electric cables to the recording equipment. Cables up to three miles long have been used to connect the instrument to shore recorders.

There has been no entirely satisfactory solution for the case of shipboard recording. The instrument must not be disturbed by even one millimeter if the recording is to be of any use. One method is to employ the electric cable for an anchoring line. The Vibrotron is attached to a one-ton concrete weight. A second one-ton weight, separated from the Vibrotron by about 300 m of slack wire along the bottom, is intended to take the strain. For depths less than 150 m this arrangement has been satisfactory in reasonable weather. But in greater depths the ship motion resulted in a vibration of the cable which was transmitted to the instrument. In our early work we used 1500 m of 48 mm-dia armored cable and anchored a cable layer (a converted LCU) in depths up to 600 m. The development of an Amergraph cable 8.6 mm in diameter with a double reverse-lay 3175 kg-strength armor has now made it possible to handle the cable from a small research vessel. About 150 kg is added to the instrument and 100 m of 2-cm chain is lashed to the cable for holding power. An additional 15 m of 2-cm chain is lashed to the cable at mid-depth to provide spring anchor and to suppress cable vibration. Successful installations have been made in water depths up to 150 m.

For water depths of less than 150 m another method has worked out satisfactorily. The instrument was set on the bottom at a distance of about 500 m from the ship with the electrical cable floated across the surface. The section of cable between the surface and the bottom was kept taut by means of chain weights and submerged buoys. The ship was anchored by a conventional bow anchor, and could swing about her anchors without tangling the electrical cable and anchor wire.

For depths exceeding 150 m we now plan to try a third method. A taut electric cable is to be connected to a surface buoy, from which the signal is to be transmitted to the ship by radio link.

Acknowledgments—Frank Peterson has been very helpful on all stages of the development of this instrument. This paper represents results of research carried out by the University of California under contract with the Office of Naval Research and the Bureau of Ships of the Navy Department.

REFERENCES

MUNK, W., F. SNODGRASS, AND G. CARRIER, Edge waves on the continental shelf, *Science*, **123**, 127–132, 1956.

MUNK, W. H., F. E. SNODGRASS, AND M. J. TUCKER, Spectra of low frequency ocean waves, *Bul. Scripps Inst. of Oceanog.* (in press).

OHMAN, J., *Vibrotron digital telemetering system*, National Telemetering Conference, Chicago, Illinois, May 1955.

POINDEXTER, R. W., *Theory and design of vibrating wire transducers*, presented at joint AIEE-IRE Symposium, Long Beach, California, Aug. 1952.

PRAST, J. W., S. H. CALHOUN, G. S. HARTLOFF, AND G. W. LISKE, *A precision pressure telemetering system with digital data handling*, National Telemetering Conference, Chicago, Illinois, May 1955.

SNODGRASS, F. E., Shore-based recorder of low-frequency ocean waves, *Trans. Amer. Geophys. Union*, **39**, 109–113, 1958.

SNODGRASS, J. M., AND J. D. CAWLEY, Temperature and depth circuitry of a telerecording bathythermometer, *Proc. National Electronics Conference*, 1956.

Scripps Institution of Oceanography, La Jolla, California.

(Communicated manuscript received May 27, 1957; open for formal discussion until July 1, 1958.)

(86)

[Reprinted from Journal of Chemical Education, Vol. 35, Page 123, March, 1958.]

Copyright, 1958, by Division of Chemical Education, American Chemical Society, and reprinted by permission of the copyright owner

• TRAINING IN CHEMICAL OCEANOGRAPHY[1]

NORRIS W. RAKESTRAW
Scripps Institution of Oceanography, University of California, La Jolla

BEFORE we can decide upon the proper training for chemical oceanographers we must agree upon the purpose and objectives of research in this field. If the chemical oceanographer is but a chemist who, for some reason, happens to undertake research involving sea water or some property or phenomenon of the marine environment, we have no problem. He is a chemist and should be trained as other chemists are.

We must raise the question whether oceanography has any place of its own in the category of sciences or whether it is merely a convenient meeting ground of many sciences. There are some of us who believe that although it involves an *object* of study rather than a *subject*, nevertheless oceanography has a methodology and subject-matter content distinctly its own. It has taken the better part of a hundred years to reach this stage and we are reluctant to retreat from it. If this view prevails, the ocean itself, its behavior, its properties and all its various phenomena are the prime considerations, and oceanographers will use all the available techniques of the various sciences in the study of the primary object. We would hold that the relation of the oceanographer is the same as that of the physician to his primary object, in the latter case the human organism. Like the physician, he is concerned with the activity of that whole organism and not merely in the opportunities which it offers for study by a specialist such as the biochemist, the pathologist, and the anatomist.

It is by no means certain that this view of oceanography will ultimately prevail, for there are some who believe that we will learn more about the ocean, and faster, by dividing its study up between respective minor subdivisions of the established sciences, physics, chemistry, biology, and geology.

If we are to train oceanographers on the basis of the unity of the subject, however, they must all of them, whatever their subdivisions, have a broad general background in the fundamental sciences. If this has not been laid during the undergraduate stage then the deficiencies must be filled during the time of specialization.

The chemical oceanographer should not only have the equivalent of an undergraduate major in chemistry but he should have also at least one solid graduate year in conventional chemistry. There are two reasons for this requirement: (1) because chemical oceanography is badly in need of all the contributions which modern chemistry can offer; and (2) because employment opportunities in this special field are still limited, and for the protection of a student's own interests his training should be broad enough to serve in more than one applied field of chemistry.

Until recently, chemistry's function in the field of oceanography has been largely to serve the interests of biology. Early interest in the study of the ocean was principally in the creatures which live there, and it is therefore not surprising that the few chemists who were attracted to the field gave their attention to the chemical conditions of life in the sea and the study of the reasons why some parts of it are fertile and others barren. This was the limited field of study of chemical oceanography until late in the 1930's, because there were too few chemists, with too little time, to do anything else.

Now, however, we are expanding our interests into the field of general geochemistry and concerning ourselves with the many chemical processes taking place in the sea water itself, in the atmosphere immediately above it, and in the bottom immediately below it, for these are all parts of the ocean. He who is to contribute productively to this area of study needs, in addition to his sound training in chemistry, a scarcely less intensive preparation in geology, as well as more than an elementary understanding of biological science. It can be assumed that his training in chemistry will include enough physics and mathematics to serve as a basis for some advanced study of physical oceanography which will frequently be found essential for the chemical oceanographer.

Evidently the chemical oceanographer must be an expert in more fields than his own specialty, chemistry. This will be a difficult specification to fulfill, and will be a sharp limitation to the number of prospective candidates. That will be all right, for this will not be a vocation which will attract great numbers, especially since it is a purely scientific one which, although it offers attractive and interesting opportunities for hard work, does not hold out great pecuniary inducements.

Specifically, chemical oceanography involves all the branches of modern chemistry except possibly organic. The complexity of sea water as a chemical system will tax to the utmost the ingenuity and the facilities of the physical and the analytical chemist. Its study involves the determination of many constituents in parts per billion, in the presence of relatively enormous quantities of disturbing and interfering constituents. Applications are many for all kinds of analytical methods, from conventional gravimetry, through numerous types of spectrographic and spectrophotometric, to the highest refined and most recent radiochemical and nuclear techniques.

---

[1] Presented as part of the Symposium on Chemistry of the Sea before the Division of Chemical Education at the 131st Meeting of the American Chemical Society, Miami, April, 1957. Contribution from the Scripps Institution of Oceanography, New Series, No. 979.

Reproduced by Permission

As a chemical system sea water is more complex than any which the physical chemist ordinarily dares to study. Its "purity" cannot even be defined, much less measured. Nevertheless we need to study its physical-chemical behavior and must devise methods to do so. If and when the physical chemist learns something about concentrated solutions he will still find great difficulty in applying his knowledge to sea water. This will frustrate him, or challenge him, depending upon his courage. Laboratory solutions have seldom if ever been under observation for more than a short time—a couple of years perhaps. The ocean, on the other hand, has been there for millions of years. Who knows what slow processes, of hitherto unsuspected nature, may have come to equilibrium there? I believe that we shall some day learn, from the study of the ocean, about a field of chemical kinetics involving entirely new orders of magnitude.

There is organic matter in the sea, of strange and unknown composition, which needs to be isolated and studied. But for the most part, the problems of marine chemistry are inorganic. Most, if not all, of the chemical elements are to be found there, although we know little about their ionic state in many cases. A solution which is at the same time concentrated with respect to many constituents and extremely dilute with respect to others is an ideal system for the existence of complex ions, and there is good reason to believe that many such combinations exist in sea water. There is plenty of work here for the trained inorganic chemist.

The chemical oceanographer's undergraduate courses should be those generally considered essential for a well-trained chemist, and should include biochemistry. At this level or at the early graduate stage he should have courses in advanced physical, analytical, and inorganic chemistry, radiochemistry, and instrumental methods, including or supplemented by a good introduction to theoretical and practical electronics. The desirability of experience in the supporting fields of geology and biology has already been referred to and need not be elaborated upon. A reading knowledge of German should have been obtained by this time; French, or preferably Russian, should be added but can be postponed until later if necessary.

Such a background will be adequate preparation for specialized graduate work in oceanography, such as is now offered by several institutions. The graduate student should first be oriented in the principal branches of oceanography: physical oceanography, marine biology, and marine geology and geochemistry. It should not take the well-trained chemist long to master the present subject matter and methods of chemical oceanography and be prepared to undertake research of his own. He should make himself familiar with some of the related specialties, such as marine microbiology, petrography, and sedimentation, by special courses or otherwise. A course in general geophysics and one in geochemistry, if not available at an earlier stage, would be valuable here.

Independent research is of course the main substance of training at the doctoral level, and the requirements for this are so well known as to need no elaboration. Closely related to this, if not an actual part, is experience in the field methods of oceanography. Actual sea-going experience should be required of all students, in which they learn something of the logistics and techniques of oceanographic expeditions. Opportunities for such participation are unfortunately to be had only at institutions which are carrying on extensive research projects, since the operation of ships is very expensive, but occasionally there are openings for young men (and even young women) from other institutions.

It should be noted that I have dealt for the most part only with such details as differentiate training in oceanography from that in other fields. We should not be unmindful of other desirable features of graduate work, such as participation in seminars, training in the preparation of oral and written reports, etc.

Furthermore, the whole treatment of this subject is based upon the assumption that it is to lead to the doctor's degree. There is of course place in oceanography for those at a lower level of training and what I have outlined may in many cases be unattainable. While we must aim at what we think is the very best, we realize that we may have to settle for less.

(88)

[AMERICAN JOURNAL OF SCIENCE, VOL. 256, APRIL 1958, P. 225-240]

American Journal of Science
APRIL 1958

PROPERTIES OF WATER, PART II. THE EQUATION OF STATE OF WATER AND SEA WATER AT LOW TEMPERATURES AND PRESSURES*

CARL ECKART

ABSTRACT. The empirical data on the equation of state of pure water have been reviewed and analyzed. Systematic errors in the isotherms are estimated at $\pm\ 2p \times 10^{-7}$ ml/gm, and the probable error of the best values of specific volume is not less than $\pm\ 2 \times 10^{-4}$ ml/gm, in the range of $0° \leqslant T \leqslant 40°C$ and $0 \leqslant p \leqslant 1000$ atm. In this region and within this error, the data can be represented by the Tumlirz equation

$$(p + p_o)\ (v - v_o) = \lambda,$$

where p = pressure, v = specific volume, while p_o, v_o and λ are empirical functions of temperature.

The quantity v_o seems to be actually independent of the temperature and p_o and λ can be sufficiently well approximated by quadratic functions of temperature. More experimental work is needed to establish these functions with the required precision.

The much less numerous data on sea water are also considered. They are certainly no more precise than the data for pure water, and can also be represneted by the above equation, provided p_o and λ are quadratic functions of temperature and linear functions of salinity; v_o appears to be independent of salinity as well as temperature. The available data do not enable the dependence of the isotherms on salinity to be determined with precision, and more experimental work is needed. Until this becomes available, the formulae derived here must be considered doubtful, but no more so than others in current use.

INTRODUCTION

The primary objectives of this work were (1) a critical examination of the present P-v-T data on sea water, and (2) the construction of a simple but currently adequate empirical formula. The ranges of interest are: pressure, 1 to 1000 atmospheres; temperature, 0 to 40°C; salinity, 0 to 40 gm/kg.

In order to achieve the first objective, it was found necessary to examine the P-v-T data on pure water, partly because the data on sea water are too few to permit an estimate of probable error and partly because the sea water measurements are all relative to distilled water. It has been assumed that the errors in the sea water data are no greater than those of the pure water data. The random errors of the sea water data, insofar as they can be estimated at all, seem to be admirably small; but it is certain that they contain larger systematic errors.

The second objective has not been fully achieved, as will appear below. After the rather lengthy computations had been finally revised, further data and information came to light. It is believed that the formulae would not be significantly changed by a recomputation at this time. The existing sets of data are inconsistent by more than the experimenters' estimates of errors, and

---

* Contribution from the Scripps Institution of Oceanography, New Series No. 980.

Reproduced by Permission

this is reflected by a corresponding uncertainty in the parameters of the equation here derived.

The P-v-T data on water and sea water have been summarized by many empirical formulae, some of them quite elaborate.[1] One of the simplest of these, first proposed by O. Tumlirz (1909),

$$(p + p_0)\ (v - v_0) = \lambda, \tag{1}$$

is entirely adequate for low temperatures and pressures. In Eq. (1), p is the pressure, v the specific volume, and p_0, v_0 and λ are functions of the temperature T. Following Dorsey (1940), v will be measured in ml/gm and p will be given in atmospheres = 1.03323 kg/cm^2 = 1.01325 bar. The quantity

$$\Delta = 10^4(1 - v) \tag{2}$$

is used by Dorsey and will be useful here.[2]

In terms of Δ, Eq. (1) becomes

$$(p - p_0\ (\Delta_0 - \Delta) = 10^4\,\lambda = K. \tag{3}$$

For many purposes, it is convenient to pick a standard pressure, p_1, and its associated Δ_1; then K may be eliminated from Eq. (3):

$$(p - p_1)\ \Delta_0 - (\Delta - \Delta_1)\ p_0 = (p\Delta - p_1\Delta_1). \tag{4}$$

Defining

$$x = (p - p_1)/(p\Delta - p_1\Delta_1), \tag{5}$$

$$y = (\Delta - \Delta_1)/(p\Delta - p_1\Delta_1), \tag{6}$$

Eq. (4) becomes

$$x\Delta_0 - yp_0 = 1. \tag{7}$$

The validity of Eq. (1) can therefore be tested by plotting x, y as the coordinates of points, and examining the deviations of these points from a straight line. If Eq. (1) is valid, the intercepts of this line are $1/\Delta_0$ and $-1/p_0$.

PURE WATER

1. *The Data.*—The most convenient tabulation of P-v-T data for pure water is given by Dorsey (1940) as Tables 95-I to 95-IX of his *Properties of Ordinary Water-Substance.* The data of V. W. Ekman (1908) on pure water appear to have escaped Dorsey's attention. A preliminary version of Kennedy's (1957) data was kindly made available to the author. This preliminary version differs from the final version, but for the reasons mentioned above, the present computations have not been correspondingly revised.

Intercomparison of these eleven sets of measurements shows that they can be divided into two groups, those in the first group being mutually consistent within ± 2 units of Δ, and those in the second being inconsistent with each other and with the first group. The first group consists of:

Dorsey's Table 95-I, due to E.-H. Amagat (1893);
Dorsey's Table 95-II, due to E.-H. Amagat;
Kennedy's preliminary data;
Ekman's data.

---

[1] W. T. Holser will summarize the formulae for pure water in another paper of this series. The standard formulae for sea water contain 37 parameters and are to be found in the book by Bjerknes and Sandström, (1910).

[2] In the oceanographic literature the quantity

$$\sigma = 10^3(1 - v)/v$$

is common, and $1 - v$ is often denoted by δ or $\Delta\alpha$.

In general, only this first group of measurements will be considered here, except that Dorsey's Table 95-III, due to P. W. Bridgman (1913), will be used for an investigation of high pressures.

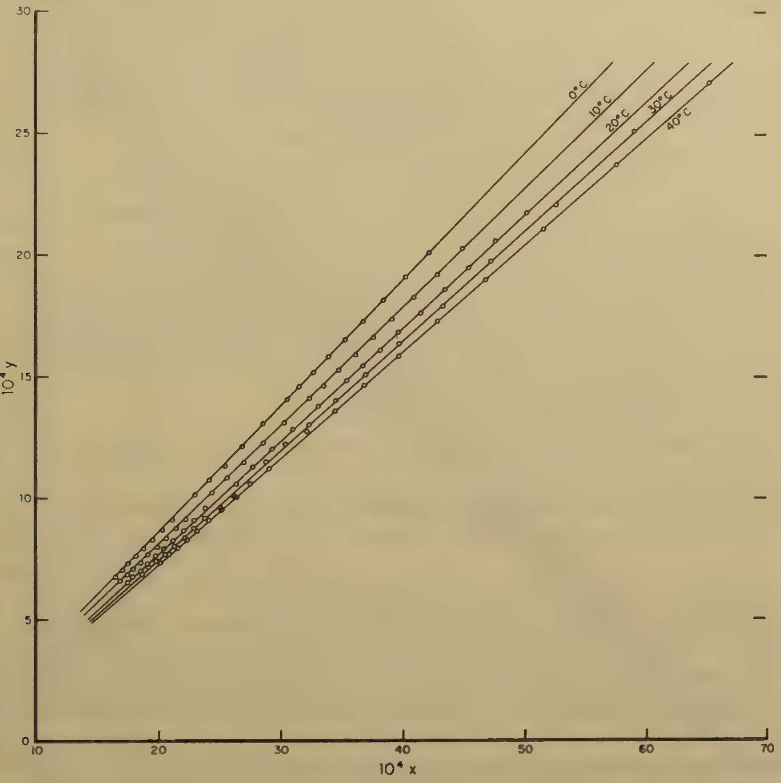

Fig. 1. Isotherms of pure water in the x – y plane: data of E.-H. Amagat (Dorsey, Table 95-I); $p_1 = 500$ atm.

After this paper was already in rough draft, the data of R. E. Gibson and O. H. Loefler (1941) were called to the author's attention by W. T. Holser.

2. *First Test of the Equation.*—Using Dorsey's Table 95-I, values of x and y were calculated using $p_1 = 500$ atm.; they are plotted as figure 1. The pressure range is 1 to 1000 atm., and the 0° to 40°C isotherms are seen to be good straight lines. Bridgman's data, Table 95-III, extend over a larger pressure range, being terminated only by the formation of Ice-VI. The x, y graphs of these data are shown as figure 2. There are systematic departures from the straight lines above $p = 3000$ atm., and there are noticeable irregularities in the spacing of the isotherms. These latter are probably due to experimental error, the former perhaps to inadequacy of the Tumlirz equation (1909).

It is to be concluded that the Tumlirz equation fits the data with some precision for $p \leqslant 3000$ atm., and $0 \leqslant T \leqslant 40°$.

3. *Second Test of the Equation.*—Figures 1 and 2 cannot be drawn on a sufficiently large scale to exhibit the detailed nature of the agreement between

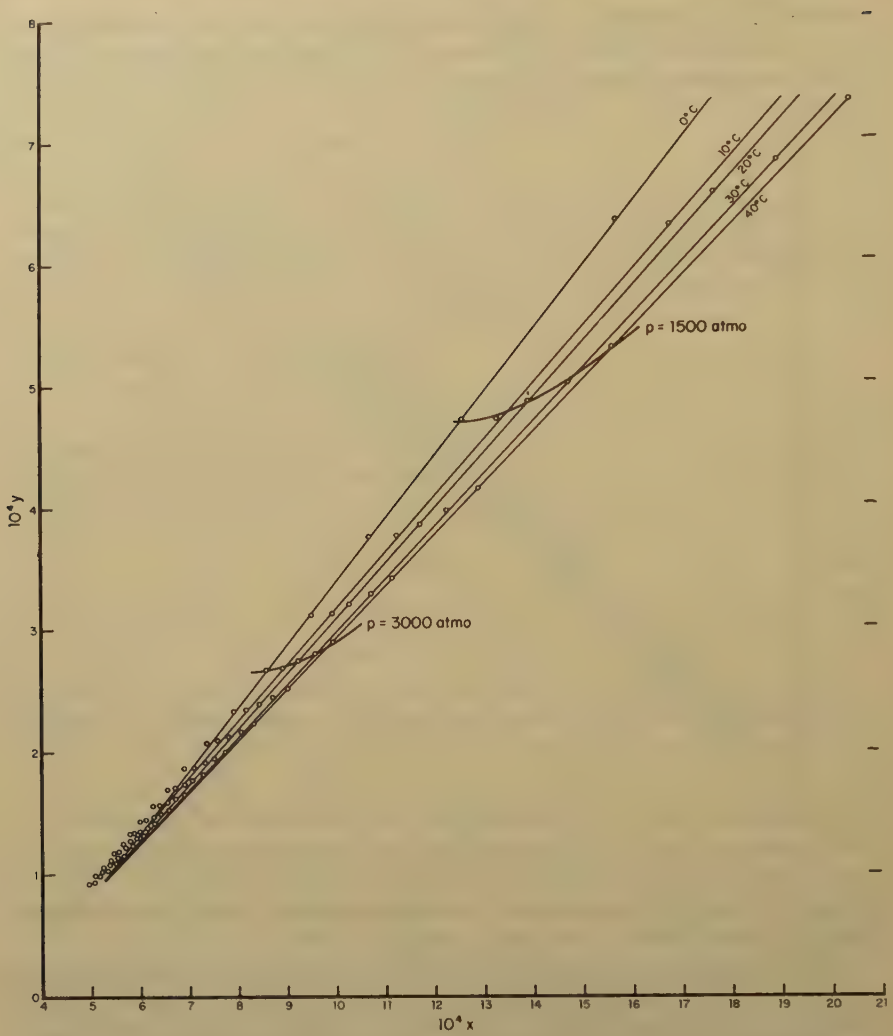

Fig. 2. Isotherms of pure water in the x – y plane: data of P. W. Bridgman (Dorsey, Table 95-III); $p_1 = 500$ atm.

the equation and the data. One would like to sight along the straight lines with a telescope. This can be accomplished mathematically by the transformation

$$\xi = \frac{1}{2}y, \qquad \eta = x - 2y. \tag{8}$$

In the ξ, η plane, the Tumlirz equation becomes

$$\alpha\xi + \beta\eta = 1, \tag{9}$$

$$\alpha = 4\Delta_o - 2p_o, \qquad \beta = \Delta_o. \tag{10}$$

Figure 3 shows the same data as figure 1, replotted in this fashion. It is seen that this provides a more searching test of the relation between the data

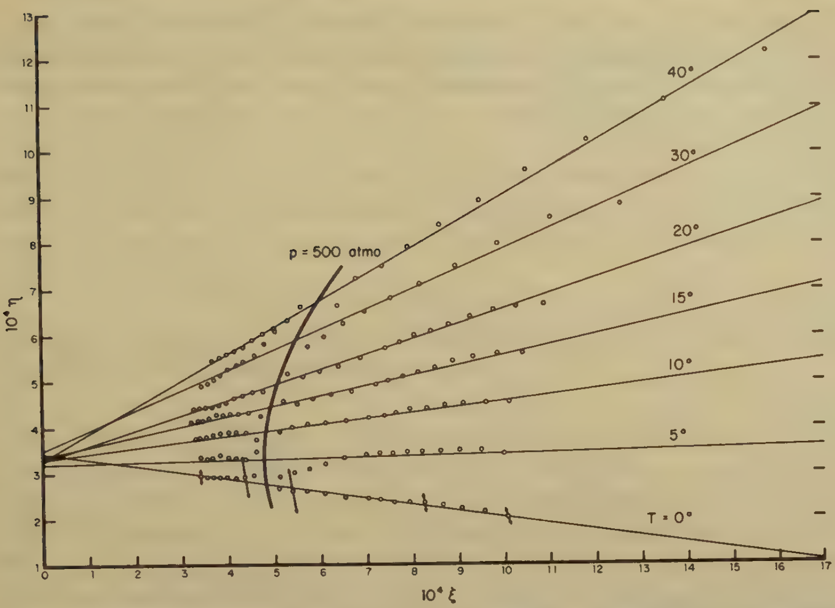

Fig. 3. Isotherms of pure water in the $\xi - \eta$ plane: same data as fig. 1. The double arrows indicate the displacements that would result from changes of ± 10^{-4} ml/gm in the specific volume.

and the equation. Systematic departures from the straight lines are apparent. The double arrows on some of the plotted points indicate the displacements that would result from changing Δ by $\pm$ 1 unit. The lengths of these arrows, and the sensitivity of the method, increase as the standard pressure $p_1 =$ 500 atm. is approached.

Figure 4 is based on Amagat's second series of measurements (Dorsey's Table 95-II). This, like the preceding figure, shows systematic departures from the straight lines—but the systems are not the same in the two cases. Both Tables 95-I and 95-II give values of Δ to 0.1 unit; one concludes, however, that there are systematic errors of at least one unit.

Figure 5 shows Kennedy's preliminary data, plotted in the same way. While Amagat smoothed his data to $\pm$ 0.1 unit of Δ while interpolating, Kennedy estimated his error at about $\pm$ 1 unit, and smoothed accordingly.

Amagat's first set of data, figure 3, yields a $\xi - \eta$ diagram that shows smaller departures of the isotherms from straight lines than do the two other sets. This might indicate that Amagat's first set is the most reliable of the three. Without more information about Amagat's method of interpolation, the writer is disinclined to adopt this view. It seems more reasonable to suppose that the differences among the three figures disclose the presence of systematic errors in all of them. It should be noted, specifically, that compatibility with the Tumlirz equation is no guarantee of the absence of such errors. More generally, experience in other fields indicates that internal consistency and smoothness do not necessarily imply lack of error, and that, while the intercomparison of independent published measurements enables the magnitude of the errors to be estimated, it rarely permits them to be located without a critical consideration of experimental procedures. Such considerations are outside the scope of this paper.

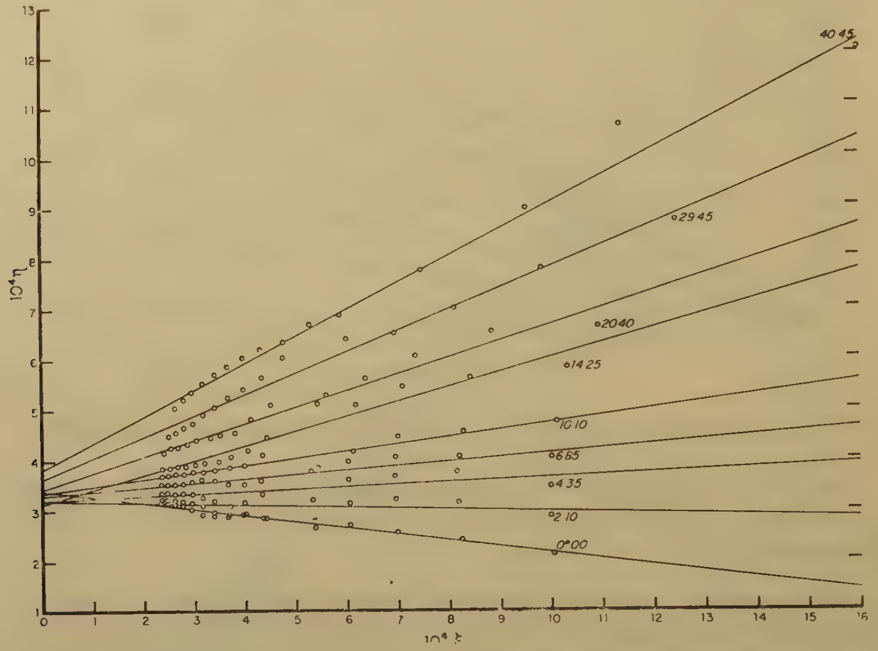

Fig. 4. Isotherms of pure water in the $\xi - \eta$ plane: second series of data of E.-H. Amagat (Dorsey, Table 95-II).

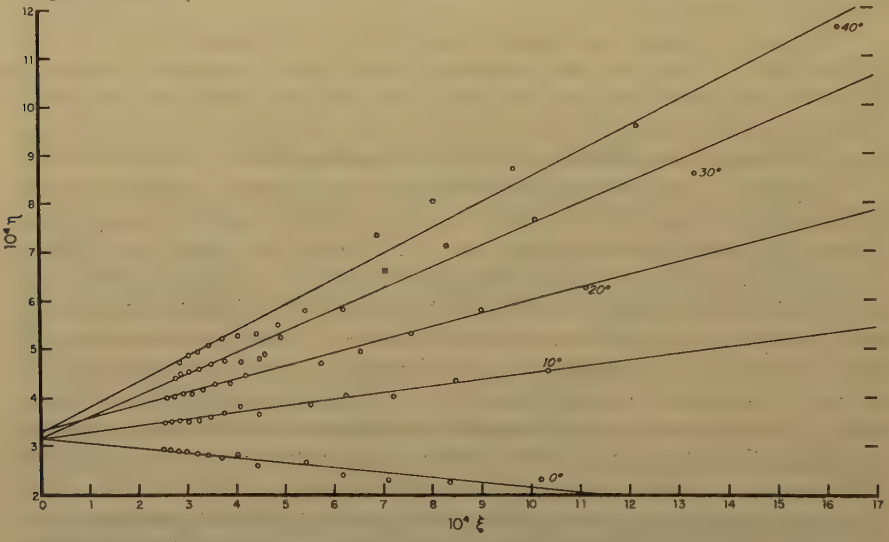

Fig. 5. Isotherms of pure water in the $\xi - \eta$ plane: preliminary data of G. Kennedy.

One may reach the provisional conclusion: the precision of the specific volume data is not better than ± 2 units of Δ, and the Tumlirz equation represents the isotherms adequately in the low pressure and temperature region. Further evidence in support of this conclusion will appear below.

4. *The Data of Ekman (1908)*.—These were not found until most of the calculations for this paper had been made. They will therefore be given separate treatment at all stages of the discussion. Ekman does not tabulate the specific volume but the "apparent compression". The compression (between 1 and p atm.) is defined as

$$k = 1 - v(p.\ T)/v(1, T), \qquad (11)$$

the apparent compression k′ differs from this because of the compressibility of the glass in which the water was contained:

$$k' = (k - k_g)/(1 - k_g), \qquad (12)$$

where k_g is the compression of glass. Ekman was uncertain of the value of k_g, and therefore published only values of k′; for distilled water, these are given in his Table 10 (Ekman, 1908, p. 32). He first suggests that $k_g = p\upsilon$, where $\upsilon = 0.225 \times 10^{-6}$ per bar; in a footnote added after correspondence with Amagat, he revises this to $\upsilon = 0.215 \times 10^{-6}$. This second value has been used here in calculating k from k′.

It is also necessary to know v(1, T) in order to obtain v(p, T): these data were taken from Dorsey's Table 94-III (revised Chappuis Table, 1937). The resulting values of Δ are given as table 1.

Ekman had no direct means of measuring pressure to the required precision. Consequently, he made indirect measurements, using the compression of distilled water at 0°C for this purpose. In order to convert these to pressures, he used a mean of Amagat's two 0° isotherms. It has been seen that these differ by several tenths of a unit in Δ, and probably contain even larger systematic errors. Ekman's values of the specific volume at T = 0°C are therefore necessarily an average of those of Amagat.

At other temperatures, they differ from those of Amagat by as much as 3 units of Δ. It is impossible to determine how the error thus disclosed is divided between the Amagat and Ekman values. Table 1 shows that Ekman's repetitions always agree to better than 0.1 unit, and often coincide to 0.01. This would lead one to give them the greater weight, were it not for their forced agreement with Amagat's 0°C isotherm: Amagat's errors influence Ekman's "measured" values in a systematic manner.

Even if the Ekman data were more accurate than the Amagat data, it would not be possible to use them for a searching test of the Tumlirz equation. Each of Ekman's isotherms is defined by just two measurements at each of three pressures: consequently the three parameters of Tumlirz' equation can always be chosen to yield the exact average of the two values of Δ at each pressure. At best, one can assume the Tumlirz equation and calculate these parameters.

5. *Temperature Dependence of the Isotherms*.—The straight lines shown on figures 1 to 5 were determined by least squares. Each yields a determination of

TABLE 1

Values of $\Delta = 10^4\ (1 - v)$ deduced from Ekman's (1908, p. 32.) Measurements on Distilled Water

T / p atm.	4° .97	9° .97	14° .96	19° .96
203.7	95.32 95.32	90.08 90.11	82.10 82.16	71.66 71.64
408.9	185.55 185.62	178.04 178.04	168.35 168.35	156.46 156.40
607.4	267.44 267.44	258.01 258.03	246.77 246.80	233.69 233.67

the parameters α and β in Eq. (9), for the corresponding temperatures. These various determinations are plotted on figure 6, a and b.

The systematic variation of β is very slight, if not negligible. The mean of the Kennedy and Amagat values is $\beta = 3020$, with a standard deviation of 158. The straight line $\beta = 3088 - 3.930T$ fits these same data with a standard deviation of 146. One is therefore justified in concluding that β is independent of temperature, and has the value

$$\beta = 3020 = \Delta_0. \tag{13}$$

The four values from the Ekman data yield $\beta = 2855 \pm 15$ and are thus barely consistent with the others. They do confirm the constancy of β, and

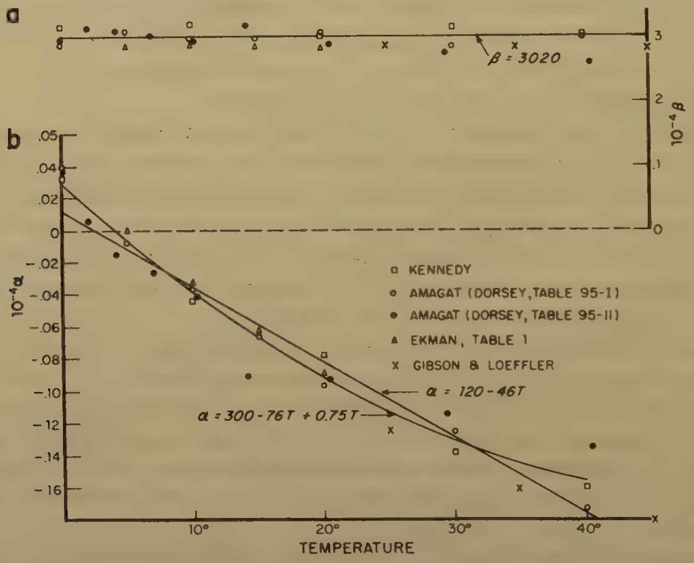

Fig. 6. Values of α and β (Eq. 9) for various temperatures and various experimenters.

(96)

would have somewhat lowered the overall average. Values of β were calculated from the Gibson and Loeffler data for T = 25°, 35°, 45° and 55°; while these data extend to 85°, it seemed undesirable to include the higher temperatures in the present study. The four selected values yielded $\beta = 2841 \pm 70$. The value of $\beta = 3020$ has been used in the following calculations, for the reasons explained above.

The values of α show a definite trend, and are represented by the linear formula

$$\alpha = 120 - 46T \tag{14}$$

with a standard deviation of 168. This is shown by the straight line on figure 6b; the values at T = 0° and 40° deviate from it by undesireably large amounts. The quadratic formula

$$\alpha = 300 - 76T + 0.75T^2 \tag{15}$$

represents the data with a standard deviation of 110. The reduction from 168 to 110 is scarcely large enough to justify Eq. (15), but the desire to reduce the deviation at T = 0°C leads to its provisional adoption.

The inclusion of the Ekman and Gibson and Loeffler values of α would have reduced the statistical significance of the quadratic term still further, and would have increased the coefficient 46 in Eq. (14). In particular, it is noted that the Ekman values trend toward Amagat's points at 0°C; in view of Ekman's method of measuring pressure, this must be somewhat discounted.

Again, Eq. (15) has been used in the following calculations. This is even less justifiable than the corresponding decision regarding Eq. (13), since it

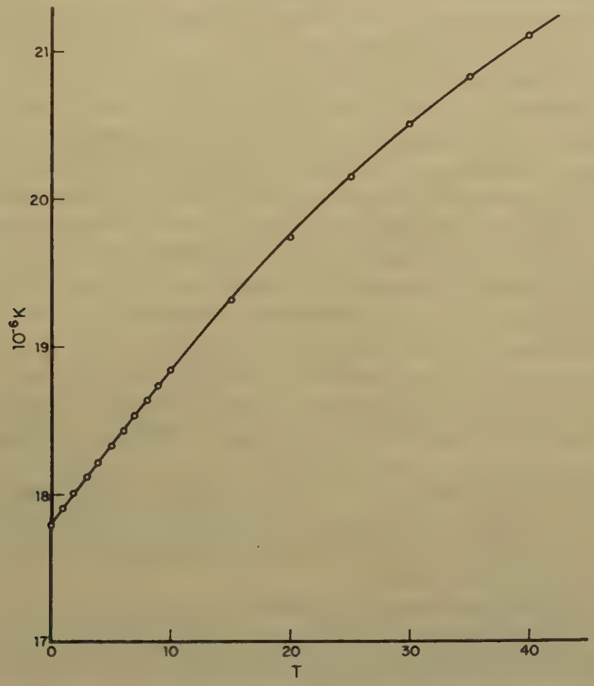

Fig. 7. Variation of K with temperature: data of Chappuis (Dorsey, Table 94-III).

gives undue weight to the three values of α at 0°C. It would be very desireable to have more measurements in the range $0° \leqslant T \leqslant 15°C$. Perhaps the use of Eq. (15) can be condoned until such measurements become available.

Since $\alpha = 4\Delta_o - 2p_o$, Eq. (13) and (15) imply

$$p_o = 5890 + 38T - 0.375T^2. \tag{16}$$

It remains to find the dependence of K, Eq. (3), on the temperature. Having shown that Eq. (3) represents the isotherms to an adequate precision, and having determined p_o and Δ_o, it suffices to consider only a single value of p and its associated value of Δ at each temperature. Since the thermal expansion at $p = 1$ atmosphere has been determined with great precision, this pressure is the logical choice. Dorsey's Table 94-III provides values of the specific volume at $p = 1$, which are probably accurate to ± 0.05 units of Δ, a greater precision than is available at any other pressure.[3] The values of K determined by substituting from this table into Eq. (3) are plotted as figure 7. They are fitted by the quadratic equation

$$10^{-6}K = 17.795 + .1125T - .000745T^2 \tag{17}$$

with a standard deviation of 0.003. The quadratic term in Eq. (17) is certainly significant.

These methods of determining the parameters Δ_o, p_o and K as functions of T are not the best. It would have been preferable to apply least squares methods directly to Eq. (3). The above methods, based on values of x and y, are not only more laborious, but give undue weight to measurements near the arbitrarily chosen pressure p_1. They were originally adopted because they are well suited for a graphical study of the data.

6. *Final Test of the Equation.*—Using Eqs. (3), (13), (16) and (17), values of Δ were calculated for various values of p and T, and compared with the tabulated values of the first group of measurements described above. As examples of the second group, the data of Smith and Keyes, from Dorsey's Table 95-VI, and those of Bridgman, from Dorsey's Table 95-III, were included. The differences are plotted on figure 8,[4] the ordinates being $\Delta - \Delta_{calc.}$. It is seen that, for a given temperature and observer, these show systematic variations with pressure. However, the systems are different for different experimenters, and are thus to be considered as systematic errors in the measurements, rather than as a failure of the equations.

It is to be noted that the systematic differences among experimenters are greatest at $T = 40°C$. The systematic departures from the equations adopted here are greatest at 0° and 40°C. This has attracted the attention of several

---

[3] Since all measurements of v at elevated pressures are relative to v(1, T) a similar choice must be made in constructing any tables of v(p, T). Dorsey has apparently used his Table 94-III in constructing most of his tables of v(p, T), but Table 95-VI, due to Smith and Keyes, is an exception. In the preliminary version of the Kennedy data studied here, the Smith and Keyes values of v(1, T) were used by mistake; in the published version of these data, Table 94-III has been used.

[4] In figure 8 the Smith and Keyes points deviate strongly from all the others. This is because their tabulated values are derived from an emprical equation that is extrapolated below 30°C, a fact which is not apparent in Dorsey's retabulation. The only experimental values of Smith and Keyes (1934, p. 297) in this range are at 30°C, and they are generally within the range of values of other investigators.

(98)

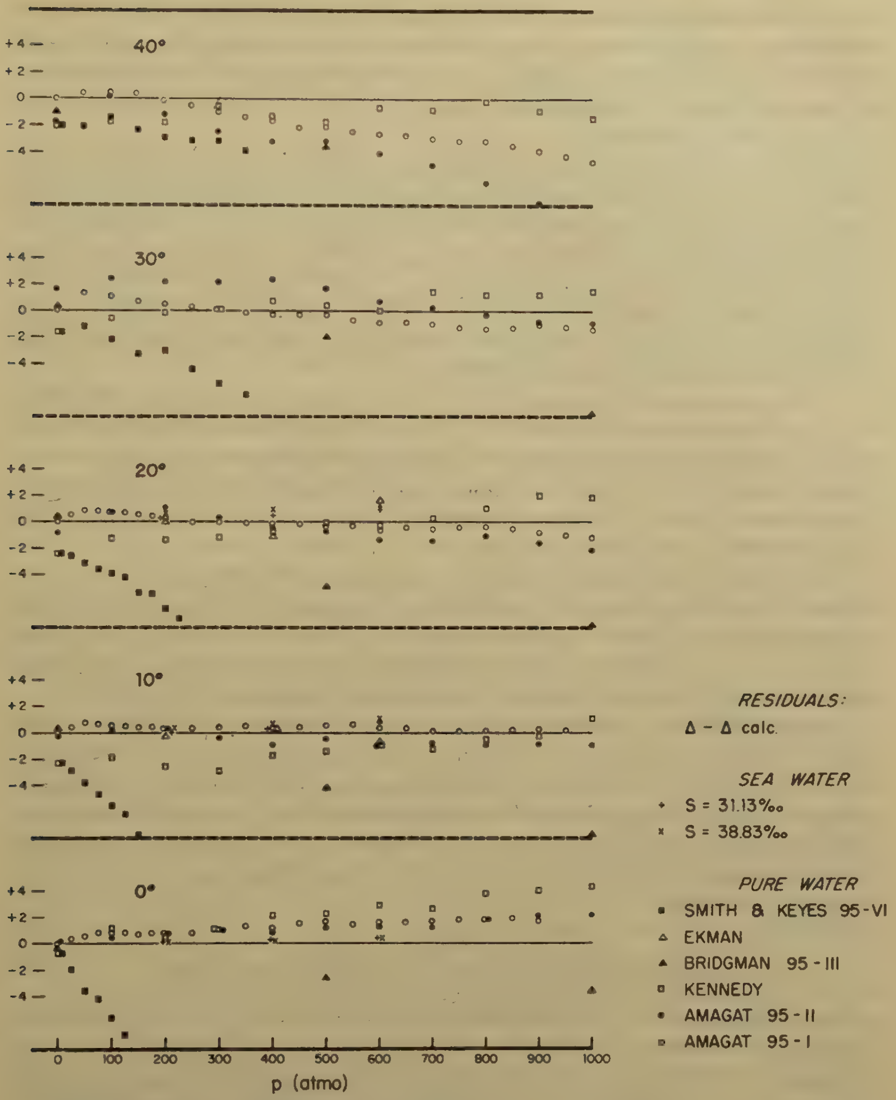

Fig. 8. Differences between observed and calculated values of $\Delta = 10^{-4}(1\text{–}v)$: various observers; Eqs. (3), (13), (16) and (17).

readers of the manuscript, and has been checked to make certain that it is not due to any arithmetic mistakes.

The systematic errors thus disclosed affect the slope of the isotherms, and may be estimated at about $\pm$ 2p x 10^{-7} ml/gm. In adition, there are more or less random errors in the data, which may be estimated at ± 2 x 10^{-4} ml/gm. There are also errors in the spacing of the isotherms, which are not disclosed by figure 8, but are treated below. These estimates of error are not very certain, and are likely to prove optimistic.

7. *The Thermal Expansion.*—The isothermal compressibility, being essentially the slope of the isotherms, is not influenced by errors in their spacing. The systematic pressure errors affect it in a manner that is roughly independent of pressure. It may be estimated that these errors in the compressibility are between 0.5 and 1.0 percent.

The coefficient of thermal expansion is essentially $a = (\partial v/\partial T)_p$, and is thus very sensitive to spacing errors. The existence of such errors is implied both by the errors in the compressibility and in p_0 and K. To investigate them, a was calculated in two ways: once using the linear Eq. (14) and once using the quadratic Eq. (15). The value of $\Delta_0 = 3020$ was used in both calculations, and interpolation of the values of K was avoided. This made it certain that the values of a at 1 atmosphere would be the accepted ones. The results of these calculations are given in table 2.

It is seen that the values at 20°C are uncertain by 3 to 5 percent at elevated pressures, while those at T = 0°C are much more seriously in doubt. This can perhaps be remedied by additional experimental work at closely spaced values of T. However, unless the precision of the compressibility measurement can be increased, not all of the error in the spacing of the isotherms will be eliminated by this.

It would be desirable to develop experimental techniques for the more or less direct measurement of a at elevated pressures. It is also possible that other methods of fitting algebraic formulae to the data would yield better values of a, but it is very doubtful whether much improvement of the present values can be achieved by modified calculational procedures alone.

The coefficient of thermal expansion is needed for the calculation of the ratio of specific heats, γ. It is known $\gamma - 1$ is proportional to a^2, so that this quantity will also be seriously in doubt at low temperatures and elevated pressures. The velocity of sound is proportional to $\gamma^{1/2}$; since a is small, the proportionate error in γ will be small. However, the adiabatic temperature gradient is proportional to $(\gamma - 1)/a$, i.e., to a. This quantity is therefore seriously in doubt.

TABLE 2

Thermal expansion, $10^5 a$, calculated in two ways

(a in cm^3 gm^{-1} deg^{-1})

p atm.	T = 0°		T = 20°	
	Linear Eq. (14)	Quadratic Eq. (15)	Linear Eq. (14)	Quadratic Eq. (15)
1	−6	−6	21	21
100	−4	−3	22	23
500	+3	+8	26	26
1000	9	19	31	30

SEA WATER

1. *The Data.*—The specific volume of sea water at elevated pressures has been determined only once, by V. W. Ekman (1908). The measurements were

all made on two halves of a single sample of sea water, one half having been diluted with distilled water, the other concentrated by evaporation. No investigation of the validity of this procedure was made. The original publication contains only values of the apparent compressibility (see above). Values of the specific volume calculated by Ekman "as directly as possible from the compressibilities measured, using the necessary additional data from Amagat and Martin Knudsen" were published[5] as Table C in Bjerknes and Sandström (1910). The need for Amagat's data has been indicated above. Knudsen (1902) measured the thermal expansion of sea water of various salinities at atmospheric pressure; Bjerknes and Sandström, in their Table B, converted this data "from the relative measure employed in the course of the experiments to the values (of specific volume) in absolute units"—i.e., presumably to cm^3/gm.

Dorsey's Table 108 gives the density of sea water at one atmosphere, for various temperatures and salinities; he comments that this table is "derived from a table by J. A. Beattie (1928) based primarily on the data given by M. H. C. Knudsen (1902) and J. Y. Buchanan (1875) but with a consideration" of a voluminous literature. These two tables have been compared in a cursory fashion: they seem to agree to about one half unit of Δ. It may therefore be supposed that the use of Bjerknes and Sandström's Table B will not introduce errors as great as those resulting from Ekman's reliance on Amagat's 0°C isotherm for the calculation of his pressures.

Bjerknes and Sandström in their Table C give values of v for p approximately 1, 200, 400 and 600 atmosphere, various values of T, and two values of the salinity: $S = 31.13$ and 38.53 gm/kg. The values of v are given to 0.01 unit of Δ: Dorsey (1940) copies this table as his Table 109, but rounds the figures to 0.1 unit of Δ. According to the above considerations, the accuracy of these data can hardly be greater than the accuracy of those for pure water.

Current oceanographic conventions require that densities and specific volume be calculated (from field measurements) to 0.1 unit of Δ; they are sometimes calculated to 0.01 unit. These conventions are not realistic, and should be reexamined, for necessity as well as for realism.

2. *The Interpolation Equation for Sea Water.*—There are thus, at most, four points on each isotherm for each of the two salinities. A test of the Tumlirz equation is barely possible by the above procedure, since one of the four points would be sacrificed as the standard. This can be avoided by averaging Eq. (4) over $p_1\ \Delta_1$, obtaining

$$(p-\overline{p})\ \Delta_0 - (\Delta - \overline{\Delta})\ p_0 = (p\Delta - \overline{p\Delta}). \qquad (18)$$

If the revised definitions

$$x = (p - \overline{p})/(p\Delta - \overline{p\Delta}), \qquad (19)$$

$$y = (\Delta - \overline{\Delta}/(p\Delta - \overline{p\Delta}), \qquad (20)$$

are used, each of the straight lines is defined by four points, and yields a

---

[5] Dorsey copies this table as Table 109 of his book; however, the pressures are in error: they should be increased by 1. atmosphere. The error arises from the oceanographic convention that p denotes "sea pressure," caused by overlying water, exclusive of the atmospheric pressure acting on the sea surface.

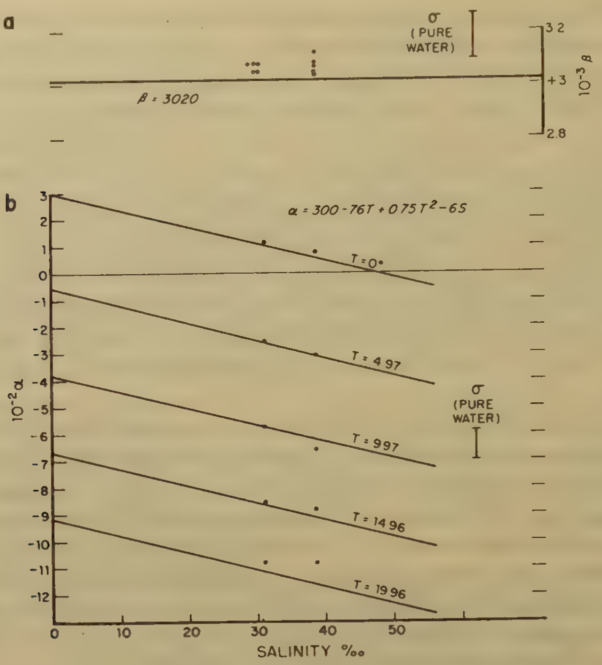

Fig. 9. Values of α and β, Eq. (9), for sea water of two salinities.

slightly less meager test of the equation. While not conclusive, this test is not inconsistent with the use of the Tumlirz equation for sea water.

Values of α and β were determined by least squares from the values of ξ, η so obtained. These are plotted as figure 9. The values of β, for all values of the temperature and the two values of salinity, all lie within one standard deviation of the value for pure water. One therefore concludes that $\beta = \Delta_0$ is independent of salinity as well as independent of temperature; obviously this conclusion should not be extrapolated to higher salinities without further study.

The values of α show a systematic downward trend with salinity. The total decrease is not more than three standard deviations, but recurs for each temperature. It may therefore be concluded that

$$\alpha = 300 - 76T + 0.75T^2 - 6S, \tag{21}$$

$$p_0 = 5890 + 38T - 0.375T^2 + 3S. \tag{22}$$

The agreement between this formula and the empirical values of α is shown on figure 9b.

Finally, by using the values of v at atmospheric pressure, from Bjerknes and Sandström, Table B, values of K were computed. To a sufficient approximation, these are given by

$$10^{-6}K = 17.795 + 0.1125T - 0.000745T^2 - (0.0380 + 0.0001T)S. \tag{23}$$

The ultimate test of these formulae is, of course, the study of $\Delta - \Delta_{\text{calc.}}$ for sea water. These values have been included on figure 8. It is seen that they are of the same order of magnitude as those for pure water. Possibly one may conclude from this that the specific volume of sea water is known to the same precision as that of pure water at 0°C. Certainly Ekman's experimental work is of high quality, and is internally consistent within narrow limits. However, his measurements were made at very few points, and have not been repeated by others. Under these conditions, the presence of unsuspected systematic errors cannot be excluded, and Eq. (22) and (23) should be used cautiously. They are uncertain, but no more so than the much more elaborate equations currently in use.

CONCLUSIONS

1. The isotherms of pure water are adequately represented by Eq. (1) in the temperature range 0° to 40°C and pressure range 0 to 1000 atm.
2. In this range, v_o is a constant, independent of temperature T, insofar as this can be determined by a statistical examination of the data.
3. In this range, p_o and λ are quadratics in T; the statistical significance of the quadratic term in p_o is very low, however.
4. Additional experimental work, at closely spaced values of T, will be required to determine the variation of p_o more precisely.
5. The random errors in the experimental specific volume determinations are not less than $\pm 2 \times 10^{-4}$ ml/gm; systematic errors, increasing with pressure, are not less than $\pm 2p \times 10^{-7}$ ml/gm.
6. The empirical isotherms of sea water are adequately represented by Eq. (1), in the same range of temperature and pressure as above, and in the salinity range 0 to 40 gm/kg.
7. In this range, v_o is independent of salinity as well as of temperature.
8. In this range, p_o and λ are linear functions of S, insofar as this dependence can be deduced from the data. The statistical significance of the variation of p_o is not great.
9. Additional experimental work is needed to establish the dependence of p_o and λ on salinity with adequate precision.
10. The errors in the experimental specific volume determinations of sea water, both random and systematic, are not less than in the corresponding measurements for pure water, and the systematic errors may be greater.
11. The systematic errors in the P-v-T data render the isothermal compressibility of water and sea water uncertain by 0.5 to 1.0 percent. Their effect on the coefficient of thermal expansion is considerably greater, especially at low temperatures and high pressures; e.g.: at $S = 0$, 0°C and 1000 atm., the thermal expansion may be 9 or 19×10^{-5} per degree, depending upon the interpretation of the data.
12. Current oceanographic conventions require that densities and specific volumes be calculated (from field measurements) to 0.1 unit of Δ; they are sometimes calculated to 0.01 unit. These conventions are not realistic, and should be reexamined, for necessity as well as for realism.

REFERENCES

Amagat, E.-H., 1893, Mémoires sur l'élasticité et la dilatabilité des fluides: Ann. de Chim. et Phys., ser. 6, v. 29, p. 68-136, 505-574.

Beattie, J. A., 1928, Int. Crit. Tables. Vol. 3: National Research Council, Washington, D. C., p. 100-101.

Bjerknes, V., and Sandström, J. W., 1910, Dynamic meteorology and oceanography, part I: Carnegie Institution of Washington, Pub. No. 88, p. 1-146.

Bridgman, P. W., 1913, Thermodynamic properties of liquid water: Amer. Acad. Arts and Sciences Proc., v. 48, p. 309-362.

Buchanan, J. Y., 1875, On the determination, at sea, of the specific gravity of sea water: Roy. Soc. London Proc., v. A23, p. 301-308.

Dorsey, N. E., 1940, Properties of ordinary water substance: Amer. Chem. Soc. Monograph Series (Reinhold, N. Y.). This work will be cited simply as "Dorsey".

Ekman, V. W., 1908, Die Zusammendrueckbarkeit des Meerwassers, nebst einigen Werten fuer Wasser und Quecksilber: Conseil Permanent pour l'exploration de la Mer, Publications de Circonstance No. 43, p. 1-47.

Gibson, R. E., and Loefler, O. H., 1941, Pressure-volume-temperature relations in solutions, V: Amer. Chem. Soc. Jour., v. 63, p. 898-906. This publication does not contain the numerical values, which are on deposit at the Library of Congress as Document 1496.

Kennedy, G., 1957, Properties of water I. Pressure-volume-temperature relations in steam to 1000 C and 100 bars pressure: AM. JOUR. SCI., v. 255, p. 724-730.

Knudsen, M., 1901, Hydrographical Tables according to the measurings of Carl Forch, J. P. Jacobsen, Martin Knudsen, and S. P. L. Sorensen: Copenhagen and London, Luno.

——————, 1902, Berichte über die Konstantenbestimmungen zur Aufstellung der hydrographischen Tabellen von Carl Forch, Martin Knudsen, and S. P. L. Sorensen: Mémoires de l'Académie Royale des Sciences de Danemark, ser. 6, no. XII-1 p. 1-151.

——————, 1903, Berechnung der hydrographischen Tabellen und Diskussion der Ergebnisse: Wissenschaftliche Meeresuntersuchungen herausgegeben von der Komission zur Untersuchung der deutschen Meere in Kiel, Band 2.

Tumlirz, O., 1909, Die Zustandsgleichung der Flüssigkeiten bei hohem Drucke: Wien Akad. Wissensch., Sitzungsberichte, Math.-Naturwiss. Kl., v. 118A, p. 203.

THE UNIVERSITY OF CALIFORNIA
SCRIPPS INSTITUTION OF OCEANOGRAPHY
LA JOLLA, CALIFORNIA
JULY 18, 1957

[Reprinted from Journal of Chemical Education, Vol. 35, Page 116, March, 1958.]

Copyright, 1958, by Division of Chemical Education, American Chemical Society, and reprinted by permission of the copyright owner

THE PROCESSES REGULATING THE COMPOSITION OF SEA WATER[1]

EDWARD D. GOLDBERG
Scripps Institution of Oceanography,[2] University of California, La Jolla

The present day composition of sea water reflects a multiplicity of chemical processes, both of an inorganic and biochemical nature. Although at the present time it is difficult to account for the absolute concentrations of most elements in the oceans, nevertheless, the dominant processes governing the distribution of chemical species between the hydrosphere and the lithosphere, biosphere, and atmosphere can be described. The importance of such considerations is evident not only in studies of the role of the oceans in the major sedimentary cycle and in the productivity of the oceans, but also in the construction of hypotheses concerned with the changes in the composition of the marine environment with time.

The ultimate sources of the chemical species found in the oceans are the igneous rocks and the gases released from the interior of the earth through heating of magmas (*1*). The former give rise to the cations while the volatile substances have condensed to furnish the water and many of the anions including chloride, sulfate, bicarbonate, and borate. The elemental abundances in the source materials provide a necessary background for investigating the facility of sea water to maintain its composition. Table 1 illustrates the striking differences in composition between these source materials and the sea water.

TABLE 1
The Composition of Sea Water, Igneous Rocks, and Gases from Fumaroles and Hot Springs (Values in Weight Percentages)

Substance	*Sea water*	*Igneous rocks (2)*	*Gases from fumaroles, steam wells and geysers (1)*
H_2O	97.5	~1	99.4
Na	1.05	2.8	....
K	0.04	2.5	....
Mg	0.13	2.0	....
Ca	0.04	3.5	....
Cl	1.9	0.03	0.12
S	0.09	0.05	0.03

It is convenient to divide the mechanisms that regulate the chemical composition of sea water into two general classes: those inorganic reactions that would occur in a sterile ocean and the reactions that arise through the existence of living matter. The inorganic reactions can in general be treated under conditions of equilibrium. It is generally believed that the bulk of ocean waters (approximately 90% of sea water exists at depths of 1000 meters or greater and at temperatures a few degrees above 0°C.) have been inaccessible to interactions with the atmosphere or sedimentary deposits for times of the order of hundreds of years. During such periods one can reasonably expect the inorganic chemical species to correspond closely to those expected from complete equilibration between all reacting substances. The first group of regulatory processes to be considered would occur in an ocean devoid of life.

INORGANIC PROCESSES

Solubility. Only calcium, among the major cations of sea water, is present in the state of saturation, and its concentration is controlled by the precipitation of calcium carbonate (*3*). The rare gases and dissolved gaseous nitrogen have their marine concentrations determined by the temperature at which their water mass was in contact with the atmosphere and are apparently in states of saturation or very nearly so. Mixed waters of warm and cold origins often contain these gases in the state of supersaturation inasmuch as mixing must of necessity lead to such a condition.

Cation Exchange and Mineral Formation. The factors that regulate the amounts of sodium, potassium, and magnesium, as well as other members of the alkali and alkaline earth metals, which are not limited by their solubility products, are to a large extent related to the cation-exchange properties of the clay minerals which have amassed upon the sea bottom (*4*). In general cation-exchange reactions are such that sodium will be replaced by potassium which in turn will be removed by magnesium. As a rule, the higher the valence of the ion, the greater its replacing power. Further, smaller ions of the same valence are held less tightly in the clay holes than the larger ions for similar conditions of ionic strength, temperature, and clay type.

Table 2 shows the relative weight ratios of sodium, potassium, and magnesium in igneous rocks, rivers and lakes, and marine waters. Both potassium and magnesium are depleted relative to sodium in river waters and this is attributed to the preferential uptake of these ions by exchange reactions upon the river solids. In the oceans magnesium remains in solution to a much higher degree than potassium and this result may be explained by the ability of clays to fix cations into nonexchangeable or difficultly exchangeable sites. It is

---

[1] Presented as part of the Symposium on Chemistry of the Sea before the Division of Chemical Education at the 131st Meeting of the American Chemical Society, Miami, April, 1957.

[2] This work was performed under contracts between the University of California and the Office of Naval Research. Contribution from the Scripps Institution of Oceanography, New Series, No. 981.

Reproduced by Permission

TABLE 2
The Distribution of Sodium, Potassium, and Magnesium in Geologic Domains
(Values on a Weight Basis Relative to Sodium)

Domain	*Na*	*K*	*Mg*
Igneous rocks	100	39	71
Terrestrial waters	100	36	59
Sea water	100	3.8	12

well known that illitic, and to a lesser extent montmorillonitic, clays build potassium into "fixed" positions rather readily. Further, chloritic micas and illites tend to form during marine diagenesis from other minerals (Ref. (*4*), p. 352).

Additional evidence that the cation-exchange reactions determine the marine concentrations of the elements of the first group of the periodic table has been pointed out by Goldschmidt (*5*). From geochemical balance computations the percentages of the amount of each alkali metal that remains in sea water, calculated from the amounts introduced into the major sedimentary cycle by the weathering of igneous rocks, can be calculated. It appears that about 65% of the sodium released now resides in solution whereas but 2.5%, 0.15%, and 0.025% of the total amounts of potassium, rubidium, and cesium that entered the hydrosphere have remained there. Such a trend follows the cited relationship between retentivity in clays and atomic radii.

Sorption Processes. The metals which are enriched in pelagic sediments relative to manganese, nickel, cobalt, zinc, copper, etc., exist in sea water in greatly unsaturated states (*6*, *7*, *8*) and it has been postulated that absorption reactions are responsible for this situation (Table 3). Two components of the pelagic deposits, the ferromanganese minerals and the apatites, apparently are the hosts for the major portion of these accumulations. The latter group of minerals is related to life in the sea and will be treated below.

TABLE 3
Comparison of Observed Concentrations of Certain Minor Elements in Sea Water with Those Concentrations Calculated upon the Basis of Their Most Insoluble Compound (*7*, *8*)

Ion	*Observed sea water concentration (M)*	*Limiting compound*	*Calculated limiting concentration (M)*
Mn^{++}	4×10^{-8}	$MnCO_3$	$\sim 10^{-5}$
Ni^{++}	4×10^{-8}	$Ni(OH)_2$	$\sim 10^{-3}$
Co^{++}	$\sim 10^{-8}$	$CoCO_3$	$10^{-6} - 10^{-7}$
Zn^{++}	2×10^{-7}	$ZnCO_3$	$\sim 10^{-4}$
Cu^{++}	6×10^{-8}	$CuCO_3$	$\sim 10^{-4}$

The ferromanganese minerals are a three-layer structure with the outer layers consisting of manganese dioxide and an inner, disordered layer of manganous hydroxide hydrate or ferric hydroxide hydrate (*9*). Substitution of the Group B metals for the ferric and manganous ions in the inner layer can occur, and Goldberg (*6*) found a whole array of such metals in such minerals in minor amounts. The ferromanganese minerals occur as components of the sedimentary deposits or as the major minerals in the so-called "manganese nodules."

Manganese exists as the divalent ion in marine waters but is found in the sediments in tetravalent as well as divalent states. Inasmuch as there is enough oxygen in all levels of the open ocean to allow oxidation to occur, the fact that it doesn't suggests a surface is necessary for the reaction. The well-known catalytic properties of iron oxides, coupled with the usual presence of large amounts of iron in these manganites, indicate that ferric oxides may supply the important initial active surface and that following a buildup of a few layers of the minerals, the reaction becomes autocatalytic. The formation of an irregular pile of these quasi-2-dimensional layer crystals allows the formation of large specific surface areas, of the order of 100 meters 2/gram (*9*), which provide sites for further accumulation and formation of the minerals as well as the incorporation of the minor elements. Table 4 shows the typical concentrations of some elements in manganese nodules and pelagic clays from the Pacific Ocean, and comparison with the corresponding abundances in igneous rocks readily illustrates the scavenging ability of the ferromanganese minerals.

TABLE 4
The Composition of Manganese Nodules and Pelagic Clays from the Pacific Ocean
(Concentrations in Parts per Million by Weight)

Element	*Manganese nodules*	*Pelagic clays*	*Igneous rocks*
Mn	193,000	12,500	1000
Ni	3,800	260	40
Co	2,600	160	20
Zn	500	200	50
Cu	4,800	740	40

Anion Exchange and Mineral Formation. Inasmuch as the anion-exchange capacities of illites and chlorites are but slightly less than the corresponding cation-exchange capacities, fractionation of the anionic species in marine waters through such processes is suggested. For example, Correns (*10*) points out that the Cl/Br ratio in sea water of 300 is displaced to values around 50 in sediments. Phosphate ion is strongly taken up by marine sediments (*11*). Such interactions may well result from the replacement of anions in clays. It is difficult to estimate the importance of anion exchange as a regulating mechanism due to the meager amount of data on the anionic composition of marine sediments and the lack of a suitable set of abundances for the amounts of such constituents introduced into the oceans.

BIOCHEMICAL PROCESSES

Primary Production. The introduction of living matter is reflected in changes in the chemical composition of all waters of the oceans. The presence of the large photosynthesizing biomass, roughly equivalent in production of organic matter to that of the terrestrial environment, is responsible for the most dramatic compositional changes in ocean water. In the surface waters where plant production occurs, carbon dioxide and oxygen, the intake and release gases of photosynthesis, respond to this biological activity. Depletion of the former and supersaturation of the latter are often observed in waters near the surface.

Certain nutrients, chemical species necessary to the growth and multiplication of the plants of the sea, vary over wide ranges of concentrations both in time and

(106)

space. Phosphate, nitrate, nitrite, ammonia and silicate ions show very low values in regions of plant productivity as compared to higher values in the deeper waters removed from photosynthetic activity. Further, decreases in the abundances of these ions coincide with the rises in plant populations during the late spring and early fall for given areas of ocean. Certain other substances concerned with plant growth, such as vitamins and some trace metal ions, may have their marine concentrations regulated by photosynthesis in the surface waters of the oceans, but as yet no such relationships have been established.

The primary production of plant material furnishes the basis of nutrition for the animal domain of the oceans. That plant material removed from the photosynthetic zones and not consumed by higher organisms, coupled with the organic debris resulting from the metabolic waste products or death of members of the biosphere, is oxidized principally in the deeper oceanic waters. This results not only in minimal values of dissolved gaseous oxygen in waters at intermediate depths, but also in maximal concentrations of inorganic phosphorus, nitrogen, and silicon compounds released simultaneously with the combustion of the organic matter.

Other Biological Processes. Arrhenius, Bramlette, and Picciotto (*12*) have established the uptake of heavy metals from sea water by bone debris which consists of microcrystalline apatite and the proteinaceous decay products. The accumulation apparently takes place after the death of the organisms and most probably at the sediment-water interface. The apatite acts as host for the rare earths, thorium, strontium, and barium, whereas the organic phases are enriched in zinc, tin, lead, titanium, copper, silver, magnesium, chromium, and nickel. These apatites, along with the ferromanganese minerals, are high-surface materials and both are responsible for the depletion of trace metals in sea water. The relative importance of each of these two processes is as yet unknown.

The oceanic concentrations of copper and barium are apparently strongly influenced by biological activity (*8*). The relationship between copper and manganese in sediments containing ferromanganese minerals is much less distinct than between nickel, cobalt, or zinc and manganese. This observation suggested other independent sources of copper-containing materials to the ocean floor. The well-known combination of copper with the organic molecules in the protein hemocyanin and the exceedingly strong ability of copper to complex with most organic functional groups pointed to biological origins. It was thus not surprising to find copper in the organic phases of fish debris (*12*). Further, copper in excess of the amounts attributed to ferromanganese minerals showed a remarkable covariance with barium, the latter element presumed to be dominantly associated with organic phases, in 400 samples of pelagic clays investigated by Revelle and co-workers (*13*).

PHYSICAL PROCESSES

Superimposed upon these chemical processes are changes in the chemical makeup of sea water by the melting of ice, evaporation, mixing with runoff waters from the continents, upwelling of deeper waters, etc. The net effects of the first three processes are changes in the absolute concentration of all of the elements but with no changes in the relative amounts of dissolved ions. Where solubility products are exceeded, as may be the case of the dissolved gases and calcium, changes in concentration not proportional to salinity are evident. In the cases of upwelling, the non-conservative nutrient elements, as well as the dissolved gases, will undergo concentration changes not related to the salinity.

CHANGES IN COMPOSITION OF THE OCEANS WITH TIME

If the chemical species in marine waters are today in a steady state with respect to concentrations, a not indelicate balance must exist between the various regulatory mechanisms. Any changes in the input of materials must be compensated by like changes in accumulation of matter on the ocean floor. Further, alterations of those parameters controlling the various inorganic and biochemical processes can readily influence the composition of ocean waters. It is upon such a basis that one may fruitfully seek out possible compositional changes in ocean waters with time. Two recently published papers involve possible changes in the temperatures of the oceans in geologic times. The concurrent changes in the chemical composition of the seas are evident.

Emiliani (*14*), from studies on the oxygen isotopic composition of the tests of *benthic foraminifera*, has suggested that the abyssal temperatures in the oceans were raised from their present values of near 0°C. to 2.2°C., 7.0°C., and 10.4°C. in the upper, middle, and lower Tertiary respectively. Such temperature increases would of necessity be accompanied by similar ones in the surface and intermediate waters. One obvious effect from such a heating of the oceans is the decrease in either or both the calcium and carbonate ions, since calcium carbonate's solubility product has a negative temperature coefficient. Further, the amounts of dissolved gases would decrease. It is easy to envisage changes in primary productivity, in the combustion of the remnants of the biosphere, in clay formations, etc., and concurrent changes in the nutrient and conservative chemical species as a function of such a temperature change.

More direct changes in the abundances of the oceanic constituents with time are available. Worthington (*15*) finds decreases in the dissolved oxygen contents of the North Atlantic deep waters of the order of 0.3 ml./l. (total dissolved oxygen is of the order of 6 ml./l.). He attributes this phenomenon to the origin of the waters containing the higher oxygen values (i.e., contact and equilibration of gases with the atmosphere) during the catastrophic cold from 1810 to 1820.

Changes in the chemical and mineral composition of sediments from the Northeast Pacific between the Quaternary and Tertiary have been reported (*8*, *13*). Higher contents of manganese and calcium are found in the older strata of such deposits and result from the presence of ferromanganese minerals and authigenic phillipsite, a zeolite with high ion-exchange capacities. The qualitative inference that such changes in the character of the ocean bottom were accompanied by at least minor changes in some of the ions of the ocean appears plausible.

LITERATURE CITED

(1) Rubey, W. W., *Bull. Geol. Soc. Am.*, **62**, 1111 (1951).
(2) Fleischer, M., *Geol. Survey Circular*, **285**, 4–5 (1953).
(3) Wattenberg, H., *Geol. Meere*, **1**, 237 (1937).
(4) Grim, R. E., "Clay Mineralogy," McGraw-Hill Book Co., Inc., New York, **1953**, p. 127.
(5) Goldschmidt, V. M., "Geochemistry," Oxford University Press, London, **1954**, p. 56.
(6) Goldberg, E. D., *J. Geol.*, **62**, 249 (1954).
(7) Krauskopf, K. B., *Geochim. et Cosmochim. Acta*, **9**, 1 (1956).
(8) Goldberg, E. D., and G. O. S. Arrhenius, *ibid.*, in press (1957).
(9) Buser, W., and A. Grutter, *Schweiz. mineral petrog Mitt.*, **36**, 49 (1956).
(10) Correns, C. W., "Physics and Chemistry of the Earth," McGraw-Hill Book Co., Inc., New York, **1956**, Vol. I.
(11) Carritt, E., and S. Goodgal, *Deep-Sea Research*, **1**, 242 (1954).
(12) Arrhenius, G., M. N., Bramlette, and E. Picciotto, *Nature*, **180**, 85 (1957).
(13) Revelle, R., M. N. Bramlette, G. Arrhenius, and E. D. Goldberg, *Geol. Soc. Am., Spec. Papers*, **No. 62**, 221 (1955).
(14) Emiliani, C., *Science*, **119**, 853 (1954).
(15) Worthington, L. V., *Deep-Sea Research*, **1**, 246 (1954).

UNITED STATES DEPARTMENT OF THE INTERIOR, Fred A. Seaton, *Secretary*
FISH AND WILDLIFE SERVICE, Arnie J. Suomela, *Commissioner*

HIGH-SPEED PLANKTON SAMPLER

By Elbert H. Ahlstrom, John D. Isaacs, James R. Thrailkill,
and Lewis W. Kidd

March 3, 1849

FISHERY BULLETIN 132

From Fishery Bulletin of the Fish and Wildlife Service

VOLUME 58

UNITED STATES GOVERNMENT PRINTING OFFICE • WASHINGTON : 1958

For sale by the Superintendent of Documents, U. S. Government Printing Office
Washington 25, D. C. - Price 50 cents

ABSTRACT

A high-speed plankton sampler is described, and performance tests are discussed in this paper. The sampler was designed to supplement, and, in certain cases, to supersede standard plankton nets. The sampler is so constructed that it can be fastened to the towing cable at any point, hence samplers can be used in series to sample different depth levels simultaneously. The samplers are towed at normal ship's speed between hydrographic stations; each sampler obtains a horizontal strip sample of the plankton at the level at which it is hauled. The usual length of haul has been 10 miles. The depth sampled and the amount of water filtered by a sampler during a haul are recorded on a strip of 35-millimeter acetate film. Tests were made to determine the comparative effectiveness of high-speed samplers and standard 1-meter plankton nets in delimiting the distribution and abundance of fish eggs and larvae. Both types of gear seem to be equally effective in delimiting the horizontal distribution of eggs and larvae. Standard nets are more versatile in depth sampling, as they can be operated to any desired depth; high-speed samplers have been operated only between about 60 meters deep and the surface, when hauled at normal ship's speed. The most marked advantage of high-speed samplers over conventional gear is that samples obtained with the former are far more representative of the mean density of plankton organisms.

CONTENTS

Page

Historical review 187

Description of high-speed sampler 189

Tests 190

- Spacing of samplers on towing wire 190
- Plankton volumes 193
- Sardine catches 195
- Anchovy catches 197
- Jack-mackerel catches 201
- Lantern fish catches 201
- Other fish catches 204

Evaluation 204

Appendix I: Operating instructions 207

Appendix II: Calibration 207

Literature cited 213

HIGH-SPEED PLANKTON SAMPLER

By E. H. AHLSTROM, *U. S. Fish and Wildlife Service*, JOHN D. ISAACS,[1] *Scripps Institution of Oceanography*, JAMES R. THRAILKILL, *U. S. Fish and Wildlife Service*, and LEWIS W. KIDD,[1] *Scripps Institution of Oceanography*

Because of the diversity in size, motility, and distribution of plankton, there is no one type of plankton sampler yet devised that can obtain a fully representative sample of all organisms in the water. Every type of plankton collector is selective in one way or another. Samples obtained with plankton-collecting gear may be classified, on the basis of distance covered in obtaining the samples, into two principal categories: spot samples and strip samples. Each has its limitations and its advantages. The conventional 1-meter plankton net used in a standard oblique tow is hauled only a short distance, seldom more than ¼ mile; hence it is regarded as a spot sampler.

The Isaacs high-speed sampler, to be described in this paper, was designed to supplement the information obtained with conventional 1-meter nets. At the time of its development, the California Cooperative Oceanic Fisheries Investigations (then the California Cooperative Sardine Research Program) was just getting under way. The plan of operation under the program was to cover a widespread grid of hydrographic stations approximately 40 miles apart. It was desired to construct a collecting device that could obtain information on plankton distribution by taking a strip sample while the ship was running full speed ahead between stations.

HISTORICAL REVIEW

A pioneer in the development of high-speed plankton sampling gear is A. C. Hardy. He has devised two instruments, one known as the Hardy Plankton Recorder, the other as the Hardy Plankton Indicator. The latter is a simple, non-quantitative instrument designed for on-the-spot assays of plankton samples. It has been widely used by fishermen in the North Sea herring fishery and by scientists (Hardy 1936a; Barnes 1951).

The Hardy Plankton Recorder (Hardy 1936b, 1939) has proved to be a successful high-speed plankton sampler. It was first used during the Discovery Expedition to the Antarctic in 1925–27. It was designed to take a continuous sample over distances as great as several hundred miles. It has been operated from both research and commercial vessels. Only one recorder is towed at a time, ordinarily at a depth of about 10 meters and a vessel speed of 8 to 16 knots. The forward end of this collector is provided with a small opening, about 1¼ inches square, which may be reduced to ½ inch square or even less. The water, after entering the instrument, flows through a wide tunnel across which is stretched a band of silk or nylon gauze. The gauze band is slowly wound across the water tunnel into a chamber where it is stored in a bath of formalin. The spooling mechanism is geared to an external propeller that is actuated by the passing water, hence the spooling is in direct relation to the distance traveled. The recorder gives a continuous line of ecological observations across an area being investigated; furthermore, since the straining band is graduated into numbered divisions, it is possible to identify any portion of the sample as to approximate location of collection. This unique feature of the Hardy Plankton Recorder makes it particularly useful for certain kinds of ecological studies. Hardy Recorders are being used by us in a study of the relation between the distribution of plankton organisms and adult sardines. The most serious disadvantages of the instrument are (1) its lack of versatility in operation, since it is designed for towing at a single depth near the surface, and (2) the difficulty of identifying the organisms caught, since they are crushed when rolled up in the filtering band.

---

[1] Contribution from the Scripps Institution of Oceanography, New Series, No. 982. This work represents in part work carried out for the Marine Research Committee of the State of California and in part work carried out by the Office of Naval Research and the Bureau of Ships under contract with the University of California.

NOTE.—Approved for publication April 23, 1957. Fishery Bulletin 132.

Reproduced by Permission

A simple type of high-speed collector was employed by personnel of the South Pacific Fishery Investigations of the U. S. Fish and Wildlife Service from the purse seiner *Pearl Harbor*, during April to June, 1946 (Smith and Ahlstrom, 1948). The idea for the collector was suggested by the work of Hardy. The cruises were made off central California, primarily to explore for sardines with echo-ranging equipment. The collector consisted of three parts: a brass towing head, a cylindrical net, and a plankton bucket (ibid., fig. 11). The towing head, shaped somewhat like an inverted funnel, was 1 inch in diameter at the mouth, expanding to 2 inches before the point of attachment of the net; the cylindrical net was 2 inches in diameter by 10 inches long, and was constructed of No. 56xxx grit gauze; the plankton bucket was the more or less standard type used for limnological work.

Most samples were obtained by towing the net at 9 knots, for a period of 20 minutes. Not only did the collector tow well at this speed, but plankton organisms were taken in fair numbers and were in excellent condition. In all, 54 samples were obtained. The analyses of the samples, including the percentage composition (by volume) of the major constituents and the distribution of fish eggs and larvae, are discussed by Smith and Ahlstrom (1948).

The results from this initial high-speed collector were so encouraging that an experimental model of a high-speed volumetric plankton sampler was built (Ahlstrom and Smith, MS.). The collector consisted of four detachable parts: a weighted forward section, a metering device, a cylindrical net, and a metal plankton bucket. The forward section, constructed of bronze, was cylindrical except for a slight taper at the forward nose: the mouth opening was 1 inch in diameter with the inner bore widening gradually to 2 inches; this section provided weight (15 lbs.) and was equipped with diving vanes and multiple attachment points. The metering section, about 1 foot long, contained an impeller and worm gear in the main tube, with the gear train of the current meter underneath. It was provided with three tail fins, with the streamlined meter box acting as a fourth. All parts were made of bronze. The cylindrical net was fastened to the "metering" section of the sampler. Nets of several lengths (10 to 24 inches) and of several mesh sizes (No. 24xxx, 40xxx and 56xxx silk grit gauze) were tried and all worked effectively. The plankton bucket was of the type used with the Clarke-Bumpus net (1950). The device was used to collect more than 150 samples during two cruises off Baja California in 1948 (Ahlstrom and McHugh, MS.).

The Ahlstrom-Smith sampler had a number of good qualities. It was easy to operate, since it could be launched or retrieved with the same ease as a bathythermograph, and was towed on the bathythermograph cable. It had good towing qualities, keeping a steady course without yawing. The plankton was recovered in excellent condition. The metering device could be accurately calibrated, and gave consistent readings when in use at sea. The mouth opening preceded the cable. This is not difficult to arrange if the sampler is attached to the end of the cable. The disadvantages of the sampler were as follows: (1) at normal vessel cruising speed it could be towed only at shallow depths, perhaps not greater than 10 meters, (2) no record was obtained of the actual depth traversed by the sampler, and (3) it was not possible to use several samplers on the same cable at one time. This type of high-speed sampler is excellent for reconnaissance work.

To overcome these disadvantages, while retaining desirable features, Isaacs and associates developed the high-speed collectors described in this paper. The qualities that the investigators sought to incorporate in the high-speed sampler described in this paper are the following:

Good towing characteristics: The sampler has been so designed that bridles are not necessary, and the mouth opening precedes the towing wire, thus eliminating water disturbance in front of the sampler; the sampler keeps a steady horizontal position without yawing while being towed at 8 to 10 knots.

Simple method of attachment: A method of fastening to the towing cable has been devised that permits attachment at any desired position on the cable, and also permits the use of any desired number of samplers at one time (in order to sample several depth layers simultaneously).

Suitable depressing force: A suitable depressing force is needed to get samplers down to desired depths; an excellent depressor has been designed, that has proven useful with many types of oceanographic gear.

Quantitative measurement of water strained: A measure of amount of water strained by each sampler has been accomplished by incorporating an impeller, gear train and recording device into the design of the sampler.

Record of depth sampled: A record of the depth traversed by a sampler has been made possible by incorporating a pressure-sensitive bellows with attached stylus. A permanent record of depth against flow is obtained on acetate film.

Plankton material should be recoverable in good condition: The high-speed sampler meets this requirement.

Rugged construction: High-speed gear must be ruggedly constructed to withstand the continuous vibration of the towing cable when hauled at high speed. A well designed sampler should operate for 100 hours or more before adjustments are needed. Ruggedness was a major consideration in the design of the Isaacs high-speed sampler.

Low cost: It is highly desirable that high-speed samplers be inexpensive, both in initial cost and maintenance. Our sampler is a fairly expensive instrument. However, the cost of the sampler could be considerably reduced if made in larger quantities. Also it is not necessary that every instrument be equipped with a depth-flow meter.

One desirable feature of the Hardy Plankton Recorder that we have not been able to incorporate into our high-speed sampler is a continuous record of plankton. Our sampler obtains an integrated sample over the distance hauled rather than a continuous line of observations.

DESCRIPTION OF HIGH-SPEED SAMPLER

The high-speed sampler is a streamlined metal tube containing a plankton filter and depth-flow meter (fig. 1). When assembled for operation, the sampler has an over-all length of 130 centimeters, a basic diameter of 7.6 cm. and a weight of 17.3 pounds (7.7 kg.). It is attached to a towing cable by means of a spherical brass clamp and socket.

The sampler is composed of three parts: an outer casing, a plankton filter, and a depth-flow meter.

The outer casing tapers from its basic diameter of 7.6 cm. to a mouth opening of approximately 2.5 cm. The anterior half of the casing is divided longitudinally to accommodate attachment to the towing cable some distance behind the mouth of the sampler. Three radially arranged stabilizing fins are attached to the rear section of the casing. A protective bumper at the back edge of the divided section protects both the towing cable and the tube. An experimental sampler which was not provided with the bumper almost severed the cable during a trial run, whereas samplers with the bumper have not injured the cable after many tows.

The plankton filter consists of two sections, the body or straining section, and a cod-end cup. The detachable straining section is made of Monel metal mesh having about 23 mesh openings to the centimeter (each opening 0.24 mm. across and 0.33 mm. on the diagonal). The straining section

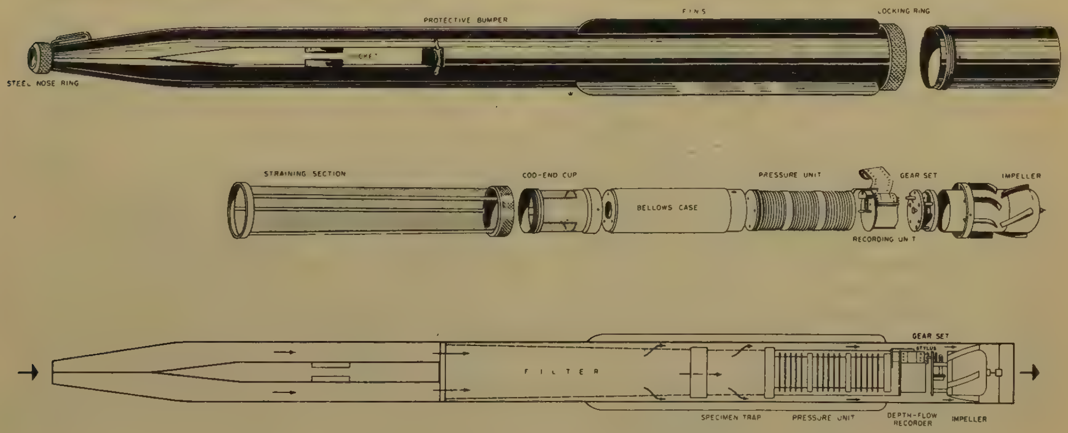

FIGURE 1.—Exploded schematic drawing of high-speed plankton sampler.

has an over-all length of approximately 36 cm.; it is supported by a brass ring at either end, and by three strengthening ribs. The cylindrical brass cod-end cup (specimen trap) is 10.5 cm. long by 5.2 cm. in diameter; two windows, approximately 5.0 cm. square, are cut out of the sides of the cup, and fitted with fine Monel metal screens (39 mesh openings to the centimeter). The cod-end cup is attached to the bellows case.

The plankton filter retains the plankton organisms in the water column entering the sampler. In present models, water is filtered at a rate of ⅙ to ¼ cubic meter per minute at 8 to 10 knots towing speed. The actual filtering rate is dependent, to some degree, on the extent of clogging of the filter by plankton organisms.

The depth-flow meter consists of three sections: a pressure unit with attached stylus, a metering unit (impeller and gear set), and a recording unit. The pressure unit makes use of bellows originally designed for the bathythermograph, which are available in different depth ranges. One type is effective to depths of 180 feet (approximately 55 meters), another to 450 feet (137 m.), and a third to depths of 900 feet (274 m.). The latter has not been used as yet with the present high-speed samplers. The bellows is housed in a brass tube. An L-shaped brass stylus is attached to the back end of the bellows.

The metering unit consists of an impeller and gear set enclosed in a brass housing. The impeller has a coaxially attached shaft which is supported at the ends in low friction bearings. Incorporated in the forward end of the shaft is a worm gear, which meshes with a gear in the gear set. The gear set is contained in a brass cylinder immediately forward of the impeller.

The recording unit is housed between the pressure unit and the gear set. It consists of a sprocket geared to the metering unit which advances a roll of 35-mm. clear acetate film. The stylus atached to the bellows produces a scratch on the 35-mm. film, recording depth of operation against quantity of water filtered. The film supply is sufficient for a one-hour tow at 10 knots when using one gear ratio, six hours when using another. After calibration, towing depths and quantity of water strained may be readily estimated by simple analysis of the record (calibration procedures are discussed in appendix II.).

TESTS

In May 1950, five high-speed samplers were tested during a regular cruise of the California Cooperative Oceanic Fisheries Investigations (cruise 5005, formerly numbered cruise 14). The tests took place in an area between Point Conception, Calif., and Point Descanso, Baja California. Standard 1-meter net hauls were made at 46 stations (Ahlstrom 1952). The high-speed samplers were towed between stations, most of which were spaced at 40-mile intervals.

Net hauls on station were taken with a standard plankton net of 1.0 meter in diameter at the mouth by approximately 5 meters in length, constructed of No. 30xxx grit gauze, a sturdy grade of Swiss bolting silk. The hauls were made obliquely from approximately 70 meters deep to the surface; a distance of approximately ½ mile was covered while making each tow.

Two series of high-speed hauls, each utilizing four samplers, were made when traveling between most stations. Locations of high-speed sampler hauls are shown in figure 2. The first series was begun immediately upon leaving a station. A depressor and three of the four samplers were attached and lowered at approximately half speed; after attachment of the fourth sampler the ship's speed was increased to normal cruising speed (approximately 10 knots), and an additional 150 to 180 meters of cable was payed out. The samplers were then towed for one hour, and retrieved.

SPACING OF SAMPLERS ON TOWING WIRE

The amount of towing cable that must be payed out to establish a sampler at a desired depth depends upon several factors, among which the following are probably the more important: amount and kind of depressing force; type and weight of the towing cable; speed of hauling; height of the boom above the water; number of samplers being hauled simultaneously.

It was possible to maintain three factors constant throughout the test operations. A ¼-inch rope-laid stainless steel towing cable was used for each test; the boom was maintained at a constant height (approximately 20 ft.) above the water; and four samplers in a series were used per tow. Only the remaining two factors could not be kept constant: (1) vessel speed of 10 knots was usually

(116)

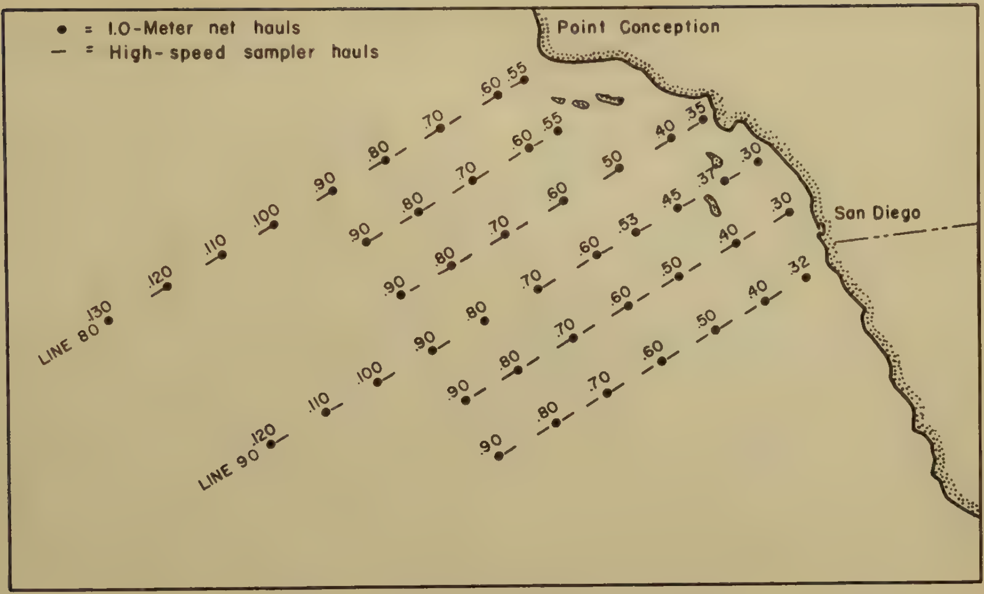

FIGURE 2.—Location of plankton hauls on cruise 5005.

maintained, but the speed varied somewhat with changing sea conditions and could not be considered constant; (2) owing to the loss of a depressor midway through the cruise, it was necessary to substitute a depressor with somewhat different depressing characteristics.

To determine the length of towing cable required to place a sampler at given depths, a single sampler was towed at normal cruising speed (10 knots) on the following lengths of towing cable: 15, 30, 50, 80, 130, 200, 300, and 450 meters. The sampler was placed approximately 6 meters above depressor. The data are summarized in table 1, and graphically presented in figure 3.

TABLE 1.—*Depths fished by a single high-speed sampler towed at a constant speed (10 knots) with selected lengths of towing cable*

Length of towing cable (meters)	Depth fished by sampler	Wire angle at vessel from vertical
	Meters	*Degrees*
15	6	-------
30	11	65
50	16	72
80	19	76
130	25	78
200	33	80
300	39	81
450	48	82

The use of several samplers instead of one changed the curve slightly; the exact spacing of samplers on the cable to obtain desired towing depths of 10, 20, 30, and 40 meters below the surface was determined by trial and error. As shown in table 2 and figure 4, the spacing that placed the four samplers at desired depths of 10, 20, 30, and 40 meters was as follows: 10 m. of cable between the depressor and the first sampler, 15 m. between the first and second samplers, 45 m. between the second and third, 80 m. between the third and fourth, and 150 m. between the fourth sampler and the ship. These trials were made with the first depressor at regular vessel speed of 10 knots.

To sample the same depths, when using the second depressor, it was necessary to change the spacing, as shown in table 3, to the following: 5 meters between the depressor and first sampler, 20 m. between the first and second samplers, 45 m. between the second and third samplers,. 80 m. between the third and fourth samplers, and 180 m. between the fourth sampler and the ship. A fairly constant angle of 82° (from the vertical) was obtained with both depressors when the samplers were fishing at the desired depths and the ship was traveling at 10 knots (fig. 5).

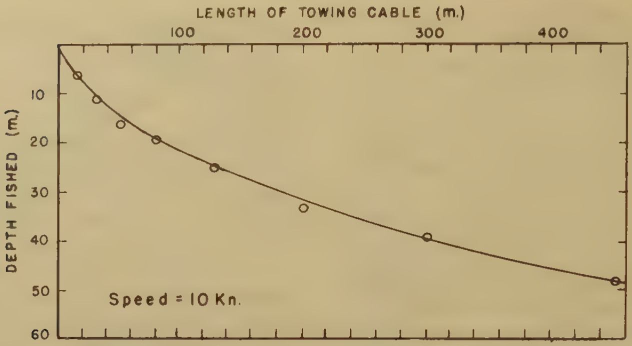

FIGURE 3.—Depths fished by a high-speed sampler with selected lengths of towing cable.

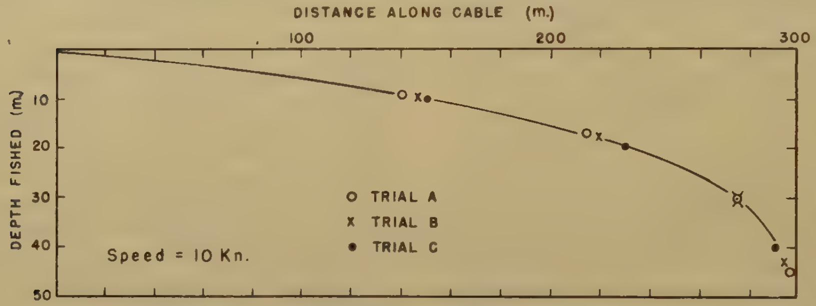

FIGURE 4.—Depths fished by four samplers at different spacings along towing cable.

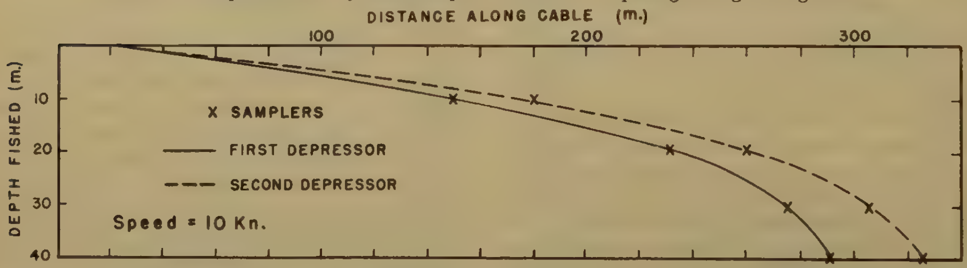

FIGURE 5.—Spacings required to place four samplers at depths of 10, 20, 30, and 40 meters when two different depressors were used.

TABLE 2.—*Depths fished by four samplers at different spacings along towing cable*

Sampler number	Trial A			Trial B			Trial C		
	Spacing between samplers	Length of towing cable	Depth fished	Spacing between samplers	Length of towing cable	Depth fished	Spacing between samplers	Length of towing cable	Depth fished
	Meters	*Meters*	*Meters*	*Meters*	*Meters*	*Meters*	*Meters*	*Meters*	*Meters*
		300			300			300	
	3			6			10		
1		297	45		294	43		290	40
	22			19			15		
2		275	30		275	30		275	30
	60			55			45		
3		215	17		220	18		230	20
	75			73			80		
4		140	9		147	9		150	10
	140			147			150		

TABLE 3.—*Spacing required to place four samplers at depths of 10, 20, 30, and 40 meters when two different depressors were used at cruising speed of 10 knots*

Sampler number	First depressor			Second depressor		
	Spacing between samplers	Length of towing cable	Depth fished	Spacing between samplers	Length of towing cable	Depth fished
	Meters	*Meters*	*Meters*	*Meters*	*Meters*	*Meters*
	10	300		5	330	
1		290	40		325	40
	15			20		
2		275	30		305	30
	45			45		
3		230	20		260	20
	80			80		
4		150	10		180	10
	150			180		

The three deeper samplers, as pointed out previously, were lowered and retrieved at half speed (5 knots). From an average of ten trials, using the first depressor, the following results were obtained: the total wire out was 150 m., the first sampler spaced 10 m. from the depressor, fished at 43 m.; the second sampler, 15 m. from the first, fished at 33 m.; and the third sampler, 45 m. from the second, fished at 13 m. (fig. 6). This shows the greater depth that can be attained at reduced vessel speed.

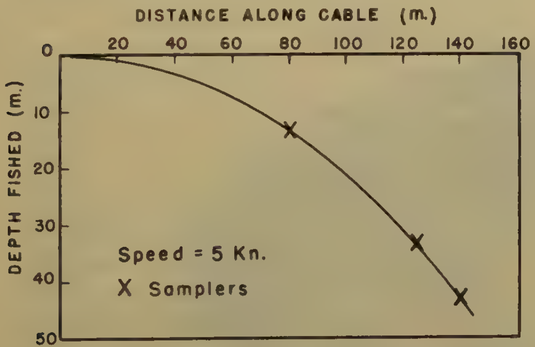

FIGURE 6.—Depths fished by three samplers towed on 150 meters of wire at ship's speed of 5 knots.

PLANKTON VOLUMES

Wet plankton volumes were determined for all samples obtained on cruise 5005. The plankton material obtained in 1-meter net hauls was standardized to the quantity in 1,000 cubic meters of water strained. This standard has been used in reporting all plankton volumes obtained on CCOFI cruises (Staff, South Pacific Fishery Investigations, 1952–56, Thrailkill, 1956).

The wet plankton volumes were determined for the individual catches obtained in high-speed samplers and standardized to the amount in 1,000 cubic meters of water strained. For comparability with standard net tows, the four plankton volumes of a series were averaged, and standardized to the amount in 1,000 cubic meters of water strained. The volumes of plankton in different parts of the area surveyed on cruise 5005, as determined by the two methods of collection, are shown in figure 7. Both methods revealed a similar outline of plankton distribution within the area. The largest individual volumes were taken by the standard 1-meter net; but a somewhat higher concentration of plankton throughout the entire area is shown in the catches of high-speed samplers. It should be noted that the two types of samplers are not entirely comparable for these reasons: (1) the standard net sampled a stratum from approximately 70 meters deep to the surface, while the high-speed samplers fished at four selected depths between 40 meters and the surface; (2) the mesh of the high-speed samplers was finer and hence retained a larger proportion of the smaller plankton material than the standard net.

The four levels sampled by high-speed samplers were found to differ in plankton density between day and night, as is shown in table 4. A similar volume of plankton was taken at all four levels during the night, but rather sharp stratification of plankton was noted during the daylight hauls, the density of plankton increasing with depth. Night hauls at 10 meters obtained a plankton volume three times greater than daylight hauls; at 20 meters twice as much plankton was taken; at 30 meters 1½ times; and at 40 meters 1¼ times as much was collected. At no level was as large a volume taken during daylight as at night. For all levels combined, the ratio of night to day was 1.75. The difference between night and day

TABLE 4.—*Comparison of plankton volumes taken at four selected depths by high-speed samplers (average plankton volume, in cc. per 1,000 m.^{3})*

Depth of sampler (meters)	All hauls	Day hauls	Night hauls	Night/day ratio
10	653	356	1,086	3
20	735	514	1,057	2
30	837	695	1,044	1.5
40	1,016	913	1,166	1.3
Average	810	619	1,088	1.75

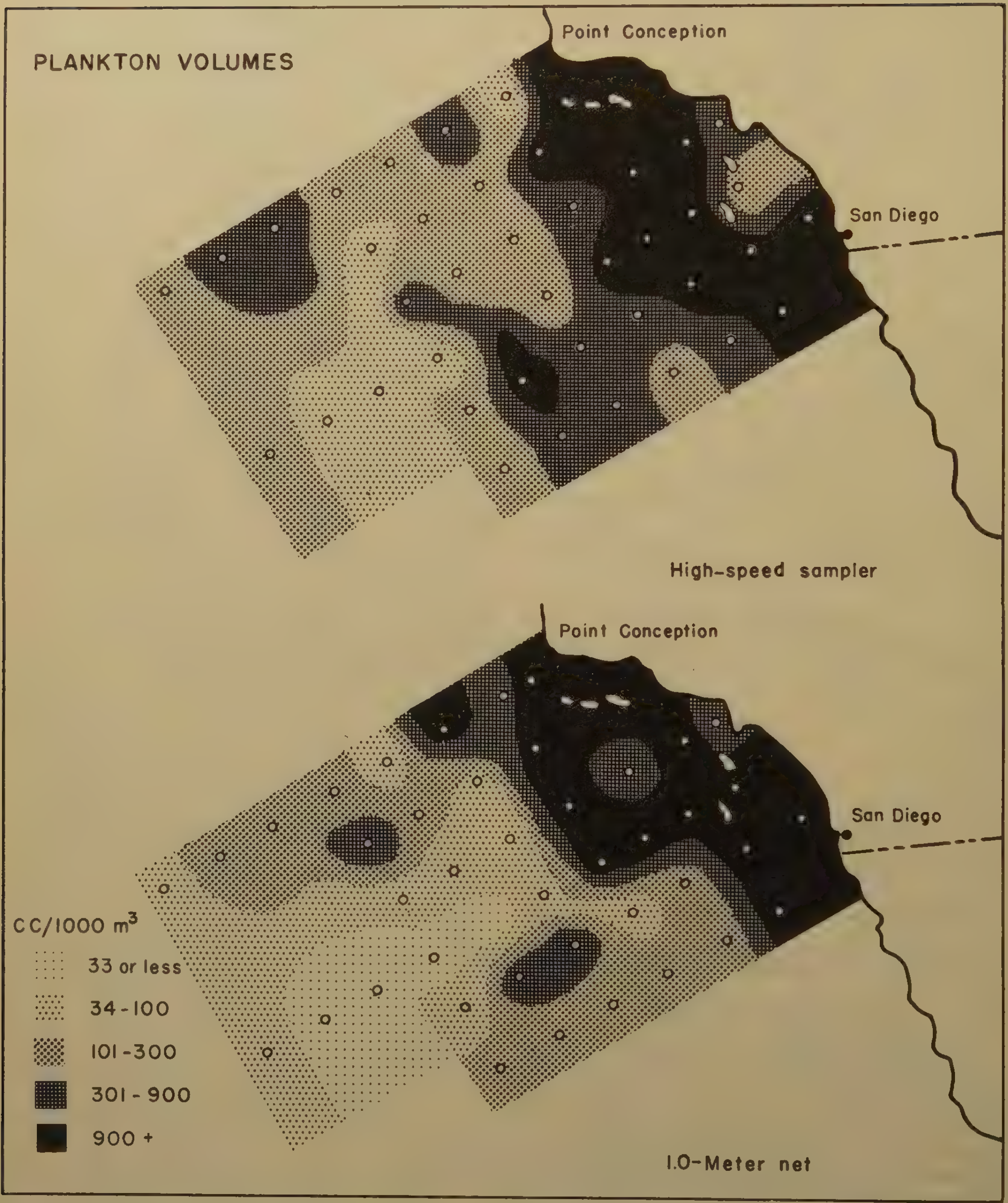
PLANKTON VOLUMES
Point Conception
San Diego
High-speed sampler
Point Conception
San Diego
1.0-Meter net
CC/1000 m³
33 or less
34-100
101-300
301-900
900 +

FIGURE 7.—Distribution of plankton volumes based on hauls made with high-speed samplers and with 1-meter net.

hauls in the levels sampled (0–40 m.) may be due to a downward migration of plankters out of the level by day, and an upward migration by night. Information of this type is not ordinarily obtained from routine hauls made with conventional nets.

Many plankton organisms tend to occur in swarms or patches. High-speed samplers obtain an average density relevant to greater distances (10 mi.) than is possible with conventional gear which samples a limited area only.

Because of the greater distance covered with high-speed samplers, it is possible to define average plankton abundance more precisely than has been possible in the past with conventional gear on similar cruise tracks.

SARDINE CATCHES

As has been indicated, the high-speed sampler facilitates the quantitative sampling of various eggs and larvae. The spawning and survival of the sardine in particular, in relation to oceanographic conditions, has been a major concern of the California Cooperative Oceanic Fisheries Investigations and is being studied on an extensive scale. The distribution and abundance of the eggs and larvae of the sardine, as well as those of the northern anchovy, jack mackerel, and lantern fish, found during cruise 5005, will be compared for the two types of gear.

Eggs.—A somewhat more extensive distribution of sardine eggs was obtained with the high-speed samplers than with conventional plankton nets, as shown in figure 8. Sardine eggs were taken at 10 stations with conventional plankton gear. They were present in one or both high-speed sampler hauls taken adjacent to these stations and, in addition, at four other stations.

The abundance of sardine eggs taken in the high-speed samplers was 3½ times greater than in the standard net hauls. Based on the high-speed samples, the estimated average number of sardine eggs spawned per day in this survey area was 642 billion eggs, as compared to 180 billion based on the standard net hauls.

Of particular interest is the sampling at and adjacent to station 97.40. At this station no sardine eggs were taken in the conventional net haul, but large numbers were taken in the high-speed sampler series made on either side of it. There can be little doubt that the sampling of sardine eggs with high-speed samplers was much more effective than with conventional gear when used to estimate the average density of eggs along cruise tracks.

Inasmuch as the high-speed samplers fished four different levels, the samples can be used to determine the level of occurrence of the largest concentrations of sardine eggs. The number of eggs (standard haul totals) taken at the different depth levels in 20 high-speed tows is shown in table 5.

TABLE 5.—*Depth distribution of sardine eggs as determined from high-speed sampler hauls*

Depth of sampler (meters)	Number of occurrences	Number of sardine eggs (standard haul totals)	Percent of total
10	16	2,741	39.9
20	13	1,541	22.4
30	14	1,350	19.6
40	13	1,246	18.1
Total		6,878	100.0

The largest number of sardine eggs collected, approximately 40 percent, were taken at the 10-meter level. The numbers taken at the 20-, 30-, and 40-meter levels were about equal. However, the depth distribution of the eggs varied greatly from series to series. The distribution between the samplers is shown in table 6 for the ten high-speed series in which most of the sardine eggs were taken.

TABLE 6.—*Depth distribution of sardine eggs in 10 high-speed sampler series*

Series taken adjacent to station numbered	Number of eggs taken (standard haul total)	Percentage of total taken at each level			
		10 meters	20 meters	30 meters	40 meters
		Percent	*Percent*	*Percent*	*Percent*
97.40a [1]	2,416	52	27	19	2
97.40b [1]	1,265	47	37	10	6
93.60	845	1	1	7	91
93.40a	676	33	16	37	14
87.60	312	32	36	29	3
90.60a	224	45	0	55	0
83.70	209	73	8	9	10
97.50	193	56	18	4	22
93.40b	161	27	0	40	33
90.60b	139	8	0	49	43

[1] When both high-speed sampler series taken adjacent to a station appear in this table, one of the series is designated a, the other b.

Larvae.—Sardine larvae, taken only in the lower half of the area surveyed, occurred mostly on the lines centering off San Diego. A somewhat wider distribution was indicated by collections taken with conventional gear than with high-speed samplers. Sardine larvae were taken at 12 sta-

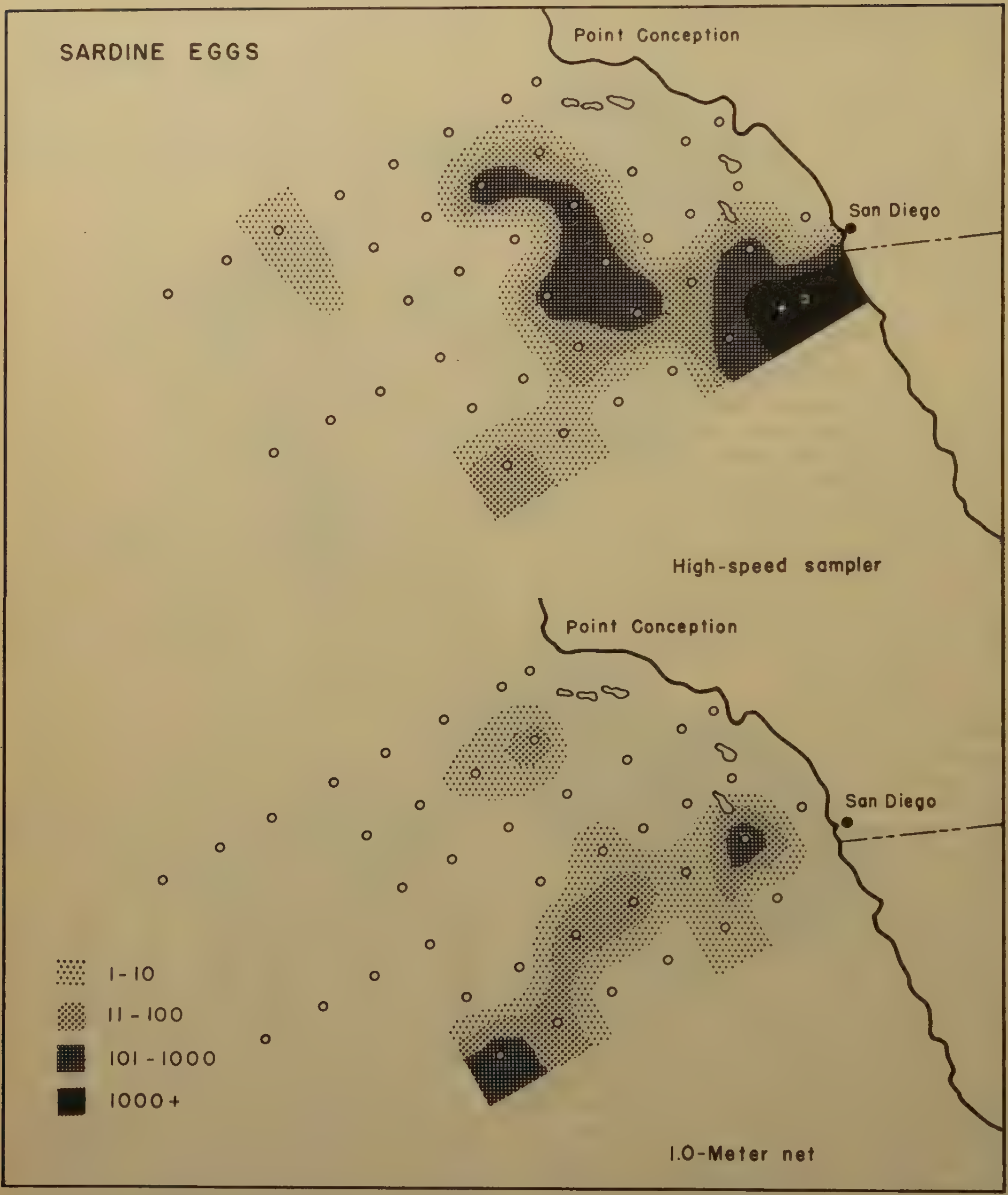
SARDINE EGGS
Point Conception
San Diego
High-speed sampler
Point Conception
San Diego
1.0-Meter net
1-10
11-100
101-1000
1000+

FIGURE 8.—Distribution of sardine eggs based on hauls made with high-speed samplers and with 1-meter net. The legend represents numbers per standard haul.

tions using conventional gear and adjacent to only 9 stations using high-speed samplers. The distributions obtained by both types of gear are shown in figure 9.

Census estimates of all sizes of sardine larvae in this area at the time of survey were similar for both types of gear: 477 billion for conventional gear as compared to 502 billion for the high-speed samplers. A comparison of the size of larvae taken by the two types of gear is shown in figure 10 and summarized in table 7. The smallest group size (2.5–5.0 mm.) and the largest group size (10.5 mm. and longer) were taken in slightly greater numbers by conventional gear, while larvae between 5.5 and 10.0 mm. long were taken in greater abundance by high-speed samplers.

Table 7.—*Abundance of sardine larvae, in billions, (census estimates) summarized by size group for 1-meter net hauls and high-speed sampler hauls*

Size of larvae (mm.)	High-speed sampler hauls	1-meter net hauls	Ratio, sampler/net
2.5–5.0	366	394	0.93
5.5–7.5	101	53	1.91
8.0–10.0	20	12	1.67
10.5 and larger	15	18	.83
Total	502	477	

These findings are, in part, contrary to expectation. It is known that the 1-meter net does not fully retain the smaller larvae, hence we would expect larger numbers of these sizes to be taken by the sampler. A possible explanation is that the 1-meter net hauls are influenced by local clumping of small sardine larvae, while the sampler catches are more representative of the mean density of these sizes.

The series of high-speed sampler hauls can be used to determine that depth within the 40-meter stratum at which sardine larvae occurred in greatest abundance. Numbers of larvae (standard haul totals) taken at the four depths sampled are tabulated in table 8. The largest number of larvae was taken at the 20-meter level. The concentration was 1.5 times as great as at the 10-meter level and nearly four times as great as at 30- and 40-meter depths. Approximately four-fifths of the larvae 8.0 mm. and longer were taken at the 20-meter level.

Table 8.—*Sardine larvae concentrations at four selected depths*

Depth of sampler (meters)	Number of larvae taken (standard haul totals)	Percent of total
10	274	29.8
20	422	45.9
30	116	12.6
40	107	11.7
Total	919	100.0

ANCHOVY CATCHES

Eggs.—Measuring only about 0.5 millimeters in their narrowest dimensions, anchovy eggs are not fully retained by our standard nets. In fact, a test conducted with a somewhat coarser mesh net than that now in use (No. 24xxx grit gauze with 0.9-mm. openings between threads when new, and shrinking to approximately 0.7 mm. after use) gave only about 1.5 percent as much retention as No. 40xxx grit gauze with pores of 0.40 mm. The net employed on cruise 5005 was constructed of No. 30xxx grit gauze, with 0.7-millimeter mesh openings when new, and approximately 0.55 mm. openings after use; this mesh retains only a small percentage of anchovy eggs. With the finer mesh used in high-speed samplers (openings 0.24 mm. across and 0.33 mm. on the diagonal) anchovy eggs were completely retained.

A census estimate of the abundance of anchovy eggs in the survey area gave 7,065 billion eggs, based on high-speed sampler hauls. The estimate based on net hauls was only 3.3 percent as large. Hence, the high-speed samplers proved effective in sampling anchovy spawning, while the conventional gear now in use is not effective for this purpose.

The depth distribution (within the upper 40-m. stratum) of anchovy eggs for hauls in which 100 or more eggs were obtained (standard number) is given in table 9. In the three hauls containing the largest number of eggs, the majority were taken below 20 meters. A portion of the eggs must have occurred below the levels fished by the high-speed samplers.

Larvae.—Anchovy larvae were taken at 10 stations with conventional gear, and adjacent to 13 stations with high-speed gear. The distribution obtained with the two types of equipment was similar; anchovy larvae occurred in a coastwise band about 125 miles wide.

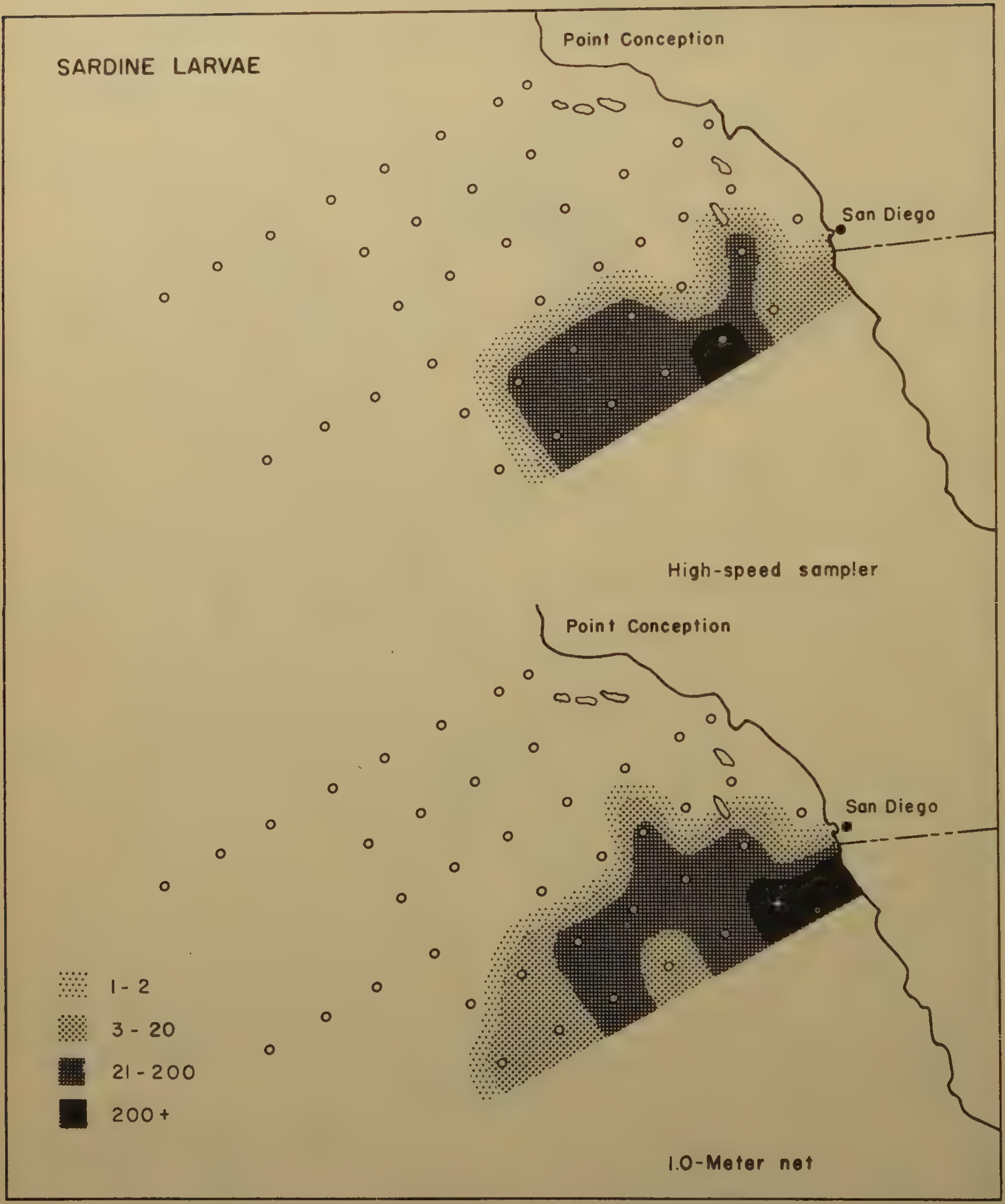
SARDINE LARVAE
Point Conception
San Diego
High-speed sampler
Point Conception
San Diego
1.0-Meter net
1 - 2
3 - 20
21 - 200
200 +

FIGURE 9.—Distribution of sardine larvae based on hauls made with high-speed samplers, and with 1-meter net. The legend represents numbers per standard haul.

(124)

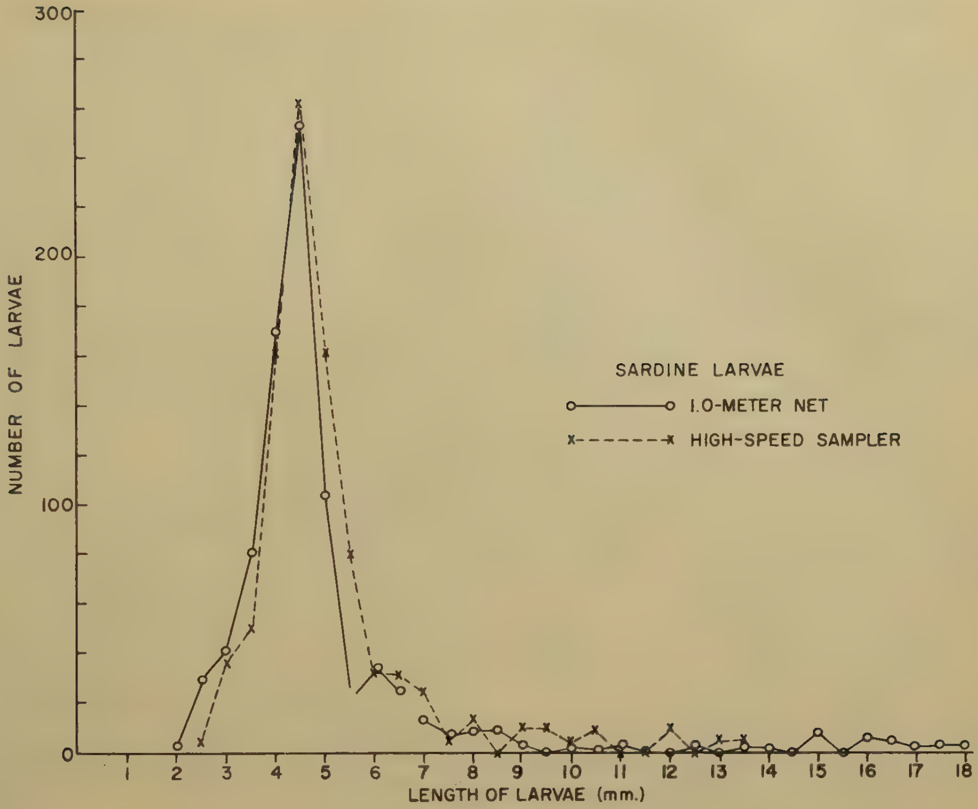

FIGURE 10.—Comparison of size composition of sardine larvae taken by high-speed sampler and 1-meter net.

TABLE 9.—*Depth distribution of anchovy eggs in 6 high-speed sampler series*

Series taken adjacent to station numbered	Number of eggs taken (standard haul total)	Percentage of total taken at each level			
		10 meters	20 meters	30 meters	40 meters
		Percent	*Percent*	*Percent*	*Percent*
93.50a [1]	15,200	2.1	2.4	56.7	38.8
93.50b [1]	8,432	3.3	2.5	8.7	85.5
93.40	1,076	3	3.3	37.1	56.5
93.30	201	60.7	39.3	0	0
90.37	183	91.8	0	8.2	0
97.50	113	8.8	37.2	35.4	18.6

[1] When both high-speed sampler series taken adjacent to a station appear in this table, one of the series is designated a, the other b.

Greater numbers of anchovy larvae were taken with high-speed samplers than with conventional gear. Census estimates of the number of anchovy larvae of all sizes in the area were more than three times as large when based on high-speed sampler collections as when based on standard net hauls: 2,156 billion as compared to 625 billion larvae. This reflects the larger numbers taken in individual hauls: nearly 2,900 anchovy larvae (standard number) were taken in one series of high-speed sampler hauls, while the largest number taken in a haul using conventional gear was 679. The size distribution of anchovy larvae taken by the two types of gear is shown in figure 11 and summarized in table 10.

TABLE 10.—*Abundance of anchovy larvae, in billions (census estimates), summarized by size group for 1-meter net hauls and high-speed sampler hauls*

Size of larvae (mm.)	High-speed sampler hauls	1-meter net hauls	Ratio, sampler/net
2.0–5.0	3,674	715	5.13
5.5–7.5	155	95	1.63
8.0–10.0	102	90	1.13
10.5–17.5	29	25	1.16
Total	3,960	925	

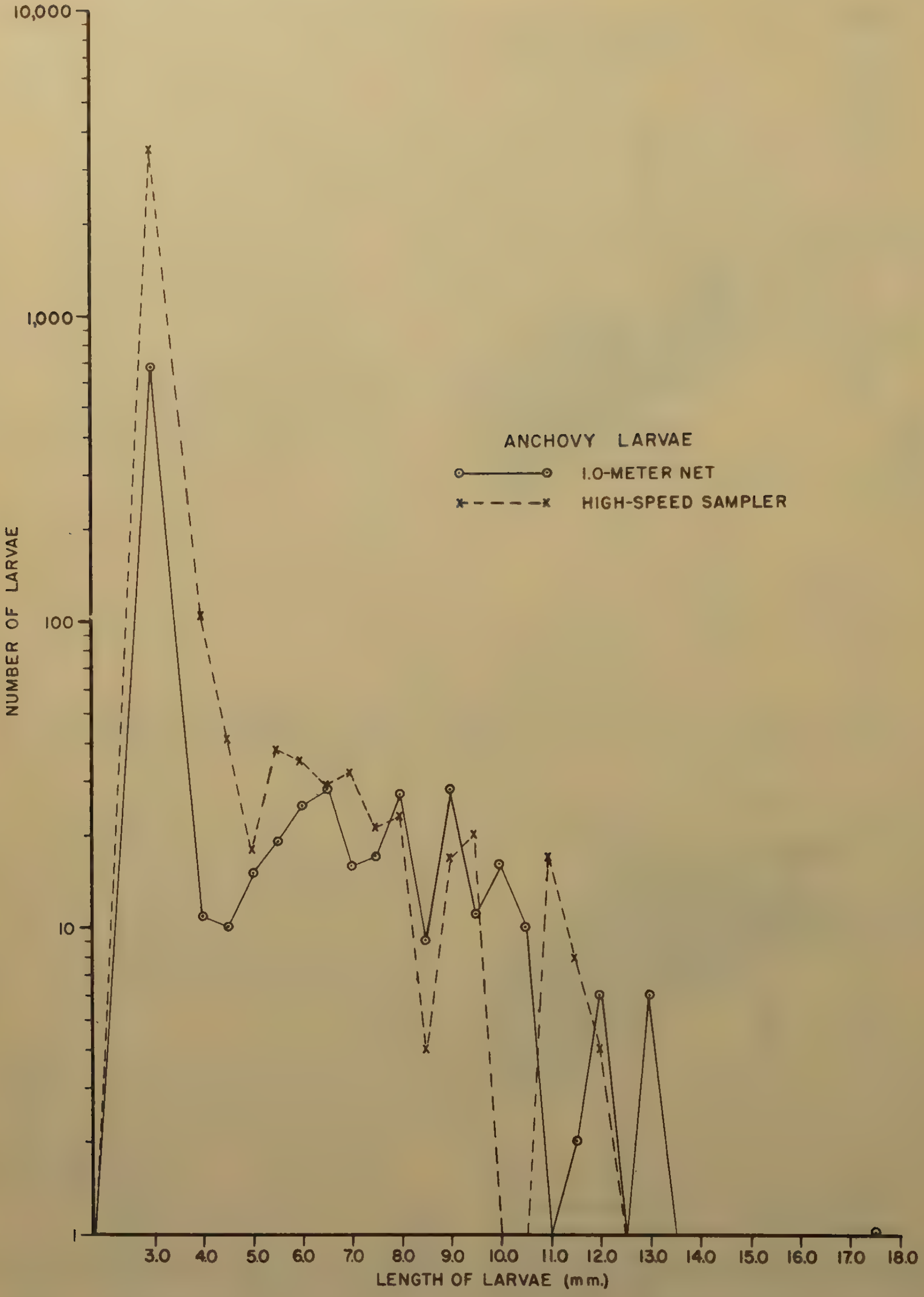

FIGURE 11.—Comparison of size composition of anchovy larvae taken by high-speed sampler and 1-meter net.

(126)

It is interesting to compare the numbers of larvae of different sizes taken by the two types of gear. More than five times as many of the smaller larvae, 2.0–5.0 mm. long, were taken in the high-speed sampler collections as in the net hauls. For larvae 5.5–7.5 mm. long, the ratio decreased to 1.63, and for larvae larger than 7.5 mm., the ratio was only slightly greater than 1. The much larger ratio of small larvae taken in high-speed sampler collections reflects, at least in part, the more complete retention of these sizes by the high-speed samplers. The Monel screen used in the high-speed samplers had pore openings of slightly less than one-fourth mm. wide, while the openings between meshes of 30xxx grit gauze used in the nets were slightly larger than one-half millimeter.

The largest concentrations of both anchovy eggs and larvae were taken at the 40-meter level in two adjacent hauls at station 93.50 representing the depth distribution at a particular locality under a specific set of conditions. In other studies of the depth distribution of anchovy eggs and larvae, eggs had not been taken in abundance as deep as 40 meters. However, at these stations there were probably many anchovy eggs and larvae below the depths reached by the lower sampler. The average depth distributions of anchovy eggs and larvae as determined from high-speed sampler hauls are summarized in table 11.

Table 11.—*Depth distribution of anchovy eggs and larvae as determined from high-speed sampler hauls*

Depth of sampler (meters)	Anchovy eggs		Anchovy larvae	
	Standard haul totals	Percent of total	Standard haul totals	Percent of total
10	941	3. 7	210	2. 7
20	741	2. 9	2, 393	30. 7
30	9, 845	39. 0	1, 820	23. 3
40	13, 742	54. 4	3, 377	43. 3
Total	25, 269	100. 0	7, 800	100 0

JACK-MACKEREL CATCHES

Eggs and larvae.—The eggs and larvae of the jack mackerel were more widely distributed than those of the sardine or anchovy, occurring throughout the area surveyed except near shore. The center of abundance was between 125 and 250 miles offshore. The distribution determined from high-speed samplers gives a more detailed picture than the distribution determined from net hauls (fig. 12).

Census estimates of the number of jack-mackerel larvae in the survey area at the time of the cruise gave 6,600 billion when based on high-speed sampler hauls, compared to 4,800 billion when based on standard net hauls. The difference may have resulted from better retention of larvae (3.0 mm. and smaller) by the high-speed sampler. Larvae more than 3.0 mm. in length are retained fully by both types of sampling gear.

Information on depth distribution of jack-mackerel eggs and larvae as determined from high-speed sampler series is summarized in table 12. Some material was probably below the nets in these series.

Table 12.—*Depth distribution of jack-mackerel eggs and larvae, based on high-speed sampler hauls*

Depth of sampler (meter)	Jack-mackerel eggs		Jack-mackerel larvae	
	Standard haul totals	Percent of total	Standard haul totals	Percent of total
10	16, 580	42. 5	3, 471	20. 2
20	9, 060	23. 2	6, 227	36. 2
30	6, 900	17. 7	4, 297	25. 0
40	6, 510	16. 7	3, 205	18. 6
Total	39, 050	100. 1	17, 200	100. 0

LANTERN FISH CATCHES

Larvae.—Larvae of the lantern fish *Lampanyctus leucopsarus* were taken throughout the survey area. They were obtained in all but two of the hauls made with conventional nets, and in 50 of the 59 series of hauls made with high-speed samplers. The distribution and abundance based on hauls made with high-speed samplers and with a 1-meter net is shown in figure 13.

Census estimates of the number of larvae of *L. leucopsarus* in the area at the time of cruise 5005 was 1,313 billion, based on high-speed sampler hauls, and 856 billion, based on 1-meter net hauls. Here again the difference may have been due to more complete retention of smaller larvae by the high-speed samplers.

There was an increase in abundance with depth, at least to the 40-meter level (table 13). Other studies made by the senior author have shown 40 meters to be the usual depth of greatest concentration, and some *Lampanyctus leucopsarus* larvae have been taken as deep as 100 meters. Hence, we may assume that larvae occurred below the level sampled by the high-speed nets.

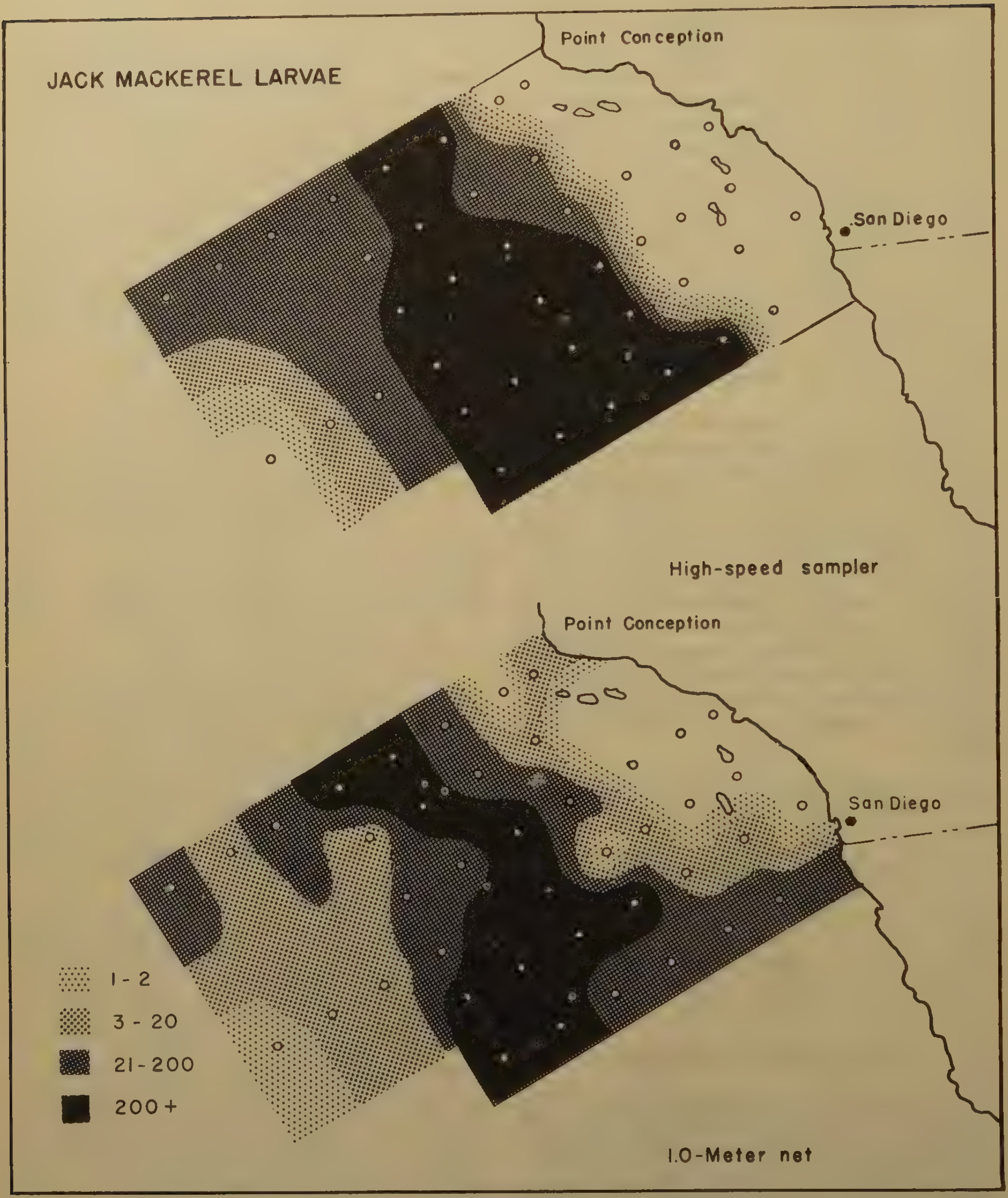
JACK MACKEREL LARVAE
Point Conception
San Diego
High-speed sampler
Point Conception
San Diego
1 - 2
3 - 20
21 - 200
200 +
1.0-Meter net

FIGURE 12.—Distribution of jack-mackerel larvae based on hauls made with high-speed samplers, and with 1-meter net. The legend represents numbers per standard haul.

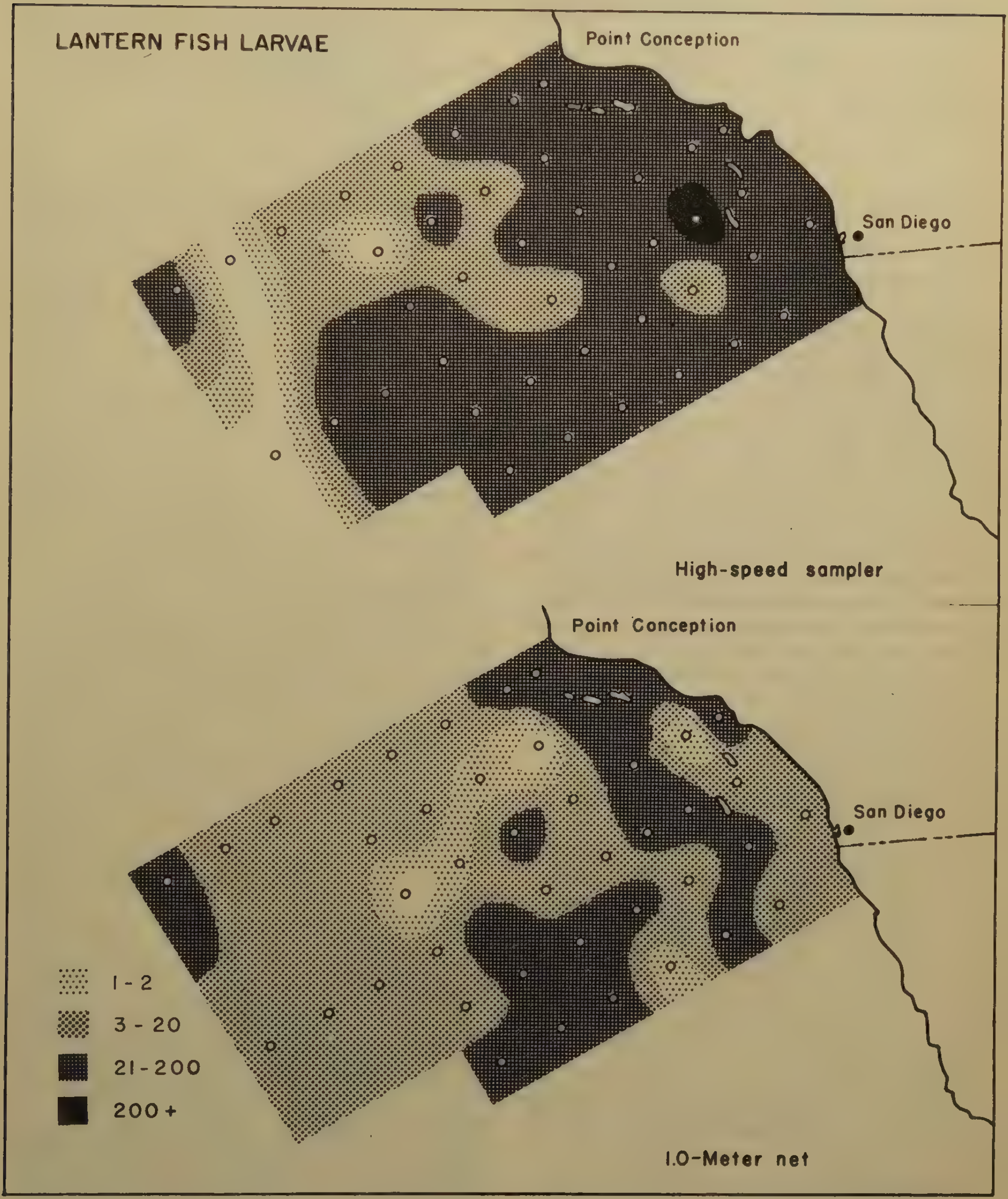
LANTERN FISH LARVAE
Point Conception
San Diego
High-speed sampler
Point Conception
San Diego
1-2
3-20
21-200
200+
1.0-Meter net

FIGURE 13.—Distribution of larvae of the lantern fish (*Lampanyctus leucopsarus*) based on hauls made with high-speed samplers and with 1-meter net. The legend is based on numbers per standard haul.

TABLE 13.—*Depth distribution of lantern fish larvae* (Lampanyctus leucopsarus), *based on high-speed sampler hauls*

Depth of sampler (meter)	Number of larvae taken (standard haul totals)	Percent of total
10	154	5.1
20	392	13.1
30	1,058	35.3
40	1,400	46.6
Total	3,004	100.1

OTHER FISH CATCHES

Small pelagic fish are occasionally taken at night in net hauls. Among those commonly caught are a number of species of lantern fish and some deep-sea smelts. Only a small fraction of the fish in the path of the net are caught, since most fish could easily avoid capture by the slow-moving standard gear. However, they have less chance of getting out of the path of the high-speed gear. This is clearly demonstrated by the fish taken during cruise 5005. Based on comparable volumes of water strained, approximately 30 times as many fish were taken in high-speed sampler hauls as with standard gear. This is a clear-cut demonstration of the greater efficiency of high-speed samplers as compared to standard nets in capturing the more agile organisms.

All fish taken with both types of gear were obtained between 8:00 p. m. and 4:00 a. m. probably as a result of the fish migrating upward for night feeding in the levels being sampled by our gear. The largest numbers were taken at 20 and 30 meters depth with high-speed samplers (table 14).

TABLE 14.—*Depths at which fish were taken in high-speed sampler hauls*

Depth of sampler (meter)	Number of fish taken (standard haul totals)	Percent of total
10	30	17.1
20	63	35.8
30	68	38.6
40	15	8.5
Total	176	100.0

The species of fish taken as juveniles or adults in both types of gear on cruise 5005 were as follows:

Myctophidae:
    Ceratoscopelus townsendi
    Diaphus theta
    Diogenichthys atlanticus
    Hygophum reinhardti
    Lampanyctus leucopsarus
    Lampanyctus mexicanus
    Notolychnus valdiviae
Gonostomatidae:
    Vinciquerria lucetia
Bathylagidae:
    Bathylagus wesethi
    Leuroglossus stilbius

EVALUATION

To sample organisms adequately, such as the larval stage of a fish, it is necessary to (1) delimit the range both horizontally and vertically; (2) obtain enough samples to estimate variation in density and (3) employ an instrument capable of quantitative measurement of water strained, retention of desired sizes (no loss of organisms through openings between meshes), capture of larger individuals in their relative proportion in the population, and in sufficient numbers for abundance and mortality estimates. The relative merits of high-speed samplers and of standard 1-meter plankton nets in fulfilling these requirements are evaluated in the following discussion.

Horizontal range.—Both types of gear seem to be equally effective in delimiting the horizontal distribution of plankton organisms. This was brought out in the discussion of the distribution of various fish eggs and larvae, as well as in figures and tables. These data are summarized in table 15. The high-speed sampler gave more information on the distribution of eggs, in the two species cited, than did the 1-meter net. The total occurrences for both eggs and larvae, however, are extremely close.

Vertical range.—High-speed samplers, used in a series, automatically give information on the distribution of organisms at the several depth zones sampled by the gear. Results of the previously discussed tests are summarized in table 16. From this information, it is obvious that the entire depth distribution of most species was not encompassed during cruise 5005 by these samplers. Hence, a somewhat deeper stratum should be sampled. It might be possible to sample as deeply as 60 meters using present equipment, but to exceed this would require changes in the depressing force and in the wire used. However, for the sardine and many other fish species, 60 meters probably would be deep enough for adequate quantitative sampling. For

(130)

some species, such as hake, this depth is not adequate.[2]

TABLE 15.—*Occurrences of fish eggs and larvae in 1-meter net hauls at stations as compared to occurrences in high-speed sampler hauls taken adjacent to stations*

Organism	1-meter net	High-speed sampler
Sardine eggs	10	14
Sardine larvae	12	9
Anchovy eggs	4	7
Anchovy larvae	10	13
Jack-mackerel larvae	34	28
Lampanyctus leucopsarus larvae	39	37
Total	109	108

TABLE 16.—*A summary of the depth distribution of eggs and larvae taken with high-speed samplers*

Organism	Percentage at each level				Total
	10 meters	20 meters	30 meters	40 meters	
Sardine eggs	39. 9	22. 4	19. 6	18. 1	100. 0
Sardine larvae	29. 8	45. 9	12. 6	11. 7	100
Anchovy eggs	3. 7	2. 9	39	54. 4	100
Anchovy larvae	2. 7	30. 7	23. 3	43. 3	100
Jack-mackerel eggs	42. 5	23. 2	17. 7	16. 7	100. 1
Jack-mackerel larvae	20. 2	36. 2	25	18. 6	100
Lampanyctus leucopsarus larvae	5. 1	13. 1	35. 3	46. 6	100. 1

Conventional gear definitely has the advantage in this phase of sampling, since it is exceedingly versatile in depth sampling. Nets can be lowered to any desired depth, even to the deepest layers of the ocean; conventional gear can also be used in series to furnish data on depth distribution of organisms. However, with nets as large as 1.0 meter in diameter, as were used on cruise 5005, such series have been taken to establish depth distribution rather than for routine sampling. Once the depth distribution of an organism has been established, then oblique hauls can be made deep enough to encompass routinely this distribution.

Variation in density.—Obtaining enough samples of organisms to determine the variation in density with range is important because organisms are seldom found to be uniformly distributed. Usually there is considerable variation in abundance in various parts of their range. Because of these variations, it is difficult to sample an organism adequately with standard plankton gear. Strip samples, covering miles at a time, are far more representative of mean density; such samples automatically average-out much of the variation in abundance. This capability of the high-speed sampler, lacking in the spot sampler, is an important advantage and was the primary consideration prompting the development of this type of gear. The results obtained on cruise 5005 point up these advantages. Very large concentrations of sardine eggs, for example, that were missed entirely by standard net hauls were picked up by means of strip sampling.

Instrument requirements.—The performance of sampling gear can seriously limit the value of plankton collections. Four aspects of gear performance will be compared for the two types of plankton samplers.

An adequate means of measuring the quantity of water strained in making a haul is an essential requirement of an instrument used for quantitative sampling. The depth-flow mechanism of the high-speed sampler automatically records both water flow and depth; the Atlas current meter used with 1-meter nets gives a reliable record of water flow.

The high-speed sampler was constructed of finer meshed netting material than the 1-meter net now being employed on cruises of the California Cooperative Oceanic Fisheries Investigations. We did not have any serious clogging of the Monel screen of the high-speed samplers (on one test, clogging retarded flow by about 10 percent after 4 hours of continuous towing), yet retention of smaller-sized fish eggs and larvae was much better than with conventional gear. However, we are now experimenting with finer-meshed synthetic netting in 1-meter nets in order to increase retention without impairing the flow of water through the nets.

Large plankton organisms are often agile enough to dodge relatively slow-moving plankton nets. The high-speed sampler was designed to prevent dodging through its speed of operation and mode of attachment to the towing wire. The mouth opening of the sampler precedes the towing wire, consequently no part of the gear can act as a scare as do both the towing wire and the bridle of our standard plankton gear. Organisms capable of moving out of the path of a conventional net being hauled at 1 to 1½ knots may have little chance of dodging the high-speed sampler moving at 10 knots. The taking of approximately 30 times as many small pelagic fishes with high-speed gear as with conventional plankton nets (based on comparable volumes of water strained) accents the effectiveness of high-speed samplers in this field.

---

[2] A newly designed depressor, given the model number 3x, permits operation to 300 meters with ⅜" and ½" towing cable (J. D. I.).

A limitation of high-speed samplers for certain purposes results from the rather small quantity of plankton collected. A group of 4 samplers hauled for 10 miles would collectively strain only about 40 cubic meters of water. This is less than one-tenth the quantity of water strained during a routine 1-meter net haul. The smaller quantity is adequate for measuring mean density of many plankton organisms, including fish eggs, but not for obtaining sufficient numbers of larvae, particularly of older stages, for mortality estimates.

The cost of constructing the Isaacs high-speed sampler may place a limitation on its widespread use. As one way of reducing the cost of equipment, it is practicable to use only one instrument with a depth-flow meter in a string of 4 or 5 samplers towed simultaneously. On cruise 5005, the three upper high-speed samplers were equipped with plankton filters of the same mesh size. Due to the time required for attaching and retrieving the samplers, the upper sampler was hauled only 83.6 percent as long, on the average, as the sampler at 30 meters, while the sampler at 20 meters was hauled 94.1 percent as long. A comparison of the volumes of water strained by the three samplers showed that the upper one strained on the average 83.2 percent as much as the sampler at 30 meters, and the 20-meter sampler strained 93.5 percent as much. We conclude from these comparisons that a fairly accurate estimate of volume of water strained by either of the upper samplers could have been obtained by using the volume of water strained by the net at 30 meters, adjusted for difference in time of hauling.

APPENDIX I: OPERATING INSTRUCTIONS

Preparing film.—Film used in the high-speed sampler is 35 mm. perforated clear No. 3 Safety Leader film. The film which is obtained in bulk must be cut into appropriate lengths (approximately 2½ ft.). To prepare the film for use, roll on a slotted brass rod (⅜" in diameter) just tight enough that the roll will come off the rod without difficulty. Wrap with a rubber band, applying sufficient tension to prevent unrolling, but not enough for tension lines to bake into the film. After the film is properly banded, remove from the rod.

The film is baked in order to set it in a tight roll, which assures that the film will automatically rewind during use. It should be baked for 4 hours at a temperature of 220° F. in a thermostatically-controlled oven.

After baking, the film is cooled to room temperature, and then rerolled. This is done so that the point of maximum tension will be on the outside of the roll, ensuring that the film will rewind on itself when in use.

Handling of samplers.—We have found from experience that careful instructions for assembling the samplers, and attaching and removing them from the towing cable may prevent costly repairs or even loss of the equipment.

Assembling.—Load the sampler with film starting the film around the film sprocket and marking the zero trace. Attach the straining section of the plankton filter to the cod-end cup. Attach the metering unit and tighten the stylus screw. Insert complete unit in the outer casing and secure.

Placing samplers on towing cable.—Attach and lower the depressor (illustrated in fig. 14) into the water with ship at half speed. Place the ball clamp on the towing cable and tighten (fig. 15). Remove the nose ring from the sampler and push the slotted nose over the wire, above or below the cable clamp. Pull the cable clamp into the cable-clamp seat and replace the nose ring. Lower the sampler the desired amount and attach (fig. 16) the second sampler in the same manner, and so on.

Removing samplers from towing cable.—The procedure for removing samplers from the towing cable is just the reverse of the preceding description. When samplers break water, they assume the mouth-up vertical position of pre-lowering, thus preventing loss of any part of the sample.

Disassembling.—Remove outer casing while keeping sampler upright to prevent loss of sample. Play a jet of salt water along the outside of the plankton filter to dislodge any adhering plankton. Detach the straining section of the filter and concentrate sample further by patting salt water on the outside of the mesh of the cod-end cup. Pour sample into a suitable container, label, and add preservative. Detach the metering unit. Remove film by slicing down through the film with a knife blade, and label (fig. 17). Wash plankton filter and metering unit with fresh water. Reload film, and reassemble sampler.

At no time during assembling or disassembling should force be used on the high-speed sampler. Gentle tapping or rocking motions will dislodge any stubborn sections without damaging the instrument. Should any section consistently stick, silicone stopcock grease can be used to overcome the tendency.

APPENDIX II: CALIBRATION

The method of standardizing hauls would require a lengthy explanation and hence would be out of place in this paper which is concerned with performance and not the technical aspects of quantitative sampling. The method of standardizing regular plankton hauls is discussed by Ahlstrom (1948), and a modification of this method was used in standardizing the high-speed sampler hauls.

The following procedures were used for obtaining depth flow calibrations:

Depth calibration.—The depth calibration was done at sea during calm weather. Instead of a

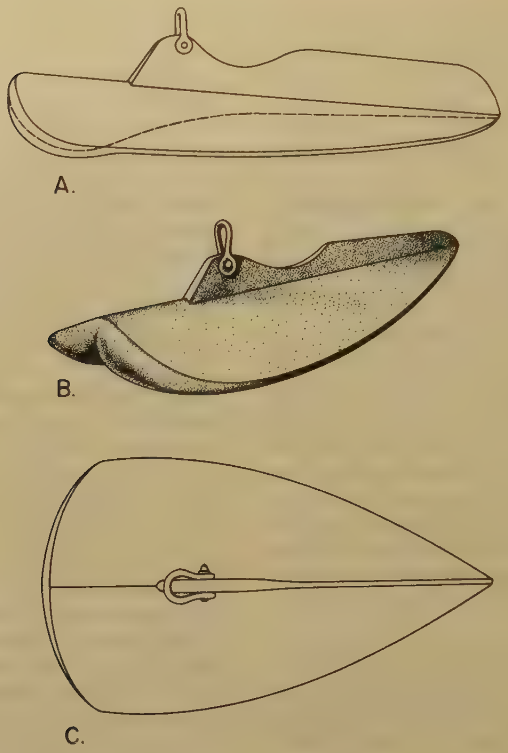

Figure 14.—Three views of depressor.

depressor, an ordinary 100-lb. weight was attached to the end of the towing cable. The sampler being calibrated for depth was attached about 10 meters above the weight. It was properly loaded with film and lowered to the water surface, at which time the meter wheel of the winch was set at zero. The sampler was then successively lowered to a number of depths. After each lowering the metering unit was removed, the depth scratched above the trace on the film, the sprocket turned about one-half a revolution, and the unit reassembled for the next lowering. Two kinds of pressure elements have been used, one type effective to approximately 55 meters, the other to approximately 137 meters. For the shallower element, lowerings were made to 10, 20, 30, 40, 50, and 60 meters, respectively. For the deeper element, lowerings were made to 10, 20, 30, 40, 50, 60, 70, 80, 100, 120, 130, and 140 meters. At the completion of a calibration the traces were measured and graphed against depth as determined by wire out, and a line was fitted to the points. Typical depth calibration graphs for the two types of pressure elements are shown in figure 18.

Flow calibration.—Flow calibration presented more of a problem. Several methods were tried before a satisfactory one was found. The most difficult problem was to find a suitable method for measuring the volume of water that passed through the sampler during the tests. Several preliminary methods did not achieve a desirable degree of either accuracy or consistency (repeatability) of results. These included rough and ready methods of either weighing or collecting and measuring the water passing through the sampler. Finally, a water meter was installed in front of the sampler in the calibration system. By this means it was possible to measure accurately the quantity and rate of flow of water passing through the sampler during each trial.

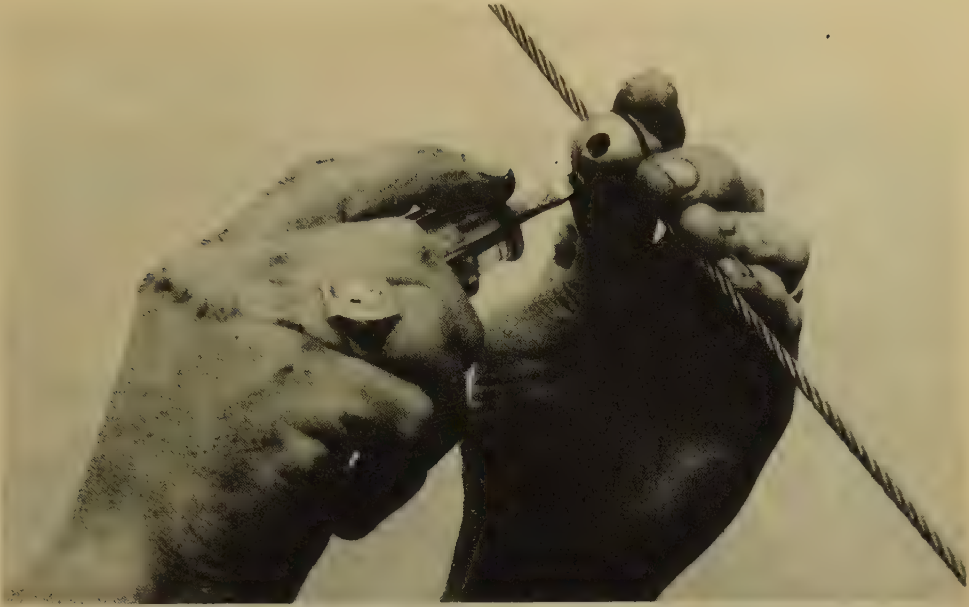

FIGURE 15.—Fastening ball clamp to towing cable.

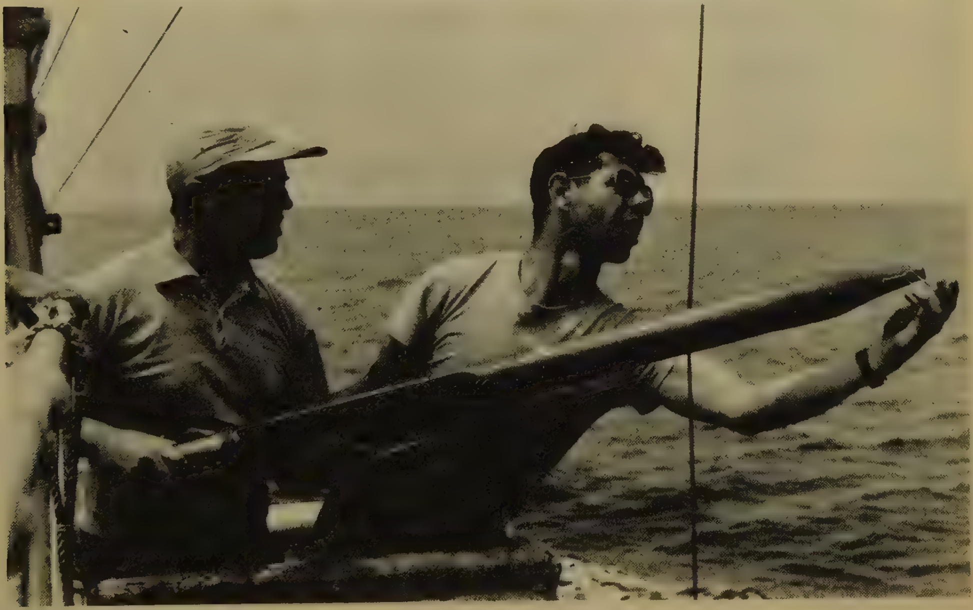

FIGURE 16.—Fastening sampler to towing cable.

NOTE:—The samplers after attachment to the towing cable, hang vertically with the mouth up. When lowered into the water, they orient themselves and assume a horizontal fishing position.

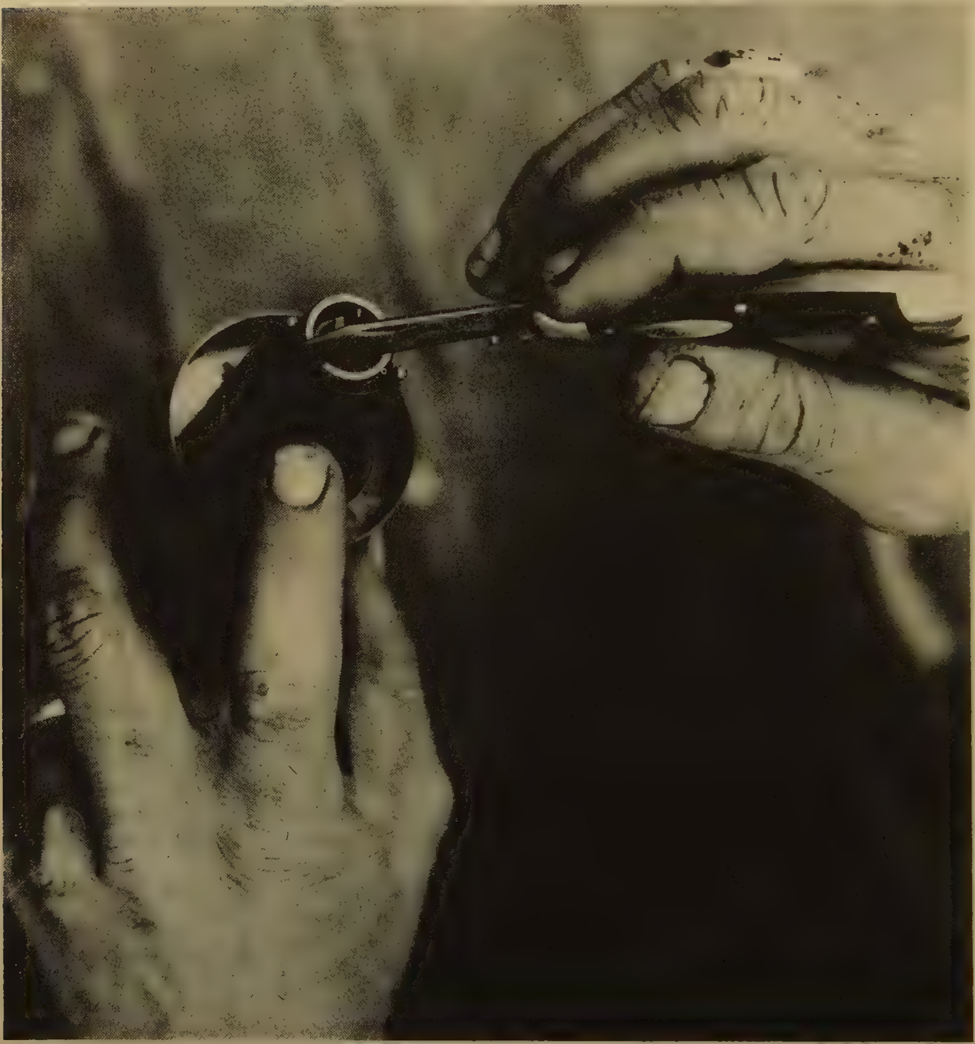

FIGURE 17.—Removal of film from sampler.

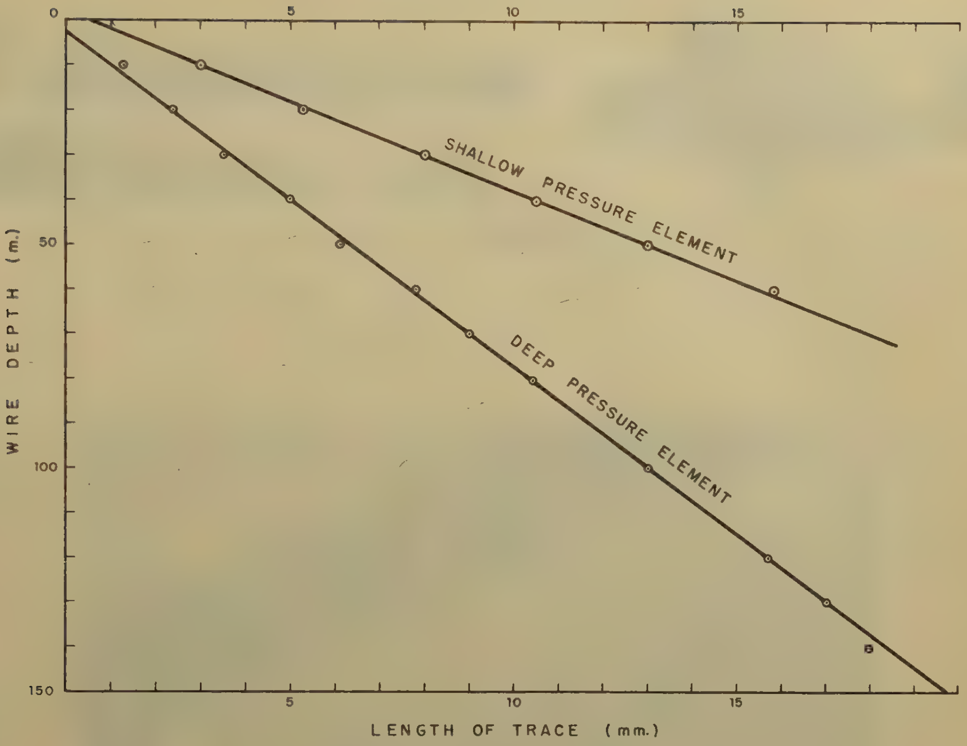

FIGURE 18.—Typical depth-calibration curves for the two types of pressure elements used.

The calibration tests were conducted in a pool. There are four important elements in the calibration system: (1) Housing for attaching essential portion of high-speed sampler to the calibration system; (2) metering device (a calibrated water meter) measuring flow; (3) water source; and (4) flow rate valve (for controlling volume of water entering system per unit of time).

Housing.—Inasmuch as the casings used with high-speed samplers at sea could not be employed conveniently during calibration tests, a cylindrical casing was substituted (fig. 19). It had a bonnet at its forward end for convenient attachment to a water meter.

Water meter.—The water meter employed had openings of 1½ inches diameter (3.8 cm.) at attachment points. It was calibrated, before use, by the Engineering Department of the San Diego Municipal Water Company (fig. 19).

Water source.—The water source was a submersible pump that drew water from the pool in which the calibration tests were made. A 1½-inch hose connected the pump to the calibration setup. The submersible pump used with this operation gave an even, steady flow of water through the calibration tube.

Valve.—A manually operated valve was used to control the rate of flow of water entering the system. In calibrating the flow-meter, it was desirable to obtain rates of flow that would bracket those obtained when in use at sea. The flow-meter being calibrated is shown in figure 20.

Because the flow-meter is directly geared to a sprocket over which is led the clear acetate film, when the flow-meter is actuated by water passing through the sampler, a trace is obtained on the film. The length of the trace is determined by two factors, the volume of water and rate of flow. In calibrating the flow unit, identical volumes of water were used on all trials, but the rate of flow was varied. A range of flow rates from 3.1 to 10.0 cubic feet per minute (0.088 to 0.283

Figure 19.—Disassembled flow calibration units.

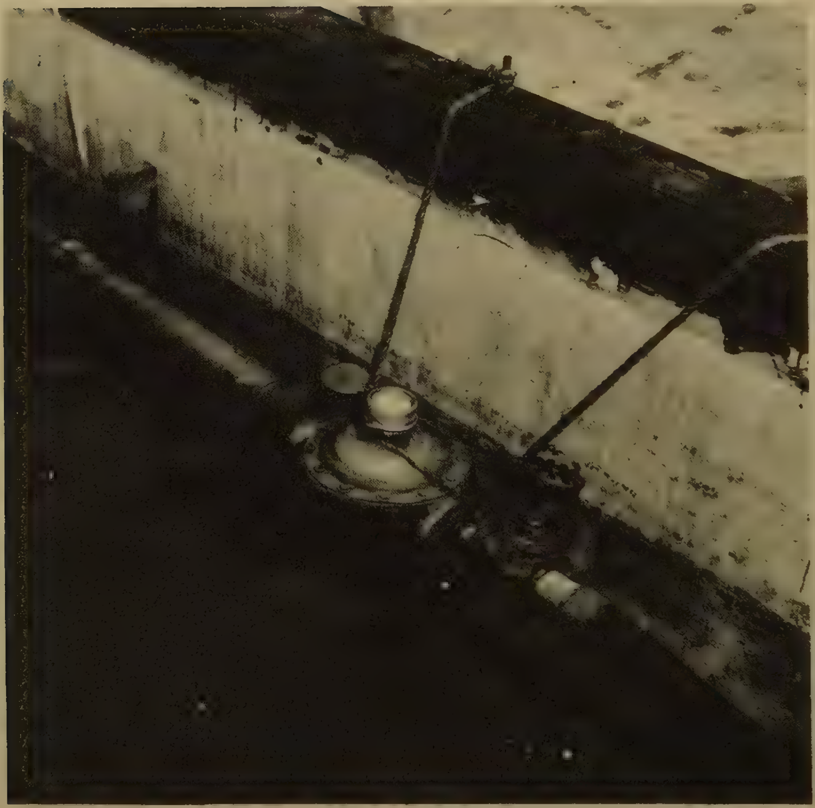

Figure 20.—Flow calibration setup in pool.

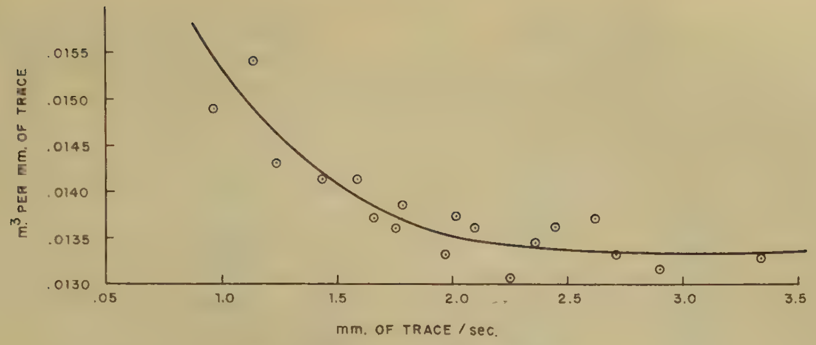

Figure 21.—A typical flow calibration.

m.^{3}/min.) was used. (The water meter used in the calibration tests recorded in ft.^{3}). The data obtained during calibration tests of one of the flow-meters are given in table 17 and graphically illustrated in figure 21.

Table 17.—*Typical flow calibration using a constant volume of water (40 ft.^{3} or 1.133 m.^{3}) and various rates of flow*

Time in seconds	Length of trace (mm.)	Millimeters trace per seconds	Cubic meters per millimeter trace
255	85.1	0.334	0.0133
297	86.0	.290	.0132
313	84.9	.271	.0133
315	82.5	.262	.0137
340	83.2	.245	.0136
356	34.1	.236	.0135
386	86.7	.225	.0131
395	83.2	.210	.0136
409	82.4	.202	.0137
430	84.9	.197	.0133
456	81.7	.179	.0139
475	83.1	.175	.0136
496	82.5	.166	.0137
503	80.0	.159	.0142
555	80.0	.144	.0142
638	79.1	.124	.0143
643	73.5	.114	.0154
780	76.0	.097	.0149

Note on flow calibration.—The following considerations were helpful in choosing the range of 3.1 to 10.0 cubic feet per minute:

The normal cruising speed of the survey vessels was 10 knots; hence the vessel would cover 1 nautical mile in 6 minutes. Assuming that the high-speed samples strained while being towed 1 nautical mile, a cylinder of water 1 mile long by 2.54 centimeters in diameter (diameter at mouth opening), it would strain 0.94 cubic meters of water or 0.157 cubic meters per minute. (This is equivalent to 5.5 ft.^{3}/min.).

Inasmuch as the collector has a 1-inch or 2.54-centimeter opening at the inlet and a 3-inch or 7.62-centimeter opening at the outlet, it was anticipated (and preliminary tests had confirmed) that the sampler would strain a somewhat greater quantity of water than the above-calculated cylinder.

However, it was also anticipated that there would be considerable variation in the volume of water strained from haul to haul, due to varying degrees of clogging of the fine-meshed net.

The flow rates at sea, measured by length of film trace per second of hauling, fell within the anticipated range of flow rates used in calibration.

LITERATURE CITED

Ahlstrom, Elbert H.

1948. A record of pilchard eggs and larvae collected during surveys made in 1939 to 1941. U. S. Dept. of Interior, Fish and Wildlife Service, Spec. Sci. Rept. No. 54, 76 pp.

1952. Pilchard eggs and larvae and other fish larvae, Pacific Coast, 1950. U. S. Dept. of Interior, Fish and Wildlife Service, Spec. Sci. Rept. Fisheries No. 80, 58 pp.

Barnes, H.

1951. A statistical study of the variability of catches obtained with two models of the Hardy Plankton Indicator. Hull Bull. Mar. Ecology, vol. II, No. 16, pp. 283–293.

Clark, G. L., and D. F. Bumpus.

1950. The plankton sampler—an instrument for quantitative plankton investigation. Limn. Soc. America, Publ. No. 5, rev. 1950, 8 pp.

Hardy, A. C.

1936a. The ecological relations between the herring and the plankton investigated with the plankton indicator. Part 1. Jour. Mar. Biol. Assn. United Kingdom, vol. XXI (n. s.), pp. 147–177.

HARDY, A. C.

1936b. The continuous plankton recorder. Discovery Reports, vol. XI, pp. 457–510.

1939. Ecological investigations with the continuous plankton recorder. Hull Bull. Mar. Ecology, vol. I, No. 1, pp. 1–57.

SMITH, O. R., and E. H. AHLSTROM.

1948. Echo-ranging for fish schools and observations on temperature and plankton in waters off central Caifornia in the spring of 1946. U. S. Dept. of Interior, Fish and Wildlife Service, Spec. Sci. Rept. No. 44, 30 pp.

STAFF of the SOUTH PACIFIC FISHERY INVESTIGATIONS.

1952. Zooplankton volumes off the Pacific Coast, 1951. U. S. Dept. of Interior, Fish and Wildlife Service, Spec. Sci. Rept. Fisheries No. 73, 37 pp.

1953. Zooplankton volumes off the Pacific Coast, 1952. U. S. Dept. of Interior, Fish and Wildlife Service, Spec. Sci. Rept. Fisheries No. 100, 41 pp.

1954. Zooplankton volumes off the Pacific Coast, 1949–50. U. S. Dept. of Interior, Fish and Wildlife Service, Spec. Sci. Rept. Fisheries No. 125, 54 pp.

1954. Zooplankton volumes off the Pacific Coast, 1953. U. S. Dept. of Interior, Fish and Wildlife Service, Spec. Sci. Rept. Fisheries No. 132, 38 pp.

1955. Zooplankton volumes off the Pacific Coast, 1954. U. S. Dept. of Interior, Fish and Wildlife Service, Spec. Sci. Rept. Fisheries No. 161, 35 pp.

1956. Zooplankton volumes off the Pacific Coast, 1955. U. S. Dept. of Interior, Fish and Wildlife Service, Spec. Sci. Rept. Fisheries No. 177, 31 pp.

THRAILKILL, JAMES R.

1956. Relative areal zooplankton abundance off the Pacific Coast. U. S. Dept. of Interior, Fish and Wildlife Service, Spec. Sci. Rept. Fisheries No. 188, 85 pp.

U. S. GOVERNMENT PRINTING OFFICE : 1958 O - 447769

(140)

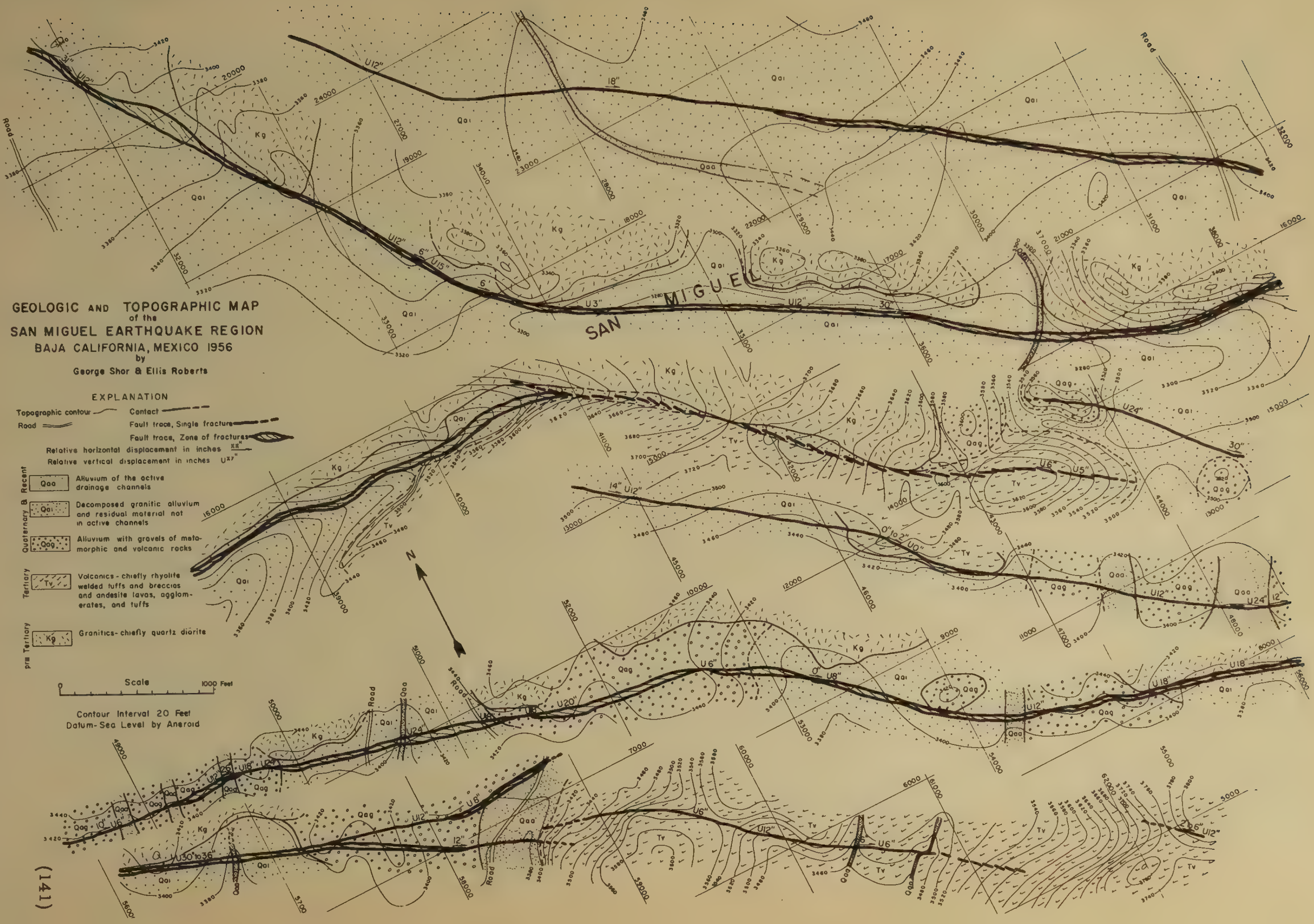

GEOLOGIC AND TOPOGRAPHIC MAP
of the
SAN MIGUEL EARTHQUAKE REGION
BAJA CALIFORNIA, MEXICO 1956
by
George Shor & Ellis Roberts

EXPLANATION
Topographic contour
Contact
Road
Fault trace, Single fracture
Fault trace, Zone of fractures
Relative horizontal displacement in inches XX"
Relative vertical displacement in inches UXX"
Quaternary & Recent
Qaa Alluvium of the active drainage channels
Qai Decomposed granitic alluvium and residual material not in active channels
Qag Alluvium with gravels of metamorphic and volcanic rocks
Tertiary
Tv Volcanics - chiefly rhyolite welded tuffs and breccias and andesite lavas, agglomerates, and tuffs
pre Tertiary
Kg Granitics - chiefly quartz diorite
Scale
0
1000 Feet
Contour Interval 20 Feet
Datum - Sea Level by Aneroid
N
SAN MIGUEL
Road
Road
Road
Road
Qai
Qaa
Qag
Kg
Tv
U12"
18"
U3"
30"
U15"
6"
U24"
U6"
U5"
14" U12"
0"to 2" U0"
U20"
0" U8"
U18"
12"
U30"to 36"
10" U6"
26" U12"
16000
24000
32000
56000

Bulletin of the Seismological Society of America. Vol. 48, pp. 101–116. April 1958

Bulletin of the
Seismological Society of America

Vol. 48 APRIL, 1958 No. 2

SAN MIGUEL, BAJA CALIFORNIA NORTE, EARTHQUAKES OF FEBRUARY, 1956: A FIELD REPORT

By George G. Shor, Jr. and Ellis Roberts

ABSTRACT

The San Miguel, Baja California Norte, earthquakes of February 9 and 14, 1956, were felt over most of northern Baja California and parts of southern California. They originated on the San Miguel fault. This newly named fault runs from the southern end of the Sierra Juárez, near the eastern end of the Agua Blanca fault, about N 60° W across the Álamo Plain. At least twelve miles of surface rupture occurred along this line during the February shocks. Cracks were uniformly open and arranged *en échelon*, stepping to the left. Magnitude of displacement was variable, but the direction was always right-lateral and up to the northeast. Surface evidence indicates that the fault is nearly vertical.

A zone of springs, linear hills and valleys, displaced drainage, and closed basins extends beyond the zone of surface rupture for fifty miles northwest to the vicinity of Guadalupe.

The main shock of February 9 occurred close to the northwest projection of the surface trace; the two major aftershocks on February 14 were near the southeast projection. This implies progressive faulting from northwest to southeast, similar to the southwest-to-northeast faulting in the Arvin-Tehachapi earthquake.

Slides occurred on the steep slopes of the Sierra Juárez. Temporary warm springs were formed a few miles from the fault, and near-by existing springs had variations in their flow.

Total property loss was small because there were few objects to be damaged. The six-building community of San Miguel, astride the fault, was severely hit: three adobe houses were destroyed and a frame schoolhouse was shifted from its inadequate foundations. Two brush shacks were relatively undamaged. Elsewhere, adobe and unreinforced concrete block structures suffered varying degrees of damage, most of which has gone unrepaired. The most common form of damage was cracking upward and outward from lintels.

The principal damage in and around the Álamo Plain, the area of surface rupture, was apparently from the shock of February 9. Beyond the southeast end of the surface trace, the only reported damage was from the aftershocks of February 14.

Introduction

At 6:32 a.m. on February 9, 1956, an earthquake which was centered near San Miguel in the sparsely inhabited central highland of the state of Baja California Norte, Mexico, shook northern Baja California and adjoining areas of southern California. Aftershocks were felt on successive days, and on February 14 two large aftershocks at 10:33 a.m. and 5:20 p.m. were again widely felt. Reports of damage were received during the following week, and, the preliminary epicenter being made available from the Pasadena Seismological Laboratory, a party from San Diego made a brief investigation of the area, where they found conspicuous fault-trace

Manuscript received for publication August 1, 1957.

Reproduced by Permission

phenomena and local damage (fig. 1). Preliminary reports were made by Richter (1956) and Shor (1956). Additional brief trips were made into the area by both authors, as well as by other interested geologists.

Preliminary epicenters, from Pasadena. are as follows:

Feb. 9, 1956	06:32:38 PST	31° 45′ N, 115° 55′ W	Mag. 6.8
Feb. 14, 1956	10:33:34 PST	31° 30′ N, 115° 30′ W	Mag. 6.3
Feb. 14, 1956	17:20:38 PST	31° 30′ N, 115° 30′ W	Mag. 6.4

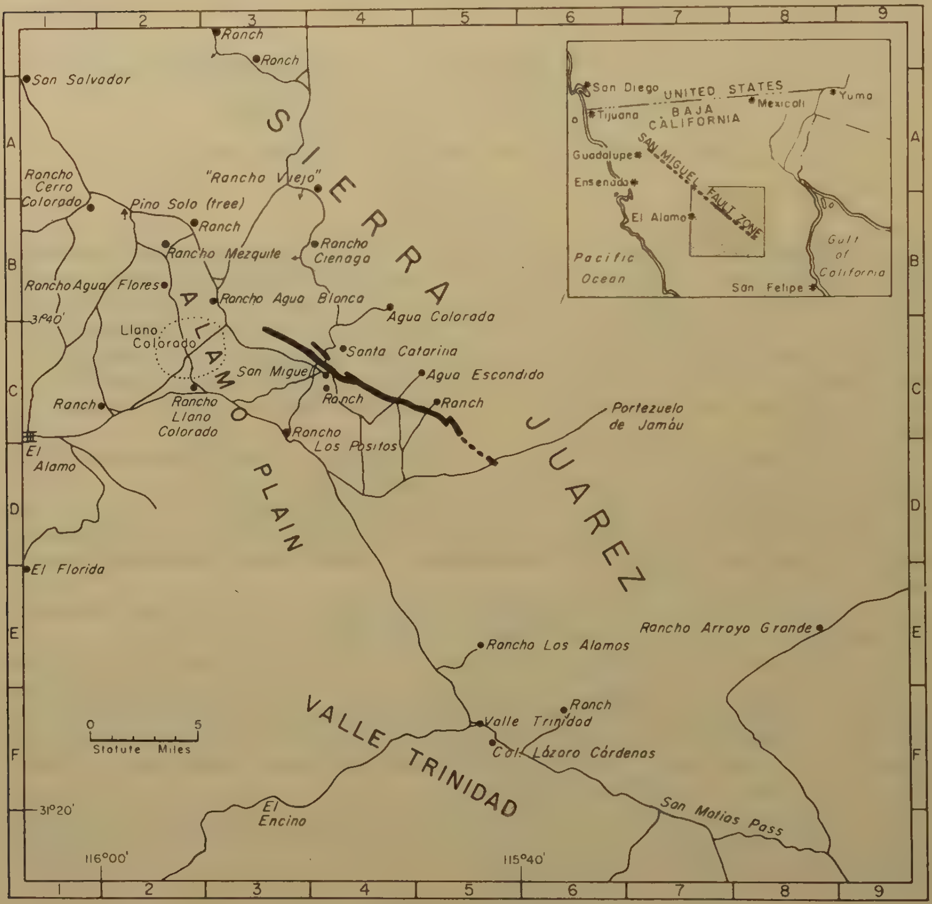
1 2 3 4 5 6 7 8 9
A B C D E F
Ranch
Ranch
San Salvador
SIERRA JUAREZ
"Rancho Viejo"
Rancho Cerro Colorado
Pino Solo (tree)
Ranch
Rancho Mezquite
Rancho Cienaga
Rancho Agua Flores
ALAMO PLAIN
Rancho Agua Blanca
Agua Colorada
31°40′
Llano Colorado
Santa Catarina
San Miguel
Agua Escondido
Ranch
Ranch
Ranch
Rancho Llano Colorado
Portezuelo de Jamáu
Rancho Los Positos
El Alamo
El Florida
Rancho Arroyo Grande
Rancho Los Alamos
Ranch
Valle Trinidad
Col. Lázaro Cárdenas
VALLE TRINIDAD
0 5
Statute Miles
31°20′
El Encino
San Matias Pass
116°00′
115°40′
San Diego
UNITED STATES
Yuma
Mexicali
Tijuana
BAJA CALIFORNIA
Guadalupe
SAN MIGUEL FAULT ZONE
Ensenada
El Alamo
Pacific Ocean
Gulf of California
San Felipe

Fig. 1. Location of fault trace and area of damage study; base map after Gerhard and Gulick (1956).

The epicenters and the zone of surface breakage lie in the Álamo Plain (Howard E. Gulick, unpublished map) and the Sierra Juárez. The Sierra Juárez is a granitic block, topped by an old erosion surface and in some areas by lava flows, now uplifted to an elevation of about 5,000 feet. The eastern face is a steep scarp, dropping to elevations below 2,000 feet in a few miles. The western face of the high block is in many places marked by cliffs, in some by gentler slopes, dropping to an elevation of about 3,500 feet on the Álamo Plain in the area under discussion. A typical view of the 5,000-foot surface is shown in figure 2, an airplane photograph taken southeast of San Miguel; the eastern scarp is to the right. The steeply sloping sides of the southern isolated sections of the high surface make them nearly inaccessible.

The Álamo Plain has topography nearly as gentle as the top of the Sierra Juárez. There are extensive areas of granitic exposure, some metamorphic rocks, and small areas of volcanic flows and tuffs, conglomerates of volcanic rocks, and fluviatile sediments. The center of the plain contains a dry lake, Llano Colorado. A view of a typical part of the plain, looking northwestward along the presumed extension of the San Miguel fault, is shown in figure 3.

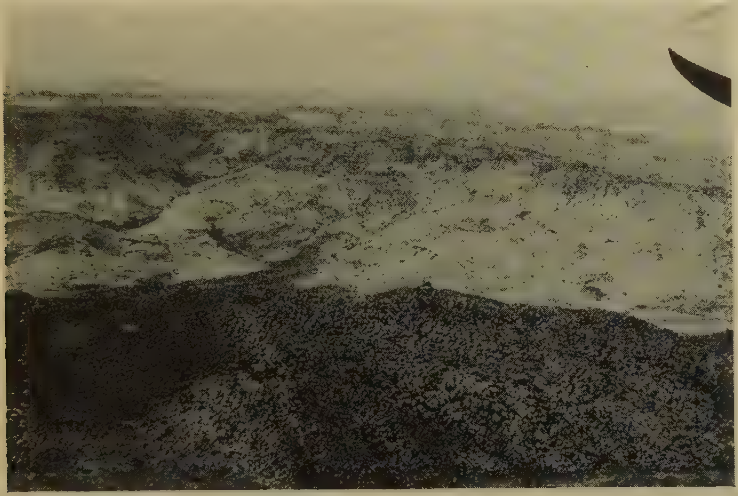

Fig. 2. Air photo of high surface on Sierra Juárez.

The two surfaces (the top of the Sierra Juárez and the Álamo Plain) were noted by Lindgren (1888) and more fully discussed by Beal (1948, pp. 14–16).

The area is difficult of access; roads from the north and northwest are passable by ordinary motor car at limited speeds, those from the east only by motor vehicles with four-wheel drive. Local roads are rudimentary and unmarked. Existing maps at the time of the first investigation were grievously inaccurate and conflicting, and it was only with the aid of the excellent road maps and logs published later by Gerhard and Gulick (1956) that the ranches and communities visited for survey of damage were placed in proper relation.

All field investigations reported here were made after the shocks on February 14. Differentiation of the effects of the main shock and the principal aftershocks must, therefore, depend upon local reports solely. Because of language barriers it was in many places impossible to make this separation.

Many smaller shocks have occurred since the major one of February 9, and preliminary epicenters have been reported by Pasadena. The three shocks listed, however, most probably account for the visible earth movement, as well as most of the damage reported. Because the instrumental results will be reported by the Seismological Laboratory, no other instrumental details will be given here.

Historical Background

Probably the most severe reported earthquake that has occurred in this part of Baja California was the shock of 1892 listed by Wood and Heck (1951, p. 13) as follows:

> **1892 February 23. This probably was the largest California shock of the interval 1873–1906. Intensity probably reached X near origin, which was apparently in the uninhabited region of northern Lower California. Intensity at least VIII along the Pacific coast of Lower California, as far south as San Quintin. Effects reported from San Diego County are as follows: At Carrizo, all adobe buildings destroyed; at Jamul, walls of stone kilns cracked; in Paradise Valley, church and schoolhouse built on stilts brought down and demolished; at San Diego, a large number of buildings cracked and plaster dislodged (VII). At Santa Ana walls were cracked and intensity was VI in Los Angeles and San Bernardino. At Campo there were 155 shocks in 12 hours. The shock was felt as far north as Visalia. Aftershocks were numerous for several days.

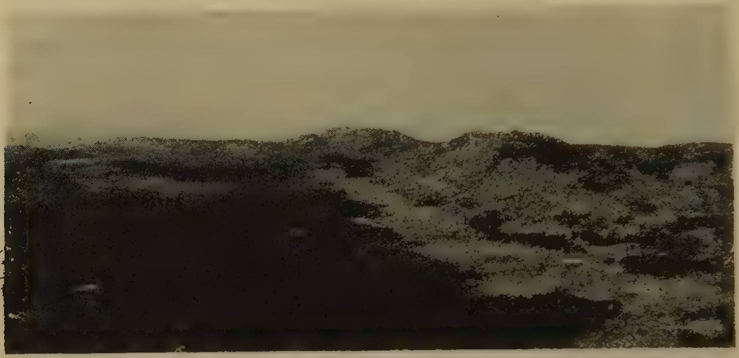

Fig. 3. Air photo of Alamo Plain, looking northwest along projection of fault trace.

No evidence of movement of so recent a date was noted on the San Miguel fault, and it is possible that this earthquake occurred on the Agua Blanca fault, a major one south of the San Miguel fault, the existence of which has been reported by Clarence Allen (Richter, 1956).

An interesting sidelight on this earthquake is the notation in the Holden catalog (1898) of a volcanic eruption in the same year, as follows:

> *1892—June 22*
>
> Messrs. Rose and Rikert, in the Santa Clara Valley, near Alamo, Lower California, last Friday, noticed two peaks four miles to the north alternately spouting smoke and flames at short intervals. The eruption was accompanied by rumbling sounds and an occasional quiver of the ground. Though frightened, they stopped long enough to satisfy themselves that two veritable volcanoes had opened. Later travelers report the volcanoes real, but not so active as at first. The region is undoubtedly volcanic, sulphur springs being in the vicinity.

The name Santa Clara is applied to several rivers in Baja California; current maps conflict both in the names and the drainage patterns. Lindgren (1888) shows a Río Santa Clara about 10 miles long flowing from El Álamo to join the Río San Carlos. As the El Álamo of the present report was the site of a gold rush at "the Santa Clara Placers" in 1889 and became a town of 5,000 inhabitants shortly thereafter (Gerhard and Gulick, 1956), it is to be presumed that a reference to Álamo in an 1892 report refers to this. The site of Rose and Rikert's report is therefore probably within 10 miles of this El Álamo. If the earthquake of 1892 occurred on the Agua Blanca fault, it is quite possible that dust clouds arising from landslides caused by aftershocks were observed, rather than volcanic eruptions.

Other earthquakes listed by Wood and Heck (1951) that may have had epicenters in the El Álamo area are those of June 23, 1843, and January 23, 1903.

Location and Extent of the San Miguel Fault

The San Miguel fault is defined primarily on the basis of surface displacement caused by the shocks of February, 1956. A zone of surface rupture trending N 60° W was observed in the vicinity of the communities of Santa Catarina and San Miguel.

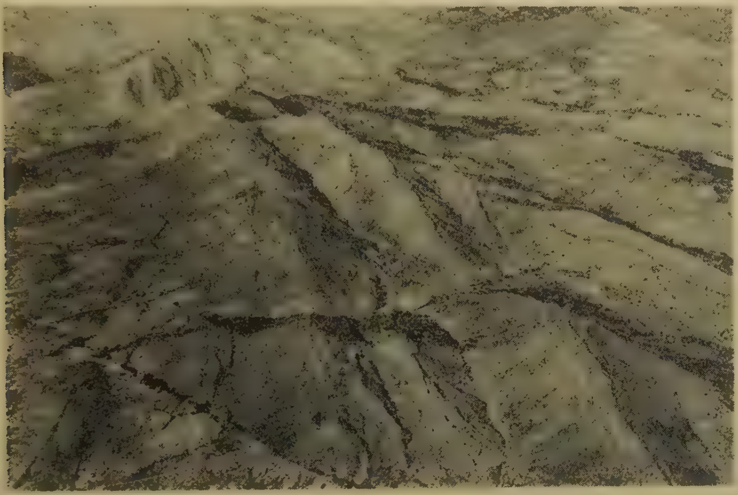

Fig. 4. Air photo of line of vegetation, east side of Valle de San Rafael, on projection of fault trace.

The zone of surface rupture lies within a wider band of fault topography running from the vicinity of San Matías Pass to the bend of the Río Guadalupe. On the southeast near San Matías Pass the only evidence for faulting is the alignment of the lower end of the Arroyo Teraizo with the upper end of the Arroyo Grande; thereafter evidence becomes more pronounced. There is a small intermontane basin now drained by Arroyo El Carrizo; then, after an unexplored interval, the recent fault trace, and near it to the west the dry lake of Llano Colorado. One-half mile northeast of the main trace of the fault on the Santa Catarina road is a kern-col through which runs a short subsidiary crack from the shock of February 9. To the northwest further evidence is found beyond Pino Solo, where a row of springs aligned N 60° W lies slightly to the east of the projection of the observed surface trace. The plain narrows here, and the mountain face to the northeast of the springs (shown in fig. 3) is straight and parallel to the direction of the zone. The plain ends in a straight valley leading over a low pass into the anomalous Valle de San Rafael. As noted by Lindgren (1888) and others, the drainage of the Valle de San Rafael (around Ojos Negros) is quite unusual, possibly in part internal. To the south it is drained by the Arroyo San Carlos, and to the north by the Río Guadalupe. A line of vegetation trending northwest on the northeast side of the valley is shown in figure 4. The Río Guadalupe continues the alignment with a straight narrow valley trending northwest until it takes a right-angle bend east of the town of Guadalupe. Lindgren (1888) suggested that the Valle de San Rafael is bounded by faults on the east and west sides; Beal (1948) suggested a major tectonic line on this general trend.

FAULT-TRACE PHENOMENA

Displacement and disruption of the ground were mapped over a distance of 12 miles. Regional location is indicated in figure 1; progressively greater detail is shown in figure 5 and on the folded map.

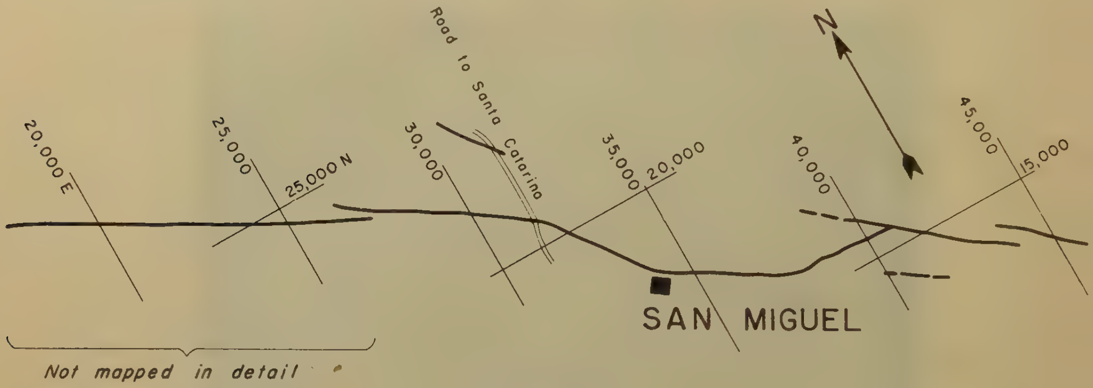

Fig. 5. Fault trace.

The surface trace consisted of one or more open cracks at all points mapped, with the exception of one 10-foot section of mole track and of some of the dry washes, where the appearance was as if someone had dragged his fingers through the sand. The cracks were *en échelon* in detail as well as on a regional scale; many sections mapped as solid single lines or wider shaded bands actually consisted of *en échelon* features of small to great length with the lateral stepping too small to show. The *en échelon* cracks always stepped left, the definition of "stepping left" being that if one follows a single crack to its end, the next crack taking up the movement will be on the left hand. It can be seen readily that open cracks stepping to the left would accompany right-lateral movement; compression ridges would necessarily step right for right-lateral movement.

Displacement was measured in a large number of places. Vertical movement could be measured with some accuracy on the ground surface alone, sometimes by direct measurement on a single crack and sometimes by making vertical profiles on dry washes; good measurements of horizontal movement were made on split bushes, matched roots, and one fence offset. Less accurate measurements were made on stream channels, road ruts, and paths. The displacement was variable over short distances. It varied from 0 to 31 inches horizontally, 0 to 36 inches vertically. In the few places where the fault trace crossed consolidated formations, the displacement was small. The direction of displacement was, however, uniformly right-lateral and up to the northeast.

In general the fault trace showed little deviation to fit topography. The attitude of the fault is therefore nearly vertical, although there is some evidence for small variations in dip to either side.

About 8 miles of the fault trace were mapped by plane-table traverse. Orientations were checked magnetically, but no triangulation control was established. The datum for elevations was by aneroid altimeter. The general dependability of this part of the mapping is estimated at one part in fifty. The main objective was to record the position of the surface trace; the geology was also plotted, but with less precision, and the topography was sketched in with rough control from the plane table. A two-mile strip to the northwest of the detailed survey was mapped by pace-and-compass traverse with a probable dependability of one part in twenty and without vertical control. Another two-mile strip to the southeast of the detailed survey was discontinuously mapped by very long stadia sights and magnetic orientation with a dependability estimated at one part in fifteen.

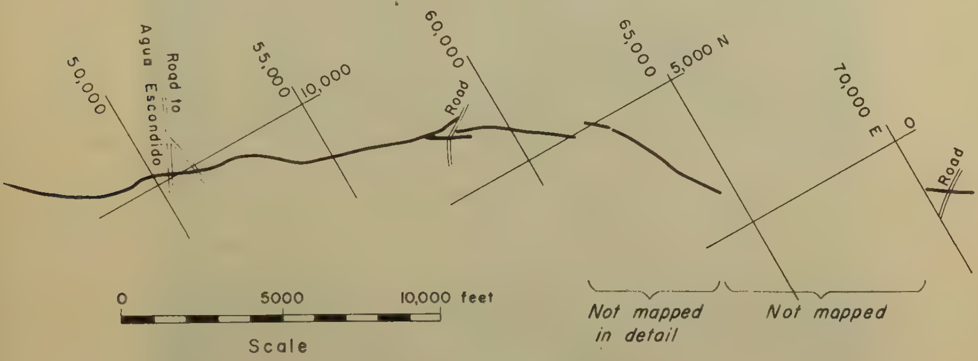

Fig. 5 (*Continued*)

Detailed description of the fault-trace features are given below, with coördinates referring to figure 5 and the folded map.

At 18,000 E, at the northwest end of the mapping, the displacement is slight and difficult to follow. Although there is some possibility that the movement has shifted to another *en échelon* crack, no such crack was seen from the air and no cracks were found crossing a road two miles beyond.

In the vicinity of coördinates 30,000 E to 35,000 E the trace crosses the Santa Catarina road on a southwest-facing hill slope. Figure 6 illustrates the appearance from the air in this vicinity. At the road crossing there is one major crack that continues for about 1,000 feet; other smaller cracks are found on both sides, ranging in width from hairline markings to 1½-inch gaps. Just east of the road the distance between the farthest cracks found on either side of the main trace was 840 feet. At this point the major crack is open to a depth of 3 feet, and is wide enough for a man to kneel inside (fig. 7). At coördinate 31,900 E a bush on the line of the major crack was split, the two halves remaining rooted on opposite sides of the crack (fig. 8). This provided a measurement of displacement of 31 inches right-lateral, 12 inches vertical up to the northeast. Similar displacements were noted in this area on the basis of offsets of road ruts and of stream bottoms.

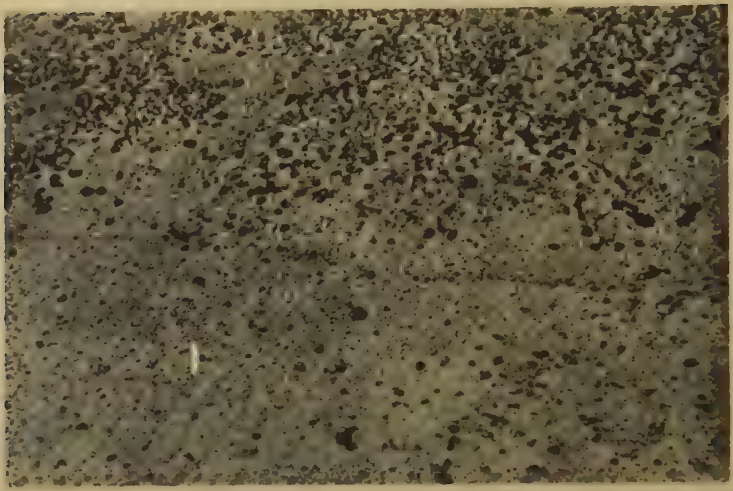

Fig. 6. Air photo of fault trace near Santa Catarina road; upper brush area is granitic, lower area alluvial.

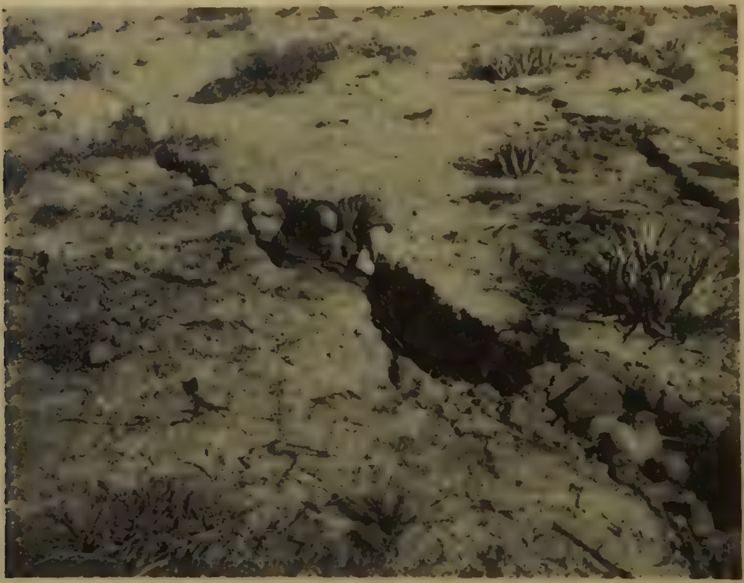

Fig. 7. Fault trace east of Santa Catarina road; man kneeling in fault crack. San Diego Union photo.

The fault trace is generally tangent to the ends of small spurs of the hills to the northeast, cutting straight across the alluvium between the spurs. Granitic outcrops are found to the northeast; to the southwest is alluvium only. At one point the trace went over the end of a spur without bending. A small graben appeared at another point, where a subsidiary crack downslope from the main trace had a 2-inch displacement down to northeast. After the earthquake, many bushes died on the northeast side of the fault, either from root damage or from change in the water table.

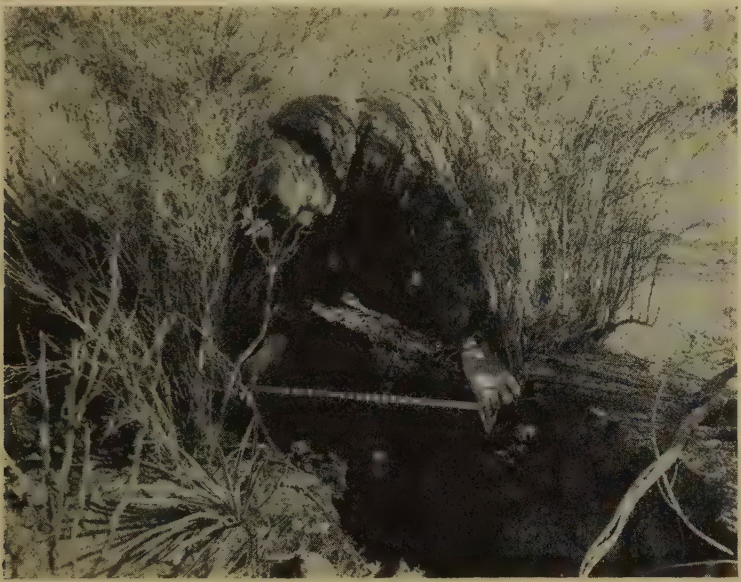

Fig. 8. Bush split by fault trace. San Diego Union photo.

One-half mile north of the crossing of the Santa Catarina road by the main trace, another zone of large cracks is found (shown in fig. 5 but not on folded map). This zone crosses the road on a southwest-facing hillslope, with approximately 9 inches of displacement up to the northeast. On the southeast side of the road there is a 6-foot-wide "plowed" band of cracks, going S 30° E up a small valley into a kern-col. The cracks fan out and disappear in the kern-col. Northwest of the road the "plowed" band turns into a single crack, which then fades out, the movement being taken up by a parallel scarp to the southwest. This *en échelon* arrangement repeats, always stepping to the left. The trace was followed for 2,100 feet to the northwest, and at this point it was still continuing across a stream bed. Over most of this distance granite outcrops on the northeast side of the trace; granitic alluvium was on the southwest side.

North of San Miguel, near coördinate 34,000 E, there were many small cracks on the top of the granitic hill. They trend N 15° W in a zone several hundred feet wide with no apparent displacement. Boulders were loosened in their sockets on the slope. Following the base of the hill is the main trace, represented by a large crack showing right-lateral and vertical displacement, down to the southwest on a southwest slope.

Beyond 34,000 E it frays out into a band of cracks which cross the flat alluvium of the stream bottom. At 36,000 E a fence is offset 30 inches.

On the far side of the stream by San Miguel, the trace turns to an east–west trend and climbs a narrow fault-controlled canyon up Dolores Mountain. The canyon separates granitics on the north from volcanics on the south; the fault trace lies entirely within broken material of the canyon floor. The zone is broad in its east–west trend and no displacement could be measured. Near coördinate 38,000 E a patch of volcanics overlies the granitics 1,000 feet north of the fault. This implies an old displacement of more than 200 feet vertically. Part way up the mountain the trace turns to a northwest–southeast trend again and becomes a series of *en échelon* cracks stepping to the left. This form of trace continues down a similar canyon on the east face of the mountain, entering the volcanics near the base. The saddle containing the fault trace and a landslide scar to the south are shown in figure 9.

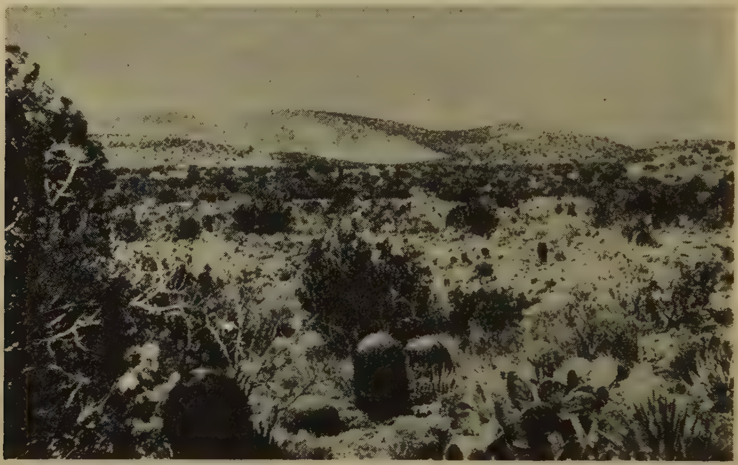

Fig. 9. Fault crosses ridge in narrow notch in right background, then across alluvial fan to observer.

At the base of the mountain, near coördinate 44,000 E, the trace steps north by a longer distance and changes its form. It crosses the broad alluvial fan (in the foreground of figure 9) with minor steps to the left. Near 46,000 E it crosses a small patch of volcanics with decreased displacement. On the southeastern edge of this area, near coördinate 49,000 E, there is a 10-foot section of mole track. Here the trace crosses a series of small ridges and gullies. It widens out to many small cracks on the ridges, and narrows down in some of the gullies where good matches of roots across the open crack were possible.

From 50,000 E to 58,000 E the trace separates an area of granitic outcrops on the northeast side from alluvial material on the southwest; no granitic outcrops were observed on the southwest side anywhere near the fault trace. Throughout this area, as elsewhere to a lesser degree, barrel cacti within a few feet of the fault trace were toppled; the root systems of these cacti are quite shallow, and the plants are heavy.

At 59,000 E, ancient displacement is estimated as more than 49 feet vertically.

(152)

The displacement on this earthquake decreases from 59,000 E on to the southeast. Because it lies in dark volcanic rocks, the fault trace could not be followed from the air beyond this point, except for a brief stretch near 70,000 E where it crosses the Portezuelo de Jamáu road. Here the trace consists of a series of small cracks and "chewed-up" ground, but with no obvious displacement or pattern of *en échelon* features. No attempt was made to follow the trace beyond this point.

PETROLOGY

The oldest unit exposed is the granitic rock which is exposed on the northeast side of the fault. It is typically a quartz diorite containing about 35 per cent of 0 to 2-mm. quartz, 55 per cent of 0 to 2-mm. plagioclase ($Ab_{32}An_{68}$), 8 per cent of 0 to 1-mm. biotite substantially altered to chlorite, and accessories including 0.1-mm. apatite. This unit also includes pegmatite and aplite dikes. The age of the quartz diorite is probably Cretaceous on the basis of its similarity and proximity to the San Pedro Mártir area 30 miles to the south, where Woodford and Harriss (1938) found Cretaceous limestones intruded by the granitics.

Overlying the granitics are volcanic rocks locally ranging in composition from andesite to rhyolite. Evidence of the nonconformable nature of this relationship can be seen on the east side of the road just north of the fault trace at coördinates 59,000 E and 7,000 N. All the volcanics are grouped into one unit for mapping purposes, but several rock types are represented.

One type is a hornblende andesite porphyry consisting of zoned phenocrysts of andesine up to 5 mm. and brown oxyhornblende up to 3 mm. in size. The groundmass consists of glass and subparallel plagioclase laths. Andesite tuff is also present. Rhyolitic rocks are chiefly welded tuffs and breccias with embayed crystals of high-temperature quartz, andesine, and brown biotite and angular fragments of felsites imbedded in a matrix of glass and recrystallized glass showing relicts of collapsed pumice.

Three alluvium units were mapped. The oldest and best consolidated of these contains gravels of vein quartz, quartzite, metachert, and volcanic rocks. The fragments are subround and up to about 6 inches in diameter. These are imbedded in decomposed granitic material with considerable clay content. Although the percentage of larger fragments is not large, weathering and erosion have concentrated these coarser fragments at the surface.

The second oldest alluvium unit consists of decomposed granitic residual material, and similar material that has been transported downslope from the adjacent granitic area. It is poorly consolidated, but sufficiently coherent to permit large fractures to be preserved. This unit also includes minor active drainage channels.

The youngest alluvium unit mapped is the material of the more prominent intermittent streams of the present drainage system. This material is loose, decomposed granitic sand.

WARM SPRINGS

Within a few hours of the shock of February 9, eruptions of warm water and gas from the ground commenced at a point west of San Miguel (position C-3 in fig. 1). These were observed by the Sub-Delegado of El Álamo about 6 P.M. on that day. Water was coming up in a fountain about 8 inches in the air at first, but subsided within a few days. On February 25 water was flowing from an area about 300 by 100 feet on a hillside, with a total flow estimated at 500 to 550 gallons per minute. Water temperature at this time was 27° C at the bottom of a pool (dug by local inhabitants) while the air temperature was 2°5 C. The springs were accompanied by actively bubbling nonodoriferous noninflammable gas. In the valley floor just north of the spring area, hairline ground cracks were accompanied by an additional flow of water, breaking out from holes in the alluvium.

By March 4 the flow had decreased slightly and the temperature of the water was reduced to approximately air temperature (about 20° C). Flow had stopped entirely by August, 1956. In other areas springs had variations in flow, increased or decreased, as noted below in the section on structural damage.

LANDSLIDES

Landslides were observed on the east and west flanks of the Sierra Juárez over a wide area, on Dolores Mountain near San Miguel, and on hills north of Valle Trinidad. Slides were reported from as far north as Palomar Canyon (about 30 miles northeast of San Miguel). Many of the slides were in areas where the hills are capped with volcanic flows overlying ash beds, an unstable situation easily disturbed. Boulders came loose and rolled down hillsides at many points along the Arroyo Grande, at one point just south of San Miguel, at San Salvador, and on the Portezuelo de Jamáu road. There was one unverified report that a boulder had crashed through a house.

STRUCTURAL DAMAGE

Structural damage was surprisingly small for an earthquake with this much surface breakage, but probably in accord with the magnitude 6.8 assigned. Marked variations in damage of poorly built adobe-block and concrete-block structures within the fault zone were more closely related to type of ground than to proximity to the surface trace. Information for the determination of intensity and construction of an isoseismal map is unfortunately meager. Many of the items that help determine the divisions of the Modified Mercalli scale could not be assessed, because of the uniform construction of the relatively few structures. The language barrier and delay in making the investigation made determination of personal reactions dubious. A list of observed and reported effects in the area surrounding the Álamo Plain is given below. Coördinates refer to the letters and numbers on the edge of the sketch map, figure 1.

A-1. San Salvador. A group of ranches. The northwesternmost house had slight damage to the poorly constructed adobe above the window lintel. Many rocks came rolling down the mountains. A spring to the southeast stopped temporarily.

A-4. "Rancho Viejo." Exterior plaster had fallen off. There was no information to indicate whether this was caused by the earthquake.

B-2. Rancho Mezquite. Alluviated area, about one mile from granite outcrop. One-room adobe-block house badly damaged, west wall leaning outward away from the rest of the building, chimney fallen, northeast corner of building badly cracked (fig. 10).

B-2. Ranch 1.7 miles north of Rancho Mezquite turnoff; granite area. No visible damage from outside of adobe-block house.

B-3. Rancho Agua Blanca. Adobe-block dwelling. Cracks in external plaster and above window lintels (fig. 11). Spring went dry.

B-4. Rancho Ciénega. Adobe dwelling. One small crack in upper corner.

C-1. El Álamo. Town of about 100 inhabitants; gold mining (lode) in near-by hills. All buildings in the town were of adobe-block construction, many of them apparently very old. This town was a

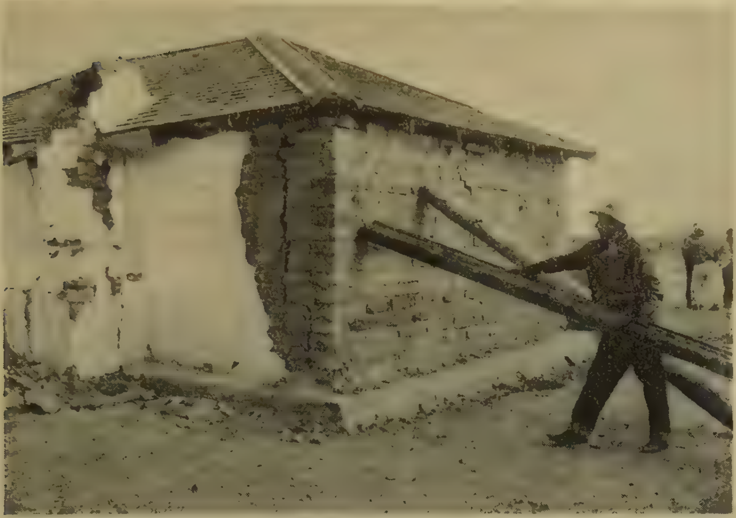

Fig. 10. Badly damaged adobe-block house at Rancho Mezquite. San Diego Union photo.

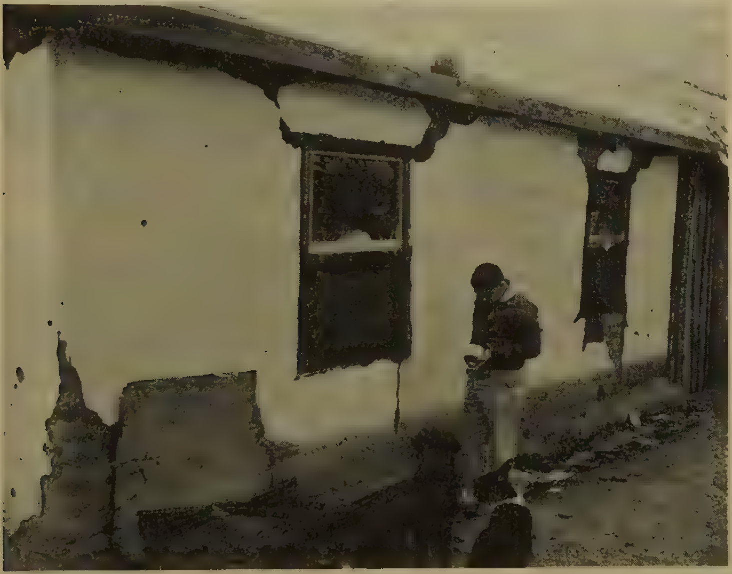

Fig. 11. Typical cracks upward and outward from window lintels in adobe-block dwelling at Rancho Agua Blanca. San Diego Union photo.

boom town of about 5,000 people in 1889; the present buildings are apparently left from that period. Every building to be seen from the main street showed some cracking, the almost universal type being cracks upward and outward from the wood lintels above windows or doors. There is some question about the date of this cracking; according to the Sub-Delegado, Jesús Menendres, the damage to the town was caused not by this series of earthquakes but by one on December 12, 1955. There may have been a mistranslation here; there is no record at the Pasadena laboratory of a shock on that date. A much later check, with the proprietor of the general store, produced the information that the cracks in his store were caused by the earthquakes in February, 1956. At that time, merchandise in this store fell off the shelves.

C-2. Rancho Llano Colorado. A small, apparently abandoned, adobe house with adobe blocks stacked within it to dry. No visible damage. This house is situated on the edge of a playa (dry lake bed).

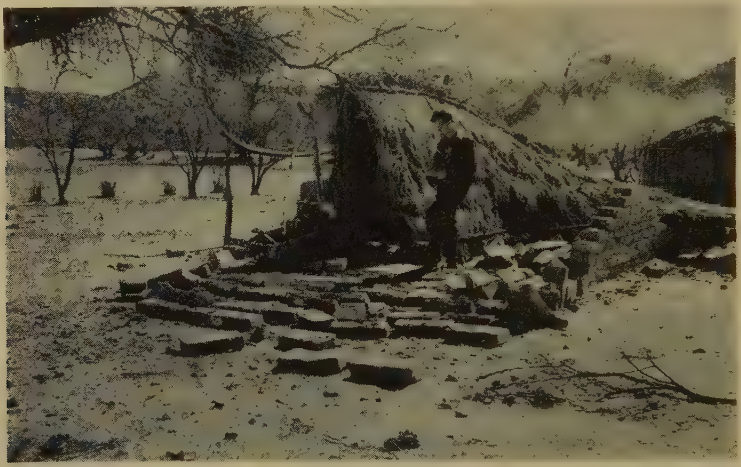

Fig. 12. Ruins of adobe-block dwelling at San Miguel. San Diego Union photo.

C-3. Rancho Los Positos (official name; shown on maps and locally known as Rancho Viejo). Four-room adobe house. The construction of this house looks somewhat different from that of the other adobe-block houses observed. The blocks are large, and seem to have no sharp dividing lines; possibly they were laid wet and dried in place. Walls 14 inches thick. Small cracks upward and outward over every window and door, starting at the upper corners of the lintels; no severe damage. The roof is wood-shingled. According to the owner, José García, these cracks were caused by "the earthquakes in February," without specification of which date.

C-4. San Miguel. The village of San Miguel lies within the Santa Catarina Reservation of the Pai-Pai Indian tribe; it consisted of three adobe-block houses, two houses of brush plastered with mud, and a frame schoolhouse. The hills on the northeast side of the valley are granitic with small patches of metamorphics. The fault trace lies at the base of these hills, separating granite from alluvium. On the southwest side of the valley are volcanic hills. Three adobe houses on alluvium 100 to 200 yards southwest of the fault trace collapsed completely, the walls falling roughly northwest. Failure was through the mud between the blocks; most of the blocks were intact. Like all the other adobe houses in the area, these had no foundations (blocks laid directly on the soil) and only mud between the blocks. The roofs were light-weight (corrugated steel or thatch) with a minimum of wood bracing. One brush-and-mud shack on alluvium and the other on granite survived with only some mud cracked off. Figure 12 shows a collapsed adobe house in the foreground, an undamaged brush shack behind.

The frame schoolhouse was built with its west end resting directly on the ground without foundations. The ground level at the east end was lower than that at the west by about one foot. To level the building, beams had been laid on the ground the long (east–west) way of the structure; upon

(156)

them 1 by 2-inch posts were set vertically like a picket fence, and the building rested upon these. The rows of posts had no bracing, either diagonally or between the longitudinal rows. The east end of the building slipped sideways to the south, tipping the posts over (fig. 13). The frame of the building was warped, but no glass was broken. The building was about 150 yards from the fault trace.

The residents of San Miguel had all been absent at the time of the earthquakes, working in the cotton fields near Mexicali, and had not returned by February 25. No one had known of the damage or visited the houses between February 9 and 14, as far as could be determined.

C-4. Ranch 0.3 mile south of San Miguel. A small ranch, with one adobe-block house and a house partly adobe block and partly brush. Parts of the adobe walls were fallen to the west, the bricks intact but the mud between separated. The brush part was unharmed.

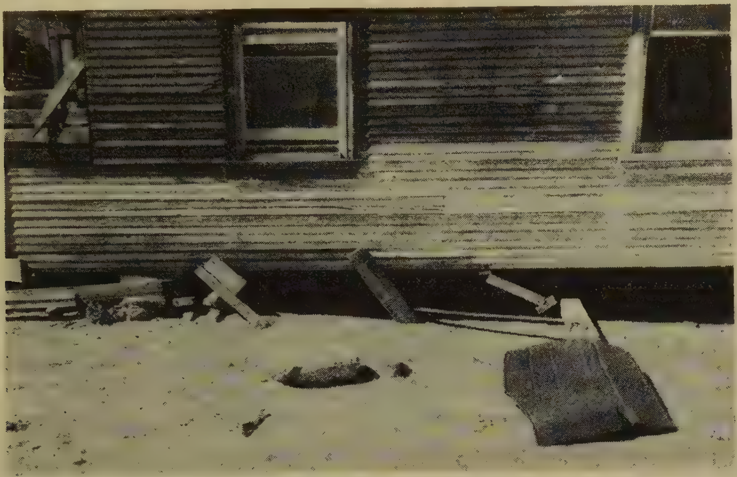

Fig. 13. Detail of schoolhouse at San Miguel, showing tipped "picket fence" foundation posts. San Diego Union photo.

C-4. Santa Catarina. A small settlement on the Santa Catarina Indian Reservation, near the site of the old Misión Santa Catalina. It consists of a few houses on each side of a small valley. The part inspected consisted of two houses, one of which was made of adobe bricks and the other of adobe brick with a brush-and-wattle lean-to. The adobe sections had suffered minor cracking. There were hairline cracks in the ground. These houses were on residual soil adjacent to an outcrop of large residual granite boulders. The tribal chief, Eugenio Albanes, aged 74, stated that he had lived there all his life and had never felt a stronger shock. On the morning of February 9 he heard an explosion and then a rumble, and was thrown to the floor of his house.

C-5. Agua Escondido. Two adobe houses. Part of one wall fallen.

C-5. House southeast of Agua Escondido. Adobe house (unoccupied) suffered minor damage.

E-5. Valle Trinidad. Consists of a store and nine houses, all adobe brick, lying on the north slope of the valley near the edge of the alluvium. The store was damaged slightly; there were open cracks between the bricks visible a year later. The nearest house to the store had cracks in the front wall around the roof beams.

E-8. Rancho Arroyo Grande. Adolf Meling, sole inhabitant of this small cattle ranch at the time of the earthquake and of the interview, stated that the first shock (February 9) shook him but did not damage the house. He had to hold the kitchen stove to keep it from falling over, and the dishes to keep them on the shelf. Large rocks rolled from the hills, and clouds of dust rose so that he could not see. The "second shock" ("three or four days later at about 10 in the morning," obviously the shock of 10:33:34, 14 February) caused major cracking in the house and blacksmith shop, dislodged some concrete blocks from the walls, and caused rocks to roll. Meling felt it while sitting on a burro. The "third shock" increased the damage to the house. Damage to the concrete-block house consisted of cracks through and around the blocks (made on the spot using coarse arkosic material for sand), the displacement of blocks from the peaks of the end walls and from the interior walls, and hairline cracks in the concrete slab floor. There was no reinforcement in the walls. The blacksmith shop, a one-room concrete-block building with a dirt floor, had the blocks of the walls shattered and bulging outward in places; they had been repaired by forcing the walls back into position with a jack against a post and then banding the building together with steel wire. There was no damage to the wood-frame barn, the openwork steel windmill tower, or the concrete water tank (nearly empty at the time of the shocks). The ranch is adjacent to a granite outcrop on a stream terrace in the bend of Arroyo Grande. Springs at the ranch were not affected by the earthquake, but the spring at "Tres Campos," in the hills west of the ranch, had an increased flow of water. On the hill just above the ranch there had been ground disturbance at one point that "looked like somebody'd been prospecting." Hairline cracks were observed by Meling in the stream bottoms. He also reported that aftershocks were still being felt in May, 1957.

ACKNOWLEDGMENTS

Information gathered by others who visited the area has been incorporated in this paper; among these are Robert Dill, James A. Noble, and Clarence Allen. Students from San Diego State College aided in surveying for the map of surface features, and Gifford Ewing flew his personal plane for an aerial reconnaissance.

Jesús Menendres, Sub-Delegado (deputy mayor) for El Álamo, guided the first party to the area and provided valuable information. The late Manuel Acosta-Meza served as interpreter on this occasion. Many of the pictures are by courtesy of the Union-Tribune Publishing Company; they were taken by Henry Kierstead. The Pacific Fire Rating Bureau has provided financial aid and drafting. Aid from Betty Shor in field work, editing, and typing is gratefully acknowledged.

REFERENCES

Beal, Carl H.
1948. "Reconnaissance of the Geology and Oil Possibilities of Baja California, Mexico," *Geol. Soc. Mem.*, 31.

Gerhard, Peter, and Howard E. Gulick
1956. *Lower California Guidebook* (Glendale, Calif.: The Arthur H. Clark Co.). 218 pages.

Holden, Edward S.
1898. "Catalog of Earthquakes on the Pacific Coast, 1769–1896," *Smithsonian Misc. Col.* 1087.

Lindgren, W.
1888. "Notes on the Geology of Baja California, Mexico," *Proc. Calif. Acad. Sci.*, 2d ser., 1: 173–196.

Richter, Charles F.
1956. "Seismological Notes: Baja California, February 9th, 1956," *Bull. Seism. Soc. Am.*, 46: 161–162.

Shor, G. G., Jr.
1956. "Seismological Notes: San Miguel, Baja California, February 9 and 14, 1956," *Bull. Seism. Soc. Am.*, 46: 162–163.

Wood, Harry O., and N. H. Heck
1951. "Earthquake History of the United States. Part II—Stronger Earthquakes of California and Western Nevada," Coast and Geodetic Survey, *Serial* No. 609, p. 13.

Woodford, A. O., and T. F. Harriss
1938. "Geological Reconnaissance across Sierra San Pedro Martir, Baja California," *Bull. Geol. Soc. Am.*, 49: 1297–1336.

MARINE PHYSICAL LABORATORY,
SCRIPPS INSTITUTION OF OCEANOGRAPHY,
LA JOLLA, CALIFORNIA.
(Contribution no. 984, New Series.)

(158)

Deep-Sea Research, 1958 Vol. 5, pp. 1 to 6. Pergamon Press Ltd., London

Deep-sea bathymetry north of Point Barrow*

R. L. FISHER†, A. J. CARSOLA‡ and G. SHUMWAY‡

Abstract—Favorable ice conditions in 1951 and 1957 allowed echo-sounding across the continental slope and into the deep basin north of Pt. Barrow, where a relatively smooth sea-floor between 2000 and 2100 fm deep was found. North-northwest of Pt. Barrow lies a continental borderland area containing a detached ridge 100 miles long with a steep (23°) southeast flank.

INTRODUCTION

CONTINUOUS echo–sounder lines from anywhere in the deep basins of the Arctic Ocean are rare due to the fact that pack ice covers most of the area the year round. During the brief Arctic summer the shallow edges of the polar sea, underlain by the continental shelf, may become ice-free; in exceptionally good years it is possible for icebreakers to penetrate a short distance into deep–water regions. Favorable ice conditions during the summers of 1951 and 1957 made it possible to obtain many continuouous echo-sounding lines running over the continental slope and well into the deep basin north of Pt. Barrow, Alsaka.

A reconnaissance cruise made in 1950 by the icebreaker *U.S.S. Burton Island* obtained sounding lines along the continental slope north of Alaska and Canada as far east as Banks Island. In 1951 the *Burton Island*, with geological observations under CARSOLA, carried out an extensive survey between Banks Island (125°W) and the 170° meridian. Some results of the 1951 cruise have been published (CARSOLA 1954, a, b, c, d, 1955). In 1954 *H.M.C.S. Labrador* carried out a survey west of 157°W between 73°N and 75°N. In 1957 two icebreakers were used for survey work: M. A. BEAL and J. H. SHERMAN III, working from *U.S.S. Staten Island*, obtained bathymetric records and bottom samples from the continental shelf and slope northeast of Barrow; two of us (R.L.F. and G.S.), working from *U.S.C.G.C. Northwind*, obtained bathymetric data on the continental slope and deep–sea floor north of Barrow.

Bathymetric data for the ocean north of Alaska have been published by CRARY, COTELL and OLIVER (1952), WORTHINGTON (1953)†, CRARY (1954) and CRARY and GOLDSTEIN (1957). A bathymetric chart of the Arctic Ocean is presented in a Soviet publication (ANONYMOUS, 1954). Earlier bathymetric studies are summarized by EMERY (1949). PANOV (1955) discussed neotectonic movements in the Arctic region.

Russian investigations, as summarized on a small-scale chart (ANONYMOUS, 1954), suggest that an extensive area shoaler than 1650 fm (3000 m) separates the deep–sea floor northeast of Barrow from the far northern basins adjacent to Lomonosov Ridge (and the Marvin Ridge of CRARY and GOLDSTEIN, 1957). The present writers propose the name Beaufort Basin to designate the region deeper than 1900 fm (or 3500 m) extending from about 140 — 160°W and northward an unspecified distance

---

*This work was supported in part by Scripps Institution of Oceanography contracts with the Arctic Institute of North America and the Office of Naval Research. Reproduction rights in whole or in part permitted for any purpose of the United States Government.

†Also reported as unpublished technical reports of the Woods Hole Oceanographic Institution: HOLMES J. F. (1951) Report 51-67; HOLMES J. F. and WORTHINGTON L. V. (1953) Report 53-23.

Reproduced by Permission

from the continental slope north of Alaska. This paper presents bathymetry of the western portion of the Beaufort Basin and its western and southwestern borders (Fig. 1).

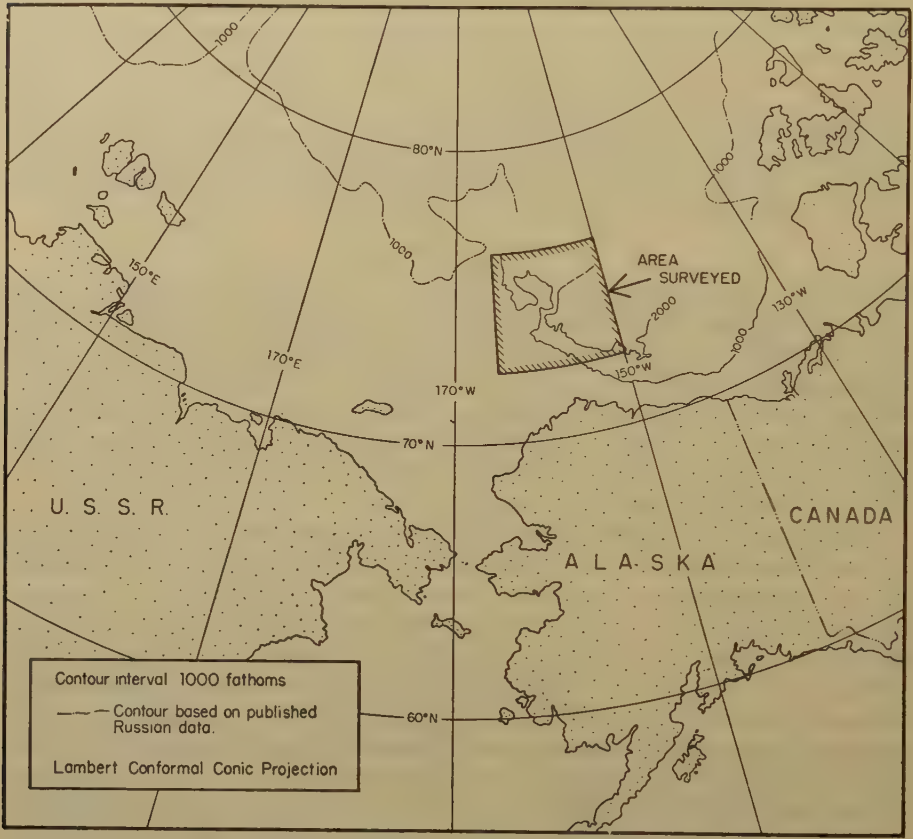
1000
80°N
1000
150°E
AREA SURVEYED
2000
130°W
1000
170°E
170°W
150°W
70°N
U. S. S. R.
CANADA
ALASKA
60°N
Contour interval 1000 fathoms
——— Contour based on published Russian data.
Lambert Conformal Conic Projection

Fig. 1. Location of survey area in the Arctic Ocean.

DISCUSSION

The detailed bathymetric chart (Fig. 2) is a product of the 1950, 1951, 1954 and 1957 investigations only, except for the four spot soundings in the northeast sector of the chart. Only these four soundings have been corrected for the dependence of sound velocity on temperature and salinity of sea–water. The continuous lines were recorded with an assumed sounding velocity of 4800 ft (1463 m) per sec. This value is within 50 ft/sec, about 1 per cent, of the velocities for the Arctic Ocean employed by Crary and Goldstein (1954, p. 187). It is greater than their shallow–water and less than their deep–water value. Slope corrections have not been applied. In traversing steep slopes, side echoes may arrive prior to returns from directly beneath the ship, resulting in an apparent sea–floor slope which is less than the true slope. This effect was noted along the N–S scarp north of 74°N, but the first recorded arrival was accepted as the depth.

During the 1951 and 1954 investigations the survey ships obtained ship's position by Electronic Position Indicator (BURMISTER, 1951, p. 4). This method is particularly convenient when operating in ice areas where poor visibility, maneuvering and frequent speed changes make dead reckoning between celestial observations uncertain, at best. In the field, the 1957 survey positions were controlled by sun lines, and intermediate positions were determined by continuous radar tracking of large, distinctive ice floes to establish ship's speed and direction. The 1957 tracks have been transposed where depth crossings with the 1951 lines indicated adjustment was necessary. Where such crossings were unavailable, the 1957 lines have a probable error of ± 2 miles in position.

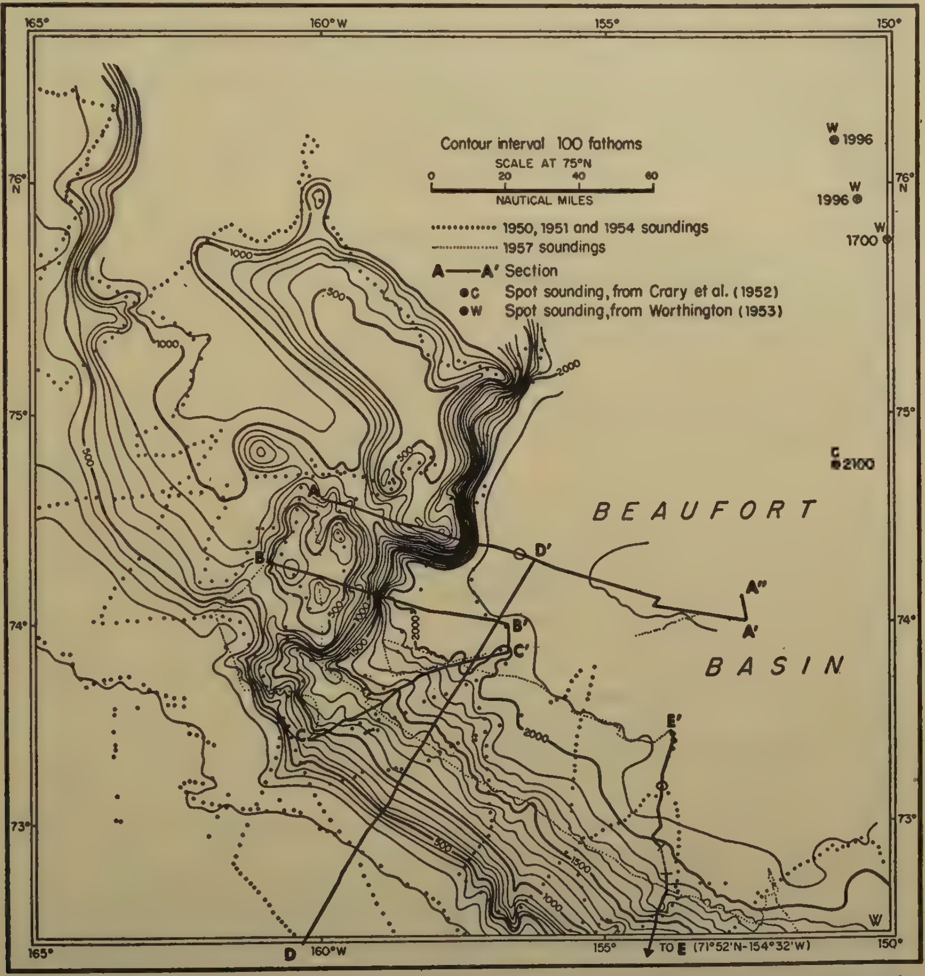
165°
160° W
155°
150°
76° N
75°
74°
73°
Contour interval 100 fathoms
SCALE AT 75°N
0
20
40
60
NAUTICAL MILES
1950, 1951 and 1954 soundings
1957 soundings
A——A' Section
●C Spot sounding, from Crary et al. (1952)
●W Spot sounding, from Worthington (1953)
W 1996
W 1996
W 1700
C 2100
BEAUFORT
BASIN
1000
500
2000
1500
A
A'
A''
B
B'
C
C'
D
D'
E'
W
160°W
TO E (71°52'N-154°32'W)

Fig. 2. Bathymetry for a portion of the Arctic Ocean north of Alaska, based on continuously-recorded echo-sounding lines. Sections A-A'', B-B', C-C'-B', and E-E' are along 1957 sounding lines. Section D-D' is along 1951 sounding line down to 1900 fm contour.

Four topographic characteristics of the area of sea–floor included in Fig. 2 should be noted; these characteristics appear clearly on the bathymetric cross-sections (Fig. 3).

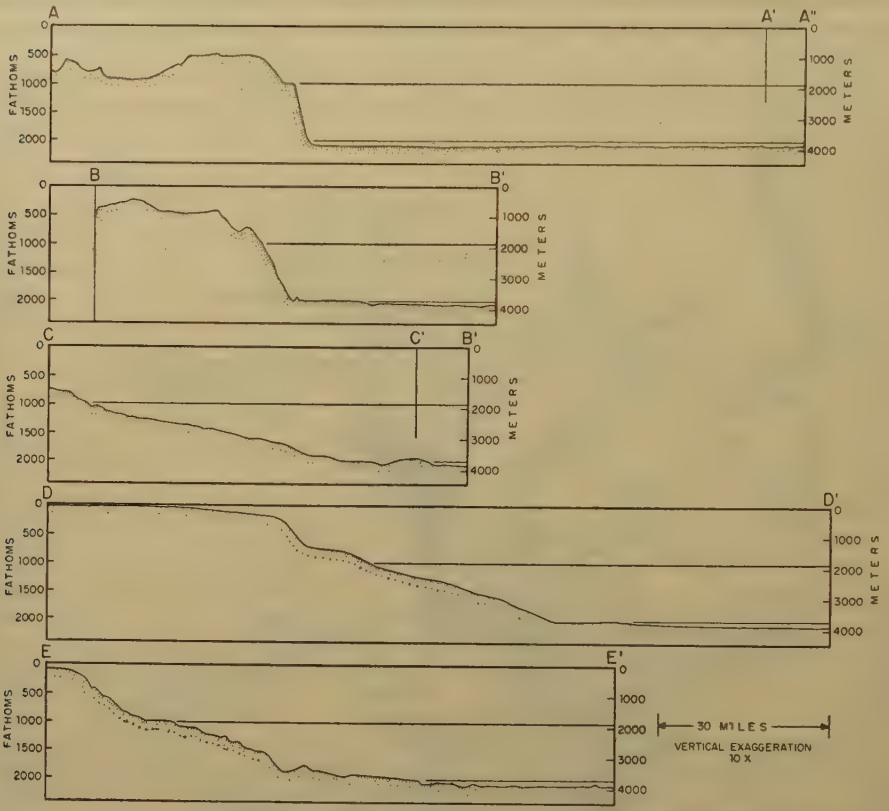

Fig. 3. Cross-sections down the continental slope north of Pt. Barrow (See Fig. 2 for locations).

First, the part of the Beaufort Basin now relatively well-explored, about 6000-8000 sq. miles in all, is nearly flat-bottomed at 2060 ± 60 fm (Fig. 3, sections A-A′, B-B′, D-D′). A slight rise lies northeast of 74°N, 155°W. The transition from continental slope to flat bottom is abrupt on the north-western sections. Apparently basement relief has been buried by a level-surfaced mass of sediment. Three of the four spot soundings (Fig. 2) suggest that this basin extends at least to 76°N, 151°W. The 1700 fm sounding may represent an isolated seamount or a ridge terminating the abyssal plain.

Second, from two normal and three oblique slope crossings in 1957 and well-controlled 1951 and 1954 soundings, the lower continental slope (below 1000 fm) is shown to be a steep scarp (23° on section A-A′) in the area west of the basin. This contrasts sharply with the lower slope to the southeast which ranges from 1°09′ to 1°56′ in three normal crossings between the vicinity of section C-C′ (Fig. 3) and the vicinity of the Mackenzie Delta. The lower slope becomes progressively gentler proceeding southeast from the vicinity of the sharp bend between sections D-D′ and B-B′; the gradient north of the bend steepens abruptly.

Third, off the Alaskan coastal plain southeast of Fig. 2, the upper continental slope is steep, ranging from 4 to 10°. Off Pt. Barrow, where the shelf-break lies near 35 fm, a very gentle upper slope appears (CARSOLA, 1954a). This upper slope extends to greater depths and widens toward the north-northwest until in the region shown in the extreme northwest portion of Fig. 2 it extends to a depth of almost 500 fm. It is possible that this feature continues to widen and deepen toward the north-west, where it may ultimately join the broad area shoaler than 1650 fm described recently by the Russians (ANONYMOUS, 1954). This upper slope province recalls the Blake Plateau off the southeast coast of the United States, where a similar region next to the shelf has a 1° gradient to depths between 300 and 500 fm (SHEPARD, 1948, pp. 176-177).

Fourth, the existence of an isolated area shoaler than 500 fm centred near 75°N, 158°W, has been established by four sounding lines, only one of which crossed a portion of its summit. The flat-topped nature of the feature as shown in Fig. 2 is an interpretation only. It is proposed that this feature be named Northwind Seahigh after the *U.S.C.G.C. Northwind* which made the southern-most crossing. A broad, flat-bottomed trough which narrows to a steep-walled gap or cleft toward the south separates this spur from the shallow area to the south-west. SHEPARD (1948, p. 105) has applied the term " continental borderland " to similar regions of intermediate depth adjacent to continental shelves.

Acknowledgments—These studies could not have been carried out without the assistance of a number of persons and organizations. For the 1951 survey the officers and men of the *U.S.S. Burton Island* (AGB-1) are thanked for their co-operation in the field; Dr. WALDO K. LYON of the U.S. Navy Electronics Laboratory and Prof. CLIFFORD A. BARNES of the University of Washington directed the 1951 survey and gave guidance and field assistance. Dr. LYON also provided sounding plots of the 1954 survey as prepared by CHARLES RICHARDSON. For the 1957 work, MAX BREWER, Director of the Arctic Research Laboratory of the University of Alaska, provided laboratory facilities and equipment. M. ALLAN BEAL and JOHN B. SHERMAN III of the Scripps Institution of Oceanography conducted the complementary survey on the *U.S.S. Staten Island*. The writers thank Capt J. A. BRESNAN, Cdr B. M. CHISWELL, Ltjg H. HAUGEN and the other officers and men of the *U.S.C.G.C. Northwind* (WAGB-282) for their enthusiastic support in the 1957 survey; the echo-sounder watch was kept by G. W. DALE, W. C. HAGEN, L. C. PARTAIN and K. C. COOK. ROBERT C. WINSETT drafted the illustrations.

†*Scripps Institution of Oceanography of the University of California, La Jolla, Calif.*
‡*U.S. Navy Electronics Laboratory, San Diego 52, Calif.*

Contribution of the Scripps Institution of Oceanography of the University of California, New Series No. 985. *U.S. Navy Electronics Contribution No.* 43.

REFERENCES

ANONYMOUS (1954) Soviet research, explorations and discoveries in the central Arctic. *Izv. Akad. Nauk., SSSR (ser. geog.)* **5**, 3–16.

BURMISTER C. A. (1951) Measuring long lines by electronic methods. *J. Coast Geod. Survey, No.* 4.

CARSOLA, A. J. (1954a) Extent of glaciation on the continental shelf in the Beaufort Sea. *Amer. J. Sci.* **252**, 366–371.

CARSOLA, A. J. (1954b) Microrelief on Arctic sea floor: *Bull. Amer. Ass. Pet. Geol.* **38**, 1587–1601.

CARSOLA, A. J. (1954c) Recent marine sediments from Alaskan and Northwest Canadian Arctic. *Bull. Amer. Ass. Pet. Geol.* **38**, 1552–1586.
CARSOLA A. J. (1954d) Submarine canyons on the Arctic slope. *J. Geol.* **62**, 605–610.
CARSOLA A. J. (1955) Bathymetry of the Arctic Basin. *J. Geol.* **63**, 274-278.
CRARY A. P. (1954) Bathymetric chart of the Arctic Ocean along the route of T-3, April 1952 to October 1953. *Geol. Soc. Amer. Bull.*, **65**, 709–712.
CRARY A. P. and GOLDSTEIN N. (1957) Geophysical Studies in the Arctic Ocean. *Deep-Sea Res.*, **4**, 185–201.
CRARY A. P., COTELL R. O. and OLIVER J. (1952) Geophysical studies in the Beaufort Sea, 1951. *Trans. Amer. Geophys. Un.*, **33**, 211–216.
EMERY K. O. (1949) Topography and sediments of the Arctic Basin. *J. Geol.*, **57**, 512–521.
PANOV D. G. (1955) Neotectonic movements in the Arctic region. *Dokl. Akad. Nauk, SSSR*, **104**, 3, 462–465.
SHEPARD F. P. (1948) *Submarine Geology*. Harper and Bros., New York.
WORTHINGTON, L. V. (1953) Oceanographic results of Project Skijump I and Skijump II in the Polar Sea, 1951-1952. *Trans. Amer. Geophys. Un.*, **34**, 543–551.

Printed in Great Britain by The Salisbury Press Ltd., Publicity House, Wilton Road, Salisbury, Wilts. (9590)

(164)

Geochimica et Cosmochimica Acta, 1958, Vol. 14, pp. 35 to 54. Pergamon Press Ltd., London

The removal of soluble silica from fresh water entering the sea*

G. S. BIEN, D. E. CONTOIS and W. H. THOMAS
Scripps Institution of Oceanography, University of California, La Jolla, California

(*Received* 25 *September* 1957)

Abstract—Determinations of soluble silica and chlorosity of water samples collected in and around the east Mississippi Delta showed that most of the soluble silica was removed from river-water by some process other than dilution with sea-water. While biological uptake by diatoms can account for part of this removal, it is more likely that a major portion is removed by inorganic precipitation.

Laboratory experiments with river-water and sea-water showed that both suspended matter from the river and electrolytes in sea-water are necessary for maximum inorganic precipitation. It is concluded that this process is an adsorption of soluble silica on suspended matter as it comes in contact with electrolytes, rather than a simple formation of salts with electrolytes. The inorganic removal can increase by a maximum of 4·5 per cent the weight of sediment in the water which may be expected to reach the bottom.

INTRODUCTION

The concentration of soluble silica in river-water is generally ten to fifteen times that of surface-water in the open ocean. The soluble silica concentration of Mississippi river-water averages 4–7·5 p.p.m., while the average concentration in Gulf of Mexico surface sea-water is 0·11 p.p.m. In spite of the large amount of soluble silica that is brought into the ocean, there is no sign of an accumulation of soluble silica in surface sea-water. Two hypotheses have been proposed to account for the depletion of soluble silica: biological removal and inorganic precipitation.

Biological removal of soluble silica from culture solutions by diatoms has been shown by JORGENSEN (1953). Also, ARMSTRONG (1954) and others have shown that following the spring "blooming" of diatoms in the English Channel the concentration of soluble silica in surface water was much reduced. KRAUSKOPF (1956) concludes that because no dissolved silica was precipitated when he added silica solutions to sea-water, biological removal must be the main factor in preventing the accumulation of silica in sea-water. Moreover, during the initial mixing of river-water, before biological removal can occur, it might be expected that the concentration of soluble silica would decrease only because of dilution. If only dilution occurred, the concentration of soluble silica would be a linear function of dilution, as measured by chlorosity determination. Any deviation from linearity would be a measure of the extent of removal.

Such a linear relationship was found by MAEDA and his associates (MAEDA 1952, 1953; MAKIMOTO *et al.*, 1955). However, their data only cover the chlorinity range from 5–17‰, which does not represent the complete range.

We have had an opportunity to test the dilution hypothesis at chlorinities of 0·1–21‰ in the area of the eastern Mississippi River Delta at Pass a Loutre, where the river empties into the Gulf of Mexico. We have also made measurements of

---

* Contribution from the Scripps Institution of Oceanography, New Series No. 986. This investigation was supported by a grant from the American Petroleum Institute, Project 51.

Reproduced by Permission

(165)

phytoplankton production from which we have attempted to calculate the magnitude of silicate removal by phytoplankton and furthermore we have studied possible inorganic removal processes in the laboratory, using water samples from the Delta. Our results are reported in this paper.

METHODS AND MATERIALS

Water samples were obtained in the field at stations shown in Fig. 1. One portion of each sample was drawn off into a glass citrate bottle, stoppered, and returned to the laboratory for the determination of chlorinity by tritation with silver nitrate. Chlorosity was calculated from this determination.

A second sub-sample was drawn from each Nansen bottle and filtered through a molecular filter (Millipore, type HA) having an average pore size of 0·45 μ. The filtrate was placed in a polyethylene bottle and returned to the laboratory for analysis of soluble silica. Experiments with sodium silicate solutions of known concentration indicated that no significant increase in soluble silica concentration occurred due to contact of water samples with the glass of the filter holders and evacuation flasks.

Soluble silica concentration was determined by the method of DIENERT and WANDENBULCKE (1923). Light absorption was measured with a Beckman Model-DU spectrophotometer at a wavelength of 360 mμ and extinction coefficients were corrected for "salt error". These "salt errors" are different for different salinities and are not a linear function of chlorosity. Beer's law slopes were, therefore, determined at different chlorosities and the "salt error" corrections applied at different chlorosities were determined from these plots. Duplicate determinations of soluble silica agreed within 5 per cent, but because of a high and variable blank correction, the values given are accurate to only ±2 μmoles/l. Soluble silica was defined as the portion of the total silica which formed silicomolybdic acid in the presence of ammonium molybdate and sulphuric acid. According to ROY (1954) and ALEXANDER, HESTON and ILER (1954), only the silicate that is in true solution and in the ionic form will react with these reagents.

The possibility that, upon contact with sulphuric acid during colour development, more silica was dissolved from colloidal material which might pass the molecular filter was tested by comparing filtered river-water with dialysed river-water. Both the filtrate and the dialysate contained the same amount of soluble silica. Thus it is unlikely that such dissolution occurred.

Phytoplankton production was determined by the method of STEEMAN-NIELSEN (1952) using ^{14}C. Phytoplankton production in the Delta will be the subject of another paper (THOMAS and SIMMONS, in preparation). Only a range of values for production obtained immediately off Pass a Loutre is used in this paper for the calculation of biological uptake of soluble silica.

A sample of surface river-water for laboratory experiments on inorganic removal was collected at Station C-2 (see Fig. 1.). It had a chlorosity of 0·035 g Cl^-/l. and contained 82·06 μmoles soluble silica/l. A surface-water sample from the Gulf of Mexico was collected east of the Delta beyond the area shown in Fig. 1. The exact location is not known. This sample had a chlorosity of 20·61 g Cl^-/l. and contained only a trace of soluble silica. Both river and Gulf samples were stored in polyethylene carboys until used. Biological activity was stopped by the addition of 1 p.p.m. $HgCl_2$ to these samples. Since soluble silica concentrations did not change during several months storage, treatment with $HgCl_2$ was successful in stopping biological activities.

RESULTS AND DISCUSSION

(a) *Field data*

Fig. 1 shows the station locations at which water samples were obtained during three different field trips. Tables 1, 2 and 3 summarize the results of the soluble silica and chlorosity determinations. Plots of soluble silica versus chlorosity for the various groups of data are shown in Figs. 2, 3 and 4.

The straight, dashed line on each graph indicates the line around which the points should group if the soluble silica of the river-water were merely diluted upon

(166)

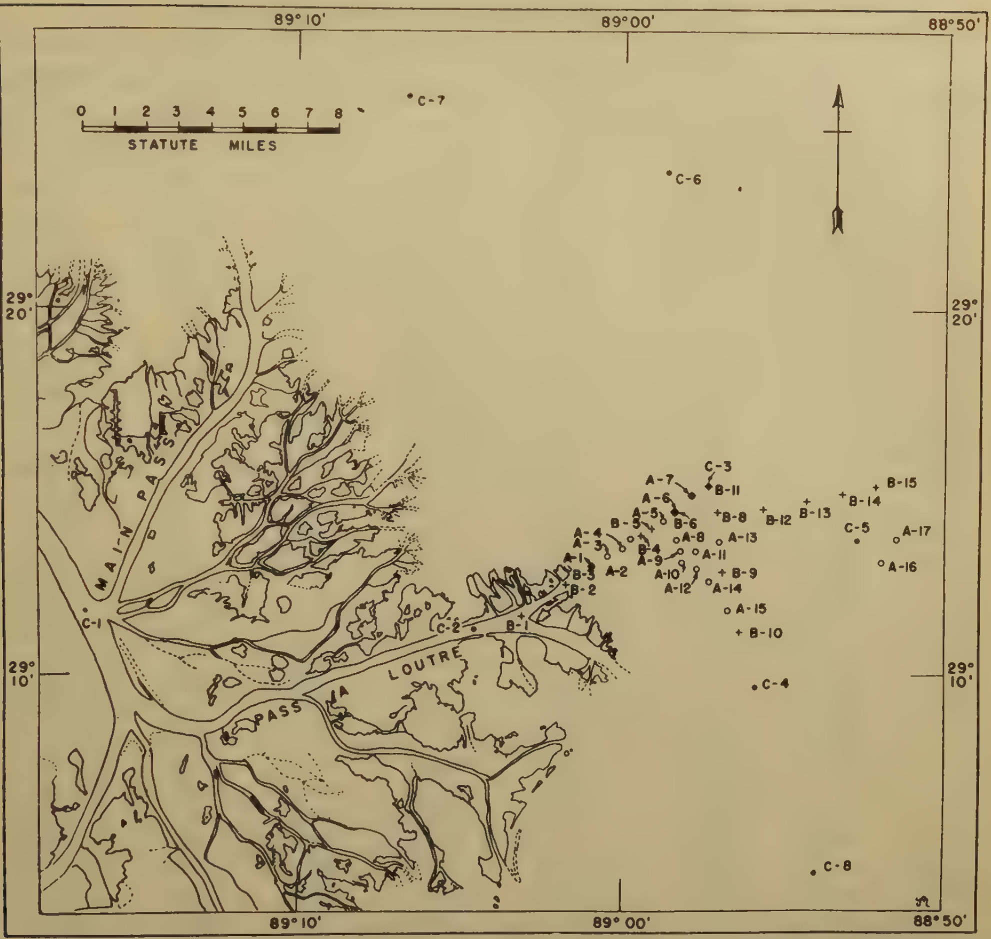
89° 10'
89° 00'
88° 50'
0 1 2 3 4 5 6 7 8
STATUTE MILES
C-7
C-6
29° 20'
29° 10'
MAIN PASS
PASS A LOUTRE
C-1
C-2
B-1
C-3
A-7
B-11
A-6
A-5
B-5
B-6
B-8
B-12
B-13
B-14
B-15
A-4
A-3
A-8
A-13
C-5
A-17
B-4
A-11
A-1
A-9
A-16
B-3
A-2
A-10
B-9
B-2
A-12
A-14
A-15
B-10
C-4
C-8

Fig. 1. Chart showing station locations in the vicinity of Pass a Loutre sub-delta of the Mississippi River. Stations B-16, B-17, and B-18 are respectively 4, 8 and 12 statute miles due east of Station B-15.

mixing with open Gulf water. This line is obtained in each instance from average values of chlorosity and soluble silica in the open Gulf water and "typical" river-water.

Determinations of the chlorosity of open Gulf water over several field seasons have shown that it varies relatively little—averaging 20·4 g Cl^-/l., with a standard deviation of 0·5 g/l. The soluble silica concentration of open Gulf water averages 4·2 μmoles/l. and has a standard deviation of 3·1 μmoles/l.

Values of chlorosity and soluble silica of river-water are constant at any given time, but vary considerably throughout the year. In general, they are proportional to the amount of river discharge. As a result, the constants of the straight lines showing the theoretical relationship between soluble silica and chlorosity are determined entirely by the characteristics of the river-water.*

---

* Our values of soluble silica in Mississippi river-water varied from 65 to 120 μmoles of silica/l. (4–7·5 p.p.m.), which is in excellent agreement with the values of Schwartz (1938) and slightly lower than the earlier values of Clarke (1924).

Table 1. Silicate and chlorosity data of June 1953

Station	Depth (ft)	Soluble silica µmoles/l.	Chlorosity (g Cl⁻/l.)	Station	Depth (ft)	Soluble silica µmoles/l.	Chlorosity (g Cl⁻/l.)
A-1	0	78·6	0·2	A-12	0	73·2	0·2
A-1	7·5	80·7	0·2	A-12	5	11·0	14·4
A-2	0	82·0	0·2	A-12	10	7·7	16·0
A-2	12	70·2	0·2	A-12	25	7·3	18·8
A-3	0	77·5	0·2	A-12	36	11·0	13·9
A-3	16	76·0	0·2	A-13	0	72·8	0·4
A-4	0	76·3	0·2	A-13	5	31·3	8·4
A-4	7·5	76·8	0·2	A-13	10	6·2	14·8
A-5	0	76·0	0·4	A-13	25	4·2	18·2
A-5	3	64·3	2·0	A-13	40	3·8	20·2
A-5	6	35·2	9·0	A-14	0	36·0	8·4
A-6	0	72·8	0·3	A-14	5	10·3	15·0
A-6	5	32·2	9·0	A-14	10	6·5	16·0
A-6	10	11·8	14·7	A-14	25	9·7	18·9
A-6	25	6·3	18·0	A-14	40	9·8	19·0
A-6	40	9·5	18·7	A-15	0	72·3	1·0
A-7	0	68·3	0·7	A-15	5	19·7	12·4
A-7	5	28·8	8·9	A-15	10	7·3	15·6
A-7	10	12·0	14·1	A-15	25	4·0	18·3
A-7	25	2·8	18·0	A-15	40	7·0	18·5
A-7	40	2·8	18·9	A-15	85	8·3	20·3
A-7	104	8·2	20·2	A-16	0	71·2	0·7
A-8	0	51·0	4·9	A-16	5	4·5	16·7
A-8	5	18·5	13·1	A-16	10	2·7	18·1
A-8	8	17·7	14·5	A-16	25	4·0	19·4
A-9	0	66·7	1·4	A-16	40	2·8	20·2
A-9	5	29·3	10·0	A-16	100	8·8	20·4
A-9	7	16·2	13·7	A-16	188	7·0	20·5
A-10	0	72·8	0·3	A-16	0	56·7	2·9
A-10	5	47·8	5·8	A-17	0	6·5	15·8
A-10	7	22·3	13·0	A-17	5	2·8	18·8
A-11	0	73·5	0·8	A-17	10	1·5	19·7
A-11	5	9·7	15·6	A-17	25	2·0	19·9
A-11	10	7·5	16·6	A-17	40	2·3	20·1
A-11	25	7·3	17·7	A-17	100	3·0	20·5
A-11	40	8·5	18·7	A-17	188	5·0	20·3

A consideration of Figs. 2, 3 and 4 leads to the conclusion that the observed distribution of soluble silica as a function of chlorosity (dilution) differs significantly from that which would be expected from the hypothesis that the soluble silica of the river-water is merely diluted upon mixing with Gulf water. Even if the slope of the theoretical dilution line shown in these figures is changed to take the error (±2 µmoles) of the determination of soluble silica into account, significant deviations from this straight line still exist and the results cannot be explained on the basis of experimental error.

Table 2. Silicate and chlorosity data of July 1955

Station	Depth (ft)	Soluble silica (μmoles/l.)	Chlorosity (g Cl^-/l.)
B-1	0	114	0·62
B-1	5	113	0·63
B-1	10	114	0·62
B-1	15	118	0·63
B-1	20	113	0·63
B-1	25	115	0·63
B-2	0	110	0·58
B-3	0	108	0·66
B-4	0	110	0·61
B-5	0	110	0·66
B-6	0	109	1·02
B-7	0	110	1·20
B-8	0	105	2·20
B-9	0	101	2·24
B-10	0	99·9	2·66
B-11	0	79·7	5·08
B-11	5	20·9	13·2
B-11	10	22·9	13·9
B-11	15	6·0	16·6
B-11	20	3·0	17·8
B-11	25	6·5	18·2
B-12	0	96·7	3·33
B-13	0	89·6	3·87
B-14	0	75·1	5·92
B-15	0	85·0	4·66
B-15	5	24·1	13·6
B-15	10	4·8	16·9
B-15	15	7·6	16·8
B-15	20	5·2	16·4
B-15	25	3·0	18·0
B-16	0	61·9	7·68
B-16	5	12·3	15·4
B-16	10	7·0	16·0
B-16	15	2·8	17·2
B-16	20	1·2	18·0
B-16	25	1·4	18·3
B-17	0	27·4	11·6
B-17	5	4·8	16·6
B-17	10	5·0	16·5
B-17	20	0·6	17·8
B-17	25	0·8	18·2
B-17	37	0·4	18·4
B-18	0	7·4	17·0
B-18	5	1·8	17·0
B-18	10	1·8	17·1
B-18	20	0·6	17·8
B-18	40	0·6	18·5
B-18	70	2·0	20·4

Table 3. Silicate and chlorosity data of October 1955

Station	Depth (ft)	Soluble silica (μmoles/l.)	Chlorosity (g Cl$^-$/l.)
C-1	0	63·9	1·6
C-2	0	59·3	2·4
C-3	0	56·1	6·1
C-4	0	41·9	7·1
C-5	0	7·5	14·8
C-6	0	8·2	16·8
C-7	0	4·6	177·5

The concentration of soluble silica as a function of chlorosity in these waters (the data of Figs. 2, 3 and 4 and Tables 1, 2 and 3) can be described (with experimental error) by the equations:

$$(SiO_2)_f = (SiO_2)_R - B\,(Cl) + C\,(Cl)^2; \qquad B > C \qquad (1)$$

where $(SiO_2)_f$ is the soluble silica concentration found, (Cl) is the chlorosity, $(SiO_2)_R$ is the initial concentration in the river and *B* and *C* are constants that vary seasonally (Bien, 1953). These data can also be expressed (within experimental error) by three lines *OA*, and *BC* in Fig. 5. Line *OA* represents the initial removal, *AB*, further removal, *BC*, the final dilution of the water and *OC*, the theoretical dilution curve. A consideration of this plot shows that nearly all of the soluble silica is removed. If only a portion were removed during the initial mixing (line *OA*)

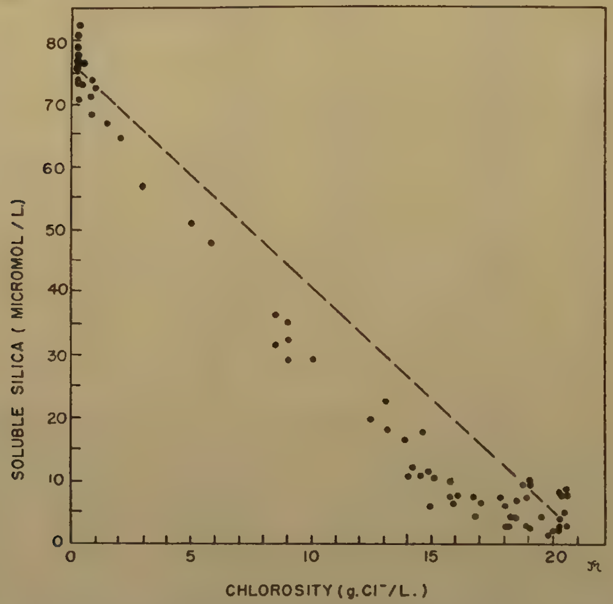

Fig. 2. Soluble silica concentration as a function of chlorosity of water samples. Data of June 1953.

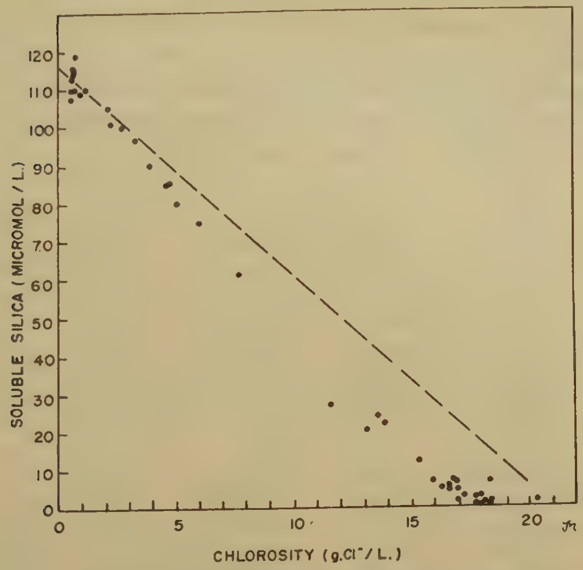

Fig. 3. Soluble silica concentration as a function of chlorosity of water samples. Data of July 1955.

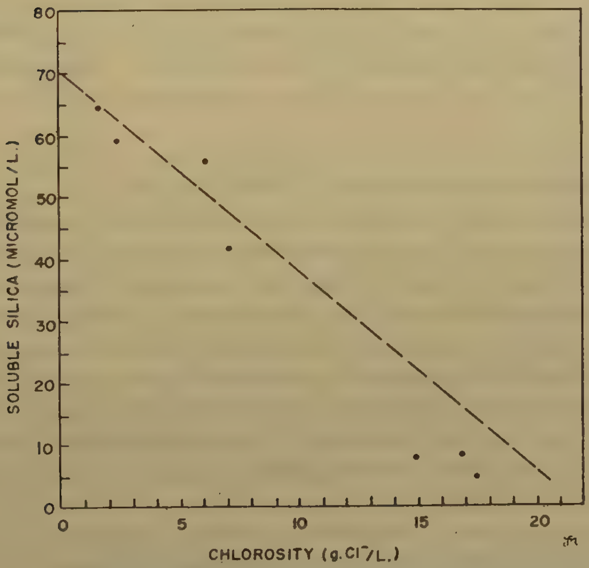

Fig. 4. Soluble silica concentration as a function of chlorosity of water samples. Data of October 1955.

and thereafter only dilution occurred, the experimental points should follow line *AC*. Instead, they do not fall on such a line, but a minimum value for soluble silica is reached before maximum dilution has occurred (at point *B*). Any further dilution with sea-water (line *BC*) results in no more removal, since the sea-water already contains this minimum amount. Since removal ceases, the removal process must be complete, and all of the soluble silica originally present must have been precipitated. This does not mean that dilution does not occur, but, that as fast as river-water is diluted, its soluble silica is removed. The possible causes of the initial removal (line *OA*) and of further removal (line *AB*) are discussed in section (c).

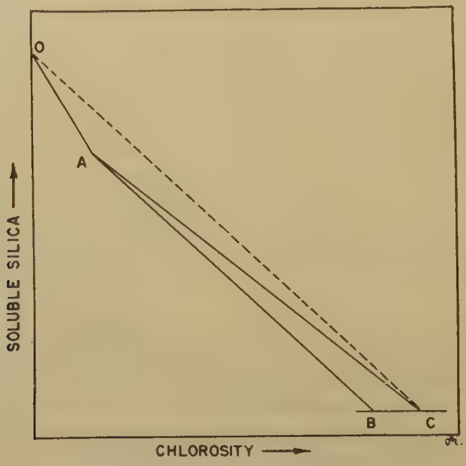

Fig. 5. Illustrative relationships of soluble silica to chlorosity.

(b) *Laboratory experiments on inorganic removal processes*

Several experiments were performed which show that results similar to the field data can be obtained by mixing turbid river-water with sea-water. The experiments were carried out by withdrawing an aliquot from a sample of river-water and adding an equivalent volume of sea-water. The process was repeated at hourly intervals and each aliquot was then filtered and its concentration of soluble silica determined. Results obtained using Mississippi river-water and Gulf sea-water are shown in Table 4 and Fig. 6. These results are not due to biological uptake, since such activity was prevented by the addition of 1 p.p.m. $HgCl_2$. It should be noted that inorganic removal occurs within 1 hr, which indicates that it will occur quite rapidly in the field.

The same experiment was performed by mixing Mississippi river-water with Pacific Ocean surface sea-water collected 60 miles east of Guadalupe Island. This sample had a chlorosity of 18·04 g Cl^-/l., and contained 20·1 μmoles soluble silica/l. The results are shown in Table 5 and Fig. 7, and are similar to those obtained with Gulf of Mexico water. Thus the phenomenon of inorganic removal is very likely a general one and is not due to anything especially characteristic of Gulf water.

Two possible mechanisms by which inorganic removal of soluble silica might

Table 4. Soluble silicate and chlorosity data of dilution Experiment A

Experiment Nos. I		II		III		IV	
Chlorosity (g Cl^-/l.)	Soluble SiO_2 (μmoles/l.)	Chlorosity (g Cl^-/l.)	Soluble SiO_2 (μmoles/l.)	Chlorosity (g Cl^-/l.)	Soluble SiO_2 (μmoles/l.)	Chlorosity (g Cl^-/l.)	Soluble SiO_2 (μmoles/l.)
0·035	82·06	0·035	82·06	0·035	82·06	0·035	82·06
2·06	65·4	0·82	76·8	2·06	69·8	2·06	70·1
4·12	61·7	1·62	70·4	3·92	68·1	3·92	61·8
6·18	52·5	2·38	67·7	5·59	52·6	5·59	64·9
8·24	41·7	3·10	63·9	7·09	46·7	7·09	46·8
10·30	36·2	3·80	61·3	8·44	44·6	8·44	42·4
11·33	31·2	4·48	58·1	9·64	37·0	9·64	37·1
12·36	27·3	5·12	70·1	10·73	34·9	10·73	34·9
13·33	25·7	5·74	52·5	11·72	29·0	11·72	26·9
14·40	20·1	6·34	51·6	12·61	24·6	12·61	24·2
15·45	16·3	6·91	48·4	13·43	20·8	13·43	20·8
16·52	11·8	7·46	45·3	14·15	18·2	14·15	18·4
17·56	9·4	8·49	43·7	14·79	17·2	14·79	18·4
18·57	5·9	9·70	40·8	15·38	15·7	15·38	15·0
19·57	1·7	10·79	33·0	15·90	13·2	15·90	13·5
20·61	0	11·76	28·1	16·37	11·4	16·37	11·5
		12·65	28·1	16·79	9·4	16·79	9·1
		13·44	22·1	17·17	8·3	17·17	8·4
		14·16	20·5	17·52	6·6	17·52	6·5
				17·83	6·0	17·83	5·1
				18·11	4·4	18·11	3·1

occur are: (1) a reaction with electrolytes in sea-water resulting in polymerization or salt formation and (2) adsorption or co-precipitation with suspended solids or colloidal material in river-water as these come in contact with electrolytes in sea-water. We have used Millipore-filtered natural waters and artificial solutions in order to distinguish between these two processes.

When filtered sea-water was diluted to various chlorosities with distilled water and known amounts of sodium metasilicate (105 μmoles/l.) were added, no loss of soluble silica was observed after storage of the solutions for 1 week. Similar results were observed using sodium chloride solutions rather than filtered sea-water. These data are shown in Table 6. Successive dilution of a sodium metasilicate solution with a sodium chloride solution also did not result in inorganic removal (see Curve I, Fig. 8). Thus, electrolytes alone do not apparently cause inorganic removal.

In a further test of this hypothesis, filtered river-water was successively diluted with filtered Gulf water. These results are shown in Curve II, Fig. 8. The deviation from linearity observed was somewhat less than that observed using unfiltered waters and may be due to incomplete removal of colloidal material by the Millipore filter. Such material has been shown to be important in inorganic removal by

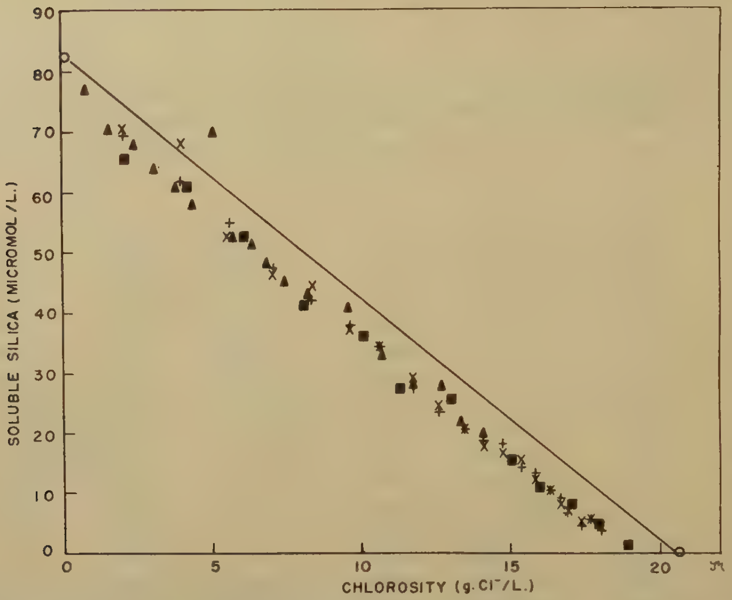

Fig. 6. Soluble silica concentration as a function of chlorosity as unfiltered river-water is mixed with Gulf of Mexico water in the laboratory.

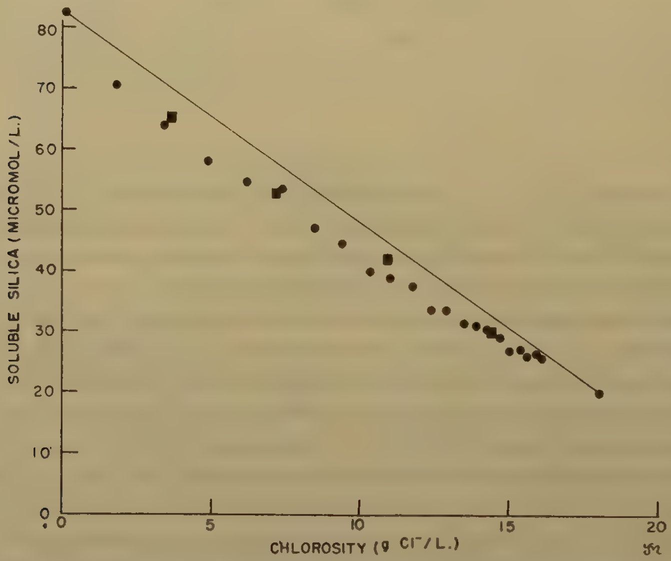

Fig. 7. Soluble silica concentration as a function of chlorosity as unfiltered river-water is mixed with Pacific Ocean water in the laboratory.

Table 5. Soluble silicate and chlorosity data of dilution Experiment B

Experiment Nos. I		II	
Chlorosity (g Cl$^-$/l.)	Soluble SiO$_2$ (μmoles/l.)	Chlorosity (g Cl$^-$/l.)	Soluble SiO$_2$ (μmoles/l.)
0·035	82·06	0·035	82·06
3·61	64·7	1·80	70·4
7·22	52·6	3·43	63·9
10·82	41·7	4·89	57·9
14·43	30·1	6·21	54·7
18·04	20·1	7·39	53·5
		8·41	46·9
		9·41	44·4
		10·28	39·9
		11·05	38·9
		11·75	37·5
		12·38	33·4
		12·95	33·4
		13·46	31·5
		13·92	31·1
		14·33	30·5
		14·70	29·5
		15·04	27·2
		15·34	27·3
		15·61	26·4
		15·85	26·8
		16·07	26·2

The sea-water used in this experiment had been standing in a glass bottle for over a year.

Table 6. Amounts of soluble silica found after storage for 1 week in the presence of filtered Gulf water or sodium chloride solutions.
Amount added = 105 μmoles/l.

A. Filtered Gulf water plus distilled water

Chlorosity (g Cl$^-$/l.)	0	1·81	3·61	5·41	7·22	9·03	10·84	12·64	14·45	16·75	18·06
SiO$_2$ soluble found (μmoles/l.)	105·4	103·0	105·0	105·0	105·2	104·0	105·5	103·6	105·0	104·5	106·0

B. Sodium chloride solutions

Chlorosity (g Cl$^-$/l.)	0	2·12	4·24	6·37	8·49	10·61	12·73	14·85	16·98	19·10	20·22
SiO$_2$ soluble found (μmoles/l.)	105·0	103·5	106·2	104·5	104·8	105·4	106·1	102·6	106·0	105·2	105·0

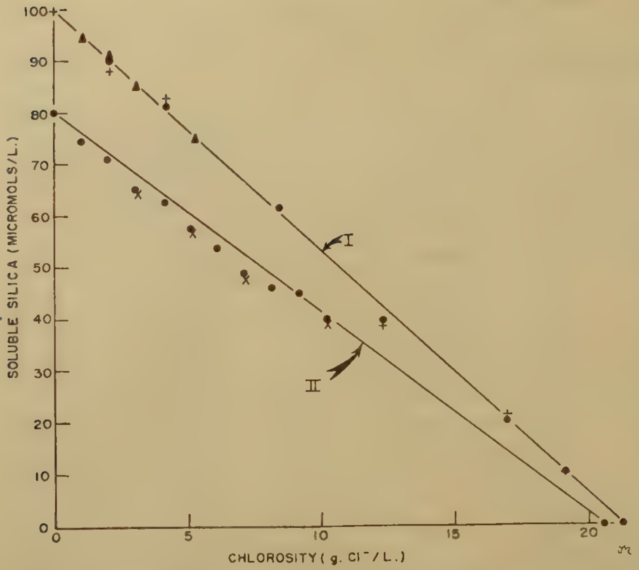

Fig. 8. Soluble silica dilution experiments. Curve I: Sodium silicate solution diluted with sodium chloride solutions. Curve II: Filtered river-water diluted with filtered sea-water. (Solid lines are calculated dilution curves.)

White *et al.* (1956). It may also mean that soluble silica is precipitated by the presence of a small amount of aluminium ions which passed the filter, formed aluminium hydroxide and co-precipitated the silica (Goto, 1956; Arrhenius, 1954; Okamoto *et al.*, 1957).

In general, these results agree with those of Krauskopf (1956), which showed that precipitation of dissolved silica does not occur when silica solutions are mixed with sea-water.

If adsorption of soluble silica could occur as suspended matter in the river reacted with electrolytes, inorganic removal would be observed when suspended solids were added to filtered sea-water enriched with sodium silicate. Such removal was observed upon addition of bentonite, aluminium oxide, and particularly, suspended solids from the Mississippi River, to enriched Gulf water. In these experiments, Gulf water was enriched, a concentrate of suspended material was added, the sample was shaken, and allowed to stand overnight. After standing, the suspension was filtered and soluble silica was determined. The results are shown in Table 7 and Fig. 9, and the data are corrected for the amount of soluble silica introduced with the concentrated suspended matter. It should be noted that suspended material from the river is more effective than either bentonite or aluminium oxide. Also, since the amount of removal increases with increasing amount of suspended solids from the river, inorganic precipitation is very likely an adsorption process.

The necessity of electrolytes as well as suspended matter for precipitation was demonstrated by adding solid sodium chloride to river-water to increase chlorosity. These results are shown in Table 8 and Fig. 10. As the chlorosity increased, an

Table 7. Removal of soluble silica by adding suspended solid matter to enriched sea-water (chlorosity = 16·27 g Cl^-/l.)

A. Bentonite suspension (suspension contains 0·102 g solid/ml; filtered solution contains 47·4 μmoles soluble silica/l.)

Wt. clay added (g/l.)	SiO_2 added (μmoles/l.)	SiO_2 found (μmoles/l.)	Per cent recovered
0	107·4	107·4	100·0
0·0204	107·6	101·6	94·3
0·0408	107·8	97·6	90·5
0·0612	108·0	96·5	89·2
0·0816	108·2	97·6	90·1
0·1024	108·4	95·2; 98·5	88·0; 90·5
0·1224	108·5	97·1	89·5
0·1530	108·7	95·6	88·0
0·204	109·3	102·5; 101·5; 97·5	93·0; 93·2; 90·5
0·306	110·4	101·2; 100·7	91·0; 90·0
0·408	111·2	102·0; 99·5	91·5; 89·5
0·510	112·1	104·3; 103·5; 101·2	98·0; 92·5; 90·0
0·612	113·0	105·0	93·0
0·714	114·0	105·3	92·5
0·816	115·0	104·8	91·0
0·918	115·9	104·8	90·5
1·02	117·0	104·8	89·5

B. Aluminium oxide suspension (suspension contains 0·120 g solid/ml; soluble silica added = 107 μmoles/l.)

Wt. Al_2O_3 added (g/l)	SiO_2 found (μmoles/l.)	Per cent recovered
0	107·0	100·0
0·024	104·0	97·4
0·048	100·0	94·0
0·072	95·5	89·0
0·096	101·0	94·5
0·12	99·5	93·5
0·144	100·3	94·1
0·168	100·3	94·1
0·192	99·7	93·5
0·216	100·0	94·0
0·240	99·7	93·5

Table 7 (*continued*)

C. River mud suspension (suspension contains 0·183 g solid/ml; filtered solution contains 95 μmoles soluble silica/l.)

Wt. Solid added (g/l.)	SiO_2 added (μmoles/l.)	SiO_2 found (μmoles/l.)	Per cent recovered
0	101·6	101·6	100·0
0·0732	101·97	98·3	96·5
0·1464	102·34	97·5	95·3
0·2196	102·72	97·5	95·0
0·2928	103·1	97·2	94·5
0·366	103·5	96·1; 95·2	93·0; 92·3
0·4392	103·8	95·2	92·8
0·5124	104·2	96·1	92·5
0·5856	104·6	96·1	92·0
0·6588	105·0	95·5	91·0
0·732	105·3	95·0; 92·5	90·2; 89·0
1·098	106·3	92·0	87·0

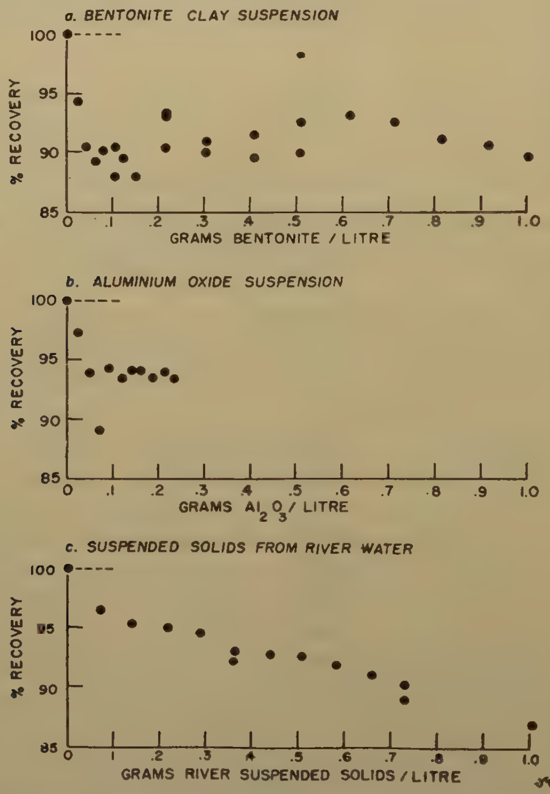

Fig. 9. The influence of suspended matter on the recovery of soluble silica from enriched Gulf of Mexico water.

Table 8. Soluble silica removal from river-water by sodium chloride

Chlorosity (g Cl⁻/l.)	SiO_2 found (μmoles/l.)	Percent recovered
0·035	90·0	100·0
0·65	84·9	94·5
1·25	83·2; 85·6	92·5; 94·5
1·86	83·0; 82·8	92·3; 92·2
2·47	83·1; 82·8	92·4; 92·2
3·07	83·2; 83·0	92·5; 92·3
3·68	82·8; 80·5	92·0; 89·5
4·29	83·0	92·3

* Original soluble silica content of this water was 82·06 μmoles/l. This was increased to 90 μmoles/l. for the experiment.

initial drop in concentration was observed, after which the concentration remained constant.

The conditions of these experiments are different from those of KRAUSKOPF (1956), who also added suspended matter to silica solutions. Little or no removal occurred in his experiments when kaolinite, montmorillonite, calcite or Fe_2O_3 were added to silica solutions made up in distilled water. Our experiments show that both electrolytes (sea-water) and suspended matter are necessary. On the other hand, in KRAUSKOPF's experiments with silica-enriched artificial sea-water, Fe_2O_3 removed about the same amount of soluble silica as in our experiments (6–9 per cent), but calcite was without effect. It should be noted that the concentrations of soluble silica used in KRAUSKOPF's experiments are 25–35 times greater than those used in our experiments or found in river-water. Also, KRAUSKOPF does not state how much suspended matter was added to his solutions. It is probable that the concentrations of silica and suspended matter are critical in such experiments. In our experiments both the concentration of silica and suspended matter from the river approximate those found in the river. A problem which remains for investigation is the role of iron and aluminium in systems which approximate the natural river–ocean complex.

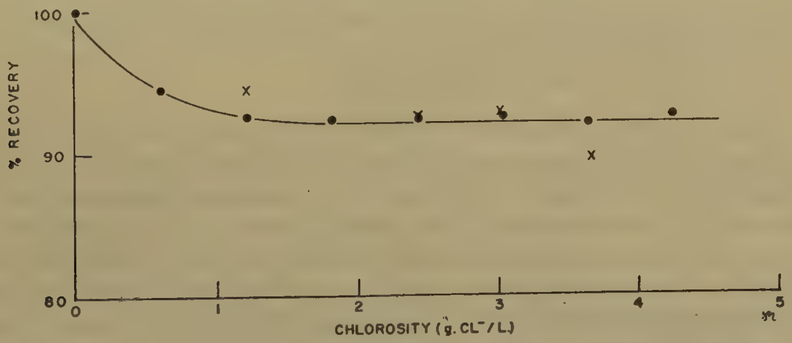

FIG. 10. The effect of sodium chloride on the soluble silica concentration of Mississippi river-water.

(c) *Biological removal of soluble silica by phytoplankton*

It is very difficult to estimate whether significant removal of soluble silica due to biological uptake by diatoms occurs during the *initial* mixing of river-water. About 15 per cent of the soluble silica in river-water or about 10–18 μmoles/l. are removed by processes other than dilution during mixing to a chlorosity of 8 g Cl^-/l. Our measurements (THOMAS and SIMMONS, 1957) show that from 1 to 7 μmoles organic carbon are formed per litre per day by surface phytoplankton off Pass a Loutre. Most of the phytoplankton off Pass a Loutre are diatoms (SIMMONS and THOMAS, 1957). Using a factor for the ratio between carbon and silica atoms in diatoms (100 : 40) calculated from SVERDRUP *et al.* (1942, p. 234), we can calculate that between 0·40 and 2·80 μmoles of silica are taken up per litre per day by diatoms. Thus about 2 per cent of the total soluble silica in river-water might be taken up in 1 day by offshore diatoms or about 20 per cent of the initial removal process might be due to diatom uptake if the assumption is made that it takes 1 day for 1 l. of fresh river-water to be diluted to a chlorosity of 8 g Cl^-/l.

This assumption is almost certain to be true during periods of high river discharge. According to SCRUTON (1956), the average surface current at the mouth of North Pass during June 1953 was 2 knots. This velocity would decrease to less than 1 knot as the water moved seaward. Thus 1 l. of water might move seaward some 24 miles during 1 day. The existence of a thin layer of relatively fresh turbid water (chlorosity 1·3 g Cl^-/l.) during the season of high river discharge even tens of miles off the delta (SCRUTON and MOORE, 1953; THOMAS and SIMMONS, 1957) indicates that mixing to a chlorosity of 8 g Cl^-/l. does not occur during the movement of the water for 24 miles.

At a period of low discharge, the above assumption is probably not true. The current velocity is less than half that measured during high river discharge (SCRUTON, 1956), so that 1 l. of river-water might move only 12 miles during 1 day. However, our measurements show that a layer of relatively fresh water does not extend that far offshore (THOMAS and SIMMONS, 1957) during the fall months.

Mixing to the *final* chlorosity probably takes several days at all seasons. Thus biological uptake may account for an appreciable amount of silica in the complete process. When the field results and the laboratory results are expressed on a comparable basis, there is a difference between the two sets of data, which may be attributed to biological uptake, since biological activities were stopped by the addition of mercuric chloride in the laboratory experiments. In comparing the sets of data, we have used the following equations:

$$(SiO_2)_{Cl} = (SiO_2)_R - K(Cl) \qquad (2)$$

is the equation describing the theoretical dilution of soluble silica in river-water with Gulf water. In this equation $(SiO_2)_{Cl}$ is the theoretical concentration which should be found at a given chlorosity (Cl); $(SiO_2)_R$ is the initial concentration in the river-water, and K is a constant. Another equation represents the soluble silica actually found, at a given chlorosity, $(SiO_2)_f$, and was given by equation (1) in section (a). The final equation used is that expressing the theoretical dilution if river-water is diluted with Gulf water containing no silica:

$$(SiO_2)'_{Cl} = (SiO_2)_R - K'(Cl) \qquad (3)$$

in which K' is slightly greater than K. This is used because we are only interested in the removal of silica from river-water and thus can neglect possible removal from Gulf water. The per cent removal is then calculated from the difference between $(SiO_2)_{Cl}$ and $(SiO_2)_f$ by dividing this value by $(SiO_2)_{Cl}$ and multiplying by 100.

Table 9 shows these calculations for the field data; Table 10, those for the experiments in which river-water was successively diluted with Gulf water. The field and experimental results are compared in Fig. 11. The difference between the two sets of data is shown by cross-hatching. It should be noted that below a chlorosity of 8 gm Cl⁻/l. little or no difference is found, but beyond this point the difference is considerable. This supports previous estimates that biological activity will occur only in waters of high chlorosity in which sufficient time for uptake has elapsed. An alternative explanation for the difference between the two curves is that in the laboratory experiments there may not be enough time for maximum removal to occur, since the river-water and Gulf water were only mixed for 1 hour before soluble silica was determined. However, if this is the reason for the difference, the initial percentage removal for one set of data should not agree so well with that for the other set.

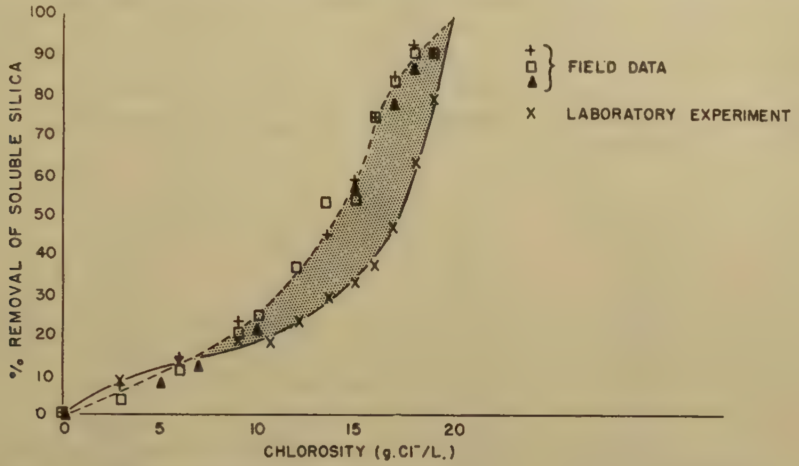

Fig. 11. The percentage removal of soluble silica as a function of chlorosity.

CONCLUSIONS

When fresh water enters the sea, it would be expected that the high concentration of soluble silica in fresh water could be reduced by dilution with sea-water having a low concentration of soluble silica. However, the soluble silica concentration is reduced by some process other than dilution. Two such processes can occur: biological uptake or inorganic precipitation.

Calculations based on phytoplankton production measurements and estimates of mixing rates of water masses in the Mississippi Delta area show that biological removal may possibly account for some of the *initial* removal during periods of high river discharge. During periods of low river discharge such removal is less possible.

However, after the initial mixing, at chlorosities greater than 8 g Cl⁻/l., biological removal may be appreciable, since enough time could elapse for uptake by diatoms to occur. Much more extensive work would be required to distinguish definitely between biological uptake and inorganic precipitation in the field.

Two mechanisms of inorganic precipitation of soluble silica have been proposed: (1) reaction of soluble silica with electrolytes in sea-water resulting in salt formation or (2) adsorption or co-precipitation of soluble silica with suspended solids or

Table 9. The difference between calculated and observed values for soluble silica as a function of chlorosity. Data from field samples

Chlorosity (g Cl⁻/l.)	$(SiO_2)_{Cl}$ (μmoles/l.)	$(SiO_2)_f$ (μmoles/l.)	$\Delta(SiO_2)$ $(SiO_2)_{Cl}-(SiO_2)_f$ (μmoles/l.)	$(SiO_2)'_{Cl}$ (μmoles/l.)	% Removal $\frac{100\,(\Delta\,SiO_2)}{(Si)'_{Cl}}$
A—Dates of June 1953					
0·2	76·4	76·4	0	76·4	0
3·0	66·4	61·8	4·6	68·8	7·0
6·0	55·7	48·0	7·7	54·5	14·0
9·0	44·9	35·0	9·8	43·1	23·0
10·0	41·4	31·2	10·2	39·3	25·7
12·0	34·2	22·5	11·7	31·8	36·8
13·5	28·8	17·0	11·8	26·0	45·0
15·0	23·5	11·5	12·0	20·9	59·0
16·0	19·9	7·5	12·4	16·6	74·7
17·0	16·4	5·6	10·8	12·8	84·3
18·0	12·8	4·4	8·9	9·1	92·3
19·0	9·2	4·4	4·8	5·3	90·6
B—Data of July 1955					
0·6	113	113	0	0	0
3·0	99·6	96·0	3·6	101·3	3·5
6·0	82·8	74·0	8·8	82·2	10·7
9·0	66·0	53·0	13·0	65·0	20·0
10·0	60·4	46·0	14·4	59·3	24·3
12·0	49·1	31·0	18·1	47·9	37·9
13·5	40·8	20·0	20·8	39·3	53·0
15·0	32·3	12·0	20·3	30·8	53·5
16·0	26·8	8·0	18·8	25·1	75·0
17·0	21·2	5·0	16·2	19·4	83·5
18·0	15·5	3·0	12·5	13·7	91·3
19·0	9·4	2·0	7·4	8·1	91·5
C—Data of October 1955					
0	70	70	0	70	0
5	54	50	4	53	7·5
7·0	47·4	42	5·4	46	12·0
10·0	37·7	30	7·7	36	21·0
15·0	21·6	11	10·6	18·5	57·0
17·0	15·0	5·6	9·4	12·0	78·0
18·0	12·0	5·0	7·0	8·0	87·0

The difference between calculated and observed values for soluble silica as a function of chlorosity. Data from laboratory experiments

Chlorosity (g Cl⁻/l.)	$(SiO_2)_{Cl} = (SiO_2)'_{Cl}$ (μmoles/l.)	$(SiO_2)_f$ (μmoles/l.)	$\Delta(SiO_2)$ (μmoles/l.)	% Removal $\frac{1000s}{SR}$
0	82·1	82·1	0	0
3	70·1	64·4	5·7	8·1
6	58·2	51·2	7·0	12·0
9	46·2	39·3	8·9	19·3
10·5	40·2	33·1	7·1	17·7
12·0	34·3	26·2	8·1	23·6
13·5	28·3	20·0	8·3	29·3
15·0	22·3	15·0	7·3	32·8
16·0	18·3	11·3	7·0	37·8
17·0	14·3	7.5	6·8	47·5
18·0	10·4	3·75	6·6	63·4
19·0	6·3	1·25	5·0	79·5

colloidal material in river-water as these come in contact with electrolytes. Our data show that both electrolytes and colloidal or suspended solids are necessary for maximum inorganic removal. The fact that increasing removal occurs when the amounts of suspended solids are increased indicates that adsorption or co-precipitation of soluble silica on these solids probably occurs.

These precipitation processes result in the removal of almost all of the soluble silica from river-water. Since this river-water contains from 4 to 7·5 mg/l. soluble silica and 160 to 1500 mg/l. of suspended solids are present in the river-water, the weight of suspended material in these waters can be slightly increased by these processes, and therefore presumably some of the silica in the deltaic sediments would also be derived from these processes.

REFERENCES

ALEXANDER G. B., HESTON W. M. and ILER R. K. (1954) *J. Phys. Chem.* **58,** 453–55.

ARMSTRONG F. A. J. (1954) *J. Mar. Biol. Ass. U.K.* **33,** 381–392.

ARRHENIUS G. (1954) *Tellus* **6,** No 3, 215–220.

BIEN G. S. (1953) *Study of nearshore sediments and their environment in the northern Gulf of Mexico.* Progress Report Amer. Pet. Inst. Project 51, No. 11, p. 51.

CLARKE F. W. (1942) The Data of Geochemistry. (5th Ed.) p. 80. *Bull. U.S. Geol. Surv.* 770.

DIENERT F. and WANDENBULCKE F. (1923) *C. R. Acad. Sci., Paris* **176,** 1478–1480.

GOTO K. (1956) *Bull. Chem. Soc. Japan* **29,** 741–742.

JORGENSEN E. G. (1953) *Physiol. Plant.* **6,** 301–315.

KRAUSKOPF K. B. (1956) *Geochim. et Cosmochim. Acta* **10,** 1–26.

MAEDA H. (1952) *Publ. Seto Mar. Biol. Lab.* **2,** 249–255.

MAEDA H. (1953) *J. Shimonoseki Coll. Fish.* **3,** 167–180

MAKIMOTO H., MEDA H. and ERA S. (1955) *Rec. Oceanogr. Wks. Japan* **2,** 106–112.

OKAMOTO G., OKURA T. and GOTO K. (1957) *Geochim. et Cosmochim. Acta* **12,** 123–132.

ROY C. J. (1945) *Amer. J. Sci.* **243,** 401–402.

SCHWARTZ M. C. (1938) *J. Amer. Wat. Wks. Ass.* **30,** 659–678.

SCRUTON P. C. (1956) *Bull. Amer. Ass. Petrol. Geol.* **40,** 2864–2952.

Scruton P. C. and Moore D. G. (1953) *Bull. Amer. Ass. Petrol. Geol.* **37,** 1067–1074.

Simmons E. G. and Thomas W. H. The phytoplankton of the Mississippi Delta. In preparation.

Steeman-neilsen E. (1952) *J. Cons. Int. Explor. Mer* **43,** 117–140.

Sverdrup H. V., Johnson M. W. and Fleming R. H. (1942) *The Oceans: Their Physics, Chemistry and General Biology.* Prentice-Hall, New York.

Thomas W. H. and Simmons E. G. Phytoplankton production in the Mississippi Delta. In preparation.

White D. E., Brannock W. W. and Murata K. J. (1956) *Geochim. et Cosmochim. Acta* **10,** 27–59.

LUMIÈRE, BIOLUMINESCENCE ET MIGRATIONS DE LA COUCHE DIFFUSANTE PROFONDE EN MÉDITERRANÉE OCCIDENTALE

par Brian P. Boden et Elizabeth M. Kampa

Université de Californie — Institution Scripps of Océanography
La Jolla, Californie.

Vie et Milieu, tome IX, fasc. 1, 1958
paru en août 1958

LUMIÈRE, BIOLUMINESCENCE ET MIGRATIONS DE LA COUCHE DIFFUSANTE PROFONDE EN MÉDITERRANÉE OCCIDENTALE (1)

par Brian P. Boden et Elizabeth M. Kampa

Université de Californie — Institution Scripps of Océanography
La Jolla, Californie.

Depuis le début de la seconde guerre mondiale, on a reconnu l'existence dans de vastes régions des Océans de couches profondes diffusant le son. Leur origine biologique probable a été suggérée par Johnson (1946) en raison du fait que le comportement de certaines d'entre elles est très comparable à celui de certains animaux marins qui selon un rythme diurne exécutent des migrations verticales étendues. La nature exacte de ces couches a fait l'objet de nombreuses spéculations et l'historique des investigations entreprises sur ce phénomène jusqu'en 1952 a été pertinemment résumé par Tchernia (1952). Les efforts les plus récents d'identification des particules diffusantes ont été exécutés au moyen d'échosondeurs immergés au sein même de la couche (Kanwisher et Volkmann, 1955) et de photographies sous-marines (Johnson et al. 1956). Depuis longtemps on pensait que la profondeur d'immersion des couches était déterminée par l'importance de l'éclairement sous-marin, et la preuve de ce fait fut présentée pour la première fois par Kampa et Boden (1954). Clarke et Backus (1956) pensent maintenant que d'autres facteurs que la lumière peuvent influencer l'immersion de ces couches. Il a été démontré qu'un certain degré de luminescence peut être détecté à des profondeurs considérables (Clarke et Wertheim, 1956) et plus récemment que cette luminescence croît aux immersions où se rencontre

---

(1) Contribution from the Scripps Institution of Oceanography, New Series, N° 987. This paper represents results of research carried out by the University of California under contract with the U. S. Office of Naval Research. Reproduction in whole of in part is permitted for any puspose of the United States Government.

Reproduced by Permission

une couche diffusante et migre verticalement avec elle (**Boden** et **Kampa**, 1957). La distribution spectrale de la lumière engendrée dans une couche diffusante a été étudiée par **Kampa** et **Boden** (1957) qui ont montré qu'elle était semblable à celle de la bioluminescence des animaux recueillis en même temps à ce niveau.

Nous pensons actuellement que dans les eaux continentales californiennes, la couche diffusante est constituée par une communauté animale mixte conduite vers la surface, la nuit, et vers les profondeurs, le jour, par un groupe d'animaux dont l'existence est associée à un « isolume » correspondant à leur éclairement optimum (**Kampa** et **Boden**, 1954). La corrélation étroite existant entre l'immersion d'une couche diffusante et la distribution verticale de la concentration des Euphausides (**Boden**, 1950), nous a amenés à penser que, dans cette région, les Euphausiacés sont les organismes phototropiques responsables de ce phénomène.

Il est déconcertant que, jusqu'à présent, on n'ait pu obtenir de preuve visuelle réelle des rapports entre les zones d'augmentation de la concentration en animaux et la présence de couche diffusante. Les observations faites en bathyscaphe ont montré un accroissement apparent des organismes de petite taille aux grandes profondeurs (**Cousteau**, 1954). Mais la plupart des plongées en bathyscaphe ont été faites dans des conditions d'éclairage artificiel et il est possible que cela suffise à effrayer les animaux les plus grands et les plus actifs et à les éloigner du champ de vision de l'observateur. **Hardy** (1956) a suggéré que l'accroissement apparent, avec la profondeur, de l'abondance des petits organismes peut être dû aux innombrables déchets exosquelettiques des Crustacés pris dans le faisceau lumineux des projecteurs du bathyscaphe pendant leur chute vers le fond. L'éclairage artificiel peut également rendre compte des résultats peu probants des investigations utilisant les techniques photographiques.

Nous avons cherché en travaillant en Méditerranée à comparer les résultats des recherches sur la réponse à la lumière des couches diffusantes à ceux que nous avions obtenus en Californie.

MÉTHODES

1° *Détection des couches diffusantes.* L'écho-sondeur du « Lacaze-Duthiers », navire de recherches du Laboratoire Arago, fonctionne sur courant continu à une fréquence de 37,5 kilocycles-sec. Il n'était pas assez puissant pour détecter les couches les plus profondes et il fut nécessaire d'employer à cet effet la technique des fréquences multiples mise au point par **Hersey** et al. (1952), technique qui est la suivante.

Par explosion à peu de distance du navire d'un pétard de 250 gr. de T.N.T., on met en œuvre une source sonore à large bande de fréquences. Un hydrophone directif à cristaux de sel de Rochelle est dirigé verticalement vers le bas et reçoit les sons diffusés qui sont enregistrés sur un magnétophone à ruban « Magnecord » 63 AH et un amplificateur « Magnecord » PT 7 P; le ruban se déroule à raison de 76,2 cm/sec. L'enregistrement sonore est filtré par un analyseur de son HH Scott type 420 A. L'enregistrement est fait au moyen d'un oscillographe à balayage déclenché, équipé d'une caméra Polaroid de Land.

2° *Mesure de l'intensité radiante* : le bathyphotomètre servant à la mesure directe de la lumière à l'immersion de la couche diffusante utilise un tube photomultiplicateur 931 A, orienté de façon telle que sa surface sensible soit tournée vers le haut. Juste devant le tube se trouve un obturateur à trois positions : la première obture complètement la photocathode de façon à ce que l'on puisse à intervalles réguliers vérifier le zéro de l'appareil. La deuxième position correspond à une ouverture en trou d'épingle qui ne laisse passer que le millième de la lumière admise lorsque l'obturateur est en position ouverte, ou position 3. Ces trois positions de l'obturateur peuvent être commandées du pont du navire lorsque l'appareil est à l'immersion désirée. Pour les mesures en lumière colorée, on utilise des filtres interférentiels et un collimateur réduit l'angle d'admission de la lumière à la photocathode, aux 5° utiles du cône des filtres. A l'extrémité distale du collimateur, se trouve un disque intégrateur en plastique opalescent ayant les caractères d'un véritable collecteur de Lambert; c'est-à-dire que sous un ciel uniforme l'intensité radiante $I\,\theta$ reçue de la direction θ est déterminée par la formule :

$$I\,\theta = Io \cos\theta \qquad (1)$$

L'instrument mesure alors l'irradiance. Cette irradiance H est calculée d'après la formule :

$$n = kH = \int_{0}^{\infty} ETS \, d\lambda \qquad (2).$$

où n est le nombre de millivolts lu sur l'enregistreur, E l'énergie de la source, T la transmission du filtre interférentiel (quand on en utilise un) et S la sensibilité spectrale du photomultiplicateur pour une bande de longueur d'onde de largeur $d\lambda$. La valeur de k fut obtenue par étalonnage sur une source de l'U.S. Bureau of Standards.

L'instrument est muni de thermistors qui permettent un enregistrement continu de la température. Il est également muni d'éléments sensibles à la pression (Boden et al; 1955). Les profondeurs indiquées dans ce travail ont donc été déterminées directement et non par le calcul.

Aussi bien les indications reçues de l'appareil immergé que les signaux transmis du pont pour déterminer la grandeur à mesurer ou la position de l'obturateur sont transmis par un câble d'acier inoxydable électro-porteur recouvert de polyéthylène. Ce câble a été éprouvé à une tension de 1270 kg.

3° *Récoltes biologiques.* Le ramasseur utilisé était un filet à plancton d'un mètre d'ouverture en gaze de nylon à mailles de 40 et 56. Il pouvait être ouvert et fermé à la profondeur désirée au moyen d'un mécanisme de Leavitt (1935). Ce mécanisme avait été modifié de façon à pouvoir être attaché au câble électrique isolé portant le bathyphotomètre. En utilisant le photomètre comme lest, il est possible d'obtenir à bord un enregistrement continu et précis de l'immersion du filet pendant un trait.

L'équipement électronique utilisé au cours de ces recherches était installé dans un petit laboratoire portatif (2 m. × 2 m. × 2 m.) qui ainsi qu'un treuil portatif et une génératrice de courant alternatif actionnée par un moteur à essence fut transporté par avion de Californie en France et installé à bord du « Lacaze-Duthiers » à Port-Vendres.

RÉSULTATS

Il n'est pas possible d'utiliser des explosifs pour la détection des couches diffusantes quand le photomètre est immergé en raison des risques de l'endommager ou de l'écraser. De ce fait, les observations exposées ici sur les variations d'immersion de la couche diffusante d'une part et les conditions de la lumière d'autre part n'ont pas été faites simultanément mais à des intervalles de temps aussi rapprochés qu'il fut pratiquement possible. Nous ne pensons pas que la valeur de nos résultats puissent être suspectée de ce fait, car en deux occasions séparées par un intervalle de temps de neuf jours, nous avons obtenu exactement les mêmes aspects pour la migration de la couche diffusante, les conditions de la lumière à la surface de la mer (observées sur le pont au moyen d'une cellule photoélectrique) étant aussi exactement les mêmes.

La figure 1 donne les variations d'immersion de la couche diffusante pendant une remontée vespérale ainsi que celle de l'isolume 5×10^{-3} microwatts-cm^2. Les mesures ont été faites les 8, 17 et 19 septembre 1955 dans le Golfe du Lion. L'isolume fut obtenue en descendant le bathyphotomètre le 19 septembre jusqu'à ce qu'il soit à la même profondeur que le sommet de la couche diffusante observée les 8 et 17 septembre. L'intensité de la lumière à cette profondeur étant déterminée, le photomètre fut alors un peu relevé et maintenu à profondeur constante jusqu'à ce que l'intensité à la nouvelle immersion fut la même qu'à la première. L'instrument était alors de nouveau remonté et l'opération répétée ainsi jusqu'à la fin du crépuscule. La courbe de températures en fonction de la profondeur obtenue le 19 septembre en même temps que la mesure des intensités de la lumière est aussi reproduite sur la figure 1.

Il ressort de ces résultats que pendant la migration vespérale, vers la surface, la courbe d'immersion de la couche diffusante coupe celle de l'isolume à laquelle elle est associée. Ceci s'est produit à 19 h. 05 au moment où la remontée de la couche était la plus rapide. Vers 19 h 22 la couche était à 35 m. au dessus du niveau de l'isolume.

On peut voir qu'après que la couche a atteint la profondeur de 46 mètres, sa migration verticale cesse assez brusquement. Ceci peut être dù à la présence d'une thermocline dont la base était à 48 mètres. Au dessus de cette profondeur la température augmentait de 2°C. pour une variation d'immersion de 13 mètres. Au dessous de la thermocline, l'eau était homogène du point de vue thermique et ne présentait aucune discontinuité pouvant, dans la limite des profondeurs étudiées, jouer un rôle de barrière pour des migrations verticales.

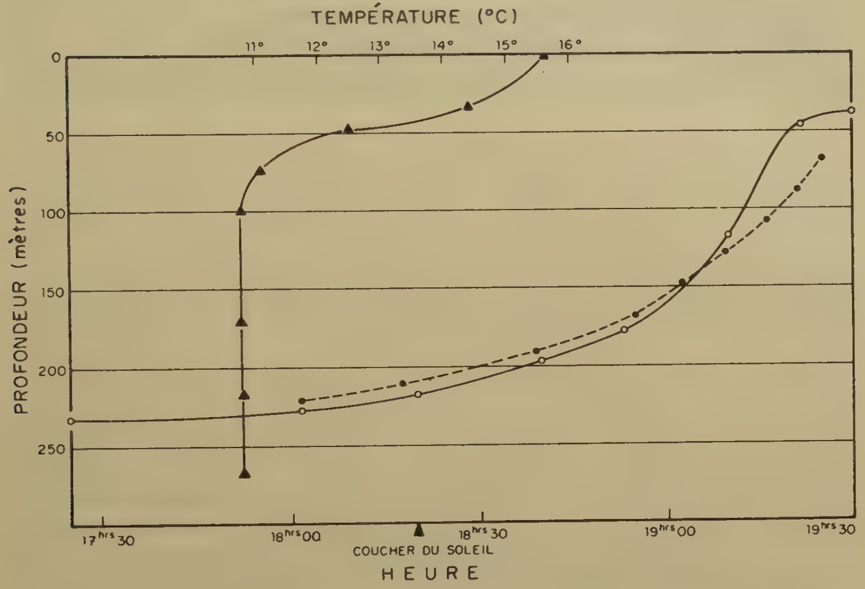

Fig. 1. — Relation entre la douche diffusante et l'isolume $5 \times 10^{-3} \mu$ W/cm² pendant une remontée vesperale.

La ligne en trait plein (o) représente les immersions successives du sommet de la couche diffusante, la ligne en tireté (.) représente celle de l'isolume. La répartition des températures à profondeurs, sur le lieu de l'observation est donnée par la courbe joignant les Δ.

Les relations entre l'irradiance totale calculée d'après l'équation (2) et la profondeur à environ 16 heures le 19 septembre sont mises en évidence par la figure 2. A l'immersion d'environ 180 mètres la courbe présente une inflexion. L'eau au dessus de cette profondeur était beaucoup moins transparente que celle de la couche sous-jacente.

Une discontinuité semblable a été rencontrée et décrite dans les eaux continentales californiennes (Kampa, 1955) à une profondeur d'environ 100 mètres. L'extension verticale de la couche supérieure dans cette région coïncide avec l'extension verticale de la zone euphotique. Le golfe du Lion est une région relativement peu profonde à fond vaseux. La station d'observation était située dans un large canyon sous-marin. Il est probable que l'augmentation d'épaisseur de l'eau optiquement dense est due aux écoulements d'eau dans ce canyon.

Un seul prélévèment de plancton fut réussi à l'immersion de la couche diffusante. Comme il n'existe aucun prélèvement de comparaison nous considérons comme sans valeur le comptage des organismes par espèce. La détermination des organismes les plus communs ou les plus caractéristiques (et en général seulement jusqu'au genre) fut regardée comme suffisante. Le plancton était rare en comparaison de celui d'autres régions, mais la Méditerranée est notoirement pauvre en plancton. Il était surtout composé de Copépodes du sous-ordre des *Calanoida* (*Acartia* sp.), plusieurs spécimens de *Candacia aethiopica* étaient présents. Il y avait aussi trois ou quatre Amphipodes (*Vibelia* sp.), alors que les *Sagitta*, Siphonophores et Salpes étaient moyennement nombreux. Un seul adulte

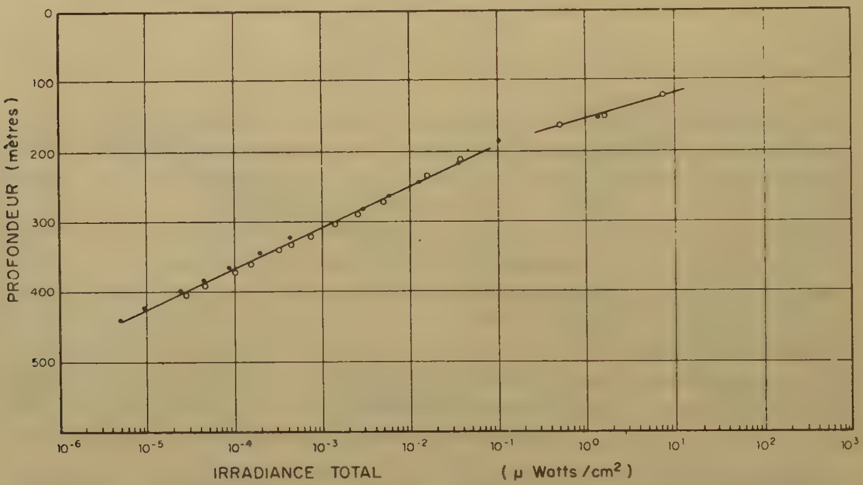

Fig. 2. — Relations entre l'irradiance totale et la profondeur. Ces renseignements furent obtenus le 19 septembre 1955 entre 15 h. 30 et 16 h. 30.

d'Euphausidé fut capturé — un mâle d'*Euphausia krohnii* — mais plusieurs larves d'*Euphausia* sp. furent trouvées. Les poissons étaient représentés par deux petits spécimens de *Cyclothone* sp. et un autre individu déchiqueté non identifiable.

DISCUSSION

Le croisement bien apparent des courbes de variation d'immersion de la couche diffusante et de l'isolume qui lui est associé marque une différence très nette entre ce qui se passe en Méditerranée et ce qui a été observé dans les eaux continentales californiennes (KAMPA et BODEN, 1954). En Californie, nous avons trouvé que les éléments diffuseurs du son et le niveau de constante intensité de lumière migraient avec la même vitesse.

CLARKE et BACHUS (1956) ont montré que dans l'Atlantique Nord, la couche diffusante coupe aussi l'isolume à laquelle elle est associée. Dans la Méditerranée, l'association entre les diffuseurs sonores et l'isolume semble être beaucoup plus intime dans la première partie de l'ascension que celle observée dans l'Atlantique. L'accord est cependant assez bon entre les distances maxima au dessus de l'isolume, atteintes par les couches dans ces deux régions (35 m. dans la Méditerranée et 40 m. dans l'Atlantique.

Il a été montré (BODEN et KAMPA, 1957) qu'une activité bioluminescente considérable était associée avec la présence de couches diffusantes et que cette activité augmentait au moment du maximum de vitesse de migration des couches (KAMPA et BODEN 1957). Des portions de tracé des enregistrements de la lumière obtenus dans le golfe du Lion le 19 septembre 1955 ont été reproduites sur la figure 3. Dans l'après-midi et durant la première partie de la migration liée au coucher du soleil, un crochet isolé occasionnel indiquant un éclat bioluminescent apparait sur le tracé. L'activité bioluminescente s'accroit fortement durant la période de migration rapide à mesure que la couche approche de la surface. Il est possible que les diffuseurs du son en mouvement de migration soient eux-mêmes responsables de cet accroisement d'activité. Mais le phénomène peut être dû aussi à des organismes de surface luminescents qui ne migrent pas du tout ou n'entreprennent que des mouvements migratoires beaucoup moins étendus que ceux des organismes composant les couches diffusantes profondes.

Cette activité accrue, quelle qu'en soit la cause, peut expliquer le croisement apparent des courbes d'immersion de l'isolume et de la couche diffusante. Le photomètre mesure l'irradiance totale et, sans filtre, il ne peut séparer les composants de la luminosité ambiante. De ce fait, durant la période de rapide migration des diffuseurs dans les couches d'eau superficielle, il mesure à la fois la lumière venant du ciel et la bioluminescence, l'intensité lumineuse cesse alors d'être une fonction de la seule lumière du ciel. En Californie, nous avons observé un accroissement de l'intensité de la lumière avec la profondeur durant des périodes d'active bioluminescence (KAMPA et BODEN, 1957). L'association étroite de la couche diffusante et de l'isolume pendant les migrations crépusculaires observée par KAMPA et BODEN (1954) était peut être expliquable par le fait que le photomètre

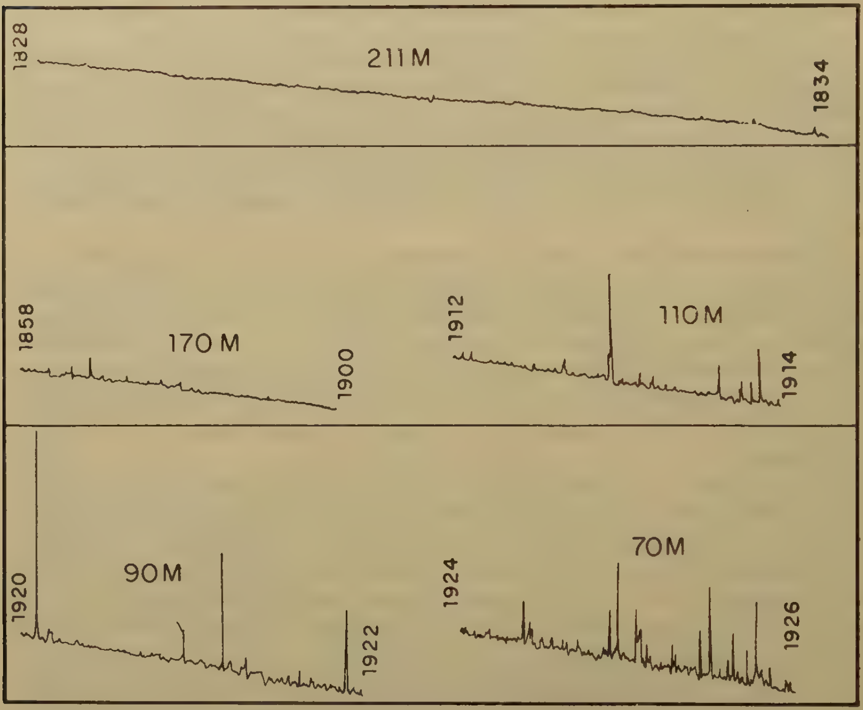

Fig. 3. — Reproduction de fragments de l'enregistrement ayant permis de suivre l'isolume de la figure 1. L'heure est indiquée au début et à la fin de chaque partie du tracé. Un accroissement de la bioluminescence put être reconnue à mesure que l'isolume approche de la surface.

alors utilisé était de réponse plus lente que l'actuel et que cet instrument ancien ne pouvait déceler les éclats luminescents. De ceci, on peut déduire soit que les organismes de la couche diffusante répondent si lentement à des stimulations lumineuses qu'ils ne sont pas affectés par des éclats luminescents transitoires ou qu'ils possèdent quelque mécanisme discriminateur qui leur permet de suivre une intensité céleste constante quels que soient les effets d'accroissement de luminescence survenant dans l'eau qui les entoure.

REMERCIEMENTS

Un don de la « National Science Foundation » permit de réaliser ce travail (NSF-G1701).

Nous remercions le colonel M. Thompson et le major J. Goodhart, 7373 Transport Group, U.S.A.F.B., Chateauroux, France, pour nous avoir accordé avec courtoisie toute facilité de transport de notre équipement à Banyuls-sur-Mer. M. F. Dwyer, Assistant Naval Attaché, Paris, nous aida également avec efficacité.

Nous sommes reconnaissants à M. le professeur G. Petit, directeur du Laboratoire Arago, Banyuls-sur-Mer, pour sa cordiale hospitalité. Il nous a généreusement accordé le temps de travailler à bord du bateau de son Institut ainsi qu'une place dans son laboratoire. Les membres de son personnel, M. C. Delamare Deboutteville, P. Bougis, et J. Paris accordèrent leur assistance, ainsi que le Capitaine et l'équipage du « Lacaze-Duthiers ».

Avant de retourner aux États-Unis, le bathyphotomètre fut recalibré à l'Université Exeter, Angleterre, sous le contrôle de M. I.-J. Linn. Nous tenons à le remercier, ainsi que M. J. Warren et M. F.-S. Russell, F.R.S., et le laboratoire de Plymouth, qui rendit possible cette assistance.

ENGLISH SUMMARY

1. The presence of a migratory sonic-scattering in the Golfe du Lion was established.

2. This layer was found to be associated with the 5×10^{-3} μ watt/cm^2 isolume during its twilight migration toward the surface.

3. As the layer approached the surface, during its period of most rapid migration it appeared to overtake this isolume. Numerous bright flashes of bioluminescence were recorded at this time, and these may have obscured the true relationship between the depth of the scattering layer and the amount of transmitted skylight. The possibility that scattering-layer organisms possess discriminatory mechanisms which enable them to distinguish components of ambient light is discussed.

4. The layer did not rise above a depth of about 48 meters. A sharp thermocline was present at this depth and it is suggested that this may have been a barrier to further migration.

BIBLIOGRAPHIE

BODEN (B.-P.), 1950. — Plankton organisms in the deep scattering layer. U. S. Navy Electronics Lab. Report, 186, 1-29 (unpublished manuscript).

BODEN (B.-P.), and (E.-M.) KAMPA, 1957. — Records of bioluminescence in the ocean. *Pacific Science*, II, 229-235.

BODEN (B.-P.), E.-M. KAMPA, J.-M. SNODGRASS, and R.-F. DEVEREUX, 1955 A depth telerecording unit for marine biology. *J. Mar. Res.*, 14 (2), 205-209.

CLARKE (G.-L.) and G.-K. WERTHEIM, 1956. — Measurements of illumination at great depths and at nigh in the Atlantic Ocean by means of a new bathyphotometer. *Deep-Sea Research*, 3, 189-205.

CLARKE (G.-L.) and R.-H. BACKUS, 1956. — Measurements of light penetration in relation to vertical migration and records of luminescence of deep-sea animals. *Deep-Sea Research*, 4, 1-14.

COUSTEAU (J.-Y.), 1950. — To the depths of the sea by bathycaphe. *Nat. Geog. Mag.*, 106, 67-79.

JOHNSON (H.-R.), R.-H. BACKUS, J.-B. HERSEY, and D.-M. OWEN, 1956. — Suspended echo-sounder and camera studies of mid-water sound scatterers. *Deep-Sea Research*, 3, 266-272.

JOHNSON M.-W, 1946. — Stratification of sound scatterers in the ocean. University of California, Division of War Research. *Report No, M* 397 (1946).

KAMPA (E.-M.), 1955. — A discrepancy between calculation and measurement of submarine illumination. *Proc. Nat. Acad. Sci.*, 41, (11), 938, 939.

KAMPA (E.-M.), and B.-P. BODEN 1954. — Submarine illumination and the twilight movements of a sonic scattering layer. *Nature*, 174, 869-870.

KAMPA (E.-M.), and B.-P. BODEN, 1957. — Light generation in a sonic-scattering layer. *Deep-Sea Research*, (4) 2 : 73-92.

KANWISHER (J.) and G. VOLKMANN, 1955. — A scattering layer observation. *Science*, 121, (3134) : 108-109.

HARDY (A.-C.), 1956. — *The open sea. The world of plankton.* Collins. London.

HERSEY (J.-B.) H.-R. JOHNSON, and L.-C. DAVIS, 1952. — Recent findings about the deep scattering layer. *J. Mar. Res.*, 11 (1) : 1-9.

LEAVITT (B.-B.), 1935. — A quantitative study of the vertical distribution of the larger zooplankton in deep water. *Biol. Bull. Woods, Hole*, 68, 115-130.

TCHERNIA (P.), 1952. — Quelques considérations sur l'état actuel du problème de la couche diffusante profonde (D.S.L.), *Bulletin d'Information du Comité Central d'Océanographie et d'Etude des Côtes*, IV, 10 décembre 1952.

Thermal and Osmotic Countermeasures Against Some Typical Marine Fouling Organisms*

By DENIS L. FOX and EUGENE F. CORCORAN

Abstract

Tests were conducted to determine the tolerance of mussels of the genus *Mytilus* to immersion in fresh water at ambient temperatures and in sea water at elevated temperatures. It was found that young bay mussels, which constitute the most serious sedentary fouling organisms in local sea conduits, may be killed in about 50 minutes at 106 F, in an hour at 100 F, in 7 hours at 95 F, and within 14 hours at 90 F. They may survive for as long as four days at 82 F and indefinitely at 77 F.

Tests results indicate that it is impractical in most cases to apply fresh water as a lethal agent for the mussels in sea water conduits. A countermeasure found to be effective was the discharge of warm sea water through conduits.
3.3.2

Fox

Corcoran

DENIS L. FOX is professor of marine biochemistry at the Scripps Institution of Oceanography, University of California, La Jolla, where he has served on the faculty for 26 years. He received a bachelors degree in chemistry from the University of California at Berkeley in 1925. After four years in industrial chemistry, he returned to graduate work at Stanford, where he received his doctorate in biological sciences (biochemistry) in 1931. Dr. Fox was a Rockefeller Research Fellow at Cambridge University in 1938-39, and a Guggenheim Foundation Fellow in 1945-46. He is the author of numerous papers dealing with marine animal life.

EUGENE F. CORCORAN is assistant professor of marine biochemistry at the Marine Laboratory of the University of Miami, Coral Gables, Florida. Formerly he was a graduate research biochemist at Scripps Institution of Oceanography, La Jolla, California, where he was primarily engaged in research on the organic constituents of sea water and marine sediments. Mr. Corcoran received a BS degree in 1940 from North Dakota Agricultural College, Fargo, North Dakota. His subsequent experience includes two tours of duty as a naval officer, three years as instructor of mathematics at San Diego State College, and one year as research assistant at Scripps Institution of Oceanography. Mr. Corcoran is a member of the American Association for Advancement of Science, Sigma Xi, and Marine Biological Ass'n of United Kingdom.

Introduction

INDUSTRIAL OPERATIONS involving the continuous use of sea water require that intake and discharge conduits be protected against fouling of their inner walls by perennial sedentary, hard-shelled marine animals, such as mussels, barnacles, tube-worms, etc. Various countermeasures have been tried, including heat, fresh water, stagnant water, chlorination, dewatering of tunnels and periodic mechanical scraping, with varying degrees of expense and effectiveness.

It has been determined that thermal treatment is the most feasible of the various countermeasures to be incorporated into the construction of a steam plant, and to be thereafter employed at regular intervals in its operation. Thermal control of marine fouling has been successfully practiced at the Redondo Steam Station of the Southern California Edison Company for nearly a decade, by discharge of the spent (i.e., warmed) circulating water through each of the pair of tunnels which serve alternately as intake and discharge conduits.[1]

Among the numerous local marine animals, mussels of the genus *Mytilus* have been found to be the most prominent members of fouling communities. They are also the most resistant of the common animals toward countermeasures such as heat,[1] osmotic changes or poisons. Therefore they were used to test organisms in investigations in which it was desirable to determine the comparative tolerance of the two most common mussel species of the Pacific coast to immersion in fresh water at ambient temperatures, and in sea water at elevated temperatures. (These marine animals are the California sea-mussel, *Mytilus californianus* and the cosmopolitan bay-mussel, *M. edulis.*)

Antifouling measures should be applied while invading mussel populations are changing, or have recently changed, from their microscopic, free-swimming larval or veliger stage, to the attached bivalve phase. For this reason very small specimens of fairly uniform length were selected for the investigation.

Groups of 10 freshly collected and carefully separated, healthy young mussels were placed into each of a series of 30-ml Gooch crucibles. The mouth of each such container was then covered with a small square of plastic screen, secured by a rubber band, to ensure the containment of the mussels throughout the experiment.

Series (usually 10) of mussel populations, thus contained in groups of 10 each, were then exposed simultaneously to the controlled experimental conditions in a large pan of water. At measured time-intervals, a crucible of mussels was removed from the common experimental environment and drained of its water. Then it was transferred immediately to fresh, daily renewed, continuously aerated sea water, and inspected at frequent intervals.

Mussels exhibit injury by (1) failure to spin new, attaching byssus threads (reattachment may sometimes be delayed, but this is diagnostic of lethality if the delay is excessive); (2) gaping apart of the paired shell-valves, especially if this persists despite mechanical shock (e.g., tapping the shell gently with a glass rod); (3) persistent "sulking" or failure to part the shell-valves for long periods (often observed in very young animals, which, unlike older ones, may, in some cases, die without their shell-valves being pulled open by the action of the tough opening hinge). Persistent gapers were safely regarded as dead or dying, and were removed, while those failing to attach byssus threads, whether sulkers or intermittently open, were given a maximum period of three days of continued observations. Sulkers or unattached individuals seldom if ever survive after exhibiting such signs of failure for a day or more.

The population of survivors (i.e., mussels that were re-attached, sensitive, and filtering water after three days) was recorded from each lot of 10, and was plotted as indicated in the accompanying charts. It will be observed that the ubiquitous bay-mussel *(Mytilus edulis)* is somewhat more tolerant toward fresh water and toward raised temperatures than is the sea mussel *(M. californianus)*.

Experiments with Fresh Water

One hundred young mussels, 7.5 to 10 mm long, were divided into groups of 10 each, in 10 Gooch crucibles. All of the crucibles were then placed in a large enamel pot completely filled with fresh water (about six liters). This pot was closed off at the top with an inverted lid, in order to exclude air space.

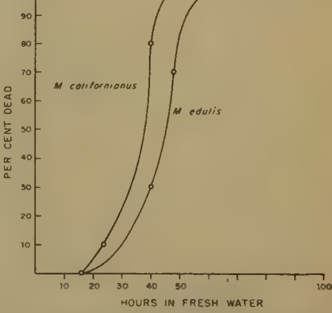

Figure 1—Death rate of *M. californianus* and *M. edulis* in fresh water.

★ Submitted for publication April 12, 1956. A paper presented at the Conference on Marine Corrosion and Fouling Problems, Scripps Institution of Oceanography, University of California, La Jolla, California, April 18-21, 1956. Contribution from the Scripps Institution of Oceanography, New Series, No. 988.

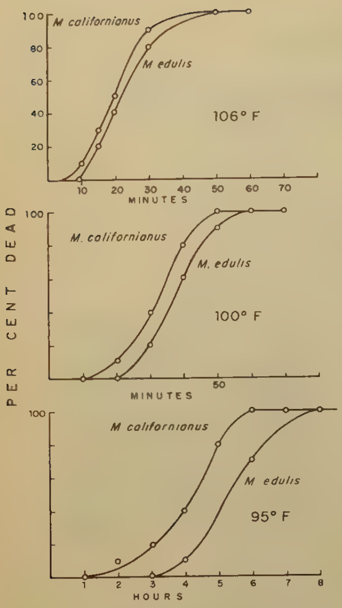

Figure 2—Death rate of *Mytilus californianus* and *M. edulis* (1 to 3 mm in length) at 95 F, 100 F and 106 F in sea water.

TABLE 1—Thermal Death Times of Mussels at Various Temperatures

TEMPERATURE		THERMAL DEATH TIME FOR 100%	
Degrees F	Degrees C	M. californianus	M. edulis
106	40.9	40 minutes	50 minutes
100	37.8	50 minutes	60 minutes
95	35.0	6 hours	7 hours
90	32.2	12 hours	14 hours
85	29.4		41 hours
82	27.8		96 hours
77	25.0		∞ (indefinite survival)

At intervals of 16, 24, 40, 48, 63, 72, 88, 96, 112 and 136 hours, a crucible was removed from the fresh water, drained, labeled and immersed in a reservoir of fresh aerated sea water. Figure 1 indicates that about 48 hours of immersion in fresh water represent a lethal period (i.e., 100 percent dead) for young sea mussels, and some 63 hours for the bay mussel. All exposures were made at ambient temperatures close to 72 F.

This comparatively greater tolerance for fresh water on the part of *Mytilus edulis* is consistent with its ability to colonize brackish waters and river mouths, wherein the other species fails. The 63-hour period required for killing the population also suggests some infeasibility of employing fresh water as an antifoulant for industrial sea water conduits.

Temperature-Time Threshold Experiments

In this series also, freshly collected juvenile mussels (1-3 mm long), differentiable as to species under low power of a stereoscopic microscope, were segregated in the customary series of screened and bottom-perforated crucibles in the usual way. They were then exposed to controlled temperature conditions for measured time-intervals, removed, drained of superfluous water, transferred to fresh, aerated sea water and inspected (see Figure 2). The thermal death times at given temperatures are given in Table 1.

It is evident from the table and the charts that young bay mussels, which constitute the most serious sedentary fouling organisms in local sea water conduits, may be killed in about 50 minutes at 106 F, in an hour at 100 F, in 7 hours at 95 F, and within 14 hours at 90 F. They may survive for as long as four days at 82 F, and indefinitely at 77 F.

In the course of these investigations, an interesting discovery was made relating to the extraordinary heat-resistant species, the so-called ribbed mussel, or Adams' mussel *Mytilus (Hormomya) adamsianus*. This species occurs along the west coast from Santa Barbara to Panama, and on the Galapagos Islands, and is easily confused with another ribbed-shell species, *Septifer bifurcatus*.

Specimens of this ribbed mussel, returned to fresh, aerated sea water after 3 hours exposure to sea water at a temperature of 106 F, remained closed for at least 48 hours, after which interval they once again moved about and spun their byssus threads for attachment. Another lot of the same species, exposed to the same warmed water for 3½ hours, resumed their activities only after some 60-72 subsequent hours in cool, aerated sea water. A thermal death interval of 2½ hours was finally established at a temperature of 113 F.

These small mussels are relatively sparse, however, apparently being crowded out by their large *Mytilus* relatives. They achieve a length of only an inch or less, and are hardly to be regarded as a threat to marine installations.

From the investigations reported here, it would hardly appear practical to apply fresh water as a lethal agent, even for very young *Mytilus* of either species, unless it were economically feasible to maintain the exposure for a 3-day period. When, on the other hand, it is feasible to warm the sea water (e.g., by recirculation, if necessary, of that which may have already acquired some heat from the condenser tubes) and to discharge this warmed wated through the conduits, this is an effective antifouling measure.

In Southern California installations, for example, sea water warmed to 100-106 F and discharged through an alternative intake tunnel for an hour, or at 95 F for 7 hours, applied say at tri-weekly intervals during the season of potential fouling by mussels* should continue to prevent the attachment of these mollusks and allied forms.

In general, thresholds of thermal tolerance may be expected to show wide variability, depending upon latitude. Marine animals inhabiting equatorial waters will exhibit a tolerance for higher temperatures than proved lethal in the present studies, and inhabitants of northerly waters will succumb at considerably lower temperatures.

Reference

1. W. L. Chadwick, F. S. Clark, and D. L. Fox. Thermal Control of Marine Fouling at Redondo Steam Station of the Southern California Edison Company. *Trans. ASME*, (1950) Feb.

---

* This period will be from about mid-March to mid-October, depending upon ambient water temperatures of 60 F and above.

Any discussions of this article not published above will appear in the June, 1958 issue

G. W. GROVES AND TOWNSEND CROMWELL

EXPERIMENTAL INVESTIGATION OF THE EFFECT OF "SECONDARY INSTABILITY" ON MIXING PROCESSES

Reprint from:

SEARS FOUNDATION: JOURNAL OF MARINE RESEARCH
Vol. 16, No. 1, November 30, 1957. Pp. 8–11.

(199)

EXPERIMENTAL INVESTIGATION OF THE EFFECT OF "SECONDARY INSTABILITY" ON MIXING PROCESSES[1]

BY

GORDON W. GROVES
University of California
Scripps Institution of Oceanography

AND

TOWNSEND CROMWELL
Inter-American Tropical Tuna Commission

Abstract. Since specific volume in the ocean is a nonlinear function of salinity and internal energy, mixing results in a change in the total volume. There is a contribution to the change in potential energy due to mixing, which depends on this change in volume and on the pressure at which mixing takes place. Fofonoff has made use of this fact in defining a "secondary stability" parameter. It might be speculated that, under conditions of (secondary) instability, turbulent mixing could be generated spontaneously or that the quality of mixing would be different from that under stable conditions. An experiment to detect this phenomenon was performed, with negative results.

Introduction. The ordinary concept of stability in the oceans, as developed by Hesselberg and Sverdrup (1914), considers the change of potential energy in a layer of water resulting from vertical displacement, up or down, of a small water parcel which is not allowed to mix with the adjacent water. If this change of potential energy is positive, the water at the point under consideration is said to be *stable,* and vice versa. Fofonoff (1956) has widened the concept of stability by including processes in which mixing occurs and by considering the potential energy of the entire vertical water column. The term *pdv* is thus introduced as an additional contribution to the potential energy change. This term results from the fact that specific volume is a nonlinear function of salinity and internal energy and is usually negative; thus an unstable configuration according to Hesselberg and Sverdrup's criterion will usually be unstable according to Fofonoff's criterion. Hesselberg and Sverdrup's stability is referred to as "primary" stability, Fofonoff's as "secondary." The experiment described in this note was an attempt to observe any possible dramatic effects associated with secondary instability (such as the

---

[1] Contribution from the Scripps Institution of Oceanography, New Series No. 989.

Reproduced by Permission

(200)

onset of turbulent motion from an initial motionless state); Fofonoff has made no such speculation.

Let us consider a configuration in which density increases with depth. Fofonoff finds that if the density gradient exceeds some *critical gradient*, then mixing can occur with loss of potential energy; in that case the system is said to exhibit secondary instability at this level. Therefore a system consisting of two homogeneous layers will almost always exhibit secondary instability at the interface.

To get a rough idea of the amount of mixing that would be necessary at the interface of a two-layer system in order to reach (secondary) stability in the system, let us assume that a fluid mass m immediately above the interface mixes thoroughly with an equal fluid mass m immediately below. Let A be the cross-sectional area of the water column under consideration and α_1 and α_2 the specific volumes of water in the upper and lower layers, respectively. For primary stability, we must have $\alpha_1 > \alpha_2$. After mixing there will be a homogeneous layer of water of mass $2m$ between the two original layers having a specific volume, say, of α. This layer is assumed thin enough so that inhomogeneity due to compressibility and pressure gradient may be neglected.

Before mixing, the center of gravity of the water to be mixed is at a distance $(m/4A)\,(3\alpha_2 + \alpha_1)$ above its lower boundary, and the potential energy relative to this level is

$$\frac{m^2 g}{2A}\,(3\alpha_2 + \alpha_1).$$

After mixing, the center of gravity will be at $\alpha m/A$ and the potential energy will be

$$\frac{2m^2\alpha g}{A} + mp\,(2\alpha - \alpha_1 - \alpha_2),$$

where the second term represents the *pdv* addition to the potential energy. Equating the potential energies before and after mixing to find the amount of water that must mix in order to reach (secondary) stability, we obtain

$$\frac{m}{A} = \frac{2p}{g} \cdot \frac{\alpha_1 + \alpha_2 - 2\alpha}{4\alpha - 3\alpha_2 - \alpha_1}, \qquad (1)$$

and it is evident that if the specific volume is governed by a linear law, no water can mix without addition of potential energy.

The Experiments. A two-layer system, consisting of pure water above and a 17% NaCl solution colored with red vegetable dye below, was put under 1000 psi pressure for 18 hours. The tank used was a rectangular aquarium 27 cm long, 17 cm wide, and 19 cm deep. In order to apply the relationship (1) to this configuration we shall neglect the change of specific volume resulting from compressibility and from conversion of potential to internal energy (which is unimportant at this pressure anyway). (Note that compressibility would play no role whatsoever if the specific volumes α, α_1 and α_2 were all affected proportionately by the pressure.) We shall therefore use the following values of specific volume for NaCl solutions at atmospheric pressure and at 20° C:

%NaCl	Specific Volume
0	1.0018
8.5	.9438
17	.8897

Taking $p = 1000\ psi = 68 \times 10^6$ dynes cm^{-2} along with the above values, we obtain $m/A = 6 \times 10^3$ gm cm^{-2} from relationship (1), which is equivalent to a thickness of 60 m. Even at atmospheric pressure, the thickness over which mixing should occur without need of additional potential energy is of the order of a meter. The motive in going to 1000 psi was to increase the secondary instability and the likelihood of a spectacular result.

At the end of 18 hours there was no visual evidence of turbulent mixing, but of course the sharpness at the interface had become considerably reduced as a result of molecular diffusion. A stirring apparatus consisting of ¼″ wire mesh mounted horizontally in the upper layer was then turned on, the mesh executing reciprocal up and down motion;[2] no qualitative difference could be detected visually in the character of mixing at 1000 psi as compared with that at atmospheric pressure.

Even if secondary instability does not induce turbulent mixing from an initial motionless state, perhaps mixing by molecular diffusion is speeded up. The first experiment would have given no indication of this, since the dye, which was used as a visual tracer, contributes negligibly to changes in specific volume and could diffuse independently of the NaCl. Therefore, a second experiment was carried out with fresh water and a concentrated solution of $CuCl_2$ (just under saturation at room temperature). This solution itself is bright green and no dye is needed as a tracer. As before, the two layer system was submitted to 1000 psi for 18 hours, at the end of which time there was no striking

[2] The junior author has used similar apparatus in a mixing experiment at atmospheric pressure.

evidence of a qualitative difference in the diffusion rate under pressure as compared with that under atmospheric pressure. It must be emphasized that we were not set up for a quantitative experiment on diffusion rates; by the methods at our disposal we could have detected only a gross difference.

Conclusions. A simple experiment, carried out in an attempt to detect a possible effect of secondary instability, gave a negative result; this, of course, does not prove that there are no such effects. It seems probable, however, that the principal result of secondary instability, if such exists at all, is a small change in the diffusion rate in unstable configurations. In the case of primary instability, it is quite evident that the potential energy lost to the system as a result of a small perturbation tends to increase the perturbation. For secondary stability this loss of energy may go somewhere else (directly into heat, for example). In any case, energy considerations in the initial and final states alone are inadequate for predicting the outcome of such an experiment. Henry Stommel (personal communication) has suggested the possible existence of a criterion for the onset of convection in this stability problem that is similar to Rayleigh's convection criterion.

Acknowledgments. A great deal of insight into the problem was obtained through many talks with Dr. Carl Eckart of the Scripps Institution of Oceanography and through correspondence with Dr. N. P. Fofonoff, who at the time was with the National Institute of Oceanography in England. The authors thank the U. S. Navy Electronics Laboratory of San Diego, especially Mr. Clarence Milligan of that establishment, for use of its high pressure tank. Instrumentation was provided through contract with the U. S. Navy Bureau of Ships. This note represents a result of research conducted by the California Cooperative Oceanic Fisheries Investigations and the Inter-American Tropical Tuna Commission.

REFERENCES

Fofonoff, N. P.

1956. Energy transformations and stability in the ocean. Unpublished manuscript.

Hesselberg, Th. and H. U. Sverdrup

1914–15. Die Stabilitätsverhältnisse des Seewassers bei vertikalen Verschiebungen. Bergens Mus. Aarb., No. 15: 1–16.

PROCEEDINGS

OF THE

CALIFORNIA ACADEMY OF SCIENCES

Fourth Series

Vol. XXIX, No. 6, pp. 257–265, 15 figs. July 10, 1958

BATHYCALANUS SVERDRUPI, N. SP., A COPEPOD CRUSTACEAN FROM GREAT DEPTHS IN THE PACIFIC OCEAN[1]

BY

MARTIN W. JOHNSON
Scripps Institution of Oceanography
University of California
La Jolla, California

Several species of unusually large, free-living copepods have been described from net hauls extending to great depths in the ocean. Among these large calanoids are the following hitherto described, closely related genera and species: *Bathycalanus richardi* Sars (1905); *Bathycalanus bradyi* (Wolfenden) (1905); *Bathycalanus princeps* (Brady) (1883); *Megacalanus princeps* Wolfenden (1904); *Megacalanus sarsi* Farran (1939); *Bradycalanus typicus* Scott (1909); *Bradycalanus gigas* Sewell (1947).

Much confusion has existed relative to the taxonomy of the group. The above grouping is based on a special analysis made by Farran (1939) in an effort to clear up the synonymy. More recently Sewell (1947) gave the group further study and in addition to describing a new species, *Bradycalanus gigas,* removed the group from the family Calanidae and created a new family, Megacalanidae, to receive it. These studies appear to have put the group on a fairly stable basis systematically though a larger series of collections is needed to establish what, if any, variations may occur.

The present study, which is being supported in part by the National

---

[1] Contribution from the Scripps Institution of Oceanography, New Series No. 990.

Reproduced by Permission

Science Foundation (no. NSF-G4993), adds a new species to *Bathycalanus*. This species is especially remarkable because of its huge size, being the largest of all free-living copepods hitherto described. Two adult females (fig. A) were found in an open trawl collection made by the Scripps Institution of Oceanography vessel *Horizon* at a towing depth of 2103 meters at 12° 33′ N., 164° 49′ E., July, 1956.

Bathycalanus sverdrupi Johnson, new species.

The chief generic characters which serve to distinguish this species from those of closely related genera are: (1) the second maxillae, which are armed with long, ribbon-like setae that bear exceedingly fine processes and sharply curved distal ends; (2) the absence of any setae on the second inner lobe of the first maxillae; (3) the cutaneous pores of the "maculae

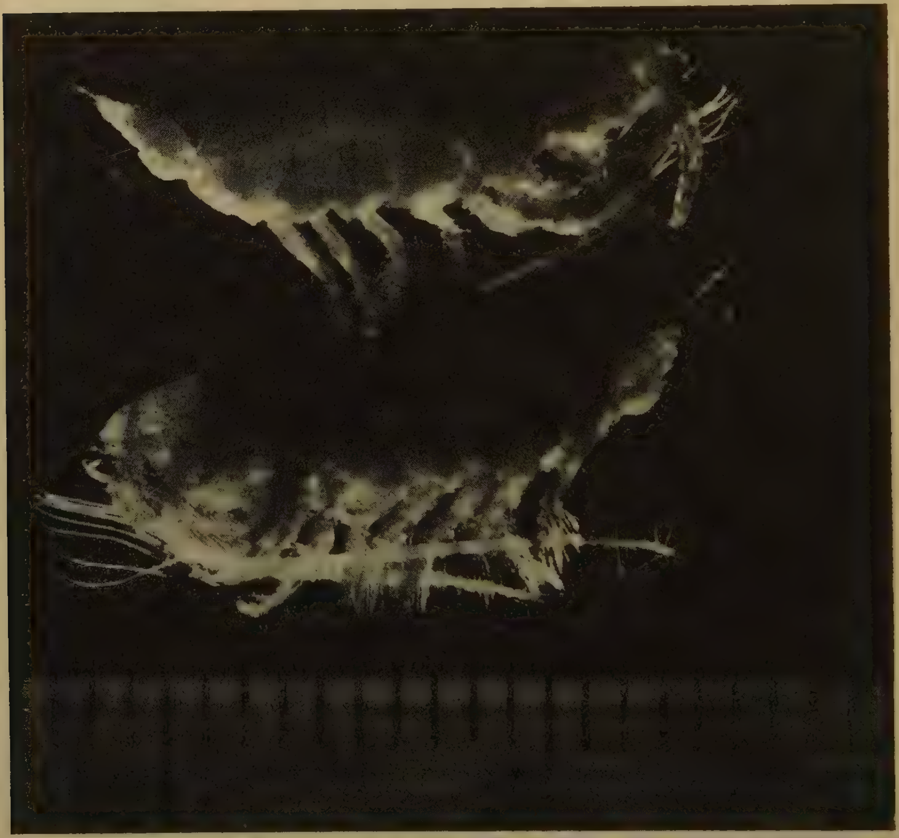

Figure A. *Bathycalanus sverdrupi*, new species. Photograph of females, to specimen has fifth feet removed. Scale in mm.

cribrosae" being arranged in clumps, not in an oval or ring; (4) only the terminal segment of the exopod of the first pair of feet is provided with external marginal spines. In the other genera the exopod bears a marginal spine on each of the three segments of the first feet.

Specific characters. Female.

Body. The body is robust and tapers rather sharply in both lateral and dorsal aspects (figs. 1 and 2). The urosome (posterior body division) is relatively short in relation to the anterior division, the ratio being about

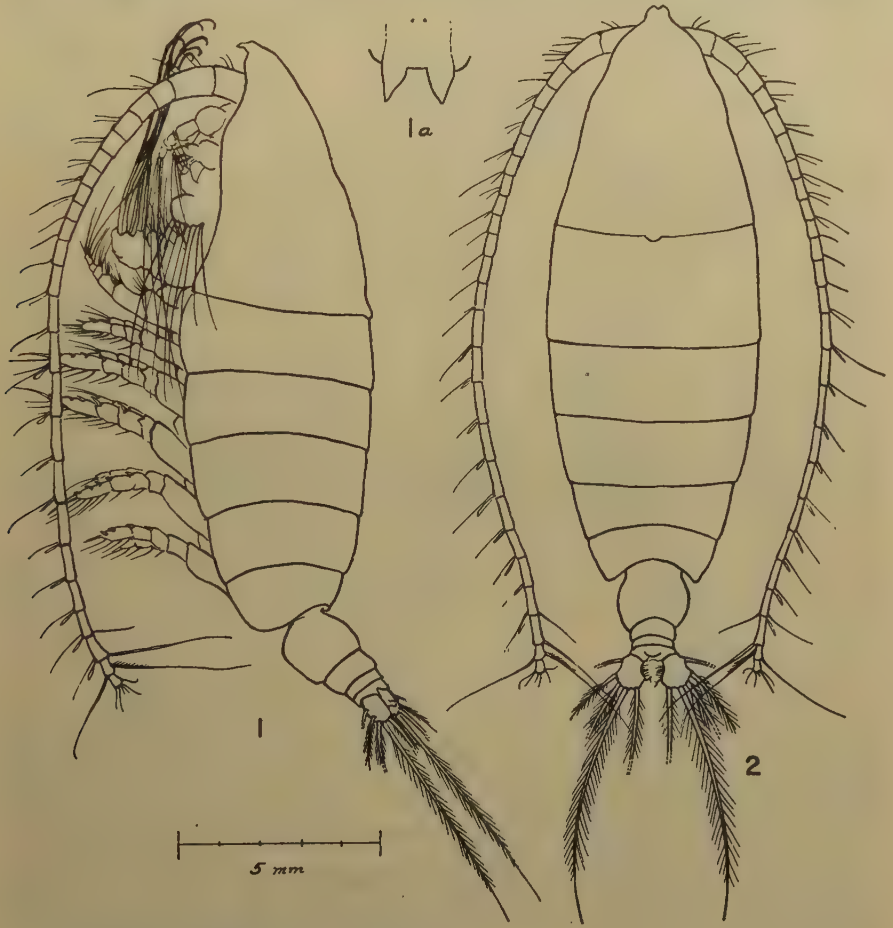

Bathycalanus sverdrupi, new species.
Figure 1. Female, lateral.
Figure 1a. Female, rostrum, anterior aspect enlarged scale.
Figure 2. Female, dorsal.

1 to 4.5 as contrasted with about 1 to 3.2 in *Bathycalanus richardi* and *Bathycalanus bradyi* and 1 to 3.7 in *Bathycalanus princeps.* The genital segment is large and tumid and there are three short abdominal segments between it and the short caudal rami. The rostrum (fig. 1a) consists of two stout tapering prongs unlike the sausage-like processes described for other known species of *Bathycalanus.* The head bears no crest as in *Bathycalanus princeps* and no horn-like process or sensory hairs were observed; however, two small pit-like spots occur just above the rostral prongs. The posterior margin of the 5th thoracic segment is rounded. The body contains much oil and the color of freshly caught specimens is deep red. The unusually large size, 16.8 and 17 mm. in length, is probably also specific. The previous maximum size record is 14.9 mm. for *Bradycalanus gigas* Sewell.

First antennae. The first antennae consist of 25 segments and hardly reach the end of the caudal rami. (These appendages were intact in only one specimen). This is in striking contrast to the long first antennae of other known *Bathycalanus* species. They overreach the caudal rami by 5 to 6 segments in *Bathycalanus bradyi* (Sewell, 1947), by ¼ of their length in *Bathycalanus princeps* (Rose, 1933), and by nearly ⅓ their length in *Bathycalanus richardi* (Sars, 1925). The terminal segment is very short.

Second antennae (fig. 6). These appendages are similar to those figured by Sars (1924) for *Bathycalanus richardi,* but lack the setae on the distal part of the first endopod segment and possess a lateral seta on the seventh (terminal) exopod segment. The second antennae appear not to have been critically studied in the other species.

Mandible (figs. 4 and 5). The second endopod segment bears only two setae and a group of cutaneous pores occurs on the second basal segment. The mandibular blade is well developed and bears teeth as shown in figure 5.

First maxillae (fig. 3). These are characteristic of the genus but have only one seta each on the second basal segment and on the first and second segments of the endopod. This differs from the arrangement on other species. Sewell (1947) has called attention to the use of setae arrangement on the first maxillae as diagnostic characters for the genera and species.

Second maxillae (fig. 8). These appendages are strongly developed and conspicuous in the species. The long heavy setae are characteristic of the genus, being armed on the distal ⅔ with very fine, closely set processes which curve into ringlets that appear to form a continuous tube. The ends of the setae are strongly curved. A distinctive feature of this

(208)

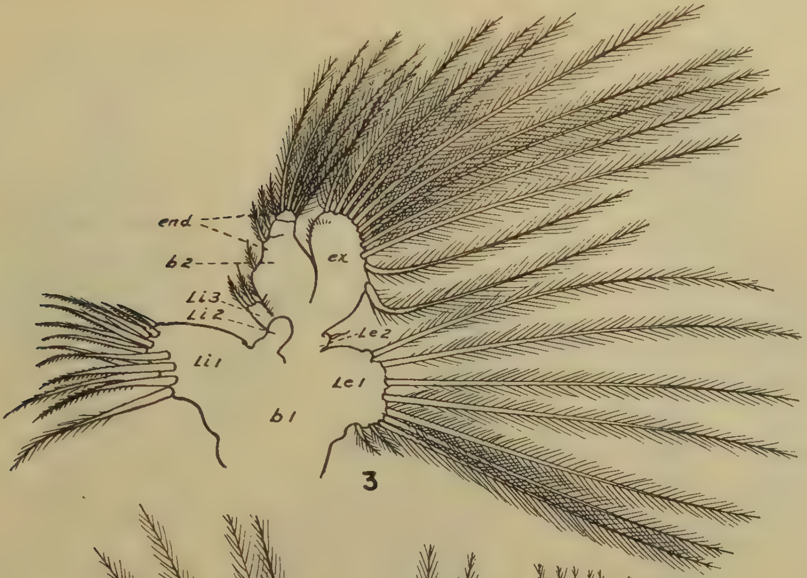
end
b2
Li3
Li2
Li1
b1
ex
Le2
Le1

3

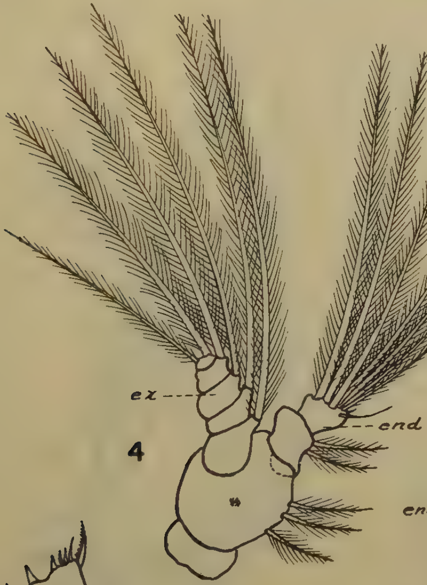

4

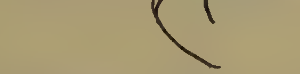

5

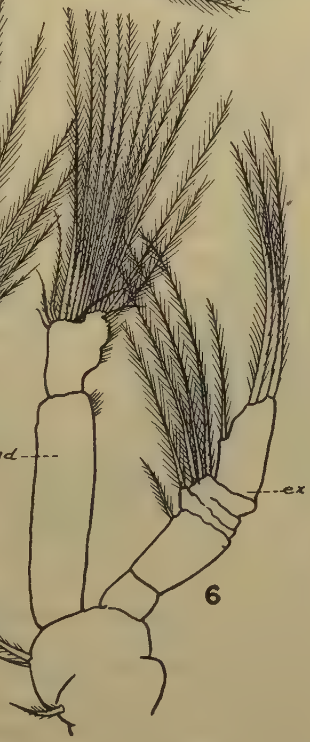

6

Bathycalanus sverdrupi, new species, female.

Figure 3. First maxilla. b 1, 1st basis; b 2, 2nd basis; end, endopod; ex, exopod; Le 1–5, external lobes; Li 1–3, internal lobes.

Figure 4. Mandibular palp.

Figure 5. Mandibular blade.

Figure 6. Second antenna. end, endopod; ex, exopod.

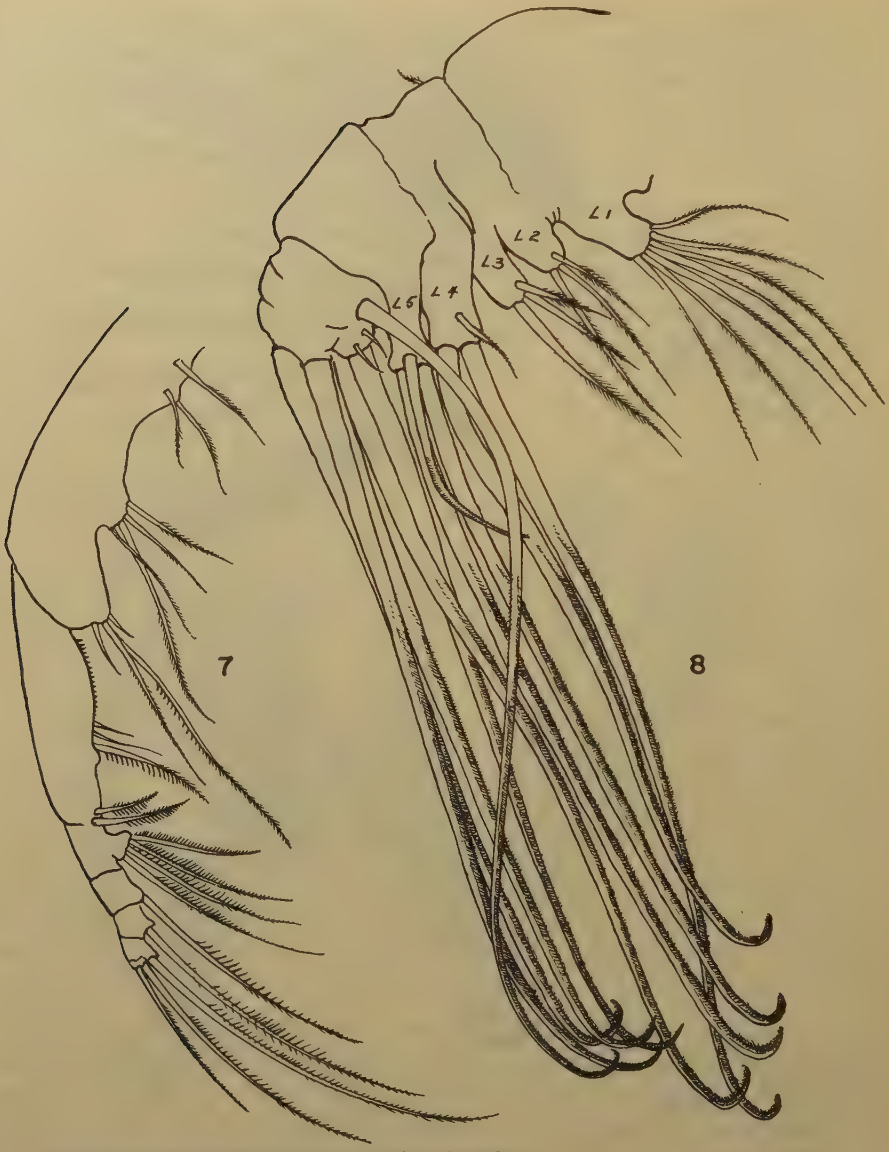

Bathycalanus sverdrupi, new species, female.
Figure 7. Maxilliped.
Figure 8. Second maxilla. L 1–L 5, lobes of the bases.

Bathycalanus sverdrupi, new species, female.
Figure 9. First leg, anterior surface.
Figure 10. Second leg. m.c., maculae cribrosae.
Figure 11. Third leg.
Figure 12. Fourth leg.
Figure 13. Exopod of first leg—abnormal.
Figure 14. Fifth leg.

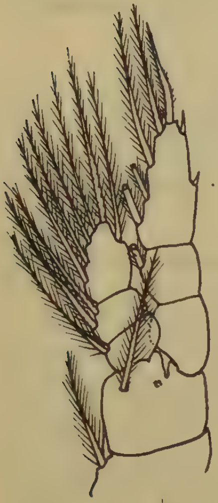

9

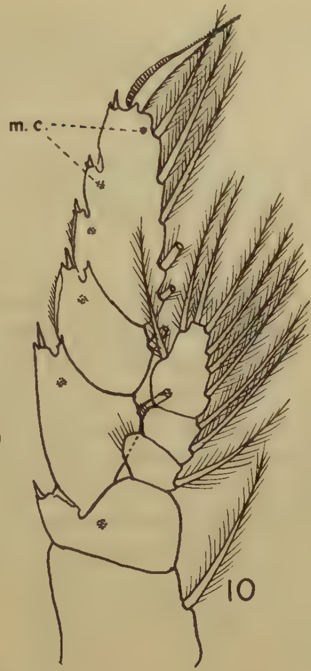

10

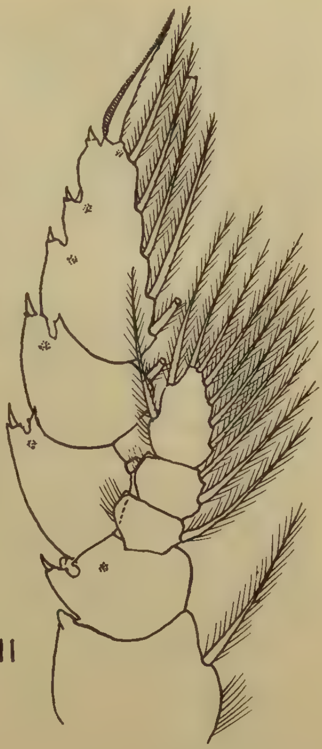

11

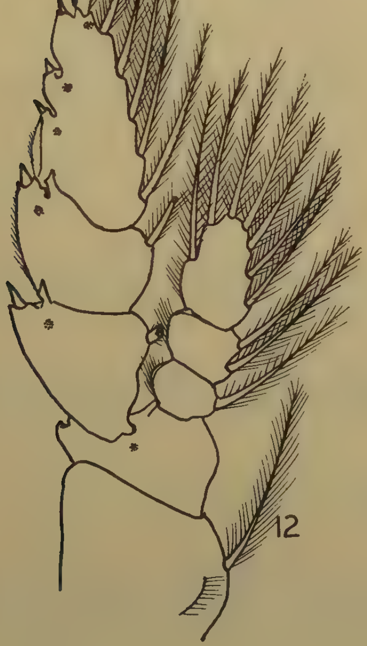

12

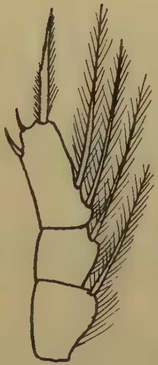

13

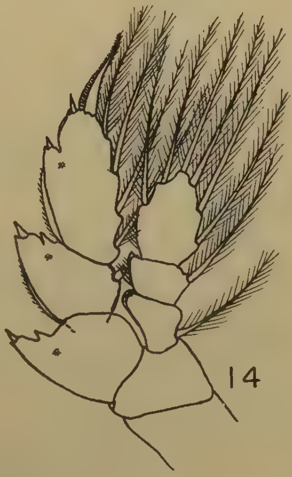

14

species appears to be the much stronger development of the setae on the fourth lobe of the second maxillae. These setae are similar to those of lobe 5 and of the endopod.

Maxillipeds (fig. 7). There appears to be but little distinction between these and the corresponding appendages of *Bathycalanus princeps.* There is but one strong seta on each of the endopod segments 2, 3, and 4. The other two species are provided with additional small setae on these segments.

Swimming feet (figs. 9–14). The first pair of feet have three-segmented exopods as in *Bathycalanus princeps* and *Bathycalanus bradyi.* The remaining feet agree closely with those of all of the known species in having three-segmented rami and in having three external spines on the terminal segment except in the fifth pair of feet which bear only two external spines. There is no retroverted spine on the second basis of the first legs. The terminal segment of the exopod of the first feet has two smooth spines and four inner setae as shown in figure 9; however, in one female the opposite foot was abnormal as in figure 13. This same female had three setae on the second endopod segment of one of the feet of the second pair instead of the normal two setae. "Maculae cribosae" occur in all of the feet.

Holotype in U. S. National Museum, No. 101078.

Paratype in California Academy of Sciences, No. 34987.

The species is named for the late Dr. Harald U. Sverdrup, renowned oceanographer.

LITERATURE CITED

Brady, G. S.

1883. Report on the Copepoda collected by H.M.S. *Challenger* during the years 1873–76. *Challenger* Reports, vol. 8, pt. 23, pp. 1–42, 55 pls.

Farran, G. P.

1939. Note on the nomenclature of the copepod genus *Megacalanus* Wolfenden and allied genera. *Annals and Magazine of Natural History*, ser. 11, vol. 4, pp. 355–361.

Rose, M.

1933. Copépodes Pélagiques. Faune de France 26, Paris, 374 pp.

Sars, G. O.

1905. Liste Préliminaire des Calanoides recueilles pendant les Campagnes de S. A. S. le Prince Albert de Monaco, avec diagnoses des genres et des espéces nouvelles, I^re^ Partie, *Bulletin du Musée Océanographique de Monaco*, no. 26, 22 pp.

SARS, G. O.—Cont.

1924–1925. Copépodes particulièrement bathypélagiques provenant des Campagnes Scientifiques du Prince Albert Ier de Monaco. Résultats des Campagnes Scientifiques, Fasc. LXIX, Planches 1924, 127 pls., Texte 1925, 408 pp.

SEWELL, R. B. S.

1947. The Free-swimming Planktonic Copepoda: Systematic Account. Scientific Reports of the John Murray Expedition 1933–34, vol. 8, no. 1, 303 pp.

SCOTT, A.

1909. The Copepoda of the "Siboga" Expedition, Part I. Free-swimming, Littoral and semi-Parasitic Copepoda, "Siboga" Expeditie Monograph, XXIXa, 323 pp., 69 pls.

WOLFENDEN, R. N.

1904. Notes on the Copepoda of the North Atlantic Sea and Faroe Channel. *Journal of the Marine Biological Association*, vol. 7, no. 1, pp. 110–146, 9 pls.

1905. Plankton Studies.—Part I. Copepoda, Rebman Ltd., London, 24 pp., 7 pls.

JOURNAL OF SEDIMENTARY PETROLOGY, VOL. 28, NO. 1, PP. 65–74
FIGS. 1–3, MARCH, 1958

HEAVY MINERAL VARIATION IN SAN ANTONIO AND MESQUITE BAYS OF THE CENTRAL TEXAS COAST[1]

DAVID M. POOLE[2]
Scripps Institution of Oceanography, University of California, La Jolla, California

ABSTRACT

As a further investigation of the sediments of the central Texas coast bays, heavy minerals in the sand-size fraction of the sediment samples were studied. The application of statistical analysis to heavy mineral studies by using chi-square to test for homogeneity of samples is shown. It was possible to divide the bays into areas where the relative amounts of heavy minerals were statistically homogeneous, and in the case of a bay with simple bottom configuration and sediment type it was possible to correlate the grain size distribution of the sediments with relative amounts of heavy minerals. This relationship, however, did not hold for a more complex bay. The accuracy of the laboratory procedures was investigated. The mineralogical differences between the various areas are probably real and not due to errors in laboratory methods. The heavy mineral distribution also showed that much of the sand-size sediment was carried into the bays from the barrier islands.

INTRODUCTION

The purpose of this paper is to show the application of statistical methods to heavy mineral studies by the use of chi-square to test for homogeneity of samples. By dividing the bays into areas where the relative amounts of heavy minerals were statistically homogeneous, significant variations of the heavy minerals could be shown. The geologic implications of these variations are not discussed in detail.

Comparisons of heavy mineral suites by statistical analysis have seldom been attempted. During the early years of sedimentary petrology the presentation of heavy mineral data was confined to estimated values of their abundance, but later the minerals were actually counted and percentage values of their abundance determined. These results were usually presented in tabular or graphic form, and each investigator would then use his personal judgment to draw conclusions as to the similarity of the samples. The first attempt to apply a statistical approach to this problem was that by Dryden (1935) who used the coefficient of correlation to compare heavy mineral suites. This idea was criticized by Eisenhart (1935a), who proposed the chi-square test in its place. It is the opinion of Eisenhart, Krumbein and Pettijohn (1938), and Robert L. Miller of the University of Chicago (personal communication) that there is no statistical theory developed for Dryden's use of the coefficient of correlation.

LOCATION AND DESCRIPTION OF THE AREA

This study was confined to San Antonio and Mesquite Bays which are located on the northwest coast of the Gulf of Mexico about 30 miles north of Corpus Christi, Texas (fig. 1). A complete description of these bays, their sediment types, and sedimentary environments can be found in Shepard and Moore (1955). These two bays were the only ones sampled in enough detail to allow a fair trial for the chi-square test. The only previous mineralogic investigation of the area was that by Bullard (1942) on the beach sands of the Texas coast.

METHOD OF STUDY

Grain size analyses were made of samples from the upper 5 ± cm of cores taken in the bays. The samples were dried, soaked in 0.025N sodium hexametaphosphate, $Na_6(PO_3)_6$(?), stirred in a malt-mixer, and then wet-sieved through a 0.061 mm sieve. The sand-size material was analyzed by the Emery settling tube and the fine material was analyzed by a hydrometer size analysis (Shepard and Moore, 1955, p. 1479). After the size analyses were completed, the sand fractions were prepared for heavy mineral separations by eliminating the coarser shelly material by sieving through a 0.210 mm

---

[1] Contribution from the Scripps Institution of Oceanography, New Series No. 991. This investigation was supported by a grant from the American Petroleum Institute, Project 51. Manuscript received October 9, 1957.

[2] Present address: The Ohio Oil Company, Denver Research Center, Littleton Colorado.

Reproduced by Permission

sieve (only 1 to 2 percent mineral grains and no heavies except mica were removed by this sieving), and then treating the material that passed through the sieve with hot 3 N HCl. The sand, freed of carbonates, was washed clear of acid, dried, and weighed.

The heavy mineral separations were made by using commercial acetylene tetrabromide (tetrabrom-ethane), sp. gr. 2.89, as the heavy liquid. Steep-walled funnels were used as the separation apparatus. The weighed sand fraction was placed in the acetylene

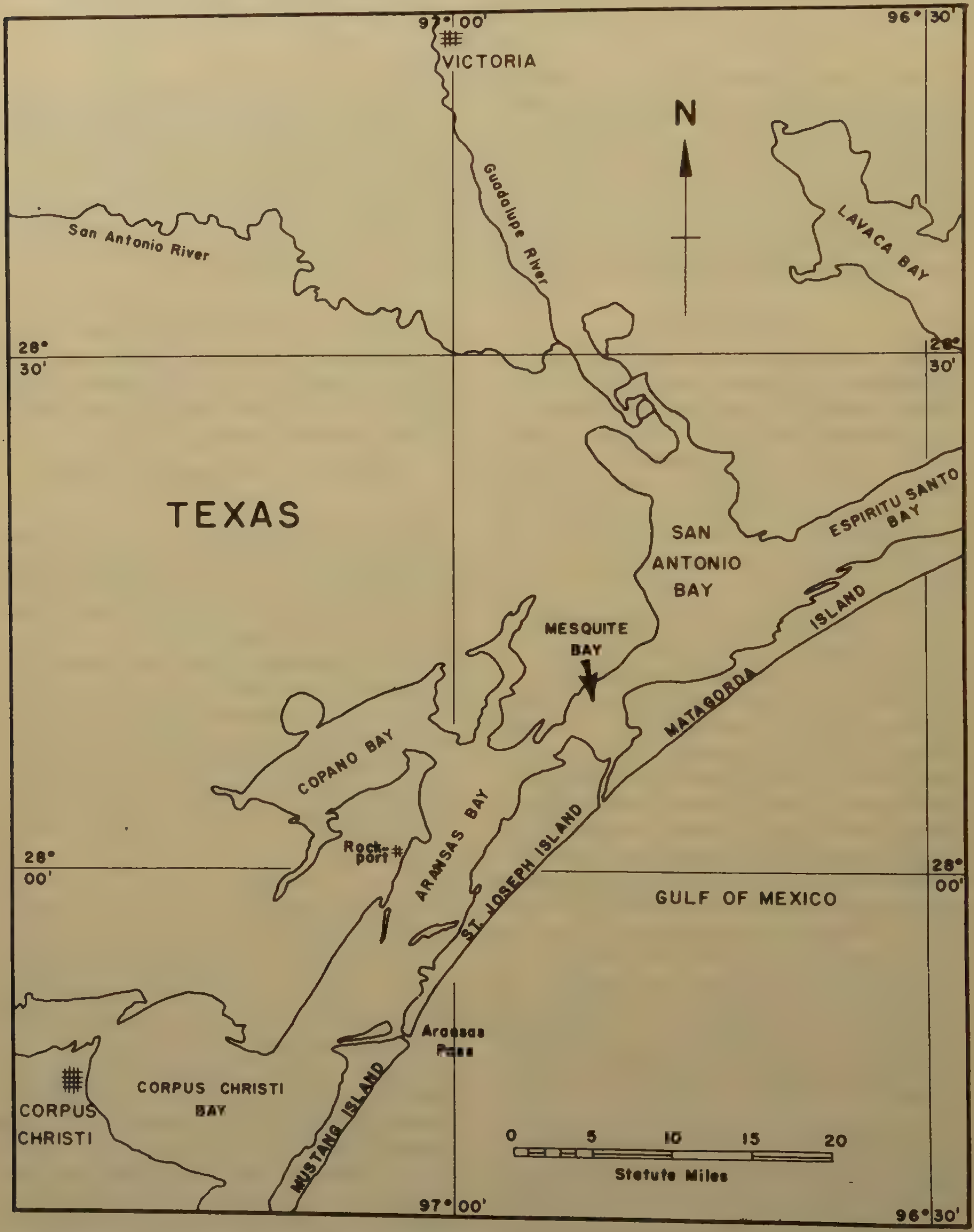
97° 00'
VICTORIA
96° 30'
N
Guadalupe River
San Antonio River
LAVACA BAY
28° 30'
TEXAS
SAN ANTONIO BAY
ESPIRITU SANTO BAY
ISLAND
MATAGORDA
MESQUITE BAY
COPANO BAY
Rockport
ARANSAS BAY
ST. JOSEPH ISLAND
28° 00'
GULF OF MEXICO
Aransas Pass
CORPUS CHRISTI
CORPUS CHRISTI BAY
MUSTANG ISLAND
0 5 10 15 20
Statute Miles

FIG. 1.—Outline map of part of Texas showing the location of the areas investigated.

TABLE 1.—*Showing loss of zircon due to sieving through 0.061 mm sieve*

Sample	Common Minerals	% Minerals in split coarser than 0.061 mm sieve	% Minerals in unsieved split	%>0.210 mm %<0.061 mm
Dune Sand (Rockport)	Black opaques	63	58	3.5%>0.210
	Tourmaline	26	8	
	Zircon	Trace	20	0.9%<0.061
	Others	11	11	
XS 387 (San Antonio Bay)	Black opaques	59	52	
	Hornblende	13	7	0.6%>0.210
	Tourmaline	15	4	
	Zircon	2	26	5.8%<0.061
	Others	11	11	

tetrabromide in the funnel, stirred thoroughly, and allowed to settle; if the sample consisted principally of very fine sand it was stirred several times during a settling period of a few hours. Acetylene tetrabromide does not completely separate the micas (specific gravities range from 2.8 to 3.1) from the light fraction so that they were not included in the heavy mineral counts. After the separation the heavy fraction was weighed and then split by means of a microsplit to a sample of about 400 grains which were mounted in Aroclor 4465. The heavy minerals from each sample were identified by traversing the slide along parallel lines and counting each grain that touched the center of the microscope cross hairs.

There are some inaccuracies in determining the heavy mineral content of the samples that are inherent in the above method of preparation because of the concentration of zircon in the finer fraction of the samples. This has been shown by Hawkes and Smythe (1931, p. 352), van Andel (1950, p. 39; 1955, p. 534), and others. The coarser silt-size material passing through the 0.061 mm sieve contains various amounts of heavy minerals that are missed in the analysis. As examples, two samples were analyzed where the separation between very fine sand and coarse silt was made by decantation using Stokes' settling velocity for quartz spheres of 0.0625 mm diameter. After being passed through a 0.210 mm sieve and treated with acid, the sand from each sample was split into two fractions. One fraction was sieved through a 0.061 mm sieve and the heavy minerals determined for the material retained on the sieve. In addition the heavy minerals were counted in the unsieved fraction. The results are shown in table 1 where it can be seen that much of the zircon is lost because of the method of size analysis. However, all the samples in this study were treated in the same manner so they are comparable one to another.

The heavy minerals in the sizes between 0.210 mm and 0.061 mm were studied, rather than a single limited size fraction or the average of two size fractions as has been advocated by some investigators. Van Andel (1950) in his study of the Rhine sediments examined the heavy minerals between 0.5 and 0.04 mm, and concluded that only in special cases was it necessary to study the various size fractions separately.

ACCURACY

The accuracy of heavy mineral studies depends on both the field sampling errors and laboratory errors. Krumbein and Rasmussen (1941) attempted to evaluate sampling and laboratory errors and concluded that they were of approximately the same order of magnitude—about 10 percent. They divided the laboratory errors into three parts: error of splitting and sieving (1.0 ±0.5%); error of bromoform separation (3.5 ±1.0%); and error of microsplitting, mounting, and counting (10.0 ±2.0%), with the counting error probably being of greatest significance.

The accuracy of mineral counts can be ascertained in several ways. Dryden (1931) prepared a chart showing the probable error for several different frequencies in samples ranging from 25 to 750 grains, and pointed out that the "law of diminishing returns" would limit to a few hundred the number of grains counted. Dryden also showed that not more than two significant figures are

TABLE 2.—*Confidence intervals (95% level) showing the precision of estimates of epidote present when a large or small number of grains are counted*

Total number of grains counted	Amount epidote present by counting		Epidote will lie between these limits 95% of time	
	No. grains epidote	% epidote	No. grains epidote	% epidote
164	3	2	1 to 7	0.5 to 4
418	8	2	3 to 14	1 to 3.5

justified even if as many as 4000 grains were counted. Manning (1953) pointed out the usefulness of confidence intervals for showing the precision of mineral frequencies determined by grain counts. Table 2 shows the variation in epidote that could be expected in an area in San Antonio Bay using the smallest and largest samples counted for that area. By using table VIII₁ of Fisher and Yates (1949) the confidence intervals can be read off with sufficient accuracy without the somewhat laborious computations used in obtaining the intervals in table 2. Since the variation between the diagnostic minerals, hornblende and black opaques (and tourmaline), which were used to delineate the mineralogical areas, was of the order of five percent or greater, the differences between these areas are probably real.

CHI-SQUARE TEST

Many texts on statistical analysis discuss chi-square and give samples of its use. These include Dixon and Massey (1951), Fisher (1950), Snedecor (1946), and others. However, Eisenhart (1935b) works out examples using chi-square to test for homogeneity with geologic data, and his examples were used as models for this study. Mineral frequencies, not percentages, were used to calculate chi-square, and following general procedure, the five percent level of significance (or probability of a larger value of chi-square, $P=0.05$) was used to determine whether the hypothesis of homogeneity was to be rejected or not. In actual practice, the values determined in this paper gave a higher P value (0.10 to 0.85). The high values of P are probably due to the fact that the data have been made more homogeneous by grouping the minerals that occurred in small quantities (Eisenhart, 1935b, p. 143). Only five mineral categories were used: black opaques (including leucoxene), hornblende (including all the amphiboles except basaltic hornblende), tourmaline (all varieties), epidote (including the colorless varieties), and "others" (a combination of all the rest of the mineral species present). This combining is recommended because the chi-square tables have been calculated on the assumption of large samples, and therefor the smallest expected frequency should be greater than five (Fisher, 1950, p. 84). It is also necessary to count approximately the same number of grains for each sample, and if exactly the same number are counted per sample the computations are greatly simplified. Snedecor (1946, p. 24) shows the effects on chi-square of varying sample sizes.

RESULTS

Heavy minerals were counted in 165 samples, of which 44 were from Mesquite Bay and 121 from San Antonio Bay (which includes Hynes and Guadalupe bays and Mission Lake). By means of testing groups of samples for homogeneity using chi-square, various areas of the bays were found to have the same relative amounts of the various heavy mineral categories, or close enough to the same amounts to be considered statistically homogeneous.

Of the 44 samples from Mesquite Bay that were analyzed for heavy minerals, only four from the main bay are not part of a statistically homogeneous group (four samples from adjoining San Carlos Bay and Cedar Bayou would not fit either). Mesquite Bay has been divided into four areas (see fig. 2): (1) an outer zone, nearest the barrier islands, high in hornblende (42%) and opaques (32%); (2) an intermediate zone somewhat lower in hornblende (35%) and higher in opaques (37%); (3) a long narrow zone that runs NW-SE down the center of the bay that is higher in opaques (46%) than the intermediate zone and somewhat lower in hornblende (32%); and (4) a zone located in the northwest corner of the bay which is very different from the other areas in that it is low in hornblende (11%) and high in tourmaline (23%) and opaques (56%). The mineralogical information is summarized in table 3, which includes average values for the five mineral categories, the range of these values, chi-square, and P values for each area. Also included are average values of median diameter, sorting (see Inman, 1952), and sand, silt, and clay. Table 3 shows a relationship between the heavy minerals and grain size distribution. The sediments with a high tourmaline content are sandier and better sorted than the hornblende-rich sediments of Mesquite Bay.

San Antonio Bay is far more complex than Mesquite Bay both in bottom configuration and sediment type (see Shepard

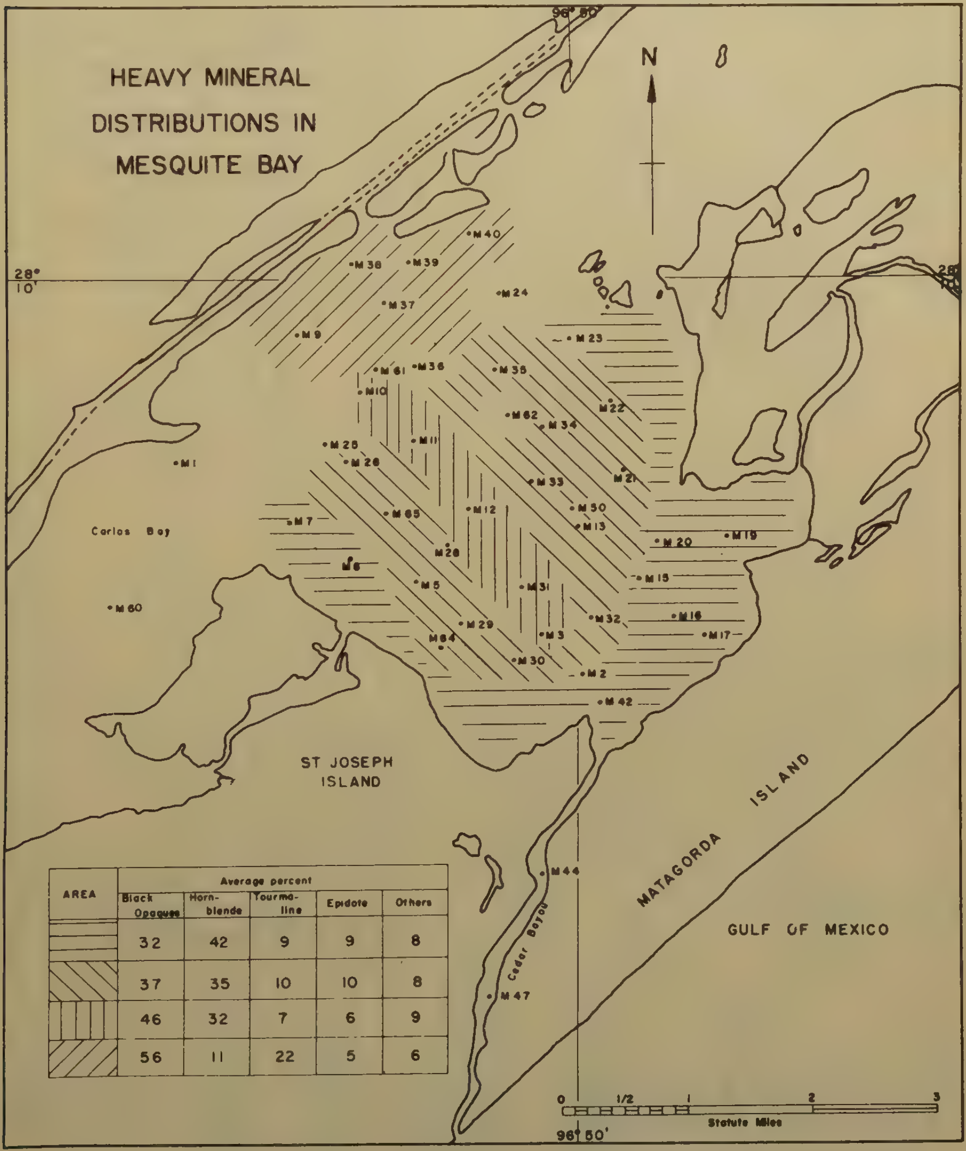
HEAVY MINERAL
DISTRIBUTIONS IN
MESQUITE BAY
N
96° 50'
28° 10'
28°
M 40
M 38
M 39
M 24
M 37
M 9
M 23
M 61
M 36
M 10
M 35
M 62
M 34
M 22
M 25
M 11
M 26
M 1
M 33
M 21
M 7
M 65
M 12
M 50
M 13
M 20
M 19
Carlos Bay
M 6
M 28
M 15
M 5
M 31
M 60
M 32
M 16
M 29
M 64
M 3
M 17
M 30
M 2
M 42
ST JOSEPH
ISLAND
MATAGORDA ISLAND
GULF OF MEXICO
M 44
Cedar Bayou
M 47
0
1/2
1
2
3
Statute Miles
96° 50'

AREA	Average percent				
	Black Opaques	Hornblende	Tourmaline	Epidote	Others
▤	32	42	9	9	8
▧	37	35	10	10	8
▥	46	32	7	6	9
▨	56	11	22	5	6

FIG. 2.—Map of Mesquite Bay showing sample locations and areas where the relative amounts of heavy minerals are statistically homogeneous.

TABLE 3.—*Summary of mineralogical data from Mesquite Bay including some size distribution measurements*

Samples in each area		Average % of Common Heavy Minerals					χ^2	Av. No. Grains Counted per Slide	Average Value		Average %		
		Range of Values					P		Range of Values		Range of Values		
	Total No.	Black opaques	Horn-blende	Tour-maline	Epidote	Others		Range	Mdϕ	$\sigma\phi$	Sand	Silt	Clay
M2A, 6A, 7A, 15, 16A, 17A, 19A, 20A, 23A, 42A		32	42	9	9	8	$\chi^2=31.64$	320	3.65	3.57	51	14	25
	10	29–35	38–45	8–10	6–12	6–10	$P \neq 0.80$	214–377	3.23–4.08	2.93–4.10	50–74	6–21	18–40
M5, 13, 21, 22, 26A, 28A, 29A, 30A, 32A, 33A, 34A, 35A, 50A, 64A, 65A		37	35	10	10	8	$\chi^2=45.41$	310	3.62	3.47	63	14	23
	15	34–41	30–39	8–13	9–12	5–10	$P \neq 0.85$	250–354	3.34–3.83	1.96–4.55	54–72	6–21	10–31
M3A, 10A, 11A, 12A, 31A		46	32	7	6	9	$\chi^2=18.52$	381	3.65	3.45	62	13	25
	5	42–50	29–36	5–9	5–7	8–10	$P \neq 0.30$	318–465	3.32–4.06	2.40–4.35	49–68	9–19	15–33
M9A, 37A, 38A, 39A, 40A, 61A		56	11	22	5	6	$\chi^2=22.24$	353	3.40	1.84	74	12	14
	6	52–62	9–12	20–25	4–7	4–7	$P \neq 0.30$	295–457	3.22–3.55	0.45–3.96	60–88	9–18	3–22

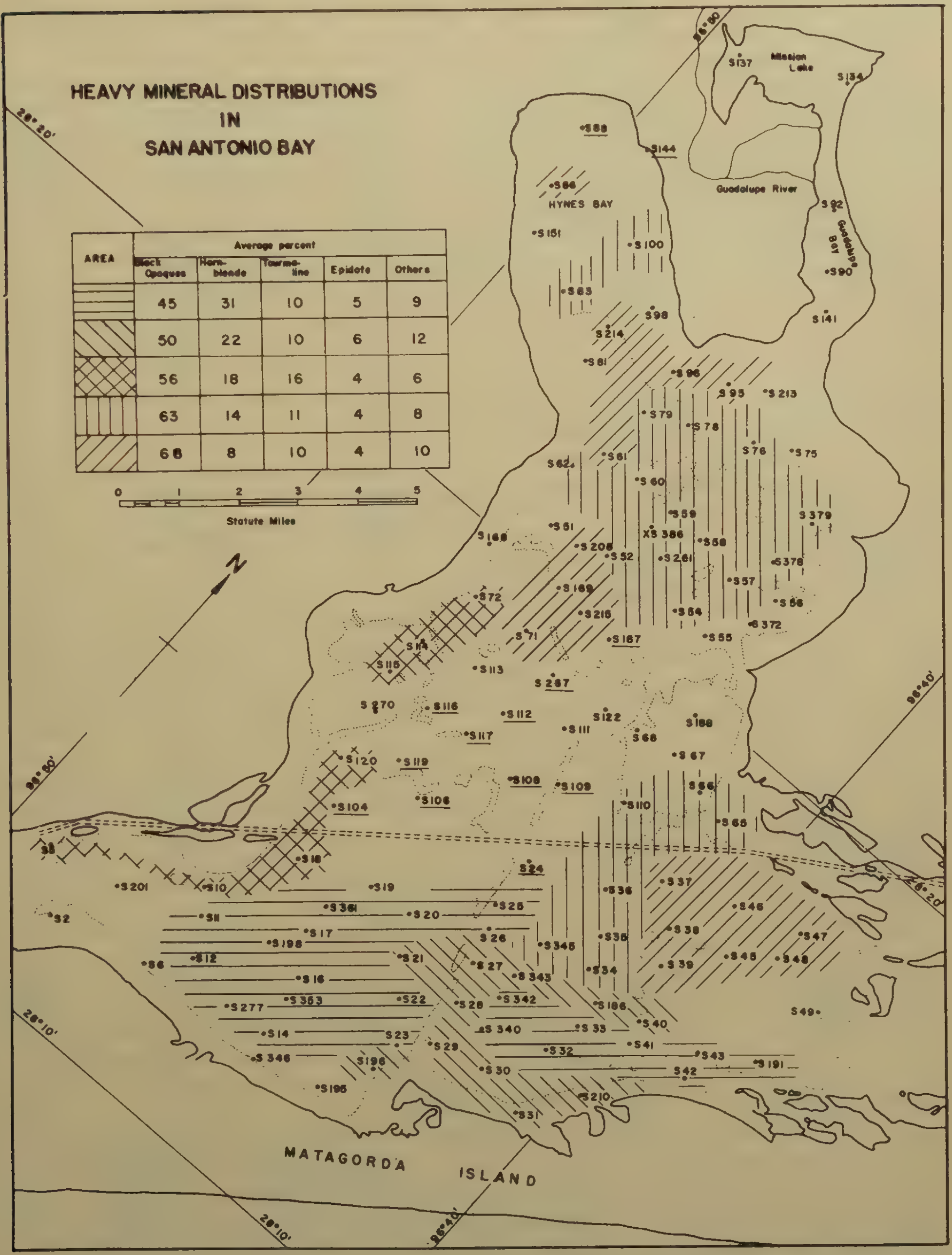
HEAVY MINERAL DISTRIBUTIONS
IN
SAN ANTONIO BAY
0 1 2 3 4 5
Statute Miles
N
28°30'
28°20'
96°30'
96°40'
28°10'
Mission Lake
Guadalupe River
Guadalupe Bay
HYNES BAY
MATAGORDA ISLAND
S137
S134
S144
S92
S90
S141
S100
S151
S63
S98
S214
S81
S96
S95
S213
S79
S78
S76
S75
S62
S61
S60
S59
S379
S386
S58
S261
S378
S57
S56
S54
S372
S55
S168
S51
S208
S52
S169
S216
S187
S72
S71
S114
S115
S113
S267
S270
S116
S112
S122
S111
S188
S68
S117
S67
S120
S119
S108
S109
S106
S66
S104
S110
S65
S18
S24
S37
S1
S201
S10
S19
S36
S2
S11
S361
S20
S25
S46
S17
S198
S26
S345
S35
S38
S47
S6
S12
S21
S27
S343
S34
S45
S48
S39
S16
S277
S353
S22
S28
S342
S186
S40
S49
S14
S23
S29
S340
S33
S41
S43
S346
S196
S32
S30
S42
S191
S195
S210
S31

AREA	Average percent				
	Black Opaques	Hornblende	Tourmaline	Epidote	Others
▤	45	31	10	5	9
▧	50	22	10	6	12
▦	56	18	16	4	6
▥	63	14	11	4	8
▨	68	8	10	4	10

FIG. 3.—Map of San Antonio Bay showing sample locations and areas where the relative amounts of heavy minerals are statistically homogeneous. Sample locations are underlined where the samples contain less than 150 heavy mineral grains and therefore were not used in this study.

TABLE 4.—*Summary of mineralogical data from San Antonio Bay including some size distribution measurements*

Samples in each area		Average % of Common Heavy Minerals					χ^2	Av. No. Grains Counted per Slide	Average Value[1]		Average %[1]		
		Range of Value							Range of Values		Range of Values		
	Total No.	Black opaques	Hornblende	Tourmaline	Epidote	Others	P	Range	Mdϕ	$\sigma\phi$	Sand	Silt	Clay
S11A, 12A, 14A, 16A, 17A, 20A, 22A, 23A, 25A, 26A, 32A, 33A, 41A, 42A, 43A, 191A, 198A, 277B, 340D, 342D, 353D, 361D		45	31	10	5	9	$\chi^2=81.83$	332	4.98	4.00?	36	31	33
	22	40–50	27–38	7–12	4–8	6–12	$P \neq 0.55$	274–418	3.45– 8.30	2.03–5.84?	12–68	10–53	16–52
S21A, 27A, 28A, 29A, 30A, 31A, 40A, 186A, 196A, 210B, 343D		50	22	10	6	12	$\chi^2=27.95$	345	4.05?	3.78?	56?	20?	24?
	11	47–54	18–26	9–13	4–8	10–13	$P \neq 0.90$	265–483	3.15– 5.55	0.27–7.89?	32–91	4–27	0–41
S5A, 10A, 18A, 72A, 114A, 115A, 120A		56	18	16	4	6	$\chi^2=34.28$	374	5.44	3.45?	36	29	35
	7	51–61	15–21	13–21	2–5	5–8	$P \neq 0.10$	297–443	3.18– 9.75	0.72–5.40?	6–82	5–55	12–60
S34A, 35A, 36A, 52A, 54A, 57A, 58A, 59A, 60A, 62A, 65A, 66A, 76A, 78A, 79A, 83A, 100A, 110A, 261B, 345D, 378D, 379D, XS386		63	14	11	4	8	$\chi^2=80.30$	319	6.76?	4.06?	27	32	41
	23	57–68	11–19	8–13	2–6	5–10	$P \neq 0.70$	164–418	3.13–10.53?	1.02–6.47?	3–70	18–47	11–74
S37A, 38A, 39A, 45A, 46A, 47A, 48A, 61A, 71A, 86A, 95A, 96A, 169A, 208B, 214B, 215B		68	8	10	4	10	$\chi^2=60.49$	367	6.83?	4.48?	26	33	41
	16	63–72	6–10	8–13	2–5	8–13	$P \neq 0.45$	265–528	356–10.92?	0.96–5.53?	7–71	16–51	13–65

---

[1] Averages follows by ? include some values determined by extrapolation of the cumulative curves.

and Moore, 1955, p. 1469 and 1484). Nevertheless, San Antonio Bay can be divided mineralogically into five main areas (fig. 3). Although there were 121 samples analyzed from San Antonio Bay only 84 could be fitted into homogeneous groups, and two of these groups consisted of small areas of homogeneous mineralogy containing two (S90 and S141 in Guadalupe Bay) and three (S55, S56, and S372) samples respectively which were not delineated in figure 3 because of their small extent. These two areas have an extremely low hornblende content, two to four percent. The region in the center of the bay consists principally of very clayey sediments which contain few heavy minerals. There were 13 samples whose total heavy mineral content was 150 grains or less. These samples were not used in this study. Twenty-four samples remained that could not be fitted into homogeneous groups. Determining the causes of this is beyond the scope of this paper.

Since the Guadalupe River carries no hornblende (Bullard, 1942, table 1, p. 1026; also checked by the writer), the source of this mineral is from the barrier islands (av. 35% hornblende) and the Pleistocene (?) cliffs (av. 20% hornblende) fringing the bay. Therefore, the areas of highest hornblende are located in the lower part of San Antonio Bay near the barrier islands. There are two areas of high hornblende (31%) located at the southern end of the bay (fig. 3), separated by a region with a slightly lower hornblende content (22%). Along the western side of the bay is a long narrow zone containing 18% hornblende, and having a higher tourmaline content (16%) than any other area of San Antonio Bay. Northward in the bay are areas containing much smaller amounts of hornblende, 8 and 14%. The regions with the lowest hornblende (8%) consist of an area in the lower bay and two small areas in the upper part of the bay, north of the clay and oyster reef region. The areas with a slightly higher hornblende content (14%) are located in the upper bay north of the clayey sediments, and also in the lower bay. The mineralogical information is summarized in table 4, including the average median diameter, sorting, and percentages of sand, silt, and clay. In San Antonio Bay there was no simple relationship between the heavy minerals and grain size distribution as was found in Mesquite Bay.

SUMMARY

A statistical method, the chi-square test, was used to compare heavy mineral samples. By means of this test it was possible to delineate statistically homogeneous heavy mineral areas in Mesquite and San Antonio bays. In Mesquite Bay, which has simple bottom topography and sediment types, the grain size distribution of the sediments could be correlated with their (relative) heavy mineral content; i. e., the sediments that were high in tourmaline and low in hornblende were coarser and better sorted than the high hornblende sediments of the bay. There was no such simple relationship in San Antonio Bay which has more complex sediment types and bottom topography. The hornblende distribution showed that some of the sand-size material of both Mesquite and San Antonio bays was derived from the barrier islands and carried into the bays by wind and overwash.

ACKNOWLEDGMENTS

The writer expresses his appreciation to Tj. H. van Andel and F. P. Shepard for their suggestions and careful reading of the manuscript.

REFERENCES

Andel, Tj. H. van, 1950, Provenance, transport and deposition of Rhine sediments: H. Veenman and Zonen, Wageningen, 129 p.

———, 1955, The sediments of the Rhone delta. II Sources and deposition of heavy minerals: Verh. Kon. Nederl. Geol. Mijnbouwk Gen., v. 15, p. 515–543.

Bullard, F. M., 1942, Source of beach and river sands on the Gulf Coast of Texas: Geol. Soc. America Bull., v. 53, p. 1021–1044.

Dixon, W. J., and Massey, F. J., Jr., 1951, Introduction to statistical analysis. McGraw-Hill Book Co., Inc., New York, 370 p.

Dryden, A. L., Jr., 1931, Accuracy in percentage representation of heavy mineral frequencies: Nat. Acad. Sci. Proc., v. 17, p. 233–238.

———, 1935, A statistical method for the comparison of heavy mineral suites: Am. Jour. Sci., 5th ser., v. 29, p. 393–408.

EISENHART, C., 1935a, A note on "A statistical method for the comparison of heavy mineral suites": Am. Jour. Sci. 5th ser., v. 30, p. 549–553.

———, 1935b, A test for the significance of lithological variations: Jour. Sedimentary Petrology, v. 5, p. 137–145.

FISHER, R. A., 1950, Statistical methods for research workers. 11th rev. ed., Oliver and Boyd, Ltd., Edinburgh, 354 p.

FISHER, R. A., AND YATES, F., 1949, Statistical tables. Hafner Publishing Co., Inc., New York, 112 p.

HAWKES, L., AND SMYTHE, J. A., 1931, Garnet-bearing sands of the Northumberland coast: Geol. Mag., v. 68, p. 345–361.

INMAN, D. L., 1952, Measures for describing the size distribution of sediments: Jour. Sedimentary Petrology, v. 22, p. 125–145.

KRUMBEIN, W. C., AND PETTIJOHN, F. J., 1938, Manual of sedimentary petrology. D. Appleton-Century Co., Inc., New York, 549 p.

KRUMBEIN, W. C., AND RASMUSSEN, W. C., 1941, The probable error of sampling beach sand for heavy mineral analysis: Jour. Sedimentary Petrology, v. 11, p. 10–20.

MANNING, J. C., 1953, Application of statistical estimation and hypothesis testing to geologic data: Jour. Geology, v. 61, p. 544–556.

SHEPARD, F. P., AND MOORE, D. G., 1955, Central Texas coast sedimentation: characteristics of sedimentary environments, recent history and diagenesis: Am. Assoc. Petroleum Geologists Bull., v. 39, p. 1463–1593.

SNEDECOR, G. W., 1946, Statistical methods. 4th Edition, Iowa State College Press, Ames, Iowa, 485 p.

Reprinted from LIMNOLOGY AND OCEANOGRAPHY
Vol. 3, No. 2, April, 1958
Printed in U.S.A.

A Comparison of Drogue and GEK Measurements in Deep Water[1]

JOSEPH L. REID, JR.

University of California, Scripps Institution of Oceanography, La Jolla, California

ABSTRACT

Two series of current measurements made with GEK and drogues are shown to agree closely, not only in the averaged results of three days' data, but in short-period variations about the mean. The variations measured are probably too large to be the ordinary tide, and the possibility of their being the orbital velocities of internal waves is discussed.

INTRODUCTION

The GEK (Geomagnetic Electrokinetograph, von Arx 1950) has been used extensively in studying the California Current. The accuracy of an average of GEK measurements over several hours in weak currents has been discussed (Knauss and Reid 1957). The validity of individual GEK measurements in a weak current system with large fluctuations in velocity has yet to be demonstrated in deep water. Von Arx (1950) has compared serial GEK measurements in the shallow water of Georges Bank with predicted tidal currents. He has used the results to estimate the effect of the conductivity of the bottom in measurements of shallow currents which extend to the bottom. Vaux (1955) has continued this work in the English Channel, comparing his GEK measurements with The Admiralty Tidal Stream data and the set of the ship as determined by the Decca Navigator system. He has derived a correction factor for use in that particular shallow (30 m) area of the English Channel, but notes that further work is needed in the velocity range below one knot.

The currents off California are slow, rarely exceeding a knot. Most of the GEK measurements fall below 30 cm/sec. Such currents are difficult to measure by GEK and not easy by any other means. The author has tried at various times to compare the results of dynamic height computations in this region with the drift of drogues. On several of these occasions the GEK has been used. It is the results of one of these attempts which allow the drogue and GEK results to be compared in total drift and variation about the mean.

THE DATA

In January of 1952 a drogue was put out in the deep water between Santa Catalina and San Clemente Islands, off California (Fig. 1), and followed for about 66 hours, at which time it was close to Catalina and its movement had almost stopped. It was recovered and set out again and followed for about 69 hours. During the tracking, GEK measurements were made around the drogue, and frequent fixes were made of its position both by bearings on the islands and by radar ranges. From their successive changes one would estimate the greatest inaccuracy of the positions to be about a quarter mile when the drogue was between the islands and about a half mile as it moved south of San Clemente Island (Figs. 2 and 3). The drogue consisted of an 8 × 8 feet biplane of canvas on a metal frame suspended below a float. The float reached about 8 inches above the water. A light

---

[1] Contribution from the Scripps Institution of Oceanography, New Series No. 993.

This paper represents one of the results of research conducted under the Marine Life Research Program, the Scripps Institution's component of the California Cooperative Oceanic Fisheries Investigations, a project sponsored by the Marine Research Committee of the State of California.

The author is indebted to Mr. James Snodgrass for a device for maintaining contact with the drogue and measuring its distance from the vessel, and to Captain E. E. Mitchell and the crew of the California Division of Fish and Game vessel YELLOWFIN, aboard which this work was done.

Reproduced by Permission

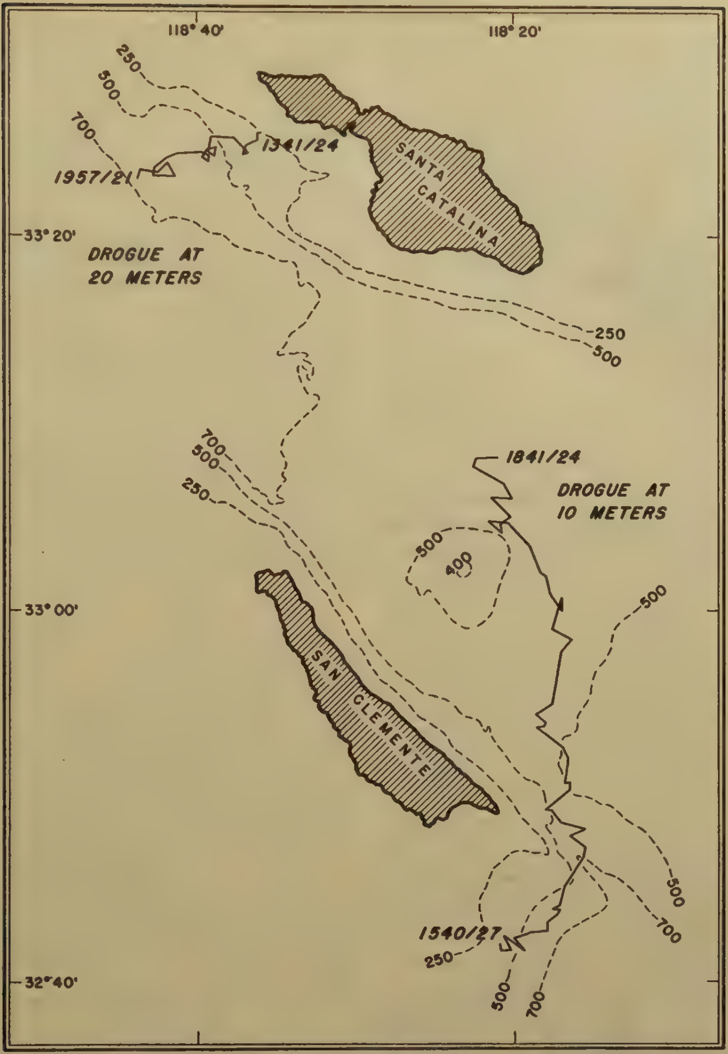
118° 40'
118° 20'
33° 20'
33° 00'
32° 40'
SANTA CATALINA
SAN CLEMENTE
DROGUE AT 20 METERS
DROGUE AT 10 METERS
1957/21
1341/24
1841/24
1540/27
250
500
700
400

FIG. 1. Trajectories of drogues, January 1952.

on a slender bamboo pole reached 6 feet above the float. Flags and radar targets were omitted to reduce wind effect.

The two observed drogue trajectories and the trajectories obtained by integrating the GEK measurements are shown by Figures 2 and 3. The depth of the thermocline and the east component of the current measured by the GEK are shown by Figure 4. In the first series there was a fairly readable thermocline. In the second the thermocline was hard to locate and the bathythermograph instrument began to give erratic surface values. The second set of thermocline measurements may be seriously in error and will not be discussed further.

THE RESULTS

The velocities measured by the GEK were corrected for the electrode-droop (Knauss and Reid 1957) and compared with the movement of the drogue. In the first case the drogue moved with an average velocity of 5.7 cm/sec, while the average of the GEK

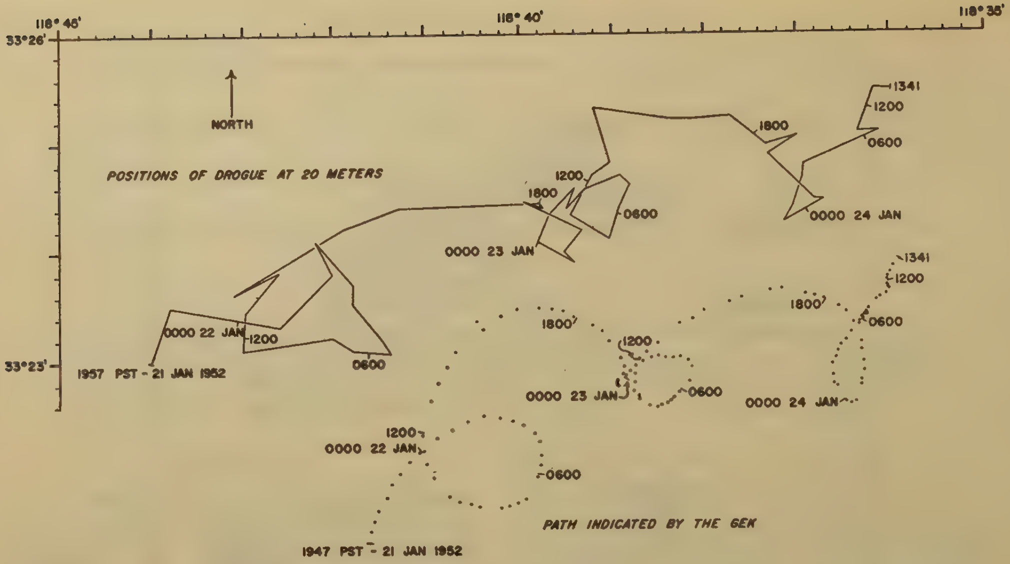
118° 45'
118° 40'
118° 35'
33°26'
33°23'
NORTH
POSITIONS OF DROGUE AT 20 METERS
1957 PST - 21 JAN 1952
0000 22 JAN
1200
0600
1800
1200
0000 23 JAN
0600
1800
0000 24 JAN
0600
1200
1341
1800
1200
0000 23 JAN
0600
1800
0000 24 JAN
0600
1200
1341
1200
0000 22 JAN
0600
PATH INDICATED BY THE GEK
1947 PST - 21 JAN 1952

FIG. 2. Trajectory of drogue near Santa Catalina Island and path indicated by the integrated GEK measurements of velocity. (Starting points offset to avoid overlap.)

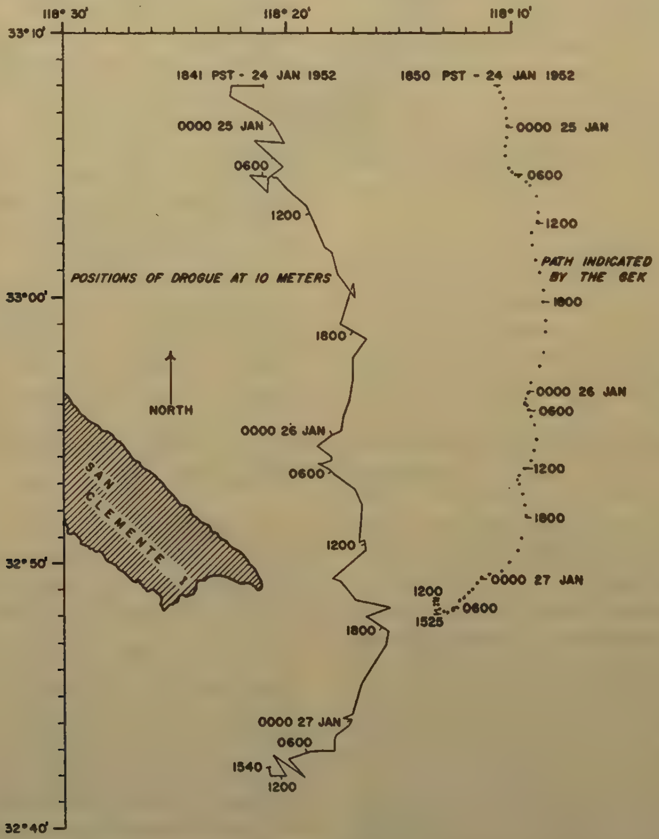
118° 30'
118° 20'
118° 10'
33°10'
33°00'
32°50'
32°40'
1841 PST - 24 JAN 1952
0000 25 JAN
0600
1200
POSITIONS OF DROGUE AT 10 METERS
1800
NORTH
0000 26 JAN
0600
1200
1800
0000 27 JAN
0600
1540
1200
SAN CLEMENTE I
1850 PST - 24 JAN 1952
0000 25 JAN
0600
1200
PATH INDICATED BY THE GEK
1800
0000 26 JAN
0600
1200
1800
0000 27 JAN
1200
0600
1525

FIG. 3. Trajectory of drogue near San Clemente Island and path indicated by the integrated GEK measurements of velocity. (Starting points offset to avoid overlap.)

measurements was 4.1 cm/sec. In the second case the drogue's average velocity was 19.3 cm/sec, while the GEK averaged 14.6 cm/sec.

The principal result of these measurements is that the GEK measurements are shown to agree closely with the drogue movement. This is true not only in total drift but in the time variations about the mean (Figs. 2, 3). On previous trials of short time-series (24 hours) with the GEK, fluctuations of the order of 12-hour period and 10 to 20 cm/sec amplitude had been seen, but it was not possible from such scanty data to call these tidal fluctuations nor even accept them as real motion. (Longuet-Higgins *et al.*, 1954, state that the natural earth-current potentials associated with geomagnetic disturbances which have been observed on land may result in a daily variation of perhaps ¼ knot if they obtain in the ocean also.)

Longer series of bathythermograph measurements (6 days) had shown semidiurnal internal waves in the region (Reid 1956). Therefore the depth of thermocline was compared (Fig. 4) with the height of tide at the coast, and the east component of current (GEK) with the rate of change of the tidal height (as a rough indication of the shape of the tidal transport current).

The two series are not long enough to confirm the tidal periodicities, but the segments show enough similarity to justify the hypothesis that they are there. (The inertial period at this latitude is 22 hours, and of course cannot be distinguished from a diurnal tide in these few data. It is the semidiurnal part which we shall discuss.) Remembering that these are not measurements made at one position but following a drogue in water of varying depth (and, in the first case, up against a barrier), a central section of 24 hours has been chosen for analysis. The 24-hourly running mean has been subtracted from the GEK data and the latitude and longitude measurements. Then curves of 24- and 12-hour periods were fitted to the north and east components of the GEK, the positions north and east, and the depth of the thermocline. (Since the variations of latitude and longitude will be the integral of the velocity components, the positions have been analysed accordingly to compare with the GEK results.) The results of analysis of the 24 hours beginning 1400 PST 22 January 1952 are given in Table 1.

Comparing the results from drogue and GEK, the differences in amplitudes (especially in the semidiurnal) are not significant. This was to be expected from Figures 2 and 3.

The likelihood that these are tidal fluctuations can be tested in certain ways for obvious contradications. As models one can take the simple cases of one- and two-layer systems.

I. *The one-layer system.* If the observed oscillation in the current is the tide, the

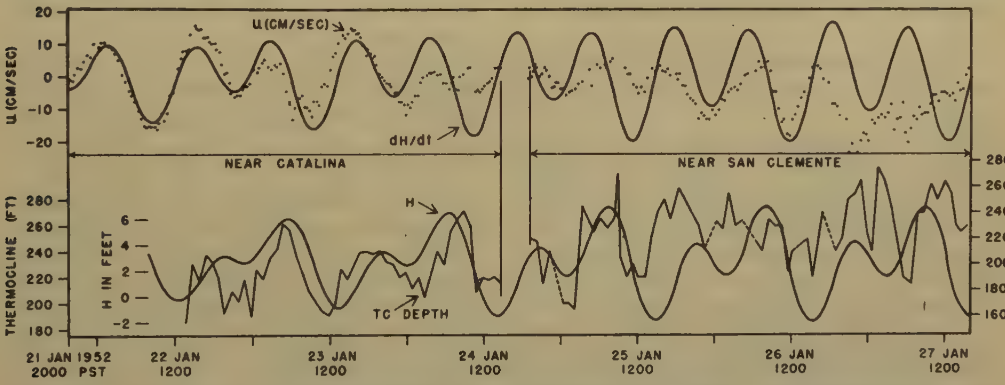

FIG. 4. Height of tide at coast (*H*), depth of thermocline (*TC* depth), east component of velocity measured by GEK (*u*), and rate of tidal rise (*dH/dt*). Scale for *dH/dt* is arbitrary and not shown.

TABLE 1. *Results of diurnal and semidiurnal analysis of 24 hours of data beginning 1400 PST 22 January 1952*

	Data	Diurnal		Semidiurnal	
		Amplitude cm/sec	Phase	Amplitude cm/sec	Phase
GEK	North component	4.5	114°	7.8	120°
	East component	6.8	39°	7.8	44°
Drogue	North component	3.3	107°	6.6	99°
	East component	11.1	39°	8.8	17°
	Depth of thermocline	3.1m	62°	6.4m	185°

water should move in its forward cycle a distance of

$$S_1 = \int_{-\pi/2m}^{\pi/2m} u \cos mt \, dt = \frac{2u}{m},$$

where u is the amplitude of the onshore current and m the frequency. If the current extends to the bottom in depth h, then the resulting rise in the height of the tide S_2 will be given by

$$S_1 h = S_2 l,$$

where l is the distance to the mainland. Using the observed value for the semidiurnal wave, $u = 7$ cm/sec, $m = 2\pi/12$ hr, $h = 1$ km, and $l = 60$ km. Total forward movement would be 1 km, and the rise in tide would be 17 m, which is about ten times too large.

Thus the currents either do not extend to the bottom or else do not obtain over a large area.

Since the oscillations were shown by the GEK as well as the drogue, a qualitative treatment by Longuet-Higgins *et al.* (1954) shows that either the velocity varies with depth or the "conductivity" of the sea bed is high. If the stream extends uniformly to the bottom, is long and straight, and the "conductivity" of the sea bed is low, the towed electrodes will record no signal. If the "conductivity" is high then the potential gradient is small and the current density at the sea surface (which is measured by the towed electrodes) will depend only upon the surface velocity. If the "conductivity" is high, $\frac{\rho D}{\rho' h} \gg 1$, where ρ and ρ' are the resistivity of the water and the sea bed, respectively, h the depth, and D the width of the current. Taking $\rho = 25$ and $\rho' = 2 \times 10^4$ ohm-cm, $h = 1$ km, $D \gg \frac{\rho' h}{\rho}$, or 800 km. This is perhaps the right order for a tidal wave, but the velocities have already been shown to be too high. The GEK disposes, in addition, of the possibility that the current extends to the bottom but is narrow.

II. *The two-layer system.* A very interesting possibility is that these currents are the orbital velocities of internal waves of tidal period. The data can be inserted in the two equations

$$c^2 = \left(\frac{\omega^2}{\omega^2 - \lambda^2}\right)\left(\frac{gh'h''}{h' + h''}\right)\left(1 - \frac{\rho'}{\rho''}\right),$$

and

$$u = \frac{-c\zeta}{h'},$$

where c is the phase velocity, u the amplitude of orbital velocity, ω the frequency, λ the Coriolis term, g the gravity term, h' and h'' the thickness of upper and lower layers, respectively, ρ' and ρ'' the density in upper and lower layers, respectively, and ζ the amplitude of rise and fall of interface. The first is the expression for an internal wave in a two-layer system on a rotating earth (Haurwitz 1950). The second derives from continuity. From the measured quantities, assuming a semidiurnal wave, u is 7.8 cm/sec, h' and h'' are 69 and 1000 m, $(1 - \frac{\rho'}{\rho''})$ is 4×10^{-3} (taking ρ'' as the mean density below the thermocline), and ζ is 6.4 m.

The first equation gives $c = 1.6$ m/sec and the second gives 0.84 m/sec. These are at least of the same order when the limitations of measurement and of the two-layer system are considered.

Longuet-Higgins *et al.* (1954) show qualitatively that if the velocity varies with depth and the "conductivity" is high, the electrodes will measure a current density which depends only upon surface current. If the values of phase velocity computed in the preceding paragraph are of the right order then $D \ll 800$ km, and the "conductivity" is almost certain to be low.

If the "conductivity" is low the towed electrodes will measure (approximately) the difference between the surface velocity and the mean velocity. In a two-layer system $u_1 h_1 = u_2 h_2$, where u_1, u_2 and h_1, h_2 are the velocities and depths of the upper and lower layers, respectively. Taking h_1 and h_2 as 69 and 1000 m

$$u_1 - u_2 = u_1\left(1 - \frac{h_1}{h_2}\right) \sim u_1$$

and the signal measured by the electrodes depends almost entirely upon the surface current.

CONCLUSION

A close agreement has been found between individual GEK measurements and the movement of a drogue in a system whose velocity varied with time. Variations of a similar order had been shown in the California Current by the GEK. Because of the possibility that these variations were geomagnetic disturbances rather than water motion, the measurements described in this paper were made. The results imply that the variations represent real water motion. In the California Current the variations in surface velocity are of the same order of magnitude as the mean.

In these data the time variation of current strongly resembles the tide. The observed current was too strong to be the orbital velocity of a wave extending to the bottom over a large area. But the GEK will not measure a current extending to the bottom which does not cover a large area. Therefore the current measured at the surface did not extend to the bottom.

In the equations of a semidiurnal internal wave phase, velocity can be computed both from the density distribution and from the observed motion at the surface and the interface. The observed quantities give results which are not contradictory.

REFERENCES

HAURWITZ, BERNHARD. 1950. Internal waves of tidal character. Trans. Amer. Geophys. Union, **31**: 47–52.

KNAUSS, J. AND J. L. REID, JR. 1957. The effects of cable design on the accuracy of the GEK. Trans. Amer. Geophys. Union, **38**(3): 320–325.

LONGUET-HIGGINS, M. S., M. E. STERN, AND H. STROMMEL. 1954. The electrical field induced by ocean currents and waves with application to the method of towed electrodes. Pap. Phys. Oceanogr. Meteor., MIT, Woods Hole Oceanogr. Inst., **13**(1): 1–37.

REID, J. L. JR. 1956. Observations of internal tides in October 1950. Trans. Amer. Geophys. Union, **37**(3): 278–286.

VAUX, DAVID. 1955. Current measuring in shallow waters by towed electrodes. J. Mar. Res., **14**(2): 187–194.

VON ARX, W. S. 1950. An electromagnetic method for measuring the velocities of ocean currents from a ship under way. Pap. Phys. Oceanogr. Meteor., MIT, Woods Hole Oceanogr. Inst., **11**(3): 1–62.

(232)

ORIGIN AND CLASSIFICATION OF CRETACEOUS, PALEOCENE, AND EOCENE SANDSTONES OF WESTERN VENEZUELA

BY

TJEERD H. VAN ANDEL

Reprinted for private circulation from
The Bulletin of the American Association of Petroleum Geologists
Vol. 42, No. 4, April, 1958

(233)

BULLETIN OF THE AMERICAN ASSOCIATION OF PETROLEUM GEOLOGISTS
VOL. 42, NO. 4 (APRIL, 1958), PP. 734-763, 13 FIGS.

ORIGIN AND CLASSIFICATION OF CRETACEOUS, PALEOCENE, AND EOCENE SANDSTONES OF WESTERN VENEZUELA[1]

TJEERD H. VAN ANDEL[2]
La Jolla, California

ABSTRACT

In western Venezuela the tectonics, facies, and paleogeography of the Cretaceous, Paleocene, and Eocene are relatively well known. A study of the sandstones of these series affords a good case history to test some of the modern concepts in sandstone petrography such as tectonic control of sandstone properties and textural and mineralogical maturity. In this case sandstone mineralogy and mineralogical maturity are functions of source area petrography, weathering, and erosion. Textural maturity on the other hand is related to environments in the depositional basin. No fixed relation between tectofacies and depositional environments seems to be present. Consequently sandstone properties do not appear to depend to any great extent on the tectofacies in the basin. The observations suggest caution in applying to the field of sandstone genetics and sandstone classification general concepts as for example the idea of tectonic control of sandstone petrography.

INTRODUCTION

In recent years the description and classification of sedimentary rocks, and of sandstones in particular, have been widely discussed. Several ideas have evolved from these discussions which have influenced modern geological thinking. Examples of this are the concepts of tectonic control of sediment properties, and sediment maturity. However, widespread disagreement on the essential points of classification and sediment genesis is a conspicuous feature of the literature on this subject. It seems that an overly theoretical approach and an absence of a sufficiently large volume of observations are partly responsible for this unfortunate state of affairs.

A classification of sediments may be designed either to convey a clear descriptive picture of the rock in question or to bring out its genesis and genetical relations with other rocks (Rodgers, 1950). The second type of classification is based on descriptive elements of genetical value, but little agreement exists on the choice of such elements. As Pettijohn (1948) points out, three main groups of factors control the genesis of sedimentary rocks: (a) the materials and processes of the source area, (b) the processes of transportation and deposition combined with the physiographic and tectonic conditions in the depositional area, and (c) the post-depositional diagenetic processes. Consequently a genetic classification encompassing all possible effects and their combinations must be large and complicated. The classifications proposed thus far are mainly of the genetic type, but are generally based on only one or a few of the groups of controlling factors.

---

[1] Contribution from the Scripps Institution of Oceanography, New Series No. 994. Manuscript received, September 5, 1957.

[2] Scripps Institution of Oceanography, University of California.

Cia. Shell de Venezuela has granted permission to publish this paper and to make use in its preparation of certain data to which the writer had access during his service with Cia. Shell de Venezuela, but the opinions expressed and conclusions reached are solely those of the writer.

The writer expresses his thanks to W. O. Gigon, K. Habicht, W. A. Mohler, J. Muller, and O. Renz for their assistance during the investigation, and to H. W. Menard, G. A. Rusnak, and F. P. Shepard.

(234)

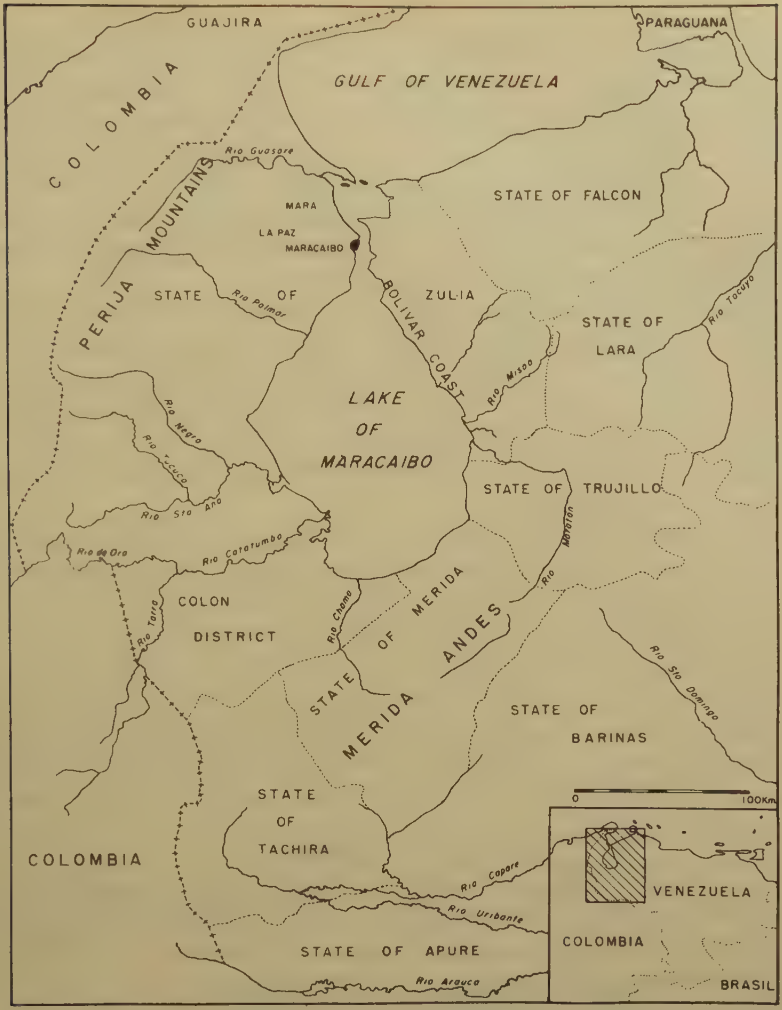
GUAJIRA
PARAGUANA
GULF OF VENEZUELA
COLOMBIA
Rio Guasare
PERIJA MOUNTAINS
MARA
LA PAZ
MARACAIBO
STATE OF FALCON
STATE OF ZULIA
Rio Palmar
BOLIVAR COAST
STATE OF LARA
Rio Tocuyo
Rio Misoa
LAKE OF MARACAIBO
Rio Negro
Rio Tucuco
Rio Sta Ana
STATE OF TRUJILLO
Rio Motatan
Rio de Oro
Rio Catatumbo
Rio Tarra
COLON DISTRICT
Rio Chama
STATE OF MERIDA
MERIDA ANDES
Rio Sto Domingo
STATE OF BARINAS
0
100Km
STATE OF TACHIRA
COLOMBIA
Rio Caparo
Rio Uribante
STATE OF APURE
Rio Arauca
VENEZUELA
COLOMBIA
BRASIL

FIG. 1.—Map of western Venezuela with place names mentioned in text.

Since the origin of many sedimentary rocks is a matter of conjecture, theoretical concepts have frequently been called upon to provide the basis for sediment genetics. At times one can hardly escape the feeling that the theory of sandstone formation has been emphasized at the expense of the study of the sandstones themselves. It is not the present intention to review and discuss extensively the voluminous literature on the subject; however, some important papers are listed at the end of this article.

It is evident that sandstone studies from areas where the depositional and tectonic history is well known would assist in clarifying some of these problems.

Recently the writer has had an opportunity to study a great many sandstone samples (more than 2,000) from the Cretaceous, Paleocene, and Eocene of western Venezuela. As a result of many modern and excellent publications and the unpublished work of numerous petroleum geologists, the depositional history of this basin is relatively well known. The basin, though not overly complicated tectonically, comprises a rather complete series of tectofacies, a varied set of depositional environments ranging from continental to deep marine, and several source areas of widely divergent character. It presents an interesting example of sediment variation under a wide range of conditions.

It is the writer's intention to present a descriptive case history of sandstone sources and deposition in western Venezuela, and to use the case history to test some basic concepts. It is not the purpose of the paper, however, to develop concepts of sediment genetics of general applicability beyond the limits of the basin of western Venezuela. Nevertheless, and notwithstanding the regional limitations, an examination of the observations may throw some light on the validity of various basic concepts.

The investigation has been restricted to sandstones, partly because of their accessibility to analysis, and partly because much of the discussion on sediment genetics and sediment classification has been built around them. As a consequence it bears only on part of the problem of sediment genetics.

The petrological part of the paper is preceded by a synopsis of the tectonic and depositional history of western Venezuela during the Cretaceous, Paleocene, and Eocene. This synopsis has been based essentially on published papers by various authors but to a certain extent also on the unpublished work of Shell geologists too numerous to mention here separately. To them the writer is deeply in debt.

METHODS OF INVESTIGATION

The investigation has been based on a study of thin sections of sandstone samples. Sandy shales and limestones have not been investigated. Many of the samples were too strongly compacted or too well cemented by silica to permit more than a microscopical investigation of thin sections.

Originally the study was designed as an investigation of sediment sources. Therefore the emphasis has been on the composition of the terrigenous fraction. An estimate of the mineralogical composition was obtained by identifying and counting 100 terrigenous grains of sand size by means of a point counter. Components recognized were quartz, the feldspars, detrital chert, and rock fragments. The presence of micas was noted, but since this flaky mineral is subject to laws of settling quite different from those controlling the deposition of the other particles, a count of micas has no great significance for a study of sand sources. Various kinds of rock fragments have been recognized; predominantly shales, fine-grained and commonly quartzitic sandstones, and low-grade metamorphic fragments. No quantitative analysis has been made of the rock fragments, however, because generally the identification of the large majority was too uncertain.

Both basic and acid feldspars, the latter predominantly orthoclase, microcline, and oligoclase, have been observed. Basic feldspars are rare and a reconnaissance study has shown that in this case feldspar ratios had no diagnostic value for source studies. Some detrital chert is difficult to recognize, especially in very fine-grained sands and in sandstones that are strongly compacted or well cemented by silica. Many chert percentages are therefore approximations.

A certain correlation of grain size and mineralogical composition has been observed, especially in the coarse-grained sands which have much higher percentages of quartz than the medium- and fine-grained sands associated with them. On the other hand, the identification of minerals and rock fragments in very fine-grained material is difficult and unreliable. Therefore, only the 0.1–0.3-mm. grade has been used for the analysis of mineralogical composition.

Characteristics not directly related to sediment source, as the presence of glauconite and pyrite, the clay content, grain size and sorting, and roundness, have received less attention, and no quantitative study has been made of them. A study of cementation was beyond the scope of the investigation. Sands have been classed as clean when they contained less than 5 per cent of clay, and as muddy when the clay matrix exceeded this figure. In thin sections the degree of sorting is not easily established without elaborate and time-consuming measurements. A simple qualitative subdivision into well, moderately, and poorly sorted sands has been made, which appears to be reasonably consistent. Sorting observations have been based on the entire thin section, not on one size grade as in the mineralogical analysis. A few tests show that the sands called well sorted generally possess Trask sorting coefficients (Trask, 1932) below 2.5, whereas the sorting coefficients of the poorly sorted group exceed 4.0. Average grain size has been noted but the data have not found application in this paper because the horizontal and vertical spacing of the samples is too wide. A study of roundness was made impossible by the predominance of strongly compacted sandstones, many of which exhibited mosaic structures.

STRATIGRAPHY AND GEOLOGICAL HISTORY

For an understanding of the trends and causes of sediment variation in a sequence of deposits, a general knowledge of the depositional and tectonic history of the basin is required. The following synopsis of the geology of western Venezuela during Certaceous, Paleocene, and Eocene time has been taken largely from recent publications by Hedberg and Sass (1937), Sutton (1946), Notestein, Hubman, and Bowler (1946), Schaub (1948), Rod and Maync (1954), Kuyl, Muller, and Waterbolk (1955), Young *et al.* (1956), and Renz (1956). For details on the geological history of the region the reader is referred to the original papers.

The petrographic data are not used here for correlation purposes. Therefore a stratigraphic subdivision at the stage or even stage-group level is sufficient. The stratigraphic framework which is summarized in Figure 2 is based on Kuyl, Muller, and Waterbolk (1955) and Renz (1956). For a convenient presentation

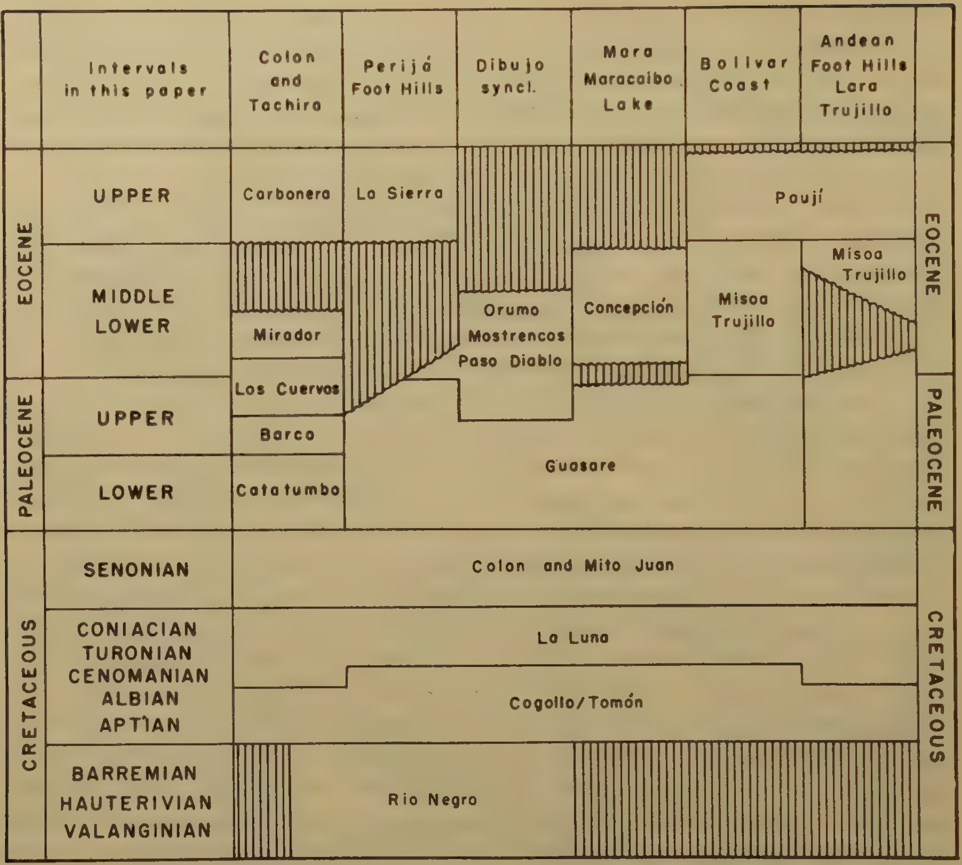
Intervals in this paper
Colon and Tachira
Perijá Foot Hills
Dibujo syncl.
Mara Maracaibo Lake
Bolivar Coast
Andean Foot Hills Lara Trujillo
EOCENE
UPPER
MIDDLE
LOWER
PALEOCENE
UPPER
LOWER
CRETACEOUS
SENONIAN
CONIACIAN
TURONIAN
CENOMANIAN
ALBIAN
APTIAN
BARREMIAN
HAUTERIVIAN
VALANGINIAN
Carbonera
La Sierra
Pauji
Mirador
Misoa Trujillo
Orumo
Mostrencos
Paso Diablo
Concepción
Misoa Trujillo
Los Cuervos
Barco
Catatumbo
Guasare
Colon and Mito Juan
La Luna
Cogollo/Tomón
Rio Negro
EOCENE
PALEOCENE
CRETACEOUS

FIG. 2.—Correlation chart and stratigraphic diagram of Cretaceous, Paleocene, and Eocene in western Venezuela. After Renz (1956) and Kuyl, Muller, and Waterbolk (1955).

of the observations, the Paleocene requires subdivision into an upper and a lower part. The limit between the two parts, as used here, is not sufficiently well established to be considered a stage boundary. However, both pollen studies and electric-log correlation suggest that the deposits taken together in this way are approximately contemporaneous.

Six principal geotectonic elements can be differentiated in the basin during Cretaceous, Paleocene, and Eocene time. Not all of these elements were active at all times and the area occupied by each has changed with time. Three moderately to strongly negative troughs are situated in the western, southwestern, and eastern parts of the basin, approximately at the present positions of the Perijá mountain range, the southwestern part of the Merida Andes, and the mountain ranges of the states of Lara and Falcón. Following Renz they are named the Machiques, Uribante, and Barquisimeto troughs respectively. Although in the first two troughs subsidence has been considerable, there is no evidence for a high degree of tectonism or for volcanic activity. They are properly classed as miogeosynclines. Comparatively little is known about the tectonics and stratigraphy of the Barquisimeto trough, especially in its central and northern parts. Its subsidence far exceeds that of the others, and metamorphic sediments are found. Intra-trough volcanics have been reported. In part and during certain periods of time it may have represented eugeosynclinal conditions.

Between the three troughs, an old and relatively stable or slowly subsiding median mass existed. This is the Maracaibo platform which is connected on the south side with the margin of the stable and largely positive Guayana Shield. West of the basin another positive area is indicated by the petrography of the sediments. It is probably identical with the Cordillera Central of Colombia. Nothing is known about the northern and eastern margins of the basin.

The early Cretaceous and probably pre-Aptian Rio Negro formation represents a period of areally restricted deposition. Sediments of this age are known with certainty only from the Machiques and Uribante troughs. They consist of coarse cross-bedded sandstones, grits, and conglomerates with subordinate claystones, and are probably largely of fluviatile origin. Stratigraphic evidence indicates that both the Maracaibo platform and the Guayana Shield were exposed to weathering and erosion during this time. The Aptian in those areas rests unconformably on granites, gneisses, and pre-Cretaceous sediments belonging to the La Quinta formation (Smith, 1956).

The Cretaceous was strongly transgressive and as early as the Albian, during deposition of the Cogollo-Tomón formation, the Maracaibo platform and a large part of the northern rim of the Guayana Shield were covered by the sea. During the Turonian, Cenomanian, and Coniacian (La Luna formation) and the Senonian (Colón) the transgression continued and at the end of the Senonian the southern shore of the sea was south of the area. The transgression apparently was very gentle, especially during the early part of Cogollo-Tomón time (Aptian), and was not accompanied by much erosion of the underlying pre-Cretaceous. This is shown by the fact that the sandy littoral belts of this period are narrow and the basal conglomerates and sandstones thin. Later, during the Albian (Cogollo-Tomón) a strong influx of sand came from the south, resulting in a broad and thick belt of marine and littoral sandstones (Tomón formation) which reached as far north as the present southern shore of Lake Maracaibo and the Rio Catatumbo. Then sand supply diminished and the La Luna formation (Cenomanian-Turonian-Coniacian) was deposited, consisting almost exclusively of shales, marls, and cherts. Marine sands of this period are restricted to the far south in the states of Táchira and Merida. This phase represents the climax of the Cretaceous transgression.

The Colón formation (Senonian) though still entirely marine, exhibits the first signs of a regressive phase which reached its maximum in the middle Eocene. Sands began spreading again in the southern and southeastern parts of the basin

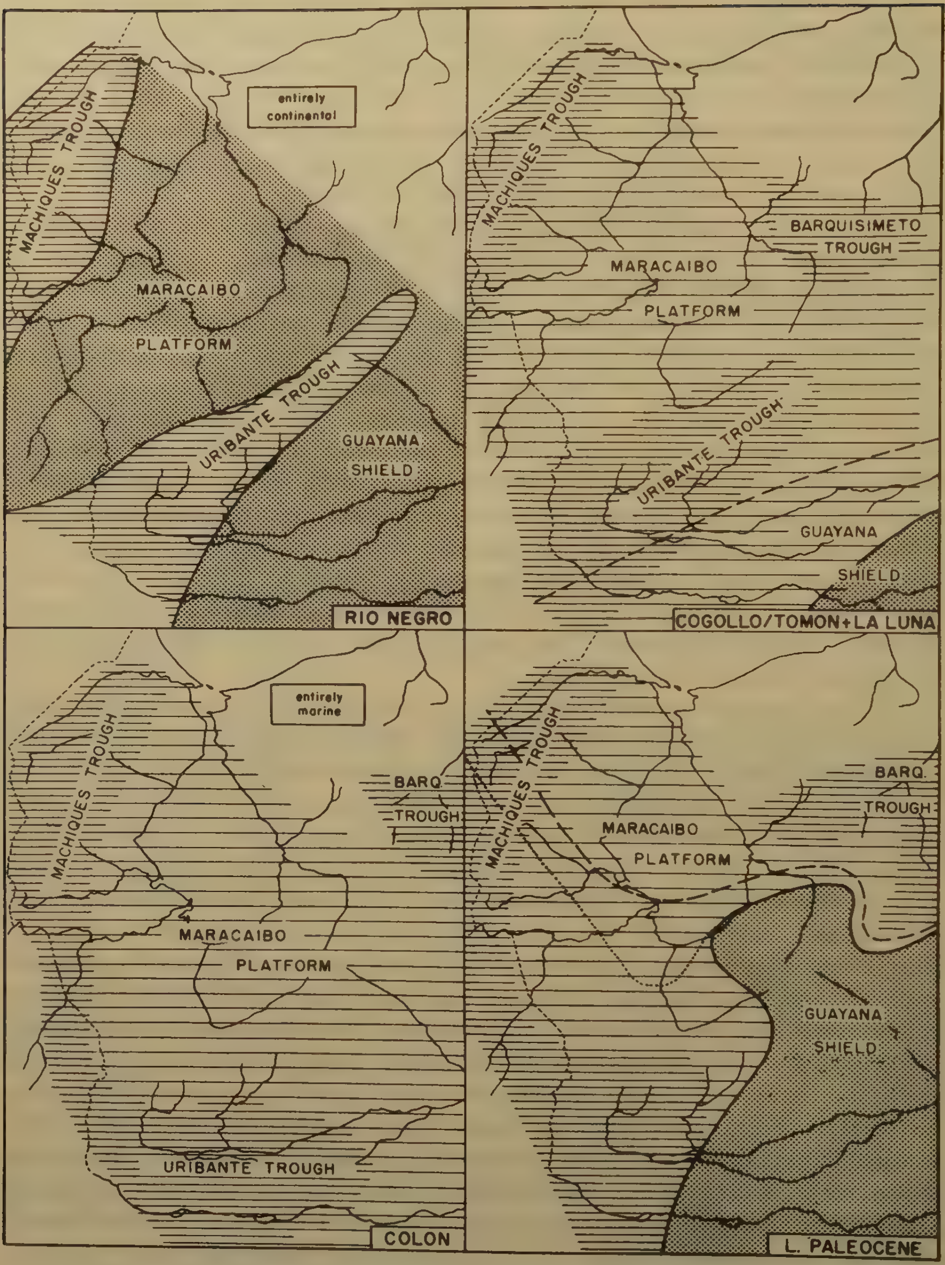
entirely continental
MACHIQUES TROUGH
MARACAIBO
PLATFORM
URIBANTE TROUGH
GUAYANA
SHIELD
RIO NEGRO
MACHIQUES TROUGH
BARQUISIMETO
TROUGH
MARACAIBO
PLATFORM
URIBANTE TROUGH
GUAYANA
SHIELD
COGOLLO/TOMON+LA LUNA
entirely marine
MACHIQUES TROUGH
BARQ.
TROUGH
MARACAIBO
PLATFORM
URIBANTE TROUGH
COLON
MACHIQUES TROUGH
BARQ.
TROUGH
MARACAIBO
PLATFORM
GUAYANA
SHIELD
L. PALEOCENE

FIG. 3.—Facies and paleotectonics of Cretaceous and lower part of Paleocene in western Venezuela. Legend in Figure 4.

(240)

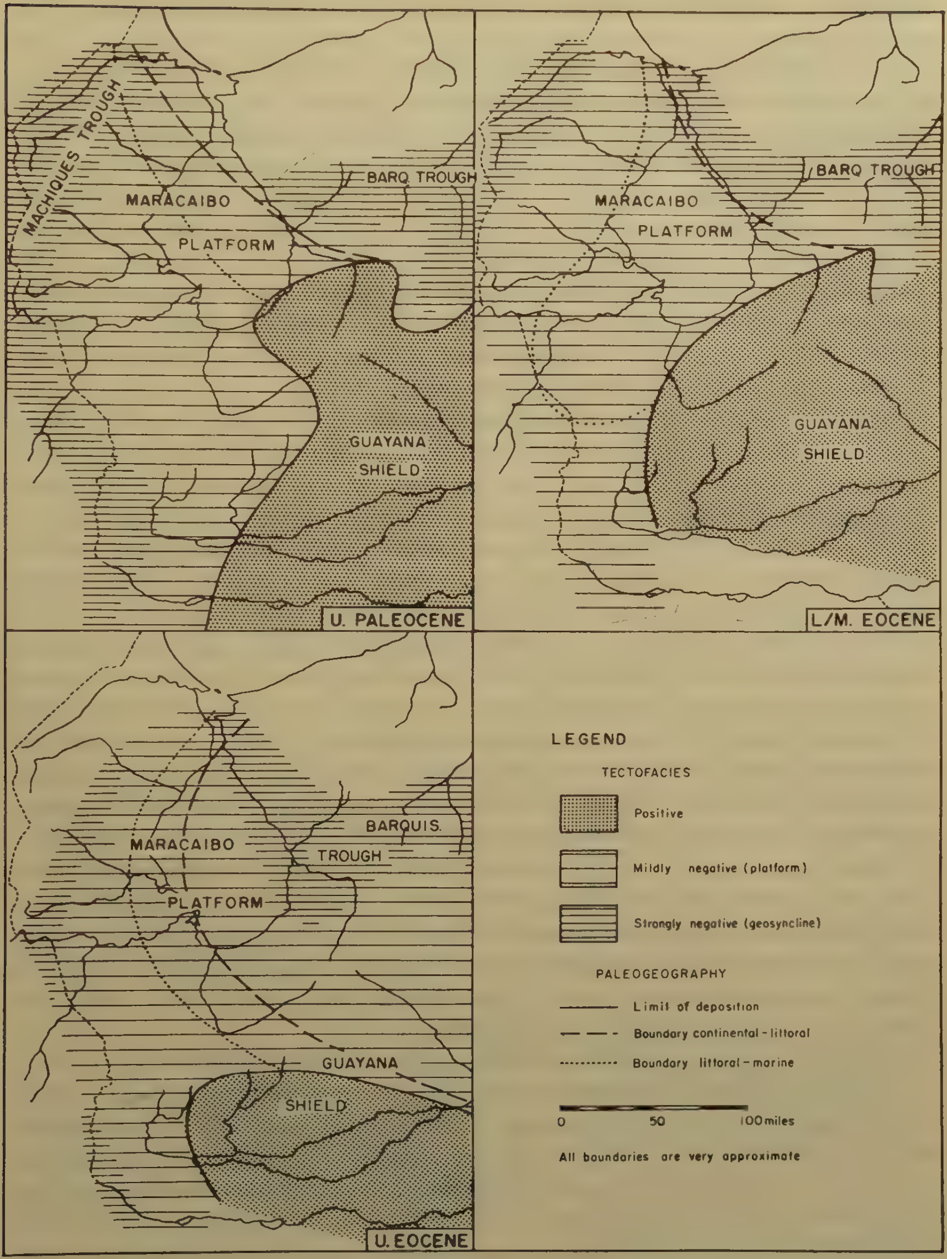
MACHIQUES TROUGH
MARACAIBO
PLATFORM
BARQ TROUGH
GUAYANA
SHIELD
U. PALEOCENE
MARACAIBO
PLATFORM
BARQ TROUGH
GUAYANA
SHIELD
L/M. EOCENE
MARACAIBO
PLATFORM
BARQUIS.
TROUGH
GUAYANA
SHIELD
U. EOCENE
LEGEND
TECTOFACIES
Positive
Mildly negative (platform)
Strongly negative (geosyncline)
PALEOGEOGRAPHY
Limit of deposition
Boundary continental - littoral
Boundary littoral - marine
0
50
100 miles
All boundaries are very approximate

FIG. 4.—Facies and tectonics of upper part of Paleocene and of Eocene in western Venezuela. Legend for Figures 3 and 4.

followed by considerable shallowing indicated by a change in microfauna of the same area.

In the Paleocene the regression became more pronounced. The shallowing of the basin and the withdrawal of the sea toward the northeast continued, resulting in the development of a wide deltaic coastal plain and littoral belt in the western and southwestern parts of the basin. Over most of the Maracaibo platform, however, and in the Barquisimeto trough and eastern border zone of the Guayana Shield marine conditions still prevailed. In the Barquisimeto trough slump and turbidity-current deposits of this period are found (Renz, Lakeman, and Van der Meulen, 1955). The northern limit of the Guayana Shield migrated northward again and parts of the arch connecting it with the Maracaibo platform appear to have been above water. Some Cretaceous and early Paleocene sediments may have been eroded there late in the Paleocene.

The Eocene sediments in the southern, central, and western parts of the basin were fluviatile, deltaic, and perhaps in part lacustrine. The unstable zone was covered with lower deltaic, beach and bay, and littoral sediments which, beyond the hinge line between platform and Barquisimeto trough, rapidly graded into fully marine depsits. The deeper parts of the trough (Barquisimeto area, Serrania de Trujillo area) were filled with a thick sequence of pelagic shales interbedded with sandstones that may have been deposited by turbidity currents.

Late in the middle Eocene another transgressive phase began, which reached its maximum in the upper Eocene. The edge of the positive part of the Guayana Shield again migrated southward and a thick series of shallow marine very sandy sediments, probably largely reworked weathered crust (Misoa), was deposited on the submerged parts. The resulting wide marine basin was rimmed by a relatively narrow belt of fluviatile and deltaic deposits. Although at present no upper Eocene deposits from the central part of the Maracaibo platform are known (probably as a result of post-Eocene erosion), it appears that the great deltaic series of the lower and middle Eocene did not continue into this stage. In the eastern trough the upper Eocene sequence is very thick and predominantly developed in the same bathyal facies as in the Paleocene. Only toward the end of the Eocene is evidence found of rapid shoaling with the appearance of littoral conglomerates and paralic sandstones and lignites.

During the entire Cretaceous and the lower Paleocene subsidence continued in the Uribante and Machiques troughs. The Barquisimeto trough about which little is known in the early and middle Cretaceous, appears as a pronounced tectonic feature from La Luna time onward. Late in the Paleocene subsidence of the Uribante trough ceased and in the lower Eocene the Machiques trough also disappeared as a separate tectonic unit. Consequently, during the later part of the lower and the entire middle Eocene the basin was tectonically simple, consisting of a large stable southern and western platform gently inclined toward the northeast, and a large and deep trough in the east. Between the stable platform and the trough an unstable transition zone occurred. The very marked hinge line between the unstable platform and the trough approximately follows the present-day Bolivar Coast. The Guayana Shield persisted as a positive mass. Evidence from the composition of the basin sediments suggests that from early Cogollo-Tomón to early Colón time no landmass in the west bordered on the Venezuelan part of the basin; but in late Colón time an important positive massif must have originated west of the border. It is probably identical with the Cordillera Central of Colombia.

CLASSIFICATION OF SANDSTONES

In order to clarify relationships, observations, measurements, and descriptions have to be arranged in groups of related units. To solve specific problems or to describe specific aspects, significant properties have to be emphasized. According to Rodgers (1950), two main types of classifications can be recognized; the descriptive and the genetic. The best descriptive classification is one which calls attention to genetically significant properties; it is an analytical descriptive classification.

The genesis of sediments involves a great many separate factors, each of which affects some of the properties of the sediment strongly, others hardly or not at all. In order to cover the entire field of sediment genesis a truly comprehensive analytical descriptive classification would have to be based on a great many characteristics. The majority of the sandstone classifications of the current literature are of the analytical type but emphasize only a few of the many potential factors; mainly source area characteristics and tectonics of the depositional basin.

It appears doubtful whether a single system which is sufficiently simple to serve the purpose of clarifying relations could, at the same time, do justice to all of the numerous aspects involved. A tabulation of the objectives of the present study and the related sediment properties and sedimentation processes demonstrates the diversity of problems and approaches (Table I).

A classification of sandstones designed to study sources would be most effective when based on the composition of the terrigenous sand fraction. A classi-

TABLE I. RELATION BETWEEN OBJECTIVES OF PRESENT STUDY AND RELEVANT SEDIMENT PROPERTIES

	Objective	*Relevant Properties of Sediments*
Sediment source	Source area petrography	Composition of terrigenous fraction
	Source area weathering	Ratio of stable to unstable minerals
	Source area tectonics (reflected in morphology and petrography)	Mineralogy and stable/unstable ratio
Transportation	Sorting, abrasion, elimination of unstable elements	Roundness; sorting; ratio of stable/unstable
Depositional basin	Depositional environments	Grain size; sorting; clay content; ratio stable/unstable; structure; authigenic minerals
	Tectonics of basin	Effective through depositional environments

fication intended to study the influence of the depositional environment and the effects of basin tectonics should stress texture and textural maturity and perhaps sediment structures as Packham (1954) does. An investigation of the influence of weathering, transportation, and reworking would have to make use of textural properties, roundness, and mineralogical maturity. The writer thinks the classification proposed by Folk (1954) is the most satisfactory one available. It is based on a tripartite nomenclature involving mineralogical composition, grain size, and textural maturity with qualifiers for special components, mainly authigenic minerals, cementation, and other aspects. In the present study this classification has been followed to a large extent, with the omission of certain elements of no direct interest in this rather special case. Since the purpose is partly a comparison with the observations and conclusions of others, classifications that are too divergent from those generally adopted are undesirable. Therefore, two other suggested solutions cannot be used: (a) a classification based on continuous variables as proposed by Rodgers (1950), and (b) a classification based on mineral associations and provinces similar to the approach of the heavy-mineral specialist (cf. Doeglas, 1940).

However, even with due attention to the various aspects of sedimentation, the problem has not been completely solved. Not all sediment source areas are petrographically similar, and adaptations in classification are required for the occurrence of prominent minerals of exceptional character. In general quartz+chert, feldspar, and the rock fragments are used as end members to define a classification framework. However, in western Venezuela feldspar is scarce in Paleocene and Eocene sediments whereas detrital chert is characteristic and abundant and merits separate treatment. Hence, for this case a quartz-chert-rock fragments diagram appears to be of more interest than the standard type (cf. Fig. 13).

It has been maintained by various authors that texture and mineralogical composition are virtually inseparable (Dapples, Krumbein, and Sloss, 1953; Bokman, 1955), and that the mineralogically most immature sediments such as graywackes and arkoses are also clayey, poorly sorted, and angular. An increase in mineralogical maturity would be accompanied by an increase in textural maturity, and orthoquartzites should generally be clean, well sorted, and well rounded. Folk (1956) has disagreed with this opinion by stating that, while parallelism

TABLE II. RELATION BETWEEN MINERALOGICAL AND TEXTURAL MATURITY IN SANDSTONES OF WESTERN VENEZUELA

Sandstone Type	*Per cent of Each Type*			*Number of Samples*
	Immature	*Submature*	*Mature*	
Graywacke	45	25	30	120
Subgraywacke	48	26	26	280
Arkose	60	28	12	38
Feldspathic ss.	58	31	11	41
Quartzose ss.	35	29	36	239

between both types of maturity is a fact in some deposits, the exceptions to the rule are numerous and genetically very important. The data from western Venezuela support this viewpoint (Table II). This table is based on the sandstone types of Figure 5 and on Folk's classes of textural maturity (immature: poorly sorted, more than 5 per cent clay, angular; submature: poorly sorted, less than 5 per cent clay, angular; mature: well sorted, less than 5 per cent clay, angular). His supermature class (well sorted, less than 5 per cent clay, rounded) has not been included since the determination of roundness in the samples that have been investigated is generally impossible because of cementation and grain deformation.

The table shows that the trend toward parallelism of textural and mineralogical maturity is only slight in the case of the graywackes and subgraywackes. No parallelism exists for the quartzose sandstones. A marked trend is indicated for the arkoses and feldspathic sandstones, but this is partly due to the fact that

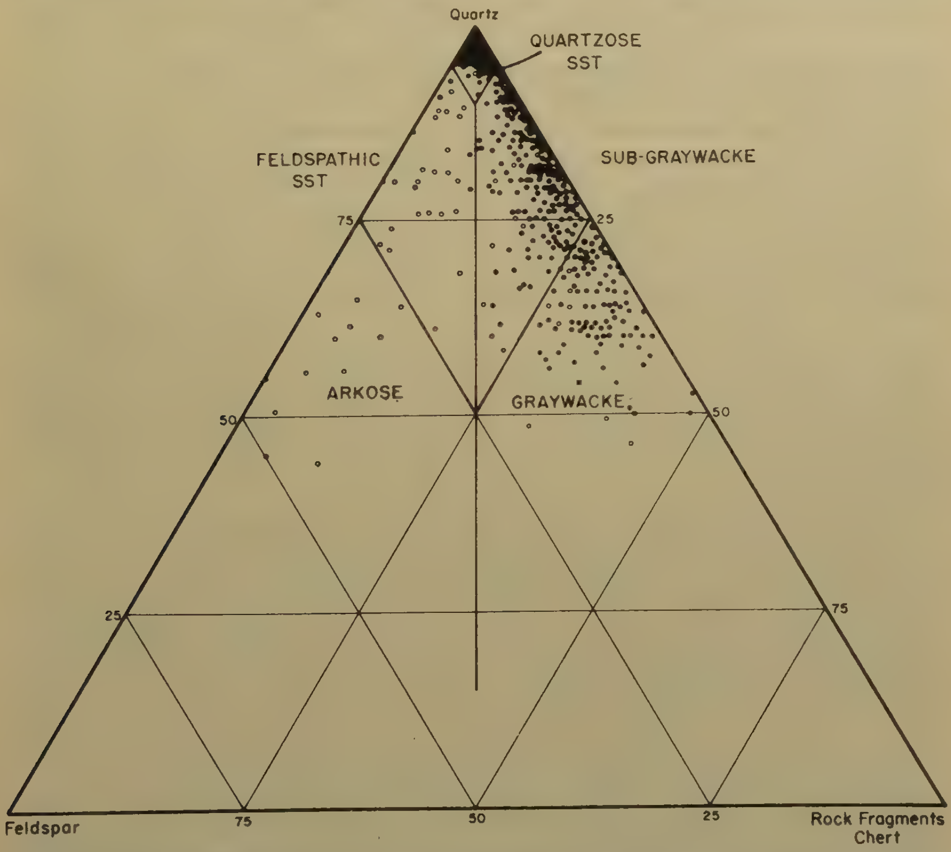

FIG. 5.—Sandstone composition and nomenclature for Cretaceous, Paleocene, and Eocene sediments of western Venezuela. Black triangle at top contains plots of approximately 400 samples.

the available samples of those groups belong almost exclusively to one single (fluviatile) environment. Consequently the assertions of the authors cited, which go so far as to equal orthoquartzites (quartzose sandstones of this study) with textural maturity and graywackes with immaturity, appear to be considerably oversimplified.

The classification of sandstones used in this paper is presented on the triangular diagram of Figure 5. Quartz, feldspar, and rock fragments+chert are used as end members.

The diagram is similar to the one used by Williams, Turner, and Gilbert (1954, pp. 292–93) but their distinction between clayey wackes and clean arenites is not used here, since clay content is related to the depositional environment and not principally to source. The concept of textural maturity is a better tool for studying environmental influence. On the basis of Figure 5 the sandstone types used in this study are defined as follows.

Quartzose sandstone: less than 10 per cent each of feldspar and of rock fragments+chert
Feldspathic sandstone: more feldspar than chert+rock fragments, feldspar between 10 and 25 per cent
Arkose: more feldspar than rock fragments+chert, more than 25 per cent feldspar
Subgraywacke: more rock fragments+chert than feldspar, rock fragments+chert between 10 and 25 per cent
Graywacke: more rock fragments+chert than feldspar, rock fragments+chert more than 25 per cent

It must be borne in mind that graywacke as defined here is approximately identical with Pettijohn's subgraywacke (1954) and that many chert-rich subgraywackes approach the second-cycle orthoquartzites of other authors. To the writer the term orthoquartzite seems to be compromised because it suggests strongly indurated or metamorphosed sandstones. It has been abandoned in favor of quartzose sandstone. Clays, the presence of which is a strictly depositional feature, have no place in a classification designed for the study of sediment sources, nor have the micas. Only after the completion of the microscopical work did the writer become aware of the fact that Folk (1951, 1954) combines metaquartzite with the rock fragments. Unfortunately it has not been possible to apply this interesting idea.

Much attention has been given to the parameters and classifications suitable to study the depositional area and the effects of tectonic control of sediment properties. Most of the proposed classifications emphasize this aspect, and mineralogical classifications which include clay have been applied widely for this purpose. Folk (1951) has pointed out that textural maturity which reflects depositional environment is one important concept in this respect, a view with which the writer agrees. Mineralogical maturity reflecting the degree of elimination of unstable components immediately before burial has also been widely used.[3]

---

[3] For this purpose Dapples, Krumbein, and Sloss (1953) have proposed the quartz index, being the ratio between quartz+chert, and clay+rock fragments+feldspar. The inclusion of clay, a stable but purely textural component, has been rejected by Pettijohn (1954). The use of chert as a stable component is also open to doubt. It is more stable than most rock fragments and feldspar, but weathered chert is often observed. The final result of deep weathering is a pure quartz sandstone and must be expressed as such.

Since a thorough discussion of the aspects of deposition in the basin must be based on observations to be described later it is postponed to the last chapter of this paper. The concepts of textural and mineralogical maturity and the classification of Figure 5 are used for this purpose.

SOURCES AND DISTRIBUTION OF SEDIMENTS

It is the purpose of this section to study the sources of the Cretaceous, Paleocene, and Eocene sediments in the basin of western Venezuela, and the effects of weathering and erosion of the source areas. The explanation of the observed petrographical variation may not seem the only one possible. An alternative is offered by the theory of tectofacies control in the basin. This possibility is discussed in the next section, together with the effects of the depositional environments.

The distribution of the various sandstone types in the basin is presented on Figure 6–12 for each of the stages and stage groups separately. The circles on the maps indicate the locations of composite stratigraphic sections.

The pre-Aptian (Rio Negro) sandstones are feldspathic and most belong to the arkoses. The predominant feldspars are orthoclase, microcline, and oligoclase. Appreciable amounts of basic feldspars are found only in the extreme northwest. Generally both altered and fresh feldspars are present in the same sample. The rock fragments are predominantly quartzitic sandstone, vein quartz, and some schist. The sandstones represent Pettijohn's (1957, p. 325) residual arkoses and are the products of stripping of a not too deeply weathered igneous and metamorphic terrane. The pre-Cretaceous basement surrounding the troughs is the most likely source.

Sands of a different composition which consist of more than 95 per cent quartz are found only along the southern edge of the Uribante trough. It does not appear likely that the absence of feldspar is due to the influence of transportation across the trough. The distance is only 20–50 miles and Russell (1937) and Koldewijn (1955) have shown that in fluviatile transportation there is no appreciable loss of feldspar over distances of 10–20 times as large as this. Hence, as suggested by their position, a sediment source on the Guayana Shield seems plausible.

The map for the Aptian-Coniacian (Cogollo-Tomón and La Luna) represents conditions at the time when the transgression had been virtually completed and the Maracaibo platform was entirely under water. The early Aptian sandstones fringing and covering the remnants of the Maracaibo platform are arkosic and of the Rio Negro type and are not shown in Figure 7. All the later sands are quartzose and contain less than 5 per cent of other constituents.

Significant mineralogical variation which might indicate sediment sources is absent in the Cogollo-Tomón and La Luna sands. However, sandstone-shale ratios increase markedly from north to south. This is conspicuous in the Albian where the dominantly sandy Tomón facies is restricted to the southern half of the basin. On a smaller scale and restricted to the extreme south of the basin, a

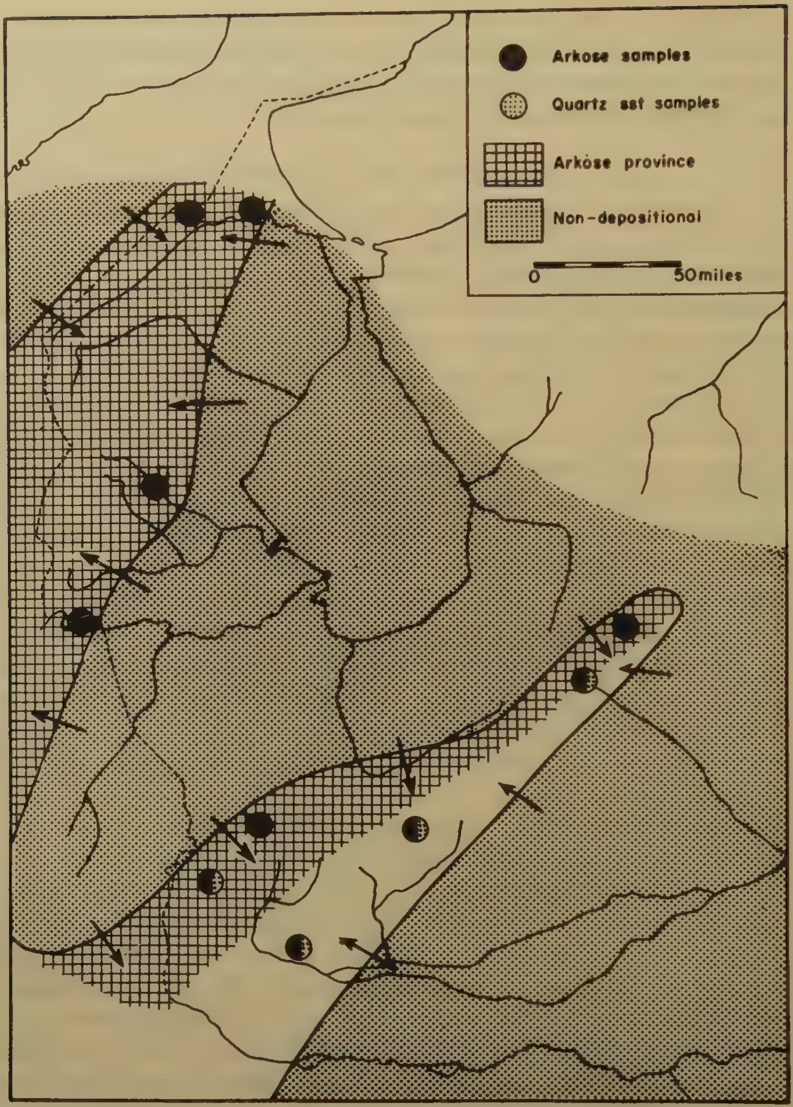
Arkose samples
Quartz sst samples
Arkose province
Non-depositional
0
50miles

Fig. 6.—Sandstone provinces of pre-Aptian stage (Rio Negro formation) in western Venezuela. Total number of samples investigated: 63.

similar increase can be observed both in the Aptian and in the Cenomanian-Turonian-Coniacian La Luna deposits, which elsewhere are predominantly shaly and calcareous. This lithofacies distribution suggests the Guayana Shield as the principal sediment source.

In the Senonian (Colón formation) also, sandstones are mainly restricted to the southern and southeastern parts of the basin, although a little sand is found in the extreme northwest. All the sandstones are marine. In marked contrast to

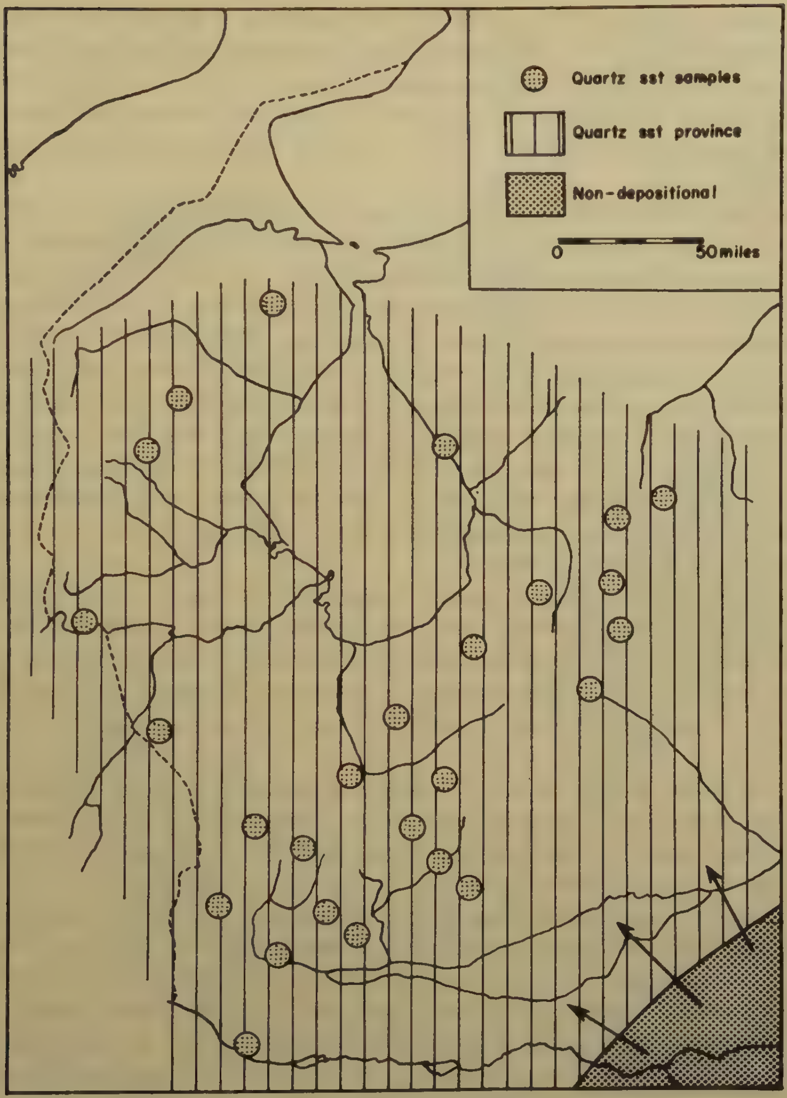

FIG. 7.—Sandstone provinces of Aptian-Coniacian (Tomón, Cogollo, and La Luna formations) in western Venezuela. Total number of samples investigated: 344.

the previous period, petrographical variation is strong and significant. Quartzose sandstones persist in the south-central part of the basin and may be attributed to the Guayana Shield. Parts of the shield must have undergone rejuvenation of relief, however, since arkoses and feldspathic sandstones, which must have had a southern source, are found in the southeastern part of the basin. They differ from the Rio Negro arkoses in having much less feldspar, predominantly slightly altered albite and oligoclase.

The most significant feature is the appearance of a belt of graywackes and subgraywackes along the southwestern and northwestern margins of the Venezuelan part of the basin. The geographical position of the graywackes points to a westerly source. They contain very little feldspar but abundant detrital chert and rock fragments (cf. Fig. 13). The rock fragments are predominantly quartzitic sandstone and shale.

From Paleocene time onward sandstones occur over the entire basin. Two main provinces can be recognized; the graywacke province along the western margin of the basin, and the quartzose sandstone province in the south and southeast. The provinces are separated by a belt of subgraywackes and interbedded subgraywacke and quartzose sandstones. Comparison of Figures 9–12 shows that in the course of the Paleocene and in the lower and middle Eocene the relative positions of the two provinces have changed considerably. From a westerly and, in the northern part of the basin, also from a northwesterly direction the graywacke province has encroached upon the territory occupied by the quartzose sandstone province since the middle Cretaceous. Geographic position and the eastward and southeastward advance of the sediments in the basin point to a source west of the Venezuelan-Colombian border.

By the end of the middle Eocene graywacke and subgraywacke sands are the most important group in the basin. The predominance of sediments from this western source over Guayana Shield detritus becomes even more apparent when volumes rather than areas are considered, since the average thickness of the sediments of the first source is approximately three or four times as great as of the second.

In the upper Eocene (Fig. 12) quartzose sandstones again become areally important because of a transgression over the border zone of the Guayana Shield. The reworked sands in this zone are widespread but thin. At the same time there is apparently no reduction in size of the graywacke province.

Most of the sandstones of the graywacke province and of the subgraywacke transitional zone are developed in fluviatile, deltaic, and littoral facies. The sands of the quartzose province are predominantly neritic. Apparently a large river system entered the basin in the west from the upper Paleocene to the middle Eocene and its sediments built a large delta. Small rivers, on the other hand, brought the erosion products from the Guayana Shield directly into the sea without building up an extensive deltaic and littoral belt. The difference in quantity of the two sediment sources thus can be explained in terms of drainage basin type and size. Differences in relief of the source areas may also have played a part.

The sandstones of the graywacke and subgraywacke group vary in grain size, sorting, and clay content, according to depositional environments. The mineralogical variation shows a clear trend. Eastward and away from the probable source of sediments the percentages of chert and rock fragments decrease, resulting in a change from graywacke to subgraywacke. This belt may be the result of dilution of graywacke material from one source with quartz sand from the other, or it

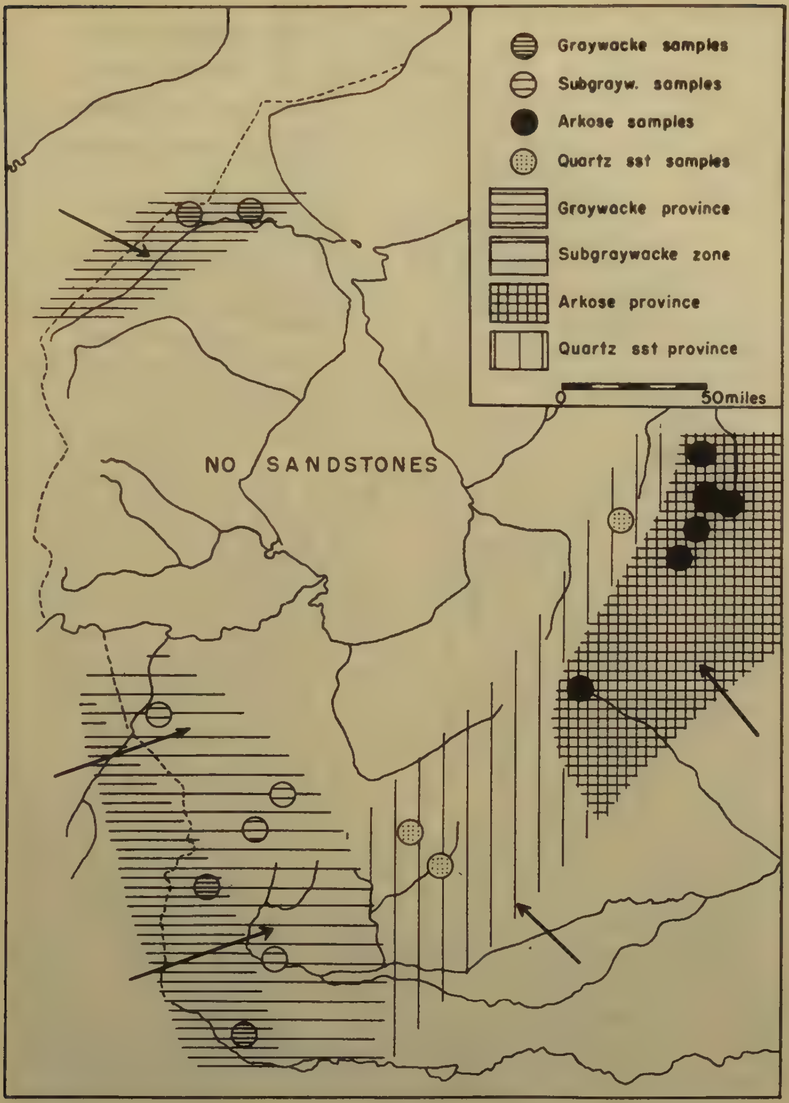
Graywacke samples
Subgrayw. samples
Arkose samples
Quartz sst samples
Graywacke province
Subgraywacke zone
Arkose province
Quartz sst province
0
50miles
NO SANDSTONES

FIG. 8.—Sandstone provinces of Senonian (Colón formation) in western Venezuela. Total number of samples investigated: 84.

nay have been caused by progressive elimination of unstable components in the ›asin. In the latter case, elimination should have been most pronounced in the ittoral belt where a maximum of energy is expended on the sediments. Examinaion of Table IV seems to suggest a sudden increase in mineralogical maturity in his zone but it is not certain whether the percentages are significant. Petrographic study of the chert and rock fragments group seems to indicate that the

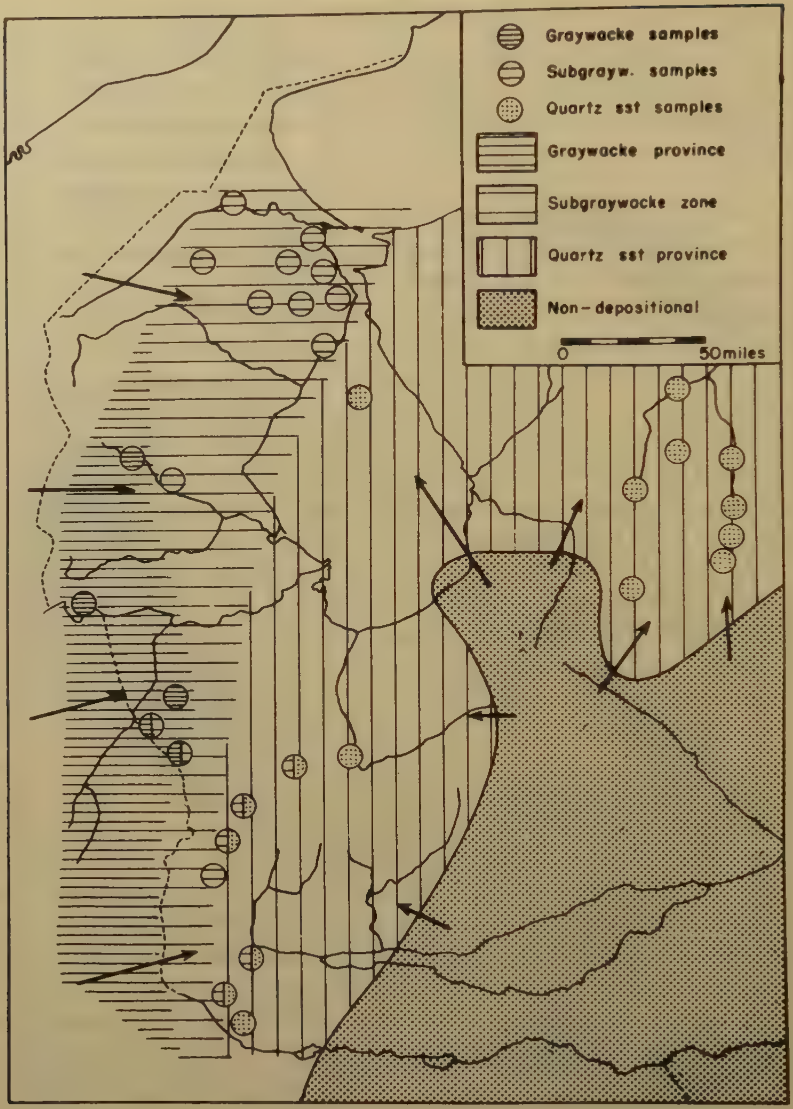
Graywacke samples
Subgrayw. samples
Quartz sst samples
Graywacke province
Subgraywacke zone
Quartz sst province
Non-depositional
0
50miles

FIG. 9.—Sandstone provinces of lower part of Paleocene in western Venezuela. Total number of samples investigated: 279.

ratio between the more stable elements in the group, for example, chert, and the unstable particles, such as shale, is no higher in the subgraywackes than in the graywackes. This points to mixing of different types of detritus as a principal cause of the increase in maturity. That mixing is possible is shown by the occurrence of interbedded subgraywackes and quartzose sandstones at the boundary between the subgraywacke belt and the quartzose sandstone province. At present

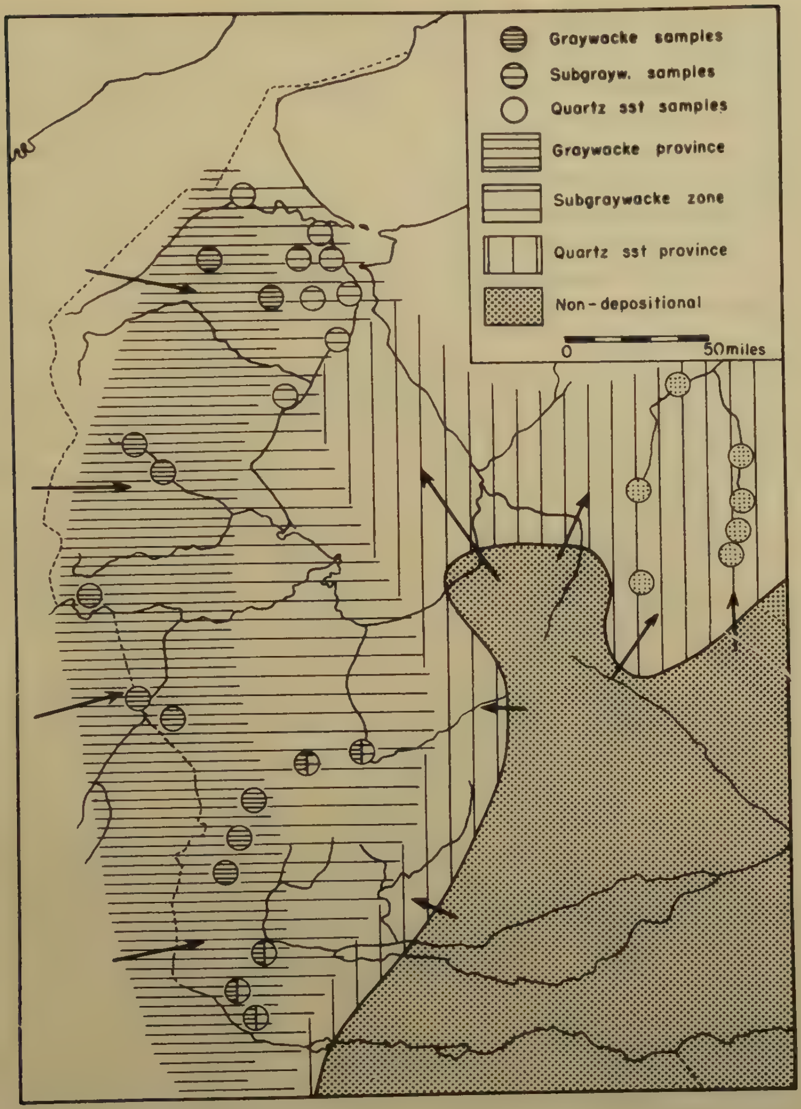
Graywacke samples
Subgrayw. samples
Quartz sst samples
Graywacke province
Subgraywacke zone
Quartz sst province
Non-depositional
0
50miles

FIG. 10.—Sandstone provinces of upper part of Paleocene in western Venezuela. Total number of samples investigated: 411.

the problem can not be solved completely; the evidence appears to be more in favor of mixing as the principal cause, but elimination of unstable elements can not be ruled out as a factor.

The composition of the sands derived from the western source varies with time. This variation is shown in Figure 13, where the composition of samples from the graywacke-subgraywacke group is plotted after converting the sum of the percentages of chert, quartz, and rock fragments to a total of 100. All samples plotted in the top triangle belong to the Senonian. They contain relatively small amounts of detrital chert and high percentages of quartz. The Paleocene sands are high in chert and contain less quartz. The Eocene samples show a broad range of chert percentages but on the whole these are lower than in the Paleocene. On the other hand, there are more samples with high percentages of rock fragments in the Eocene than in the Paleocene. The change in gross composition is accompanied by changes within the rock-fragments group where particles of low-grade metamorphics, such as phyllites and andalusite schist, become gradually more important in the course of the late Paleocene and the Eocene.

The only possible source of the detrital chert in the sediments is the middle Cretaceous terrane, the only series in western Venezuela and eastern Colombia which contains large quantities of this mineral. The sequence of sandstone types here described appears to reflect in reverse order the strata of an orogenic massif. First, in the late Senonian, the upper shaly beds of the early Senonian were eroded, resulting in graywackes that are relatively poor in chert; subsequently, during the Paleocene, erosion of the middle Cretaceous produced graywackes with abundant chert; and finally, in the Eocene, when erosion cut into the metamorphic core of the massif, deposits were formed which contain metamorphic rock particles.

From the geology of Colombia it is known that uplift of the Cordillera Central began in the late Cretaceous. Therefore, it may be assumed that the sediments belonging to the graywacke province of western Venezuela are the erosion products of this range.

One might suppose that these changes in mineralogical composition reflect progressive weathering and reworking of the source material. This explanation, however, conflicts with the fact that, both in the early and late stages of the depositional history of this sediment group, unstable rock fragments predominate. Hence, there is no increase in mineralogical stability. On the other hand, the fact that the mineralogy of the sequence of deposits in the basin conforms with an erosion history which is logical for the Colombian range, supports the view that petrographic changes at the source and not weathering are the cause of petrographic variation of the deposits. On the whole, the abundance of unstable components in the sediments from the western source shows that in this area mechanical erosion was predominant over chemical weathering. If a tropical climate is assumed, rapid erosion and steep relief are suggested.

The other sedimentary province is very homogeneous throughout its history and its detritus is mineralogically mature. Hence, either the petrography of the source area has never changed in the course of a long erosion history (an unlikely assumption), or weathering has been so rigorous that only the most stable components have reached the sea. Little is known about the petrography of the Guayana Shield in this area. It may be assumed, however, that during the Cretaceous

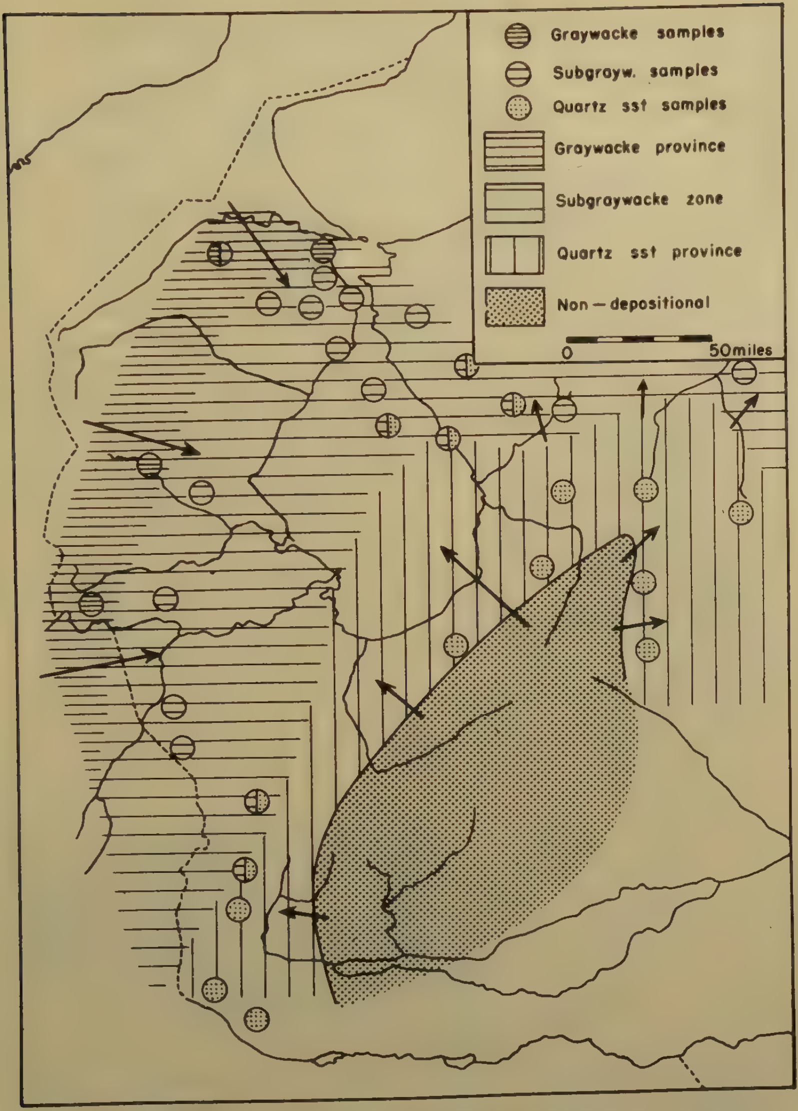
Graywacke samples
Subgrayw. samples
Quartz sst samples
Graywacke province
Subgraywacke zone
Quartz sst province
Non—depositional
0
50miles

FIG. 11.—Sandstone provinces of lower and middle Eocene in western Venezuela. Total number of samples investigated: 734.

nothing but sediments belonging to the pre-Cretaceous La Quinta or Girón series and the igneous and metamorphic basement rocks were cropping out. The La Quinta, within the basin, is very incompletely known but seems to be variable in composition. Also, shales and claystones are abundant in this formation and the presence of rock fragments should be expected in fresh detritus. The igneous and metamophic basement should have provided both feldspars and rock frag-

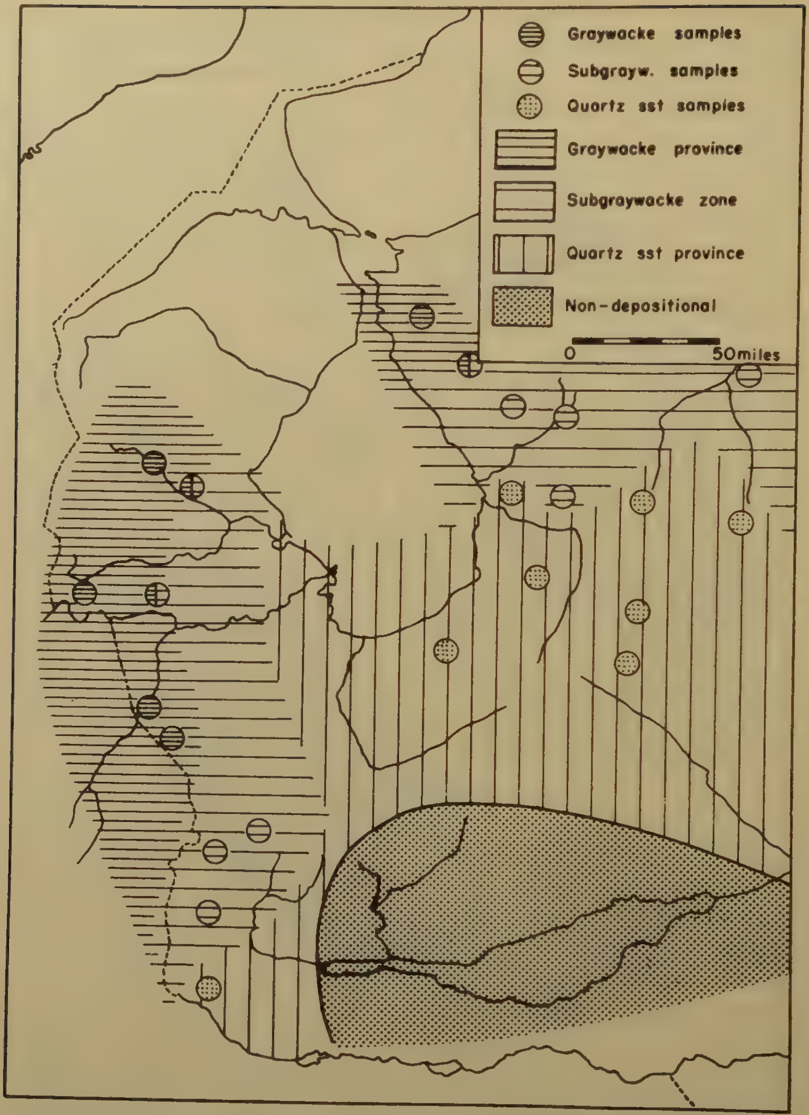
Graywacke samples
Subgrayw. samples
Quartz sst samples
Graywacke province
Subgraywacke zone
Quartz sst province
Non-depositional
0
50miles

FIG. 12.—Sandstone provinces of upper Eocene in western Venezuela. Total number of samples investigated: 537.

ments. Since these constituents are absent, deep and intense weathering in the Guayana Shield area must be assumed. This implies low relief.

During the late Paleocene, upper Cretaceous and lower Paleocene sediments (mostly sandstones) were subject to erosion on the arch connecting the Maracaibo platform with the Guayana Shield. The sandstones that were eroded have not changed the composition of the sediment stream because they were quartzose and can not be traced separately.

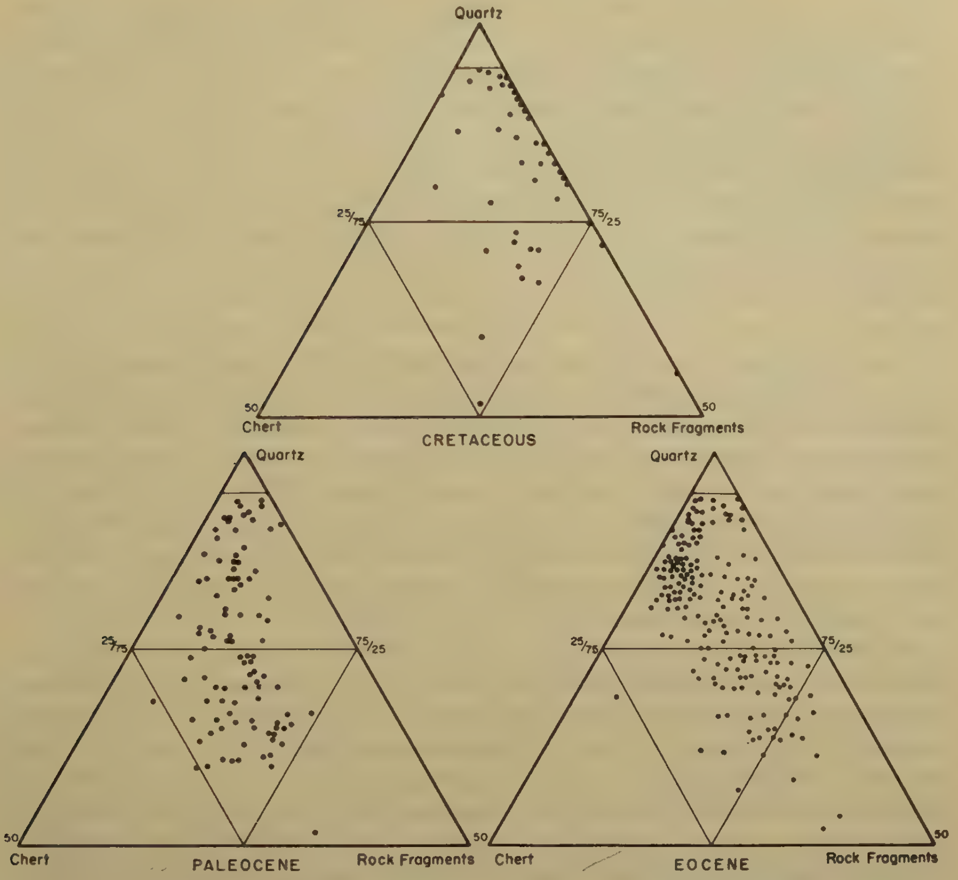

FIG. 13.—Composition of Cretaceous, Paleocene, and Eocene sandstones belonging to graywacke-subgraywacke group. Sum of percentages of quartz, chert, and rock fragments in original analyses is converted to total of 100.

In the foregoing discussion the petrography of the marginal sands of the basin has been used to arrive at conclusions concerning the petrography, the conditions of weathering and erosion of the source areas. The marginal sands are the end products of a history of weathering and erosion in the source, and between source and depositional area, plus an additional and unknown amount of abrasion and weathering during deposition. The mineralogically immature sands of the graywacke group have been considered as the products of low energy expenditure in the source area, whereas the mineralogically mature quartzose sandstones are supposed to represent the results of rigorous weathering at the source. The implicit assumption that abrasion during transportation is of minor importance can not be fully proved but is supported by the results of studies of recent sediments (Burri, 1929; Russell, 1937; van Andel, 1950; Koldewijn, 1955), which show that strong abrasion is not common.

Similarly the effects of reworking in the depositional basin before final burial have been ignored. If this is not correct, a quite different explanation of the distribution of mature and immature sandstones in the basin might be given which might for example attribute differences in sandstone petrography to differences in tectofacies. Quartzose sandstones are often considered indicative of a stable platform facies and the graywackes of geosynclinal conditions. This possibility which frequently has been advocated in the literature is discussed in the next chapter as it is related to processes in the depositional area. In the present case tectofacies control does not appear to be important.

SANDSTONES IN DEPOSITIONAL BASIN

The characteristics of a basin are expressed in its sediments through its depositional environments. This is true also for tectonics. There is no direct influence of tectofacies on sediments; it is only possible through control of depositional environments. The idea of tectonic control of sediment characteristics has drawn much attention in recent literature (Krynine, 1941a, b, c, 1942, 1948; Dapples, Krumbein, and Sloss, 1948; Dapples, Krumbein, and Sloss, 1953; Folk, 1954, 1956; Bokman, 1955; Pettijohn, 1957, pp. 611–32). It is the purpose of this chapter to examine the effect of tectofacies on the Cretaceous, Paleocene, and Eocene sediments of western Venezuela.

Tectofacies in this respect has often been used in a broad sense involving both source area and depositional basin tectonics. This requires assumptions concerning natural links between negative and positive tectonic elements. The specific character of the sediments of each tectofacies would then be the result of a varying degree of preservation in the depositional area of the properties inherited from the associated source. Dapples, Krumbein, and Sloss (1953) recognize three main tectonic couples: (a) basins in stable tectofacies linked with an epeirogenic source, (b) moderately negative basins with an epeirogenic-orogenic source, and (c) eugeosynclinal basins with an orogenic source.

These assumptions do not appear to be true in all conditions. Sediments available in sufficient quantities to fill large basins have generally been derived from vast source areas comprising a variety of tectofacies. The present Gulf of Mexico derives its sediments from the entire drainage basin of the Mississippi and from the basins of several other rivers. Geosynclines are sometimes remote from orogenic sources and receive their sediments from wide stable platforms. On the other hand, orogenic belts, for example, the mountain ranges of Java and Sumatra, may supply a large part of the sediments deposited on stable platforms (in this case the Sunda shelf). The tectofacies maps of western Venezuela (Figs. 3, 4) illustrate the point. The geosynclinal Barquisimeto trough is adjacent to a stable shelf and has received a large part of its sediments from this source. The sediments derived from the orogenic belt of the Colombian Andes on the other hand have been deposited both in the moderately negative Machiques trough and on the stable Maracaibo platform. Therefore, it appears necessary to consider separately the influences of basin and source area tectonics.

To explain the influence of basin tectofacies, Bokman (1955) has postulated three generalized depositional environments correlatable with tectofacies types: the undisturbed geosyncline, the partly reworked unstable platform, and the intensely reworked stable platform. Folk (1956) has pointed out that reworking is a process which is rapid compared with subsidence. The time needed to sort a sand on a beach is infinitely short compared with the time needed for subsidence and burial beyond the range of surface processes. Therefore, a close relation between reworking and subsidence as assumed by Bokman seems an oversimplification. It may be added that the rate of subsidence is not the only factor controlling depositional environment. Actually it is the ratio between the rates of sediment supply and of subsidence which is of prime importance, and to less extent also the morphology of the basin and of the adjacent land areas. Except for the rate of subsidence, none of these factors is exclusively controlled by basin tectofacies.

In order to investigate the importance of tectofacies control, it is necessary first to establish the degree to which depositional environment controls sediment characteristics and second to determine the relations between environment and tectofacies. The influence of transportation in the basin may conveniently be included in the study of the environments since transportation in a depositional area is largely a matter of reworking and redeposition.

Many properties of the sediments are due to or modified by the depositional environment. For the purpose of this study the principal ones are sorting, clay content, and the presence of unstable minerals. For an evaluation of grain size the samples are too widely spaced; and roundness can not be studied because of strong compaction and cementation with silica in many samples. Structure has been used as a base for an environmental classification of sediments by Packham (1954) and should merit more attention, but in the present study insufficient observations have been made.

A great many environments can be recognized in the Cretaceous, Paleocene and Eocene of western Venezuela. For the present purpose these have been grouped into four broad categories comparable with the broad tecto-facies elements: (a) terrestrial (fluviatile and upper deltaic), (b) littoral (lower delta, beaches, bays, lagoons, mud flats, shallow offshore belt), (c) neritic marine, and (d) bathyal marine. The regional distribution of these groups is shown in Figures 3 and 4.

In Table III sediment characteristics are compiled for each of the four facies

TABLE III. COMPARISON BETWEEN DEPOSITIONAL FACIES GROUPS AND SEDIMENT PROPERTIES OF CRETACEOUS, PALEOCENE, AND EOCENE SANDSTONES IN WESTERN VENEZUELA
(Percentages of total number of samples in each facies group)

Facies	*Mineralogical Composition*				*Texture*				*No. of Samples*
	Gray-wacke	*Sub-gray-wacke*	*Arkose*	*Quartz-ose Ss.*	*Clean*	*Clayey*	*Well Sorted*	*Poorly Sorted*	
Terrestrial	45	40	All	15	51	49	35	65	283
Littoral	30	45	are	25	50	50	63	37	248
Neritic	20	45	fluvia-	35	35	65	42	58	223
Bathyal	40	60	tile	—	15	85	25	75	68

groups. The parameters are expressed in per cent of the total number of samples investigated for each facies group. It is felt that the sets of data arc sufficiently large and varied to avoid over-representation of specific environments within each facies group (for example, an excess of well sorted clean beach sand samples in the littoral group).

Graywackes, subgraywackes, and quartzose sandstones are found in all facies groups, but there is a marked seaward decrease of the first two. A relation between mineralogical maturity as expressed by sandstone types and depositional environments appears to exist. If progressive elimination of unstable elements would be the cause, a sudden increase in maturity in the littoral belt might be expected. This is not the case; the change is very gradual. On the other hand, it has been shown in the previous section that probably two mineralogically different sources have supplied the sediments, one primarily to the neritic zone, the other to a full range of facies. Hence the data in Table III may not be homogeneous as to source. Therefore, it is more appropriate to consider only the data from the graywacke-subgraywacke area which are all from the same source. Table IV shows that in this case there is very little relation between mineralogical composition and facies. Therefore, it may be concluded that differences in mineralogical maturity in western Venezuela are mainly due to differences in source. When large groups of samples are taken together as in Table III significant differences in sorting and clay content are found between the different facies groups. Well sorted sandstones are most abundant in the littoral zone, rare in bathyal sediments. Clayey sands on the other hand are very prominent in bathyal deposits and common in the neritic zone. In terms of textural maturity this implies that in this area: (1) terrestrial sands are predominantly submature; (2) littoral sands are predominantly mature; (3) neritic sands are submature-immature; and (4) bathyal sands are predominantly immature.

TABLE IV. RELATION BETWEEN MINERALOGICAL MATURITY AND FACIES. SAMPLES FROM LOWER AND MIDDLE EOCENE SERIES IN GRAYWACKE-SUBGRAYWACKE PROVINCE
(Expressed in per cent of total number of samples per facies group)

Facies Group	*Graywacke*	*Subgraywacke*	*Quartzose Ss.*
Terrestrial	65	33	2
Littoral	54	42	4
Neritic	55	43	2
Bathyal	50	42	8

Many sands are both well sorted and clayey. Such sediments can not be placed in Folk's (1954) scheme of textural maturity. They represent well sorted beach and dune sands washed over into areas of clay deposition.

In summary, there is no evidence to suggest a relation between sandstone types or mineralogical maturity and depositional environment. On the other hand, with a sufficiently large set of data, a clear correlation between textural maturity and environment groups appears to exist.

The relations between depositional facies and tectofacies must now be examined. It has been pointed out before that only some of the factors controlling depositional environment are related to tectofacies. The importance of tectofacies may therefore vary from case to case. In some places, the tectofacies is reflected in depositional environment, as in the Barquisimeto trough which was a deep sea throughout the Paleocene and Eocene. In other places there is no apparent relation between tectofacies and depositional environment. The Uribante trough in the Paleocene and the Machiques trough in the lower Eocene were both rapidly subsiding basins, but they are not reflected in the depositional environment. In Table V the various tectofacies elements that occurred in the basin of western Venezuela in Cretaceous, Paleocene, and Eocene time have been tabulated, together with the associated depositional environments and source areas. This table shows no fixed relation between tectofacies and depositional facies and no fixed association between the tectofacies of positive and negative areas.

TABLE V. TECTOFACIES ELEMENTS AND ASSOCIATED DEPOSITIONAL ENVIRONMENTS IN CRETACEOUS, PALEOCENE, AND EOCENE OF WESTERN VENEZUELA

Basin Tectofacies	*Stage*	*Depositional Environments*	*Associated Source Tectofacies*
Stable platform	U. Eocene	Terrestrial-littoral-neritic	Epeirogenetic orogenetic
	U. Paleoc.-M. Eoc.	Terrestrial-littoral	Epeirogenetic-orogenetic
	U. Cret.-L. Pal.	Predominantly neritic	Epeirogenetic-orogenetic
	M. Cretac.	Littoral-neritic-bathyal	Epeirogenetic
	L. Cretac.	Terrestrial	Epeirogenetic
Unstable platform	U. Eocene	Neritic	Epeirogenetic-orogenetic
	U. Paleoc.-M. Eoc.	Littoral-neritic	Epeirogenetic-orogenetic
	L. Paleoc.	Neritic-bathyal	Epeirogenetic-orogenetic
Troughs	L. Paleoc.-U. Eoc.	Terrestrial and bathyal	Epeirogenetic-orogenetic
	U.-M. Cret.	Neritic-bathyal	Epeirogenetic
	L. Cretac.	Terrestrial	Epeirogenetic

It is therefore not surprising that an arrangement of sample characteristics according to tectofacies does not show any relation between either textural or mineralogical maturity and tectofacies (Table VI).

TABLE VI. COMPARISON BETWEEN TECTOFACIES AND SEDIMENT PROPERTIES IN CRETACEOUS, PALEOCENE, AND EOCENE OF WESTERN VENEZUELA
(Expressed in per cent of total number of samples per tectofacies type)

Tectofacies	*Sandstone Types*				*Texture*				*No. of Samples*
	Graywacke	*Subgraywacke*	*Arkose*	*Quartzose Ss.*	*Clean*	*Clayey*	*Well Sorted*	*Poorly Sorted*	
Stable platform	32	36	4	28	42	58	46	54	255
Unstable platform	34	31	7	28	57	43	68	32	179
Geosyncline	35	24	8	33	44	56	51	49	364

Therefore, it may be concluded that: (a) depositional environment and textural maturity appear to be closely related; (b) tectofacies and depositional environment are related only in certain cases; (c) there is no general relation between tectofacies and textural maturity; and (d) there is no relation between tectofacies and mineralogical maturity or sandstone types.

CONCLUSIONS

The following conclusions are applicable in the Cretaceous, Paleocene, and Eocene of western Venezuela.

1. Detrital mineralogy, sandstone types, and mineralogical maturity appear to reflect source area petrography, weathering and erosion in the source area, and the mixing of sediments from different sources in the basin. Insofar as the morphology in the source area is controlled by tectonics, the petrography of the sediments also reflects the latter.
2. Mineralogical maturity does not reflect the tectofacies of the depositional basin.
3. No general relation exists between the tectonics of the source area and the depositional basin.
4. Sediment texture and textural maturity are controlled by depositional environment.
5. Depositional environments are controlled by numerous factors in addition to basin tectofacies, such as the morphology of the basin and the surrounding land, and the ratio between rate of supply and rate of subsidence.
6. Consequently, there is no systematic tectofacies control of texture and textural maturity.

A comparison with other studies of the relation between tectofacies and sediment characteristic that are based on sufficiently numerous observations, such as those of Pettijohn (1947) and Krynine (1941, 1942), shows little agreement with the conclusions of the present investigation. It seems to the writer that an explanation of these divergences can not be attempted yet on the basis of the available information. The results of the present study, however, show the need for caution in the application of theories concerning sediment genesis and for much additional work in this field.

REFERENCES

BOKMAN, J., 1955, "Sandstone Classification; Relation to Composition and Texture," *Jour. Sed. Petrology*, Vol. 25, No. 3, pp. 201–06.

BURRI, C., 1929, "Sedimentpetrographische Untersuchungen an alpinen Flusssanden, I: Die Sande des Tessin," *Schweiz. Min. Petr. Mitt.*, Vol. 9, pp. 205–41.

DAPPLES, E. C., W. C. KRUMBEIN, AND L. L. SLOSS, 1948, "Tectonic Control of Lithologic Associations," *Bull. Amer. Assoc. Petrol. Geol.*, Vol. 32, pp. 1924–47.

———, ———, AND ———, 1953, "Petrographic and Lithologic Attributes of Sandstones," *Jour. Geol.*, Vol. 61, No. 4, pp. 291–317.

DOEGLAS, D. J., 1940, "The Importance of Heavy Mineral Analysis for Regional Sedimentary Petrology," *Natl. Research Council Committee on Sedimentation Report 1939–1940*, pp. 102–21.

FOLK, R. L., 1951, "Stages of Textural Maturity in Sedimentary Rocks," *Jour. Sed. Petrology*, Vol. 21, No. 3, pp. 127–30.

———, 1954, "The Distinction between Grain Size and Mineral Composition in Sedimentary Rock Nomenclature," *Jour. Geol.*, Vol. 62, No. 4, pp. 344–59.

———, 1956, "The Role of Texture and Composition in Sandstone Classification," *Jour. Sed. Petrology*, Vol. 26, No. 2, pp. 166–71.

HEDBERG, H. D., AND L. C. SASS, 1937, "Synopsis of the Geological Formations of the Western Part of the Maracaibo Basin," *Bol. Geol. Miner. Caracas*, Vol. 1, Nos. 2–4, pp. 73–114.

KRYNINE, P. D., 1941a, "Paleogeographic and Tectonic Significance of Arkoses," *Bull. Geol. Soc. America*, Vol. 52, No. 12, p. 1918.

———, 1941b, "Paleogeographic and Tectonic Significance of Graywackes," *ibid.*, p. 1916.

———, 1941c, "Paleogeographic and Tectonic Significance of Sedimentary Quartzites," *ibid.*, p. 1916.

———, 1942, "Differential Sedimentation and Its Products during One Complete Geosynclinal Cycle," *Proc. 1st Pan Amer. Congr. Mining Eng. Geol.*, Vol. 1, pp. 537–61.

———, 1948, "The Megascopic Study and Field Classification of Sedimentary Rocks," *Jour. Geol.*, Vol. 56, pp. 130–65.

KOLDEWIJN, B. W., 1955, "Provenance, Transport and Deposition of Rhine Sediments. II, an Examination of the Light Fraction," *Geologie en Mijnbouw*, Vol. 17, No. 2, pp. 37–45.

KUYL, O. S., J. MULLER, AND H. TJ. WATERBOLK, 1955, "The Application of Palynology to Oil Geology with Reference to Western Venezuela," *ibid.*, Vol. 17, No. 3, pp. 49–76.

NOTESTEIN, F. B., C. W. HUBMAN, AND J. W. BOWLER, 1944, "Geology of the Barco Concession, Colombia," *Bull. Geol. Soc. America*, Vol. 55, pp. 1165–1216.

PACKHAM, G. H., 1954, "Sedimentary Structures as an Important Factor in the Classification of Sandstones," *Amer. Jour. Sci.*, Vol. 252, pp. 466–76.

PETTIJOHN, F. J., 1943, "Archean Sedimentation," *Bull. Geol. Soc. America*, Vol. 54, pp. 947, etc.

———, 1948, "A Preface to the Classification of Sedimentary Rocks," *Jour. Geol.*, Vol. 56, No. 2, pp. 112–17.

———, 1954, "Classification of Sandstones," *ibid.*, Vol. 62, No. 4, pp. 360–65.

———, 1957, *Sedimentary Rocks*. 2d ed. New York.

RENZ, O., R. LAKEMAN, AND E. VAN DER MEULEN, 1955, "Submarine Sliding in Western Venezuela," *Bull. Amer. Assoc. Petrol. Geol.*, Vol. 39, No. 10, pp. 2053–60.

———, 1956, "Cretaceous in Western Venezuela and the Guajira (Colombia)," *Proc. 20th Intern. Geol. Congr. Mexico.*

ROD, E., AND W. MAYNC, 1954, "Revision of Lower Cretaceous Stratigraphy of Venezuela," *Bull. Amer. Assoc. Petrol. Geol.*, Vol. 38, No. 2, pp. 193–283.

RODGERS, J. D., 1950, "The Nomenclature and Classification of Sedimentary Rocks," *Amer. Jour. Sci.*, Vol. 248, pp. 297–311.

RUSSELL, R. D., 1937, "Mineralogical Composition of Mississippi River Sands," *Bull. Geol. Soc. America*, Vol. 48, pp. 1307–48.

SCHAUB, H. P., 1948, "Outline of Sedimentation in Maracaibo Basin, Venezuela," *Bull. Amer. Assoc. Petrol. Geol.*, Vol. 32, No. 2, pp. 215–27.

SMITH, J. E., 1956, "Basement Reservoir of La Paz-Mara Oil Fields, Western Venezuela," *ibid.*, Vol. 40, No. 2, pp. 380–86.

SUTTON, F. A., 1946, "Geology of Maracaibo Basin, Venezuela," *ibid.*, Vol. 30, No. 10, pp. 1621–1741.

TRASK, P. D., 1932, *Origin and Environment of Source Sediments of Petroleum*. Houston.

VAN ANDEL, TJ. H., 1950, *Provenance, Transport and Deposition of Rhine Sediments, I, a Heavy Mineral Study on River Sands from the Drainage Basin of the Rhine*. Groningen.

WILLIAMS, H., F. J. TURNER, AND C. M. GILBERT, 1954, *Petrography*. San Francisco.

YOUNG, G. A., A. BELLIZZIA, H. H. RENZ, F. W. JOHNSON, R. H. ROBIE, AND J. MAS VALL, 1956, "Geologia de las cuencas sedimentarias de Venezuela y de sus campos petroliferos." *Symposium sobre Yacimientos de Petroleo y Gas*, Vol. IV, XX Congr. Geol. Intern. Mexico.

(264)

Reprinted from Biological Bulletin, Vol. 114, No. 2, pp. 247–254, April, 1958
Printed in U. S. A.

THE PRODUCTION OF TWIN EMBRYOS IN DENDRASTER BY MEANS OF MERCAPTOETHANOL (MONOTHIOETHYLENE GLYCOL)[2]

DANIEL MAZIA[1]

Scripps Institution of Oceanography, University of California,
La Jolla, California, and Department of Zoology,
University of California, Berkeley, California

The problem of individuation in the earliest embryonic development of certain animal groups resolves itself into questions concerning the interaction of blastomeres. Some transaction *between* the blastomeres determines that the first division will produce an individual composed of two cells rather than two individual embryos. Physical contiguity is a factor by definition, for, in those cases where the blastomeres are capable of producing complete embryos, such "twinning" can always be achieved by complete separation of the blastomeres. But complete physical separation is not necessary for functional isolation of the blastomeres; from studies of echinoid eggs we have a variety of experimental conditions under which twin embryos are produced from sister blastomeres in contact with each other (summarized by Schleip, 1929; Harvey, 1940). The experimental problem is to define the means—not necessarily a single one—whereby adjacent cells can mutually influence or restrict each other's behavior. The question is of interest in research on cell division as well as on developmental problems, and probably has much broader implications relative to the behavior of multicellular systems. In the case of echinoid eggs, it has received a good deal of attention, particularly in studies on cell division, and some of the ideas regarding the mechanisms are reviewed in a paper by Dan and Ono (1952).

Our chemical insights into the mechanisms of blastomere interaction are rather rudimentary, centering on the study of "extracellular coats" or "intercellular cements" which have, for good reasons, been characterized as calcium proteinates.

The present work is part of a series of studies in which mercaptoethanol (monothioethylene glycol) was employed as an agent which was expected to interfere with the association of protein molecules through thiol groups. The considerations underlying the study and the selection of this agent are discussed in another paper (Mazia, 1958). It was found, with the eggs of *Dendraster excentricus*, that treatment with mercaptoethanol at the proper time would produce twins in very high yields even though the blastomeres remained in contact within the fertilization

---

[2] Contributions from the Scripps Institution of Oceanography, New Series, No. 995.

[1] Permanent address: Department of Zoology, University of California, Berkeley. The major part of this work was done during the tenure of a visiting professorship at the Scripps Institution of Oceanography, University of California, La Jolla, California. The author thanks the director and staff of that institution for this opportunity and for their valued cooperation. The work was completed during the tenure of a research professorship in the Adolph C. and Mary Sprague Miller Institute for Basic Research in Science at Berkeley. Material support from the American Cancer Society and the Office of Naval Research is gratefully acknowledged.

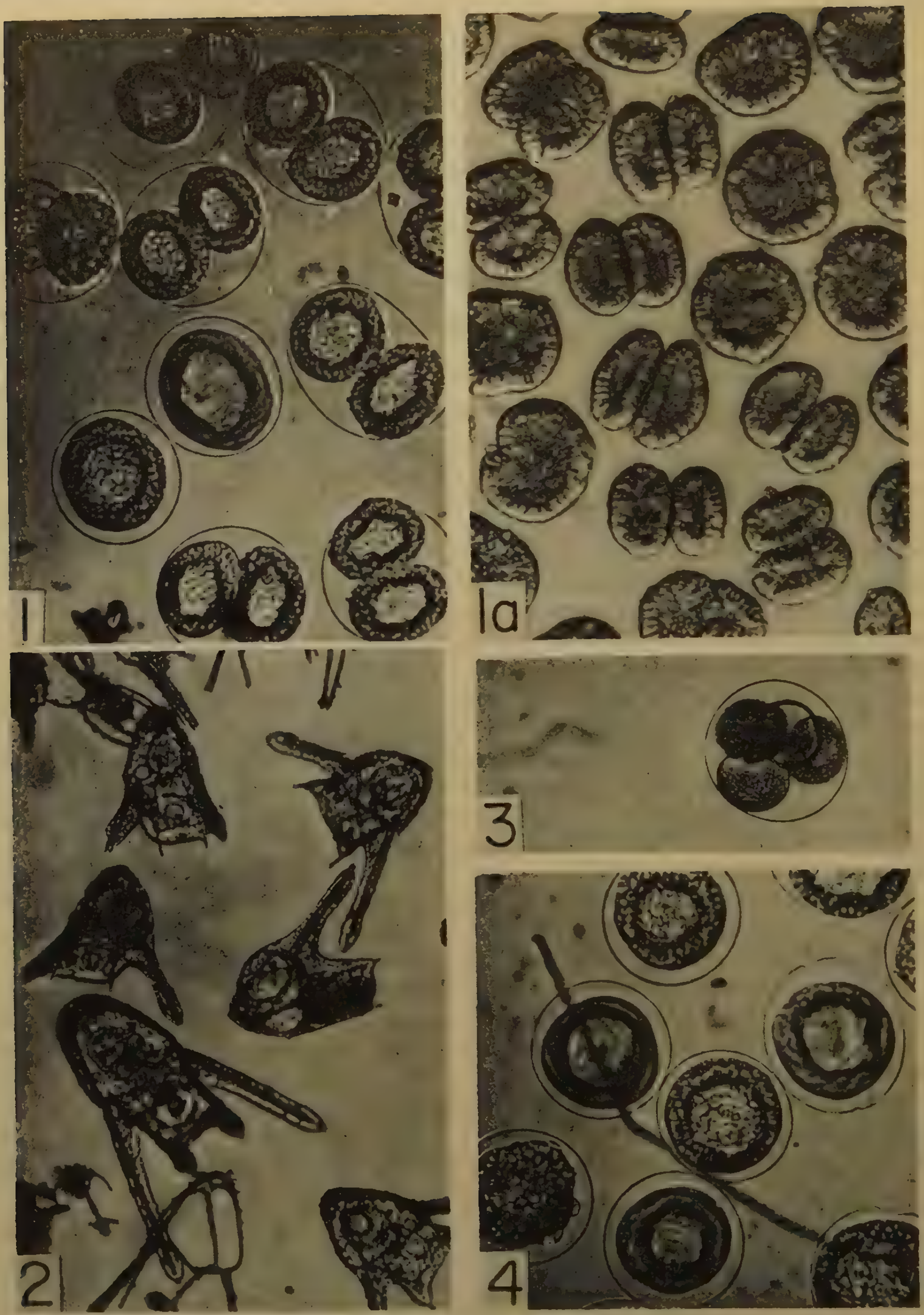

FIGURE 1. Twin blastulae. *Dendraster* eggs had been placed in 0.1 *M* mercaptoethanol in sea water at 41 minutes after insemination, and exposed for 28 minutes. Photographed alive at 7 hours 15 minutes after insemination. Twins are hatching in embryo at top of photograph.

membrane. The points of interest in the following discussion are not only the interpretation of the effect as one implicating thiol groups in blastomere interaction, but also the fact that processes determining the twinning or non-twinning may be restricted to a short period *during* the cleavage of the eggs.

METHODS

The details of the methods used will be found in a previous paper (Mazia, 1958). The eggs of *Dendraster excentricus,* obtained in Mission Bay, San Diego, California, were used. At various times after fertilization, nine volumes of egg suspension were mixed with one volume of 1 *M* 2-mercaptoethanol (Eastman) in sea water. A common synonym for mercaptoethanol ($HSCH_2CH_2OH$) is monothioethylene glycol. After various times of exposure, the eggs were washed in sea water and their development was followed. When the fertilization membrane was to be removed, this was done by treatment with a solution of Worthington "Crude Protease" in sea water (0.1 mg. per ml.). In the case of the *Dendraster* egg, the protease may be introduced a few minutes after fertilization, and the dissolution of the fertilization membrane may be observed visually. The fact that the membrane of *Dendraster* eggs is susceptible to protease for some time after fertilization was called to my attention by Dr. William E. Berg.

RESULTS

The over-all study of which this is a part concerned the blockage of mitosis by mercaptoethanol. The essential finding was that 0.1 *M* solutions would block division completely if applied at any time up to the time of metaphase, which takes place at about 35–40 minutes after fertilization, at 24° C. If the mercaptoethanol is applied at any time after this critical point, the cells divide without delay, and if left in the mercaptoethanol are blocked reversibly in the two-cell stage. In the course of observations on the reversibility of the block it was noted that a large proportion of those eggs which had cleaved while in the mercaptoethanol gave rise to twin blastulae when returned to sea water. Such a population containing the twin blastulae is shown in Figure 1. These blastulae gastrulate and develop into normal plutei (Fig. 2).

In order to obtain twinning, the mercaptoethanol must be applied during the period of furrowing. This is shown in Table I, where the yield of twins from eggs placed in mercaptoethanol at various times from metaphase to the completion of furrowing is given. At 35 minutes after fertilization, half of the eggs are blocked

---

FIGURE 1A. Another group of twin blastulae, fixed in 1 per cent formaldehyde in sea water. In this experiment, evidence of incomplete twinning is seen in some individuals.

FIGURE 2. Plutei produced by twinned embryos. The small plutei are the products of twinning. The large pluteus, from an egg which failed to produce twins, serves as a control.

FIGURE 3. Second cleavage of *Dendraster* egg in Ca-free sea water, showing irregular positions of blastomeres. Eggs had been placed in Ca-free sea water at 30 minutes after fertilization and exposed for 60 minutes, during which time the first and second cleavages occurred.

FIGURE 4. Blastulae from eggs that had been exposed to Ca-free sea water from thirtieth to ninetieth minute after fertilization (*cf.* Fig. 3). This experiment paralleled that shown in Figure 1, used the same lot of fertilized eggs and was photographed at the same time as Figure 1. Rotating blastulae gave blurred photographs.

and half have passed into the insensitive stage following metaphase. The latter are blocked in the two-cell stage. Upon return to sea water after 30 minutes in mercaptoethanol, those that had divided in the mercaptoethanol gave rise to twin embryos. Those that were blocked before the first division gave single embryos. By the thirty-eighth minute after fertilization, all of the cells had passed the critical stage, divided in mercaptoethanol and gave rise to a large proportion of twin embryos. Around 45 minutes after fertilization, when most of the cells were well advanced in cleavage at the time the mercaptoethanol was introduced, the yield of twin embryos began to decrease rapidly. If mercaptoethanol was introduced 10 minutes later, the number of twins produced was small.

The critical time for twinning thus comes immediately after the critical time for mitotic blockage, as determined in the previous study (Mazia, 1958). The maximum yield of twins is obtained when the mercaptoethanol is introduced just at the time of the mitotic elongation of the cleavage furrows. The duration of the exposure to mercaptoethanol seems to have relatively little significance. What is important is that it acts during the brief effective period: the 5–10 minutes during which mitosis is completed and furrowing is going on.

TABLE I

Production of twin embryos from Dendraster eggs placed into 0.1 M mercaptoethanol at various times after fertilization

Time after fertilization when mercaptoethanol was introduced* (minutes)	Per cent cleavage in mercaptoethanol	Per cent twin blastulae**
35	50	50
38	90	85
41	95+	90
44	95+	45
47	95+	30
50	95+	8
53	95+	8

* Duration of mercaptoethanol treatment: 30 minutes.

** These percentages are relative to the total number of blastulae, and do not take into consideration individuals which degenerated before reaching the blastula stage. In the particular experiment from which Table I is taken, about 15 per cent of the eggs treated at 38, 41 and 44 minutes degenerated.

Another kind of variation of "sensitivity" to mercaptoethanol with time should be mentioned, though it has not yet received adequate study. This is evidenced by the failure of some of the eggs to form normal blastulae, single or double. This was not recorded in Table I, where the fraction of twin blastulae is given relative to the total number of blastulae. To illustrate, in the experiment given in Table I, a yield of 90 per cent twins from eggs exposed at 41 minutes after fertilization was given. In the whole population, 15 per cent of the eggs failed to form normal blastulae, so that the yield of twins could also be given as 78 per cent—still a very high figure.

The best-studied methods of obtaining multiple embryos from echinoderm eggs involve modification of the ionic content of the environment, whether by removing

Ca or other ions or by varying the concentration of the sea water in the direction of hypotonicity or hypertonicity. In the present study, the effects of Ca-free sea water were compared with those of mercaptoethanol. A small volume of fertilized eggs (less than 0.5 ml.) was washed by centrifuging and re-suspending in 15 ml. of Ca-free sea water four times, beginning at 30 minutes after fertilization. The

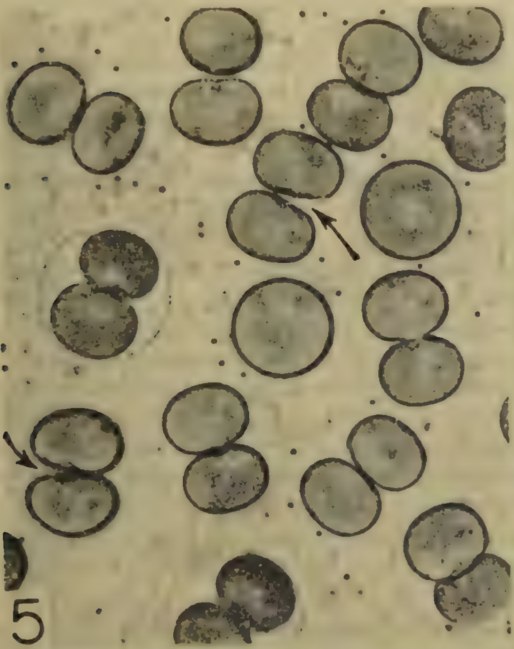

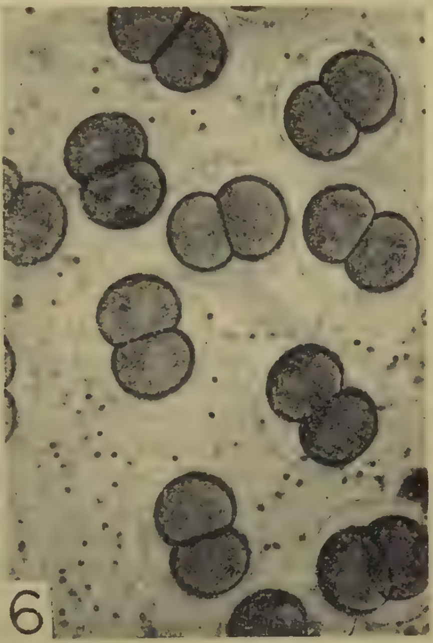

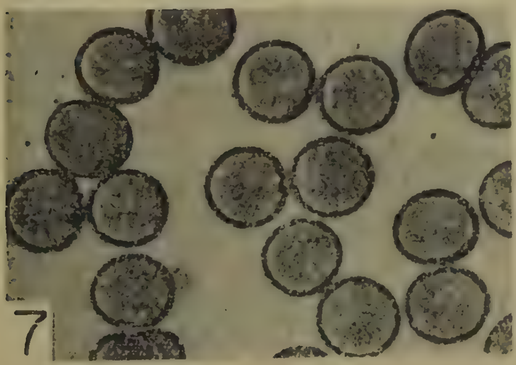

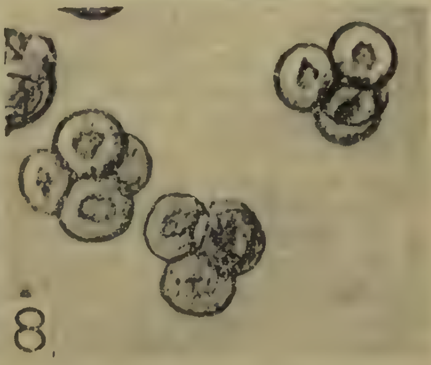

FIGURE 5. *Dendraster* eggs with fertilization membranes cleaving in 0.1 *M* mercaptoethanol. Blastomeres are not so firmly apposed as in control (Fig. 6), but appear to be connected by strands of clear material (arrows).

FIGURE 6. Control for Figure 5. Eggs have just completed cleavage in normal sea water.

FIGURE 7. *Dendraster* eggs without fertilization membranes just after cleavage in 0.1 *M* mercaptoethanol.

FIGURE 8. Quadruplets produced when mercaptoethanol treatment is applied at both the first and second divisions.

fertilization membranes were not removed. The eggs were permitted to go to the four-cell stage in Ca-free sea water before being returned to normal sea water. It was clear by this time that the Ca-deficiency was having its expected effect on blastomere adhesion. The first cleavage blastomeres were not flatly apposed, as was the case in the control, and the planes of the second cleavages did not coincide (Fig. 3). Nevertheless, long treatment with Ca-free sea water did not cause twinning (Fig. 4). Apparently, the embryo can organize itself to form a single blastula, following the treatment with Ca-free sea water, as long as the blastomeres are held together within the fertilization membrane. This corresponds with Harvey's (1940) experience with hypertonic sea water. It should be mentioned that the results in Figure 1 and Figure 4 were obtained with the same lot of eggs.

The mercaptoethanol does visibly affect the adhesion of the blastomeres. Figure 5 shows eggs that have cleaved in mercaptoethanol, the fertilization membrane being present. While they are compressed together, we do see rather more separation than in the controls (Fig. 6), and also see strands of glassy-appearing material between the blastomere surfaces in the furrow. If the fertilization membranes have been removed by protease, the cleavage in mercaptoethanol gives fully spherical blastomeres (Fig. 7), connected by tenuous strands, an appearance almost identical with that of membrane-free eggs that have cleaved in Ca-free sea water.

It would be predicted that if the mercaptoethanol was applied again at the time of the second cleavage, quadruplets would be produced. This was the case, as shown in Figure 8. The yield of quadruplets was never as high as that of twins. This would be expected from the fact that the eggs were not as synchronous in their second cleavage. In a desynchronized population a good many of the embryos will either be in a stage earlier than metaphase, at which they will merely be blocked, or at a stage later than the sensitive part of cleavage (Table I), in which case the mercaptoethanol will not be effective.

Finally, it should be mentioned that the effect of mercaptoethanol could not be duplicated with ethanol or with ethylene glycol, the analogs lacking the SH group. The latter may be considered the active center, and other SH compounds might have similar effects. The writer has found none that is comparably nontoxic and therefore usable at such high concentrations.

DISCUSSION

Two questions demand discussion: (1) the chemical interpretation of the effect of mercaptoethanol in inducing twinning, and (2) the relation of the results to the earlier observations on twinning and on blastomere adhesion. The most reasonable interpretation of the chemistry of the observed effect is that the mercaptoethanol is affecting some interaction between the blastomeres that involves the formation of S—S bonds. This reagent is commonly used for reducing S—S bonds in proteins (Olcott, 1942). It has been seen that its analogs lacking the SH group are ineffective in inducing twinning. The results would be in accord with the hypothesis that the blastomere interaction depends on the formation of a gel serving as a cement between the blastomeres, and would fit equally well with a hypothesis calling for the establishment of fibrous connections between the blastomeres. The formation of protein gels by the establishment of intermolecular S—S bonds has been described by Huggins *et al.* (1951). The role of S—S bonds in the formation of protein fibers is well known from studies on the keratins. Mercaptoethanol would be expected to block such intermolecular bonding by preventing the oxidation of the SH or by competing with protein SH.

The fact that the mercaptoethanol is effective only during a short period and is ineffective later would lead to the conclusion that we are dealing with the formation of the inter-blastomere links during the cleavage process itself. The mercaptoethanol is effective in preventing the formation of the links but not in splitting them once they are formed. This might mean that it acts by competition with protein SH in the formation of S—S bonds, not by reduction of S—S. It might also mean that the protein S—S becomes inaccessible to the reagent or that sufficient secondary bonds are formed, following the establishment of the intermolecular S—S links, to hold the structure together in the face of the reduction of the latter. In any event, the results imply that during cleavage, connections are formed between the blastomeres. The alternative explanation is that pre-existing factors tending to hold the blastomeres together (*e.g.* the hyaline layer as envisaged by Dan and Ono, 1952) undergo a change that renders them susceptible to mercaptothanol during the brief period of cleavage.

These results do not stand in contradiction to any of the previous observations regarding the induction of twinning by other means and especially by variations in the ionic environment. These have been interpreted, with some difference of opinion as to the details, as reflecting the significance of extracellular layers having the character of calcium proteinates (Moore, 1949; Hagström and Hagström, 1954). The physical properties of such layers are known to be affected by the ionic composition of the medium; obviously they will also depend on the protein-to-protein links that make their existence as stable masses possible. The contrast between the effects of Ca-free sea water and of mercaptoethanol in the present experiments is explicable on the assumption that the Ca-free sea water softens the layers but does not dissolve them quickly, while the mercaptoethanol actually solubilizes newly-appearing or pre-existing protein that would normally function in holding the blastomeres together. Thus the effect of Ca-free sea water might be reversible where the effect of mercaptoethanol was not.

The most striking feature of the mercaptoethanol effect is its complete irreversibility with respect to the division during which the reagent was applied, and its complete lack of effect on subsequent divisions. If it is applied at first cleavage, the blastomeres are "isolated" but subsequent divisions are normal, and the end result is fully normal twins in a large proportion of the population. If it is applied again at the second division, there is a fair yield of normal quadruplets. The results are not perfect: some incomplete twinning and occasional quadruplets are observed when the treatment takes place at the first division and some triplets are obtained when the treatment is given at the first and second divisions. On the whole, however, the results may be described as the effective and irreversible isolation of blastomeres by chemical means.

SUMMARY

1. When *Dendraster* eggs are permitted to cleave in 0.1 M mercaptoethanol in sea water and then restored to normal sea water, a large proportion of the embryos develops as twins, producing normal twin plutei.

2. The effectiveness of the mercaptoethanol treatment is restricted to the short period during which the first cleavage furrows are forming.

3. If the treatment is repeated at the time of the second cleavage, quadruplets are produced.

4. Twins are not produced when the eggs cleave in Ca-free sea water.

5. The results are discussed in terms of the significance of the thiol groups of proteins for the interactions of blastomeres.

LITERATURE CITED

Dan, K., and T. Ono, 1952. Cyto-embryological studies of sea urchins. I. The means of fixation of the mutual positions among the blastomeres of sea urchin larvae. *Biol. Bull.,* **102**: 58–73.

Hagström, B., and Britt Hagström, 1954. The action of trypsin and chymotrypsin on the sea urchin egg. *Exp. Cell Res.,* **6**: 532–534.

Harvey, E. B., 1940. A new method of producing twins, triplets, and quadruplets in *Arbacia punctulata,* and their development. *Biol. Bull.,* **78**: 202–216.

Harvey, E. B., 1956. The American *Arbacia* and Other Sea Urchins. Princeton University Press, Princeton, New Jersey.

Huggins, C., D. F. Tapley and E. V. Jensen, 1951. Sulphydryl-disulphide relationships in the induction of gels in proteins by urea. *Nature,* **167**: 592–593.

Mazia, D., 1958. SH compounds in mitosis. I. The action of mercaptoethanol on the eggs of the sand dollar *Dendraster excentricus. Exp. Cell Res.* (in press).

Moore, A. R., 1949. On the precursors of the fertilization and the hyaline membranes in the eggs of the sea urchin *Stronglycentrotus purpuratus. Biodynamica,* **6**: 197–212.

Olcott, H. S., 1942. Monothioglycol. *Science,* **96**: 454.

Schleip, W., 1929. Die Determination der Primitiventwicklung. Akademische Verlagsgesellschaft, Leipzig.

Sedimentation of the northwestern Gulf of Mexico

By

F. P. Shepard
La Jolla

With 10 figures

Sonderdruck
aus der
Geologischen Rundschau
Bd. 47, Heft 1, Seite 150—167. 1958

FERDINAND ENKE VERLAG STUTTGART

(273)

SEDIMENTATION OF THE NORTHWESTERN GULF OF MEXICO[1]

By FRANCIS P. SHEPARD [2]), *La Jolla, California*

With 10 figures

Abstract

Six years of intensive study of the shallow water sediments of the northwestern Gulf of Mexico have indicated that there are many criteria by which ancient sediments deposited under similar conditions can be recognized. Thus the presence of echinoid fragments and of glauconite-filled Foraminifera tests favors marine shelf deposition over bay deposits; calcareous aggregates and grains of gypsum suggest high salinity bay deposits; abundance of wood fibers, high mica content, ferruginous aggregates, and well laminated sediments all are suggestive of deposition near river mouths; greater roundness distinguishes

---

[1]) Contribution from the Scripps Institution of Oceanography, New Series No. 997. Investigation supported by a grant from American Petroleum Institute, Project 51.

[2]) Scripps Institution of Oceanography, University of California, La Jolla, California.

Reproduced by Permission

(274)

dunes from adjacent beach sands; and coarser grain size distinguishes beach sands from shallow shelf sands in the vicinity.

Faunal assemblages of Foraminifera, Ostracoda, and Mollusca all serve to distinguish between bay and shelf deposits. Within the bays the faunas show a close relationship to salinity conditions whereas on the shelf the faunas are arranged in bands parallel to the shore and to the depth contours. Certain generalizations concerning the relation of faunas to environment can be made without detailed knowledge of the species.

Introduction

In 1951 a project supported by the American Petroleum Institute was initiated at Scripps Institution for the purpose of studying the characteristics of recent marine sediments as they are related to depositional environments. The hope has been that this information could be used to help distinguish the environments of deposition of ancient sediments. Most of this work has been carried on at Scripps Institution of Oceanography, although a few projects have centered elsewhere.

The first locality used for a concentrated study was the northwestern Gulf of Mexico, extending from the Mexican border to the Mississippi Delta. Here investigations have centered around the Mississippi Delta, the bays of the central Texas coast, the Laguna Madre, which is located along the southern Texas coast, and the continental shelf. Approximately 4,000 samples have been taken during the past six years and most of these have now been analyzed by a variety of methods. In addition, borings have been made into the bays and barrier islands of the Texas coast, reaching to depths of about 25 meters. Shoaler borings have been made into the Mississippi Delta and samples have been studied from borings made by various federal and state agencies. All of this work has helped round out the third-dimensional picture of these sedimentary environments and has given some insight into the early stages of diagenesis during the burial of sediments.

The study of the sediments, although not as complete as could be desired, has gone somewhat further than many other investigations of recent sediments since it has involved the joint efforts of scientists in the fields of physical aspects of sediments, Foraminifera, Ostracoda, macroorganisms, microfossils, organic productivity, clay mineralogy, chemistry, petrography, and physical oceanography.

In the sediment studies there has been particular emphasis on estimating the percentages of coarse fraction constituents, as determined from the microscopic examination and counting of fractions sieved to standard sizes of 62—125, 125—250, 250—500, 500—1,000 microns and larger than 1,000 microns. To date, 36 papers, many of which are included in the bibliography, have been published concerning the results of this work. Others are in various stages of completion. The present paper represents a summary of the work on the project with especial attention to phases of sedimentation.

The areas chosen for the study have proven fruitful since they represent environments in which sedimentation has been continuing for a long time under conditions which appear to have been similar to those of the present day. The coastal areas along the Gulf Coast are sinking slowly so that at least 6,000 meters of sediments were deposited during the Tertiary along most of this coast (Murray et al. 1952, and various personal communications from oil geologists). Much of this thick column can be compared directly with the shallow water sediments now being deposited.

Texas Bays

The coast of Texas from the Mexican border almost to the Louisiana line is flanked by a series of sandy barrier islands (offshore bars) enclosing elongate lagoons, which run parallel to the islands, and rather stubby partly filled estuaries which extend into the coast at right angles to the barriers (fig. 1). All of these bays are shallow, with water rarely exceeding 5 meters in depth. Inlets connect all of the northern bays to the open Gulf, whereas to the south the Laguna Madre extends for over 62 kilometers with Gulf connections only to the north and south. Most of the northern bays receive large supplies of fresh water from Texas rivers, although this supply is extremely variable in amount, having been very low in recent years[3]. To the south there are virtually no rivers entering the extensive Laguna Madre, partly because of the low rainfall in the adjacent portion of Texas and partly because the main drainage coming down from the southern Rocky Mountains enters the sea by the way of the Rio Grande to the south of the Laguna. Because of the combination of inlets and entering rivers to the north, the salinity is extremely variable, both in point of time and according to position in the bay. Normally there is very low salinity near the deltas at the heads of the bays and relatively high salinity near the inlets. During dry periods evaporation raises the salinity of the lower bays above that of the Gulf. To the south, in the Laguna Madre, where under normal conditions there are no entering streams, the salinity is raised well above that of the Gulf of Mexico, especially in the northern portions of the lagoon where it commonly reaches about 60—80‰.

Considering first the sediments of the northern type of bay, we find that there are several influences which determine the character of the sediment (see Shepard and Moore 1955, pp. 1488—1497). In the first place, the rivers are supplying large amounts of fine material in which clay predominates, although silt is also an important constituent. The lower bays, on the other hand, are receiving considerable sediment from the beaches and from the open Gulf introduced through inlets and by way of washover fans during times of high storm tides which traverse low passes in the barrier island. This lower bay sediment is predominantly sand-sized but in a zone between the upper bays, where clayey sediments predominate, and the lower bays with their sandy sediments, there are areas where clay and sand are mixed. Silt-size material is less abundant than either clay or sand.

---

[3] As this is being written this condition has been radically changed as the result of the tremendous Texas floods of the spring of 1957.

In some of the deeper bays at a distance from the river mouths, the clayey sediments from the rivers are introduced only in small quantities and little sand is washed in from the inlets or from the overwash channels. As a result, sedimentation proceeds very slowly and microscopic examination of the coarse fraction of the sediment often shows that Foraminifera constitute a major fraction of the sand-sized material. Oyster reefs provide another special sediment of these northern bays.

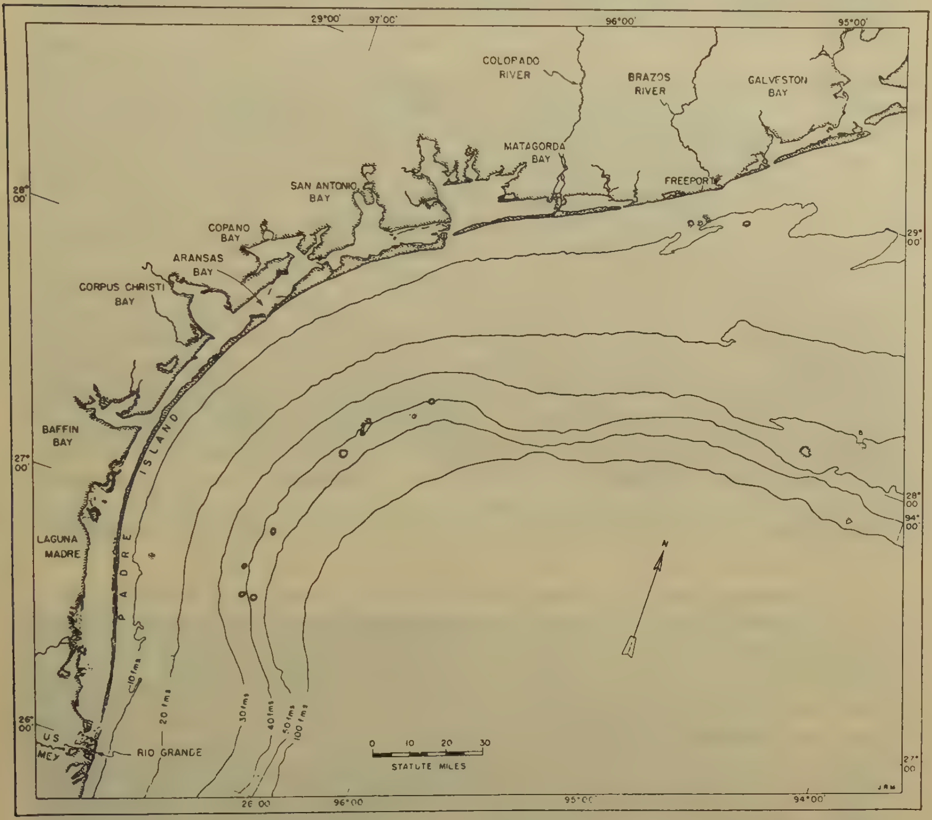
29°00'
97°00'
96°00'
95°00'
COLORADO RIVER
BRAZOS RIVER
GALVESTON BAY
MATAGORDA BAY
FREEPORT
SAN ANTONIO BAY
COPANO BAY
ARANSAS BAY
CORPUS CHRISTI BAY
BAFFIN BAY
LAGUNA MADRE
PADRE ISLAND
28° 00'
27° 00'
26° 00'
29° 00'
28° 00'
94° 00'
27° 00'
10 fms
20 fms
30 fms
40 fms
50 fms
100 fms
US
MEX
RIO GRANDE
0 10 20 30
STATUTE MILES
N
26 00
96°00
95°00
94°00
J.R.M.

Fig. 1. Indicating the geographic nature of the Texas bays and of the principal rivers which come into the coast. The extensive Laguna Madre is seen to the south with its virtual absence of entering streams

Since the common oyster *Crassostrea virginica* is largely confined to waters of intermediate salinity, these reefs develop principally in the central portions of the bays. The sediment in the reefs consists predominantly of oyster shells with an admixture of clayey sediments and of various small organisms which prey on the oysters. If consolidated, these reefs would become bioherms of impure limestones cutting across the clayey and sandy shales constituting the other bay deposits. The shales formed from the deposits of the northern bays would show little structure and would be largely devoid of stratification except near the river mouths.

The sediments of the Laguna Madre 4) in the semi-arid area to the south differ quite strikingly from those of the northern bays. Most of the material is derived from the barrier islands, partly by overwashes and partly by windblown sand from the extensive dunes of Padre Island where vegetative cover is very scanty. Accordingly, sand-size material predominates in the Laguna, although there are local areas with high clay content. The sediments of the Laguna Madre commonly have calcareous aggregates apparently related to the high evaporation. Locally aragonite has coated the sand grains, particularly along the shoreline, developing calcareous ooliths. The Laguna Madre, unlike the northern bays has stratified sediments in many places (fig. 2). The benthonic organisms which stir up the bottom of the northern bays and destroy stratification are lacking in much of the Laguna, apparently because of the sterile condition for burrowing organisms existing under the waters of this bay. A constituent of the Laguna sediments rarely found to the north is gypsum. Small amounts of this mineral are scattered through the upper sediments, and gypsum rosettes have been found at depths of one or two meters below the surface. The latter represent slow authigenic development within the shallow subsurface sediments (Masson 1955).

The sediments of the barrier islands of the Texas coast are predominantly sandy. Where the islands reach a width of several kilometers, they usually contain three divisions or facies: broad beaches along the Gulf shore; extensive dune tracts; and barrier flats which have numerous lakes and are cut by channels (fig. 3). The beaches and dunes have sediments that are virtually indistinguishable except for a greater roundness in the dune sands than in the sands of the adjacent beaches (Beal and Shepard 1956). The dunes also have a somewhat smaller quantity of shell material and a somewhat larger quantity of plant remains than the beach sands. The sediment in both the beaches and dunes consists of almost 100 percent sand with a diameter from 62 to 250 microns. The barrier flats on the other hand have small percentages of silt and clay, generally not more than 30 percent. Stratification is found in the barrier island sediments in all three of the facies. The beach sands are not as well stratified as in many other areas because of the scarcity of layers of dark minerals which produce the excellent lamination in beach sands. The dunes have

---

4) Currently under study by G. A. Rusnak.

Fig. 2. A. Cores in San Antonio Bay in which the stratification has been destroyed by organisms. B. Stratified sediments of the Laguna Madre where organisms are less active

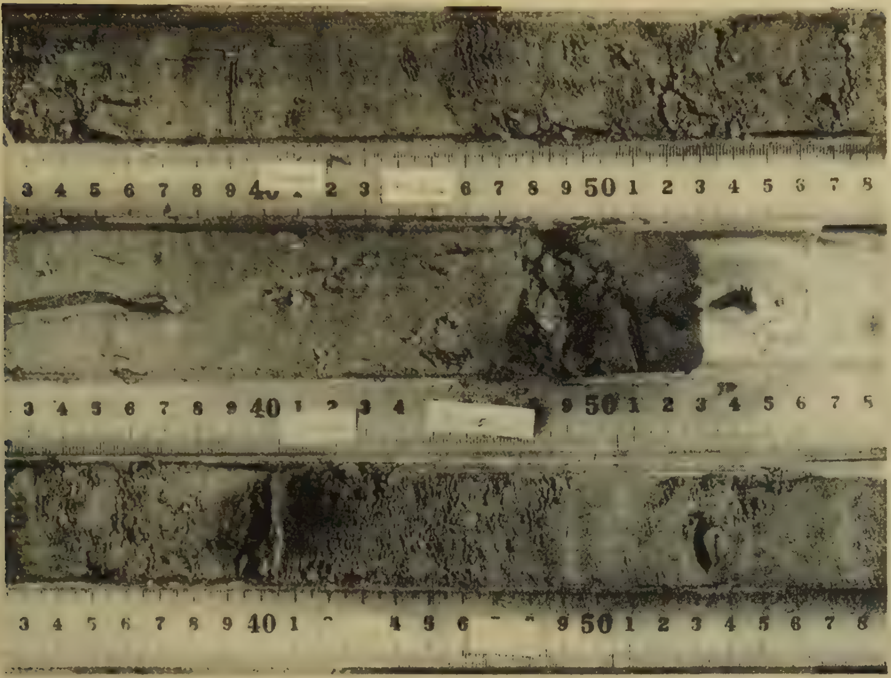

Fig. 2A

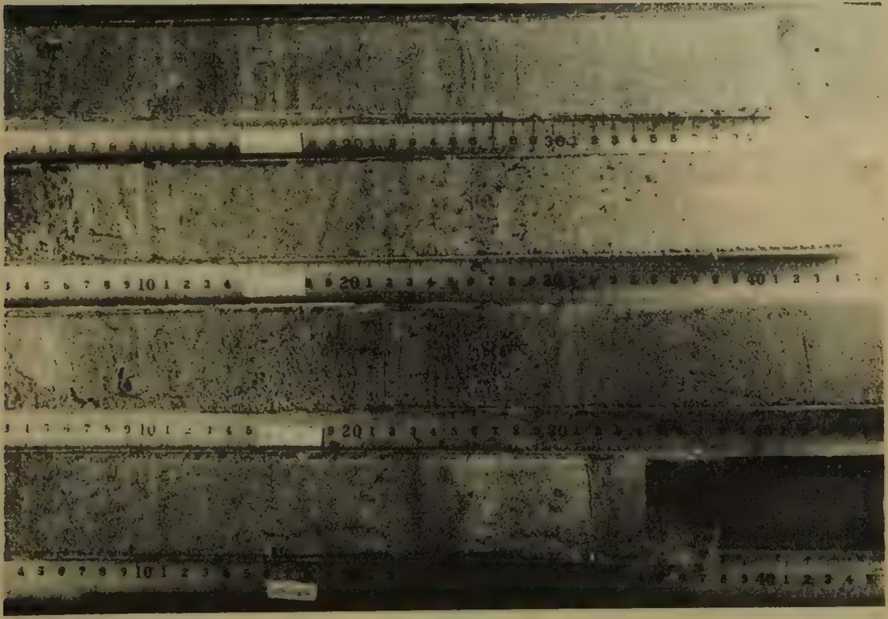

Fig. 2B

the cross lamination characteristic of other dune areas, although here again the lamination is not as easy to see because of the absence of distinctive layers in most places. Lamination is brought out by etching of a windstorm acting on the dunes, but does not show very well in cores. The stratification in the barrier flats is not always evident, but in some places where ditches have been cut into the overwash fans, the stratification can be plainly seen. In these places the beds are essentially horizontal, contrasting with the dunes and the foreshore of the beaches.

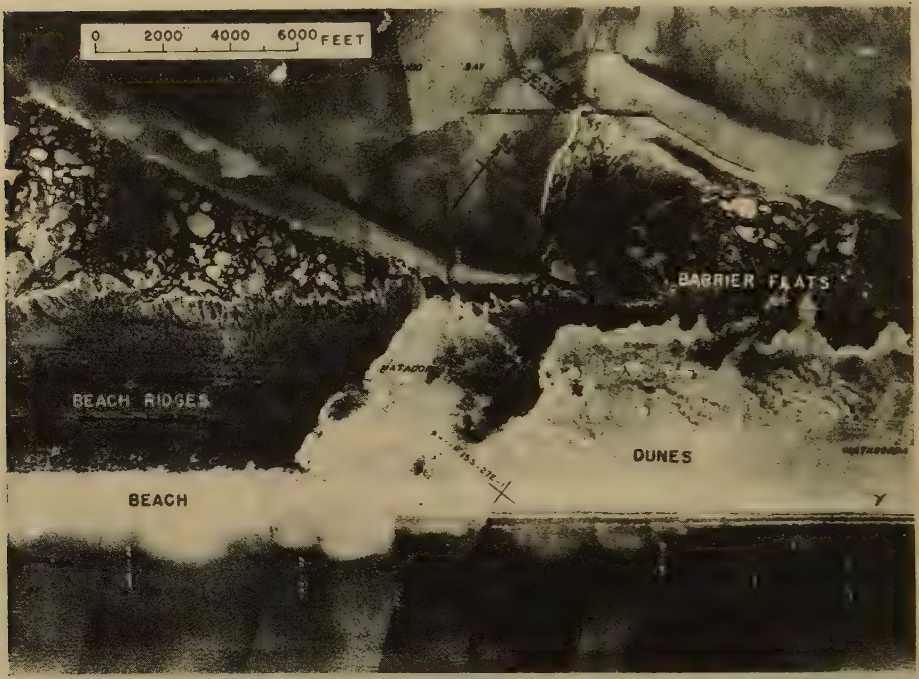

Fig. 3. Air photo of Matagorda Island showing the three principal facies of the Texas barrier islands. The "beach ridges" have been determined to be actually dune ridges

Borings in the Texas Bays and Barrier Islands

A series of shallow borings have been made in the Texas bays and barrier islands (Shepard and Moore 1955, pp. 1546—1577). One line with 11 holes (fig. 4) extended down the Guadalupe Delta, along the length of San Antonio Bay, and across the adjacent barrier island. The cores from these holes show that present day conditions of bay and barrier island can be traced back into the past for almost 9,000 years. Thus the intermediate salinity necessary for oyster reefs seems to have existed in the central portions of these bays over long periods because as much as 12 meters of oyster reef material was encountered in one hole in the central portion of the bay and a carbon 14 age of about 8700 years (Kindly supplied by Magnolia Petroleum Company) was determined from the base of the reef. During this same time in the lower bays fine-grained sediments containing bay faunas have accumulated to thicknesses of as much as 25 meters. Below these bay sediments river deposits of an older cycle were encountered. In the upper bay, indications of deposition near a river mouth are found in most of the underlying sediments. The Guadalupe Delta is only about 1 or 2 meters thick, but the true deltaic sediments are underlain by low salinity bay deposits. In the barrier island borings, beach, dune, and barrier flat deposits are found to depths of as much as 18 meters. A shell layer in these sands found at 14 meters yielded a carbon 14 age of about 6,500 years.

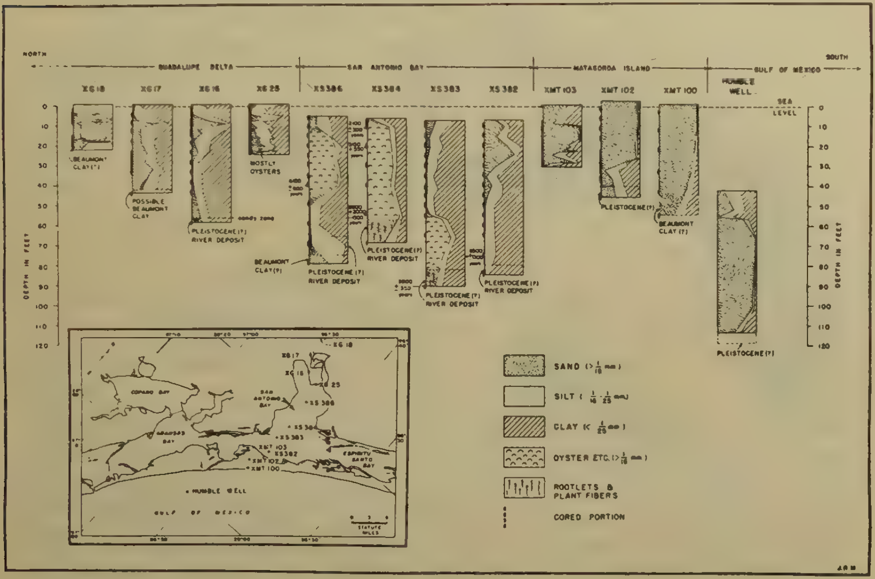
NORTH
GUADALUPE DELTA
SAN ANTONIO BAY
MATAGORDA ISLAND
GULF OF MEXICO
SOUTH
XG 18
XG 17
XG 16
XG 25
XS 386
XS 384
XS 383
XS 382
XMT 103
XMT 102
XMT 100
HUMBLE WELL
SEA LEVEL
DEPTH IN FEET
0
10
20
30
40
50
60
70
80
90
100
110
120
BEAUMONT CLAY (?)
POSSIBLE BEAUMONT CLAY
MOSTLY OYSTERS
sandy zone
PLEISTOCENE (?) RIVER DEPOSIT
BEAUMONT CLAY (?)
PLEISTOCENE (?)
COPANO BAY
SAN ANTONIO BAY
ARANSAS BAY
ESPIRITU SANTO BAY
HUMBLE WELL
GULF OF MEXICO
STATUTE MILES
SAND (> 1/16 mm)
SILT (1/16 - 1/256 mm)
CLAY (< 1/256 mm)
OYSTER ETC. (> 1/16 mm)
ROOTLETS & PLANT FIBERS
CORED PORTION

Fig. 4. A north-south section through the Guadalupe Delta, San Antonio Bay, and the adjacent barrier island indicating the relative uniformity of material extending to considerable depths below the present surface in most borings. Dates at several points were determined by Magnolia Petroleum Co. by a Carbon 14 technique

Some indications of diagenesis are found in the borings. Thus, there is a small decrease in water content. Some of the clays develop parting planes at about 20 meters. Calcium carbonate content shows a net decrease but organic carbon and nitrogen remain the same.

These borings indicate a history of barrier islands developing during the time of rising sea level some 9,000 years ago and growing upward and keeping pace with the rise so that protected bays could exist throughout this long period. A complication of all available carbon 14 dates from the Gulf coast and elsewhere indicates that the rise of sea level may have continued virtually up to the present time (early version in Shepard and Suess 1956). The detailed study of the sediments in the Texas coast borings favors such a history.

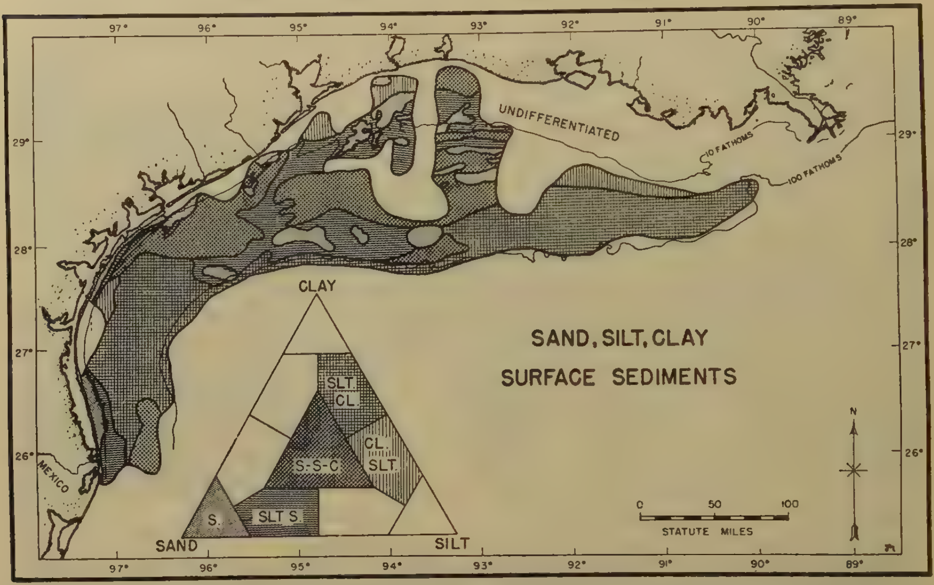
97°
96°
95°
94°
93°
92°
91°
90°
89°
29°
28°
27°
26°
UNDIFFERENTIATED
10 FATHOMS
100 FATHOMS
MEXICO
CLAY
SLT.
CL.
CL.
SLT.
S-S-C
S.
SLT S.
SAND
SILT
SAND, SILT, CLAY
SURFACE SEDIMENTS
N
0
50
100
STATUTE MILES

Fig. 5. Showing the variation of textures in the sediments of the continental shelf extending from the Mexican border to the Mississippi Delta. The relative percentages of sand, silt and clay are based on the triangle diagram shown in the lower left. Blank areas undifferentiated

Continental Shelf

The extensive samples obtained by the American Petroleum Institute project have been coordinated with the sediments collected by Stetson and Trask (1953) and with those of various petroleum companies. This has provided a broad basis for the understanding of the sedimentation conditions along this coast (fig. 5)[5]. In general these investigations have shown that the sedimentation is related to (1) nearness to rivers, (2) general circulation resulting from the predominant currents, (3) the existence of a series of small elevations rising above the general level of the shelf and concentrated along the outer margin.

The largest source of sediment for the shelf is the Mississippi River, which has provided fine material for a distance of about 125 kilometers to the west of the delta and 20 kilometers to the east. The heavy mineral assemblage from the Mississippi is distinctive from those of rivers both to the east and west (GOLDSTEIN 1942). Also this river material can be recognized by an abundance of land plant debris, mica, and small ferruginous aggregates. River-derived deposits are also found off the Brazos, which is building a delta into the open Gulf; off the Rio Grande, which enters directly into the Gulf; and possibly off the Colorado River, which was diverted in 1936 from Matagorda Bay to the open Gulf. Indirectly such rivers as the Sabine supply a considerable abundance of sediment to the shelf despite the intervention of a bay separating the river mouth from the Gulf. During high water the finer sediments cross these bays, pass out through the strait, and are deposited as fine sediment along the inner shelf.

---

[5] The shelf sediments are being studied by J. R. Curray.

Another source of shelf sediment is the barrier beaches at least during storms. Waves breaking on these beaches transport very fine sand seaward. This very fine sand constitutes the dominant sediment out to depths of about 9 meters, although some of it may come directly from rivers. Small amounts of this beach-derived sand is carried into much deeper water by the waves and currents. Still another source of shelf sediment is the Pleistocene deposits left on the continental shelf by the rivers during glacial stages when the sea level was much lower. This sandy sediment is being actively reworked by present day currents in some places, notably on the broad shelf off the Galveston area.

Banks rise above the shelf with a concentration along the outer margin. Many of these appear to be the result of salt dome intrusion (SHEPARD 1937; PARKER and CURRAY 1956; and LANKFORD and CURRAY in press). These banks provide a small source of sediment, due primarily to slumping but also to washing of material from the bank surfaces by strong currents.

Organisms yield a rather small percentage of the shelf sediment, but on the outer shelf the Foraminifera, particularly planktonic, become important constituents. Also locally various types of mollusks contribute to the total of the sediment. Much of the sediment of the outer shelf is of uncertain origin although the dominant clays and silts are presumably material transported from distant river mouths and carried to some extent out of coastal bays through the inlets.

In a central area off Galveston deposition seems to be very slow or non-existent. In many places the macroinvertebrates [6] are characteristic of a much shallower environment than is now found, and the same is true to some extent of the Foraminifera [7]. Presumably these organisms lived here during a time of lowered sea level thousands of years before the present.

Among the distinctive characteristics of shelf sediments are (1) the abundance of echinoids, which are very rare in the bays; (2) the occurrence of glauconite, especially as fillings of Foraminifera tests, and (3) the presence of a fauna which is very distinctive from the restricted fauna of the bays with their variable salinities (PARKER et al. 1953, SWAIN 1955). Sediments containing an abundance of planktonic Foraminifera can always be referred to the outer shelf in this Gulf of Mexico province; in fact, the ratio of planktonic to benthonic Foraminifera shows a definite relationship to the depth of water in crossing the shelf (fig. 6). The stratification of shelf sediments is rather poor, although stringers or lenses of sandy sediments are found in many of the cores, particularly at intermediate depths beyond the sandy fringes of the barrier islands and inside the clayey sediments of the outer shelf (fig. 7). The sandy sediments on the portions of the continental shelves bordering the barrier islands are easily distinguished from the beach and dune sands by their size characteristics. The shelf sediments have almost all of their sand in the 62 to 125 micron size, whereas most of the beaches and dunes have sands rather evenly divided between the 62 to 125 and the 125 to 250 micron fractions. So far as we know this same distinction is found all along the Gulf coast from the Mississippi Delta to the Mexican border. On the other hand some of the outer sands, which are believed to be remnants of Pleistocene low sea level conditions, have a predominance of the 125—250 micron fraction which may indicate that they also were deposited as beaches or barrier islands.

---

[6] From data being studied by R. H. PARKER.

[7] Personal communication of F. B. PHLEGER.

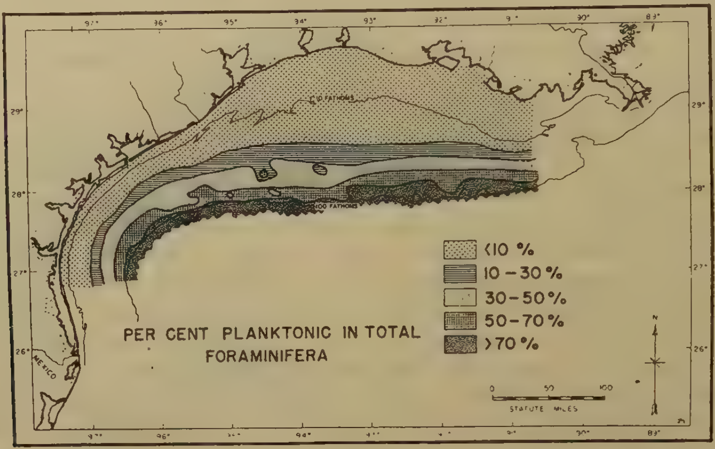

Fig. 6. Indicating the general increase in planktonic Foraminifera in the total percentage of Foraminifera in crossing the continental shelf off the coast of Texas and southwestern Louisiana. It will be seen that the boundaries are approximately parallel to the submarine contours

Shelf Third-dimensional Studies

Third-dimensional studies of the continental shelf are not as advanced as in the bays. In a few cases shallow borings have been made by oil companies and some of the material given to us, but elsewhere information has had to come from the longest cores taken in our own sampling operations. Where the outer shelf cores have reached a length of 5 meters or more, they have usually reached deposits indicative of colder water and hence of late glacial epoch conditions. This gives a rough estimate of the rate of postglacial accumulation. In two oil company borings, a few miles from shore, sediments indicative of barrier islands have been encountered at depths of $3^1/_2$ and 20 meters below the bottom, showing that islands like the present Texas barriers developed during the past, probably during the time when the sea level was rising. Also beach rock has been found on the tops of many of the shallow

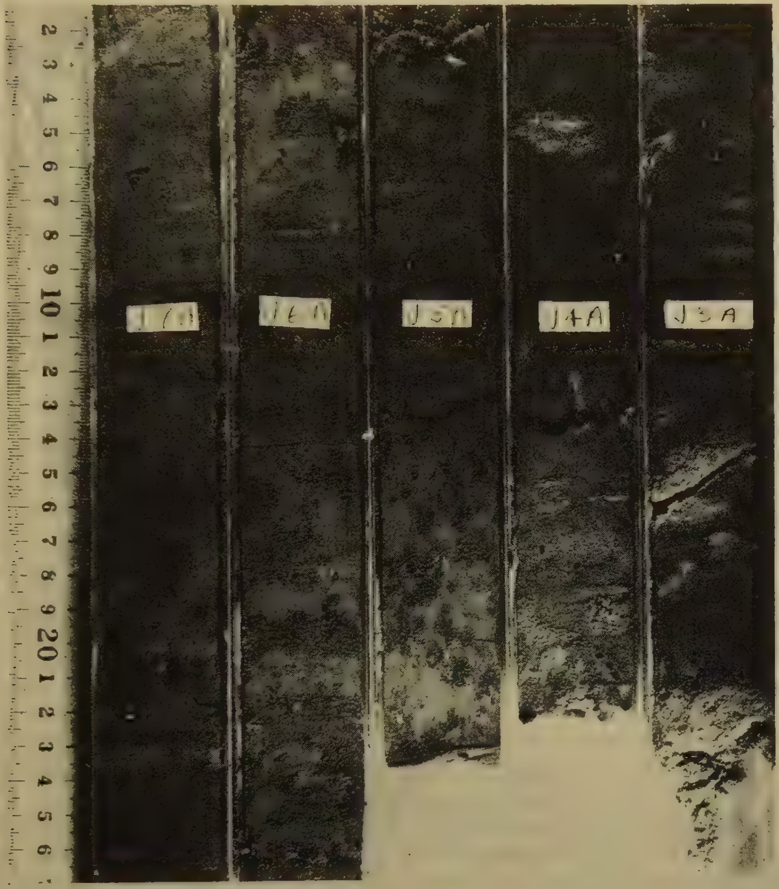

Fig. 7. Typical sand stringers and lenses in cores from the inner portion of the continental shelf. Samples come from increasing depth from J3A at 35 feet to J7A at 56 feet

banks [8]), apparently developed during halts in the rising sea level. Carbon 14 determinations from these banks have yielded dates of 9,000 to 13,000 years (kindly supplied to us by Shell Development Company of Houston).

Mississippi Delta Marginal Deposits

Along the margins of the Mississippi Delta large numbers of samples have been obtained from the river mouths and the adjacent shelf (SCRUTON 1955, SHEPARD 1956). Most work has been concentrated on the east side of the Mississippi Delta where several passes have been building actively into the Gulf of Mexico in recent years. The changes in the Mississippi Delta on the east side during the past hundred years are indicated in Figure 8. From this information it is clear that the delta margin is an area of extremely rapid deposition, at a rate far exceeding any of the other environments along the Gulf coast.

The delta deposits appear to be best described in terms of the old concept of topset, foreset, and bottomset beds (fig. 9). In the Mississippi Delta the topset beds include the deposits in the subaerial portions and those of the shallow marine platform which directly border the delta margin. Beyond the platform the foreset beds are being deposited very rapidly on a gentle slope, rarely more than one percent. Farther seaward is a broad zone of low relief where the bottomset beds are forming at a much slower rate. The bottomset beds are in turn encroaching onto older sediments of an entirely different nature from those of the Mississippi Delta.

In the topset beds the subaerial deposits, in addition to channel and natural levee, include those forming in the extensive marshes which lie between the various active distributary passes. Here sedimentation is relatively slow, large quantities of organic material, mostly plant remains, are found in the coarser fraction of the sediment. Silt, clay, and small quantities of detrital sand are also introduced by occasional stream overflows of the natural levees. The roots of the marsh plants tend to destroy the stratification developed by these overflows, so that the sediments are mostly unstratified and are traversed by numerous rootlets (fig. 10 a). The levee deposits also are rather high in plant remains but the plants were introduced as flood deposits. Sand content is extremely variable, the sediments are generally stratified, and lamination (fig. 10 b) is found in most of the cores which we obtained from these natural levees. The channel deposits are even more variable than the levees, so that locally they are almost a pure sand, but in a neighboring area may consist predominantly of clay and silt. Lamination is also found in many of the channel deposits. In all of the subaerial delta, organisms are very scarce, although shells are found locally (PARKER 1956), as are also Foraminifera [9]). Ostracods which live in fresh water as well as salt environments are fairly common in some places. On the shallow marginal platforms and in the distributary bays beyond the delta margin, sediments are usually laminated. Plant remains, ferruginous aggregates, and mica are very important constituents. In these platform deposits Foraminifera are found, although they are extremely scarce, and have a different assemblage from those at greater distance from the delta (PHLEGER 1956).

---

[8]) This beach rock was discovered by J. R. CURRAY and is being investigated by him.

[9]) The Foraminifera move up river in the salt wedge which intrudes under the fresh water at the river mouth (see SCRUTON 1956, fig. 12).

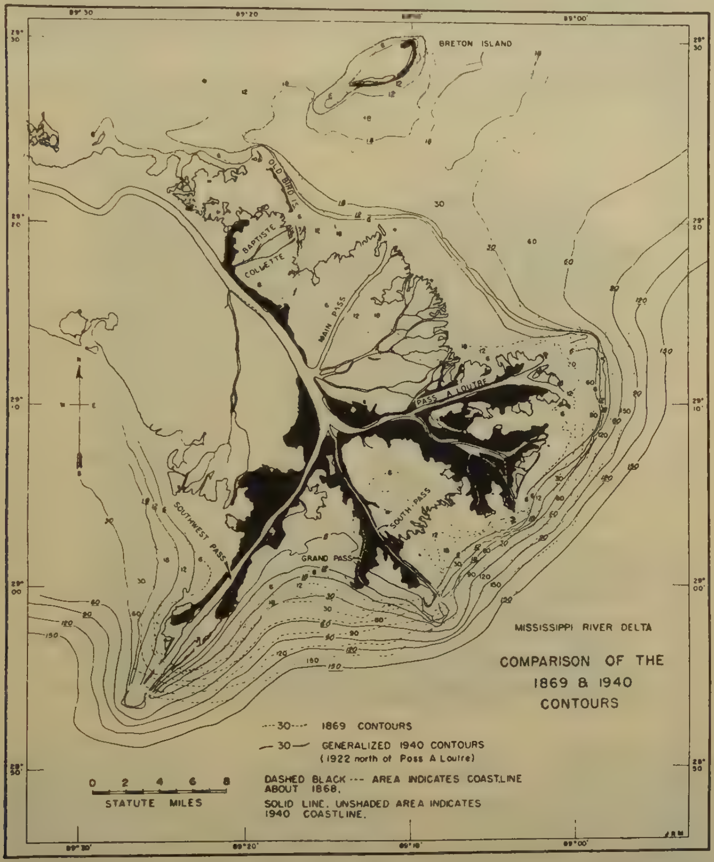
89°30
89°20
89°00'
29° 30
29° 20
29° 10
29° 00
28° 50
89°30'
89°20'
89°10'
89°00'
BRETON ISLAND
OLD BIRD IS.
BAPTISTE
COLLETTE
MAIN PASS
PASS A LOUTRE
SOUTH PASS
SOUTHWEST PASS
GRAND PASS
MISSISSIPPI RIVER DELTA
COMPARISON OF THE
1869 & 1940
CONTOURS
---30--- 1869 CONTOURS
—30— GENERALIZED 1940 CONTOURS
(1922 north of Pass A Loutre)
DASHED BLACK --- AREA INDICATES COASTLINE ABOUT 1868.
SOLID LINE. UNSHADED AREA INDICATES 1940 COASTLINE.
0 2 4 6 8
STATUTE MILES

Fig. 8. Showing growth of the Mississippi Delta since 1869 and depth changes. Because the 1869 soundings were not sufficiently detailed to show submarine gullies, the 1940 contours were generalized for comparative purposes

The slope deposits are much less stratified than those of the topset beds. Sand and coarse silt lenses are found locally, particularly in the upper portions of these slopes, but many of the cores have no apparent stratification. Silt and clay form the predominant constituents of the slope deposits and in many samples only a fraction of one percent consists of sand-sized material. Foraminifera and other types of organisms are scarce even in the coarse fraction. The inclination of the bedding in these foreset beds is very low, rarely exceeding one percent except at the very edge of the platform where it may locally be two three times this amount. In general, where the deltas are building forward into the deep Gulf of Mexico, the slopes are very close to one percent, although they are less where the deltas are advancing over the shallow shelf.

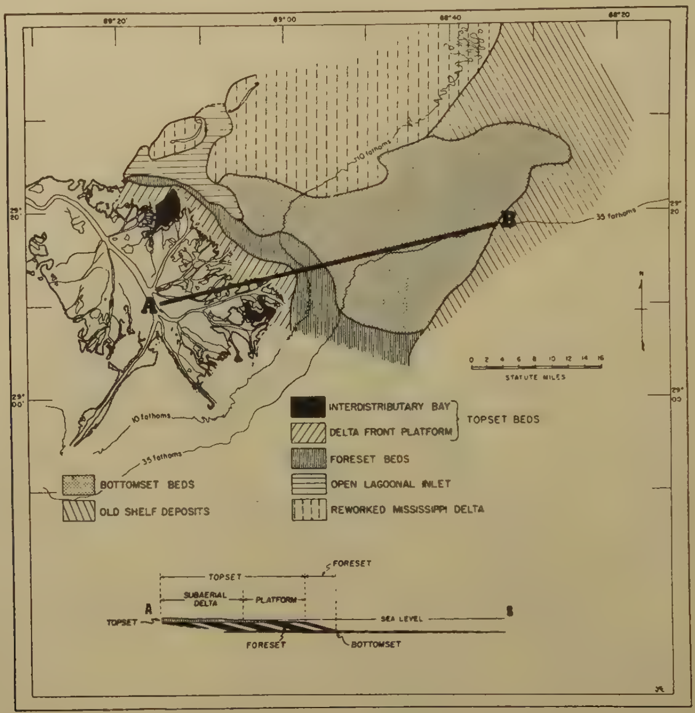
89° 20'
89° 00
88° 40
88° 20
29° 20'
29° 00'
10 fathoms
35 fathoms
A
B
0 2 4 6 8 10 12 14 16
STATUTE MILES
N
INTERDISTRIBUTARY BAY
DELTA FRONT PLATFORM
TOPSET BEDS
FORESET BEDS
OPEN LAGOONAL INLET
REWORKED MISSISSIPPI DELTA
BOTTOMSET BEDS
OLD SHELF DEPOSITS
TOPSET
FORESET
SUBAERIAL DELTA
PLATFORM
SEA LEVEL
FORESET
BOTTOMSET

Fig. 9. Sediment environments to the east of the outer Mississippi Delta. The relation of these environments to topset, foreset and bottomset beds is indicated by comparison with the inset at the lower part of the figure. In this section the vertical has been exaggerated and actually the slopes rarely exceed one per cent

Bottomset beds differ from the foresets in having a much higher quantity of organisms, so that the Foraminifera are often quite abundant among the sand-sized constituents. Sand in the bottomset beds, instead of being scarcer than in the foresets, as might be expected, is actually more abundant. Probably most of this sand is introduced into the bottomset beds by currents transporting material from the old sand deposits which remain uncovered farther east on the shelf. Stratification of the bottomset beds is virtually unknown. The wood fibers, mica, and aggregates found in the topset and foreset beds are still present although in

(288)

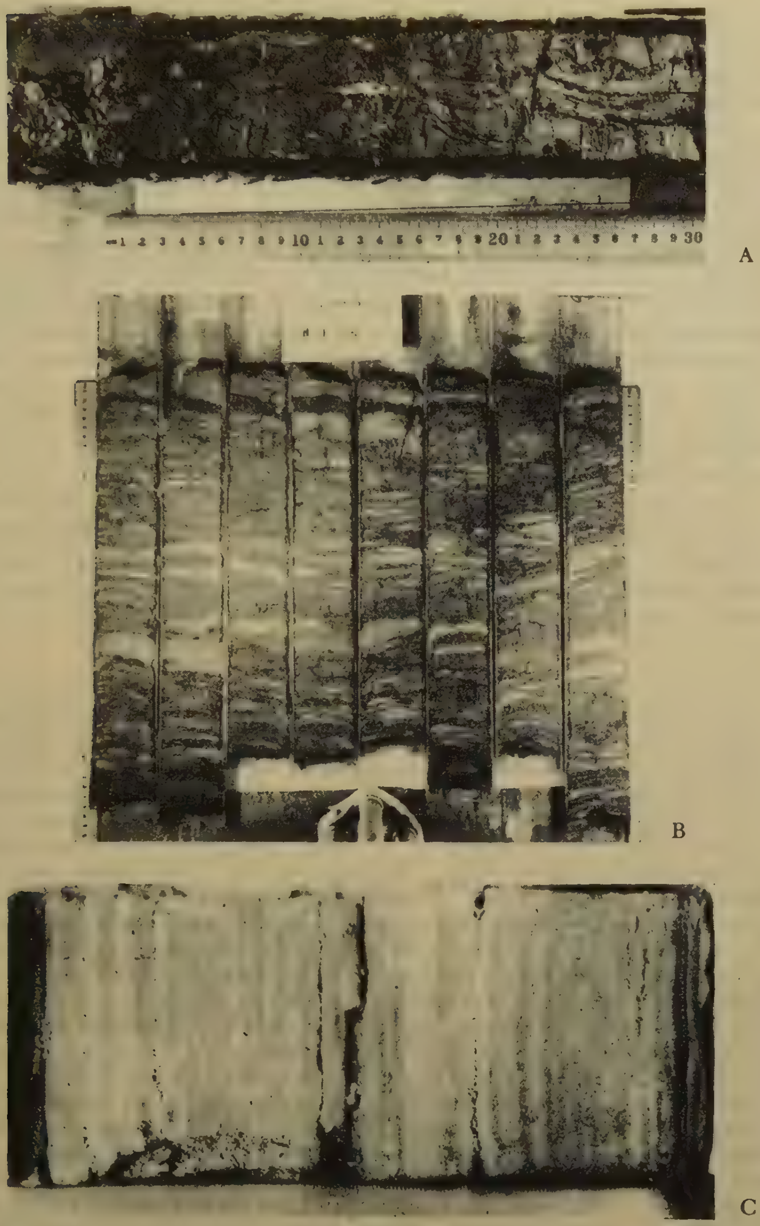

Fig. 10. A. Core indicating the rootlets and general structureless character of the marsh environment. B. Lamination from eight adjacent cores from the submarine platform showing continuity of laminations. C. Laminations similar to the above taken from boring obtained in Chandeleur Sound by the U.S. Army Engineers from a depth of 58 feet

somewhat smaller quantities in the bottomset beds. Much helpful information concerning the delta facies has been obtained from the faunal relations (PHLEGER 1955, and PARKER 1956). Studies of the live population of the Foraminifera are being made by R. R. Lankford and of the Ostracoda by Doris Malkin Curtis.

Borings in the Mississippi Delta have shown sediments that were deposited in the subaerial delta down to depths of as much as 31 meters below sea level in some localities [10]). In some places the borings in the delta have penetrated into bay deposits at as little as 5 meters, and at depths of about 18 meters borings have encountered deposits that are presumably both foreset and bottomset in origin, judging from their general constituents and the nature of the Foraminifera. The lamination characteristic of the topset beds is encountered in various places in the borings under the Mississippi Delta (fig. 10 c). The borings of greater depth obtained by the Army Engineers (FISK 1944, 1952, FISK and McFARLAN 1955) show that a series of cyclic changes have developed in these Mississippi Delta sediments during the Pleistocene.

It seems probable that delta deposits like those forming at the mouths of the Mississippi could be recognized in ancient sedimentary columns, although it should be borne in mind that the foreset beds of these old deltas, probably like those of the present day Mississippi and other large deltas, would have very low dips.

References

BEAL, M. A., and SHEPARD, F. P. (1956): A use of roundness to determine depositional environments. Jour. Sed. Petrol., Vol. 26, No. 1, p. 49—60. — FISK, H. N. (1944): Geological investigation of the alluvial valley of the lower Mississippi River. Miss. River Comm., 78 p. – (1952): Geological investigation of the Atchafalaya Basin and the problem of Mississippi River diversion. Ibid. — FISK, H. N., and McFARLAN, E., jr. (1955): Late Quaternary deltaic deposits of the Mississippi River. From "The Crust of the Earth". Geol. Soc. Amer. Spec. Paper 62, p. 279—302. — GOLDSTEIN, AUGUST, jr. (1942): Sedimentary petrologic provinces of the northern Gulf of Mexico. Jour. Sed. Petrol., Vol. 12, No. 2, p. 77—84. — LANKFORD, R. R., and CURRAY, J. R. (in press): Mid-Tertiary outcrops on the continental shelf, northwest Gulf of Mexico. — MASSON, P. H. (1955): The occurrence of gypsum in southwest Texas. Jour. Sed. Petrol., Vol. 25, p. 72—77. — MURRAY, G. E., et al. (1952): Sedimentary volumes in Gulf coastal plain of United States and Mexico. Bull. Geol. Soc. Amer., Vol. 63, No. 12, p. 1157—1228. — PARKER, F. L., PHLEGER, F. B., and PEIRSON, JEAN (1953): Ecology of Foraminifera from San Antonio Bay and environs, southwest Texas. Cushman Found. Spec. Pub. 2, 75 p. — PARKER, R. H. (1956): Macro-invertebrate assemblages as indicators of sedimentary environments in east Mississippi Delta region. Bull. Amer. Assoc. Petrol. Geol., Vol. 40, No. 2, p. 295—376. — PARKER, R. H., and CURRAY, J. R. (1956): Fauna and bathymetry of banks on continental shelf, northwest Gulf of Mexico. Bull. Amer. Assoc. Petrol. Geol., Vol. 40, No. 10, p. 2428—2439. — PHLEGER, F. B. (1955): Ecology of Foraminifera in southeastern Mississippi Delta area. Bull. Amer. Assoc.

---

[10]) These were derived from cores taken by the U. S. Army Engineers.

Petrol. Geol., Vol. 39, No. 5, p. 712—752. – (1956): Significance of living foraminiferal populations along the central Texas coast. Cushman Found., Vol. VII, Part 4, p. 106—151. — Scruton, P. C. (1955): Sediments of the eastern Mississippi Delta. Symposium on "Finding Ancient Shorelines". Soc. Econ. Paleon. and Mineral. Spec. Pub., 3, p. 21—50. — Shepard, F. P. (1937): Salt domes related to Mississippi submarine trough. Bull. Geol. Soc. Amer., Vol. 48, p. 1349—1362. – (1956): Marginal sediments of Mississippi Delta. Bull. Amer. Assoc. Petrol. Geol., Vol. 40, No. 11, p. 2537—2623. — Shepard, F. P., and Moore, D. G. (1955): Central Texas coast sedimentation: characteristics of sedimentary environment, recent history, and diagenesis. Bull. Amer. Assoc. Petrol. Geol., Vol. 39, No. 8, p. 1463—1593. — Shepard, F. P., and Suess, H. E. (1956): Rate of postglacial rise of sea level. Science, Vol. 123, No. 3207, p. 1082—1083. — Stetson, H. C., and Trask, P. D. (1953): The sediments of the western Gulf of Mexico. Papers in Phys. Oceanog. and Meteorol., M.I.T. and Woods Hole Oceanog. Inst., Vol. 12, No. 4, 45 p. — Swain, F. M. (1955): Ostracoda of San Antonio Bay, Texas. Jour. Paleon., Vol. 29, No. 4, p. 561—646.

STUDIES OF THE
CALIFORNIA CURRENT SYSTEM

by
JOSEPH L. REID, JR., GUNNAR I. RODEN,
and JOHN G. WYLLIE

Contributions from the Scripps Institution of Oceanography, New Series No. 998

CONTENTS

Page

THE WINDS OVER THE NORTHEASTERN PACIFIC OCEAN AND THEIR EFFECT UPON THE WATER ---- 29

THE CURRENTS ---- 30

THE NATURE OF THE WATERS ENTERING THE MAIN STREAM ---- 34

RESULTANT DISTRIBUTION OF PROPERTIES AND THEIR VARIATION WITH SEASON ---- 35

RELATION OF THE ENVIRONMENT TO THE PLANTS AND ANIMALS ---- 47

NON-SEASONAL VARIATIONS IN THE CALIFORNIA CURRENT SYSTEM SINCE 1916 ---- 49

POSSIBLE EFFECTS OF VARIATION IN THE CURRENT SYSTEM UPON THE ORGANISMS ---- 53

CONCLUSION ---- 55

REFERENCES ---- 55

ILLUSTRATIONS

Figure — Page

1. Average monthly atmospheric sea level pressure over the eastern North Pacific Ocean and the western coast of North America during four months of the year ---- 29
2. Variations of wind speed with distance from coast, May, 1953 ---- 30
3. Ocean currents off the western coast of North America 32
4. Ocean temperature at 10 meters, August, 1955 and March (composite) ---- 35
5. Vertical profiles of temperature, salinity, oxygen, and phosphate from the surface to 600 meters, August, 1955 ---- 36
6. Seasonal variation of temperature in the upper 125 meters at four locations ---- 40
7. Seasonal variation of temperature at the sea surface off the western coast of North America ---- 41
8. Frequency distribution of monthly average temperature, Scripps Pier, 1917-56 ---- 41
9. Monthly average temperature at North Farallon Island in 1940 and 1955 ---- 42
10. Salinity at 10 meters in August, 1955, March (composite), January (average of three years), and June (average of three years) ---- 43
11. Seasonal variation of salinity in the upper 125 meters at three locations ---- 45
12. Seasonal variation of salinity at the sea surface off the western coast of North America ---- 46
13. Dissolved oxygen at 200 meters, August, 1955 ---- 46
14. Distribution of phosphate-phosphorus and zooplankton volumes, August, 1955 ---- 48
15. Distribution of phosphate-phosphorus and zooplankton volumes, April, 1950 ---- 48
16. Distribution of phosphate-phosphorus and zooplankton volumes, July, 1950 ---- 48
17. Distribution of certain zooplankton and certain temperature and oxygen values, August, 1955 ---- 50
18. Monthly differences from average sea surface temperature at three locations and monthly difference from average northerly wind components at one location ---- 51
19. Average surface temperature and salinity at Pacific Grove and Scripps Pier for the periods 1949-56 and 1920-48 ---- 52
20. Average northerly wind component and temperature in recent period compared to averages for 1920-38 ---- 52
21. Temperature anomalies, 1949 to 1957, at four locations as referred to 1949-56 mean ---- 53
22. Temperatures in 1956 and 1957 at four locations as compared to long-term means ---- 54
23. Temperature at 10 meters and zooplankton volumes averaged from February through August for each year from 1949 through 1956 ---- 54

THE WINDS OVER THE NORTHEASTERN PACIFIC OCEAN AND THEIR EFFECT UPON THE WATER

The most important force moving the surface waters of the ocean is the wind. Upon comparing a current chart of the North Pacific Ocean with a chart of the winds, one is immediately struck by the similarities in direction of motion. The strong westerly winds in high latitudes move the water eastward and the strong and constant trade winds farther south push the water westward. Both the winds and the water go through an enormous clockwise circulation in the North Pacific Ocean. The California Current lies at the eastern, southward-flowing side of the circulation.

The circulation is of course not quite so simple as this. There are countercurrents and subsurface currents which are harder to understand and to measure, and there are seasonal changes in the circulation of the air which are reflected in the motion of the water. The California Current flows southeastward between a cell of high atmospheric pressure to the west and a cell of low pressure on the landward side. The winds over the California Current are mostly from the north and west and are strong when these two cells are close together and intense, weak when the cells are farther apart and moderate.

Both these cells are weakest in winter; that is, the high pressure cell is less high and the low is less low. The high to the west moves north in spring and summer as it grows slightly stronger and moves south again in the fall as it weakens. The low over the land is a semi-permanent feature with a wider range of seasonal variation. The pressure differences between these two cells afford the best data available for the

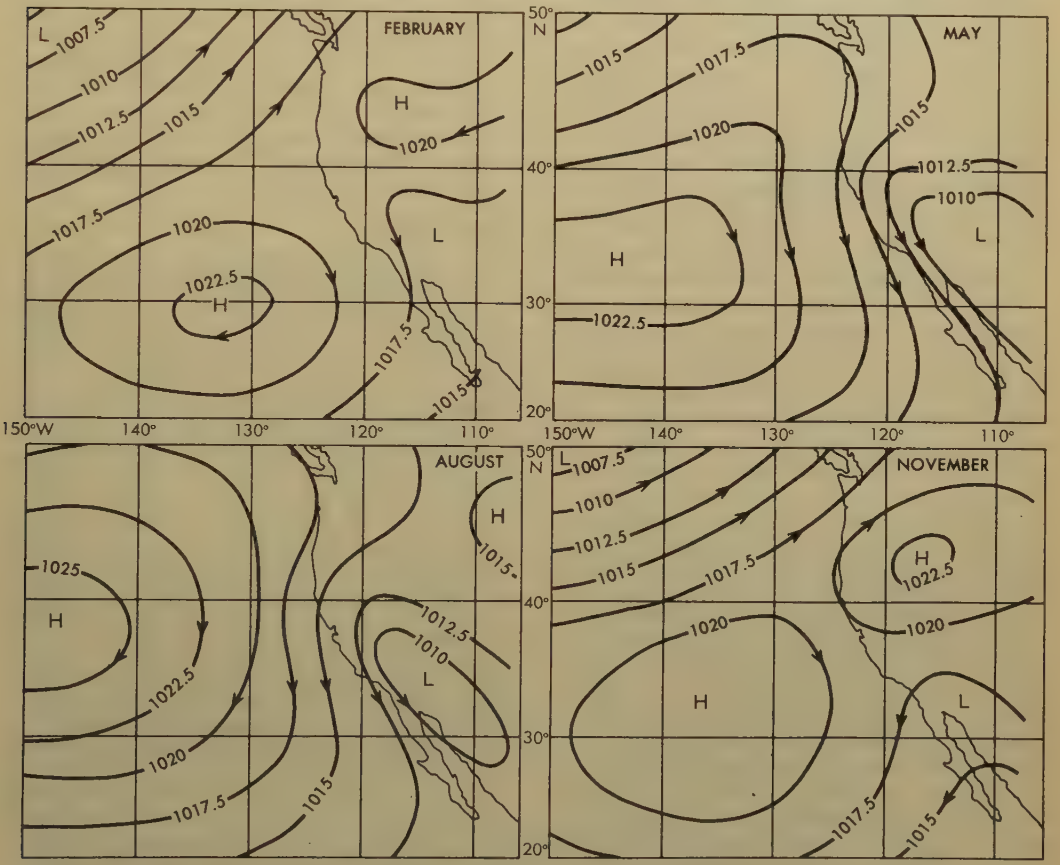
FEBRUARY
L
1007.5
1010
1012.5
1015
1017.5
1020
1022.5
H
H
1020
L
1017.5
1015
MAY
1015
1017.5
1020
H
1022.5
1015
1012.5
1010
L
AUGUST
H
1015
1025
H
1022.5
1020
1017.5
1015
1012.5
1010
L
NOVEMBER
L
1007.5
1010
1012.5
1015
1017.5
1020
H
H
1022.5
1020
L
1017.5
1015
50° N
40°
30°
20°
150°W
140°
130°
120°
110°

FIGURE 1. Average monthly atmospheric sea level pressure (in millibars) over the eastern North Pacific Ocean and the western coast of North America during four months of the year.

Reproduced by Permission

study of wind variations over the California Current region, since not enough direct measurements of wind are available to permit the study of year-to-year changes. Under certain assumptions winds can be calculated from the difference in atmospheric pressures at two places. Such calculated winds are called geostrophic. In some parts of this discussion the pressure gradients have been expressed as meters per second of (geostrophic) wind.

The changes in strength and location of the cells cause seasonal changes in the winds (Fig. 1). From spring through fall over most of the California Current the winds have a northerly component which tends to push the current along but in winter this northerly component either weakens or reverses. In winter when the north winds are less effective a countercurrent develops at the surface near the coast from Baja California to some distance beyond Point Conception.

Along the coast of California and Baja California winds from the north and northwest are of peculiar importance. Under the force of these winds and the earth's rotation the surface waters are turned from their movement along the coast to a direction offshore. Some part of the waters which move offshore are then replaced by water from below. This replacement is known as upwelling, and it is important because it brings to the surface waters which are richer in nutrient material than the waters they replace. Since upwelling is the result of the north and northwest winds it will be most marked when these winds are strongest. They are strongest off Baja California in April and May, off southern and central California in May and June, off northern California in June and July, and off Oregon in August. In winter the winds south of Point Conception are still northerly but north of Point Conception they are westerly and southwesterly. In the south upwelling will be strongest in spring and in the north it will be strongest in summer.

These two features, upwelling in spring and summer and countercurrent in fall and winter, will be referred to frequently in the sections on currents, water properties, and the relation of these to the plants and animals of the current system.

In any discussion of wind Point Conception stands out. Mariners have long known that strong winds are found to the west-southwest of the Point. Typical wind strengths, from measurements made by a CCOFI cruise in May, 1953, show the local intensification (Fig. 2). About one day was spent on each line shown. The strongest winds were found just beyond Point Conception where their strength was about twice the average along the line. This feature seems to be confined to the months from April to August. It may occur to the south also but the evidence is not conclusive.

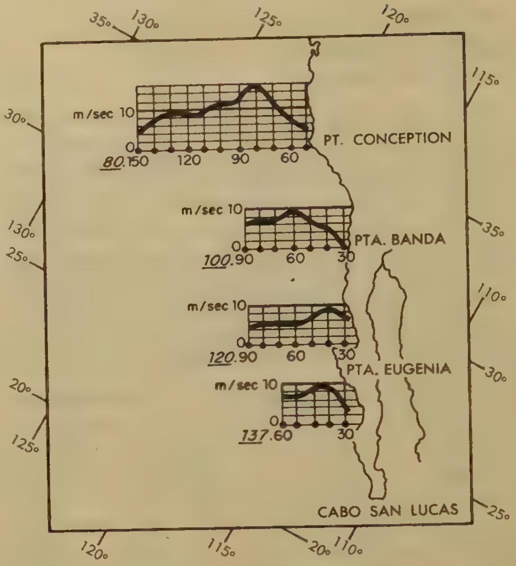

FIGURE 2. Variations of wind speed with distance from coast, May 1953. Measurements made along Station Lines 80, 100, 120, and 137, on CCOFI Cruises. Wind expressed as meters per second. Strongest winds occur off Point Conception.

THE CURRENTS

The California Current system is a part of the great clockwise circulation of the North Pacific Ocean. At high latitudes the waters move eastward under the influence of the strong westerly winds (the "roaring forties") and near the coast of North America divide into two branches. The smaller part turns northward into the Gulf of Alaska, and the larger part turns southeastward to become the California Current. In general the temperatures in the open ocean are lower toward the north so that the branch turning northward into the Gulf of Alaska is known as a warm current. The water which is brought south by the California Current system is cooler than the waters farther offshore. As it moves slowly south at speeds generally less than half a knot it becomes warmer under the influence of the sun and by mixing with the warmer waters to the west. As it nears the latitude of 25° N it begins to turn westward and its waters become part of the west-flowing North Equatorial Current. On the inshore side of the current some disturbances in the circulation are found.

A small eddy is usually found offshore from Cape Mendocino through most of the year (Fig. 3a). A similar eddy is found between Guadalupe Island and the mainland. A permanent eddy, the Southern California Countercurrent (Sverdrup and Fleming, 1941), is found inside the submerged peninsula that extends southeast from Point Conception and includes

Santa Rosa Island, San Nicolas Island, and Cortes Bank. The waters on the eastward side of this are protected from the northwest winds by the land and separated in part from the strong southeasterly-flowing offshore current. The currents are weaker and usually to the north. The waters remain off the coast of southern California for a considerable time and become much warmer than those offshore, which are constantly replaced by cooler water from the north.

The area off southern California was studied by Sverdrup and Fleming (1941) using the data taken by the California Division of Fish and Game vessel *Bluefin* in the late '30s and the University of California vessel *E. W. Scripps* in 1940 and 1941; and until the CCOFI program began it was the only area which had received any detailed attention. The small area covered by these cruises made speculations about the continuity of the northward flow around Point Conception extremely difficult. Only one extensive cruise was made from Punta Eugenia to Cape Mendocino. As this was conducted in the summer of 1939, it did not bear upon the problem of the continuity of the winter countercurrent. However, many of the results of the CCOFI program in the regions where Sverdrup and Fleming had little or no data had been anticipated to a remarkable degree by their speculations.

A deep countercurrent, below 200 meters, flows to the northwest along the coast from Baja California to some point beyond Cape Mendocino. It brings warmer, more saline water great distances northward along the coast. When the north winds are weak or absent in late fall and early winter the countercurrent forms at the surface well on the inshore side of the main stream and extends from the tip of Baja California to north of Point Conception, where it has been called the Davidson current. The causes of the deep countercurrent and its appearance at the surface in winter are not understood. Rossby (1936) derived a theory of oceanic circulation in which a large ocean current has associated with it on its lefthand side looking downstream a countercurrent; and Sverdrup *et al.* (1942) mentioned the possibility that the California Current system is an example of this sort of circulation. However, the assumptions are not all fulfilled and this theory cannot be applied with any confidence at present.

The process of upwelling, in which winds parallel to the coast move the waters offshore, has been mentioned. This effect seems to be intensified south of capes and points which extend out into the stream. Thus Cape Mendocino, Point Conception, and Punta Eugenia are regions of more intense upwelling than the rest of the coast.

Some of the current measurements made by the CCOFI program are shown in figure 3. They are computed from the density distribution of the water, measured at the points indicated. In order to express these density distributions as currents it is necessary to make certain assumptions. These are that the currents and density distribution are steady, there is no effect of friction either at the bottom or from wind at the surface, there is some depth (perhaps 1000 meters) at which there is no motion and to which the density measurement can be referred, and above this level all movement is horizontal and east-west. These assumptions are no doubt best fulfilled farther upstream where the west wind drift at 160° W longitude is very nearly east-west and where the ocean is deep. At any rate the currents computed from the density distribution in that area have been in agreement with the many measurements made by the set and drift of merchant vessels (University of California (in press) and U. S. Hydrographic Office, 1947).

Offshore in the California Current system these measurements are equally in agreement with the set and drift results and present a coherent picture of the clockwise circulation of the North Pacific. Near the coast, however, the assumptions are not so well fulfilled. The effect of the irregular coastline cannot be entirely ignored, nor the varying depth. These and the winds, which sometimes reinforce and sometimes oppose the current, and the significant vertical motion in the regions of upwelling and the oscillations of internal waves (Reid, 1956) all combine to make the measurement of currents by density distribution less accurate and less useful.

The currents computed from density are less clear near the coast (Fig. 3). Indeed it is not upon the density measurements alone that our knowledge of the countercurrent is based, but upon the observed effect of the countercurrent in moving large quantities of water of a distinct type far up the coast, and upon various direct measurements obtained by drogues, drift bottles, and an electronic current-measuring instrument, the Geomagnetic Electrokinetograph (von Arx, 1950).

Because of the doubtful validity of computing currents from density in the nearshore regions, especially around the Channel Islands, work was done as early as 1937 with drift bottles (Tibby, 1939) and in 1950 with drogues. The density distribution indicated a movement to the northwest inside the islands. Measurements of the currents made at the same time (in June 1950) by both the density method and drogues showed a northwesterly flow. Whether this flow reached as far as Point Conception and proceeded northward around the Point in summer has been more recently inquired into by using drift bottles. These have been put over on all the CCOFI cruises made in the last three years. The results have been very informative. They have indicated a flow northwestward from the Channel Islands region around Point Conception only in late fall and winter. In summer the

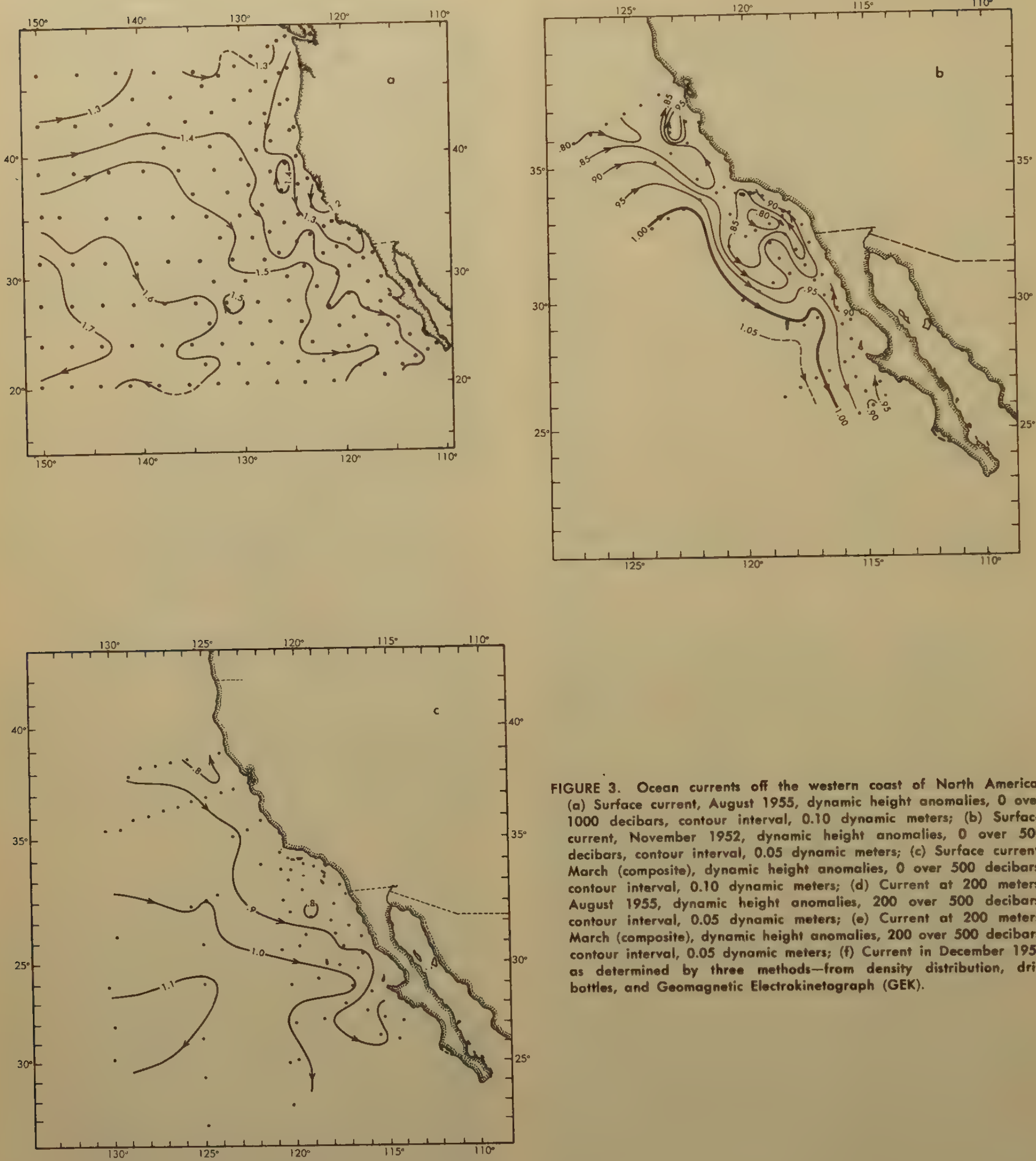
a
150°
140°
130°
120°
110°
40°
30°
20°
1.3
1.4
1.2
1.5
1.6
1.7
b
125°
120°
115°
110°
35°
30°
25°
.80
.85
.90
.95
1.00
1.05
c
130°
125°
120°
115°
110°
40°
35°
30°
25°
.8
.9
1.0
1.1

FIGURE 3. Ocean currents off the western coast of North America. (a) Surface current, August 1955, dynamic height anomalies, 0 over 1000 decibars, contour interval, 0.10 dynamic meters; (b) Surface current, November 1952, dynamic height anomalies, 0 over 500 decibars, contour interval, 0.05 dynamic meters; (c) Surface current, March (composite), dynamic height anomalies, 0 over 500 decibars, contour interval, 0.10 dynamic meters; (d) Current at 200 meters, August 1955, dynamic height anomalies, 200 over 500 decibars, contour interval, 0.05 dynamic meters; (e) Current at 200 meters, March (composite), dynamic height anomalies, 200 over 500 decibars, contour interval, 0.05 dynamic meters; (f) Current in December 1954 as determined by three methods—from density distribution, drift bottles, and Geomagnetic Electrokinetograph (GEK).

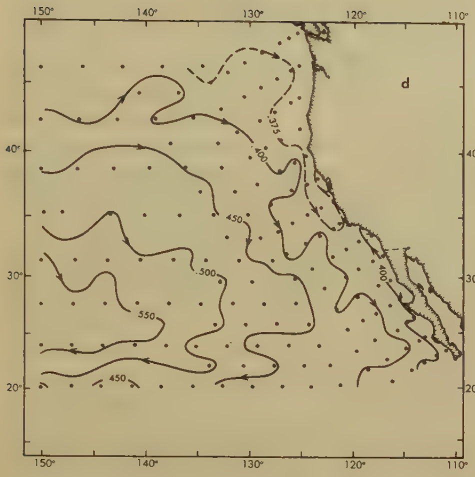
d
150°
140°
130°
120°
110°
40°
30°
20°
.375
400
450
.500
550
450
400

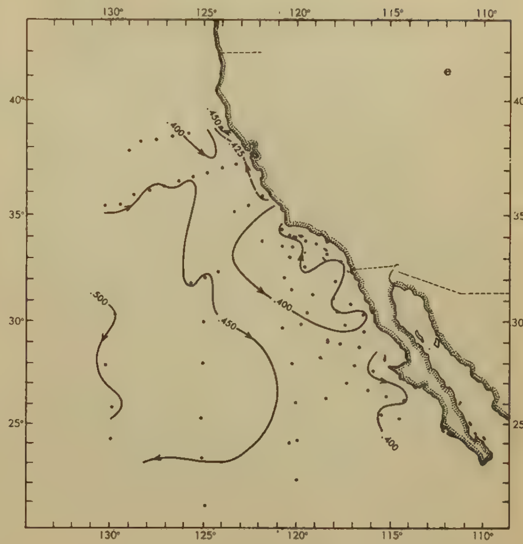
e
130°
125°
120°
115°
110°
40°
35°
30°
25°
400
450
425
.500
400
450
400

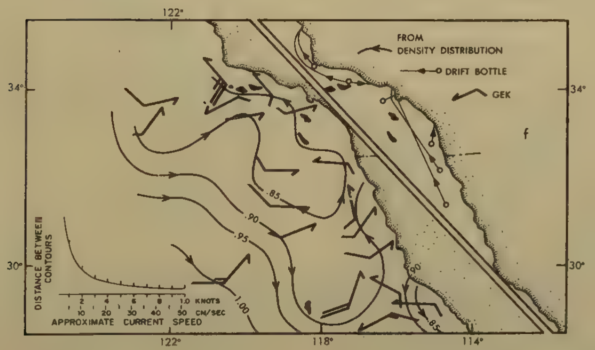
f
FROM DENSITY DISTRIBUTION
DRIFT BOTTLE
GEK
122°
118°
114°
34°
30°
.85
.90
.95
1.00
.90
.85
DISTANCE BETWEEN CONTOURS
.2 .4 .6 .8 1.0 KNOTS
10 20 30 40 50 CM/SEC
APPROXIMATE CURRENT SPEED

drift bottles have moved short distances northwestward along the coast between San Diego and Port Hueneme but none has rounded the corner. There is reason to believe that they turn southward again in summer as they near the Point and are carried down with the main current. An interesting feature of the drift bottle results is that few of the bottles put over more than 40 miles offshore have returned to the coast. This result is consistent with the assumption that the surface waters are nearly always moved slightly offshore by the prevailing winds.

The currents were measured in December 1954 by the distribution of density, by drift bottles, and by means of an electronic current-measuring device (Fig. 3f). The three methods are in general agreement, all of them showing a northwestward flow past Point Conception. The electronic measuring instrument has revealed many short-period changes in the surface currents off California (Reid: in press). Some of these variations appear to be tidal. There is so much variation over a 12-hour period that a single measurement is difficult to interpret. A clearer picture is found when some averaging system is introduced either by area or by time (Knauss and Reid, 1957).

THE NATURE OF THE WATERS ENTERING THE MAIN STREAM

The waters of the California Current come from four water masses distinguishable by their content of heat, salt, oxygen, and phosphate. (The deeper circulation is excluded from this discussion.) Processes of mixing and surface effects cause these properties to change as the water moves. We shall identify them by their descriptions as they enter the area of interest.

From the North

A great part of the water mass which moves eastward across the North Pacific has been called Subarctic water. At 147° W longitude this eastward-moving mass is centered at about 48° N latitude in summer. It is this water mass which gives to the offshore waters of the California Current their characteristic surface properties of low temperature, low salinity, high oxygen and, in part, their high phosphate. These properties distinguish this water mass sharply from the waters to the southwest with which it mixes as it moves down the coast of North America. Mixing alters the properties of the Subarctic water considerably before the Current begins to turn southwest at about 25° N latitude. But it is still clearly recognizable, especially by the low salinity, as it turns westward and becomes part of the North Equatorial Current.

From the West

In the central part of the North Pacific lies water whose properties are in sharp contrast to those of the Subarctic water mass. This water has remained in the central part of the North Pacific gyral long enough for its temperature to be raised, its salt content to be raised by evaporation, and the nutrients in the surface layer nearly exhausted. These two bodies of water move eastward side by side until they approach the coast of North America. Some mixing takes place as they move to the eastward, though the boundary still remains relatively sharp. But as the Subarctic water turns southeastward to become the California Current much more horizontal mixing takes place near the surface. This continues down the coast so that the upper waters have attained quite different characteristic values by the time the Current begins to turn southwest. The mixing does not take place equally at all levels but is most intense near the surface, so that the upper waters come to be dominated more nearly by the Central Pacific characteristics than do the waters below 100 meters. This effect will be shown later on vertical profiles.

From the South

To the far south lies a great body of water called Equatorial Pacific, which has been defined by a certain easily recognizable temperature-salinity relation. In the upper levels these waters are very warm and salty. The major influx of these waters into the California Current system occurs along the coast well beneath the surface. At the tip of Baja California the temperature-salinity relation below 200 meters coincides with that of the definition of Equatorial Pacific water. This water also fills the lower levels of the Gulf of California. The water which moves up the western coast of Baja California at depth must have been beneath the surface for a long period because it is low in oxygen and high in phosphate. This implies a great deal of decomposition of organic matter fallen from the surface, and no extensive mixing with the surface waters.

From Below

The strong northwesterly winds near the coast of the Californias combine with the earth's rotation to effect an offshore transport of the surface waters. These are replaced by colder, more saline waters from below. Having been below the surface for a long time, the water thus upwelled contains nutrients which have been both produced in it by decay and by mixing with the still richer, untapped reservoirs below. Some part of these upwelling waters comes from the lower levels of Subarctic water and some parts are a transitional form of the Equatorial Pacific water which has flowed far up the coast beneath the surface and mixed with the lower levels of Subarctic water.

The wind charts (Fig. 1) have shown that winds are more likely to cause upwelling in spring and early summer but that there is some tendency for upwelling at other times of the year. The predominance of the wind from the northwest even when weak and the general southeastward movement of the current combine with the irregularities in the sea bottom and with such sharp breaks in the coastline as Cape Mendocino, Point Conception, and Punta Eugenia to cause spots of cold, salty water near the coast through a great part of the year though, as will be seen, spring and early summer are the periods of strongest upwelling.

RESULTANT DISTRIBUTION OF PROPERTIES AND THEIR VARIATION WITH SEASON

The properties of the water are shown by the horizontal charts and vertical profiles. Some have smooth patterns, some change abruptly, some are characterized by maxima and minima which appear as tongues or fingers penetrating other waters.

Temperature

In general ocean temperatures become higher toward the equator and lower toward the poles. Over most of the Pacific Ocean the lines of constant temperature run east-west. The clockwise circulation of the North Pacific Ocean, however, causes the isotherms to bend sharply toward the south as the currents approach North America. The southward flowing cooler Subarctic water collides with much warmer water toward the tip of Baja California (Fig. 4a) where a sharp front is nearly always found near the coast (Cromwell and Reid, 1956). In the southwest are found the high temperature values of the central part of the great North Pacific gyral. Even these high values, however, are surpassed by the warm water at the tip of Baja California.

The coldest water in the area shown on figure 4a, however, is not in the north, but off California. An isolated cold area extends from the Columbia River to Point Conception. In August the only possible origin of such waters is from below. This water then is upwelled and will later be seen to be high in salinity as well. Weaker upwelling takes place at numerous points from San Diego to Magdalena Bay. In August, the upwelling off Baja California is weak, as its maximum occurs earlier in the year, but off northern California upwelling is at its strongest and the temperatures are affected correspondingly.

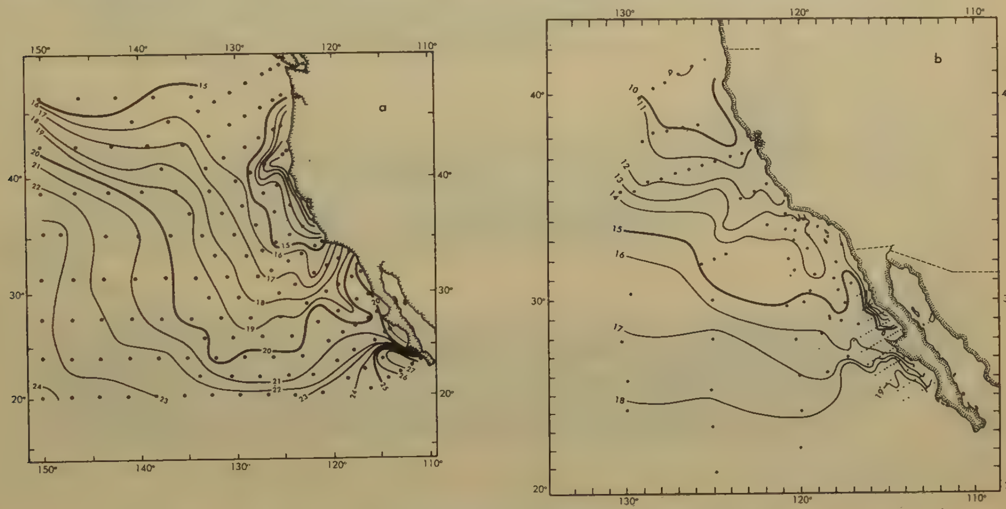

FIGURE 4. Ocean temperatures at 10 meters (degrees Centigrade). (a) August 1955. (b) March (composite).

The great eddy off southern California results at this time of year in a local high temperature between San Diego and San Clemente Island. This water is moving very slowly to the northwest and is warmed to these high temperatures as it moves.

Four profiles of the upper 600 meters of water drawn roughly perpendicular to the direction of flow are shown in figure 5a. The high temperatures at the surface diminish very rapidly with depth and at 600 meters the difference between the northern and southern temperatures is of the order of a degree. At the surface this difference may be as high as 10° C. Near the tip of Baja California, where the deep waters reach their maximum temperature, a small inversion in the temperature is nearly always found. The cool and less saline waters of the California Current here have overridden the warmer and more saline waters of the deep countercurrent to such an extent that over

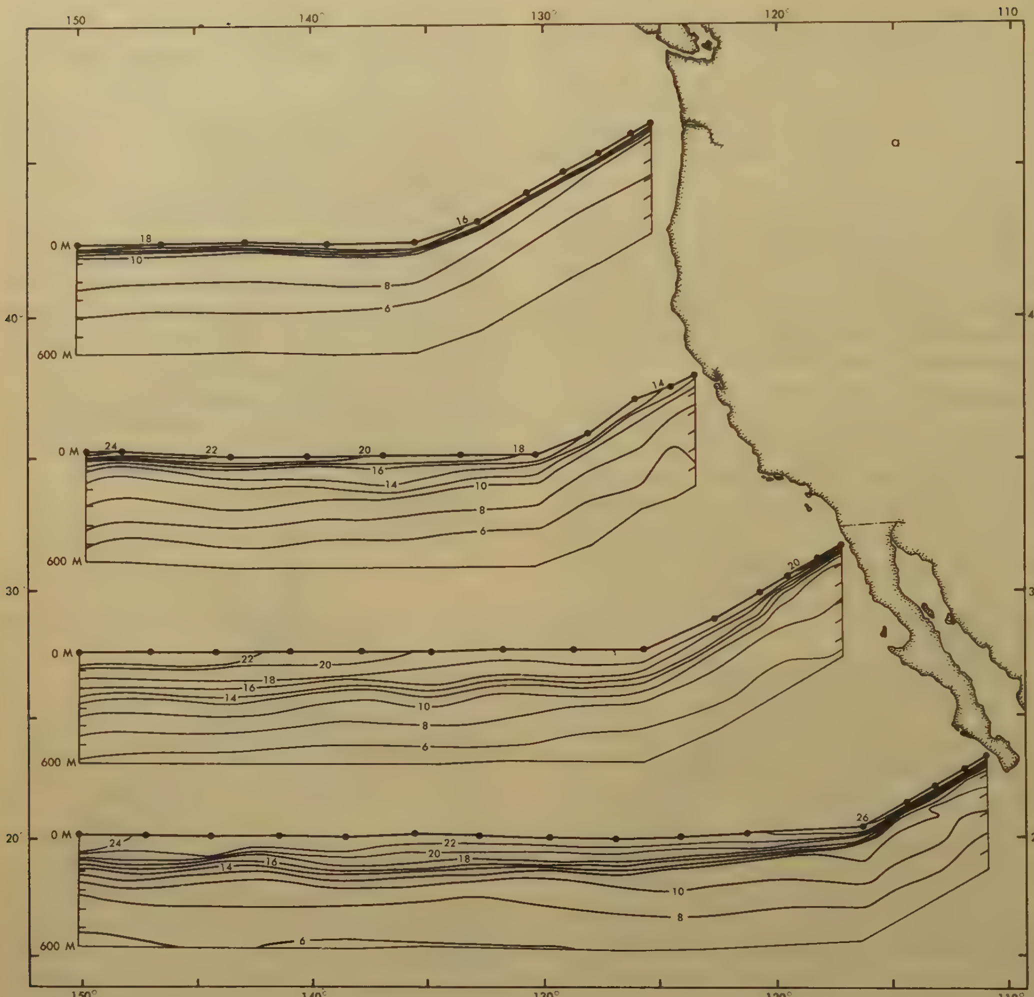

FIGURE 5. Vertical profiles of temperature, salinity, oxygen and phosphate from the surface to 600 meters, August 1955.

(a) Temperature, degrees Centigrade.

a small area and through a narrow range of depth the temperatures may actually increase with depth at about 100 to 150 meters.

Offshore the upper waters vary seasonally in a rather smooth and regular pattern (Fig. 6.). In January and February a well-mixed surface layer is found with the water becoming colder quite suddenly beneath it. The region of sharp change is called the thermocline. In spring the water receives more heat from the sun and a thin layer of warmer water appears at the surface. A new thermocline is formed near the surface and this strengthens and becomes deeper as the summer passes, and the original winter thermocline loses its identity. The surface is warmest from August to October but the new thermocline continues to deepen until finally it reaches the depth of

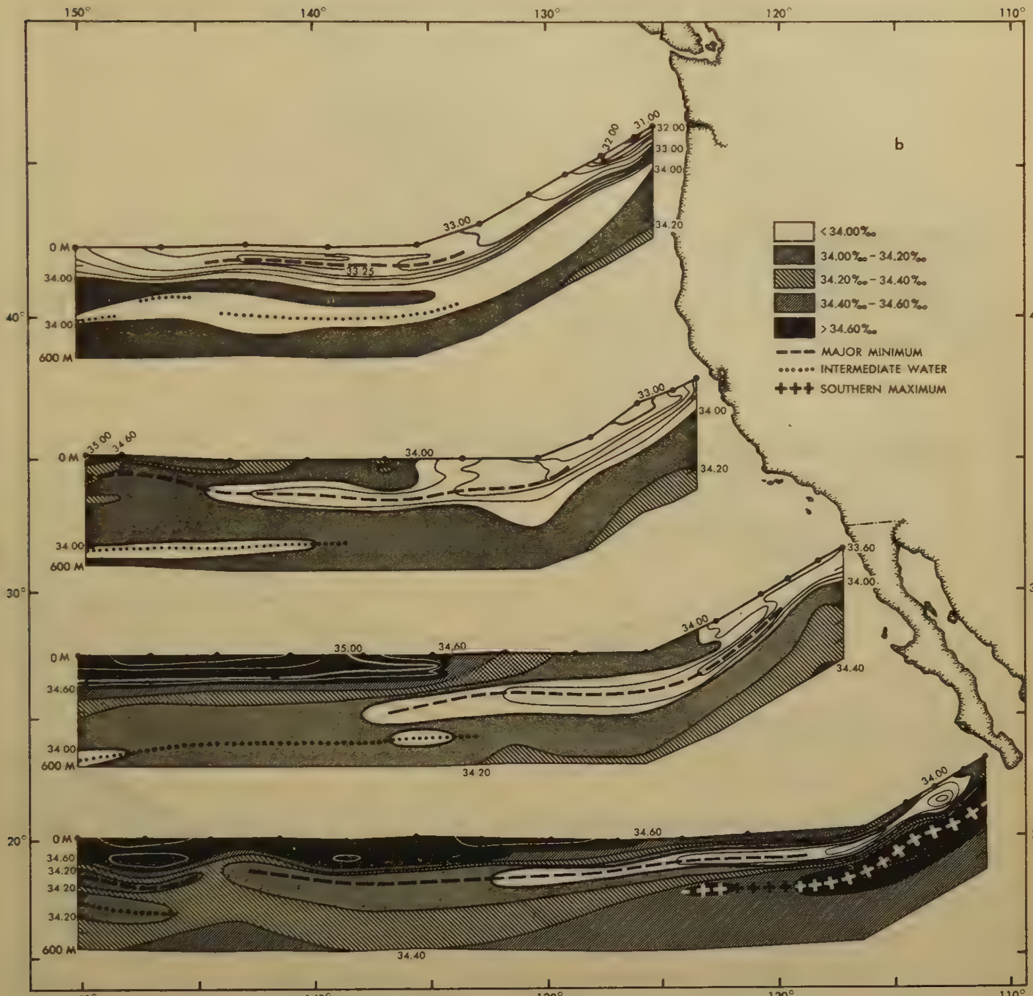
150°
140°
130°
120°
110°
40°
30°
20°
b
< 34.00‰
34.00‰ - 34.20‰
34.20‰ - 34.40‰
34.40‰ - 34.60‰
> 34.60‰
MAJOR MINIMUM
INTERMEDIATE WATER
SOUTHERN MAXIMUM
0 M
600 M
34.00
33.00
33.25
32.00
31.00
34.20
35.00
34.60
34.40
33.60

FIGURE 5—Continued

(b) Salinity, parts per mille.

the original thermocline. A curious result of this sequence is that the high temperatures are found later in the year at deeper levels than at the surface. Heat is still conducted downward by the process of mixing long after the highest surface temperatures are past. This circumstance may be of some importance in the distribution of dissolved oxygen and will be mentioned again. (The upper left-hand section of figure 6 is taken from Robinson, 1957, and Mrs. Robinson also prepared the rest of the data for the figure.)

Near the coast two entirely different causes of seasonal change are found, and these alter the simple offshore sequence. The first is upwelling, which occurs earlier south of Point Conception than northward. To the south it occurs at about the time of the offshore seasonal low in temperature. Upwelling and seasonal

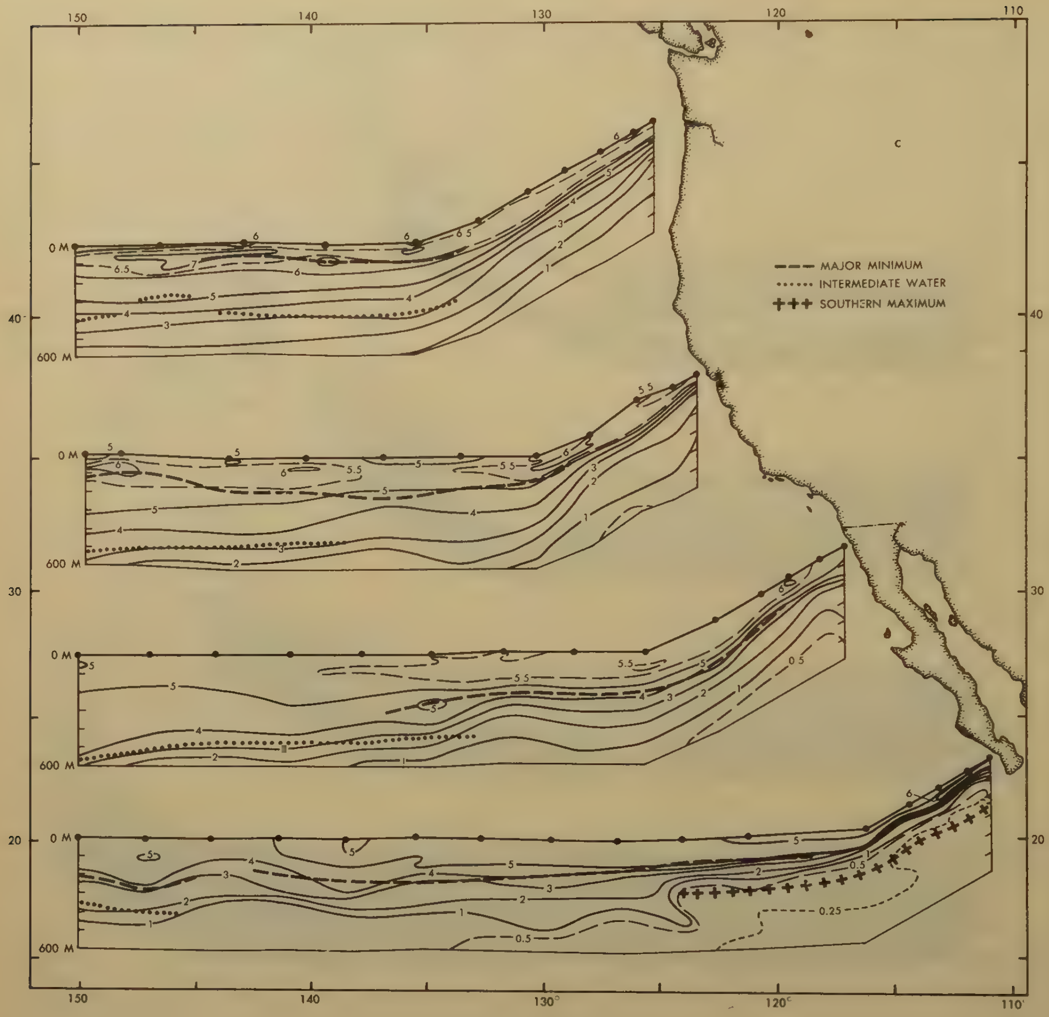

FIGURE 5—Continued

(c) Oxygen, milliliters per liter.

cooling combined result in a wider range in temperature than is found offshore. North of Point Conception upwelling occurs later and lengthens the cold period, and diminishes the seasonal range well below that of the offshore waters. Thus the March and August temperatures off Cape Colnett (30° N) are 12° C and 19° C while off Cape Mendocino they are both between 10° C and 11° C (Figs. 4a and 4b).

The second principally coastal cause is the seasonal ebb and flow of the countercurrent. This current, which is found off Baja California in the fall, brings warmer water from the south northwestward along the coast. It increases the fall high in temperature and extends it long enough to delay the spring low. It will be seen to be even more effective in altering the salinity.

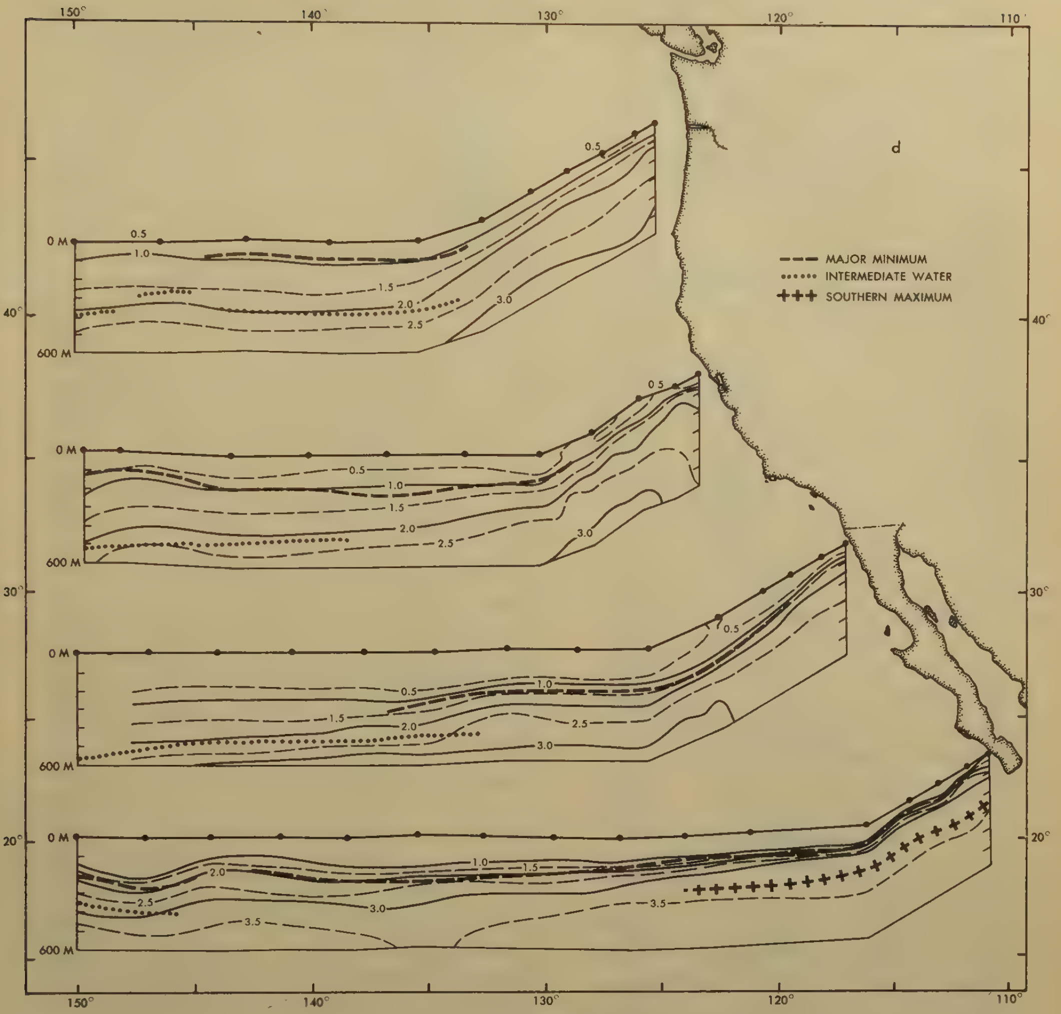

FIGURE 5—Continued

(d) Phosphate-phosphorus, microgram atoms per liter.

The results of the various seasonal forces are shown in figure 7 for the surface temperatures. Offshore the seasonal variation is largely the result of radiation and exchange with the atmosphere. A simple pattern is found with the ranges greatest in the north, where the variation of sunlight is greatest. Near the continent north of Point Conception the seasonal range is decreased and the cool period lengthened by upwelling. Between Point Conception and Punta Eugenia upwelling increases the seasonal range. South of Punta Eugenia the fall countercurrent raises the range above that offshore and delays the low until late spring. (Data for the areas 40-45° N 127-130° W, and 45-50° N 124-127° W, are from Robinson, 1957.)

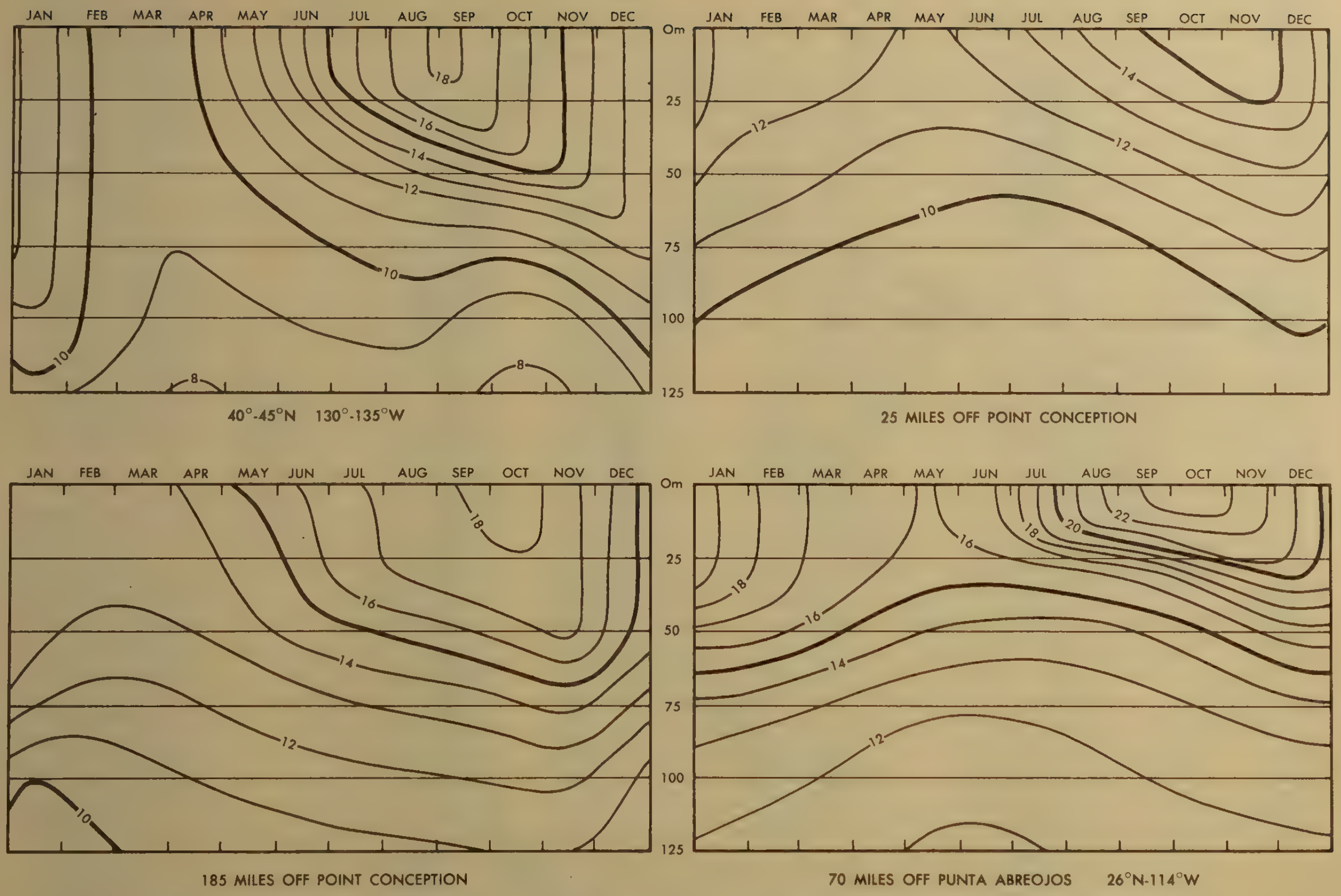

40°-45°N 130°-135°W

25 MILES OFF POINT CONCEPTION

185 MILES OFF POINT CONCEPTION

70 MILES OFF PUNTA ABREOJOS 26°N-114°W

FIGURE 6. Seasonal variation of temperature in the upper 125 meters at four locations. Temperature in degrees Centigrade, depth in meters. The upper left-hand section is from Robinson (1957); the other sections are from CCOFI data, 1949-55.

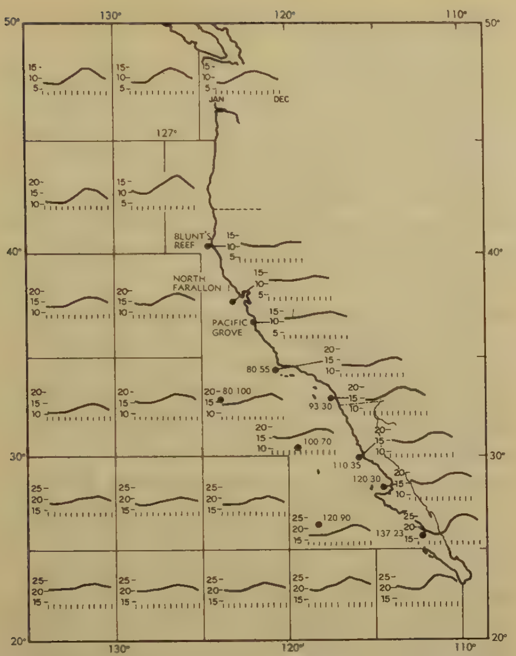

FIGURE 7. Seasonal variation of temperature at the surface off the western coast of North America. Temperature in degrees Centigrade. Values over five-degree squares are from Robinson (1957); values at Blunt's Reef, North Farallon Island and Pacific Grove are from U. S. Coast and Geodetic Survey (1956); values at numbered stations are from CCOFI data, 1949-55.

There are marked year-to-year differences in monthly average temperature. Such differences are indicated in the long and continuous (40 years) data for the Scripps Pier (Fig. 8). (Temperatures at this position will later be shown to represent to a high degree the general fluctuations in conditions off southern California and northern Baja California.) The maximum observed range of average monthly temperature is about 7° C and the average range is nearer 5° C. The frequency distributions are not symmetrical, especially during the months of minimum temperature (February through April). In this period the mean temperature is closer to the minimum than to the maximum of the range. This can be interpreted to mean that large temperature departures in the cold months are caused by an intrusion of warm rather than cold water. In late summer an opposite asymmetry is less clearly suggested.

In regions of small seasonal range the highest temperatures in one year may be lower than the lowest in another. Thus the monthly temperature averages at North Farallon Island (where the seasonal range is reduced by upwelling) in 1940 were higher throughout the year than in any month in 1955 (Fig. 9).

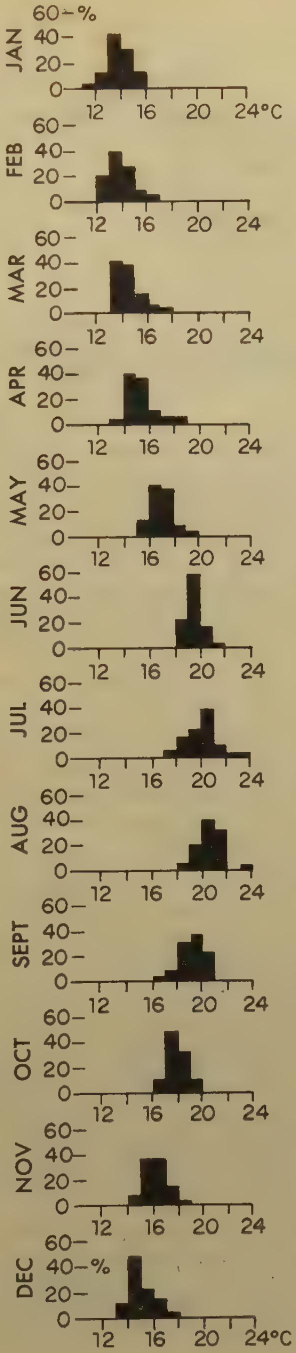

FIGURE 8. Frequency distribution of monthly average temperature at Scripps Pier, La Jolla, from 1917 to 1956. Temperature in degrees Centigrade.

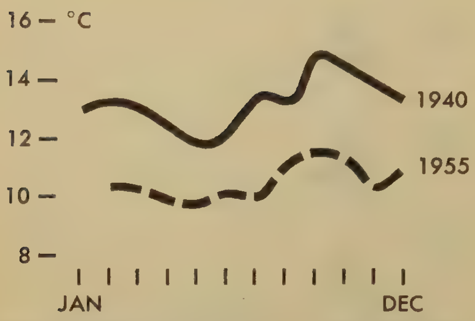

FIGURE 9. Monthly average temperature at North Farallon Island in 1940 and 1955. Temperature in degrees Centigrade.

Salinity

The California Current brings water of low salt content (about 32.5 parts per mille is the minimum value farther upstream) from higher latitudes down the coast where it mixes with water of higher salinity from below, from the west, from the inshore upwelling areas and the south (Figs. 10a and 10b). At times (Fig. 10a) the Columbia River makes an appreciable contribution of fresh water and at other times the countercurrent in the south contributes very salty water (Fig. 10c).

This history of the low-salinity Subarctic water as it moves down the coast is shown by the vertical profiles of figure 5b. On the upper line the water of low salinity is shown coming in above 200 meters. Already the horizontal mixing (which takes place faster in the upper layer) has caused the surface layer to be increased more than that below the permanent thermocline, and a slight but clearly detectable and continuous minimum can be seen (it is indicated by the long dashes). Values greater than 34.00 parts per mille (the shaded areas) are found over most of the deeper waters of the North Pacific (Sverdrup *et al.*, 1942) except where they are interrupted by Intermediate Water (dotted line). This water is generally supposed to form (*ibid.*) in the western Pacific at the intersection of the warm salty Kuroshio and cold, low-salinity Oyashio Currents in the winter, and it sinks to a depth corresponding to its density after mixing and spreads over nearly all the North Pacific. In the upper profile it loses its identity in the low-salinity Subarctic water of the California Current, and in the other profiles its low value is gradually increased by mixing with the higher salinities of the Equatorial Pacific and transition water to the east.

Before the water reaches the latitude of San Francisco much more east-west mixing has taken place, and the influx of salty water from the west has greatly intensified the difference between the surface values and the minimum. The effect of the Columbia River, shown to be small by the first profile, has now almost entirely disappeared.

Still farther south the amount of water of low salinity has diminished and the minimum has been gradually eroded by vertical mixing. The California Current does not terminate here, however, but can be traced to the west by its low salinity into the westward-flowing North Equatorial Current.

The effect of the subsurface countercurrent is most strongly seen in the last profile. The water, as it enters, has the temperature-salinity relation characteristic of the Equatorial Pacific water. The salinity is sufficiently greater than that of the California Current water above it and the deeper Pacific water below it to produce a maximum which continues as far north as Guadalupe Island. After the local maximum has been mixed away the Equatorial Pacific water can still be identified in a state of transition along the coast possibly as far north as the Gulf of Alaska, and in offshore waters as far as 40° N latitude.

The direct effect of the seasons upon salt content at the surface is limited to processes of precipitation and evaporation. Jacobs (1951) has estimated the difference between these terms in each season. Over the northern part of the current, rainfall predominates throughout the year, and evaporation in the south, with the boundary at San Francisco in summer and at Point Conception in winter. The seasonal changes are not large compared to other areas of the ocean. The largest difference is found off Washington and Oregon where rainfall exceeds evaporation in the winter by 14 centimeters per month and in the summer by only 3 centimeters per month. If this difference of 11 centimeters of rainfall were mixed into the upper 30 meters of water of about 32.5 parts per mille the salinity would drop by 0.12 part per mille, and this might be the order of the seasonal variation expected from exchange with the atmosphere.

Such a small range is difficult to detect against a background of strong vertical and horizontal variation (Figs. 5b and 10a-d). The minimum value would fall at about the time of year when the winds off Washington are from the southwest, and these may bring in enough salty, offshore water to cancel or reverse the trend. In any case, no such consistent minimum has been found in the offshore waters of the California Current. Although several large changes are indicated in the data taken by the CCOFI program in this region, they occur in such a scattered fashion as to present no coherent pattern at this writing. This may mean that offshore the seasonal variations are small compared to changes of other periods, and this will be taken up in the section on long-term variations.

Near the coast, however, several sorts of seasonal change are found. In the far north the runoff from the Columbia River has a seasonal variation, with the

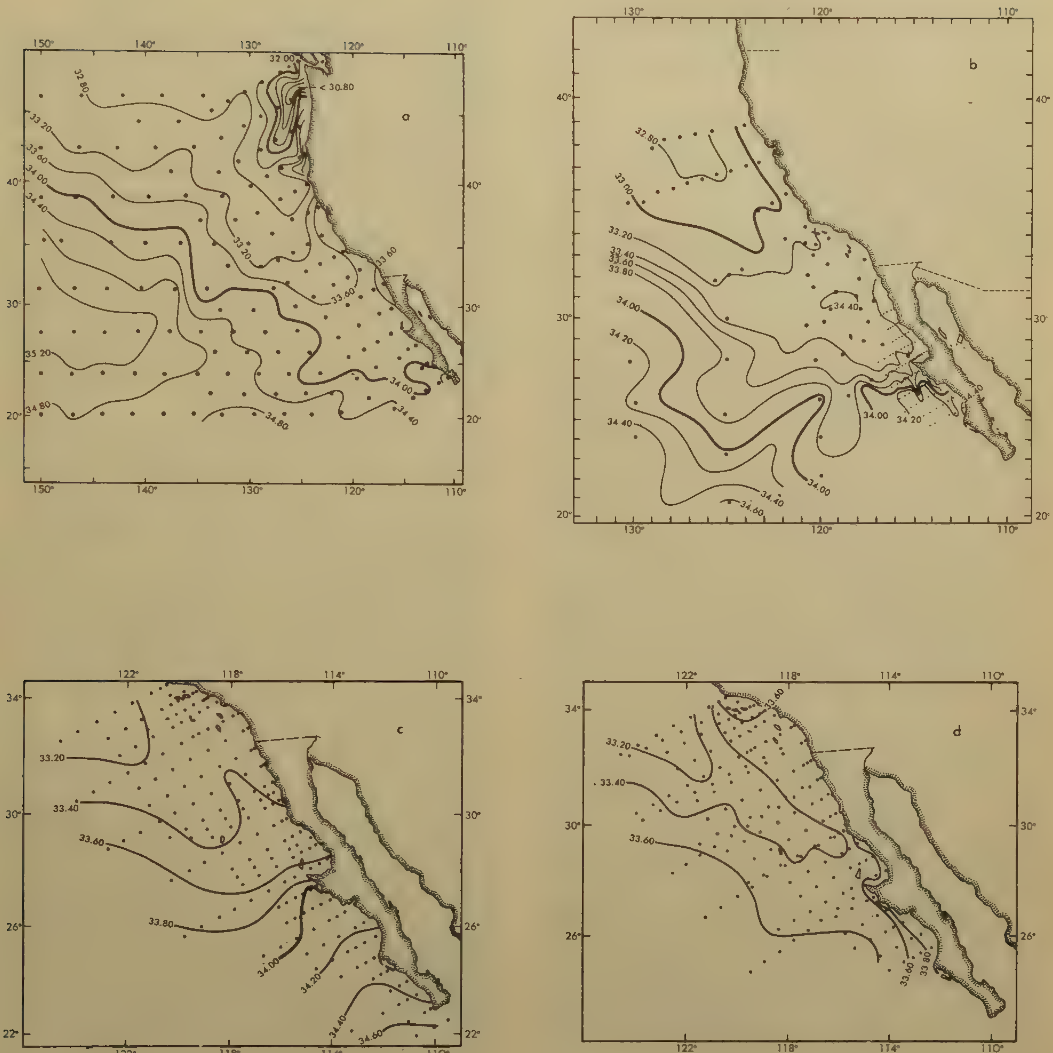
a
150°
140°
130°
120°
110°
32.00
< 30.80
32.80
33.20
33.60
34.00
34.40
40°
33.20
33.60
33.60
30°
35.20
34.00
34.80
34.80
34.40
20°
b
40°
32.80
33.00
33.20
33.40
33.60
33.80
34.40
34.00
34.20
34.40
34.00
34.20
34.40
34.60
30°
20°
c
122°
118°
114°
110°
34°
33.20
33.40
33.60
33.80
34.00
34.20
34.40
34.60
26°
22°
d
33.60
33.20
33.40
33.60
33.60
33.80

FIGURE 10. Salinity at 10 meters, in parts per mille. (a) August 1955. (b) March (composite). (c) January (average of three years). (d) June (average of three years).

highest outflow in May and June and the lowest from November through February. The U. S. Geological Survey (1952) reported that in 1951 and 1952 the rate of outflow ranged from 1800 to 7000 cubic meters per second. Although the greatest outflow is about a thousandth part of the California Current (Sverdrup, *et al.*, 1942), the fresh water is lighter and lies upon the top of the ocean water until it loses its identity by mixing.

It is in the salinity that the effect of the river water is most obvious. It spreads over the surface of the southward-moving current in a thin layer affecting noticeably only the upper 10 meters. In this thin surface layer the salinities may be reduced from the offshore value of 32.5 parts per mille to as low as 30 parts per mille. This is at once noticeable as a local minimum in salinity (Fig. 10a).

In temperature and oxygen measurements the effects of the river water are much less obvious, since the values in the river water are not so vastly different from those of the ocean water. The amount of dilution which has taken place by the time the waters have moved 100 miles offshore (in the above case 8 percent of river water to 92 percent of ocean water), obscures any difference. The same situation apparently holds true for the phosphate. Although the effect of the river water stands out on the charts of salinity, the charts of temperature, oxygen, and phosphate do not show any corresponding offshore peculiarities.

The CCOFI program has not measured the salinity north of Cape Blanco in the period December through February. The salinity in the area well south of the river shows a drop in July, which would be consonant with a maximum outflow in May and June, and the values are below oceanic from July through September.

Southward the two great causes of seasonal variation in salinity are upwelling and current. The values change as the upper waters are moved offshore by the wind at Point Conception and the countercurrent ebbs and flows south of Punta Eugenia (Fig. 11). The salty southern water advances in the fall and retreats in the spring.

North of Point Conception where the range of temperature from March to August is reduced by upwelling the range of salinity is increased (Figs. 10a and 10b). South of Point Conception the range is less. March and August are not the extreme months in the south. It is in January and June that the 10-meter salinities show the greatest effects of the countercurrent (Figs. 10c and 10d).

There are striking differences in seasonal variation at the surface over the whole area (Fig. 12). The extreme effect of upwelling is seen north of Point Conception and of the countercurrent south of Punta Eugenia, with their high and low values at different periods. In the intermediate area these effects combine and reduce the seasonal range. In the south the seasonal effects extend well offshore, but in the north the range is small and the nature of the variation is not clear.

Oxygen

Oxygen will dissolve in sea water up to a limit (saturation value) which depends upon the temperature and salinity. Over most of the California Current the oxygen above the thermocline is concentrated to about 100 percent saturation. Oxygen is produced by the photosynthetic activities of plants in the upper levels of the ocean to which light can penetrate, and it is consumed by processes of respiration and decay. Since there are no new sources of oxygen at depth, the deeper waters become depleted in oxygen. The concentration of oxygen has been used as an indicator of the "age" of the water, that is, the length of time it has been away from any contact with the surface; and it is partly because of its low oxygen values that the deep Pacific water is thought to be older than the deep Atlantic water and to have originated in the Atlantic (Sverdrup *et al.*, 1942).

Most of the time the content of oxygen at the surface is at or slightly above 100 percent of the saturation value. Less often it is slightly below saturation. The saturation value of oxygen depends upon both temperature and salinity, but over the range of variation of these two quantities in the upper layers of the California Current, the temperature effect is several times larger than the effect of salinity. The saturation value of oxygen is higher at low temperatures; thus the deep waters, which are colder than the surface waters, could hold more oxygen, but they rarely do since the supply at depth is limited to mixing from above or vertical movement.

In summer the upper waters entering from the northwest are high in oxygen, containing greater than 7 milliliters per liter (Fig. 5c). In the southwest they hold generally less than 5.5. A striking feature of the upper-layer oxygen distribution is the shallow subsurface maximum found over most of the area in summer and fall. Below this maximum, and at a level corresponding to the salinity minimum, the oxygen shows a sharp drop. The percentage of saturation value, which has been at or above 100, drops as markedly. This may mean that the water above the permanent thermocline has relatively free access to the atmospheric oxygen, but that the stability of the water at the level of the salinity minimum (which allows a thin layer to preserve its low salinity over so many miles of motion) severely limits the transfer of oxygen downward from the rich layers.

In the deeper layers very low values are found off southern Baja California and extending northward along the coast. Values at 200 meters off the tip of the peninsula are less than one-tenth as high as those in the northwest (Fig. 13). This water of low oxygen

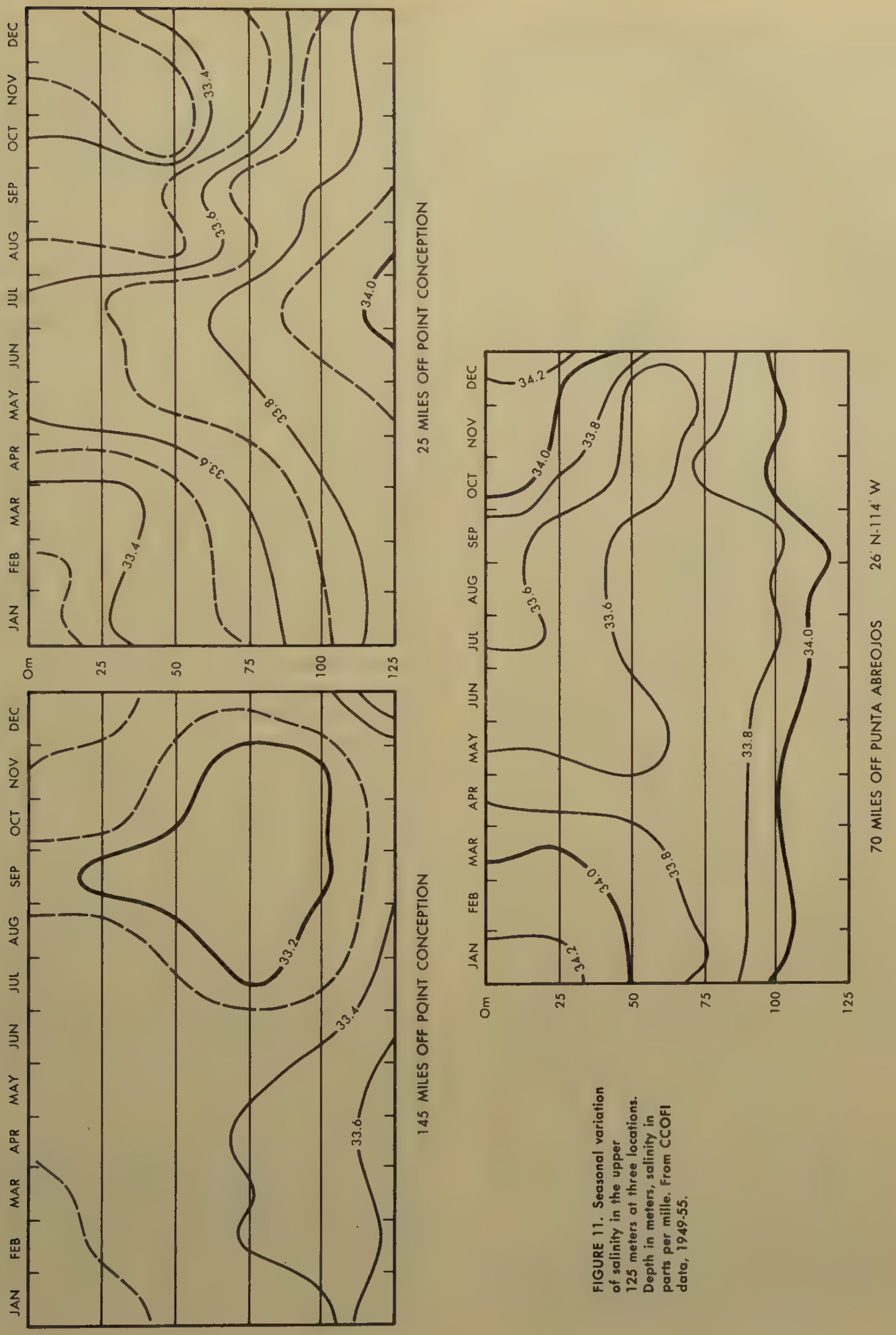

FIGURE 11. Seasonal variation of salinity in the upper 125 meters at three locations. Depth in meters, salinity in parts per mille. From CCOFI data, 1949-55.

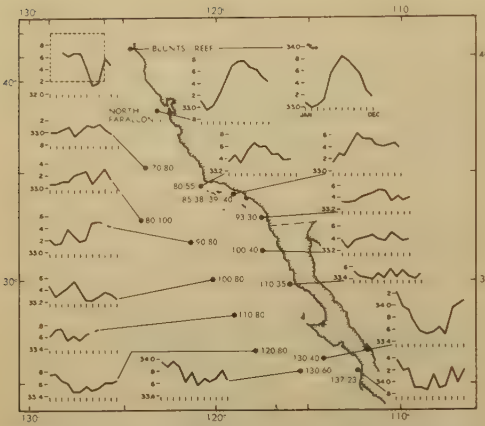

FIGURE 12. Seasonal variation of salinity at the surface off the western coast of North America. Salinity in parts per mille. Values at Blunt's Reef and North Farallon Island are from U. S. Coast and Geodetic Survey (1954); all other values are from CCOFI data, 1949-55.

has been discussed with the salinity and seen to be water from far south gradually weakening in distinction as it moves northwest. It is of high salinity and high phosphate as well (Fig. 5d). It must have been below the surface for a long period, for its oxygen has nearly been consumed in the decay of organic matter from the upper layer.

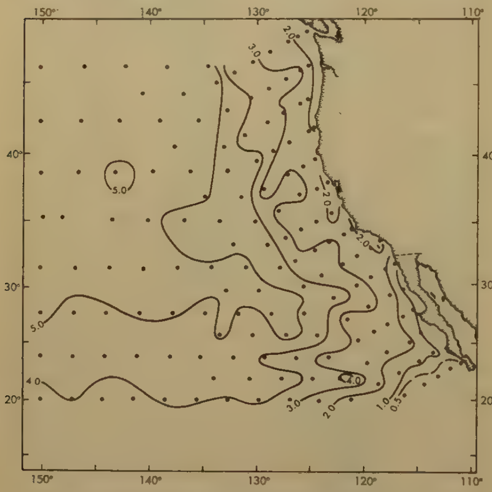

FIGURE 13. Dissolved oxygen, in milliliters per liter, at 200 meters, August 1955.

The seasonal variations of oxygen at the surface occur generally in response to the seasonal change in temperature (and thus saturation value); that is, in the cold months the water has more oxygen than in the warm months. The average range of this variation is about one milliliter per liter, though it may sometimes be higher. Thus the surface oxygen values offshore from Point Conception are usually slightly over 6 milliliters per liter from March to May and slightly under 5.5 from August through November. The occurrence of the high values is delayed over a month off Punta Eugenia, corresponding to the delayed minimum of temperature. The high and low values are about 6 and 5 milliliters per liter.

The surface values are sometimes less than 100 percent saturation. In periods of intense upwelling the water of low oxygen content from below may arrive at the surface and remain below saturation (as its temperature increases) for several days before saturation is attained.

The slight subsurface maximum (Fig. 5c) has been referred to as a summer and fall occurrence. Such a maximum is rarely found in the winter or spring. The sequence of formation of the maximum is generally as follows: In winter the oxygen values in the mixed layer are fairly constant with depth at about 100 percent saturation or very slightly above. In spring the surface values begin to fall. The oxygen content at 30 to 70 meters depth does not begin to fall until July or August; thus a maximum value is found around 50 meters from late spring until winter, nearly always slightly supersaturated.

A possible cause of the subsurface oxygen maximum is the subsurface production by phytoplankton. A more likely one might be the "entrapment" of oxygen by the water during the cold periods. If the values near the surface, which is in contact with the air, decrease more rapidly from their common winter maximum, then the subsurface water will for some period contain more oxygen. The lag of the deeper values behind the surface in the period of minimum and maximum temperature has been mentioned. This would cause the saturation limits of oxygen to decrease later at depth than at the surface. Redfield (1948), after examining the seasonal changes in the Gulf of Maine, concluded that over the whole year photosynthesis there has considerably less effect than changes of saturation value, but that at the period of minimum temperature (and small change) photosynthesis may dominate.

Phosphate

Phosphate is important to life in the sea as one of the principal nutrients. The North Pacific contains higher phosphate concentrations than the Atlantic or Indian Oceans. Its maximum values are well below the surface, usually just below the oxygen minimum, which places them at a depth of 1000 to 1200 meters (Wooster, 1953). Values greater than 1 microgram atom per liter are found in the Subarctic water at the surface north of 45° N latitude, increasing to values as great as 3 at a depth of 200 meters. At corresponding latitudes in the Central Atlantic Ocean the surface values are less than 0.1 microgram atom per liter (Sverdrup *et al.*, 1942). It has been shown, in fact, that for certain organisms the phosphate is present in sufficient quantity for growth everywhere in the North Pacific (Goldberg *et al.*, 1951). This has not been shown, however, for all organisms and for other nutrients. The phosphate continues to be investigated in the Pacific, not only because of its own possibly critical value, but because it may be an indicator of other nutrients.

The high phosphate values of the Subarctic water at 147° W longitude drop off sharply to the south (Fig. 5d). Below 35° N in that longitude they are less than 0.5 microgram atom per liter in the mixed layer. The average value over the southwest part of the region is about 0.3 microgram atom per liter. Phosphate is concentrated at depth (Fig. 5d) and its upward diffusion is found to be limited, as was the downward diffusion of the oxygen, by the stable layer below the seasonable thermocline. In regions where there is a salinity minimum below the mixed layer, the first marked increase of phosphate is almost invariably found at the minimum value of salinity. In the California Current system the mixed layer is shallower near the land. Some photosynthesis may take place beneath the mixed layer in the nearshore regions, and the nutrients used in the process can be more easily replaced than those in the mixed layer by diffusion from below.

Over the Northeastern Pacific the horizontal distribution of phosphate at 100 meters depth and the horizontal distribution of zooplankton are very much alike (Figs. 14 to 16). The higher zooplankton volumes are found in the Subarctic waters where they lie near the surface in the California Current region, and especially in the regions of upwelling. Farther offshore the high values of phosphate are found at greater depths, where no photosynthesis can take place, and where replenishment of the surface waters is very slow.

The close relation of phosphate to zooplankton is somewhat baffling if, as has been suggested, the phosphate values in the Pacific are high enough everywhere to promote normal growth. The relation holds however not only in a rough fashion over large areas (Figs. 14a and 14b) but in a remarkable station-to-station coherence (Figs. 15a-b and 16a-b). This indicates that the zooplankton growth takes place in the areas of high phosphate near the coast, and that parcels of this water moving outward into the main stream contain both high phosphate and high zooplankton volumes.

The seasonal variations of phosphate are more difficult to understand in the California Current system than they have been in the Atlantic. Redfield (1948) and Redfield, Smith, and Ketchum (1937) have discussed the seasonal variation of phosphate in the Gulf of Maine; and Atkins (1923-30) and Cooper (1933 and 1938) have discussed the variation in phosphate in the English Channel. In both regions a marked change occurred in the upper levels in summer owing to the consumption of the phosphate by the phytoplankton. However, the lowest values near the California coast at any time of year are generally higher than the highest values ever attained in the two Atlantic areas mentioned. The same consumption of phosphate in the California Current would cause a proportionately smaller drop in phosphate. Furthermore, the periods of minimum phosphate found by the authors mentioned above occur in summer as the result of heavy plant growth. This same period in the California Current is one of great replenishment of phosphate by upwelling. In a discussion of the seasonal variation of oxygen in the Gulf of Maine, which has already been mentioned, Redfield (1948) made use of a relation between the oxygen and phosphate transformation in the biological processes of photosynthesis and respiration. He accounted in part for the seasonal change in oxygen by the change in phosphate. Using this relation, and taking into account the maximum effect of photosynthesis allowed by the observed values of chlorophyll "a" in the region south of Point Conception (Holmes, personal communication), an absolute maximum consumption of phosphate of the order of 0.4 microgram atom per liter per month might be attained. The actual value is likely to be much less than this, and the amount of upwelling necessary to produce the observed temperature and salinity effects near the coast could easily counterbalance this consumption.

On the other hand, the phosphate values have not shown the effects of upwelling as clearly as have temperature and salinity. The measurement of phosphate has not been carried on as successfully by the program as have the measurement of temperature, salinity, and oxygen; and the measurement has not been so continuous nor covered so wide an area. Higher values near the surface are found at the appropriate times as the result of upwelling, but the appearances are not so regular or simple as those of temperature and salinity.

RELATION OF THE ENVIRONMENT TO THE PLANTS AND ANIMALS

The previous discussion has shown that the California Current system contains a band of cool water reaching from high latitudes far down the coast of North America. It brings in waters of relatively high phosphate content (Fig. 14a), in sharp contrast to the waters farther offshore. Along the coast this

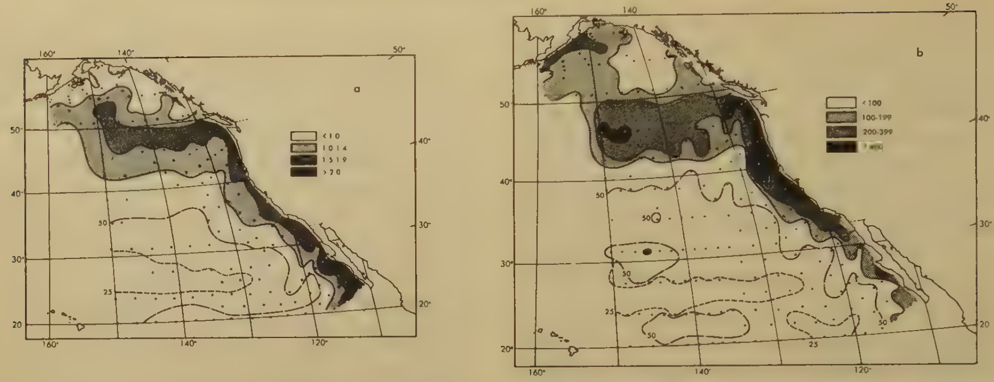
a
<1.0
1.0-1.4
1.5-1.9
>2.0
b
<100
100-199
200-399
160°
140°
120°
50°
40°
30°
20°
50
25

FIGURE 14. Distribution of phosphate-phosphorus and zooplankton volumes, August 1955. (a) Phosphate-phosphorus, microgram atoms per liter at 100 meters. (b) Zooplankton volumes, cubic centimeters per 1000 cubic meters.

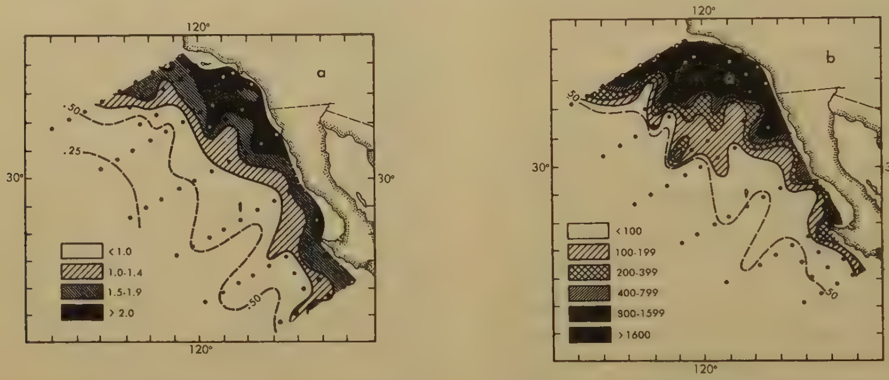
a
120°
30°
.50
.25
<1.0
1.0-1.4
1.5-1.9
> 2.0
b
<100
100-199
200-399
400-799
800-1599
>1600
50

FIGURE 15. Distribution of phosphate-phosphorus and zooplankton volumes, April 1950. (a) Phosphate-phosphorus, microgram atoms per liter at 100 meters. (b) Zooplankton volumes, cubic centimeters per 1000 cubic meters.

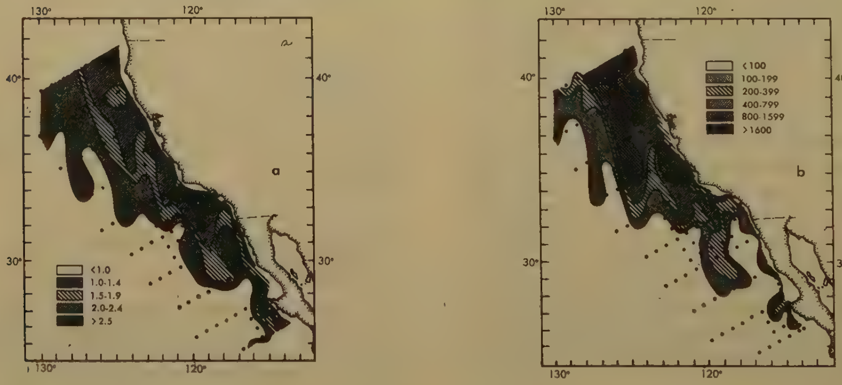
a
130°
120°
40°
30°
<1.0
1.0-1.4
1.5-1.9
2.0-2.4
>2.5
b
<100
100-199
200-399
400-799
800-1599
>1600

FIGURE 16. Distribution of phosphate-phosphorus and zooplankton volumes, July 1950. (a) Phosphate-phosphorus, microgram atoms per liter at 100 meters. (b) Zooplankton volumes, cubic centimeters per 1000 cubic meters.

higher value of phosphate is reinforced by the upwelling of deeper waters whose nutrient properties have not been exhausted. From the south at a depth of about 200 meters another current, also high in phosphate content, moves northward. This water has but little dissolved oxygen left (Figs. 5c and 13). This indicates that the oxygen has been depleted by respiration and the decay, over a long period, of organic material. The product of this decay is nutrient material, which is transported up the coast immediately below the surface layer and becomes available to the plants by mixing and upwelling.

The result, then, is a narrow band of waters all along the coast which are high in phosphate and presumably other nutrients. One effect of the richness of these waters is seen in the high volumes of zooplankton along the coast (Figs. 14 to 16), which are highest in regions where the upwelling and mixing are strongest. These high volumes contrast sharply with those of the less abundant waters of the west and southwest, and it is this great mass of living matter which accounts for the coastal fisheries.

This living matter, however, is of vastly different kinds, each with its own particular needs, so that within the region the species have quite different sorts of distributions. Most of the planktonic animals prefer the nearshore waters, but some have particular needs which cause them to live in greatest quantity offshore.

Relations have been found between the character of water masses and currents off southern California and the marine plants, diatoms (Sverdrup and Allen, 1939). Of particular interest is the finding that the offshore waters contain few diatoms, whereas the eddies of inshore water may contain large numbers. They found that the "age" of the surface water was an important factor. Newly upwelled water is high in nutrients, but after it has been at the surface for a long time, as is the case with the offshore waters, its nutrients have been consumed.

The planktonic animals have little power to move through the water and are transported largely by the currents. Different species and different stages of one species may live at different depths and have different limitations. Some must live near the surface and some avoid light and some move up and down. Some thrive at high temperature, some at low and some over a wide range of temperature. The charts showing the distribution of properties have shown that the properties vary in different manners. It does not seem impossible that an organism may be limited on one side of its distribution by temperature and on another side by some other properties, such as nutrients. Certain interesting examples of the regions inhabited by particular species are shown in figures 17a to e, on which are drawn certain other properties, which seem to coincide with their boundaries. The examples cover the larger part of the California Current system. Some species are distributed in the very cold, rich, waters of the northeast; others limited perhaps by a need for higher temperatures, are found to the southwest and may have an upper temperature limitation farther west.

The requirements of the organisms shown are not well enough understood for us to conclude that the properties illustrated at the boundaries are the effective ones. The euphausiids, in particular, are difficult to understand since they undergo a diurnal migration, and are deep in the daytime and near the surface at night. As they must move back and forth across a wide range of temperature in their migration, it is difficult to think that some temperature at a particular depth should be the major limiting factor. Work has been done upon this (Boden, *et al.*, 1955) and is being continued. The euphausiid distributions (Figs. 17a to d) are from work made available by Dr. Edward Brinton and the salp distribution (Fig. 17e) is from Dr. Leo D. Berner.

NON-SEASONAL VARIATIONS IN THE CALIFORNIA CURRENT SYSTEM SINCE 1916

The dependence of specific organisms on certain properties of the water masses has been assumed and to some extent measured. If conditions in the water are different in one year from another, certain organisms which thrive in the one year might not do well in the other. If long series of data were available for both the organisms and the current, the dependence might be explored statistically. The length of time this series would have to cover would depend upon the simplicity of the relation and upon the nature of the variations in condition and distribution. If the period since 1949 contained several highly unusual years, which were different from each other, the dependence could be much more easily established than if the years were more nearly alike.

In order to have some background against which the period of the CCOFI program can be examined, certain previous data have been used. In the late '30s and early '40s the cruises of the California Fish and Game vessel *Bluefin* and the Scripps Institution vessel *E. W. Scripps* made many measurements near the Channel Islands area of southern California. The *E. W. Scripps* also made one long cruise in 1939 from Cape Mendocino to Punta Eugenia and two cruises into the Gulf of California, in 1939 and 1940.

In addition to these data, surface temperatures had been measured by merchant vessels for many years, and various agencies have collected these and arranged them by monthly averages for 5-degree squares of latitude and longitude for each year. Principal among these agencies is the Kobe Imperial Marine Observatory in Japan to which we are indebted for

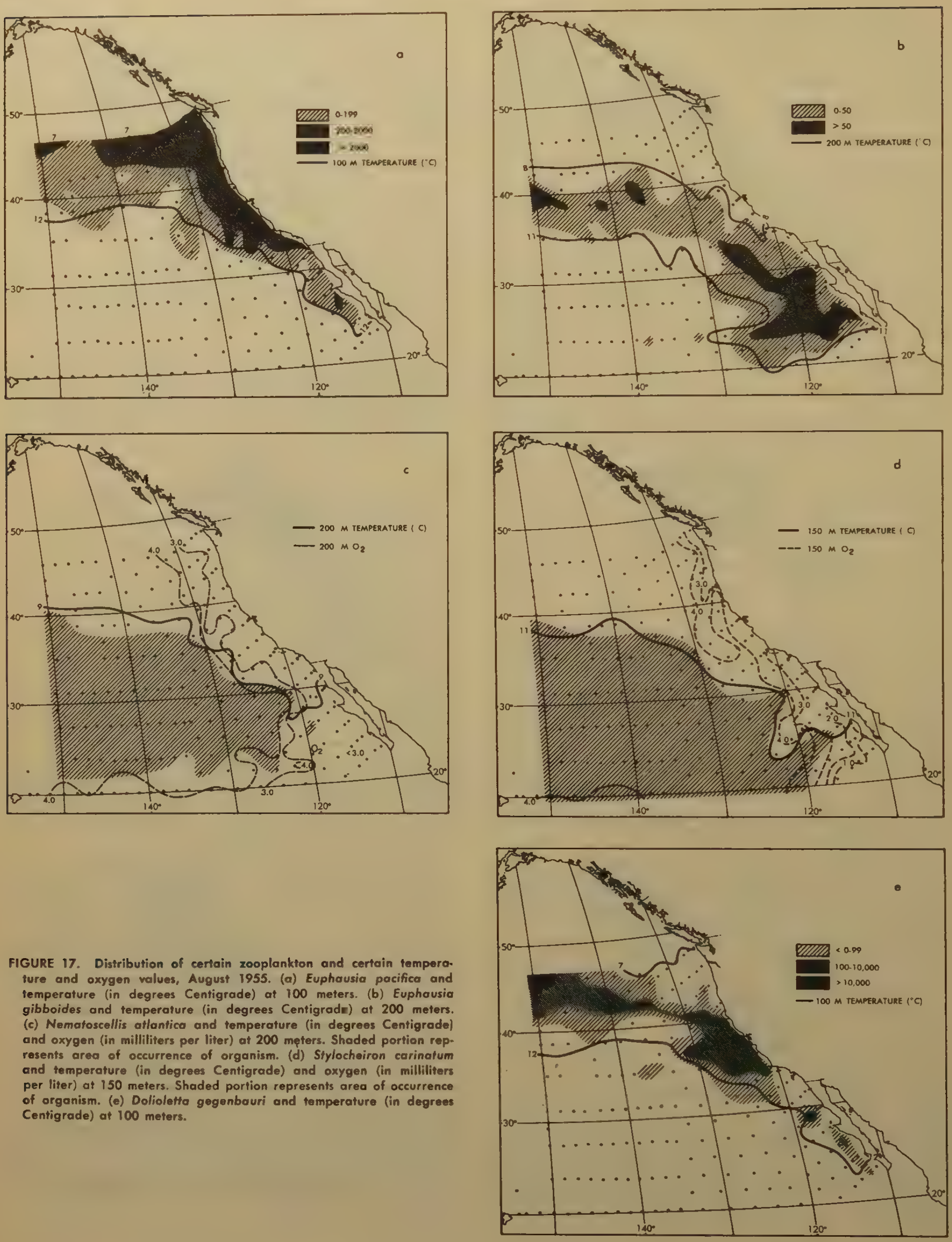
a
0-199
200-2000
> 2000
100 M TEMPERATURE (°C)
b
0-50
> 50
200 M TEMPERATURE (°C)
c
200 M TEMPERATURE (C)
200 M O2
d
150 M TEMPERATURE (C)
150 M O2
e
< 0.99
100-10,000
> 10,000
100 M TEMPERATURE (°C)
50°
40°
30°
20°
140°
120°

FIGURE 17. Distribution of certain zooplankton and certain temperature and oxygen values, August 1955. (a) *Euphausia pacifica* and temperature (in degrees Centigrade) at 100 meters. (b) *Euphausia gibboides* and temperature (in degrees Centigrade) at 200 meters. (c) *Nematoscelis atlantica* and temperature (in degrees Centigrade) and oxygen (in milliliters per liter) at 200 meters. Shaded portion represents area of occurrence of organism. (d) *Stylocheiron carinatum* and temperature (in degrees Centigrade) and oxygen (in milliliters per liter) at 150 meters. Shaded portion represents area of occurrence of organism. (e) *Dolioletta gegenbauri* and temperature (in degrees Centigrade) at 100 meters.

the publication of such data over the North Pacific Ocean from 1911 through 1938. In addition, for many years, the U. S. Coast and Geodetic Survey has taken sea level temperature and salinity measurements at various of its tide gauge installations along the west coast of North America and Alaska. Observations of surface temperature and salinity from 1923 through 1940 are available for the Blunt's Reef light vessel and from North Farallon Island. Surface temperature and salinity measurements have been made daily at Pacific Grove and at Scripps Pier for many years.

Meteorological data are available from the U. S. Weather Bureau in the form of sea level atmospheric pressure averaged by months from 1899 to the present.

With these data in hand, it has been possible to compare the variations from year to year of temperature, salinity, and wind at various places. With the exception of the surface temperatures from merchant vessels, however, the hydrographic data are almost entirely from the *Bluefin* and *E. W. Scripps* cruises 20 years ago and the CCOFI cruises which began in 1949.

These data would seem rather scanty for an analysis of variations in a major current over a long period, but certain of the initial results have been encouraging. The variations in temperature at points along the coast of North America show considerable coherence over great distances. The major anomalies in temperature, high or low, seem to last several months, implying that monthly averages are not an unlikely method of approach. Certain of these data are shown by monthly anomalies (Fig. 18); that is, the value plotted in June of a given year represents the amount by which the average temperature in June of that year was higher or lower than the average of all the Junes from 1920 to the present. (Some of the data are from the Japanese sources and are available only through 1938.)

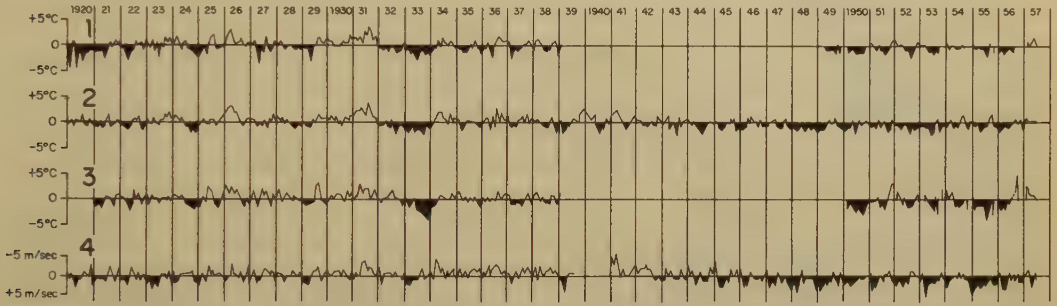

FIGURE 18. Monthly differences from average sea surface temperatures (degrees Centigrade) at (1) 30°-35° N, 115°-120° W, (2) Scripps Pier, and (3) 25°-30° N, 110°-115° W; and (4) monthly differences from average northerly wind component (in meters per second) at 30° N, 110°-130° W.

The principal cold periods were from 1920 to 1924, in 1932 and 1933, and from 1948 through 1956. The warmest groups of years were from 1926 through 1931, and from 1934 through 1944. The variation in the strength of the north wind from its monthly mean over the same period is also shown (Fig. 18, part 4) and a certain similarity in long-term variation is seen between wind and temperature anomalies.

The last few years stand out from the long-term mean both in temperature and salinity (Figs. 19 and 20). The winter and spring temperatures are low and the summer values more normal or high. The salinity values are high in winter and spring and more nearly normal the rest of the year. Although there is some variation from year to year since 1949, the deviations have not been extreme (Fig. 18) except possibly south of Punta Eugenia. From 1949 through 1956 there were no years as extreme as 1926, 1931, 1933, or 1941.

A cause for this behavior has been sought in the variations of the strength of the wind. The northerly component of wind (computed from atmospheric pressure difference at 30° N latitude between 110° W and 130° W longitude) was generally stronger in the last decade (Fig. 20). A significant correlation has been found between the wind anomalies and the temperature and salinity anomalies in the spring and early summer months where as many as 18 years of data are available (Roden and Reid, Ms. in preparation). It is in these months that the greatest variations from the mean are found in the wind data. In August, although the winds are strong, the variation of monthly averages about the long-term mean is much smaller. The mechanism of this relation may be an increased amount of upwelling, and possibly an increased amount of Subarctic water being brought south by the northerly winds. The correlation holds in all the data from Blunt's Reef to Magdalena Bay during these months. In the latter part of the year the winds have varied less, and no significant correlation has been found.

The fact that temperature has been lowered and salinity raised during this period implies that at least

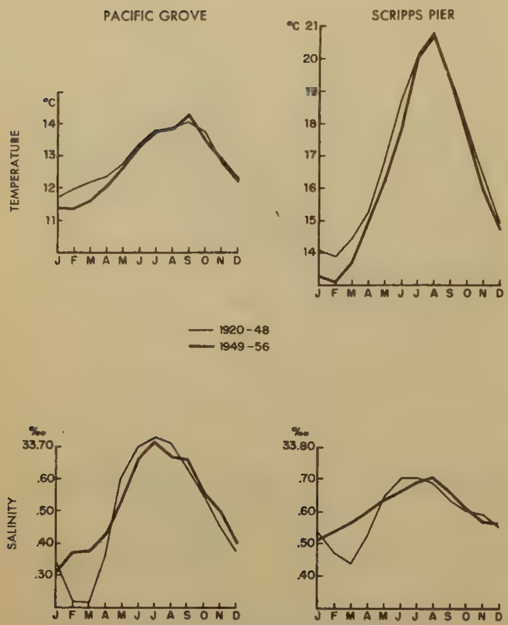

FIGURE 19. Average surface temperature (degrees Centigrade) and salinity (parts per mille) at Pacific Grove and Scripps Pier for the periods 1949-56 and 1920-48.

part of this process is upwelling, since the evaporation minus precipitation values here (Jacobs, 1951) are quite small. There are no earlier phosphate data with which the CCOFI data can be compared.

It may then be concluded that the period from 1949 to 1956 is distinguished from the previous 15 or 20 years by substantially colder waters in the first few months of the year. There are differences in the years from 1949 to the present (which will be taken up later), but they have nearly all exhibited this colder feature in the early months.

The sea surface temperature in the period from 1945 to 1956 showed no values extreme enough to compare with those of the intensity and endurance of 1926, 1931, 1933, 1940, or 1941 (Fig. 18). A certain coherence of the system is at once obvious from the data from 1949 to the present (Fig. 21). These data allow one to generalize somewhat about the difference in the various years. South of Punta Eugenia the data in the 5-degree square show some greater irregularities and indicate some difference in behavior from those to the north. They generally show the same phenomenon of cold springs which have a significant correlation with the northerly winds. The most remarkable variations in this period have been south of

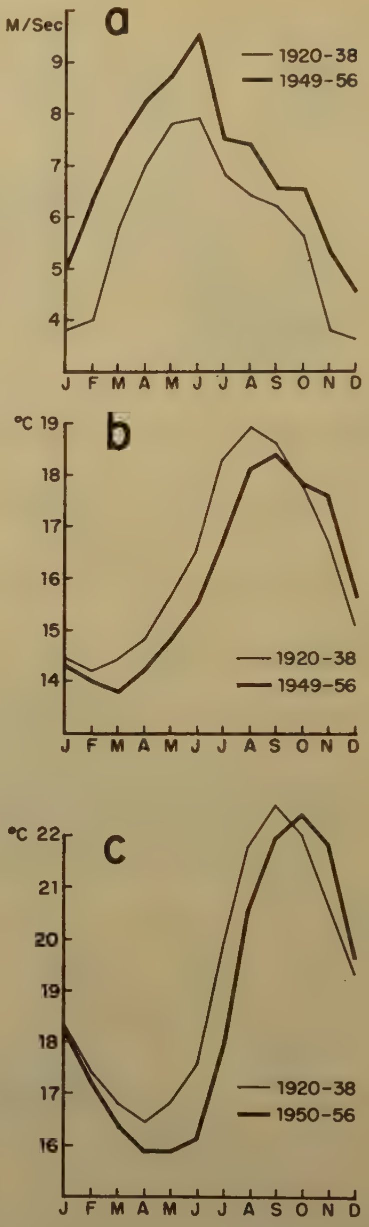

FIGURE 20. Average northerly wind component and temperature in recent period compared to averages for 1920-38. (a) Northerly wind component in meters per second at 30° N in years 1949-56. (b) Temperature in degrees Centigrade at 30°-35° N, 115°-120° W, 1949-56. (c) Temperature in degrees Centigrade at 25°-30° N, 110°-115° W, 1950-56. No data 1939-48.

Punta Eugenia where the late fall of 1951 was unusually warm and the summer of 1955 was unusually cold. It is unfortunate that in 1940 and 1941, when the temperatures over all the west coast north of San Diego are known to have been at their highest in the last 25 years, no data are available from the vicinity of Punta Eugenia. A comparison of 1951 with 1940 and 1941 might be of interest.

Over most of the area, 1954 was the warmest year, though there was at least one cold month toward the end of the year. The year 1949 began well below normal in winter and spring and was somewhat above normal in the early fall. Likewise, 1950 was below normal in winter and spring but did not show the same summer and fall warming as had 1949. The year 1951 was more normal during the first few months but at different places showed both warming and cooling toward the end of the year. In most places, 1952 began somewhat above normal but dropped below normal in the fall. The year 1953 began slightly above normal and in the north was above normal again in the fall but in the south was cooler in the fall. The year 1954, in most of the data, was well above normal most of the year dropping below only in November and December in most places. The year 1955, in much of the data, was well below the normal and 1956 was likewise generally cool. In 1957, the southern California waters seem to be at or above normal through June (Fig. 22). North Farallon Island shows temperatures slightly below normal averaged through June, and data from Blunt's Reef through April show values generally below normal.

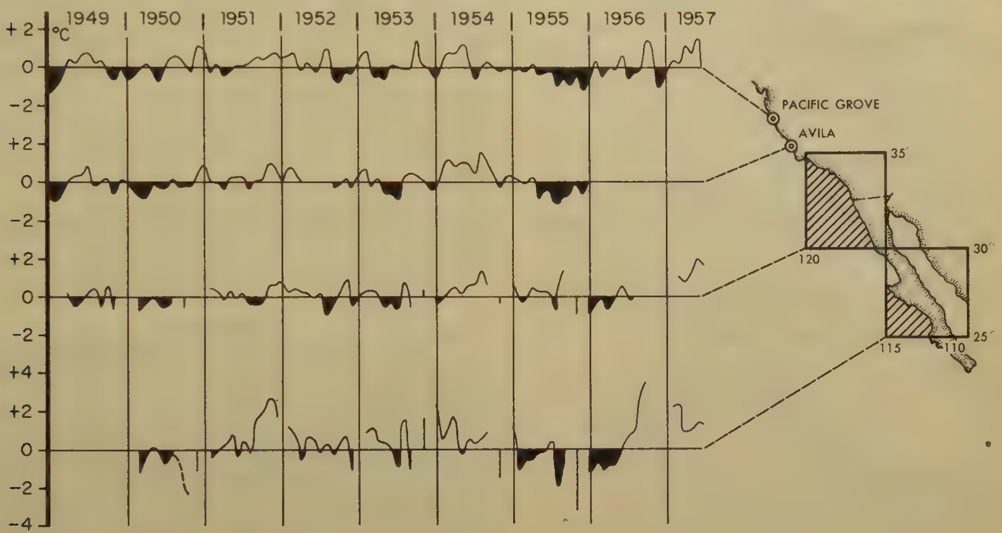

FIGURE 21. Temperature anomalies, 1949 to 1957, at four locations as referred to 1949-56 mean. Temperature in degrees Centigrade.

POSSIBLE EFFECTS OF VARIATION IN THE CURRENT SYSTEM UPON THE ORGANISMS

Before 1949 only a few measurements of the plant and animal populations of the California Current system had been made. Since 1949 the volume of zooplankton has been measured over a great part of the current nearly every month, and much has been learned about the distribution in space and time. Because different methods of measuring zooplankton were used before 1940, it is not easy to compare present populations with those in the past, yet some significant indications have been obtained. The nature of the waters of the California Current has been discussed, and the distribution of the properties, especially phosphate as an index to the nutrients, has been described. A simple relation between zooplankton and phosphate has been shown (Figs. 14-16). Phosphate has not been measured regularly, and very few measurements in this region were made before 1949; therefore in using the available data any significant relation of zooplankton to the environment which can account for changes in time of the population must involve some other parameter than phosphate or nutrients—some parameter for which data exist over a longer period.

In previous discussion of the current system and its variation it was mentioned that the only property for which any long series of data exist is temperature. The general relation of temperature to phosphate has not yet been mentioned, but an examination of the

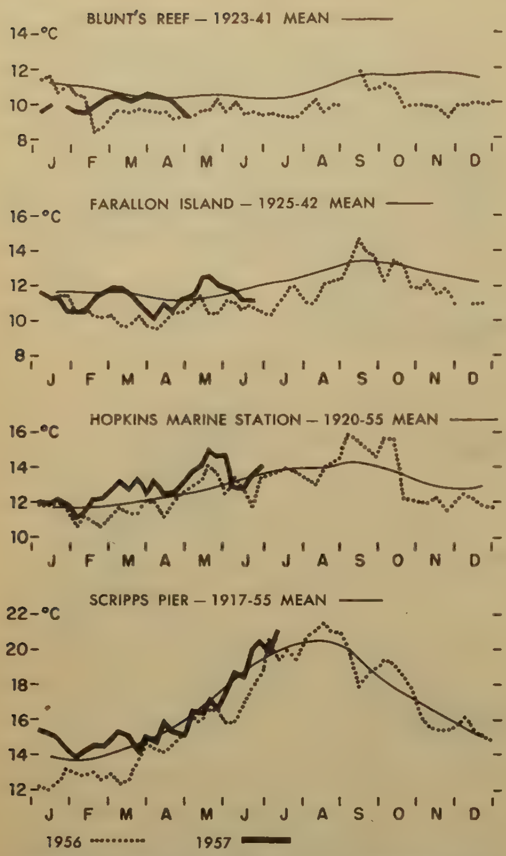

FIGURE 22. Temperatures in 1956 and 1957 at four locations as compared to long-term means. Temperature in degrees Centigrade.

charts of temperature and phosphate shows that over a vast area, including the nearshore waters of Baja California and the west coast of the United States, high phosphate values are generally accompanied by low temperatures. This holds not only vertically, where the deeper waters contain the products of decayed organic matter, but horizontally as well. The Subarctic waters of the north, which form a great part of the surface waters of the California Current system, are both cool and high in phosphate. Therefore, in the regions of the California Current one may with some confidence use the low temperature in the mixed layer as an indicator of higher nutrient properties.

The succession of relatively cool years from 1946 has been mentioned. Where data have been available salinities have been found to be higher near the coast in the same period. If one assumes that the cooling of the surface waters of the California Current and the increase in their inshore salinities are due to an internal redistribution of the heat and salt, as would result from upwelling, rather than a loss of heat and water to the atmosphere, then the accompanying redistribution of phosphate and other nutrients would have considerably enriched the surface waters.

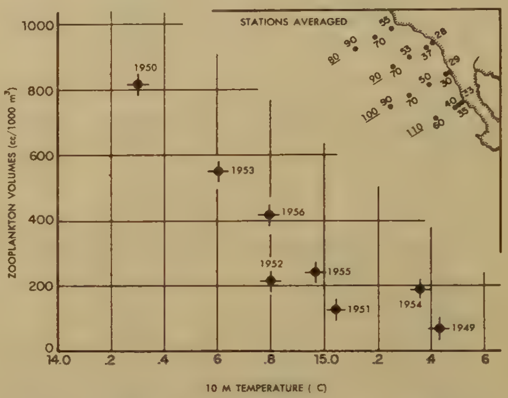

FIGURE 23. Temperature at 10 meters (in degrees Centigrade) and zooplankton volumes (in cubic centimeters per 1000 cubic meters) averaged from February through August for each year from 1949 through 1956.

The dependence of zooplankton upon the nutrients is, of course, an indirect one via the phytoplankton. If it had been consistently measured, the phytoplankton might be expected to yield a better correlation than zooplankton with the nutrients. In the region between Point Conception and Punta Eugenia, however, a satisfactory relation has been found during the seven years for which data are available (Fig. 23). (Zooplankton data were prepared for figure 23 by Mr. James Thrailkill of the U. S. Fish and Wildlife Service.) Indeed, if there is no direct relation between zooplankton growth and temperature, the relation shown between the temperature as an indirect measure of nutrients and zooplankton as an indirect measure of phytoplankton is better than would be expected, and greater irregularities will almost certainly be found in subsequent data.

Within certain limits of temperature, the zooplankton volumes were lowest when the temperatures were high and highest when the temperatures were low (Fig. 23). Data from 1940 and 1941 cannot be plotted on this chart, since the cruises made in those years covered only a small part of the area. However, there is qualitative agreement in that the plankton volumes measured in the region of southern California in 1941 (E. H. Ahlstrom, personal communication) averaged only 103 cubic centimeters per 1000 cubic meters, and 1941, as has been shown (Fig. 21), had also the highest temperatures observed in any year from 1931 to the present.

South of Punta Eugenia, where the zooplankton volumes have generally been smaller and the temperatures higher, a similar plot of zooplankton volumes against temperature is not nearly so regular. Although a similar trend can be seen, these data are hardly convincing.

Correlations of this type are difficult to make not only because the temperatures and zooplankton are not sampled as completely as we should desire, but because the zooplankton varies from year to year in a fashion more complex than gross amount. There are data to suggest, at least, that the response of the zooplankton to changing hydrographic conditions is not only in mass but in change of species as well. Salps, for example, may predominate one year and other groups in other years, with the volumes not changing significantly. All of the area is inhabited (Figs. 17a-e), and it can well be imagined that a change in conditions could cause the boundaries to move so that the species would inhabit slightly different regions, without a great change occurring in gross amount.

CONCLUSION

The waters of the California Current and their manner of flow in the fishery region of California, both horizontal and vertical, have been briefly described. The seasonal variations and long-term variations have been mentioned, and some attempt at relating the environment to the organisms has been made. The bearing of these matters upon the central problem of the CCOFI program, that is, the fluctuations in the catch of the sardine and other oceanic fishes, has not yet been mentioned. One difference between the last decade and the previous period when the sardine fishery was at its height has been pointed out. The temperatures during the early months of the year—the sardine spawning months—have been consistently lower in the last ten years and with certain assumptions inferences bearing upon the sardine problem can be drawn. These cooler months seem to be cooler because the winds were stronger and caused more upwelling. Assuming this relation to hold, and that the low temperatures are indicative of high nutrients, then the result of the enrichment has been higher zooplankton volumes. If this relation between temperature and zooplankton is a real one and has held over the last 20 years, as it did in 1941 and from 1949 through 1956, then we must assume that plankton volumes were smaller in the great period of the sardine fishery than they are now when the sardine catch is much reduced. How the zooplankton and sardines could be so inversely related is beyond the purpose of this report to speculate. It is unfortunate that we do not have a coverage of the area in years when the catch was high or when at least there was a high survival rate. Until such a year occurs any correlations of this sort will be severely limited.

REFERENCES

Atkins, W. R. G.

1923. The silica content of some natural waters and of culture media. *J. Mar. Biol. Assn. U. K.*, vol. 13, pp. 151-159.

1926. Seasonal changes in the silica content of natural waters in relation to the phytoplankton. *J. Mar. Biol. Assn. U. K.*, vol. 14, pp. 89-99.

1928. Seasonal variations in the phosphate and silicate content of sea-water during 1926 and 1927 in relation to the phytoplankton crop. *J. Mar. Biol. Assn. U. K.*, vol. 15, pp. 191-205.

1930. Seasonal variation in the phosphate and silicate content of sea-water in relation to the phytoplankton crop. Part V. November 1927 to April 1929, compared with earlier years from 1923. *J. Mar. Biol. Assn. U. K.*, vol. 14, pp. 821-852.

Berner, Leo D., Jr.

1957. Studies on the Thaliacea of the temperate northeast Pacific Ocean. Unpublished doctoral dissertation on file in the Library, University of California, Scripps Institution of Oceanography. 144 pp., 26 figs.

Boden, Brian P., Martin W. Johnson, and Edward Brinton

1955. The Euphausiacea (Crustacea) of the north Pacific. *Univ. Calif., Scripps Inst. Oce., Bull.*, vol. 6, pp. 287-400, 55 figs.

Canadian Joint Committee on Oceanography

1956. Physical, chemical and plankton data record. Project NORPAC, July 26 to September 1, 1955. Prepared by Pacific Oceanographic Group, Nanaimo, B. C., Duplicated report. File N 6-17-4(2). 202 pp., 4 figs.

Cooper, L. H. N.

1933. Chemical constituents of biological importance in the English Channel. Part I. Phospate, silicate, nitrate, ammonia. Part II. Hydrogen ion concentration, excess base, carbon dioxide, and oxygen. *J. Mar. Biol. Assn. U. K.*, vol. 18, pp. 677-753.

1938. Phosphate in the English Channel, 1933-8, with a comparison with earlier years, 1916 and 1923-32. *J. Mar. Biol. Assn. U. K.*, vol. 23, pp. 181-195.

Cromwell, Townsend, and Joseph L. Reid, Jr.

1956. A study of oceanic fronts. *Tellus*, vol. 8, no. 1, pp. 94-101.

Goldberg, Edward D., Theodore J. Walker, and Alice Whisenand

1951. Phosphate utilization by diatoms. *Biol. Bull.*, vol. 101, no. 3, pp. 274-284.

Imperial Marine Observatory, Kobe, Japan

1925. The mean atmospheric pressure, cloudiness and sea surface temperature of the north Pacific Ocean and the neighboring seas for the lustrum, 1916 to 1920. Kobe, Imp. Mar. Obs., 581 pp.

1927. The mean atmospheric pressure, cloudiness and sea surface temperature of the north Pacific Ocean and the neighboring seas for the year, 1926. Kobe, Imp. Mar. Obs., 171 pp., 20 figs.

1929a. The mean atmospheric pressure, cloudiness and sea surface temperature of the north Pacific Ocean and the neighboring seas for the lustrum, 1921 to 1925. Kobe, Imp. Mar. Obs. 623 pp.

1929b. The mean atmospheric pressure, cloudiness, air temperature and sea surface temperature of the north Pacific Ocean and the neighboring seas for the year, 1928. Kobe, Imp. Mar. Obs., 176 pp., 20 figs.

1930. *Ibid.* 1929. 173 pp., 20 figs.

1931. *Ibid.* 1930. 176 pp., 22 figs.

1932. *Ibid.* 1931. 167 pp., 16 figs.

1933. *Ibid.* 1932. 167 pp., 16 figs.

1934. *Ibid.* 1933, 168 pp., 16 figs.

1935. *Ibid.* 1934. 160 pp., 16 figs.

1936. *Ibid.* 1935. 168 pp., 16 figs.

1937. *Ibid.* 1911 to 1935. 197 pp.

1938. The mean air temperature, cloudiness and sea surface temperature of the north Pacific Ocean and the neighboring seas for the year, 1936. Kobe, Imp. Mar. Obs., 195 pp., 12 figs.

1939a. *Ibid.* 1937. 195 pp., 9 figs.

1939b. *Ibid.* 1938. 195 pp., 12 figs.

Jacobs, Woodrow C.

1951. The energy exchange between sea and atmosphere and some of its consequences. *Univ. Calif., Scripps Inst. Oce., Bull.*, vol. 6, no. 2, pp. 27-122, 67 figs.

Knauss, John A., and Joseph L. Reid, Jr.

1957. The effects of cable design on the accuracy of the GEK. *Am. Geophys. Un., Trans.*, vol. 38, no. 3, pp. 320-325.

Redfield, A. C.

1948. The exchange of oxygen across the sea surface. *J. Mar. Res.*, vol. 7, pp. 347-361.

Redfield, Alfred C., Homer P. Smith, and Bostwick Ketchum

1937. The cycle of organic phosphorus in the Gulf of Maine. *Biol. Bull.*, vol. 73, pp. 421-443.

Reid, Joseph L., Jr.

1956. Observations of internal tides in October 1950. *Am. Geophys. Un., Trans.*, vol. 37, no. 3, pp. 278-286.

(In press.) A comparison of drogue and GEK measurements in deep water. *Limnol. and Oceanogr.*

Robinson, Margaret K.

1957. Sea temperature in the Gulf of Alaska and the northeast Pacific Ocean, 1941-1952. *Univ. Calif., Scripps Inst. Oce., Bull.*, vol. 7, no. 1, pp. 1-98, 61 figs., 1 chart.

Roden, Gunnar I.

(In press.) Oceanographic and meteorological aspects of the Gulf of California. *Pac. Sci.*

Roden, Gunnar I., and Joseph L. Reid, Jr.

(ms.) On a relation between atmospheric pressure and sea surface temperatures in the north Pacific Ocean.

Rossby, C. G.

1936. Dynamics of steady ocean currents in the light of experimental fluid mechanics. *Papers in Phys. Oceanogr. and Meteorol.*, vol. 5, no. 1, 44 pp.

Staff, South Pacific Fishery Investigations

1952. Zooplankton volumes off the Pacific Coast, 1941. *U. S. Fish and Wildl. Serv., Spec. Sci. Rept.: Fish.*, no. 73, 37 pp.

1953. *Ibid.* 1952; no. 100, 41 pp.

1954a. *Ibid.* 1949-50; no. 125, 54 pp.

1954b. *Ibid.* 1953; no. 132, 38 pp.

1955. *Ibid.* 1954; no. 161, 35 pp.

(ms.) Biological results of the portion of NORPAC occupied by agencies participating in the California Cooperative Oceanic Fisheries Investigations.

Sverdrup, H. U., and E. W. Allen

1939. Distribution of diatoms in relation to the character of water masses and currents off southern California. *J. Mar. Res.*, vol. 2, no. 2, pp. 131-144.

Sverdrup, H. U., and R. H. Fleming

1941. The waters off the coast of southern California, March to July, 1937. *Univ. Calif., Scripps Inst. Oce., Bull.*, vol. 4, no. 10, pp. 261-378, 66 figs.

Sverdrup, H. U., Martin W. Johnson, and Richard H. Fleming

1942. *The oceans, their physics, chemistry and general biology.* New York: Prentice-Hall, Inc., 1087 pp., 265 figs., 7 charts.

Tibby, Richard B.

1939. Report on returns of drift bottles released off southern California, 1937. *Calif. Div. of Fish and Game. Fish Bull.*, no. 55, 36 pp., 22 figs.

U. S. Coast and Geodetic Survey

1954. Density of sea water at tide stations. Pacific Coast. North and South America and Pacific Ocean islands. Spec. Pub. No. 281, 64 pp.

1956. Surface water temperatures at tide stations. Pacific Coast. North and South America and Pacific Ocean islands. Spec. Pub. No. 280, 74 pp.

U. S. Geological Survey

1952. Quality of surface waters of the United States. Colorado River basin to Pacific slope basins in Oregon and lower Columbia River basin. Geol. Surv. Water-Supply Paper 1253. Part 9-14, 344 pp., 1 fig.

U. S. Hydrographic Office

1947. *Atlas of surface currents. Northeastern Pacific Ocean.* H. O. Pub. No. 570.

University of California, Scripps Institution of Oceanography

1957. *Oceanic observations of the Pacific, 1949.* Berkeley: Univ. Calif. Press, 363 pp., 6 figs.

(In press.) *Oceanic observations of the Pacific, 1955. NORPAC Vols. I, and II.* Berkeley: Univ. Calif. Press.

(In preparation.) *Oceanic Observations of the Pacific, 1950-57.* Berkeley: Univ. Calif. Press.

University of Washington, Dept. of Oceanography

1956. Special Report No. 22. Preliminary Data Report. NORPAC 1955. Duplicated report. Ref. 56-4, 104 pp., 1 fig.

von Arx, William S.

1950. An electromagnetic method for measuring the velocities of ocean currents from a ship under way. *Papers in Phys. Oceanogr. and Meteor.*, vol. 11, no. 3, 62 pp., 17 figs.

Wooster, Warren Scriver

1953. Phosphate in the eastern north Pacific Ocean. Unpublished doctoral dissertation on file in the Library, Univ. Calif., Scripps Inst. Oce., 83 pp., 16 figs.

PUBLICATIONS

(Annotated list of publications arising from the California Cooperative Oceanic Fisheries Investigations, 1 July 1956 to 30 June 1957)

Ahlstrom, Elbert H., and Harold D. Casey

1956. Saury distribution and abundance, Pacific coast, 1950-55. *U. S. Dept. Interior, Fish and Wildl. Service, Spec. Sci. Rept.: Fisheries,* no. 190, 69 pp.

Information on the saury, obtained on CCOFI cruises, is of two kinds: (1) collections of saury eggs in plankton hauls and (2) visual observations of saury abundance. This report gives the basic data on saury eggs for six years, 1950-1955, and on visual observations of saury abundance at night stations for the period September 1951 through December 1955.

Ahlstrom, Elbert H., and David Kramer

1956. Sardine eggs and larvae and other fish larvae, Pacific coast, 1954. *U. S. Dept. Interior, Fish and Wildl. Serv., Spec. Sci. Rept.: Fisheries,* no. 186, 79 pp.

Basic data on abundance of sardine eggs and larvae in the area surveyed on CCOFI cruises during 1954. Also included are records of abundance of the larvae of northern anchovy (*Engraulis mordax*), jack mackerel (*Trachurus symmetricus*), hake (*Merluccius productus*), Pacific mackerel (*Pneumatophorus diego*), and rockfish (*Sebastodes* spp.).

Barham, E. G.

1957. The ecology of sonic scattering layers in the Monterey Bay area. Technical Report No. 1 under N6onr 25127, NSF G911 and NSF G1708, 182 pp., 31 figs.

This report is primarily concerned with deep sea ecology investigated on other programs. However, it does utilize and discuss briefly phytoplankton data accumulated on the CCOFI program and the influence of productivity in modifying and shifting the deep scattering layer.

Bieri, Robert

1956. A method for the microscopic examination and manipulation of plankton on board ship. *J. Cons. Int. Explor. Mer,* vol. XXII, no. 1., pp. 38-41, 3 figs..

The under-way plankton tray, a device for the microscopic examination of plankton on board ship, is described.

Dales, R. Phillips

1957. The pelagic polychaetes of the Pacific Ocean. *Univ. Calif. Scripps Inst. Oce., Bull.,* vol. 7, No. 2, pp. 99-168, 64 figs.

The author has examined many of the CCOFI collections, among others, in this paper, which described the distribution and life histories of several species of marine worms.

Farris, David A.

1956. Diet-induced differences in the weight-length relationship of aquarium fed sardines (*Sardinops caerulea*). *J. Res. Bd. Can.,* vol. 13, no. 4, pp. 507-513.

Sardines which were fed two markedly different types of diet—one a high protein diet, the other a carbohydrate diet—showed differences in weight-length relationship.

Holmes, Robert W., and Theodore M. Widrig

The enumeration and collection of marine phytoplankton. *J. Cons. Int. Explor. Mer,* vol. XXII, no. 1, pp. 21-32, 2 figs.

Methods of enumerating and collecting phytoplankton are discussed in this study, which arose directly out of the CCOFI program.

Johnson, Martin W.

1956. The larval development of the California spiny lobster, *Panulirus interruptus* (Randall), with notes on *Panulirus gracilis* Streets. *Calif. Acad. Sci., Proc.,* vol. XXIX, no. 1, pp. 1-19, 22 figs.

The author draws on data from the CCOFI cruises to describe stages of the spiny lobster larva.

Joseph, David C.

1956. New techniques in ocean electro-fishing are developed. *Outdoor Calif.,* vol. 17, no. 9, p. 13, September.

A report on the preliminary series of electro-fishing experiments conducted by personnel of the Marine Fisheries Branch, California Department of Fish and Game. Reasons for the work, obstacles to using this gear in salt water, and other items are briefly discussed in a non-technical report.

Knauss, John A., and Joseph L. Reid

1957. On the accuracy of the GEK for measuring surface current. *Amer. Geophys. Un., Trans.,* vol. 38, no. 3, pp. 320-325, 2 figs.

The GEK (geomagnetic-electrokinetograph) is one of the standard tools used in the CCOFI program to measure surface currents. The authors made simultaneous observations of GEK measurements and of drifting drogues in order to test the validity of the GEK for surface current measurements. Good agreement was obtained.

Marine Research Committee

1956. *California Cooperative Oceanic Fisheries Investigations, Progress Report, 1 April 1955 to 30 June 1956.* Sacramento: The State Printer. 1 July 1956. 44 pp., 21 figs.

This progress report consists of a review of activities for the period and separate sections on the anchovy, jack mackerel, Pacific mackerel, and eggs and larvae of these species. Publications for the period are listed.

Miller, Daniel J.

1956. Anchovy study shows gain in Southern waters. *Outdoor Calif.,* vol. 17, no. 12, p. 3, 8-9, December.

A short discussion of the anchovy situation in Californian waters has been presented. Catch, population densities, aerial surveys, laws, spawning populations, and movements are mentioned in a non-technical terminology.

Robinson, Margaret K.

1957. Sea temperature in the Gulf of Alaska and the northeast Pacific Ocean, 1941-52. *Univ. Calif. Scripps Inst. Oce., Bul.,* vol. 7, no. 1, pp. 1-98, 61 figs., 1 chart.

In her study of sea temperatures in the northeast Pacific Ocean, the author has utilized data collected in the course of some of the CCOFI cruises.

Thrailkill, James R.

1956. Relative areal zooplankton abundance off the Pacific coast. *U. S. Dept. Interior, Fish and Wildl. Serv. Spec. Sci. Rept. Fisheries,* no. 188, 85 pp.

Contained in the report are distribution charts showing abundance of zooplankton for every CCOFI hydrographic-biological cruise during the seven-year period 1949 through 1955. In addition, there are yearly distribution charts showing the average plankton volumes obtained at each station.

United States Fish and Wildlife Service, South Pacific Fishery Investigations

1956. Zooplankton volumes off the Pacific coast, 1955. *U. S. Dept. Interior, Fish and Wildl. Serv. Spec. Sci. Rept.: Fisheries,* no. 177, 32 pp.

This report deals with zooplankton volumes obtained on 1955 CCOFI survey cruises. This is the sixth report in a continuing series, which, with this report, covers the period 1949-1955. In addition to wet plankton volumes (reported as volume per 1000 cubic meters of water strained), this report contains the basic data on all plankton hauls made during the year, including location, date, duration of haul, depth of haul, and volume of water strained.

o

printed in CALIFORNIA STATE PRINTING OFFICE

71181 2-58 6M

(324)

Reprinted from THE JOURNAL OF THE ACOUSTICAL SOCIETY OF AMERICA, Vol. 30, No. 5, 442–448, May, 1958
Copyright, 1958 by the Acoustical Society of America.
Printed in U. S. A.

Effect of High Pressure on Sound Absorption and Chemical Equilibrium*

F. H. FISHER†
University of California, Marine Physical Laboratory of the Scripps Institution of Oceanography, San Diego 52, California
(Received December 23, 1957)

Interest in acquiring more definite knowledge of the mechanism of sound absorption in electrolytic solutions led to this experimental investigation of the pressure dependence of this phenomenon. A technique was evolved to measure sound absorption in liquids as a function of pressure at frequencies of 100–600 kc. The following properties of a 0.5-molar solution of $MgSO_4$ were measured up to 20 000 psi at 26°C: absorption, relaxation frequency and velocity. The absorption at 20 000 psi is less than one quarter that at atmospheric pressure and the relaxation frequency remains constant at 1.2×10^6 rad/sec over this pressure interval within the estimated experimental error of $\pm10\%$. The velocity increases linearly with pressure at the rate 0.1588 m/atmos. From these data the chemical and adiabatic compressibilities are computed.

In an effort to secure quantitative agreement with experimental results some new aspects of the dissociation theory are discussed.

INTRODUCTION

THE anomalous sound absorption exhibited by $MgSO_4$ solutions has spurred the interest of many researchers[1–6] in the general problem of sound absorption in solutions. In treating this phenomenon Liebermann[1] proposed two relaxation mechanisms to account for the observed excess absorption; (1) a partial specific heat, and (2) a partial chemical compressibility. For the particular case of a 0.02-molar solution of $MgSO_4$ in water he showed that the partial chemical compressibility could account for virtually all of the excess absorption while the partial specific heat accounted for only five percent. Presumably this chemical compressibility arises from the lack of pressure equilibrium between the molecule and its ions; neither $MgCl_2$ nor Na_2SO_4 exhibits this phenomenon which indicates both the magnesium and sulfate ions are involved in the absorption mechanism.

Sound absorption resulting from lack of equilibrium between a molecule and its ions is particularly significant in that it offers a means of exploring experimentally the kinetics of chemical equilibria in electrolytic solutions. For example, whenever pressure dependent chemical reactions are responsible for excess absorption a change in hydrostatic pressure should produce a shift in chemical equilibria and therefore a corresponding change in acoustic absorption.

Liebermann[1] showed that a liquid exhibiting a chemical compressibility will have an unusual property in that its total compressibility, β, depends on the rate of compression; that is

$$\beta=\beta_0-\beta_0'+\beta_0'/(1+i\omega/\kappa), \qquad (1)$$

where β_0 is the isothermal compressibility, β_0' the chemical compressibility and κ the relaxation frequency associated with β_0'. Suppose the pressure on such a liquid is varied by a sound wave of angular frequency ω.

---

* This paper represents one of the results of research carried out under contract NObsr-72512 with the Bureau of Ships, Department of the Navy. The material presented is extracted from a thesis submitted as partial fulfillment for the requirements for the degree of Doctor of Philosophy at the University of Washington, Seattle, Washington.

† Now at the Cruft Laboratory, Laboratory of Applied Physics, Harvard University, Cambridge, Massachusetts. Contribution from the Scripps Institution of Oceanography, New Series, No. 999.

[1] Liebermann, Phys. Rev. 76, 1520 (1949).

[2] Leonard, Technical Report No. I, UCLA Physics Dept. (1950).

[3] Kurtz and Tamm, Acustica 3, 33 (1953).

[4] Milton Manes, J. Chem. Phys. 21, 1791 (1953).

[5] David A. Bies, J. Chem. Phys. 23, 428 (1955).

[6] O. B. Wilson and R. W. Leonard, J. Acoust. Soc. Am. 26, 223 (1954).

Reproduced by Permission
Contributions from the Scripps Institution of Oceanography, New Series, No 999

From Eq. (1) it is seen that the compressibility is greatest when $\omega=0$, the static case for which $\beta=\beta_0$. As ω increases the total compressibility decreases until $\beta=\beta_0-\beta_0'$ for $\omega=\infty$. Physically this means that the volume change due to the chemical reaction diminishes as the frequency increases because the finite rate of the chemical reaction gradually renders the reaction less sensitive to the more rapid pressure variations.

A fluid whose compressibility is of the form shown in Eq. (1) (complex compressibility) exhibits acoustic absorption which is related to chemical compressibility by the following equation[1]:

$$2\alpha=\frac{\beta_0'}{\beta_0 c}\left(\frac{\omega^2\kappa}{\omega^2+\kappa^2}\right), \qquad (2)$$

where α is the acoustic absorption coefficient and c is the sound velocity. It will be shown later how β_0' is related to equilibrium properties of the chemical reaction.

EXPERIMENTAL WORK

Resonator Technique

In order to obtain the relaxation frequency of magnesium sulfate solutions as a function of pressure the absorption should be measured above and below the relaxation frequency if possible. Leonard,[2] Kurtz and Tamm,[3] and Wilson and Leonard[6] have measured the relaxation frequencies of magnesium sulfate solutions at atmospheric pressure and found them to be relatively insensitive to concentration. For solutions up to 0.1 molar concentration the relaxation frequencies lie in the 140-kc region.

The method chosen for absorption measurements in this frequency region was the resonator technique.[2] Basically this technique consists of exciting a single normal mode of the resonator, stopping the excitation and measuring the rate of decay of the sound field for this mode. The decay measured is the sum of losses due to the liquid and the resonator. Losses due to the resonator can be determined by using a liquid with negligible absorption.

Apparatus

The resonator was the most crucial piece of apparatus. It had to withstand high pressure, not corrode in water or salt solutions, and yet have thin walls to minimize absorption losses.

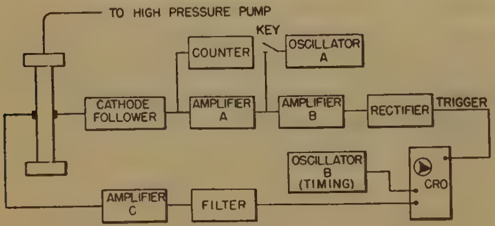

FIG. 1. Block diagram of apparatus.

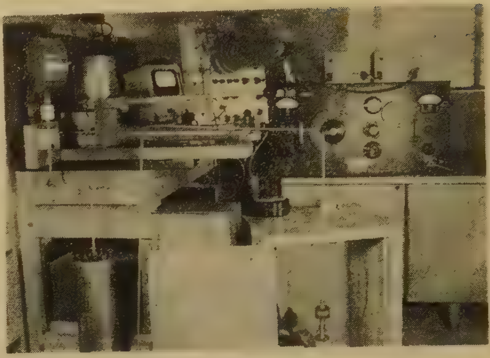

FIG. 2. High pressure absorption apparatus.

Consideration of machining problems led to the choice of a cylinder for the resonator. It was made long compared to its diameter in order to lessen end effects. The radius of the cylinder was determined by estimating the desired spacing of radial modes which should have the lowest losses. A cylinder with approximately a one inch inside radius proved to be satisfactory in the 100-kc region but exploded before satisfactory measurements could be made near 500 kc. Another cylinder, essentially a four-to-one reduction of the one which exploded, was built to make measurements in the 400–600-kc region.

Except for the resonant cylinders and the exchanger necessary for applying the hydrostatic pressure to them the apparatus consisted almost entirely of commercially available equipment. Figure 1 is a block diagram of the apparatus which is shown in Fig. 2. Filters were used in the receiver circuit.

The high pressure gauge, connectors, and one-fourth inch tubing were stock items from the American Instrument Company. The pressure calibration of the gauge was checked by measuring the velocity of sound in water as a function of pressure, correcting for expansion of the resonator walls and comparing results with known values.[7,8] As a precaution against explosions the resonators were enclosed in a box shown in Fig. 2 which also facilitated maintaining the temperature at 26±0.5°C.

Each cylinder was excited by a barium titanate transducer attached as shown in the block diagram and in Fig. 3. The response to the excitation was observed on the oscilloscope by means of a similar transducer mounted approximately opposite the other one.

High Pressure Technique

To measure absorption as a function of pressure required that a normal mode be followed as the pressure

---

[7] Gerald Holton, J. Appl. Phys. 22, 1407 (1951).

[8] T. A. Litovitz and E. H. Carnevale, J. Appl. Phys. 26, 816 (1955).

(326)

increased; that is, the oscillator frequency had to be increased as the resonant frequency of the mode varied according to the change in sound velocity of the solution and the expansion of the resonator walls (see Fig. 4). Positive identification of liquid modes was assured by the sound velocity *vs* pressure data for water[7,8] and sound velocity *vs* concentration data at atmospheric pressure for aqueous solutions.[9–11]

Because the wall losses of the cylinders were large, it was necessary to use high concentrations of $MgSO_4$ in order to observe the effect of pressure on absorption. The concentration had to be great enough so that the absorption could still be measured at high pressures where it was less than one-third the value measured at atmospheric pressure. For this reason a concentration of 0.5 molarity was selected.

Ideally resonator loss data for a given mode should be obtained at the identical frequency using the non-absorbing liquid. In previous work at lower concentrations water has been used to obtain correction data because the resonant frequencies in water and the solution of interest were practically identical. In this experiment the difference between the resonant frequencies in water and in 0.5 molar $MgSO_4$ is approximately four percent, too great to obtain valid correction data (see Fig. 4). Aqueous solutions of sodium chloride show negligible absorption; hence, the velocity of such solutions can be adjusted independently of absorption by varying concentration. By selecting the proper concentration the resonant frequencies in NaCl could be matched with those in $MgSO_4$ and correction data could be obtained satisfactorily. The match was not perfect over the entire pressure range (Fig. 4) but the difference was very small, less than 1.7 kc at 20 000 psi for the high frequency mode.

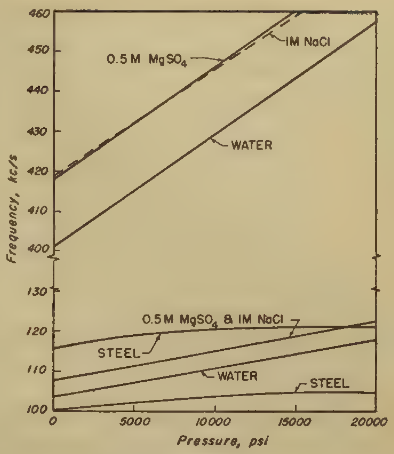

FIG. 4. Typical graph of shift of resonant frequency *vs* pressure for various solutions.

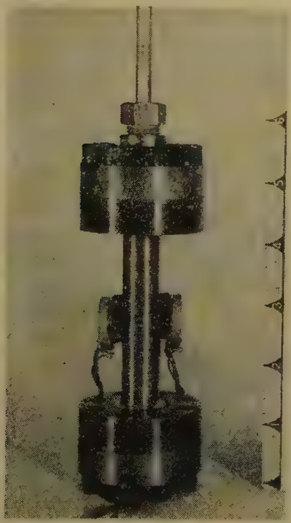

FIG. 3. Small stainless steel resonant cylinder.

A major difficulty in measuring absorption as a function of pressure arises from the existence of resonant steel modes (modes in the walls of the cylinder) which at various pressures were observed to cross the liquid modes and make impossible the identification of liquid modes. Figure 4, which shows some typical steel and liquid modes as a function of pressure, illustrates this interfering behavior. Fortunately, it was found that the *Q* of the steel modes was lowered greatly by touching the cylinder at various places while the *Q* of the liquid modes was lowered only slightly. In order to exploit this damping the cylinder was wrapped with a layer of masking tape, a device which proved to be successful in permitting modes to be followed up to 20 000 psi. This procedure was resorted to only for the large cylinder. The effect of mode crossing for the large cylinder was still apparent [notice the large hump in Fig. 5(a) for both $MgSO_4$ and NaCl data] but the mode could be followed.

EXPERIMENTAL RESULTS

Absorption measurements were made in two frequency regions: in the 100-kc region with the large cylinder and in the 500-kc region with the small one. The resonant frequencies at atmospheric pressure, f_0, were 107.7 kc and 495.8 kc. All measurements were made at 26°C. The absorption measurements were made at 1000 psi intervals for both the 0.5-molar solution of $MgSO_4$ and the 1.0175-molar‡ NaCl solution. These absorption measurements are shown in Fig. 5.

---

[9] Romard Barthel, J. Acoust. Soc. Am. **26**, 227 (1954).
[10] Schaafs, Z. Physik **105**, 658–75 (1937).
[11] A. Weissler and V. A. Del Grosso, J. Acoust. Soc. Am. **23**, 222 (1951).

‡ Velocity *vs* concentration data at various temperatures for $MgSO_4$[10,11] and NaCl[9,11] were used to compute concentration of NaCl solution which would have same velocity as 0.5 molar $MgSO_4$ solution.

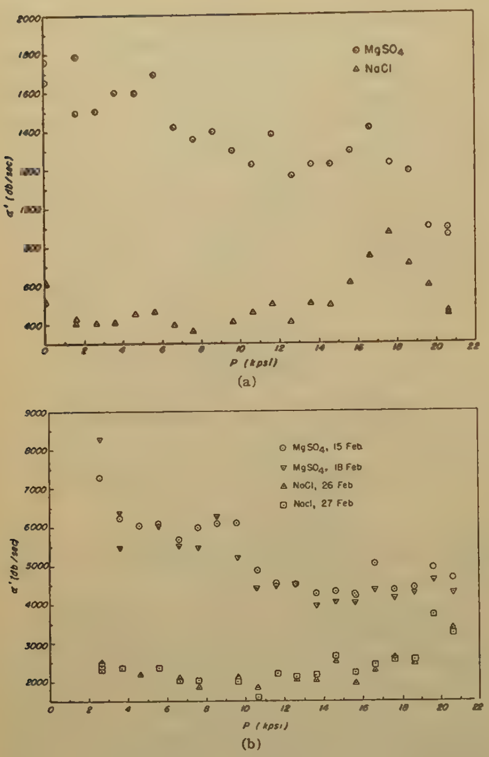

(a)

(b)

FIG. 5. Raw absorption data, 26°C. (a) Low frequency: Note the absorption peak at 18 000 psi for both solutions where a steel mode crosses the liquid mode. (b) High frequency: The mode for both solutions could not be followed down to atmospheric pressure.

The absorption of the magnesium sulfate was found by subtraction of the NaCl data point-by-point from the MgSO$_4$ data; where more than one absorption measurement was made the average was used in computation. The large cylinder exploded before more data could be taken in the low-frequency region.

The observations of the absorption of MgSO$_4$ are shown in Fig. 6 for both the low and high frequencies. The line in each figure, drawn by eye, is somewhat arbitrary because equal weight was not given to all points, especially in regions where steel modes cross the liquid ones; whenever data showed relatively slow variations with pressure these points were given more weight. Absorption is not observed for a fixed frequency because, as mentioned earlier, the frequency must be increased as the pressure is elevated in order to observe the same mode.

The relaxation frequency was calculated from the above data and Eq. (2). It was found that within the estimated accuracy of the absorption measurements, ±10%, there was no change in κ, as the pressure increased; its value was found to be 1.2×10^6 rad/sec. In Fig. 7 this result is compared with those of Wilson and Leonard[6] as a function of the square root of concentration.

Once the relaxation time was known, the absorption measurements could be reduced to absorption as a function of pressure at a fixed frequency. The absorption results at fixed frequencies, Fig. 8, show that the absorption decreases approximately by a factor of four for a change of 20 000 psi.

To calculate the chemical compressibility using Eq. (2) the isothermal compressibility and sound velocity must be known in addition to the absorption and relaxation frequency which were measured. Using instead the adiabatic compressibility[12] $(\rho c^2)^{-1}$ for β_0 in Eq. (2), one obtains

$$\beta_0' = \frac{2\alpha}{\rho c}\left(\frac{\omega^2+\kappa^2}{\omega^2\kappa}\right). \tag{2a}$$

The experiment itself yields sound velocity *vs* pressure; density *vs* pressure at 25°C can be calculated.[13] The

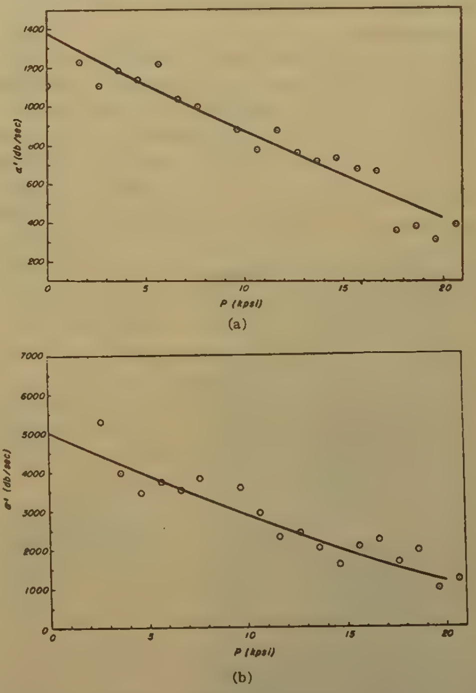

(a)

(b)

FIG. 6. Absorption of 0.5 molar MgSO$_4$ solution, 26°C. Note that as the pressure increases the frequency of the resonant mode increases from the atmospheric pressure frequency, f_0. (a) f_0 = 107.7 kc. (b) f_0 = 495.8 kc.

---

[12] Harned and Owen, *Physical Chemistry of Electrolyte Solutions* (Reinhold Publishing Corporation, New York, 1950). For aqueous solutions at 25°C the adiabatic and isothermal compressibilities differ by only about one percent.

[13] Gibson, J. Am. Chem. Soc. **56** : 1, 4 (1934).

chemical compressibility was computed from the fixed frequency absorption results at both the high and low frequencies. The discrepancy between values shown in Fig. 9 at 26°C is an indication of the accuracy of the experiment. No attempt was made to reconcile the differences. Note that at atmospheric pressure the chemical compressibility is approximately a factor of 1000 smaller than the isothermal compressibility.

It has been mentioned earlier that it was necessary to increase the frequency in order to follow a given mode as the pressure was increased. By calculating the change in the dimensions of the cylinder as a function of pressure it was possible to obtain relative velocity measurements accurate to one part in a thousand. Although the experiment was done at 26°C the velocity is presented in Table I as a function of pressure at 25°C since chemical and physical data are usually determined at this temperature. The velocity of sound at 25°C for $MgSO_4$ was found by interpolation from the data of Schaafs[10] and Weissler and Del Grosso.[11] In doing so it has been assumed that variation of velocity with pressure is the same at the two temperatures.

Since the velocity and density are known as a function of pressure the adiabatic compressibility can be computed; the results at 25°C are presented in Fig. 10.

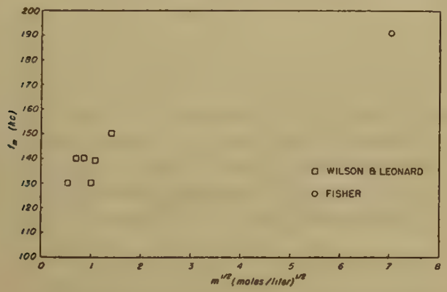

FIG. 7. Relaxation frequency *vs* (concentration)$^{\frac{1}{2}}$, 23–26°C.

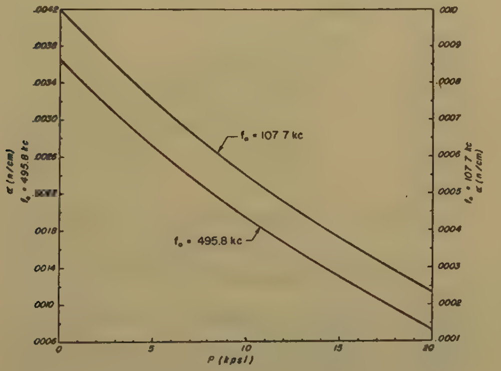

FIG. 8. Absorption of 0.5 molar $MgSO_4$ solution at 26°C.

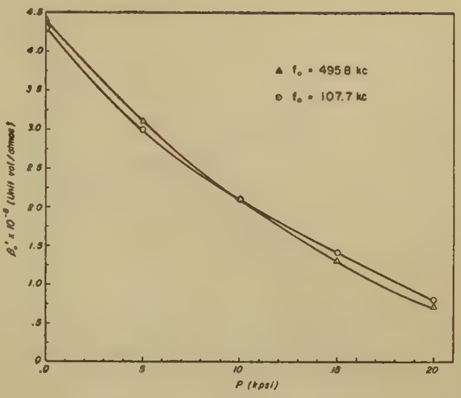

FIG. 9. Chemical compressibility *vs* pressure, 26°C.

COMPARISON OF THEORY AND EXPERIMENT

The chemical compressibility, β_0', can be related to chemical thermodynamic properties as was pointed out by Liebermann.[1] For example,

$$\beta_0' = -\frac{1}{V}\left(\frac{\partial V}{\partial p}\right)_T = -\frac{1}{V}\left(\frac{\partial V}{\partial \ln K}\right)_{T,p}\left(\frac{\partial \ln K}{\partial p}\right)_T, \quad (3)$$

which relates the volume, V, of the solution and the equilibrium constant K to chemical compressibility. The pressure dependence of K is expressed by the standard thermodynamic equation[14]

$$\left(\frac{\partial \ln K}{\partial p}\right)_T = -\frac{\Delta V^0}{RT}, \quad (4)$$

where ΔV^0 is the algebraic difference between the partial molal volumes of the products and reactants in their standard states. A more specific expression for β_0' for the case of a salt dissociating into two ions has been given by Bies.[5] However, his expression for β_0' includes the explicit ratio of two kinetic quantities, reaction rate and relaxation frequency, in spite of the fact that β_0' is an equilibrium property; he subsequently shows an equilibrium relation between these two quantities. A more direct relation can be derived from the Manes[4] expression for relaxation frequency and for this case it can be shown that the ratio of the specific reaction rate for dissociation, k_1, to relaxation

TABLE I. Velocity *vs* pressure, 25°C 0.5 molar $MgSO_4$.

P (psi)	c(m/sec)
15	1558
5 000	1612
10 000	1666
15 000	1720
20 000	1774

---

[14] Owen and Brinkley, Chem. Revs. 29, 461 (1941). A detailed discussion is given of Eq. (4).

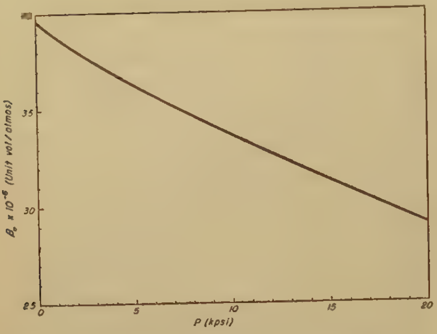

FIG. 10. Adiabatic compressibility *vs* pressure, 25°C.

frequency, κ, is

$$\frac{k_1}{\kappa}=1+\frac{\bar{V}_2-\bar{V}_2^0}{\Delta V^0}, \tag{5}$$

where $\bar{V}_2$ is the partial molal volume of the solute at the concentration to which κ refers and $\bar{V}_2^0$ is the partial molal volume of the solute at infinite dilution.

By evaluating the Manes[4] expression for β_0' the chemical compressibility is expressed as

$$\beta_0'=\frac{\Delta V'\Delta V^0 c_s(1-\theta)}{RT}\left[1+\frac{\bar{V}_2-\bar{V}_2^0}{\Delta V^0}\right], \tag{6}$$

in which unit volume has been assumed, c_s is the concentration in moles/cc,§ and θ is the degree of dissociation. The quantity $\Delta V'$ is closely related to ΔV^0.‖ Liebermann, Bies, and Manes set $\Delta V'=\Delta V^0$ in their work although Bies,[15] as well as Manes, suggested that this may not be true. In the absence of any data by which $\partial\bar{V}_1/\partial\xi$ can be accurately evaluated in the expression for $\Delta V'$ given in the footnote below, it will be assumed that $\Delta V'$ is independent of pressure.

Whenever the dissociation reaction is responsible for sound absorption its pressure dependence can be calculated by combining Eqs. (2) and (6); the result is

$$2\alpha=\frac{\Delta V'\Delta V^0 c_s(1-\theta)}{c\beta_0 RT}\left[1+\frac{\bar{V}_2-\bar{V}_2^0}{\Delta V^0}\right]\left[\frac{\omega^2\kappa}{\omega^2+\kappa^2}\right]. \tag{7}$$

Equation (7) may be rearranged by lumping terms independent of pressure ($\Delta V'$, ω and κ) into a constant; hence

$$\alpha=\text{constant}\times|\Delta V^0|\rho c c_s(1-\theta)\left[1+\frac{\bar{V}_2-\bar{V}_2^0}{\Delta V^0}\right], \tag{8}$$

in which β_0 is expressed as $(\rho c^2)^{-1}$. A numerical evaluation of the effect of pressure on sound absorption using Eq. (8) can be made provided data on the pressure dependent variables are known.

Some of the pressure dependent variables are readily calculated, namely, ρ, c_s, and c. The pressure dependence of ΔV^0 and of the dissociation constant, K, is obtained by the method of Owen and Brinkley[14] up to 15 000 psi.

In order to calculate the degree of dissociation, θ, it is necessary to use the equation for thermodynamic equilibrium

$$K=c_s'\gamma_\pm^2/(1-\theta), \tag{9}$$

in which c_s' is in units of moles/liter and $\gamma_\pm$ is the stoichiometric activity coefficient.[16]

The pressure dependence of $\gamma_\pm$ may be calculated[17] by making use of the equation

$$\partial\ln\gamma_\pm/\partial p=(\bar{V}_2-\bar{V}_2^0)/2RT, \tag{10}$$

in which account is taken of the pressure dependence of $(\bar{V}_2-\bar{V}_2^0)$. Once K, $\gamma_\pm$ and c_s' are known as functions of pressure, the degree of dissociation can be calculated. All calculations have been made on the assumption that the activity coefficient of the undissociated solute is unity.

The effect of pressure on some of these quantities is by no means negligible. For example, in a 0.5-molar $MgSO_4$ solution the following changes are found for a pressure increase from atmospheric pressure to 15 000 psi: K increases by a factor of approximately 6.6; ΔV^0 increases from −51.7 cc/mole to −39.9 cc/mole; if one uses the atmospheric pressure values of 0.0882 for $\gamma_\pm$ [18] and 0.00616 for K,[19] the degree of dissociation

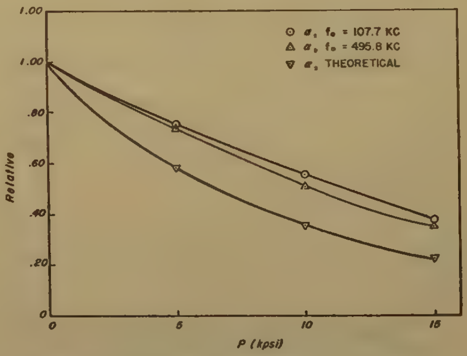

FIG. 11. Comparison of experiment and theory.

---

§ Bies[5] incorrectly uses moles/liter.

‖ Manes defined $\Delta V'=\partial V/\partial\xi$, where ξ is the degree of advancement of the reaction expressed in number of moles of any key component. Taking $\xi=n_2\theta$, where n_2 is the number of moles of the solute, it can be shown that $\Delta V'=n_1(\partial\bar{V}_1/\partial\xi)+(\bar{V}_2^m/\theta)+\Delta V^0$, where n_1 is the number of moles of solvent and $\bar{V}_1$ is the partial molal volume of the solvent and $\bar{V}_2^m$ the molar volume of the anhydrous solute.

[15] David A. Bies, Technical Report, No. VI, UCLA Physics Department, p. 47 (1953).

[16] Robinson and Stokes, *Electrolyte Solutions* (Academic Press, Inc., New York, 1955), p. 403.

[17] Robinson and Harned, Chem. Revs. 28, 419 (1941).

[18] Robinson and Jones, J. Am. Chem. Soc. 58, 961 (1936).

[19] Dunsmore and James, J. Chem. Soc. Pt. 4, 2925 (1951).

if found to increase from 0.37 to 0.84; $(\bar{V}_2-\bar{V}_2^0)$ decreases from 12.9 cc/mole to 9.1 cc/mole. The decrease in $(\bar{V}_2-\bar{V}_2^0)$ has nearly the same pressure dependence as the decrease in the magnitude of ΔV^0, within three percent over the entire range; hence, by Eq. (5), the ratio k_1/κ is nearly independent of pressure. At atmospheric pressure k_1 is calculated to be 0.90×10^6 rad/sec or $k_1/2\pi$ is 143 kc. At infinite dilutions, therefore $f_m=\kappa/2\pi$ is 143 kc which may be compared with the results shown in Fig. 7.

The predicted pressure dependence of sound absorption using Eq. (8) is shown in Fig. 11. The slope of the predicted curve agrees with experiment fairly well from 5000–15 000 psi, but there is a discrepancy between observed and theoretical behavior below 5000 psi. This discrepancy undoubtedly stems from the assumption that $\Delta V'$ is independent of pressure. Unfortunately it is not possible to evaluate this quantity at higher pressures or even at atmospheric pressure with accuracy sufficient to permit quantitative interpretation of results. Until the pressure dependence of $\Delta V'$ is known it will not be possible to discuss this discrepancy more fully. Another source of discrepancy may arise from inaccuracies in the value of θ calculated at atmospheric pressure. Variations as large as 30% in the value of θ might be expected from the reported data.

CONCLUSION

The marked pressure dependence of acoustic absorption in $MgSO_4$ solution offers additional proof that chemical equilibrium in this solution is affected by pressure.

Since κ and the ratio k_1/κ were found to be nearly independent of pressure, it must be concluded that k_1, the specific reaction rate for dissociation, is influenced very little by pressure.

The nature of the pressure-sensitive reaction is still uncertain. It has been shown that the dissociation reaction can be responsible. Other reactions, however, cannot yet be excluded. For example, the variation with pressure of the concentration of the associated ions, $c_s(1-\theta)$, is the major factor in the predicted absorption shown in Fig. 11; the parameters $|\Delta V^0|$ and ρc vary in opposite directions such that their net influence is small. Thus, the quantity $c_s(1-\theta)$ would appear in an analogous manner if a purely monomolecular reaction involving only the associated molecules rather than the dissociation process were responsible.

Owen and Brinkley[14] indicated that ΔV^0, a negative number, becomes more positive with increasing temperature for some electrolytes. If this were true for $MgSO_4$ there may be some temperature at which $\Delta V^0=0$. A crucial test of the theory would be to measure absorption at this temperature to observe whether excess absorption persists.

ACKNOWLEDGMENTS

The author's interest in this problem stemmed from the published work of Professor Leonard Liebermann. To him the author is deeply indebted for his stimulating discussions and support.

The author also wishes to thank the staff of the Marine Physical Laboratory whose cooperation made this work possible, Mr. Dan Andrews of the U. S. Navy Electronics Laboratory for his assistance and many helpful discussions, and Mr. Norman Pintchuck of Solar Aircraft Company for his help with metallurgical problems.

Finally, the author wishes to thank his wife, Julie, for her assistance in data processing and preparation of the manuscript.

(331)

Atmospheric Limitations on Missile Photography

By SEIBERT Q. DUNTLEY

Optical data taken from an aircraft in flight as well as data secured at ground level have enabled the obscuration of high-flying missiles by the atmosphere to be ascertained and the requirements to be met by telescopic finders and cameras to be specified for several typical weather and lighting conditions.

MISSILE photography encounters atmospheric limitations whenever the object-to-camera distance is long. This paper is concerned primarily with the long-range case. If missile photography were conducted in the absence of deleterious effects due to the atmosphere, sufficiently large high-quality optics and sufficiently accurate mountings would enable any required level of detail to be resolved in the resulting photographs. The atmosphere, however, sets a fundamental limit on resolution, and this limitation comes about in two ways. First, the atmosphere scatters light in such a manner as to lower the apparent contrast of the distant objects and cause them to merge with their background. Second, the atmosphere contains refractive imperfections which may obscure fine detail in somewhat the same way that ripples on the surface of a pond obscure small stones on the bottom.

Because the atmosphere is usually in motion, the presence of these refractive imperfections, due primarily to small-scale variations in temperature, often exhibit a dynamic manifestation called *shimmer* or *boil;* thus stars are seen to twinkle and extended objects to distort and appear blurred. All who have used telescopes are acquainted with the fact that the effects of atmospheric boil are more pronounced and more serious as magnification is increased. Exactly the same situation occurs in long-lens photography. Atmosphere which exhibits no shimmer effect which can be discerned by the naked eye or by ordinary cameras may cause distant objects to appear as a swirling blur in pictures taken with missile-tracking cameras having focal lengths of several hundred inches. No discussion of the limitations imposed by the atmosphere on missile photography would be complete without consideration of both the effects due to atmospheric scattering and those due to atmospheric boil.

Atmospheric Scattering

In the absence of effects due to atmospheric boil, the apparent luminance of any distant object seen through the atmosphere is the sum of two independent components: (1) residual image-forming light originating at the object and traversing the intermediate space without experiencing scattering or absorption; (2) luminance generated by scattering processes throughout the path of sight, including contributions due to scattered sunlight, sky light, earth shine, etc. The second of these components contains no information concerning the object but serves only to mask it by lowering the contrast available to the camera. At sufficiently low levels of contrast, details cannot be resolved.

A quantitative description of contrast reduction due to scattering within the atmosphere is given by Equation (1).*

$$\frac{B_{\text{missile}}}{B_{\text{sky}}} = 1 + T\left[\frac{B'_{\text{missile}}}{B_{\text{sky}}} - \frac{B'_{\text{sky}}}{B_{\text{sky}}}\right]$$

It states that the apparent contrast-ratio of a missile as photographed from the ground is given by unity plus the transmittance of the atmospheric path between the missile and the camera multiplied by a factor composed of two terms: the first of these is the ratio of the inherent luminance of the missile to the apparent luminance of the sky as seen by the camera; and the second term, which enters by subtraction from the first, is the ratio of the luminance of the sky above the missile in the direction of the path of sight to the apparent luminance of the sky as seen by the camera.

In Eq. (1) the primed luminances are to be thought of as measured by a photometer located close to the missile, whereas luminances without the prime

---

A contribution from the Scripps Institution of Oceanography, New Series No. 1000, presented on May 2, 1957, at the Society's Convention at Washington, D.C., by Seibert Q. Duntley, Visibility Laboratory, Scripps Institution of Oceanography, Univ. of Calif., San Diego 52, Calif., and received in written form on June 19, 1957. This paper represents results of research which has been supported by the Bureau of Ships, U.S. Navy.

*For derivation, see Equation (6) of S. Q. Duntley, A. R. Boileau and R. W. Preisendorfer, "Image transmission by the troposphere," *J. Opt. Soc. Am., 47:* 499–506, 1957.

Reproduced by Permission

Copyrighted, 1958, by the Society of Motion Picture and Television Engineers, Inc.

Contributions from the Scripps Institution of Oceanography, New Series, No. 1000

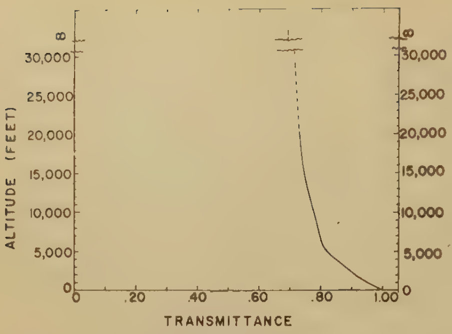

Fig. 1. Transmittance of the atmosphere for image-forming rays along a vertical path of sight from any altitude to the ground on a typical clear day. The solid portion of the curve is based upon experimental data; the dotted portion is an extrapolation based upon a standard atmosphere.

are as measured at the camera; all luminances are measured in the direction in which the camera is aimed; T is the transmittance of the atmospheric path from missile to camera for image-forming rays. Strictly, Eq. (1) should be written in terms of monochromatic radiance N, rather than in terms of luminance B, because all of the radiometric quantities are functions of wavelength. The flight research which has been conducted by the Visibility Laboratory at the University of California has demonstrated, however, that under virtually all circumstances the scattering processes in the atmosphere are sufficiently nonselective so that the equation can be used within the precision requirements of missile photography either with luminance (B) or with data obtained by means of a photometer having the same spectral sensitivity as the missile-tracking camera. There is, therefore, a practical right to use the equation in the form in which it is written.

In the case of a high-flying missile the luminance of the sky above it may be so small compared to the luminance of the sky as seen from the ground that the second term of Eq. (1) is negligible.

Equation (1) is the only expression necessary for a quantitative description of the reduction of contrast caused by atmospheric scattering along any upward-looking path of sight. It must, however, be supplied with experimentally measured data. For this reason the Visibility Laboratory has been engaged for some time in an extensive flight research program aimed at providing the data required for the practical utilization of this equation. As an example of such data, Fig. 1 shows transmittance versus altitude for an observer looking vertically upward on a typical clear day. Thus the transmittance of a vertical path of sight from an object at 20,000 ft to a camera located at sea level is read from this graph as 0.73. If the path of sight is not vertically upward but at some zenith angle θ, then the transmittance of the path from the camera to the 20,000-ft elevation will be 0.73 raised to the secant θ power. Thus, when photographing a missile which is flying at 20,000 ft, but which appears to be 10° above the horizon (zenith angle = 80°), the path transmittance is 0.73 raised to the 5.76 power or 0.16. If the camera has its back to the sun, the sky in the direction of the object will appear to have a luminance of 2,100 ft-L. A photometer just above the missile directed upward in the direction of the line of sight would measure a luminance of 1,400 ft-L. The missile, if painted white, might have a luminance of 8,400 ft-L. When these numbers are substituted in Eq. (1) it will be found that the apparent contrast ratio at the camera will be 1.53, i.e., $1.53 = 1 + 0.16\left[\frac{8400}{2100} - \frac{1400}{2100}\right]$.

It is obvious that sky luminance data are required for the use of Eq. (1). There are a number of sources of applicable information in the public literature.[1] Scientists who have taken photometers to high altitudes in balloons report that the luminance of the sky is approximately proportional to atmospheric pressure. Thus, tables such as those of Packer and Lock, which relate to the luminance of the sky in the neighborhood of 35,000 ft, can be extrapolated upward or downward by means of pressure ratios. The principal uncertainty in this process arises from the possible existence of layers of tenuous high altitude clouds which are difficult or impossible to see from the ground but which affect sky luminance.

Fortunately, the only requirement for knowing the sky luminance at high altitude is set by the second term of the equation, and this term becomes progressively less important as the missile goes higher. Since the second term is often small and can be regarded merely as a correction to the first term, it usually suffices to use tabulated high-altitude sky luminance data for this correction.

Under marginal atmospheric conditions, it sometimes develops that photography is successful although visual tracking fails; or, alternatively, under some circumstances the missile can be followed through the telescopic finder but the camera records nothing. Advance information concerning the probability of success in the photographic and visual tracking of the missile is obviously desirable. This information can be calculated from the known properties of photographic equipment and of the human eye provided the apparent contrast of the missile is known. Equation (1) provides a basis for obtaining this required information. The techniques for such calculations are well known. A typical result is illustrated by Fig. 2. This is a plot of magnifying power of a telescopic finder required to track a certain missile on a typical low-altitude flight. The required magnification is plotted as the function of the azimuth toward which the camera is pointed during the process of tracking the missile. In the case illustrated, it will be observed that more than 35-power is required in order to track the missile throughout the entire path. A 30-power tracking telescope will be able to follow it throughout the section of the path lying between azimuth 25° and 60°, and it can be found again at azimuth 91° and tracked to azimuth 101°. A telescope of lesser power will, of course, provide coverage through a lesser part of the path. For example, a 20-power telescope will track the sectors shown by the heavy line, and a 10-power telescope will enable the missile to be seen only in a region between azimuth 32° and azimuth 42°.

Atmospheric Boil

Ordinarily the missile subtends from the camera an angle larger, by far, than the root-mean-square (rms) random deviation of image-forming rays by atmospheric refractive processes. Missile photographers, on the other hand, are seldom content to have the image appear as a shapeless dot in the film. They desire to resolve details such as control fins and other structures. These subtend very much smaller angles at the camera, and these angles, fractions of seconds of arc, often correspond in size with the rms ray deviations due to boil. In such cases atmospheric boil limits the ability of cameras to record these details even though the focal length of the camera and the resolving power of the film are sufficient to provide adequate resolution if the atmosphere were free from refractive imperfections. The cameras in use at the missile test centers usually fulfill this basic resolution requirement; it is often the shimmer-state of the atmosphere that sets the resolution limit.

Apparatus has been devised that enables the rms deviation of image-forming rays due to boil to be measured from the camera station. It is found that rms ray deviations of a few tenths of a second of arc are commonly observed for near-vertical paths of sight and that values up to several seconds of arc typify near-horizontal paths.

The rms ray deviation depends upon the diameter of the entrance pupil (lens diameter) of the camera and upon shutter speed. Typical data are shown by

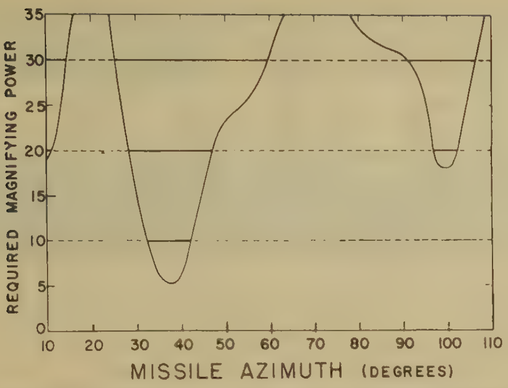

Fig. 2. Magnifying power required to enable a typical missile to be tracked visually by means of the telescopic finder on a missile camera.

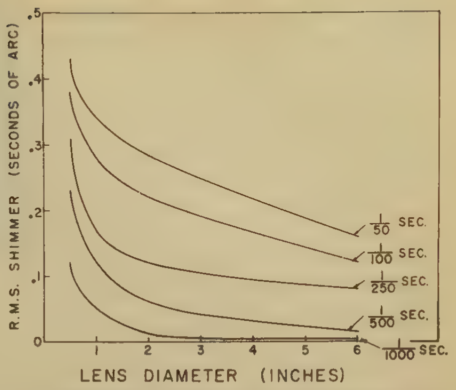

Fig. 3. Illustrating the dependence of rms shimmer upon lens diameter and shutter speed for a nearly vertical path of sight on a typical clear day.

Fig. 3. The effective rms shimmer can be markedly reduced by using the optimum aperture and a fast shutter.

A theoretical equation by means of which the rms ray deviation may be interpreted in terms of contrast loss for any item of fine detail has been published.[2] This equation is repeated here as Eq. (2).

$$\left[\frac{\bar{B}_{\text{missile}}}{B_{\text{sky}}}-1\right]=\left[\frac{B_{\text{missile}}}{B_{\text{sky}}}-1\right]\left[1-e^{-\frac{1}{2}\left(\frac{\psi}{\sigma}\right)^2}\right]$$

In Eq. (2) the contrast ratio $B_{\text{missile}}/B_{\text{sky}}$ has the same significance as in Eq. (1); i.e., the ratio of missile luminance to sky luminance at the camera without regard to contrast degradation due to atmospheric boil. The contrast ratio $\bar{B}_{\text{missile}}/B_{\text{sky}}$ in Eq. (2) is the corresponding ratio at the camera but including the effect of boil. The symbol ψ represents the apparent angular radius of the object, assumed circular, and σ is the root-mean-square ray deviation characteristic of the path of sight, the lens diameter, and the shutter speed. This equation is a sufficient geometrical approximation for most practical problems in missile photography.

The reduction of contrast is seen to be controlled by the ratio of ψ to σ. When these two angles are roughly equal, the contrast loss due to shimmer becomes important. The relation is illustrated by Table I. Thus, if the rms shimmer is half a second of arc, details subtending half a second of arc will be reduced in their contrast to the order of 40% of the contrast which they would have if there were no refractive imperfections in the atmospheric path. The dependence upon the angular size of the target is quite sharp. Objects subtending angular radii three times greater than the rms shimmer have their contrast essentially unaffected, details whose angular radii are one-third the rms shimmer are wiped out entirely. By virtue of these rules-of-thumb, it is seldom necessary to use the equation.

Table I

ψ/σ	$[1 - e^{-\frac{1}{2}(\psi/\sigma)^2}]$
3	0.99
2	0.86
1	0.39
$\frac{1}{2}$	0.12
$\frac{1}{3}$	0.05

References

1. D. M. Packer and C. Lock, "The brightness and polarization of the daylight sky at altitudes of 18,000 to 38,000 feet above sea level," *J. Opt. Soc. Am., 41:* 473–478, July 1951.
2. S. Q. Duntley, W. H. Culver, F. R. Culver and R. W. Priesendorfer, *J. Opt. Soc. Am., 42:* 877A, Nov. 1952.

Discussion

Floyd Kinder (*Naval Ordnance Test Station, China Lake, Calif.*): You commented that you needed larger lenses as well as faster shutter speeds. Might not the larger lenses take in more "boil" area? Or what effect might there be?

Dr. Duntley: The plot I showed went up to 6 in. in diameter because my experiments were made with a 6-in. diameter lens. I have tests scheduled next week for an optical system of larger diameter, but right now I don't know if there is a deterioration of quality at larger apertures. It may depend on geographical location and circumstance; what really counts, I think, is the relation between the size of the optics and the size of the turbulent parcels in the atmosphere.

michigan fish

Number 1
October 31, 1957

DEPARTMENT OF FISHERIES, SCHOOL OF NATURAL RESOURCES
UNIVERSITY OF MICHIGAN ANN ARBOR

LIST OF FISHES OF THE GREAT LAKES AND TRIBUTARY WATERS

Carl L. Hubbs and Karl F. Lagler

- LAMPREY FAMILY - Petromyzontidae
  - SILVER LAMPREY - *Ichthyomyzon unicuspis* Hubbs and Trautman
  - NORTHERN BROOK LAMPREY - *Ichthyomyzon fossor* Reighard and Cummins
  - CHESTNUT LAMPREY - *Ichthyomyzon castaneus* Girard
  - SEA LAMPREY - *Petromyzon marinus* Linnaeus
  - HOLARCTIC BROOK LAMPREY - *Entosphenus lamottenii* (LeSueur)
    - AMERICAN BROOK LAMPREY - *E. l. lamottenii* (LeSueur)
- PADDLEFISH FAMILY - Polyodontidae
  - PADDLEFISH - *Polyodon spathula* (Walbaum)
- STURGEON FAMILY - Acipenseridae
  - LAKE STURGEON - *Acipenser fulvescens* Rafinesque
- GAR FAMILY - Lepisosteidae
  - SPOTTED GAR - *Lepisosteus productus* (Cope)
  - LONGNOSE GAR - *Lepisosteus osseus* (Linnaeus)
    - NORTHERN LONGNOSE GAR - *L. o. oxyurus* Rafinesque
- BOWFIN FAMILY - Amiidae
  - BOWFIN - *Amia calva* Linnaeus
- MOONEYE FAMILY - Hiodontidae
  - MOONEYE - *Hiodon tergisus* LeSueur
- HERRING FAMILY - Clupeidae
  - ALEWIFE - *Pomolobus pseudoharengus* (Wilson)
  - AMERICAN SHAD - *Alosa sapidissima* (Wilson)
  - GIZZARD SHAD - *Dorosoma cepedianum* (LeSueur)
- SALMON FAMILY - Salmonidae
  - ATLANTIC SALMON - *Salmo salar* Linnaeus
    - SEARUN ATLANTIC SALMON - *S. s. salar* Linnaeus
    - LANDLOCKED ATLANTIC SALMON - *S. s. sebago* Girard
  - EUROPEAN TROUT - *Salmo trutta* Linnaeus
    - BROWN TROUT - *S. t. fario* Linnaeus
  - CUTTHROAT TROUT - *Salmo clarkii* Richardson
    - YELLOWSTONE CUTTHROAT TROUT - *S. c. lewisi* (Girard)
  - RAINBOW TROUT - *Salmo gairdnerii* Richardson
    - COAST RAINBOW TROUT - *S. g. irideus* Gibbons
  - CHINOOK SALMON - *Oncorhynchus tshawytscha* (Walbaum)
  - BROOK TROUT - *Salvelinus fontinalis* (Mitchill)
  - LAKE TROUT - *Salvelinus namaycush* (Walbaum)
    - COMMON LAKE TROUT - *S. n. namaycush* (Walbaum)
    - SISCOWET - *S. n. siscowet* (Agassiz)
    - RUSH LAKE TROUT - *S. n. huronicus* (Hubbs)

Contributions from the Scripps Institution of Oceanography, New Series, No. 1001
Reproduced by Permission

- WHITEFISH FAMILY - Coregonidae
  - SHALLOWWATER CISCO - Coregonus artedii LeSueur
    - TORCH LAKE CISCO - C. a. greeleyi (Koelz)
    - RUSH LAKE CISCO - C. a. huronicus (Koelz)
    - LAKE ANNE CISCO - C. a. annensis (Koelz)
    - SARGENT LAKE CISCO - C. a. sargenti (Koelz)
    - ONEIDA LAKE CISCO - C. a. hankinsoni (Koelz)
    - GREEN LAKE CISCO - C. a. birgei (Wagner)
    - PINE LAKE CISCO - C. a. russeli (Koelz)
    - WHITEFISH LAKE CISCO - C. a. atikamek (Koelz)
    - ONTARIO CISCO - C. a. mackayi (Koelz)
    - GREAT LAKES CISCO - C. a. artedii LeSueur
    - SENECA LAKE CISCO - C. a. osmeriformis Smith
    - CLEAR LAKE CISCO - C. a. clarensis (Koelz)
    - NIPIGON CISCO - C. a. clemensi (Koelz)
    - HULBERT LAKE CISCO - C. a. lowei (Koelz)
    - RAWSON LAKE CISCO - C. a. bisselli Bollman
    - LAKE ERIE CISCO - C. a. albus LeSueur
    - LAKE SUPERIOR CISCO - C. a. arcturus (Jordan and Evermann)
    - TIPPECANOE LAKE CISCO - C. a. sisco (Jordan)
    - GOGEBIC LAKE CISCO - C. a. microcephalus (Koelz)
    - NORTH CHANNEL TULLIBEE - C. a. manitoulinus (Jordan and Evermann)
    - TWIN LAKE CISCO - C. a. woodi (Koelz)
    - LAKE WINNIPEGOSIS CISCO - C. a. winnipegosis (Koelz)
  - IVES LAKE CISCO - Coregonus hubbsi (Koelz)
  - NIPIGON TULLIBEE - Coregonus nipigon (Koelz)
  - SISKIWIT LAKE CISCO - Coregonus bartletti (Koelz)
  - SHORTNOSE CISCO - Coregonus reighardi (Koelz)
    - MICHIGAN SHORTNOSE CISCO - C. r. reighardi (Koelz)
    - SUPERIOR SHORTNOSE CISCO - C. r. dymondi (Koelz)
  - SHORTJAW CISCO - Coregonus zenithicus (Jordan and Evermann)
  - LONGJAW CISCO - Coregonus alpenae (Koelz)
  - GREAT LAKES BLOATER - Coregonus hoyi (Gill)
  - DEEPWATER CISCO - Coregonus johannae (Wagner)
  - KIYI - Coregonus kiyi (Koelz)
    - MICHIGAN KIYI - C. k. kiyi (Koelz)
    - ONTARIO KIYI - C. k. orientalis (Koelz)
  - BLACKFIN CISCO - Coregonus nigripinnis (Gill)
    - MICHIGAN BLACKFIN CISCO - C. n. nigripinnis (Gill)
    - SUPERIOR BLACKFIN CISCO - C. n. cyanopterus (Jordan and Evermann)
    - NIPIGON BLACKFIN CISCO - C. n. regalis (Koelz)
    - ONTARIO BLACKFIN CISCO - C. n. prognathus Smith
  - LAKE WHITEFISH - Coregonus clupeaformis (Mitchill)
    - GREAT LAKES WHITEFISH - C. c. clupeaformis (Mitchill)
    - ERIE WHITEFISH - C. c. latus Koelz
    - INLAND LAKES WHITEFISH - C. c. neohantoniensis Prescott
    - MEDORA LAKE WHITEFISH - C. c. medorae Koelz
    - LAKE DESOR WHITEFISH - C. c. dustini Koelz
    - GULLIVER LAKE WHITEFISH - C. c. gulliveri Koelz
  - ROUND WHITEFISH - Prosopium cylindraceum (Pennant)
    - ROUND WHITEFISH - P. C. quadrilaterale (Richardson)
  - PYGMY WHITEFISH - P. coulteri Eigenmann and Eigenmann
- GRAYLING FAMILY - Thymallidae
  - ARCTIC GRAYLING - Thymallus arcticus (Pallas)
    - SAILFIN ARCTIC GRAYLING - T. a. signifer (Richardson)
- SMELT FAMILY - Osmeridae
  - AMERICAN SMELT - Osmerus mordax (Mitchill)
- SUCKER FAMILY - Catostomidae
  - BIGMOUTH BUFFALO - Ictiobus cyprinellus (Valenciennes)
  - BLACK BUFFALO - Ictiobus niger (Rafinesque)

- SMALLMOUTH BUFFALO - Ictiobus bubalus (Rafinesque)
- QUILLBACK CARPSUCKER - Carpiodes cyprinus (LeSueur)
  - CENTRAL QUILLBACK CARPSUCKER - C. c. hinei Trautman
  - NORTHERN QUILLBACK CARPSUCKER - C. c. cyprinus (LeSueur)
- RIVER CARPSUCKER - Carpiodes carpio (Rafinesque)
  - NORTHERN RIVER CARPSUCKER - C. c. carpio (Rafinesque)
- HIGHFIN CARPSUCKER - Carpiodes velifer (Rafinesque)
- WHITE SUCKER - Catostomus commersonnii (Lacépède)
  - COMMON WHITE SUCKER - C. c. commersonnii (Lacépède)
  - DWARF WHITE SUCKER - C. c. utawana Mather
- LONGNOSE SUCKER - Catostomus catostomus (Forster)
  - EASTERN LONGNOSE SUCKER - C. c. catostomus (Forster)
  - DWARF LONGNOSE SUCKER - C. c. nannomyzon Mather
- LAKE CHUBSUCKER - Erimyzon sucetta (Lacépède)
  - WESTERN LAKE CHUBSUCKER - E. s. kennerlii (Girard)
- CREEK CHUBSUCKER - Erimyzon oblongus (Mitchill)
  - EASTERN CREEK CHUBSUCKER - E. o. oblongus (Mitchill)
  - WESTERN CREEK CHUBSUCKER - E. o. claviformis (Girard)
- SPOTTED SUCKER - Minytrema melanops (Rafinesque)
- BLACK REDHORSE - Moxostoma duquesnii (LeSueur)
- GREATER REDHORSE - Moxostoma valenciennesi Jordan
- GOLDEN REDHORSE - Moxostoma erythrurum (Rafinesque)
- SILVER REDHORSE - Moxostoma anisurum (Rafinesque)
- SHORTHEAD REDHORSE - Moxostoma macrolepidotum (LeSueur)
  - NORTHERN SHORTHEAD REDHORSE - M. m. macrolepidotum (LeSueur)
- RIVER REDHORSE - Moxostoma carinatum (Cope)
- COPPER REDHORSE - Moxostoma hubbsi Legendre
- HARELIP SUCKER - Lagochila lacera Jordan and Brayton
- NORTHERN HOG SUCKER - Hypentelium nigricans (LeSueur)

MINNOW FAMILY - Cyprinidae

- CARP - Cyprinus carpio Linnaeus
- GOLDFISH - Carassius auratus (Linnaeus)
- FALLFISH - Semotilus corporalis (Mitchill)
- CREEK CHUB - Semotilus atromaculatus (Mitchill)
  - NORTHERN CREEK CHUB - S. a. atromaculatus (Mitchill)
- PEARL DACE - Semotilus margarita (Cope)
  - ALLEGHENY PEARL DACE - S. m. margarita (Cope)
  - NORTHERN PEARL DACE - S. m. nachtriebi (Cox)
  - HARVEY LAKE PEARL DACE - S. m. koelzi (Hubbs and Lagler)
- NORTHERN CHUB - Hybopsis plumbea (Agassiz)
  - LAKE NORTHERN CHUB - H. p. plumbea (Agassiz)
  - CREEK NORTHERN CHUB - H. plumbea, subspecies
- HORNYHEAD CHUB - Hybopsis biguttata (Kirtland)
- RIVER CHUB - Hybopsis micropogon (Cope)
- SILVER CHUB - Hybopsis storeriana (Kirtland)
- BIGEYE CHUB - Hybopsis amblops (Rafinesque)
- GRAVEL CHUB - Hybopsis x-punctata Hubbs and Crowe
  - EASTERN GRAVEL CHUB - H. x. trautmani Hubbs and Crowe
- BLACKNOSE DACE - Rhinichthys atratulus (Hermann)
  - EASTERN BLACKNOSE DACE - R. a. atratulus (Hermann)
  - WESTERN BLACKNOSE DACE - R. a. meleagris Agassiz
- LONGNOSE DACE - Rhinichthys cataractae (Valenciennes)
  - GREAT LAKES LONGNOSE DACE - R. c. cataractae (Valenciennes)
- TONGUETIED MINNOW - Parexoglossum laurae Hubbs
  - EASTERN TONGUETIED MINNOW - P. l. laurae Hubbs
- CUTLIPS - Exoglossum maxillingua (LeSueur)
- FINESCALE DACE - Chrosomus neogaeus (Cope)
- NORTHERN REDBELLY DACE - Chrosomus eos Cope
- SOUTHERN REDBELLY DACE - Chrosomus erythrogaster Rafinesque
- REDSIDE DACE - Clinostomus elongatus (Kirtland)

- PUGNOSE MINNOW - Opsopoeodus emiliae Hay
- GOLDEN SHINER - Notemigonus crysoleucas (Mitchill)
  - WESTERN GOLDEN SHINER - N. c. auratus (Rafinesque)
  - EASTERN GOLDEN SHINER - N. c. crysoleucas (Mitchill)
- EMERALD SHINER - Notropis atherinoides Rafinesque
  - RIVER EMERALD SHINER - N. a. atherinoides Rafinesque
  - LAKE EMERALD SHINER - N. a. acutus (Lapham)
- SILVER SHINER - Notropis photogenis (Cope)
- ROSYFACE SHINER - Notropis rubellus (Agassiz)
- REDFIN SHINER - Notropis umbratilis (Girard)
  - NORTHERN REDFIN SHINER - N. u. cyanocephalus (Copeland)
- COMMON SHINER - Notropis cornutus (Mitchill)
  - CENTRAL COMMON SHINER - N. c. chrysocephalus (Rafinesque)
  - NORTHERN COMMON SHINER - N. c. frontalis (Agassiz)
- RIVER SHINER - Notropis blennius (Girard)
  - NORTHERN RIVER SHINER - N. b. jejunus (Forbes)
- SPOTTAIL SHINER - Notropis hudsonius (Clinton)
  - GREAT LAKES SPOTTAIL SHINER - N. hudsonius, subspecies
  - NORTHERN SPOTTAIL SHINER - N. h. hudsonius (Clinton)
- IRONCOLOR SHINER - Notropis chalybaeus (Cope)
- WEED SHINER - Notropis roseus (Jordan)
  - NORTHERN WEED SHINER - N. r. richardsoni Hubbs and Greene
- BLACKCHIN SHINER - Notropis heterodon (Cope)
- BIGEYE SHINER - Notropis boops Gilbert
- SATINFIN SHINER - Notropis analostanus (Girard)
- SPOTFIN SHINER - Notropis spilopterus (Cope)
- BIGMOUTH SHINER - Notropis dorsalis (Agassiz)
  - EASTERN BIGMOUTH SHINER - N. d. keimi Fowler
  - CENTRAL BIGMOUTH SHINER - N. d. dorsalis (Agassiz)
- SAND SHINER - Notropis deliciosus (Girard)
  - SOUTHERN SAND SHINER - N. d. deliciosus (Girard)
  - NORTHEASTERN SAND SHINER - N. d. stramineus (Cope)
- SWALLOWTAIL SHINER - Notropis procne (Cope)
  - NORTHERN SWALLOWTAIL SHINER - N. p. procne (Cope)
- MIMIC SHINER - Notropis volucellus (Cope)
  - NORTHERN MIMIC SHINER - N. v. volucellus (Cope)
- BLACKNOSE SHINER - Notropis heterolepis Eigenmann and Eigenmann
  - NORTHERN BLACKNOSE SHINER - N. h. heterolepis Eigenmann and Eigenman
  - HARVEY LAKE BLACKNOSE SHINER - N. h. regalis Hubbs and Lagler
- BRIDLED SHINER - Notropis bifrenatus (Cope)
- PUGNOSE SHINER - Notropis anogenus Forbes
- SUCKERMOUTH MINNOW - Phenacobius mirabilis (Girard)
- SILVERJAW MINNOW - Ericymba buccata Cope
- BRASSY MINNOW - Hybognathus hankinsoni Hubbs
- SILVERY MINNOW - Hybognathus nuchalis Agassiz
  - EASTERN SILVERY MINNOW - H. n. regia Girard
  - WESTERN SILVERY MINNOW - H. n. nuchalis Agassiz
- FATHEAD MINNOW - Pimephales promelas Rafinesque
  - NORTHERN FATHEAD MINNOW - P. p. promelas Rafinesque
  - HARVEY LAKE FATHEAD MINNOW - P. p. harveyensis Hubbs and Lagler
- BULLHEAD MINNOW - Pimephales vigilax (Baird and Girard)
  - NORTHERN BULLHEAD MINNOW - P. v. perspicuus (Girard)
- BLUNTNOSE MINNOW - Pimephales notatus (Rafinesque)
- STONEROLLER - Campostoma anomalum (Rafinesque)
  - LARGESCALE STONEROLLER - C. a. oligolepis Hubbs and Greene
  - OHIO STONEROLLER - C. a. anomalum (Rafinesque)
  - CENTRAL STONEROLLER - C. a. pullum (Agassiz)

NORTH AMERICAN CATFISH FAMILY - Ictaluridae

- CHANNEL CATFISH - Ictalurus punctatus (Rafinesque)
  - NORTHERN CHANNEL CATFISH - I. p. punctatus (Rafinesque)

- WHITE CATFISH - *Ictalurus catus* (Linnaeus)
- BLACK BULLHEAD - *Ictalurus melas* Rafinesque
    - NORTHERN BLACK BULLHEAD - *I. m. melas* (Rafinesque)
- BROWN BULLHEAD - *Ictalurus nebulosus* (LeSueur)
    - NORTHERN BROWN BULLHEAD - *I. n. nebulosus* (LeSueur)
- YELLOW BULLHEAD - *Ictalurus natalis* (LeSueur)
    - NORTHERN YELLOW BULLHEAD - *I. n. natalis* (LeSueur)
- FLATHEAD CATFISH - *Pylodictis olivaris* (Rafinesque)
- STONECAT - *Noturus flavus* Rafinesque
- TADPOLE MADTOM - *Schilbeodes gyrinus* (Mitchill)
- EASTERN MADTOM - *Schilbeodes insignis* Richardson
    - COMMON EASTERN MADTOM - *S. i. insignis* Richardson
- (?) SLENDER MADTOM - *Schilbeodes exilis* (Nelson)
- BRINDLED MADTOM - *Schilbeodes miurus* (Jordan)
- FURIOUS MADTOM - *Schilbeodes furiosus* (Jordan and Meek)

MUDMINNOW FAMILY - Umbridae
- CENTRAL MUDMINNOW - *Umbra limi* (Kirtland)

PIKE FAMILY - Esocidae
- GRASS PICKEREL - *Esox americanus* Gmelin
    - WESTERN GRASS PICKEREL - *E. a. vermiculatus* LeSueur
- CHAIN PICKEREL - *Esox niger* LeSueur
- NORTHERN PIKE - *Esox lucius* Linnaeus
- MUSKELLUNGE - *Esox masquinongy* Mitchill
    - GREAT LAKES MUSKELLUNGE - *E. m. masquinongy* Mitchill

FRESHWATER EEL FAMILY - Anguillidae
- AMERICAN EEL - *Anguilla bostoniensis* (LeSueur)

KILLIFISH FAMILY - Cyprinodontidae
- BANDED KILLIFISH - *Fundulus diaphanus* (LeSueur)
    - EASTERN BANDED KILLIFISH - *F. d. diaphanus* (LeSueur)
    - WESTERN BANDED KILLIFISH - *F. d. menona* Jordan and Copeland
- STARHEAD TOPMINNOW - *Fundulus nottii* (Agassiz)
    - NORTHERN STARHEAD TOPMINNOW - *F. n. dispar* (Agassiz)
- BLACKSTRIPE TOPMINNOW - *Fundulus notatus* (Rafinesque)

LIVEBEARER FAMILY - Poeciliidae
- COMMON GAMBUSIA - *Gambusia affinis* (Baird and Girard)
    - WESTERN COMMON GAMBUSIA - *G. a. affinis* (Baird and Girard)
    - EASTERN COMMON GAMBUSIA - *G. a. holbrookii* Girard

COD FAMILY - Gadidae
- BURBOT - *Lota lota* (Linnaeus)
    - AMERICAN BURBOT - *L. l. lacustris* (Walbaum)

TROUTPERCH FAMILY - Percopsidae
- TROUTPERCH - *Percopsis omiscomaycus* (Walbaum)

PIRATEPERCH FAMILY - Aphredoderidae
- PIRATEPERCH - *Aphredoderus sayanus* (Gilliams)
    - WESTERN PIRATEPERCH - *A. s. gibbosus* LeSueur

BASS FAMILY - Serranidae
- WHITE BASS - *Lepibema chrysops* (Rafinesque)
- YELLOW BASS - *Morone interrupta* Gill
- WHITE PERCH - *Morone americana* (Gmelin)

PERCH FAMILY - Percidae
- YELLOW PERCH - *Perca flavescens* (Mitchill)
- SAUGER - *Stizostedion canadense* (Smith)
- WALLEYE - *Stizostedion vitreum* (Mitchill)
    - YELLOW WALLEYE - *S. v. vitreum* (Mitchill)
    - BLUE WALLEYE - *S. v. glaucum* Hubbs
- RIVER DARTER - *Hadropterus shumardi* Girard
- BLACKSIDE DARTER - *Hadropterus maculatus* (Girard)
- SLENDERHEAD DARTER - *Hadropterus phoxocephalus* (Nelson)
- GILT DARTER - *Hadropterus evides* (Jordan and Copeland)
- CHANNEL DARTER - *Hadropterus copelandi* (Jordan)

- LOGPERCH - Percina caprodes (Rafinesque)
  - OHIO LOGPERCH - P. c. caprodes (Rafinesque)
  - NORTHERN LOGPERCH - P. c. semifasciata (DeKay)
- NORTHERN SAND DARTER - Ammocrypta pellucida (Baird)
- JOHNNY DARTER - Etheostoma nigrum Rafinesque
  - TESSELLATED JOHNNY DARTER - E. n. olmstedi Storer
  - SCALY JOHNNY DARTER - E. n. eulepis (Hubbs and Greene)
  - CENTRAL JOHNNY DARTER - E. n. nigrum Rafinesque
- BLUNTNOSE DARTER - Etheostoma chlorosomum (Hay)
- BANDED DARTER - Etheostoma zonale (Cope)
  - EASTERN BANDED DARTER - E. z. zonale (Cope)
- IOWA DARTER - Etheostoma exile (Girard)
- RAINBOW DARTER - Etheostoma caeruleum Storer
- ORANGETHROAT DARTER - Etheostoma spectabile (Agassiz)
  - NORTHERN ORANGETHROAT DARTER - E. s. spectabile (Agassiz)
- FANTAIL - Etheostoma flabellare Rafinesque
  - BARRED FANTAIL - E. f. flabellare Rafinesque
  - STRIPED FANTAIL - E. f. lineolatum (Agassiz)
- LEAST DARTER - Etheostoma microperca Jordan and Gilbert
- GREENSIDE DARTER - Etheostoma blennioides Rafinesque
  - NORTHERN GREENSIDE DARTER - E. b. blennioides Rafinesque

- SUNFISH FAMILY - Centrarchidae
  - SMALLMOUTH BASS - Micropterus dolomieui (Lacépède)
    - NORTHERN SMALLMOUTH BASS - M. d. dolomieui Lacépède
  - LARGEMOUTH BASS - Micropterus salmoides (Lacépède)
    - NORTHERN LARGEMOUTH BASS - M. s. salmoides (Lacépède)
  - WARMOUTH - Chaenobryttus gulosus (Cuvier)
  - GREEN SUNFISH - Lepomis cyanellus Rafinesque
  - PUMPKINSEED - Lepomis gibbosus (Linnaeus)
  - REDEAR SUNFISH - Lepomis microlophus (Günther)
    - WESTERN REDEAR SUNFISH - L. microlophus, subspecies
  - BLUEGILL - Lepomis macrochirus Rafinesque
    - COMMON BLUEGILL - L. m. macrochirus Rafinesque
  - ORANGESPOTTED SUNFISH - Lepomis humilis (Girard)
  - LONGEAR SUNFISH - Lepomis megalotis (Rafinesque)
    - NORTHERN LONGEAR SUNFISH - L. m. peltastes Cope
  - ROCK BASS - Ambloplites rupestris (Rafinesque)
    - NORTHERN ROCK BASS - A. r. rupestris (Rafinesque)
  - WHITE CRAPPIE - Pomoxis annularis Rafinesque
  - BLACK CRAPPIE - Pomoxis nigromaculatus (LeSueur)
- SILVERSIDE FAMILY - Atherinidae
  - BROOK SILVERSIDE - Labidesthes sicculus (Cope)
    - NORTHERN BROOK SILVERSIDE - L. s. sicculus (Cope)
- DRUM FAMILY - Sciaenidae
  - FRESHWATER DRUM - Aplodinotus grunniens Rafinesque
- SCULPIN FAMILY - Cottidae
  - FOURHORNED SCULPIN - Myoxocephalus quadricornis (Linnaeus)
    - GREAT LAKES FOURHORNED SCULPIN - M. q. thompsonii (Girard)
  - SPOONHEAD SCULPIN - Cottus ricei (Nelson)
  - MOTTLED SCULPIN - Cottus bairdii Girard
    - NORTHERN MOTTLED SCULPIN - C. b. bairdii Girard
    - GREAT LAKES MOTTLED SCULPIN - C. b. kumlieni (Hoy)
  - SLIMY SCULPIN - Cottus cognatus Richardson
    - EASTERN SLIMY SCULPIN - C. c. gracilis Heckel
- STICKLEBACK FAMILY - Gasterosteidae
  - BROOK STICKLEBACK - Eucalia inconstans (Kirtland)
  - NINESPINE STICKLEBACK - Pungitius pungitius (Linnaeus)
  - THREESPINE STICKLEBACK - Gasterosteus aculeatus Linnaeus:
aculeatus × cuvieri Girard

Reprinted from the Proceedings of the NATIONAL ACADEMY OF SCIENCES
Vol. 44, No. 4, pp. 320–323. April, 1958.

*INVARIANT IMBEDDING RELATION FOR THE PRINCIPLES OF INVARIANCE**

BY RUDOLPH W. PREISENDORFER

UNIVERSITY OF CALIFORNIA, LA JOLLA, CALIFORNIA

Communicated by S. Chandrasekhar, February 13, 1958

1. *Introduction.*—The *principle of invariant imbedding*, recently stated by Bellman and Kalaba,[1] is a rule of action which may be followed in the mathematical formulation of any of a wide class of problems concerned with transfer phenomena in general media. The statement of the principle generalizes the methodology originally developed by Ambarzumian[2, 3] and extended by Chandrasekhar[4, 5] in their studies of the transfer of radiation through scattering and absorbing media. In this note we exhibit an explicit analytic embodiment of the principle for radiative-transfer and neutron-transport processes. This symbolic statement of the principle—which we shall call the *invariant imbedding relation*—yields in particular the general symmetric forms of the principles of invariance[5] for these processes. The semigroup features which are generally associated with an invariantly imbedded process are also implicit in the invariant imbedding relation.

The present discussion will be limited to the steady-state case on a class of inhomogeneous one-parameter carrier spaces[6] (e.g., plane-parallel, cylindrical, spherical, and general one-parameter space-filling families of surfaces). Additional features of the invariant imbedding relation such as those associated with time-dependence, polarization, and more general carrier spaces, will be reserved for subsequent discussions.

2. *Invariant Imbedding Relation.—Let* $\Phi = X \times \Xi$ *be a one-parameter carrier space in* E_3, *i.e.,* $X = \{X_x: \ x \in [a, b]\}$, *where* $[a, b]$ *is a closed interval in the extended real-number system, and* Ξ *is the unit sphere in* E_3. *For each* $y \in [a, b]$ *there is a pair* $[N_+(y), N_-(y)]$ *of (real or vector-valued) functions on* $\Phi_y = X_y \times \Xi_+$. *Let* $\mathcal{N}$ *denote the collection of all ordered pairs of functions* $[N_+(z), N_-(x)]$, $[x, z] \subset [a, b]$, *with subcollections* $\mathcal{N}_+$ *and* $\mathcal{N}_-$ *defined as* $\{N_+(z);\ z \in [a, b]\}$ *and* $\{N_-(x):\ x \in [a, b]\}$, *respectively. Then for each* $y \in [x, z] \subset [a, b]$, *there is a map* $\mathcal{M}(x, y, z)$ *of* $\mathcal{N}$ *into* $\mathcal{N}$ *such that*

$$[N_+(y), N_-(y)] = [N_+(z), N_-(x)]\mathcal{M}(x, y, z), \tag{1}$$

where

$$\mathcal{M}(x, y, z) = \begin{pmatrix} \mathfrak{J}(z, y, x), & \mathcal{R}(z, y, x) \\ \mathcal{R}(x, y, z), & \mathfrak{J}(x, y, z) \end{pmatrix},$$

in which $\mathcal{R}(x, y, z)$ *is the complete reflectance operator with domains* $\mathcal{N}_+$, $\mathcal{N}_-$, *and ranges* $\mathcal{N}_-$, $\mathcal{N}_+$, *respectively;* $\mathfrak{J}(x, y, z)$ *is the complete transmittance operator with domains* $\mathcal{N}_+$, $\mathcal{N}_-$, *and ranges* $\mathcal{N}_+$, $\mathcal{N}_-$, *respectively. In addition,* $\mathfrak{J}(x, z, z) = \mathrm{T}(x, z)$ *is the standard transmittance operator and* $\mathfrak{J}(x, x, z) = I$, *the identity operator;* $\mathcal{R}(x, x, z) = \mathrm{R}(x, z)$ *is the standard reflectance operator and* $\mathcal{R}(x, z, z) = O$, *the zero operator.*

Expression (1) is the *invariant imbedding relation* for the radiative-transfer and neutron-transport contexts. The pair of functions $N(y) = [N_+(y), N_-(y)]$ is the abstract version of the classical intensity (or radiance) function on a surface X_y, y units of depth "below" the upper boundary of the medium. $N_+(y)$ is a *function*

Reproduced by Permission

Contributions from the Scripps Institution of Oceanography, New Series, No. 1002

which physically describes the "outward"-directed flux and $N_-(y)$ describes the "inward"-directed flux at each point of X_y (Fig. 1). $N(y)$ need not be constant over X_y. Starting with the S and T functions of Chandrasekhar, one may obtain concrete examples of the various operators and of relation (1) in the classical case of a finitely deep plane-parallel medium.

3. *Principle of Invariant Imbedding.*—In the present context, the *invariant process* mentioned in the general statement of the principle is represented by the collection $\{\mathfrak{M}(x, y, z): y \in [x, z] \subset [a, b]\}$ of transformations, and the *state vectors* are the elements of the collection $\mathfrak{N}$.

4. *Semigroup Properties of the Imbedding Relation.*—The semigroup relations are obtained by setting $N_+(b) = 0$ (the zero function on $X_b \times \Xi_+$). By equation (1), for all $y \in [a, b]$,

$$[N_+(y), N_-(y)] = [N_+(b), N_-(a)]\mathfrak{M}(a, y, b) = [N_-(a)\mathfrak{R}(a, y, b), N_-(a)\mathfrak{T}(a, y, b)],$$

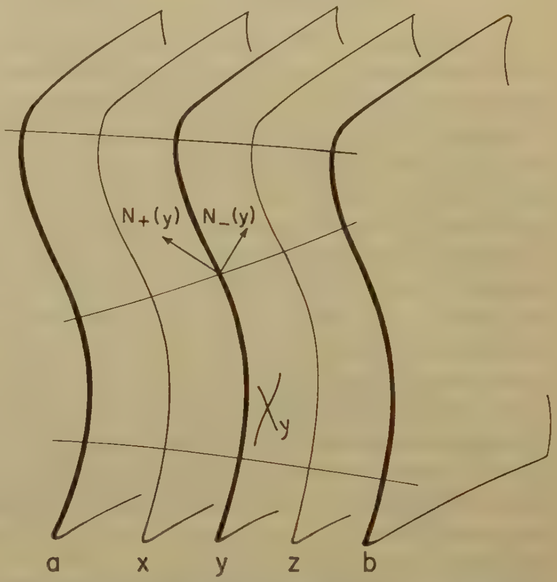

FIG. 1.—$N_+(y)$ and $N_-(y)$ describe the outward- and inward-directed flux across the surface X_y, respectively. Ξ_+, not explicitly shown, is the "outward" hemisphere of the unit sphere Ξ.

and for $b \in [y, b]$,

$$[N_+(b), N_-(b)] = [N_+(b), N_-(y)]\mathfrak{M}(y, b, b) = [0, N_-(y)\mathfrak{T}(y, b, b)],$$

whence

$$N_-(b) = N_-(a)\mathfrak{T}(a, b, b) = N_-(a)\mathfrak{T}(a, y, b)\mathfrak{T}(y, b, b),$$

so that

$$\mathfrak{T}(a, b, b) = \mathfrak{T}(a, y, b)\mathfrak{T}(y, b, b), \qquad y \in [a, b]. \tag{2}$$

In a similar way it may be shown that

$$\mathfrak{R}(a, z, b) = \mathfrak{T}(a, y, b)\mathfrak{R}(y, z, b), \qquad y \in [a, z]. \tag{3}$$

The complementary set of semigroup relations are obtained by setting $N_-(a) = 0$.

5. *Principles of Invariance.*—The four general principles of invariance associated with X are obtained by first writing out in full the matrical relation (1) and then suitably choosing the spread of the interval $[x, z]$ and the location of the parameter y in $[x, z]$. Thus, from (1):

I. Let $x = y$, use component $N_+(y)$:

$$N_+(y) = N_+(z)T(z, y) + N_-(y)R(y, z).$$

II. Let $z = y$, use component $N_-(y)$:

$$N_-(y) = N_-(x)T(x, y) + N_+(y)R(y, x).$$

III. Use I twice: Let $y = a$, $z = b$; then $y = a$, z arbitrary:

$$N_+(a) = N_+(b)\mathrm{T}(b, a) + N_-(a)R(a, b) = N_+(z)T(z, a) + N_-(a)R(a, z).$$

IV. Use II twice: Let $y = b$, $x = a$; then $y = b$, x arbitrary:

$$N_-(b) = N_-(a)T(a, b) + N_+(b)R(b, a) = N_-(x)T(x, b) + N_+(b)R(b, x).$$

Three observations may be made here: (1) the four principles of invariance stated above are in *undecomposed* operator form. The advantage gained by retaining this form is the resultant general symmetry of the statements. (2) Principles III and IV are special cases of I and II, respectively, and the latter in turn are obtained by the appropriate permutation of $+$, $-$, and x, z, in a single basic statement derived from expression (1). (3) The invariant imbedding relation and the principles of invariance refer (as do their classical counterparts) to an arbitrary source-free subset of X defined by the interval $[x, z]$. This is in keeping with the original purpose[2–6] of defining and characterizing the inherent reflecting and transmitting properties of source-free subsets of a space. Thus the problem of formulating the general principles of invariance is, by definition, independent of the boundary-value problem associated with *internally* distributed sources. It should be observed, however, that if sources are present *in* X, relation (1) and its corollaries I–IV continue to hold for all those subsets (defined by $[x, z]$) which are free of sources.

The classical forms of the principles of invariance are obtained by: (1) decomposing the functions $N(y)$, $y \in [a, b]$ into the sum of their reduced and diffuse components: $N(y) = N^\circ(y) + N^*(y)$; (2) imposing the boundary conditions: $N_-(a) = N^\circ(a)$ with Dirac-delta structure over Ξ_+, and $N_+(b) = 0$; (3) assuming X to be a plane-parallel homogeneous slab, so that $R(x, y) = R(y, x) = R(|x - y|)$ and $T(x, y) = T(y, x) = T(|x - y|)$.

The decomposition of $N(y)$ carries through to the general case, and the classical boundary conditions may be imposed on $N_-(a)$ and $N_+(b)$. However, the general inhomogeneity and curvilinear structure of X, first of all, give rise to the *polarity* of the R and T operators: $R(x, y) \neq R(y, x)$, $T(x, y) \neq T(y, x)$; and, second, remove some of the original invariant features of the R and T operators such as those associated with the physical operations of adding or subtracting finite layers of the media. The general functional relations satisfied by the R and T operators will be considered at a later time.

---

* *Contribution from the Scripps Institution of Oceanography*, New Series. This paper represents results of research which has been supported by the Bureau of Ships, U.S. Navy.

[1] R. Bellman and R. Kalaba, "On the Principle of Invariant Imbedding and Propagation through Inhomogeneous Media," these PROCEEDINGS, **42**, 629–632, 1956.

[2] V. A. Ambarzumian, "Diffuse Reflection of Light by a Foggy Medium," *Compt. Rend.* (Doklady) *Acad. Sci. U.R.S.S.*, **38**, 229–232, 1943.

(345)

[3] V. A. Ambarzumian, "On the Problem of the Diffuse Reflection of Light," *J. Phys. Acad. Sci. U.S.S.R.*, **8**, 65–75, 1944.

[4] S. Chandrasekhar, "On the Radiative Equilibrium of a Stellar Atmosphere. XIV," *J. Astrophys.*, **105**, 164–203, 1947.

[5] S. Chandrasekhar, *Radiative Transfer* (Oxford, 1950).

[6] Carrier spaces are the measure-theoretic settings for transfer phenomena. A complete definition may be found in Rudolph W. Preisendorfer, "A Mathematical Foundation for Radiative Transfer Theory," *J. Math. and Mech.*, **6**, 685–730, 1957.

Reprinted from the Proceedings of the NATIONAL ACADEMY OF SCIENCES
Vol. 44, No. 4, pp. 323–327. April, 1958.

*FUNCTIONAL RELATIONS FOR THE R AND T OPERATORS ON PLANE-PARALLEL MEDIA**

BY RUDOLPH W. PREISENDORFER

UNIVERSITY OF CALIFORNIA, LA JOLLA, CALIFORNIA

Communicated by S. Chandrasekhar, February 13, 1958

1. *Introduction.*—In the classical theory of radiative transfer, one may associate with a separable plane-parallel medium—i.e., a medium in which the phase function $p = 4\pi\sigma/\alpha$ is independent of depth—two functions, S and T, which analytically characterize the diffuse reflectance and transmittance of the medium. Explicit knowledge of the S and T functions is tantamount to a solution of an important class of multiple-scattering problems associated with the medium. Whereas the volume-scattering function, σ, and the volume-attenuation function, α, summarize the *local* optical properties of the medium, the S and T functions summarize the *global* optical properties of the medium. Furthermore, as the local behavior of the light field is described by the equation of transfer in terms of σ and α, so is the global behavior of the light field described by the principles of invariance in terms of S and T. The global approach was initiated by Ambarzumian, but it remained for Chandrasekhar to formulate the four principles of invariance and deduce from them the requisite integral equations for S and T for the case of finite, separable plane-parallel media. The importance of the global formulation has been illustrated by its role in many successful solutions of multiple-scattering problems which were intractable under the local formulation.

In this note we consider the case of finite, *non-separable* plane-parallel media. As is shown below, the study of these media requires not two but four functions: a reflectance-transmittance pair for each of the two boundaries of the medium. The four principles of invariance for a non-separable plane-parallel medium are formulated and are found to be just sufficient to yield the appropriate integrodifferential equations governing the four functions.

It is of some interest to observe that the following derivations can be patterned after the procedure used by Chandrasekhar for the separable case, namely, the procedure which makes explicit use of the principles of invariance in conjunction with the equation of transfer. This procedure promises to be adequate, under appropriate extensions, for use in the formulation of the functional relations governing the scattering functions in general one-parameter carrier spaces. In this way a useful methodology already extant in classical theory is retained and is extended to

Reproduced by Permission
Contributions from the Scripps Institution of Oceanography, New Series, No. 1003

more general settings. In addition, this procedure appears to be pertinent to an important question in the mathematical foundations of radiative-transfer theory, namely, the question of the apparent mathematical abiogenesis of the S and T functions and the principles of invariance. In short, are the principles of invariance part of the basic laws of radiative-transfer theory or merely consequences of them? In this connection, we observe that the operator form of the equation of transfer adopted during the course of the present derivations yields a pair of statements which clearly represent what might be termed the *local* forms of the principles of invariance. These in turn may possibly supply a key, by means of the general theory of Green's functions for linear operators, to an existence proof for the S and T functions and perhaps a *derivation* of the statements of the principles of invariance themselves. If this or any coterminous procedure is possible, then the general equation of transfer may serve as the sole starting point of an unbroken network of deductions covering all salient mathematical features of modern radiative-transfer theory.

The operators used in the present note are left in undecomposed form in order to secure maximum symmetry and compactness of the formulations.

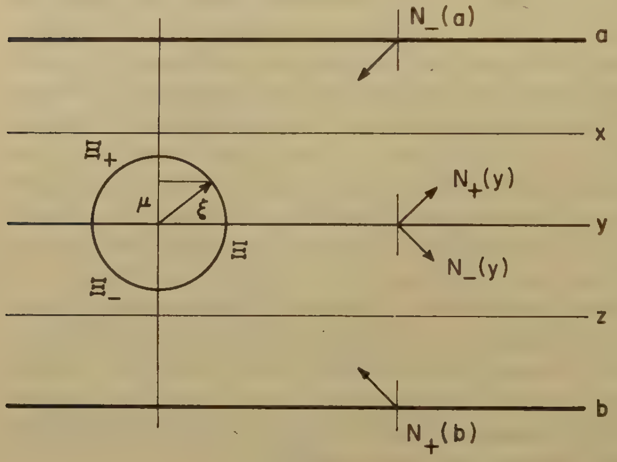

FIG. 1

2. *Equation of Transfer and the Local Forms of the Principles of Invariance.*—We begin with a plane-parallel medium imbedded in Euclidean three space (Fig. 1), namely, that subset contained by two planes at geometric depths a and b from some datum plane. Several intermediate planes at depths x, y, z will also be considered: $a \leq x \leq y \leq z \leq b$. The volume-attenuation and volume-scattering functions, α and σ, along with the radiance function (specific intensity) N, will depend spatially only on the depth parameters and in an arbitrary way. The steady-state, emission-free equation of transfer for radiance may be written

$$\mu \frac{dN(y, \mu, \phi)}{dy} = -\alpha(y)N(y, \mu, \phi) + N_*(y, \mu, \phi), \tag{1}$$

where

$$N_*(y, \mu, \phi) = \int_{\Xi} \sigma(y; \mu, \phi; \mu', \phi')N(y, \mu', \phi')d\mu'd\phi'.$$

We adopt the concepts of outward and inward radiances: $N(y, +\mu, \phi)$; $N(y, -\mu, \phi)$, $0 < \mu \leq 1$, and write the outward and inward radiance distributions at level y as

(348)

$$N_+(y), \qquad N_-(y);$$

these are *functions* which assign to the pair (μ, ϕ), $0 < \mu \leq 1$, $0 < \phi \leq 2\pi$ the appropriate radiance values at level y in the indicated directions. If Ξ_+ and Ξ_- are the totalities of outward and inward unit vectors at each level y, the equation of transfer may be written in the following operator form:

$$-\frac{dN_+(y)}{dy} = N_+(y)\tau(y) + N_-(y)\rho(y),$$

$$\frac{dN_-(y)}{dy} = N_-(y)\tau(y) + N_+(y)\rho(y), \tag{2}$$

where, for each y, $a \leq y \leq b$, and arbitrary (μ, ϕ), $0 < \mu \leq 1$, $0 \leq \phi < 2\pi$,

$$\rho(y) = \frac{1}{\mu}\int_{\Xi_+} \sigma_-(y; \mu, \phi; \mu', \phi')[\quad]d\mu' d\phi',$$

$$\tau(y) = \frac{1}{\mu}\int_{\Xi_+} \sigma_+(y; \mu, \phi; \mu', \phi')[\quad]d\mu' d\phi' - \frac{1}{\mu}\alpha(y).$$

Thus $\rho(y)$ and $\tau(y)$ evidently play the role of local reflectance and transmittance operators, and σ_- and σ_+ are appropriate restrictions of σ chosen so that their μ-arguments are positive. (Such restrictions are possible because of the implicitly assumed isotropy of the medium.) The pair (2) clearly represents the *local* (or integrodifferential) forms of the principles of invariance.

3. *Principles of Invariance for Non-separable Plane-Parallel Media.*—In an earlier note[1] the classical principles of invariance were generalized to the context of general one-parameter carrier spaces. These generalizations were based directly on considerations of the classical forms as given by Chandrasekhar and resulted in an explicit analytical embodiment of the principle of invariant imbedding[2] for the radiative-transfer context. The two main statements of the principles of invariance were shown to be of the forms:

$$\left.\begin{array}{ll} \text{I.} & N_+(y) = N_+(z)T(z, y) + N_-(y)R(y, z) \\ \text{II.} & N_-(y) = N_-(x)T(x, y) + N_+(y)R(y, x) \end{array}\right\} a \leq x \leq y \leq z \leq b. \tag{3}$$

The structural similarity of sets (2) and (3) can be noted. By suitably choosing the spread of the interval $[x, z]$ and the location of y within it, the operator forms of four principles of invariance for the present context may be obtained from (3):

$$\begin{array}{lll} \text{I.} & N_+(y) & = N_+(b)T(b, y) + N_-(y)R(y, b), \\ \text{II.} & N_-(y) & = N_-(a)T(a, y) + N_+(y)R(y, a), \\ \text{III.} & N_+(a) & = N_+(b)T(b, a) + N_-(a)R(a, b) = N_+(y)T(y, a) + N_-(a)R(a, y), \\ \text{IV.} & N_-(b) & = N_-(a)T(a, b) + N_+(b)R(b, a) = N_-(y)T(y, b) + N_+(b)R(b, y). \end{array}$$

For every pair of depths (x, z) in the closed interval $[a, b]$ we have

$$R(x, z) = \frac{1}{\mu}\int_{\Xi_+} R(x, z; \mu, \phi; \mu', \phi')[\quad]d\mu' d\phi'.$$

Furthermore,

$$T(x, z) = T^\circ(x, z) + T^*(x, z),$$

where

$$T^*(x, z) = \frac{1}{\mu}\int_{\Xi_+} T(x, z; \mu, \phi; \mu', \phi')[\quad]d\mu' d\phi',$$

$$T^\circ(x, z) = \int_{\Xi_+} T_r(x)\delta(\mu - \mu')\delta(\phi - \phi')[\quad]d\mu' d\phi',$$

in which

$$T_r(x) = \exp\left\{-\frac{1}{\mu'}\left|\int_x^z \alpha(y)dy\right|\right\}, \qquad r = |z - x|/\mu', \qquad 0 < \mu' \leq 1.$$

$T(x, z)$ is the *transmittance operator:* $T^\circ(x, z)$, $T^*(x, z)$ are its *reduced* and *diffuse* components. $R(x, z)$ is the *reflectance operator*, and, since the reflected flux is, by definition, entirely of diffuse character, the corresponding reduced component $R^\circ(x, z)$ of $R(x, z)$ is the zero operator, so that $R^*(x, z) = R(x, z)$. It may be shown that, in analogy to the S and T functions of the classical theory, the present R and T functions have the properties:

$$\begin{aligned} \lim_{z \to x} R(x, z; \mu, \phi; \mu', \phi')/|z - x| &= \sigma_-(x; \mu, \phi; \mu', \phi'), \\ \lim_{z \to x} T(x, z; \mu, \phi; \mu', \phi')/|z - x| &= \sigma_+(x; \mu, \phi; \mu', \phi'). \end{aligned}$$

4. *Functional Relations for the R and T Operators.*—In what follows, let $N_-(a)$ be of arbitrary angular structure and set $N_+(b) = 0$ (the zero function); furthermore, all functions and operators will be assumed continuously differentiable with respect to the depth parameter, y. Now from I, with the adopted boundary conditions in force,

$$\frac{dN_+(y)}{dy} = \frac{dN_-(y)}{dy} R(y, b) + N_-(y)\frac{dR(y, b)}{dy}. \tag{4}$$

Since interest is at present centered on the functional relations for the slab defined by the planes at depths a and b, we consider

$$\lim_{y \to a} \frac{dN_+(y)}{dy},$$

which, by (2), has the form

$$-[N_+(a)\tau(a) + N_-(a)\rho(a)] = -N_-(a)[R(a, b)\tau(a) + \rho(a)],$$

where the latter relation follows from use of the left-hand equality of III. Similarly,

$$\lim_{y \to a} \frac{dN_-(y)}{dy} = N_-(a)[\tau(a) + R(a, b)\rho(a)].$$

Since

$$\lim_{y \to a} \frac{dR(y, b)}{dy} = \frac{\partial R(a, b)}{\partial a},$$

and $N_-(a)$ is arbitrary, the limit operation $\lim_{y \to a}$ applied to (4) yields

$$\text{I}'. \quad -\frac{\partial R(a, b)}{\partial a} = \rho(a) + \tau(a)R(a, b) + R(a, b)\tau(a) + R(a, b)\rho(a)R(a, b).$$

Now, from II,

$$\frac{dN_-(y)}{dy} = N_-(a)\frac{dT(a, y)}{dy} + \frac{dN_+(y)}{dy}R(y, a) + N_+(y)\frac{dR(y, a)}{dy}. \tag{5}$$

By (2) and the left-hand equality of IV,

$$\lim_{y \to b}\frac{dN_-(y)}{dy} = N_-(a)T(a, b)\tau(b),$$

$$\lim_{y \to b}\frac{dN_+(y)}{dy} = -N_-(a)T(a, b)\rho(b).$$

Applying the limit operation $\lim_{y \to b}$ to (5), setting

$$\frac{\partial T(a, b)}{\partial b} = \lim_{y \to b}\frac{dT(a, y)}{dy},$$

and recalling that $N_-(a)$ is arbitrary, we have

$$\text{II}'. \quad \frac{\partial T(a, b)}{\partial b} = T(a, b)\tau(b) + T(a, b)\rho(b)R(b, a).$$

The procedure is now clear. By applying this procedure in turn to the right-hand equalities of principles III and IV, we have the results:

$$\text{III}'. \quad \frac{\partial R(a, b)}{\partial b} = T(a, b)\rho(b)T(b, a),$$

$$\text{IV}'. \quad -\frac{\partial T(a, b)}{\partial a} = \tau(a)T(a, b) + R(a, b)\rho(a)T(a, b).$$

In conclusion, several general observations may be made. (1) For non-separable spaces, i.e., spaces in which the phase function $p = 4\pi\sigma/\alpha$ is dependent on depth, I′–IV′ show that the R and T operators possess *polarity:* $R(a, b) \neq R(b, a)$; $T(a, b) \neq T(b, a)$. (2) The system I′–IV′ is a simultaneous system of the simplest kind. It can be solved, in principle, by successively considering the individual relations in either of the following orders: I′, IV′, III′, II′; I′, IV′, II′, III′. (3) To obtain the equations governing the R and T *functions,* one must first assume, as in the classical case, a Dirac-delta structure for $N_-(a)$: $N_-(a) = N^\circ\delta(\mu - \mu')\delta(\phi - \phi')$. Then, by successively applying the operators on each side of the statements I′–IV′ to $N_-(a)$ and making the appropriate reductions, the requisite integrodifferential equations for the R and T functions are obtained.

---

* *Contribution from the Scripps Institution of Oceanography,* New Series. This paper represents results of research which has been supported by the Bureau of Ships, U.S. Navy.

[1] R. W. Preisendorfer, "Invariant Imbedding Relation for the Principles of Invariance," these PROCEEDINGS, **44**, 320–323, 1958.

[2] R. Bellman and R. Kalaba, "On the Principle of Invariant Imbedding and Propagation through Inhomogeneous Media," these PROCEEDINGS, **42**, 629–632, 1956.

Reprinted from the Proceedings of the NATIONAL ACADEMY OF SCIENCES
Vol. 44, No. 4, pp. 328–332. April, 1958.

TIME-DEPENDENT PRINCIPLES OF INVARIANCE*

BY RUDOLPH W. PREISENDORFER

UNIVERSITY OF CALIFORNIA, LA JOLLA, CALIFORNIA

Communicated by S. Chandrasekhar, February 13, 1958

1. *Introduction.*—Radiative-transfer phenomena, whether in the transient or stationary states, may be classified according to the relative importance of the roles played by the three general processes of conduction, convection, and radiation. *Strict radiative transfer* refers to the transfer by radiation processes alone. In 1926 work on time-dependent strict radiative-transfer processes had been carried out by Milne and later extended by Chandrasekhar.[1] In these studies the time-dependent radiation field is considered to be governed principally by the various decay rates of excited atoms. This is in contrast to the time-dependent process initiated and sustained by the mechanism of simple scattering and the speed of propagation of radiant energy through the medium (the multiple-scattering process). In another early study, simultaneous consideration of time-dependent convection and radiation processes was made by Rosseland.[2] Aside from these studies, the time-dependent case of strict radiative-transfer theory has been relatively unexplored. This is particularly true for the time-dependent multiple-scattering problem.

Most of the tools presently available for the study of time-dependent multiple-scattering phenomena are imports from neutron-transport theory. In this field the approach to the transient case has been successfully effected by means of the linearized Boltzmann transport equation—the exact counterpart to the equation of transfer in radiative-transfer theory. The approach may be analyzed into two alternate procedures: the direct and the indirect. The direct procedure, as exemplified in the papers of Lehner and Wing,[3] is based on the transport equation, in which the time-dependence is explicitly retained throughout. In the indirect procedure, the time-dependent problem is immediately shunted to a stationary problem by means of the Laplace transform, is solved in that context, and then is switched back to a non-stationary problem by an inverse Laplace transform. Examples may be found in the works of Grosjean,[4] Case, de Hoffman, and Placzek,[5] and Davison.[6] We note that this procedure is possible only if the attenuation and scattering functions are time-independent. The mathematical questions of the existence of solutions sought in the time-dependent case by these methods can be settled, for example, by applications of the results obtained by Kurth.[7]

There remains, however, to explore a potentially useful approach to the time-dependent multiple-scattering processes—an approach based on the principle of invariance formulations which have been instrumental in the exact solution of a large class of stationary multiple-scattering problems in radiative-transfer theory. In this note we exhibit the formulation of the requisite statements of the four time-dependent principles of invariance and show that they are sufficient to derive the functional relations governing the time-dependent R and T functions and their corresponding integral operators. The derivations follow closely the pattern used in some earlier studies of the stationary case.[8] In this way we add to the evidence that the classical procedures initiated by Chandrasekhar can be extended to more general settings. For brevity, the present discussion is limited to plane-parallel

*Contributions from the Scripps Institution of Oceanography, New Series, No. 1004

Reproduced by Permission

media. However, the media will be assumed finite, non-separable, and such that the attenuation and scattering functions are generally dependent on time.

2. *Local Forms of the Time-dependent Principles of Invariance.*—With the exception of the explicit incorporation of time parameters, the geometrical setting and the notation used in the present investigation are the same as those used in the study of the steady-state case.[8] In particular, the time-dependent equation of transfer will be written

$$\frac{\mu\,\partial N(y, t, \mu, \phi)}{\partial y} + \frac{1}{v}\,\frac{\partial N(y, t, \mu, \phi)}{\partial t} = -\alpha(y, t)N(y, t, \mu, \phi) + N_*(y, t, \mu, \phi) \quad (1)$$

where

$$N_*(y, t, \mu, \phi) = \int_{\Xi} \sigma(y, t; \mu, \phi; \mu', \phi')N(y, t, \mu', \phi')d\mu' d\phi'.$$

As before, we use the notions of outward and inward radiance distributions:

$$N_+(y, t), \qquad N_-(y, t).$$

The local reflectance and transmittance operators are defined as

$$\rho(y, t) = \frac{1}{\mu}\int_{\Xi_+} \sigma_-(y, t; \mu, \phi; \mu', \phi')[\quad]d\mu' d\phi',$$

$$\tau(y, t) = \frac{1}{\mu}\int_{\Xi_+} \sigma_+(y, t; \mu, \phi; \mu', \phi')[\quad]d\mu' d\phi' - \frac{1}{\mu}\,\alpha\,(y, t),$$

so that the local forms of the time-dependent principles of invariance may be written thus:

$$\frac{D_-N_+(y, t)}{Dy} = -\frac{\partial N_+(y, t)}{\partial y} + \frac{1}{\mu v}\,\frac{\partial N_+(y, t)}{\partial t} = N_+(y, t)\tau(y, t) + N_-(y, t)\rho(y, t), \quad (2)$$

$$\frac{D_+N_-(y, t)}{Dy} = \frac{\partial N_-(y, t)}{\partial y} + \frac{1}{\mu v}\,\frac{\partial N_-(y, t)}{\partial t} = N_-(y, t)\tau(y, t) + N_+(y, t)\rho(y, t).$$

3. *Time-dependent R and T Operators and Principles of Invariance.*—For every pair (x, z) of geometric depths and ordered pair (t', t) of times, $t' \leq t$, we define two non-negative real-valued functions $R(x, z, t', t;\ ;\ )$, $T(x, z; t'; t;\ ;\ )$, on $\Xi_+ \times \Xi_+$ and their associated integral operators:

$$R(x, z, t', t) = \frac{1}{\mu}\int_{\Xi_+} R(x, z, t', t; \mu, \phi; \mu', \phi')[\quad]d\mu' d\phi',$$

$$T^*(x, z, t', t) = \frac{1}{\mu}\int_{\Xi_+} T(x, z, t', t; \mu, \phi; \mu', \phi')[\quad]d\mu' d\phi'.$$

These are clearly analogous to the operators $R(x, z)$ and $T^*(x, z)$ considered in the steady-state case. In addition, we define

$$T^\circ(x, z, t', t) = \int_{\Xi_+} T_r(x)\delta(\mu - \mu')\delta(\phi - \phi')\delta\left(t - \frac{r}{v} - t'\right)\ [\quad]d\mu' d\phi',$$

where $T_r(x)$, $r = |z - x|/\mu'$, is defined as in the stationary case. Set

$$T(x, z, t', t) = T^\circ(x, z, t', t) + T^*(x, z, t', t).$$

In addition to the usual analytic conditions imposed on the R and T functions in the stationary context, we require at present three additional properties: (i) If $N_-(x, \cdot)$ is arbitrary and $N_+(z, \cdot) = 0$, then

$$N_+(x, t) = \int_{-\infty}^{t} N_-(x, t')R(x, z, t', t)dt' = N_-(x, \bar{t}')R(x, z, \bar{t}', t),$$

$$N_-(z, t) = \int_{-\infty}^{t - \frac{|z-x|}{v}} N_-(x, t')T(x, z, t', t)dt' = N_-(x, \bar{t}')T(x, z, \bar{t}', t).$$

The right-hand equalities define a convenient integration convention. (ii) In particular, if $N_-(x, \cdot)$ is constant over $(-\infty, t)$, t finite, and α and σ are independent of t, then

$$\begin{aligned} N_+(x) &= N_-(x, \bar{t}')R(x, z, \bar{t}', t) = N_-(x)R(x, z), \\ N_-(z) &= N_-(x, \bar{t}')T(x, z, \bar{t}', t) = N_-(x)T(x, z), \end{aligned}$$

where $R(x, z)$ and $T(x, z)$ are the steady-state operators considered earlier. (iii) Finally,

$$R(x, z, t, t) = 0 \qquad \text{for all } t,$$

and

$$\mathrm{T}(x, z, t', t) = 0 \qquad \text{for} \qquad t - t' \leq |z - x|/v.$$

These adopted conditions are sufficient to allow the formulation of both the time-dependent principles of invariance and the necessary functional relations governing the time-dependent R and T operators which reduce, under steady-state conditions, to their respective steady-state counterparts.

The two main time-dependent principles of invariance may then be written:

$$\begin{aligned} &\text{I.} \quad N_+(y, t) = N_+(z, \bar{t}')T(z, y, \bar{t}', t) + N_-(y, \bar{t}')R(y, z, \bar{t}', t), \\ &\text{II.} \quad N_-(y, t) = N_-(x, \bar{t}')T(x, y, \bar{t}', t) + N_+(y, \bar{t}')R(y, x, \bar{t}', t), \\ &\qquad\qquad a \leq x \leq y \leq z \leq b. \end{aligned} \tag{3}$$

The structural similarity of sets (2) and (3) can be noted. Set (3) yields, after appropriate choices of the spread of $[x, z]$ and the location of y within it, the operator forms of the four principles of invariance for the present context. The general resultant forms, being structured similarly to the steady-state set considered earlier, need not be given here. Instead, for brevity, we assume that the usual boundary conditions are already in force, namely, $N_-(a, \cdot)$ is arbitrary, and $N_+(b, \cdot) = 0$ (the zero function). The appropriate principles then follow directly from set (3):

$$\begin{aligned} &\text{I.} \quad N_+(y, t) = N_-(y, \bar{t}')R(y, b, \bar{t}', t), \\ &\text{II.} \quad N_-(y, t) = N_-(a, \bar{t}')T(a, y, \bar{t}', t) + N_+(y, \bar{t}')R(y, a, \bar{t}', t), \\ &\text{III.} \quad N_+(a, t) = N_-(a, \bar{t}')R(a, b, \bar{t}', t) = N_+(y, t')T(y, a, \bar{t}', t) \\ &\qquad\qquad + N_-(a, \bar{t}')R(a, y, \bar{t}', t), \\ &\text{IV.} \quad N_-(b, t) = N_-(a, \bar{t}')T(a, b, \bar{t}', t) = N_-(y, \bar{t}')T(y, b, \bar{t}', t). \end{aligned}$$

4. *Functional Relations for the Time-dependent R and T Operators.*—In what follows, let $N_-(a, \cdot)$ be of arbitrary angular structure, but of Dirac-delta time-dependence: $N_-(a, t) = N_-(a, t_0)\delta(t - t_0)$. This procedure results in relatively simple relations for the R and T *operators* [cf. with the adoption of a Dirac-delta angular structure for $N_-(a)$ in the steady-state formulation which results in the relatively simpler relations for the R and T *functions*]. The subsequent operations involving the Dirac-delta functions, their products, and derivatives are governed by the usual conventions.[9]

We begin by applying the operator D_-/Dy to I:

$$\frac{D_-N_+(y, t)}{Dy} = \frac{D_-N_-(y, \bar{t}')}{Dy} R(y, b, \bar{t}', t) + N_-(y, \bar{t}') \frac{D_-R(y, b, \bar{t}', t)}{Dy}. \tag{4}$$

To this we apply in turn the operation $\lim_{y \to a}$. The left side of equation (4) yields, by means of (2),

$$N_+(a, t)\tau(a, t) + N_-(a, t)\rho(a, t) = N_-(a, t_0)[R(a, b, t_0, t)\tau(a, t) + \delta(t - t_0)\rho(a, t)],$$

the alternate expression comes from the left-hand side of III and the adopted form of $N_-(a, \cdot)$. Further, by (2),

$$\frac{D_-N_-(y,t')}{Dy} = -\frac{\partial N_-(y, t')}{\partial y} = \frac{1}{\mu v}\frac{\partial N_-(y, t')}{\partial t} - N_-(y, t')\tau(y, t') - N_+(y, t')\rho(y, t'),$$

so that

$$\lim_{y \to a}\frac{D_-N_-(y, t')}{Dy} = N_-(a, t_0) \left[\frac{1}{\mu v}\delta'(t' - t_0) - \delta(t' - t_0)\tau(a, t') - R(a, b, t_0, t')\rho(a, t')\right],$$

where $\delta'(t' - t_0)$ is the symbolic derivative of the Dirac-delta function with respect to t'. Finally,

$$\lim_{y \to a}\frac{D_-R(y, b, t', t)}{Dy} = -\frac{\partial R(a, b, t', t)}{\partial a} + \frac{1}{\mu v}\frac{\partial R(a, b, t', t)}{\partial t}.$$

Using these results and the fact that $N_-(a, \cdot)$ is of arbitrary angular structure, we have

$$\text{I}'.\quad -\frac{\partial R(a, b, t_0, t)}{\partial a} + \frac{1}{\mu v}\left[-\frac{\partial R(a, b, t_0, t)}{\partial t_0} + \frac{\partial R(a, b, t_0, t)}{\partial t}\right] = \delta(t - t_0)\rho(a,t) + \tau(a, t_0)R(a, b, t_0, t) + R(a, b, t_0, t)\tau(a, t) + R(a, b, t_0, \bar{t}')\rho(a, \bar{t}')R(a, b, \bar{t}', t).$$

Now starting with II, applying in turn the operations D_+/Dy and $\lim_{y \to b}$ and then making use of (2) and the left side of IV, we have, in a similar way,

$$\text{II}'.\quad \frac{\partial T(a, b, t_0, t)}{\partial b} + \frac{1}{\mu v}\frac{\partial T(a, b, t_0, t)}{\partial t} = T(a, b, t_0, t)\tau(b, t) + T(a, b, t_0, \bar{t}')\rho(b, \bar{t}')R(b, a, \bar{t}', t).$$

The third relation follows from the right-hand equality of III by applying the procedure used for I′. The result is

$$\text{III}'. \qquad \frac{\partial R(a, b, t_0, t)}{\partial b} = T(a, b, t_0, \bar{t}')\rho(b, \bar{t}')T(b, a, \bar{t}', t).$$

The fourth relation follows from the right-hand equality of IV by applying the procedure used for II′. The result is

$$\text{IV}'. \qquad -\frac{\partial T(a, b, t_0, t)}{\partial a} - \frac{1}{\mu v}\frac{\partial T(a, b, t_0, t)}{\partial t_0} = \tau(a, t_0)T(a, b, t_0, t) + R(a, b, t_0, \bar{t}')\rho(a, \bar{t}')T(a, b, \bar{t}', t).$$

We conclude by observing that (1) the time-dependent R and T operators will be homogeneous with respect to time (i.e., will depend on time differences $t - t'$) if and only if the attenuation and scattering functions are independent of t; (2) furthermore, for non-separable spaces, the time-dependent R and T operators exhibit polarity: $R(a, b, t', t) \neq R(b, a, t', t)$, $T(a, b, t', t) \neq T(b, a, t', t)$; (3) the solution procedures for the time-dependent relations are, in principle, the same as those followed in the stationary case.

---

* *Contribution from the Scripps Institution of Oceanography,* New Series. This paper represents results of research which has been supported by the Bureau of Ships, U.S. Navy.

[1] S. Chandrasekhar, *Radiative Transfer* (Oxford, 1950), pp. 354–364.

[2] S. Rosseland, "On the Transmission of Radiation through an Absorbing Medium in Motion, with Applications to the Theory of Sunspots and Solar Radiation," *Astrophys. J.*, **63**, 342–367, 1926.

[3] J. Lehner and G. M. Wing, "Solution of the Linearized Boltzmann Transport Equation for the Slab Geometry," *Duke Math. J.*, **23**, 125–142, 1956.

[4] C. C. Grosjean, *The Exact Mathematical Theory of Multiple Scattering of Particles in an Infinite Medium* ("Verhandelingen van de Koninklijke Vlaamse Academie voor Wetenschappen, Lettern en schone Kunsten van België" [Brussels: Paleis der Academiën, 1951]).

[5] K. M. Case, F. de Hoffman, and G. Placzek, *Introduction to the Theory of Neutron Diffusion,* (Los Alamos, New Mexico: Los Alamos Scientific Laboratory, 1953), Vol. I, chap. iii.

[6] B. Davison, *Neutron Transport Theory* (Oxford, 1957), chap. iii.

[7] R. Kurth, "Das Anfangswertproblem der Stellardynamik," *Z. Astrophys.*, **30**, 213–229, 1952.

[8] R. Preisendorfer, "Functional Relations for the R and T Operators on Plane-parallel Media," these PROCEEDINGS, **44**, 000, 1958.

[9] B. Friedman, *Principles and Techniques of Applied Mathematics* (New York: John Wiley & Sons, 1956), chap. iii.

Ecology of Sulfate Reducing Bacteria

By Claude E. ZoBell*

Ecology of Sulphate Reducing Bacteria[1]

In the sense that they can assimilate sulfate as a source of sulfur essential for cell synthesis, most bacteria, yeasts, molds and algae as well as higher green plants reduce sulfate. It is incorporated in organic sulfur compounds constituting protoplasm, which upon decomposition may yield hydrogen sulfide. Only a specialized few bacterial species, however, reduce sulfate directly to hydrogen sulfide. It is to these specialized microorganisms that use sulfate primarily as an hydrogen acceptor that the term "sulfate reducer" is ordinarily applied. Hydrogen for the reaction may be supplied by organic compounds, such as lactate, for example:

$$2C_3H_5O_3Na + MgSO_4 \rightarrow H_2S + 2C_2H_3O_2Na + MgCO_3 + CO_2 + H_2O$$

or by molecular hydrogen for autotrophic varieties of sulfate reducers:

$$4H_2 + MgSO_4 \rightarrow H_2S + MgO + 3H_2O$$

The classical example of a sulfate-reducing bacterium is **Desulfovibrio desulfuricans Beijerinck** (1895). Although other species have been named and there may be other genera of sulfate reducers, neither their ~~tavomic~~ taxonomic position nor their importance in the sulfur cycle has been established. **Desulfovibrio aestuarii** van Delden (1904), **D. thermodesulfuricans** Elion (1924), **D. rubentschickii** Baars (1930), **D. hydrocarbonoclasticus** ZoBell (1947a), and **D. sulfurgenii** Subba Roa (1950) may all be physiological artifacts or adaptive variants of **D. desulfuricans. Vibrio halobicus desulfuricans,** described by Horowitz-Wlassowa and Sontag (1931) as a halophile found in salted anchovies, is probably a salt-tolerant **Desulfovibrio species.**

In many published reports on the occurrence, distribution, control, and activity of sulfate-reducing bacteria, the species have not been identified. Though tacitly assumed to be species of **Desulfovibrio** (previously termed **Spirillum, Microspira, Vibrio,** or **Sporovibrio**), the cultures may have consisted of or contained species of **Clostridium, Desulphoristella,** or possibly other genera. Technical difficulties in obtaining and maintaining pure cultures of sulfate-reducing bacteria, their variability, complex life cycles, plemorphism, adaptability, transmutability, physiological versatility, and ecological capriciousness, coupled with differences of opinions among various investigators regarding what constitutes a variety, strain, species, or genus, have complicated the taxonomic picture.

Sporogenous varieties, designated **Sporovibrio** by Starkey (1938), are claimed by Campbell, Frank, and Hall (1957) to be identical with **Clostridium nigrificans.** Cultures of **Cl. nigrificans** were found to produce from 191 to 244 mg H_2S per liter of medium from the reduction of sulfate in 48 hours at 55°C. The reduction of sulfate to H_2S by **Cl. caproicum, Cl. cauteretsensis,** and **Cl. flabelliferum** has been reported by Prevot (1949). According to Bromfield (1953), **Bacillus megatherium** reduces sulfate to H_2S, but it is not clear from his protocols whether the reduction is direct or indirect.

Desulphoristella hydrocarboniblastica, described by Hvid-Hansen (1951) as a new species belonging to the family Ristellaceae, is a short gram-negative rod which reduces sulfate to H_2S. It was found in H_2S-bearing waters in Denmark associated with **Desulfovibrio** species. The obligately barophilic sulfate reducer isolated from deep-sea sediments by ZoBell and Morita (1957a) is morphologically more akin to **Desulphoristella** than to **Desulfovibrio** species, but it differs from both in being unable to grow unless compressed to about 700 atm, it requires sea water for growth, and it is killed in a few minutes at 25° to 30°C. Neither pressure, salinity, nor temperature tolerance, however, is a sufficiently distinctive property of bacteria to delineate species.

Employing H_2S formation as the criterion for detecting the occurrence and activity of sulfate-reducing bacteria is another technical and taxonomic pitfall. A common source of error is H_2S from substances other than sulfate such as peptone, cystine, yeast extract, sulfite, thiosulfate, thioglycollate, and other sulfur compounds sometimes used in nutrient media (Fig. 1). On the other hand, Stokvis (1899), Saltet (1900), and more recently Oppenheimer (1957) have observed cultures which reduce sulfate only to sulfite; pure cultures produced no H_2S. This is not surprising in light of the observations of Ishimoto and Koyama (1953) which suggest that strains of **D. desulfuricans** have enzymes specific for the reduction of either sulfate, sulfite, or thiosulfate. A good many microbial species which are unable to use sulfate as an hydrogen acceptor reduce sulfite and thiosulfate to H_2S (Tanner, 1917, 1918).

Although Datta (1946), Subba Roa (1950), and others have described species which allegedly reduce sulfate to elemental sulfur without H_2S formation, the direct microbial formation of sulfur from sulfate has yet to be established. From present concepts of metabolic pathways of sulfate reducers (Postgate, 1957), more likely H_2S is oxidized to yield sulfur. There may be oxidizing components in certain systems or, if H_2S comes into contact with air, O_2 may serve as the hydrogen acceptor:

$$2H_2S + O_2 \rightarrow 2H_2O + 2S$$

In the vicinity of strains which reduce sulfate only to sulfite, elemental sulfur could be formed as follows from the oxidation of H_2S produced by other strains:

$$H_2SO_3 + 2H_2S \rightarrow 3H_2O + 3S$$

As a group sulfate reducers are ecologically versatile and capricious. Native habitats of constituent members embrace a wide range of salinity or osmotic pressure, temperature, hydrostatic pressure, pH, Eh, and other environmental conditions. Certain varieties occur in bog water at pH 4.2 with less than 100 ppm of dissolved salts; other varieties have been found growing in concentrated salt solutions and at ph 10.4 (Baas, Becking and Wood, 1955). Some are active at near 0°C; others grow at temperatures exceeding 100°C when compressed to 1000 atm. Though generally regarded as strict anaerobes which do best at redox

TABLE 1
SALT TOLERANCE OF SOME SULFATE-REDUCING BACTERIA FROM DIFFERENT HABITATS

Observer or reference	Habitat or material in which found	Salinity as NaCl in per cent
Chait (1924)	Russian salt limans	8 to 20
Baranik-Pikowsky (1927)	Russian salt limans	2 to 25
Saslowsky (1928)	Russian salt limans	up to 30
Rubentschick (1946)	Russian salt limans	5 to 30
Ginsberg-Karagitscheva (1933)	Oil field brines	up to 18
Horowitz-Wlassowa and Sontag (1931)	Salted Anchovies	up to 25
Hof (1935)	Salt works brines	up to 30
Iya and Sreenivasaya (1945)	Sulfur deposits	6 to 13
Kimata et al. (1955b)	Marine sediments	1.5 to 6
van Delden (1904)	Coastal marine muds	3 to 10
Baas Becking and Wood (1955)	Estuarine environments	up to 30

---

*Professor of Microbiology and Chairman Division of Marine Biology.

[1] Contribution from the Scripps Institution of Oceanography. University of California, New Series No. 1005

Paper prepared for presentation at symposium sponsored by the Biology Department. Saint Bonaventure University, October 23, 1957.

Reproduced by Permission

potential more reducing than Eh-100mv at pH 7, aerobic growth of certain varieties has been reported (Butlin et al., 1949; Sturm, 1950; Grossman and Post gate, 1953).

Salinity Requirements. — Sulfate-reducing bacteria found in most soil, sewage, and freshwater (river and lake) sediment samples are active in nutrient solutions hypotonic to or less saline than physiological saline (0.85 per cent NaCl) and are inhibited by from 1.5 to 3.0 per cent NaCl. Others commonly called **D. aestuarii**, found in brackish waters, sea water, and marine sediments, seem to require either sea water or mineral solutions made isotonic with sea water by the addition of NaCl.

Immediately following initial isolation from marine materials, cultures of **D. aestuarii** tolerate hypertonicity (with reference to sea water having a salinity of from 3 to 3.5 per cent) no better than they tolerate hypotonicity. They do not grow in nutrient medium having a salinity of 5 to 6 per cent. However, there are true halophiles which reduce sulfate in nutrient solutions containing from 6 to 30 percent salt (Table 1). Such salt-tolerant varieties occur in salt lakes, marine salterns, oil-well brines, salted foods, and salt flats.

Whether the halophilic, marine, and freshwater varieties represent strains which are interconvertible by acclimatization or adaptation is ~~intermediate~~ indeterminate. Baars (1930) claims to have adapted by gradual transitions the marine species **D. aestuarii** to a salt-free medium and, by successive transplantations to media of progressively increasing salinity, the freshwater species **D. desulfuricans** was adapted to grow in 3 per cent salt solutions. Neither Rittenberg (1941) nor others who have worked in my laboratory could duplicate Baars' results when starting with single-cell isolates, although with prolonged laboratory cultivation mutants developed, some of which were more salt tolerant and some were less salt tolerant than the parent culture. Cultivating these organisms in nutrient media hypertonic or hypotonic to solutions to which they were accustomed had a selective action, but failed to favor transmutation.

Results with acclimatized cultures, mutants, different species, or with mixed cultures may account for the rather wide variance observed in the salt tolerance of marine sulfate reducers reported by different workers. For example, van Delden (1904) reported that cultures isolated from coastal marine muds developed in nutrient media containing from 3 to 10 per cent salt. The sulfate reducers found in marine muds by Kimata et al. (1955b) were active only within the range of 1.5 to 6 per cent salt, 3 per cent salt providing for optimal conditions. Microbiologists working at the Scripps Institution of Oceanography have noted considerable difference in the salt tolerance of sulfate-reducing bacteria isolated from the sea at stations remote from possibilities of terrestrial or freshwater influence. Most of our recently isolated cultures exhibited maximum activity in media containing from 2 to 3.5 per cent salt. Very few of our marine cultures developed in nutrient media containing less than 1.5 per cent or more than 5.0 per cent salt. However, in marine salterns, Great Salt Lake, and certain oil-well brines we have found sulfate reducers which developed in the presence of from 20 to 30 per cent salt. In salt-saturated brines from Lake Eyre, Australia, Baas Becking and Kaplan (1956) found both autotrophic and heterotrophic sulfate reducers.

While working under the auspices of the American Petroleum Institute, the Pennsylvania Crude Oil Association, and certain oil companies, we have examined several hundred carefully collected samples of reservoir fluids, produced waters, and oil-well brines for the occurrence of bacteria. These oil-well waters or brines ranged in salinity from 1.2 to 28 per cent. Sulfate-reducing bacteria were detected in approximately half of the samples by inoculating 120 ml of nutrient medium with 1.0 ml of the produced water or brine sample. The media had the following composition per liter:

$MgSO_4 \cdot 7H_2O$	2.0 gm	NaCl	0.5 gm
K_2HPO_4	0.2 gm	Agar	3.0 gm
Mohr's salt	0.2 gm	Asparagine	0.2 gm
Ca lactate	3.5 gm	Ascorbic acid	0.1 gm

Media were prepared with three different kinds of water; viz., distilled, sea, and autogenous (or corresponding) produced water or oil-well brine itself. As a rule, but not invariably so, the most positive results were obtained in media prepared with produced water or brine (Table 2). This suggests that the bacteria were adapted to grow in the solution (produced water) in which found. There was no apparent relationship between either the occurrence or abundance of bacteria in produced waters and salinity. However, the lag phase was usually much longer in high salinity media. From two to six weeks' incubation at 28°C was commonly required for evidence of growth or activity of sulfate-reducing bacteria in media containing more than 6 per cent salt. The inoculated media were not discarded as negative until after at least 12 weeks' incubation.

Negative results were obtained in 209 out of a total of 396 samples of produced waters or brines in any medium tried. When media prepared with these produced waters showing no growth were inoculated with active cultures of sulfate-reducing bacteria pooled from freshwater medium, sea water medium and medium containing 15 per cent salt, growth occurred in 84 of the produced waters; no growth in 125. Here positive results indicate the absence of growth-inhibiting properties of produced water unless perchance such inhibitors were neutralized by sampling and media-making manipulations. Negative results show that certain produced or formation waters inhibit the growth of sulfate-reducing bacteria, which may be due to the presence of bacteriostatic minerals, phenols, or other substances. Certainly, though, salinity per se or osmotic pressure is not the determining factor.

TABLE 2

Number of samples produced water or oil-well brines out of a total of 396 examined in which 1.0-ml inocula carried sulfate-reducing bacteria which developed in nutrient media prepared with either distilled water, sea water, or with the produced water.

Growth of sulfate reducers in medium prepared with			
Distilled water	Sea water	Produced water	Total number
+	+	+	38
+	+	O	8
+	O	O	3
O	+	O	27
O	O	+	26
O	+	+	71
+	O	+	14
O	O	O	209
Totals 63	144	149	187

TABLE 3

H_2S produced in 18 hours at different pressures at 30°C by washed cell suspensions of an autotrophic strain of Desulfovibrio from the following reaction: $CaSO_4 + 4H_2 \rightarrow H_2S + CaO + 3H_2O$

Pressure in atmospheres	H_2S produced mg/L	Pressure-in atmospheres	H_2S produced mg/L
1	22	800	53
200	21	1000	79
400	27	1400	8
600	39	1800	3

Natural selection of salt tolerant strains is illustrated by the observations of Rubentschick and Goicherman (1936), who noted that the abundance and proportion of halophilic sulfate reducers in limans increased with the seasonal increase in salinity and vice versa. Freshening of certain limans during the rainy season resulted in a 10- to 1,000-fold increase in the population of sulfate reducers and a lowering of their mean salt optima. Between 1932 and 1934 when input of freshwater exceeded evaporation, the salt optima of sulfate reducers dropped from 5-8 per cent to 2-4 per cent NaCl. Such observations led Rubentschick (1946) to conclude that classification of bacteria according to salinity requirements is arbitrary, because their salt requirements appear to be a function of environmental conditions.

The salt tolerance of sulfate reducers is influenced by temperature, hydrogen-ion concentration, hydrostatic pressure, chemical composition of the medium, and by other environmental factors. Although sulfate reducers occur in salt lakes and brines and many cultures are able to grow slowly in nutrient media containing from 15 to 30 per cent NaCl, we have yet to find a halophilic strain whose optimum salinity exceeded 10 to 12 per cent.

Cells of **D. desulfuricans** are not freely permeable by either chloride or sulfate, according to Littlewood and Postgate (1957). Wet cells suspended in 3 per cent (w/v) NaCl solution did not dilute the salt solution. Dilution of 4 to 6 per cent NaCl was due to plasmolytic dehydration of the cells, not osmotic breakdown. Up to 15 per cent Na_2SO_4 solution was not diluted by intact cells.

Not much work has been done to determine the extent to which the dissolved mineral content of the milieu provides for favorable osmotic conditions or for specific inorganic ion requirements of halophilic bacteria (Flannery, 1956). Sulfate reducers recently isolated from marine materials grow better in nutrient media prepared with sea water than in ordinary media made isotonic with sea water by the addition of NaCl, but it has not been determined whether the beneficial effect of sea water is attributable to trace elements, to combination of minerals, or to accessory growth factors.

Certain groups of marine bacteria studied by Dianova and Voroshilova (1935) required NaCl, being unable to grow when either potassium, magnesium, or calcium was substituted for sodium in equimolar concentrations. Species of marine **Flavobacterium, Pseudomonas,** and **Spirillum** examined by MacLeod and Onofrey (1956, 1957) required sodium, potassium, magnesium, and ferrous iron as well as chloride. The magnesium requirements were dependent upon the calcium content of the medium. According to Baas Becking and Wood (1955), the ratio of monovalent to bivalent cations does not seem to be critical for sulfate reducers, nor does the relative concentrations of chloride, bicarbonate, and sulfate ion. At high salt concentrations sulfate reducers become sensitive to magnesium. Enrichment cultures of **D. aestuarii** were found by Updegraff and Wren (1952) to require potassium, magnesium, ferrous iron, and phosphate phosphorus. The essentiality of magnesium and ferrous iron for **Desulfovibrio** species has also been reported by Kimata et al. (1955). Butlin (1947) obtained no growth of sulfate reducers in nutrient medium rendered "biologically free" of iron; normal development occurred on addition of 0.002 per cent $FeSO_4 \cdot 7H_2O$.

Temperature Range of Growth—The growth and activity of sulfate-reducing bacteria has been observed throughout the range of 0° to 100°C. Mesophilic strains, which have received the most attention of investigators, grow best between 25° and 45°C. Obligate psychrophiles have not been reported, although certain cultures reproduce slowly and produce H_2S at refrigeration temperatures. Apparently the activities of such cultures are stopped by cold only when water is removed from solution by ice formation at temperatures dependent upon osmotic and hydrostatic pressures. The slow growth of marine bacteria at -3° to -11°C has been reported by ZoBell (1934).

Sulfate reducers which are active at refrigeration temperatures are hardly biological curiosities. A world-wide census would probably reveal the existence of more sulfate-reducing bacteria in nature at temperatures below 5°C than at higher temperatures. This estimate is based upon the fact that more than 80 per cent of the ocean floor, where sulfate reducers are commonly found in abundance, is colder than 5°C and the ocean floor covers more than two-thirds of the earth's surface.

Despite the low temperature of their native habitat, most of the sulfate reducers coming from cold climates grow better in the laboratory at 20°C to 30°C than at lower temperatures. Warming deep-sea sediment samples to 30° or 40°C for ten minutes kills many sulfate-reducing bacteria, but such bacteria in shallow marine sediments tolerate somewhat higher temperatures. Cultures isolated by Kimata et al. (1955b) grew well over the range of 20° to 40°C, but failed to grow at 15° or at 45°C.

The maximum temperature at which Rittenberg (1941) was able to get marine sulfate-reducing bacteria to grow was between 40° and 45°C. Reducing the salinity of the medium decreased the maximum temperature at which the marine cultures would grow. Diluting sea water medium 1:1 with distilled water reduced the maximum temperature at which sulfate reducers would grow to between 35° and 40°C, and to between 30° and 35°C for a 1:4 dilution. All attempts to acclimatize the marine cultures to grow at higher temperatures were unsuccessful.

From ditch mud Elion (1924) isolated a thermophilic culture which rapidly reduced sulfate to sulfide at 55°C. To this organism he applied the species name **thermodesulfuricans.** Although in its native habitat in ditch mud it had probably never been subjected to a temperature higher than 25°C, it grew throughout the range of 25° to 65°C; optimally at 55°C. From such observations plus getting sub-cultures to reduce sulfate as rapidly at 25 to 30°C as at 55°C Baars (1930) concluded that Elion's **thermodesulfuricans** was an adaptive variety of Beijerinck's mesophilic **D. desulfuricans.** However, since Baars did not start with single cell isolations, he may have merely selectively produced enrichment cultures having different temperature optima from the parent culture which seems to have contained both mesophilic and thermophilic strains, if not species.

Upon demonstrating the growth of sulfate reducers at 30°, 35°, 40°, 45°, 50° and 55°C in nutrient media inoculated with portions of the same soil samples and finding no pure culture capable of growing at all of these temperatures without acclimatization or adaptation, Butlin et al. (1949) concluded that the soil contained different strains of **Desulfovibrio.** Iya and Sreenivisaya (1945) studied a culture of **D. desulfuricans** from soil which produced H_2S at 30°C but not at 37°C. Some cells from this culture survived for ten minutes at 55°C, for five minutes at 60°C, and for one minute at 70°C. All cells of this culture were killed in ten minutes at 60°C, in five minutes at 70°C, and in one minute at 80°C.

In oil-well waters ranging in temperature from 44° to 47°C at the surface, Gahl and Anderson (1928) found sulfate-reducing bacteria, described as **Desulfovibrio** species, which were active at temperatures ranging from 28° to 50°C. None was active at 60°C. Both gram-negative (probably **D. thermodesulfuricans**) and gram-positive (probably **Clostridium** species) were found at temperatures up to 58°C in geothermal regions of New Zealand by Kaplan (1956).

In cores from oil and sulfur wells, produced waters, and drilling muds we have occasionally encountered thermophilic sulfate reducers some of which developed at temperatures ranging from 65° to 85°C. These samples came from depths of 6,000 to 12,000 feet where the in situ temperature was 60° to 105°C and the hydrostatic pressure 200 to 400 atm. The maximum temperature at which the thermophilic cultures are active is increased by compression. At 1,000 atm one culture reproduced and produced H_2S at 104°C. No attempt has been made to ascertain whether bacteria will grow at temperatures higher than 104°C when compressed, but indications are highly suggestive of the possibilities in view of the protective effect of high pressure on the thermal tolerance of bacteria (ZoBell and Johnson, 1949; Johnson, 1957).

Hydrostatic Pressure—Except for minor anomalies, the hydrostatic pressure in the water-containing crust of the earth, as ~~is~~ the sea, increases with depth by approximately 0.1 atm per meter or about ½ psi per foot. This appears to be an ecological factor of importance in the sea where pressures exceeding 1000 atm occur and perhaps even more important in oil-bearing formations in the earth's crust where temperature increases with depth by approximately 0.01°F per foot or 0.02°C per meter. Thus at a depth of 12,000 feet the bottom-hole temperature of an oil well in the Gulf Coast area may be around 100°C and the hydrostatic pressure about 6000 psi or 400 atm.

When compressed to 400 atm in nutrient medium, none of the bacteria commonly found at shallow depths in soil, sediments, sewage, or water grew normally. The growth of many was inhibited at 300 atm or at even lower pressures. Some were killed by being held for a few days at 600 atm at 30°C. These generalizations are based upon observations on more than a hundred different species, including some cultures of **Desulfovibrio.** No culture, however, was sterilized by being subjected for a few minutes to pressures up to 1000 atm. In fact, some cultures have survived being compressed to 1000 atm followed by decompression ten successive times within ten minutes without affecting their viability in nutrient media. In the presence of appreciable quantities of dissolved gases, however, sudden decompression is an effective way of rupturing cell walls of microbes.

When held for a few days at high pressures most common bacteria slowly perish in nutrient medium incubated at their normal optimum temperature. Their pressure tolerance is generally greater when held at temperatures from 5° to 20°C higher than their normal optimum at 1 atm. As pointed out by Johnson et al. (1954), appreciably higher temperatures are required to kill living cells or to inactivate various biological systems at elevated pressures. Just as we find differences in the temperature optima and tolerance of different species, strains, or ecotypes of bacteria, similar differences have been observed in the pressure tolerance of bacteria from different environments.

In contrast with the bacteria of soil, sewage, and shallow water which generally fail to grow when compressed to 400 or 600 atm, deep-sea deposits are inhabited by many bacteria which grow in nutrient media only when compressed to 700 to 1000 atm. Such pressure-requiring or barophilic bacteria, including some sulfate reducers, have been demonstrated in a large number of sediment samples collected from depths of 7,000 to 10,000 meters (ZoBell and Morita, 1957a, b).

A few cultures of barophilic sulfate reducers have been recovered from sulfur and oil wells at depths exceeding 3,000 meters or 9,000 feet. All of these barophiles were thermophilic, growing preferentially or exclusively at 55°C or higher. However, the majority of the bacteria found in oil-well cores and reservoir fluids were neither barophilic nor thermophilic, although many tolerate pressures to 600 atm and temperatures to 85°C. In most cases it could not be determined whether they were species indigenous to the oil-bearing formations or if they were adventitiously introduced during drilling or sampling operations, by the movement of ground water, by migration, or otherwise. Finding obligate thermophiles and barophiles at great depths in samples of reservoir fluids and oil-well cores is highly suggestive but not conclusive evidence of indigenity.

Certain physiological processes besides growth, reproduction, and death are affected by pressure. A clear-cut example is hydrogen utilization by an autotrophic sulfate reducer. As shown by the data summarized in Table 3, washed cells of a **Desulfovibrio** species grown at 1 atm oxidized hydrogen, reduced sulfate, and produced H_2S from 3 to 4 times faster at 1000 atm than at 1 or 300 atm. At between 1400 and 1800 atm, these reactions were stopped, presumably due to the irreversible inactivation of the catalyzing enzyme system. Pressure affected differently the reaction rates and enzyme systems of strains from different depths.

Besides being influenced by temperature, the effect of pressure on biological systems is also a function of the chemical composition of the medium, its osmotic pressure, its redox potential, and its pH. Additional information on pressure as an ecological factor is outlined by Johnson (1957).

Eh/pH Relationships—The reaction of marine bottom deposits in which sulfate reducers occur ranges from pH 6.4 to 9.5; the Eh ranges from +350 to —500 mv (ZoBell, 1946a). Soil, swamps, sewage, and nearly all other natural habitats of such bacteria have reactions within the extreme ranges of pH 4.2 and 10.4.

Cultures of **D. desulfuricans** examined by Starkey and Wight (1945) grew over the range of pH 5.5 to 8.5; best near pH 7. Their cultures failed to grow below pH 5 or above pH 9. After noting that sulfate reducers are not active below pH 5 or above pH 9.5, Bunker (1942) proposed controlling iron corrosion caused by them by employing fill material more alkaline than pH 10. In investigating caustic-treated drilling mud as a means of moderating oil-well casing corrosion, Snedden (1951) found no evidence of sulfate reducers in mud of pH 9.5 or higher. Similarly Hunter et al. (1948) reported that a reaction about pH 9 inhibited sulfate reducers in drilling muds. Acidifying the water of an ammonia-synthesizing plant to pH 4.3 with H_2SO_4 prevented the production of H_2S by sulfate reducer (Katagiri et al., 1947).

As pointed out by Baas Becking and Wood (1955) and elaborated by Bass Becking and Kaplan (1956a), the pH tolerance of sulfate-reducing bacteria both in their natural habitats and in enrichment or purified cultures under controlled laboratory conditions is affected by the Eh or redox potential of the environment, the chemical composition of the medium, and by other factors. In milieu more reducing than Eh -150 mv sulfate reducers were found to be active up to pH 9.5; in milieu as acidic as pH 4.2 at Eh 0. Most of their cultures, however, grew best between pH 6.2 and 7.9 and at Eh -50 to -150 mv.

The optimum Eh for the initiation of growth of sulfate reducers has not been established owing to technical difficulties in measuring this property of milieu and because it is difficult to maintain the redox potential of milieu at a fixed value. When large inocula are used, reducing materials such as H_2S may be introduced into culture medium in quantities sufficient to affect the Eh, particularly in microspheres or micoenvironments within the medium. Not infrequently raw or enrichment cultures may carry aerobic bacteria which create reducing conditions. In our laboratory small inocula and single cells of **Desulfovibrio** species isolated with micropipettes have developed in nutrient medium only when the initial Eh was 0 to -100 mv or more reducing. Other workers, however, have reported the growth of sulfate reducers in nutrient media having positive Eh values and, indeed, the aerobic reduction of sulfate has been reported (Sturm, 1950). According to Grossman and Postgate (1953), growth under aerobic conditions is possible only in the presence of reducing agents such as ascorbic acid, sodium sulfide, glutathione, or cysteine or when a large inoculum is used so that conditions in the immediate vicinity of growing cells are anaerobic. Butlin et al. (1949) recorded the growth of "pure strains aerobically in shallow (1 cm) layers of medium to which 0.025 per cent ascorbic acid had been added. Sulfate reducers in most soils are active in nutrient medium even if no anaerobic precautions are taken, presumably because the aerobic organisms also present deoxygenate the medium. Nevertheless, growth is much better when oxygen is rigorously excluded."

Although found most commonly and abundantly in black reducing muds, muck, sediments, soil, swamps, and sewage having redox potentials ranging from Eh -100 to -350 mv., sulfate reducers also occur in soil and marine bottom deposits having apparent redox potentials of Eh +50 to +350 mv. Whether such sulfate reducers are actually active in oxidizing environments, active only in more reducing microspheres therein, or merely passively present is indeterminate. The redox potential of the culture media used by Starkey and Wight (1945) for the cultivation of **D. desulfuricans** was initially 300 to 400 mv and dropped to —200 to —300 mv during the growth of the bacteria. Sulfate reducers generally lower the redox potential of the milieu, primarily by the formation of H_2S.

Theoretically the reduction of sulfate either to sulfite, elemental sulfur, or to sulfide results in an increase in pH of the medium. Whether sulfate-reducing bacteria affect the reaction of the medium in which they are growing depends in part upon the buffer capacity of the milieu and partly upon concurrent oxidation-reduction processes and end products. Autotrophic strains, which oxidize molecular hydrogen while reducing both sulfate and carbon dioxide or bicarbonate, have been observed to change the reaction of poorly buffered medium from an initial pH 7.5 to pH 8.5 or slightly higher. The reduction of sulfate by an autotroph in a mineral salts steel wool medium resulted in an increase of pH from 8.1 to 8.5 (Bass Becking and Wood, 1955).

Heterotrophic sulfate reducers have a variable effect upon pH, depending upon the kind and concentration of organic matter in the medium, its buffer capacity, period of incubation, and other factors. In one series of experiments, for example, Rittenberg (1941) found the final reaction of unbuffered lactate media to be pH 6.8 to 6.9 as a result of the activity of sulfate reducers for 35 days in media having initial reactions of pH 6.0, 7.0, and 7.8 respectively.

The growth of sulfate-reducing bacteria in sewage was found by Allen (1949) to be favored by neutral or slightly alkaline conditions and retarded by acidic conditions. Addition to sewage of nitrobenzene, dinitrobenzene, picric acid, or trinitrotoluol in amounts to give from 2 to 200 ppm retarded H_2S formation, ostensibly because these nitro-compounds kept the redox potential of the sewage at levels too high for the development of sulfate-reducers.

Energy Sources—The activities, abundance, and kinds of sulfate-reducing bacteria occurring in nature must be affected by the availability of substances that they can oxidize as energy sources. Although different strains or species utilize different substances, as a class sulfate reducers utilize a large variety of organic compounds, including lactate, malate, citrate, pyruvate, tartrate, fatty acids ranging from formic to stearic, amino acids, peptone, simple alcohols above methyl, monosaccharides, certain disaccharides, and a good many other organic substances. Evidence for the direct assimilation of cellulose, starch, and other complex carbohydrates is lacking, but associated organisms in soil or sediments attack such substances with the formation of metabolites that can be used by sulfate reducers (Rubentschick, 1928). A lack or low concentration of utilizable carbon compounds limits the abundance and activity of sulfate reducers in many environments.

The utilization of petroleum hydrocarbons by sulfate-reducing bacteria has been reported by Tausson and Aleshina (1932), Tausson and Vesselov (1934), Maliyantz (1935), Novelli and ZoBell (1944), ZoBell (1946b), and by Rosenfeld (1947). On the other hand, Baars (1930) was unable to demonstrate the utilization of either crude oil or paraffin oil by his cultures. Jones (1955) noted the slow formation of H_2S by certain sulfate reducers growing in sulfate medium enriched with crude oil, but he questioned whether these organisms utilized hydrocarbons or some other constituent, such as fatty acids. Beck (1947a) questioned whether **Desulfovibrio** species could attack pure hydrocarbons, but his cultures grew in oil-bearing sands from Pennsylvania oil fields without additional nutrients. It is my present belief that a good many crude oils support the growth and activity of certain sulfate-reducing bacteria, provided the oil is dispersed throughout appropriate mineral salts solutions. Even under optimum conditions sulfate reducers develop very slowly owing to the low solubility of oil in water. Whether pure hydrocarbons are attacked by sulfate reducers seems questionable in the light of recent observations.

Evidence for the oxidation of molecular hydrogen by sulfate-reducing bacteria has been reviewed by ZoBell (1947b), Sisler and ZoBell (1950), Postgate (1951), and by Senez (1955). Hydrogen for the reaction in nature may come from the fermentation of organic compounds, from the reaction of water on iron as around iron pipes or other structures buried in soil or submerged in water, and to a lesser extent from other reactions. Hydrogen is a minor constituent of natural gases if it occurs at all. Its absence or low concentration may be a reflection upon the facility with which hydrogen is oxidized by bacteria. The rather common occurrence of autotrophic sulfate reducers in soil and marine sediments suggests the availability of hydrogen in such environments.

Hydrogen Acceptors—Sulfate is usually in adequate supply in sea water and in most marine sediments and oil-field waters to provide for the growth of sulfate-reducing bacteria which use sulfate as an hydrogen acceptor. Analyses of profile sections of recent marine sediments indicate that the total sulfate content or the ratio of sulfate to chloride decreases with age or core depth, thereby suggesting that sulfate reducers have been active. A similar decrease in the sulfate:chloride ratio with increasing geological age has also been observed in a good many oil-field waters, some of which now contain little or no sulfate. The gradual disappearance of anhydrite and gypsum with increasing abundance of sulfur and limestone in the vicinity of sulfur deposits around salt domes may be another manifestation of the activities of sulfate-reducing bacteria. The fractionation of stable istopes of sulfur by sulfate reducers coupled with the S^{32}/S^{34} ratios found in samples of natural sulfur from salt domes supports the theory that such sulfur has resulted from the bacterial reduction of sulfate (Jones and Starkey, 1957).

In soil, freshwater sediments, sewage, and other materials a lack or depletion of sulfate not infrequently limits the abundance and activities of sulfate-reducing bacteria. For example, in the Takana Estuary in Maizuru Bay, Japan, Kimata et al. (1957) found that the production of sulfides in bottom mud by sulfate reducers was influenced by both the sulfate and organic content of the mud or overlying water. In the freshwater zone where the sulfate content of bottom water was very small, sulfide production was restricted by the availability of sulfate, whereas in the sea water zone where sulfate was sufficient the production of sulfides in mud was controlled primarily by the availability of utilizable organic matter. Sulfate reducers and sulfides were most abundant in the intermediate brackish water zone where both sulfate and organic matter were in good supply. According to Postgate (1951b), 100 mg sulfate per liter provides for the optimal growth of **D. desulfuricans.** We find, however, that the rate of H_2S production by either proliferating or "resting" cells is not retarded until the sulfate content is less than 10 mg/L. In certain freshwater lakes the rate of H_2S production by sulfate reducers is a linear function dependent on the concentration of sulfate. The concentration ranges from nil to 100 mg/L. The mean sulfate content of most freshwater lakes is less than 5 mg/L, although certain salt lakes and brines contain up to 60 gmL. The sulfate content of normal sea water is 2.65 gm/L.

The use of sulfite ($SO_3^{=}$), thiosulfate ($S_2O_3^{=}$), and dithionate or hydrosulfite ($S_2O_4^{=}$) as hydrogen acceptors by certain **Desulfovibrio** strains was demonstrated by Baars (1930). These substances as well as tetrathionate ($S_4O_6^{=}$), perdisulfate ($S_2O_8^{=}$), and metabisulfite ($S_2O_5^{=}$) were used as hydrogen acceptors by **D. desulfuricans,** strain 'Hildenborough' (Postgate, 1951b). The ability of sulfate-reducing bacteria to grow and produce H_2S in the absence of sulfate is of significance in considering their ecology to the extent that other hydrogen acceptors occur in nature or can be used to demonstrate the presence of sulfate reducers. It is reiterated, though, that a good many microbes besides sulfate reducers produce H_2S from sulfite, thiosulfate, tetrathionate, etc. Being readily oxidized or reduced biologically or otherwise, these oxides of sulfur intermediate between sulfate and elemental sulfur probably occur only ephemorally in the biosphere, but conceivably they could provide for the growth of sulfate reducers in certain localized environments.

Because of its more common occurrence in the biosphere, elemental sulfur may play an important role in affecting the ecology of sulfate reducers if they can use it as an hydrogen acceptor. Some do, according to Baars (1930). However, in the hands of Postgate (1951b) neither the 'Hildenborough' strain nor any of the five other strains of **D. desulfuricans** grew in media containing pure elemental sulfur as the only hydrogen acceptor, but colloidal sulfur provided for slow hydrogen absorption by resting cell suspensions of autotrophic strains.

Carbon dioxide or bicarbonate ion is used as an hydrogen acceptor by actively growing cultures of autotrophic sulfate reducers. During three weeks' incubation in purely inorganic media cultures of autotrophs consumed much more molecular hydrogen than could be accounted for either by the amount of sulphate reduced or the amount of H_2S formed (Sisler and ZoBell, 1951a). Carbon balance determinations showed that these cultures reduced from 0.8 to 6.4 ml of CO_2 per 100 ml of medium:

$$CO_2 + 2H_2 \rightarrow (CH_2O) + H_2O$$

The reduction product of the reaction symbolized as (CH_20) occurred primarily as bacterial protoplasm. Washed cell suspension (so-called "resting" cells) of **Desulfovibrio** consumed hydrogen more rapidly in the presence of sulfite or thiosulfate than of sulfate. No measurable amount of CO_2 was reduced by "resting" cells during 9 days at 28°C. Fumarate was rapidly reduced and hydrogen consumed by "resting" cells. Suspensions of this strain were found by Grossman and Postgate (1955) to reduce fumarate quantitatively in the presence of H_2; malate was reduced slowly.

The utilization of fumarate and malate as hydrogen acceptors and the growth of several strains of **Desulfovi-**

brio in sulfate-free media containing pyruvate as the only hydrogen acceptor, reported by Postgate (1952), raises the question as to whether these or similar organic compounds can provide for the growth of sulfate reducers in nature without involving either sulfate or H_2S.

Neither ethylsulfone, butylsulfone, ethylsulfoxide, ethanesulfonate, benzenesulfonate, toluenesulfonate, peptone, nitrate, nor phosphate was used as hydrogen acceptors for the growth of sulfate reducers studied by Rittenberg (1941). The moderate amount of growth occurring in peptone medium was shown to be proportional to the amount of sulfate present as an impurity.

Nitrate reduction by enrichment cultures of sulfate reducers, which probably contained bacteria besides **D. desulfuricans**, has been reported by Beckwith and Moser (1932) and by Baumann and Denk (1950). Whether nitrate could provide for the growth of these cultures in the absence of sulfate was not determined.

Washed cell suspensions of an autotrophic strain of **D. desulfuricans** were found by Senez et al. (1956) to reduce both nitrate and hydroxylamine to ammonia in the presence of H_2. From a brackish water pond in Messina, Genovese et al. (1957) isolated a strain of **D. desulfuricans**, resting cells of which reduced sulfite and hydroxylamine more actively than sulfate in the presence of H_2. Thiosulfate was not reduced by this strain and nitrite was reduced only slowly.

Nitrogen Requirements — Beijerinck (1895) and van Delden (1904) added from 0.1 to 0.25 per cent of either asparagin or peptone to nutrient media to satisfy the nitrogen requirements of enrichment cultures. Rank (1907) showed that ammonium sulfate was a better nitrogen source and moreover the elimination of peptone and asparagin minimized the occurrence of contaminating organisms in enrichment cultures. Most modern-day media specify from 0.02 to 0.1 per cent of either ammonium chloride or ammonium sulfate to provide for the optimum growth of **Desulfovibrio** cultures. Some strains can obtain adequate nitrogen from certain amino acids for slow growth. Complex proteinaceous compounds supply neither available nitrogen nor energy for these bacteria, which is a reflection upon a general lack of proteolytic enzymes.

Neither nitrate nor nitrite is utilized as a nitrogen source by **Desulfovibrio** species. Negative results have also been obtained with urea. From 20 to 200 mcg/L ammonium-nitrogen is adequate for the optimum growth of sulfate reducers. They will grow and reduce sulfate in an otherwise complete medium until the ammonium content has been deleted to less than 0.2 mcg/L.

There is no evidence that a lack of available nitrogen in soil, in marine sediments, in reservoir fluids, or elsewhere in nature is a factor which limits the occurrence, growth, or activity of sulfate reducers.

Nitrogen fixation by autotrophic cultures was demonstrated by Sisler and ZoBell (1951b).

Effect of Sulfide Concentration — Is the abundance or activity of sulfate-reducing bacteria in nature or in the laboratory limited by the accumulation of H_2S? The toxicity of H_2S for a good many forms of life, including many species of microbes and enzyme systems, poses this question.

In media containing sufficient sulfate and lactate to provide for the formation of at least 2,000 mg of H_2S per liter, Baars (1930) found the maximum concentrations produced were 566 mg/L by **D. thermodesulfuricans**, 794 mg/L by **D. desulfuricans**, and 1448 mg/L by **D. aestuarii**. In Rittenberg's (1941) experiments, cultures of **D. aestuarii** produced H_2S in maximum concentrations ranging from 740 to 1140 mg/L, the maxima being influenced by temperature and salinity of the medium. By increasing the amount of lactate and sulfate in the medium, Miller (1949, 1950) increased the maximum yield of H_2S produced by sulfate reducers to 1750 to 2600 mg/L for different cultures. In media treated with cadmium carbonate to combine with H_2S as formed, concentrations equivalent to 3300 mg/L were produced. Up to 3120 mg sulfide/L was produced by the 'Hildenborough' strain of **D. desulfuricans** in sulfate medium enriched with yeast extract and Bacto-tryptone (Butlin and Postgate, 1953).

Experimental results summarized in the preceding paragraph tell us something about how much H_2S may be produced by sulfate-reducing bacteria, but they fail to delineate the tolerance of such bacteria for H_2S, because in the media sulfide may occur partly as H_2S, sulfide ions, or largely as insoluble sulfides. Regardless of the amount produced, the concentration of H_2S present will be influenced by the pH and chemical composition of the medium, temperature, pressure, and other factors.

In the Black Sea, where sulfate reducers were first demonstrated by Zelinski (1893), the concentration of H_2S ranges from 1.1 mg/L at a depth of about 200 meters (Kriss and Rukina, 1949) to nearly 10 mg/L at 2000 meters (Kriss, 1949). Such concentrations of H_2S make deep waters of the Black Sea inhospitable to virtually all other forms of life except sulfate-reducing bacteria, the abundance and activities of which are probably limited by the H_2S. Cultures of sulfate reducers isolated from the Black Sea, some from depths as great as 2,118 meters, produced from 300 to 500 mg H_2S/L in laboratory media, but not as free H_2S.

Oil-field or formation waters, in which sulfate-reducing bacteria may have been active, have been reported by Ginter (1934) to contain H_2S in concentrations up to 2400 mg/L, probably as total sulfides rather than as free H_2S.

Habitats of Sulfate Reducers — From what has been recorded in the preceding paragraphs regarding the ecological factors affecting the growth and survival of sulfate-reducing bacteria, it should be evident that they are widespread in occurrence. Besides participating in the sulfur cycle in both salt and freshwater environments and in all soils generally, sulfate reducers may have contributed to the formation of sulfur deposits and certain metallic sulfides. They may have played a part in the origin of oil by affecting environmental conditions, including redox potential, pH, H_2, H_2S, sulfate, organic matter content, etc., in source sediments of petroleum. Their activities may have influenced the permeability of sediments or the movements of reservoir fluids therein. They may have produced some hydrocarbons (ZoBell, 1952) as part of their cell substance or protoplasm.

Although present, sulfate-reducing bacteria are generally much less abundant in freshwater environments than in marine materials which are richer in sulfate. In sea water the growth, activity, and abundance of sulfate reducers are limited primarily by available organic matter and the high oxygen tension; not by lack of sulfate. Except in localized areas as in blooming diatom fields, in the vicinity of sewage outfalls, or on the sea floor, the organic carbon content of sea water is rarely more than 5 mgm/L and the oxygen tension is usually more than 5 mgm/L. In places where conditions are anaerobic, as in stagnant water basins or where the oxidation of exceptionally large amounts of organic matter has depleted oxygen, sulfate reducers dominate the scene, producing sufficient H_2S to extend reducing conditions. Highly reducing conditions occur below the euphotic zone in the Black Sea (Issatchenko, 1924, 1929; Kriss, 1949), in the Caspian Sea (Butkevich, 1938), and in many fjords and deep ocean basins. Copenhagen (1934) described an area covering a few thousand square miles in the Atlantic Ocean off Walvis Bay, Africa, where at times sulfate reducers produce H_2S in concentrations that become lethal to flora and fauna almost to the water's surface.

The discoloration of painted fishing craft and houses by H_2S produced in the Bay of Callao and other harbors along the Peruvian Coast is described by Mears (1943) as the "Callao Painter," presumably due to the activities of sulfate-reducing bacteria in organic-rich waters during certain seasons. Similarly the "stinking putrefaction" during summer months in the Little Kiel, Germany, was attributed by Baier (1935) primarily to H_2S produced by sulfate reducers. In organic polluted bays sulfate-reducing bacteria often gain the ascendancy. H_2S, which they produce, removes dissolved oxygen thus creating anaerobic conditions favorable for their growth in an expanding area. The growth of aerobic organisms is inhibited or certain organisms may be killed by H_2S, thus leaving more organic matter to feed sulfate reducers, which then produce more H_2S. The expansion of this vicious cycle in all dimensions is limited primarily by the lack of organic matter, the depletion of sulfate, and by the introduction of oxygen by water movements and/or by the activities of photosynthetic organisms.

Large numbers of sulfate reducers were found by Bavendamm (1932) in nearly all samples of calcareous mud from the Bahama Banks. Such bacteria were common inhabitants of deep-sea bottom deposits off the Russian coasts examined by Ginsburg-Karagitscheva and Rodionova (1935). In marine bottom deposits off the coast of California, ZoBell (1938) demonstrated thousands of sulfate reducers per gram (wet weight) in certain samples. In nearly half of the 450 2- to 3-gram samples (wet weight) from 160 stations off the California coast, Rittenburg (1941) detected viable sulfate reducers. Their abundance decreased with core depth and with decreasing organic content of the sediment samples. From the northwestern part of the Pacific Ocean, Limberg-Ruban (1952) collected a good many mud samples from depths to 3500 meters containing sulfate-reducing bacteria. Their occurrence is not limited by water depth nor by the resultant hydrostatic pressure, because ZoBell and Morita (1957a, b) found sulfate reducers in deep-sea deposits at depths from 7,000 to 10,000 meters. Though sparse in numbers, sulfate reducers were present in a good many of the 236 samples of red clay and globigerina oozes collected by Morita and ZoBell (1955) on the Mid-Pacific Expedition, some at the bottom of cores from 400 to 750 cm in length.

Though sporadic in abundance, the general trend is for the numbers of sulfate-reducing bacteria, the concentration of sulfate, and the organic carbon content of long cores of marine sediments to decrease with core depth or geological age (Morita, 1954). The sulfide and carbonate content generally increase with core depth. Sulfate reducers in such sediments are believed to get their energy from the oxidation of either organic matter or molecular hydrogen. Sisler and ZoBell (1950) detected heretotrophic sulfate reducers in 187 out of a total of 245 sediment samples collected from various parts of the Antarctic, Arctic, Atlantic, and Pacific Oceans, employing 1-gram (wet weight) inocula. In some samples 1:100 and 1:1,000 dilutions yielded positive results, indicating the presence of at least 100 to 1,000 sulfate reducers per gram of sediment. Hydrogen-consuming autotrophs were demonstrated in 108 of the 245 samples analyzed.

In water samples from Hiroshima Bay, Kimata et al. (1955a) found from 0 to 10^4 sulfate reducers per ml of sea water and from 0 to 10^6 per gram of mud. A direct correlation was observed between the population of sulfate reducers and the sulfide and organic content of the mud samples. Marine sands and muds examined by Perkins (1957) were blackened by sulfides below depths of from 1 to 10 cm beneath the mud-water interface, the black boundary layer being closer to the surface during summer months when there was more organic matter for sulfate-reducing bacteria and deeper during the winter months.

In sulfur-bearing soils of India, Iya and Sreenivasaya (1945) noted the presence of sulfate reducers which were believed to contribute to the formation of sulfur. Supporting evidence for the bacterial origin of certain commercial sulfur deposits is given by Jones (1955) and Jones and Starkey (1957). Miller (1949a) tells of finding sulfate-reducing bacteria in drill cores from sulfur-producing salt domes in Texas from depths of 700 to 900 feet.

The occurrance of sulfate reducers in medicinal or sulfurous muds has been reported by Tausson et al. (1933) and by Salimovskaja-Rodina and Neschaeva (1940). Sturm (1937) detected them in sulfur-bearing rocks. Among the many workers who have found sulfate reducers in natural mineral waters are Goslings (1904), Rank (1907), Kupsis (1928), Richard (1946), and Embil (1956). Edington (1938) found them in drainage waters from lead mines.

Cultures of hydrogen-consuming **Desulfovibrio** were obtained from artesian well water in Tunis by Berkalof and Cabasso (1940) and by Menard and Berkalof (1940), but whether the bacteria occurred in the aquifer prior to the pipes' being placed there is problematical. This qualifying clause applies wherever man may have modified or contaminated the environment, including water, oil, and sulfur wells.

In his critique on the occurrence of sulfate reducers in deep Danish well waters, Hvid-Hansen (1951) points out that some of the wells in which appreciable numbers of such bacteria were demonstrated by rigorous sampling procedures had been producing water for 15 or more years. During this period any originally introduced inocula would have been washed away. The presence of H_2S in the ground water, its low content of sulfate, the high percentage of bicarbonate, and other properties of the water strongly suggest that bacteria had been reproducing and physiologically active in situ.

From the side walls of well shafts dug in sands and intercalated clay layers in North Holland, von Wolzogen Kuhr (1922) recovered sulfate-reducing bacteria from depths of 10 to 37 meters. Later he (1938) reported finding such bacteria to a depth of 71 meters. In post-glacial sediments Baier (1938) demonstrated the presence of sulfate reducers to a depth of 11.8 meters. Their abundance, the concentration of sulfate, and the organic content of the sediment samples decreased and the carbonate content increased with depth, which indicated activity of the bacteria. **Desulfovibrio** species, which they found in most sediment samples from soda lakes in West Siberia, were believed by Gubin and Tzeohomskaya (1930) to be responsible for the reduction of sulfate with the concurrent formation of sulfide and the oxidation of organic matter to carbonates.

Sulfate reducers are commonly present in anaerobic soils surrounding buried iron or steel structures (von Wolzogen Kuhr and van der Vlugt, 1934; Bunker, 1936; Hadley, 1940; Starkey and Wight, 1945; Butlin, 1948). They are also present and frequently harmful in sewage sludge or treatment plants (Agar, 1935; Allen, 1949; Barr and Buchanan, 1912; Beckwith and Moser, 1932; Butlin et al., 1956; Heukelekian, 1948). The control of sulfate-reducing bacteria has also been a problem in slow sand filter beds (Dey and Ganapati, 1934), trickling gas coolers (Kegel, 1940), Baier, 1942), cable storage tanks and gas holders (Rogers, 1945), ceramic slurries (Johnson et al., 1949), washing plant in a flour mill (Barton-Wright, 1945), water in a synthetic ammonia plant (Katagiri et al. 1947), and in oil-well drilling muds (Cannon, 1939; Hunter et al., 1948; Menaul and Dunn, 1956; Sneddon, 1951). The occurrence and control of sulfate reducers in oil-well flood or input waters have received the attention of Allred (1954), Anderson (1956), Beck (1947b), Hitzman et al., (1957), Morris (1943), Plummer and Walling (1946), Sloat et al., (1957), Williams (1953), and many other workers.

Sulfate Reducers in Oil-bearing Formations—The occurrence of sulfate-reducing bacteria in oil-well or formation waters and reservoir fluids as well as in cores from oil wells has been reported by several investigators. From finding such bacteria in produced waters or brines from 43 different oil wells in California and Illinois ranging in depth from 400 to 1,866 feet, Bastin (1926) concluded that the bacteria were probably responsible for reduction of sulfate to sulfide. Similar conclusions were reached by Gahl and Anderson (1928), who found sulfate reducers in 17 out of 40 California oil-well waters, some from depths as great as 3,090 feet. Bastin and Greer (1930) noted a direct correlation between the occurrence of sulfate reducers and the sulfide content of water from producing oil wells in Illinois fields. Ginter (1930, 1934) noted that many oil-well brines having a high content of carbonate and sulfide had a correspondingly low content of sulfate, which he attributed to the reduction of sulfate to sulfide by bacteria which oxidize organic matter to carbon dioxide.

Ginsburg-Karagitscheva (1933) reported the occurrence of sulfate reducers in produced waters from several oil wells. Such bacteria were found in 14 out of 15 samples of oil sands from the Grozny oil field. The bacteria were believed to be indigenous to the petroleum formation and responsible for the low sulfate content, the presence of sulfide, and the modification of the associated oil.

Employing Bastin's methods and media, Young (1936) reported finding sulfate-reducing bacteria in produced water from shallow oil wells in Alberta fields. Sulfide in these oil-field waters was attributed to the activity of the sulfate reducers, which were said to utilize napthenic acids as a source of energy.

Sulfate reducers, detected in produced waters from appreciable depths in the oil fields of Baku and Kirgiziya by Issatchenko et al. (1945), were credited with affecting the chemical composition of the water (sulfate $\rightarrow$ sulfide) and also the chemical composition of the associated oils.

Muller and Schwartz (1949) found sulfate reducers in about half of the samples collected in oil fields, including 105 samples of oil-bearing sediments and 6 oil-well brines. Freedom of the samples from aerobes, indicative of the general absence of surface contamination, together with other evidence led these workers to believe that some of the oil-bearing formations harbored sulfate reducers. Hitzman and Whitesell (1957) found from 0 to 175 sulfate-reducing bacteria per ml of reservoir fluids from producing wells, usually none, as compared with counts of up to 10,000 sulfate reducers per ml of injection water.

From personal communications and unpublished reports I am aware of many workers having failed in their attempts to find sulfate-reducing bacteria in oil-well waters or cored samples. This is mentioned in trying to present and assess the facts in proper perspective, because negative results and conclusions generally are not reported or emphasized to the same extent as positive results. Actually our own negative results outnumber, but do not outweigh, our positive findings.

As outlined above in the section on "Salinity Requirements" and summarized in Table 2, I have found sulfate-reducing bacteria in 187 different samples of oil-well brines or produced waters using 1.0-ml inocula. No such bacteria could be demonstrated in 209 samples. Of these 396 samples I personally collected 66 at well heads, usually from bleeder valves, in California, Texas, Louisiana, Oklahoma, Illinois, and Pennsylvania oil fields. The perforation or production zones ranged from 2,680 to 10,470 feet below the earth's surface. Rigorous precautions were exercized both in collecting the samples, their transportation to the laboratory, and aseptic handling. Sulfate-reducing bacteria were detected in 29 of the 66 samples when 10 ml was used to inoculate the medium, 25 with 1.0 ml inocula, 15 with 0.1 ml inocula, and only 4 samples with 0.01 ml inocula. From my own observations and the experiences of others, I am convinced that in certain oil fields sulfate-reducing bacteria are present and reproducing in formation waters, perhaps at the oil-water interface. However, whether they were introduced by the movement of ground waters or by the activities of man during drilling or other operations remains problematical in my mind.

In an effort to resolve this problem we have examined a good many cores drilled from sulfur-limestone-anhydrite and oil-bearing rocks; some from depths of nearly 10,000 feet representing sediments from 10^6 to 10^8 years old. Enrichment cultures of sulfate-reducing bacteria were recovered from some, but not all, of the cores. Negative results or finding no bacteria proved that it was possible to obtain aseptic samples despite possibilities of contamination from drilling mud, handling, etc. Positive results indicated that sulfate reducers were associated with some of the cored material but failed to prove the presence of an indigenous microflora.

Through the cooperation of the Shell Oil Company in 1950 an attempt was made to drill an oil well aseptically. Company engineers were concerned with learning whether living bacteria indigenous to the oil-bearing formation were responsible for the bacterial corrosion of oil-well casings at depths of a few thousand feet in the Ventura, California, field as reported by Doig and Wachter (1951) and Sneddon (1951). Extraordinary precautions were taken to minimize the possibilities of contamination, including the use of alkaline (pH 11.5) drilling mud to drill a new well and the generous use of germicides and blow torch. All stages of the sampling operation were personally supervised or conducted by Dr. F. D. Sisler and myself in cooperation with Shell Oil Company corrosion engineers. At the well head, cores of oil-bearing sand about 3 inches in diameter and 8 to 18 inches long were received with heat-sterilized tongs and given a quick dip in boiling paraffin wax to destroy surface contaminants and to retain the fluid content of the cores. Thus protected the cores were rushed to the laboratory where radially central subsamples were removed aseptically with heat-sterilized instruments. Viable sulfate-reducing bacteria were detected in many 10-gram (approximate weight) samples and in some 1-, 0.1- and 0.01-gram samples of the crushed oil-bearing rock taken from strata 4337 to 4412 feet deep. No such bacteria could be detected in the alkaline drilling mud. The absence of heterotrophic aerobes indicated freedom from contamination from soil or other common surface sources. Extensive tests demonstrated the ability of the sulfate reducers to grow in the oil-bearing formation. It possessed all of the prerequisites for such growth, including water, essential minerals, nutrients, energy sources, favorable pH, tolerable temperature, and other conditions. There was no way, however, to ascertain how long the bacteria had been present in the formation or the extent of their activity in situ prior to disturbance by drilling operations. The sulfate reducers may have been introduced in relatively recent years by the movements of ground water or by their own movements.

Factors Affecting Dissemination of Sulfate Reducers—It is difficult to evaluate the influence of the movements of underground waters on the occurrence of bacteria in subterranean formations. Such movements are affected by faults, fissures, fractures, bedding planes, pore spaces, hydrostatic heads, and many other factors. Whether the bacteria move with or through the water is influenced by environmental as well as by geological and hydrological conditions. Most bacteria are effectively filtered out of water passing through sediments or, for various reasons, fail to survive for long periods of time at appreciable depths in sedimentary materials. Sulfate reducers, however, are different from most bacteria in that they can utilize sulfate as an hydrogen acceptor when energy sources and other cultural conditions are favorable.

Besides being carried by moving water, certain sulfate reducers slowly propel themselves through fluids by flagella or they may grow through nutrient water-wet sediments by protoplasmic extrusion. The rate of self-induced or vital movement is rather slow, ranging from a few microns to a few centimeters per day. The rate is influenced by nutrient properties of interstitial fluids in sediments, the size of channels or pore spaces, temperature, and other factors. They do not migrate into environments that are unfavorable for their growth. Extremes of temperature, pressure, pH, redox potential, toxic constituents, adsorptive capacity of solids, and mechanical barriers in sediments may restrict the movements of bacteria.

Most crude oil deposits occur in aquifers or water-saturated rocks; mainly sandstones, limestones, and dolomite. Water fills the smaller interstitial or pore spaces and forms films on sedimentary particles making up the reservoir rocks. Interstitial water in oil reservoirs is seldom less than 10 per cent and it may fill more than 50 per cent of the pore space (Levorsen, 1954). Besides the water held by capillary attraction or adhering to solid surface, there may be some water emulsified in oil. The main body of water, though, is under the oil pool or at its boundaries, this being the so-called bottom or edge water respectively. Being heavier than most oils, water tends to percolate down through oil-bearing formations, or oil tends to rise above the water in reservoirs.

In such reservoirs neither a lack of water nor pore space is incompatible with the occurrence or the movement of sulphate-reducing bacteria. Actually we have demonstrated the migration of **Desulfovibrio** species through many paraffin- or plastic-coated cores of diamond-drilled oil-bearing sands. When flooded with various kinds of nutrient media, the sulfate reducers moved through the cores at average rates ranging from 1.8 mm to 3.7 cm per day. From these results it is calculated that the bacteria might move from 2 to 40 feet per year through such materials. Although such laboratory results give only rough approximations of what may happen in the field, they do demonstrate the possibilities of microbial migration in oil-bearing sediments. In the face of such possibilities it seems unwarranted to guess from the occurrence of sulfate-reducing bacteria how long they may have been present in the formation where found. Those which we found in the "aseptically-drilled" Ventura oil-field sands may be progeny of sulfate reducers introduced into the formation a hundred or so yards away when other wells were drilled there with **Desulfovibrio**-laden drilling mud 20 or 30 years earlier.

Sulfate-reducing bacteria may be widely disseminated by water movements above ground. In oxygenated sea water and freshwater streams, conditions may not be conducive to their growth, but their occasional presence is indicative of their prolonged survival in moving waters. In one series of experiments we held raw, enriched, and pure cultures of sulfate reducers in bottles of sea water through which air was bubbled for several weeks. Although the organisms gradually died off, some of them remained viable for 12 weeks.

It was necessary to filter the air before bubbling it through the cultures, because analyses revealed the presence of sulfate-reducing bacteria in the air. There are many mechanisms by which bacteria in soil or water become airborne. Bacteria occur in air over the ocean at all elevations and distances from land where careful tests have been made for their presence (ZoBell, 1942). Many of the bacteria suspended in the air survive the adversities of the atmospheric environment for prolonged periods.

According to Hvid-Hansen (1951), sulfate-reducing bacteria are not singularly sensitive to radiations. His cultures grew just as well in nutrient media when incubated in daylight as in absolute darkness. Some cultures were extraordinarily tolerant of ultra-violet radiations, growing after being irradiated for 30 minutes twice daily by a mercury vapour lamp at a distance of 25 cm.

Association with Other Organisms—Sulfate reducers commonly occur in close association with other microorganisms. Enrichment cultures as well as discrete colonies growing in agar or gelatin medium were observed by Beijerinck (1895), van Delden (1904), and Elion (1924) to consist frequently of a mixture of **Desulfovibrio** species and other bacteria, one of which was characterized as being coli-like. Similar observations have been recorded by Rank (1907), Kupsis (1928), Baars (1930), and by many contemporary investigators who have attempted to develop selective media or procedures for the elimination of associated organisms. The persistence of the latter makes it difficult to obtain and maintain pure cultures. Although **Desulfovibrio** species are highly pleomorphic, physiologically variable, and purportedly adaptable, it is often open to question how much of their apparent morphological, physiological, or cultural capriciousness is due to experimental irregularities, transmutations, or to the presence of contaminants.

Baas Becking (1925) applied the term sulfuretum to aquatic ecosystems where active sulfate reducers are intimately associated with various kinds of heterotrophs and autotrophs, including purple bacteria, thiobacteria, and many others which affect the availability of organic matter or the state of sulfur. The shallow sulfur-producing Cyrenaican lakes investigated by Butlin and Postgate (1954) contained massive mats of **Chromatium** and **Chlorobium** intermixed with cellulose decomposers, sulfate reducers, and several other morphological and physiological types of bacteria. Ostensibly the sulfate reducers depended upon the activities of other organisms for utilizable organic matter and to a lesser extent for sulfate, sulfite, thiosulfate, etc.

Associated organisms aid sulfate reducers primarily by creating reducing conditions and by providing certain essential metabolites. The latter may consist of simple organic acids, alcohols, or sugars resulting from the hydrolysis or partial oxidation of cellulose, chitin, proteins, or other complex carbon compounds. Hydrogen may be supplied from fermentations. Accessory growth factors are unproved possibilities. The most obvious benefit from associated organisms, however, is oxygen depletion by aerobes and the creation of redox potentials favorable for the growth of sulfate reducers.

Less well understood is why sulfate reducers are attractive to certain facultative anaerobes until H_2S accumulates in inhibitory concentrations. There are many ways in which microorganisms are mutually beneficial. Perhaps sulfate reducers are unique in providing reduced sulfur (possibly nascent HS^- ion) in a form that is more readily available to intimately associated organisms than sulfate. Reduced sulfhydryl groups are required for the activation of many enzyme systems. The exploration of these possibilities may reveal facts of fundamental physiological and ecological significance.

Some microorganisms are antagonistic towards sulfate reducers and, indeed, a good many commercial antibiotic preparations inhibit their growth. Finding antagonistic or antibiotic-producing organisms that will thrive in environments where sulfate reducers are unwanted may be a practical means for their control.

Summary

Widespread in distribution are bacteria which utilize sulfate as the terminal electron acceptor with the production of H_2S. They are most abundant in marine bottom deposits and around buried cast iron or steel structures. Sulfate reducers also occur in soil, sewage, swamps, and freshwater sediments. They are found in oil-well flood waters, certain industrial cooling waters, waste waters, and bottom waters over which petroleum products are stored. Drilling muds, ceramic slurries, filter beds, and anaerobic mucks may harbor hundreds of sulfate-reducing bacteria per ml. Such bacteria are also associated with oil and sulfur deposits.

Sulfate reducers may produce H_2S in concentrations which adversely affect other bacteria, plants, and animals. They play an important role in the carbon and sulfur cycles. They are believed to contribute to the formation of sedimentary sulfur deposits and metallic sulfides. They may have played a part in the origin of oil, its migration, and in its modification.

Sulfate reducers have been incriminated in the corrosion of cast iron, steel, and concrete structures. In many places they are responsible for foul odors, the discoloration of painted buildings or boats, the catastrophic killing of marine fauna, and for oil-well flood water problems.

Sulfate reducers have been found in and cultivated in solutions having salinities ranging from 0.1 to 30 per cent, although separate strains are rather restricted in their salt tolerances. Most strains grow best at temperatures ranging from 25° to 45°C. Some grow slowly at O°C and other strains grow at 65°C or higher. When compressed to 1000 atm, one thermophilic culture reproduced and produced H_2S from the reduction of sulfate at 104°C. Hydrostatic pressures exceeding 400 atm generally inhibit the growth or slowly kill most surface-dwelling strains, but from the deep-sea floor (7,000 to 10,000 meters) have been recovered sulfate reducers which grow preferentially or exclusively at 700 to 1000 atm.

Though found in natural habitats at hydrogen-ion concentrations ranging from pH 4.2 to 10.4, most sulfate reducers grow best in nutrient media at pH 6.5 to 7.5. They appear to be strict anaerobes, growing best at redox potentials of Eh -50 to -300 mv. The amount of sulfide which sulfate-reducing bacteria produce and tolerate is influenced by the pH of the medium, the presence of cations which may form insoluble sulfides, available sulfate, and the source of energy. Autotrophs can utilize molecular hydrogen as an energy source. Heterotrophs oxidize a large variety of organic compounds. Ammonium satisfies their nitrogen reqirements. Some varieties fix nitrogen. Neither nitrate, nitrite, nor complex proteinaceous compounds are utilized as nitrogen sources by **Desulfovibrio** species.

Sulfate-reducing bacteria have been detected in cores and reservoir fluids from petroliferous sediments. It is virtually impossible, however, to prove whether they are adventitious or indigenous. Unquestionably some are now active at the oil-water interface at depths of several thousand feet, but whether they were introduced by man or the movements of ground waters is problematical. Sulfate-reducing bacteria are believed to have been present and active either sporadically or continuously in certain petroliferous or sulfurous aquifers throughout the geological ages. In such formations the bacteria probably grow in accordance with Malthusian principles, populations being restricted by the availability of food and by the accumulation of toxic metabolic products. The concentration of metabolites is probably in a state of dynamic equilibrium affected both by diffusion and the migration of fluids. The bacteria themselves may move through certain formations.

References

Agar, C. C., 1935. Sulphates to sulphides. Water Works and Sewerage, 82: 189-191.

Allen, L. A., 1949. The effect of nitro-compounds and some other substances on production of hydrogen sulphide by sulphate-reducing bacteria in sewage. Proc. Soc. Appl. Bact., 2:26-38.

Allred, R. C., 1954. The role of microorganisms in oil field water flooding operations. Producers Monthly, 18: 18-22.

Anderson, K. E., 1956. Standardization of bacteriological testing. World Oil, 142: 176, 180, 182.

Baars. J. K., 1930. Over Sulfaatreductie door Bacterien. Dissertation, Delft, Holland, 164 pp.

Baas Becking, L. G. M., 1925. Studies on the sulfur bacteria. Ann. Bot., 39: 613-650.

Baas Becking, L. G. M., and Kaplan, I. R., 1956a. Biological processes in the estuarine environment, III. Electrochemical considerations regarding the sulphur cycle. Proc. Kon Ned. Ak. v. Wet. Amsterdam, 59: 86-96.

Baas Becking, L. G. M., and Kaplan, I. R., 1956b. The microbiological origin of the sulphur nodules of Lake Eyre. Trans. Roy. Soc. S. Austral., 79: 52-65.

Baas Becking, L. G. M., and Wood, E. J. F., 1955. Biological processes in the estuarine environment. I. Ecology of the sulphur cycle. Proc. Kon. Ned. Ak. v. Wet. Amsterdam, 58: 160-181.

Baier, C. R., 1935. Studien zur Hydrobakteriologie stehender Binnengewasser. Arch Hydrobiol. 29: 183-264.

Baier, C. R., 1938. Chemisch-mikrobiologische Beobachtungen zur Sedimentdiagenese an postglazialen Sedimenten der Eckernforder Bucht (Ostsee). Geol. Rundschau, 29: 316-321.

Baier, C. R., 1942. Sulfatreduzierende Bakterien in technischen Anlagen. Gas u. Wasserfach, 85, 25-29.

Baranik-Pikowsky, M. A., 1927. Uber den Einfluss hoher Salzkonzentrationen auf die Limanbakterian. Zentr. Bakt. Parasitenk., II, 70: 373-383.

Barton-Wright, C. E., 1945. Treatment of sulfate-reducing bacteria in a flour mill. Jour. Soc. Chem. Indust., 64: 295.

Barr, W. M., and Buchanan, R. E., 1912. The production of excessive hydrogen sulide in sewage disposal plants and consequent disintegration of the concrete. Iowa State College Engin. Exper. St. Bull., 26: 1-16.

Bastin, E. S., 1926. The problem of the natural reduction of sulphates. Bull. Amer. Assoc. Petrol. Geol., 10: 1270-1299.

Bastin, E. S., and Greer, F. E., 1930. Additional data on sulphate-reducing bacteria in soils and waters of Illinois oil fields. Bull. Amer. Assoc. Petrol. Geo., 14: 153-159.

Baumann, A., and Denk, V., 1950. Zur Physiologie der Sulfatreduktion. II. Zur Kenntnis der biologischen Sulfatreduktion. Arch. Mikrobiol., 15: 283-307.

Vavendamm, W., 1932. Die mikrobiologische Kalkfallung in der tropischen See. Arch Mikrobiol., 3: 205-276.

Beck, J. V., 1947a. Penn Grade progress on use of bacteria for releasing oil from sands. Producers Monthly, 11: 13-20.

Beck, J. V., 1947b. Prevention of microbiological growths in water flood operations. Producers Monthly, 11: 21-26.

Beckwith, T. D., and Moser, J. R., 1932. The reduction of sulphur containing compounds in wood pulp and paper manufacture. Jour. Bact., 24: 43-52..

Beijerinck, M. W., 1895. Uber Spirillum desulfuricans als Ursache von Sulfatreduction. Zentr. Bakt. Parasitenk., 11, 1: 1-9, 49-59, 104-114.

Berkalof, E., and Cabasso, V., 1940. Sur une souche de vibrion redusteur des sulfates isolec de l'eau d'eau d'un puits artesien, en Tunis. Arch. inst. Pasteur, Tunis, 29; 262-284.

Bromfield, S. M., 1953. Sulphate reduction in partially sterilized soil exposed to air. Jour. Gen Microbiol., 8: 378-390.

Bunker, H. J., 1936. A review of the physiology and biochemistry of the sulphur bacteria. His Majesty's Stationery Office, London, 48 pp.

Bunker, H. J., 1942. The control of bacterial sulfate reduction by regulation of hydrogen-ion concentration. Proc. Soc. Agric. Bact., 13: 8-10.

Butkevich, V. S., 1938. On the bacterial population of the Caspian and Azov seas. Microbiology, U.S.S.R., 7: 1005-1021.

Butlin, K. R., 1947. Report of the microbiology section for 1947. Chemistry Research, Dept. Sci. and Indust. Res., pp. 24-28.

Butlin, K. R., 1948. Report of the microbiology section for 1948. Chemistry Research, Dept. Sci. and Indust. Res., pp. 19-26.

Butlin, K. R., Adams, M. E., and Thomas, M., 1949. The isolation and cultivation of sulphate-reducing bacteria. Jour. Gen. Microbiol., 3: 46-59.

Butlin, K. R., and Postgate, J. R., 1953. Micobiological formation of sulphide and sulphur. Proc. Istit. Superiore di Sanita, Rome, pp. 126-143.

Butlin, K. R., and Postgate, J. R., 1954. The microbiological formation of sulphur in Cyreniacan lakes. Biol. Deserts Symposium, Inst. Biol., London, pp. 112-121.

Butlin, K. R., Selwyn, S. C., and Wakerley, D. S., 1956. Sulphide production from sulphate-enriched sewage sludges. Jour. Appl. Bact. 19: 3-15.

Campbell, L. L., Frank, H. A., and Hall, E. R., 1957. Studies on thermophilic sulfate reducing bacteria. I. Identification of Sporovibrio desulfuricans as Clostridium nigrificans. Jour. Bact., 73: 516-521.

Cannon, G. E., 1939. Summary on work of isolating sulfate reducing bacteria from drilling muds. Proc. Amer. Petrol. Inst., 20, 134-135.

Chait, S. Z., 1924. Microspira desulfuricans des Kujalnitzky Limanes. Zhur Nauchno-issledov. Kafedry, Odessa, 1: 39-48.

Copenhagen, W. J., 1934. Occurrence of sulphides in certain areas of the sea bottom on the South African Coast. Fish. Mar. Biol. Surv., Un. S. Afr. Rep. No. 11: 3-18.

Datta, S. C., 1946. Sulphate reduction and production of elemental sulphur by bacteria. Jour. Sci. Indus. Res., 5B: 28-30.

Dey, B. B., and Ganapati, S. V., 1934. The production of sulphuretted hydrogen in the slow sand filters at the Madras waterworks. Water and Water Engin., 36: 107-111.

Dianova, E., and Voroshilova, A., 1935. Salt composition of medium and specificity of marine bacteria. Microbiology, U.S.S.R., 4: 393-402.

Doig, K., and Wachter, A., 1951. Bacterial casing corrosion in the Ventura Field. Corrosion, 7: 212-216.

Edington, J. W., 1938. Hydrogen sulfide by bacteria in a lead mine. Jour. Hyg., 38; 683-687.

Elion, L., 1924. A thermophilic sulfate-reducing bacterium. Zentr. Bakt. Parasitenk., II, 63: 58-67.

Embil, J., 1956. Las Bacterias del azufre y la posible genesis del acido sulfhidrico de las agaus de los manantiales de los bancos de San Diego de los Banos, en Pinar del Rio. Bol. Ext. Inst. Nac. Hidrol. Climatol. Med., 3: 165-190.

Flannery, W. L., 1956. Current status of knowledge of halophilic bacteria. Bact. Rev. 20: 49-66.

Gahl, R., and Anderson, B., 1928. Sulphate reducing bacteria in California oil waters. Zentr. Bakt. Parisitenk., II, 73: 331-338.

Genovese, S., Pinchionoty, F., and Senez, J. C., 1957. Sui Batteri solfato-riduttori del lago di Faro. Atti, Soc. Peloritana Sci. Fisic. Matemat. e Nat., 3: 303-319.

Ginsberg-Karagitscheva, T. L., 1933. Microflora of oil waters and oil-bearing formations and biochemical processes caused by it. Bull. Amer. Assoc. Petrol. Geol., 17: 52-65.

Ginsberg-Karagitscheva, T., and Rodionova, K., 1935. Beitrag zur Kenntnis der im Tiefseeschlamm stattfindenden biochemischen Prozesse. Biochem. Zeitscher., 25: 296-404.

Ginter, R. L., 1930. Causative agents of sulphate reduction in oil-well waters. Bull. Amer. Assoc. Petrol. Geol., 14: 139-152.

Ginter, R. L., 1934. Sulphate reduction in deep subsurface water. Problems of Petroleum Geology, Amer. Assoc. Petrol. Geol., Tulsa, Oklahoma, pp. 907-924.

Goslings, N., 1904. Ueber schwefelwasserstoffbildende Mikroben in Mineralwassern. Zentr. Bakt. Parasitenk., II, 13: 385-394.

Grossman, Joy P., and Postgate, J. R., 1953. Cultivation of sulphate-reducing bacteria, Nature, 171: 600-605.

Grossman, Joy P., and Postgate, J. R., 1955. The metabolism of malate and certain other compounds by Desulphovibrio desulphuricans. Jour. Gen. Microbiol., 12: 429-445.

Gubin, V., and Tzechomskaya, V., 1930. Ueber die biochemische Sodabildung in den Sodaseen. Zentr. Bakt. Parasitenk., II, 81: 396-401.

Hadley, R. F., 1940. Studies in microbiologicel anaerobic corrosion. Proc. Amer. Gas Assoc., 22: 764-788.

Heukelekian, H., 1948. Some bacteriological aspects of hydrogen sulfide production from sewage. Sewage Works Jour., 20: 490-498.

Hitzman, D. O., and Whitsell, L. B., Jr., 1957. The effects of seasonal variations and various treatments on counts of sulfate-reducing bacteria in a water flood. Preprint of API Paper No. 851-31-E.

Hitzman, D. O., Whitsell, L. B., Jr., and Mills, A., 1957. A rapid method for determining bactercidal activity of compounds against sulfate reducing bacteria. Producers Monthly, 21: 28-30.

Hof, T., 1935. Investigations concerning bacterial life in strong brines. Rec. Trav. botan. neerlandias, 32: 92-173.

Horowitz-Wlassowa, L. M., and Sontag, A. D., 1931. Zur Mikrobiologie der Fischkonserven. Vibrio halobiscus desulfuricans. Arb. a. d. Staatl. wissensch. Nahrungsmittel-Institute (Russian); see Ztschr. f. Unters. d Lebenim., 62: 597-610.

Hunter, J. B., McConomy, H. F., and Weston, R. F., 1948. Environmental pH as a factor in control of anaerobic bacterial corrosion. Oil and Gas Jour., 47: 249-250.

Hvid-Hansen, N., 1951. Sulphate-reducing and hydrocarbon-producing bacteria in ground water. Acta Path. Microbiol. Scandinavica, 29: 314-334.

Ishimoto, M., and Koyama, J., 1953. Biochemical study of sulfate-reducing bacteria. I. Reduction of sulfate by lactate. Jour. Chem. Soc. Japan, 84: 853-857.

Issatchenko, B. L., 1924. Sur la fermentation sulfhydrique dans la mer Noire. Compt. rend. Acad. Sci., 178: 2204-2206.

Issatchenko, B. L., Reinfel'd, E. A., and Sturm, L. D., 1945. Microorganisms in oil fields. Bull. Acad. Sci., U.S.S.R., 95:

Iya, K K., and Sreenivasaya, M., 1945. Studies in the formation of sulphur at Kona (Masulipatem). Curr. Sci., 14: 243-244; 267-269.

Johnson, A. L., Postlewaite, D. E., and Rittenberg, S. C., 1949. Bacteria, a factor in slip control. Jour. Amer. Ceramic Soc., 32: 347-350.

Johnson, F. H., 1957. The action of pressures and temperature. Microbial Ecology, Cambridge Univ. Press., pp. 134-167.

Johnson, F. H., Eyring, H., and Polissar, M. J., 1954. The Kinetic Basis of Molecular Biology. John Wiley and Sons, Inc., New York. 874 pp.

Jones, G. E., 1955. Fractionation of the stable isotopes of sulfur by microorganisms with particular reference to the sulfate-reducing bacteria. Doctorate Dissertation, Rutgers Univ., 187 pp.

Jones, G. E., and Starkey, R. L., 1957. Fractionation of stable isotopes of sulfur by microorganisms and their role in deposition of native sulfur. Appl. Microbiol., 5: 111-118.

Kaplan, I. R., 1956. Evidence of microbiological activity in some of the geothermal regions of New Zealand, N.Z. Jour. Sci. and Tech., 37: 639-662.

Katagiri, H., Kanie, M., and Ishida, T., 1947. Sulfur bacteria. Repts. Chem. Res. Inst., Kyota Univ., 16: 25-26.

Kegel, 1940.Biologische Reduktion von Sulfaten in direkt berieselten Gaskuhlern. Chem. Ztg., 64: 507.

Kimata, M., Kadota, H. Hata, Y., and Miyoshi, H., 1957. Studies on the marine sulfate-reducing bacteria. VI. Production of sulfides in the estuarine region of the river receiving a large amount of organic drainage. Bull. Jap. Soc. Scient. Fish., 22: 701-707.

Kimata, M., Kadota, H., Hata, Y., and Tajima, T., 1955a. Studies on the marine sulfate-reducing bacteria. I. Distribution of sulfate-reducing bacteria in the costal region of the sea. Records Oceanographic Works Japan, 2: 85-93.

Kimate, M., Kadota, H. Hata, Y., and Tajima, T., 1955b. Studies on the marine sulfate-reducing bacteria. II. Influences of various environmental factors upon the sulfate-reducing activity of marine sulfate-reducing bacteria. Bull. Jap. Soc. Scient. Fish., 21: 109-112.

Kimata, M., Kadota, H., Hata, T., and Tajima, T., 1955c. Studies on the marine sulfate-reducing bacteria. III. Influences of various environmental factors upon the sulfate- reducing of marine sulfate-reducing bacteria. Bull. Jap. Soc. Scient. Fish., 21: 113-118.

Kriss, A. E., 1949. Microorganisms and accumulation of H_2S, ammonia, and nitrogen in the Black Sea. Priorda, 6: 35-46.

Kriss, A. E., and Rukina, E. A., 1949. Sources of H_2S in the Black Sea. Microbiology, U.S.S.R., 18: 332-345..

Kupsis, J., 1928. Die biochemischen Vorgange im Schwefel—und Moorbade Kemmern in Lettland. Zent. Bakt. Parasitenk., II, 76: 48-65.

Levorsen, A. I., 1954. Geology of Petroleum. W. H. Freeman and Co., San Francisco, 703 pp.

Limberg-Ruben, E. L., 1952. Number of bacteria in the water and floor of the northwestern part of the Pacific Ocean. Acad. Nauk. SSSR. Zool. Inst., 3: 138-141.

ittlewood, Dorothy, and Postgate, J. R., 1957. On the osmotic behaviour of Desulphovibrio desulphuricans. Jour. Gen. Microbiol., 16: 596-603.

MacLeod, R. A., and Onofrey, E., 1956. Nutrition and metabolism of marine bacteria. II. Observations on the relation of sea water to the growth of marine bacteria. Jour Bact., 71: 661-667.

MacLeod, R. A., and Onofrey, E., 1957. Nutrition and metabolism of marine bacteria. VI. Quantitative requirements for halides, magnesium, calcium, and iron. Canad. Jour. Microbiol., 3: 753-759.

Maliyantz, A. A., 1935. Bacteriological method of desulphurizing crude. Azerb. Neft. Khoz., 6: 89-93.

Mears, E. G., 1943. The Callao Painter. Scient. Monthly, 57: 331-336.

Menard, P., and Berkalof, E., 1940. Corrosion biologique dans les puits artesiens en Tunisie. Arch. inst. Pasteur, Tunis, 29: 455-462.

Menaul, P. L., and Dunn, T. H., 1946. Formaldehyde as an inhibitor of corrosion caused by hydrogen sulphide. Amer. Inst. Mining and Metal. Eng. Tech. Publ. 1970, pp. 1-9.

Miller, L. P., 1949a. Rapid formation of high concentrations of hydrogen sulfide by sulfate-reducing bacteria Contrib. Boyce Thompson Inst., 15: 437-465.

Miller, L. P., 1949b. Stimulation of hydrogen sulfide production by sulfate-reducing bacteria. Contrib. Boyce Thompson Inst., 15: 467-474.

Miller, L. P., 1950. Tolerance of sulfate-reducing bacteria to hydrogen sulfide. Contrib. Boyce Thompson Inst., 16: 73-83.

Morita, R. Y., 1954. Occurrence and significance of bacteria in marine sediments. Doctorate Dissertations, Univ. of Calif., Los Angeles, 80 pp.

Morris, W. S., 1943. Subsurface dispocal of salt water in the East Texas field. Petrol. Engin., July, 10 pp.

Muller, A., and Schwartz, W., 1949. Untersuchungen zur Erdolbakteriologie I. Arch. Mikrobiol., 14: 291-308.

Novelli, G. D., and ZoBell, C. E., 1944. Assimilation of petroleum hydrocarbons by sulfate-reducing bacteria. Jour. Bact., 47: 447-448.

Oppenheimer, C. H., 1957. Personal Communication, Inst. Mar. Sci., Aransas Pass, Texas.

Perkins, E. J., 1957. The blackened sulphide-containing layer of marine soils, with special reference to that found at Whitstable, Kent. Ann. and Mag. Nat. Hist., 10: 25-35.

Plummer, F. B., and Walling, I. W., 1946. Laboratory investigations of chemical changes in East Texas water affecting its injection into subsurface sands. Amer. Inst. Mining. and Metal Eng. Tech. Pub. No. 2019, pp. 1-14.

Postgate, J. R., 1951a. On the nutrition of Desulphovibrio desulphuricans. Jour. Gen. Microbiol., 5: 714-724.

Postgate, J. R., 1951b. The reduction of sulphur compounds by Desulphovibrio desulphuricans. Jour. Gen. Microbiol.. 5: 725-738.

Postgate, J. R., 1952. Growth of sulphate-reducing bacteria in sulfate-free media. Research 5:189-191.

Postgate, J. R., 1957. The psychiology of sulphate reducing bacteria. Saint Bonaventure Centennial Symposium on Sulfate Reducing Bacteria.

Prevot, A. B., 1949. Anaerobies reducteurs des sulfates et formation des petroles. Ann. inst. Pasteur, 77: 400-418.

Rank, A., 1907. I. Beitrage sur Kenntnis der sulfatreduzierenden Bakterien. 2. Schwefelwasserstoff bildung im Passuger Mineralwasser. Dissertation, Zurich. 66 pp.

Richard, O., 1946. Das Vorkommen van Schwefelwasserstoff in Gewassern als Folge bakteriellen Sulfatreduktion. Zeitscher. Hydrol., 10: 124-151.

Rittenberg, S. C., 1941. Studies an marine sulfate-reducing bacteria. Doctorate Dissertation, Univ. of Calif., Los Angeles, 115 pp.

Rogers, T. H., 1945. The inhibition of sulphate-reducing bacteria by dyestuffs. Part II. Practical applications in cable storage tanks and gas holders. Jour. Soc. Chem. Induct., 64: 292-295.

Rosenfeld, W. D., 1947. Anaerobic oxidation of hydrocarbons by sulfate-reducing bacteria. Jour. Bact., 54: 664-665.

Rubentschick, L. I., 1946. Sulfate reducing bacteria. Microbiology. U.S.S.R. 15: 443-456.

Rubentschick, L. I., and Goicherman, D. G., 1936. The influence of a decrease in salt-content in limans on the microflora of medicianl muds. Arkh. biol. nauk, 43 (ser. 2-3): 217-227.

Salimovskaja-Rodina, A. G., and Neschaeva, N. B., 1940. The desulfatation process in Stararusska medicinal mud. Microbiology U.S.S.R., 9: 695-701..

Saltet, R. H., 1900. Ueber Reduktion von Sulfaten in Brackwasser durch Gakterien. Znter. Bakt. Parasitenk., II, 6: 648-651; 695-703.

Saslawsky, A. S., 1928. Zur Frage der Wirking hoher Salzkonzentrationen auf die biochemischen Prozesse im Limanschlamm. Zentr. Bakt. Parasitenk., II, 73: 18-27.

Senez, J. C., 1955. Consommation de l'hydrogene moleculaire par les suspensions nonproliferantes et par les extraits cellulaires de Desulfovibria (Sporovibrio) desulfuricans. Bull. Soc. Chim. Biol., 37: 1135-1146.

Senez, J. C., Pinchinoty, F., and Konovaltchikoff-Mazoyer, M., 1956. Reduction des nitrates et de l'hydrozylamine par les suspensione et les extraits de Desulfovibrio desulfuricans. Comp. rend. Acad. Sci., 242: 570-573.

Sisler, F. D., and ZoBell, C. E., 1950. Hydrogen-utilizing, sulfate-reducing bacteria in marine sediments. Jour. Bact., 60: 747-756.

Sisler, F. D., and ZoBell, C. E., 1951a. Hydrogen utilization by some marine sulfate-reducing bacteria. Jour. Bact., 62: 117-127.

Sisler, F. D., and ZoBell, C. E., 1951b. Nitrogen fixation by sulfate-reducing bacteria indicated by nitrogen/argon ratios. Science, 113:511-512.

Sloat, B., Clayton, J. M., and Ellenberger, A. R., 1957. Water treatment in water flooding. Producers Monthly, 21: 38-43.

Sneddon, R., 1951. Casing failures traced to bacterial action. Petrol. Engin., August, pp. 7-12.

Starkey, R. L., 1938. A study of spore formation and other morphological characteristics of Vibro desulfuricans. Arch Mikrobiol., 9: 268-304.

Starkey, R. L., and Wight, K. M., 1945. Anaerobic corrosion of iron in soil. Tech. Rep. Distrib. Comm., No. 1945, Amer. Gas. Assoc., 108 pp.

Stokvis, C. S., 1899. Bijdrage tot verklaring der zwavelwaterstofvorming in het Amsterdamsche grachwater. Dissertation, Univ. of Amsterdam, pp. 1-82.

Sturm, L. D., 1937. A study of the microflora of sulfur-containing rocks. Microbiology, U.S.S.R., 6: 481-497.

Sturm, L. D., 1950. Some observations in the growth of Vibrio desulfuricans. Microbiology, U.S.S.R., 19: 289-293.

Subba, Roa, M. S., 1950. A biochemical study of the microbiological formation of elemental sulphur in coastal areas. Dissertation, Indian Inst. Sci., Bangalore, 110. pp.

Tanner, F. W., 1917. Studies on the bacterial metabolism of sulfur. I. Formation of hydrogen sulfide from certain sulfur compounds under anaerobic conditions. Jour. Bact., 2: 585-593.

Tanner, F. W., 1918. Studies on the bacterial metabolism of sulfur. II. Formation of hydrogen sulfide from certain sulfur compounds by yeast-like fungi. Jour. Amer. Chem. Soc., 40: 663-669.

Tausson, W. O., and Aleshina, W. A., 1932. Uber die bakterielle Sulfatreduktion bei Anwesenheit der Kohlenwasserstoffe. Microbiology, U.S.S.R., 1: 229-261.

Tausson, W. O., and Veselov, I. J., 1934. On the bacteriology of the decomposition of cyclical compounds at the reduction of sulphates. Microbiology. U.S.S.R., 3, 360-369.

Tausson, W. O., Vesselov, I. J., Aleshina, V. I., and Golden, M. I., 1933. The anaerobic microflora of mud-volcano mud. Microbiology U.S.S.R., 2: 303-345.

Updegraff, D. M., and Wren, G. B., 1952. The mineral element requirements of Desulfovibrio aestuarii in enrichment cultures. Bact. Proc., p. 136.

van Delden, A., 1904. Beitrag zur Kenntnis der Sulfatreduktion durch Bäkterian. Zentr. Bakt. Parasitenk., II, 11: 81-95; 113-119.

von Wolzogen Kuhr, C.. A. H., 1922. On the occurrence owf sulfate-reduction in the deeper layers of the earth. Proc. Kon. Ned. Ak. v. Wet. Amsterdam, 25: 188-198.

von Wolzogen Kuhr, C. A. H., 1938. De eenheid van het anaerobe en aerobe ijzercorrosieproces in den grond. Water (Netherlands) 22: 33-38; 45-47.

von Wolzogen Kuhr, C. A. H., and van der Vlugt, L. S., 1934. De grafiteering van gietijzer als electrobiochemisch proces in anaerobe gronden. Water (Netherlands) 18: 147-165.

Williams, O. B., 1953. Little bugs . . . big problems. World Oil, 136(6): 170-175.

Young, J. W., 1936. The bacterial reduction of sulphates. Canad. Jour. Res. Sec. B., 14: 49-54.

Zelinski, N. D., 1893. On hydrogen formation in the Black Sea and the Odessa estuaries. Proc. Russ. Phys. Chem. Soc., 25: 298-303.

ZoBell, C. E., 1934. Microbiological activities at low temperatures with particular reference to marine bacteria. Quart. Rev. Biol., 9: 460-466.

ZoBell, C. E., 1938. Studies on the bacterial flora of marine bottom sediments. Jour. Sed. Petrol., 8: 10-18.

ZoBell, C. E., 1942. Microorganisms in marine air. Aerobiology, Amer. Assoc. Adv. Sci., Washington, D. C., Pub. No. 17: 55-68.

ZoBell, C. E., 1946a. Studies on redox potential of marine sediments. Bull. Amer. Assoc. Petrol. Geol., 30: 477-513.

ZoBell, C. E., 1946b. Action of microorganisms on hydrocarbons. Bact. Rev., 10: 1-49.

ZoBell, C. E., 1947a. Bacterial release of oil from sedimentary materials. Oil and Gas Jour., 46, 62-65.

ZoBell, C. E., 1947b. Bicrobial transformation of molecular hydrogen in marine sediments, with particular reference to petroleum. Bull. Amer. Assoc. Petrol. Geol., 31: 1709-1751.

ZoBell, C. E., 1952. Part played by bacteria in petroleum formation. Jour. Sed. Petrology, 22: 42-49.

ZoBell, C. E., and Johnson, F. H., 1949. The influence of hydrostatic pressure on the growth and viability of terrestrial and marine bacteria. Jour. Bact., 57: 179-189.

ZoBell, C. E., and Morita, R. Y., 1957a. Barophilic bacteria in some deep sea sediments. Jour. Bact., 73: 563-568.

ZoBell, C. E., and Morita, R. Y., 1957b. Deep sea bacteria. Galathea Report, Copenhagen, 1: 139-154.

Reprinted from the May 1958 issue of Producers Monthly, Vol. 22, No. 7, Pages 12-29.

Reprinted from GEOPHYSICS AND THE IGY, Geophysical Monograph No. 2,
American Geophysical Union, Washington, D. C., July 1958

Sun, Sea, and Air: IGY Studies of the Heat and Water Budget of the Earth *

ROGER R. REVELLE

The great saga of the Norse kings, the *Heimskringla,* begins with the words "Earth's round face, whereon mankind dwells." The Vikings, like other primitive peoples, thought of Earth as their home and of themselves as its creatures. Today we know that Earth is the only planet of our solar system on which human life could have developed, for no other satellite of our Sun has land masses surrounded by an ocean of liquid water or an atmosphere containing abundant free oxygen.

Our bodies are made up almost entirely of four elements drawn from sea water and air: hydrogen, carbon, oxygen, and nitrogen. The narrow temperature range in which we can survive is maintained by the great heat capacity of the sea and the atmosphere. The waste products that otherwise would suffocate us are continuously dispersed by the easy motions of the atmosphere. We can exist as land animals only because the Sun's deadly ultraviolet and x-rays are fended off by the protective shield of the air, and because the great natural engine of the sea and the atmosphere pumps water continuously from the sea surface and pours it gently down upon the land.

Yet from our point of view, the Earth is a careless mother. Large areas of her surface are too hot or too cold, too dry or too wet to support any large number of human beings. Moreover, she is unreliable. Areas where there was once sufficient water for men to build civilizations are now so dry that only a few desperate nomads can live in them. Elsewhere, a mile-thick blanket of ice has crept down and obliterated once green farms and forests. Millions of our species suffer when a slight change in the running of the sea-atmosphere engine causes drought or flood. Sometimes the engine runs with unpleasant violence. Then thunder storms and hurricanes, tornadoes and typhoons bring destruction and death to many of us.

Because of our dependence on events taking place in the air, almost everyone is an amateur meteorologist. Wherever two or more people are gathered together the first topic of conversation is the weather, and this was probably just as true in the time of Hammurabi or Amenhotep as it is today. Professional weathermen are a new development, however, and it has only been within the last few decades that we have begun to gain an understanding of the great interrelated mechanisms of the air and the oceans.

We know that the sun pours a flood of particles and visible and invisible light into the top of our atmosphere. The amount of visible light appears to be nearly constant, but the intensity of ultraviolet and x-rays and the number of particles varies by at least a hundred-fold [*Chapman,* 1956, p. 19]. The particles are chiefly electrons and protons. The average number of hydrogen nuclei entering our atmosphere is surprisingly large, perhaps a billion per square centimeter per second. During the geological lifetime of the Earth, if all this hydrogen were combined with oxygen as water, it would correspond to a layer over the ocean about twenty meters thick. The energy carried to the Earth by these particles from the Sun during periods of sunspot activity may be as much as one tenth of the total energy of sunlight [*Chapman,* 1956, p. 17].

In addition to particles of ordinary hydrogen, there is new evidence that most of the tritium or radioactive hydrogen on Earth also comes from the Sun [*Craig,* 1956, p. 1125]. It was formerly thought that all the tritium was produced by cosmic rays bombarding nitrogen and oxygen molecules in the upper air, but recent calculations indicate that the amount present is nearly ten times too large to be produced in this way.

The marked variations in ultraviolet radiation and in the number of particles coming from the Sun cause large variations in the temperature and in the electrical and magnetic behavior of the upper atmosphere, because there is such a small amount of air at these high levels. Neither the majority of particles nor the ultraviolet rays penetrate very deeply, however, and

---

* Contribution from the Scripps Institution of Oceanography, New Series. 1006

Reproduced by Permission

it is not clear whether the variations in the amounts coming from the Sun have appreciable effects near the Earth's surface. Visible light is the dominant form of solar energy entering the lower atmosphere. Part of this light is reflected back to space, chiefly from the surface of clouds, snow, and ice. Most of it is absorbed in the atmosphere and the sea, from which it is ultimately re-radiated as infrared radiation.

In this respect, the atmosphere behaves much like the glass in a greenhouse. It easily transmits visible light but is rather opaque to the infrared or heat radiation coming from the ground and the sea surface. Just as in a greenhouse, the air temperature must be considerably warmer than it would be in the absence of materials that absorb infrared, in order to allow a balance between incoming and outgoing radiation. In the greenhouse the absorbing material is the glass roof. The corresponding materials in the atmosphere are three substances present in quite minor amounts: water vapor, carbon dioxide, and ozone.

The temperatures in the upper air do not vary markedly with latitude and consequently the amount of back radiation is roughly the same all over the globe. But the amount of incoming sunlight is greater in the tropics than in high latitudes. As a consequence, air and water warmed in the tropics must move toward the poles. Part of the energy received from the Sun is thus used to carry the excess heat absorbed in low latitudes to high latitudes where it can be re-radiated. The amount of heat transported across the parallels of 30° is 10 to 20 pct of the total incoming radiation [*Starr* and *White*, 1954], but the mechanical work involved is less than one per cent [*Starr*, 1948, p. 193].

The situation can be thought of as if the sea and the atmosphere were interlinked heat engines of very low efficiency. These engines do mechanical work against friction by carrying the working fluids, sea water and air, from the 'firebox' of the tropics to the radiation-cooled 'condenser' of the polar regions. The circulation of the working fluids is manifest in the winds of the air and the currents of the sea. In the atmosphere, it takes place through the coupling of rotary current patterns of all possible shapes and sizes. These include the trade-wind cells of ocean-wide dimensions, the large scale high and low pressure areas of mid-latitudes, the wavelike jet stream, hurricanes, tornadoes, tiny whirls and vortices. In the sea, major units of the circulation include the Gulf Stream and the Kuroshio, the fast moving equatorial currents and the sluggish currents of the abyssal depths. These circulation patterns are partly unstable, and this shows itself to those of us who live in mid-latitudes as the radical changes in weather with which we are all familiar. In low latitudes over the ocean the instability produces the terrifying hurricanes of the western Pacific and of our own east coast.

The behavior of the interlinked heat engines of the sea and the atmosphere is profoundly influenced by four facts: first is their peculiar shape; they are essentially two thin sheets wrapped around a sphere; second, the sphere is rotating; the lower layers of air are dragged along by the rotation, and the movements of both the sea and the air are largely determined by the forces generated by the rotation (at a height above our heads of several hundred miles there is a transition to a zone where the sparse atoms of gas no longer move around the Earth's axis); third, the ocean is not a continuous sheet like the atmosphere, but is broken up by the relatively dry areas we call continents; fourth, like an invisible *pousse café*, the atmosphere is stratified in thin layers that do not mix readily with each other and each of these layers has to a considerable extent a separate behavior of its own. The same is true of the ocean but with the marked difference that while the temperatures of the different layers of the atmosphere are alternatively lower and higher as we go upward, the temperature of the ocean decreases continuously nearly to the freezing point at great depths. It increases slightly near the bottom because of the heat coming from the interior of the Earth.

The energy needed to drive the sea-air circulation is only a small portion of the incoming solar radiation, but it is still enormous on a human scale. The winds of the Earth have a total kinetic energy estimated to equal seven million atomic bombs, or more electric power than all the power plants in the United States could produce in a hundred years. This energy must be replenished every nine to twelve days because of the loss by friction between the winds and the Earth's surface [*Wexler*, 1955].

Although there is general agreement about the foregoing generalizations, our mental model of the sea-atmosphere system is so inadequate in many essentials that meteorologists are unable to predict anything very useful for more than a few days in advance about the circulation of the atmosphere.

Even more fundamentally, we do not know the factors that determine the average conditions. Consequently, we are quite unable to forecast changes in climate. Yet we know that such changes have occurred in the relatively recent past. Only about ten thousand years ago the Earth emerged from a dark age of snow and ice; less than five thousand years ago, Greenland offered a fair and pleasant habitation for human beings. Within the last fifty years, the climate over eastern North America and northern Europe has again become slightly warmer and the Arctic waters are perhaps again becoming accessible to human beings, while elsewhere prolonged droughts are destroying the work and hopes of decades. For the farmer, the strategist and the statesman, an accurate forecast of climatic change over the next fifty years would be of immeasurable value. But such a forecast is completely beyond our present ability. Ability to forecast depends on understanding, and this comes in two interrelated ways: by constructing small models in our heads of the two great Earth fluids, and by testing and refining these models through observations. This second method is one of the major objectives of the International Geophysical Year. In particular, we are concerned with measurements in areas that have never been adequately explored and of phenomena that have never been adequately studied.

To increase our understanding of climatic change we can ask first, what changes have occurred in the past and how did they happen? Second, because a change in climate is essentially a change of average air temperature, we need to examine the ways in which the heat content of the air can vary. The heat content must be that required to give a balance between incoming and outgoing radiation, hence it can vary if there is a change in the amount of incoming radiation from the Sun, in the proportion of sunlight reflected versus that absorbed, or in the amount of the infrared back radiation absorbed by carbon dioxide, water vapor and ozone. A change of one per cent in the intensity of the incoming sunlight or in the amount of sunlight reflected back to space would give about a one degree centigrade change in the average air temperature [*Plass,* 1956, p. 141].

The total solar radiation seems to be remarkably constant. The most recent continuous observations are those made at the Lowell Observatory since 1953 [*Evans,* 1956, p. 2]. During this period of sunspot minimum no solar variations in the blue region of the spectrum greater than 0.3 pct have occurred. Ionospheric observations show, however, that ultraviolet components of the solar radiation are larger during periods of sunspot maxima and the visual spectrum observations must therefore be continued throughout at least one sunspot cycle before we can say definitely that solar radiation is virtually constant over decades.

In contrast to the apparent constancy of the incoming radiation, the reflectivity of the Earth would appear to be easily changeable. Clouds, snow, and ice reflect most of the sunlight that fails on them, whereas the ocean surface, vegetation and bare ground are highly absorbing for visible light. At present about 50 pct of the earth's surface is normally covered with clouds, while large areas are capped with snow and ice, particularly during winter. An average of 36 pct of the incoming sunlight is reflected back to space without being absorbed [*Danjon,* 1954, p. 734; *Byers,* 1954, p. 303]. The average air temperature would decrease by one degree centigrade if the reflection increased to 37 pct through increased cloudiness or a spreading of the snow- and ice-covered areas [*Wexler,* 1956, p. 488].

Dust in the upper air also scatters and reflects sunlight before it can reach the ground and ocean surfaces. After the explosion of the Volcano Krakatoa in 1883, the incoming radiation from Sun and sky decreased by five to ten per cent for three years [*Wexler,* 1956, p. 485]. Changes in the water vapor, ozone, or carbon dioxide content of the air change the amount and character of the infrared absorption. Calculations by *Plass* [1956, p. 141] indicate that a 25 per cent change in the carbon dioxide content of the air would change the average air temperature by roughly one degree centigrade.

The factors affecting the average air temperature are interrelated; there are in fact what electronic engineers call 'feedback' relationships between them. These feedback linkages are both positive and negative. For example, an increase of air temperature from whatever cause would result in a melting of part of the snow and ice cover of the Earth and a corresponding reduction in the reflection. Consequently, the amount of absorbed radiation would increase and the temperature would rise still further. This is a positive feedback. Similarly, an increase of average air temperature would increase the evaporation from the oceans, hence the water-vapor content of the air and the absorption of infrared radiation. The temperature would not increase without limit, however, because an increase in evaporation must eventually result in an increase of cloudiness as the water vapor condenses, hence an increase in the proportion of reflected sunlight. This is a negative feedback. Such complex feedback linkages tend to hunt or oscillate, with time constants determined by the speed of the different processes involved.

Thus far we have been discussing comparatively small changes in average air temperature over the Earth. Such changes may be of great significance; it is generally estimated by meteorologists that a four-degree drop in average air temperature would be sufficient to bring on a new ice age [*Wexler,* 1956, p. 488; *Wundt,* 1933, p. 241]. But with present meteorological observing facilities they would be almost impossible to measure. What is observed are local changes of much greater magnitude. These must be brought about chiefly by variations in atmospheric and perhaps oceanic circulation, specifically in the locations of north-south transport of heat and matter.

For example, the January mean temperature at Spitzbergen increased by 24° from 1913 to 1937, whereas during almost the same period there was a three- to five-degree drop in January mean temperature in the Great Basin of the western United States [*Wexler,* 1956, p. 485].

Because of the complex relationship between the amounts of insolation and infrared absorption on the one hand and the circulation patterns of north-south transport on the other, it is by no means certain whether an increase of insolation or absorption would bring on a colder or a warmer climate.

The circulation patterns are profoundly affected by the distribution of continents and oceans, and therefore it is of great importance to make comparative studies of past climatic changes in the northern and southern hemispheres, because of their markedly different patterns of sea and land. Since changes in the intensity of the north-south circulation should have different effects in high and low latitudes, it is also necessary to attempt to determine the nature of simultaneous climatic changes in different latitude zones.

The great ice caps of Antarctica and Greenland and the mountain glaciers throughout the world are remarkable indicators of climatic change. During periods of warming or reduced precipitation the glaciers retreat; when the atmosphere is cooled or snowfall increases, they thicken and rapidly advance. Moreover, the layers of ice laid down in successive years constitute an unrivalled record of events on Earth during past millenia.

Many aspects of glaciers will be studied during the IGY. Among the most significant from the standpoint of the heat and water budget of the Earth will be the thickness of the ice. This will be measured by the seismic techniques used in prospecting for oil. Bore holes and cores will also be taken to study the frozen record of the past.

Ice caps now cover about three per cent of the Earth's surface. A melting of two feet per year over these surfaces seems quite possible from present data. This would result in a rise of sea level of about an inch per year or roughly ten feet in one hundred years. Even such a rise as this would bring serious consequences to many thickly populated coastal areas.

The sediments of the deep-sea floor, like the ice caps, contain a detailed climatic record extending back over many thousands of years. For example, variations in the numbers of limy shells of the tiny animals called foraminifera reflect variations in the oceanic circulation near the surface. The ratios of oxygen isotopes in these shells tell us something about past ocean temperatures. At least part of the present temperature differences we can measure between different layers in deep-sea sediments may be the result not of heat flow from the Earth's interior but of warmer temperature of the deep ocean waters a few hundreds or thousands of years ago. Studies of these sediments and their significance for climatic change will be an important part of the series of oceanographic expeditions to be conducted during the International Geophysical Year.

The meteorologist and the oceanographer can seldom use that peerless tool of the laboratory scientists, the controlled experiment. As substitutes for experiment they must attempt to make comparative investigations of the behavior of the Earth fluids under different conditions. For this reason a major part of the IGY meteorological program will be focussed on comparisons between the southern and the northern hemispheres.

Because the Earth is closer to the Sun in January than in July, the southern hemisphere receives about six per cent more radiation in summer than does the northern. The geometry of the two hemispheres is also quite different. In the north, the polar sea with its thin, cracked skin of ice is surrounded by continents; in the south a continent nearly twice the size of the United States, having an ice-covered surface two miles above sea level, lies at the pole and is surrounded by the great southern ocean. This high central plateau, sheathed in darkness for six months each year, is a focal point for inward-circling storms and outward surges of cold air. The weather conditions in the Antarctic are nearly incredible; for example, wind velocities at Adelie land have averaged 110 mi/hr for a day, more than 60 mi/hr for a month and about 40 mi/hr for an entire year. The American IGY party now maintaining a vigil at the South Pole have already recorded temperatures below −100°F with 15- to 20-knot winds.

As is well known, the testing of large atomic weapons produces considerable amounts of radioactive substances, some of which decay rather slowly. A large part of the radioactive material produced by atomic weapons tests is injected into the upper strata of the air and can be used by meteorologists as a tracer of atmospheric movements, for example to determine the rate at which the air at different levels is carried from the northern to the southern hemisphere and vice versa, and the rate of mixing between the upper and the lower atmosphere. An important IGY objective will be world-wide measurements of these artificially radioactive substances.

A slight excess or deficit in the input of solar energy over the output of infrared radiation from the Earth may cause large changes in weather and, if long continued, in climate. At present we are unable to determine whether such differences between income and outgo exist. Here the Earth satellite program shows great promise; one of the first satellites will carry relatively simple equipment for measuring the difference between the amounts of incoming and outgoing radiation at all points over its path [*Wexler*, 1957, p. 144]. Later satellite experiments will include actual mapping of the Earth's cloud and snow cover, allowing accurate and continuous measurements of the amount of sunlight reflected from the Earth, a quantity that can at present only be rather crudely estimated.

A change in average air temperature represents, of course, a gain or loss of heat from the air, but it need not represent a gain or loss from the ocean-atmosphere-glacier system of the Earth. On the other hand, an excess of heat could be stored for long periods on the Earth without much change in the temperature of the lower air. There are two great mechanisms for this: one is the melting of ice caps, the other is the heating of the deep waters of the ocean. The latter has by far the larger capacity. The energy required to melt all the ice in Antarctica is equivalent to about two and a half years' supply from the Sun reaching the Earth's surface at the present rate of 175,000 cal/cm^2 yr. This same amount of energy would raise the average temperature of the ocean by only a little more than one degree C. (On the other hand, the melting of ice caps would be somewhat more obvious to everyone, since it would result in a rise of sea level by at least 200 ft, and the consequent destruction of most of the world's largest cities!)

Because of the great heat capacity of the ocean, many meteorologists and oceanographers now believe that climatic changes lasting over decades or centuries may be intimately related to changes in the circulation of the deep sea. Effective techniques for studying this circulation have become available only in the last few years, and it is little understood. We know that cold water sinks to great depths from the surface in high latitudes, moves slowly toward the equator and perhaps across it, and returns by an unknown path to the starting point. The time required for the round trip is not known; it may be measured in decades or millenia. Nor do we know whether the circulation is steady, or intermittent like the flushing of water in a bowl.

One of the major enterprises of the International Geophysical Year will be a series of great oceanographic expeditions, conducted by 70 ships belonging to many countries. Their principal objective will be to obtain a comprehensive picture of the temperature and other properties of the deep sea waters, and to make direct and indirect measurements of their motions.

President Eisenhower has said that water is rapidly becoming our most critical natural resource. During the last few years, serious attempts have been made to develop inexpensive machines for converting sea water into fresh water. The fact is, of course, that nature herself operates a most effective distillation system. Nearly one-third of all the energy of sunlight falling on the sea surface is utilized in converting sea water to fresh water by evaporation. The immense quantity of solar power used in this way is several thousand times all the power produced by our industrial society from hydroelectric power and the burning of coal, oil, and natural gas.

The total quantity of water evaporated, if all of it fell on the surface of the land and were uniformly distributed, would result in an average rainfall of over one hundred inches a year. Evidently the trouble with the natural distillation process is not the quantity of fresh water produced, but rather that nature's pipe lines are badly placed. Too much water moves to some areas and not enough to others; moreover, the valve system seems to be capriciously managed. Sometimes the discharge is too great, bringing floods, while at other times there is only a trickle and droughts occur. Can anything be done about this faulty distribution system?

The quantity of solar energy used in driving the engine of the sea and the atmosphere is so great compared to any of the energy sources under man's control that it would seem impossible for us to affect weather or climate materially by any human action. Yet a close look shows there may be some things we could do. Many of the processes in the atmosphere are metastable: a slight action may initiate a very large scale process. We might learn how to regulate climate if we could find the right lever to pull.

One may predict that with the coming of greater understanding promising methods for control of weather and climate will be found. The average reflectivity of the ground surface over large areas might be reduced, for example, by rapid melting of the snow cover, thus increasing the percentage of sunlight absorbed. On the other hand, it might be possible to shut off some of the Sun's radiation before it reaches the Earth's surface, for example, by injecting a small amount of absorbing or reflecting substances into the upper atmosphere.

During our lifetime we may be witnessing an example of one way in which human actions can affect weather and climate. Since the beginning of the industrial revolution, an amount of carbon dioxide equal to about 12 pct of the total already present in the atmosphere has been produced by the burning of coal, oil, and natural gas. The ability of the ocean to absorb carbon dioxide is very great and probably most of the amount added to the atmosphere during the last century has gone into the sea. During the next hundred years, however, the increasing use of fossil fuels in our world-wide industrial civilization should result in the production of about 1700 billion tons of carbon dioxide, 70 pct of the amount now in the atmosphere [*Revelle* and *Suess,* 1957, p. 19]. Because of the rapid increase in the production rate, the fraction of the added carbon dioxide absorbed by the ocean will be lessened and an increase of perhaps 20 pct in atmospheric carbon dioxide can be expected. The effect of such an increase is not easy to predict, but there is some theoretical reason to believe that it could result in a warming of the lower atmosphere by several degrees. Thus by consuming, within a few generations, the fossil fuels laid down in sedimentary rocks over many hundreds of millions of years, we are conducting, more or less in spite of ourselves, a great geophysical experiment. It is of vital importance to keep accurate records of this experiment in order to increase our understanding of the mechanisms controlling climate. With this in mind, careful measurements will be made during the IGY of the carbon dioxide content of the atmosphere, and studies will be initiated to refine our estimates of the absorption of carbon dioxide in the sea.

REFERENCES

BYERS, HORACE R., The atmosphere up to 30 kilometers, *The Earth as a Planet,* pp. 299–370, 1954.

CHAPMAN, SYDNEY, Solar influences on the upper atmosphere, *The Sun's effects on the Earth's atmosphere,* Tech. Rep. 2, High Altitude Obs. Univ. Colorado, pp. 11–20, Oct. 1956.

CRAIG, HARMON, Distribution, production rate and possible solar origin of natural tritium, *Phys. Rev.,* 105, 1125–1127, 1957.

DANJON, ANDRÉ, Albedo, color, and polarization of the Earth, *The Earth as a Planet,* pp. 726–738, 1954.

EVANS, JOHN W., Variations of the Sun, *The Sun's effects on the Earth's atmosphere,* Tech. Rep. 2, High Altitude Obs. Univ. Colorado, pp. 1–10, Oct. 1956.

Plass, G. N., The carbon dioxide theory of climatic change, *Tellus,* **8**, 140–154, 1956.

Revelle, R., and Hans E. Suess, Carbon dioxide exchange between atmosphere and ocean, and the question of an increase of atmospheric CO_2 during the past decades, *Tellus,* **9**, 18–27, 1957.

Starr, V. P., On the production of kinetic energy in the atmosphere, *J. Met.,* **5**, 193–196, 1948.

Starr, V. P., and R. M. White, Balance requirements of the general circulation, *Studies of the atmospheric general circulation,* Mass. Inst. Tech. Final Rep., pt. 1, General Circulation Proj., pp. 186–242, 1954.

Wexler, Harry, The circulation of the atmosphere, *Sci. Amer.,* Sep. 1955.

Wexler, Harry, Variations in insolation, general circulation and climate, *Tellus,* **8**, 480–494, 1956.

Wexler, Harry, Meteorology in the International Geophysical Year, *Sci. Mon.,* **84**, 141–145, 1957.

Wundt, W., Änderungen der Erdalbedo während der Eiszeit, *Met. Zs.,* **50**, 241–250, 1933.

Scripps Institution of Oceanography, University of California, La Jolla, California

Reprinted from GEOPHYSICS AND THE IGY, Geophysical Monograph No. 2, American Geophysical Union, Washington, D. C., July 1958

The Seasonal Budget of Water

WALTER H. MUNK

Suppose one were to examine the Baltimore tide record after suppressing daily and semi-daily tides by a suitable scheme of averaging. The record would then show a pronounced seasonal trend. The mean level in March would be lower by something like 20 cm than in September. This result is not an isolated instance, but part of a coherent picture in the entire North Atlantic Ocean. A relatively low sea level in February to May by a sizable fraction of a foot can be found along the East Coast from Florida to Maine, at Bermuda and the Azores, from the Mediterranean to Norway, along Greenland and Iceland [*Pattullo* and others, 1955]. In general terms this holds also for the North Pacific Ocean. In the southern hemisphere the relation appears to be reversed, with sea level high in March and low in September. "Sea level is low in spring" may serve as a very rough first approximation.

What are the causes of this seasonal variation in sea level? It is far easier to say what cannot be the principal causes. The gravitational attraction of Sun and Moon give rise to a seasonal tide about ten per cent of the observed value. The yielding of the sea surface under the direct effect of atmospheric pressure likewise amounts to only about one-tenth the observed amount. Apparently the largest effect, at least in moderate latitudes, is the heating and cooling of the water by solar radiation, back radiation, evaporation, etc. [*Pattullo,* 1957].

In turn this means that most of the observed variation in sea level represents a thermal expansion and contraction of the water rather than a shifting water mass. A pressure recorder at the sea bottom would note a relatively small seasonal variation, that is, conditions are nearly 'isostatic.'

In high latitudes the situation is apparently different. From what one can tell on the basis of the present very inadequate data, conditions there are not at all isostatic. It looks as if during winter in each hemisphere, water is moved from the polar and subpolar seas into the subtropical regions; in summer the transport is in the opposite sense. (The fact that the Arctic Ocean partakes in this seasonal trend is known to us due to the cooperation of Russian oceanographers who made available some observations in response to a request at the Brussels IGY meeting, 1955. Previously no Arctic tide observations of sufficient duration had been known to us.)

Our present picture is based on something like 500 tide gage stations. During IGY we expect to occupy an additional 200 to 250 stations. The positioning of these stations has been determined largely by the gaps in the present distribution. Accordingly the emphasis is, in the order given, on (1) islands, (2) the southern hemisphere, and (3) measurements of the specific volume of water so that the degree of isostasy can be computed.

The international scale of this undertaking is noteworthy. At the time of this writing, the United States and Argentina have plans for 20 stations each, New Zealand, South Africa, and Spain plans for 15 stations each, Mexico 14, Australia 11, Italy and USSR 10 each, etc. The present total is 226 stations to be established by 27 countries. One of the American stations will be located at Pt. Barrow, Alaska, with special efforts to obtain records even when the sea is frozen.

So far we have dealt with shifts in water mass within the oceans. On the basis of the present data we have attempted also to find out whether the total mass of ocean water varies appreciably throughout the year. Our best guess is that between October and March the northern hemisphere oceans lose 2×10^{19} grams, while southern hemisphere oceans gain 1×10^{19} grams, leaving a net loss of 1×10^{19} grams, equivalent roughly to a sea level drop by 4 cm [*Munk,* 1956]. The uncertainty is such that the total loss may be twice as large or there might be none at all. We do hope that the IGY effort will narrow the uncertainty by a good deal.

Suppose we accept the above values for the moment. Where can one store 10^{19} grams of water during March? The atmosphere contains two to three grams of water per square centimeter, and the seasonal variation is only about ten per cent of this value. This is inadequate.

Contribution from the Scripps Institution of Oceanography, New Series. 1007

Reproduced by Permission

Snow over Siberia alone amounts to about one-third of the required amount, and maximum storage does occur at the required time, in northern spring. Recently, *van Hylckama* [1956] has completed a global survey of variable detention of moisture in the form of snow, organic material, moisture in the soil and ground water. His estimates are that maximum detention for the Earth is during March and April, minimum detention in September and October, and that the total range equals 0.5 to 0.75×10^{19} grams. In magnitude as well as phase this agrees with our rough estimates based on oceanic measurements. Thus there is some hope that the global water budget might be balanced in a rough way on the basis of the IGY effort.

There is, moreover, opportunity for making a rough check as to whether such a budget is in accord with other considerations. Clearly a shift of water mass towards the equator increases the Earth's moment of inertia, and accordingly, if angular momentum is to be conserved, the Earth's angular velocity must decrease or the length of day increase. The expected seasonal range in the length of day due to shifts in water mass is of the order of 0.1 milliseconds. Astronomic measurements indicate a total range of about 0.7 milliseconds. Most of this range is due to winds [*Mintz* and *Munk*, 1954] but the amount due to shifts in water is evidently not negligible. Inasmuch as the meterologic and astronomic observations will be taken with particular care during IGY, there is a possibility that the effect of shifts in water can be isolated.

There is yet another astronomic effect. On account of the asymmetrical distribution of sea and land, a shift in water mass will tilt the axis of rotation with respect to the body of the Earth. The expected amount is of the order 0″.03, or roughly a shift of the pole of rotation by three feet. The observed annual wobble is about ten times larger and caused principally by shifts in air mass. Here again there might be a chance to isolate the water term.

In closing one must emphasize that there are some difficulties associated with the water-budget problem that have not been discussed here. The reason for emphasizing this particular portion of the oceanographic program is that it fits rather well into the framework of the International Geophysical Year, for the following reasons: (1) global observations are definitely required; (2) the observations must be synchronous; (3) the period of the phenomenon is one year; (4) cooperation of various geophysical disciplines are required: oceanography, meteorology, glaciology, and hydrology; and (5) there is a relation to the IGY program involving precise determinations of longitude and latitude.

REFERENCES

MINTZ, YALE, AND WALTER MUNK, The effect of winds and bodily tides on the annual variation in the length of day, *Mon. Notes R. Astron. Soc., Geophys. Sup.*, **6**, 566–578, 1954.

MUNK, WALTER, Geophysical Discussion, R. Astr. Soc., *Observatory*, **76**, 56–57, 1956.

PATTULLO, JUNE, The seasonal heat budget of the oceans, Dissertation, University of California, 1957.

PATTULLO, JUNE, WALTER MUNK, ROGER R. REVELLE, AND ELIZABETH STRONG, The seasonal oscillation in sea level, *J. Marine Res.*, **14**, 88–155, 1955.

VAN HYLCKAMA, T. E. A., The water balance of the Earth, *Pub. in Climatology*, Drexel Inst. Tech., Lab. Climatology, Centerton, N. J., **9**, 57–117, 1956.

Scripps Institution of Oceanography, La Jolla, California

(380)

Reprinted from SCIENCE, July 25, 1958, Vol. 128, No. 3317, pages 204–205.

Thorium Content of Ocean Water

Two samples of ocean water from the Pacific, one collected at the surface, near the coast, outside San Diego Bay in the summer of 1956, and the other taken at a depth of 3500 m from longitude 124° 41.0′ W, latitude 33° 54.5′ N on 25 March 1957, have been analyzed for total thorium alpha activity.

Each sample was approximately 25 liters in volume. Three hundred milliliters of concentrated HCl, 25 ml of $0.18M$ $Fe(NO_3)_3$ solution, and approximately 5000 count/min of Th^{234} beta tracer were added to each sample at the time of collection. The samples (in polyethylene containers) were stored for several weeks before they were analyzed.

The method of analysis was as follows. To carry the thorium, ferric hydroxide was precipitated by adding slight excess of ammonium hydroxide to the sample solution. The hydroxide precipitate was dissolved in dilute hydrochloric acid. Nitric acid and perchloric acid were added to the solution, which was then evaporated to fumes of perchloric acid. Addition of hydrofluoric acid and repeated fuming served to remove silica. The final solution was diluted to decrease the concentration of perchloric acid to $3N$ and was then transferred to a 4- by 100-mm Dowex-50 resin column to separate the thorium from carrier and extraneous ions (*1*). The thorium on the column was washed repeatedly with $3N$ hydrochloric acid. It was then eluted from the column with $0.5M$ oxalic acid. This eluant was treated with nitric acid and perchloric acid, heated to fumes of perchloric acid three times, diluted, and again transferred to the resin column. After washing with $3N$ hydrochloric acid, the carrier free thorium was eluted with $0.5M$ oxalic acid, and the eluant was collected on a tantalum plate. The plate was taken to dryness under a heat lamp, flamed, and counted for alpha and beta activity. The beta count served to determine the fraction of added Th^{234} which was recovered. From the observed alpha activity the total thorium alpha activity in the sample was calculated assuming complete exchange of thorium with the Th^{234} tracer.

In each of the samples analyzed, additional thorium was obtained from the first eluant and hydrochloric acid washings by taking these through further perchloric acid fumings and resin-column treatments. These second fractions of thorium which were separated from the surface water and deep ocean samples are designated below as S-2 and D-2, respectively.

Samples were counted on an alpha proportional counter at 51-percent geometry. The observed activities, corrected for yield, geometry, background, and reagent blank, are listed in Table 1.

The half-life values of Th^{232}, Th^{230}, Th^{228}, and Th^{227} (the only thorium alpha emitters which occur naturally) are 1.39×10^{10} years, 80,000 years, 1.90 years, and 18.6 days, respectively. Using these values, we calculate the following upper limits of concentration of thorium isotopes in the deep ocean sample (*2*): Th^{232}, less than 5×10^{-11} g/ml; Th^{230}, less than 3×10^{-16} g/ml; Th^{228}, less than 7×10^{-21} g/ml; Th^{227}, less than 2×10^{-22} g/ml.

Some information concerning the approximate isotopic composition of the thorium which was isolated from our surface water sample was obtained by observing the change in its alpha activity with time. The data for sample S-2 are shown in Table 2. The growth of alpha activity during the first 20 days indicates the presence of Th^{227} or Th^{228}, or both.

The fact that the activity at 73 days is higher than the initial activity shows that Th^{228} is present. If we represent the initial activities (in disintegrations per hour per liter of water) of the individual nuclides by $A_{Th^{232}}$, $A_{Th^{228}}$, and so forth, we may write for the total initial alpha activity

$$9.6 = A_{Th^{232}} + A_{Th^{230}} + A_{Th^{228}} + A_{Th^{227}}.$$

Table 1. Thorium alpha activity in Pacific Ocean water.

Sample	Th^{234} tracer recovered (%)	Th alpha activity (disintegration/hr liter)
	Surface	
Fraction S-1	10	9 (± 2)
Fraction S-2	40	9.6 (± 0.5)
	Deep ocean	
Fraction D-1	28	0.3 ± 0.3
Fraction D-2	45	0.4 ± 0.4

Table 2. Alpha activity in thorium isolated from surface water, sample S-2.

Elapsed time after chemical processing (day)	Total alpha activity in sample (disintegration/hr liter)	
	Observed	Calcd.
0	9.6 (± 0.5)	
3	13.5 (± 1.0)	13.5
4	15.2 (± 0.9)	14.6
7	16.6 (± 0.6)	16.7
18	18.5 (± 0.6)	19.0
21	19.1 (± 0.6)	
35	18.7 (± 0.6)	18.3
73	16.7 (± 0.6)	16.0
161	14.8 (± 0.6)	14.3
221	13.7 (± 0.5)	13.7
363	12.8 (± 0.5)	

At 363 days over 99.99 percent of Th^{227} and daughters will have decayed. Allowing for Th^{228} and daughter activity growth and decay during the 363-day interval (*3*) and assuming 100 percent Rn^{220} retention, we write for the total alpha activity at 363 days

$$12.8 = A_{Th^{232}} + A_{Th^{230}} + 3.5\, A_{Th^{228}}.$$

At 21 days the activity of Th^{228} and its daughters will be 4.84 times the initial Th^{228} activity (*3*). The activity of Th^{227} and its daughters will be 2.31 $A_{Th^{227}}$. Hence we write for the activity at 21 days

$$19.1 = A_{Th^{232}} + A_{Th^{230}} + 4.8\, A_{Th^{228}} + 2.3\, A_{Th^{227}}.$$

Solving the above equations, we find:

$A_{Th^{227}} = 1.6$ disintegration/hr liter
$A_{Th^{228}} = 1.9$ disintegration/hr liter
$A_{Th^{232}} + A_{Th^{230}} = 6.1$ disintegration/hr liter

Calculated total alpha activities at various times for a sample which initially had this composition are shown in Table 2 alongside the observed activities in the S-2 surface sample. The calculated and observed values are in good agreement.

Taking the uranium content (*4*) of ocean water as 3.0×10^{-6} g/liter ($A_{U^{238}} = 130$ disintegration/hr liter), we see that in both samples the Th^{230} content is far below the amount required for secular equilibrium with the U^{238} pres-

Contributions from the Scripps Institution of Oceanography, New Series, No. 1008

Reproduced by Permission

ent. In the surface water we find 5 percent or less of the equilibrium quantity of Th^{230}; in the deep sample less than 1 percent of the equilibrium amount.

The equilibrium Th^{227} activity corresponding to a uranium content of 3.0×10^{-6} g/liter is 6 disintegration/hr liter. A comparison with the experimental values listed above shows that the Th^{227} concentration in both the deep water and surface water samples is also below its equilibrium concentration with respect to U^{235}, indicating that not only Th^{230} but apparently also Pa^{231} or Ac^{227}, or both, are precipitated with the sediments.

Using the value 1.3×10^{-13} g/liter for the radium (*5*) content of deep ocean water, we calculate $A_{Ra^{226}} \simeq 17$ disintegration/hr liter. Hence, for the deep sample,

$$A_{Th^{230}}/A_{Ra^{226}} < 0.05$$

The radium content of the water is far in excess of the amount which can be supported by the Th^{230} which is present. Koczy, Picciotto, Poulaert, and Wilgain (*2*) report a similar situation in their Skagerak and Gullmerfjord samples. They suggest that the excess radium may arise from redissolution of radium originating from Th^{230} in the sediments (*6*).

William M. Sackett
Herbert A. Potratz
Department of Chemistry, Washington University, St. Louis, Missouri
Edward D. Goldberg
Scripps Institution of Oceanography, University of California, La Jolla

References and Notes

1. J. W. Barnes, E. J. Lang, H. A. Potratz, *U.S. Atomic Energy Comm. Rept. LA-1845* (1955).
2. These data on the deep ocean sample are in essential agreement with values reported recently by F. F. Koczy, E. Picciotto, G. Poulaert, and S. Wilgain for samples of coastal waters collected in the Skagerak and Gullmerfjord [*Geochim. et Cosmochim. Acta* 11, 103 (1957)]. The total thorium alpha activity in our surface water sample, however, is considerably higher than the average value reported by Koczy *et al.* Our surface water sample was collected near the coast and may not be a truly representative specimen of ocean surface water.
3. The growth factors 3.5, 4.8, and 2.3 were calculated by the method of H. Bateman [*Proc. Cambridge Phil. Soc.* 15, 423 (1910)]. Tables of these values for the naturally occurring radioactive series have been published by H. W. Kirby [*Anal. Chem.* 26, 1063 (1954)].
4. M. Nakanishi, *Bull. Chem. Soc. Japan* 24, 36 (1951); E. Rona, L. O. Gilpatrick, L. M. Jeffy, *Trans. Am. Geophys. Union* 37, 697 (1956).
5. H. Faul, Ed., *Nuclear Geology* (Wiley, New York, 1955), p. 116.
6. Contribution from the Scripps Institution of Oceanography, New Series No. 1008. This investigation was supported in part by a fellowship grant from the Aluminum Company of America to W. M. Sackett and was aided further by facilities provided by the Los Alamos Scientific Laboratory and by funds supplied under contract No. AT(11-1)-581 between Washington University and the U.S. Atomic Energy Commission.

19 February 1958

Reprinted from The Journal of the Acoustical Society of America, Vol. 30, No. 5, 470–477, May, 1958
Copyright, 1958 by the Acoustical Society of America.
Printed in U. S. A.

Arrays for the Investigation of Ambient Noise in the Ocean*

Victor C. Anderson
University of California, Marine Physical Laboratory of the Scripps Institution of Oceanography, San Diego 52, California
(Received November 17, 1957)

A discussion of the important parameters to be considered in the use of directional arrays for the study of noise fields in the ocean leads to specialized array designs. Some properties of circular and spherical arrays composed of omnidirectional elements are presented. Consideration of these properties leads to an optimum selection of geometry and element spacing for each of two cases: a distributed noise source, and a set of point noise sources.

The calculation of directivity index for a spherical array is carried out by the use of the space-correlation functions of an isotropic noise field.

The measured, broad-band directivity pattern of a model circular plane array as a function of frequency is also shown.

INTRODUCTION

The study of ambient noise in the ocean forms a fundamental part of the Navy's sonar problem. Considerable effort has been expended on the measurement of the spectral distribution of the noise received from a hydrophone suspended in the ocean.[1] Such measurements constitute an important facet of our present knowledge of the acoustic properties of the ocean. However, for a more complete description of the ambient noise it is necessary to extend these measurements beyond the frequency domain, determining, in addition to the power spectrum of the ambient noise, the dependence of ambient noise energy on direction of arrival and the variation or fluctuation of the received energy with time. A number of theoretical studies based on various statistical models have been made,[2,3] but few experimental measurements of these properties have been carried out.

If the ambient noise observed in the ocean followed the convenient Gaussian noise model, the directivity of the noise could be readily determined by a series of measurements with a trainable directional transducer. Unfortunately, the variation from measurement to measurement is so large that the noise cannot be treated as a stationary process over the period of observation. Hence, to obtain a meaningful measurement of the directivity it is necessary to make simultaneous measurements of noise energy received from a number of different directions, preferably all possible directions. The complexity of the instrumentation required to make measurements of this type is a deterrent which has delayed the determination of the bearing dependence of the noise. With recent technological developments it is now feasible to undertake the instrumentation for a noise study of this type. This paper deals with one aspect of the instrumentation.

The obvious solution to the problem of simultaneous bearing observations is to use a multiple hydrophone array system which incorporates a multiple tap delay line at the output of each hydrophone. Suitable interconnection of different delay combinations would then electrically steer or phase the array for each preferred direction. This paper is not concerned with the technical problems associated with the construction of such an array, but rather, presents the consideration of the optimum configuration for such an array designed to measure the ambient noise.

BASIC ARRAY PARAMETERS

Number of Elements

There are three basic parameters to consider in the design of an ambient noise array; the number of elements, the geometry, and the inter-element spacing. The first of these three may be determined simply. The choice of the number of elements is based on practical considerations of the acceptable complexity of the steering system. These practical considerations have led to the selection of 30 and 32 element arrays for the ambient noise study underway at the Marine Physical Laboratory. Selection of the remaining two parameters, the geometric distribution of the elements and the element spacing, is a bit more complicated.

Array Geometry

Assuming small deviations from an isotropic noise field are to be measured, it is desirable to maintain a high order of symmetry in the geometrical distribution so that the directivity patterns formed by electrical steering are nearly identical. It is also desirable to have a uniform density of elements in the region of space occupied by the array, thereby keeping the distance between any element and its nearest neighbor as large as possible. This will reduce the correlation between

---

* This work represents one of the results of research carried out under Contract NObsr-72512, NE 120221-4-5-6 with the Bureau of Ships, Navy Department. Contribution from the Scripps Institution of Oceanography, New Series. No. 1009

[1] Knudsen, Alford, and Elming, J. Marine Research Sears Foundation 7, 410–429 (1948).

[2] R. E. Roberson, J. Acoust. Soc. Am. 23, 353–358 (1951).

[3] C. Eckart, J. Acoust. Soc. Am. 25, 195–199 (1953).

Reproduced by Permission

elements, and in that way effect maximum array gain as will be brought out later.

As will be shown later, the expected distributions of noise sources in the ocean lead to a choice of two element configurations; one spherical, and the other a plane circular configuration. The actual configurations are based on regular geometric figures; a great stellated icosohedron for the three-dimensional array and a hexagonal distribution for the plane array. These two configurations are shown in Fig. 1. A hydrophone is located at each vertex in the figure, 32 hydrophones for the icosohedron, and 30 for the plane array. The icosohedron has two sets of axes of symmetry, one set of 10 and one set of 6, giving rise to a complete set of 32 preformed beams which may be described by two very similar beam patterns. The plane array has six axes of symmetry, and, by symmetrically dividing steering directions between the six axes, a full set of 48 preformed beams in the horizontal plane may be described by five typical directivity patterns.

Inter-Element Separation

Selection of the inter-element spacing requires a consideration of the effect of the spacing on the electrical output of the array. Typically, it is necessary to assume, for the purpose of analysis, a stationary process. Although this appears to contradict the earlier statement as to the true nature of the ambient noise, it is a legitimate assumption to make in the selection of array parameters. The voltage output of an n-element array is given by the general expression

$$E=\sum_{1}^{n} e_i(\gamma_i,\tau_i), \qquad (1)$$

where E is the voltage output of the "steering line," i.e., phasing and summing networks, $e_i(\gamma_i,\tau_i)$ is the voltage output of the ith hydrophone, which is located at a vector distance γ_i and delayed by a time delay τ_i.

The power output is then proportional to

$$\langle E^2\rangle=\langle\sum_{1}^{n}\sum_{1}^{n} e_i(\gamma_i\tau_i)e_j(\gamma_j\tau_j)\rangle, \qquad (2)$$

where the brackets $\langle\,\rangle$ signify a time average.

$$\langle E^2\rangle=\langle\sum_{1}^{n} e^2\rangle+2\sum_{i=1}^{i=j}\sum_{j=1}^{n} P_{ij}(\gamma_i-\gamma_j,\ \tau_i-\tau_j), \qquad (3)$$

where P_{ij} is the cross correlation or time averaged product of the ijth element pair.

For signals arriving on the axis of the electrically steered beam, the P_{ij}'s are equal to unity, and $\langle E^2\rangle=\langle n^2e^2\rangle$, while, if the outputs of each element are completely random and statistically independent, the P_{ij}'s are equal to zero, and $\langle E^2\rangle=n\langle e^2\rangle$.

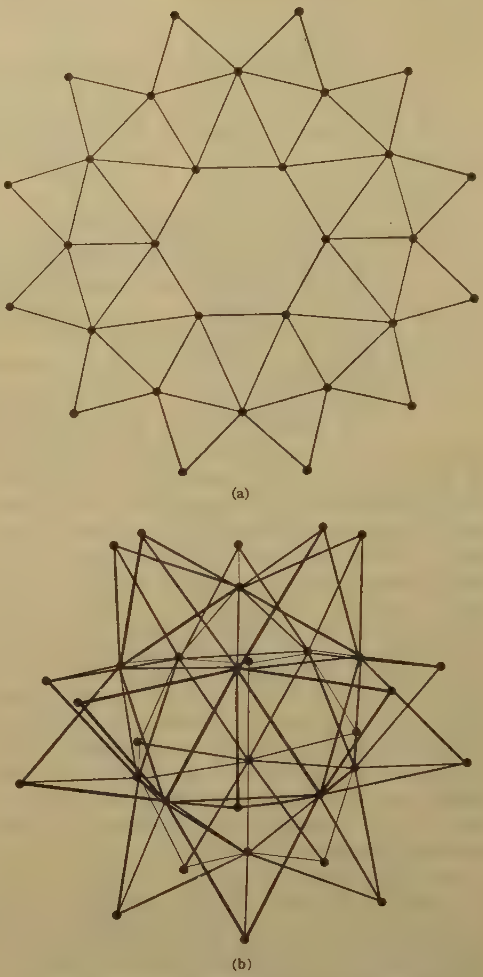

Fig. 1. Geometry of the great stellated icosohedron and the hexagonal plane array.

In order to determine an optimum inter-element spacing for these two arrays it is convenient to use a simplified analysis of the array performance.

The following simplifying assumptions will be made in this analysis: (1) the outputs of each element-delay-line-compensator pair of the array are correlated and add amplitude-wise for noise coming from directions within the major lobe (ψ_0) while they are uncorrelated and add power-wise for noise arriving from directions outside of the major lobe. (2) The major part of the noise is generated by an infinite number of randomly distributed sources so that the energy received within any solid angle is given by the product of the noise density $(N+S)$ and the solid angle ψ, where N represents a uniform isotropic noise field and S is a measure of deviation from an isotropic distribution for different directions.

One may now define the signal-to-noise ratio S'/N' at the output of the array as the ratio of the contribution of the desired signal S within the beam width of the array to the undesired noise composed of the contributions from the N within the beam, and the N and S outside of the beam; i.e.,

$$S'/N' = \left[n^2 \int_0^{\psi_0} S d\psi\right] \Big/ \left[n^2\psi_0 N + n\int_{\psi_0}^{4\pi} S d\psi + (4\pi-\psi_0)nN\right]. \quad (4)$$

Assuming n large and S/N small, and further assuming $S=S_0$ over a solid angle Ψ, and $S=0$ elsewhere, this expression may be further simplified to

$$S'/N' \simeq n\psi_0/(4\pi+n\psi_0)S_0/N \quad \text{for} \quad \psi_0<\Psi \quad (5)$$

$$S'/N' \simeq n\Psi/(4\pi+n\psi_0)S_0/N \quad \text{for} \quad \psi_0>\Psi. \quad (6)$$

It is now convenient to define an array efficiency

$$\alpha = (S'/N')/(S_0/N), \quad (7)$$

which is the bracketed terms of Eqs. (5) and (6). The function α is plotted in Fig. 2 for $n=32$, and for two values of Ψ. These curves show a maximum array efficiency for beam widths ψ_0 equal to the angle subtended by the source. Thus the conclusion is reached that, for maximum efficiency, the beam width of the array should be matched to the width of the source, a conclusion analogous to the choice of an optimum filter in the frequency domain.

However, the angular distribution of the sources in the ocean is unknown at this point, and further, even if known, it might not be possible to match beam widths in practice because of other considerations. There actually are two probable source distributions which should be considered; (1) a large scale distribution, such as that caused by surface distributed sources, and (2), a distribution of point sources in a horizontal plane due to distant ship traffic. In the one case the beam width of the array will of necessity be less than the extent of the source, while in the other it will always be greater.

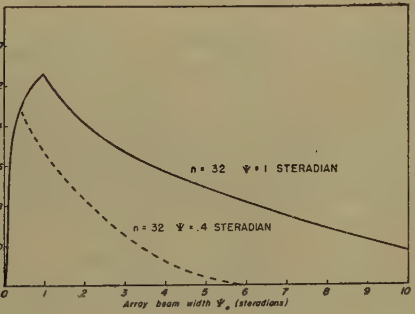

FIG. 2. Array efficiency, finite source.

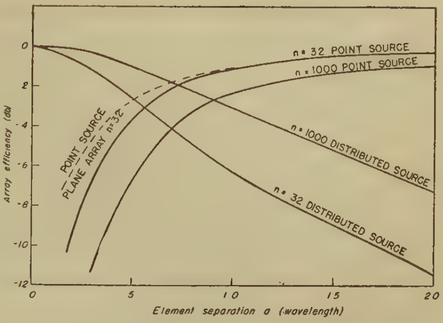

FIG. 3. Array efficiency, point and distribution source.

For these cases, it is possible to obtain from the previous Eqs. (5) and (6) for S'/N', a relation for the array efficiency in terms of the inter-element spacing a in wavelengths.

An approximate expression for the directivity ψ_0 of an array of n elements spaced a wavelengths apart in a cubic lattice, is given by

$$\psi_0 \simeq (1.2/n^{\frac{2}{3}}a^2), \quad (8)$$

where n = number of elements, a = element spacing in wavelengths. The approximation of Eq. (8) is remarkably good, giving the 6 db beam width to ±5% for all solid angles over the range of 0 to 4π. This relationship may be introduced into Eqs. (5) and (6) to obtain S'/N' as a function of a. The array efficiencies for these two cases are then;

$$\alpha_1 = (S'/N')/(S_0/N) = 1/(4\pi a^2/1.2n^{\frac{2}{3}}+1) \quad (9)$$

for the distributed source, and

$$\alpha_2 = (S'/N')/(nS_0\psi/4\pi n) = 1/(1+1.2n^{\frac{2}{3}}/4\pi a^2) \quad (10)$$

for the point source. Note that a slightly different definition for α is used for the point source; Eq. (10), where n = number of elements = theoretical array gain, $S_0\psi$ is the total point source power, and $4\pi N$ is the total noise power.

These equations give rise to the curves of Fig. 3 which indicates a different direction of optimization for the two cases. For a distributed source, the array efficiency rises with decreasing a, corresponding to an increase in beam width, while for a point source the array efficiency rises with increasing a, or, narrowing beam width.

The approximations used to obtain the curves of Fig. 3 begin to break down for small values of element separation where the correlation between outputs of element pairs can no longer be considered negligible. Introduction of the effect of the interelement correlation would cause the efficiency to drop off for low values of a. For a one-half octave band of noise the correlation becomes important for separations approaching values of $a=0.5$. The array dimensions which have been chosen for the MPL spherical array for the investigation of large distributed sources are based on a value of $a=0.6$. This value of a according to the approximate analysis would result in an array efficiency of -3.4 db and would correspond to a beam width of 36 degrees between -6 db points.

CALCULATION OF ARRAY GAIN FOR THE SPHERICAL ARRAY

If quantitative measurements of the directivity of a distributed source are to be made, it is particularly important to establish the array gain since the element spacing is small enough to introduce correlation between element pairs. In order to determine this one must return to the general expression of Eq. (3) and investigate the P_{ij}'s as a function of both element spacing and relative time delay. This may be done for the case of an isotropic noise field of predetermined band width by making use of the equation

$$P(d,\tau)=\frac{c}{2d}\int_{-d/c+\tau}^{d/c+\tau}\rho(\tau')d\tau' \qquad (11)^{4}$$

where d is the distance between the element pair, c is the velocity of sound, and ρ is the autocorrelation function of the noise. The manner in which this function has been computed for the half-octave noise field being considered here is as follows: First, the impulse response of the filter used to determine the band width of the noise was obtained by recording oscillographically its response to a very narrow pulse. The impulse response is shown in Fig. 4. From the impulse response the autocorrelation function of a noise having a power spectrum determined by the filter is obtained by use of the following convolution:

$$\rho(\tau)=\int_0^\infty a(t-\tau)a(t)dt\Big/\int_0^\infty a^2(t)dt. \qquad (12)$$

Carrying out this convolution by numerical integration, the autocorrelation of Fig. 5 is obtained from the impulse response of Fig. 4. From the autocorrelation the space correlation P_{ij} may be determined by numerical integration of Eq. (11).

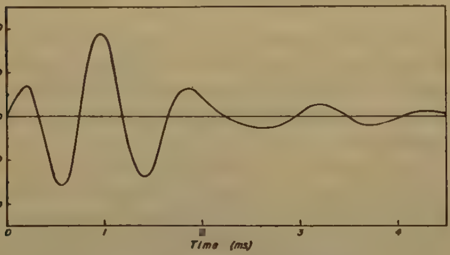

FIG. 4. Impulse response of band pass filter.

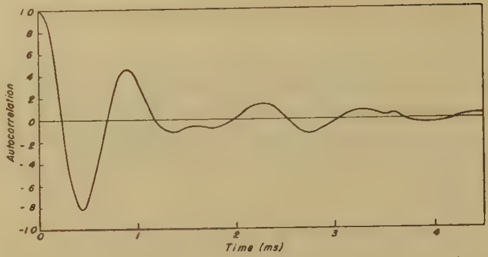

FIG. 5. Autocorrelation function.

Results of these computations are shown in the contour plot of Fig. 6. This function has some very interesting properties. Along the abscissa for $d/r=0$ the function is identical to the autocorrelation function of the half-octave noise field while along the ordinate for $\tau=0$ the function is the simplified space correlation obtained by plotting the time average product of the output of the two elements as a function of separation in an isotropic noise field. The remaining portion of the plot then represents all possible combinations of time delay and element separation. It is interesting to note that the correlation is, in general, highest for values of separation and time delay which are nearly equal to each other. Once having obtained the function of P_{ij} one may now proceed to determine the output of the steered array for a horizontal noise field by enumerating the number of possible element pair combinations, plotting them as points on the d/c, τ plane, obtaining the values of P_{ij} at each of these points and completing the double summation of Eq. (3). The set of points for the spherical array is shown in Fig. 6 superimposed on the plot of P_{ij}. The numbers along side of each point represent the number of element pairs for the particular combination of values of d/c, τ. This summation can now be carried out, and in so doing it is found that the noise output from the array is 0.8 db higher than the noise output predicted for the simple theory wherein the array gain would be equal to n. The actual array gain is 14.25 db.

Directivity Patterns for the Plane Array

For the investigation of point noise sources, the curves of Fig. 3 indicate that it is desirable to use as large a

---

[4] Faran and Hills, *The Application of Correlation Techniques to Acoustic Receiving Systems* (Harvard University Technical Memorandum, 1 November 1952), No. 28.

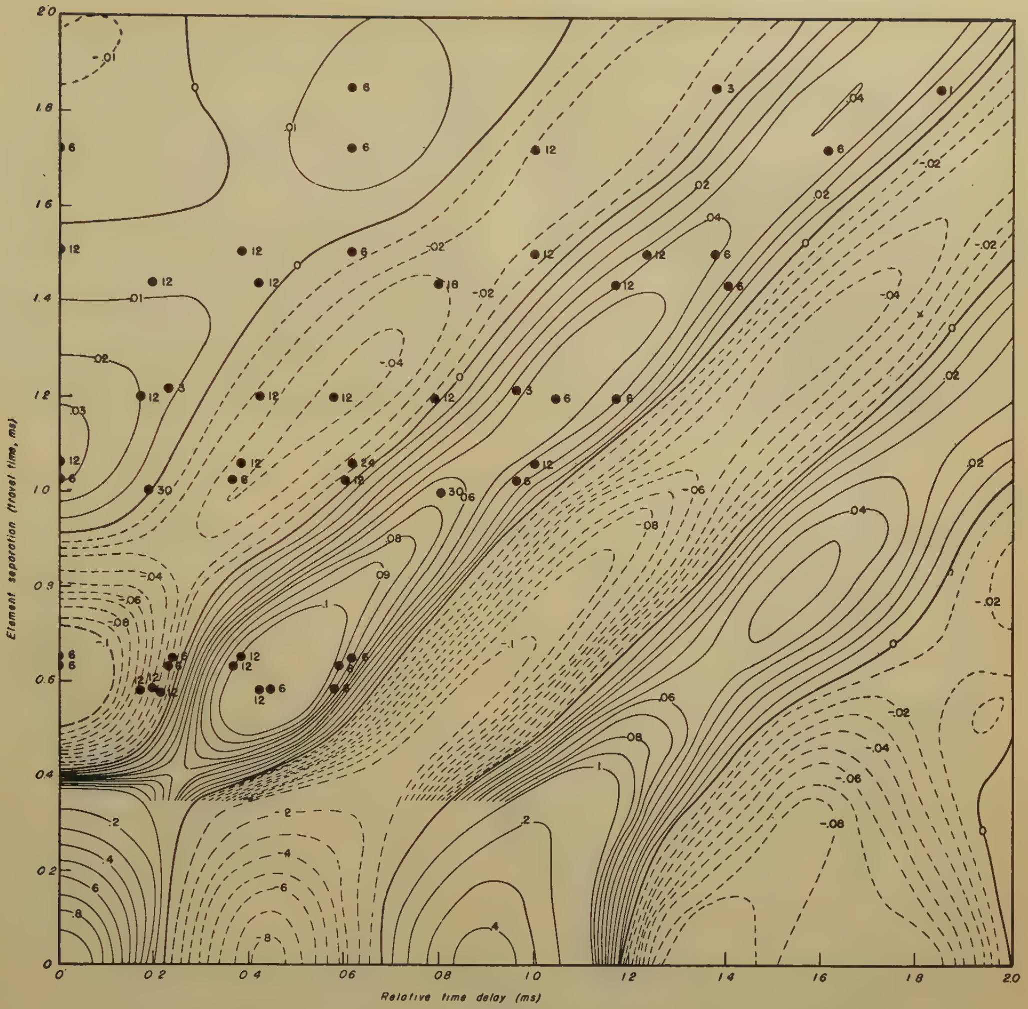

FIG. 6. Space correlation.

spacing as possible to obtain the highest array efficiency. There is a limitation, however, in the narrowness of beams which may be used for such an investigation because of the strong vertical refraction which is always present in the ocean. The refraction causes a spreading in the probable direction of arrival in the vertical plane for a distant target; which is considerably greater than the expected variation in the horizontal direction. Thus, it is desirable to use an array configuration which will give rise to a narrow horizontal beam width and a relatively broad vertical beam width. A horizontal plane array has a desirable characteristic in that its beam width in the vertical direction corresponds to the relatively broad directivity of an end-fire array, while in the horizontal direction it corresponds to the narrower directivity of a broadside element array. If such an array configuration is to be used, it is wise to reconsider the approximate analysis used to obtain the array efficiency of Eq. (10). The dependence of ψ_0 on element separation for a square plane lattice is given by the approximate expression

$$\psi_0 \simeq 1.6/n^{\frac{3}{4}}a^{\frac{3}{2}}. \qquad (13)$$

Introducing this relationship into Eq. (6), a slightly different functional relation for array efficiency is obtained for a plane array,

$$\alpha = 1/(1+1.6n^{\frac{1}{4}}/4\pi a^{\frac{3}{2}}). \qquad (14)$$

This is plotted as the dotted line in Fig. 3. It can be seen that the effect of change in symmetry from spherical to plane is most apparent for values of small element spacing; for values above $a=1$ the efficiency is approximately the same for both the plane and spherical arrays.

Thus, the selection of the inter-element spacing for a plane array to be used in the study of point noise sources will be determined by the desired directivity rather than by the array efficiency inasmuch as very little change in array efficiency occurs for values greater than $a=1$.

The hexagonal structure of Fig. 1 provides a uniform inter-element spacing and reduces the number of different beam patterns by its inherent sixfold symmetry. Using this geometry, it was determined that 48 shoulder-to-shoulder beams would be a desirable number to use in the investigation of the horizontal directivity, giving adequate resolution in the horizontal plane without requiring unduly complex instrumentation.

In order to obtain the relation between element separation and horizontal beam width, a number of directivity patterns were obtained with the use of an analog computer. The computer consisted of a conventional steering line for a sonar array composed of an *L-C* delay line in which uniform incremental delay taps are brought out to a corresponding set of equally spaced parallel conductors on a flat plate. Two such steering lines were used. Each was fitted with a rotatable plate upon which 30 independent brushes were mounted in the hexagonal geometry of the array. The signal was sent into the end of one of the lines, which served as a receiving array simulator. Each brush output of the

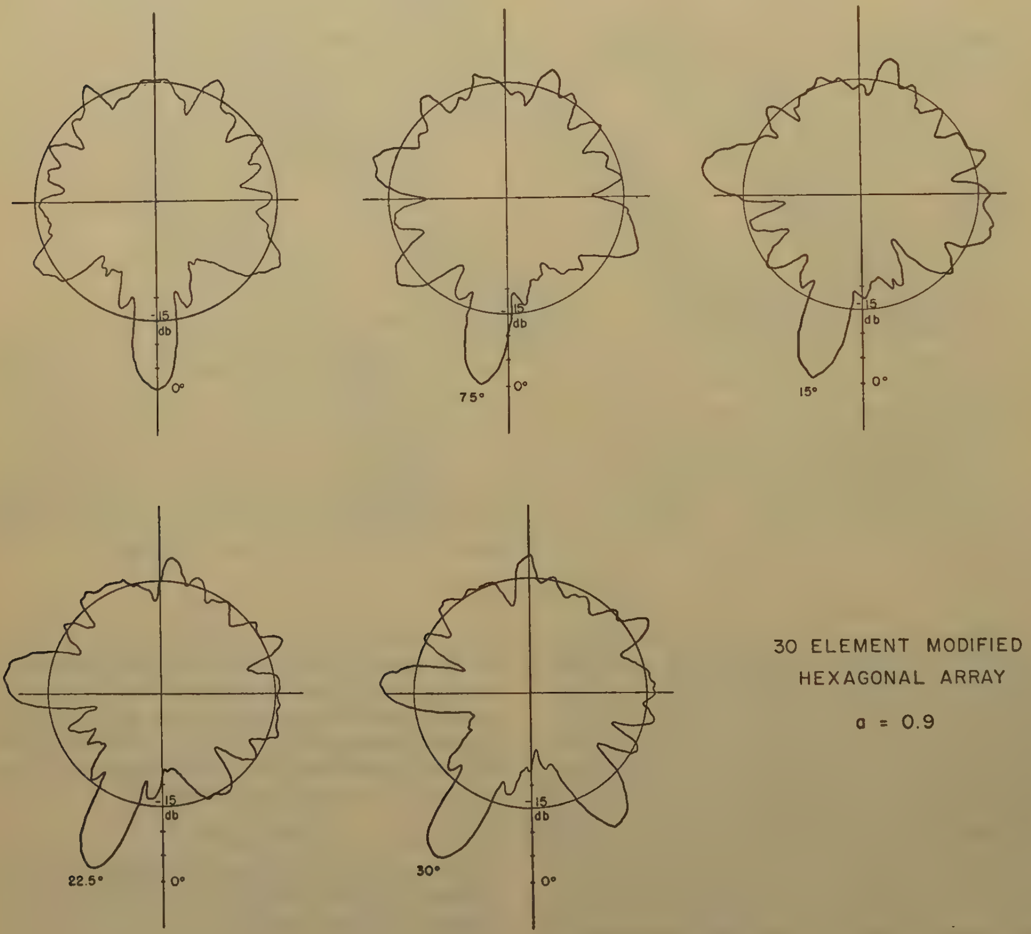

Fig. 7. Directivity patterns, $a=0.9$.

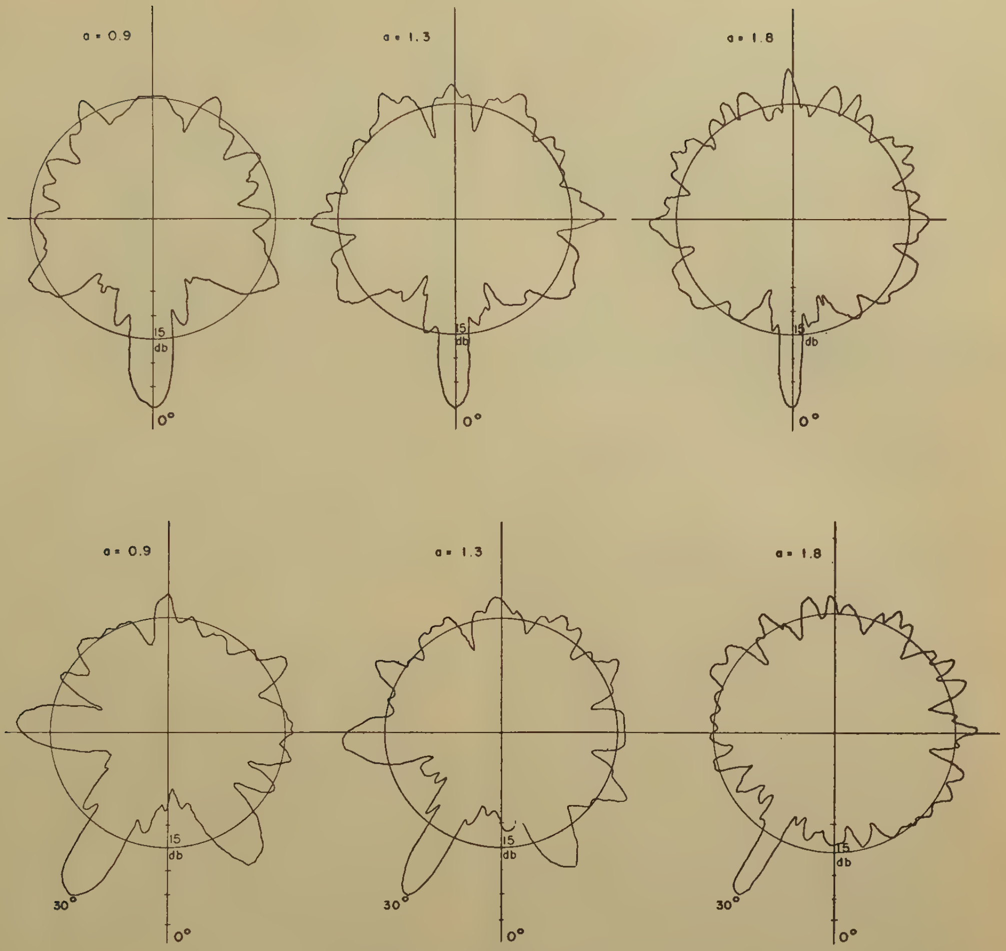

FIG. 8. Directivity patterns, $a=0.9$, 1.3, 1.8.

simulated array was sent through a special variable gain buffer amplifier having a nearly infinite input and output impedance to a corresponding brush on the plate of the second steering line. This second steering line serves its normal purpose of phasing the array outputs for a particular direction of arrival.

The procedure for obtaining the directivity pattern was as follows: The plate on the second steering line was oriented for the desired electrically steered direction and fixed in position. A half-octave band of thermal noise was fed to the input end of the first steering line. The arrival of a signal at an angle θ from the steered direction was then simulated by off-setting the orientation of the first plate by an angle θ from the orientation of the second plate. At each such value of θ the buffer amplifier gains were individually adjusted to give the same signal level at the output of the second delay line. After each channel was adjusted, all amplifiers were connected and the array response for this angle was given by the combined output. These measurements were carried out as a function of center frequency of the noise band and steered direction.

Some of these results are shown in Fig. 7. These directivity patterns of Fig. 7 correspond to $a=0.9$, and are the five directivity patterns which describe 48 preformed beams for the full 360 degrees. The beam widths shown here are somewhat larger than the 7.5 degrees required for 48 shoulder-to-shoulder beams. The directivity patterns of Fig. 8 correspond to values of $a=0.9$, 1.3, and 1.8. Note that increasing a

decreases the side lobes of the directivity patterns. This increased side lobe suppression reflects the effect of operating farther out on the space correlation curve, thereby approaching the ideal array gain of 15 db for a 30 element array. A value of $a=1.3$ gives the correct beam width for 48 shoulder-to-shoulder beams, however, practical considerations of manageable size for handling at sea dictate a maximum separation of $a=1.1$, the separation selected for the ambient noise plane array.

SUMMARY

The optimum design of a receiving array for the study of the anisotropic properties of ambient noise depends on the actual distribution of noise sources. In general the optimum array is one whose beam width is equal to the angle subtended by the noise source. For expected noise source distributions in the ocean, two array configurations are obtained. A three-dimensional spherical array appears to be the best choice for investigation of distributed noise sources while, for point noise sources, a two-dimensional circular array appears to have more desirable properties. An exact solution of the broad band output of the spherical array by the use of the space correlation function is required in view of the small inter-element spacing. This exact solution yields a noise output which is only 0.8 db higher than the −15.45 db obtained with the idealized analysis.

JOURNAL OF SEDIMENTARY PETROLOGY, VOL. 28, NO. 2, PP. 234–235
JUNE, 1958

DISCUSSION

A DEFENSE OF THE TERM ALTERITE

TJEERD H. VAN ANDEL[1]
Scripps Institution of Oceanography, University of California, La Jolla, California

Recently Dorothy Carroll (1957) has discussed and condemned the use of the term "alterite" in heavy mineral studies. The present author coined this term in 1950 for the special needs of a study of the heavy minerals of the Rhine. The alterites in the Rhine are fine-grained, frequently rounded translucent grains of unknown composition. They are very characteristic for sediments of alpine derivation. Later work with sediments of various ages from different parts of the world has shown that alterites are common and often diagnostically important. A few words in defense of the term may therefore be said.

The author is in complete agreement with Miss Carroll where she criticizes the indiscriminate use of the term without proper definition. As a group term "alterite" is necessarily vague and it is virtually meaningless without a description of the grains included. It is also true, as Miss Carroll states, that such group terms might become a convenient "sack" for anything not easily identified and that its use might encourage lazy mineralogists. The present author, however, prefers to believe that most students of heavy minerals seriously strive to identify each grain before resorting to the extreme measure of group classification. It appears to be Miss Carroll's experience that in such an attempt few if any grains would remain unidentified.

It is on this point that we must disagree. In the Rhine study several types of alterites have been distinguished according to parent minerals (epidote-alterite, hornblende-alterite, etc.). This does not imply that it is possible to apply this subdivision to all alterites. On the contrary, most of the grains definitely defy every attempt to identify the parent mineral. Since the coining of the term the author has seen many thousands of alterites. For the very large majority of these an identification of the parent mineral was absolutely impossible. It may be stated here in passing that the alterite group never was meant to be a collective name for all unidentifiables, unknowns or dirty minerals, but is definitely restricted to one specific group.

Although mineralogically of unsatisfactory character, the alterite group is often of diagnostic value (see, for example, de Jong 1956, Groot 1955, van Andel 1955). In this respect we may compare the alterites to the opaque group. Opaque percentages are often important; still, the number of cases where separate opaque minerals have been, or easily could have been, identified is small.

If the use of the term alterite would not be permitted, what should we do? Should the individual alterites be forced into mineralogical species although most often one cannot be sure about the correct identification? The present author would much rather encounter the term alterite with all its implied vagueness and be sure that species identification has been difficult than to have to doubt all hornblende, epidote, or pyroxene percentages. Or should we simply omit all deeply altered grains from our counts? That would deprive us of a group of diagnostically valuable elements. After all, most of us are studying heavy minerals not for their mineralogy, but in order to investigate sediment sources, stratigraphy, and related problems.

Therefore, it is the author's considered opinion that the use of group terms like alalterite is not only justifiable but in many cases desirable if applied with caution and if properly defined for each case.

---

[1] Contribution from Scripps Institution of Oceanography. New Series 1010

Reproduced by Permission

REFERENCES

Carroll, D., 1957, Use of the term "alterite": Am. Mineralogist, v. 42, p. 110–113.

De Jong, J. D., 1956, Sedimentpetrographische Untersuchungen in Terrassenschottern im Gebiet zwischen Krefeld und Kleve: Geologie en Mijnbouw, v. 18, p. 389–394.

Groot, J. J., 1955, Sedimentary petrology of the Cretaceous sediments of northern Delaware in relation to paleogeographic problems: Delaware Geol. Survey Bull. 5, 157 p.

van Andel, Tj. H., 1950, Provenance, transport and deposition of Rhine sediments. Wageningen, 130 p.

———. 1955, Sediments of the Rhone Delta II. Ver. Nederl. Geol. Mijnb. Gen., v. 15, no. 3, p. 515–556.

(*Reprinted from Nature, Vol.* 182, *p.* 42 *only, July* 5, 1958)

The Annual Pole Tide*

THE annual variation in latitude[1] causes a disturbance in the gravitational potential with an amplitude :

$$U = a^2\,\Omega^2\,m \sin\theta\cos\theta = 880 \sin\theta\cos\theta \text{ cm.}^2 \text{ sec.}^{-2}$$

where a is the radius and Ω the angular velocity of the Earth, and where m is the angular displacement of the pole along the meridian of a station located at co-latitude θ. For the annual term, Jeffreys[1] obtained $m \approx 0{\cdot}084'' = 4{\cdot}07 \times 10^{-7}$ radians, and the numerical value 880 follows from this. In comparison, the equilibrium tide S_a associated with the annual variation of the heliocentric distance has a potential[2] :

$$472(\tfrac{1}{3} - \cos^2\theta)\text{cm.}^2 \text{ sec.}^{-2}$$

The mean square values, $\int_0^{\pi/2} U^2 \sin\theta\, d\theta$, are equal to (321 cm.^{2} sec.$^{-2}$)^2 for the 'pole tide', and (141 cm.^{2} sec.$^{-2}$)^2 for the S_a, so that the pole tide is larger. Yet it appears to have been overlooked. This simply means that there is a larger effect from a movement, north or south, by 10 ft. than from a variation by 2 per cent of the Sun's distance.

The annual oceanic pole tide has an amplitude :

$$(1 + k - h)U/g = 0{\cdot}62 \sin\theta\cos\theta \text{ cm.}$$

where $k = 0{\cdot}29$, $h = 0{\cdot}59$ are the Love numbers. This is negligibly small compared to the observed tide, which has amplitude of the order of 10 cm. and is due largely to meteorological factors[3].

The disturbance in gravity due to the bodily pole tide has an amplitude :

$$\Delta g = 2(1 - \tfrac{3}{2}k + h)U/a = 3{\cdot}2 \sin\theta\cos\theta \text{ microgal.}$$

which will be difficult to observe. There is barely a possibility[4] of observing the difference in time kept by a pendulum clock (frequency $\sim \sqrt{g}$) and a quartz crystal clock. This time-difference has an amplitude :

$$\tfrac{1}{2}(\Delta g/g)(T/2\pi) = 0{\cdot}01 \text{ sec.} \sin\theta\cos\theta$$

for $T = 1$ year. The corresponding error in time-keeping for the semi-annual tide is 0·006 sec. at the equator, according to Jeffreys[5].

Thus the annual disturbance in the gravitational potential resulting from the Earth's wobble is small

---

* Contributions from the Scripps Institution of Oceanography, New Series. 1011

Reproduced by Permission

indeed, and worthy of note only because it exceeds the annual solar tide which is included in all text-books on the subject.

WALTER MUNK
RICHARD HAUBRICH

Institute of Geophysics,
University of California,
Los Angeles, California,
and the Scripps Institution of Oceanography,
California. May 12.

---

[1] Jeffreys, H., "The Earth" (Cambridge, 1952).

[2] Doodson, A. T., and Warburg, H. D., "Admiralty Manual of Tides" (Hydrographic Dept., Admiralty, 1941).

[3] Pattullo, J., Munk, W., Revelle, R., and Strong, E., *J. Mar. Res.*, **14**, 88 (1955).

[4] Stoyko, N., *Bull. Astron.*, **15**, Fasc. 3, 14 (1951).

[5] Jeffreys, H., *Mon. Not. Roy. Astron. Soc., Geophys. Supp.*, **2**, 58 (1928).

Printed in Great Britain by Fisher, Knight & Co., Ltd., St. Albans

(394)

PART 10

RADIOLARIA

IN

ANTARCTIC SEDIMENTS

By

WILLIAM R. RIEDEL

[B.A.N.Z.A.R.E. Reports, Series B, Vol. VI., Part 10, Pages 217–255]
Issued April, 1958

7425/57.

CONTENTS

Page

INTRODUCTION 219

MATERIAL STUDIED AND SPECIES ENCOUNTERED 220

ECOLOGICAL CONSIDERATIONS 221

LATITUDINAL EFFECTS 221

DEPTH RELATIONSHIPS 222

TAXONOMY 223

Cenosphaera cristata Haeckel ? 223

Diploplegma banzare n. sp. 223

Actinomma imperfecta Popofsky 224

Echinomma sp. 225

Prunopyle antarctica Dreyer 225

Stylatractus neptunus Haeckel ? 226

Spongurus pylomaticus n. sp. 226

Spongopyle osculosa Dreyer 226

Spongotrochus ? glacialis Popofsky 227

Lithelius nautiloides Popofsky 228

Phorticium pylonium (Haeckel ?) Cleve 229

Triceraspyris antarctica (Haecker) 230

Peripyramis circumtexta Haeckel 231

Cornutella profunda Ehrenberg 232

Mitrocalpis araneafera Popofsky 232

Dictyophimus gracilipes Bailey 233

Dictyophimus mawsoni n. sp. 234

Helotholus histricosa Jörgensen 234

Peromelissa denticulata (Ehrenberg) 236

Dictyocephalus papillosus (Ehrenberg) 236

Pterocorys hirundo Haeckel 238

Theocalyptra davisiana (Ehrenberg) 239

Theocalyptra bicornis (Popofsky) 240

Stichopilium variabile Popofsky 240

Artostrobus annulatus (Bailey) 241

Lithomitra arachnea (Ehrenberg) 242

Siphocampium sp. 243

Cyrtocapsa sp. 244

Botryopyle ? antarctica (Haecker) 244

LITERATURE CITED 246

EXPLANATION OF PLATES 248

RADIOLARIA

IN

ANTARCTIC SEDIMENTS

By WILLIAM R. RIEDEL*

Scripps Institution of Oceanography

(With 4 Plates and 13 Text Figures)

(*Received for Publication, October*, 1957)

INTRODUCTION

Previous work on antarctic spumelline and nasselline Radiolaria can be reviewed in a very few sentences. The first record of antarctic Radiolaria is that of Ehrenberg (1844, 187, 189, 190), based on material collected during the voyage of Sir James Clark Ross in 1841–43 to the sea which now bears his name. Haeckel (1887), in his report on the Radiolaria collected by the "Challenger" Expedition, described some twenty species from Station 157 at Lat. 53° 55′ S., Long. 108° 35′ E. Haecker (1908) described the species collected by the Deutsche Tiefsee Expedition on the "Valdivia", which took plankton samples south of Africa; and Popofsky (1908) studied the Radiolaria collected between the Wilhelm II. Coast and Kerguelen Island by the Deutsche Südpolar Expedition on the "Gauss". Most of the efforts of these earlier workers were directed toward the discovery of the species present, many of which were described on the basis of few individuals from plankton samples.

When Sir Douglas Mawson, leader of the British, Australian and New Zealand Antarctic Research Expedition, suggested that the present author undertake the study of the Radiolaria in the collections of that expedition, it was realized that the nature of the available material would permit a study on a somewhat broader scale than the almost purely descriptive work of the earlier authors. Of the reasons for this, the most important is that the B.A.N.Z.A.R.E. material includes several sediment samples from which rather large numbers of radiolarian skeletons can be readily isolated. Thus the ranges of variation of the species present can be determined with much more accuracy than would be possible on the basis of isolated examples from plankton hauls: this understanding of the ranges of variation of the species is of the utmost importance in taxonomic work on the Radiolaria, as will be illustrated in a subsequent section of this report. Moreover, a single sediment sample may be expected to contain representatives of all spumelline and nasselline radiolarians which have populated an area of the sea over a considerable length of time, whereas a single plankton sample will contain only those species present at the time of the haul and at the depths fished. Finally, the present-day worker enjoys an advantage over earlier investigators in that oceanographic expeditions in recent years have collected deep-sea sediments from a large number of widely scattered localities, and the ease and rapidity of modern methods of international communication facilitate the acquisition of material for comparison. For all of these reasons, it is possible in this report to define more precisely the species comprising the antarctic radiolarian fauna, to determine their distribution in the Pacific and Indian oceans, and thus to arrive for the first time at a broad comparison between the assemblage of the Antarctic and that of the warmer waters in general.

For support and encouragement during this study, the author is grateful to authorities and colleagues at the South Australian Museum and at the University of California Scripps Institution of Oceanography. At the latter institution, the investigation was sponsored in part by the U.S. Office of Naval Research under contract with the University of California. Portions of the manuscript have been read critically by Miss Frances L. Parker, Dr. M. N. Bramlette and Dr. F. B Phleger, and some nomenclatural problems were discussed with Dr. Carl L. Hubbs; to these colleagues the author is especially grateful.

---

* Contribution from the Scripps Institution of Oceanography. NEW SERIES, No. 1012

Reproduced by Permission

MATERIAL STUDIED AND SPECIES ENCOUNTERED

This report is based on a study of the Radiolaria from six sediment samples, of which one was taken near Kerguelen Island and the others from the vicinity of the Antarctic continent between longitudes 54° E. and 115° E. The depths from which the samples were taken range from 150–1,718 metres. General descriptions of these sediments have already been published in Parr's (1950) report on the B.A.N.Z.A.R.E. Foraminifera, so that it is here necessary only to list the station positions of the samples studied.

Station 30. Lat. 66° 48′ S., Long. 71° 24′ E., 540 metres.
Station 42. Lat. 65° 50′ S., Long. 54° 23′ E., 220 metres.
Station 47. Lat. 49° 50′ S., Long. 69° 33′ E., 150 metres.
Station 94. Lat. 64° 28′ S., Long. 114° 59′ E., 1,718 metres.
Station 97. Lat. 65° 10′ S., Long. 108° 12′ E., 474 metres.
Station 103. Lat. 67° 03′ S., Long. 74° 29′ E., 437 metres.

The radiolarian skeletons were isolated by the usual method for recent pelagic sediments (Riedel, 1957, 64). The only species recorded are those of which the number of specimens found was considered sufficient to show the range of intraspecific variation; by applying this restriction, it is hoped that erroneous identifications and the introduction into the literature of confusing names which will later have to be placed in synonymy have been minimized. In the following tabulation (Table I.) of the species found in each sample, the assemblage from near Kerguelen is placed in the first column, and the samples from near the Antarctic continent are placed in order of increasing depth.

TABLE I

Species	Station Number					
	47	42	103	97	30	94
Cenosphaera cristata Haeckel ?	—	—	+	+	+	+
Diploplegma banzare n. sp.	+	—	+	+	+	+
Actinomma imperfecta Popofsky	—	—	+	+	+	+
Echinomma sp.	—	—	—	+	+	+
Prunopyle antarctica Dreyer	—	—	—	—	—	+
Stylatractus neptunus Haeckel ?	—	—	—	—	—	+
Spongurus pylomaticus n. sp.	—	—	—	+	+	+
Spongopyle osculosa Dreyer	—	—	—	+	+	+
Spongotrochus ? glacialis Popofsky	+	+	+	+	+	+
Lithelius nautiloides Popofsky	+	+	+	+	+	+
Phorticium pylonium (Haeckel?) Cleve	+	—	+	+	+	+
Triceraspyris antarctica (Haecker)	+	+	+	+	+	+
Peripyramis circumtexta Haeckel	—	—	—	+	+	+
Cornutella profunda Ehrenberg	—	—	—	—	—	+
Mitrocalpis araneafera Popofsky	+	—	+	+	+	+
Dictyophimus gracilipes Bailey	—	—	—	+	—	+
Dictyophimus mawsoni n. sp.	—	—	—	+	+	+
Helotholus histricosa Jörgensen	+	+	+	+	+	+
Peromelissa denticulata (Ehrenberg)	+	+	+	+	+	+
Dictyocephalus papillosus (Ehrenberg)	—	—	—	+	+	+
Pterocorys hirundo Haeckel	—	—	+	+	+	+
Theocalyptra davisiana (Ehrenberg)	+	—	+	+	+	+
Theocalyptra bicornis (Popofsky)	+	—	—	+	+	+
Stichopilium variabile Popofsky	—	—	—	—	—	+
Artostrobus annulatus (Bailey)	—	—	—	—	—	+
Lithomitra arachnea (Ehrenberg)	—	—	—	—	—	+
Siphocampium sp.	—	—	+	+	+	+
Cyrtocapsa sp.	—	—	—	—	—	+
Botryopyle ? antarctica (Haecker)	+	+	+	+	+	+

Radiolaria were obtained in considerably larger numbers from the sediment taken at Station 94 than from the samples collected at the other stations. All of the species discussed in this report were found at Station 94, and most of them were not encountered at every station; this may be due in part to the fact that a larger number of individuals was found at Station 94, but it is believed to be due at least in some degree to a real difference between the faunas of the different localities, as discussed below under the heading " Depth relationships ".

ECOLOGICAL CONSIDERATIONS

Although there is a considerable literature on the Spumellina and Nassellina of all oceans, very little is known of the ecology of these groups. Popofsky (1908) and a few other authors have distinguished several cold- and warm-water forms, but most workers have done no more than describe the species which they encountered. The present author has at his disposal a large number of radiolarian assemblages from sediments of the tropical parts of the Indian and Pacific Oceans, and from the northern Pacific, as well as a few from the American sector of antarctic waters; it is thus possible to compare the B.A.N.Z.A.R.E. Radiolaria with the assemblages from these other widely distributed localities, in order to reach a general understanding of the distribution of some species.

LATITUDINAL EFFECTS

The distribution of each species encountered in the B.A.N.Z.A.R.E. sediments is discussed below in the taxonomic section. For the various reasons there indicated, it is not yet possible to determine the distribution of some of the species, but for the majority the information is considered sufficient to indicate their geographic ranges. It will be seen that some species have been found only in the Antarctic, others occur in both northern and southern cold waters, and still others are apparently cosmopolitan. Determination of a species as being definitely cosmopolitan is impossible at present because the author has insufficient Atlantic samples at his disposal. Nevertheless, there are records of some Atlantic Radiolaria in the literature, and there are indications that the cold- and warm-water assemblages of the Atlantic are not greatly different from those of corresponding latitudes of the other oceans; thus it is considered justifiable to describe a species as being probably cosmopolitan if it occurs in both high and low latitudes of the Pacific and Indian Oceans.

The species which have been found only in the Antarctic are :—

Spongurus pylomaticus n. sp.
Lithelius nautiloides
Triceraspyris antarctica
Peromelissa denticulata.

Bipolar cold-water forms, which are apparently not distributed continuously across the tropical Pacific by being submerged below the warmer surface waters, are—

Actinomma imperfecta
Mitrocalpis araneafera
Dictyophimus mawsoni n. sp.
Helotholus histricosa
Theocalyptra bicornis
Botryopyle ? antarctica

and perhaps

Prunopyle antarctica

and

Spongotrochus ? glacialis.

The species which appear to be cosmopolitan are :—

Spongopyle osculosa
Peripyramis circumtexta
Cornutella profunda
Dictyophimus gracilipes
Dictyocephalus papillosus
Pterocorys hirundo
Theocalyptra davisiana
Stichopilium variabile
Artostrobus annulatus
Lithomitra arachnea

and perhaps

Diploplegma banzare n. sp.
Stylatractus neptunus ?

and *Cyrtocapsa* sp.

No listing such as the above can indicate clearly the striking differences between the antarctic radiolarian assemblage and that of the tropical oceans. There is such a great difference between the aspects of the assemblages that there seems no reason to doubt that further investigations will reveal transitional stages between the two, and the Radiolaria may become as useful as the Foraminifera (see, for example, Phleger, Parker and Peirson, 1953) for the palaeoceanographic interpretation of sediments. The antarctic assemblage is characterized by abundant *Spongotrochus ? glacialis*, *Lithelius nautiloides*, *Helotholus histricosa*, *Peromelissa denticulata*, *Theocalyptra davisiana* and *Botryopyle ? antarctica*, and by the complete absence of such groups as the panartids, the euchitoniins, *Pterocanium praetextum* (Ehrenberg) and related species, *Anthocyrtidium cineraria* Haeckel and its relatives, species of the genus *Carpocanium* and many others which form conspicuous elements of the tropical assemblage.

It is interesting to note that the Radiolaria from Station 47, near Kerguelen, are typically antarctic. Little is known of the fauna of intermediate latitudes of the southern hemisphere, but it seems not unlikely that a rather sharp faunal boundary separates antarctic from subantarctic Radiolaria to the north of Station 47. Ekman (1953, 218–219), on the basis of an analysis of the echinoderms and fishes of that area, considers the Kerguelen fauna to be subantarctic in the sense that it is transitional and includes a mixture of antarctic and temperate species.

DEPTH RELATIONSHIPS.

It can be seen from Table 1 that certain of the species present in the deepest sample (from Station 94) were not found in some of the other samples. Although, as has been stated above, this may be due partly to the fact that more individuals were found at Station 94 than at the other stations, there are indications that there is probably a real difference between the species assemblages inhabiting the water-columns at the different localities. There is little difference between the latitudes of the positions of the five antarctic samples, and it is probable that the differences between their radiolarian assemblages are related to depth rather than to latitude. It must be emphasized that the number of samples available is too small to permit of reaching any definite ecological conclusions, but it does seem justifiable to speculate along these lines.

Two facts which seem particularly significant are that—

(1) the majority of the species which are found consistently in the shallower samples are either restricted to Antarctic waters or have a bipolar cold-water pattern of distribution—*Spongotrochus ? glacialis*, *Lithelius nautiloides*, *Triceraspyris antarctica*, *Helotholus histricosa*, *Peromelissa denticulata* and *Botryopyle ? antarctica* ; and

(2) many of the species which are apparently cosmopolitan are found only in the deeper samples—*Spongopyle osculosa*, *Peripyramis circumtexta*, *Cornutella profunda*, *Dictyophimus gracilipes*, *Dictyocephalus papillosus*, *Stichopilium variabile*, *Artostrobus annulatus* and *Lithomitra arachnea*.

Thus there appear to be two sets of species, one of which is restricted to high latitudes and can inhabit the upper part of the antarctic water-column (perhaps the Antarctic Surface Water of Sverdrup, Johnson and Fleming, 1942), and the other of which has a wider distribution in warmer water and is able to live in the deeper Antarctic Circumpolar Water but not in the colder Antarctic Surface Water. This submergence of warm-water species in high latitudes (below the Antarctic Surface Water) may be regarded as a corollary to the submergence of cold-water forms in low latitudes which Haecker (1904) found during his study of the distribution of tripylean Radiolaria.

This general picture deduced from the radiolarian assemblages in the sediments is not necessarily invalidated by Popofsky's (1908) report of the occurrence of two of the cosmopolitan species (*Stichopilium variabile* and *Lithomitra arachnea*) in plankton hauls from shallow depths on the 15th and 23rd March, 1903, at Lat. 64–65° S., Long. 80–85° E. These occurences may have been the result of the warmer, deeper water being brought nearer the surface because of certain meteorological or oceanographical conditions. If one could be certain that the apparent absence of the cosmopolitan radiolarian species at B.A.N.Z.A.R.E. Stations 42 and 103, for example, is not due to the fact that relatively few individuals were found in these samples, but to the real absence of those species at those stations, it would be justifiable to speculate that the warmer Antarctic Circumpolar Water *never* intruded at those localities.

TAXONOMY

In the following descriptions of species, measurements were made where possible on at least ten specimens of each species from each sediment sample; in the cases in which the number of specimens measured is less than ten, only the indicated number of individuals was found in the sample. Types and figured specimens will be temporarily in the custody of Sir Douglas Mawson at the University of Adelaide, pending a decision as to the disposal of the Expedition's collections. Throughout this report, the general arrangement of Haeckel's system of radiolarian classification is used, with some of the modifications proposed by Campbell (1954).

Genus Cenosphaera Ehrenberg 1854

Cenosphaera cristata Haeckel ?

(Pl. 1, figs. 1, 2.)

Cenosphaera cristata Haeckel, 1887, 66.

Spherical shell thick-walled, thorny. Pores subcircular or circular, variable in size, 10–24 on the half-equator, as wide to five times as wide as the intervening bars. Pores surrounded by raised polygonal frames bearing short thorns at the corners—in rare specimens the polygonal frames are absent but the thorns present. Diameter of shell 115–230 μ.

Measurements based on 5 specimens from Sta. 30, 25 from Sta. 94, and one each from Stas. 97 and 103.

This form can be identified only doubtfully with Haeckel's species, because of the brevity of the original description and lack of an illustration. The question can be settled only by re-examination of specimens from the type locality, namely the North Pacific "Challenger" Sta. 254. The Antarctic specimens show greater variability than is indicated in Haeckel's description. The Antarctic species resembles to some extent *Cenosphaera favosa* Haeckel (1887, 62, Pl. 12, fig. 10) and *C. globosa* Popofsky (1908, 207, Pl. 22, fig. 2), from both of which if differs in the irregularity of the pores.

Rather similar thorny, thick-walled species of this genus have been recorded from the Antarctic by Haeckel (1887, 65; *C. solida*) and Popofsky (1908, 207; *C. globosa* and *C. solida*). However, a large number of species of *Cenosphaera* have been described, in many instances inadequately, from both high and low latitudes, and the pattern of distribution of members of this group cannot be determined until the relationships between the various species are more satisfactorily understood.

Genus Diploplegma Hinde 1890

Diploplegma banzare n. sp.

(Pl. 1, figs. 3, 4.)

Shell consisting of a spherical, thick-walled, rough cortical shell which has in some specimens a somewhat spongy structure, joined by numerous radial beams to an inner sphere of loose spongy network which apparently has no central cavity. Outer shell, though spongy in some specimens, always has a definite surface with rounded pores of different sizes separated by heavy intervening bars; usually approximately 12-16 pores on the half-circumference. Numerous delicate radial beams, which are always branched proximally and in some specimens also distally, extend between the inner surface of the outer sphere and the inner spherical or subspherical mass of loose spongy meshwork. Diameter of outer sphere 225–315 μ, of inner spongy mass 105–155 μ.

Measurements based on 7 specimens from Sta. 30, 10 from Sta. 47, 25 from Sta. 94, 4 from Sta. 97 and 2 from Sta. 103.

Type locality Sta. 94.

The assignment of this species to the genus *Diploplegma* is based on those specimens in which the cortical shell has a spongy structure, because it is these which are considered to be the most completely developed individuals. The antarctic species differs from *Diploplegma cinctum* Hinde

(1890, Pl. 3, fig. 10) in less spongy outer sphere, and longer radial beams between inner and outer spheres. It shows considerable resemblance to the figures of *Plegmosphaera churchi* Campbell and Clark (1944, 10, Pl. 1, figs. 6–10), from the Miocene of California, but the description of that species states that the thickness of its spongy wall is greater than the radius of its hollow sphere. The name *banzare* is derived from the initial letters of the name of the Expedition, and is proposed as a noun.

Although this species occurs in several samples from the Indian Ocean sector of Antarctic waters, the author has not found it in sediments from the American sector. A somewhat similar form, differing in having a more delicate cortical shell which is rarely spongy, is widespread in the tropical parts of the Pacific and Indian Oceans, and in the northern Pacific. Thus members of this species-group may be cosmopolitan.

Genus Actinomma Haeckel 1861

Actinomma imperfecta Popofsky

(Pl. 1, fig. 5.)

Actinomma imperfecta Popofsky, 1908, 215, Pl. 24, fig. 4.

Shell consisting of usually three, or less commonly four, concentric lattice-shells, connected by radial spines, some of which project beyond the surface of the outermost sphere. Innermost lattice-shell approximately spherical, or represented by only a few loose meshes. Second lattice-shell spherical or subspherical, with pores circular or subcircular, approximately 8–10 on the half-equator. Radial beams connecting first lattice-shell to second are difficult to distinguish, probably approximately 4–8 in number; those connecting second lattice-shell to third, and projecting beyond the surface of the latter, are usually 10–16 in number and three-bladed. Third lattice-shell spherical, with rather large round pores somewhat variable in size and shape, separated by heavy intervening bars. In specimens having only three lattice-shells, the outer surface has approximately 15–40 acute, three-angled spines, which in some examples show the beginnings of a fourth shell as lateral branches on the spines. Fourth shell, when present, is spherical and thin-walled, with numerous circular or subcircular pores which are considerably smaller than those of the third shell; it has usually numerous, acute, three-bladed spines of different lengths on the surface, representing prolongations of at least some of the rods connecting it with the third shell. Diameter of innermost shell 12–20 μ, of second shell 37–50 μ, of third shell 85–125 μ, of fourth shell 110–145 μ. Length of free surface spines 5–60 μ.

Emended description based on 6 specimens from Sta. 30, 25 from Sta. 94, 3 from Sta. 97, and one from Sta. 103.

The single specimen described under this name by Popofsky from the edge of the Antarctic pack-ice was an apparently immature individual with only the two innermost shells developed. Besides the third shell, the presence of which Popofsky inferred from the lateral branches on the radial spines, a fourth shell is present in some of the numerous specimens found in the B.A.N.Z.A.R.E. sediments. The presence of a fourth shell does not appear to be sufficiently constant to justify transfer of the species to the genus *Cromyomma* or *Cromyechinus*. It is impossible at present to classify this species according to the system proposed by Mast (1910) because of the difficulty of determining which lattice-sphere is to be regarded as the primary shell.

Forms identical with or similar to this species occur in both the American and Indian Ocean sectors of Antarctic waters, and are widely distributed in the northern Pacific. No similar form has been found in the sediments of the tropical parts of the Pacific or Indian Oceans. *Echinomma leptodermum* Jörgensen, recorded by Jörgensen (1905, 116, Pl. 8, fig. 33) and Mielck (1913, 363) as occurring commonly at some localities in the northern Atlantic, may be closely related to *Actinomma imperfecta*. A more thorough investigation of this general group is necessary before it will be possible to draw conclusions regarding the distribution of its members.

Genus ECHINOMMA HAECKEL 1882

ECHINOMMA sp.

(Pl. 1, fig. 6.)

Shell consisting of three concentric lattice-shells, of which the outer two are spherical and the innermost somewhat irregular. Outermost shell usually very thick-walled, thorny or rarely with bristle-like by-spines, with hexagonally framed circular pores of sometimes variable size separated by wide intervening bars, and approximately 10–20 long, delicate, cylindrical or weakly three-bladed main-spines (broken short in all observed specimens). Second lattice-shell thin-walled, with small circular or subcircular pores separated by narrow intervening bars. Outer two lattice-shells joined by approximately 20 radial beams, which are three-bladed in at least some specimens. Innermost lattice-shell in most specimens irregular, with few large, angular meshes. Diameter of innermost lattice-shell 15–30 μ, of second shell 38–45 μ, of outermost shell 100–150 μ. Thickness of outermost shell-wall approximately 15–20 μ. Maximum observed length of main-spines 75 μ.

Description based on 10 specimens from Sta. 30, 25 from Sta. 94 and 4 from Sta. 97.

It seems that this species may be identical with that figured by Popofsky (1908, 209, Pl. 22, fig. 4) as *Hexalonche regularis*, but the two are not identified because Popofsky described his form as possessing only one medullary shell and six regularly arranged main-spines. The systematics of species more or less closely resembling this are in such a confused state that a thorough re-examination of a large number of forms would be necessary in order to determine their relationships and distributions.

Genus PRUNOPYLE DREYER 1889

PRUNOPYLE ANTARCTICA Dreyer

(Pl. 1, figs. 7, 8.)

Prunopyle antarctica Dreyer, 1889, 24–25, Pl. 5, fig. 75.

Skeleton consisting of four concentric shells connected by numerous radial bars. The three inner shells are spherical, or approximately so, while the fourth is ovate. The two inner and the two outer shells lie rather close together, and a larger space separates the second shell from the third. Pores of the second shell (counting outward) subcircular, separated by relatively thin bars. Pores of the third shell rather large, of irregular size and form, separated by rather heavy bars. Pores of the fourth (outermost) shell small, circular or subcircular, in many specimens arranged in groups over the pores of the third shell in such a manner that 2–8 pores of the fourth shell overlie one larger pore of the third shell. Fourth shell apparently rather thick, with smooth or ridged surface, in some individuals partially united with the third shell. Short, thorn-like spines are sparsely distributed over the shell surface; those surrounding the large pylome are longer and stronger, and some specimens have a group of large spines also on the aboral pole. Diameter of the innermost shell approximately 15–17 μ, of second shell 35–42 μ (occasionally to 61 μ ?), of third shell 75–98 μ, of fourth shell (major axis) 115–160 μ, (minor axis) 105–140 μ.

Emended description, differing principally in the ranges of variation of the shell diameters, based on 15 specimens from Sta. 94. Although Dreyer stated that the diameter of the second shell is approximately 61 μ, the present author has found no specimen in which it exceeds 42 μ.

This species, first described from the southern Indian Ocean, occurs in both the American and Indian Ocean sectors of antarctic waters. A rather similar form, which may belong to the same species, occurs in the northern Pacific—the material at present available is however insufficient for accurate identification of the northern form. No form resembling *P. antarctica* has been found in the tropical parts of the Pacific or Indian Oceans. Thus this species may possibly be restricted to high northern and southern latitudes.

Genus Stylatractus Haeckel 1887

Stylatractus neptunus Haeckel ?

(Pl. 1, fig. 9.)

Stylatractus neptunus Haeckel, 1887, 328, Pl. 17, fig. 6.

Shell ellipsoidal, consisting of three concentric lattice-shells and two unequal polar spines. Innermost shell spherical or subspherical, thin-walled, with numerous circular or subcircular pores, joined to the second shell by few radial beams. Second lattice-shell somewhat ellipsoidal, usually thick-walled, with large subcircular or angular pores, joined to the outermost lattice-shell by numerous radial beams. Outermost lattice-shell ellipsoidal, thick-walled, thorny, with irregular pores (7–16 on a half-equator) which are large when few in number, and are in many specimens subdivided by centripetal ingrowths from the pore-walls to form numerous smaller pores. Polar spines heavy, usually cylindro-conical and fluted at the base, rarely weakly three-bladed. Major diameter of outermost lattice-shell 130–150 μ, its minor diameter 115–140 μ. Major diameter of second lattice-shell 75–85 μ, of innermost lattice-shell 30–40 μ. Length of longer polar spine 55–95 μ, of shorter polar spine 30–75 μ.

Description based on 21 specimens from Sta. 94.

Positive identification of this form as *S. neptunus* is impossible at present, because of the inadequacy of Haeckel's description of that species, and the fact that the present author has not enough specimens from its type locality to determine its range of variation. Specimens closely resembling those from the Antarctic have been found in the northern Pacific, and in the tropical parts of the Pacific and Indian oceans—it may thus be a cosmopolitan species.

Genus Spongurus Haeckel 1861

Spongurus pylomaticus n. sp.

(Pl. 1, figs. 10, 11.)

Shell subcylindrical or elongate ellipsoidal, approximately twice as long as broad. An inner, densely spongy core is surrounded by a narrow mantle of less dense meshwork. Entire surface usually sparsely covered with bristle-like spines, which in many specimens tend to be longer at the two poles of the main axis. At one pole is a pylome, usually surrounded by short, irregular teeth. Length 150–255 μ, breadth 78–125 μ. Length of surface spines 5–40 μ (usually broken off).

Description based on 3 specimens from Sta. 30, 25 from Sta. 94 and one from Sta. 97.

Type locality Sta. 94.

This species differs from all others of the genus in the presence of a pylome. The specific name is derived from the Greek πύλωμα (gate or gateway).

As indicated by Haeckel (1887, 343–345), the genus *Spongurus* is apparently cosmopolitan : this species, the only pylomatic member of the genus, has not been found anywhere but in the Antarctic, where it occurs in both the American and Indian Ocean sectors.

Genus Spongopyle Dreyer 1889

Spongopyle osculosa Dreyer

(Pl. 1, fig. 12.)

Spongopyle osculosa Dreyer, 1889, 42–43, Pl. 6, figs. 99, 100.

This species is well described by Dreyer on the basis of abundant specimens from the sediment sample collected at "Challenger" Station 157 in the southern Indian Ocean, and other examples from the northern and tropical parts of the Pacific Ocean. The diameter of the shells of 25 apparently fully developed specimens from B.A.N.Z.A.R.E. Sta. 94, and 7 specimens from Sta. 30, ranged from

150–275μ. In the 7 specimens found at Sta. 97, the diameter of the shell was less (130–180μ), and the internal spongy material was less dense than usual near the margin of the disc. Rare specimens were found with a few short spines on the margin, but they apparently belong to this species and not to *Spongopyle setosa* Dreyer.

Dreyer's records of this species from the southern Indian Ocean, the tropical and northern Pacific Ocean, and several other unspecified localities, indicate that it may be cosmopolitan.

Genus SPONGOTROCHUS HAECKEL 1861

SPONGOTROCHUS ? GLACIALIS Popofsky

(Pl. 2, figs. 1, 2 ; text-fig. 1.)

Sponogtrochus glacialis Popofsky, 1908, 228–229, Pl. 26, fig. 8 ; Pl. 27, fig. 1 ; Pl. 28, fig. 2.

Shell biconvex-discoidal, consisting of a spiny disc of spongy structure which is in some (fully developed ?) individuals surrounded by a lenticular lattice-shell. Spongy disc thickened in its central portion (a quarter to a half of its total diameter), with numerous acicular or acutely conical spines of different lengths around its circumference and in most specimens also on the two surfaces, particularly on the thickened central portion. When present, the enclosing lenticular lattice-shell is apparently in contact with the spongy disc at or near its circumference, but is separated by a distinct space from its two surfaces. In most specimens, the spines arising from the thickened central part of the spongy disc penetrate the lattice-shell. The lattice-shell has an uneven surface, with subcircular or circular pores of varying sizes, the diameters of which are a half to ten times as great as the breadth of the intervening bars. Diameter of shell 195–465 μ. Length of free parts of spines on circumference 5–170 μ (often about 70 μ).

Emended description based on 25 specimens from Sta. 94, 10 from each of Stations 97 and 103, and two specimens from each of Stations 30, 42 and 47.

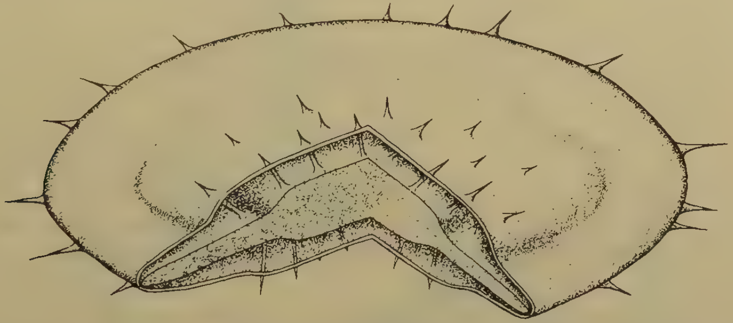

Fig. 1. *Spongotrochus ? glacialis* Popofsky. Diagram to illustrate the relation of the skeletal elements. One quarter of the skeleton is represented as being cut away. The external lattice-shell does not extend to the edge of the spongy disc in all specimens.

Some specimens among the B.A.N.Z.A.R.E. material have long, acicular spines as illustrated by Popofsky (1908, Pl. 27, fig. 2), but in others the spines are considerably stouter and shorter (my Pl. 2, fig. 2). As here interpreted, this species shows a wide range of variation and may also include the abundant antarctic form which Popofsky (1908, 227–228, Pl. 26, figs. 5–7 ; Pl. 28, fig. 1) identified as *Stylotrochus arachnius* (Haeckel). It also appears probable that at least some of the specimens which Popofsky (1908, 226–227, Pl. 26, fig. 4) identified as *Spongodiscus favus* Ehrenberg var. *maxima* are no more than incompletely developed forms, specifically identical with *Spongotrochus glacialis*. In view of these uncertainties, which can be resolved only by a thorough investigation of a large number of named spongodiscids, the present author has treated the less developed individuals (which are common in the sediment samples) as possible "juvenile" representatives of *S. glacialis*, without making the nomenclatural changes which will be necessary if a more exhaustive study proves this to be the more acceptable view.

Popofsky's description of *S. glacialis* is apparently based on specimens which are appropriately placed in the genus *Spongotrochus* in Haeckel's system. However, examination of numerous skeletons in the sediments leaves little doubt that in the completely developed individuals a lenticular lattice-shell surrounds the spongy disc (text-fig. 1), and a form with this structure cannot readily be assigned to any known genus. Nevertheless, re-examination of forms already described may reveal a similar structure in some of the coccodiscids, porodiscids or spongodiscids, and for this reason erection of a new genus is not considered advisable at present.

This species occurs in both the American and Indian Ocean sectors of Antarctic waters. A somewhat similar form, differing principally in that the central area of the disc is not so pronouncedly thickened, is widely distributed in the northern Pacific. All members of the subgenus *Spongotrochiscus* hitherto found in sediments of the tropical parts of the Pacific and Indian Oceans are smaller (usually less than 240 μ in diameter) and more delicately constructed.

Genus LITHELIUS HAECKEL 1861

LITHELIUS NAUTILIODES Popofsky

(Pl. 2, figs. 3, 4; text-fig. 2.)

Lithelius nautiloides Popofsky, 1908, 230–231, Pl. 27, figs. 2–4.

Shell subspherical, consisting of a small, spherical medullary shell surrounded by a completely involute spiral of approximately four or five whorls. The whorls of the spiral increase in width outward, and are penetrated by numerous radial bars which extend as radial spines on the shell

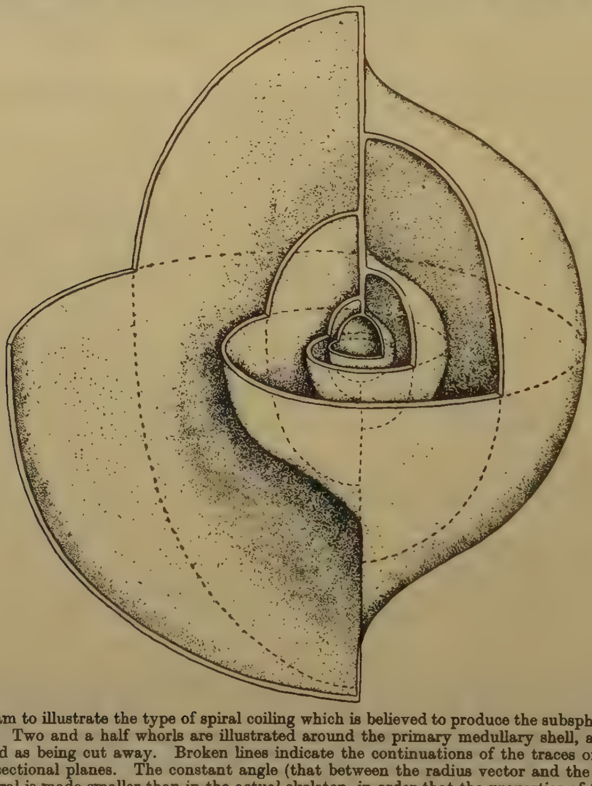

Fig. 2. Diagram to illustrate the type of spiral coiling which is believed to produce the subspherical shell of *Lithelius nautiloides* Popofsky. Two and a half whorls are illustrated around the primary medullary shell, and one quarter of the skeleton is represented as being cut away. Broken lines indicate the continuations of the traces of the shell-wall on the axial and equatorial sectional planes. The constant angle (that between the radius vector and the tangent to the curve) of the equiangular spiral is made smaller than in the actual skeleton, in order that the properties of the figure may be seen more easily.

surface. Radial spines mostly broken off in the examples from the sediments, but according to Popofsky they are approximately as long as the shell radius or shorter, needle-like, and of varying thickness. Shell wall of moderate thickness, with rounded pores of different sizes. Diameter of medullary shell 10–15 μ, of entire shell of approximately four to five whorls 110–220 μ.

Measurements based on 15 specimens from Sta. 30, 4 from Sta. 42, 15 from Sta. 47, 25 from Sta. 94, 15 from Sta. 97 and 15 from Sta. 103.

The specimens from the B.A.N.Z.A.R.E. sediments are considerably larger than those described by Popofsky from plankton samples. There is little doubt, however, that they are of the same species, and that fully formed specimens may have more whorls than indicated in the original description. Popofsky's description does not indicate the overall subspherical form. The method of formation of the subspherical shell cannot readily be seen under the microscope: text-figure 2 is an attempted representation of the details of the structure. Optical sections visible microscopically are (1) a series of alternating concentric semicircles increasing in diameter outward, surrounding a small central sphere, on sectional planes including the polar axis of the spiral, or (2) an equiangular (logarithmic) spiral beginning at a small central sphere, on sectional planes passing through the centre of the skeleton but not including the polar axis.

Together with common examples readily identifiable as *L. nautiloides*, the assemblages from the Antarctic sediments also contain a relatively few specimens which appear to have a similar structure enclosed in a thick-walled final whorl (Pl. 2, fig. 4). These dense specimens are considered as questionably belonging to the same species, though later studies based on more extensive material may prove the desirability of separating them specifically.

Neither this species, nor any closely resembling it, has been found anywhere except in the Antarctic, where it occurs in both the American and Indian Ocean sectors.

Genus PHORTICIUM HAECKEL 1882

PHORTICIUM PYLONIUM (Haeckel?) Cleve

(Pl. 2, fig. 5.)

? Phorticium pylonium Haeckel, 1887, 709, Pl. 49. fig. 10.

Phorticium pylonium Haeckel; Cleve, 1899, 31, Pl. 3, figs. 2a–d.

Octopyle octostyle Haeckel f. *minor* Jörgensen, 1900, 64.

Tetrapylonium clevei Jörgensen, 1900, 64.

Phorticium pylonium (Haeckel ?) Cleve; Jörgensen, 1905, 120–121, Pl. 10, figs. 42a–d; Pl. 11, figs. 42e–f, 43–45d.

The correct taxonomic position of this species, which has been recorded as occurring rather abundantly at a number of localities in the North Atlantic, cannot at present be determined satisfactorily. Cleve (1899) identified, as *Phorticium pylonium* Haeckel, a variable form which he found at several localities near Spitzbergen. Jörgensen (1900) described the same form, found off the west coast of Norway, as *Octopyle octostyle* forma *minor* ("less developed forms") and *Tetrapylonium clevei*, though he later (1905), as a result of a detailed re-examination of the species, reverted to Cleve's designation as *Phorticium pylonium* Haeckel ?. Jörgensen pointed out that Haeckel's descriptions of this and related forms are not sufficiently precise, and that a revision of the group is necessary.

Specimens found in the Antarctic sediments have the major and minor diameters of the outermost lattice-girdle 120–200 μ and 90–155 μ respectively, in well developed individuals. Measurements based on 2 specimens from Sta. 30, 8 from Sta. 47, 16 from Sta. 94, 11 from Sta. 97 and 2 from Sta. 103.

In the present unsatisfactory state of the taxonomy of this group, it is impossible to determine the distribution of one species relative to another.

Genus Triceraspyris Haeckel 1882

Triceraspyris antarctica (Haecker)

(Pl. 2, figs. 6, 7 ; text-fig. 3.)

Phormospyris antarctica Haecker, 1907, 124, fig. 9.

Triceraspyris antarctica (Haecker) ; Haecker, 1908, 445–446, Pl. 84, fig. 586.

Tripospyris biloculata Popofsky, 1908, 269, Pl. 30, fig. 7.

Tripospyris bicornis Popofsky, 1908, 269–270, Pl. 30, fig. 6.

Shell of rather heavy construction, nut-shaped, with unequal rounded pores, generally smooth surface, and slight or pronounced sagittal constriction. Four large basal pores. Usually three basal feet, circular or three-bladed in section, of approximately the same length as the cephalis : of these, the unpaired one is usually simply latticed proximally, and in many specimens all three are forked distally. In a few specimens, secondary spines or a small amount of lattice-work are developed between the proximal parts of these basal feet. Sagittal ring approximately D-shaped, from which a short, free apical spine arises subapically, and a thorn-like vertical spine arises from the more curved part of the ring near the basal pores. In most specimens, two more thorn-like spines are present, one to either side of the apical part of the sagittal ring, and in some specimens several more thorns are scattered over the apical surface. Height of sagittal ring 63–90 μ ; maximum breadth of bilocular cephalis 80–125 μ.

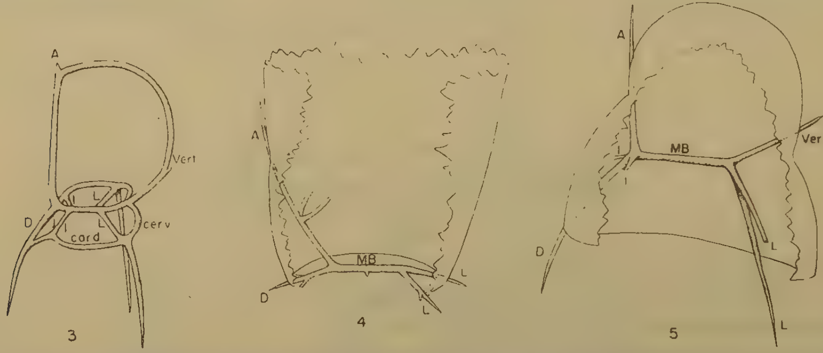

Figs. 3–5. Diagrams to illustrate the primary skeletal structures of the collar and cephalic regions of (3) *Triceraspyris antarctica* (Haecker), (4) *Mitrocalpis araneafera* Popofsky and (5) *Dictyophimus gracilipes* Bailey. For explanations see text.

Emended description based on examination of 15 specimens from Sta. 30, 2 from Sta. 42, 4 from Sta. 47, 25 from Sta. 94, 18 from Sta. 97 and 20 from Sta. 103. Haecker and Popofsky described their three forms from one specimen of each, and the range of variation is now found to be sufficient to include all three.

The generic name *Triceraspyris* is not replaced by *Triospyris* (as recommended by Campbell, 1954, 112) because Haeckel is clearly to be considered as the first reviser of this genus, and his action in establishing *Triceraspyris* in preference to *Triospyris* is to be upheld according to the Copenhagen decisions of the International Commission on Zoological Nomenclature.

The general basal structure of the shell of this species is apparently analogous to that which Popofsky (1913) termed the "*Tripospyrissa*-type" (text-fig. 3). The three main basal feet correspond to the dorsal (D) and two primary lateral spines (L, L), the free portions of the apical (A) and vertical (Vert.) spines are small, and the four large basal pores paired on either side of the median bar (MB) are probably best regarded as the cervical (cerv.) and cardinal (card.) pores, with the jugular pores (j) bounded by the secondary lateral spines (l, l) forming the 'latticed' proximal part of the unpaired basal foot.

This species occurs in both the American and Indian Ocean sectors of antarctic waters, and no form resembling it has been found at any other locality. Thus it appears to be an exclusively southern cold-water species.

Genus PERIPYRAMIS HAECKEL sens. emend.

Peripyramis Haeckel, 1882, 428.

Spongopyramis Haeckel, 1887, 1260.

Sethophormidinae with numerous straight or slightly curved radial ribs in the wall of the conical or pyramidal thorax. Surface of thorax covered by secondary arachnoidal or spongy meshwork which surrounds the heavier primary lattice-shell. Cephalis with or without horn.

This emendation of the definition of the genus *Peripyramis* is necessitated by the finding that its type species (*P. circumtexta*, see below) has a cephalis and thorax. The generic name *Spongopyramis* becomes a junior synoym.

PERIPYRAMIS CIRCUMTEXTA Haeckel

(Pl. 2, figs. 8, 9.)

Peripyramis circumtexta Haeckel, 1887, 1162, Pl. 54, fig. 5.

Cephalis small, ovate, hyaline, bearing a short, excentric, vertical apical spine. Collar stricture slight, with four collar pores in the one specimen which could be examined from the apex. In some specimens, one to three (?) short, downwardly-directed spines penetrate the thoracic wall near the collar stricture. Thorax rather acutely conical, in some specimens subcylindrical below, consisting principally of 8–11 longitudinal rods joined by transverse bars which are usually not continuous around a circumference. Thoracic pores thus formed are rounded-quadrangular, increasing in size distally. From the longitudinal and transverse skeletal bars of the thorax arise numerous short, forked spines; the terminations of these spines are in some specimens joined by delicate siliceous threads which thus form a loose, irregular, incomplete network surrounding the main surface of the thorax. Total length usually 100–270 μ (to 320 μ according to Haeckel); maximum breadth 85–150 μ.

Emended description based on one specimen from Sta. 30, 10 from Sta. 94, 2 from Sta. 97, and 5 from a depth of 5–5.5 cm. in the Swedish Deep-Sea Expedition Core No. 74B collected at 00° 29′ S., 151° 33′ W. (see Riedel, 1957, 63, 68).

The examples of this species found in the B.A.N.Z.A.R.E. sediments show some resemblance to Haeckel's description and figure of *P. circumtexta*, and it was therefore considered desirable to compare them with specimens from the type locality (" Challenger " Sta. 271). No material from the original " Challenger " sample was available to the author, but the Swedish Deep-Sea Expedition Core 74B was collected less than 5 nautical miles from " Challenger " Sta. 271, and available material from near the top of this core might be expected to contain the same species as Haeckel described from the " Challenger " sample.

A search through a large number of Radiolaria from a depth of 5–5.5 cm. in the above-mentioned core did not yield any specimens agreeing with Haeckel's definition of *Peripyramis* in lacking a cephalis. However, five specimens were found which agreed with the original description of *P. circumtexta* except in that a small cephalis was present, bearing an apical horn, and the total length of the largest example was 270 μ. There is little doubt that these five specimens belong to Haeckel's species *P. circumtexta*, and that Haeckel either overlooked the presence of the small cephalis or based his description on an abnormal example. As *P. circumtexta* is the type species of its genus, the generic definition is emended accordingly. It seems probable that subsequent thorough investigation will prove many of Haeckel's phaenocalpids (Archiphormididae according to Campbell, 1954) to be actually dicyrtid.

This species occurs in the tropical parts of the Pacific and Indian Oceans, as well as in the American and Indian Ocean sectors of antarctic waters and in the northern Pacific. Thus it may be a cosmopolitan species.

Genus CORNUTELLA EHRENBERG 1839

CORNUTELLA PROFUNDA Ehrenberg

(Pl. 3, figs. 1, 2.)

Cornutella clathrata β profunda Ehrenberg, 1856, Pl. 35B, fig. 21 ; Bailey, 1856, 2, Pl. 1, fig. 23.

Cornutella profunda Ehrenberg, 1859, 31.

Sethoconus profundus (Ehrenberg) ; Haeckel, 1887, 1294.

Cornutella hexagona Haeckel, 1887, 1180, Pl. 54, fig. 9.

Shell slender, conical, with smooth surface. Cephalis small, hyaline, poreless, with conical, acute apical horn. Pores of thorax regularly arranged, subcircular, increasing in size distally, 4–7 on the half-circumference. Proximal part of thorax usually poreless. Some specimens have a heavier shell-wall, with wider intervening bars between the pores which are fewer in number, and tend to be subcylindrical or slightly contracted in the distal one-third or one-quarter. Length of apical horn 2–30 μ, of cephalis 7–20 μ, of thorax 110–200 μ. Maximum shell breadth 45–65 μ.

Measurements based on 18 specimens from Sta. 94.

After examining the Radiolaria of a large number of sediment samples from the Pacific and Indian Oceans, the author has reached the following conclusions :—That there is probably only one common, widespread species of *Cornutella* of this general form in those two oceans at the present day ; that the species of this genus (including the type species) are probably best regarded as dicyrtid ; that the antarctic form is identical with specimens from the warmer regions of the Pacific and Indian Oceans ; and that there are no separate cosmopolitan Recent species which can be distinguished as *Sethoconus clathratus* and *Cornutella clathrata* in the sense of Haeckel (1887). Only the possibility that the form occurring in the late Tertiary sediments of Caltanisetta in Sicily is consistently curved or different in some minor but constant respect from that which is here called *C. profunda*, prevents this author from applying the name *Cornutella clathrata* Ehrenberg to the antarctic (and apparently cosmopolitan) species.

Investigation of the synonymy of this species has been hampered by the present unavailability of topotypic material of several other described species resembling *C. profunda*. Re-examination of the Radiolaria from portions of the original sediment samples from "Challenger" Sta. 265, 266 and 270 showed that transitional stages exist between thin-walled forms with long apical spines and thick-walled forms with short spines, so that there appears to be no justification for separating *C. hexagona* Haeckel as a different species. But no topotypic material is available for the following species which may later prove to be identical with *C. profunda* :—*Cornutella stylophaena* Ehrenberg (1872, 305 ; 1873, Pl. 6–III., fig. 1), *C. trichostyla* Ehrenberg (1872, 305 ; 1873, Pl. 6–III., fig. 2), *C. distenta* Ehrenberg (1872, 304 ; 1873, Pl. 6–III., fig. 3), *C. tumens* Ehrenberg (1872, 305 ; 1873, Pl. 6–III., fig. 4), *C. trochus* Ehrenberg (1872, 305 ; 1873, Pl. 9, fig. 14), *C. longiseta* Ehrenberg (1872, 304 ; 1873, Pl. 9, fig. 15), *C. verrucosa* Ehrenberg (1872, 305–306 ; 1873, Pl. 9, fig. 16), *C. sethoconus* Haeckel (1887, 1180, Pl. 54, fig. 10), *Sethoconus orthoceras* Haeckel (1887, 1294, Pl. 54, fig. 11) and *S. bimarginatus* Haeckel (1887, 1295, Pl. 54, fig. 12).

Besides its occurrence in the Indian Ocean sector of antarctic waters, this species has been found at widespread localities in the tropical parts of the Pacific and Indian Oceans, and in the northern Pacific. Ehrenberg (1856) described it from the North Atlantic. It thus appears to be cosmopolitan.

Genus MITROCALPIS HAECKEL 1882

MITROCALPIS ARANEAFERA Popofsky

(Pl. 3, figs. 3, 4 ; text-figs. 4.)

Mitrocalpis araneafera Popofsky, 1908, 273–274, Pl. 30, fig. 11.

Shell consisting of a large ovate cephalis, contracted toward the mouth, broader toward the aboral pole, with its wall composed of irregular subcircular or rounded-polygonal meshes. Pores very variable in size, separated by rather thin intervening bars ; in at least some specimens, the meshes are widest at the oral pole. From the surface of the cephalic shell-wall arise short spines, which in some specimens anastomose to form a loose, delicate, arachnoidal covering over the shell: the surface of this secondary meshwork not smooth, but irregular. The secondary meshwork decreases and disappears toward the mouth. Around the mouth are approximately 4–6 spines, all similar in form, conical and acute, of which three are the primary basal spines separating three collar pores. In the shell-wall of the cephalis of some specimens are 5–7 ill-defined longitudinal ribs, which extend upward from the main skeletal elements of the oral region. Length of shell 138–182 μ, of oral spines 20–40 μ. Maximum shell breadth 90–140 μ.

Emended description based on 5 specimens from Sta. 94, and one specimen from each of Stations 30, 47, 97 and 103.

The original description of this species was based on a single specimen from an antarctic plankton sample, and the examination of nine more specimens from the B.A.N.Z.A.R.E. sediments results in a more thorough understanding of its structure. The skeletal elements of the oral region (see text-fig. 4) are found to include the usual median bar (MB), two primary lateral spines (L, L), a dorsal spine (D) and an apical spine (A). Although the primary lateral and dorsal spines extend beyond the oral aperture as three short basal feet, they are not markedly different in length or form from the other (secondary) oral spines.

This species occurs in both the American and Indian Ocean sectors of antarctic waters, and rare examples of the same species or a closely similar form have been found in northern Pacific sediments. Thus its distribution may be bipolar.

Genus Dictyophimus Ehrenberg 1847

Dictyophimus gracilipes Bailey

(Pl. 3, fig. 5; text-fig. 5.)

Dictyophimus gracilipes Bailey, 1856, 4, Pl. 1, fig. 8: Haeckel, 1887, 1197: Cleve, 1899, 29, Pl. 2, fig. 2: Popofsky, 1908, 274–275, Pl. 30, figs. 12, 13; Pl. 31, fig. 15; Pl. 34, fig. 6: Bernstein, 1932, 221, Pl. 3, figs. 4, 5.

Dictyophimus clevei Jörgensen, 1900, 80, Pl. 5, fig. 26; Mielck, 1913, 370–371.

Cephalis subglobular to cap-like, in some specimens thorny, with numerous circular to subcircular pores, bearing an excentric apical spine and an oblique laterally-situated "vertical" spine; cephalic spines variable in length, circular or three-bladed in section. In some specimens the vertical spine is not sufficiently developed to project beyond the wall of the cephalis. Thorax usually broadly campanulate, in some specimens constricted distally. Thoracic pores subcircular, variable in size. In the wall of the thorax are three ribs prolonged to form the three feet which are divergent, three-bladed or circular in section, and usually more or less curved with convexity outward. The internal skeleton in the cephalic region is of the type which Popofsky (1913) termed the "*Plagiocarpa*-type", with the dorsal (D) and two lateral spines (L, L) continuous with the three thoracic ribs, and a vertical (Vert.) and an apical spine (A) projecting (usually) beyond the surface of the cephalis (text-fig. 5). In some specimens, two short accessory spines (l, l, secondary lateral spines) extend from the junction of the apical and dorsal spines to the adjacent shell-wall. Length of apical horn 7–55 μ, of cephalis 13–35 μ, of thorax 25–40 μ, of feet 27–95 μ. Breadth of cephalis 30–46 μ, of thorax 48–70 μ.

Measurements based on 18 specimens from Sta. 94 and 2 from Sta. 97.

Dictyophimus platycephalus Haeckel (1887, 1198, Pl. 60, figs. 4, 5), *D. brandtii* Haeckel (1887, 1198, Pl. 60, fig. 6) and *D. elegans* Dogiel (Dogiel and Reschetnjak, 1952, 14–15, fig. 7) may be identical with *D. gracilipes*, but it would be necessary to examine topotypic material of these forms to determine whether or not this is so. There is little doubt that the variable form found in the B.A.N.Z.A.R.E. sediments is identical with the species first described from the western Bering Sea by Bailey, and later recorded from the north-eastern Pacific (Haeckel), the northern Atlantic (Cleve; Jörgensen; Mielck), the Barents and Kara Seas (Bernstein) and the Indian Ocean sector of the Antarctic (Popofsky).

It occurs in the sediments off the American and Indian Ocean sectors of Antarctica, and is also found to be widespread in the northern Pacific, and in the tropical parts of the Pacific and Indian Oceans. It is thus apparently cosmopolitan.

DICTYOPHIMUS MAWSONI n. sp.

(Pl. 3, figs. 6, 7.)

Shell large, of heavy construction, spiny, generally subhemispherical in form. Cephalis cap-like, with subcircular pores and short, acute, thorn-like spines scattered over its surface. Apical horn stout, cylindro-conical, vertical or oblique. Collar stricture indistinct. Thorax subhemispherical, with large subcircular or subangular pores separated by heavy intervening bars from which arise numerous acute, conical spines. Three ribs, which in some specimens are not distinct, extend along the entire length of the thoracic wall and terminate in three sub-parallel or divergent, stout, cylindro-conical feet. At the collar region, three spines extend inward from the shell-wall, but do not connect with each other; these apparently represent all that remains of the reduced internal spicular skeleton. Length of apical horn 113–166μ, of cephalis 33–40 μ, of thorax 125–175 μ, of feet 100–187 μ. Breadth of cephalis 53–76 μ, of thorax 196–225 μ.

Description based on one specimen from Sta. 30, 9 from Sta. 94 and one from Sta. 97.

Type locality Sta. 94.

This species is distinguished from all others of the genus *Dictyophimus* by the combination of characters: heavy construction, spiny surface, long and stout apical horn, and subhemispherical thorax. Although the number of observed specimens is less than that desirable for the description of a new species, the naming of this species seems justifiable because of the apparent constancy of the skeletal structure, and the distinct differences between this and other described species. This species is named for Sir Douglas Mawson, leader of the B.A.N.Z.A.R. Expedition and my teacher, mentor and friend, who was responsible for my deciding to study the Radiolaria.

Apart from its occurrence in the B.A.N.Z.A.R.E. sediments, *D. mawsoni* has been found in no other locality except the far northern Pacific. It is thus apparently a bipolar cold-water species.

Genus HELOTHOLUS JÖRGENSEN 1905

HELOTHOLUS HISTRICOSA Jörgensen

(Pl. 3, fig. 8; text-fig. 6.)

Helotholus histricosa Jörgensen, 1905, 137, Pl. 16. figs. 86–88: Popofsky, 1908, 279–281, Pl. 32, figs. 1–5; Pl. 36, fig. 2.

Helotholus histricosa micropora Popofsky, 1908, 282, Pl. 33, figs, 2, 3.

Helotholus longus Popofsky, 1908, 282–283, Pl. 34, fig. 2.

Shell consisting principally of a relatively large, approximately hemispherical cephalis and a broad, irregularly campanulate thorax which in some specimens tends to be closed distally by a lattice-plate. Collar stricture usually not very pronounced. Pores of both the cephalis and thorax subcircular to circular, irregularly arranged and of variable size; those of the cephalis not markedly different in size from those of the thorax. Surface of the cephalis, and in many specimens also that of the thorax, beset with numerous, irregularly arranged, thorn-like or acicular spines which are usually shorter than the cephalis. In some specimens, the lower margin of the thorax terminates in a large number of irregular thorns which are not sharply differentiated from the shell-wall. Total length of shell 90–185 μ, its maximum breadth 70–125 μ.

Measurements based on 13 specimens from Sta. 30, 16 from each of Stations 42 and 47, 24 from Sta. 94, and 14 from each of Stations 97 and 103.

This species was first described from Norwegian waters (Jörgensen, 1905), and was subsequently found to be one of the most abundant Radiolaria in the plankton samples collected in the Antarctic by the Deutsche Südpolar-Expedition (Popofsky, 1908). It is abundant in the sediment samples collected by the B.A.N.Z.A.R.E. The forms observed here are outwardly less spiny than those described and figured by Jörgensen and Popofsky, but as this may be due to solution or attrition during sedimentation no taxonomic differentiation is proposed.

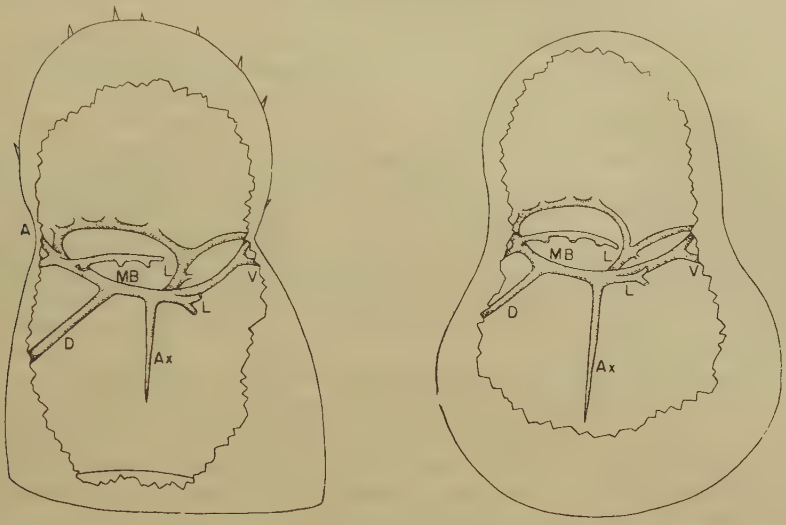

6 7

Figs. 6, 7. Diagrams to illustrate the primary skeletal structures of (6) *Helotholus histricosa* Jörgensen and (7) *Peromelissa denticulata* (Ehrenberg). For explanations see text.

The internal skeletal structure has been described by previous authors, but the large number of specimens now available has made possible a more accurate determination of its nature (text-fig. 6). Using the nomenclature proposed by Popofsky, its most conspicuous elements are the median bar (MB), dorsal spine (D) and two lateral spines (L, L). When the shell is viewed along its main axis, these bars are seen to separate four large collar pores. Near the junction of the lateral spines with the median bar arises an axial spine (Ax) which projects freely into the thoracic cavity. The median bar branches near either end, to form near one extremity a short ventral spine (V), and at the other an apical spine (A) which in some specimens projects beyond the surface of the cephalis. Where the dorsal spine meets the shell wall, there is in most specimens an external longitudinal furrow which extends along a considerable length of the thorax. Near the origin of the apical spine arise two supplementary lateral spines which extend close to the shell wall, to which they are connected at intervals to form a type of ridge along the junction between cephalis and thorax. In the specimens observed, none of the main-spines extends as conspicuously beyond the shell-wall as indicated by Popofsky and Jörgensen.

As a result of the examination of a large number of specimens of *Helotholus* from the B.A.N.Z.A.R.E. sediments, the author is left with little doubt that *Helotholus longus* Popofsky should be synonymized with *H. histricosa*, and that it is impossible to separate *H. histricosa micropora* as a different subspecies. *H. histricosa* is found to be more variable in length and breadth than indicated by Popofsky, and the cephalis, both in its degree of separation from the thorax and in the size of its pores, presents all transitional stages between the form which Popofsky considered typical and the " subspecies *micropora* ".

This species occurs abundantly in both the American and Indian Ocean sectors of Antarctic waters. No closely similar form has been found in the tropical Indian Ocean, nor in the tropical or northern Pacific, and only Jörgensen's (1905) record of its occurrence in Norwegian waters indicates its bipolar distribution.

Genus PEROMELISSA HAECKEL 1882

PEROMELISSA DENTICULATA (Ehrenberg)

(Pl. 3, fig. 9; text-fig. 7.)

Lithobotrys ? denticulata Ehrenberg, 1844, 203.

Lithopera denticulata (Ehrenberg); Ehrenberg, 1873, Pl. 12, fig. 7.

Pylospyris denticulata (Ehrenberg); Haeckel, 1887, 1083; Haecker, 1907, 123–124, fig. 8.

Peromelissa denticulata (Ehrenberg); Haecker, 1908, 448–452, Pl. 84, figs. 582, 583 and 591, text-fig. 83.

Helotholus histricosa Jörgensen *clausa* Popofsky, 1908, 281–282, Pl. 33, fig. 1; Pl. 34, fig. 1.

This species has been well described by Popofsky (1908) and particularly by Haecker (1908). In a long discussion, Haecker gave reasons for its inclusion in the genus *Peromelissa*, and although this is not entirely satisfactory it seems desirable to retain it there until a more natural system of classification is proposed to replace Haeckel's largely artificial system. Popofsky, not realizing that his form is identical with that of Ehrenberg, described it as a variety of *Helotholus histricosa*: this indicates the similarity and probably very close relationship between *Peromelissa denticulata* and *Helotholus histricosa*, and it is unfortunate that expediency dictates the generic separation of these two forms for the present. The internal skeletal structure is similar in the two forms (compare text-figs. 6 and 7).

The three free external spines described by Haecker have not been observed in any of the numerous examples found in the B.A.N.Z.A.R.E. sediment samples, and the three longitudinal furrows on the thorax are neither as distinct nor as constant as Haecker's description indicates. Longitudinal thoracic furrows are absent in some specimens, and in others are associated with the distal terminations of any or all of the following elements of the internal skeleton: the two lateral spines, the dorsal spine, and the ventral spine. In many specimens the axial spine is joined distally to the antapical shell wall.

Total length of shell 80–145 μ, its maximum breadth 75–118 μ. Measurements based on 18 specimens from Sta. 30, 14 from Sta. 42, 5 from Sta. 47, 20 from each of Stations 94 and 97, and 14 from Sta. 103.

This species occurs in both the American and Indian Ocean sectors of Antarctic waters, and no form closely resembling it has been found at any other locality. Thus it appears to be an exclusively southern cold-water species.

Genus DICTYOCEPHALUS EHRENBERG 1861

DICTYOCEPHALUS PAPILLOSUS (Ehrenberg)

(Pl. 3, fig. 10; text-fig. 8.)

Eucyrtidium papillosum Ehrenberg, 1872, 310–311; 1873, Pl. 7, fig. 10.

Dictyocephalus papillosus (Ehrenberg); Haeckel, 1887, 1307.

Dictyocephalus tabulatus Haeckel, 1887, 1307.

Cephalis approximately hemispherical, with small subcircular pores in a hyaline shell-wall, set off from thorax by a pronounced change in contour. Many specimens have a small, inconspicuous lateral tubule projecting slightly from the cephalis near its junction with the thorax, and a short, acute apical horn. Thorax ovate, usually with a rough surface, and with a conspicuous subcylindrical or flared peristome surrounding the mouth which is approximately one-half to two-thirds as broad as the thorax. Thoracic pores subcircular to circular, usually of different sizes and without regular arrangement, separated by rather wide and often thick intervening bars. In the upper part of the thoracic wall are three, usually conspicuous longitudinal ribs, which in many specimens terminate in three short, solid, triangular lateral wings at or above the level at which the thorax reaches its maximum breadth. Length of cephalis 18–25 μ, of thorax (including peristome) 60–90 μ. Maximum breadth of thorax 58–70 μ.

Measurements based on one specimen from Sta. 30, 20 from Sta. 94 and one from Sta. 97.

At the collar stricture are four large collar pores. The bars separating these pores, and their relations with the lateral cephalic tubule, the apical spine, and the three lateral wings, are shown diagrammatically in text-fig. 8. According to the nomenclature used by Popofsy (1913), the bars separating the large collar pores are the median bar (MB), the vertical spine (Vert.) which terminates at the lateral tubule, and the two lateral spines (L, L). In some specimens can be distinguished two short, secondary lateral spines (1, 1) which bound two smaller collar pores. The apical spine (A) penetrates the cephalic wall in some specimens. The three lateral wings represent the terminations of the two primary lateral spines and the dorsal spine (D).

The decisions to identify this species as *Dictyocephalus papillosus* and to place *D. tabulatus* in synonymy are reached after examination of a number of widely separated samples from the Pacific and Indian oceans, but are nevertheless made rather hesitantly. Ehrenberg described *D. papillosus* from a sediment sample collected at Lat. 18° 03′ N., Long. 129° 11′ E. The nearest localities from which the present author has samples available for comparison are those of the "Challenger" Stations 226 and 228 (Lat. 14° 44′ N., Long. 142° 13′ E. and Lat. 19° 24′ N., Long. 141° 13′ E.). It might be expected that the Recent Radiolaria of these two "Challenger" samples would not differ greatly from those at Ehrenberg's locality, but no specimens were found which agreed well with that part of the original description of *D. papillosus* which states: "Articulus secundus maximus papillarum rotundarum seriebus irregularibus margine prominulis obsessus". The specimens observed could better be described as having a generally rough rather than a papillate surface, and in this as in other respects the specimens from the Philippine Sea agree with those from the antarctic samples. Ehrenberg's description and figure do not indicate the apical spine, lateral cephalic tubule and thoracic spines, but this is probably the result of his having overlooked these inconspicuous structures.

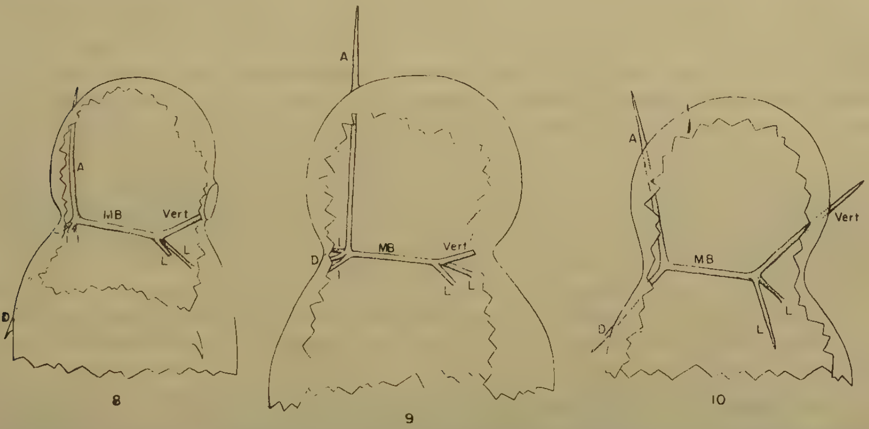

Figs. 8–10. Diagrams to illustrate the primary skeletal structures of the collar and cephalic regions of (8) *Dictyocephalus papillosus* (Ehrenberg), (9) *Pterocorys hirundo* Haeckel and (10) *Theocalyptra davisiana* (Ehrenberg). For explanations see text.

There seems little doubt that *D. tabulatus* is synonymous with *D. papillosus*. The type locality of *D. tabulatus* is "Challenger" Station 271, and although the author has been unable to examine the original sample from that station, it seems reasonable to expect that the recent assemblage from the top of the nearby Swedish Deep-Sea Expendition Core No. 74 (Riedel, 1957) is identical with that of the "Challenger" sample. Specimens agreeing well with the above emended description of *D. papillosus* were found near the top of this core, and no specimens were found to differ sufficiently to justify their being placed in a separate species as *D. tabulatus*. It seems possible that *D. australis* Haeckel (1887, 1306–1307, Pl. 62, fig. 1) and *D. mediterraneus* Haeckel (1887, 1307, Pl. 62, fig. 2) may also have to be placed in synonymy with *D. papillosus*, but as specimens from the type localities of these species are not at present available for comparison, the question is left in abeyance.

Although the presence of an apical spine and three lateral wings on the thorax is incompatible with the placement of this species in the genus *Dictyocephalus*, it seems advisable to leave it in that genus until a thorough revision of related forms results in a more natural classification. Stöhr (1880, 100, Pl. 3, fig. 19) described a rather similar form as *Lithomelissa amphora*, and if Haeckel's classification is applied strictly that species is widely separated taxonomically from the apparently closely related *Sethocorys amphora* (Stöhr).

D. papillosus occurs at widely separated localities in the Indian Ocean sector of antarctic waters, but has not been found in the American sector–though it appears probable that this species will eventually prove to have an almost cosmopolitan distribution. It occurs in the tropical parts of the Pacific and Indian oceans, and in the northern Pacific. Specimens from the antarctic sediment samples are generally more heavily constructed, with consequently more prominent thoracic spines, than those from more northerly localities, but this does not seem to be sufficient reason to separate them taxonomically.

Genus PTEROCORYS HAECKEL 1882

PTEROCORYS HIRUNDO Haeckel

(Pl. 3, fig. 11 ; Pl. 4, fig. 1 ; text-fig. 9.)

Pterocorys hirundo Haeckel, 1887, 1318, Pl. 71, fig. 4.

Cephalis subglobular, with smooth or slightly spiny surface, and numerous small pores which in some specimens are secondarily closed by siliceous lamellae. Apical horn thin, acute, vertical, excentrically situated, usually approximately as long as the cephalis. In some specimens the "vertical spine" element of the primary spicular skeleton (Vert. in text-fig. 9) extends beyond the cephalis surface as a second, oblique cephalic horn. Thorax truncate-conical to campanulate, with rather large subcircular or circular pores, its surface usually bearing short, thorn-like spines. Abdomen short, narrower than widest part of thorax, in many specimens rudimentary or consisting of only one or two rows of subcircular pores separated by narrow intervening bars, with no distinct peristome. In the wall of the thorax are three ribs, continuous with the three three-bladed, acute, divergent, straight or slightly curved feet which arise subterminally from the thorax. At the collar stricture are two pairs of large collar pores separated by the primary lateral spines (L, L), and it is often possible to distinguish also a pair of smaller pores, enclosed by the dorsal (D) and the secondary lateral (l, l) spines in front of the origin of the apical spine (A, text-fig. 9). Length of apical horn 7–36 μ, of cephalis 16–27 μ, of thorax 30–70 μ, of feet 35–125 μ. Breadth of thorax 50–90 μ.

Emended description based on two specimens from B.A.N.Z.A.R.E. Sta. 30, 20 from Sta. 94, and one from each of Sta. 97 and 103, as well as 9 specimens from the sediment collected at "Challenger" Sta. 272.

Re-examination of a large number of Radiolaria from a portion of the original sediment sample from "Challenger" Stas. 272, the type locality of this species, did not reveal any specimen agreeing with the original description and figure in having a long, heavy, pyramidal apical horn and a thorax and abdomen each 80 μ long and 100 μ broad. However, nine specimens found at that locality apparently belong to this species, and the discrepancies are probably due to the fact that Haeckel had a specimen with an abnormally developed skeleton.

As this species is now described, it differs from *Pterocorys aquila* Haeckel (1887, 1317–1318, Pl. 71, fig. 5) principally in having a narrower thorax, and in the feet not being latticed proximally. It is distinguished from *Dictyophimus arabicus* (Ehrenberg) (Ehrenberg, 1872, 316 ; 1873, Pl. 10, fig. 3 ; Haeckel, 1887, 1198) by the usually spiny thorax and pronouncedly three-bladed feet.

This species occurs in both the American and Indian Ocean sectors of Antarctic waters, in the tropical parts of the Pacific and Indian Oceans, and in the northern Pacific. It may thus be cosmopolitan.

Genus THEOCALYPTRA HAECKEL 1887

THEOCALYPTRA DAVISIANA (Ehrenberg)

(Pl. 4, figs. 2, 3; text-fig. 10.)

Cycladophora ? davisiana Ehrenberg, 1862, 297; 1873, Pl. 2, fig. 11.
Eucyrtidium davisianum (Ehrenberg); Haeckel, 1862, 328–329.
Stichopilium davisianum (Ehrenberg); Haeckel, 1887, 1437–1438.
Pterocodon davisianus Ehrenberg, 1862, 300–301; 1873, Pl. 2, fig. 10.
Pterocanium davisianum (Ehrenberg); Haeckel, 1862, 332.

Shell conical-campanulate, of moderately heavy structure, consisting of two, three or four segments. Cephalis subglobose, with small, sparse pores, and bearing two short, acicular spines—one vertical, approximately apical, and the other lateral, oblique. Collar stricture slight. Subsequent part of shell, comprising its main bulk, will be termed the thorax, though in some specimens it appears to be divided by an ill-defined internal transverse ridge into an upper and a lower portion. Thorax approximately conical, in many specimens flared at a wider angle distally than proximally. Thoracic pores subcircular proximally, becoming polygonal distally, arranged in usually 4–7 transverse rows which are indefinite in some specimens. In most specimens, three short, downwardly directed acicular spines penetrate the thoracic wall near its junction with the cephalis. In many specimens a further shell-segment is present, marked off from the thorax by an internal septal ring. When present, this abdomen is short, truncate-conical, usually flared at a wider angle than the thorax, with usually 2–4 transverse rows of polygonal pores separated by more delicate bars than those of the thorax. Length of cephalis usually 17–25 μ, of thorax 40–80 μ, of abdomen 15–35 μ. Maximum breadth of shell 70–130 μ.

Measurements based on 7 specimens from Sta. 30, one from Sta. 47, 25 from Sta. 94, 8 from Sta. 97 and 2 from Sta. 103.

There seems to be little doubt that the two forms from Davis Strait, which Ehrenberg described as *Pterocodon davisianus* and *Cycladophora davisiana*, belong to a single species, as was suggested by Haeckel (1887). Judging from Ehrenberg's figures, the Antarctic specimens are almost certainly identical with the species described from Davis Strait.

The correct generic assignment of this species, however, is difficult. Ehrenberg's description of his *Cycladophora davisiana* indicates that the shell consists of three segments, while that of his *Pterocodon davisianus* states that its shell has four segments. Haeckel (1887) writes that *Stichopilium davisianum* has four segments. In the Antarctic specimens, the cephalis can be clearly distinguished in all individuals, but subsequent segmental divisions are neither distinct nor constant. In rare individuals, no segmental divisions can be distinguished in the post-cephalic part of the shell; in others, a subterminal internal septal ring clearly separates a "thorax" from an "abdomen"; while in still others the main "thoracic" portion of the shell is apparently divided into two by yet another internal septal ring. Thus it is virtually impossible to place this species, with confidence, in any of the genera of Haeckel's system. Its assignment to *Theocalyptra* is based on the following considerations:—(1) it is probably best regarded as having three segments, and (2) it is apparently closely related to *Theocalyptra bicornis* (Popofsky), which in turn is probably congeneric with *Theocalyptra veneris* Haeckel, the type species of its genus. Many species apparently closely related to *T. davisiana* have been described in the genus *Clathrocyclas*.

The internal skeletal structure of this form corresponds to that which Popofsky (1913) described as the "*Lithomelissa brevispicula*" type. The two cephalic spines are the free portions of the apical (A, in text-fig. 10) and vertical (Vert.) spines, while the three spines which project below the collar stricture are the unpaired dorsal (D) and paired lateral (L, L) spines.

T. davisiana occurs in the American and Indian Ocean sectors of Antarctic waters, as well as in the northern Pacific and in the tropical parts of the Pacific and Indian Oceans. These occurrences, together with the previous records from the northern Altantic, indicate that it may be cosmopolitan. It appears to be more common in sediments from high and middle latitudes than in those from tropical regions.

Theocalyptra bicornis (Popofsky)

(Pl. 4, fig. 4.)

Carpocanium cornutum (Bailey) ; Ehrenberg, 1862, 296 ; 1873, Pl. 2, fig. 9.
Lophophaena cornuta (Bailey) ; Haeckel, 1862, 299.
Theocalyptra cornuta (Bailey) ; Haeckel, 1887, 1398.
Pterocorys bicornis Popofsky, 1908, 288–289, Pl. 34, figs. 7, 8.

Shell conical-campanulate, consisting usually of two or three segments. Cephalis subglobose, with numerous small pores, bearing two three-bladed spines of approximately the same length as the cephalis—one vertical, approximately apical, and the other lateral, oblique. Collar stricture slight. Major portion of the shell in most specimens not showing segmental division, and therefore termed the " thorax ". Thorax conical proximally, campanulate distally, with subcircular to polygonal pores separated by rather narrow intervening bars. Thoracic pores increase in size distally, and are arranged in usually 9–11 transverse rows. Three short, downwardly directed acicular spines penetrate the wall of the thorax near the collar stricture. In some specimens, there is a marked change in thoracic contour at the position of the rather abrupt transition from subcircular proximal thoracic pores to more regular polygonal distal thoracic pores ; it is apparently this change in contour, which in some specimens gives the impression of a segmental division, which Popofsky regarded as a lumbar stricture. In many specimens, one or two rows of pores are marked off from the distal end of the thorax by an internal septal ring ; these may be considered to constitute an abdomen. Length of cephalis 15–27 μ, of thorax 80–97 μ ; maximum breadth 95–120 μ.

Measurements based on 2 specimens from each of Stas. 30 and 47, 9 from Sta. 94 and one from Sta. 97. This species differs from *T. davisianum* principally in more delicate structure and larger thorax.

Theocalyptra bicornis appears to be closely related to *T. davisiana*, and the distinction of its segments involves the same difficulties as described for that species. Because an internal septal ring dividing the major portion of the shell is not constantly present, it is considered advisable to regard that large part of the shell as a thorax. This species is thus placed in the genus *Theocalyptra* for the same reasons as given above for *T. davisiana*. It appears that the form which Ehrenberg (1873) figured as *Carpocanium cornutum* (Bailey) may not belong to the same species as that which Bailey (1856, 5, Pl. 1, figs. 13, 14) named *Halicalyptra ? cornuta*—for this reason, Popofsky's specific name is retained, at least temporarily.

The internal skeletal structure of this species is exactly similar to that described for *T. davisiana* in all specimens examined from the B.A.N.Z.A.R.E. sediments. No trace was found of the ventral spine which Popofsky (1913) described as characteristic of his " *Pterocorys bicornis* type ".

T. bicornis occurs in the American and Indian Ocean sectors of Antarctic waters ; it also occurs in the northern Pacific, but has not been found in the tropical parts of the Pacific and Indian Oceans. These findings, together with Ehrenberg's record of its occurrence in Davis Strait, indicate that its distribution may be bipolar.

Genus Stichopilium Haeckel 1882

Stichopilium variabile Popofsky

(Pl. 4, fig. 5 ; text-fig. 11.)

Stichopilium (?) *variabilis* Popofsky, 1908, 290–292, Pl. 35, figs. 4–7.

Shell cylindro-conical, consisting generally of four segments of which the third or fourth is broadest. Cephalis subglobular, with numerous, small, subcircular pores and a short, acute apical spine. Collar stricture distinct. Thorax truncate-conical, with subcircular pores separated by intervening bars of variable width. Three radial ribs extend in the wall of the thorax, and in some specimens are continued to the wall of the third segment. In some specimens, the distal portions of these ribs are raised above the shell surface as latticed wings. Lumbar stricture distinct in some specimens but barely discernible in others. Post-thoracic part of shell in some specimens distinctly divided into a third and a fourth segment, but in others not obviously subdivided. Pores of post-thoracic part of shell variable in size, subcircular to subangular, without regular arrangement, separated by intervening bars of variable width. As indicated in text-fig. 11, there are four collar pores separated by elements of the internal spicular skeleton—the median bar (MB), the vertical spine (Vert.), and the two lateral spines (L, L) which are prolonged to form two of the thoracic ribs. The third thoracic rib and the apical spine represent the dorsal (D) and apical (A) spines of the primary spicular skeleton, respectively. Length of apical horn 5–12 μ, of cephalis 14–21 μ, of thorax 22–42 μ, of post-thoracic part of shell 50–140 μ. Maximum breadth of shell 60–92 μ.

Measurements based on 14 specimens from Sta. 94.

In reversing Campbell's (1954) decision to use the name *Triacartus* for this genus, the author is acting in accordance with the Copenhagen decision of the International Commission on Zoological Nomenclature to uphold the action of the first reviser (in this case undoubtedly Haeckel, 1887). The termination of the specific name is altered to correspond to the neuter generic name.

Besides its occurrence in the Indian Ocean sector of Antarctic waters, this species has been found in sediments from the tropical parts of the Pacific and Indian Oceans, and the northern Pacific. It thus appears to be cosmopolitan.

Genus Artostrobus Haeckel 1887

Artostrobus annulatus (Bailey)

(Pl. 4, fig. 6.)

Cornutella ? annulata Bailey, 1856, 3, Pl. 1, figs. 5a, b ; Ehrenberg, 1862, 297 ; Ehrenberg, 1872, Pl. 2, fig. 16.

Eucyrtidium annulatum (Bailey) ; Haeckel, 1862, 327–328.

Artostrobus annulatus (Bailey) ; Haeckel, 1887, 1481 ; Cleve, 1899, 27, Pl. 1, fig. 6.

Cornutella annulata Ehrenberg ; Haeckel, 1887, 1182.

Shell narrowly conical or subcylindrical, reaching its maximum breadth at or near the distal end. Cephalis subglobular, hyaline, poreless, bearing an eccentric, vertical apical spine. Collar stricture indistinct. Remainder of the shell (regarded as the thorax) usually conical proximally, subcylindrical distally, with 9-16 transverse rows of subcircular to subquadrangular pores which increase in size distally. Near the collar stricture in most specimens, three small, downwardly

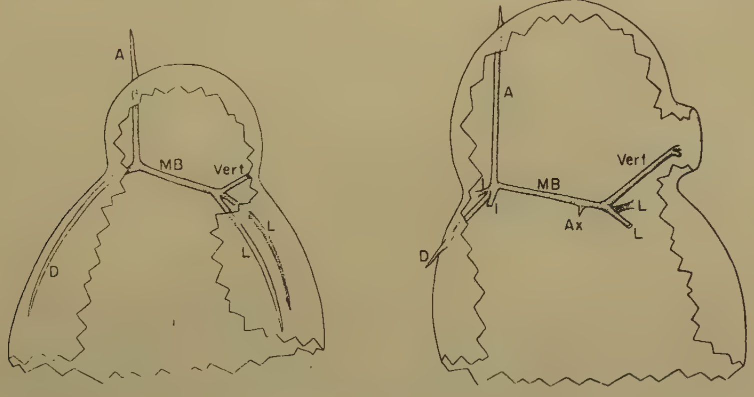

11 12

Figs. 11, 12. Diagrams to illustrate the primary skeletal structures of the collar and cephalic regions of (11) *Stichopilium variabile* Popofsky and (12) *Siphocampium* sp. For explanations see text.

directed spines penetrate the thoracic wall; these spines represent the terminations of the dorsal and two lateral spines of the internal spicular skeleton. The apical spine arises from the median bar of the internal skeleton near the origin of the dorsal spine. Collar pores are three or four in number, not all examples showing a continuation of the median bar bisecting the angle between the two lateral spines. Length of apical horn 8–42 μ, of cephalis 15–17 μ, or thorax 66–120 μ. Maximum breadth of shell 32–42 μ.

Measurements based on 16 examples from Sta. 94.

There is little doubt that the Antarctic form is identical with that described by Bailey from the western Bering Sea—the general form and dimensions are similar, and one of Bailey's figures shows a downwardly directed spine similar to those found in the Antarctic specimens. It also appears that the specimen which Ehrenberg figured from the Davis Strait as *Cornutella annulata*, and which Haeckel considered to be a different species from *Artostrobus annulatus* (Bailey), is in fact the same species. The present author has found this species in many widely scattered localities, and in some specimens it is difficult or impossible to distinguish downwardly directed spines penetrating the shell wall near the collar stricture.

It seems that the entire post-cephalic portion of the shell should best be regarded as a thorax with a number of transverse rows of pores, rather than as a number of segments each having one row of pores. If this view is accepted, it is unfortunate that '*Cornutella annulata* Bailey' has been made (Campbell, 1954, 140) the type species of the genus *Artostrobus*, which is supposed to be an eradiate stichocyrtid.

Besides its occurrence in the Indian Ocean sector of Antarctic waters, *A. annulatus* has been found in the tropical parts of the Pacific and Indian oceans, and in the northern Pacific. Thus it may be cosmopolitan.

Genus LITHOMITRA BÜTSCHLI 1882

LITHOMITRA ARACHNEA (Ehrenberg)

(Pl. 4, figs. 7, 8.)

Eucyrtidium lineatum arachneum Ehrenberg, 1862, 299.

Lithomitra lineata (Ehrenberg); Haeckel, 1887, 1484 (*partim*); Cleve, 1899, 30, Pl. 2, fig. 7.

Lithomitra nodosaria Haeckel, 1887, 1484, Pl. 79, fig. 1.

Lithomitra vanhöffeni Popofsky, 1908, 296, Pl. 36, fig. 9.

Shell subcylindrical, with 4–9 segments. Cephalis hemispherical, with few small, round pores and no apical horn, but with an inconspicuous lateral or subapical tubule. Inside the cephalis, near its junction with the thorax, are the apical, dorsal, vertical and two lateral spines. Collar stricture not pronounced; lumbar and subsequent constrictions distinct. Thorax subcylindrical, with 2–3 transverse rows of small subcircular pores. Subsequent segments each have one transverse row of similar pores at the level at which their diameter is greatest, with the exception that in some specimens the first two post-thoracic segments appear to be fused together, so that there is in effect a rather broad third segment with two rows of pores. Longitudinal ridges, in many specimens connected by transverse ridges to form a network, ornament the surface of the thorax and subsequent segments. Shell terminally open, not pronouncedly constricted. Total length of shell 73–160 μ, of cephalis 13–22 μ, of thorax 17–26 μ, of subsequent segments each 10–30 μ. Maximum breadth of shell (at fourth or fifth segment) 34–57 μ.

Measurements based on 17 specimens from B.A.N.Z.A.R.E. Sta. 94, 10 from the northern Pacific (Lat. 49° 39.5′ N, Long. 177° 39′ W), 10 from the tropical Pacific (Lat. 00° 20′ N, Long. 150° 36′ W) and 10 from the tropical Indian Ocean (Lat. 01° 56′ N, Long. 88° 12′ E).

The determination of the correct name of this species is a rather complicated problem. Both Haeckel (1862, 316) and Stöhr (1880, 101) pointed out that Ehrenberg had applied the name *Lithocampe lineata* (later *Eucyrtidium lineatum*) to a number of different species from various Tertiary localities. Haeckel (1887, 1484) gave a somewhat fuller description of the 'species', and restricted the sense in which the name, which he changed to *Lithomitra lineata* (Ehrenberg), was to be used. The two earliest of Ehrenberg's figures which Haeckel admitted to the restricted definition of *L. lineata* were of an example from Caltanisetta (Sicily) and one from the Nicobar Islands. In the opinion of the present author, these two figures are of different species, and it is necessary to restrict the definition of *L. lineata* still further. It is proposed that the name be confined to the form which Ehrenberg (1856, Pl. 22, fig. 26) figured from Caltanisetta. The form which Haeckel found to have a cosmopolitan distribution in the 'Challenger' samples is apparently different from the species occurring in the Miocene sediments of Caltanisetta, and therefore requires a different name. It seems that the cosmopolitan Recent form might most appropriately be called *Lithomitra arachnea* (Ehrenberg), as this is apparently the form which Ehrenberg described from a marine sediment near Greenland as *Eucyrtidium lineatum arachneum*: 'loricae lineis longitudinalibus aliis lineolis transversis in opus reticulatum contextis'. Although a small lateral tubule is present on the cephalis, it is considered advisable to retain the species for the present in the genus *Lithomitra*, because it may be more closely related to *Lithomitra pachyderma* (Ehrenberg) (the type species of *Lithomitra*) than to the type species of the genus *Siphocampium*, *S. accrescens* Rüst. The termination of the specific name is changed to correspond with the femine generic name.

It seems necessary to place *Lithomitra nodosaria* Haeckel in synonymy with *L. arachnea*. The type locality of *L. nodosaria* is the central Pacific ('Challenger' Stations 263–274), but examination of a large number of Radiolaria from the original 'Challenger' sediment samples from Stations 263, 265, 266, 270 and 272 did not reveal the existence of a form corresponding to Haeckel's description of this species, sufficiently different to justify specific separation from *L. arachnea*.

Popofsky was apparently unaware of Ehrenberg's description of *Eucyrtidium lineatum arachneum* when he described his single antarctic specimen as a new species *Lithomitra vanhöffeni*, which he states is to be distinguished from *L. lineata* by its size and the network of ridges on the shell surface.

L. arachnea has been found in the American and Indian Ocean sectors of Antarctic waters, in the tropical parts of the Pacific and Indian Oceans, and in the northern parts of the Pacific and Atlantic Oceans. It is thus apparently cosmopolitan.

Genus SIPHOCAMPIUM HAECKEL 1882

SIPHOCAMPIUM sp.

(Pl. 4, figs. 9, 10; text-fig. 12.)

Subcylindrical shell consisting of 4–6 segments, of which the third or fourth is broadest. Cephalis approximately hemispherical, with a short, inconspicuous lateral tubule, scattered subcircular pores, and usually a tiny, thorn-like apical spine. Collar stricture indistinct. Thorax short, truncate-conical, with small subcircular to circular pores arranged approximately in transverse rows. Subsequent segments annular, separated by usually distinct constrictions, and having subcircular to circular pores arranged in regular transverse rows in the smooth, thin, hyaline shell wall. Thorax has 3–6 transverse rows of pores, the third segment 4–8 rows, the fourth segment 3–15 rows, and the fifth segment (in the specimens in which it is complete) 2–4 rows. Although part of a sixth segment was found in some specimens, it was not observed to terminate at a definite peristome, and thus was apparently incomplete. In many specimens, the fourth or fifth segment terminates in a clear, annular peristome with a smooth margin, somewhat narrower than the terminal segment. Total length of shell 92–172 μ, its maximum breadth 46–75 μ. Length of cephalis 14–22 μ, of thorax 15–32 μ, of third segment 20–36 μ, of fourth segment 18–98 μ, of fifth segment 12–40 μ.

Description based on 7 specimens from Sta. 30, 25 from Sta. 94, 5 from Sta. 97 and 10 from Sta. 103.

The internal skeleton of the cephalis and collar region is rather difficult to see, and is apparently not completely similar in all individuals. The general structure appears to be as illustrated in text-figure 12. From a median bar (MB) arise eight spines: an apical spine (A) which in most specimens penetrates the cephalic wall excentrically, a downwardly directed dorsal spine (D) which in many examples penetrates the thoracic shell-wall, a vertical spine (Vert.) directed obliquely upward toward the lateral tubule, a short spine (Ax) directed downward, and two pairs of lateral spines (LL, ll) connecting the median bar with the shell-wall of the collar region.

The taxonomic position of this species cannot at present be determined satisfactorily. It may be identical with one or more of the superficially similar species which Popofsky (1908, 293–296) described from antarctic waters—*Poroamphora paradoxa*, *Lithamphora furcaspiculata*, and perhaps *Dictyomitra meridionalis* and *D. drygalskii*—but on the other hand the presence of a lateral tubule on the cephalis suggests its placement in the genus *Siphocampium*. Earlier workers did not describe the minute structure of the cyrtoid cephalis in detail, and thus a large number of the stichocyrtids are difficult to identify and require re-examination. Determination of the structure and true relationships of this and similar species, and of their distributions, will require a thorough study which will necessarily be of monographic proportions, and is considered beyond the scope of the present paper.

Genus CYRTOCAPSA HAECKEL 1882

CYRTOCAPSA sp.

(Pl. 4, fig. 11.)

Shell rather thin-walled, slender, conical, consisting of 5–14 segments increasing gradually in breadth and separated by distinct constrictions. Cephalis subspherical, with few small pores and a curved, excentrically placed apical horn which is usually as long to three times as long as the cephalis. Four collar pores. Subsequent segments annular or truncate-conical, with subcircular to subhexagonal pores generally showing alignment in transverse rows. On the second segment are 2–3 transverse rows of pores, on the third, fourth and fifth segments 2–4 rows, on the sixth and seventh segments (when present) 2–5 rows, and on subsequent segments (when present) 3–8 rows. On the segments other than the cephalis, most specimens have a few short spines, which are not arranged in longitudinal rows. Terminal segment subglobular, closing the shell aperture. Total length of shell (excluding apical spine) 140–210 μ, its maximum breadth 45–85 μ.

Description based on five complete (closed) and several incomplete examples, all from Sta. 94.

This form is not described as a new species because the number of examples found seems too small to establish the range of variation. Moreover, it appears possible that it may be identical with several forms previously described as having " open " shells, as for example *Lithostrobus cornutella* (Ehrenberg) (Ehrenberg, 1862, 298 ; 1873, Pl. 2, fig. 14) and the form which Ehrenberg called " *Eucyrtidium cuspidatum* Bailey " (Ehrenberg, 1862, 298 ; 1873, Pl. 2, fig. 15).

Fragments of the skeletons of this or closely related species are widely distributed in the sediments of the tropical Pacific and Indian Oceans, and of the northern Pacific. However, it will not be known whether we are here dealing with one cosmopolitan species or a group of species, until it is possible more closely to define this species and other rather similar forms such as *Lithostrobus cornutella* (Ehrenberg), *L. cuspidatus* (Ehrenberg), *L. tetrastichus* Haeckel, *Cyrtopera laguncula* Haeckel, *Stichopera pectinata* Haeckel and Haeckel's species of the subgenus *Sticholagena*.

Genus BOTRYOPYLE HAECKEL 1882

BOTRYOPYLE ? ANTARCTICA (Haecker)

(Pl. 4, fig. 12 ; text-fig. 13.)

Saccospyris antarctica Haecker, 1907, 124, figs. 10a, b ; 1908, 447–448, Pl. 84, figs. 584, 589, 590.

Haliphormis antarctica (Haecker) ; Campbell, 1954, 116, fig. 56 (12).

From the material collected in antarctic waters by the " Valdivia " in 1898-99, Haecker (1907) described this species for which he erected the genus *Saccospyris* within the subfamily Rhodospyrinae. Campbell (1954) indicated that *Saccospyris* is a junior synonym of Ehrenberg's genus *Haliphormis*. However, examination of this species from the B.A.N.Z.A.R.E. material shows that it does not belong among Haeckel's Triospyrida (superfamily Triospyridicae according to Campbell, 1954) but rather among his Botryodea (superfamily Cannobotrydicae according to Campbell).

Although Haecker apparently took considerable pains to determine the internal structure of this form, his description and figures are somewhat inadequate. The following description (and text-figure 13) are based on a close examination of several specimens, which varied in some details but in all of which the general plan of the internal structure was similar. Externally, the shell exhibits five main parts :—the thorax (A) which in some specimens is closed distally, a larger (B) and a smaller (C) cephalic lobe, an inconspicuous chamber (D) between A and C, and some rather irregular shell material (E) laterally from D. Pores which are generally regular in form and arrangement connect the chambers of A and B, B and C, C and D, D and A, and D and B. Between A and B are two large, constant pores (a, a′) and usually one or two smaller pores (b, b′). An almost constant feature of the wall separating B and C is a pair of pores c and c′, and in some specimens other pores also penetrate this wall. C communicates with D by a simple opening (d), which is constricted by a ledge (e). Between the chamber D and A are four main pores, two larger (f, f′) and two smaller (g, g′), and a number of peripheral pores (h) which are inconstant in size and arrangement. Near the junction of the bars separating f, f′, g and g′ arises a spine (k) which projects downward into the thorax A. Two large pores (j, j′) connect D with B. Close to the wall of the chamber D, bars extend between C and A.

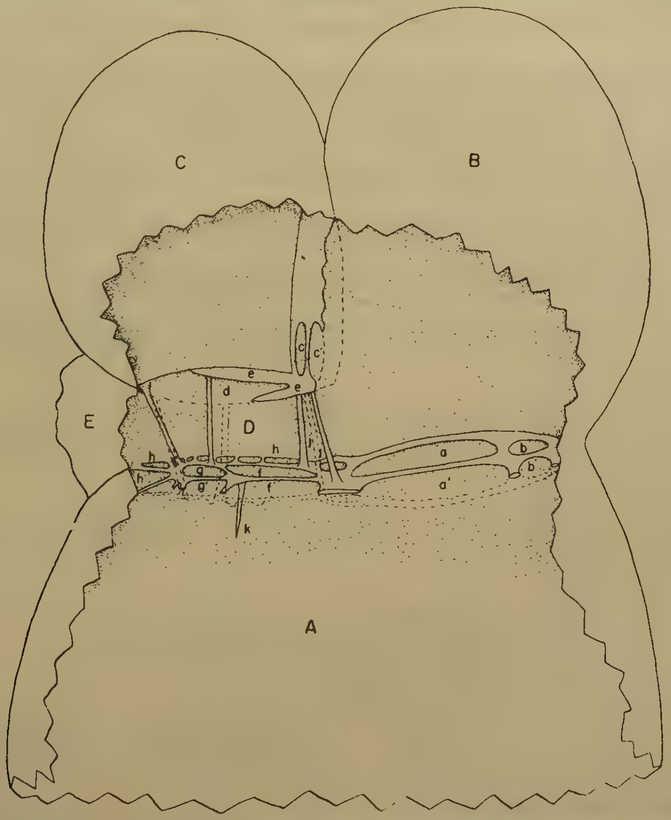

Fig. 13. Diagram to illustrate the internal skeletal elements of the cephalic region of *Botryopyle ? antarctica* (Haecker). For explanation see text.

Thus the structure is more complicated than indicated by Haecker's description, and comparison with that described by Bütschli (1882, 520, Pl. 33, figs. 27a–c) for *Lithobotrys geminata* Ehrenberg leaves little doubt that the antarctic form belongs among the Cannobotrydicae. Haeckel's descriptions of members of this group are inadequate, and it is difficult at present to assign this species to a genus with any confidence. *Botryopyle* ? *antarctica* may be identical with *Bisphaerocephalus minutus* Popofsky (1908, 284–285, Pl. 33, fig. 9), described from a single specimen collected in Antarctic waters.

Total length of shell of *B.* ? *antarctica* 80–155 μ, its maximum breadth 70–100 μ. Measurements based on 11 specimens from Sta. 30, 3 from Sta. 42, 9 from Sta. 47, 24 from Sta. 94, 17 from Sta. 97 and 5 from Sta. 103.

This species occurs in both the American and Indian Ocean sectors of Antarctic waters, as well as at several widely separated localities in the northern Pacific. It has not been found in the tropical parts of the Pacific and Indian Oceans. Thus it appears to have a cold-water bipolar distribution.

LITERATURE CITED

Bailey, J. W., 1856. Notice of microscopic forms found in the soundings of the Sea of Kamtschatka. American Jour. Sci. Arts, ser. 2, 22, 1–6, Pl. 1.

Bernstein, T., 1932. Über einige arktische Radiolarien. Archiv für Protistenkunde, 76, 217–226, Pls. 1, 2.

Bütschli, O., 1882. Beiträge zur Kenntnis der Radiolarienskelette, insbesondere der der Cyrtida. Zietschr. Wissensch. Zool., Leipzig, 36, 485–540, Pls. 31–33.

Campbell, A. S., 1954. Radiolaria. In Moore, R. C., and Campbell, A. S., Treatise on Invertebrate Paleontology, D, Protista 3, 11–163.

——and Clark, B. L., 1944. Miocene radiolarian faunas from Southern California. Geol. Soc. America, Spec. Papers, 51, 1–76, Pls. 1–7.

Cleve, P. T., 1899. Plankton collected by the Swedish Expedition to Spitzbergen in 1898. Kongl. Svenska Vetensk.-Akad., Handl., 32., (3), 1–51, Pls. 1–4.

Dogiel, V. A., and Reschetnjak, V. V., 1952. Materialy po radioljarijam severo-zapadnoj chasti tikhogo okeana. Issledovanija Dalnevostochnykh Morej SSSR, 3, 5–36.

Dreyer, F., 1889. Die Pylombildungen in vergleichend-anatomischer und entwicklungsgeschichtlicher Beziehung bei Radiolarien und bei Protisten überhaupt. Jenaische Zeitschr. Naturwiss., 23, N. F. 16, 1–138, Pls. 1–6.

Ehrenberg, C. G., 1844. Einige vorläufige Resultate seiner Untersuchungen der ihm von der Südpolreise des Capitain Ross, so wie von den Herren Schayer und Darwin zugekommenen Materialien über das Verhalten des kleinsten Lebens in den Oceanen und den grössten bisher zugänglichen Tiefen des Weltmeers. K. Preuss. Akad. Wiss., Berlin, Ber., 1844, 182–207.

———1856. Mikrogeologie. Leipzig.

———1859. Kurze Characteristik der 9 neuen Genera und der 105 neuen Species des ägäischen Meeres und des Tiefgrundes des Mittel-Meeres. K. Preuss. Akad. Wiss. Berlin, Monatsber., 1858, 10–41.

———1862. Die Tiefgrund-Verhältnisse des Oceans am Eingange der Davisstrasse und bei Island. K. Preuss. Akad. Wiss. Berlin, Monatsber., 1861, 275–315.

———1872. Mikrogeologische Studien als Zusammenfassung seiner Beobachtungen des kleinsten Lebens der Meeres-Tiefgründe aller Zonen und dessen geologischen Einfluss. K. Preuss, Akad. Wiss. Berlin, Monatsber., 1872, 265–322.

——1873. Mikrogeologische Studien über das kleinste Leben der Meeres-Tiefgründe aller Zonen und dessen geologischen Einfluss. K. Akad. Wiss. Berlin, Abh., 1872, 131–399, Pls. 1–12.

Ekman, S., 1953. Zoogeography of the Sea. London.

Haeckel, E., 1862. Die Radiolarien. Berlin.

——1882. Entwurf eines Radiolarien-Systems auf Grund von Studien der Challenger-Radiolarien. Jenaische Zeitschr. Naturwiss., 50, N. F. 8, 418–472.

——1887. Report on the Radiolaria collected by H.M.S. "Challenger" during the years 1873–1876. Challenger Exped. Repts., Zool., 18, clxxxviii + 1803 pp., 140 pls., 1 map.

Haecker, V., 1904. Bericht über die Tripyleen-Ausbeute der Deutschen Tiefsee-Expedition. Deutschen Zool. Gesell., Verh., Jahrg. 14, 122–157.

——1907. Altertümliche Sphärellarien und Cyrtellarien aus grossen Meerestiefen. Archiv für Protistenkunde, 10, 114–126.

——1908. Die Tripyleen, Collodarien und Mikroradiolarien der Tiefsee. Wiss. Ergeb. Deutsche Tiefsee-Expedition, 14, (1), 1–476, Pls. 1–85.

Hinde, G. J., 1890. Notes on Radiolaria from the Lower Palaeozoic rocks (Llandeilo-Caradoc) of the South of Scotland. Ann. Nat. Hist., (6), 6, 40–59, Pls. 3, 4.

Jörgensen, E., 1900. Protophyten und Protozoen im Plankton aus der norwegischen Westküste. Bergens Museums Aarbog, 1899, 6, 1–112 + lxxxiii pp., Pls. 1–5.

——1905. The protist plankton and the diatoms in bottom samples : Radiolaria. Bergens Museum Skrifter, 1905, 114–151, Pls. 8–18.

Mast, H. 1910. Die Astrosphaeriden. Wiss. Ergeb. Deutsche Tiefsee-Expedition, 19, (4), 125–190, Pls. 14–21.

Mielck, 1913. Résumé des observations sur le plankton : Radiolaria. Conseil Permanent Internat. pour l'Exploration de la Mer, Bull. Trimestriel, 3, 303–402.

Parr, W. J., 1950. Foraminifera. B.A.N.Z. Antarctic Research Expedition Repts., ser. B. 5, (6), 234–392, Pls. 3–15.

Phleger, F. B, Parker, F. L., and Peirson, J. F., 1953. North Atlantic Foraminifera. Swedish Deep-Sea Expedition Repts., 7, (1), 1–122, Pls. 1–12.

Popofsky, A., 1908. Die Radiolarien der Antarktis (mit Ausnahme der Tripyleen). Deutsche Südpolar-Expedition, 10, (3), 185–305, Pls. 20–36.

——1913. Die Nassellarien des Warmwassergebietes. Deutsche Südpolar-Expedition, 14, (2), 217–416, Pls. 28–38.

Riedel, W. R., 1957. Radiolaria : a preliminary stratigraphy. Swedish Deep-Sea Expedition Repts., 6, (3), 61–96 Pls. 1–4.

Stöhr, E., 1880. Die Radiolarienfauna der Tripoli von Grotte, Provinz Girgenti in Sicilien. Palaeontographica, 26, 69–124, Pls. 1–7.

Sverdrup, H. U., Johnson, M. W., and Fleming, R. H., 1942. The oceans : their physics, chemistry and general biology. New York.

EXPLANATION OF PLATES

All figured specimens are from the sediment sample collected at B.A.N.Z.A.R.E. Station 94.

PLATE 1.

Figs. 1, 2. *Cenosphaera cristata* Haeckel ?. x205.

Figs. 3, 4. *Diploplegma banzare* n. sp. Fig. 3, Holotype. Fig. 4, Paratype. Both x205. Portion of the outermost meshwork is broken away in both specimens.

Fig. 5. *Actinomma imperfecta* Popofsky. x203. Portion of the outermost (fourth) shell is broken away. The innermost shell cannot be seen.

Fig. 6. *Echinomma* sp. x205. The two inner lattice-shells cannot be seen through the thick-walled outer shell.

Figs. 7, 8. *Prunopyle antarctica* Dreyer. x205. The second and third shells are seen as shadowy outlines through the outermost shell.

Fig. 9. *Stylatractus neptunus* Haeckel ?. x205.

Figs. 10, 11. *Spongurus pylomaticus* n. sp. Fig. 10, Holotype. Fig. 11, Paratype. Both x205.

Figs. 12. *Spongopyle osculosa* Dreyer. x205.

PLATE I.

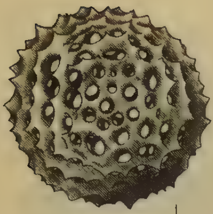
1

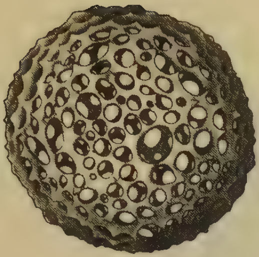
2

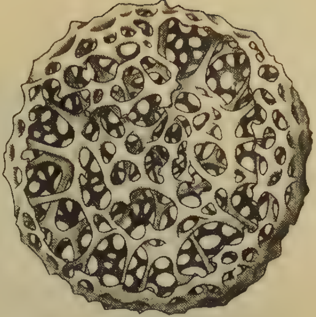
3

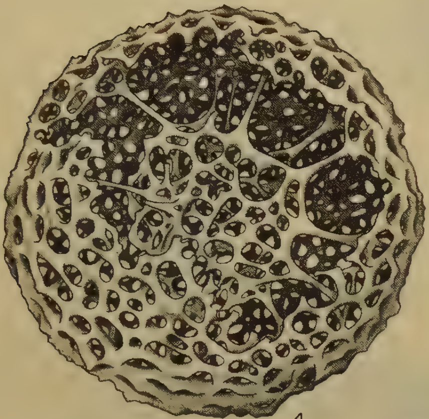
4

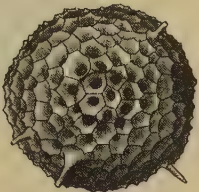
6

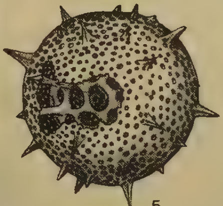
5

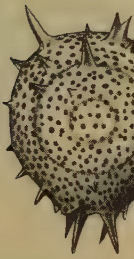
7

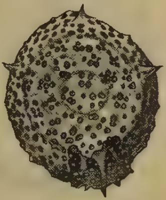
8

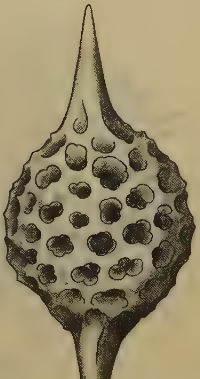
9

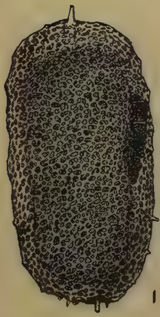
10

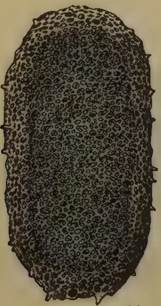
11

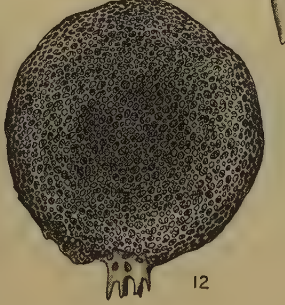
12

PLATE II.

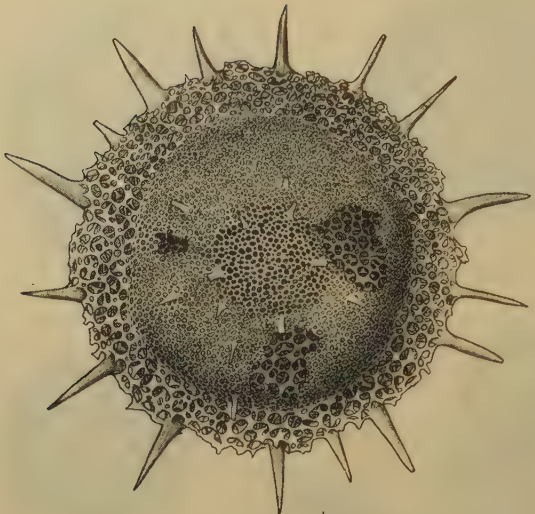

1

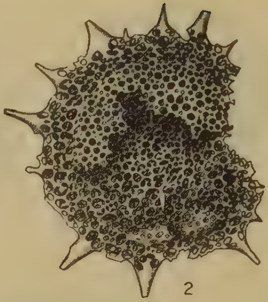

2

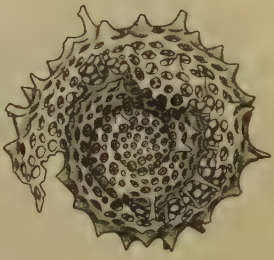

3

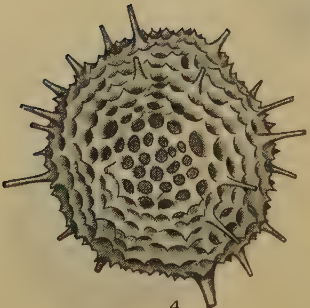

4

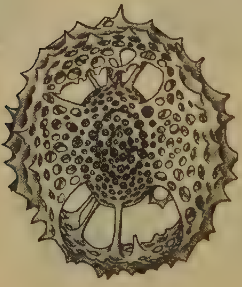

5

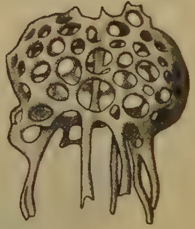

6

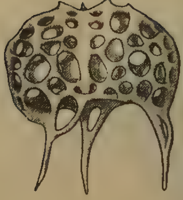

7

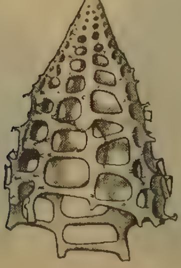

8

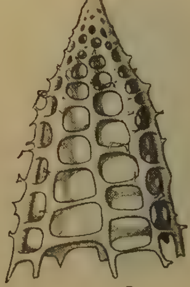

9

PLATE 2.

Figs. 1, 2. *Spongotrochus ? glacialis* Popofsky. x95.

Fig. 3. *Lithelius nautiloides* Popofsky. x205. A broken specimen viewed along the polar axis of the spiral.

Fig. 4. *Lithelius nautiloides* Popofsky ?. x205. Thick-walled form, viewed perpendicularly to the polar axis of the spiral.

Fig. 5. *Phorticium pylonium* (Haeckel ?) Cleve. x205.

Figs. 6, 7. *Triceraspyris antarctica* (Haecker). x205.

Figs. 8, 9. *Peripyramis circumtexta* Haeckel. x205.

PLATE 3.

Figs. 1, 2. *Cornutella profunda* Ehrenberg. x205.
Figs. 3, 4. *Mitrocalpis araneafera* Popofsky. x205.
Fig. 5. *Dictyophimus gracilipes* Bailey. x205. One of the three feet (that facing the observer) is broken off.
Figs. 6, 7. *Dictyophimus mawsoni* n. sp. Fig. 6, Paratype. Fig. 7, Holotype. Both x160.
Fig. 8. *Helotholus histricosa* Jörgensen. x205.
Fig. 9. *Peromelissa denticulata* (Ehrenberg). x205.
Fig. 10. *Dictyocephalus papillosus* (Ehrenberg). x315.
Fig. 11. *Pterocorys hirundo* Haeckel. x315.

(430)

PLATE III.

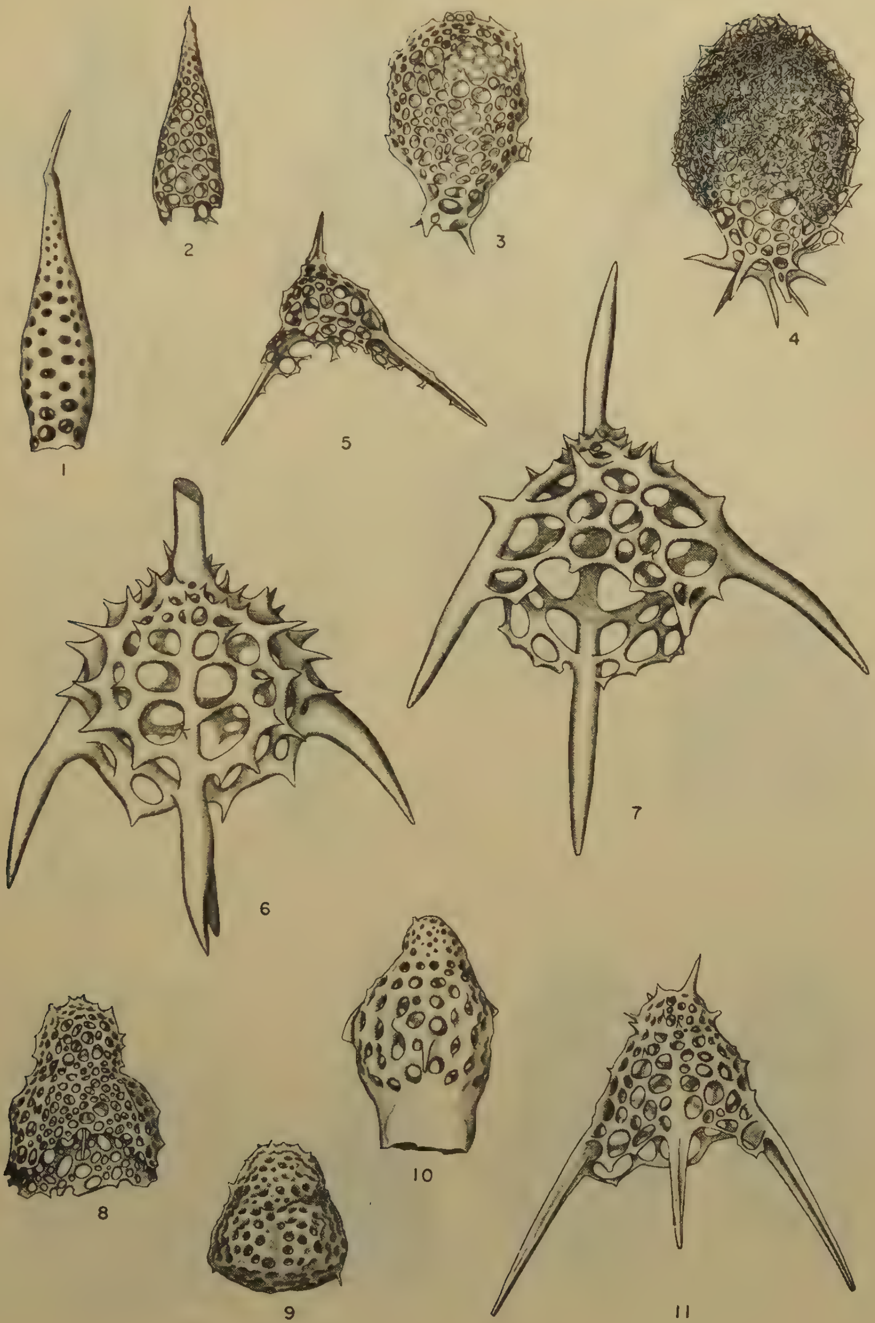
1
2
3
4
5
6
7
8
9
10
11

PLATE IV.

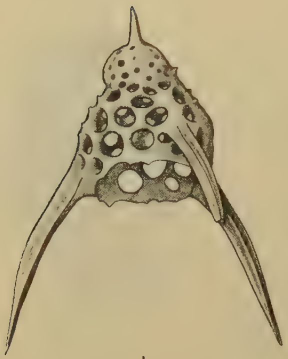

1

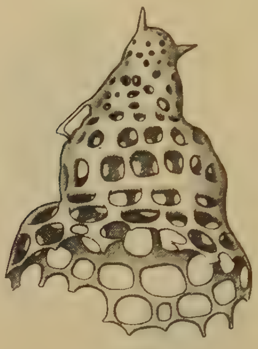

2

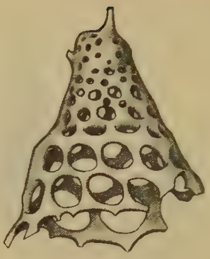

3

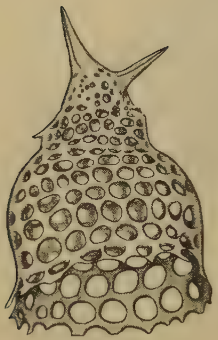

4

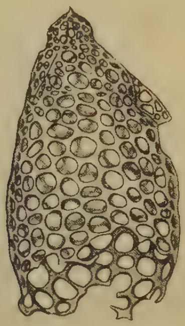

5

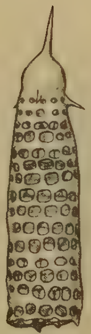

6

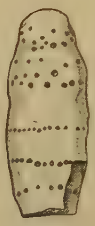

7

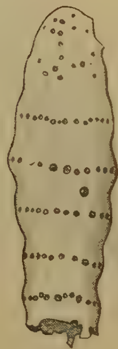

8

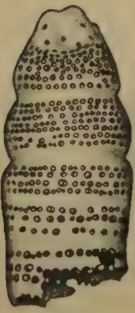

9

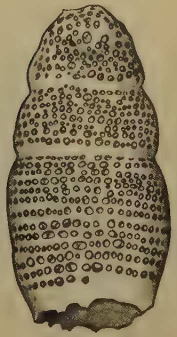

10

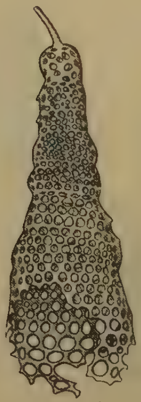

11

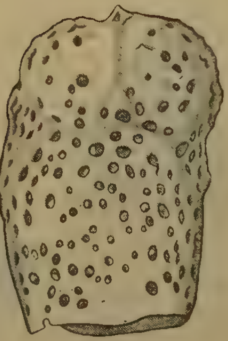

12

(432)

PLATE 4.

Fig. 1. *Pterocorys hirundo* Haeckel. x315.
Figs. 2, 3. *Theocalyptra davisiana* (Ehrenberg). x315.
Fig. 4. *Theocalyptra bicornis* (Popofsky). x315.
Fig. 5. *Stichopilium variabile* Popofsky. x315.
Fig. 6. *Artostrobus annulatus* (Bailey). x315.
Figs. 7, 8. *Lithomitra arachnea* (Ehrenberg). x315.
Figs. 9, 10. *Siphocampium* sp. x315.
Fig. 11. *Cyrtocapsa* sp. x315.
Fig. 12. *Botryopyle ? antarctica* (Haecker). x315.

By Authority: A. J. ARTHUR, Commonwealth Government Printer, Canberra.

(433)

(434)

E X T R A I T

Rapp. et Proc.-Verb. Vol. 144, 1958
Cons. Internat. Explor. de la Mer

C. 9.

Surface Chlorophyll "A", Surface Primary Production, and Zooplankton Volumes in the Eastern Pacific Ocean

By Robert W. Holmes
Scripps Institution of Oceanography, University of California

Introduction

In the first section of this paper nearly all of the simultaneously observed surface chlorophyll *a*, surface primary production, and zooplankton volume data, regardless of differences in time of collection, have been summarized in an attempt to present a picture of the "productivity" of the north-eastern Pacific Ocean. These observations are related in a qualitative manner to the physical and chemical regime in these waters. In the second section an attempt is made to compute the daily organic carbon requirement of the zooplankton captured by the meter net in the upper 300 metres and to compare this with the daily production of organic carbon by the phytoplankton. Lastly, photosynthetic rates per unit chlorophyll *a* observed in sea-water samples are compared to similar rates measured in the laboratory by other investigators.

Geographical variations in surface chlorophyll *a*, surface primary production, and zooplankton volume

In Figures 1 and 2 the values of surface chlorophyll *a* and surface *in situ* primary production are presented. The data have been averaged over each 5° square of latitude and longitude, regardless of the date of sampling; the number of observations used in obtaining this average is given in the upper right hand corner of each square. The zooplankton volume data, presented in a somewhat different manner, are illustrated in Figure 3. In spite of the rather patchy series of observations, a few qualitative generalizations may be made about them and their relation to the physical and chemical environment.

Let us first consider the region offshore of the western United States and Mexico north of about 15° N. and extending northward to about 40° N. In this region we find low concentrations of chlorophyll *a* (0·100 mg./m^3., or less), low surface primary production (less than approximately 2 mg.C/m^3./day, with a number of individual values less than 0·50 mg. C/m^3./day), and low zooplankton volumes in the upper 300 m. (generally less than 50 ml./1000 m^3.). In the south-eastern portion of this area the mixed layer is low in soluble inorganic phosphate (about 0·3 μg.-at. PO_4-P/l.), and nitrate is present in trace quantities only. The water is likewise quite transparent, averaging greater than 96 % transmission per metre in the blue-green spectral region (480 ± 50 mμ). Scattered observations throughout the remaining portion of the area also indicate the existence of the same general conditions although phosphate-phosphorus concentrations appear somewhat greater to the north.

The region under consideration appears to lie in the eastern edge of a gyra discernible in the Sverdrup *et al.* (1942) current chart (Fig. 4). While the existence of this gyra cannot yet be said to be a permanent feature of the circulation in the north-eastern Pacific, evidence from different sources seems to support this idea. This gyra appeared from Munk's (1950) calculations, and the U.S. Hydrographic Office Atlas of surface currents in this region (H.O. No. 570) yields no information contrary to this supposition. This is also the area occupied by the atmospheric "high" in the north Pacific. This current (and biological) boundary likewise corresponds to the eastern edge of an extensive red clay deposit (see Sverdrup *et al.*, p. 972 and Fig. 253, p. 975). Although data are not available, it is tempting to suggest that the entire area of the gyra is likewise poor with respect to chlorophyll *a*, surface production, and zooplankton.

Contribution from the Scripps Institution of Oceanography, New Series, No. 101

Reproduced by Permission

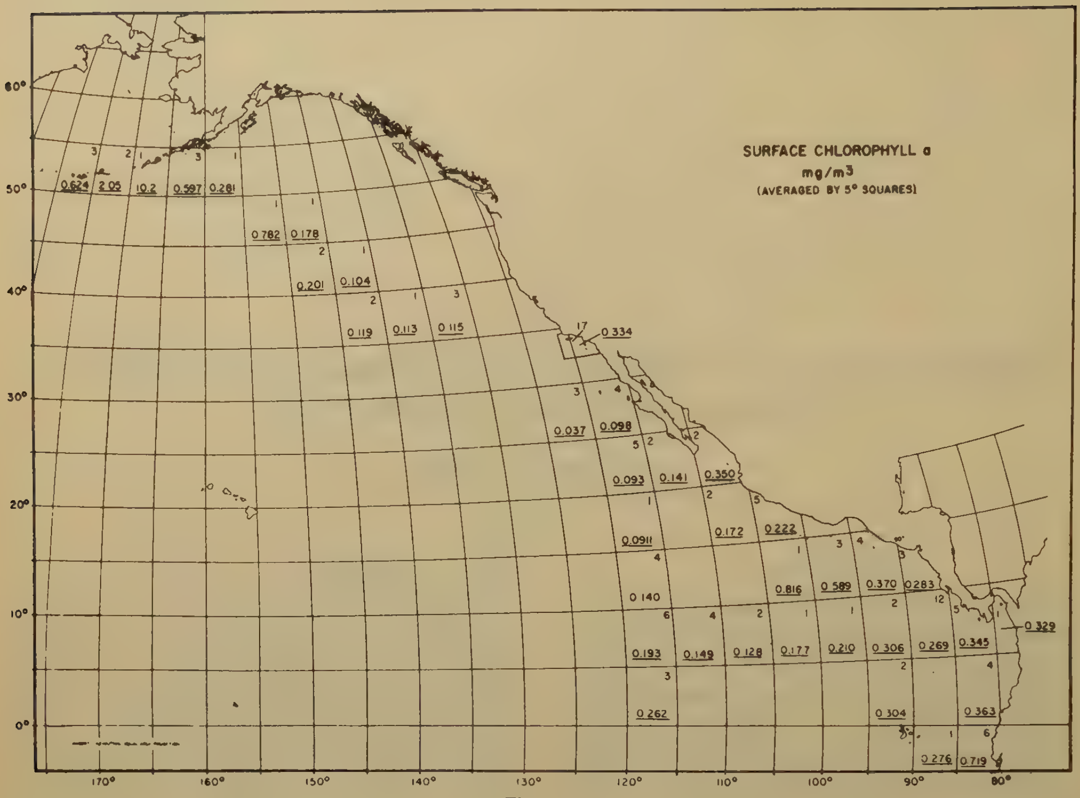
SURFACE CHLOROPHYLL a
mg/m3
(AVERAGED BY 5° SQUARES)
60°
50°
40°
30°
20°
10°
0°
170°
160°
150°
140°
130°
120°
110°
100°
90°
80°
0.624
2.05
10.2
0.597
0.281
0.782
0.178
0.201
0.104
0.119
0.113
0.115
0.334
0.037
0.098
0.093
0.141
0.350
0.0911
0.172
0.222
0.140
0.816
0.589
0.370
0.283
0.329
0.193
0.149
0.128
0.177
0.210
0.306
0.269
0.345
0.262
0.304
0.363
0.276
0.719

Figure 1.

Higher values of surface chlorophyll *a*, surface primary production, and zooplankton volumes are found in the region of the northern boundary of the Equatorial Countercurrent (*ca.* 10° N.) and these values trend upward from west to east toward the coast of Central America. This phenomenon seems to be related to the thermocline, which is elevated close to the surface as a ridge along this boundary, and which shoals from west to east. For example, in 1955 the mixed layer had a thickness of about 30 metres at about 115° W., while at about 90° W. it was only 18 metres thick. At the inshore end, this ridge appears to spread out into a broad "dome" off the Central American coast, the thermocline becoming slightly deeper again close inshore. In the region of this "dome" we find relatively high values of surface chlorophyll *a* (0·269 to 0·345 mg./m^3.), surface primary production (9·0 to 20 mg.C/m^3./day), and zooplankton volumes (200 ml./1000 m^3. and higher). In 1956, phosphate-phosphorus concentrations were moderately high (0·7—1·0 μg.-at. PO$_4$-P/l.) and nitrate values, though quite variable, were generally higher than those encountered in the waters to the north-west. Water transparency was also moderately low, averaging 90—94 $^0/_0$ transmission per metre in the blue-green spectral region (480 ± 50 mμ).

In the region of the northern boundary of the Peru Current, off northern South America and in the vicinity of the Galapagos Islands high surface chlorophyll *a* (0·719 mg./m^3.), surface productivity (15 and 15 mg.C/m^3./day) and zooplankton volumes (up to 600 ml./1000 m^3.) are found.

Moderately high levels of chlorophyll *a*, primary production, and zooplankton volumes are shown for the South Equatorial Current in the vicinity of the equator near 115° W. longitude. Hydrographic data indicate the presence of upwelling along the equator (unpublished results).

Moderate to high values of cholorophyll *a*, production, and zooplankton volume appear in the area just off the coast of Mexico from the Gulf of Tehuantepec northward to the vicinity of Cape Corrientes. Nutrient concentrations are generally moderately high in the mixed layer in this region. Some of this is probably

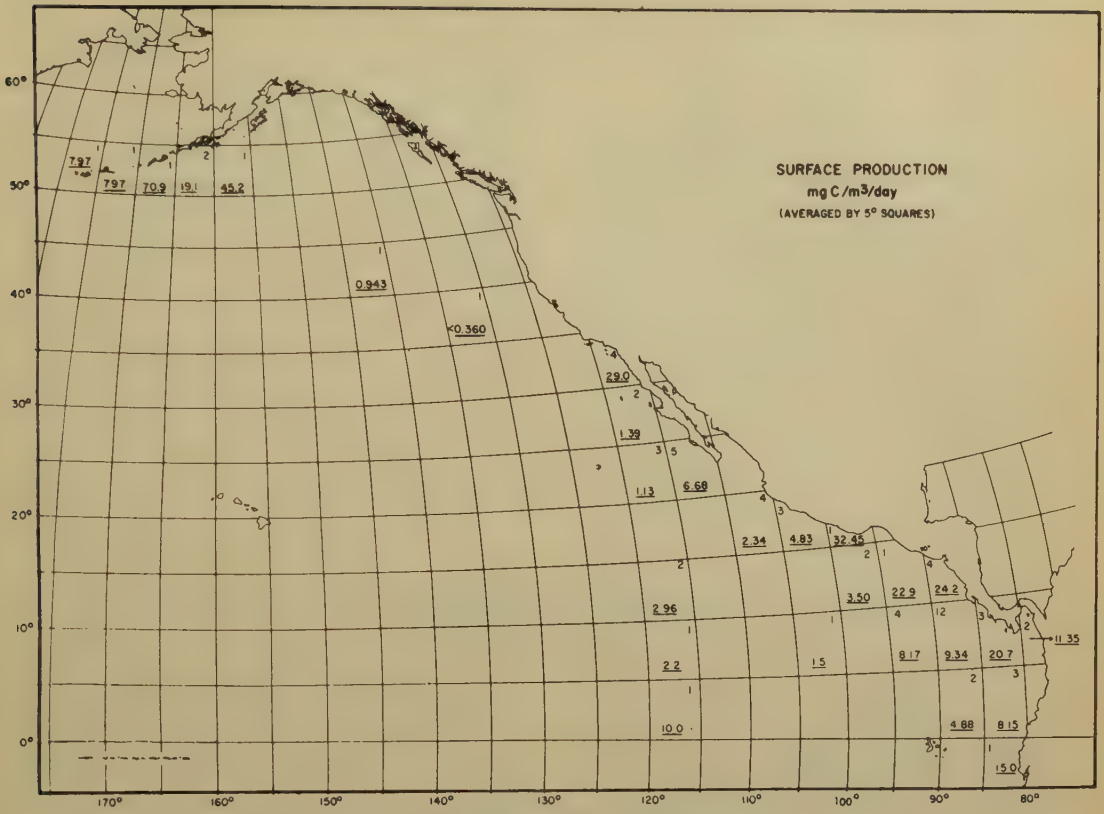

Figure 2.

the result of coastal upwelling, especially in the vicinity of the Gulf of Tehuantepec, but in general the causes of the biological activity cannot be said to be completely understood at present.

The Channel Island area off the coast of southern California seems to maintain about the same level of productivity (29 mg.C/m³./day) and surface chlorophyll *a* (0·334 mg./m³.) as the area off Central America, although there appears to be considerable spatial and temporal variation in these California waters. This area, like the Tehuantepec region, is one of upwelling. The upwelling is generally centered about Point Conception and is nearly a continuous phenomenon but with seasonal trends in magnitude.

The area lying just north and south of the Aleutian Islands, west of about 155° W. is quite rich (data from August 1953) and the phosphate-phosphorus concentration generally exceeds 1·10 μg.-at./l. in the mixed layer. The highest chlorophyll *a* and surface productivity values the author has observed in Pacific waters occurred in the Bering Sea (10 mg./m³. and 71 mg.C/m³./day, respectively). The causes for this richness at this time of year are not presently understood.

The general agreement between these three biological measurements is surprisingly good and in sub-temperate and tropical waters any one will serve as a rough estimator of the other two.

The above observations, within the limits of the sampling programme, substantiate the predictions of Sverdrup (1955) which were largely based on physical oceanographic data. Deviations from the productivity pattern he predicted do occur but mostly involve the location of boundaries. Such differences may be the result of the incomplete coverage of the author's data. In general, agreement between predicted and observed productivity is remarkably good and supports Prof. Sverdrup's thesis that, other things being equal, productivity is closely related to the rate of replenishment of nutrients to the mixed layer.

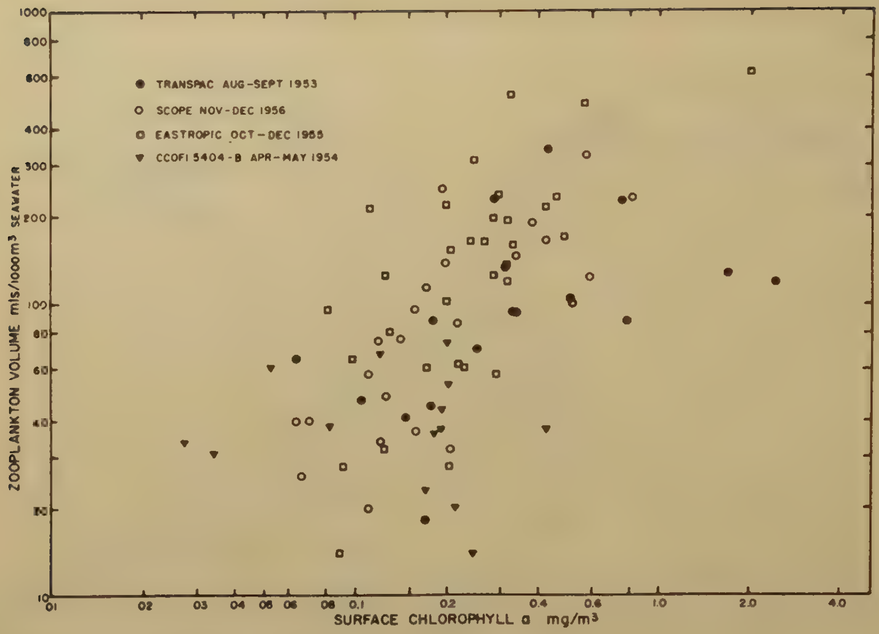

Figure 3.

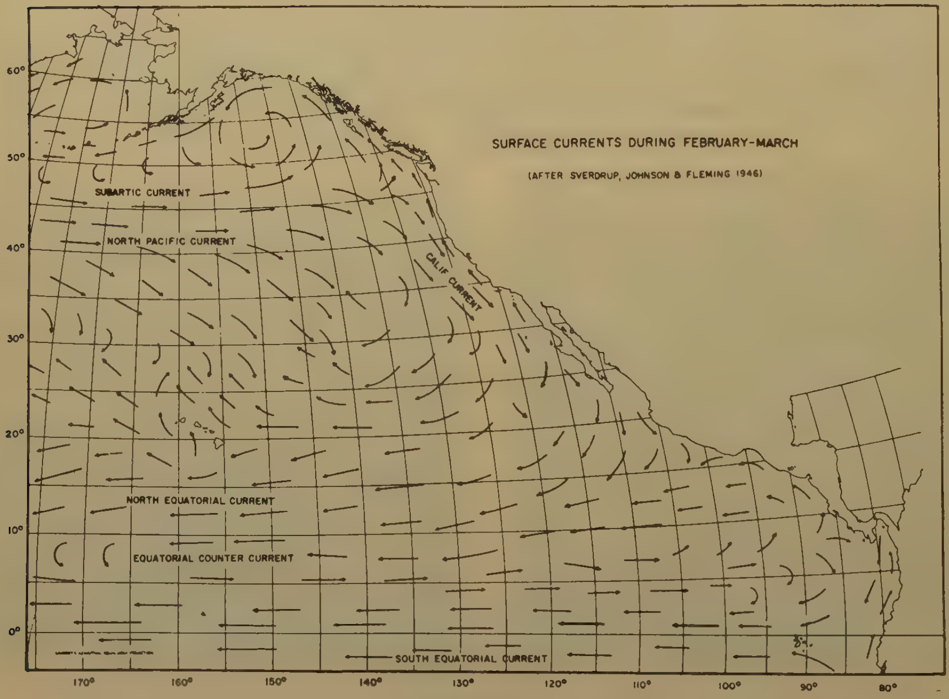
SURFACE CURRENTS DURING FEBRUARY-MARCH
(AFTER SVERDRUP, JOHNSON & FLEMING 1946)
SUBARTIC CURRENT
NORTH PACIFIC CURRENT
CALIF. CURRENT
NORTH EQUATORIAL CURRENT
EQUATORIAL COUNTER CURRENT
SOUTH EQUATORIAL CURRENT
60°
50°
40°
30°
20°
10°
0°
170°
160°
150°
140°
130°
120°
110°
100°
90°
80°

Figure 4.

Surface chlorophyll *a* — zooplankton relationships

In Figure ~~4~~ 3 the zooplankton volume is presented as a function of surface chlorophyll *a* concentration for each station. While there is some scatter, the observations reveal that a relationship exists between these two quantities. The correlation might have been improved had we had available a sufficient number of vertical chlorophyll *a* profiles for integration and comparison with zooplankton volumes. Thus the variation seen in Figure ~~4~~3 is considerably less than might have been expected—especially if certain observations from northern waters ("Transpac" data) are excluded. This lack of extreme variation indicates that in our southern waters we may well have a situation approaching a steady state. If we assume a steady state, the *in situ* water column productivity (g.C/m^2./day) minus the daily particulate organic carbon requirements of zooplankton not captured in the meter net, minus any particulate carbon metabolized by bacteria, minus the fallout, should equal the daily particulate organic carbon requirements of the zooplankton retained by the meter net.

During 1955 and 1956 the median value of *in situ* water column production observed at seven stations off Central America (see Table 1) was 0·442 g.C/m^2./day (range, 0·163—1·02); the median zooplankton volume in the upper 300 metres was 166 ml./1000 m^3. (range, 161—250). If we assume a steady state, then 0·442 mg.C/m^2./day, less the above mentioned three unknown quantities, should equal the grazing rate. To obtain an estimate of the grazing rate in terms of organic carbon it has been necessary to use the results of laboratory feeding experiments. Dr. R. Lasker of the Scripps Institution of Oceanography has kindly provided me with the necessary information obtained in a recent series of experiments with *Euphausia pacifica*, as yet unpublished. Dr. Lasker reports the following:—

(1) the wet weight of an adult *E. pacifica* averages 0·025 mg. (density assumed to be unity in calculations),

(2) the filtering rate in an adult averages 1·0 ml./hr. over a 24 hour period, and

(3) the median value for the amount of particulate organic carbon filtered by a starved adult *E. pacifica* is 0·05 mg./24 hours (range, 1·0—0·005).

If we convert the median zooplankton volume observed at the seven stations (see Table 1) to an equivalent volume of *E. pacifica* and compute the daily particulate organic carbon requirement of the number of individuals contained in this column, we obtain 0·385 mg.C. This requirement is 0·090 g. less than the median daily production. This excess is then available for fallout, etc., and represents some 20 % of the particulate carbon produced per day. Unfortunately we have no adequate estimates of the amount of zooplankton not captured by the net, nor of the bacterial requirements, nor of the fallout in these tropical waters, and this makes it impossible to determine how the remaining carbon is partitioned.

While these observations and calculations reveal that the daily production by the phytoplankton exceeds the demands of the zooplankton captured in the upper 300 metres, it is also apparent that the concentration per unit volume of particulate organic carbon must be considerably greater than that amount produced per day by the phytoplankton if the zooplankton are to survive. Based on a filtering rate of 1 ml. per hour, an adult *E. pacifica* would need a particulate organic carbon concentration of 2·1 mg./l. Fox *et al.* (1952) give the concentration of particulate organic carbon for a station in waters off San Diego: from 0·47—0·16 mg./l. in the depth range 100—300 metres and 5·0 mg./l. at or near the surface. If these values hold for tropical waters it would appear that the zooplankton cannot survive in the 100—300 m. depth range for any length of time and must migrate to the surface where food is available in sufficient quantity. If the zooplankton spend one half of each day in the upper layers, then the particulate carbon concentration would need to be twice the above figure, or 4·2 mg./l.—a value quite close to the average concentration for surface water given by Fox *et al.* (1952).

If 4·2 mg./l. may be considered a minimal value for the concentration of particulate organic carbon in the surface layer, and we believe this material to be of autochthonous photosynthetic origin, it is evident

Table 1

Date	Lat.	Long. °W.	*In situ* productivity g.C/m.^{2}/day	Zooplankton volume ml./1000 m.^{3} (in the upper 300 m.)	Equiv. no. *E. pacifica* per 1000 m.^{3}	Daily requirement of *E. pacifica* g.C/day	Excess (+) Deficit (—) mg.C/m.^{2}/day
13 Oct. 1955 ...	0°04′ N.	115°39′	0·510	166	6640	0·352	+(0·158)
3 Nov. 1955 ...	10°39′ N.	89°51′	0·163	193	7720	0·409	—(0·246)
4 Nov. 1955 ...	9°27′ N.	87°53′	0·442	164	6560	0·338	+(0·104)
5 Nov. 1955 ...	7°33′ N.	87°21′	0·779	161	6440	0·341	+(0·438)
23 Nov. 1955 ...	4°03′ S.	84°11′	1·02	219	8760	0·464	+(0·736)
20 Nov. 1956 ...	9°08′ N.	89°16′	0·316	135	5400	0·270	+(0·046)
21 Nov. 1956 ...	9°33′ N.	89°13′	0·368	250	10000	0·500	—(0·138)
		Median :...	0·442	166	6640	0·352	+(0·090)
		Mean	0·513	184	7360	0·368	+(0·146)

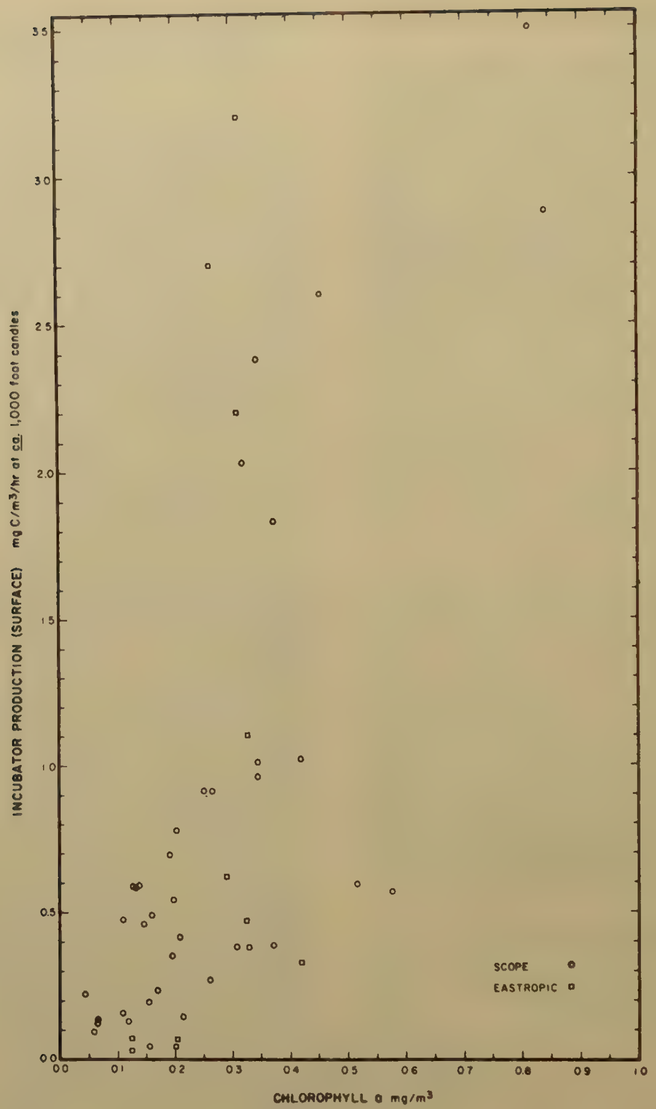

Figure 5.

that the daily production represents only a small fraction of the total carbon. In the waters off Costa Rica for example, the daily surface production averages 21 mg.C/m³./day, or only 0·05 $^0/_0$ of the postulated carbon content of the surface water.

Productivity per unit chlorophyll *a* in surface waters

The relationship between chlorophyll *a* concentration and photosynthesis has been investigated and discussed by a number of people—see for instance

(440)

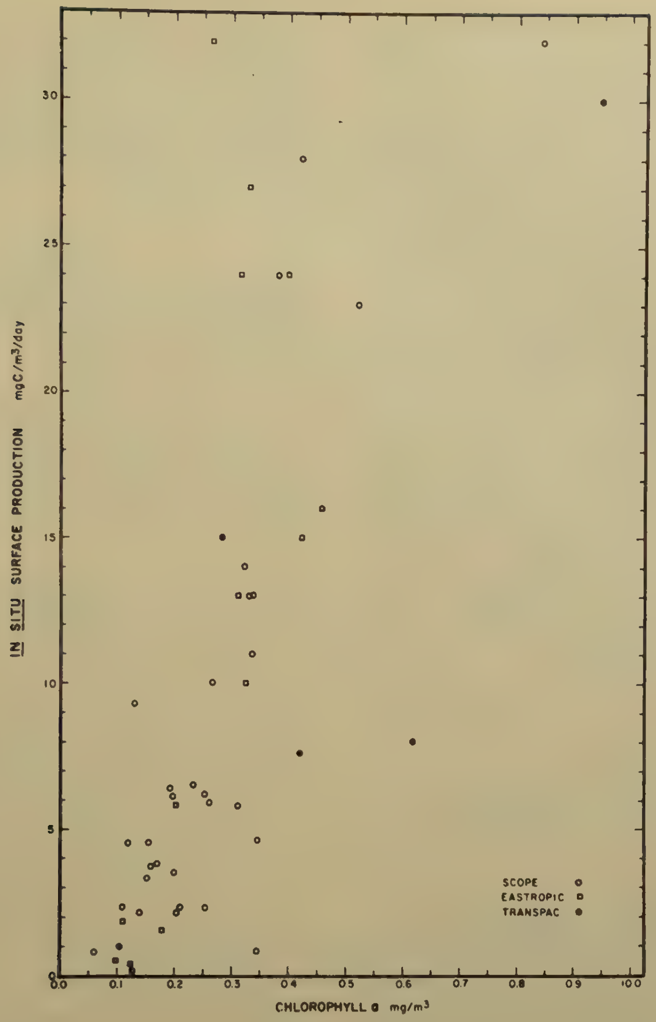

Figure 6.

Clendenning, *et al.*, 1956; Rytheb, 1956; and Rabinowitch, 1951. Since most of these observations were obtained with laboratory cultures it should be interesting to compare productivity per unit chlorophyll *a* as observed in nature with that obtained under controlled conditions in the laboratory.

The data available for this comparison are of two types: (a) the photosynthetic rates obtained with surface samples incubated for four hours under constant light (1000 ± 40 foot candles) at sea surface temperatures and (b) the rates per day of surface samples trailed astern of the vessel for about six hours (sunrise to noon, or noon to sunset). Chlorophyll *a* determinations were made from water samples collected at, or nearly at, the same time as the samples for the photosynthesis studies.

In Figure 5 the photosynthetic rates obtained with surface samples placed in the incubator and the corresponding chlorophyll *a* concentrations are illustrated. These data appear to fall into two groupings, each exhibiting different rates per unit chlorophyll *a*. Eye-fitted best fit lines drawn through these two groups of data yield the following average rates: 7+ mg.C/hr./mg. chlorophyll *a* for the data exhibiting the high rates (all data from the "dome" area off Central America) and 2 mg.C/hr./mg. chlorophyll *a* for the majority of observations. Assuming a photosynthetic quotient of 1·00, equivalent values in terms of oxygen production would be 13 and 3·7 ml. oxygen/hr. respectively, per mg. chlorophyll *a*. CLENDENNING *et al.* (1956) give rates on this same basis for a number of algae grown at 25° C. under conditions of light saturation, and compare their values with those obtained in higher plants and other algae by other investigators. These ranged from 2·64 to 14·77 ml. oxygen/hr./mg. chlorophyll *a*. The average rate observed by RYTHER (1956) for 15 species of algae grown under undefined conditions was 22·7 ml. oxygen/hr./mg. chlorophyll *a*. At the depth of maximum photosynthesis in nine Wisconsin lakes, MANNING and JUDAY (1941) found an average rate of 6·7 ml. oxygen/hr./mg. chlorophyll.

The average rate for the three stations which yielded the highest rate per unit chlorophyll *a* was nearly 20 ml. oxygen/hr. and is close to the average value given by RYTHER (1956).

The six hour *in situ* ocean measurements (Fig. 6) yield an average rate somewhat higher than that obtained from the samples incubated on shipboard. Also the scatter of points is somewhat less with these *in situ* observations.

It is impossible to state why some of the rates observed in the incubator and *in situ* experiments are so low. The cause might be nutrient deficiencies and/or a large percentage of inactive chlorophyll *a*. But on the whole these data yield further confirmation of RYTHER's suggestion (1956) that it should be possible to estimate productivity, at least at the surface, from the concentration of chlorophyll *a*, when the light saturation intensity for the population under consideration is known.

Appendix I

A multiple regression equation has been calculated using log-transformed "*Scope*" and "*Eastropic*" data. In all some 30 sets of observations were available and the following equation was obtained:—

$$\hat{Y} = 0{\cdot}161 + 0{\cdot}369\ X_1 + 0{\cdot}832\ X_2$$

where $\hat{Y}$ is the logarithm of the zooplankton volume in ml./1000 m³., X_1 the logarithm of the surface *in situ* productivity (mg.C/m³./day), and X_2 the logarithm of surface clorophyll *a* concentration (mg./m.³). The standard error of the estimate is 0.0151 which corresponds to about 10 %. Both surface *in situ* production and surface clorophyll *a* may be employed individually to estimate zooplankton volume although the precision is not great (standard error: 17 % and 13 %, respectively).

Appendix II

If we exclude the data obtained in northern waters and consider only the "*Scope*" and "*Eastropic*" data, the regression for these is:—

$$\hat{Y} = 0{\cdot}584 + 1{\cdot}012\ X$$

where X is the logarithm of the surface clorophyll *a* concentration (mg./m³.) and $\hat{Y}$ is the logarithm of the zooplankton volume (ml./100 m³.). The standard error of the estimate is 0·226 which corresponds to 1·68 %.

References

CLENDENNING, K. A., BROWN, T. E., & EYSTER, H. C., 1956. "Comparative studies of photosynthesis in *Nostoc muscorum* and *Chlorella pyrenoidosa*". Can. J. Bot., **34**: 943—66.

FOX, D. L., ISAACS, J. D., & CORCORAN, E. F., 1952. "Marine leptopel, its recovery, measurement and distribution." J. Mar. Res., **11** (1): 29—46.

HARDY, A. C., & GUNTHER, E. R., 1935. "The plankton of the South Georgia whaling grounds and adjacent waters, 1926—27." Discovery Rep., **11**: 1—146.

HARVEY, H. W., 1955. "The chemistry and fertility of sea waters." Cambridge Univ. Press, 224 pp.

MANNING, W. M., & JUDAY, R. E., 1941. "The chlorophyll content and productivity of some lakes in northern Wisconsin." Trans. Wisc. Acad. Sci., Arts and Let., **33**: 363—93.

MUNK, W. H., 1950. "On the wind-driven ocean circulation." J. Meteor., **7**: 79—93.

RABINOWITCH, E. I., 1956. "Photosynthesis and related processes. Vol. II, Part 2, Kinetics of Photosynthesis." Interscience Publishers, N. Y., pp. 1211—2088.

RYTHER, J. H., 1956. "The measurement of primary production." Limn. and Oceanogr., **1** (1): 72—84.

STEEMANN NIELSEN, E., 1937. "On the relation between the quantities of phytoplankton and zooplankton in the sea." J. du Cons., **12** (2): 147—54.

SVERDRUP, H. U., JOHNSON, M. W., & FLEMING, R. H., 1942. "The Oceans, their Physics, Chemistry, and General Biology." Prentice-Hall Inc., 1087 pp.

SVERDRUP, H. U., 1955. "The place of physical oceanography in oceanographic research." J. Mar. Res., **14** (4): 287—94.

BIANCO LUNO A/S, KBH

(442)

Reprinted for private circulation from
THE JOURNAL OF GEOLOGY
Vol. 66, No. 3, May 1958
PRINTED IN U.S.A.

CLIPPERTON FRACTURE ZONE IN THE NORTHEASTERN EQUATORIAL PACIFIC[1]

H. W. MENARD AND ROBERT L. FISHER
Scripps Institution of Oceanography of the University of California, La Jolla, California

ABSTRACT

The Clipperton fracture zone is divisible as follows:

(127°–113° W. long.). A broad, low welt, 900 miles long, has a central trough 10–30 miles wide and at most 4,200 feet deep. North of the welt the sea floor is 150–200 fathoms deeper than to the south.

(113°–107° W. long.). Clipperton Island is one peak on a volcano-studded ridge, 60 miles wide and 330 miles long, with a deep, narrow trough on the north side. Local relief is 18,000 feet, and for 8,300 feet the slope is 40°.

(107°–101° W. long.). A low welt with a central trough 1,200–2,400 feet deep transects the Albatross Plateau.

(101°–96° W. long.). The east-west trend of the fracture zone appears offset 60 miles to the north; a great branching feature, the Tehuantepec Ridge, trends 400 miles northeast to the continental margin.

Great submarine ridges like Clipperton Ridge are found in other places where major lineations intersect. This may indicate that a northwest-trending lineation intersects the Clipperton fracture zone near Clipperton Island.

Transcurrent faults and submarine fracture zones are associated with most oceanic trenches. Lineations are much longer than trenches and intersect them at random angles. Lineations appear older than trenches.

INTRODUCTION

The Clipperton fracture zone, a band of unusually mountainous submarine topography, trends roughly east-west for 3,300 miles in the equatorial part of the northeastern Pacific Basin. When the zone was first described (Menard, 1955, p. 1170–1172), twelve echograms crossing the fracture zone were available from the Mid-Pacific, Shellback, Shuttle, and Capicorn expeditions, and 11,000 miles of expedition sounding lines were available to show the bathymetry in the area from the equator to 17° north latitude and from 84° to 129° west longitude. Nevertheless, the continuity of the fracture zone was still questionable, and more field work was clearly needed. Since the the Acapulco Trench, Eastropic, and Acapulco Geological expeditions have increased the number of crossings fivefold and have more than tripled the length of sounding lines. It is now apparent that the Clipperton fracture zone is continuous for at least 1,500 miles. Therefore, the original question can be dismissed, but, as might be anticipated, many new structures have been discovered and many new questions have arisen.

REGIONAL BATHYMETRY

The regional bathymetry of the equatorial part of the northeastern Pacific Basin is sufficiently well known that the outlines are clear. Broad swells and swales are relatively subdued compared to such local features as ridges, troughs, and seamounts; this disparity in relief makes it impossible to prepare a bathymetric chart of uniform quality at present. Instead of a chart, a physiographic diagram (fig. 1) has been made to show the general shape of the sea floor and the relative positions of small-scale features.

Proceeding westward from Central America, one finds the following north- or northwest-trending features:

1. The Middle America Trench, discussed by Heacock and Worzel (1955) and Fisher and Shor (1958).
2. The Albatross Plateau, a broad swell that appears to be the northernmost part of the vast East Pacific Rise.
3. The Albatross Basin, a small basin crossed by few sounding lines.
4. The Mathematicians Seamount Range,

---

[1] Contribution from the Scripps Institution of Oceanography, Manuscript received July 22, 1957.

New Series, No. 1014.

Reproduced by Permission

(443)

discovered and explored in the course of this investigation. A group of high seamounts are separated by deep, narrow troughs. The range is named after the example of the Presidential Range in New England and the Emperor Seamount Range in the North Pacific (Dietz, 1954, p. 1209).

Farther west the sea floor grades into the great bowl of the North Pacific Basin.

Transecting the area from east to west is the Clipperton fracture zone, which varies in character from a low, elongate swell with a central trough to an enormous, volcano-capped ridge. The fracture zone appears to bifurcate slightly east of the crest of the Albatross Plateau, forming the great Tehuantepec Ridge trending northeast and a smaller ridge trending east.

DESCRIPTION OF FRACTURE ZONE

The best-explored part of the Clipperton fracture zone is now divisible into four sections having markedly different topography. The westernmost section extends roughly 900 miles, from 127° to 113° west longitude. It may continue without change for 1,000 miles to the west, where the zone has been tentatively recognized (Menard, 1955, p. 1170), but details are lacking. The general slope in this region of the Pacific Basin is toward the southwest. Superimposed on the regional slope is the broad, low swell of the east–northeast-trending fracture zone (fig. 1). Along the crest of the swell is a trough, 10–30 miles wide, flanked by narrow ridges and low seamounts. Maximum local relief from the crest of a ridge to the base of the trough is 4,200 feet, but most crossings show considerably less relief (fig. 2). The sea floor to the north of the swell is 150–200 fathoms deeper than to the south. The regional slope is so gentle, however, that even such a small difference in depth causes a horizontal offset of the 2,200-, 2,300-, and 2,400-fathom contours by several hundred miles.

All these characteristics are typical of the fracture zones of the northeastern Pacific (Menard, 1955, p. 1182–1183). The best-known example of an elongate welt with a central trough flanked by narrow ridges is the Murray fracture zone west of Erben Guyot, but the western sections of the Mendocino and Clarion fracture zones appear to be similar. Likewise, regional differences in depth of 250 and 500 fathoms exist across the Murray and Mendocino fracture zones, respectively.

Between 113° and 107° west longitude, the fracture zone appears as an enormous, somewhat sinuous, asymmetrical ridge, roughly 60 miles wide and 330 miles long (fig. 3). This submarine structure, here named the Clipperton Ridge, is 8,000–10,000 feet high. A trough about 10 miles wide and a mile deeper than the surrounding region borders the ridge. The over-all easterly trend of the ridge is complicated by a southeasterly cross trend indicated by the alignment of volcanoes, by orientation of minor ridges on the south side of the main ridge, and by the marked change in trend of the main ridge at its eastern end. Clipperton Island, the only feature in the whole Clipperton fracture zone that reaches the sea surface, is one volcano on a cross trend. The maximum relief of the Clipperton Ridge is 18,000 feet from Clipperton Island to the deepest spot in the trough at 2,960 fathoms. The asymmetrical ridge is steeper on its north side, where the maximum relief along a continuous slope is 13,200 feet (fig. 4). This flank is a seascarp with an average slope in most places as great as 17° (fig. 5). In one place the slope is 45° for a fall of 4,300 feet and 40° for 8,300 feet.

East of the Clipperton Ridge the relief of the fracture zone is subdued, but it continues as a distinct east-trending swale at least to 101° west longitude (fig. 1). In the western part of this section the swale is about 20 miles wide and 2,400 feet deeper than the surrounding region. Its greatest depth is about 2,200 fathoms. Between 105° and 104° west longitude the swale still has a relief of about 1,200 feet, but its axial depth shoals to 1,800 fathoms because the regional depth decreases across the Albatross Plateau. From 104° to 101° west longitude the swale broadens to the east and the

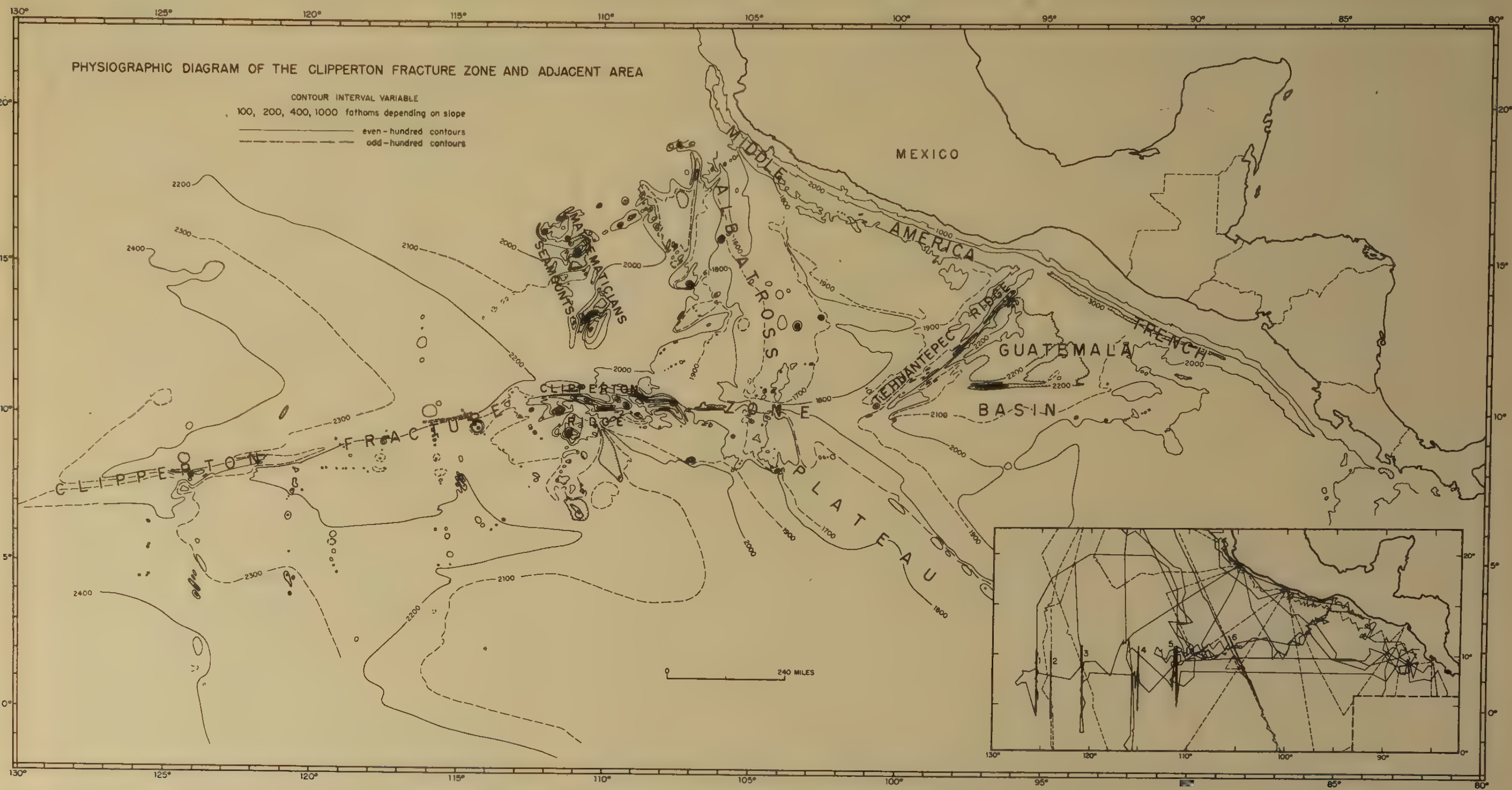
PHYSIOGRAPHIC DIAGRAM OF THE CLIPPERTON FRACTURE ZONE AND ADJACENT AREA
CONTOUR INTERVAL VARIABLE
100, 200, 400, 1000 fathoms depending on slope
even-hundred contours
odd-hundred contours
MEXICO
MIDDLE AMERICA TRENCH
MATHEMATICIANS SEAMOUNTS
ALBATROSS PLATEAU
CLIPPERTON FRACTURE ZONE
CLIPPERTON RIDGE
TEHUANTEPEC RIDGE
GUATEMALA BASIN
0 240 MILES
130° 125° 120° 115° 110° 105° 100° 95° 90° 85° 80°
0° 5° 10° 15° 20°
2400 2300 2200 2100 2000 1900 1800 1700 1000 3000
1 2 3 4 5 6

FIG. 1.—Physiographic diagram of the Clipperton fracture zone and adjacent area. *Insert:* track lines of Scripps Institution of Oceanography and Navy Electronics Laboratory expeditions; solid lines indicate sounding lines discussed for the first time in this report. Profiles along the heavy numbered lines in the insert appear in fig. 2.

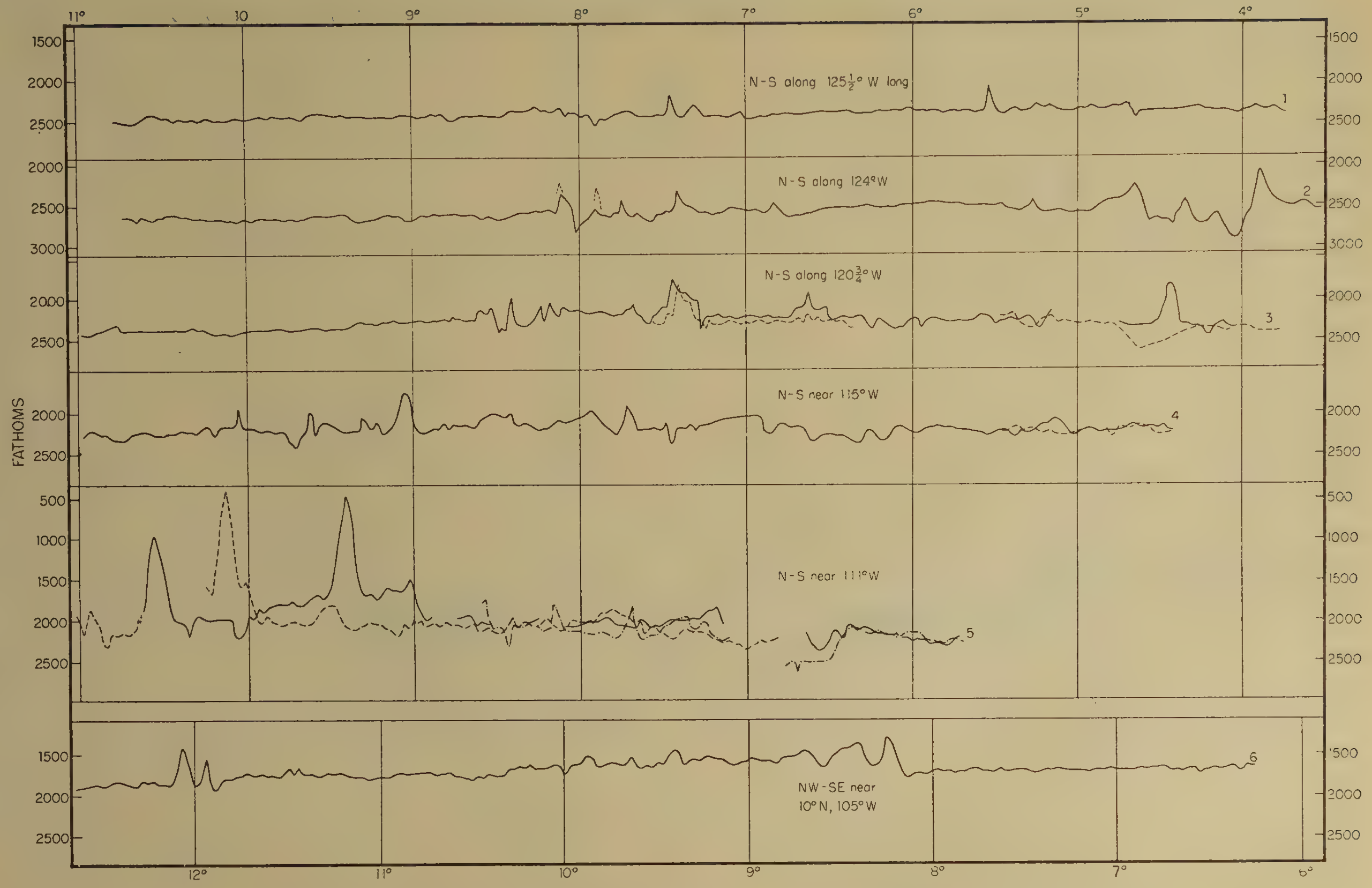

FIG. 2.—Transverse profiles of the Clipperton fracture zone. Locations appear on the insert on fig. 1

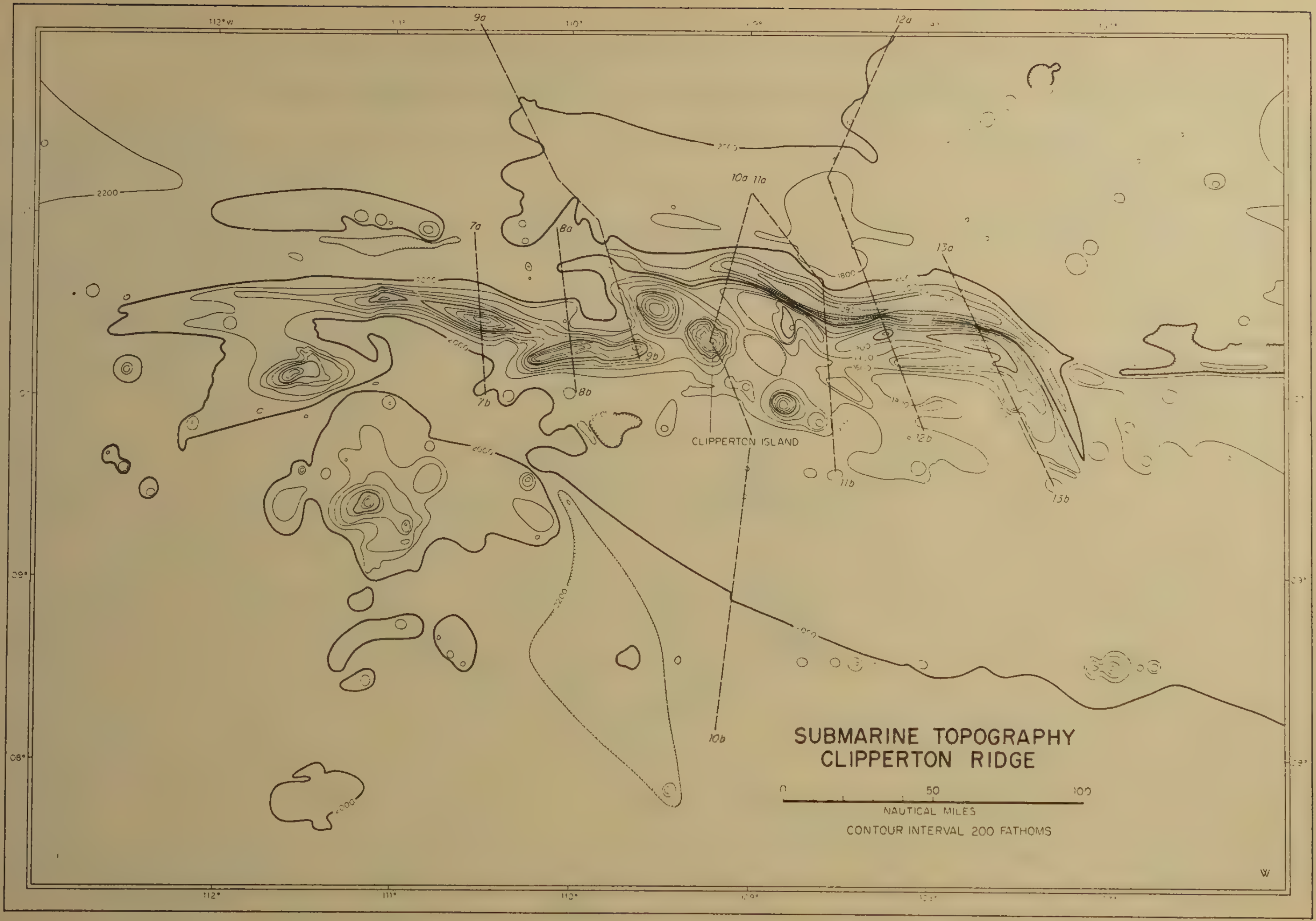
SUBMARINE TOPOGRAPHY
CLIPPERTON RIDGE
0
50
100
NAUTICAL MILES
CONTOUR INTERVAL 200 FATHOMS
CLIPPERTON ISLAND
7a
7b
8a
8b
9a
9b
10a
10b
11a
11b
12a
12b
13a
13b
2200
1800
112°W
110°
112°
111°
110°
09°
08°
W

Fig. 3.—Submarine topography of Clipperton Ridge. Numbered lines show positions of profiles appearing in fig. 5

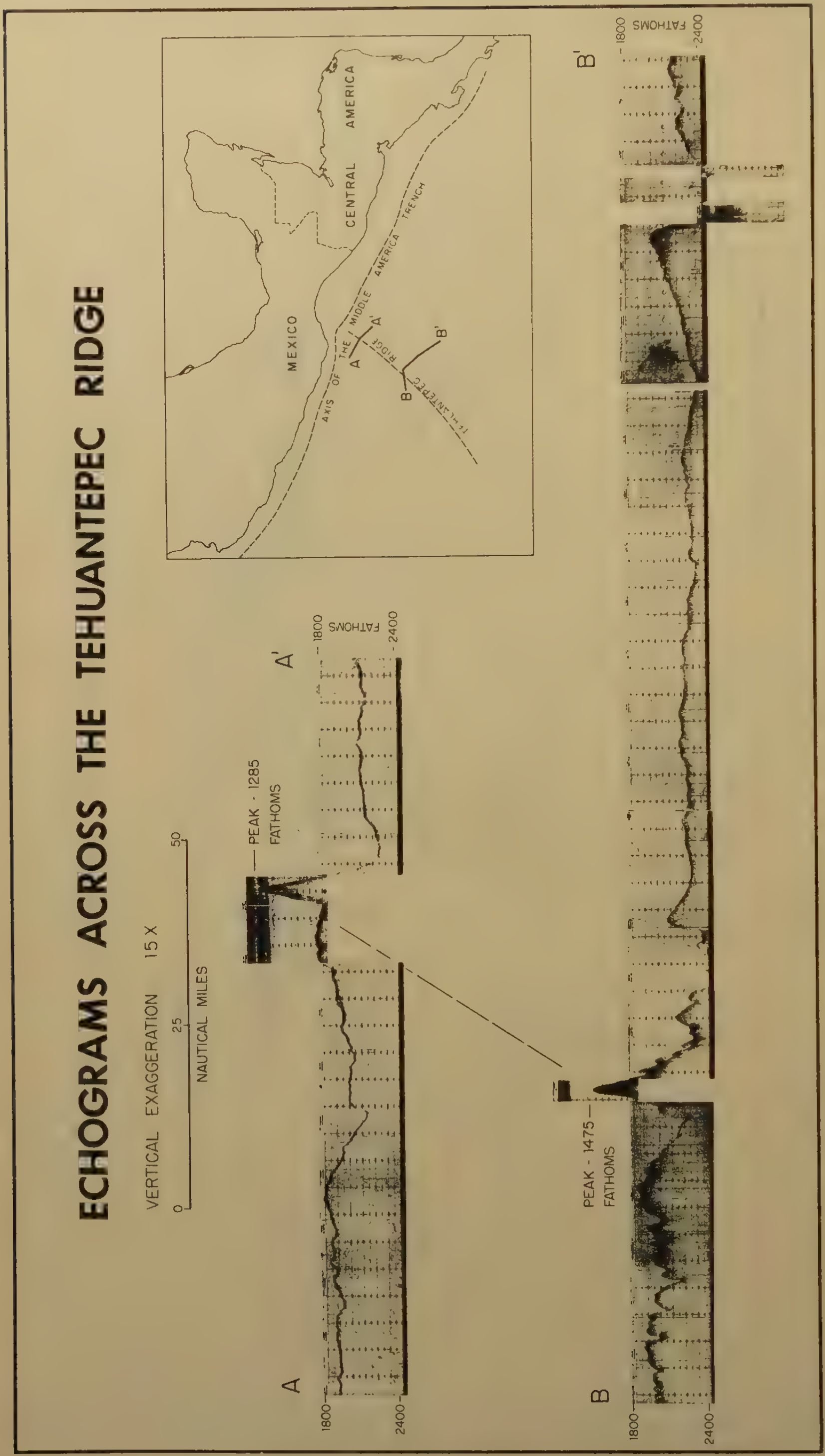
ECHOGRAMS ACROSS THE TEHUANTEPEC RIDGE
VERTICAL EXAGGERATION 15 X
0
25
50
NAUTICAL MILES
MEXICO
CENTRAL
AMERICA
AXIS OF THE MIDDLE AMERICA TRENCH
TEHUANTEPEC RIDGE
A
A'
B
B'
PEAK - 1285 FATHOMS
PEAK - 1475 FATHOMS
1800
2400
FATHOMS

Echograms

1,700-, 1,800-, 1,900-, and 2,000-fathom contours resemble chevrons.

The Clipperton fracture zone was thought to extend along a great circle farther east than 101° west longitude because echograms showed irregular topography with unusual deeps (Menard, 1955, p. 1171). An echogram from the Acapulco Trench Expedition (pl. 1) confirms the existence of an east-trending lineation between 97°30′ and 96° west longitude. There an asymmetrical ridge, steeper on the south side, is bordered on the south by a narrow trough. Local relief is about 3,000 feet. The lineation continues to 94° west longitude, as shown by the 2,200-fathom contour, but the relief is much more subdued. In this area the continuity and great-circle trend of the fracture zone suggested by earlier soundings is not confirmed, however, by more detailed reconnaissance. Where it crosses the Albatross Plateau, the fracture zone curves more to the south than the earlier soundings suggested; consequently, an offset of 60 miles of latitude separates the east-trending swale at 101° west longitude from the east-trending ridge at 97°30′ west longitude. Any details of the offset are wholly obscured by the intersection of the northeast-trending Tehuantepec Ridge. Some influence of the fracture zone is suggested by the easterly trend of the southern margin of the Guatemala Basin, particularly by the 2,100-fathom contour, but the similarity of trend may be fortuitous.

Between 94° west longitude and the coast of Central America the density of expedition soundings is adequate to show that no east-trending band of exceptionally mountainous topography exists.

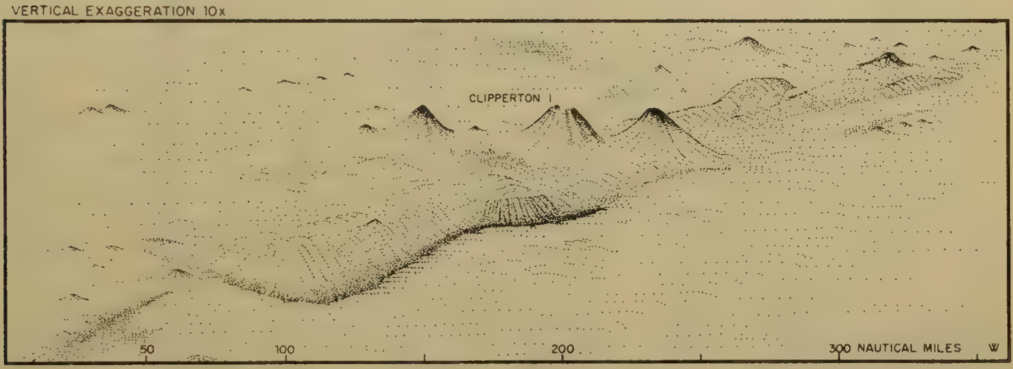

FIG. 4.—View to southwest toward Clipperton Island and the Clipperton Ridge

The Tehuantepec Ridge extends 440 miles in a northeasterly direction from the Clipperton fracture zone at 101° west longitude almost to the Gulf of Tehuantepec in southern Mexico (fig. 6, 7). The Ridge is the most prominent feature in a band of mountainous topography about 60 miles wide. Crossing from south to north, the band consists of a subdued ridge about 20 miles wide; a trough 5–10 miles wide; the main 20-mile-wide ridge, which is more or less asymmetrical with a steep side on the south; and a shallow swale (pl. 1). In its western half the main ridge is split longitudinally by a very narrow trough. In a general way the Tehuantepec Ridge rises toward the east, and the trough on the south side deepens. Consequently, the average relief on the steep south side

---

PLATE 1

Echograms across the Tehuantepec Ridge, showing the high, narrow ridge separating two regions with different average depths. The asymmetrical ridge crossed just northwest of *B* has an east-west trend.

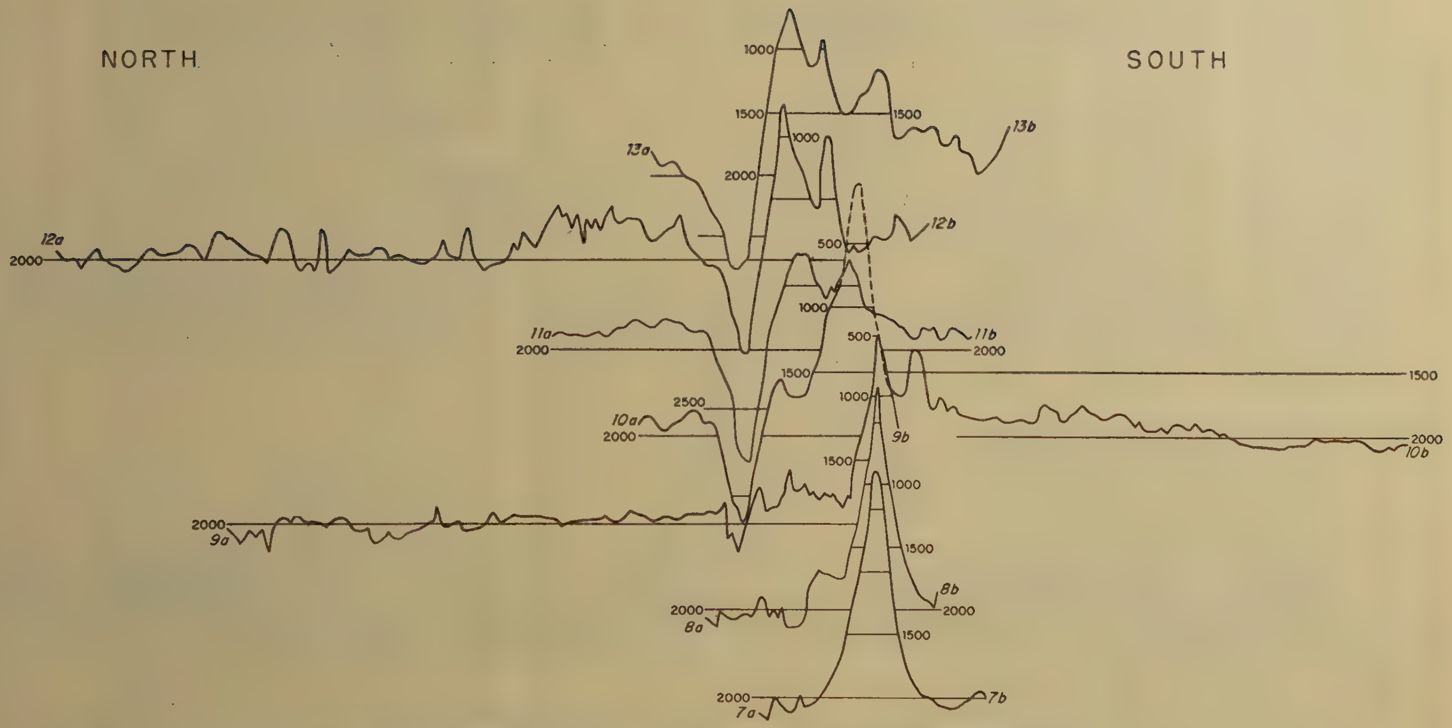

Fig. 5.—Transverse profiles of the Clipperton Ridge (see fig. 3 for locations)

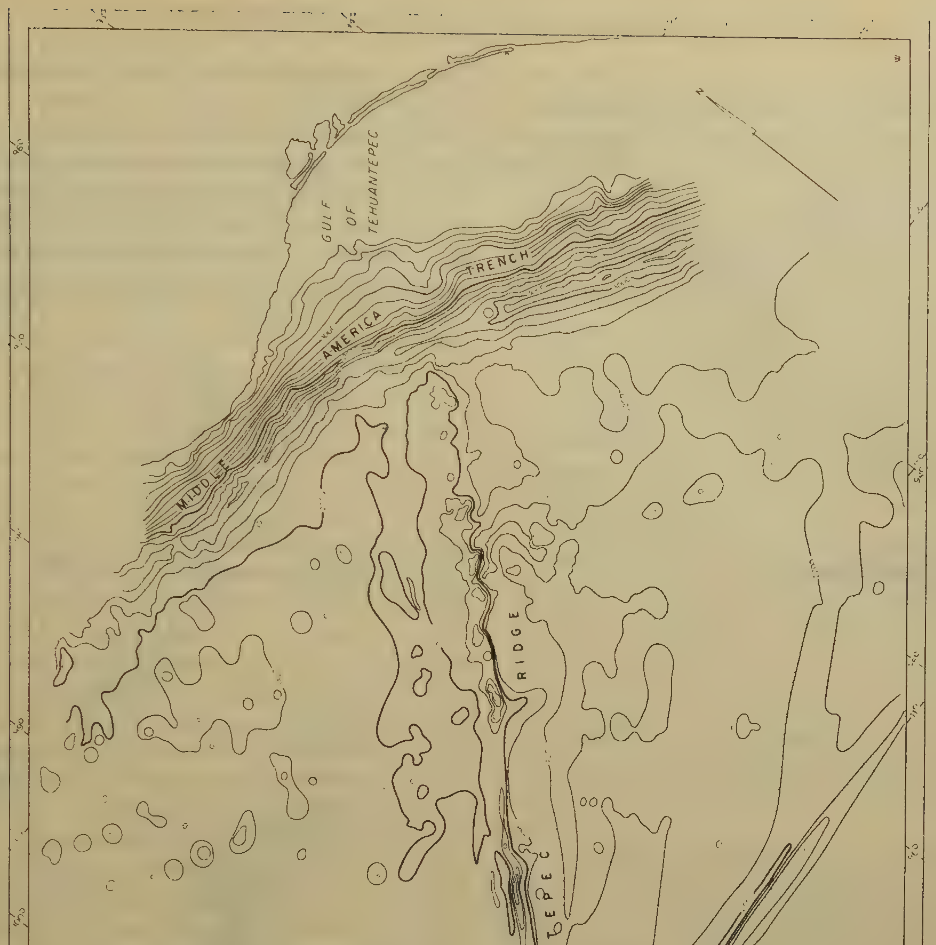
SUBMARINE TOPOGRAPHY
TEHUANTEPEC RIDGE
0
50
100
NAUTICAL MILES
CONTOUR INTERVAL 200 FATHOMS
MIDDLE
AMERICA
TRENCH
GULF OF TEHUANTEPEC
TEHUANTEPEC
RIDGE
N
120
110
100

Fig. 6.—Submarine topography of the Tehuantepec Ridge

of the ridge increases eastward from about 2,000 feet to about 6,000 feet, reaching a local maximum of 8,100 feet. Slopes on this scarp are as much as 15°–21° for falls of 4,000–5,000 feet.

The Tehuantepec Ridge and related topography form the northwestern boundary of the Guatemala Basin (Agassiz, 1906, p. 2), which deepens from about 2,100 fathoms to about 2,300 fathoms along the base of the ridge. Northwest of the low swale lying on the west edge of the ridge, the regional depth is relatively constant at about 1,850 fathoms. The ridge, therefore, is the boundary between regions that differ in depth by 250–450 fathoms.

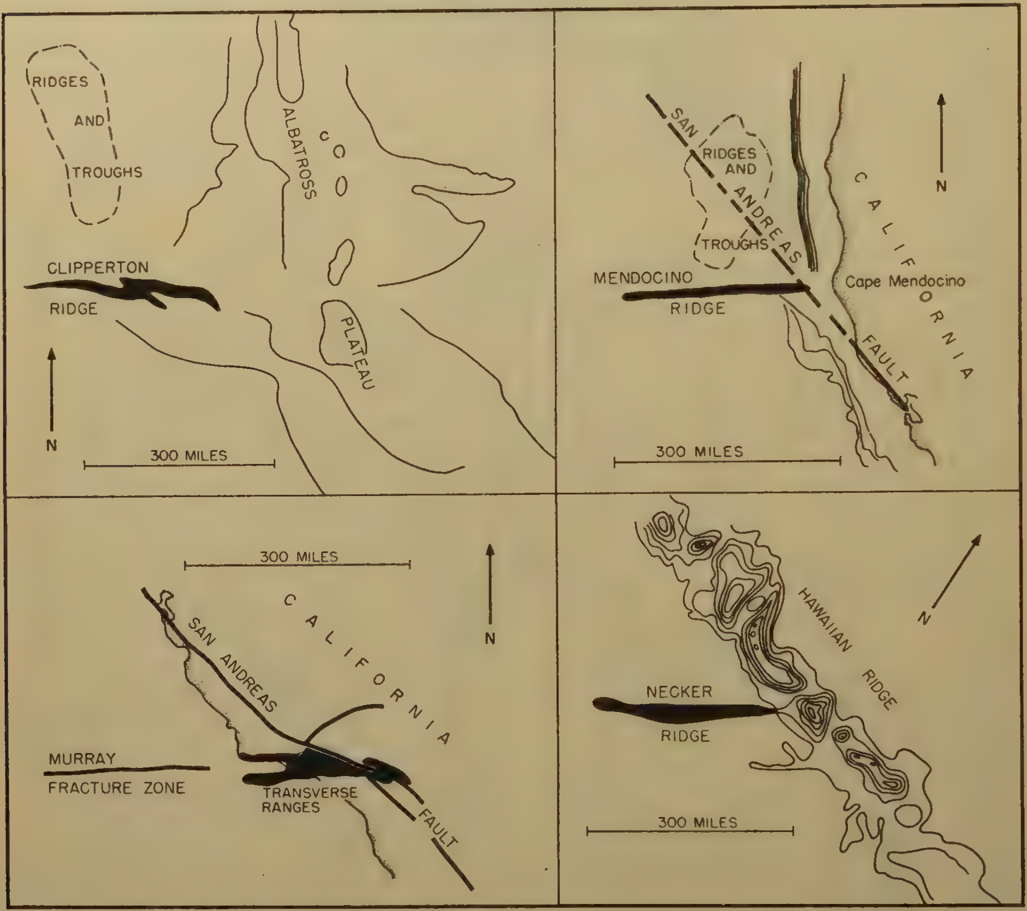
RIDGES
AND
TROUGHS
CLIPPERTON
RIDGE
ALBATROSS
C
O
C
O
PLATEAU
N
300 MILES
SAN
RIDGES
AND
ANDREAS
TROUGHS
MENDOCINO
RIDGE
C
A
L
I
F
Cape Mendocino
O
R
N
I
A
FAULT
N
300 MILES
300 MILES
C
A
L
I
F
O
R
N
I
A
N
SAN
ANDREAS
MURRAY
FRACTURE ZONE
TRANSVERSE
RANGES
FAULT
HAWAIIAN
RIDGE
N
NECKER
RIDGE
300 MILES

Fig. 7.—Great east-west ridges in the northeastern Pacific, showing the similarities in regional topography and structure in the vicinity of the ridges. It is inferred that a northwest-southeast transcurrent fault may once have been active just east of the Clipperton Ridge.

This long band of parallel asymmetrical ridges, troughs, and swales separating large areas with different regional depths is topographically a typical fracture zone like those found in the northeastern Pacific Basin. Its trend, however, is quite exceptional. All four of the great fracture zones so far discovered in the northeastern Pacific are subparallel and appear to follow great circles (Menard, 1955, p. 1163). The Tehuantepec Ridge has a very different trend, with a relatively short radius of curvature.

The zone connects with and may logically be considered to be a branch of the Clipperton fracture zone. Inasmuch as it is a far more prominent feature than the poorly developed east-trending topography in the area, it may also be considered as the Clipperton fracture zone bending away from the great-circle trend observed elsewhere. It may, however, be a fracture zone that is conjugate to, or wholly unrelated to, the four subparallel zones that were first discovered. In any event, it is the first of its kind; no other submarine branch, sharp bend, conjugate, or unrelated fracture zone has been found in the Pacific Basin. The Tehuantepec Ridge trend may extend in both directions. Sounding lines crossing the area to the southwest (fig. 1) show irregular topography but are not adequate to show trends. From the existing soundings, charts could be drawn that would carry the ridge for about 200 miles to the southwest and show a regional change in depth across it. Equally plausible charts indicate no ridge and no regional change in depth (fig. 1), so that the issue remains in doubt.

To the northeast, the trend of the ridge intersects the Middle America Trench in the Gulf of Tehuantepec. The immediate area of the intersection is unsounded, but detailed charts (Fisher, 1957) show the following changes in topography at the intersection: (1) the axis of the trench deepens to the south by 300–500 fathoms or about the same amount as the regional change in depth found elsewhere on opposite sides of the ridge; (2) the bottom of the trench is flat in most places to the north and V-shaped to the south. In the vicinity of the intersection the trench is constricted, and a few miles to the south a seamount rises from the axis of the trench. The intersection also marks a major change in the structure of the Middle America Trench. Northwest of the ridge the crust under the trench is thinner (Fisher and Shor, 1958), and no active volcanoes line the coast. Southeast of the ridge the crust is thicker, and a line of active volcanoes lies parallel to the trench on land.

SMALL TROUGHS AND RIDGES IN AREA OF FRACTURE ZONE

Five isolated troughs have been discovered in the course of the present exploration of the northeastern equatorial Pacific (fig. 1). A group of four widely spaced, northwest-trending troughs lies parallel to and 150–200 miles south of the Clipperton fracture zone. The fifth trough, about 180 miles north of the fracture zone, trends northeast. The southern troughs have not been purposely surveyed, but the trends are known either because two ships were traveling in company on parallel courses or because one ship approximately reversed its course for hundreds of miles while studying ocean currents. The northern trough has been crossed by three expeditions; the most recent track was laid out to clarify the topography. The trough proved to be unexpectedly complex, and further sounding will be required for the preparation of an adequate chart. Despite these limitations, a brief description of the features seems warranted because local deep troughs are so very rare in ocean basins.

A trough centered at 4° N., 123°50′ W. has a known length of 10 miles and an apparent trend of N. 41° W. The regional depth is 2,350 fathoms, and the trough is about 3,000 feet deeper. An asymmetrical ridge to the southwest rises to 1,825 fathoms, and the steep northeast side slopes into the trench at an average angle of 10° for 6,000 feet.

A trough at 4°30′ N., 120° 45′ W. trends N. 20° W. for at least 20 miles. Regional depth is 2,300 fathoms, and the trough is 2,000 feet deeper. Beside the trough is a peak at 1,835 fathoms, giving a local relief of 4,700 feet.

A trough at 7°40′ N., 114°50′ W. trends N. 41° W. for at least 20 miles. The trough is 1,500 feet deeper than the regional depth of 2,200 fathoms. An asymmetrical ridge, its steep side toward the trough, rises to 1,515 fathoms northeast of the trough. Local relief is 5,700 feet.

The trough centered at 6°45′ N., 111° W

trends N. 43° W. for at least 40 miles and is much wider than the three troughs to the west. Regional depth is 2,150 fathoms; the trough is 3,000 feet deeper. It is bounded by ridges; the higher, to the southwest, rises to 1,830 fathoms. Local relief is 4,900 feet.

The trough centered at 13°30′ N., 110°30′ W., north of the fracture zone, is at least 100 miles long and as much as 30 miles wide. The trend is ill defined but lies between N. 20° E. and N. 40° E. The maximum depth of 3,030 fathoms is 5,600 feet below the regional depth of 2,100 fathoms. Local relief is much greater because the trough is flanked by ridges rising to 1,020 and 900 fathoms, and a seamount rising to 780 fathoms lies within the trough. The ridge to the southeast is asymmetrical, with its steep side toward the trough; local relief is 12,800 feet.

STRUCTURAL INTERPRETATION OF TOPOGRAPHY IN AREA OF FRACTURE ZONE

The area of the present study is a band about 700 miles wide and 2,400 miles long, centered on the Clipperton fracture zone. The topography in the fracture zone itself resembles the topography in other fracture zones in the northeastern Pacific. Near the fracture zone lie several linear topographic features that may be related to it but have not been found near other zones.

The largest topographic unit is the broad, low swell of the Clipperton fracture zone. All the submarine fracture zones of the northeastern Pacific Basin display reasonably similar swells. The swells have been interpreted as first-order welts produced by compressional stresses acting in the whole northeastern Pacific (Menard, 1955, p. 1182). In the approximate center of the swell is a trough, commonly bounded by asymmetrical ridges, which also has its counterpart in all the other fracture zones. The topography of the troughs and the bounding ridges have two characteristics giving some indication of the type of faulting that produced them: they have relief of a few thousand feet, and, in most places, they are straight. The topography can be explained by superficial normal keystone faulting, at the crests of the welts, along the straight fault lines produced as shears by the first-order compressional stress.

The extraordinary Clipperton Ridge, 40–60 miles wide, 330 miles long, and 8,000–10,000 feet high, is matched in approximate size, relief, and position within a known fracture zone by several other ridges (fig. 7). The Mendocino Ridge is 10 miles wide, 240 miles long, and has a relief up to 10,700 feet. The Necker Island Ridge is 25 miles wide, 300 miles long, and 10,800 feet high. Likewise, the Transverse Ranges and Channel Islands—which have been described as a possible continental extension of the Murray fracture zone (Menard, 1955, p. 1166–1167)—are an east-trending group of mountains that have nearly the same dimensions as the Clipperton Ridge. Unnamed ridges in the central part of the Mendocino fracture zone and of the Murray fracture zone around Erben Bank are also similar. Even the southeasterly cross trends found on the Clipperton Ridge have counterparts elsewhere. At Cape Mendocino, where the Mendocino Ridge reaches the continent, both the shore line to the south and a late Tertiary basin to the north curve toward the southeast; and southeasterly trends are common on the south side of the Transverse Ranges and Channel Islands. Clipperton Island, moreover, is matched by Erben Guyot, a drowned ancient island (Carsola and Dietz, 1952, p. 493) that rises above a great ridge in the Murray fracture zone.

All these ridges are parts of one deformation pattern, comprising the approximately east-trending fracture zones of the northeastern Pacific. Two complementary fracture zones with northwesterly trends have been suggested—the San Andreas fault system (Menard, 1955, p. 1193–1194) and the Hawaiian Islands (Hamilton, 1957). Supposedly complementary fractures intersect in only three places: Cape Mendocino, the Transverse Ranges, and Necker Island. It would appear more than coincidental that three of the known great ridges are found at the points of intersection. If the existence of a ridge of this type can be taken tentatively as marking the intersection of two fracture zones, then at least one otherwise unindicated fracture zone with a northwesterly trend intersects the Clipperton fracture zone east of Clipperton Island.

All the known troughs and ridges in the vicinity of the fracture zone appear related. The relatively small troughs south of the fracture zone all trend northwesterly; and the large trough and the Tehuantepec Ridge north of the fracture zone trend northeasterly. It is by no means certain that any of the troughs or even the Tehuantepec Ridge was produced by the same stress as the fracture zone or that any other causative relationship exists. It seems worthwhile, however, to see whether any single stress distribution is capable of forming the observed pattern. In this connection a knowledge of the relative movement on at least one of the faults is almost indispensable. Without it, and considering that the trends of the troughs are not resolved with more definition than about 10°, almost any stress-strain relationship is suitable. For example, the troughs south of the fracture zone may be first-order shears complementary to the fracture zone or second-order shears if the movement in the fracture zone is left-lateral or the complementary second-order shears if movement in the fracture zone is right-lateral. If all the fracture zones in the northeastern Pacific were produced by a northeast-southwest compression, the fracture zone is left-lateral; the troughs south of the fracture zone may be second-order right-lateral faults; and the trough and ridge north of the fracture zone may be complementary second-order left-lateral faults.

The distribution of earthquake epicenters in the area (Gutenberg and Richter, 1954, p. 36–37) suggests another possibility. The Tehuantepec Ridge is the locus of many earthquakes, and almost certainly the faults that formed the ridge are active. The epicenters continue southwestward of the known extent of the ridge, and two lie far to the west-southwest in the region of the troughs. It may be possible, therefore, that the troughs represent an early stage in the formation of a new zone of fracturing and that this "Tehuantepec" zone crosses the older, inactive, Clipperton fracture zone. If so, the troughs are simple tension cracks (de Sitter, 1956, p. 172), and the primary motion in the zone is right-lateral.

Any attempt to deduce a large-scale stress pattern relating one fracture zone to another in this area may be of little value because the age of the faulting is not known. The stress pattern has reversed since the Pliocene in the Volcanic Province of Mexico (F. Mooser, personal communication). It may also have reversed in the related Clarion fracture zone or elsewhere in the area. Mooser's important observation suggests once again that the faults in a crustal mosaic remain active almost without regard for any changes in the stress pattern in the area. In this connection, reversal of motion may explain an apparent anomaly in the fracture pattern in the Central America region. The great transcurrent faults that bound the Caribbean Sea to north and south (Bucher, 1952, p. 82–83; Hess and Maxwell, 1953*a*, p. 5; Rod, 1956, p. 457) lie along extensions of the trends of the Clarion and Clipperton fracture zones and appear to be part of the same pattern (Menard, 1955, p. 1170–1171). It would be expected that the Caribbean faults would show the same sense of motion, but at present the motion is left-lateral on the northern fault and right-lateral on the southern.

NOTES ON SPATIAL AND TEMPORAL RELATIONS OF FRACTURE ZONES, ISLAND ARCS, AND OCEANIC TRENCHES

Fracture zones bound the ends of many island arcs and oceanic trenches. Elsewhere the trend, water depth, depth to the *M* discontinuity, seismicity, or vulcanism of an island arc or trench may change where a fracture zone intersects it. The frequency with which fracture zones determine the shape and linear dimensions of trenches is suggested by the following examples (fig. 8), in which many of the features have not been previously identified as "fracture zones" but all have many characteristics of such zones:

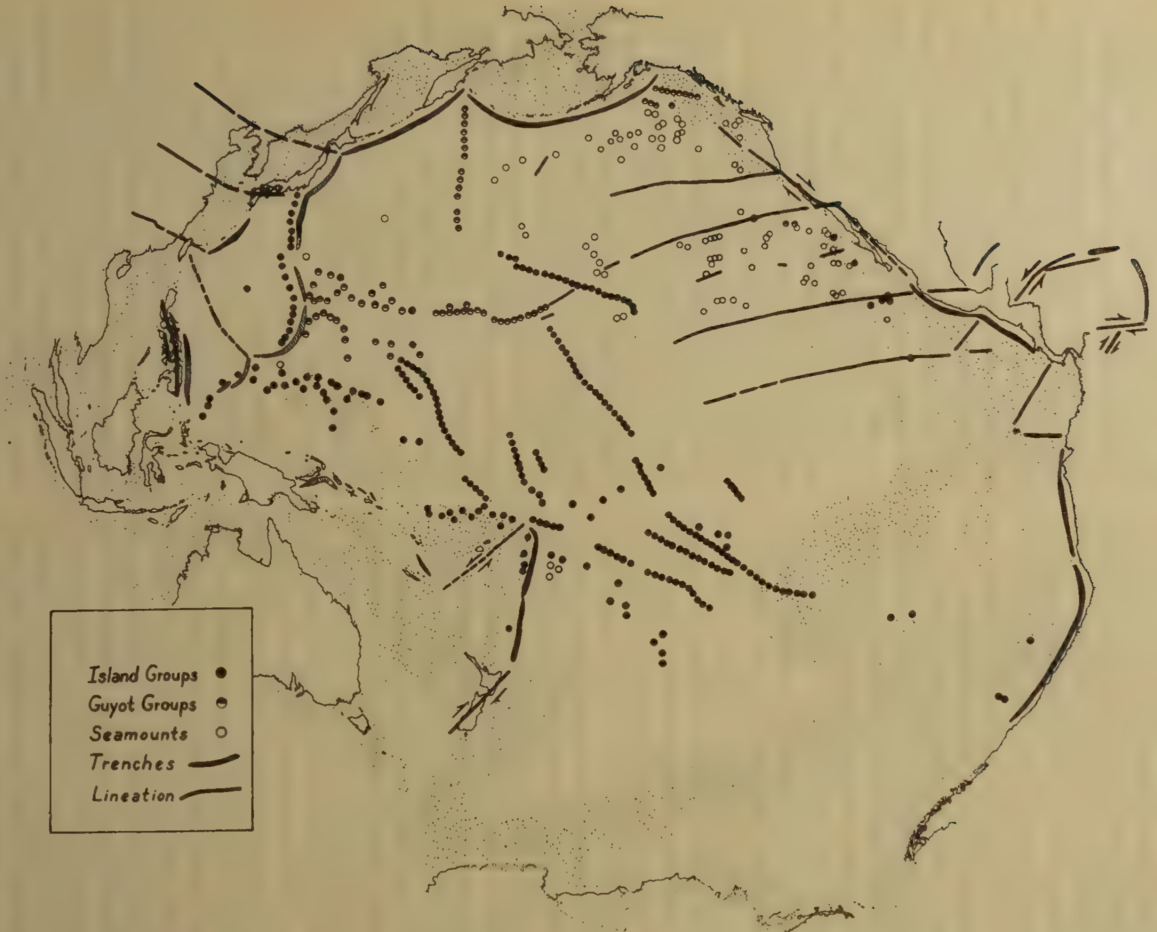
Island Groups ●
Guyot Groups ◉
Seamounts ○
Trenches
Lineation

FIG. 8.—Lineations and trenches in the Pacific Basin, shown on equal-area projection. Island and guyot symbols are diagrammatic and merely show the location and trend of groups rather than individual islands and guyots. Stippled area is shallower than 4,000 meters.

1. Where the Tehuantepec Ridge intersects the Middle America Trench, the depth of the trench, the depth to the *M* discontinuity, and the vulcanism related to the trench are completely changed (Fisher and Shor, 1958).

2. The Clarion and Clipperton fracture zones form the approximate limits of the whole Middle America Trench (Menard, 1955, p. 1192). If the same trends are extended across Central America, they are found to limit the Lesser Antilles arc. The continuity of the individual structures is somewhat in question, however, because of the pronounced change in trend on both sides of Central America, indicated by the Cayman Trough, Tehuantepec Ridge, and Cocos Ridge. The Puerto Rico Trench lies along the Clarion fracture zone trend (Ewing and Heezen, 1955, p. 257).

3. The Aleutian and Kurile Island arcs intersect at nearly a right angle. The long, straight Emperor Seamount Range intersects the margin of the Pacific Basin where the two arcs meet.

4. If the trend of the Median Trough in the Philippine Sea "is extended to the northwest it terminates in the junction of the Nansei Shoto and Taiwan-Philippine arcs, and if extended to the southeast it terminates in the junction of the Marianas and West Caroline arcs" (Hess, 1948, p. 427).

5. The Marcus-Necker Rise terminates at the junction of the Japan Trench and the Marianas Trench. This rise continues as a trend to the east through the Mid-Pacific Mountains, the Necker Ridge, and the Murray fracture zone 5,000 miles across the Pacific Ocean to the Transverse Ranges of California.

6. The section of the Caroline Swell from which Ulithi Atoll rises terminates at the intersection of the Marianas Trench and the West Caroline Trench.

7. Completing the circuit of the Pacific, the Carnegie Ridge (Shumway, 1954, p. 574–580) east of the Galapagos Islands bounds the Peru-Chile Trench on the north.

Remarkable similarities between the east-west tectonic zones of China (Lee, 1939, p. 247–281) and the fracture zones of the northeastern Pacific have been pointed out to the writers by K. O. Emery. The obvious inference may be drawn that the two types of zones differ only to the extent that might be expected for structures in different types of crust. It is particularly interesting, therefore, that Lee observes that the east-west zones deflect and alter the northeasterly geosynclinal and geoanticlinal trends of eastern China (1939, p. 247). He infers that the zones extend along the same trends at least as far as the Japan-Formosa line of island arcs. At the points of intersection, he finds the junctions of individual arcs corresponding to the change in geosynclinal trends in China.

Turning to a slightly different type of evidence for the relation between island arcs, trenches, and fracture zones, it has been proposed that the San Andreas fault zone is complementary to and similar to the fracture zones of the northeastern Pacific. It may also be argued that the Clarion and Clipperton fracture zones of the Pacific continue in the Caribbean area as major transcurrent faults. If fracture zones and major transcurrent faults are merely different expressions of the same features, the relation of major transcurrent faults to trenches is pertinent to the discussion. The following relations have been observed in addition to the ones in the Caribbean:

1. The southern end of the San Andreas fault zone lies near the northern end of the Middle America Trench, although they appear to have no direct topographic connection. The change in trend at the junction is no more than 30°.

2. The Alpine fault zone (Wellman, 1955, p. 249) ends as an identifiable feature at the southern end of the Kermadec Trench. The change in trend is about 30°.

3. Hess and Maxwell (1953*a*, *b*, p. 15–16) have proposed that a major transcurrent fault zone lies south of the Fiji Islands. It forms the northern terminus of the Tonga Trench and the southern terminus of the New Hebrides arc.

4. The transverse faulting of the Visayan

rift zone in the Philippine Islands (Willis, 1944, p. 70) is almost parallel to the Mindanao Trench.

In short, most of the trenches and island arcs of the world are closely associated either with major transcurrent faults or with linear structures or topographic features that probably were formed by transcurrent faulting. Three explanations have been advanced to account for the association in different local areas: (1) the faults are part of a pattern produced by the fracturing of the whole crust in early geological history (Vening Meinesz, 1948, p. 32–35); (2) the faults are part of a global pattern of ancient east-west tectonic zones (Lee, 1939, p. 337–339); and (3) the faults mark the lateral boundaries of convection currents that formed the associated trenches (Hess, 1938, p. 88). Considering the evidence from all the faults and trenches, it appears that Vening Meinesz' hypothesis is the most general, that Lee's hypothesis deals with a local coincidence in trend, and that Hess's hypothesis applies to special situations. Lee's hypothesis may be dismissed for the present discussion without prejudice toward its general validity. Many of the transcurrent or linear features are far too long to have been formed by a local convection current such as may have formed an individual trench. The Marcus–Necker Rise–Murray fracture zone trend is a notable example, and the Clarion and Clipperton fracture zones, with their extensions in the Caribbean and even in the Atlantic Ocean (Hess, 1955, p. 427), are also disproportionately large compared to the associated island arcs and trenches. Moreover, the transverse structures lie at all angles from parallel to perpendicular to the island arcs, hardly suggesting a causative relationship.

It appears that the crust of the Pacific Basin and of eastern China has been broken into very large blocks. Moreover, the boundaries between blocks are so fundamental that not even the great structures of island arcs or of geosynclines ordinarily cross them. The forces, here unidentified, that form the island arcs may possibly act on an area larger than a block, but the structures they produce are discontinuous at the edges of the blocks. They may also act at random orientations to the boundaries of the blocks. Deformation apparently occurs most often along the boundaries, and the type of deformation depends on the orientation. Off Mexico and also New Zealand as slight a change in trend as 30° appears sufficient to change a transcurrent fault zone into a rather straight island "arc." If the orientation of forces is parallel or even roughly parallel to the block boundaries, then Hess's hypothesis may apply. The direction of movement is produced by the forces acting at the moment; the orientation of the faults does not necessarily change.

Acknowledgments.—The writers are indebted to the scientific leaders of expeditions in this area for their co-operation in laying out ships' tracks to fill in unexplored areas. E. L. Hamilton and J. F. T. Saur led the Shuttle Expedition; John Knauss and Townsend Cromwell the Eastropic Expedition; Roger Revelle the Capricorn Expedition; and Warren Wooster the Shellback Expedition. The masters and officers of "Baird," "Horizon," and the Navy Electronics Laboratory ship "EPCE (R) 857" were responsible for celestial navigation. Much of the plotting was done by Shirley Fisher, Ann Hartswick, and Carol Ingram, and drafting by J. R. Moriarty, H. F. Taylor, and R. C. Winsett. Funds for ship operations were provided on various contracts by the Office of Naval Research and the Bureau of Ships.

REFERENCES CITED

Agassiz, A., 1906, General Report of the expedition (Albatross Expedition 1904–1905): Mus. Comp. Zoölogy Mem., v. 26.

Bucher, W. H., 1952, Geologic structure and orogenic history of Venezuela: Geol. Soc. America Mem. 49.

Carsola, A. J., and Dietz, R. S., 1952, Submarine geology of two flat-topped northeast Pacific seamounts: Am. Jour. Sci., v. 250, p. 481–497.

Dietz, R. S., 1954, Marine geology of northwestern Pacific: Geol. Soc. America Bull., v. 65, p. 1199–1224.

Dietz, R. S., and Menard, H. W., 1953, Hawaiian swell, deep, and arch, and subsidence of the Hawaiian Islands: Jour. Geology, v. 61, p. 99–113.

Ewing, M., and Heezen, B. C., 1955, Puerto Rico Trench topographic and geophysical data; in A. Poldervaart (ed.), Crust of the earth, p. 255–268: Geol. Soc. America Special Paper 62.

Fisher, R. L., 1957, Geomorphic and seismic-refraction studies of the Middle America Trench, 1952–1956: unpublished Ph.D. thesis on file, Scripps Institution ot Oceanography and University of California at Los Angeles.

——— and Shor, G. G., 1958, Topography and structure of the Middle America Trench: XX Internat. Geol. Cong. Proc. (in press).

Gutenberg, B., and Richter, C. F., 1954, Seismicity of the earth: Princeton, Princeton Univ. Press.

Hamilton, E. L., 1957, Marine geology of the southern Hawaiian Ridge: Geol. Soc. America Bull., v. 68, p. 1011–1026.

Heacock, J. G., and Worzel, J. L., 1955, Submarine topography west ot Mexico and Central America: Geol. Soc. America Bull., v. 66, p. 773–776.

Hess, H. H., 1938, Gravity anomalies and island arc structure with particular reference to the West Indies: Am. Philos. Soc. Proc., v. 79, p. 71–96.

——— 1948, Major structural features of the western North Pacific, an interpretation of H.O. 5485, bathymetric chart, Korea to New Guinea: Geol. Soc. America Bull., v. 59, p. 417–446.

——— 1955, The oceanic crust: Jour. Marine Research, v. 14, p. 423–440.

——— and Maxwell, J. C., 1953*a*, Caribbean research project: Geol. Soc. America Bull., v. 64, p. 1–6.

——— — ——— 1953*b*, Major structural features of the south-west Pacific: Seventh Pacific Sci. Cong. Proc., v. 2, p. 14–17.

Lee, J. S., 1939, The geology of China: London, Thomas Murby & Co.

Menard, H. W., 1955, Deformation of the northeastern Pacific Basin and the west coast of North America: Geol. Soc. America Bull., v. 66, p. 1149–1198.

——— 1956, Archipelagic aprons, Am. Assoc. Petroleum Geologists Bull., v. 40, p. 2195–2210.

——— and Dietz, R. S., 1951, Submarine geology of the Gulf of Alaska: Geol. Soc. America Bull., v. 62, p. 1263–1285.

Rod, E., 1956, Strike-slip faults of northern Venezuela: Am. Assoc. Petroleum Geologists Bull., v. 40, p. 457–476.

Shumway, G., 1954, Carnegie Ridge and Cocos Ridge in the east equatorial Pacific: Jour. Geology, v. 62, p. 573–586.

de Sitter, L. U., 1956, Structural geology: New York, McGraw-Hill Book Co.

Vening, Meinesz, F. A., 1948, Gravity expeditions at sea, 1923–1938: Pub. Netherlands Geog. Comm., Delft, v. 4.

Wellman, H. W., 1955, New Zealand Quaternary tectonics: Geol. Rundschau, v. 43, p. 248–257.

Willis, B., 1944, Philippine earthquakes and structure, Seismol. Soc. America Bull., v. 34, p. 69–81.

(461)

(462)

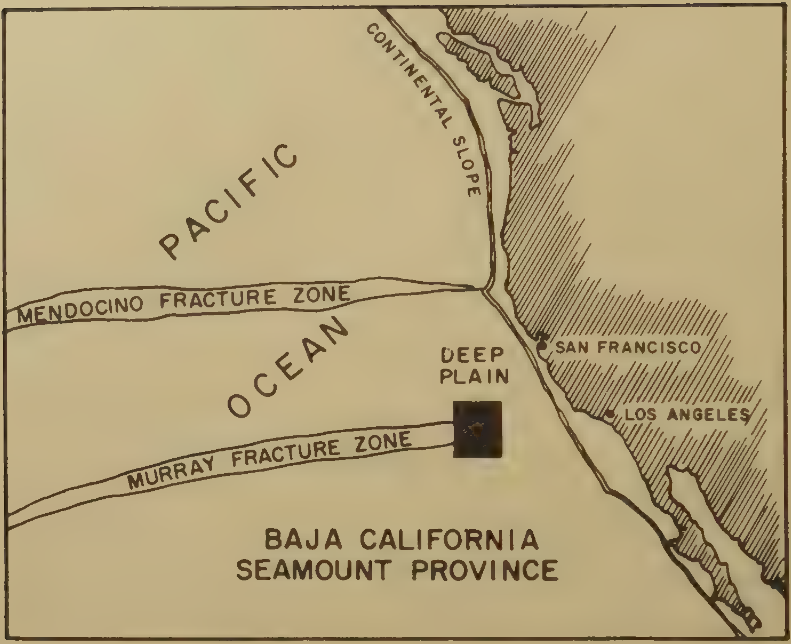
CONTINENTAL SLOPE
PACIFIC
OCEAN
MENDOCINO FRACTURE ZONE
MURRAY FRACTURE ZONE
DEEP
PLAIN
SAN FRANCISCO
LOS ANGELES
BAJA CALIFORNIA
SEAMOUNT PROVINCE

Figure 1 - Index map of a part of the northeastern Pacific Ocean and West Coast of United States, showing location of area covered by magnetic survey (black rectangle).

Figure 2 - The USC&GS ship PIONEER.

Magnetic Survey of Part of the Deep Sea Floor Off the Coast of California

Henry W. Menard
Victor Vacquier
Scripps Institution of Oceanography

Measurements made of the depths of the ocean by echo-sounding devices have revealed the existence of many mountains, valleys, and plains on the ocean floors. Because these features have been protected by the sea from powerful erosive agents, and therefore have been preserved for much longer periods of time than similar features on exposed surfaces of the earth, they have aroused much interest among marine geologists and other investigators (see Research Reviews, August 1957). Primarily, this interest has centered on the geologic structures in which the record of the forces responsible for the topography is "written." These structures have been well preserved also, but as they are inaccessible, indirect means of identifying and mapping them have had to be utilized.

One of these approaches relies on geophysical techniques—the same ones used so widely in prospecting for oil and minerals over the land surfaces of the earth. For example, by timing the travel of elastic waves generated by earthquakes and explosions, seismologists have shown that the earth's crust, which is about 20 miles thick under the continents, thins out to about three miles under oceanic basins. This establishes the fundamental difference between continents and ocean basins and suggests that continental and oceanic areas of the world have retained their identity throughout geologic time.

Another method for investigating the ocean floor utilizes sonic waves. By measuring the velocities of these waves after they have been reflected from the ocean bottom to listening stations, it is often possible to determine the approximate thickness of the crustal layers and the kinds of rock that constitute them.

A third method involves the collection of magnetic data. This information is applicable to the study of geologic structures because of the fact that the crustal rocks, both of the land and the ocean floors, are magnetized by the earth's magnetic field. Thus, contacts of rock bodies of different mineralogical composition and surface and subsurface topography create measurable anomalies of the field at the surface of the ocean. By measuring these anomalies, important clues as to the nature of the crustal rocks can often be found.

Utilizing the latter method of study primarily, but applying data collected by the other methods to interpret the results obtained, the authors recently made a survey of a portion of the floor of the Pacific Ocean (Figure 1). One of the objectives was to learn more about a very prominent structure called the Murray fracture zone—a break in the earth's crust extending 1,800 nautical miles from a point near the

Contribution from the Scripps Institution of Oceanography, New Series, No. 1015.

Reproduced by Permission

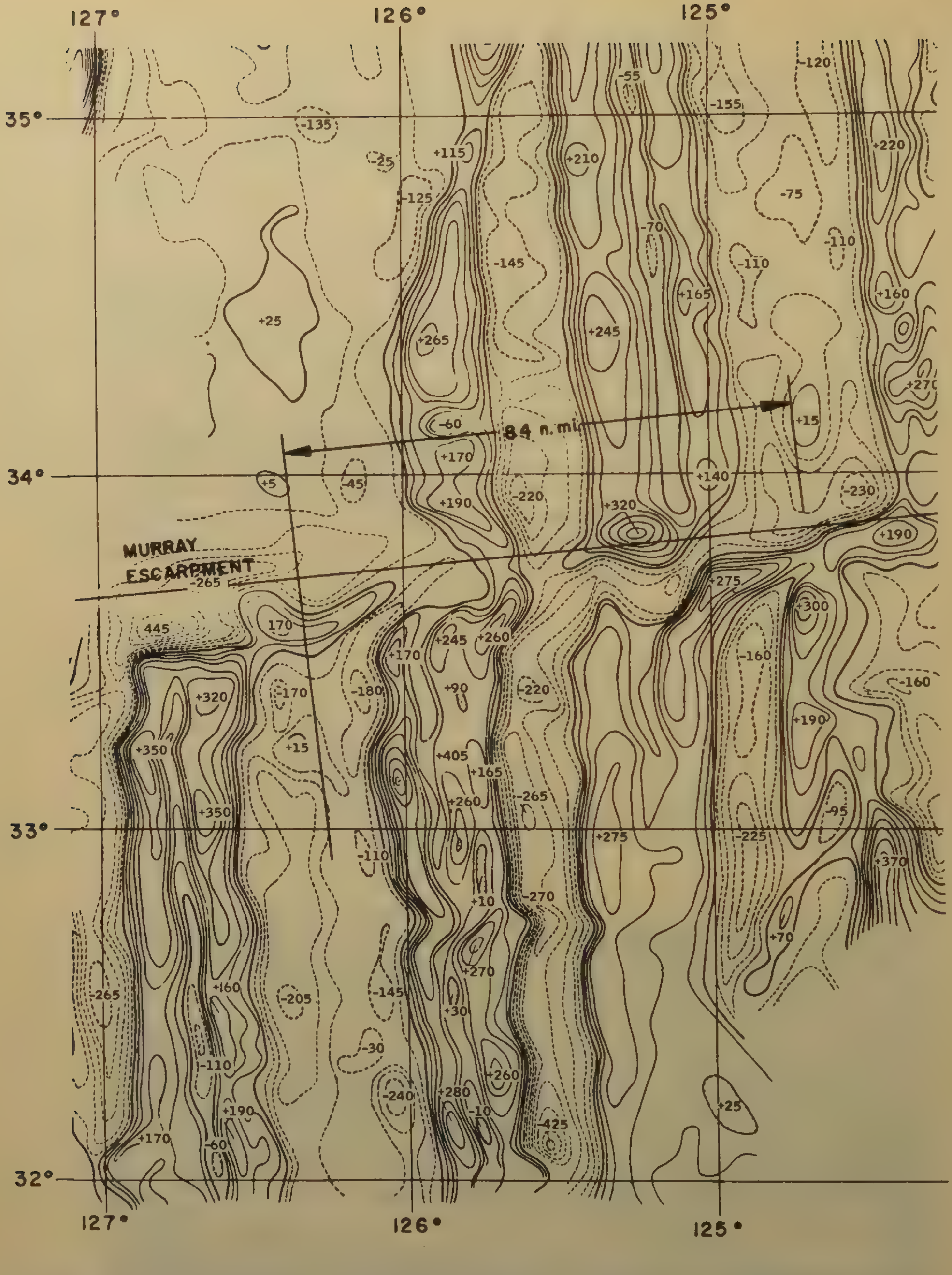
127°
126°
125°
35°
34°
33°
32°
-55
-120
-155
-135
+220
-25
+115
+210
-75
-125
-70
-110
-110
-145
+25
+165
+160
+265
+245
+270
+15
-60
84 n.mi
+170
+5
-45
+140
-230
-220
+190
+320
MURRAY
ESCARPMENT
-265
+190
+275
+300
170
445
+245
+260
+170
-160
-160
+320
-170
-180
+90
-220
+190
+15
+350
+405
+165
-265
+350
+260
-95
+275
-225
-110
+370
+10
-270
+70
+270
-265
+160
-205
-145
+30
-30
-110
+260
-240
+280
+25
+190
-10
-425
+170
-60

Figure 3 - Map showing the total magnetic intensity of the area outlined in Figure 1. The contour interval is 50 gammas (1 gamma equals 10^{-5} gauss). The north-south trending features are interpreted as being lava flows that fill the linear depressions of old topography. Note the horizontal shift along the Murray escarpment.

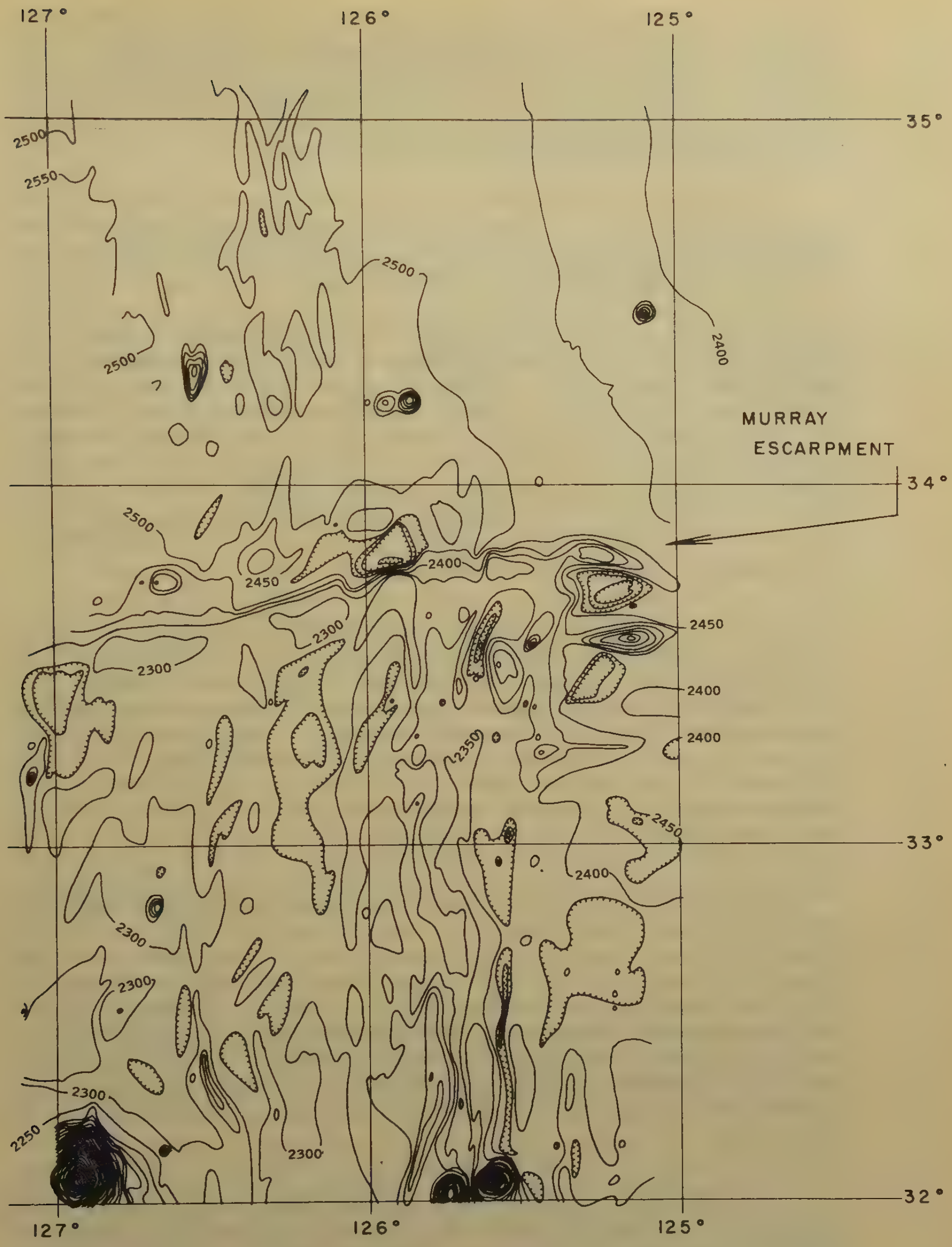
127°
126°
125°
35°
2500
2550
2500
2500
2400
MURRAY
ESCARPMENT
34°
2500
2450
2400
2450
2300
2300
2400
2400
2350
2450
33°
2400
2300
2300
2300
2250
2300
32°
127°
126°
125°

Figure 4 - Map showing generalized bottom topography of the area of Figure 3. The contour interval is 50 fathoms. Except for the northeastern corner of the map, where the ocean floor consists of sediments derived, apparently, from the continent, most of the topography shown is oriented north-south.

Pacific Coast almost to the Hawaiian Islands. The original observations were made mostly along east-west lines, about 5 nautical miles apart, with a magnetometer towed behind the USC&GS ship PIONEER (Figure 2), which was then engaged in a detailed hydrographic survey. The work was done under the sponsorship of the Office of Naval Research and with the cooperation of the Coast and Geodetic Survey.

Figure 3 is a map of the area surveyed, showing contour lines of equal magnetic intensity. The lines have been adjusted so that they do not reflect the increase in intensity of the earth's magnetic field that occurs from south to north across the area.

In Figure 4, the general ocean-bottom topography of the area is shown. The most conspicuous feature on this map is the escarpment of the Murray fracture zone. It trends east-northeast across the whole area. Not only does the escarpment have prominent relief of its own, but it also marks the boundary between two topographic provinces—a shallow, irregular one to the south and a deep, smooth one to the north. In this particular area, which is near the eastern end of the fracture zone, the maximum relief of the escarpment is only about 2,400 feet, and the average relief is only 1,200 feet. West of the area the relief of the escarpment is as great as 6,840 feet.

South of the Murray escarpment is the Baja California Seamount Province, a vast region consisting entirely of seamounts and hills. The seamounts in this province that have been dredged are volcanoes, and all the other large peaks appear to be volcanoes because of their typical conical shape (a few can be seen at the bottom of Figure 4). The origin of these countless hills is not well understood. Most of those in the area of Figure 4 do not resemble small, low volcanoes, but instead are long and narrow like the topography one would expect to be produced by folding and faulting.

Extending northward from the Murray escarpment to the Mendocino escarpment, and a few hundred miles westward from the continental slope off the coast of central California, is an abyssal plain called the Deep Plain (see Figure 1). At its western edge, the plain is interrupted by an increasing number of low hills (see Figure 4). These are part of the transition zone between the Deep Plain and the more rugged topography to the west. Most of the low hills north of the Murray escarpment have the same northerly trend as the hills to the south. However, some comparatively small volcanic cones rise above even the smoothest parts of the plain.

The magnetic expressions of the volcanoes vary greatly. This suggests that the more magnetic ones contain larger amounts of massive lavas than the less magnetic ones, most of which are probably cinder cones. The map of Figure 3 is drawn to too small a scale to permit adequate study of the volcanoes.

The northerly trend of the topography is reflected prominently by the larger magnetic features shown on Figure 3. Some of these magnetic features are known to extend 370 miles north of the Murray escarpment. They are also present over the smooth abyssal plain of the northeastern quarter of the topographic map of Figure 4, indicating that in that area the north-south ridges are covered by a layer of sediment which was deposited, in all probability, by turbidity currents—high-density mixtures of water and suspended sediment that flow down ocean-bottom slopes.

The sharpness of some of the large magnetic anomalies that trend north-south, coupled with the knowledge of the depth of the ocean and the thickness of sediment indicated by seismic shooting, suggests that the anomalies are caused by lava sheets which fill the valleys of the old topography. The total thickness of the lavas must be at least 2,000 feet in order to be consistent with the likely value of the magnetic polarization of such rocks. The lavas may be less magnetic if one assumes that some of the anomalies are due to intrusive bodies several miles thick, rather than thin lava flows piled one on top of another. However, the absence of erosional agencies, and the lack of correspondence between magnetic and topographic features, except for trend, suggest that the lava-flow hypothesis is the more likely one.

The Murray escarpment is reflected clearly on the magnetic map of Figure 3. It interrupts the great north-south trending features. The continuity of the latter is reestablished by slipping the area north of the Murray escarpment 84 nautical miles to the west along the line of the escarpment. The magnetic survey thus shows that, in addition to the vertical displacement of 1,200 feet, there is a right lateral displacement along the Murray escarpment which occurred after the pouring out of lavas on the ocean floor.

This evidence of recent relative motion in the sub-oceanic crust some 200 miles off the continental shores raises interesting questions with regard to the relationship between the deformations of the oceanic crust and adjacent continental margins in response to mountain-building forces in the depths of the earth.

The Material Sciences Division at ONR has a new Director—Dr. J. H. Shenk, formerly Head of the Research Department of the Naval Ordnance Test Station. He replaces Dr. I. Estermann, who will now give full time to his duties as Deputy Director of the Research Group for Coordination.

Dr. Shenk graduated from Kansas State College in 1929 with a degree in chemistry. Later, he obtained a Master's degree from that school and a Doctor's degree from the University of Illinois. He has been on the faculty of Kansas State College, University of Illinois, and Ohio State University. Before going to NOTS in 1946, he was a Research Associate with the Ohio State University Research Foundation.

More than 4,500 Navy personnel have taken part in the Navy's two Antarctic operations, DEEPFREEZE I and DEEPFREEZE II. Through their efforts, an area the size of the United States and Western Europe combined has been explored, much of it never before seen by man.

CHAPTER 13

A WAVE HEIGHT AND FREQUENCY METER

Frank E. Snodgrass and Robert R. Putz
Scripps Institution of Oceanography
and Institute of Engineering Research
University of California

INTRODUCTION

During World War II a group of Naval officers conducted visual measurements of ocean waves simultaneously with instrumental recordings. A comparison of the visual and instrumental values indicated ".... the natural tendency for the observer .... to record not the average wave height but a wave height based on some kind of average of the highest waves. The general experience is that an observer will give a value for the wave height which represents the average of the highest 20 to 40 per cent of the waves" (SIO, 1944). The average height of the highest one-third of the waves, $H_{1/3}$, was therefore suggested as the characteristic (or significant) wave height. "Characteristic wave period" was given a corresponding definition as the average period of the highest one-third waves.

An interpretation of characteristic wave height in terms of standard statistics was made by Putz (1952) and Longuett-Higgins (1952). They related theoretically rms height, mean absolute ordinate a_o, and the average height of the highest "p" per cent. It turns out that $H_1 = 5.02a_o$. Underlying assumptions are that the ordinates are Gaussian and the spectrum moderately narrow. A summary of observations relating to statistical properties of wave heights was recently made by Wiegel and Kukk (1957).

Measurement of the average absolute ordinate can easily be accomplished. In this paper we describe two systems which lead to a direct measurement of $5a_o$ ($=H_{1/3}$). The overall situation is therefore satisfactory inasmuch as a naturally reported quantity, the characteristic wave height, can be defined in terms of fundamental statistics and objectively recorded by automatic means.

The situation is not nearly as satisfactory with regard to wave period. The original definition of characteristic wave period as the period of the highest of one-third waves could not be interpreted in terms of standard statistics, nor is it possible to design reasonably simple devices for recording this quantity. An alternate definition is

Contribution from the Scripps Institution of Oceanography, New Series, No. 1016.

Reproduced by Permission

based on the average time between zero crossings. This can be interpreted in terms of standard statistics, and instruments can be devised for recording it. Moreover, a definition based on zero crossings is as much in accord with the natural tendency of observers as the previous definition of characteristic period. It would seem that characteristic period is not a useful concept and should be dropped. In this paper we describe two instruments for directly measuring the average zero crossing frequency.

OCEAN WAVE RECORD ANALYSIS

Recent research on ocean wave record analysis has dealt with two problems: (1) the description of data obtained from wave meters which record the time history of surface elevation or subsurface pressure fluctuation and (2) the formulation of a theoretical model for the analysis of the data. Two points of view have often been taken in the work on these problems, resulting in the methods of "wavewise" analysis and "ordinatewise" analysis. The first considers the record as a sequence of oscillations defined by the successive points on it which correspond to relative maxima and minima. The second treats the record as a continuous function of the time variable which may be considered either on its own merits as an isolated piece of data or as a particular sample of finite length from a continuing process. Thus, from the second viewpoint, the given time history may be analyzed by taking into account all of the information which is present in it - corresponding to the information in the ordinary Fourier spectrum (specifying amplitude and phase vs. frequency), or it may be analyzed by taking into account all the information present except that which depends upon the value of the absolute time variable - corresponding to the power spectrum (specifying amplitude, but not phase.) The latter method thus seeks to describe the record in terms of the statistical distributions of the various ordinates on the time-history curve. Such a description for a stationary Gaussian process may be considered complete if the correlation function is specified.

A wavewise analysis is often convenient to apply, whereas the ordinate-wise analysis furnishes a more complete and sophisticated description of the data. The existence of the two methods of description creates the problem of relating the measured parameters which result from the two types of analysis. It is thus of interest to see how to obtain information about the power spectrum (or, equivalently, about the correlation function) from a wavewise analysis.

Wavewise analyses of time-history records have been reported by many observers. In these analyses measurements were made on the empirical distributions of wave height and wave period, referred, in each case, to troughs and crests. Certain regularities were found in these distributions, particularly those for wave heights. From measured inter-zero-crossing period distributions the correlation function and hence, in principle, the power spectrum, has been estimated (Putz, 1957).

Studies of the Fourier spectrum of observed wave records have been made by Barber and Ursell (1948), using analog computer methods. The results of those studies are useable spectral curves, which, however, reflect the finite length of the analyzed record and the finite resolving power of the analyzing instrument.

The introduction of the notion of a stochastic process to describe ocean wave records was pioneered by Seiwell (1951) and Rudnick (1951), among others. The usefulness of the Gaussian model was recognized by Rudnick, who also computed for a number of wave records the correlation function - the element remaining to complete the picture given by the stationary stochastic process model. The study of the applicability of this stationary Gaussian model was taken up by Pierson (1952) and Putz (1953), among others.

The stationary Gaussian model was found to be in reasonably good agreement with data and to explain a number of the previously-observed relations brought to light by wavewise analyses. These relations were found to be derivable from the mathematical model, which had, in fact, been discussed earlier in some detail by Rice (1944-5). Wave-height distributions, predicted for a narrow-band spectrum, were found to agree with observed distributions, both as to shape and relative values of parameters. The distributions of wave periods, redefined in terms of zero-axis crossings, were found to be directly related to the power spectrum of the individual wave record, and a means of estimating the spectrum from these distributions was developed. Putz (1957a, b). In addition, various relations between parameters of these zero-crossing period distributions and the power spectrum (or, equivalently, the correlation function) were shown to hold.

RELATIONS INVOLVING a_o AND $f_{z.c.}$

The present report considers techniques for the measurement of two quantities, and shows how these may be used to obtain information about the power spectrum and the wave-height distribution. The first of these is the so-called mean deviation a_o of the time-history ordinate, f(t), i.e., the value of $\overline{|f(t) - \xi_o|}$, averaged over time, where ξ_o is the mean ordinate, such that $\xi_o T = \int_o^T f(t)\,dt$, where T is the total duration of the record. The second is the so-called mean upcrossing frequency, f_o, i.e., the number of times the time-history curve crosses the mean ordinate level per unit time. It is convenient to define also the corresponding angular frequency, ω_o. Thus if N_o is the total number of crossings (in both directions), then $f_o = N_o/(2T)$, and $\omega_o = 2\pi f_o = \pi N_o/T$. The notation "$f_{z:c:}$" is also used below for the quantity $N_o/(2T)$.

If $\underline{\omega}$ is the general angular frequency and $\Phi(\omega)$ is the spectral density function describing the power spectrum, we define the absolute spectral moment M_k of order $\underline{k}$ by the expression $M_k = \int_{-\infty}^{+\infty} |\omega|^k \Phi(\omega)\, d\omega$, $k = 0, 1, 2, \ldots$. Thus the zero-order moment M_o is the total power in the spectrum. The first-order absolute moment becomes, after division by M_o, the mean angular spectral frequency, $\mu_\omega = M_1/M_o$. From μ_ω and the reduced second-order moment, $\mu_2 = M_2/M_o$, is derived the concept of the spectral bandwidth σ_ω defined by the expression $\sigma_\omega^2 = \mu_2 - \mu^2_\omega$. Further, the relative spectral bandwidth, δ_ω, may be defined as σ_ω/μ_ω, with the result that $\sqrt{\mu_2} = \sqrt{\sigma_\omega^2 + \mu_\omega^2} = \mu_\omega \sqrt{1 + \delta_\omega^2}$.

It is well known (Rice, 1944-5) that for a Gaussian process, $a_o = (2/\pi)^{1/2}\sqrt{M_o}$, and $\omega_o = \sqrt{M_2/M_o} = \sqrt{\mu_2}$, so that $M_o = (\pi/2)a_o^2$ and $\mu_\omega = \mu_o\,(1 + \delta_\omega^2)^{-1/2}$. It is seen that observation of a_o and ω_o (or f_o) leads to the determination of M_o and, in the case of small relative bandwidth, of an approximation (on the high side, within 5% if δ_ω does not exceed a value of 1/3, approximately) to μ_ω.

To obtain information regarding the wave-height distributions in a wave record, additional theoretical relations may be used. Thus it follows from the theory of the stationary Gaussian stochastic process that the mean height of the envelope to the time-history graph is $(\pi/2)^{1/2}(M_o)^{1/2} \mp (\pi/2)\, a_o$. In the case of small relative bandwidth the height of the double envelope may be taken to be the mean trough-to-crest wave height; in this case, then, $\pi\, a_o$ is the mean wave height. More generally, it is known that the mean height of the ordinates at the relative maxima (or the mean depth of the ordinates at the relative minima) is given by $\mu_M = \alpha\,(\pi/2)\, a_o$, where $\alpha = f_o/f_1$, and f_1 is the mean up-crossing frequency for the first derivative curve. The mean trough-to-crest wave height will be given by $2\mu_M = \alpha\pi a_o$. A typical value of $\underline{\alpha}$ for ocean swell is 0.85. It follows also from the theory of the stationary Gaussian process that the doubled mean height of the highest one-third of the ordinates on the envelope curve is $2(2.00\sqrt{M_o}) = 5.02\, a_o$.

More general relationships holding for the total spectral power and the reduced second spectral moment may be obtained by considering measurement of mean ordinate deviation and mean up-crossing frequency made about an arbitrary ordinate level. Thus, if we measure the average value, a_h, of $|f(t) - h|$, where $h = \xi_o + k\sqrt{M_o}$, we find that $a_h/a_o = \exp(-k^2/2) + k \cdot \Psi(k)$, where $\Psi(k) = \int_o^k \exp(-t^2/2)\,dt$. Also, for the mean up-crossing frequency, f_h, at ordinate level $\underline{h}$, we have $f_h/f_o = \exp(-k^2/2)$, where, as before, $k = (h-\xi_o)/\sqrt{M_o}$.

It will be noted that both ratios reduce to unity when $k = o$. Further, the differences $a_h - a_o$ and $f_h - f_o$ are of higher order in k, so that the effect of a small error in locating the mean ordinate level vanishes rapidly with k. In fact, for values of k not in excess of about 0.4, the approximations $a_h/a_o\ (\doteq)\ 1 + k^2/2\ (=)\ f_o/f_h$ may be used. For example, an error of 5 or 10% in the determination of ξ_o should not correspond to a value of over 0.4 for k, which yields a relative error of 8% in the value of a_o.

DESCRIPTION OF THE ANALYZER

The block diagram of the wave analyzer is shown in Figure 1. The wave data enters a point A as an electrical signal which varies about a zero potential in proportion to the amplitude of the wave about the mean pressure level. This signal is simultaneously applied to two channels of the analyzer. The first channel reverses the polarity of the signal each time it becomes negative to produce a full wave rectification of the incoming signal. By averaging the rectified signal with an appropriate filter a measure of the average absolute ordinate, a_o, is obtained.

The second channel produces a unit pulse for each positive zero-axis crossing of the incoming signal. By again averaging these pulses with an appropriate low-pass filter a mean zero-axis crossing frequency can be obtained.

AN ELECTRONICALLY OPERATED ANALYZER

This analyzer (Figure 2) operates as shown in the block diagram Figure 1). All amplifiers indicated are type K2W Philbrick functional d-c amplifiers and the circuits are discussed by Philbrick (1955).

The rectifier circuit provides full-wave rectification about the zero axis with d-c coupling and a common ground between input and output. With the input connected to ground the zero adjustment potentiometer is set for zero output of the rectifier for rectification at zero input voltage level.

The pulse generator circuit consists of an overdriven amplifier and relay operated pulsing circuit. The amplifier has positive feedback with a loop gain of slighly greater than unity and therefore tends to assume one of two stable states. When the input exceeds a critical voltage, the amplifier output is positive and the relay is energized. When the input voltage returns to a value slightly below the critical voltage the amplifier output becomes negative. With negative voltage the relay is de-energized due to the action of the shunting diode.

The difference between the level at which a positive-going voltage causes the relay to energize and a negative-going voltage causes the relay to de-energize is the circuit hysteresis. The hysteresis prevents chattering of the relays when the input voltage is zero. The amount of hysteresis is controlled by the 50M feedback resistor. For zero axis adjustment the zero adjustment potentiometer is set in the center of the hysteresis range with the amplifier input connected to ground.

Relay operated pulse generators are used in preference to electronic circuits. When relay A is de-energized a 300 μfd electrolytic condenser is charged to 10 volts; when relay is energized the condenser is discharged through relay B energizing it for 3 seconds. A 1.35 volt pulse is therefore applied to the input of the filter for each positive zero-axis crossing.

Stability of the two filter circuits is the primary concern of their design. All electrical components must be of high quality with low temperature and aging coefficients. Sufficient stability was obtained only by using heavy negative feedback.

The time constant of the filter, being essentially equal to RC, can be made equal to 2 seconds for adjusting the circuit and 600 seconds for normal operation. With a 600 second time constant the high frequency cutoff occurs at $1/2\pi\ 600) = 1$ cyc/hr. Recording millimeters can be driven directly from the output of the filter. Sensitivity of the circuits is adjusted by potentiometers connected in series with the recorders.

A RELAY-OPERATED ANALYZER

This wave analyzer, designed to operate with a Mark IX Pressure Head (Snodgrass, 1955), consists of a thyratron-operated relay circuit which drives two panel meters filled with 12,500 centistoke silicone fluid (Figure 3). The viscous damping of the meter movement provides a response time-constant of twenty minutes. These meters are equivalent to a single stage RC filter with a high frequency cutoff at $1/(2\pi\ 20\ \text{min}) = 0.5$ cyc/hr. (Snodgrass, Putz 1954).

The second meter receives as an input the rectified current of the a-c wave signal driving the Esterline-Angus recorder. The wave height meter is 10 times more sensitive than the Esterline-Angus recorder; its full scale reading corresponds to an average absolute

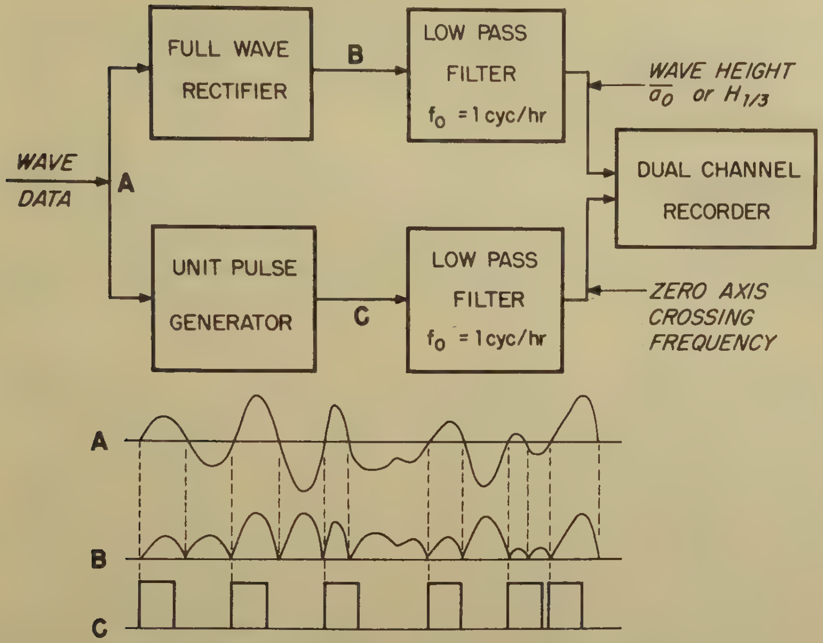
FULL WAVE RECTIFIER
B
LOW PASS FILTER f_0 =1 cyc/hr
WAVE HEIGHT $\overline{a_0}$ or $H_{1/3}$
WAVE DATA
A
DUAL CHANNEL RECORDER
UNIT PULSE GENERATOR
C
LOW PASS FILTER f_0 = 1 cyc/hr
ZERO AXIS CROSSING FREQUENCY
A
B
C

Fig. 1. Block diagram of the analyzer. Voltage signal from wave gage enters A; the average values of the rectified wave record at B and zero-axis-crossing unit pulses at C are recorded as wave height and frequency.

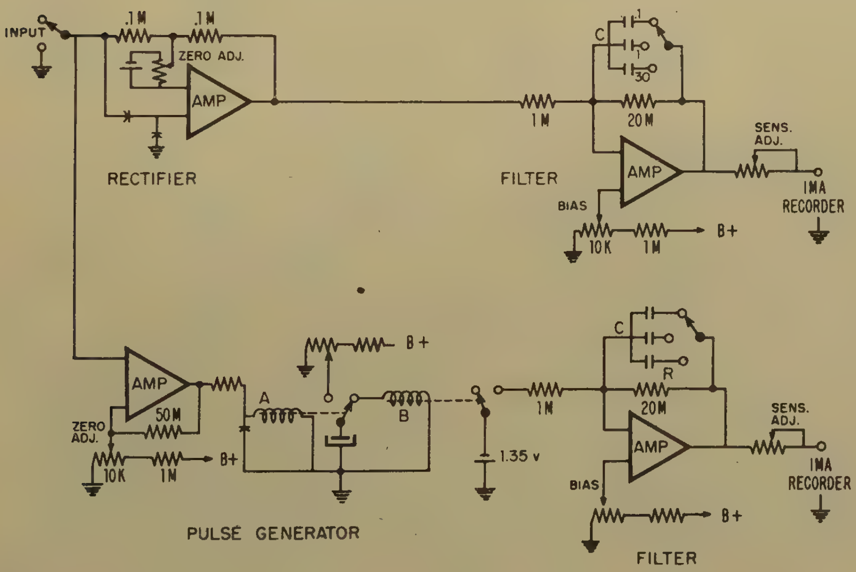
INPUT
.1M
.1M
ZERO ADJ.
AMP
RECTIFIER
C
1
1
30
1M
20M
FILTER
AMP
SENS. ADJ.
1MA RECORDER
BIAS
10K
1M
B+
AMP
ZERO ADJ.
50M
10K
1M
B+
B+
A
B
1.35 v
PULSE GENERATOR
C
R
1M
20M
AMP
SENS. ADJ.
1MA RECORDER
BIAS
B+
FILTER

Fig. 2. Functional diagram of an electronically operated analyzer. AMP symbols are Philbrick d-c operational amplifiers.

ordinate value of 0.1 of full scale of the Esterline-Angus. If $H_{1/3}$ is assumed to be equal to approximately $5a_o$, the characteristic wave height $H_{1/3}$ is $(5CR_h)/10$ where C is the full scale calibration of the Esterline-Angus recorder and R_h is the reading of the wave height meter assuming full scale to be unity.

The first meter receives a pulse of current each time the wave record passes through the zero axis in a positive direction. By proper adjustment of the circuit the meter reads one milliampere for an input signal with a frequency of 0.1 cyc/sec. The zero crossing frequency then equals 0.1 R_f, where R_f is the reading of the frequency meter.

Circuit operation - A combination of a d-c bias voltage and a 90° leading a-c bias voltage connected in a cathode circuit of the thyratron tube (Figure 4) prevents the tube from conducting unless the grid voltage exceeds a given value. The exact value of the grid voltage necessary to cause conduction is determined by the setting of potentiometer P_1. This voltage will be approximately 12 volts with respect to the negative side of the d-c bias supply, since the "wave-recorder potentiometer" is in its center position with no ocean-wave signal applied. Resistor R_1 and Condenser C_1 in the grid of the thyratron decouple the thyratron grid from the recording circuit of the wave recorder and prevent high-frequency noise from firing the tube.

Resistor R_2 and Condenser C_2 shift the filament voltage 90° leading with respect to the plate voltage. With this voltage connected in the bias circuit, the tube will conduct the entire positive half of the plate voltage swing as soon as grid voltage exceeds the critical value. With only the d-c bias connected in the circuit, the tube would conduct only one-half of the positive plate voltage.

Relay operation - The relay circuit operation is as follows: Assume the thyratron grid voltage is below the critical value, the tube is not conducting, and the relays are de-energized. If a signal is supplied from the wave recorder which causes the grid voltage to increase above the critical value, the tube will conduct and relay A will be energized, closing contacts A_1 and A_2. Contact A_1 energizes Relay B, which closes contacts B_2 and B_3 and opens contact B_1. Contact B_1 disconnects relay A, but relay A will remain energized because of the charge in condenser C_3. The contacts of relay A remain closed for 1.4 seconds each time the circuit is actuated. Contact A_2 causes a unit pulse current of 7.1 ma for 1.4 seconds to flow through the "wave period" meter each time the grid signal exceeds the critical value. Contact B_2 prevents relay B from de-energizing when contact A_1 opens. Relay B, therefore, will remain energized as long as the

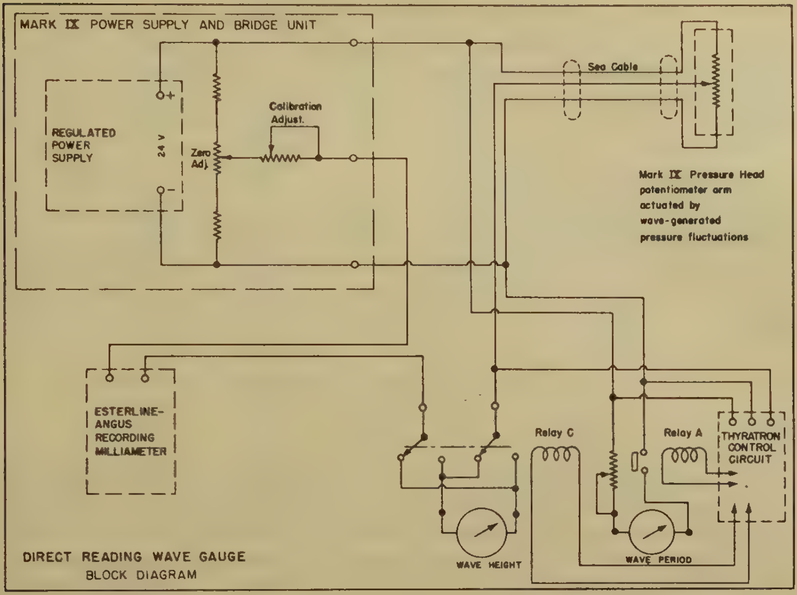
MARK IX POWER SUPPLY AND BRIDGE UNIT
REGULATED POWER SUPPLY
24 V
+
−
Zero Adj.
Calibration Adjust.
Sea Cable
Mark IX Pressure Head potentiometer arm actuated by wave-generated pressure fluctuations
ESTERLINE-ANGUS RECORDING MILLIAMETER
Relay C
Relay A
THYRATRON CONTROL CIRCUIT
WAVE HEIGHT
WAVE PERIOD
DIRECT READING WAVE GAUGE
BLOCK DIAGRAM

Fig. 3. Functional diagram of the relay operated analyzer for the Mark IX pressure gage.

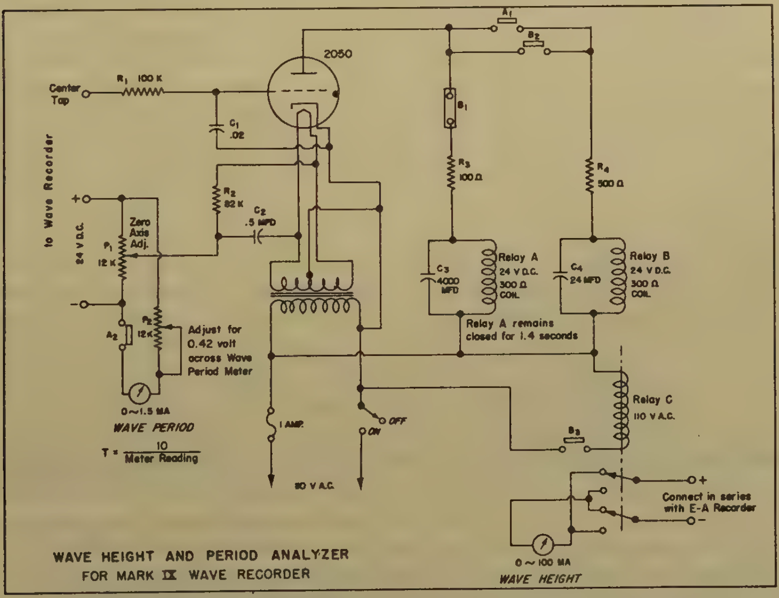
A_1
B_2
2050
Center Tap
R_1 100 K
C_1 .02
B_1
R_3 100 Ω
R_4 500 Ω
to Wave Recorder
24 V D.C.
+
−
Zero Axis Adj.
P_1 12 K
R_2 82 K
C_2 .5 MFD
C_3 4000 MFD
Relay A 24 V D.C. 300 Ω COIL
C_4 24 MFD
Relay B 24 V D.C. 300 Ω COIL
Relay A remains closed for 1.4 seconds
A_2
P_2 12 K
Adjust for 0.42 volt across Wave Period Meter
0~1.5 MA
WAVE PERIOD
$T = \frac{10}{\text{Meter Reading}}$
1 AMP.
OFF
ON
110 V A.C.
Relay C 110 V A.C.
B_3
Connect in series with E-A Recorder
0 ~ 100 MA
WAVE HEIGHT
WAVE HEIGHT AND PERIOD ANALYZER
FOR MARK IX WAVE RECORDER

Fig. 4. Schematic diagram of the relay operated analyzer. The wave height and period meters are submerged in 20,000 centistoke oil for averaging of signals.

TABLE I*. TEST RESULTS

DATE 1954	$1/f_{z.c.}$	$T_{1/3}$	a_o	$H_{1/3}$	DATE 1954	$1/f_{z.c.}$	$T_{1/3}$	a_o	$H_{1/3}$
1/26$^{(1)}$	-	10.9	-	18	2/5	-	12.5	-	11
	11.1	12.0	3.2	17		12.5	12.3	3.5	17
	11.5	12.9	3.0	15		14.7	11.9	3.8	20
	-	13.3	-	16		-	11.9	-	20
1/27	-	13.7	-	17	2/6$^{(2)}$	-	11.9	-	17
	14.1	13.9	2.6	15		12.5	12.8	3.6	19
	13.2	14.6	2.9	16		14.8	11.5	2.4	13
	-	13.8	-	17		-	11.9	-	16
1/28$^{(2)}$	-	13.4	-	16	2/7$^{(2)}$	-	13.0	-	13
	14.1	13.9	2.7	16		14.7	13.2	3.2	17
	15.4	13.2	2.8	14		13.5	12.9	2.9	17
	-	14.6	-	15		-	12.6	-	16
1/29$^{(2)}$	-	14.9	-	17	2/8	-	12.9	-	14
	15.4	15.2	2.7	15		13.3	13.5	2.7	15
	13.2	14.1	3.2	16		13.0	13.3	3.1	16
	-	15.1	-	16		-	13.6	-	16
1/30	-	16.3	-	20	2/9	-	13.2	-	16
	14.7	17.3	4.0	23		14.3	13.9	3.2	17
	12.5	16.9	4.5	19		14.5	14.9	3.6	19
	-	17.9	-	18		-	14.2	-	17
1/31	-	16.1	-	24	2/10	-	14.5	-	20
	12.7	16.2	4.2	22		12.5	13.9	3.0	18
	12.0	16.1	3.4	20		11.7	13.5	3.6	19
	-	14.6	-	18		-	13.2	-	18
2/1	-	-	-	15	2/11$^{(1)}$	-	14.5	-	22
	14.3	15.7	3.0	15		12.5	13.9	6.0	30
	14.9	14.7	2.6	14		11.7	13.5	6.3	30
	-	13.7	-	16		-	13.2	-	26
2/2	-	15.1	-	17	2/12$^{(1)}$	-	13.9	-	28
	13.3	14.4	4.0	22		12.7	13.6	4.8	23
	14.1	13.6	3.4	17		12.5	14.0	5.1	25
	-	14.5	-	16		-	16.0	-	24
2/3	-	14.3	-	16	2/13$^{(1)}$	-	16.0	-	22
	14.1	13.3	3.2	18		12.3	15.2	11.6	58
	12.8	13.5	3.0	16		7.7	12.0	10.0	43
	-	12.7	-	15		-	14.0	-	52
2/4	-	13.2	-	13	2/14$^{(1)}$	-	13.3	-	44
	13.3	12.1	3.0	16		10.7	13.9	9.2	48
	12.8	13.3	2.4	14					
	-	13.1	-	16					

*Four measurements were made at 0415, 1015, 1615, and 2215 of each day.

$f_{z.c.}$ and a_o were read from the relay-operated analyzer. $H_{1/3}$ and $T_{1/3}$ were measured from 20-minute wave records by the personnel of the Surf and Weather Station, Camp Pendleton, California.

[1] Local storm present which generated strong secondary waves.

[2] Sections of the record were nearly flat making zero axis crossings difficult to measure.

grid signal exceeds the critical value. Contact B_3 causes relay C to operate as a rectifier by reversing the polarity of the "wave height" meter. The critical grid voltage is adjusted so that the meter polarity is reversed as the current in the Esterline-Angus recorder passes through zero current.

Condenser C_4 prevents relay B from chattering due to the half-wave rectified current flowing in the 2050 thyratron tube. Resistor R_4 limits the current so that 24 volts appear across Relay B with the thyratron conducting. Resistor R_3 limits the current in the thyratron to its maximum allowable value, while Relay A is being energized.

TESTS AND RESULTS

The relay operated analyzer was tested for 23 consecutive days at the Surf and Weather Station, Camp Pendleton, California. The readings of wave height and period obtained from the oil immersed meters were compared to the values determined by the standard manual analysis. The test indicated that $H_{1/3}$ is approximately equal to $5a_o$ (Figure 5).

The frequency meter indicated a wave period that was generally less than the significant wave period particularly during local storms as indicated in Table I. At the outset of the local storm high frequencies could be seen in the wave record which would considerably affect a reading on the zero crossing meter; the manual analysis of the record would fail, however, to indicate this change in sea state until the amplitude of the high frequency waves was appreciable in comparison to the underlying sea swell.

Figure 6 indicates results obtained by comparing the value of the zero-axis crossing frequency, measured by the electronic analyzer, to the value computed from the spectrum. The spectra were obtained from data consisting of 3000 values at one-second intervals read from a 50-minute wave pressure record (gage depth 14 feet), (Munk, 1957). The value at A is the mean frequency of the record, while the value at B is the theoretical zero-axis crossing frequency. The arrow labeled C indicates the range of values obtained from the analyzer during the 50-minute period of the spectrum data. Good agreement was found between the computed and measured zero-axis crossing frequency.

The continuous recording of wave height (or energy) and frequency is perhaps more important than the determination of the average values of $H_{1/3}$ and $f_{z.c.}$ discussed above. Large variations in $H_{1/3}$ and $f_{z.c.}$ can occur in relatively short periods of time as shown in Figures 7 and 8. This record indicates that 15-minute records taken a half hour apart could differ by 30 or 40 per cent.

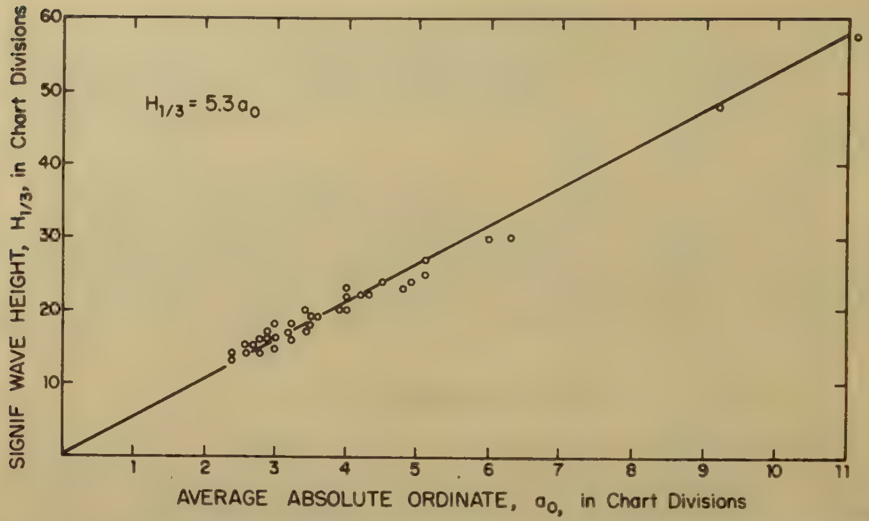

Fig. 5. Experimental data comparing the average absolute ordinate, a_o, to the characteristic wave height $H_{1/3}$.

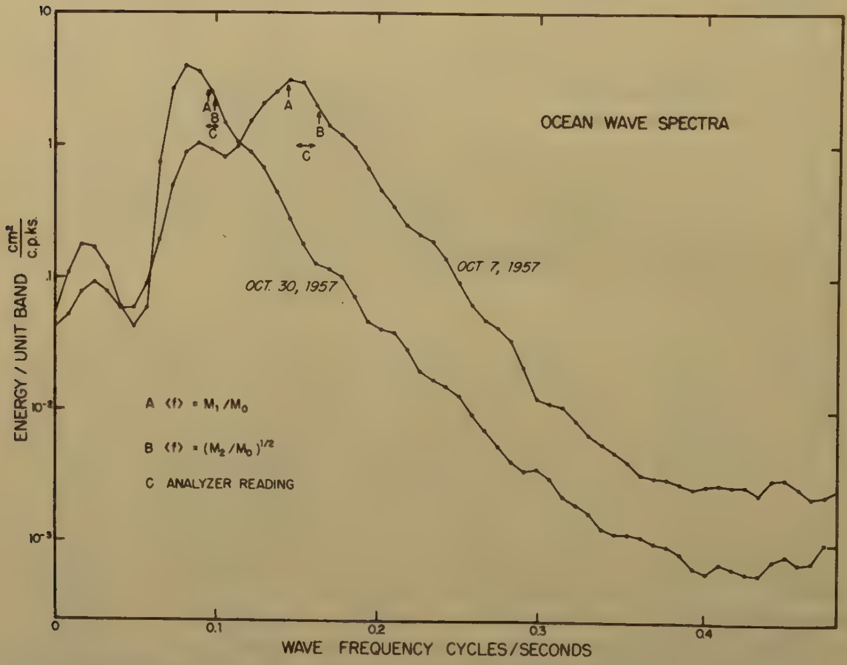

Fig.6. Experimental data comparing wave spectra, calculated mean frequency (A) and zero crossing frequency (B), to measured zero crossing frequency (C).

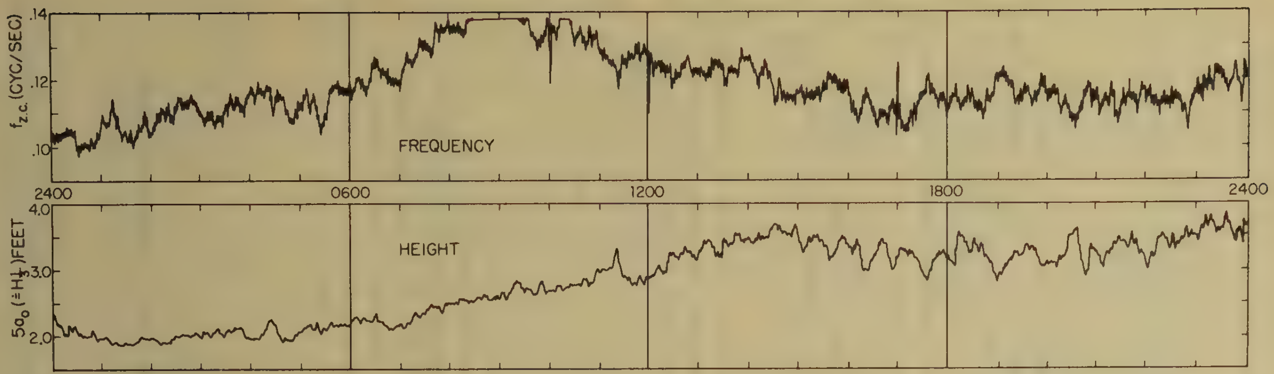

Fig. 7. Analyzer output Nov. 1, 1957. The input signal was obtained from a pressure head 12 feet below MLLW at Scripps Pier. The waves were generated by 15-knot winds that started late October 31 and lasted through November 1.

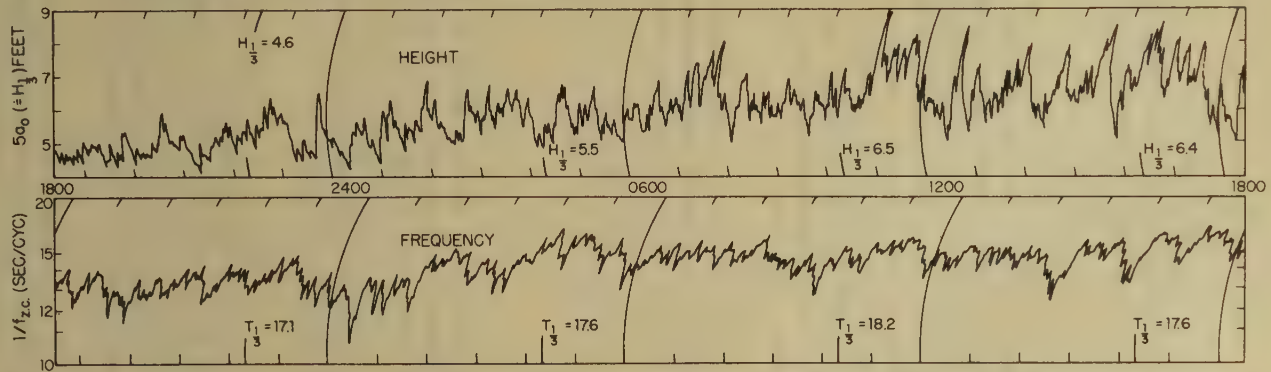

Fig. 8. Analyzer output July 4 - 5, 1956. Local winds were less than 7 knots. Waves were typical "heavy southern swell." Values of $H_{1/3}$ and $T_{1/3}$ were obtained by manual analysis of twenty-minute records at the time indicated.

The change in sea state indicated in Figure 7 was caused by a local 15-knot wind which started late October 31 and lasted through November 1. The wave record was obtained from a pressure gage 12 feet below MLLW in 20 feet of water at Scripps Pier. The zero crossing frequency increased sharply, reached a peak and then decreased before the wave energy increased appreciably.

The record shown in Figure 8 was obtained from a pressure gage 30 feet below MLLW in 35 feet of water at Camp Pendleton, California. The local winds were less than 7 knots. The waves were described as "heavy southern swell" being very low frequency and from the south. Characteristic of southern swell recordings from the analyzer, the zero crossing frequency is low and steady with large variations in wave height. Some correlation is apparent between the frequency and height recordings, with low frequency occurring at times of high energy. The values of $H_{1/3}$ and $T_{1/3}$, indicated in Figure 8, were obtained by manual analysis of twenty-minute records at the time indicated.

The fluctuations of the records pose some interesting questions. Can the fluctuations be predicted for various sea states or for an aging storm? What are the expected correlations between the height and frequency records? Can the spectrum of the analyzer output be predicted from the raw wave record?

ACKNOWLEDGMENT

The authors wish to thank Walter Munk for his many helpful suggestions, both during the study and in the preparation of the manuscript. The assistance given by L. G. Boyd, CWO Marine Corp, and the staff at the Surf and Weather Station, Camp Pendleton, in obtaining wave data was greatly appreciated.

REFERENCES

Barber, N. F. and Ursell, F. (1948). Phil. Trans. A, 240, 527.

Longuett-Higgins, M. S. (1952). On the statistical distribution of the heights of sea waves: J. Mar. Res., vol. 9, pp. 245-266.

Munk, W. H., Snodgrass, F. E., Tucker, M. J., (in press). Spectra of low frequency waves: Bulletin of the Scripps Inst. of Oceanog., Univ. of Calif. Press.

Putz, R. R. (1952). Statistical distributions for ocean waves: Trans. Amer. Geophys. Union, vol. 33, no. 5, pp. 685-692.

Putz, R. R. (1953). The analysis of wave records as random processes: (abstract) Translation of the American Geophysical Union, vol. 34, p. 807.

Putz, R. R. (1953). Ocean wave record analysis - ordinate distributions and wave heights; Technical Report, Series 3, Issue 351, Institute of Engineering Research, Univ. of Calif., Berkeley, Calif.

Putz, R. R. (1957a). A method for the measurement of the correlation function and ordinate distributions for two time-history functions: Technical Report, Series 61, Issue 11, Institute of Engineering Research, Univ. of Calif., Berkeley, Calif.

Putz, R. R. (1957b). A relay-operated device for the measurement of distribution and correlation functions: Technical Report, Series 61, Issue 12, Institute of Engineering Research, Univ. of Calif., Berkeley, Calif.

Pierson, W. J. (1952). A unified mathematical theory for the analysis, propagation, and refraction of storm generated ocean surface waves: Report, Department of Meteorology, N. Y. Univ.

Rice, S. O. (1944-5). Mathematical analysis of random noise, Parts I-IV, Bell System Technical Journal, vol. 23, pp. 282-332, vol. 24, pp. 46-156.

Rudnick, P. R. (1951). Correlograms for Pacific Ocean waves: Proceedings of the Second Berkeley Symposium in Mathematical Probability and Statistics, University of California Press, Berkeley and Los Angeles, Calif.

Scripps Institution of Oceanography (1944). Proposed uniform procedure for observing waves and interpreting instrument records: Waves Project Report No. 26.

Seiwell, H. R. (1951). Experimental correlogram analyses of artificial time series (with special reference to analyses of oceanographic data): Proceedings of the Second Berkeley Symposium in Mathematical Probability and Statistics, University of California Press, Berkeley and Los Angeles, Calif.

Snodgrass, F. E. (1955). Mark IX shore wave recorder: Proc. of the First Conference on Coastal Engin. Instr., Council on Wave Research, The Engineering Foundation, Chap. 6.

Wemelsfelder, P. J. (1954). Wave measuring by means of the Integrator: Technical Report, Rykswaterstaat, The Hague, The Netherlands.

Wiegel, R. L., Kukk, J. (1957). Wave measurements along the California Coast: Trans. Amer. Geophys. Union, vol. 38, no. 5, pp. 667-674.

Wilkie, M. J., King, R. F. (1953). A wave-height analyzer: J. of Scien. Inst., vol. 30, pp. 311-314.

Snodgrass, F E., Putz, R. R. (1954). A direct reading wave meter. Institute of Engineering Research, Wave Research Laboratory, Technical Report, Series 3, Issue 37.

Philbrick (1955). Application manual for Philbrick octal plug-in computing amplifiers, George A. Philbrick Researchers Inc., Boston, Mass.

Reprinted for private circulation from
THE JOURNAL OF GEOLOGY
Vol. 66, No. 4, July 1958
PRINTED IN U.S.A.

SOME REMARKS ON GEOMORPHOLOGY OF CONTINENTAL SHELVES OFF NORWAY, LABRADOR, AND SOUTHEAST ALASKA[1]

HANS HOLTEDAHL[2]
Bergen, Norway

ABSTRACT

Studies of the continental shelves off Labrador and the west coast of southeast Alaska suggest that there are marked topographical similarities between these and the Norwegian shelf. A large longitudinal channel or depression is present outside the northeast coast of Labrador, running almost parallel to the coast for more than 400 km., with depths of 300–400 fathoms. Another submarine arcuate channel of smaller dimensions runs parallel to the coast for about 140 km. north of Belle Isle. In the Yakutat Bay region of Alaska and in the Cross Sound area similar, but less significant, channels are present. Both in the Labrador and in the Alaskan area large transverse depressions on the shelf terminate landward in a relatively steep slope which is located along the line of the longitudinal channels. The features are thought to indicate that these present land areas are bordered by major fracture zones along which dislocations took place during the Cenozoic uplift.

INTRODUCTION

In a number of papers O. Holtedahl (1933, 1935*a*, 1940, 1950, 1953) has drawn attention to some rather striking geomorphologic features of the shelf area off the northwest coast of the Scandinavian peninsula. Relatively long and narrow depressions are found parallel to the main trend of the coast line, forming a marked boundary between the irregular, rocky "skjaergaard" area and the even shelf outside. Most of the transverse submarine channels which cross the outer part of the shelf terminate landward at the relatively steep inner slope of the longitudinal depression (fig. 1). A series of profiles obtained by echo-sounding across this boundary zone has been described by the present writer (1955, p. 27–32).

It has been suggested that the long, narrow depressions can best be explained as marginal fracture lines along which the topography has been carved out, mainly during periods when sea levels were lower than at present. It was also thought very probable that the supposed tectonic fracturing had a close relation to the fairly recent, mainly Tertiary oblique uplift of the Scandinavian land mass, during which a more or less peneplained region was transformed into a highly dissected land block of great height.

It was suggested that during Pleistocene time the shelf was highly modified by the erosional and depositional action of the ice, the former river channels being remodeled into troughlike basins and the old topography obscured to a great extent by the deposition of drift material.

The presence of marginal channels has been shown also in other shelf areas off glaciated coasts, where the present high relief is due to fairly recent uplift, namely, off the coasts of Spitzbergen, Greenland, Labrador, and Scotland (O. Holtedahl, 1935*b*, 1936, 1950, 1951).[3] The present writer has also suggested the presence of fault lines crossing the Norwegian shelf, with certain major depth differences of the shelf due to differential movements of blocks bounded by these lines.

The purpose of the present contribution is to draw attention to the shelf areas off the Labrador peninsula and off southeast Alas-

---

[1] Contribution from the Scripps Institution of Oceanography. Manuscript received January 31, 1958.

[2] Geological Institute, University of Bergen, Bergen, Norway.

[3] Recently a bathymetric chart of the continental shelf off the north coast of Ellesmere Island has been published by A. P. Crary (Arctic, v. 9, 1956, p. 155–165), showing very similar features.

Contributions from the Scripps Institution of Oceanography, New Series, No. 1017
Reproduced by Permission

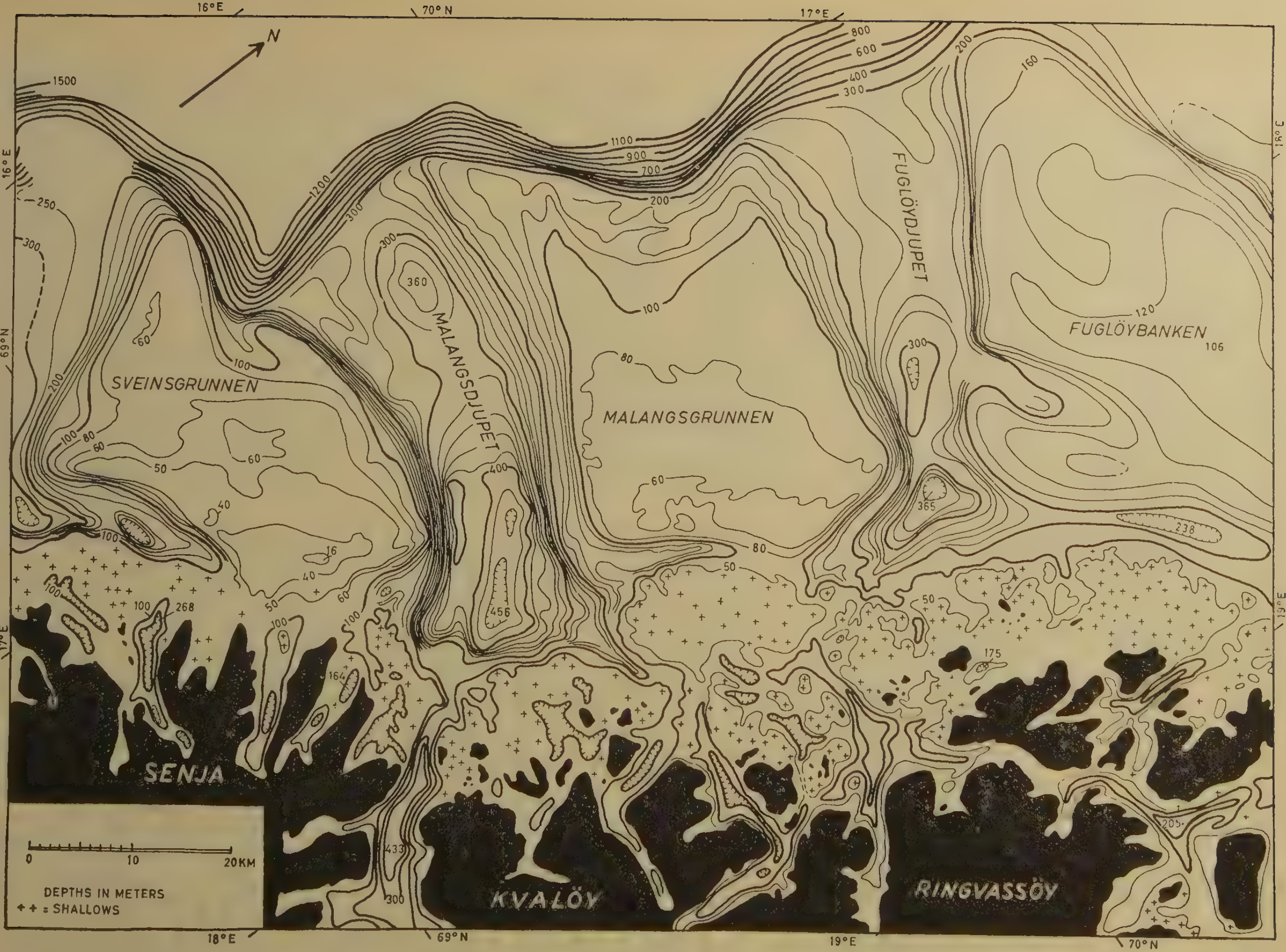
16°E
70° N
17°E
18°E
16°E
69°N
17°E
18°E
69°N
19°E
70°N
19°E
N
FUGLÖYDJUPET
FUGLÖYBANKEN
MALANGSGRUNNEN
MALANGSDJUPET
SVEINSGRUNNEN
SENJA
KVALÖY
RINGVASSÖY
0
10
20KM
DEPTHS IN METERS
+ + = SHALLOWS

FIG. 1.—Shelf area outside Tromsö district, northern Norway. Transverse depressions and longitudinal channels. Drawn from maps II and III, O. Holtedahl (1940).

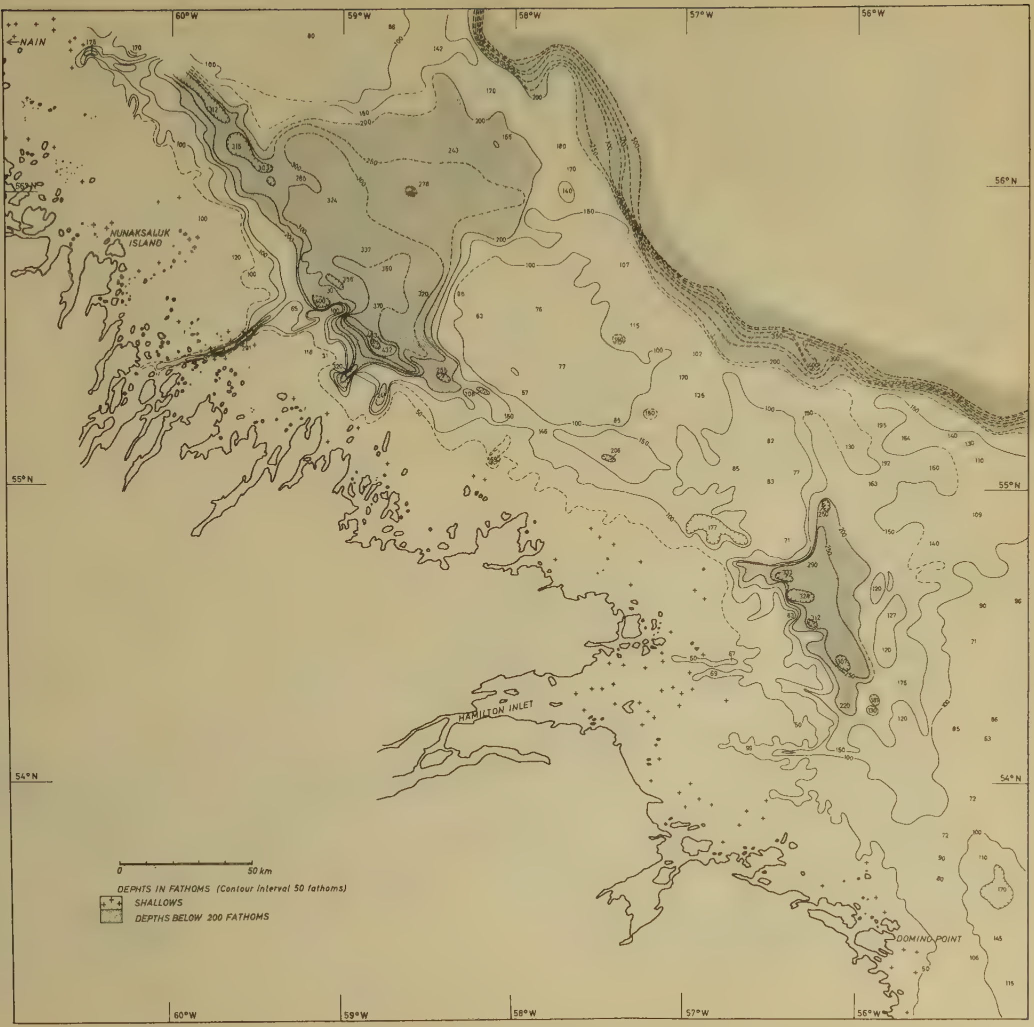
NAIN
NUNAKSALUK ISLAND
HAMILTON INLET
DOMINO POINT
60°W
59°W
58°W
57°W
56°W
56°N
55°N
54°N
0
50 km
DEPTHS IN FATHOMS (Contour Interval 50 fathoms)
SHALLOWS
DEPTHS BELOW 200 FATHOMS

FIG. 2.—Main bathymetric features of continental shelf between Nain and Domino Point, Labrador. Note the deep longitudinal depression separating the outer shelf from the inner. Chart drawn from H. O. Chart 811 (1st ed. 1955; revised 1956).

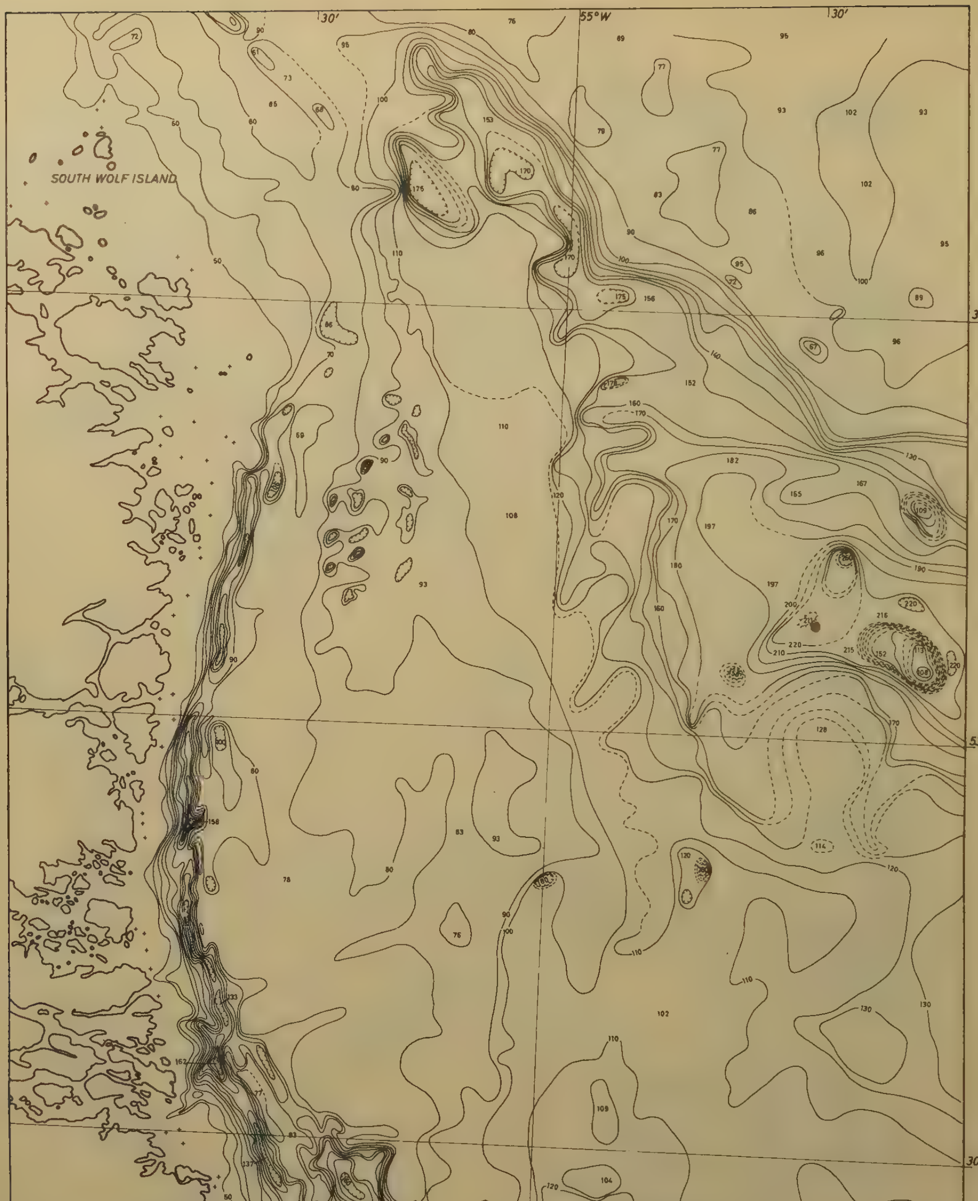
30'
55°W
30'
SOUTH WOLF ISLAND
30'
53° N
30'
52°N
STRAIT OF BELLE ISLE
0
10
20 km
DEPTHS IN FATHOMS
+ + + SHALLOWS

FIG. 3.—Main bathymetric features of the inner part of the continental shelf between South Wolf Island and Belle Isle, Labrador. Note inner arcuate channel and the outer depression which forms a continuation of the longitudinal depression in fig. 2.

ka, where recently published charts show geomorphologic features which closely resemble those off the west coast of Norway.

THE LABRADOR SHELF

Figure 2 shows the main bathymetric features of the continental shelf between Nain and Domino Point. The most striking feature here is a depression or channel running almost parallel to the coast and separating the inner part of the shelf, which is highly irregular and to a great extent corresponds to the Norwegian "skjaergaard" area, from the outer, major part of the shelf. The channel can be traced more or less continuously throughout the area—a distance of more than 400 km.—and has an irregular and undulating bottom relief, with depressions in certain places exceeding 400 fathoms (730 m.) in depth.

The shelf outside consists of bank areas with depths of 50–100 fathoms (90–180 m.) more or less separated by transverse depressions or troughs. The most extensive depression is seen in the northwestern part, where it extends across the shelf and has a width of at least 60 km. It has features in common with similar depressions of the Norwegian shelf in that (1) it terminates abruptly landward with a relatively steep slope situated along the continuation of the inner slope of the longitudinal depression and (2) it shows some shallowing in its outer parts. Another shallower and less significant transverse trough is seen in the central area, and farther south a third depression branches off from the longitudinal channel in a northerly direction.

Figure 3 shows the inner part of the continental shelf off the coast of Labrador farther south, between South Wolf Island and Belle Isle. The longitudinal depression found off the northern coast continues southeastward and then widens into a broad depression which extends northeastward to the edge of the shelf (fig. 5). Another, very marked, longitudinal channel is seen to exist close to the coast and almost parallel to it, extending from east of Domino Point to north of Belle Isle, a distance of about 140 km. The width of this channel is mostly less than 2 km., and its deepest portions lie between 130 and 160 fathoms (240–290 m.). Noticeable is its arcuate form, which also corresponds to the general form of the adjoining coast line.

SHELF BETWEEN CROSS SOUND AND YAKUTAT BAY, SOUTHEAST ALASKA

The bathymetric features of the continental shelf roughly between Cross Sound and Yakutat Bay are shown in figure 4. Northwestward from Cross Sound the continental shelf is fairly broad (between 60 and 100 km.), while to the south of the sound it becomes considerably narrower (about 18 km.). Three very marked submarine channels cross the shelf: one off Cross Sound, another off Dry Bay, and a third (only inadequately sounded) off Yakutat Bay. The depression off Cross Sound has a width of about 22 km. and has, according to the soundings available, a fairly flat bottom with a depth of about 240 fathoms (440 m.). A ridge about 200 fathoms (370 m.) in depth, which protrudes from the northern rim, partly closes the outer entrance to the depression. Both this submarine channel and its surrounding area show a strong morphological similarity to certain areas of the Norwegian shelf (see fig. 1). It terminates landward in a fairly steep slope, and narrow, shallow channels extend from the northeastern and northern corners: one inland as a typical fiord, the other off the coast and roughly parallel to it so that it is more similar to the Norwegian marginal channels. Farther to the northwest, southeast of Lituya Bay, a relatively steep slope leads from the foreland to a depression in the shelf and appears to form a natural continuation of the channel farther south.

The shelf northwest of Lituya Bay is rather different from that off Norway. The submarine transverse channel off Dry Bay has a very smooth relief and lacks the steep, abrupt back wall of the Norwegian transverse channels; nor is there any shallowing

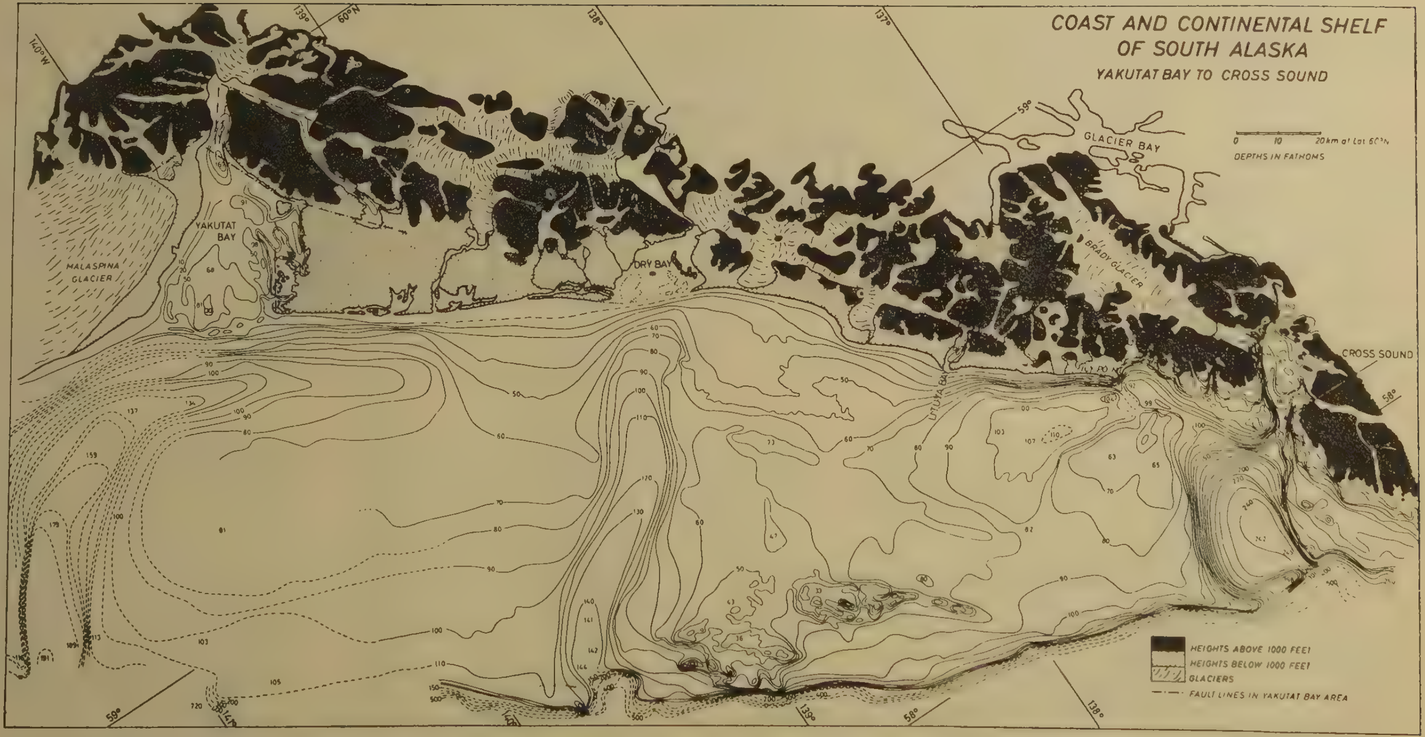
COAST AND CONTINENTAL SHELF
OF SOUTH ALASKA
YAKUTAT BAY TO CROSS SOUND
0 10 20 km at Lat 60°N
DEPTHS IN FATHOMS
GLACIER BAY
BRADY GLACIER
CROSS SOUND
LITUYA BAY
DRY BAY
YAKUTAT BAY
MALASPINA GLACIER
140° W
139°
60° N
138°
137°
59°
58°
HEIGHTS ABOVE 1000 FEET
HEIGHTS BELOW 1000 FEET
GLACIERS
FAULT LINES IN YAKUTAT BAY AREA

FIG. 4.—Shelf and coastal area between Cross Sound and Yakutat Bay, southeast Alaska. Chart drawn mainly from U.S. Coast and Geodetic Survey chart 8402 (1st ed. 1949; revised 1956).

of its outer parts. The sounding data available for the shelf off Yakutat Bay are not sufficient to convey more than a rough indication of the submarine channel which crosses the shelf in that area. It seems, however, to have much the same trend as the channel off Dry Bay and to have a fairly flat bottom.

Of special interest is the continuation of the transverse channel into a longitudinal channel extending southeastward parallel to the shore. This may indicate a pronounced depression of the shelf floor, with, however, the original features covered to a great extent by later sedimentation.

ORIGIN OF SHELF FEATURES

In view of these striking similarities in the submarine relief of the continental shelves off Norway, Labrador, and Alaska, it may be well to give a brief summary of the major geologic events which would seem to be of significance in the morphological development of the corresponding land areas.

Of the greatest importance was, no doubt, the vertical uplift which affected the three areas in relatively recent times. Western Scandinavia and Labrador both show physiographic evidence of an extensive oblique upwarping, with maximum elevation of the coastal areas, during the later parts of Tertiary times. Both areas consist mainly of old, pre-Cambrian or Paleozoic crystalline rocks. In the southeast Alaska region the present mountains show evidence of regional upwarping of more than 1,000 m. on the coast, and this elevation is assumed to have taken place in late Pliocene and Pleistocene times (Peacock, 1935). In the Cross Sound area the high mountains, consisting of metamorphic and igneous rocks of pre-Tertiary age, border the coast; north of the sound, however, through Lituya Bay to Yakutat Bay and beyond, a narrow coastal plain exists outside the mountain range, consisting of strata most probably of Pliocene and Pleistocene age.

The Cenozoic elevation and the successive epoch of extensive glaciation which affected the three areas must be major factors to consider in discussing the geomorphology of the present land areas as well as that of their adjoining continental shelves.

LABRADOR SHELF

It seems very likely that the longitudinal channel, which runs off the northeast coast of Labrador and more or less parallel to it for a distance of more than 400 km., represents a major crustal fracture zone. The same is probably also true with regard to the narrower and shallower channel which runs in a southerly direction from Domino Point. Probably this fracturing of the crust was connected with the Cenozoic upwarping of the land mass.

The supposition of the presence of fracture zones on the continental shelf is supported by the existence of numerous facture zones or fault zones on land, fault zones which can with great certainty be connected with the late Tertiary epeirogenic movements (Cooke, 1929, 1930, 1931). Thus the Melville–Double Mer Basin near the Hamilton inlet appears to be a downfaulted block; other examples from other parts of the Canadian Shield are the basins of Lake St. John and that of Lake Timiskaming. These faults are in all cases marked by high, straight scarps, which, in certain instances at least, are clearly not formed by differential erosion (Cooke, op. cit.). The old, peneplained surface of Labrador has been unequally warped, some parts attaining higher elevations than others. Therefore, it seems reasonable to assume that the continental shelf has developed a fracture pattern with major fault zones intersected by others and that differential movements of blocks have taken place.

Between Newfoundland and the Quebec coast the deep channel of the Straight of Belle Isle is supposed to follow a fault line (Cooke, 1930). On the west coast of Newfoundland a series of fault zones runs more or less parallel to the coast line and is assumed to be of Tertiary age, related to the late Tertiary upwarping and tilting of the island (Twenhofel, 1912; Twenhofel and MacClintock, 1940). If these fault lines continue in the sea area northeastward, then they must intersect the assumed lines which run parallel to the east and northeast coast. Figure 5 shows the major submarine channels and depressions in the shelf area off the Labrador peninsula and Newfoundland, supposed fracture lines on the shelf, and some of the major fault lines on land.

It has been suggested that the longitudinal marginal depressions outside the Norwegian coast, which supposedly represent fracture lines, have been carved out by erosional agencies, mainly during periods when sea levels were lower than at present (O. Holtedahl, 1940). A similar origin may be suggested for the longitudinal marginal depressions off the Labrador coast, with initial preglacial valley erosion, being particularly active along the weak fractures, and subsequent denudation by ice. The transverse depressions across the shelf may also have been initiated as river-cut valleys, thus being part of the same preglacial drainage system and later greatly modified by the influence of the inland ice. Initial valley erosion by running water would, however, presuppose a considerable relative lowering of sea level—a lowering which would exceed the 100–130 meters suggested by Cooke (1929, 1930, 1931).

Denudation by ice has no doubt played a great role in the formation of the present topographical features off Labrador, as also elsewhere on shelves off glaciated coasts. As Shepard has pointed out in a number of papers (Shepard, 1930, 1931, 1948; Shepard *et al.*, 1934), the unusual character of almost all shelves off glaciated areas and the contrast observed in the shelves adjacent to these areas seem to leave little doubt that glaciation has been of great significance in causing these characteristics.

No doubt, ice occupied and also to some extent excavated the longitudinal marginal channels as well as the transverse depressions of the shelf off Labrador. Their great depth and the fact that the direction of the former is almost at right angles to the general direction of ice movement would, however, indicate that valleys of considerable depth existed prior to glaciation. Even with this assumption, however, it seems difficult to explain the great difference in magnitude between the erosional features outside and those inside the major marginal channel. There are depressions in the sea floor of the "skjaergaard" area, but these are usually narrow submarine fiords of quite different dimensions from the features outside. To account for the great depressions, which extend from the inner marginal channel toward and to the shelf edge, as being formed mainly by ice erosion, one would have to assume that this outer part of the shelf consists of rocks very different in lithologic character from those of the inner shelf area—viz., either very soft rocks or rocks with a great concentration of fractures. Even on this assumption the abrupt drop from the level of the inner shelf at a depth of less than 100 fathoms to the inner deep of the transverse depressions at a depth of over 450 fathoms, over a distance of about 5 km., seems to suggest additional factors, other than ice erosion for the formation of this feature.

There would seem to be good grounds for considering the landward slope of the transverse depressions and of the longitudinal channel as primarily a fault scarp, with a downdrop of the outer shelf in relation to the inner shelf. The slightly sloping bottom of the northern depression toward the marginal channel may indicate tilting toward the southwest but may also be explained by glacial action.

A feature which may support the hypothesis of faulting is the difference in depth between the shelf off the northeastern coast of Labrador and Newfoundland and that off the east coast farther southwest (fig. 5). While the shelf area between Cape Cod and Avalon Peninsula is relatively shallow, with extensive bank areas of less than 50 fathoms and with the major part of the shelf less than 100 fathoms in depth, the shelf northwest of the Grand Banks is definitely deeper, with the major part of the shelf deeper than 100 fathoms. The greatest deeps of the shelf between the Grand Banks

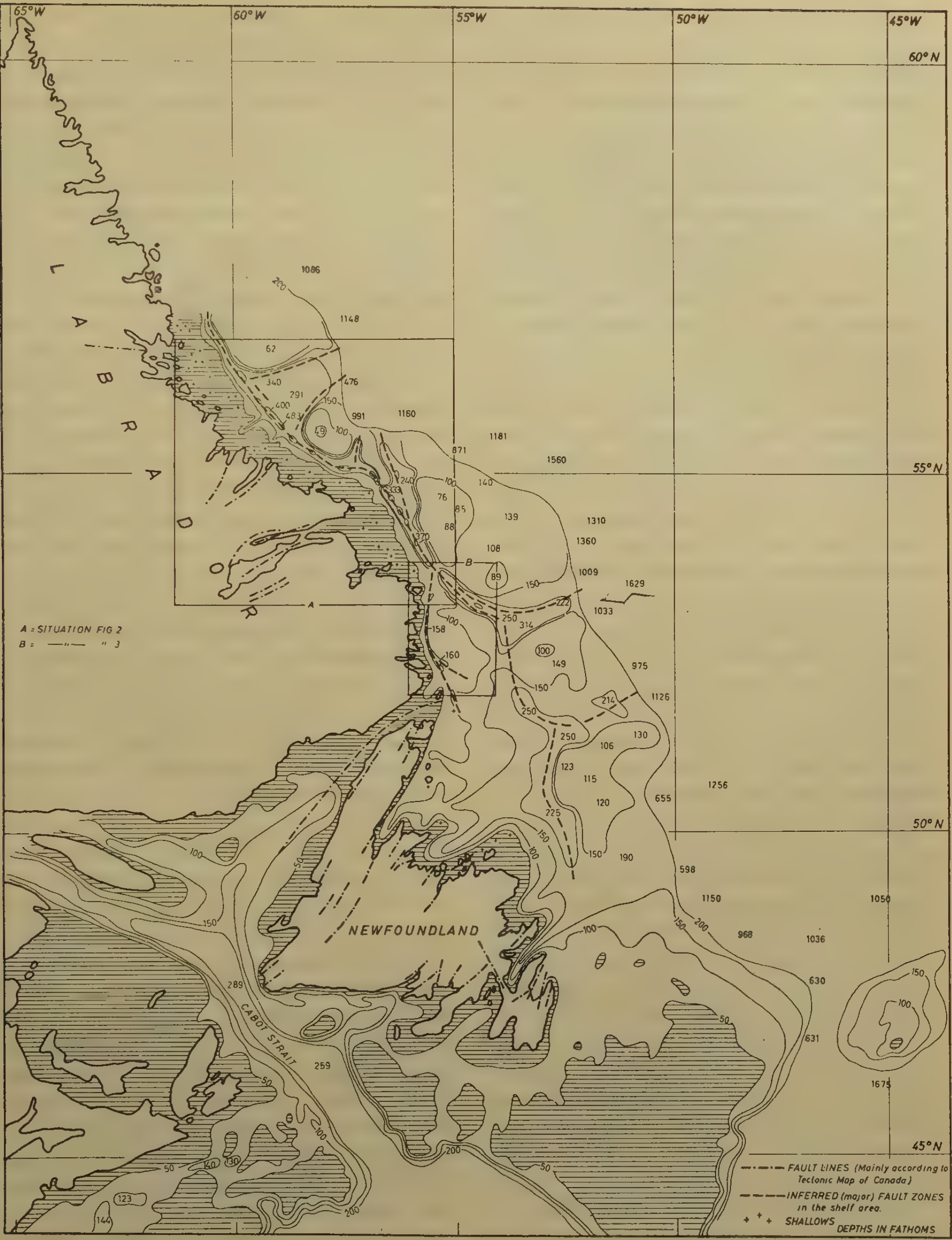
65°W
60°W
55°W
50°W
45°W
60° N
55° N
50° N
45° N
LABRADOR
NEWFOUNDLAND
CABOT STRAIT
A = SITUATION FIG 2
B = —"— " 3
A
B
1086
200
1148
62
340
291
400
483
476
150
991
1160
49
100
1181
871
1560
240
100
140
33
76
85
139
1310
88
370
1360
108
1009
89
150
1629
222
1033
250
314
100
158
160
100
149
975
150
214
1126
250
250
130
106
123
1256
115
120
655
225
150
190
50° N
598
100
150
50
100
150
1150
1050
200
968
1036
100
150
100
289
630
50
631
259
1675
50
100
200
50
40
30
50
123
144
200
FAULT LINES (Mainly according to Tectonic Map of Canada)
INFERRED (major) FAULT ZONES in the shelf area.
SHALLOWS
DEPTHS IN FATHOMS

Fig. 5.—Map showing bathymetric features of the continental shelf off Labrador and Newfoundland, with major submarine channels and depressions, supposed fault lines, and major fault lines on land. Hatched areas have depths less than 50 fathoms.

and Cape Cod are found along the transverse submarine troughs of Cabot Strait, with maximum depths of nearly 300 fathoms, and in the submarine channel which extends to the shelf edge between George's Bank and Brown's Bank, with a maximum depth of less than 200 fathoms. Both these submarine channels, which show definite glacial characters (Shepard, 1931; Shepard *et al.*, 1934), have continuations in inland seas, i.e., the Gulf of St. Lawrence and the Gulf of Maine, respectively. In these areas, therefore, one would expect a concentration of ice flow, which would account for the excavation of submarine channels extending to the shelf edge. Between these major troughs, depressions on the shelf do not exceed 150 fathoms. Along the northeast coast, however, from the Grand Bank and northwestward, the greatest deeps are found along longitudinal channels which run almost parallel to the coast and with depths far exceeding even the greatest depths of the Cabot Strait trough. There are no transverse channels on the outer shelf which have continuations inland, either in inland seas or in fiords, but, as will have been seen, the transverse depressions terminate landward in steep slopes which are in line with the marginal channels.

It is generally stated that continental shelves off glaciated coasts are deeper than shelves off non-glaciated coasts (Shepard, 1931, 1948). If this difference is due mainly to glacial erosion, it means that ice activity has been much more effective in eroding the shelf northwest of the Grand Banks than the shelf farther southwest. As the whole area was presumably covered by the Laurentide ice sheet and since there is reason to believe that ice activity has been less, rather than greater—at least on the outer shelf—off Labrador than farther southwest and as the inner shelf off Labrador does not show any evidence of particularly strong ice erosion, the greater depths of the outer shelf off Labrador and northeast Newfoundland must be considered as being due to either (*a*) a great difference in lithologic character or (*b*) tectonic dislocation. In the opinion of the present author, the last alternative seems to offer the most satisfactory explanation of these features. With regard to the major transverse depressions, these may be related to fault lines crossing the continental shelf, as has been suggested in figure 5. For the northern depression two hypothetical fault lines are drawn along the northwestern and southwestern slopes to suggest that this very wide and deep basin may be primarily tectonic in origin.

The conclusion, then, is, as it was in the case of the Norwegian shelf (H. Holtedahl, 1955) that the east coast of Labrador and probably also northern Newfoundland are bordered by longitudinal fault zones which run off the present coast and more or less parallel it and that the shelf is probably also traversed by transverse fracture lines, or fault lines, which cut across the shelf. In connection with the late Tertiary upwarping of the Labrador and Newfoundland area, major dislocations are assumed to have taken place along the longitudinal fracture zones, probably with lesser dislocations and block faulting of the shelf outside. Subsequently, during the Pleistocene, the shelf was greatly modified primarily by glacial erosion and deposition.

SHELF OFF SOUTHEAST ALASKA

In the shelf region between Cross Sound and Yakutat Bay there are no marginal channels corresponding to those off Labrador. The transverse trough off Cross Sound and the immediate shelf area to the northwest do, however, show features which are very similar to certain features of the Norwegian shelf, which in turn have been related to lines of dislocation. The landward termination of the depression in a wide and fairly steep slope which extends northwestward and forms a distinct boundary between the narrow foreland and the shelf may indicate that this slope marks the position of a marked line of dislocation. The broad trough with its long axis parallel to the shore outside Yakutat Bay may indicate the presence of a similar line in this area.

Ice erosion has no doubt played an important role in the formation of a trough such as that off Cross Sound. The ridge, which partially blocks its entrance, seems to indicate that its basin was occupied by ice. Its great dimensions may, however, be explained on the assumption that the area is traversed by a series of intersecting fracture lines and possibly also by assuming the presence of softer and weaker rocks, which would offer less resistance to ice erosion than would the rock inland. It is interesting to note that the boundary line between the mountainous coastal range, consisting of complexly deformed metamorphosed pre-Tertiary rocks, and the flat foreland, consisting of Quaternary deposits and underlying Pliocene strata (Smith, 1939), continues into the sea near Icy Point and is very much in line with the inner wall of the transverse channel off Cross Sound. This contact takes the form farther northwest of a marked tectonic boundary formed when, in late Tertiary or Pleistocene time, the pre-Tertiary eastern rock complex, including the Chugach and St. Elias Mountains, was thrust upward and southward against the bordering belt of Tertiary rocks along several high-angle faults. Thus in the Yakataga and Katalla districts northwest of Yakutat Bay, the Chugach–St. Elias fault has been traced with reasonable certainty for a distance of 270 km. and may extend farther southeast (Miller, 1951, p. 28).

The nature of the contact of the Tertiary rocks with the older rocks at Lituya Bay has not been determined with certainty, but a high-angle fault within the older rocks probably forms part of the same arcuate fault system (Miller, 1953). The faults of this system are either nearly vertical or dip away from the Gulf of Alaska. In the Yakataga and Katalla area the Tertiary rocks have been displaced along many thrust faults that approximately parallel the Chugach–St. Elias fault.

The Yakutat area is very instructive with regard to crust movements along fault lines (Tarr and Martin, 1912). In connection with the 1899 earthquake there was a renewal of mountain growth, with uplift of that part of the mountain front which borders the Yakutat Bay inlet, by amounts ranging from 7 to 10 feet on the southeast side of the bay and from 40 to 47 feet on the northwest side. This uplift was complicated by movements along secondary fault lines, which produced at least three and perhaps more distinct blocks with roughly parallel sides. In figure 4 the inferred fault lines are shown according to Tarr and Martin. It will be seen that fault lines have directions both parallel to the main coast direction and transverse to it and that the physiography is related to these lines. It therefore seems likely that a similar tectonic pattern has also been of importance in shaping the submarine shelf features, even though the tectonic features have been greatly obscured by subsequent deposition.

DIFFERENT STAGES OF SHELF DEVELOPMENT

The coast and shelf area of Cross Sound–Yakutat Bay is instructive as a stage of shelf development where the mountain-building processes are still active and may help toward comprehension of the development of such shelf areas as those off Labrador and Norway, where epeirogenic forces, except those connected with the disappearance of the ice sheet, are no longer at work. In Figure 6 is shown very schematically a series of profiles across different shelf areas. In the Yakutat Bay region (1*A*), a higher relative sea level, in conjunction with glacial action, would form a submarine platform corresponding to the Norwegian "strandflat"; and the fault separating pre-Tertiary and Tertiary and Pleistocene formations would be marked by a steep slope in the submarine topography (1*B*). Profile 2 is of the shelf south of Cross Sound, where the width is notably less than north of the sound. Farther south, off Moresby Island (3), the continental shelf is almost nonexistent, but a submarine platform with a depth of about 400 fathoms is present, separated from the mainland by a deep trench. A fault line is suggested along this trench. Profiles 4, 5, and 6 across the shelf off Labrador, and, for comparison, two profiles off Norway—one off the west coast in the Möre area and another across the Fuglöy Depression in northern Norway—are shown.

CONCLUSION

Major marginal zones of dislocation parallel to the coast, as well as transverse fracture zones, are assumed to be present on the continental shelves off Norway, Labrador, and southeast Alaska. The fracturing is thought to be related to the late Cenozoic upwarping of the crust, which resulted in the present high elevation of the peripheral parts of the three land areas. The evolution of the present shelf relief was greatly influenced by these lines of dislocation, first by preglacial river erosion and later by the work of glaciers. Certain morphological features of the shelf are thought to be tectonic forms produced mainly by faulting.

The bathymetric data on which the present study of the shelf areas off the coasts of Labrador and southeast Alaska is based

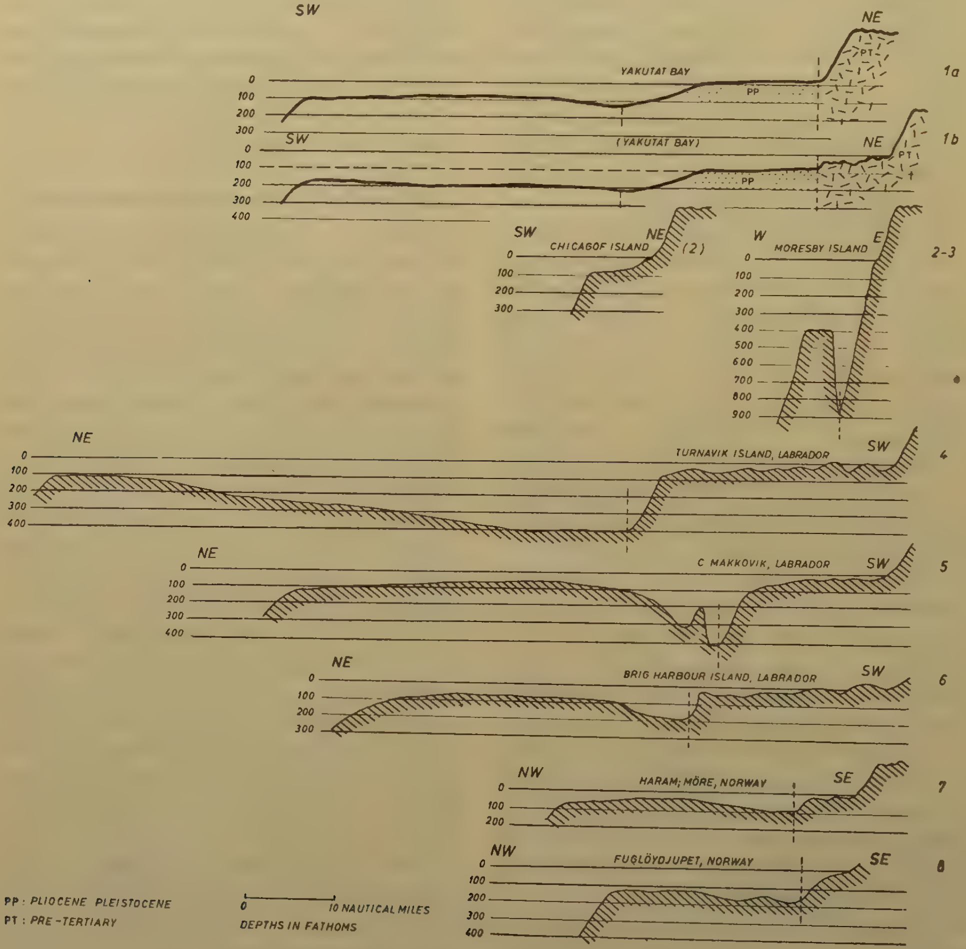
SW
NE
YAKUTAT BAY
PT
PP
1a
0
100
200
300
SW
(YAKUTAT BAY)
NE
PT
PP
1b
0
100
200
300
400
SW
NE
CHICAGOF ISLAND
(2)
0
100
200
300
W
E
MORESBY ISLAND
2-3
0
100
200
300
400
500
600
700
800
900
NE
TURNAVIK ISLAND, LABRADOR
SW
4
0
100
200
300
400
NE
C MAKKOVIK, LABRADOR
SW
5
0
100
200
300
400
NE
BRIG HARBOUR ISLAND, LABRADOR
SW
6
0
100
200
300
NW
HARAM; MÖRE, NORWAY
SE
7
0
100
200
NW
FUGLÖYDJUPET, NORWAY
SE
8
0
100
200
300
400
PP : PLIOCENE PLEISTOCENE
PT : PRE-TERTIARY
0
10 NAUTICAL MILES
DEPTHS IN FATHOMS

FIG. 6.—Profiles across continental shelf areas off southeastern Alaska, British Columbia, Labrador, and Norway. Observed and hypothetical fault lines marked with dotted line.

show only the major features. It is to be hoped that further bathymetric work will be carried out and that sampling of bedrock and seismic refraction studies can be undertaken so that further information can be acquired from this important "fringe zone" of the continents.

ACKNOWLEDGEMENTS.—The writer is happy to acknowledge the help and assistance given him during his stay at Scripps Institution of Oceanography. Special thanks are due to Dr. F. P. Shepard and to Dr. H. W. Menard for helpful discussions with regard to the manuscript, and to Miss E. Irgens, University of Bergen, for preparation of the figures.

REFERENCES CITED

COOKE, H. C., 1929, Studies of the physiography of the Canadian Shield: Trans. Royal Soc. Canada, ser. 3, sec. 4, v. 23, p. 91–120.

——— 1930, Studies of the physiography of the Canadian Shield: *ibid.*, v. 24, p. 51–87.

——— 1931, Studies of the physiography of the Canadian Shield: *ibid.*, v. 25, p. 127–180.

HOLTEDAHL, H., 1955, On the Norwegian continental terrace, primarily outside Möre-Romsdal: its geomorphology and sediments, with contributions on the Quaternary geology of the adjacent land and on the bottom deposits of the Norwegian sea: Univ. Bergen Aarb. naturv. r., v. 14.

HOLTEDAHL, O., 1933, Eine unterseeische Dislokations-Linie ausserhalb der norwegischen Kuste: Zeitschr. ges. Erdk. Berl., p. 198–204.

——— 1935*a*, Den norske landmasses begrensning mot havet (English summary): Norsk. geog. Tidsskr., v. 5, p. 453–466.

——— 1935*b*, A new example of a submarine fault-line along a continental border: K. norsk. vidensk. Selsk. Forh., v. 8, p. 91–93.

——— 1936, On faultlines indicated by the submarine relief in the shelf area west of Spitsbergen: Norsk. geog. Tidsskr., v. 6, p. 214–221.

——— 1940, The submarine relief off the Norwegian coast, with bathymetical map in seven sheets: Norsk. Vidensk. Ak. Oslo, Special paper.

——— 1950, Supposed marginal fault lines in the shelf area off some high northern lands: Bull. Geol. Soc. America, v. 61, p. 493–500.

——— 1951, A comparison of a Scottish and a Norwegian shelf area: Trans. Edinburgh. Geol. Soc., v. 15, p. 214–220.

——— 1953, On the oblique uplift of some northern lands: Norsk. geog. Tidsskr., v. 14, p. 132–139.

MILLER, D. J., 1951, Preliminary report on the geology and oil possibilities of the Yakataga district, Alaska: U.S. Geol. Survey mimeo. rept.

——— 1953, Late Cenozoic marine glacial sediments and marine terraces of Middleton Island, Alaska: Jour. Geology, v. 61, p. 17–40.

PEACOCK, M. S., 1935, Fiord-land of British Columbia: Bull. Geol. Soc. America, v. 46, p. 633–696.

SHEPARD, F. P., 1930, Fundian faults or Fundian glaciers: Bull. Geol. Soc. America, v. 41, p. 659–674.

——— 1931, Glacial troughs of the continental shelves: Jour. Geology, v. 39, p. 345–360.

——— 1948, Submarine geology: New York, Harper & Bros.

——— and EMERY, K. O., 1941, Submarine topography off the California coast: Geol. Soc. America Special Paper 31.

——— TREFETHEN, J. M., and COHEE, G. V., 1934, Origin of Georges Bank: Bull. Geol. Soc. America, v. 45, p. 281–302.

SMITH, P. S., 1939, Areal geology of Alaska: U.S. Geol. Survey Prof. Paper 192.

TARR, R. S., and MARTIN, L., 1912, The earthquakes at Yakutat Bay, Alaska, in September, 1899: U.S. Geol. Survey Prof. Paper 69.

TWENHOFEL, W. H., 1912, Physiography of Newfoundland: Am. Jour. Sci. (4), v. 33, p. 1–24.

———and MCCLINTOCK, P., 1940, Surface of Newfoundland: Bull. Geol. Soc. America, v. 51, p. 1665–1728.

Reprinted from **ANALYTICAL CHEMISTRY**, Vol. 30, Page 1525, September 1958
Copyright 1958 by the American Chemical Society and reprinted by permission of the copyright owner

Salt Effect Correction in Determining Soluble Silica in Sea Water by the Silicomolybdic Acid Method

GEORGE S. BIEN
Scripps Institution of Oceanography, University of California, La Jolla, Calif.

▶ When the silicomolybdic acid method is used for the analysis of a given amount of soluble silica, the presence of salt causes less silicomolybdate color to be developed in sea water than in distilled water solution. This effect varies with the salt concentration and is corrected by plotting the micromolar absorbance coefficient at different chlorosities against chlorosity. From the empirical relations obtained, the micromolar absorbance coefficient of the desired chlorosity is computed. Then the silica content of this solution is calculated directly from the absorbance measured by Beer's law.

During the determination of a given amount of soluble silica by the silicomolybdic acid method (*2*, *3*, *5*), less silicomolybdate color is developed in sea water than in distilled water. This is attributed to the effect of various salts dissolved in the saline water and is called the salt effect. To correct for this effect, some authors have used the salt factor, which is the ratio of the silica content determined gravimetrically to that determined colorimetrically. Because the absorbance as a function of concentration obeys Beer's law within a definite concentration range, the salt factor can also be determined by the ratio of the molar absorbance coefficient of distilled water solution to that of the sea water (*2*, *5*). Values of the salt factor reported in the literature (*1*, *2*, *5*, *6*) vary from 1.16 to 1.66.

For determinations of soluble silica in sea water where the salt concentration has no appreciable change, Robinson and Spoor (*5*) found that the salt factor changed very little and it was sufficient to use only one value for the salinity range they covered. When salt concentration varies from practically zero to that of sea water, as in the study of soluble silica content of river water as it flows into the sea, the problem is not so simple. When chlorosity of the sea water dropped from 20 to 5 grams of Cl⁻ per liter, the salt factor decreased only a little more than 5%. Below 5 grams of Cl⁻ per liter, the salt factor decreases very rapidly.

In determining salt effect corrections over a wide range of salt concentration, solutions of known silica content and chlorosity were made by diluting a standard sodium silicate solution with artificial sea water (*4*) and distilled water. The soluble silica was determined spectrophotometrically with a Beckman Model DU spectrophotometer. The procedure is essentially that of Chow and Robinson (*2*), ex

Table I. Absorbance at Different Silica Concentrations in Solutions of Different Chlorosities

Soluble SiO_2, µmole/Liter	Chlorosity, Grams Cl^- per Liter						
	0	2.06	4.12	8.24	12.36	16.49	20.20
0	0	0	0	0	0	0	0
20	0.125	0.115	0.116	0.109	0:107	0.099	0.097
40	0.246	0.243	0.230	0.220	0.213	0.211	0.205
60	0.363	0.356	0.336	0.326	0.315	0.307	0.306
80	0.477	0.467	0.444	0.428	0.413	0.395	0.418
100	0.606	0.585	0.564	0.557	0.542	0.529	0.528
120	0.740	0.698	0.680	0.667	0.655	0.644	0.636
140	0.840	0.808	0.785	0.779	0.764	0.747	0.741
150	0.902	0.868	0.842	0.826	0.801	0.791	0.789

Table II. Average Values of Micromolar Absorbance Coefficients, *a*, and Salt Factors

	Chlorosity, Grams Cl^- per Liter						
	0	2.06	4.12	8.24	12.36	16.49	20.20
$a \times 10^3$	6.07	5.67	5.55	5.45	5.36	5.23	5.23
Salt factor	1.00	1.07	1.09	1.11	1.13	1.16	1.16

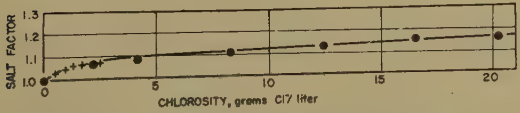

Figure 1. Salt factor as a function of chlorosity

X Points from other sets of determinations

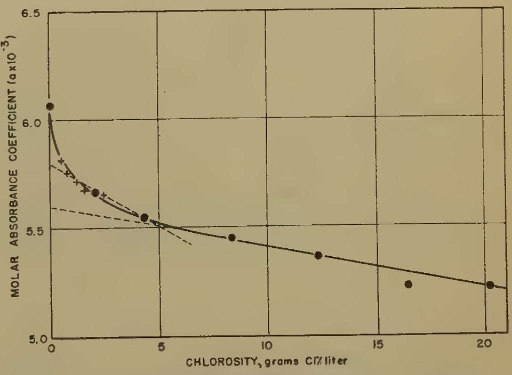

Figure 2. Molar absorbance coefficient as a function of chlorosity

Effective slopes for determining absorbance coefficients at different chlorosities X Points from other sets of determinations

Reproduced by Permission

cept that a 1-cm. cell and a wave length of 360 mμ were used. In Table I are given the data for one set of determinations. Absorbance values were corrected for the reagent blanks at the chlorosities in question. Reagent blanks vary very little and have no relation to chlorosity. The average values of the micromolar absorbance coefficients at different chlorosities and the salt factors obtained are given in Table II. Salt factor as a function of chlorosity is shown in Figure 1.

It is simpler to utilize the functional relation between micromolar absorbance coefficient and chlorosity to correct for the salt effect. In Figure 2, the micromolar absorbance coefficient is plotted as a function of chlorosity. Above a chlorosity of 5 grams of Cl^- per liter, a linear relationship is obtained. Between chlorosities of 0.5 to 5 grams of Cl^- per liter, another straight line may be approximated without seriously sacrificing accuracy. When the concentration of silica is in micromoles per liter, two empirical linear relationships are obtained:

$k_{Cl} = 0.0058 - 0.00006\ Cl$; for Cl from 0.5 to 5 grams of Cl^- per liter

$k_{Cl} = 0.0056 - 0.0000185\ Cl$; for Cl greater than 5 grams of Cl^- per liter

where k_{Cl} stands for the micromolar absorbance coefficient at chlorosity Cl. The silica content of the solution at this chlorosity may be calculated directly from the absorbance at 360 mμ by

$$SiO_2\ (\mu\text{mole/liter}) = A_{360}/k_{Cl} \times l$$

where l = 1 cm.

Printed in U. S. A.

LITERATURE CITED

(1) Brujewicz, S. V., Blinov, L. K., *State Oceanog. Inst., Moscow, U.S.S.R.*, Bull. 14 (1933).
(2) Chow, D. T. W., Robinson, R. J., Anal. Chem. 25, 646 (1953).
(3) Dienert, F., Wandenbulke, F., *Compt. rend.* 176, 1478 (1923).
(4) Lyman, J., Fleming, R. H., *J. Marine Research* (*Sears Foundation*) 3, 134 (1940).
(5) Robinson, R. J., Spoor, H. J., Ind. Eng. Chem., Anal. Ed. 8, 455 (1936).
(6) Saeki, A., *J. Oceanog. Soc. Japan* 6, 39 (1950).

Received for review November 18, 1957. Accepted May 5, 1958. Work supported by a grant from the American Petroleum Institute, Project 51. Contributions from the Scripps Institution of Oceanography, New Series. 1018

Second United Nations
International Conference
on the Peaceful Uses of
Atomic Energy

A/CONF.15/P/1979
U.S.A.
June 1958

ORIGINAL: ENGLISH

A CRITICAL EVALUATION OF RADIOCARBON TECHNIQUES FOR DETERMINING MIXING RATES IN THE OCEANS AND THE ATMOSPHERE

H. Craig*

In this communication an attempt will be made to summarize the present status of our knowledge of the distribution of carbon 14 in the atmosphere and the sea, and the exchange rates which are implied by this distribution.

The natural fractionation of the stable isotopes C^{12} and C^{13} produces a C^{13}/C^{12} ratio in surface ocean water bicarbonate and shell carbonate which is about $2.5^{\circ}/_{\circ}$ higher than the C^{13}/C^{12} ratio in terrestrial plants, and thus the C^{14} concentration in the oceanic material should be about $5^{\circ}/_{\circ}$ higher than in the terrestrial plants. However it is well established that wood and shell actually have about the same C^{14} concentration (Suess, 1954, 1955; Rafter, 1955). Some years ago it was pointed out that this effect can only be explained by an exchange rate of CO_2 between atmosphere and sea which is slow enough to produce an apparent radiocarbon age of 400 years for surface ocean bicarbonate, corresponding to $5^{\circ}/_{\circ}$ of the radiocarbon mean life of 8,033 years (Craig, 1954). Detailed calculations based on various models have been made by Arnold and Anderson (1957), Craig (1957 and in press), and Revelle and Suess (1957).

The total amount of carbon in the active reservoirs of the atmosphere, biosphere, and sea, called the exchangeable system, is about 7.9 grams of carbon per square centimeter of earth surface (cm^2). Table I shows the amounts of carbon assumed for the various components of the exchangeable system, the characteristic carbon 13 concentration in each of the components, and the carbon 14 fractionation factor relative to modern wood, computed as the square of the equivalent factor for carbon 13. The values of α are the C^{14} concentration factors relative to modern wood which would be observed if carbon 14 were stable, i.e. if the relative concentrations were unaffected by radioactive decay.

---

* University of California, Scripps Institution of Oceanography, La Jolla, California. Contribution from the Scripps Institution of Oceanography, New Series. No. 1019

Reproduced by Permission

TABLE I

Amounts of carbon, characteristic C^{13} concentration, and C^{14} fractionation factor relative to terrestrial wood, of the various components of the exchangeable system of natural carbon

	δ C^{13}(‰) (1)	α 14 (2)	Carbon content grams/cm^2 (3)
Atmospheric CO_2	- 7	1.037	0.126
Terrestrial biosphere (living)	-25	1	0.06
Terrestrial humus	-25	1	0.215
Marine biosphere	-13.5	1.024	0.002
Dissolved organic carbon in sea	-13.5	1.024	0.533
Total inorganic carbon in sea	- 1.5	1.049	6.94
Total exchangeable system			7.88

(1) Data from H. Craig (1953, 1954). $\delta = \left[(R\ \text{sample}/\ R\ \text{standard}) - 1\right] \times 1000$, where $R = C^{13}/C^{12}$ and the standard is the Chicago isotopic standard.

(2) Fractionation factor for C^{14} relative to terrestrial wood; i.e. the expected C^{14}/C^{12} ratio in the component material, divided by the C^{14}/C^{12} ratio of modern wood. From column 1, the C^{13} fractionation factors relative to modern wood (-25‰) were computed for each component; these values squared give the values in column 2, α is the factor which would give the C^{14} concentration relative to wood if the mixing between components were infinitely fast.

(3) Sources of data given by Craig (1957).

Figure 1 shows the simplest model used for calculation; the exchangeable system is divided into five reservoirs containing amounts of carbon relative to N_a, the amount in the atmosphere, as shown in the various boxes. For convenience the term biosphere is restricted to denote the living terrestrial plants. The transfer between units is assumed to be determined by first order rate constants except in the case of biosphere assimilation. The amounts of carbon in the atmosphere, biosphere, humus, and in the entire ocean, are taken directly from Table I. However, the ocean has been taken as consisting of two reservoirs, a mixed layer and the deep sea, separated by the thermocline. The average depth of the thermocline is taken as 75 meters, on the basis of a study by W. Wooster, and the average depth of the ocean is taken as 3800 meters from Kossinna's data. Thus the mixed layer and the deep sea reservoirs are assumed to contain respectively 2°/₀ and 98°/₀ of the total carbon in the sea (including the marine biosphere entirely in the mixed layer).

Figure 1 also shows the values of the assumed present-day radiocarbon concentrations in the various reservoirs, relative to R_w, the C^{14}/C^{12} ratio in terrestrial wood undiluted by industrially produced CO_2 which contains no C^{14}. The absolute value of R_w is taken as 1.24×10^{-12} from the measurements of Suess (1955) on 19th century wood normalized for age and isotopic fractionation. Rafter (1955) has shown that atmospheric CO_2 differs in C^{14} content from wood by the expected factor of 1.037; thus for steady-state calculations we take the atmospheric C^{14}/C^{12} ratio as 1.037 R_w, and assume R_w equal to R_b, the ratio in the biosphere. However, the value of R_m, the ratio in the mixed layer, which is now about the same as R_w is probably somewhat lower than its normal value due to dilution with industrial CO_2 (the Suess effect). The measurements of Suess on 19th century and modern tree rings, indicate that, neglecting trees which grew in areas of heavy industrial contamination, a weighted average value for the world-wide atmospheric radiocarbon dilution in 1947 (year of Suess' average tree ring) is 1.25°/₀. Since we shall show that the atmospheric residence time of CO_2 is quite short and that there is a significant holdup at the thermocline, it appears reasonable to assume a comparable dilution in the mixed layer and to take the pre-dilution value of R_m to be 1.0125 R_w and use this value in calculations. The average radiocarbon activity in humus is not known, but must lie within limits of 0-1 R_w; the effect of this uncertainty on the calculations is negligible.

The notation used is as follows:

N_i = amount of $(C^{12} + C^{13})$ in reservoir i.

k_{i-j} = rate constant for transfer of carbon from reservoir i to reservoir j, (first order process assumed) years^{-1}.

$\tau_{i-j} = 1/k_{i-j}$ = residence time (years) of a stable carbon atom in reservoir i before transfer to reservoir j.

$R_i = C^{14}/C^{12}$ ratio in carbon in reservoir i.

The model shown in Figure 1, in which the surface mixed layer of the sea covers the entire ocean, is termed the "chain model" since the reservoirs are connected as links on a chain. We can calculate the exchange rate of CO_2 between the atmosphere and the sea in two quasi-independent ways. The first method is based on the steady-state material balance of C^{14} in the atmosphere as a function of the production rate of radiocarbon and the rate at which carbon enters the sea. The measured radiocarbon production rate is taken as $Q = (2 \pm 0.5) C^{14}$ atoms/cm^{2}sec, and with the values of N and R given above we obtain an atmospheric residence time of about 5 years, with an estimated uncertainty of about 3 years (Craig, 1957 and *in press*).

A more general calculation of the atmospheric residence time can be made by eliminating the production rate of C^{14} and writing out the general rate equations for the steady-state distribution of radiocarbon and stable carbon between the various reservoirs. In this case we can show the explicit dependence of the C^{14} concentration in each reservoir on the various exchange rates involved, and this can be seen most easily by comparing the concentrations with those which would be observed if the exchange rates were infinitely fast relative to the decay rate of radiocarbon. If the atmosphere and sea were uniformly and rapidly mixed in a time short compared to the C^{14} half life, the C^{14}/C^{12} ratio, normalized for isotopic fractionation, would be everywhere the same, just as if C^{14} were a stable isotope of carbon. If we now interpose a mixing barrier at the sea surface, the radiocarbon will pile up in the atmosphere where it is produced, until the concentration increases enough so that the increased radioactive decay rate brings the system back to steady state. Similarly, if we then add a mixing barrier within the sea, the concentrations in both the atmosphere and the portion of the sea above the new barrier will increase until the steady state is reached. Thus the concentrations of C^{14} within each reservoir are a function of the exchange rates and the amounts of carbon in each reservoir.

We define δ_i as the percentage increase in radiocarbon activity (C^{14}/C^{12} ratio) in a reservoir i due to slow mixing, relative to the hypothetical state in which mixing is infinitely faster than the rate of radioactive decay. In Table II we tabulate the calculated δ_i values for atmospheric residence times, relative to the mixed layer, of 5, 10, and 20 years, and deep sea residence times, relative to the mixed layer, of 0 (rapidly mixed sea), 500, and 1000 years. For the case of rapid mixing of the sea, the C^{14} activity in the atmosphere is increased by about 0.74°/o for each year of atmospheric residence time, relative to the condition of rapid atmospheric exchange with the sea, while the activity in the sea is reduced by 1/60 of the atmospheric increase. If the internal mixing within the sea is slow, corresponding to a deep-sea residence time of 500 years relative to the mixed layer, the effect is to increase the activity in both the atmosphere and the mixed layer by 6°/o, while reducing the deep-sea activity by 0.28°/o; thus the difference in the observed activities in the atmosphere and mixed layer remains about the same. As the table shows, the atmospheric and mixed-layer activities are each increased by about 1.2°/o, relative to the condition of a rapidly mixed sea, for each 100 years of residence time in the deep sea, or "age" of the deep sea water relative to the mixed layer. The residence times shown are for C^{14} but these differ by only a few percent from those for C^{12}.

As discussed below, radiocarbon measurements and heat flux considerations indicate that the deep sea residence time is of the order of a thousand years and so does not strongly affect the percentage difference in C^{14}/C^{12} ratio between the atmosphere and sea for a given exchange rate with the atmosphere. From Table I we see that the bicarbonate in the sea should be about 4.9°/o higher in C^{14} concentration than the ratio in wood as a result of isotopic fractionation. Since the C^{14}/C^{12} ratio in the mixed layer of the sea is approximately the same as R_w, the 19th century wood standard

TABLE II

Effect of the residence times of CO_2 in the atmosphere and deep sea, both relative to exchange into the mixed layer, on the specific activity of radiocarbon in the atmosphere, mixed layer, and deep sea. δ = percent difference in activity (C^{14}/C^{12} ratio) from the condition of infinitely fast mixing relative to the radioactive decay rate.

		$\tau_{a-m} = 5$ y.	$\tau_{a-m} = 10$ y.	$\tau_{a-m} = 20$ y.
$\tau_{d-m} = 0$	δ_a	+ 3.7	+ 7.4	+ 14.7
	δ_m, δ_d	- 0.06	- 0.12	- 0.24
$\tau_{d-m} =$ 500 y.	δ_a	+ 9.7	+ 13.4	+ 20.7
	δ_m	+ 5.93	+ 5.86	+ 5.73
	δ_d	- 0.28	- 0.34	- 0.46
$\tau_{d-m} =$ 1000 y.	δ_a	+ 15.6	+ 19.3	+ 26.6
	δ_m	+ 11.88	+ 11.81	+ 11.67
	δ_d	- 0.51	- 0.57	- 0.69

mentioned above, the difference between the predicted and observed concentration gives the percentage increase in atmospheric C^{14} content, relative to the mixed layer, due to slow exchange of carbon between atmosphere and sea. As shown in Table II, an increase of 4.9°/o in atmospheric activity, relative to the mixed layer, corresponds to an atmospheric residence time τ_{a-m} of about 6.5 years. However, we noted above that about 1.2°/o of this effect is probably due to dilution of mixed layer carbon with dead CO_2 from industrial combustion. Thus we have a net difference, $\delta_a - \delta_m$, of about 3.7°/o, which, from Table II, reflects an atmospheric residence time of about 5 years, regardless of the deep sea residence time which increases the atmosphere and mixed layer activities by about the same factor.

We conclude therefore, that for the chain model shown in Figure 1, the 4.9°/o difference between the expected and observed radiocarbon activity in the mixed layer of the sea reflects about 1.2°/o of dilution of mixed layer carbon with industrial CO_2, and a 3.7°/o increase in activity of atmospheric CO_2 due to an atmospheric residence time of about 5 years, which agrees with the figure calculated above from the estimated production rate of radiocarbon. The 25°/₀ uncertainty in Q, the radiocarbon production rate, from the limits cited above, means that the estimated production rate is consistent with any deep sea residence time up to about 2500 years. Thus the uncertainty is such that no significant information on the mixing rate in the sea can be obtained from the figure for the production rate.

Figure 2 shows a more detailed model of the atmosphere and sea, in which the mixed layer is assumed from oceanographic data to cover the oceans in a belt between latitudes 45° north and south. This amounts to 75°/₀ of the area of the sea being covered by the mixed layer, which floats on the deep sea reservoir and is separated from it by the thermocline, which because of its great stability, represents the major barrier to mixing between the two reservoirs. The deep sea reservoir "outcrops" and is exposed directly to the atmosphere over about 25°/₀ of the sea surface. This model will be called the "cyclic" model, and we shall discuss the equilibrium case in which there is no net flux of carbon across any boundary between reservoirs.

In the chain model, all of the carbon entering the deep sea does so by exchange with the mixed layer. However, in the cyclic model, carbon also enters directly from the atmosphere, and we may ask what the proportions of carbon entering from the mixed layer and from the atmosphere must be, assuming for this model that the exposed areal ratio of the mixed layer to deep sea is 3.

Assume for the moment that there is no exchange at all between the mixed layer and the deep sea, so that all the carbon entering the deep sea must do so by direct exchange with the atmosphere. In the first place, the ratio k_{2-m}/k_{a-d} must be about 3, i.e. the flux of CO_2 into the sea per cm^2 must be about the same over the surface of the sea. This is so because the flux of carbon dioxide into the sea is simply proportional to the number of molecules striking the sea surface, and thus depends only on partial pressure and temperature. Slight deviations should occur because of seasonal partial pressure differences over the sea surface, effects of roughness of the sea on surface area and the reflection coefficient, differences in surface films over the two areas, and temperature differences, but these effects must be small and they probably do not change the ratio by even as much as a factor of two. Using this ratio of the atmospheric exchange constants, and the values of R_m/R_a given above, we can calculate the ratio R_d/R_m, the activity ratio in the two uncoupled oceanic reservoirs, from the ratio of stable carbon in these reservoirs; this gives $R_d/R_m = 0.17$, which corresponds to a radiocarbon "age" of deep sea carbon, relative to the mixed layer, of 14,000 years.

A lower limit for R_d/R_m can be obtained from the measured production rate of radiocarbon. The lowest figure is that of Soberman, which corrected for resonance capture of neutrons by nitrogen gives a production rate Q of about 1.3 radiocarbon atoms/cm^2sec; this is almost certainly a minimum figure, since all other estimates give a figure of about 2. Using the value of R_m given above, and taking the amounts of carbon in the terrestrial biosphere and humus as given in Table I, the minimum value of R_d/R_m consistent with $Q = 1.3$ is obtained by assuming all the humus to have the activity of modern wood; this value is 0.64, corresponding to a maximum deep sea carbon "age" of only 3600 years. In fact the radiocarbon measurements so far available, made by Rubin, and by Broeker and coworkers, indicate that the radiocarbon "age" of deep Atlantic water is not more than 500-1000 years relative to surface waters. Heat flux considerations by Revelle and Maxwell imply that deep Pacific water cannot be a great deal older and thus the average figure for the oceans as a whole is of the order of about 1000 years.

The figure of 14,000 years for the necessary age of deep sea carbon, relative to the mixed layer, for a system in which there is no exchange between the mixed layer and deep sea, is a minimum value which would be observed if internal mixing in the deep sea were rapid on the radiocarbon time scale. For slow mixing between the surface and depths of the deep sea reservoir, the situation would be exactly analagous to development of a second "mixed layer" interposed between the deep sea and the atmosphere and exchanging with the deep sea. Thus it is clear that a large fraction of the carbon dioxide flux into the deep sea must come from the mixed layer, even if the system resembles the cyclic model shown in Figure 2.

We may now calculate the residence times for the cyclic equilibrium model, using the values given for the chain model and assuming that the reservoirs exchange as shown in Figure 2. In these calculations the radiocarbon flux from the deep sea to the atmosphere has been multiplied by a factor β, defined as the C^{14}/C^{12} ratio in the surface layer of the exposed deep sea reservoir divided by R_d, the average ratio in the deep sea reservoir, in order to allow for a radiocarbon concentration gradient, with depth, in the deep sea, which would produce a back flux of C^{14} into the atmosphere greater than that calculated without the use of β. (β is not applied to the flux from the deep sea into the mixed layer, as it is not certainly known that this exchange takes place only at the surface, and in any case the effect is small).

Table III gives the values of τ_{a-m} computed for two assumed values of R_d/R_m, with values of $\tau = 1$ (no gradient) and 1.04 (carbon in surface layer of deep sea 320 years younger than average deep sea carbon). With $R_d = R_m$, and $\beta = 1$, τ_{a-m} would be calculated as 6.2 years. The dependence of τ_{a-m} on the age of carbon assumed for the deep sea is greater than in the case of the chain model, but it appears reasonable to choose a value from the table of about 10 years.

TABLE III

Values of τ_{a-m} (in years), the residence time of CO_2 in the atmosphere relative to the mixed layer, in the cyclic model.

	R_d/R_m and "age" of deep sea carbon	
	(640 y) 0.920	(960 y) 0.880
$\beta = 1$	10.5	12.9
$\beta = 1.04$	8.7	11.2

The values derived from steady-state considerations of the cyclic equilibrium model are then:

$\tau_{a-m} =$ 10 years $k_{a-m} = 0.100$

$\tau_{a-d} =$ 30 years $k_{a-d} = 0.033$

$\tau_{a-s} =$ 7.5 years $k_{a-s} = 0.133$

where the subscript a-s indicates the total atmospheric residence time relative to transfer into the sea. The value of τ_{a-s} obtained is about the same as the value of τ_{a-m} calculated from the chain model, and this agreement emphasizes the fact that the calculation of the exchange time of carbon dioxide between atmosphere and sea is simply not very sensitive to assumptions about the structure of the sea.

The values of τ_{m-d} calculated as a function of R_d/R_m for the same two values of β are shown in Table IV, together with values calculated from the chain model for comparison. The cyclic model calculation roughly doubles the value of τ_{m-d} calculated from the chain model. The total flux of carbon into the deep sea is the same, but because some of the carbon comes in directly from the atmosphere, the residence time in the mixed layer, relative to the deep sea is increased. We conclude that for the cyclic equilibrium model ${}_{m-d}$ is of the order of 40 years, and τ_{d-m}, the residence time in the deep sea relative to the mixed layer, is of the order of 2000 years (i.e. 50 times τ_{m-d}, because $N_d/N_m = 50$). From the values for τ_{a-d} and τ_{m-d} derived from Tables III and IV, we see that for these values of R_d/R_m, about half of the carbon entering the deep sea comes directly from the mixed layer with the other half entering directly from the atmosphere.

TABLE IV

Values of τ_{m-d} (in years), the residence time of carbon in the mixed layer relative to the deep sea, in the cyclic equilibrium model, and in the chain model.

	R_d/R_m and "age" of deep sea carbon	
	(640 y) 0.920	(960 y) 0.880
Cyclic Model $\beta = 1$	30.6	57.1
Cyclic Model $\beta = 1.04$	25.3	49.2
Chain Model	14.4	22.6

For a measured value of R_d/R_m, the radiocarbon activity in the deep sea relative to the activity in the mixed layer, the computed radiocarbon "age" relative to mixed layer carbon t_d, is defined by the relationship: $R_d/R_m = \exp[- t_d]$. As in the case of the chain model t_d is essentially equal to the residence time of carbon in the deep sea relative to all routes of removal. In the case of the cyclic equilibrium model, this total residence time, τ_{d-T}, is defined by the relationship $\tau_{d-T} = 1/k_{d-T}$, where $k_{d-T} = k_{d-m} + k_{d-a}$, and for $t_d =$ 1027 years, $\tau_{d-T} = 1076$ years. We shall neglect such differences and assume them to be equivalent.

However, since τ_{d-T} is the residence time relative to both routes of removal of carbon from the deep sea, τ_{d-m}, the residence time relative to removal only into the mixed layer, is necessarily greater than τ_{d-T}. Now since τ_{d-m} refers to physical mixing in the sea, it is apparent that τ_{d-m} is also the oceanographic flushing time of water in the deep sea, or, more precisely, the residence time of water in the deep sea relative to transfer into the mixed layer. Thus the residence time for water in the deep sea relative to transfer into the mixed layer is considerably greater than the "age" of deep sea water computed from a radiocarbon measurement. Another way to state this is that since carbon is replenished from both the atmosphere and mixed layer, the average age of a carbon atom in the deep sea is much less than the age of a water molecule calculated with respect to renewal from the mixed layer of the sea. In Table V we show the various residence times for carbon in the different reservoirs, computed from the cyclic equilibrium model with $\beta = 1.04$, for two values of R_d/R_m, together with the computed radiocarbon "age" of the deep sea carbon. Comparison of t_d with τ_{d-m} shows the relationship of the radiocarbon "age" of the water with the actual oceanographic flushing time relative to renewal from the mixed layer. The values in Table V show that over the range of radiocarbon activity most likely to be encountered in the deep sea, the radiocarbon "age" of deep sea water is about half the average time required for physical exchange between the deep sea and the mixed layer.

TABLE V

Residence times (in years), and computed radiocarbon age of deep sea carbon relative to mixed layer carbon, calculated for the cyclic equilibrium model with $\beta = 1.04$.

Residence time	R_d/R_m ($\beta = 1.04$)	
	0.920	0.880
τ_{a-m}	8.7	11.2
τ_{a-d}	26.1	33.6
τ_{a-s}	6.5	8.4
τ_{m-a}	10.4	13.4
τ_{m-d}	25.3	49.2
τ_{m-T}	7.4	10.5
τ_{d-a}	1520	1960
τ_{d-m}	1230	2390
t_d	670	1030

It now becomes clear that the interpretation of the radiocarbon age of a given mass of seawater is strongly dependent on the model of the ocean assumed. In the zero order model of a completely uniform ocean, the radiocarbon concentration is assumed to be constant throughout the sea, and the residence time of carbon in the sea refers only to exchange with the atmosphere. In the "chain" model we took the extreme case of a mixed surface layer entirely covering a homogeneous "deep sea" reservoir. In this case carbon enters the deep sea only by physical exchange with the surface mixed layer, and the deep-sea residence times of carbon and water are necessarily the same because of the nature of the model.

The cyclic model is a second order approximation, intermediate in character between the uniform-sea model and the chain model.

If one takes the uniform sea model and adds a small surface mixed layer covering only a small area, the residence time of carbon in this mixed layer, relative to transfer into the rest of the sea, is very much larger than in the mixed layer of the chain model, because the estimated radiocarbon content of the deep sea and the calculated atmospheric exchange rate require a large hold-up in the carbon exchange with the mixed layer. As the area covered by the mixed layer is increased, the direct atmospheric flux into the deep sea decreases, and thus τ_{m-d} decreases and approaches the value calculated for the chain model.

The residence time τ is difficult to define precisely except in the statistical sense of the average lifetime of a particle in a well-defined reservoir, relative to removal into one or more other well-defined reservoirs. The residence time calculated for a non-conservative element which is being consumed at a significant and known rate in an area will not be the same as the "mean displacement time" calculated from the flux of water by currents, because of renewal of the non-conservative element by turbulent exchange and convective mixing at the boundaries. Of course in this case the residence time of the element in question, relative to the rest of the ocean, is actually the same as the true "residence time" of the water, but this will not be the time calculated from the mass transport by currents. If a difference in radiocarbon content exists between two bodies of water, the net flux of radiocarbon from one to the other is generally not even approximately given by the product of the concentration in the upstream water mass and the mass of water transported per unit time by the current, although similar assumptions are often made in oceanographic calculations on the balance of non-conservative elements.

In the case of the cyclic model, the concentration of radiocarbon in the deep sea is no longer directly related to physical mixing within the sea, because the model assumes direct exchange of carbon between the atmosphere and a homogeneous deep sea in high latitudes. In this model the two defined reservoirs in the sea are the mixed layer and the deep sea, and if such a model were an actual representation of the sea, the only "mixing rate" or "exchange time" which could be obtained from radiocarbon data would be the exchange rate of water between the defined mixed layer and the rest of the sea, which is not given directly by the relative concentrations of radiocarbon.

The closest approximation to a generalized structure of the oceans as a whole is probably intermediate between the chain and cyclic models, due to slow mixing in the reservoir designated as the "deep sea". As noted in an earlier section, the principal result of slow vertical mixing in the sea would be to extend the effective mixed layer over a larger portion of the sea surface. Thus, depending on the rates of vertical mixing in high latitudes, the percentage difference in C^{14}/C^{12} ratio between deep waters and the mixed layer, multiplied by the radioactive mean life of radiocarbon, is a rough measure of the residence time of water in the deep sea relative to exchange with the total surface waters over the total sea surface, or it is roughly the residence time of carbon in the deep sea relative to exchange with both the mixed layer, as defined by the extent of the thermocline, and with the atmosphere in high latitudes, this figure differing by the order of a factor of two from the exchange time of water between deep sea and the mixed layer bounded by the thermocline. The distinction between these two approximations will be made by detailed measurements of radiocarbon concentration over the surface of the sea, by comparison of data from high and mid-latitudes.

In summary, then, the atmospheric residence time of CO_2, relative to exchange into the sea, appears to be about 7 years, and this result is relatively independent of assumptions about the sea structure. It is probably correct to better than ± 5 years. Suess has previously calculated the atmospheric residence time in a different way, using his data on the dilution of the activity of wood by industrial CO_2, and Revelle and Suess (1957) have discussed the relationships between the exchange rate, the Suess effect, the effect of an increase in the atmospheric CO_2 content on the atmospheric and oceanic reservoirs, and the buffering effect of the sea water alkalinity on carbon transients. They conclude that the residence time of CO_2 in the atmosphere, relative to exchange with the sea, is of the order of 10 years. Though the uncertainty in their estimate is larger than in the case of the steady-state considerations discussed above, the close agreement of the figures obtained by these different considerations is gratifying. Revelle and Suess also consider the steady-state relationships in a simple model with a uniform sea, and Arnold and Anderson (1957) have calculated residence times from the steady-state case and the Suess effect. All these considerations yield figures which are very similar.

The size of the terrestrial biosphere and the annual rate of photosynthesis on land have been estimated by Schroeder and Noddack, and from their figures it appears that the terrestrial plants consume about 3°/₀ of the atmospheric CO_2 per year, corresponding to an atmospheric residence time before entrance into the biosphere of 33 years. With a residence time of 7 years, prior to exchange into the sea, the total residence time of a CO_2 molecule in the atmosphere is 6 years, after which it goes either into the sea (9 chances out of 11) or into the terrestrial biosphere (2 chances out of 11). Thus the carbon dioxide flux into the sea is about 4.5 times larger than the flux into the biosphere, and about 82°/₀ of the CO_2 leaving the atmosphere goes into the sea, while only about 18°/₀ goes into the terrestrial plants. This ratio represents a considerable departure from previous estimates, and indicates that the spatial distribution of plants and soils is probably not the dominant factor in determining the CO_2 concentration in the atmosphere. The absorption and release of CO_2 by the sea are more probably the controlling factors.

The evaluation of the internal mixing rate of the sea is much more complicated and depends strongly on the model of the sea which is used. There is no direct relationship between mixing times for water and elements such as carbon or oxygen unless the only processes involved are those of physical mixing between water masses. On the other hand the two models discussed are probably extreme cases which fairly well bracket the average behavior of the oceans as a while, and as such they should be useful for estimating limits in geochemical calculations involving the oceans and the atmosphere.

REFERENCES

Arnold, J. R. and Anderson, E. C., *The Distribution of Carbon-14 in Nature*, Tellus, 9:28-32, (1957).

Craig, H., *The Geochemistry of the Stable Carbon Isotopes*, Geochim. et Cosmochim. Acta, 3:53-92, (1953).

Craig, H., *Carbon 13 in Plants and the Relationships Between Carbon 13 and Carbon 14 Variations in Nature*, Journ. Geology, 62:115-149, (1954).

Craig, H., *The Natural Distribution of Radiocarbon and the Exchange Time of Carbon Dioxide Between Atmosphere and Sea*, Tellus, 9:1-17, (1957).

Craig, H., *The Natural Distribution of Radiocarbon: II. Mixing Rates in the Sea and Residence Times of Carbon and Water*, Tellus, *in press*.

Rafter, T. A., *C^{14} Variations in Nature and the Effect on Radiocarbon Dating*, N. Zealand Journ. Sci. Tech. B 37:20-38, (1955).

Revelle, R. and Suess, H., *Carbon Dioxide Exchange Between Atmosphere and Ocean, and the Question of an Increase of Atmospheric CO_2 During the Past Decades*, Tellus, 9:18-27, (1957).

Suess, H., *Natural Radiocarbon Measurements by Acetylene Counting*, Science, 120:5-7, (1954).

Suess, H., *Radiocarbon Concentration in Modern Wood*, Science, 122: 415-417, (1955).

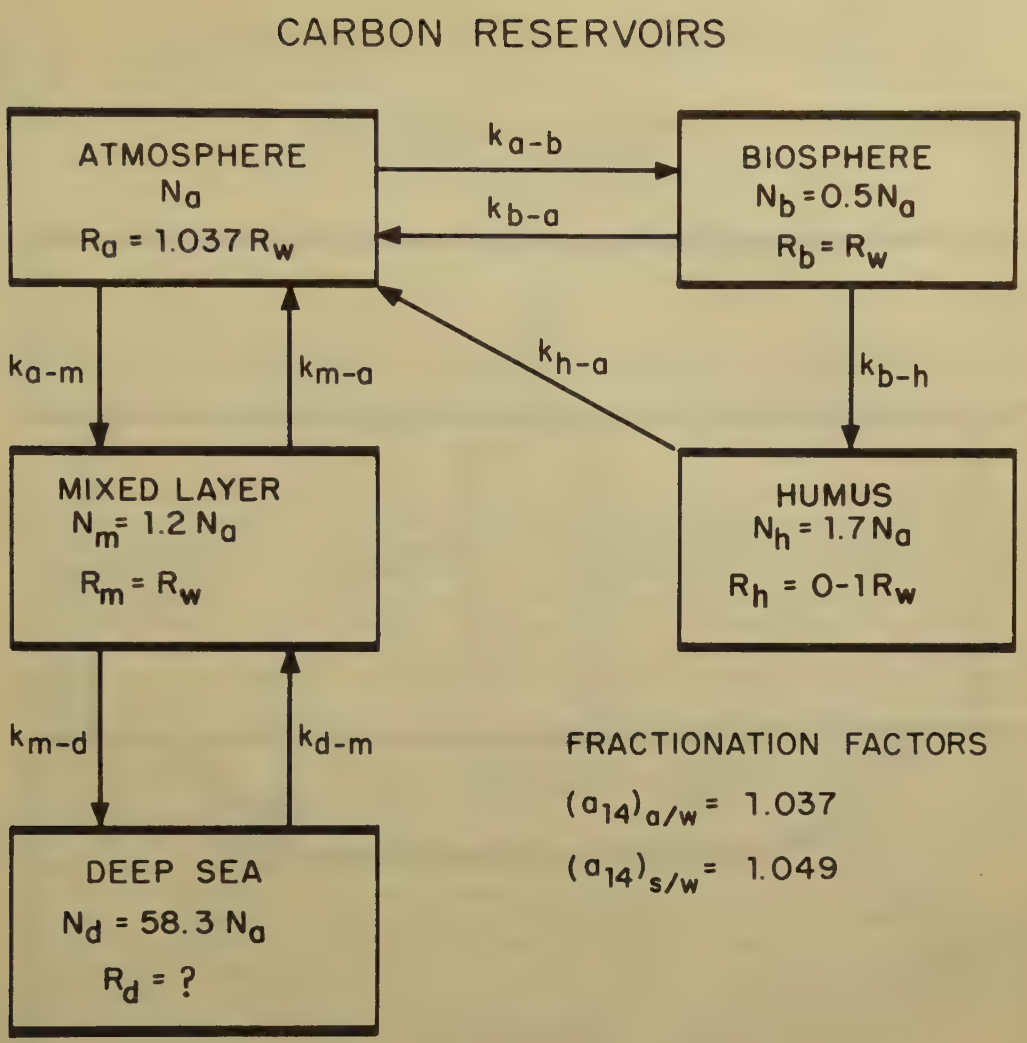
CARBON RESERVOIRS
ATMOSPHERE
N_a
$R_a = 1.037 R_w$
k_{a-b}
k_{b-a}
BIOSPHERE
$N_b = 0.5 N_a$
$R_b = R_w$
k_{a-m}
k_{m-a}
k_{h-a}
k_{b-h}
MIXED LAYER
$N_m = 1.2 N_a$
$R_m = R_w$
HUMUS
$N_h = 1.7 N_a$
$R_h = 0-1 R_w$
k_{m-d}
k_{d-m}
DEEP SEA
$N_d = 58.3 N_a$
$R_d = ?$

FRACTIONATION FACTORS

$(\alpha_{14})_{a/w} = 1.037$

$(\alpha_{14})_{s/w} = 1.049$

$N = 7.60$ grams Carbon $/\mathrm{cm}_e^2$

$N_a = .126\ \mathrm{g}/\mathrm{cm}_e^2$

$R_w = 1.24 \times 10^{-12}\ C^{14}/C^{12}$

Figure 1. CARBON RESERVOIRS IN THE "CHAIN" MODEL OF THE EXCHANGEABLE SYSTEM.

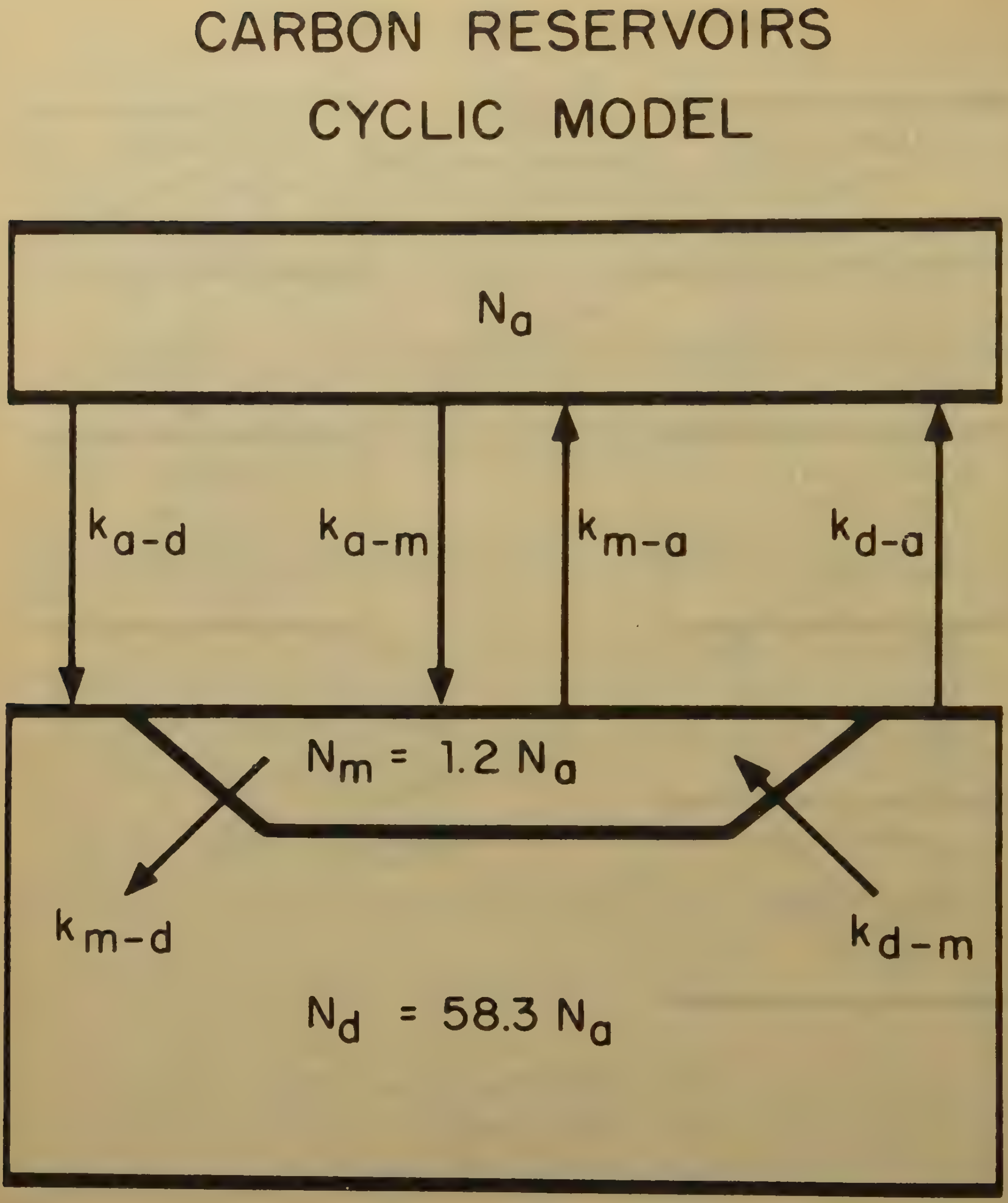
CARBON RESERVOIRS
CYCLIC MODEL
N_a
k_{a-d}
k_{a-m}
k_{m-a}
k_{d-a}
$N_m = 1.2\ N_a$
k_{m-d}
k_{d-m}
$N_d = 58.3\ N_a$

Figure 2. CARBON RESERVOIRS IN THE "CYCLIC MODEL". THE MIXED LAYER IS ASSUMED TO COVER 75°/₀ OF THE SURFACE OF THE SEA.

* U. S GOVERNMENT PRINTING OFFICE : 1958 O—467683

Second United Nations
International Conference
on the Peaceful Uses of
Atomic Energy

A/CONF. 15/P/1980
U.S.A.
June 1958

ORIGINAL: ENGLISH

IONIUM-THORIUM AND LEAD ISOTOPE RATIOS AS INDICATORS OF OCEANIC WATER MASSES

E. D. Goldberg[1], C. Patterson[2] and T. Chow[2]

There are two popular techniques for the study of the present day circulation of deep-water masses. The first involves the direct measurement of the velocity of the water body under consideration (Swallow, 1955). Secondly, the systematic variations in the temperature and/or the concentrations of the dissolved constituents as a function of the distance of the water mass from a given location, coupled with bottom topography, have been used with some success (Sverdrup, Johnson and Fleming, 1946, p. 751; Wooster and Volkman, unpublished manuscript, presented at Eleventh General Assembly of IUGG, Toronto, Canada, 1957).

A complementary technique may be the use of the isotopic analyses of certain elements in components of the deep-sea sediments underlying the water masses. The transfer of dissolved chemical species, characteristic of a given water mass, to one or more of the solid phases on the ocean floor, may well record the travels of bottom waters. Further, the possibility of studying the character and behavior of deep oceanic waters in past ages presents itself in the depth distribution of isotopes of certain elements in deep-sea cores. The purpose of this paper is to present some preliminary results on the distribution of the isotopes of both lead and thorium in the surface layers of recent sediments from the Pacific Ocean and to compare these distributions with oceanic circulation patterns derived from other approaches.

RESULTS

Ionium and thorium: The two alpha-emitting isotopes of thorium, Th-232 and Th-230 (ionium) have been assayed in pelagic sediments of the Pacific using an alpha spectrometric technique which will be described elsewhere (Goldberg and Koide, manuscript in preparation). Th-232, natural thorium, has a half-life of 1.4×10^{10} years, whereas ionium, one of the daughter products in the U-238 decay series, has a half-life of 80,000 years. Th-232 hereafter will be designated as Th.

---

[1] Scripps Institution of Oceanography, University of California, La Jolla, California. Contribution from the Scripps Institution of Oceanography, New Series. No. 1020

[2] Division of Geologic Sciences, California Institute of Technology, Pasadena, California

Reproduced by Permission

The Io/Th ratios in the surface samples of analyzed cores from the Pacific Ocean fall into two distinct groups: a set in the region between the Aleutian Islands and Hawaii with values averaging about 15 and a second group between 120° and 140° West Longitude from 40° N to 20° S with a ratio varying around 35 (Figure 1). The fall-off in the ratio with depth is continuous within the cores. An example from each group is presented in Table I. The values are reproducible to within ten percent of the tabulated numbers.

Table I: Io/Th ratios in two cores from the Northeast Pacific Ocean. The ratios are given in terms of disintegrations of Io per disintegration of Th per unit time.

Capricorn 50 BG	Io/Th	Chinook 11	Io/Th	Depth Interval in Core in Cm.
14°55' N		49°39.5'N		
124°12' W		177°39' W		
4270 meters	30	4850 m	16	0-4
	23		18	4-8
	16		11	8-12
	9.0		10	12-16
	8.4		7.0	16-20
	6.1		6.2	20-24
	5.3		4.4	24-28

Lead Isotopes: There are four stable lead isotopes: Pb-208, Pb-207 and Pb-206, the end products of the radioactive decay of Th-232, U-235 and U-238 respectively; and Pb-204, which has no known radioactive parent. Changes in the relative abundances of lead isotopes within geologic systems depend upon the uranium, thorium and the initial abundances of the lead isotopes as well as the age of the system. Oceanic leads represent a mixture of leads from different geologic systems on the continents. The isotopic analyses of lead in manganese nodules and in pelagic sediments were accomplished by mass spectrometric techniques. A detailed description of the analyses will be given elsewhere (Chow and Patterson, manuscript in preparation).

The lead results are presented in Figure 1 where values of a parameter, proportional to the Pb-206 content in the lead isolated from the samples, are plotted at the location of the point of collection. The measurement error is equivalent to approximately 7 units of the parameter given. A general feature of the data is an increase of the Pb-206 abundance in the isolated leads from West to East across the Pacific. In addition, the concentration of this isotope is always less in Pacific Ocean leads than in Atlantic Ocean leads. The parameter has a range of 48.2 to 74.7 in Atlantic Ocean manganese nodules.

DISCUSSION

It will be of interest to consider the results against a background of present ideas concerning the composition and formation of pelagic sediments. The components of deep-sea sediments fall into three principal genetic classes:

(1) Lithogenous. Those solid phases which arise from the weathering of continental rocks or volcanic debris and which undergo no change in chemical composition during their travels through the atmosphere and hydrosphere to the deep-sea sediment site. Quartz and volcanic glasses are typical examples within this group.

(2) Biogenous. The skeletal remains of members of the marine biosphere. Included within this group are the opal, calcium carbonate and apatite phases.

(3) Hydrogenous. The solid phases which precipitate or form from the dissolved species in seawater. The ferro-manganese minerals, the zeolite phillipsite and the clay minerals are examples of this group.

The sediments considered in this presentation are composed nearly entirely of phases from the first and last classes. Only one lithogenous component was present in significant quantities -- quartz, whose abundance varied from less than one to twenty percent by weight (Rex and Goldberg, in press, 1958). The amounts of thorium and lead in this detrital quartz was negligible with respect to their concentrations in the clay and ferro-manganese minerals.

Of particular interest are the ferro-manganese minerals which occur as components of the sediments or as the major minerals in the so-called "manganese nodules". They consist of a three-layer structure with the outer layers formed of manganese dioxide and an inner, disordered layer of manganese hydroxide hydrate or ferric hydroxide hydrate (Buser and Grütter, 1956). The formation of these layer lattice minerals is accompanied by the build-up of large surface areas of the order of 100 m^2/g, which provide sites for the accumulation of such elements, which exist in trace amounts in seawater, as lead, cobalt, zinc, cadmium, copper and thorium. All of these metals occur in concentrations one to two orders of magnitude greater than the corresponding average values in crustal rocks. The unique chemical and mineralogical composition of the ferro-manganese minerals reflects their hydrogenous character (Goldberg and Arrhenius, 1958).

The uptake of elements from seawater to form such authigenic phases as the ferro-manganese minerals probably occurs at the sediment-water interface (Arrhenius, 1954; Goldberg and Arrhenius, 1958). Quantitative descriptions of such processes involve the residence times of elements in the oceans which may be defined by $T = A/(dA/dt)$. A is the standing crop of the element in the oceans and dA/dt is the rate of introduction or the rate of removal of the element from the marine hydrosphere. A steady state system is obviously assumed. Two methods for arriving at residence times have been proposed: one based upon the rate of supply of elements to the oceans by the rivers (Barth, 1952); and one based upon the rate of sedimentation of the elements in the marine environment (Goldberg and Arrhenius, 1958). A remarkable agreement is observed between these two sets of calculations and residence times for a selected group of elements given below (Table II) based upon the second method:

Table II Residence times of elements in the Oceans

Element	Amount in Oceans (grams)	Residence Time (years)
Na	1.5×10^{22}	2.6×10^{8}
Ca	5.6×10^{20}	8.0×10^{6}
U	5.2×10^{15}	6.5×10^{5}
Cu	5.2×10^{15}	6.5×10^{4}
Si	5.2×10^{18}	1.0×10^{4}
Mn	1.4×10^{15}	7.0×10^{3}
Pb	4.0×10^{14}	1.0×10^{4}
Th	2.8×10^{13}	1.4×10^{3}
Ti	1.4×10^{15}	1.6×10^{2}
Al	1.4×10^{16}	1.0×10^{2}

Ferguson (1958) reports radiocarbon ages on deep waters from the South Pacific Ocean in the range of thousands of years. Such ages are related to the times since the water masses were last in contact with the atmosphere. Further, contact with the atmosphere implies a steady state between the dissolved gases in the water and the atmosphere. The order of magnitude correspondence between the transport ages of waters and the residence times of lead and thorium in ocean waters suggests that the transfer of ions of these elements from a water mass to sediment components over a large area of the sea floor is possible.

The long-term isotopic stability of these systems (i.e. the isotopic compositions of the lead and thorium in the waters above a given depositional site have been relatively constant over time periods longer than the residence times of the elements or the transport times of waters) is indicated by the exponential decreases in the Io/Th ratio in the two cores with depth (Table I). On the basis of this data, the approximate rates of accumulation for the Capricorn and Chinook cores are 1 and 2 mm/1000 years respectively; and the lower sections of the cores were deposited several hundred thousand years ago.

It is of interest now to consider these results on lead and thorium isotopes in context with present ideas on the deep water circulation in the Pacific. Wooster and Volkman (op. cit.) have analyzed the chemical and physical characteristics of selected waters from the Pacific, and, combining such data with the bottom topography of the areas, have proposed one flow line for deep water (5000 meters). This path is shown in Figure 2 with temperatures at this depth at various points. The bottom water is presumed to originate in the Antarctic, entering the Pacific from the west between Australia and the Antarctic continent. Along this route, the five thousand meter water passes through four basins, all containing water at depths of 5000 meters or greater. The water is presumably heated along its travels by the heat flow through the floor of the ocean and by the exothermal oxidation of organic matter. In the more easterly portions of the Pacific, the depths are shoaler, with an average close to 4000 meters. Temperatures taken at four thousand meter depths on the Scripps Institution of Oceanography IGY Expedition DOWNWIND, suggest a northward component of flow, apparently from a different point of origin.

Corresponding to these two areas are the two groups of lead and ionium isotopes taken from the sedimentary deposits:

	Io/Th	Pb-206 (arbitrary units)
Eastern Area	30-35	28.7-41.5
Western Area	13-19	22.9-28.9

A third set of lead results, off the coast of Japan, with values of 6.4 and 7.5 appears to constitute another group.

These tentative results and conclusions strongly invite more studies on the chemical and physical characteristics of the deep waters of the Pacific, as well as the other oceans. Questions as to the origins of the deep water masses, the introduction of chemical species from the continents into the oceanic waters, and the chemical interplay between the seawater and the sediments may receive some satisfying answers upon the basis of such investigations.

REFERENCES

Arrhenius, G., Significance of carbonate stratification in pelagic sediments, Bull. Geol. Soc. Amer., 65: 1228-9, (1954).

Barth, T. W., Theoretical Petrology, John Wiley, New York, (1952).

Buser, W. and Grütter, A., Über die Natur der Manganknollen, Schweiz. Min. Petrogr. Mitt., 36: 49-62, (1956).

Ferguson, G. J., Reduction of atmospheric radiocarbon concentration by fossil fuel carbon dioxide and the mean life of carbon dioxide in the atmosphere. Proc. Roy. Soc., 243A: 561-74, (1958).

Goldberg, E. D. and Arrhenius, G. O. S., Chemistry of Pacific Pelagic Sediments, Geochim. Cosmochim. Acta, 13: 153-212 (1958).

Sverdrup, H., Johnson, M., and Fleming, R., The Oceans, Prentice-Hall Inc., New York, (1946).

Swallow, J. C., A neutral buoyant float for measuring deep currents, Deep-Sea Research, 3: 74-81 (1955).

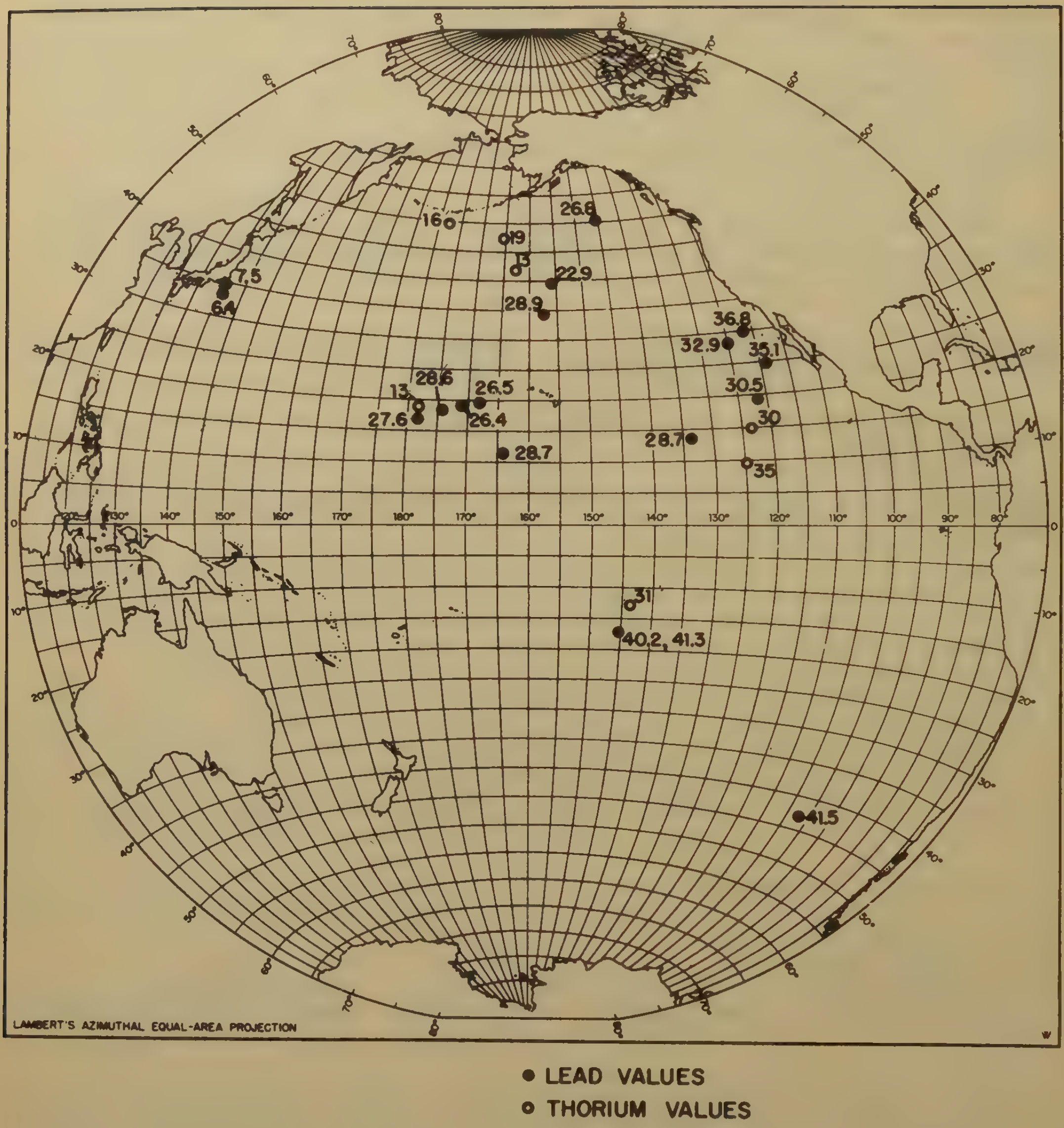
LAMBERT'S AZIMUTHAL EQUAL-AREA PROJECTION
16
19
13
26.8
22.9
28.9
7.5
6.4
36.8
32.9
35.1
30.5
30
28.7
35
13
28.6
26.5
27.6
26.4
28.7
31
40.2, 41.3
41.5
130°
140°
150°
160°
170°
180°
170°
160°
150°
140°
130°
120°
110°
100°
90°
80°
● LEAD VALUES
○ THORIUM VALUES

Figure 1. The isotopic composition of lead and thorium from the Pacific Ocean floor. The ionium/thorium ratio in surface sediment samples is given in terms of disintegrations of ionium per disintegration of thorium per unit time. The Pb-206 abundance in leads isolated from manganese nodules is given in terms of an arbitrary parameter.

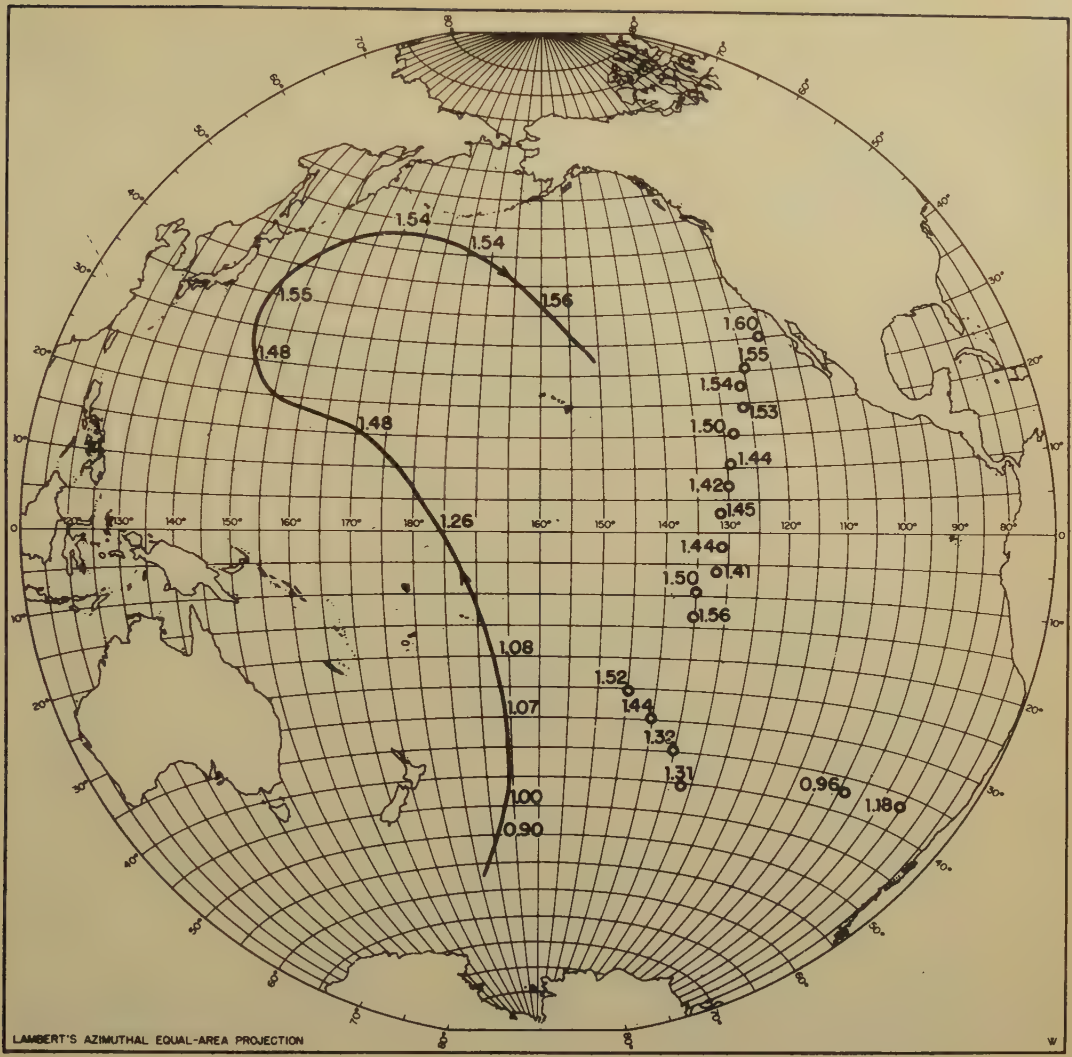
1.54
1.54
1.55
1.56
1.48
1.48
1.26
1.08
1.07
1.00
0.90
1.60
1.55
1.54
1.53
1.50
1.44
1.42
1.45
1.44
1.41
1.50
1.56
1.52
1.44
1.32
1.31
0.96
1.18
130°
140°
150°
160°
170°
180°
160°
150°
140°
130°
120°
110°
100°
90°
80°
LAMBERT'S AZIMUTHAL EQUAL-AREA PROJECTION
W

Figure 2. Bottom water temperatures in the Pacific Ocean. The left hand flow curve (with associated water temperatures at 5000 meters in degrees centigrade) is taken from an unpublished manuscript of Wooster and Volkman (op. cit.). The right hand temperatures at 4000 meters are from the Scripps Institution of Oceanography IGY Expedition DOWNWIND (1957-58).

★ U. S. GOVERNMENT PRINTING OFFICE : 1958 O—467682

Second United Nations
International Conference
on the Peaceful Uses of
Atomic Energy

A/CONF.15/P/2357
U.S.A.
June 1958

ORIGINAL: ENGLISH

EXPERIMENTS WITH RADIOACTIVE SAND AS A TRACER OF BEACH SAND MOVEMENT*

by

D. L. Inman and T. K. Chamberlain[1]

INTRODUCTION

Until recently there has been no satisfactory means of tagging sand size material so that the movement of sand could be studied in the beach and nearshore zone. The advent of readily available high flux neutron sources for activating sand samples has given impetus to studies involving the tracing of sediment movements. The purpose of this investigation was to perfect a field technique using low levels of radioactivity in sands that would be suitable for studying sand movements on populated swimming beaches, and to apply this technique in studying the rate of dispersion of sand under wave action near shore.

Previous work with radio isotopes as tracers of sand has principally been confined to the use of foreign particles such as ground glass, which are added to the sand under study, and which in general have employed levels of activity too high for use along California beaches (Hours, et al, 1955; Inose and Shiraishi, 1956; Putman and Smith, 1956; Arlman et al, 1957). Also, foreign particles are not usually suitable for beach sand tracers because their hydraulic behavior may be different from that of the natural sands. To be satisfactory, the natural tracer of sand movements should be: (1) not a health hazard, (2) of the same size distribution, density, and shape as one of the major components under study, (3) easily and rapidly distinguishable from the sand mass, (4) inexpensive and available in relatively large amounts, (5) able to retain its distinguishing properties over times comparable to the times of the fluid processes. Thus, the problem was to seek out a tracer that would fulfill these requirements, and to develop field techniques that could be used in the difficult conditions encountered near the surf zone.

---

[1] Scripps Institution of Oceanography of the University of California, La Jolla, California

* Contribution from Scripps Institution of Oceanography, New Series. No. 1021

Reproduced by Permission

Since quartz is one of the dominant components of most sands, a method of tagging it was highly desirable. The technique of Goldberg and Inman (1955) utilizing phosphorus-32, which is formed when normally occuring phosphorus in quartz sand is subjected to slow neutron irradiation, satisfactorily fulfills the requirements for a tracer, including that of not constituting a health hazard when used near populated beaches. Goldberg and Inman found that phosphorus-32 is the principal radioisotope formed from the slow neutron irradiation of natural quartz sand. Phosphorus, which occurs as a minor impurity in the order of hundreds of parts per million in quartz, is a low level beta emiter. Since each radioactive quartz particle can be detected on photosensitive film, sensitivity of the assay is limited only by size of sample and size of film. Single irradiated quartz particles can easily be detected when mixed with about one million inactive particles. Phosphorus-32 has a half-life of 14.6 days and irradiated quartz particles could be detected for several months.

To carry out the study, a natural sample of sand was obtained from the environment to be studied. The quartz grains were concentrated by partial removal of other constituents, the resulting concentrate irradiated, and then reintroduced back into the natural environment by swimmers equipped with self-contained underwater breathing apparatus. After reintroducing the irradiated sand on the bottom, the area was periodically sampled to determine the rate of dispersion of irradiated particles. Two types of samples were obtained: (1) the surface layer of sand, by impressing a grease-coated 3 x 5 inch card on the bottom, and (2) cores, obtained by forcing small plastic vials into the bottom. The activity of the surface sample was assayed by laying the sample card on photosensitive film and, after exposure and development, counting the exposed spots. The cores were lithified and sectioned before assaying.

Since it was desirable to use an area that was convenient to reach from the laboratory and one in which good wave and tidal data could be obtained, the sandy beach and shelf immediately adjacent to the Scripps Institution of Oceanography was chosen as the field locality in which to carry out the experiments (Figure 1). The shelf is flat and is uniformly covered with fine and very fine sand. The irradiated sand was released on the bottom by swimmers at a point where the water depth was about 10 feet. During the observations the surface waves were about 1¼ feet high and the wave period was about 14 seconds (Table I).

LABORATORY METHOD

The natural sand collected from the experiment site was composed of about 74% quartz, 14% feldspar, 10% heavy minerals, and 2% shell fragments (Inman, 1953). Thus it was necessary to process the sample in order to concentrate the quartz. The sample was first washed and treated with dilute HCl to remove the calcareous shell material, then dried and sieved, and the smallest size group discarded because it contained little quartz. The magnetic minerals were removed with an electromagnetic separator, after which the sample was placed in hot *aqua regia* for 24 hours. The sample resulting from the above treatment was nearly 98% quartz and feldspars and compared closely in size distribution with the natural sand of the experimental area (Figure 3).

The concentrate of 860 grams of sand, prepared as outlined above, was sent for irradiation to the Union Carbide Nuclear Company, Oak Ridge National Laboratory, Oak Ridge, Tennessee. There it was placed in the atomic pile and subjected to slow neutron irradiation with a nominal flux of 10^{12} neutrons/cm^2/sec for 14 days. Following irradiation and prior to shipping, the sample was cooled for seven days to allow the removal of the induced Na and K activities in the feldspar impurities. After receipt at the laboratory, the irradiated sand measured approximately 16 mr/hr at the surface of the container. Beta absorption measurements were taken and showed the presence of the phosphorus 1.7 Mev beta particle. Measurement on half-life indicated that the short life contaminants did not contribute significantly to the over-all activity.

The sample was dyed an intense blue with analin dye (Night Blue, National Analin No. 598) before introduction to the experiment site. Coloring the tracer permitted the first stages of the dispersion to be followed visually.

COUNTING TECHNIQUE

To determine the quantity of irradiated sand in each sample collected, the 3 x 5 inch sampling cards, covered with sand grains, were brought from the field and wrapped face to face with No-Screen X-Ray film in a light-tight package. The film was exposed 24 hours in this manner, then developed and fixed. The irradiated sand grains showed themselves quite easily as black spots on the resulting transparent film negative.

The small cores collected in the field were brought into the laboratory and solidified by the injection of plastic resin. They were then sectioned lengthwise and laid upon photosensitive film for the required exposure period. The result was similar to that of the surface samples, and counts could easily be made of the irradiated grains.

SENSITIVITY

Tests were conducted on a portion of the irradiated sample to determine the sensitivity of the photosensitive film in recording individual radioactive sand grains, and to determine the most desirable exposure time to use at various decay times. It was found that thin wrapping paper placed between the irradiated particles and the X-Ray film absorbed most of the radiation, but that "Saran Wrap", an extremely thin sheeting of vinylidene chloride made by Dow Chemical Company, allowed the radiation to penetrate and register on the film. Saran Wrap was used to protect the film from the greased sand sample in all experiments. Thirty days after irradiation an exposure time of 4 hours gave weak returns from the control sample, while 12 hours was adequate to give strong signatures from all irradiated grains. Four months after irradiation, strong exposure could still be obtained from all particles in the control sample with an exposure time of 16 hours. Exposure times longer than 48 hours were excessive and resulted in clouding the film, thereby obscuring particle counts.

Prior to the release of irradiated sand, 32 samples of sand were collected from the area of investigation to determine the natural background activity of the region. These were processed in the usual way with an exposure time of 24 hours. Although each sample contained about 100,000 particles of natural sand, no positive exposures were found. Supporting this assumption of no detectable background activity were the results of the actual sampling itself. The last irradiated grains were detected from the sampling at 24 hours. Subsequent to this, 84 surface samples were taken in the area, none of which showed the presence of irradiation.

FIELD PROCEDURE

The field work was carried out by swimmers equipped with self-contained underwater breathing apparatus, operating from a small boat. Concurrent with the sand sampling a pressure type wave meter was used to record wave conditions, and current measurements were taken using a captive drogue. Principal operations were concluded in 24 hours, although background sampling was continued for 23 days. A total of 311 surface samples and 39 cores were collected and processed (Table II).

The irradiated sand was carried to the center of the grid in a plastic bottle by a swimmer. There the plastic bottle was opened and the irradiated sand poured out onto the bottom, covering an area of about 3 square feet. Samples were taken at predetermined positions on the grid at ¼, 1, 3½, 7½, and 24 hours, (Figure 1, Table II). Also, background samples were obtained throughout the area 7 and 23 days after the release, but did not show the presence of irradiated particles.

A permanent sampling grid was established prior to the actual experiment. It consisted of a series of reference stakes driven into the bottom at 10 foot intervals along eight ranges radiating from the release point. The major onshore-offshore range extended through the breaker zone onto the beach, and is shown in Figure 1. The beach profile and it's changes are shown in Figure 2.

The principal sampling was performed with 3 x 5 inch paraffin-coated paper cards, covered on one side with Varcon #4-1645 Water Pump Grease. Each sample was taken by pressing a sampling card onto the bottom so that the surface layer of sand grains adhered to the coating of grease. In addition, subsurface samples were obtained by forcing small plastic vials into the bottom. The plastic vials were approximately one inch in diameter by 3 inches long and were quite efficient in obtaining relatively undisturbed sediment samples.

The distribution patterns of irradiated grains showed extremely rapid rates of dispersion; far greater than were expected under such low wave conditions. The transport rate for some particles was as high as 1.5 feet per minute during the first 1/4 hour period. The initial distribution pattern of surface counts showed dispersion in all directions, with an elongate offshore-onshore axis. In 7 to 24 hours the net onshore transport of sand overshadowed the lateral and offshore dispersion and the entire surface distribution pattern indicated an onshore migration. Of 26 surface samples collected from the beach at 24 hours, four showed single irradiated particles. The locations of these samples are shown by triangular symbols on the inset of Figure 1. Both the surface and subsurface samples showed an increase in irradiated grains with time in a shoreward direction, and for the most part the highest counts were found shoreward of the release point at all sampling times.

Accurate measurements of the change in sand level were obtained by comparing the length of reference rods exposed along the major axis of the sampling grid, following the procedure of Inman and Rusnak, 1956. The sand level measurements show that erosion occurred in the vicinity of the release point and that deposition of sand occurred on the beach and to a lesser extent offshore (Figure 2).

The 39 cores taken in the sampling area showed the occurrence of vertical mixing of sand. The subsurface concentration at the release point decreased with time while the depth of mixed sand increased. At 24 hours, irradiated sand was found as deep as 0.2 foot below the surface of the core taken at the release point. This may in part result from the disturbance of previous coring. Cores taken away from the release point showed a decrease in concentration of irradiated material following the one hour sampling, except cores in the onshore direction where a maximum concentration occurred 10 feet from the release point at 7½ hours. A maximum depth of mixing of 0.06 foot was observed at this time.

SUMMARY AND CONCLUSIONS

1. The procedure used in this radioactive tracer experiment was: (a) collection of natural sand samples from the area under investigation, (b) processing sample to concentrate quartz grains, (c) irradiation of processed sample, (d) reintroduction of irradiated sample as a point source on the bottom by swimmers, (e) collection and assay of samples for radioactive particles by radioautography. The irradiated sand did not constitute an apparent health hazard.

2. The sensitivity for this experiment was one particle per 100,000 particles. However, greater sensitivity is practical, and is limited only by size of photosensitive film and size of sample. Sensitivity tests showed that irradiated particles could be detected for periods of several months.

3. The field experiment indicated a rapid rate of dispersion of sand from the point of release, where the waves were about 1¼ feet high and the water depth was about 10 feet. A net sand transportation rate of 1½ feet per minute was measured near the release point.

4. Dispersion of sand was most rapid in the onshore and offshore directions. Irradiated grains were detected on the beach approximately ¼ mile from the release point in 24 hours.

5. Sampling indicated a net onshore transportation of irradiated particles, and that the particles were dispersed over an area as great as one square mile in 24 hours (Table II).

6. Cores near the release point showed irradiated particles as much as 0.06 foot below the surface of the sand.

7. Measurements of sand level change show that a net erosion of about 0.1 foot occurred in the vicinity of the release point, while deposition of sand occurred on the beach foreshore (Figure 2). It seems probable that the rate of dispersion of sand would be quite different for irradiated material released in a zone of net deposition.

ACKNOWLEDGEMENTS

The field phase of the investigation was performed principally by Earl Murray. Assistance in the field work and analysis of data was given by Helene Flanders. Valuable suggestions and guidance during the course of the study were contributed by E. D. Goldberg and J. D. Frautschy, all on the staff of the Scripps Institution of Oceanography.

LITERATURE CITED

Arlman, J. J., P. Santema and J. N. Svasek, Movement of Bottom Sediment in Coastal Waters by Currents and Waves; Measurements with the Aid of Radioactive Tracers in the Netherlands, Deltandienst, Rijkswaterstaat, Ministry of Transport and Waterstaat, The Netherlands, Progress report, June: 1-56, (1957).

Goldberg, E. D. and D. L. Inman, Neutron-irradiated Quartz as a Tracer of Sand Movements, Bulletin of the Geological Society of America, 66:611-13, (1955).

Hours, R., W. D. Nesteroff, and V. Romanovsky, Methode D'Etude de L'Evolution des Plages par Traceurs Radio-Actifs, Centre de Recherches et D'etudes Oceanographiques, v. 1, no. 11:1-7, (1955).

Inman, D. L., Areal and Seasonal Variations in Beach and Nearshore Sediments at La Jolla, California, Beach Erosion Board, Corps of Engineers, Tech. Memo. 39:1-134, (1953).

Inman, D. L. and G. A. Rusnak, Changes in Sand Level on the Beach and Shelf at La Jolla, California, Beach Erosion Board, Corps of Engineers, Tech. Memo. 79:1-72, (1956).

Inose, S. and N. Shiraishi, The Measurement of Littoral Drift by Radio-Isotopes, The Dock and Harbour Authority, Hokkaido Development Bureau, Japan, January: 284-88, (1956).

Putman, J. L. and D. B. Smith, Radioactive Tracer Techniques for Sand and Slit Movements Under Water, International Journal of Applied Radiation and Isotopes, 1:24-32, (1956)..

TABLE I

Wave and tide data

Time After Release	Depth of water at Release Point ft	Wave Height[a] ft	Wave Period[a] sec
¼ hr	11.3	1.3	15.0
1 hr	11.6	1.2	14.3
2 ½ hrs	11.9 (highest water)		
3½ hrs	11.7	1.1	13.9
7½ hrs	8.6	1.4	13.3
10 hrs	7.7 (lowest water)		
24 hrs	11.0	1.9	13.0

[a] Height and period of the highest one-third of the waves measured during a 20 minute interval. The maximum wave measured during each interval was about 1.6 times greater.

Table II. Distribution of irradiated sand particles (2.44×10^8 irradiated particles were released).[b]

Time after release	Number of surface samples	Number of cores	Number of Particles Accounted for by Sampling			Area of distribution, square feet[c]
			Surface	Subsurface	Total	
$\frac{1}{4}$ hr	32	0	3.25×10^6	1.19×10^8	1.22×10^8	0.73×10^3
1 hr	37	9	0.93×10^6	1.19×10^8	1.19×10^8	1.5×10^3
$3\frac{1}{2}$ hrs	42	5	0.19×10^6	0.77×10^8	0.79×10^8	5.3×10^3
$7\frac{1}{2}$ hrs	42	11	0.24×10^6	0.31×10^8	0.31×10^8	17.2×10^3
24 hrs	74	5	scattered returns			24×10^6 [d]
7 to 23 days	84	9	no positive returns			indeterminate

[b] 860 grams of very fine sand were released

[c] Area over which concentration of irradiated particles was equal or greatern than one per 1/10 ft^2. This is a surface concentration of 1 in 10^5 particles.

[d] Assuming total number of irradiated particles to be dispersed so that concentration is equal or less than one particle per 1/10 ft^2 as indicated by sampling.

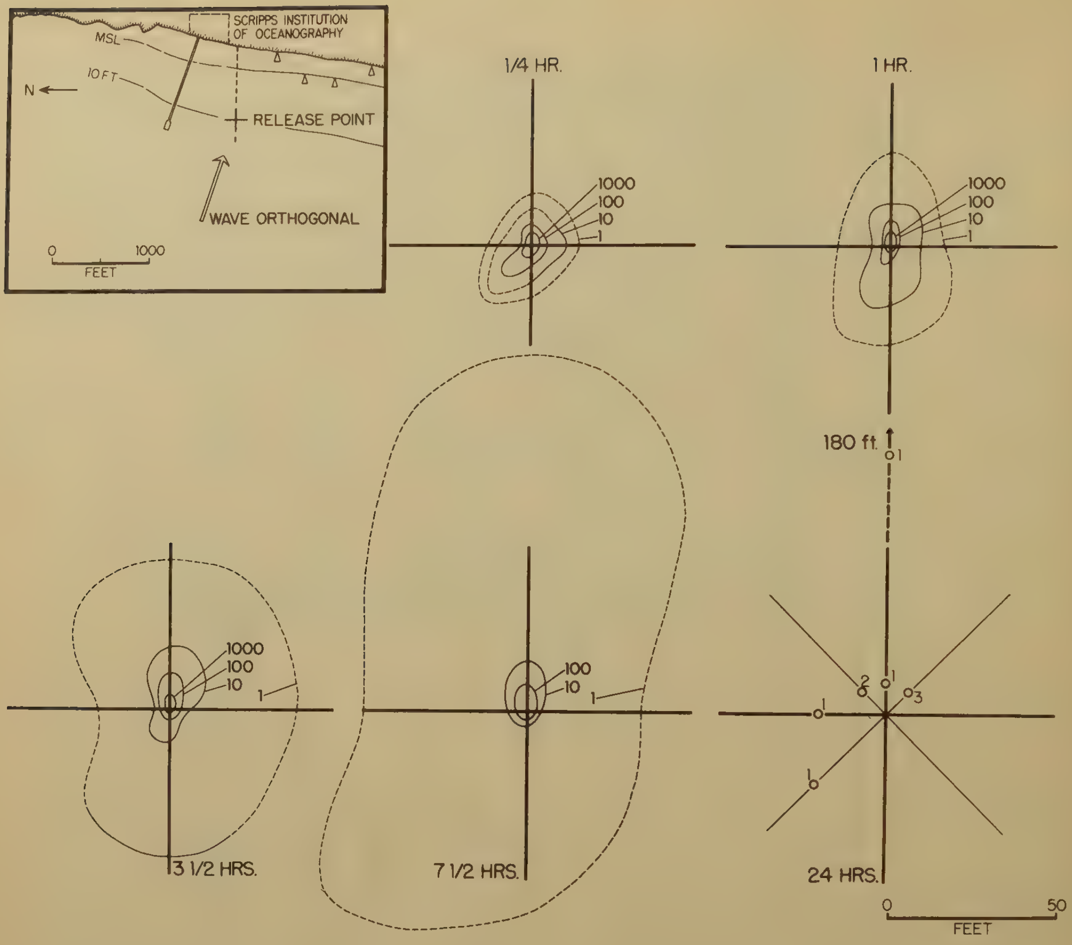

Figure 1. Distribution of irradiated sand particles with time. The contours are lines of equal concentration of surface particles, and their value is expressed in number of irradiated particles per 0.1 square foot (100 cm^2). At 24 hours only six offshore samples gave returns, which are shown as individual points. The four positive beach counts for the 24 hour sampling are plotted in the inset. Orientation of grid is shown in the inset.

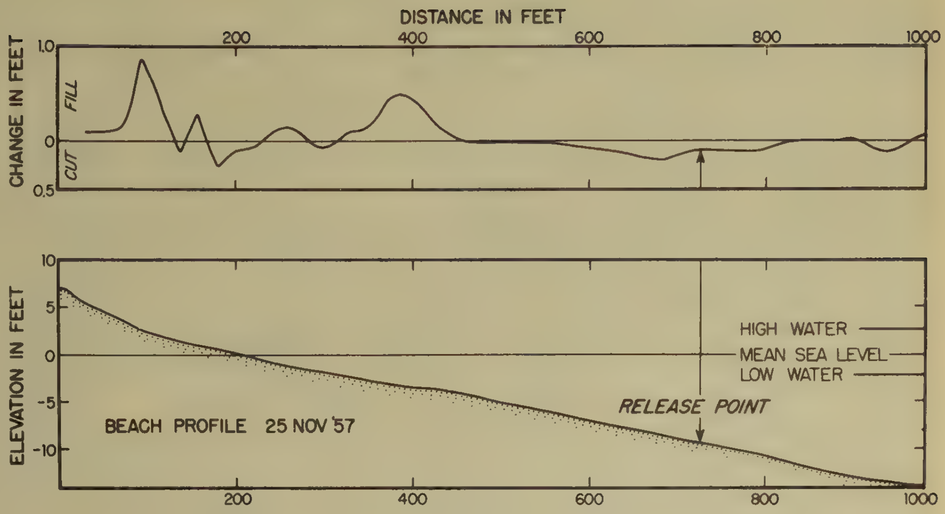

Figure 2. Changes in sand level along the beach profile during first 40 hours of the experiment. Erosion (cut) occurred in the vicinity of the release point; deposition (fill) occurred on the beach. Location of profile shown in Figure 1.

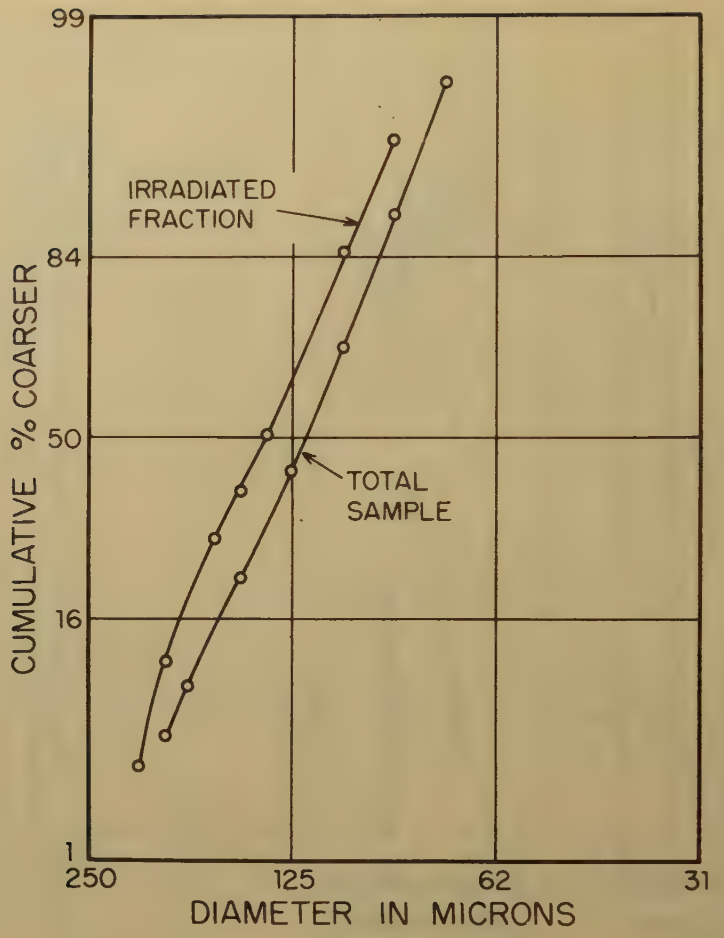

Figure 3. Particle size distribution curves for the total sample of natural sand and the concentrate of quartz sand which was irradiated and reintroduced into the area of investigation.

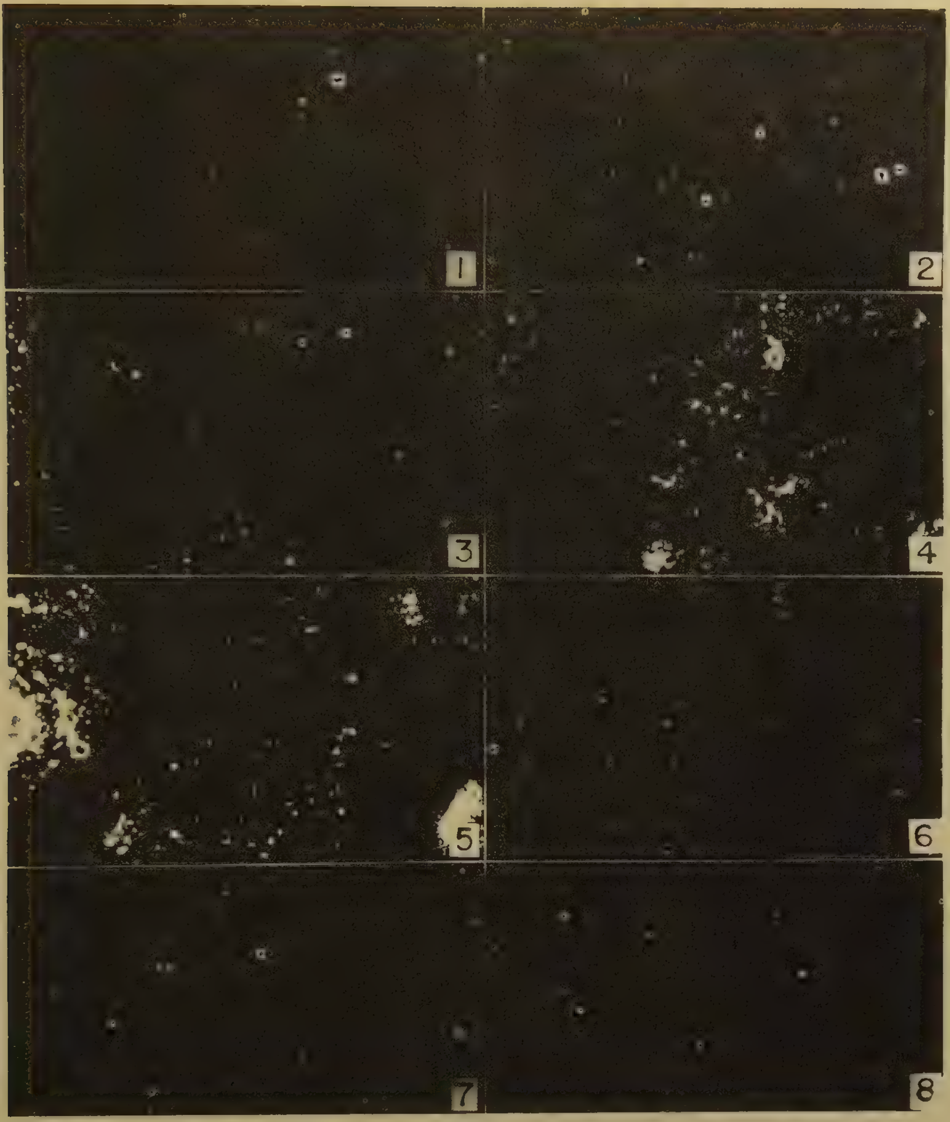

Figure 4. Eight representative surface samples taken along the onshore-offshore range line of Figure 2. Samples were taken 1/4 hour after the release of irradiated material. These are prints from photosensitive film negatives used in counting the irradiated grains. Each white dot represents one irradiated sand grain. The location of the samples relative to the release point is as follows: (1) 10 ft shoreward, (2) 7½ ft shoreward, (3) 5 ft shoreward, (4) 2½ ft shoreward, (5) 2½ ft seaward, (6) 5 ft seaward, (7) 7½ ft seaward, (10) 10 ft seaward.

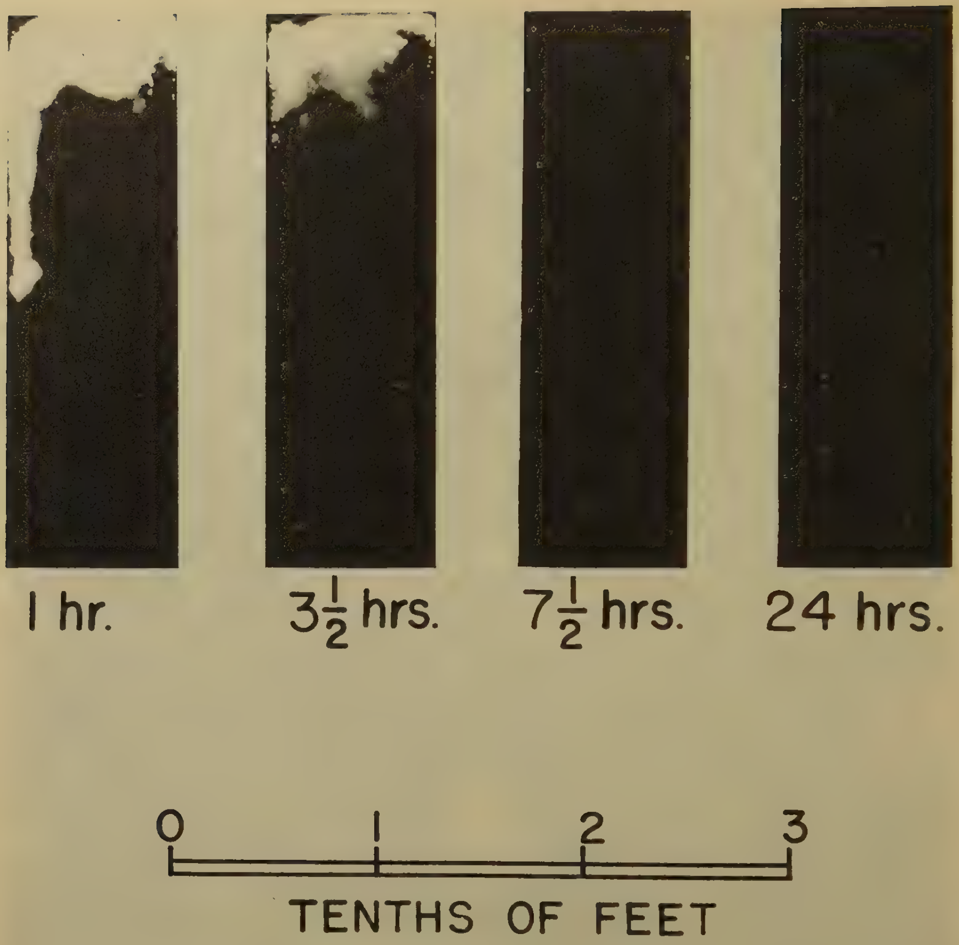
1 hr.
3½ hrs.
7½ hrs.
24 hrs.
0
1
2
3
TENTHS OF FEET

Figure 5. Representative subsurface profiles of cores taken at the release point. Each core was lithified, sectioned, then exposed to photosensitive film. Each white dot represents an irradiated sand grain. The extension of the zone of irradiated sand down along the side of the coring tube is the result of coring method.

★ U. S. GOVERNMENT PRINTING OFFICE : 1958 O—468352

Reprinted from Limnology and Oceanography
Vol. 3, No. 2, April, 1958
Printed in U.S.A.

Particulate Iron in Offshore Waters of the Panama Bight and in the Gulf of Panama

Milner B. Schaefer and Yvonne M. M. Bishop

Inter-American Tropical Tuna Commission, Scripps Institution of Oceanography, La Jolla, California

ABSTRACT

Particulate iron is reported from replicate samples taken at two depths at several locations in the Panama Bight during November 1955, and in replicate samples taken at two depths at a single inshore location in the Gulf of Panama at bimonthly intervals from December 1954 through December 1955. In addition, a few samples were taken at other locations in the Gulf of Panama and from a river flowing into the Gulf. The content of particulate iron, both in the Panama Bight and in the Gulf, shows highly contagious distributions, necessitating a logarithmic transformation to make the data amenable to statistical analysis. All samples from the Panama Bight could have arisen from a single log-normal distribution with a mean of 12.2 μg/L. In the Gulf of Panama, there is significantly higher iron in the surface (115.2 μg/L) than at 30 meters (62.1 μg/L) during the early part of the year when the standing crops of plankton organisms are high. Particulate iron content is higher inshore in the Gulf of Panama than offshore in the Panama Bight, and two samples from the Río Escota, containing 692 and 863 μg/L, were much higher than in the Gulf, indicating that possibly the iron is being brought in by runoff. From comparison of iron content in inshore and offshore waters, in both of which biological production is high, it is inferred that particulate iron cannot be a limiting factor on phytoplankton growth in the inshore waters.

INTRODUCTION

Particulate iron in marine waters is of considerable interest because it is the form in which iron is utilized by phytoplankton organisms (Goldberg 1952, Harvey 1937). It may, in some circumstances, be a limiting constituent for the growth of these microscopic plants.

Lewis and Goldberg (1954) investigated the iron content of waters at different depths from a number of stations in the North Pacific. They concluded that particulate iron tends to be more abundant in the upper layers (less than 500 meters) than in deeper layers, at least at some stations in the Northeast Pacific, and that the variability of results from replicate samples from the upper layer is quite high. It was inferred that "the marine biosphere acts as a reservoir for iron particles and accentuates the high scatter of the particulate iron and distribution."

In order to investigate the content of particulate iron in near-surface waters in an offshore and an inshore situation in the Tropical Eastern Pacific, and in order to investigate in somewhat more detail the nature of the distribution of particulate iron, two series of data have been collected: (1) replicate samples at two depths (ca. 10 meters and 65 meters) at nine stations in the Panama Bight, offshore from Panama and Colombia, occupied during November 1955 on the "Eastropic" expedition of the Scripps Institution of Oceanography; (2) replicate samples at two depths (10 meters and 30 meters, near the bottom) at a fixed inshore station in the Gulf of Panama occupied at biweekly intervals from December 1954 to December 1955. The latter series of data was part of a time-series observation of a number of physical and biological properties at this station made by personnel of the Inter-American Tropical Tuna Commission in connection with a study of the ecology of the Gulf of Panama. Replicate samples were also taken on one occasion at two other locations in the Gulf of Panama, and from a river flowing into the Gulf.

In every case, the analysis for particulate iron was made on a sample of approximately one liter of seawater, following the procedures of Lewis and Goldberg (1954). The

Contributions from the Scripps Institution of Oceanography, New Series, No. 1022

Reproduced by Permission

analyses were made by Mr. Minoru Koide, Research Chemist of the Scripps Institution of Oceanography, whose assistance in this study is gratefully acknowledged. The basic data are presented in Tables 1, 3, and 5, the concentrations of particulate iron being expressed as micrograms per liter of water.

TABLE 1. *Particulate iron content of replicate samples at nine stations in the Panama Bight*

Station No.	Position Lat. N	Position Long. W	Date		Particulate iron micrograms per liter "Shallow"	Particulate iron micrograms per liter "Deep"
ET-H-46	5° 00′	78° 09′	14 Nov. 1955		9.7	1.5
					12.6	13.0
					72.8	9.6
				mean	31.7	8.0
ET-H-47	5° 49′	78° 31′	15 Nov. 1955		18.2	11.1
					9.1	22.9
					16.1	12.9
				mean	14.5	15.6
ET-H-48	6° 52′	78° 54′	15 Nov. 1955		4.6	2.2
					8.4	8.4
					5.6	7.1
				mean	6.2	5.9
ET-H-49	7° 42′	79° 20′	16 Nov. 1955		8.8	14.7
					30.2	6.3
					5.1	6.2
				mean	14.7	9.1
ET-H-49A	8° 20′	79° 21′	16 Nov. 1955		6.4	6.7
					2.6	4.1
					9.3	10.7
				mean	6.1	7.2
ET-H-52	5° 43′	80° 31′	19 Nov. 1955		22.0	4.4
					82.0	11.9
					10.9	12.4
				mean	38.3	9.6
ET-H-53	4° 37′	81° 02′	20 Nov. 1955		9.1	4.2
					0	4.0
					6.6	6.2
				mean	5.2	4.8
ET-H-54	4° 08′	81° 48′	20 Nov. 1955		12.4	3.6
					9.1	9.1
					41.1	2.4
				mean	10.9	5.0
ET-H-55	3° 01′	82° 15′	21 Nov. 1955		6.6	2.8
					2.0	2.8
					7.2	3.0
				mean	5.3	2.9
			Arithmetic means of all observations		15.9	7.7
			Means of all observations, derived from transformed data		19.5	7.4
					$\underbrace{19.5 \quad 7.4}_{12.2}$	

OBSERVATIONS AT STATIONS IN THE PANAMA BIGHT

The positions of the nine stations, which were located in the Panama Bight, are given in Table 1 and are shown by solid circles in Figure 1. At each of these stations three one-liter samples were taken from each of the two depths. The "shallow" samples were taken in the mixed layer, with a wire length of 10 meters, except for ET-H-48 where only 5 meters were used. The "deep" samples were all taken with 65 meters of wire out, which, at every station, corresponded to a point within the thermocline, below the mixed layer (Anon. 1956). The content of particulate iron is shown in Table 1 for each sample, together with the means for each depth at each station, and the grand mean of all observations for each of the two depths. The average content of particulate iron at these stations appears to be very similar to that found by Goldberg and Lewis in the upper layer of the sea near the coast of California (their Figure 1) and and at their stations 7, 12, and 20 in the Northeast Pacific.

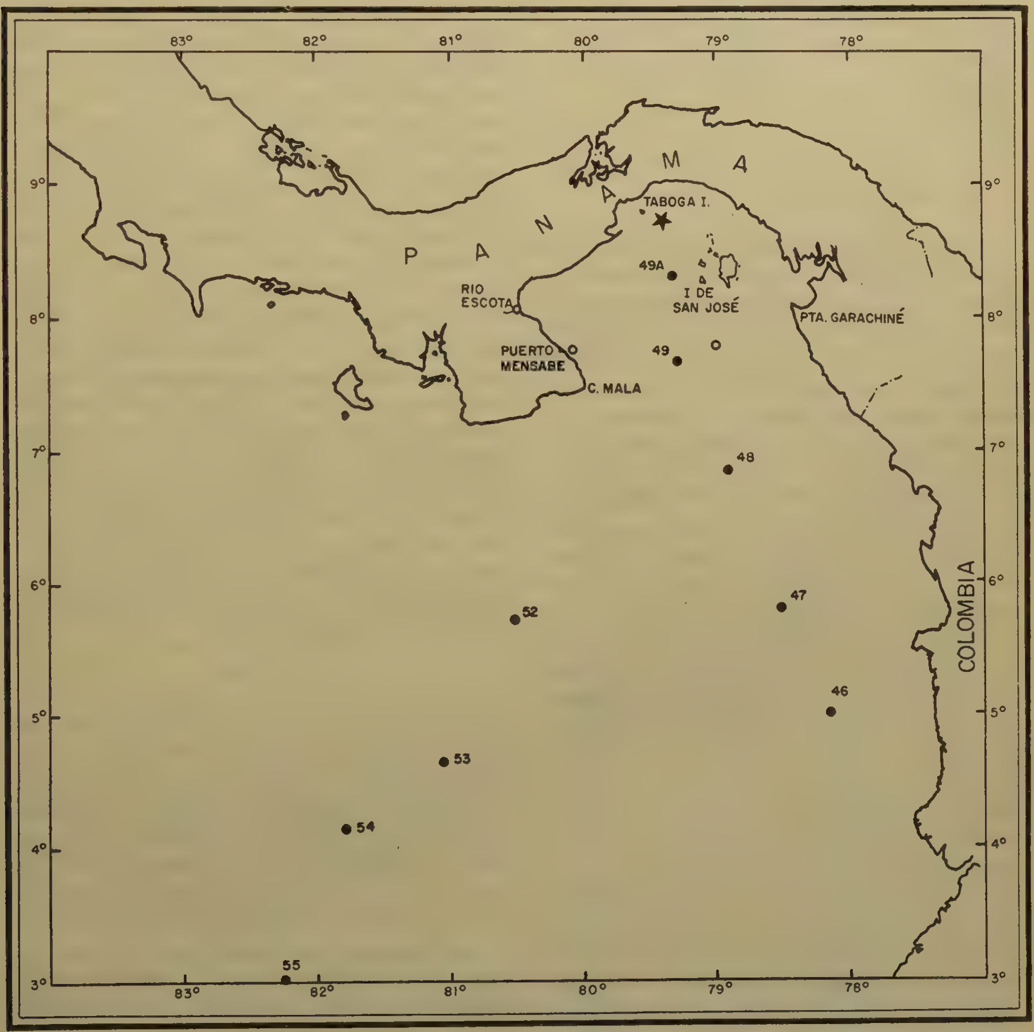
83°
82°
81°
80°
79°
78°
9°
8°
7°
6°
5°
4°
3°
PANAMA
TABOGA I.
49A
I DE SAN JOSÉ
RIO ESCOTA
PUERTO MENSABE
C. MALA
49
PTA. GARACHINÉ
48
52
47
COLOMBIA
46
53
54
55

FIG. 1. Gulf of Panama and Panama Bight, showing locations at which samples were taken for particulate iron.

TABLE 2. *Analyses of variance of samples from the Panama Bight*

Source of variation	Degrees of freedom	Sum of squares	Mean square	Variance ratio
Raw data				
Total	53	11,751		
Depths	1	932	932	4.86*
Stations	8	2,338	292	1.53
Interaction	8	1,583	198	1.03
Samples at same position	36	6,897	192	
Transformed data				
Total	53	10.7011		
Depths	1	0.5451	0.5451	3.12
Stations	8	2.5938	0.3242	1.86
Interaction	8	1.2796	0.1599	0.92
Samples at same position	36	6.2832	0.1745	

* Significant at 5% level

An analysis of variance[1] of the raw data (Table 2) indicated that there was possibly a difference in the mean iron content at the two depths, but that there was no reason to suspect any differences between stations, and there was apparently no significant station-depth interaction. Comparing the variances among all samples for each of the two depths, a ratio of 15.85 was obtained, which is highly significant and indicates that possibly there was a difference in the variance about the mean values of the two depths. This analysis assumes, of course, normality in the distribution which was in fact not true. Since, however, deviations from normality tend to err in the direction of giving significant results when they do not really exist (Barnes 1952, p. 63), rather than the contrary, the conclusions from the analysis of variance of the raw data that there was no significant difference between stations was deemed sufficient basis for amalgamating all observations at each depth to examine the nature of the distributions. The variances among all samples at each depth (judged by a Chi-square test) were clearly larger than the mean, so that the iron content was not distributed according to a single Poisson distribution. It was apparent that the iron content follows some type of "contagious" distribution.[2]

To describe observations of this kind there have been proposed several types of distribution functions, which may be employed to transform the data so that they will satisfy the conditions for analysis of variance. A suitable transformation may be selected from examination of the relationships between the means and variances of the observations. For discussion of the various types of transformations that may be employed to normalize "contagious" distributions, and the criteria upon which they may be selected, the reader is referred to Barnes (1952) and Anscombe (1950). We have, therefore, computed the means and variances for each of the sets of three replicate observations given in Table 1. In Figures 2 and 3 are plotted the means and standard deviations (square root of the variance) for the nine sets of observations at the "shallow" and "deep" sampling levels, respectively. It may be seen that, in each case, the standard deviation is roughly proportional to the mean, although the proportionality constant appears to be smaller for the deep than for the shallow observations. This suggests that a logarithmic transformation will stabilize the variance in each case (Barnes 1952). Since there is one zero value, it is necessary to add a constant to all the values before taking the logarithms. We have, therefore, employed the transformation

$$X' = \log_{10}(10X + 1)$$

where X is the particulate iron in μg/liter and X' is the transformed variate.

The effect of this transformation in stabilizing the variances is shown in Figure 4, where the standard deviations of X' are plotted against the mean values of X' for each set of three replicates. It may be seen that these means and standard devia-

---

[1] Analysis of variance in this paper follows the methods of Snedecor, 1946, Chapter 11.

[2] A distribution is "contagious" when the occurrences of the variate measured are not random in space, but are "clumped" so that the probability of occurrence is not uniform throughout the space.

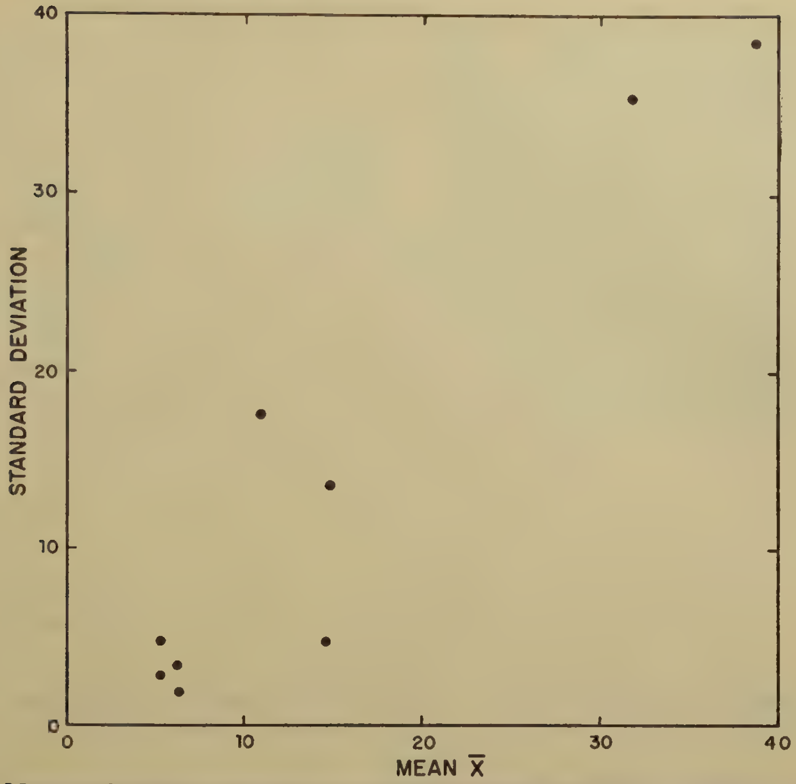

FIG. 2. Means and standard deviations of replicate "shallow" samples for particulate iron in the Panama Bight.

tions are not correlated. Furthermore, comparison of the variances about the means of all samples at each depth indicated no significant difference.

The analysis of variance of the transformed data (Table 2) indicates that there are no significant differences between stations or between depths, and no significant interaction.

It may, therefore, be concluded that the observed values at all stations at both depths in the Panama Bight could have been drawn from a single "population" of iron particles with a contagious distribution. The best estimate of the mean value, obtained from the transformed data, is 12.2 μg/L. This is computed by taking the mean of the transformed values, adding 1.15 times the variance and transforming back (Barnes 1952). This value and similar estimates of the means for the "shallow" and "deep" series are also shown in Table 1.

OBSERVATIONS IN THE GULF OF PANAMA

Serial data from a fixed location in the Gulf

One-liter water samples were taken in replicate, by repeated casts, from two different depths, at bimonthly intervals between December 24, 1954, and December 12, 1955, at a single location in the Gulf of Panama (79°23′ W, 8°45′ N) about 10 miles southeast of Taboga Island, shown by a star in Figure 1. At this location the depth of the Gulf is about 40 meters, varying with the stage of the tide, which has a spring range in the Gulf of Panama of about 5 meters. With a few exceptions three samples were taken from the surface and three from 30 meters. The exceptions were the omissions of one surface sample on April 5 and one deep sample each on May 3 and August 22. The deep samples on April 19 were taken at 40 meters instead of 30 meters, but this has been disregarded in subsequent

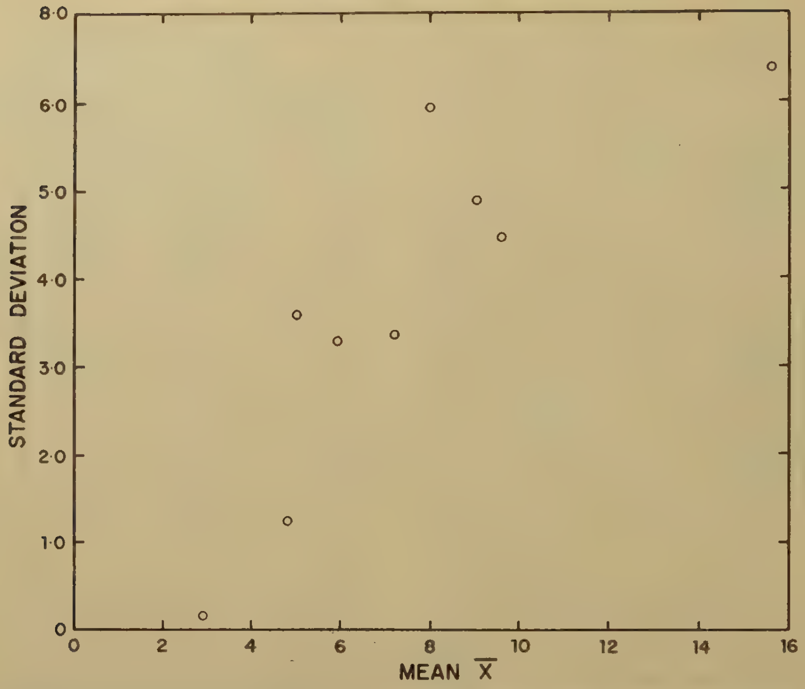

FIG. 3. Means and standard deviations of replicate "deep" samples for particulate iron in the Panama Bight.

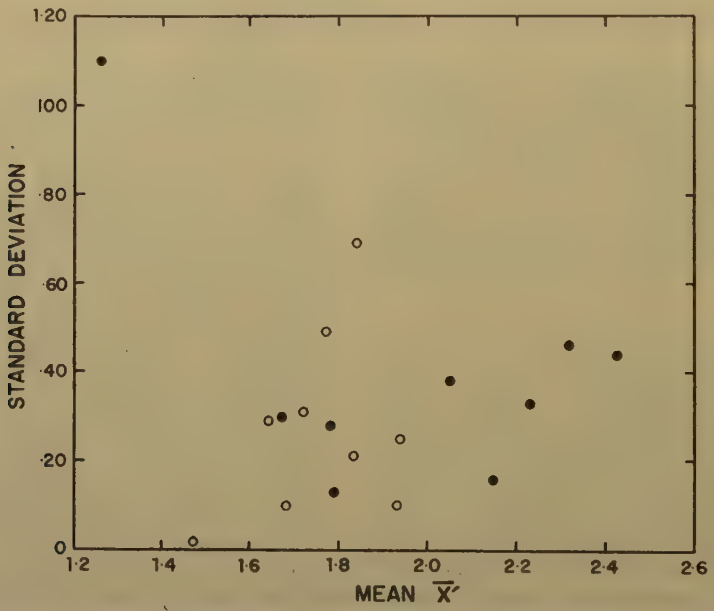

FIG. 4. Means and standard deviations of logarithmic transformation of values of particulate iron in sets of replicate samples in the Panama Bight. Solid circles represent "shallow" samples; open circles represent "deep" samples.

(546)

analyses, since the values of the iron content were well within the range of those obtained at 30 meters on other dates. The basic data, together with the mean values for each depth at each station and the grand means of all observations at each depth, are given in Table 3. Salinity values at the surface and 30 meters are also tabulated; salinities were determined by the standard method of titration with silver nitrate.

It may be noted that the average particulate iron content of these inshore waters is several times higher than that of offshore waters in the Panama Bight. It also appears that the particulate iron is, on the average, more abundant in the surface samples than at 30 meters. Here again, however, there is rather considerable variation among replicates and among the means of the samples taken on different dates.

The large variability among replicates suggests that we are again dealing with some contagious distribution. Therefore, we have plotted in Figures 5 and 6 for the surface and 30-meter samples, respectively, the means and standard deviations of each set of replicate samples. It may be seen from these figures that the variances are too large relative to the means to apply the Poisson distribution, and that the standard

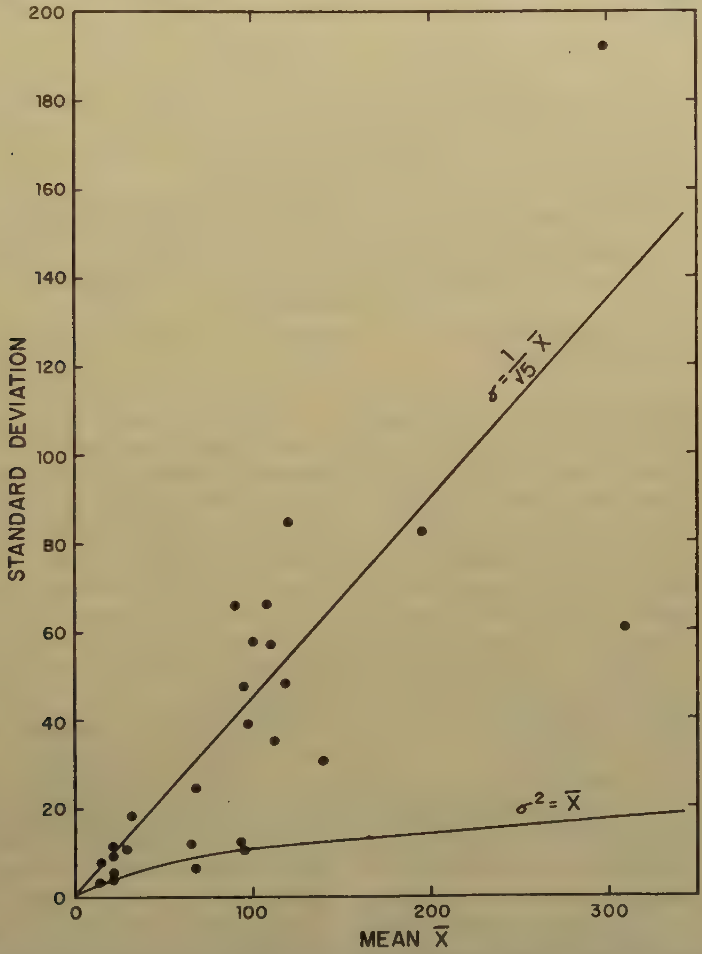

FIG. 5. Means and standard deviations of replicate surface samples for particulate iron at the fixed location in the Gulf of Panama.

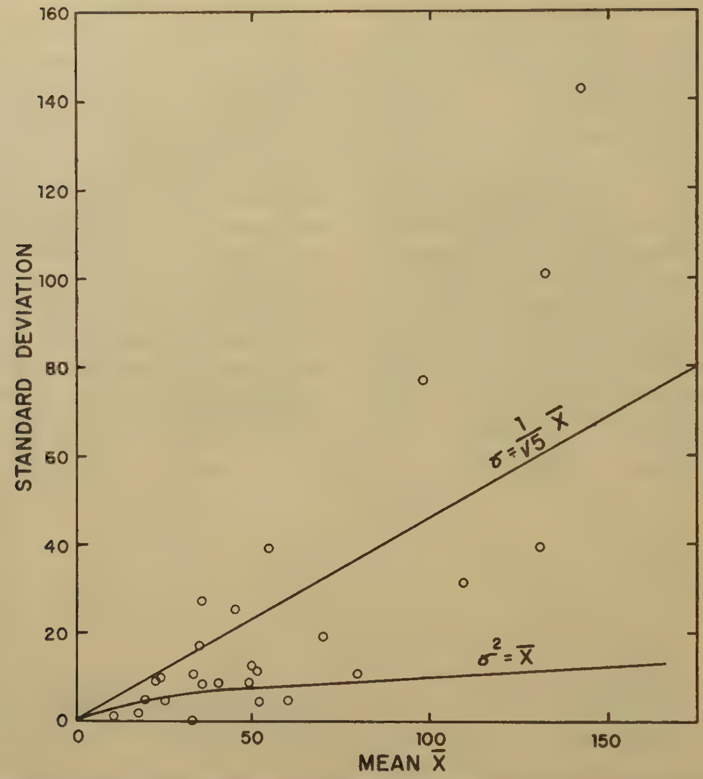

FIG. 6. Means and standard deviations of replicate 30-meter samples for particulate iron at the fixed location in the Gulf of Panama.

deviations appear to be roughly proportional to the means, the proportionality constant being, in each case, close to $1/\sqrt{5}$. A logarithmic transformation should, therefore, stabilize the variance and permit the use of analysis of variance to compare depth and time differences. We have, therefore, employed the transformation $X' = \log_{10} X$.

In Figure 7 are shown graphically the means of the logarithms of the measurements of particulate iron, at each depth at each station, and also the salinities at corresponding stations and depths.

In Figure 8 are plotted, for each set of replicate samples, the mean of X' against the standard deviation. It may be seen that, while the standard deviations show much scatter, they are no longer correlated with the means. We have employed this transformed variate in analysis of variance to examine differences among stations and depths (Table 4).

It may be seen that, considering all observations, there were much greater differences between the average values at each of the two depths, and among the average values from station to station, than could be expected from the variability observed among replicate samples. That the difference between depths is not consistent at different stations (dates) is shown by the significantly high depth-station interaction.

It may be noted, however, from Figure 7 that up to July or August the iron content seems to be consistently higher at the surface than at 30 meters. It has been shown by Schaefer (1957, Fig. 10) that the plankton organisms are more abundant at this location in the Gulf of Panama during the first half of the year than subsequently, presumably due to the effects of upwelling from January to April. It may be, therefore, that the particulate iron content is

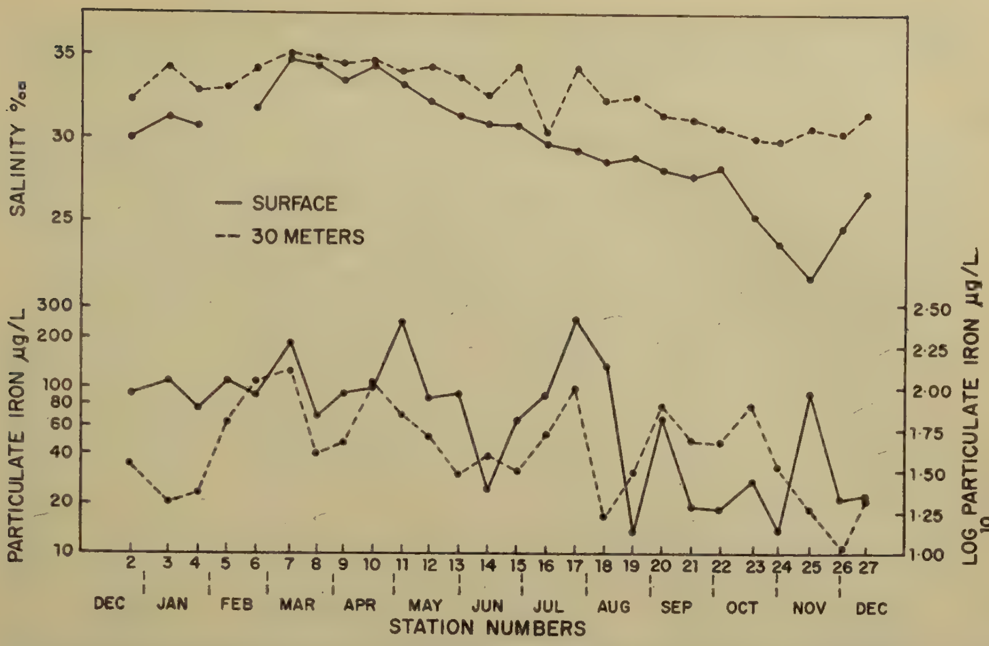

FIG. 7. Mean values of logarithm of particulate iron and values of salinity at the surface and 30 meters at the fixed location in the Gulf of Panama.

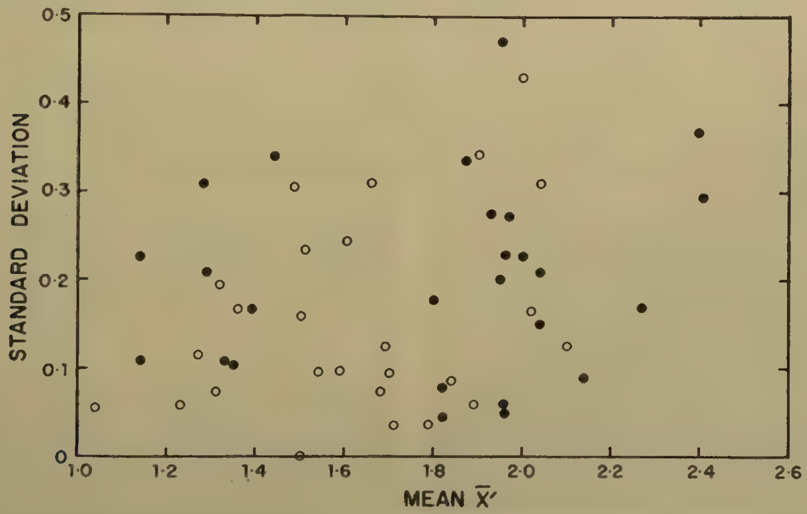

FIG. 8. Means and standard deviations of logarithmic transformation of values of particulate iron in sets of replicate samples taken at the fixed location in the Gulf of Panama. Solid circles represent surface samples; open circles represent 30-meter samples.

maintained at a higher level near the surface during the early part of the year by biological action, but that later in the year this effect is no longer evident. In order to examine this, we have made separate analyses of the particulate iron data for Stations 2–16 (24 December 1954 through 11 July 1955) and for Stations 17–27 (25 July 1955 through 12 December 1955).

During the early part of the year the mean

TABLE 3. *Particulate iron content of replicate samples at a fixed location in the Gulf of Panama (79° 23′ W 8° 45′ N.) occupied at bimonthly intervals from December 1954 to December 1955*

Station number	Date	Particulate iron, micrograms per liter								Salinity ‰[2]	
		Surface			Means (arithmetic)	Deep (30 meters)			Means (arithmetic)	Surface	30 meters
2	24 Dec. 1954	167.0	69.2	64.8	100.3	45.5	29.9	32.5	36.0	30.01	32.4
3	11 Jan. 1955	133.0	72.8	134.0	113.3	21.9	31.0	24.8	25.9	31.16	34.2
4	25 Jan. 1955	163.0	35.9	70.2	89.7	17.9	35.6	18.4	24.0	30.77	32.9
5	8 Feb. 1955	153.3	138.3	63.1	118.2	55.6	62.5	65.2	61.1	(lost)	33.0
6	22 Feb. 1955	105.0	129.0	53.2	95.7	82.3	249.0	65.2	132.2	31.76	34.2
7	10 Mar. 1955	166.0	135.0	290.0	197.0	175.0	117.0	100.0	130.7	34.67	35.0
8	23 Mar. 1955	77.4	68.8	53.1	66.4	23.9	73.3	37.5	44.9	34.41	34.8
9	5 Apr. 1955	101.0	83.6	—	92.3	39.9	24.0	98.4	54.1	33.21	34.5
10	19 Apr. 1955	60.6	95.8	172.0	109.5	113.0[1]	145.0[1]	67.8[1]	108.6	34.20	34.6
11	3 May 1955	359.0	468.0	96.4	307.8	84.0	56.7	—	70.4	33.16	34.0
12	16 May 1955	122.0	125.0	41.0	96.0	47.7	63.8	41.9	51.1	32.10	34.3
13	30 May 1955	180.0	89.5	51.0	106.8	67.7	19.8	20.3	35.9	31.42	33.6
14	13 Jun. 1955	21.1	38.0	18.3	25.8	41.6	47.5	30.6	39.9	30.99	32.6
15	27 Jun. 1955	70.2	89.1	40.3	66.5	21.5	42.9	33.4	32.6	30.86	34.4
16	11 Jul. 1955	189.0	144.0	25.6	119.5	47.4	55.9	52.0	51.8	29.59	30.4
17	25 Jul. 1955	255.0	128.0	507.0	296.7	306.0	76.3	44.2	142.2	29.29	34.2
18	8 Aug. 1955	132.0	173.0	113.0	139.3	16.4	19.5	15.0	17.0	28.65	32.3
19	22 Aug. 1955	11.1	18.5	13.1	14.2	31.6	31.4	—	31.5	28.98	32.5
20	5 Sept 1955	69.6	68.9	58.2	65.6	83.2	86.5	66.9	78.9	28.16	31.5
21	19 Sept 1955	12.0	31.6	19.1	20.9	41.4	64.2	44.2	49.9	27.84	31.1
22	3 Oct. 1955	8.1	24.8	31.0	21.3	42.6	58.0	44.8	48.5	28.33	30.6
23	19 Oct. 1955	44.9	11.5	40.5	32.3	37.9	184.7	71.2	97.9	25.20	30.0
24	31 Oct. 1955	13.8	8.1	23.1	15.0	51.9	17.8	36.0	35.2	23.61	29.9
25	15 Nov. 1955	104.4	90.0	83.3	90.6	13.9	24.0	18.7	18.9	21.68	30.6
26	1 Dec. 1955	27.7	21.5	16.8	22.0	10.5	9.9	12.5	11.0	24.61	30.4
27	12 Dec. 1955	17.1	24.1	27.3	22.8	12.6	30.2	23.7	22.2	26.82	31.5
Arithmetic means					94.2				56.0	29.66	32.67
Means derived from transformed data					86.4				55.9		

[1] Taken at 40 meters

[2] Surface salinities are observed values. 30 meter salinities are interpolated values.

logarithms of particulate iron content were 1.9569 at the surface and 1.6863 at 30 meters. Corresponding means of 115.2 and 62.1 μg/L respectively are obtained when each mean logarithm is added to 1.15 times its variance and transformed back to the original units. It is shown clearly by Table 4 that this difference is highly significant. The analysis of variance for these stations shows also that there was, during this period, more variation among the values obtained on different dates than could be expected from the variation among replicates, but the fact that the depth-station interaction is non-significant demonstrates that the depth difference is consistent from station to station.

During the latter part of the year the mean logarithms of particulate iron content were 1.5708 at the surface and 1.5491 at 30 meters. Corresponding means of 64.2 and 46.6 μg/L respectively are obtained when each mean logarithm is added to 1.15 times its variance and transformed back to the original units. It is evident from the analysis of variance that this small difference is no greater than could be expected from the variability among replicates. During this period, however, there is a significantly high variation among station means and significant station-depth interaction. This indicates that the differences between values obtained at the two depths on different dates were significantly high with respect to the variations among replicates, but that the depth differences were not consistent from station to station.

It may be seen from Figure 7 that the

salinity at this location in the Gulf of Panama declined progressively during the period May-November, the decline being more rapid at the surface than in the deeper layers. This corresponds to the period of heavy rainfall, which reaches a maximum in October. It seemed possible that the precipitation differentially diluting the surface layer might sufficiently decrease the particulate iron per unit volume to mask any effect of biological activity in maintaining a concentration near the surface. We have, therefore, also calculated the iron/salinity ratio for each of our samples. The station means of the logarithms of this ratio for each depth are shown graphically in Figure 9. It may be seen that this graph exhibits the same general features as Figure 7, indicating a higher iron/salinity ratio at the surface than at 30 meters during the early part of the series, but no apparent difference in the latter part of the year. To examine this critically, we have made an analysis of variance of these data, again treating separately the observations for Stations 2–16 and 17–27. Results were the same as before, *i.e.*, a highly significant difference between depths for the first period and no significant difference between depths for the last part of the series. The differential concentration of particulate iron in the surface water is, therefore, demonstrable only during the early part of the year, and is very likely due to the biological activity of the large numbers of plankton organisms present during that time.

TABLE 4. *Analyses of variance of logarithms of particulate iron in samples taken at the fixed location in the Gulf of Panama*

Source of variation	Degrees of freedom	Sum of squares	Mean square	Variance ratios
All observations:				
Total	152	21.7028		
Depths	1	1.0153	1.0153	1.0153/0.0454 = 22.36† 1.0153/0.2083 = 4.87*
Stations (dates)	25	10.8919	0.4357	0.4357/0.0454 = 9.60†
Interaction	25	5.2076	0.2083	0.2083/0.0454 = 4.59†
Replicates (samples at same position)	101	4.5880	0.0454	
Early (Stations 2–16)				
Total	87	8.7068		
Depths	1	1.6112	1.6112	1.6112/0.0487 = 33.08†
Stations (dates)	14	3.1970	0.2284	0.2284/0.0487 = 4.69†
Interaction	14	1.0739	0.0767	0.0767/0.0487 = 1.57
Replicates (samples at same position)	58	2.8247	0.0487	
Late (Stations 17–27)				
Total	64	10.4394		
Depths	1	0.0077	0.0077	0.0077/0.0410 = 0.19
Stations (dates)	10	5.1385	0.5139	0.5139/0.0410 = 12.53†
Interaction	10	3.5300	0.3530	0.3530/0.0410 = 8.61†
Replicates (samples at same position)	43	1.7632	0.0410	

* Significant at 5% level.
† Significant at 1% level.

Other data from the Gulf of Panama

On 29 and 30 November 1955 replicate samples of approximately one liter each were taken at a depth of 10 meters at two other locations in the Gulf of Panama and analyzed for particulate iron. The data are reported in Table 5 and the positions of the stations shown in Figure 1 by open circles.

Puerto Mensabe is located on the western shore of the Gulf, about 20 miles inside Cape Mala. Results from the samples from this inshore location are quite similar to the values obtained during the latter part of the year at the location near Taboga Island (Table 3), which is also fairly well inshore; the mean logarithm for the Puerto Mensabe station is 1.4262, whereas for the fixed station in the Gulf of Panama during the latter part of the year the mean logarithms were 1.5708 at the surface and 1.5491 at 30 meters.

The location off San José Island is, on the contrary, well out in the Gulf, being not far from Station ET-H-49 of the Panama Bight sampling series. At this offshore location the particulate iron values are similar to those obtained at 10 meters at other locations in the Panama Bight (Table 1). However, the difference between the mean logarithm of the values at this single location (1.1517) and the mean logarithm of surface samples at the fixed location near Taboga Island in the latter part of the year (1.5708) cannot be judged as necessarily significant in the light of the sampling variance of 0.5139 (Table 4) among values obtained at the same location on different dates.

These results suggest that there may be

an offshore gradient of particulate iron in the Gulf of Panama, and this together with the obvious difference between the values obtained inshore in the Gulf and offshore in the Panama Bight, further suggests that the iron is coming in from the land.

This appears to be confirmed by samples taken from the Río Escota, a tributary of the Río Santa María, which flows into the west side of the Gulf of Panama (Bahía Parita). The position is shown by an open circle in Figure 1. These samples were from estuarine waters, since the lower reaches of these rivers are actually estuaries. Two samples of one liter each were taken on 20 November 1955. Because of the turbidity it was not possible to pass the entire samples through a millipore filter. Consequently, the particulate iron was measured in aliquots of 370 ml for one sample and 300 ml for the other, giving 692 and 863 $\mu g/L$ respectively (Table 5). It may be seen that the particulate iron content of these samples is a great deal higher than that of samples taken in the Gulf.

TABLE 5. *Other particulate iron samples from the Gulf of Panama*

Position	Date	Depth	Particulate iron micrograms per liter	$\log_{10}$
28 miles SSE of Southern end of San José Island	29 Nov., 1955	10 meters	18.6 13.1 11.7	1.2695 1.1173 1.0682
			mean 14.5	1.1517
5 miles E of Puerto Mensabe	30 Nov., 1955	10 meters	26.3 25.7 28.1	1.4200 1.4099 1.4487
			mean 26.7	1.4262
Rio Escota (8° 04′ 30″ N, 80° 29′ 30″ W)	20 Nov., 1955	Surface	692 863	
			mean 778	

DISCUSSION

It has been shown that both in the offshore waters of the Panama Bight and in the inshore waters of the Gulf of Panama the content of particulate iron exhibits "contagious" distributions. For the statistical analysis of samples from such distributions by the analysis of variance, it is necessary to employ a transformation to approximately normalize the distributions. A logarithmic transformation appears to be adequate for this purpose in the case of our data on particulate iron. Re-examination of the data of Lewis and Goldberg (1954) from their Stations 7, 12, 20, and 47 in the Northeast Pacific also indicates that the sampling distributions of particulate iron at these locations were of a similar type.

It may be that the contagious type of distributions of particulate iron is due in

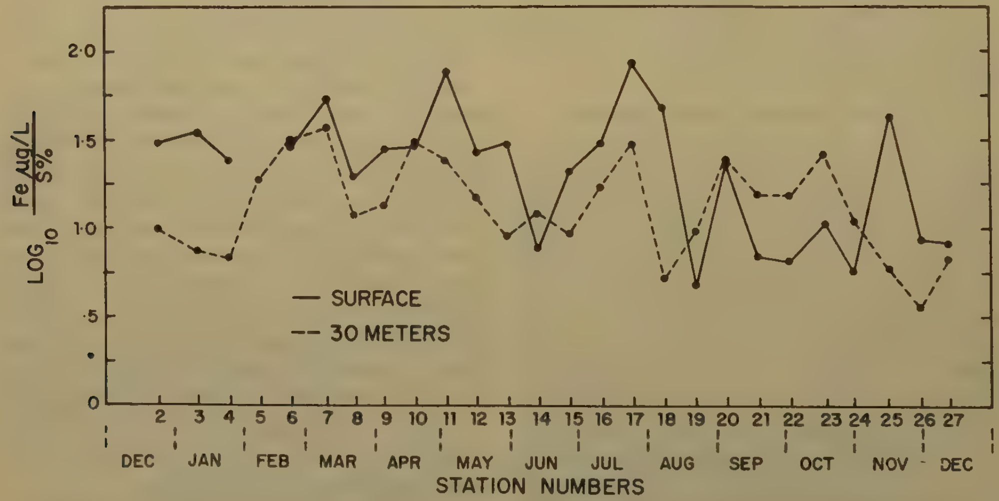

FIG. 9. Logarithms of iron-salinity ratio at the fixed location in the Gulf of Panama.

large part to the activity of the marine biosphere, as concluded by Lewis and Goldberg. This, however, is not *necessarily* true. Such distributions *could* arise from the occurrence of particles of iron of a variety of sizes, each size being distributed in the water completely at random (Anscombe 1950). It would be desirable to examine the distributions of particle sizes in order to investigate this matter further.

On the other hand, the occurrence of significantly higher average particulate iron content, at least on some occasions, associated with the marine biosphere, indicates that the organisms do modify the distribution of iron due to purely physical processes. Lewis and Goldberg's data show that the iron content of the upper 500 meters at some stations in the Northeastern Pacific is significantly greater than in deeper layers. (This result is obtained even when their data are re-analyzed employing a logarithmic transformation to normalize the sampling distribution.) The observations from off Taboga Island in the Gulf of Panama indicate clearly that the particulate iron content at the surface is higher than at 30 meters during the period of high standing crops of plankton organisms.

There is rather good evidence that the iron in the region of the Gulf of Panama and Panama Bight is being brought into the sea by runoff from the land. Particulate iron in the lower reaches of one of the rivers flowing into the Gulf was found to be much higher than the iron content at an inshore location in the Gulf, and the latter in turn is significantly greater than the iron content at offshore stations in the Panama Bight. A single group of 3 replicates from the outer part of the Gulf of Panama off San José Island showed a mean iron content comparable to the values encountered elsewhere in the Panama Bight; however, since this value was within the range of sampling variation at the inshore station near Taboga Island, this particular evidence of an offshore gradient of particulate iron in the Gulf is not conclusive.

Since the particulate iron content of inshore waters in the Gulf is higher than at locations offshore in the Panama Bight, and since the latter are biologically very productive (Holmes, Schaefer, and Shimada 1957), it seems unlikely that iron can be a limiting factor on phytoplankton growth in these inshore waters.

REFERENCES

ANONYMOUS. 1956. Data collected by Scripps Institution vessels on "Eastropic" expedition, September–December 1955. Univ. Cal., Scripps Inst. Oceanogr.; SIO Reference 56–28, 15 October 1956 (mimeographed). 156 pp.

ANSCOMBE, F. J. 1950. Sampling theory of the negative binomial and logarithmic series distributions. Biometrika, **37**: 358–382.

BARNES, H. 1952. The use of transformations in marine biological statistics. J. Cons. Int. Explor. Mer, **18** (1): 61–71.

GOLDBERG, E. D. 1952. Iron assimilation by marine diatoms. Biol. Bull., Woods Hole, **102**: 243–248.

HARVEY, H. W. 1937. The supply of iron to diatoms. J. Mar. Biol. Assoc. U. K., **22**: 205–219.

HOLMES, R. W., M. B. SCHAEFER, AND B. M. SHIMADA. 1957. Primary production, chlorophyll, and zooplankton volumes in the tropical Eastern Pacific. Inter-Am. Trop. Tuna Comm., Bull., **2** (4): 127–169.

LEWIS, G. J., AND E. D. GOLDBERG. 1954. Iron in marine waters. J. Mar. Res., **13** (2): 183–197.

SCHAEFER, M. B. 1957. Report on the investigations of the Inter-American Tropical Tuna Commission for the year 1956. Inter-Am. Trop. Tuna Comm., Ann. Rep. for 1956. *In press.*

SNEDECOR, GEORGE W. 1946. Statistical methods. Iowa State College Press: Ames, Iowa, USA. 485 pp.

(*Reprinted from Nature, Vol.* 182, *pp.* 601–602, *August* 30, 1958)

Observations of the Pacific Equatorial Undercurrent

We have succeeded in measuring the flow of the Pacific Equatorial Undercurrent first described by Cromwell, Montgomery and Stroup[1]. Taut-wire buoys[2] were anchored in 2,300 fathoms as reference points. Measurements at different depths were made by suspending a modified Roberts current meter[3] from a drifting ship. A vibrotron pressure element was used to give the depth of the meter, and the drift of the ship relative to the anchored buoy was measured by radar. To define the bottom of the undercurrent four measurements were made with Swallow type neutral buoyant floats[4]. These measurements were the principal object of the Dolphin Expedition March 27–June 10, 1958, one of the special cruises of the International Geophysical Year oceanographic programme.

Five buoys were laid on long. 140° W. at latitudes 2° N., 1° N., 0°, 1° S. and 2° S. Measurements were made from two ships, *Horizon* of the Scripps Institution of Oceanography, University of California, and *Hugh M. Smith* of the Pacific Oceanic Fisheries Investigation, U.S. Fish and Wildlife Service. The equator station was monitored by one ship during April 6–28. The second ship made measurements at the other four buoys in rotation.

On the second half the expedition *Horizon* made measurements with the Roberts meter at 180-mile intervals along the equator from long. 137° W. to 89° W. For these measurements the reference buoy was a free floating parachute drogue[5] with the parachute suspended at 1,000 m. Parachutes at this depth were occasionally used for reference at long. 140° W. and their motion with respect to the anchored buoys was about 0·2 knots.

The Undercurrent is an east-flowing current centred at the equator just below the west-flowing South Equatorial Current. Measurements at long. 140° W. indicate a transport of the order of 30 million cubic meters a second or about the same as the transport of the Florida Current. Measurements along the current indicate that it is at least 3,500 miles long.

At long. 140° W. the Undercurrent is symmetrical about the equator. During the 22-day observational period the highest velocities toward the east were always recorded at the equator and at a depth of 100 ± 13 m. The velocities in this core were between

Contributions from the Scripps Institution of Oceanography, New Series, No. 1023
Reproduced by Permission

two and three and a half knots. During this period the South Equatorial Current was flowing westward at speeds between half a knot and one and a half knots.

The top and bottom of the Undercurrent are at about 30 and 300 m. respectively for 0°, 140° W. The Swallow drogues indicate a small flow to the west between 500 and 700 m.

The Undercurrent becomes thinner and weaker on either side of the equator. At 2° N. and S. the average thickness was 30 m. and the average maximum velocity was 0·6 knots.

Measurements made along the equator showed no diminution in the core velocity between long. 140° and 95° W. At 92° W. (25 miles west of San Isabela Island in the Galapagos) the core velocity was 1·2 knots. At 89° W. (east of the Galapagos) the Undercurrent was missing. The depth of the core rose from 100 m. at 140° W. to 52 m. at 98° W., a slope of $1 \cdot 3 \times 10^{-5}$. Stations of 95° and 92° W. showed the core dipping down. It was at 92 m. at 92° W.

Three days after the completion of these measurements, Townsend Cromwell, who discovered the Pacific Equatorial Undercurrent in 1952 and gave it its present name, was killed in an aeroplane crash near Guadalajara, Mexico, on June 2, 1958, on his way to join another Scripps Institution oceanographic expedition at Acapulco. We would like to suggest that this current be called the Cromwell Current.

JOHN A. KNAUSS

Scripps Institution of Oceanography,
La Jolla, California.

JOSEPH E. KING

Pacific Oceanic Fisheries Investigation,
Honolulu, Hawaii.

July 1.

---

[1] Cromwell, T., Montgomery, R. B., and Stroup, E. D., *Science*, **119**, 648 (1954).

[2] Isaacs, J., Huffer, R. P., and Kidd, L. W., *Science*, **125**, 341 (1957).

[3] Roberts, E. B., "Roberts Radio Current Meter Modified II Operating Manual", 32 (U.S. Dept. of Commerce, Washington, D.C., 1952).

[4] Swallow, J. C., *Deep Sea Res.*, **3**, 74 (1955).

[5] Volkmann, G., Knauss, J., and Vine, A., *Trans. Amer. Geophys. Union*, **37**, 573 (1956).

Printed in Great Britain by Fisher, Knight & Co., Ltd., St. Albans.

DISTURBANCES IN AN IDEALIZED ATMOSPHERE ON A FLAT PLANET WITHOUT ROTATION

By Prof. C. Eckart

The Scripps Institution of Oceanography,
La Jolla, California

I will confine my remarks to the oscillations of a perfect gas about a state of stratified equilibrium. The stratification is assumed to have been produced by gravity. Both the curvature and rotation of the earth's surface have been neglected. The equilibrium pressure, P_0 , and the equilibrium density, ρ_0 , are functions of the vertical coordinate only and are connected through the relation

$$\frac{dP_0}{dZ} = -\rho_0 g \qquad (1)$$

In order to solve this equation, it is necessary to know both the equation of state and the temperature distribution. The equation of state of an ideal gas can be written in the form

$$P_0 V_0 = R\theta_0 \qquad (2)$$

The equation of the adiabatics will also be needed—it is

$$PV^\gamma = (\gamma - 1)Ae^{(\gamma-1)\eta/R} \qquad (3)$$

where γ = ratio of specific heats, η = entropy per gram, and A = chemical constant.

I have investigated several quite general temperature distributions, but will here consider only the simplest cases.

$$\frac{d\theta_0}{dZ} = 0 \qquad (4a)$$

$$\frac{d\theta_0}{dZ} = \nu, \qquad \theta_0 = a + \nu Z \qquad (4b)$$

The linear relation may be a fairly good approximation above 80 km. Above this altitude, the temperature gradient is known to be about three degrees per kilometer. At lower levels, the temperature variation is somewhat erratic. In what follows, we will consider that the temperature gradient is positive. A special case of the negative gradient is the so-called adiabatic atmosphere, in which the entropy density does not vary with altitude. Such an atmosphere is on the verge of instability. It follows that all gravitational effects will be exaggerated. There is an additional difficulty which stems from the fact that the temperature goes to absolute zero at some finite altitude.

If the gas executes small oscillations about the equilibrium state, the basic equations can be written in the following linearized form:

(557)

Contributions from the Scripps Institution of Oceanography, New Series, No. 1024
Reproduced by Permission

$$\frac{\partial \vec{U}}{\partial T} + c_0(\nabla + \Gamma\vec{k})P - N^2 Q\vec{k} = 0 \qquad (5a)$$

$$\frac{\partial P}{\partial T} + c_0(\nabla - \Gamma\vec{k})\cdot\vec{U} = 0 \qquad (5b)$$

$$\frac{\partial Q}{\partial T} + \vec{U}\cdot\vec{k} = 0 \qquad (5c)$$

$\vec{k}$ is a unit vector in the vertical direction. N, Γ, and c_0 are the three quantities which introduce the characteristics of the state about which the oscillation is taking place. N has the units of a frequency and is commonly referred to as Väisälä's (or Brunt's) frequency. In an isothermal atmosphere at a temperature of 300°, the Väisälä frequency is one radian per minute. This corresponds to a period of about six minutes. Γ has the dimensions of a reciprocal length and c_0 is the sound velocity in the equilibrium state. The quantities $\vec{U}$, P, and Q are related to the particle velocity $\vec{u}_1$, the differential pressure p_1, and the local entropy variation η_1 through the equations

$$\vec{U} = \vec{u}_1(\rho_0 c_0)^{1/2} \qquad (6a)$$

$$P = p_1(\rho_0 c_0)^{1/2} \qquad (6b)$$

$$Q = (\eta_1/\eta_0')(\rho_0 c_0)^{1/2} \qquad (6c)$$

η_0' is the entropy gradient in the equilibrium state. It is evident that in a nearly adiabatic atmosphere a small oscillation in the local entropy will cause a large oscillation in Q. This may be taken as an indication of the singular character of the adiabatic atmosphere.

(5a) and (5b) are simply statements of the equations of motion and of mass conservation. (5c) states that the entropy of a given mass of gas does not change as it moves. This does not mean that the entropy at a fixed point is constant. In the course of time, a fixed volume will be occupied by gas from neighboring regions which have different entropy densities. Thus, the entropy at a fixed point will change due to advection.

In the isothermal case, the basic equations are linear with constant coefficients. If we assume a solution of the type

$$\vec{U} = \vec{U}(Z)e^{i(\alpha X + \beta Y - WT)} \qquad (7)$$

the three basic equations can be reduced to two which have the form

$$C_0\left(\frac{d}{dZ} + \Gamma\right)P = (N^2 - W^2)Q \qquad (8a)$$

$$C_0\left(\frac{d}{dZ} - \Gamma\right)Q = \left(1 - \frac{K^2C_0^2}{W^2}\right)P, \qquad (K^2 = \alpha^2 + \beta^2) \qquad (8b)$$

The boundary conditions require that P and Q remain finite as Z approaches infinity and that the vertical velocity vanish at the earth's surface. The second requirement implies that there is no variation in the entropy at the earth's surface.

The region of the W–K plane in which permissible solutions lie is indicated in Figure 1. The points which lie on the 45° line correspond to surface gravity waves. These waves have been investigated by Lamb. They are characterized by a pressure amplitude which decays exponentially with altitude and by no entropy change.

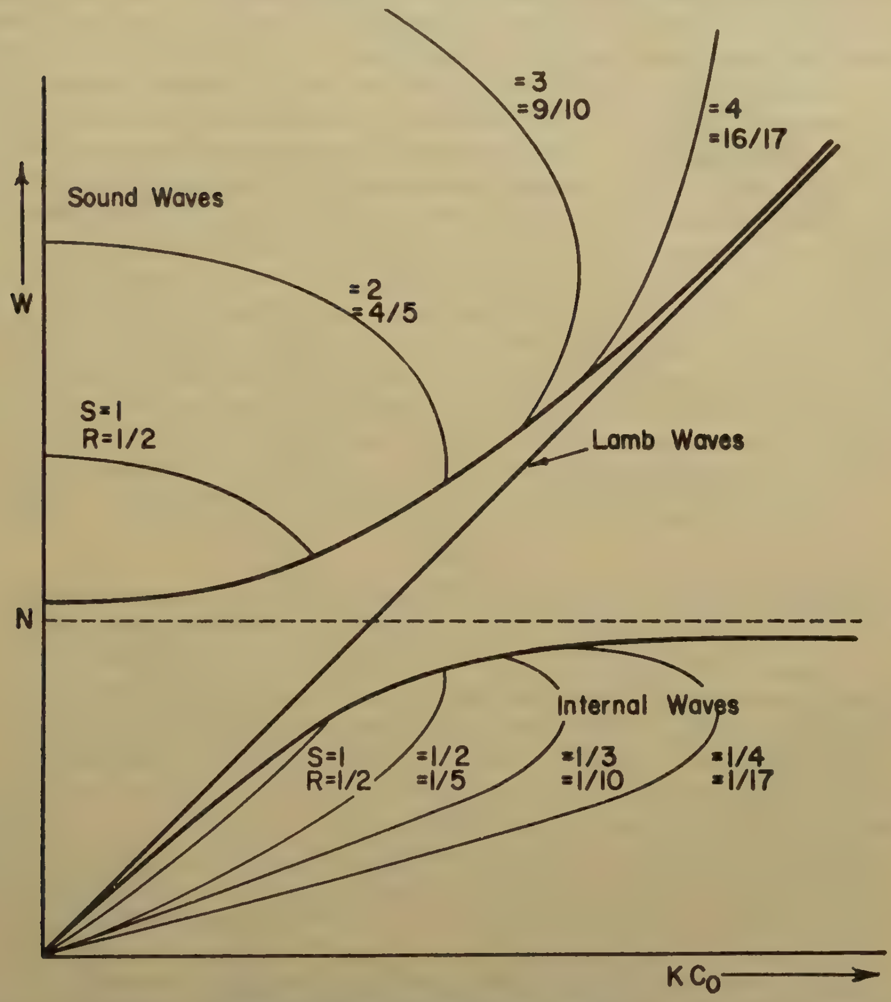

FIG. 1—Points which fall within the "sound wave" and "internal wave" areas and on the line labeled Lamb waves are permissible solutions for the isothermal atmosphere

Points which lie in the forbidden region between the 45° line and the upper and lower curves correspond to solutions which become infinite at high altitudes.

Curves of constant R and S have also been plotted in Figure 1. R is the dimensionless ratio of pressure amplitude to particle velocity, and S is the dimensionless ratio of pressure amplitude to local entropy variation. In the isothermal case, S is a function of R. For large values of W, the quantity R approaches unity and S approaches infinity. This is characteristic of what we ordinarily call sound

(559)

waves. In other words, these are waves in which the pressure and velocity amplitudes are comparable and in which there is no variation of the entropy. In the lower part of the diagram, both R and S can become quite small. This means that a small fluctuation in pressure will produce high velocities and relatively large entropy and temperature oscillations. Both of these phenomena are characteristic of wind and weather. Therefore, even this simplified isothermal case exhibits the most striking characteristics of wind and weather.

If the temperature increases in a linear fashion with altitude, the situation changes radically. The first thing to notice is that the sound rays are no longer straight lines but cycloids. If the frequency is high compared to the Väisälä frequency, the cycloids will be characterized by large curvature at low altitudes and small curvature at high altitudes. If the frequency is less than the Väisälä frequency,

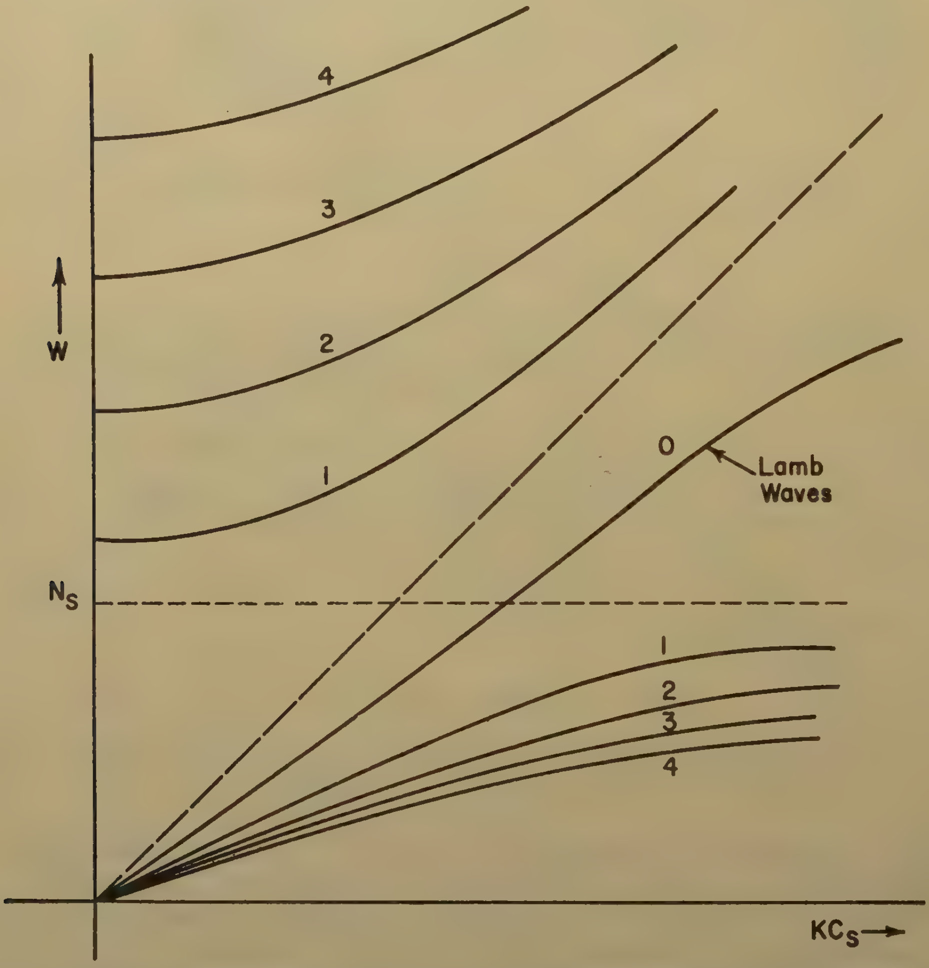

Fig. 2—Points which fall on the curves represent permissible solutions for an atmosphere in which the temperature increases linearly with altitude. The numerals represent the number of pressure nodal planes which lie above the earth's surface in the different modes.

the cycloids will be characterized by large curvature at high altitudes and small curvature at low altitudes. In the second case, the energy propagates in a nearly horizontal direction at low altitudes. In other words, the temperature gradient effectively holds in the mechanical energy. The second thing to notice is that now the points in the W–K diagram (Fig. 2) which lead to permissible solutions lie on a family of curves rather than in certain regions. The quantities N_s and c_s are the values of the Väisälä frequency and the sound velocity at the earth's surface. These curves correspond to oscillations in a sinusoidal sound field which is being propagated along a cycloidal path. Points which lie on a particular curve correspond to a particular mode of oscillation. The label on each curve indicates the number of pressure nodal planes which lie above the surface.

Observations made within the last ten years indicate that the highest layers of the atmosphere actually do exhibit a characterisitc temperature increase. It is probable that the thermosphere, as it is called, is actually the lid on the atmosphere—the thing that prevents the mechanical energy from leaking out. In an isothermal atmosphere, the pressure amplitude decreases and the velocity amplitude increases with decreasing density in such a way that the energy flow remains constant. In the non-isothermal case, both the pressure and velocity amplitudes go to zero with decreasing density. Of course, even if there were no temperature increase, the mechanical energy would be converted to thermal energy at altitudes where the wavelength becomes comparable to the mean free path.

DISCUSSION

F. Press: Why is it that a pulse like that from Krakatoa, which had a predominant period of about an hour, propagated with a velocity which was very close to that of sound in air at sea level?

C. Eckart: In the lower part of the atmosphere, there are low velocity channels. It may be that the energy was trapped in one or more of these low altitude channels. One thing that is fairly clear from the theory is that any disturbance which is localized in the lower part of the atmosphere will travel at the surface with a velocity which is fairly close to the surface value. It is also possible that it was a Lamb wave. In fact, a very low frequency Lamb wave would propagate with a velocity fairly close to the surface value.

J. C. Savage: Is the condition that P and Q remain finite at infinity a sufficient condition?

C. Eckart: One has to become a little sophisticated on this point. In order to demonstrate that these are the right boundary conditions, one must resort to the Hilbert-space theory of differential equations.

J. C. Savage: But physically are they the right boundary conditions? If $\vec{u}_1$ blows up at infinity, it would contradict your linearized theory of sound propagation.

C. Eckart: Not at all. You have several kinds of solutions to deal with, some of which have physical significance. Those which have physical significance contain a finite amount of total energy. The Hilbert-space theory tells you under what conditions you can construct a solution from periodic solutions which contain an infinite amount of total energy. Sometimes you have to deal with physically inadmissible solutions in order to arrive at the physically admissible ones. In other words, you have to make a detour into the Hilbert-space theory of abstract mathematics in order to construct the solutions that you are after. In the course of this detour, you will study solutions which have an infinite amount of energy. All the solutions for the isothermal case, except the Lamb wave, do have an infinite amount of energy. None the less, these solutions do have significance, since you need them in order to construct the physically admissible solutions.

A. T. de Hoop: You have stated that in the non-isothermal atmosphere the rays are cycloids and that the shape of these cycloids is frequency dependent. The usual definition of a ray makes no reference to frequency.

C. Eckart: That is for non-dispersive media.

A. T. de Hoop: It has nothing to do with dispersion.

C. Eckart: I see; you are referring to Hadamard's theory of characteristics, which is often called a theory of rays. This is a theory that can be established rigorously, but applies only to infinite frequencies. That is, it applies to shock waves and to "first arrivals." There is another theory of rays, which was introduced into modern physics by de Broglie, although its roots go back to Hamilton and Jacobi. This theory is approximate, but it is often a very good approximation. It does make the rays dependent on the frequency, and it is this second ray theory to which I refer.

BULLETIN OF THE GEOLOGICAL SOCIETY OF AMERICA
VOL. 69, PP. 1179-1186, 2 FIGS. SEPTEMBER 1958

DEVELOPMENT OF MEDIAN ELEVATIONS IN OCEAN BASINS

BY H. W. MENARD

Introduction

Recent geophysical measurements reveal that ocean basins are profoundly different from continents. The hypothesis that continents formerly existed in some places where ocean basins are now found is correspondingly less acceptable. The hypothesis of epeirogeny in ocean basins, however, is not adversely affected by the geophysical measurements; on the contrary, it is supported, although the evidence is not everywhere compelling.

Geological evidence for widespread epeirogeny in ocean basins dates back to Darwin's theory of the origin of atolls and barrier reefs. The distribution of drowned ancient islands or guyots (Hess, 1946) indicates large additional areas in the ocean basins where great changes in depth have occurred. Epeirogeny may have produced the trans-oceanic land bridges, required by paleontologists and paleogeographers, in the form of transient links (Willis, 1932). Hess (1955) has recently emphasized the role of epeirogeny in ocean basins by proposing that the many oceanic rises and ridges are produced by this mechanism. He suggests that serpentine is formed by the reversible reaction of water with olivine in the mantle, and that the resulting volume change causes epeirogeny.

The evidence and the hypotheses here proposed have been discussed with many colleagues. Comments by Robert Arthur, Walter Elsasser, E. L. Hamilton, R. R. Revelle, and Walter Munk have been particularly helpful. Pre-publication copies of Plate 120, a bathymetric chart of the Pacific Basin, from the new Times Atlas were made available through the kindness of John C. Bartholomew, Jr. This paper represents in part results of research supported by the Office of Naval Research and the National Science Foundation.

Concentration of Submarine Elevations along the Median Line of Ocean Basins

The writer has attempted to locate the median lines of all ocean basins in order to compare them with the locations of submarine elevations. The technique used is to draw a family of lines approximately parallel to and equidistant from the 1000-m contour by swinging arcs, with string and chalk, on a 50-cm diameter globe. The intersections of arcs with equal radii are taken as midpoints, and the midpoints are connected to establish median lines. Thus, not only an entire ocean but also any major convexity of the margin of an ocean has a median line. Examples of convexities are found on the west side of Africa and in the western Pacific in the great curve bounded by New Guinea, the Philippines, and Japan.

The results of this construction (Fig. 1) are shown on a Mercator projection chart along with the best-known locations of the crests of oceanic rises and ridges, and the position of the 1000-m contour used in the construction where it does not closely correspond to a continental margin. In most places the 1000-m contour can be taken, without question, from a good chart. Elsewhere, particularly along the western border of the Pacific, a choice must be made within a zone of islands and basins. The contour selected lies on the continental side of the oceanic basin nearest the continent. Oceanic basins are identified by the rule of Ewing and Press (1955, p. 2), based on earthquake surface waves, that any place deeper than 2000 fathoms is underlain by an oceanic type of crust. Even with the help of this rule, the position of New Zealand remains a puzzle. It may be regarded as a small "continent" or a continental island. It is here considered a continent, and the median lines south of 20°S. Lat. are relative to

Contributions from the Scripps Institution of Oceanography, New Series, No. 1025
Reproduced by Permission

(563)

New Zealand. North of 20° S. Lat. the median lines are relative to Australia and New Guinea although New Zealand would give almost the same position.

basins. However, the process that ceters then rises between continents may not be sensitive to minor bends in the continental margin, or the margins may have shifted since the process began. These uncertainties may justify some experimentation in attempting to obtain an exact fit between the median line and the crest of a rise. For example, by smoothing off relatively pointed continental projections into the Indian Ocean, such as India and Madagascar, and by removing Sumatra and Java, the median line can be superimposed on the crest of the rise and on the main branches of the rise. It would be profitless at this time to attempt to attach meaning to this particular adjustment on geological grounds.

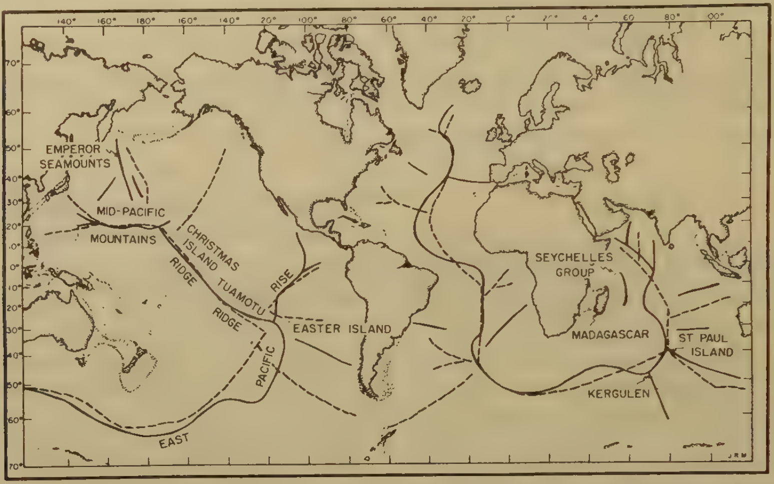

FIGURE 1.—LOCATION OF THE CRESTS OF SUBMARINE MEDIAN RIDGES AND RISES (solid line) COMPARED WITH THE GEOMETRICAL MEDIAN LINE (dashed line) OF THE OCEAN BASINS

Points on the geometrical median line are equidistant from the margins of the continents as indicated by the 1000-m contour. The 1000-m contour is shown by dotted shading where it does not almost coincide with the shore line and where it is pertinent to the construction of the geometrical median line.

Median Elevations of the Atlantic, Antarctic, Indian, and South Pacific Oceans

The median line follows the sinuous crest of the oceanic rises and ridges through the Atlantic, Indian, and Antarctic oceans with remarkable consistency. Even in the south Pacific the two lines agree in trend although they are as much as 1000 km apart. The agreement is particularly noteworthy in the south Indian Ocean where both the crest and the median line branch. Elsewhere the minor branches from the main rise have the same trends and in many places the same positions as the spurs from the central median line. Several prominent features such as the Walvis Ridge and the Newfoundland Rise are not duplicated by spurs, and several spurs are not duplicated by known rises in the south Atlantic. On the whole, however, the discrepancies merely emphasize the generally close agreement in the lines. It is at least not improbable that the agreement signifies a causative relationship—that is, the rises are in the middle because it is the middle.

An objective comparison is possible only if some well-defined line, such as the 1000-m contour, is selected as the edge of the ocean

In the southeastern Pacific the trend and position of the median line and the three spurs toward South America show a close correspondence to the known topography. The crest between New Zealand and Antarctica lies near the median line, at about 55° S. Lat.; however, the crest bends sharply to the east and is about 1000 km east of the median line from the bend to Easter Island. Submarine topography suggests that the bend may be an offset caused by faulting. The spurs of the median line are almost superimposed on the two northern branches of the rise as drawn, but the branches are not in the positions shown on most charts. The positions are based on closely spaced sounding lines taken during the Navy HIGH-

JUMP and DEEPFREEZE expeditions, and on the unpublished soundings of the Scripps SHELLBACK, CAPRICORN, and EASTROPIC and DOWNWIND expeditions. The southernmost branch of the rise and the corresponding median line are roughly parallel but widely separated. As in the Indian Ocean, it is possible to obtain an exact agreement, but the whole of South America south of the Brazilian shield must be removed—which appears unjustified unless the rise is thought to be very old.

The rises and ridges shown on the chart essentially are all parts or branches of one great median elevation. To this extent the chart supports the conclusion of Heezen (1957) that there is a world-girdling rise. However, the existence of the rise may be questioned in some places, and the position of the crest elsewhere may be poorly defined. For this reason the location of the crest as shown in Figure 1 does not agree everywhere with the location shown by Heezen.

Median Elevations of the Central and North Pacific

The median line of the central and north Pacific has four main divisions (Fig. 1): a line trending northwest from Mangareva Island to Johnston Island, and three spurs from Johnston Island trending west, northwest, and northeast. The line is followed from Mangareva to Johnston and thence along the western spur by a series of great submarine ridges which appear to be connected. The southernmost ridge is the extraordinary Tuamotu Ridge with an area of approximately 200,000 sq. km shoaler than 3 km. About 100 atolls and seamounts including guyots are distributed on the ridge. To the northwest is the Christmas Island Ridge which has an area of roughly 100,000 sq. km at or less than 3 km depth and an almost continuous line of atolls, banks, and seamounts along its crest. This ridge abuts the west-trending Marcus-Necker Rise which, in its eastern half (the Mid-Pacific Mountains), has an area of roughly 60,000 sq. km shoaler than 3 km. The Mid-Pacific Mountains includes about 50 seamounts, most of which are guyots, distributed all over the ridge. The Mid-Pacific Mountains and the Tuamotu Ridge and atolls are similar in every respect except that coral has capped the Tuamotu peaks. The three connecting ridges lying along the median line of the Pacific Basin for almost 10,000 km probably would have been named the "Mid-Pacific Ridge" if they had all been discovered at the same time. As it is, the separate names seem adequate. The northwest-trending spur lies somewhat east of, but parallel to, the Emperor Seamounts which include a number of large guyots (Dietz, 1954, p. 1209–1211). The seamounts rise above a continuous narrow ridge at least 1 km high (Bezrukov and Udincev, 1955, translation by E. R. Hope available through the courtesy of the Defense Research Board of Canada). The northeast-trending spur lies in a relatively well-explored part of the Pacific Basin, and it does not appear to be related to any continuous ridge or line of seamounts, although the eastern end of the Mid-Pacific Mountains has a conspicuous northeasterly trend and lies just north of the spur.

Differences in Morphology of Median Elevations

Median elevations of ocean basins include a variety of types which are gradational from very broad rises with gentle slopes to narrow, steep-sided ridges (Fig. 2). If these essentially continuous elevations are produced by the same process, why do different types of topography exist? They might be produced because of regional crustal differences, but seismology attests to the remarkable uniformity of the oceanic crust. Size of basins might have an effect, but the broadest rises and narrowest ridges in the Pacific are at the same distance from continents.

The various gradational forms of median elevations may be stages in development. The following sequence of forms is suggested:

(1) A very broad, seismically active rise with many volcanic islands and seamounts but few if any guyots. The southern East Pacific Rise is an example. Absence of known guyots may somewhat reflect sparse soundings, but many seamounts have been found on this rise, and none are guyots.

(2) A narrower, steeper, seismically active rise with volcanic islands and guyots side by side. The Mid-Atlantic Ridge in the North Atlantic is an example of this stage.

(3) Narrow, steep-sided, seismically inactive ridges lacking volcanic islands but with many guyots and atolls. Examples are the Tuamotu Ridge and Mid-Pacific Mountains.

It is difficult to fix in this sequence the position of the 45,000-mile-long trough that is said to exist on the crest of all oceanic rises (Ewing and Heezen, 1956, p. 80). The writer and his colleagues at Scripps Institution have not observed a continuous trough in the supposed position in the northeastern Pacific. A special survey during the Downwind Expedition did not find any apparant trough for 300 miles along the crest of the East Pacific Rise.[1] It appears that a median trough may not be characteristic of all rises and ridges but only of the intermediate form. The central trough may not yet have formed in the young stage, but what happens to it in the old stage? It may be filled by volcanic rocks. However, parallel troughs have been found in the southern section of the Mid-Atlantic Ridge (Heezen, personal communication). It is possible that the flanks of a broad rise subside on the outside of each trough and that a narrow central ridge remains.

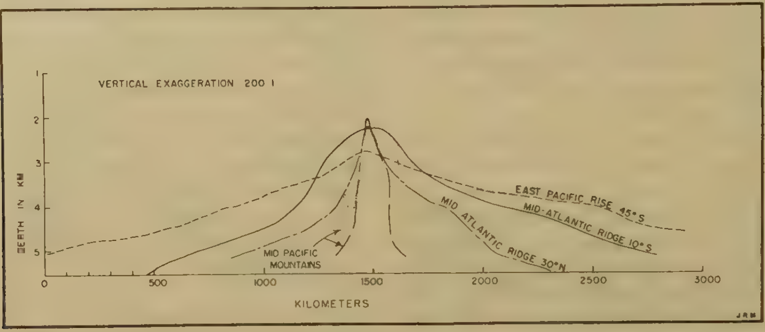

Figure 2.—Transverse Profiles of Submarine Median Elevations

Showing the gradation from the broad East Pacific Rise to the steep-sided, narrow Mid-Pacific Mountains.

Permanence of Oceanic Rises

The proposed sequence of development from rises to ridges implies that oceanic rises are not permanent features. Impermanence is suggested by other lines of evidence. One of the great belts of earthquakes is centered on the crest of the world-girdling oceanic rise (Gutenberg and Richter, 1954; Ewing and Heezen, 1956, p. 78). Volcanoes abound on rises, and many have subsided to form guyots and atolls. Heat-flow measurements have been made on the East Pacific Rise, the Albatross Plateau, and the Mid-Atlantic Ridge, and values as great as twice the heat flow characteristic of continents and ocean basins are common (Bullard *et al.*, 1956; Roger Revelle, personal communication; R. P. von Herzen, personal communication). If these widely distributed measurements are typical of the intervening areas of the rise, the high values indicate an active process and instability.

The permanence of continents and ocean basins is in dispute, but there can be little doubt that each has some highly stable characteristics, namely:

(1) A distinct topographic level that is so widespread as to dominate the hypsographic curve of the earth (Kossinna, 1921, p. 36).

(2) A characteristic suite of rocks that is statistically different if not completely so (Gilluly, 1955, p. 8–10).

(3) A typical, apparently layered, crustal structure as revealed by seismic methods (Ewing and Press, 1955, p. 2–4).

A continent cannot be changed into an ocean basin without changing 35 km of one type of rock into 5 km of another type and lowering the surface by more than 5 km.

In contrast, an oceanic rise appears to have few if any stable characteristics. Rises are, on the average, 1 km shallower than ocean basins, but there is no distinct boundary between the two. Rises characteristically have the cross sections of broad arches, although in most places the arch is apparently faulted. The top is not level. Rises cover a sizable portion of the earth's surface. If any distinct intermediate level existed, it would be reflected in the hypsographic curve of the earth, but it is not.

Except for the Indian Ocean, the petrology of igneous rocks on oceanic rises is based almost wholly on samples collected subaerially from the island peaks of large submarine volcanoes. The peaks of volcanoes are, notoriously, the locus of magmatic differentiates that are not representative of the main volume of the cone so that the petrology of most rises remains obscure. Efforts have been made to show that all oceanic rises are composed of rocks that are not typical of oceanic basins, but the efforts are based on emphasizing the atypical differentiates on the peaks at the expense of the main volume of the subaerial part of the volcanoes. Gilluly (1955, p. 9), for example, gives a table of examples of oceanic occurrences of rocks more siliceous than basalt and refers to a "rhyolite" on Easter Island citing Bandy (1937). Bandy in the cited work makes it clear that the rhyolitic obsidian is merely a differentiate of basalt, and states (p. 1607) "... the amount of obsidian on the island is 0.02 per cent of the amount of basalt that has crystallized." Hess (1954, p. 344) generalizes that basaltic vulcanism is typical of oceanic rises.

---

[1] Doctor Heezen has inspected all the Downwind echograms in this area with the writer, in a preliminary attempt to standardize topographic terminology in the Pacific and Atlantic basins. Heezen believes that the soundings may show a small median trough and certainly do not rule out the possibility of one.

The Mid-Indian Ridge may have exceptional rocks in considerable volume. The difficulty in drawing a firm conclusion comes not in identifying the rocks but in identifying the Mid-Indian Ridge. The western half of the ocean floor is mountainous (Fairbridge, 1955, p. 161), and the Mid-Indian Ridge is not easily distinguished from the Seychelles and Maldive ridges. As drawn by Fairbridge (1954, unnumbered figure) the Mid-Indian Ridge is a normal oceanic rise capped by volcanoes. The Seychelles Islands and Maldive and Laccadive islands, however, rise from very shallow, extensive ridges; the Seychelles Islands contain granite and may have continental structure (Darwin, 1889, p. 146, 260). If the various ridges are all similar features or parts of one feature, granitic rocks occur in at least one place in an oceanic rise. However, the Seychelles Ridge appears to be a separate topographic feature perhaps a small continental outlier not unlike near-by Madagascar except that it has been truncated. The granite proves that continental rocks may be produced in ocean basins (Gilluly, 1955), but it does not prove that it is any more likely to occur on an oceanic rise than elsewhere in the basins.

The East Pacific Rise at 45° S. Lat. has a normal oceanic crust and mantle, although the second layer is unusually thick (George Shor, personal communication). This confirms the indications of surface-wave dispersion in the area (Oliver *et al.*, 1955, p. 936). The Albatross Plateau west of Central America likewise has a normal oceanic crust and mantle (R. W. Raitt, personal communication). At 10° S. lat. on the East Pacific Rise, and on the Mid-Atlantic Ridge normal mantle velocities have not been observed. Instead, the maximum velocities are 7.2 to 7.7 km/sec (Raitt, 1956, p. 1636; Ewing and Ewing, 1957). Normal oceanic crustal velocities are found at 10° S. Lat. on the East Pacific Rise, but they are lacking in some places on the Mid-Atlantic Ridge.

Abnormal velocities under rises are intriguing, but the normal crustal sections are more significant with regard to the permanence of rises. The southern part of the East Pacific Rise is 2000 km wide and 2 km high—one of the largest oceanic rises in the world—yet the crustal section is essentially the same as that under the deep basins of the oceans.

In summary, oceanic rises do not have a distinct topographic level, nor do they appear to have a characteristic suite of rocks or crustal section. Observations do not rule out the possibility that broad rises may be temporary features which are elevated and then subside, leaving narrow ridges capped with guyots and atolls.

Origin of Median Topography

Features as large as oceanic rises must be isostatically compensated. Inasmuch as some rises have a normal oceanic crustal section, the compensation occurs in the mantle. The indicated horizontal differences in the mantle have not been detected except by the fact that rises exist. Nevertheless, it appears that some process in the mantle causes localized density changes adequate to produce epeirogenic uplift of the sea floor by 2 km.

Ewing and Ewing (1957) suggest that the low maximum seismic velocities found under the Mid-Atlantic Ridge are caused by a physical mixing of mantle and crustal material. This process does not explain the relief of rises where the crustal section is of normal oceanic type.

Hess (1954, p. 346–347) proposes that serpentinization of the mantle is a common cause of oceanic epeirogeny. The reaction has the virtue of occurring wholly within the mantle and being reversible, and because it is exothermic it also offers an explanation for the high heat flow associated with rises.

The process that centers rises in ocean basins has the following characteristics:

(1) It is sensitive to the margins of the basins.

(2) It is capable of acting at distances as great as half the width of the Pacific Basin—more than 5000 km or 50° of arc.

(3) It acts on both sides of a basin at one time.

(4) It appears to be ephemeral or intermittent.

One possible process is the convection current. If so, the high heat flow along seismically active rises implies rising currents in the middle (Bullard *et al.*, 1956, p. 177). Continuity requires sinking currents near the margins of the basins with horizontal movement toward the margins under the crust. This is the direction of movement advocated by proponents of the convection origin of island arcs and Pacific fracture zones.

Corollaries

The hypothesis of epeirogenic uplift and subsidence of median oceanic elevations has several corollaries which can be used to test its validity and the validity of other hypotheses. Some of the most important ones are briefly discussed.

Faunal migration. Although not continental, if the median ridges of the Pacific were once elevated and were contemporary they would have produced many of the effects normally attributed to continents. Individual ridges are less than 1 km deeper than many of the guyots that rise above them, so that, when the guyots were islands, the ridges were deep banks, each 1000–2000 miles long. Whether the ridges were contemporary is unknown, but the distribution of existing rises suggests that single median elevations the length of an ocean basin are normal whereas shorter detached elevations are not. The only indication of the age of the ridges is the Late Cretaceous dating of the final truncation of the guyots in the Mid-Pacific Mountains (Hamilton, 1956, p. 42). Assuming approximate contemporaneity, the median line of the Pacific Basin was marked in Mesozoic time by an almost continuous deep bank capped by numerous closely spaced islands and shallow banks. The general picture closely resembles the isthmian links of Willis (1932) and is no more than a geographical extension of the dense island chains of the Mid-Pacific Mountains (Hamilton, 1956, p. 50–52). Island stepping stones and almost continuous shallow water may have been available for faunal migration from Japan to Easter Island or even to South America. A branching structure reached almost to Kamchatka.

Continental drift. Evidence in support of continental drift is derived from the similar shapes of the Mid-Atlantic Ridge and the adjacent shores of Africa and South America. This evidence can be dismissed as not pertinent to the hypothesis because both Africa and South America are almost circled by rises that are roughly parallel to the shore lines. If the Mid-Atlantic and Mid-Indian ridges are fragments left by the drift of South America and Australia, respectively, what are the rise and ridge structures of the Pacific? If the continents have only begun to drift in Early Tertiary time, how did the Cretaceous rise of the Mid-Pacific Mountains become centered relative to the present margins of the Pacific?

References Cited

Bandy, M. C., 1937, Geology and petrology of Easter Island: Geol. Soc. America Bull., v. 48, p. 1589–1609

Bezrukov, P. L. and Udincev, G. B., 1955, The northern end of the Hawaiian suboceanic ridge (in Russian): Dok. Akad. Nauk, v. 103, p. 1077–1080. Defense Research Board of Canada, translation T226R by E. R. Hope

Bullard, E. C., Maxwell, A. E., and Revelle, R. R., 1956, Heat flow through the deep sea floor: Advances in Geophysics, v. 3, p. 153–181

Darwin, C., 1889, Structure and distribution of coral reefs, 3d ed: New York, D. Appleton and Co., 366 p.

Dietz, R. S., 1954, Marine geology of northwestern Pacific: description of Japanese bathymetric chart 6901: Geol. Soc. America Bull., v. 65, p. 1199–1224

Ewing, J., and Ewing, M., 1957, Seismic-refraction measurements in the Atlantic Ocean basins, in the Mediterranean Sea, on the Mid-Atlantic Ridge, and in the Norwegian Sea: Paper presented to the Annual Meeting of the Seismol. Soc. America

Ewing, M., and Heezen, B., 1956, Some problems of Antarctic submarine geology: Geophys. Mon. no. 1, p. 75–81

Ewing, M., and Press, F., 1955, Geophysical contrasts between continents and ocean basins, p. 1–6 *in* Poldervaart, A., Editor, Crust of the earth: Geol. Soc. America Special Paper 62, 762 p.

Fairbridge, R., 1954, Report on limits of the Indian Ocean: Indian Ocean Science Cong. Proc., Perth, p. 18–28

——1955, Some bathymetric and geotectonic features of the eastern part of the Indian Ocean: Deep-Sea Research, v. 2, p. 161–171

Gilluly, James, 1955, Geologic contrasts between continents and ocean basins, p. 7–18, *in* Poldervaart, A., Editor, Crust of the earth: Geol. Soc. America Special Paper 62, 762 p.

Gutenberg, B., and Richter, C. F., 1954, Seismicity of the earth: Princeton, N. J., Princeton Univ. Press, 310 p.

Hamilton, E. L., 1956, Sunken islands of the Mid-Pacific Mountains: Geol. Soc. America Mem. 64, 97 p.

Heezen, B. C., 1957, Deep-sea physiographic provinces and crustal structure: Paper presented to the 38th Annual Meeting of the Am. Geophys. Union

Hess, H. H., 1946, Drowned ancient islands of the Pacific Basin: Am. Jour. Sci., v. 244, p. 772–791

—— 1954, Geological hypotheses and the earth's crust under the oceans: Royal Soc. London, Proc., v. 222, p. 341–348

—— 1955, Serpentines, orogeny, and epeirogeny, p. 391–408 *in* Poldervaart, A. *Editor*, Crust of the earth: Geol. Soc. America Special Paper 62, 762 p.

Kossinna, E., 1921, Die Tiefen des Weltmeeres: Inst. f. Meereskunde, H. 9, 70 p.

Oliver, J., Ewing, M., and Press, F., 1955, Crustal structure and surface-wave dispersion, Pt. IV: Atlantic and Pacific Ocean basins: Geol. Soc. America Bull., v. 66, p. 913–946

Raitt, R. W., 1956, Seismic-refraction studies of the Pacific Ocean Basin, Pt. I: Crustal thickness of the central equatorial Pacific: Geol. Soc. America Bull., v. 67, p. 1623–1640

Willis, B., 1932, Isthmian links: Geol. Soc. America Bull., v. 43, p. 917–952

SCRIPPS INSTITUTION OF OCEANOGRAPHY, UNIVERSITY OF CALIFORNIA, LA JOLLA, CALIF.

MANUSCRIPT RECEIVED BY THE SECRETARY OF THE SOCIETY, FEBRUARY 8, 1958

CONTRIBUTION FROM THE SCRIPPS INSTITUTION OF OCEANOGRAPHY

(569)

Population Studies on Juvenile Herring in Barkley Sound, British Columbia[1,2]

By Alan S. Hourston
Fisheries Research Board of Canada
Biological Station, Nanaimo, B.C.

ABSTRACT

Population studies were carried out on herring in the juvenile (first year, post-metamorphosis) stage in Barkley Sound in the summers of 1951 to 1954. Their chief objective was to detect and estimate yearly changes in relative abundance. The juveniles were found mostly in shallow, sheltered bays, inlets and channels, mainly on the southeast side of the sound. The stocks apparently arose from different mixtures of the progeny of a series of spawnings extending over two months and located mainly on the northwest side of the sound. Mixing between localities averaged less than one-third. The 1953 and 1954 juvenile populations were above average (both about 640 million fish), while the 1952 population was below average. Upon recruitment to the fishery, the relative strength of these three year-classes was comparable to that observed in the juvenile stage. Thus, surveys of herring abundance at the juvenile stage provide an index of year-class strength at recruitment.

CONTENTS

Introduction 909
Distribution of Juvenile Herring in Barkley Sound 912
Composition of the Barkley Sound Juvenile Herring Population 917
Abundance of Juvenile Herring in Barkley Sound 938
Relationship of Juvenile Herring Stocks to Those of the Eggs and Larvae 944
Summary and Conclusions 945
Acknowledgments 948
References 948
Appendices 950

INTRODUCTION

The Pacific Herring, *Clupea pallasi* Valenciennes, goes through egg, larval, immature and adult stages. In southern British Columbia, the eggs are deposited on vegetation in the intertidal zone in late winter or early spring (mid-January to mid-April). They hatch in about 2 weeks (Stevenson, *et al.*, 1952) into larvae, which metamorphose in 6 to 8 weeks (Stevenson, 1955a) into the adult form. These young herring remain inshore until September or October, when they migrate offshore. During this inshore stage, the herring are referred to as juveniles. Except for rare inshore appearances of schools of second-year fish, older herring remain offshore until they join the spawning stocks as mature adults, usually in the third year (Stevenson, 1955b).

Appreciable fluctuations occur in the abundance of herring in British Columbia (Taylor, 1955, and previous reports in that series). Once a year-class

---

[1] Received for publication November 27, 1957.

[2] Based on portions of a thesis accepted by the School of Graduate Studies, University of California, Los Angeles, in partial fulfilment of the requirements for the degree of Doctor of Philosophy.

Contributions from the Scripps Institution of Oceanography, New Series, No. 1027

Reproduced by Permission

enters the fishery (i.e. matures for the first time), its future strength may be predicted on the basis of fishing mortality and calculated rates of natural mortality (Tester, 1955). As these two factors do not appear to appreciably alter relative year-class strength from year to year, it must thus be established prior to maturity. Since the newly recruited year-class usually makes up more than half of the adult population in southern British Columbia stocks, it is both the major source of variation in population abundance and the key to the prediction of population size.

Considerable attention has been given to determining mortality in the early stages of the life history of the herring in British Columbia waters. Studies on egg mortality (Tester, 1948; Stevenson, 1952; McMynn and Hoar, 1953) give estimates of mortality varying from 35% to 65%, due mainly to bird predation. Losses due to other factors are small (less than 10%). A re-analysis of experimental data from these and other studies conducted at the Biological Station, Nanaimo, B.C., indicated a total mortality of about 79%. However, year-class strength has shown no correlation to the amount of spawn deposited (Tester, 1948). This is well illustrated by the exceptionally strong 1947 year-class on the west coast of Vancouver Island, which was produced from a lower-than-average spawning (Stevenson *et al.*, 1951) and the very poor 1940 year-class, which was produced from an above-average spawning (Tester, 1948).

Stevenson (1955a), on the other hand, has been able to establish a correlation between year-class strength and conditions affecting larval survival in Barkley Sound. On the basis of these data, and data on the amount of spawn deposited and the extent of mortality between metamorphosis and recruitment, he estimated mortality during the larval stage to be 99.3 to 99.7% (Stevenson, 1955b). He concluded that mortality during this vulnerable stage is the major factor involved in fluctuations in year-class strength. It would thus appear that the earliest stage in the development of the Pacific herring at which year-class strength may be assessed is that immediately following the larval stage—namely, as juveniles. Since the herring migrate offshore and scatter at the end of their first summer, the early juvenile stage is the last stage before recruitment at which they are relatively accessible for population studies.

THE BARKLEY SOUND HERRING STOCKS

Barkley Sound (Fig. 1) is one of the major herring rearing grounds on the British Columbia coast. The sound is about 12 miles square and lies in a southwest–northeast direction between 48° 47′ and 49° 02′ North Latitude and between 124° 35′ and 125° 35′ West Longitude. The Barkley Sound herring stocks form the major portion of the herring population on the lower west coast of Vancouver Island subdistrict. This population is one of the ten major migratory populations making up about 95% of the total British Columbia stock (Taylor, Hourston and Outram, 1956). These populations were established on the basis of average differences in meristic characters and on the returns of tagged fish (Thompson, 1917; Tester, 1937, 1949; McHugh, 1954; Stevenson, 1955c). Intermixture between these major populations amounts to about 25% on the average, and is greatest between contiguous populations.

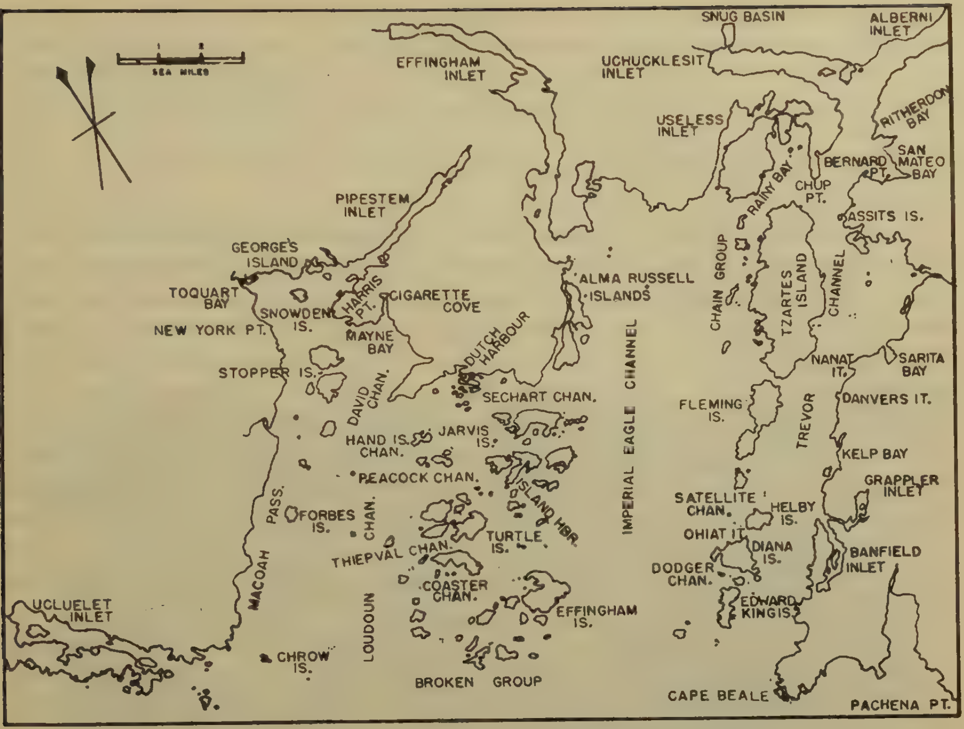
SEA MILES
SNUG BASIN
ALBERNI INLET
EFFINGHAM INLET
UCHUCKLESIT INLET
USELESS INLET
RITHERDON BAY
SAN MATEO BAY
BERNARD PT.
CHUP PT.
RAINY BAY
ASSITS IS.
PIPESTEM INLET
GEORGE'S ISLAND
TOQUART BAY
SNOWDEN IS.
HARRIS PT.
CIGARETTE COVE
ALMA RUSSELL ISLANDS
CHAIN GROUP
TZARTES ISLAND
CHANNEL
NEW YORK PT.
MAYNE BAY
DUTCH HARBOUR
STOPPER IS.
NANAT IT.
SARITA BAY
DAVID CHAN.
SECHART CHAN.
FLEMING IS.
TREVOR
DANVERS IT.
HAND IS. CHAN.
JARVIS IS.
IMPERIAL EAGLE CHANNEL
KELP BAY
PEACOCK CHAN.
ISLAND HBR.
GRAPPLER INLET
PASS.
FORBES IS.
CHAN.
SATELLITE CHAN.
HELBY IS.
TURTLE IS.
OHIAT IT.
THIEPVAL CHAN.
DIANA IS.
BANFIELD INLET
MACOAH
DODGER CHAN.
COASTER CHAN.
UCLUELET INLET
LOUDOUN
EFFINGHAM IS.
EDWARD KING IS.
CHROW IS.
BROKEN GROUP
CAPE BEALE
PACHENA PT.

Figure 1. Map of Barkley Sound showing the major localities mentioned in the text.

The lower west coast population spawns in coastal waters between Pachena Point and Esteban Point. The summer feeding grounds are considered to be located off the outer entrance of the Strait of Juan de Fuca, and to extend southward off the northern coast of Washington (Stevenson, 1955c). Tagging studies (Stevenson, 1955c) have shown that about 83% of the herring that survive until the following year return to the inshore waters in which they spawned previously. Of the remainder, about 11% join runs of the population on the upper west coast of Vancouver Island (a population of comparable size whose summer feeding grounds are considered to be located off Nootka Sound and Esperanza Inlet) and 6% join runs of the population on the lower east coast of Vancouver Island (a larger population which migrates through the Strait of Juan de Fuca to feeding grounds off the northern coast of Washington).

Approach to the Problem

The practical objective of this study was to obtain estimates of relative population size in the juvenile stage which might foreshadow fluctuations in year-class strength in the adult stage. However, before the size of a population can be reliably estimated, the extent of its distribution and the unit to which estimation procedures can be applied must be determined. To this end, a study of these aspects of the population dynamics of the juvenile herring was launched in Barkley Sound in 1951.

The problem of relating this information on the juvenile herring stocks to that on the adult populations was tackled at the same time by tagging juveniles with body cavity tags and recovering tags from the fishery after the fish were recruited to the spawning populations. These results will be reported later.

DISTRIBUTION OF JUVENILE HERRING IN BARKLEY SOUND

METHODS

SCOUTING. The simplest and most direct approach to determining the distribution is to look for or attempt to catch fish throughout the area under study. During the summer months schools of juvenile herring may be seen in the early morning and evening "flipping" at the surface in many of the sheltered inlets and bays in Barkley Sound. An experienced observer can distinguish the young herring schools from those of other species by the appearance of the rings formed by fins breaking the water surface and by the swimming motion and body shape of the fish. Juvenile herring "flips" generally show in groups of 6 to 20 in a small circle 1 to 3 feet in diameter. The rings formed by finning are distinct and usually have a single or double rim; the initial ring is about 2 inches in diameter. The school as a whole is usually 2 to 3 feet below the surface at dawn and dusk. The young herring swim with a smooth, graceful motion; their backs are green to purple in colour.

Other species present as schools of small fish may be distinguished as follows. Salmon (*Oncorhynchus* spp.) tend to flip singly and often jump right out of the water. Their backs are usually a lighter green in colour and the schools tend to stay more than 3 feet below the surface. Sand lance (*Ammodytes tobianus personatus*) swim with a distinctive undulating motion, generally just below the surface of the water. They break surface less often and the type of ring formed is more irregular and variable. Sticklebacks (*Gasterosteus aculeatus*) and sea-perch (*Cymotogaster aggregatus*) are usually smaller in size and swim just below the surface with a more leisurely motion. They produce very small, weak rings when they break surface. Anchovies (*Engraulis mordax*) are readily identified by a characteristic flashing of their gill covers.

DIP-NETTING WITH LIGHT. Various methods of capturing samples of fish were employed to identify fish located and to locate fish where none were observed. In 1951, samples of herring in the early juvenile stage were captured by a dip-net from schools attracted to a light at night. A 200-watt light backed by a reflector and hung just over the surface of the water proved more effective than less powerful or more powerful lights, and more effective also than submerged lights. The effectiveness of this method decreased rapidly as the fish grew and by mid-June, when the juveniles were close to 2 inches (5 cm.) in size, it had to be discarded. By this time, however, samples could be readily obtained by seining. Subsequent surveys were therefore concentrated in this period of greater accessibility of the juveniles.

HERRING RAKE. When the schools of juveniles were concentrated 6 inches to 3 feet (15–100 cm.) below the surface, samples of a few fish were obtained by use of a herring rake. This is a long flat pole about 10 feet × 2 inches × ½ inch (3 m. × 5 cm. × 12 mm.) with a comb-like projection of sharp 2-inch pins set along the long axis of the pole at half-inch intervals for about 3 feet from the end. The rake is passed quickly through a school of fish, prongs first, with a motion similar to that employed in paddling a canoe (Fig. 2). The direction of motion through the water is perpendicular to the direction of motion of the school so that the prongs will have an opportunity to impale some fish through the side. Up to about 20 fish may be caught per stroke, but in most cases the catch is 1 to 6 fish. This instrument is commonly employed by sport fishermen to obtain fresh bait, and stems directly from aboriginal models. Samples were raked in all years, mainly for the purpose of identifying schools.

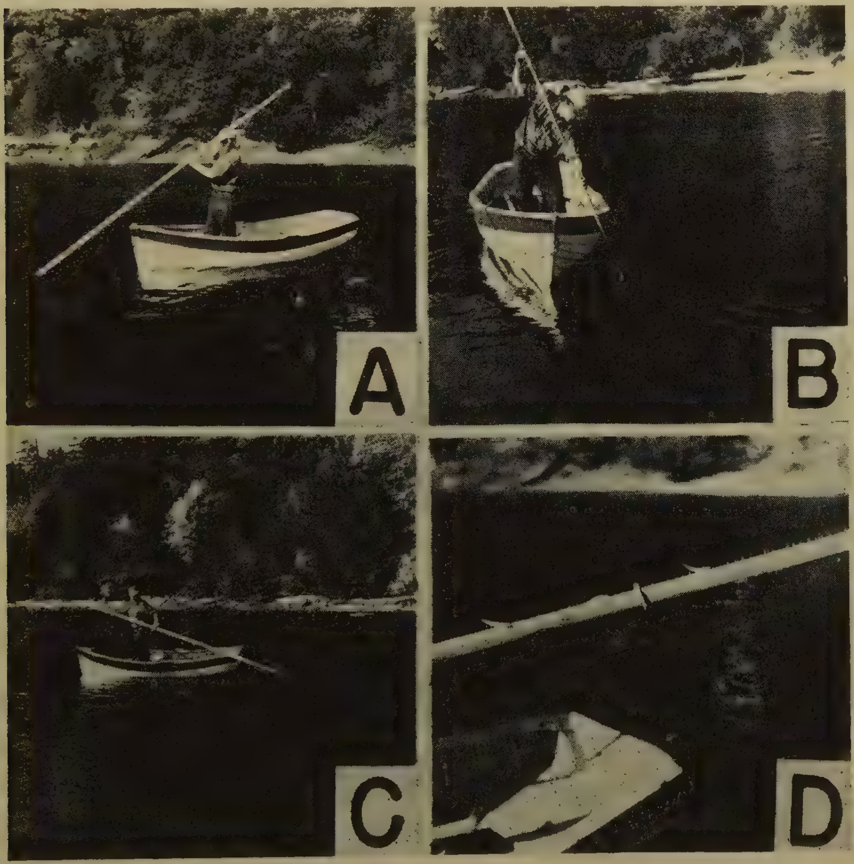

FIGURE 2. Raking juvenile herring.

A. Rake poised for action.
B. Rake in midst of stroke through a school of juvenile herring.
C. Rake emerging from water with juveniles on prongs.
D. Juveniles impaled on prongs.

SEINING. The most successful method of capturing juvenile herring was seining. Various mesh sizes, web preservatives and seine designs and sizes were tried throughout the 4-year period. Most of the seining was carried out with two types of net. The first was a drag seine of ¾-inch cutched web 20 by 3 fathoms (36.5 × 5.5 m.), "hung in" 25%. Sets of 2,000–3,000 fish were readily made in the shallow waters (less than 5 fathoms) inhabited by the juveniles in early summer. In 1953 purse rings were attached to this net and it fished even more effectively. However, toward the end of the summer, as the juveniles grew larger and became more effective swimmers, they were found in deeper waters and tended to sound before this net could be closed. The second net, a 2-strip purse seine of similar web 37 by 6 fathoms (68 × 11 m.), was then employed. It proved effective on the larger fish in deeper waters and provided larger catches (up to 30,000 fish), which were more satisfactory for the marking and tagging programs.

Attempts to capture fish by other methods, including fyke net and miniature trawl, were unsuccessful.

In 1951, localities where appreciable numbers of juvenile herring were reported (Banfield Inlet, Uchucklesit Inlet and Pipestem Inlet—Fig. 1) were scouted visually throughout the day. When weather conditions were favourable, schools were almost always observed for 2 or 3 hours following dawn, and from about an hour before sunset to 1 to 2 hours afterward. Schools were occasionally observed during the day, mainly around docks and in well-shaded inlets, especially during the early part of the summer (the last week in June and the first two weeks in July). However, these daytime showings were sporadic and small compared to those at dawn and dusk. Scouting during the actual surveys was therefore confined to dawn and dusk.

Even when weather conditions were good for observation, schools sometimes failed to show where they were observed a few hours previously or afterwards. When weather conditions were poor they seldom showed at the surface at all. In partial compensation, scouting was also carried out with an echo-sounder during the 1952 and subsequent surveys. Schools were often observed at the surface at the same time, making the identification of the marks on the sounder as juvenile schools highly probable. Such schools usually made small shallow marks on the sounder paper (Fig. 3). Larger and deeper marks were observed where the fish were most abundant and at greater depths. Sets made on typical sounder marks usually yielded juveniles. Since young herring appear to make up the bulk of the small fish in this area, any marks that looked like juvenile herring and which could not be identified as arising from other sources were recorded as herring.

RESULTS

Juvenile schools were found mainly in inlets and bays, and in the back-eddies behind islands and points, and in channels (Fig. 4). In these localities the water was usually relatively shallow (less than 100 feet deep) and currents were relatively weak but definitely present. The 1951 and 1952 observations were based on visual scouting only. In 1953 and 1954 echo-sounder observations were also

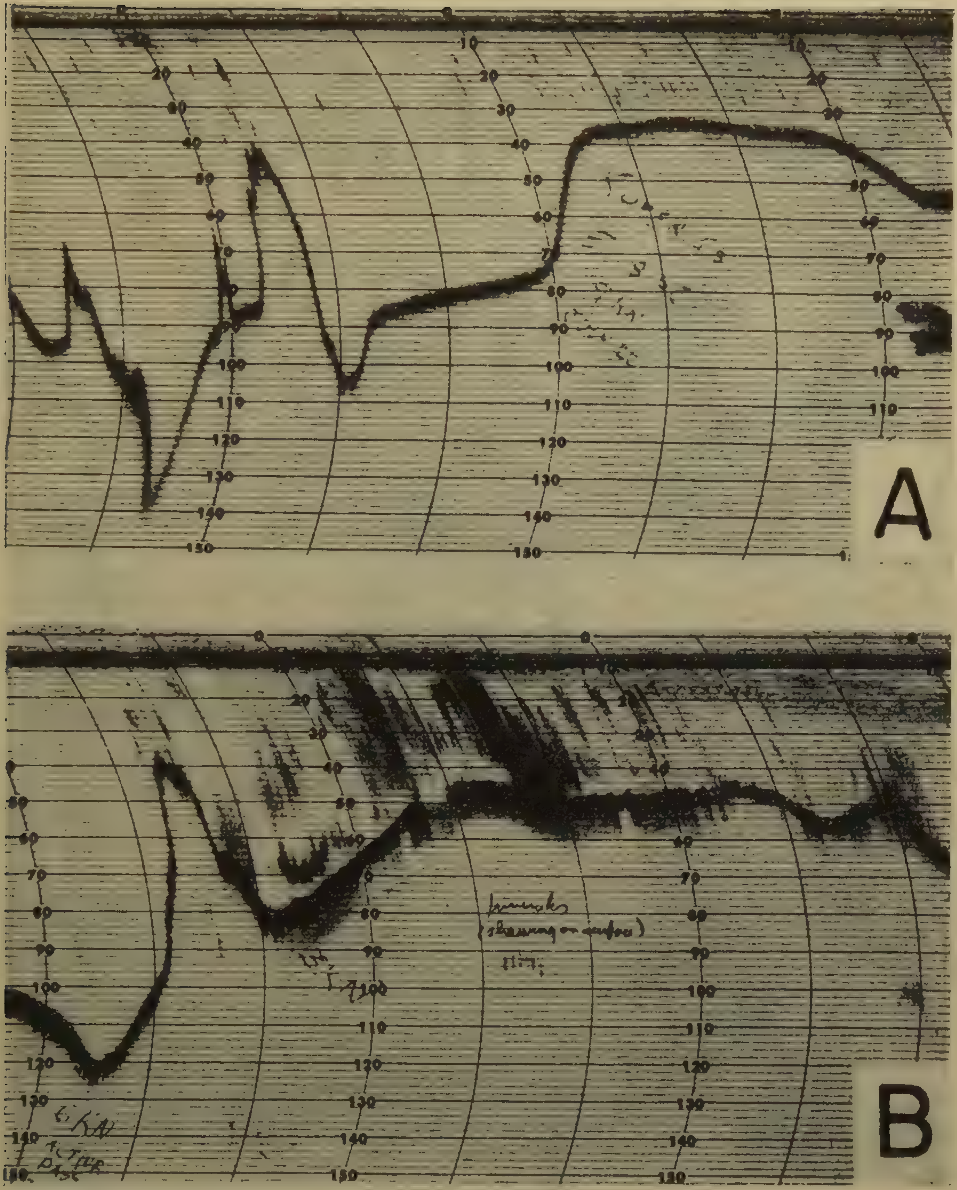

FIGURE 3. Echo-sounder tracings showing schools of juvenile herring. A—Standard type marks; B—Very dense schooling.

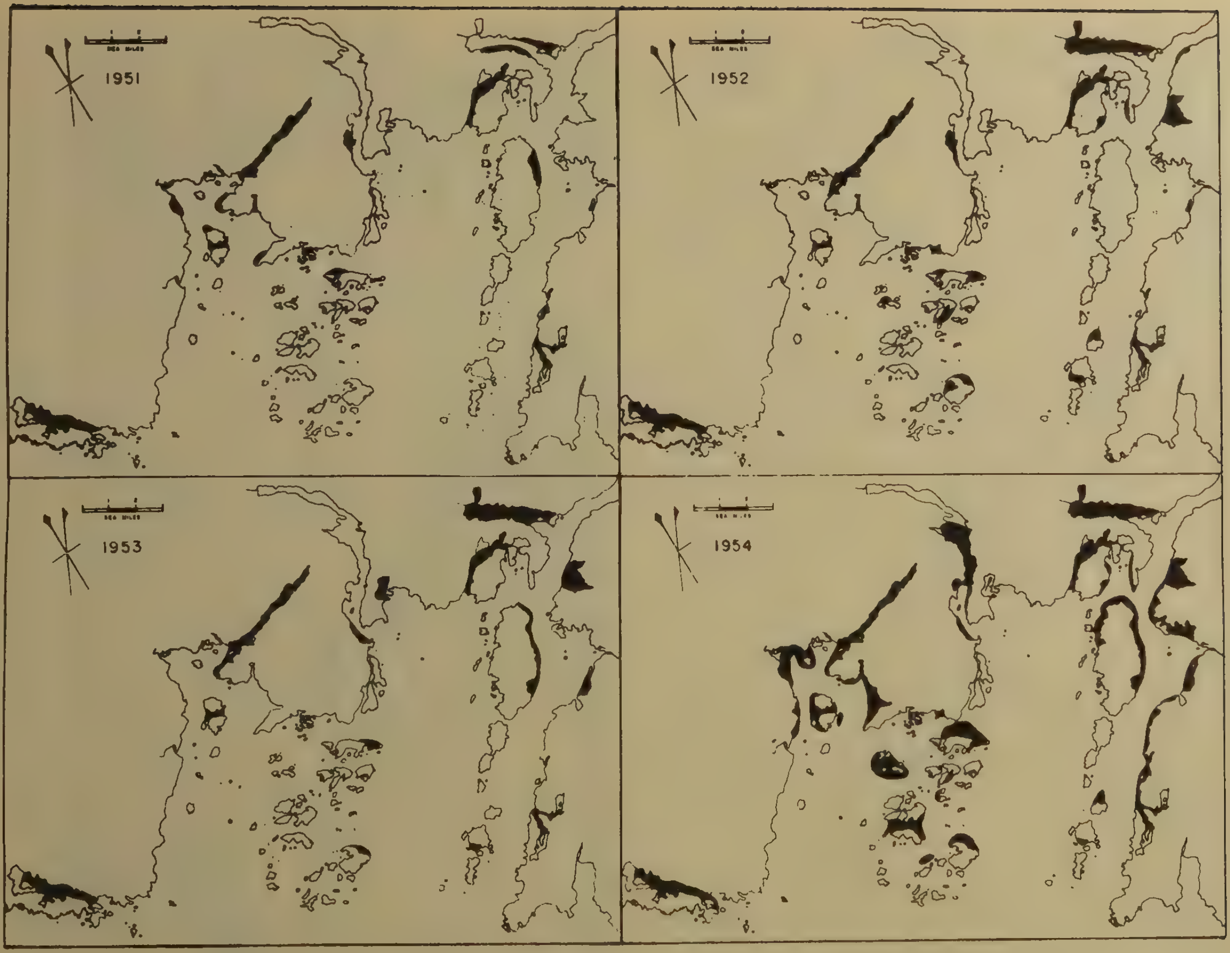
1951
1952
1953
1954
SEA MILES

FIGURE 4. Localities in Barkley Sound where juvenile herring were found.

employed. Scouting in 1951 was of a preliminary nature and only localities in which juveniles had been reported, or which appeared to be good rearing grounds, were visited. Scouting was extended to cover some other localities in 1952 and 1953, but commitments to other aspects of the program precluded complete coverage. Not until 1954 was the whole sound thoroughly scouted; each locality was visited several times that year. The more extensive showing of fish in 1954 resulted more from finding stocks missed previously than from the presence of new stocks.

Both visual and sounder showings in thickly populated localities dropped off abruptly on leaving sheltered bays and back-eddies, and upon entering isolated spots in these localities where the wind had sufficient force to appreciably ruffle the surface.

Extensive scoutings of the large open channels failed to show any juveniles. Conditions for visual observation were generally poor, but even when conditions were good, few schools were observed. The echo-sounder tracings showed correspondingly few schools under all conditions. All coast lines were thoroughly scouted but fish were found consistently only in the more sheltered localities.

COMPOSITION OF THE BARKLEY SOUND JUVENILE HERRING POPULATION

One of the fundamental considerations in the population dynamics of the juvenile herring in Barkley Sound is the extent to which the juveniles form relatively discrete local populations or stocks within the sound or, conversely, the extent to which these stocks mix with one another. In the section on distribution it was shown that some groups of fish appear to be more or less isolated from each other geographically, which suggests the possibility of the existence of local populations or stocks within the sound. Two methods were used to investigate this possibility: (1) the recovery of marked fish, and (2) the analysis of the various stocks for differences in length composition.

Marking Program

Fish from several of the larger concentrations in the sound were marked by the removal of different combinations of the paired fins. Fish captured by seining were transferred into a live pound at the site of capture by attaching the lead line of the seine to the rim of the live pound and "drying up" the net into the pound. Fish handled in this manner showed less injury than those transferred into the pound by dip-net. Every effort was made to avoid towing the pounds as this usually resulted in the removal of a considerable number of scales. Experiments on adults have shown that previous scaling increases tagging mortality tremendously. However, it was occasionally necessary to move the fish to a more sheltered spot. This was generally accomplished with little apparent damage by towing the pound very slowly (about one knot).

The pounds were rectangular enclosures of half-inch web. Tarred web was used (although it damaged fish scraping against it), as it was the only type of preservative that withstood the prolonged submergence these pounds were subjected to. A frame of 4 × 4-inch lumber, 3 × 4 feet in size, floated on the surface. The web was attached to this frame and fell down 5 feet to a bottom of similar meshed web attached to a 3 × 4-foot frame of half-inch metal pipe. Thus the pound was collapsible for easy storage. Ropes attached to the four corners of the metal frame and drawn up through the corners of the wooden frame enabled the gradual drying up of the pound to reduce the size of the enclosure as the number of fish became less.

During the marking operations (Fig. 5), groups of about 100 fish were transferred by dip-net into a tray of half-inch Cuprinoled web joining two "sticks" of 1-inch square lumber just over 4 feet long. These were set just inside one side of the pound and rested on the 4 × 4's forming either end of the pound's frame. By rolling the web onto either stick the desired depth of the tray could be obtained.

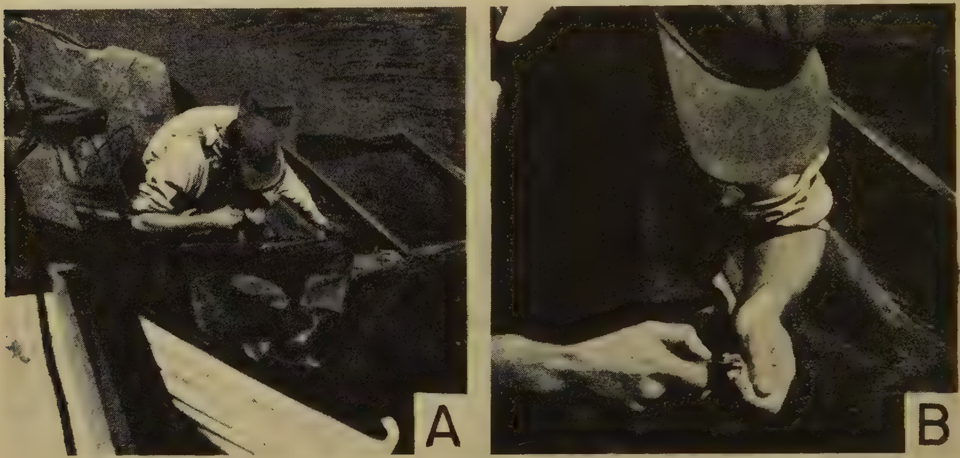

FIGURE 5. Marking juvenile herring.
A. Markers, pound and tray.
B. Marking a fish by clipping off the left pelvic fin.

The side of the pound with the tray along it was lashed to the side of a rowboat. The markers sat in the boat facing lengthwise to the pound so that the tray was on their left side. A quick scoop of the left hand into the tray captured a fish in the palm of the hand. The fish was grasped belly up with the head pointing toward the marker's body and was held steady by the thumb on one side and the fingers on the other. In this manner all paired fins could be checked at a glance for previous marks without moving the fish, and the prescribed fins could be clipped off (Fig. 5b). The fish was then released immediately. In this manner up to 500 fish could be marked per hour by a skilled marker, and each fish remained out of water for less than 5 seconds. Mortality under these conditions proved relatively small (Appendix 1).

The most vulnerable period from the point of view of predation was immediately after release. The fish shot wildly off in any direction for the first few seconds, and then appeared to settle down to normal swimming behaviour and sought the nearest school. Predators, principally rockfishes (*Sebastodes* sp.) and sea-perches (Embiotocidae) congregated while marked fish were being released. However, concentrated hand-line fishing simultaneous with the marking seemed to remove the worst of this threat. Since the fish swam close to the surface until they regained their normal behaviour, any predation that occurred during this period was readily observed. On one occasion, in an effort to protect the freshly-marked fish from predation, some were released into a live pound. However, most of these fish injured themselves by dashing into the web sides of the pound during the initial shock, and this procedure had to be abandoned.

Experiments were carried out to determine the mortality caused by the marking operation. These indicated a mortality of from 1% to 16% (Appendix 1). It seems improbable that marking mortality under natural conditions exceeded 15%; and where experienced markers worked with fish that were in good condition, it appears to have been virtually negligible. Consequently no correction factor was applied to the numbers of fish marked.

Individual markings and recoveries (Tables I–IV) were summarized by locality for each year (Tables V–VIII for 1951 to 1954 respectively) and for the entire 4-year period (Table IX). With a few exceptions, more than two-thirds of the recoveries from each marking were in the locality of marking (Fig. 6). The exceptions are of three types:

(1) Groups of fish that disappeared from the locality during the summer after a strong early showing (Toquart Bay, 1951; Sechart Channel and Island Harbour, 1952).

(2) A population which showed a high degree of dispersion but continued to exist locally (Uchucklesit Inlet, 1952, 1954). This may have been a single stock behaving somewhat abnormally, or these fish, with others nearby, may have formed part of a larger stock.

(3) Two localities marked separately that appeared to contain the same population (Banfield Inlet and Kelp Bay, 1954).

TABLE I. Markings and recoveries of juvenile herring in Barkley Sound during 1951.

Marked at	Date	Number marked	Marked fish at large		Recoveries from					
			Locality	Sound	Banfield Inlet	Cigarette Cove	Pipestem Inlet	Toquart Bay	Useless Inlet	All
Toquart Bay	July 18	946	...	...	...	...	...	...	...	...
Banfield Inlet	July 25	6,000	...	946	...	...	...	...	...	...
Cigarette Cove	July 30	1,000	...	6,946	...	...	...	...	...	...
Banfield Inlet	Aug. 2	273	6,000	7,946	...	...	...	...	...	...
Toquart Bay	Aug. 7	1,011	946	8,219	...	...	...	...	...	...
Cigarette Cove	Aug. 8	1,926	1,000	9,230	7	4	...	7	...	18
Useless Inlet	Aug. 15	2,348	...	11,156	...	...	...	...	...	...
Banfield Inlet	Aug. 20	8,650	6,273	13,504	7	1	...	1	...	9
Pipestem Inlet	Aug. 23	687	...	22,154	...	...	...	...	...	...
Useless Inlet	Aug. 25	2,185	2,348	22,841	...	...	...	1	...	1
Banfield Inlet	Aug. 27	1,430	14,923	25,026	...	...	...	...	...	...
Uchucklesit Inlet	Sep. 5	(3,188)	...	26,456	...	...	...	2	...	2
Banfield Inlet	Sep. 10	1,110	16,353	26,456	10	1	...	2	...	13
Useless Inlet	Sep. 12	5,000	4,533	27,566	...	...	...	1	5	6
Useless Inlet	Sep. 13	560	9,533	32,566	...	...	...	...	...	...
Useless Inlet	Sep. 14	860	10,093	33,126	...	...	...	...	...	...
Uchucklesit Inlet	Sep. 22	(1,607)	...	33,986	...	...	...	...	...	...
Uchucklesit Inlet	Sep. 26	(1,014)	...	33,986	2	...	...	2	...	4
Tzartes Island	Oct. 3	(4,164)	...	...	...	...	...	5	...	5
All localities		33,986 (9,973)			26	6	...	21	5	58

TABLE II. Markings and recoveries of juvenile herring in Barkley Sound during 1952.

Marked at	Date	Number marked	Marked fish at large: Locality	Marked fish at large: Sound	Recoveries from: Banfield Inlet	Effingham Island	San Mateo Bay	Sechart Channel	Uchucklesit Inlet	Ucluelet Inlet	All
San Mateo Bay	July 9	1,350	...	...	...	...	...	...	...	...	...
Uchucklesit In.	July 10	1,940	...	1,350	...	...	...	...	...	...	...
Effingham Is.	July 12	2,600	...	3,290	...	...	...	...	...	...	...
SechartChannel	July 13	3,982	...	5,890	...	...	...	...	...	...	...
Island Harbour	July 14	3,140	...	9,872	...	...	...	1	...	...	1
Ucluelet Inlet	July 15	1,667	...	13,012	...	...	...	...	...	...	...
Banfield Inlet	July 19	1,320	...	14,679	...	...	...	...	...	...	...
Banfield Inlet	July 20	4,490	...	15,999	...	...	...	...	...	...	...
Ucluelet Inlet	July 29	2,590	1,667	20,489	...	...	3	...	...	1	4
Uchucklesit In.	Aug. 6	4,979	1,940	23,079	...	...	...	...	...	...	...
Banfield Inlet	Aug. 7	1,420	5,810	28,058	...	...	...	...	...	...	...
Banfield Inlet	Aug. 8	4,107	5,810	29,478	...	...	...	...	...	...	...
Ucluelet Inlet	Aug. 10	2,615	4,257	33,585	...	...	...	...	...	2	2
Banfield Inlet	Aug. 11	2,230	11,337	36,200	2	...	...	1	2	...	5
San Mateo Bay	Aug. 13	6,654	1,350	38,430	...	...	...	...	1	...	1
Uchucklesit In.	Aug. 15	7,027	6,919	45,084	...	...	...	...	1	...	1
Banfield Inlet	Aug. 17	7,121	13,567	52,111	1	...	...	2	...	...	3
San Mateo Bay	Aug. 18	3,336	8,004	59,232	...	...	6	...	1	...	7
Ucluelet Inlet	Aug. 21	1,980	6,872	62,568	...	...	...	...	...	...	...
Banfield Inlet	Aug. 26	818	20,688	64,548	...	...	...	...	...	...	...
San Mateo Bay	Aug. 27	9,544	11,340	65,366	...	...	2	1	...	...	3
San Mateo Bay	Sep. 23	2,033	20,884	74,910	...	...	...	...	...	...	...
Effingham Is.	Sep. 25	2,056	2,600	76,943	...	...	...	...	...	...	...
Ucluelet Inlet	Sep. 27	2,017	8,852	78,999	...	...	...	...	...	...	...
Ecoole Cannery	Oct. 1	2,064	...	81,016	...	...	...	...	...	...	...
All localities		83,080			3	0	11	5	5	3	27

TABLE III. Markings and recoveries of juvenile herring in Barkley Sound during 1953. Numbers bracketed under "Number marked" were checked only.

Marked at	Date	Number marked	Marked fish at large: Locality	Marked fish at large: Sound	Recoveries from: Banfield Inlet	Pipe stem Inlet	San Mateo Bay	Sarita Bay	Uchucklesit Inlet	Ucluelet Inlet	Vernon Bay	All
Banfield In.	July 10	5,250	...	...	...	...	...	...	...	...	...	...
Uchucklesit Inlet	July 12	4,690	...	5,250	...	...	...	...	...	...	...	...
Uchucklesit Inlet	July 12	530	...	9,940	...	...	...	...	...	...	...	...
Banfield In.	July 16	7,030	5,250	10,470	2	...	...	...	...	...	...	2
Ucluelet In.	July 19	950	...	17,500	...	...	...	...	...	...	...	...
San Mateo B	July 20	2,010	...	18,450	...	...	...	...	1	...	...	1
San Mateo B	July 21	4,510	2,010	20,460	...	...	...	...	...	...	...	...
Banfield In.	July 23	10,400	12,280	24,970	7	...	...	...	...	...	...	7
Banfield In.	July 24	4,100	22,680	35,370	1	...	2	...	...	...	...	3
Banfield In.	July 25	1,730	26,780	39,470	1	...	...	...	...	...	...	1
Banfield In.	July 27	3,340	28,510	41,200	3	...	1	...	2	...	...	6
San Mateo B	July 28	5,340	6,520	44,540	...	...	1	...	...	...	...	1
Banfield In.	July 31	10,020	31,850	49,880	3	...	...	...	...	...	...	8
San Mateo B	Aug. 2	8,470	11,860	59,900	2	...	3	...	3	...	...	3
San Mateo B	Aug. 2	5,780	20,330	68,370	1	...	2	...	...	...	...	3
Useless In.	Aug. 4	5,030	...	74,150	1	...	...	...	1	...	...	2
Sarita Bay	Aug. 4	2,630	...	79,180	...	...	...	...	...	...	...	...
Uchucklesit Inlet	Aug. 6	5,000	5,220	81,810	...	...	...	...	2	...	...	2
Vernon Bay	Aug. 8	6,020	...	86,810	...	...	...	...	...	...	...	...
Pipestem In.	Aug. 9	5,700	...	92,830	...	...	...	...	...	...	...	...
Stopper Is.	Aug. 10	1,070	...	98,530	...	...	...	...	...	...	...	...
Banfield In.	Aug. 11	4,141	41,870	99,600	7	...	...	...	1	...	...	8
San Mateo B	Aug. 11	4,431	26,110	103,741	1	...	...	...	...	...	...	1
Sarita Bay	Aug. 13	4,298	2,630	108,172	3	...	...	1	1	...	...	5
Ucleulet In.	Aug. 13	1,850	950	112,470	...	...	...	...	...	1	...	1
Vernon Bay	Aug. 14	3,030	6,020	114,320	...	...	...	...	...	...	2	2
Uchucklesit Inlet	Aug. 15	4,240	10,220	117,350	...	...	...	...	...	...	...	...
Pipestem In.	Aug. 17	4,500	5,700	121,590	...	1	...	...	...	...	...	1
Banfield In.	Aug. 18	4,150	46,011	126,090	2	...	...	...	...	...	...	2
San Mateo B	Aug. 19	2,626 (7,020)	30,541	130,240	1	...	1	...	...	...	...	2
Sarita Bay	Aug. 21	3,629 (6,440)	6,928	132,866	...	...	...	...	...	...	...	...
Uchucklesit Inlet	Aug. 22	1,538 (5,180)	14,460	136,495	...	...	...	...	1	...	...	1
Pipestem In.	Aug. 23	3,155 (5,580)	10,200	138,033	1	...	...	...	...	...	...	1
Pipestem In.	Aug. 24	3,093 (4,320)	13,555	141,188	...	...	...	...	...	...	...	...
All localities		144,281 (28,540)			36	1	10	1	12	1	2	63

TABLE IV. Markings and recoveries of juvenile herring in Barkley Sound during 1954. Numbers bracketed under "Number marked" were checked only.

Marked at	Date	Number marked	Marked fish at large		Recoveries from							
			Locality	Sound	Banfield Inlet	Kelp Bay	Pipestem Inlet	San Mateo Bay	Uchucklesit Inlet	Ucluelet Inlet	Useless Inlet	All
Banfield In.	Jul. 21	5,510	...	...	...	...	...	...	...	...	...	...
Banfield In.	Jul. 22	4,970	5,510	5,510	2	...	...	...	...	...	...	2
Ucluelet In.	Jul. 24	7,240	...	10,480	...	...	...	...	...	...	...	...
Ucluelet In.	Jul. 25	2,980	7,240	17,720	...	...	...	...	...	...	...	...
Uchucklesit Inlet	Jul. 27	10,070	...	20,700	...	...	...	...	...	...	...	...
San Mateo B	Jul. 28	10,110	...	30,770	...	...	...	...	...	...	...	...
Pipestem In.	Jul. 30	6,910	...	40,880	...	...	...	...	...	...	...	...
Banfield In.	Jul. 31	6,230	10,480	47,790	3	...	...	...	...	...	...	3
San Mateo B	Aug. 3	8,130	10,110	54,020	...	...	...	3	...	...	...	3
Uchucklesit Inlet	Aug. 5	4,620	10,070	62,150	...	...	...	...	4	...	...	4
Pipestem In.	Aug. 6	8,330	6,910	66,770	...	...	5	...	...	...	...	5
Ucluelet In.	Aug. 8	3,630	7,240	75,100	...	...	...	...	...	1	...	1
Banfield In.	Aug. 9	6,050	16,710	78,730	2	...	...	...	...	...	...	2
San Mateo B	Aug. 10	10,210	18,240	84,780	...	...	...	4	...	...	...	4
Uchucklesit Inlet	Aug. 18	8,190	14,690	94,990	...	...	...	...	...	...	...	...
Pipestem In.	Aug. 19	6,790	15,240	103,180	...	...	5	...	...	...	...	5
Ucluelet In.	Aug. 20	2,060	13,850	109,970	...	...	...	...	...	...	...	...
Banfield In.	Aug. 21	3,300	22,760	112,030	...	...	...	...	...	...	...	...
Banfield In.	Aug. 22	4,220	26,060	115,330	...	...	...	...	...	...	...	...
Uchucklesit Inlet	Aug. 25	6,210	22,880	119,550	1	...	...	1	1	...	...	3
Pipestem In.	Aug. 26	6,420	22,030	125,760	...	...	5	...	...	...	...	5
Ucluelet In.	Aug. 27	8,970	15,910	132,180	...	...	...	...	...	6	...	6
Ucluelet In.	Aug. 28	1,960	24,880	141,150	...	...	...	...	...	...	...	...
Banfield In.	Aug. 30	4,750	30,280	143,110	2	...	...	1	...	...	...	3
Kelp Bay	Sep. 1	6,190	...	147,680	...	...	...	...	...	...	...	...
Useless In.	Sep. 2	5,270	...	153,870	...	...	...	...	...	...	...	...
Kelp Bay	Sep. 3	4,210 (2,030)	6,190	159,140	...	3	...	...	...	...	...	3
Ucluelet In.	Sep. 3	(2,450)	26,840	163,350	2	...	...	...	2	2	...	6
Useless In.	Sep. 6	(6,050)	5,270	163,350	...	...	...	...	...	...	3	3
Kelp Bay	Sep. 7	(10,810)	10,400	163,350	2	1	...	...	...	...	...	3
All localities		163,350 (21,340)			14	4	15	9	7	9	3	61

TABLE V. Summary of markings and recoveries of juvenile herring in Barkley Sound in 1951.

Marked at	Number marked	Recoveries from					
		Banfield Inlet	Cigarette Cove	Tzartes Island	Useless Inlet	Uchucklesit Inlet	All
Banfield Inlet	17,463	17	7	...	...	2	26
Cigarette Cove	2,926	2	4	...	...	...	6
Pipestem Inlet	687	...	...	...	...	...	...
Toquart Bay	1,957	3	7	5	2	4	21
Useless Inlet	10,953	...	...	...	5	...	5
Totals	33,986	22	18	5	7	6	58

TABLE VI. Summary of markings and recoveries of juvenile herring in Barkley Sound in 1952.

Marked at	Number marked	Recoveries from					
		Banfield Inlet	San Mateo Bay	Sechart Channel	Uchucklesit Inlet	Ucluelet Inlet	All
Banfield Inlet	21,506	3	...	...	...	...	3
Ecoole Cannery	2,064	...	...	...	...	...	...
Effingham Island	4,656	...	...	...	...	...	...
San Mateo Bay	22,917	...	8	...	...	3	11
Sechart Channel and Island Harbour	7,122	3	1	1	...	...	5
Uchucklesit Inlet	13,946	2	1	...	2	...	5
Ucluelet Inlet	10,869	...	...	...	...	3	3
Totals	83.080	8	10	1	2	6	27

Table VII. Summary of markings and recoveries of juvenile herring in Barkley Sound in 1953.

		Recoveries from								
Marked at	Number marked	Banfield Inlet	Pipestem Inlet	San Mateo Bay	Sarita Bay	Uchucklesit Inlet	Ucluelet Inlet	Useless Inlet	Vernon Bay	All
Banfield Inlet	50,161	26	1	5	3	...	...	1	...	36
Pipestem Inlet	16,448	...	1	...	...	...	...	...	...	1
San Mateo Bay	33,167	3	...	7	...	...	...	...	...	10
Sarita Bay	10,557	...	...	...	1	...	...	...	...	1
Stopper Islands	1,070	...	...	...	...	...	...	...	...	...
Uchucklesit Inlet	15,998	3	...	4	1	3	...	1	...	12
Ucluelet Inlet	2,800	...	...	...	...	...	1	...	...	1
Useless Inlet	5,030	...	...	...	...	...	...	...	...	...
Vernon Bay	9,050	...	...	...	...	...	...	...	2	2
Totals	144,281	32	2	16	5	3	1	2	2	63

Table VIII. Summary of markings and recoveries of juvenile herring in Barkley Sound in 1954.

		Recoveries from						
Marked at	Number marked	Banfield Inlet	Kelp Bay	Pipestem Inlet	San Mateo Bay	Uchucklesit Inlet	Ucluelet Inlet	Useless Inlet	All
Banfield Inlet	34,850	9	2	...	...	1	2	...	14
Kelp Bay	10,400	...	4	...	...	...	...	...	4
Pipestem Inlet	28,450	...	...	15	...	...	...	...	15
San Mateo Bay	28,450	1	...	...	7	1	...	...	9
Uchucklesit Inlet	29,090	...	...	...	...	5	2	...	7
Ucluelet Inlet	26,840	...	...	...	...	...	9	...	9
Useless Inlet	5,270	...	...	...	...	...	...	3	3
Totals	163,350	10	6	15	7	7	13	3	61

Table IX. Summary of markings and recoveries of juvenile herring in Barkley Sound over the period 1951–1954.

		Recoveries from												
Marked at	Number marked	Banfield Inlet	Cigarette Cove	Kelp Bay	Pipestem Inlet	San Mateo Bay	Sarita Bay	Sechart Channel	Tzartes Island	Uchucklesit Inlet	Ucluelet Inlet	Useless Inlet	Vernon Bay	All
Banfield Inlet	125,380	55	7	2	1	5	3	...	...	3	2	1	...	79
Cigarette Cove	2,926	2	4	...	...	...	...	...	...	...	...	...	...	6
Effingham Island	4,656	...	...	...	...	...	...	...	...	...	...	...	...	...
Kelp Bay	10,400	...	...	4	...	...	...	...	...	...	...	...	...	4
Pipestem Inlet	45,585	...	...	...	16	...	...	...	...	...	...	...	...	16
San Mateo Bay	84,534	4	...	...	...	22	...	...	...	1	3	...	...	30
Sarita Bay	10,557	...	...	...	...	...	1	...	...	...	...	...	...	1
Sechart Channel	7,122	3	...	...	...	1	...	1	...	...	...	...	...	5
Stopper Islands	1,070	...	...	...	...	...	...	...	...	...	...	...	...	...
Toquart Bay	1,957	3	7	...	...	...	...	...	5	4	...	2	..	21
Tzartes Island	4,164	...	...	...	...	...	...	...	...	...	...	...	...	...
Uchucklesit Inlet	64,843	5	...	...	...	5	1	...	...	10	2	1	...	24
Ucluelet Inlet	40,509	...	...	...	...	...	...	...	...	...	13	...	...	13
Useless Inlet	21,253	...	...	...	...	...	...	...	...	...	...	8	...	8
Vernon Bay	9,050	...	...	...	...	...	...	...	...	...	...	...	2	2
Totals	436,070	72	18	6	17	33	5	1	5	18	20	12	2	209

(584)

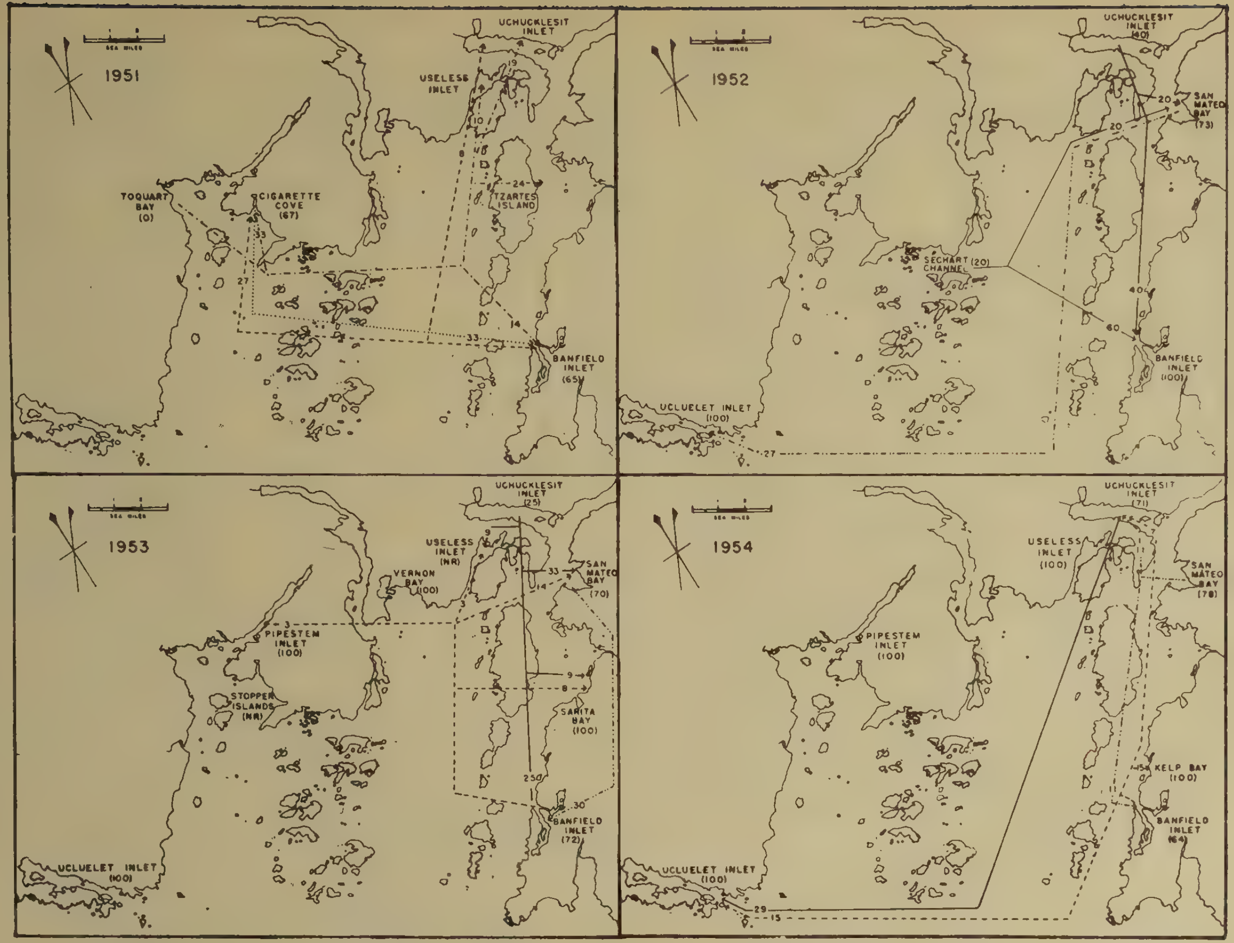
1951
UCHUCKLESIT INLET
USELESS INLET
TOQUART BAY (0)
CIGARETTE COVE (67)
TZARTES ISLAND
BANFIELD INLET (65)
19
10
48
24
33
27
14
33
1952
UCHUCKLESIT INLET (40)
SAN MATEO BAY (73)
SECHART CHANNEL (20)
BANFIELD INLET (100)
UCLUELET INLET (100)
20
20
40
60
27
1953
UCHUCKLESIT INLET (25)
USELESS INLET (NR)
VERNON BAY (100)
SAN MATEO BAY (70)
PIPESTEM INLET (100)
STOPPER ISLANDS (NR)
SARITA BAY (100)
BANFIELD INLET (72)
UCLUELET INLET (100)
9
33
14
3
3
9
8
250
30
1954
UCHUCKLESIT INLET (71)
USELESS INLET (100)
SAN MATEO BAY (78)
PIPESTEM INLET (100)
KELP BAY (100)
BANFIELD INLET (64)
UCLUELET INLET (100)
29
15
SEA MILES

FIGURE 6. Migrations of the juvenile herring in Barkley Sound in 1951, 1952, 1953 and 1954 as indicated by the recoveries of marked fish. (Figures in parentheses by locality names indicate percentage of recoveries from markings made there which were taken in the locality of marking.)

The last-named situation is fairly well established since scoutings in 1954 showed that, at times, the schools of young herring extended along the entire one-mile coast between Banfield Inlet and Kelp Bay, and individual schools were observed from one of these localities to the other. Also, the composition of the two stocks is virtually identical (see length-frequency analysis).

The Uchucklesit Inlet picture is not as clear. This inlet is only two miles from San Mateo Bay, but the two are separated by a deep channel. The 1954 data (Table VIII) show no indications of extensive mixing between these two localities but in 1953 (Table VII) more Uchucklesit Inlet marks were taken in San Mateo Bay than in Uchucklesit Inlet itself. The movement seems to be more in the direction of San Mateo Bay than the reverse. If these two localities are considered to contain the same stock it too would fit the general pattern of less than one-third of the population emigrating. On the other hand the Uchucklesit Inlet fish may form a highly migratory stock which dispersed into the other localities in that general region, namely, into San Mateo Bay, Sarita Bay, Useless Inlet and Banfield Inlet. The fact that the San Mateo Bay fish, themselves, behaved like an individual stock favours this hypothesis. Mixing between these two localities would be expected to be greatest since they are closest geographically. The length-group analysis of the fish in these two regions favours this alternative.

A certain amount of mixing between the fish of Uchucklesit Inlet, San Mateo Bay and Banfield Inlet was apparent from the data from all years (Fig. 6). The 1953 data suggest that Sarita Bay and Useless Inlet fish also contributed to this mixing. Markings in Useless Inlet were also carried out in 1951 and 1954 but failed to show any mixing. However, only three markings were carried out in other localities after the 1954 marking, and the fish would scarcely have had time to migrate in that short period (1 to 5 days). In 1951 the only nearby locality in which markings were carried out was Banfield Inlet, and since only five recoveries were made from the Useless Inlet marking it is not surprising that none was made outside the inlet.

The 1952 recoveries suggest that the Sechart Channel–Island Harbour fish also participated in the general mixing in this region. Since these fish disappeared early in the summer and no appreciable numbers of fish were found there in other years, it is difficult to assess their role in the general picture unless it is assumed that these fish were transients on their way to form the stocks along the southeast side of the sound.

Considering the combined data for all years (Table IX), the fish in each locality (except the two transient groups in Sechart Channel and Toquart Bay, and the Uchucklesit Inlet fish discussed above) showed emigration by less than one-third of the stock. A limited amount of longer range cross-sound migration (i.e., movement across or around the sound to the opposite side) is indicated in all years. In 1951, seven (29%) of the Banfield Inlet recaptures were taken in Cigarette Cove, and movement in the reverse direction was 33% (7 marks); Toquart Bay marks were found in Cigarette Cove (33%) and in all localities studied on the southeast side of the sound (Banfield Inlet, 14%; Trevor Channel, 24%; Uchucklesit Inlet, 19%; and Useless Inlet, 10%). In 1952, three (27%) of the San Mateo Bay

(586)

marks were taken in Ucluelet Inlet. In 1953, one (3%) of the Banfield Inlet marks was recovered in Pipestem Inlet. In 1954, two (14.5%) of the Banfield Inlet, and two (29%) of the Uchucklesit Inlet marks were recovered in Ucluelet Inlet.

Over the 4-year period, emigration from the southeast to the northwest side of the sound amounted to 2.5% from Banfield Inlet to Pipestem Inlet; 2.5% from Banfield Inlet to Ucluelet Inlet; 10% from San Mateo Bay to Ucluelet Inlet; and 8% from Uchucklesit Inlet to Ucluelet Inlet. In the opposite direction, the emigration from Toquart Bay was 14% to Banfield Inlet, 24% to Trevor Channel, 19% to Uchucklesit Inlet and 10% to Useless Inlet. In addition, 33% of the Cigarette Cove fish emigrated to Banfield Inlet.

It would thus appear that there is some cross-sound migration, although the length-frequency analysis of the sampling data fails to indicate any extensive mixing. However, with the exception of the movement observed in 1951 eastward from the Toquart Bay–Cigarette Cove region to the southeast shore, these migrations appear to be less extensive than those between localities along either side of the sound. The 1951 migration may represent a late movement of juveniles into their natural rearing grounds as these fish disappeared from the Toquart Bay–Cigarette Cove region early in August and did not reappear. Thus, considering the results for the last three years only, the cross-sound migration is only about one-fifth that between localities on the same side of the sound (Table X).

TABLE X. Percentage movement of marked fish from one locality to other localities on the same side of the sound and from one side of the sound to the other. Actual numbers are given in parenthesis.

	1951	1952	1953	1954	1951–54	1952–54
Between localities SE side	8 (2/24)	33 (7/21)	35 (21/60)	15 (5/33)	25 (35/138)	29 (33/114)
Between localities NW side	64 (7/11)	. .	0 (0/2)	0 (0/24)	19 (7/37)	0 (0/26)
SE side to NW side of sound	23 (7/31)	13 (3/24)	12 (1/61)	11 (4/37)	10 (15/153)	7 (8/122)
NW side to SE side of sound	59 (16/27)	0 (0/3)	0 (0/2)	0 (0/24)	29 (16/56)	0 (0/29)
Total movement on one side of sound	26 (9/35)	33 (7/21)	34 (21/62)	9 (5/57)	24 (42/175)	24 (33/140)
Total movement across sound	25 (23/58)	11 (3/27)	2 (1/63)	7 (4/61)	15 (31/209)	5 (8/151)

The extent of mixing between stocks bears a relationship to distance. Using the data for all four years, the number of recoveries taken at 5-mile intervals was as below. Distances measured followed shorelines and islands except where

Distance moved	Recoveries	
miles	*number*	%
0–1	137	66
1–5	28	12
5–10	17	8
10–15	14	7
15–20	11	5
20–25	5	2

major detours would have been involved. Thus the number of migrants decreases by about one-fifth each 5-mile interval from the area of tagging. These movements are, therefore, probably random. Fewer cross-sound migrations were observed because the distance is greater across the sound than between localities on one side. Indeed, no migrations were observed across the 10 miles separating the two major stocks on the northwest side (Pipestem Inlet and Ucluelet Inlet).

SAMPLING PROGRAM

Samples of over 100 of these fish were taken periodically from the major stocks located and preserved in 5% formalin. One hundred fish from each sample were later measured and weighed. The standard length of each fish (distance from the tip of the snout to the end of the fleshy part of the tail) was measured to the nearest half-millimeter, and each fish was weighed to the nearest twentieth of a gram. Sampling data were checked in three ways (Appendix 2). Randomness of selection of the fish preserved as a sample was checked by comparing two independent samples from the same catch. Average weights were checked by weighing the sample as a whole. (The average of these two determinations was taken as the sample average.) As a check on the randomness of selection of the fish sampled, the remainder of the fish preserved were weighed as a unit and their average weight calculated. Generally this average corresponded closely with that found for the sample. The number of samples taken in Barkley Sound in all years is given below along with the number of fish examined.

Year	1951	1952	1953	1954	All
Number of samples	56	65	91	76	288
Number of fish	3,700	8,276	12,306	9,667	33,949

Samples were also taken from other areas on the west coast of Vancouver Island (1952), the lower east coast of Vancouver Island (1951, 1952, 1953), from mortality experiments (1952, 1953) and from the fishery (1951, 1952). The total sampling for all years may be summarized as follows:

Year	1951	1952	1953	1954	All
Number of samples	116	90	192	76	474
Number of fish	8.247	16,834	15,621	9,667	44,369

LENGTH-FREQUENCY ANALYSES

Analysis of the sampling data indicated the presence of more than one size-group of juvenile herring in Barkley Sound, presumably reflecting the different ages of the various hatchings (Hourston, 1956). Since a frequency distribution from a single hatching usually forms a normal curve, frequency distributions of lengths of fish in samples from the various localities may be inspected for the presence of more than one normal distribution. This may be accomplished by direct inspection of the frequency plot for polymodal tendencies or by a graphic analysis of the various plots. Where the stocks in two localities are represented by

(588)

samples differing markedly in the number or size of the length groups, these stocks are not likely to have mixed to any great extent. Stocks that showed similar frequency distributions could have intermixed more freely (but need not have done so).

DIRECT ANALYSIS. Length-frequency distributions for the individual samples were plotted by locality in a time-scale series for each year (Fig. 7–10). When several samples were taken in the same locality over a short period of time, some plots overlapped each other and had to be displaced slightly in the time-scale to be distinguished. However, this displacement never exceeded two days.

In 1951 a particularly wide scatter was shown by the Banfield Inlet samples. At least four size-groups were prominent in the various samples and many more may have been present. At least two size-groups were apparent in the Cigarette Cove and Toquart Bay data. A single size-group dominated the other plots, but their wide size-range (e.g. in Pipestem Inlet) or skewed shape (e.g. in Trevor Channel) indicated the probable presence of other groups. It appeared from the size-range and the position of the major modes that the Banfield Inlet fish did not emigrate appreciably to other localities, although fish from the other localities could have joined the Banfield Inlet stock. However, the Cigarette Cove and Toquart Bay fish showed sufficiently similar distributions to admit of considerable mixing, as did the Uchucklesit Inlet, Useless Inlet and Trevor Channel fish. The latter group of fish appeared to be longer than the former. The single Pipestem Inlet sample was scarcely sufficient for adequate comparison but could have showed some mixing with the Cigarette Cove and Toquart Bay fish.

In 1952 considerable scatter and variability was again demonstrated by the Banfield Inlet samples; at least three modes were apparent. In the Broken-Group samples the distribution was similar to that in Banfield Inlet, but was less erratic, indicating that migration from the Broken-Group to Banfield Inlet was quite possible. The San Mateo Bay samples also showed a wide scatter and at least three modes, but these tended to be at a greater length than those for the Banfield Inlet fish. Migration from Uchucklesit Inlet to San Mateo Bay was compatible with the length-frequency distributions, but, due to the smaller range in size and the unimodal distribution of the former fish, migration in the opposite direction was less likely. The Ucluelet Inlet fish had a more or less unimodal distribution and tended to be much smaller than those in other localities. The single Useless Inlet sample resembled the Uchucklesit Inlet ones in distribution but was characterized by a larger size-range. The Cigarette Cove fish resembled the Ucluelet Inlet fish in their mode but exhibited a wider size-range. On this basis, neither the Banfield Inlet fish nor the San Mateo Bay fish joined other stocks in appreciable numbers although these two stocks may have intermixed. The Broken-Group fish could have joined the Banfield Inlet stocks or the Uchucklesit Inlet stocks in appreciable numbers early in the season. There may have been some emigration from Uchucklesit Inlet to San Mateo Bay. The Ucluelet Inlet fish appear to have remained more or less isolated.

In 1953 sampling was concentrated in a shorter time period and major trends were therefore more evident. Again the Banfield Inlet and San Mateo Bay plots showed considerable scatter and variability; each indicated a minimum of four size-groups. Mixing between these two groups was quite possible, although the main modes tended to be at greater lengths in San Mateo Bay. The Useless Inlet samples were also characterized by a considerable scatter, although one major mode was evident. This scatter could be accounted for by limited emigration from the Banfield Inlet or San Mateo Bay stocks, or from both. Ucluelet Inlet fish also varied considerably but from the last week in July were dominated by one size-group of relatively small fish. About the same time a dominant group of fish of similar size appeared in Pipestem Inlet; it also appeared in the Stopper Islands, although a larger size-group dominated one of these samples. The ubiquitous presence of this size-group in localities along the northwest side of the sound could indicate a general mixing in this area, or could indicate that these localities shared the results of the same spawnings more or less equally. In any event, this

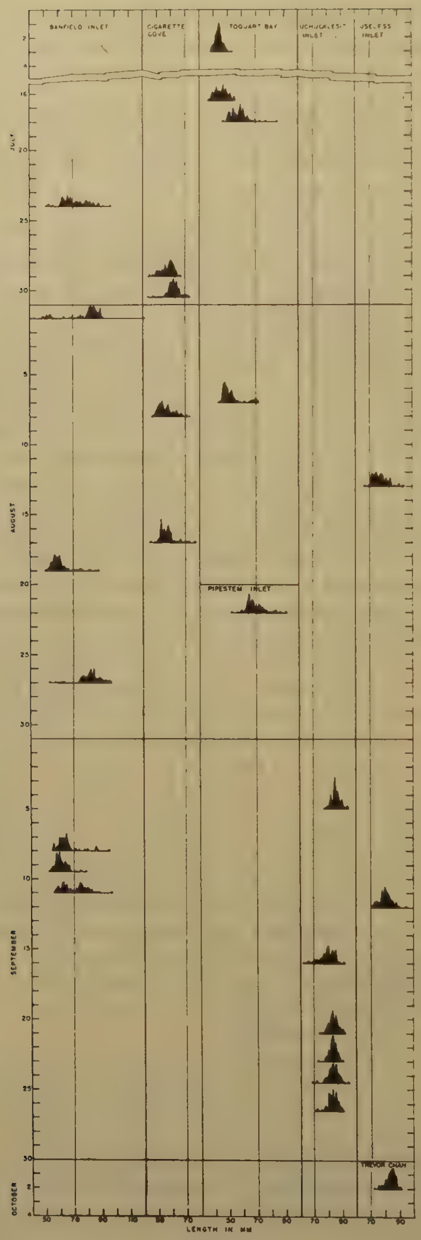

FIGURE 7. Frequency distributions of the standard lengths of juvenile herring in the 1951 samples plotted on a time scale according to date of capture.

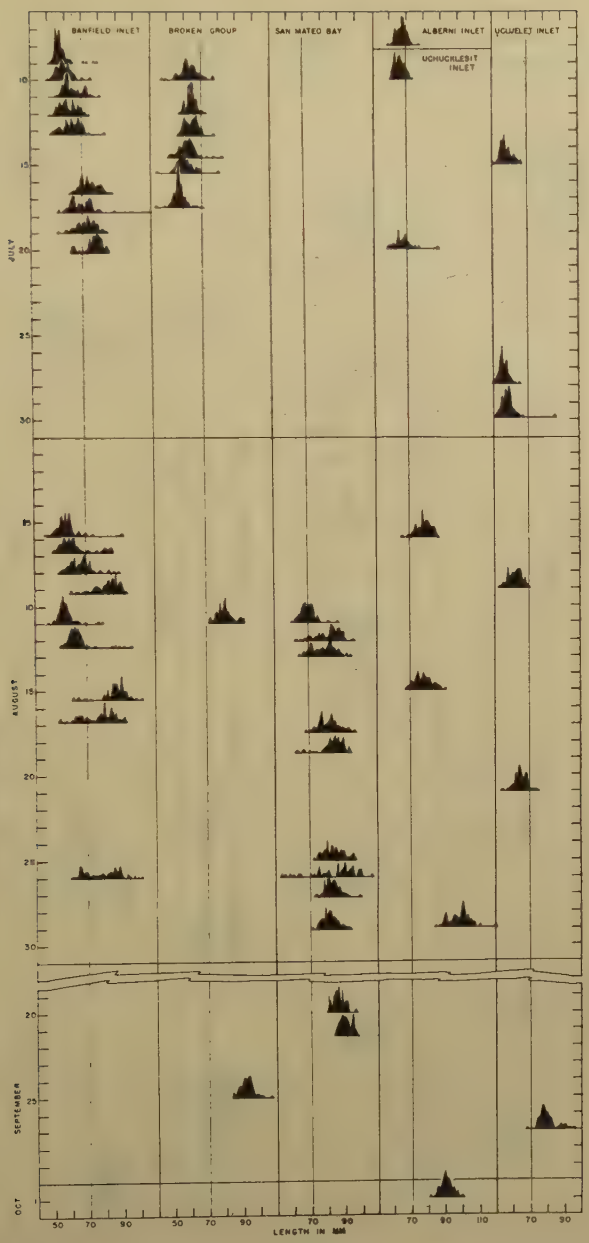

Figure 8. Frequency distributions of the standard lengths of juvenile herring in the 1952 samples plotted on a time scale according to date of capture.

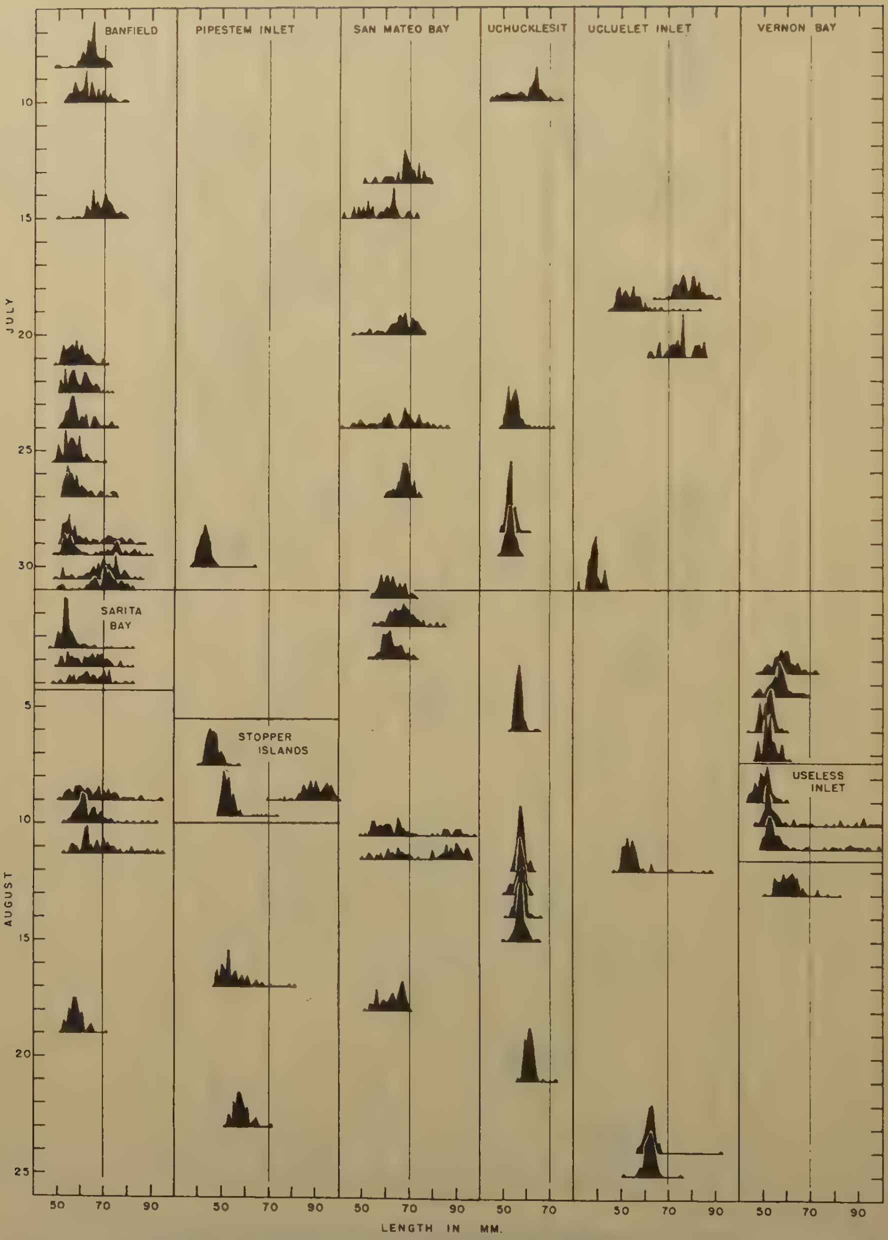

FIGURE 9. Frequency distributions of the standard lengths of juvenile herring in the 1953 samples plotted on a time scale according to date of capture.

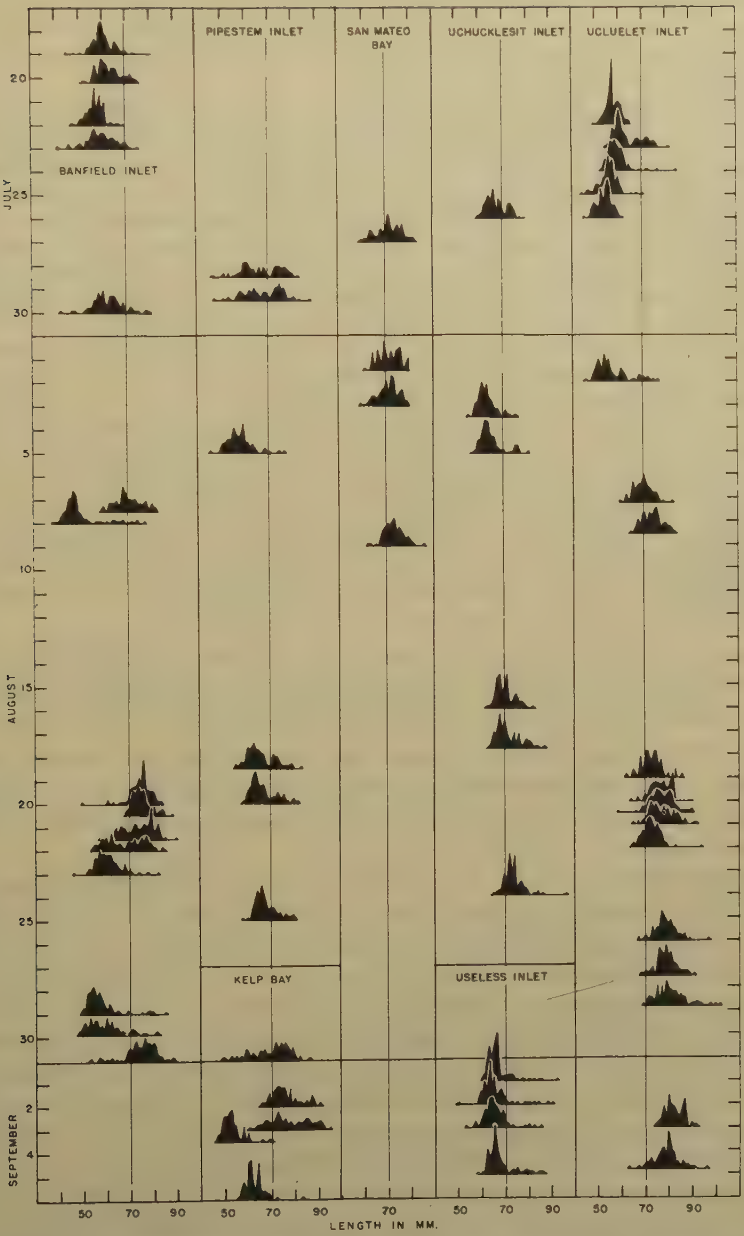

FIGURE 10. Frequency distributions of the standard lengths of juvenile herring in the 1954 samples plotted on a time scale according to date of capture.

size-group distinguished the stocks on that side of the sound and indicated that mixing was relatively limited with the stocks elsewhere. A slightly larger but slower-growing size-group markedly dominated the Uchucklesit Inlet stock and appears to have been present but less dominant in the Useless Inlet and Vernon Bay stocks. Mixing between these three localities was also quite possible, but the small size-range shown by the Uchucklesit Inlet fish indicates little immigration into this locality.

In 1954 the samples were again concentrated in a short time interval. A wide size-range and considerable variability were again demonstrated by the Banfield Inlet samples. This feature is shared with the Kelp Bay fish, and the fish in these two localities could have mixed freely. At least three size-groups were present in each. The San Mateo Bay samples failed to show the scatter and variability noted in other years. One size-group dominated throughout, although at least two others were probably present. These fish appeared to be larger than the dominant size-groups in Banfield Inlet. A single smaller size-group dominated in Uchucklesit Inlet although at least two others were present there. In Useless Inlet an even smaller size-group dominated; considerable scatter was evident, made up of at least three size-groups of larger fish. Thus, each of the stocks on the southeast side of the sound appeared to be characteristically different. The scatter evident in all may reflect limited immigration from the other stocks. Ucluelet Inlet and Pipestem Inlet fish also showed considerable scatter in their length-frequency plots, with one size-group dominating. In Pipestem Inlet this was the smaller size-group (which was roughly about the same size as the smaller dominant group in Banfield Inlet). In Ucluelet Inlet, a slightly larger size-group dominated, but at least one smaller and two larger size-groups were included. Limited mixing between these two localities was likely, as the dominant size-group in each was evident as a secondary size-group in the other. Some mixing between Ucluelet Inlet and San Mateo Bay and/or Uchucklesit Inlet was also possible on this basis.

In all years, the extensive scatter shown by the Banfield Inlet samples could reflect immigration from any and all other localities.

PROBABILITY PLOT ANALYSIS. A method of separating a frequency-distribution plot into its theoretical normal curve components by plotting probability graphs has been described by Harding (1949) and discussed by Cassie (1950, 1954). Since the length-frequency distribution for the progeny of a single spawning should form a normal curve, this procedure seemed promising as a method of sorting out size-groups of juveniles resulting from the contributions of different hatchings.

The procedure is to plot the cumulative percentage length-frequencies for the sample on probability graph paper. Single size-groups or normal curves are "probably" represented by a single unbroken line. Where the trend line shifts in slope or position, a new size-group is indicated, with the point of inflection of the sigmoid curve joining two succeeding lines representing the division between the two size-groups. Plots showing the presence of one, two, three and five size-groups (Fig. 11) illustrate the procedure. It was sometimes difficult to determine whether a series of points represented a new size-group or merely the sigmoid curve joining two other size-groups; when the number of fish involved was relatively large, the points were considered to represent a new size-group.

Each size-group determined in this manner is then replotted as a single frequency distribution (Fig. 11) with the ordinate (length) corresponding to 50% representing the mean of the group, and the range between 16.7% and 88.3% representing two standard deviations. The normal curves represented by these lines may then be plotted over a histogram of the observed frequencies to indicate the length-group composition of the sample (Fig. 11).

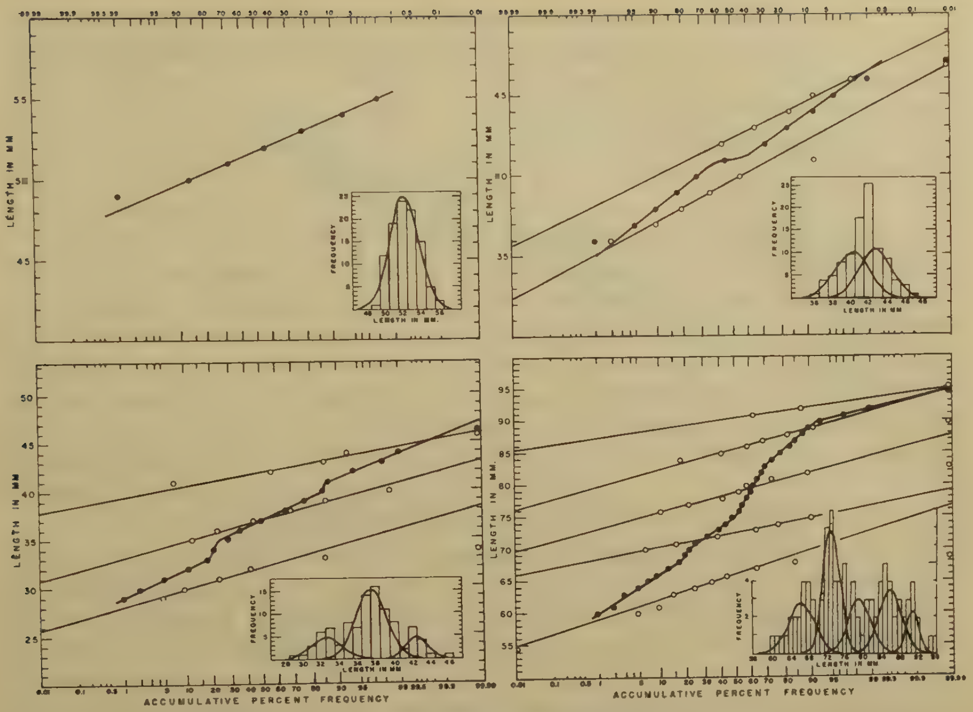

FIGURE 11. Probability plots of length-frequency distributions for a unimodal sample, a bimodal sample, a trimodal sample and a pentamodal sample.

There were a large number of spawnings (13 to 19) each year in Barkley Sound, and a certain amount of mixing throughout the sound was indicated by the marking studies. Detecting as large a number of size-groups as this in probability plots, and relating them to the various spawnings would be exceedingly difficult, if not impossible.

Therefore, as a test of the method, an analysis was run on the Departure Bay samples from 1950 to 1953 inclusive (Appendix 3). There were only three or four major spawnings per year in this region and it should be reasonably easy to detect that number of size-groups by this method. In each year the number of size-groups found corresponded with the number of major spawnings in the region. It would therefore appear that these size-groups were due to the age differential resulting from spawnings at different times, and thus that this graphic analysis probably detected real differences. Indeed, the size-group means determined in this manner for the Departure Bay data for 1950 and 1951 formed four and three relatively clear cut lines with very little scatter in a semi-logarithmic plot of length against date of capture (Fig. 12), whereas a similar plot of the sample means for 1950 and 1951 showed a considerable amount of scatter.

The method has a number of limitations, namely:

(1) Lines were fitted by sight to the probit plots. On some diagrams more than one set of lines could be interpreted. If the scatter of the points about the

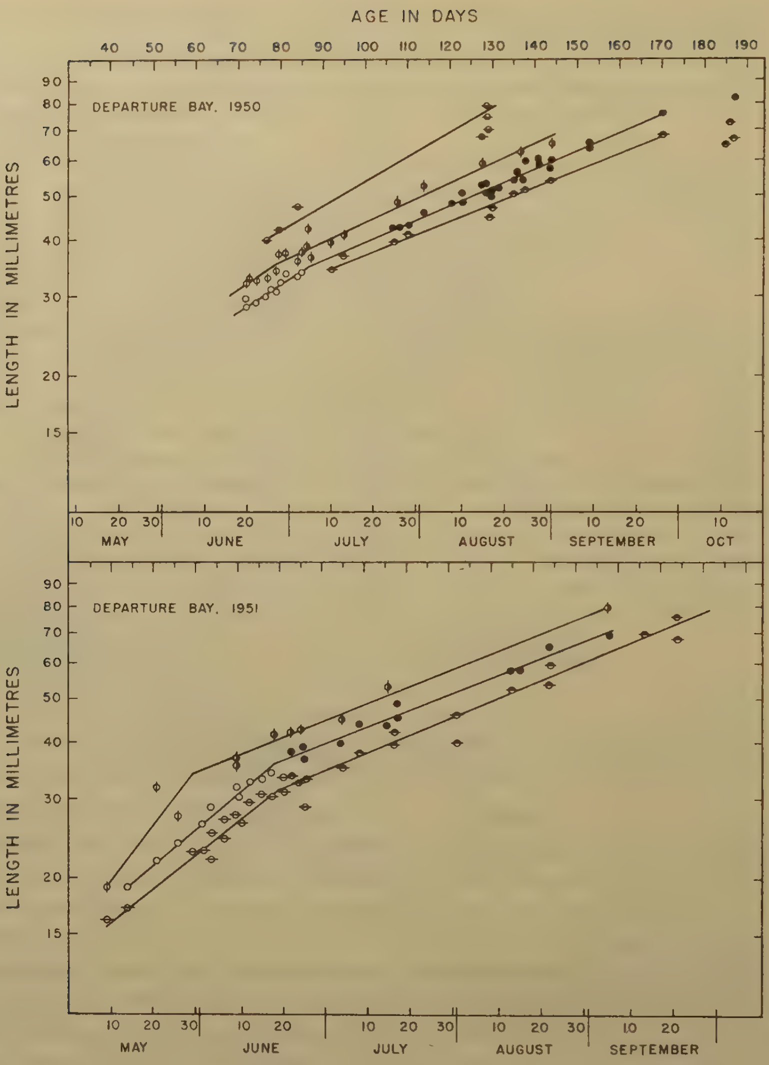

FIGURE 12. The relationship of the logarithm of length to date of capture, for different size-groups of juvenile herring in Departure Bay during 1950 and 1951.

proposed lines was relatively large, a questionable break was usually considered unreal but if the scatter was small, the questionable group was accepted.

(2) When a frequency distribution showed considerable variation in the "tails" of the curve, it was often impossible to sort out more than one group with any degree of confidence as the number of fish involved was usually very small.

(3) Since the size-range in some samples taken at approximately the same time differed widely, the maximum number of size-groups in any one sample

would not represent the maximum number in any locality. Consequently it was necessary to plot the size-group means and fit growth curves (straight lines on a semi-logarithmic plot) to the points to estimate the number of size-groups found in the locality. When a large number of points were involved, the number of lines represented was not clear. In such plots, the minimum probable number of lines were drawn. This was sufficient to indicate lack of mixing with stocks containing only a few size-groups.

(4) Individual size-groups may not be represented by normal curves in a frequency distribution. Predation could be rather specific to size, distorting the normal curve so that probit analysis would indicate more than one size-group.

Thus erroneous conclusions could easily have been drawn for individual samples. However, when a series of samples shows consistent trends, as for the juvenile samples from Departure Bay, it is highly probable that real differences are being detected. The fact that the number of size-groups found in the juvenile samples from Departure Bay corresponds with the number of major spawnings in that locality lends additional validity to the results.

The method was therefore applied to the Barkley Sound data. The means of the length-groups were plotted logarithmically against time for the six most heavily sampled localities (Fig. 13). Lines were fitted visually to these means in an effort to clarify the number of size-groups involved. In some diagrams other sets of lines could have been drawn but would not have affected materially the number of size-groups. While the maximum number of size-groups in any one sample was six, different samples were taken on the same or successive days indicated groups beyond the size-range of other samples and thus the presence of a larger number of groups in some localities. In all diagrams the number of size-groups indicated was greater than could clearly be observed in the direct analysis of the length-frequency plots.

Sampling was not sufficiently intensive in 1951 to permit much comparison between localities. In Banfield Inlet, the only locality where sampling was sufficiently intensive to permit an estimate of the number of size-groups, six size-groups were detected. Scanty sampling in Pipestem, Uchucklesit and Useless Inlets showed three size-groups in each. Thus appreciable immigration to the latter localities from Banfield Inlet appears unlikely as the smaller size-groups in Banfield Inlet were not detected elsewhere.

In 1952, nine size-groups were found in Banfield Inlet, precluding extensive emigration of these fish to other localities, all of which contained fewer size-groups. Six size-groups were found in San Mateo Bay, but they tended to be larger than those in Banfield Inlet, in mid-August at any rate. However, their apparently slower growth rate would eliminate this difference by mid-September. Thus some intermixture may have taken place between these two localities. Similar slopes to those found in Banfield Inlet were shown by the Uchucklesit Inlet size-groups but these fish were larger, more the size of the San Mateo Bay fish. Some of these fish could have joined the San Mateo Bay fish but the large number of size-groups in the latter locality precludes appreciable movement in the opposite direction. The four Useless Inlet size-groups were also found in Banfield Inlet so some of these fish could have moved to Banfield Inlet. The four size-groups found in Ucluelet Inlet were smaller than those found elsewhere, except for the smaller size-groups in Banfield Inlet. Since the latter had a greater slope, mixing either way could not have been extensive. These conclusions are all in agreement with those found in the direct analysis.

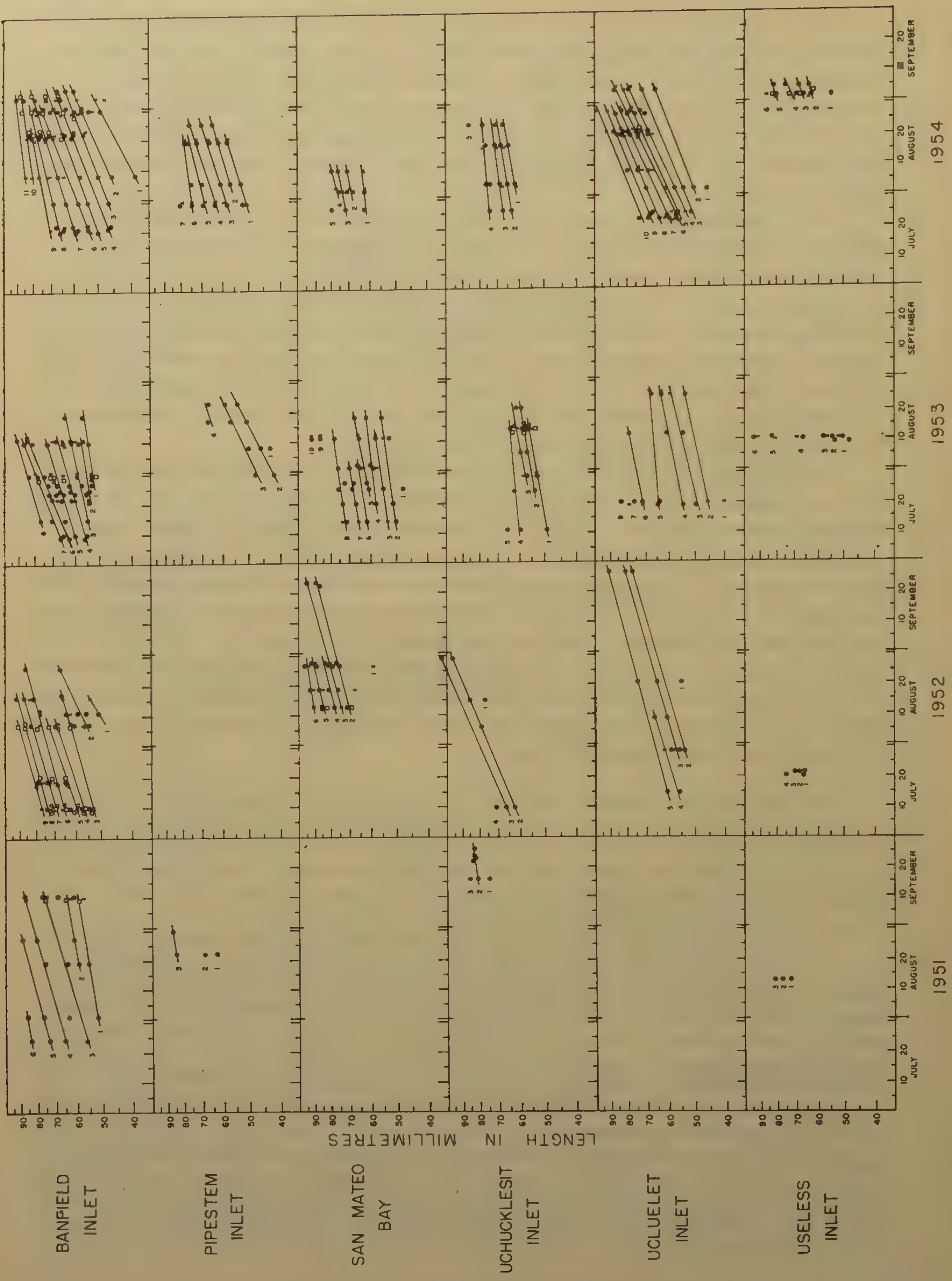

FIGURE 13. The relationship of the logarithm to length to date of capture, for size-groups within samples from six of the most extensively sampled localities in Barkley Sound.

In 1953, eight size-groups were found in the Banfield Inlet data. Ten were found in San Mateo Bay but these had smaller slopes. However, because of the complexity of both diagrams the slopes could have been interpreted differently in either case, and consequently these two stocks could have intermixed. The Uchucklesit Inlet plots showed slopes comparable to those found in the San Mateo Bay plots, and their five length-groups were all represented in San Mateo Bay (numbers 2, 3, 4, 6 and 7). Consequently, Uchucklesit Inlet fish could have migrated to San Mateo Bay in appreciable numbers, but movement in the opposite direction could not have been extensive. The Ucluelet Inlet samples had the widest size-range early in the season with eight size-groups appearing. The Pipestem Inlet fish were small; three of the four size-groups found corresponding roughly to numbers 1, 2 and 4 in Ucluelet Inlet. Thus there may have been some migration from Pipestem Inlet to Ucluelet Inlet but little movement in the opposite direction was likely. The smaller size-groups in these two localities were not found elsewhere, indicating very little emigration to localities on the other side of the sound. The six size-groups in Useless Inlet were again found in Banfield Inlet, indicating some Useless Inlet fish may have migrated to Banfield Inlet. This is in agreement with the results of direct analysis.

In 1954 the Banfield Inlet data again showed a large number of size-groups (eleven). Ten size-groups were found in Ucluelet Inlet, but these covered a smaller size-range and tended to be bigger fish. Their trend lines had greater slopes than those for Banfield Inlet. The Kelp Bay fish seemed to fit the pattern shown by the Banfield Inlet fish and were plotted on the same graph. The six size-groups found in Useless Inlet corresponded fairly closely with numbers 2, 5, 6, 7, 9 and 10 in the Banfield Inlet–Kelp Bay plot; Useless Inlet fish may therefore have migrated in appreciable numbers to Banfield Inlet, but migration in the opposite direction would have been limited. Both the San Mateo Bay and Uchucklesit Inlet plots were again characterized by smaller slopes. The five Uchucklesit Inlet groups corresponded roughly with the five groups in San Mateo Bay and the two groups of fish could have mixed freely. These size-groups could also have corresponded to the larger size-groups in Useless Inlet, although the difference in the time of sampling precludes accurate comparison. A relatively large number (seven) of size-groups was also found in Pipestem Inlet, representing a wide size-range. These size-groups did not correspond closely with those in any of the other localities.

The direct analysis of the length-frequency distributions indicated some mixing between San Mateo Bay, Uchucklesit Inlet and Useless Inlet but the dominance of different size-groups in these localities showed that this mixing was limited, not relatively free as indicated above. On the other hand, the former analysis shows some mixing between Pipestem Inlet and Ucluelet Inlet was likely, whereas the probability plot analysis shows this was unlikely. Mixing between Ucluelet Inlet and San Mateo Bay and Uchucklesit Inlet was also not very probable according to the latter analysis.

CONCLUSIONS ON COMPOSITION

On the whole, the results of the length-frequency analysis support the conclusions from the marking experiment. These include:

(1) The Banfield Inlet and Kelp Bay fish form a single stock.

(2) The Toquart Bay fish mix freely with those in Cigarette Cove, possibly forming a single stock.

(3) Other localities appear to contain relatively discrete stocks.

(4) These stocks mix to some extent.

(5) The 1952 Sechart Channel and Broken Group fish that disappeared in mid-summer moved to the southeast side of the sound, mainly to Banfield Inlet.

(6) The 1951 Toquart Bay–Cigarette Cove fish that disappeared early in the summer migrated to various localities on the southeast side of the sound.

(7) The results of the marking program left the status of the Uchucklesit Inlet fish unsettled. However, the difference in composition of the Uchucklesit

Inlet and San Mateo Bay fish found every year except 1954, indicates that these two groups of fish did not form a single stock. Uchucklesit Inlet fish migrated to San Mateo Bay in 1952 and especially 1953 but only one San Mateo Bay mark was recovered in Uchucklesit Inlet, and that was in 1954 when the composition of these two stocks was more similar than in other years. The Uchucklesit Inlet fish may, therefore, be considered to have formed a single stock which showed stronger migratory tendencies than the other stocks studied.

Thus the Barkley Sound juvenile herring population during these years was made up of a series of individual stocks which mixed somewhat, but not enough to destroy their identity. These stocks contained varying numbers of size-groups, presumably the progeny of different spawnings, so that they differed somewhat in the average length of the fish and in growth-rates. Growth patterns varied from year to year and may have differed significantly from those observed in other major herring populations.

ABUNDANCE OF JUVENILE HERRING IN BARKLEY SOUND

A general estimate of the juvenile herring population in Barkley Sound was made each year from a scouting survey. More precise estimates of some of the major stocks were made by Schnabel-type marking experiments. These more precise estimates were then employed to provide a correction factor for the general estimate, which was invariably low, since all the fish in any locality were seldom observed in any scouting.

Scouting Surveys

Scouting for juvenile herring consisted mainly of visual observations of schools flipping at the surface. The juvenile schools were readily observed when they broke surface, usually in the early morning (dawn to sunrise) and late evening (sunset to dusk). They occasionally appeared during the day also, especially when they were abundant, but such appearances were not consistent. Many of these schools were seined to obtain fish for marking and thus enabled counts of the number of fish in these schools. The results were applied in estimating the number of fish seen in a locality. General estimates according to a scale of abundance were made at first but these were soon supplemented by absolute estimates of abundance. Since the extent to which the fish show at the surface varies with weather conditions, these conditions were also recorded at the time of observation. Observations made under poor weather conditions were repeated under good conditions in order to obtain more reliable estimates of distribution and abundance.

Early in the summer the schools tended to be relatively small, consisting of a few hundred fish. As time passed the schools grew larger and by mid-July most contained several thousand fish (averaging about 10,000). When these schools showed at the surface in calm water, several flips could be seen at one time, generally in a circle 1 or 2 feet in diameter. The surface area actually occupied by such schools appeared to be about 20 to 30 feet square (6–9 m.). In late summer and early fall (mid-August on) the schools often mingled to form large masses of fish; sometimes over a million fish would be schooled together in this manner. Such bodies of fish were estimated in terms of the number of "normal" (10,000 fish) schools they contained from the number of "groups" of flips showing (several flips in a small circle) and by the area they occupied.

The problem of weather conditions during observation was alleviated somewhat in 1952 and succeeding years by the application of the echo-sounder to these surveys. When the fish were right at the surface, the echo-sounder would not pick them up, but below a depth of about ten feet (3 m.) they produced marks on the sounder paper. At a speed of 7 to 9 knots (13–17 km./hr.) many such marks appeared as tiny lines about 1.5 mm. deep (the distance between two fine lines on Bendix sounder paper), and one to three scratches wide (Fig. 3). Sets by purse-seine on some of these marks showed that the schools contained about 10,000 fish. Fish observed in this manner were included in the total estimates. Adult herring populations have been estimated by this means, although certain difficulties are intrinsic in the method (Hourston, 1953a,b). Sometimes it was difficult to identify marks as juveniles, but since juvenile herring made up the largest portion of the fish in this area at this time, marks were concluded to represent juveniles unless there was reason to believe otherwise (e.g. salmon, sand lance or adult herring observed in the vicinity).

From tables of the estimated numbers of juvenile herring seen during each observation, the maximum single estimates (i.e. the largest number of fish observed at one time in each locality) were summarized for each year (Table XI). With the exception of 1953, the estimates increased yearly. It is thought that the observed increase stems from more extensive and efficient scouting rather than a general increase in abundance of the juveniles. In 1953 efforts to make the scouting more critical in order to standardize procedures apparently resulted in a general underestimate of abundance. Also, since weather conditions were poorer in 1953 than in other years, a smaller portion of the fish may have been seen that year. The number of localities scouted was not increased over 1952. In any case the drop in the total number of fish observed in 1953 is not regarded as significant.

A more representative index of relative annual abundance may be obtained by comparing the abundance in localities which were scouted both years. On this basis 4 localities out of 12 showed an increase in 1952 over 1951, 8 showed a decrease, and 2 showed no change. In 1953 there was an increase in the estimates for 3 of the 11 localities over the 1951 estimates, a decrease in 10 localities, and no change in the remaining one. In 1954 more fish were observed in 10 localities than in 1951, whereas fewer fish were observed in 4 localities; no change was indicated in the other locality. In 5 out of 21 localities the stocks were larger in 1953 than in 1952; in 14 they were smaller, and there was no change in 2. In 1954 the number of fish seen was greater than in 1952 in 16 localities; it was less in 3 localities and there was no change in the 3 other localities. In 21 out of 23 localities the estimates were higher in 1954 than in 1953; in the other 2 localities a decrease was indicated. On this basis the 1954 year-class was much stronger than any of the others. The 1951 year-class was the next strongest, followed by 1952 and 1953. However, since the 1953 year-class is thought to have been underestimated, the order of abundance could read 1954, 1953, 1951 and 1952. In any event, the 1954 year-class appears to be relatively strong, the 1952 year-class relatively weak and the other two probably intermediate.

MARKING EXPERIMENTS

Schnabel-type marking experiments (Schnabel, 1938) were carried out on several of the larger stocks each year in order to estimate the number of juveniles present. A marking and recovery program of this type, where the recoveries are made while marking is in progress, lends itself well to the conditions of this study, since fishing mortality is relatively low, and the only opportunity to search for marked fish occurs in the experimental catches. Thus fish are examined for previous marks with each marking after the first. Fish were marked by the removal of various combinations of the paired fins.

Since the Barkley Sound population was made up of a series of local stocks, as determined above, a single experiment for the whole sound would not satisfy the assumption of a homogeneous population. However, as a method of estimating the size of the individual stocks this assumption was satisfied. Other prerequisites of this type of experiment (Ricker, 1948) were approximated by this study. The marked fish could not lose their mark over the period of the investigation, and were readily recognized. It is presumed that marked and unmarked fish were equally vulnerable to capture by seining. Some mortality of marked fish did occur but was comparatively small (Appendix 1) and, presumably, rather constant. Consequently, the mortality would not have affected comparative estimates, and would have affected absolute estimates only slightly. Some migration took place in and out of these localities but it would not have been sufficient to mask major differences in population size, although it could have affected somewhat the absolute value of the population estimate.

In population estimates of this nature, the number of marked fish recovered must be sufficiently large to provide reasonably small confidence limits for the population estimate. Also, the number of times recoveries are made should be sufficient to establish a "levelling off" of the estimate. In some tests these conditions were not satisfied, especially in the earlier years when techniques were being developed.

TABLE XI. The maximum single estimates of the number of juvenile herring in each locality surveyed during the study in thousands.

Locality	Thousands of juvenile herring			
	1951	1952	1953	1954
Alberni Inlet	..	203	..	..
Assits Island to Congreve Island	..	..	..	250
Banfield Inlet	1,000	1,150	200	600
Banfield Inlet to Kelp Bay	..	..	..	200
Bernard Point to Assits Island	..	..	..	250
Chrow Island	..	..	..	50
Chup Point	..	..	..	100
Cigarette Cove[a]	300	5	0	150

Locality	Thousands of juvenile herring			
	1951	1952	1953	1954
Coaster Channel	..	..	..	10
David Channel	..	[b]	[b]	50
Diana Island	..	..	..	0
Dodger Channel	..	1	10	50
Dutch Harbour[a]	..	200	0	150
Ecoole Cannery	..	300	0	500
Edward King Island	..	..	..	0
Effingham Inlet	300	3	1	600
Effingham Island	..	200	5	1,000
Fleming Island	..	..	..	75
Forbes Island	..	..	..	0
Georges Island[a]	[c]	[c]	[c]	250
Grappler Inlet	[d]	[d]	[d]	200
Hand Island Channel[a]	..	100	..	500
Harris Point	0	0	400	80
Helby Island	..	..	..	0
Island Harbour	..	500	0	50
Island Harbour to Coaster Channel	..	..	..	30
Jaques Island	..	..	..	0
Jarvis Island	..	..	..	0
Kelp Bay[a]	35	..	..	2,000
Kelp Bay[a] to Danvers Inlet	..	..	..	1,000
Loudoun Channel	..	..	..	2,000
Macoah Passage	..	..	..	1,000
Mayne Bay	10	0	0	2,000
Nanat Islet	..	..	..	0
Nanat Islet to Danvers Islet	..	..	..	30
New York Point[a]	200	[c]	[c]	200
Numukamis Bay	..	..	..	150
Ohiat Island	..	..	..	0
Peacock Channel	..	..	..	300
Pipestem Inlet	500	5	1,010	1,500
Rainy Bay	..	20	0	300
Rainy Bay to Vernon Bay	..	..	..	0
Ritherdon Bay	..	..	..	0
San Mateo Bay	..	1,000	300	1,000
Sarita Bay[a]	..	..	10	1,100
Satellite Passage	..	50	0	100
Sechart Channel	100	1,000	15	1,000
Snowden Island	[c]	[c]	[c]	500
Snug Basin	..	..	..	30
Stopper Islands	35	5	10	700
Swaile Rock	[e]	[e]	[e]	70
Swaile Rock to Island Harbour	..	[e]	[e]	50
Thiepval Channel	..	..	..	1,000
Toquart Bay	400	0	0	250
Turtle Island	..	..	..	0
Tzartes Island (east side)	2,000	0	500	1,000
Tzartes Island (west side)	..	[f]	[f]	100
Uchucklesit Inlet	400	5,000	300	900
Ucluelet Inlet	80	300	100	1,000
Useless Inlet	300	1	200	300
Vernon Bay	..	..	30	250
Totals	5,660	10,043	7,611	24,975

[a] Local name
[b] Included in Mayne Bay
[c] Included in Toquart Bay
[d] Included in Banfield Inlet
[e] Included in Sechart Channel
[f] Included in Tzartes Island, east side.

Estimates of the total population in the localities covered by the marking operation each year (Table XII) were made from the basic marking and recovery data (Tables I–IV). Confidence limits, based on random distribution of marks, were determined according to Ricker (1937). Since different stocks were marked in different years these total estimates are not directly comparable, with the possible exception of 1953 and 1954. These years have six localities in common. Markings and populations in the other localities were relatively small. The 1953 estimate should exceed that of 1954 for populations of comparable size, since it covers more of the total population of the sound. The 1954 estimate slightly exceeds that of 1953 and thus the 1954 juvenile herring population in Barkley Sound may have been larger than that of 1953. This is in accord with the estimates based on scouting.

TABLE XII. Estimates of the abundance of juvenile herring in localities in Barkley Sound in which Schnabel-type marking experiments were carried out. Limits of confidence are based on the assumption of random mixing of marked and unmarked fish and may be too narrow insofar as this condition is not met.

Year	No. of fish marked	No. of fish examined	No. of recoveries	Population	
				Estimate	95% limits
		All localities marked		*millions*	*millions*
1951	33,986	44,413	58	11.7	9.0– 15.2
1952	81,016	81,730	30	67.3	47.1– 99.9
1953	141,188	167,571	65	166.5	130.6–212.2
1954	163,350	179,170	59	188.3	147.1–239.9
		Banfield Inlet			
1951	18,863	12,863	17	4.4	2.7– 7.5
1952	20,688	20,186	3	40.6	13.9–203.0
1953	46,011	44,911	26	41.6	28.5– 63.7
1954	26,060	24,770	7	43.5	21.2–108.8
		Banfield Inlet and Kelp Bay			
1954	40,680	48,010	13	74.4	43.4–140.1
		San Mateo Bay			
1952	20,884	21,567	8	16.9	8.5– 39.7
1953	30,541	38,177	7	71.2	34.6–178.0
1954	18,240	18,340	7	38.3	18.6– 95.9
		Uchucklesit Inlet			
1953	14,460	16,488	3	41.1	14.0–205.4
1954	22,880	19,020	5	37.7	16.1–117.9
		Ucluelet Inlet			
1952	8,852	9,202	3	5.2	1.8– 25.7
1954	26,840	22,050	9	27.3	14.4– 61.4
		Useless Inlet			
1951	10,953	8,605	5	4.5	1.9– 14.2
1954	5,270	6,050	3	10.6	3.6– 53.1

A further indication of the relative strength of these year-classes may be derived from a comparison of local stocks whose abundance estimates were based on more than one recovery (Table XII). Estimates for all four years are available for Banfield Inlet, while 1952 to 1954 estimates are available for San Mateo Bay. The 1954 stocks in Uchucklesit Inlet, Ucluelet Inlet and Useless Inlet may be compared with those in 1953, 1952 and 1951 respectively.

The 1951 markings were not sufficiently extensive to enable adequate estimates. In addition techniques were in the process of development, and marking mortality was probably rather variable. The 1952 year-class appears to have been definitely weaker than the two succeeding ones in two of the three localities in which estimates could be made. The 1953 and 1954 year-classes were of comparable size in Banfield and Uchucklesit Inlets, while the 1953 year-class was stronger in San Mateo Bay.

Considering the results of both comparisons of relative abundance, the 1953 and 1954 year-classes appear to have been approximately equal in numbers, while the 1952 year-class was definitely smaller.

ABSOLUTE POPULATION ESTIMATES

An index of the extent to which a stock of juveniles was observed in a survey of a locality, may be obtained by comparing the population estimates from the marking experiments with the scouting estimates for these localities. The latter were invariably smaller, as even an extensive visual survey would not likely discover all the fish in a locality. Consequently the visual estimates for the entire sound must be low; the true level of abundance probably lies closer to that which could be obtained by marking extensively throughout the sound. Such a program was beyond the scope of this study but an approximation to this type of estimate was obtained by calculating an "adjustment factor" for the scouting estimates in the localities included in the marking program, and applying it to the scouting estimate for the sound (Table XIII). Thus the 1953 and 1954 year-classes in Barkley Sound apparently constituted about 640,000,000 fish in the juvenile stage. Coverage of the other two year-classes was not sufficiently complete to consider the estimates quantitatively.

TABLE XIII. Estimates of the 1951–1954 juvenile herring populations in Barkley Sound from the scouting survey coverage adjusted to the extent indicated by marking experiments.

Year	Estimate for localities marked		Adjustment factor	Estimate for Barkley Sound	
	From marking	From scouting		From scouting	Adjusted
	millions	*millions*		*millions*	*millions*
1951	10.91	2.00	5.5	5.66	31.1
1952	67.26	8.95	7.5	10.04	75.3
1953	166.50	1.97	84.5	7.61	643.0
1954	188.29	7.30	25.8	24.98	644.4

CONCLUSIONS ON ABUNDANCE

Calculations based on recruitment and natural mortality rates (Appendix 4) show the average recruitment of the 1942–1952 year-classes would have been provided by a juvenile population of 403 million fish (ignoring the 1951 year-class which was not subject to a fishery at recruitment). The smallest year-class (1948) would have had a population of 269 million in the juvenile stage, whereas the largest year-class (1947) would have sprung from 575 million juveniles. On this basis, the 1953 and 1954 year-classes (about 640 million fish each) were well above average in strength. Although the coverage of the 1952 survey was not complete enough to permit comparison with the above determinations, it was sufficient to indicate that this year-class was appreciably weaker than the two succeeding year-classes.

The 1952 year-class was well below average strength when recruited to the 1954–55 fishery (Taylor, 1955) and the 1953 year-class was above average strength when it entered the fishery in 1955–56 (Taylor *et al.*, 1956). The 1954 year-class had an above-average recruitment as II-year fish and appears to be at least comparable to that of 1953. Thus, in general, relative abundance at recruitment appears to coincide with predictions based on juvenile abundance.

RELATIONSHIP OF JUVENILE HERRING STOCKS TO THOSE OF THE EGGS AND LARVAE

DISTRIBUTION

The Barkley Sound juvenile herring stocks are concentrated in inlets and bays and around islands, mainly on the southeast side of the sound (Fig. 4). However, spawning occurs mainly on the opposite side of the sound. Thus, either there is high mortality in the spawnings along the northwest side and low mortality in the spawnings along the southeast side, or a large portion of the fish migrate across the sound sometime before mid-summer. The first alternative seems unlikely since:

(1) There is no evidence of such differential mortality either in the egg or larval stages. Larvae are considerably more abundant on the northwest side of the sound (Stevenson, 1955a).

(2) Some juvenile stocks on the northwest side (e.g. Toquart Bay), and in the middle of the sound (Broken Group) disappeared early in the summer. Recoveries of marked fish in these stocks were taken mainly along the southeast side, indicating migration in that direction.

(3) At least some (Banfield Inlet, San Mateo Bay) of the stocks along the southeast side appear to contain numerous size-groups, presumably reflecting the age differences involved in the hatchings from several spawnings. Since the number of these size-groups could not be accounted for by the number of spawnings along the southeast side (4 to 7), but could be accounted for by the number of spawnings on the northwest side (9 to 12) or in the sound as a whole (13 to 19), migration from the northwest to the southeast side is indicated.

Thus, the juvenile stocks located apparently arise from the hatchings of spawn throughout the sound and not just local spawnings. Sometime prior to the intensive schooling stage of juveniles in mid-summer, a large portion of the young herring migrate from the northwest to the southeast side of the sound. Since the larvae are more abundant on the northwest side up to the late post-larval stages, after which they can escape capture by plankton nets, this movement must take place during or shortly after metamorphosis.

ABUNDANCE

The juvenile herring population in Barkley Sound has been estimated in excess of 640 million fish (minimum estimate from surveys and marking programs) in the two years for which adequate data are available. How many eggs and larvae would be required to produce this population? Since it appears that mixing among the various hatchings was relatively extensive prior to mid-summer, the population for the entire sound is treated as a unit.

Estimates of the length, width and intensity of spawn depositions are available from the reports of the Department of Fisheries in this area, and from special surveys made by scientists of the Fisheries Research Board of Canada (Taylor and Outram, 1954, and other reports in this series). From these reports the area covered by spawnings of each intensity can be calculated. These estimates, particularly of intensity, are rather rough but they permit an estimate of the number of eggs deposited after the method outlined by Hourston (1953b). Estimates for 1951 to 1954 were 417, 404, 335 and 476 billions (Table XIV). Thus, about 400 billion eggs were deposited annually over the 4-year period of this study. Mortality in the egg stage has been estimated at 65% (Stevenson, 1955b) and during the larval stage at 99.5% (Stevenson, 1955a). Applying these rates to the above egg estimates:

Number of eggs = 400,000 million
Number of newly-hatched larvae = 140,000 million
Number of metamorphosed juveniles = 700 million

Agreement of the juvenile estimate with the 1953 and 1954 survey estimates (640 million) is striking. The 700 million estimate should be high, as it includes no mortality during the early juvenile stage, whereas the 640 million may be low because some small stocks may have remained undetected. However the 1953 and 1954 year-classes are thought to be above average in size and consequently the average juvenile population may be somewhat less than 600 million fish. Thus Stevenson's mortality estimates may be slightly low, but an absolute error of 0.1% in larval survival or 9% in egg survival (either of which is not unreasonable) would account for the difference in estimates.

SUMMARY AND CONCLUSIONS

The population dynamics of the Pacific herring in the juvenile (first year) stage were investigated in Barkley Sound on the west coast of Vancouver Island during the summer months of 1951 through 1954. The primary objective was the assessment of relative population size in the juvenile stage with a view to predicting recruitment to the fishery 2 years later. This information, of importance in efficient management of the fishery, forms an integral part of special population studies now in progress on Pacific herring in British Columbia waters. In order

TABLE XIV. Area and intensity of herring spawnings in Barkley Sound, 1951–1954. Estimates of the number of eggs involved were obtained using the best available data on the average number of eggs per acre for each intensity category.

Date	Place	Area of spawn	Spawning intensity	Number of eggs
1951		*acres*		*millions*
Feb. 11	Macoah Passage	26.03	L	33,266
Feb. 15	Banfield Inlet	1.32	VL	45
Feb. 15	Useless Inlet	4.65	VL	158
Mar. 8	Mayne Bay	.26	VL	9
Mar. 8	Toquart Bay	33.69	M	164,542
Mar. 10	Banfield Inlet	1.24	VL	42
Mar. 12	Macoah Passage	24.79	VL	842
Mar. 12	Macoah Passage	2.48	VL–L	1,627
Mar. 15	Forbes Island	1.05	L	1,342
Mar. 16	Useless Inlet	4.34	M	21,197
Mar. 17	Kelp Bay	0.31	VL	11
Mar. 26	Toquart Bay	1.24	M	6,056
Apr. 1	Snowden Island	0.14	L–M	431
Apr. 2	Toquart Bay	28.23	H	187,052
Total for 1951		129.77		416,620
1952				
Feb. 8	Macoah Passage	6.65	VL	226
Feb. 10	Banfield Inlet	4.21	VL	143
Feb. 28	Useless Inlet	8.81	L	11,259
Feb. 29	Macoah Passage	3.95	L	5,048
Mar. 1	Kelp Bay	2.07	M	10,110
Mar. 6	Toquart Bay	9.09	M	44,396
Mar. 10	Grappler Inlet	1.18	M	5,763
Mar. 11	Macoah Passage	6.52	M	31,844
Mar. 14	Toquart Bay	20.21	L–M	62,267
Mar. 17	Banfield Inlet	5.58	L–M	17,192
Mar. 17	Macoah Passage	34.00	M	166,056
Mar. 25	George's Island	5.25	M	25,641
Mar. 25	Snowden Island	1.90	M	9,280
Apr. 9	Hillier's Cove	0.99	M	4,835
Apr. 9	Toquart Bay	2.09	M	10,208
Total for 1952		112.50		404,268
1953				
Feb. 22	Macoah Passage	18.90	L	24,154
Feb. 24	Banfield Inlet	1.13	L	1,444
Feb. 24	Mayne Bay	0.52	VL	18
Feb. 24	Useless Inlet	0.47	M	2,295
Mar. 1	Macoah Passage	0.47	VL	16
Mar. 1	Useless Inlet	8.06	VL	274
Mar. 2	Toquart Bay	64.57	VL	2,195
Mar. 7	Macoah Passage	3.72	L	4,754
Mar. 9	Banfield Inlet	24.38	M	119,072
Mar. 9	Macoah Passage	3.49	VL	119
Mar. 10	Kelp Bay	0.09	H	596
Mar. 16	Toquart Bay	64.95	L	83,006
Mar. 20	Useless Inlet	73.70	VL	2,506
Mar. 23	Snowden Island	0.83	VL	28
Mar. 26	Banfield Inlet	1.24	M	6,056
Mar. 27	Hillier's Cove	1.61	M–H	9,266
Mar. 28	Macoah Passage	5.81	L	7,425
Mar. 28	New York Point	.52	VL	18
Mar. 30	Stopper Islands	10.85	H	71,892
Total for 1953		128.48		335,134

Date	Place	Area of spawn	Spawning intensity	Number of eggs
1954		*acres*		*millions*
Feb. 26	Toquart Bay	14.46	VL	492
Feb. 27	Roquefeuil Bay	1.76	M	8,596
Mar. 3	Macoah Passage	59.30	L	75,785
Mar. 5	Useless Inlet	6.20	L	7,924
Mar. 9	Toquart Bay	21.59	L	27,592
Mar. 10	Useless Inlet	13.00	L	16,614
Mar. 15	Macoah Passage	28.20	M	137,729
Mar. 17	Rainy Bay	.41	L	524
Mar. 18	Snowden Island	.83	L	1,061
Mar. 19	New York Point	9.92	M	48,449
Mar. 28	Banfield Inlet	29.44	M	143,785
Mar. 28	Toquart Bay	.83	L	1,061
Mar. 29	Hermit Island	.98	H	6,493
Apr. 3	Useless Inlet	.10	VL	3
Apr. 14	Toquart Bay	7.81	VL	266
Total for 1954		194.83		476,374

to assess the abundance of juveniles in Barkley Sound, an important rearing ground, it was was first necessary to determine there the distribution of the population and its composition. Relating the results of this study to studies on the preceding (larval and egg) stages permits their application to general population studies. These objectives may now be considered in the light of the data presented on the population of juvenile herring in Barkley Sound.

Distribution of the juvenile herring in Barkley Sound. Scouting, seining and light fishing programs indicated that the juvenile herring in Barkley Sound live mainly in the shallow and protected waters in bays and inlets, and around islands. Some relatively large groups occur offshore, especially in the late summer and fall when the fish begin to move to offshore feeding grounds, but these fish appear to be transients.

Composition of the juvenile herring population. On the basis of results from a marking program and a study of differences in size-groups present in samples, the Barkley Sound juvenile herring population appears to comprise a number of individual stocks that mix somewhat, but not enough (less than one-third of the stock emigrating) to destroy their identity. Emigration is generally to adjacent and nearby localities but some fish wander to distant parts of the sound. Most of these fish remain on the same side of the sound rather than moving to the other side, possibly indicating that they customarily follow the shore rather than venturing into deep waters. The extent of migration appears to be directly related to distance moved, decreasing by about one-fifth to one-half for each additional 5 miles.

Abundance of juvenile herring. Estimates of the relative abundance of juveniles were made during each scouting survey. Absolute juvenile abundance was estimated for several localities each year by Schnabel-type marking experiments, and these estimates were compared with those obtained by scouting for the same localities to arrive at a "correction factor" for the scouting estimates. The correction factor for each year was then applied to the scouting estimate for the entire sound. The results indicate that the 1953 and 1954 juvenile populations were apparently in excess of 640 million fish (the minimal estimates). Two additional independent estimates of average year-class strength at the juvenile stage were based on extent of spawn deposition and mortality during the egg and larval stages, and on recruitment and mortality between the first summer and maturity. These rough estimates of 700 million and 403 million juveniles respectively compared rather well with the direct estimate. Relative juvenile abundance indicates that the 1953 and 1954 year-classes are above average in strength whereas the 1952 year-class is below average. The results of the 1953–54 and 1954–55 fisheries support this conclusion, indicating that this method of predicting recruitment has practical value.

ORIGIN OF THE STOCKS OF JUVENILE HERRING (relationship to earlier stages in the life history). Each local stock of juvenile herring in the sound apparently comprised the progeny of several hatchings as each contained several size-groups. The majority appear to have been hatched on the northwest side of the sound, as most of the spawnings took place there and the number of size-groups in samples from the southeast side could not be accounted for by the spawning on the southeast side. The larger portion of the progeny from the spawnings on the northwest side presumably migrated to the southeast side early in the summer, as fish marked in stocks which disappeared from the northwest side during June and July were recovered on the southeast side. Also there were relatively few stocks located on the northwest side. Extensive mortality in the egg (65%) and larval (99.5%) stages reduces a population of about 400,000 million eggs to about 700 million juveniles.

ACKNOWLEDGMENTS

The stimulation and suggestions provided by Dr. C. L. Hubbs of the Scripps Institution of Oceanography throughout the preparation of this paper are gratefully acknowledged. Drs. W. E. Ricker, J. C. Stevenson and F. H. C. Taylor of the Biological Station, Dr. M. B. Schaefer of the Inter-American Tropical Tuna Commission, Dr. A. L. Tester, then of the University of Hawaii, and Mr. T. Widrig of the United States Fish and Wildlife Service read early drafts of the entire report and offered many helpful suggestions. Capt. W. Egeland of the *Grassholm* brought a wealth of practical experience to the field program and gave unstintingly of his efforts and abilities. Thanks are also expressed to the many scientists, technicians and boat crews of the Biological Station staff who assisted in the program.

The study was financed by the Fisheries Research Board of Canada as part of the Biological Station's investigation of the herring resource. Thanks are extended to Dr. A. W. H. Needler, Director of the Biological Station, and to his predecessor as Director, Dr. J. L. Hart, for provision of facilities for the research.

REFERENCES

CASSIE, R. M. 1950. The analysis of polymodal frequency distributions by the probability paper method. *New Zealand Science Review*, 8: 89–91.

1954. Some uses of probability paper in the analysis of size frequency distributions. *Australian J. Marine and Freshwater Res.*, 5(3): 513–522.

Harding, J. P. 1949. The use of probability paper for the graphical analysis of polymodal frequency distributions. *J. Mar. Biol. Assoc.*, **28**(1): 141–153.

Hourston, A. S. MS, 1951. Preliminary studies of the juvenile stage of the Pacific herring (*Clupea pallasii*). *Fish. Res. Bd. Canada, MS Rept. Biol. Sta.*, No. 411, 28 pp. (multigraphed).

1953a. The spawning population of herring in Northern British Columbia in 1952. *Fish. Res. Bd. Canada, Pacific Prog. Rept.*, No. 97: 21–26.

1953b. Estimation of herring population size by means of echo-sounder tracings, and its application to herring research. *Fish. Res. Bd. Canada, Nanaimo Sta., Circ.* No. 26, 76 pp. (multigraphed).

MS, 1956. Population dynamics of juvenile herring in Barkley Sound, British Columbia, as an integral part of the life history. Doctoral dissertation, University of California, Los Angeles, 176 pp.

Larkin, P. A., G. C. Anderson, W. A. Clemens and D. C. G. MacKay. 1950. The production of Kamloops trout (*Salmo gairdnerii kamloops* Jordan) in Paul Lake, British Columbia. *Sci Publ. British Columbia Game Dept.*, No. 1, 37 pp.

McHugh, J. L. 1954. Geographic variation in Pacific herring. *Copeia*, 1954(2): 139–151.

McMynn, R. G., and W. S. Hoar. 1953. Effects of salinity on the development of the Pacific herring. *Canadian J. Zool.*, **31**(4): 417–432.

Milne, D. J. MS, 1953. Growth studies on spring and coho salmon. 2 pp. Fish. Res. Bd. of Canada, Nanaimo, B.C.

Shetter, D. S. 1952. The mortality and growth of marked and unmarked lake trout fingerlings in the presence of predators. *Trans. Am. Fish. Soc. for 1951*, **81**: 64–67.

Stevenson, J. C. MS, 1955a. Distribution and survival of herring larvae (*Clupea pallasi* Valenciennes) in British Columbia waters. Ph.D. Thesis, Univ. of Toronto, 161 pp.

MS, 1955b. Herring mortality at various stages in the life history. 15 pp. Fish. Res. Bd. of Canada, Nanaimo, B.C.

(In press). The movement of herring in British Columbia waters as determined by tagging. *Rapp. et Proc.-Verb., Cons. Explor. Mer*, **140**(2): 33–34.

Stevenson, J. C., A. S. Hourston, K. J. Jackson and D. N. Outram. 1952. Results of the west coast of Vancouver Island herring investigation, 1951–52. *Rept. British Columbia Fish. Dept.* for 1951, pp. 57–87.

Stevenson, J. C., A. S. Hourston and J. A. Lanigan. 1951. Results of the west coast of Vancouver Island herring investigation, 1950–51. *Rept. British Columbia Fish. Dept.* for 1950, pp. 51–84.

Taylor, F. H. C. 1955. The status of the major herring stocks in British Columbia in 1954–55. *Rept. British Columbia Fish. Dept.* for 1954, pp. 51–73.

Taylor, F. H. C., A. S. Hourston and D. N. Outram. 1956. The status of the major herring stocks in British Columbia in 1955–56. *Rept. British Columbia Fish. Dept.* for 1955, pp. 51–80.

Tester, A. L. 1937. Populations of herring (*Clupea pallasii*) in the coastal waters of British Columbia. *J. Biol. Bd. Canada*, **3**(2): 108–144.

1948. The efficacy of catch limitations in regulating the British Columbia herring fishery. *Trans. Royal Soc. Canada*, Sec. V, **42**: 135–163.

1949. Populations of herring along the west coast of Vancouver Island on the basis of mean vertebral number, with a critique of the method. *J. Fish. Res. Bd. Canada*, **8**(7): 403–420.

1955. Estimation of recruitment and natural mortality rate from age composition and catch data in British Columbia herring populations. *J. Fish. Res. Bd. Canada*, **12**(5): 649–681.

Thompson, W. F. 1917. A contribution to the life history of the Pacific herring: its bearing on the condition and future of the fishery. *Rept. British Columbia Commissioner of Fish.* for 1916, pp. 39–87.

APPENDIX 1: MARKING MORTALITY

A series of 14 experiments was carried out in order to determine the extent of mortality suffered by juvenile herring as a result of marking (Table A). Fish marked by removing fins, in the various combinations employed in the marking program, were placed in a live pound or tank along with "controls" (unmarked fish which had received minimal handling). The dead of each type were removed and counted every day. The probable percentage survival of the marked fish was taken to be the percentage survival of the marked fish plus the percentage mortality of the controls. This correction should allow for mortality due to causes other than marking, such as poor feeding conditions, disease and adverse environmental conditions. However, the controls were subjected to handling that would not occur under natural conditions (seining, transportation in a boat live pound, and transfer to the experimental pounds or tank), and to shock resulting from an abruptly restricted environment. Any fish noticeably suffering from this treatment were discarded, but probably some minor injuries escaped notice.

TABLE A. Survival of marked fish in mortality experiments. Corrected survival discounts mortality due to causes other than marking, as indicated by the survival of the control (unmarked) fish.

Experiment Number	Duration	No. of fish		Observed survival		Corrected survival of marked fish
		Controls	Marked	Controls	Marked	
	days			%	%	%
1	12	44	45	98	78	80
2	10	31	38	71	71	100
3	18	18	20	83	55	66
4	18	19	20	58	45	78
5	18	20	20	75	50	67
6	18	6	6	100	33	33
7	18	46	44	96	82	85
8	20	50	49	92	88	96
9	28	40	200	100	81	81
10	19	41	180	100	89	89
11	16	200	234	91	44	48
12	16	100	98	92	91	99
13	16	100	102	97	96	99
14	51	116	20	49	70	100+
Average					70	80

Handling mortality should be included in marking mortality. Presumably its major component is that resulting from picking the fish up in the hand and holding it out of water for several seconds during the marking. Chances of loss of scales and shock to the system are greatest at this point, and the fish would be expected to be damaged far more then than during seining, transportation and transfer, provided these operations are carried out with due care. Consequently, the exclusion of these latter factors from marking mortality is not serious, especially since the average over-all mortality of the controls in good condition was only about 3% to 15%.

It seems reasonable, therefore, to consider the percentage mortality of the controls as representing the mortality due to causes other than the general marking operation, and thus to add this percentage to the percentage survival of the marked fish in order to estimate the probable survival of marked fish in nature, assuming that the marked fish are no more susceptible to predation than are the unmarked ones (Shetter, 1952).

Experiments 1, 7 and 8 were carried out in a "web" live pound similar to that employed in marking in the field (3 × 4 × 5 ft., of half-inch tarred web, Fig. 14A). Experiments 3, 4, 5 and 6 were carried out simultaneously in each of four chambers of a "box" type pound. This was a wooden box, 8 × 2 × 2 ft., divided into four chambers, with stout quarter-inch wire

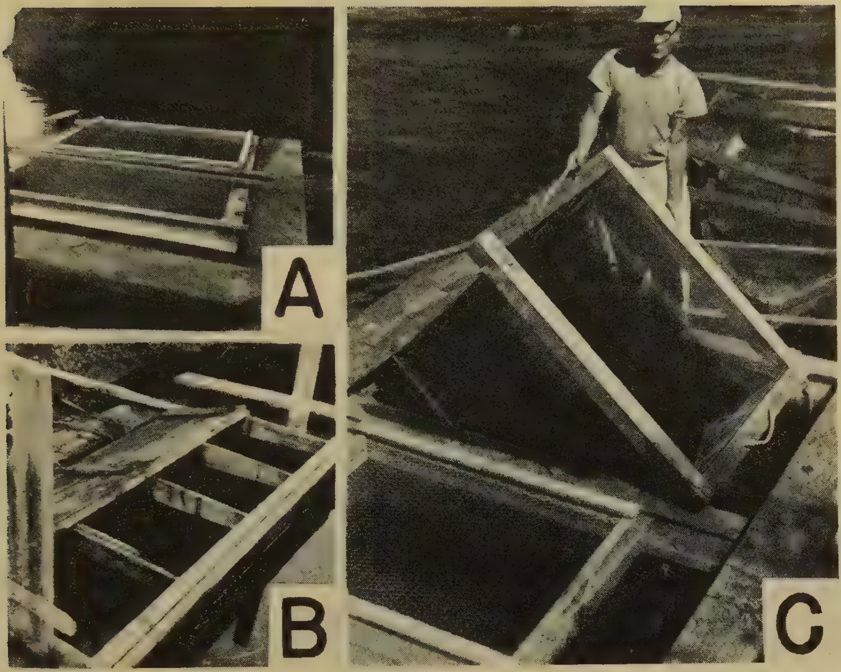

FIGURE 14. Live pounds used to hold fish for mortality experiments.

A. "Web" live pound.
B. "Box" live pound.
C. "Wire" and "boat" live pounds.

mesh forming the two long sides of the box (Fig. 14B). All of these chambers were employed in Experiment 2. During the above experiments, the live pound was attached to the float at the Biological Station dock in Departure Bay. Although this location was relatively sheltered, the pounds were occasionally subject to considerable rocking, because the whole float moved with the stronger waves. Furthermore the water in the pounds was churned by the wash of boats coming into and leaving the dock. Consequently, for Experiments 9 to 13 the location was shifted to a specially constructed float anchored in the lee of a small island in Departure Bay. These experiments were carried out in a "wire" live pound, a structure similar to the "web" pound, but with wire mesh substituted for the web (Fig. 14C). This substitution was necessary as the web rotted quickly under constant immersion and was difficult to scrub clean of growth.

Experiment 14 was conducted in a circular laboratory tank, with a diameter of 37 inches and a depth of 22.5 inches (Fig. 15A). It was supplied with a constant flow of sea water. Survival conditions in this tank were checked by two control experiments. During the first check the methods of introducing new water and draining off the overflow were modified. In the final arrangement, the water flowed in through five holes, punctured by a 2-inch nail, on one side of a plastic tube inserted vertically in the tank about midway between the edge and the center (Fig. 15B). The inflow of approximately 3.5 litres per minute resulted in a slow circular movement of water around the tank. The overflow spilled into a 1¼-inch or 32 mm. (outside diameter) pipe in the centre of the tank, rising 20 inches (50 cm.) from the drain on the bottom. This free overflow facilitated the escape of the scum that collected at the surface (mainly from the food given to the fish).

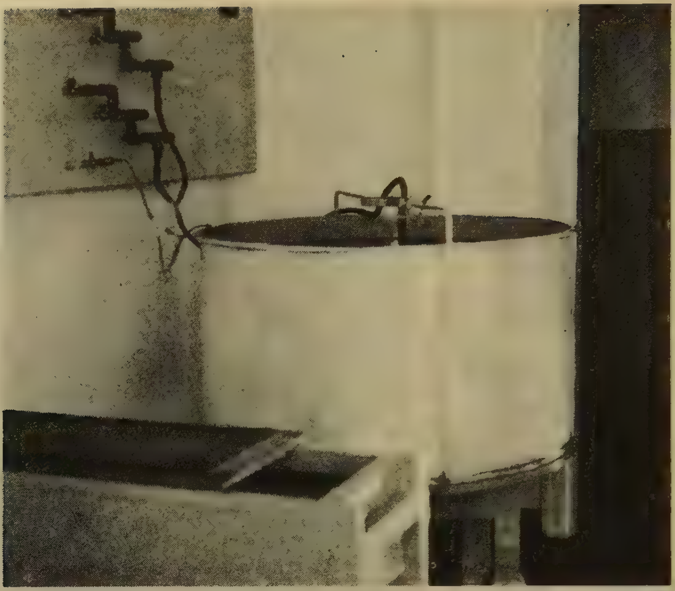

FIGURE 15A. Photograph of the laboratory tank used to hold fish during mortality experiments.

Juveniles seined in Departure Bay were transferred to a "boat" live pound (an old 12-foot dinghy with a large number of small slits, 1½ × ¼ inch or 38 × 6 mm., cut in the bottom) for transport to the Biological Station dock, about a quarter of a mile away. The fish were carried in bait pails from the dock to the laboratory, about 500 ft., where they were transferred into the circular tank.

The fish used in laboratory experiments were fed finely ground beef liver twice a day during the week and once a day on weekends. They did not feed for the first 2 or 3 days in either of the control experiments, but fed actively thereafter, breaking their school (orientated to the flow within the tank) immediately after encountering the liver. In spite of this regular feeding activity and a controlled environment, the herring died at the rate of about one a day for the first three weeks of the first control experiment. After the 21st day of the experiment, the liver diet was supplemented with brine shrimp. The bulk of the diet was still provided by ground liver, but the inclusion of one quart of brine shrimp culture in each feeding seemed to relieve some diet deficiency, since only one death occurred in the next ten days. On the 31st day, a failure in the water pump resulted in death of all the juveniles. Throughout the second control experiment, the water exchange was as outlined above, and the juveniles were fed ground liver supplemented by brine shrimp. Two of the 157 juveniles died the first day, presumably as a result of injury during transit, but no further mortality was observed that week. Rearing conditions were then considered suitable and the mortality experiments begun.

Survival was extremely variable between experiments (Table A). In the earlier experiments this probably reflected the skill of the markers and the variability of conditions in the box pound. Since the fish used in Experiment 11 seemed rather sluggish at the time of marking, this experiment cannot be considered representative. Ignoring the box pound experiments and Experiment 11, all of which were probably atypical, the average corrected survival was 91%. Thus mortality due to marking was probably less than 10%. Indeed in the tank experiment, where rearing conditions were best controlled, the mortality of the marked fish was less than that of the fish used as controls. In the two experiments which were carried out in the wire pound in 1953, marking mortality was only 1%. Since the skill of the markers and environmental

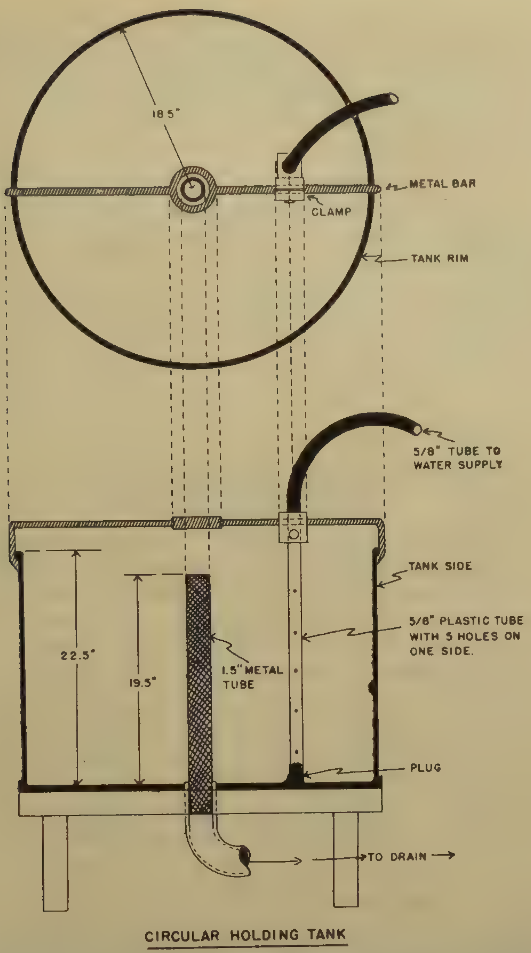
18.5"
METAL BAR
CLAMP
TANK RIM
5/8" TUBE TO WATER SUPPLY
TANK SIDE
5/8" PLASTIC TUBE WITH 5 HOLES ON ONE SIDE.
22.5"
19.5"
1.5" METAL TUBE
PLUG
TO DRAIN
CIRCULAR HOLDING TANK

FIGURE 15B. Diagram of the laboratory tank used to hold fish during mortality experiments.

conditions probably approached conditions of field operations most during these latter three experiments, marking mortality may be considered negligible. In any case it is probably less than the 9% average for the web and wire pound experiments (ignoring Experiment 11).

APPENDIX 2: SAMPLING TECHNIQUE

Various checks were empolyed from 1952 through 1954 to test randomness in selection of fish preserved as a sample, randomness in selection of fish to be measured and weighed from the preserved sample, and average weights for the samples.

RANDOMNESS OF SELECTION OF FISH FOR SAMPLE

Nine times, a catch was sampled in duplicate (Table B). Five of the 9 pairs of samples show length differences of less than 1%, two show less than 2%, and two show less than 4%. Consistent biases are lacking. It may therefore be assumed that the fish taken from the catch as a sample are representative of it.

Table B. Average length and weight of fish in nine duplicate samples used to check sampling technique. Average weight was determined (1) from the sums of the individual weights (column 7); (2) from the weight of the sample as a whole (column 8); and (3) from the weight, as a whole, of the remainder of the fish after 100 had been sampled (column 9). The average weight employed (column 10) was the mean of the first two determinations.

1	2	3	4	5	6	7	8	9	10
						Average weight			
Sample number	Date	Locality	No. of fish	Average length	Difference	Individuals	Sample	Remainder	Average
				mm.	*mm.*	*g.*	*g.*	*g.*	*g.*
52–59A	27/8/52	San Mateo Bay	123	81.42	1.19	6.94	6.82	6.87	6.88
52–59B			123	82.61		7.50	7.38	7.35	7.44
53–37A	22/7/53	Banfield Inlet	312	58.84	0.63	2.34	2.27	2.24	2.31
53–37B			340	58.11		2.22	2.18	2.12	2.20
53–39A	29/7/53	Uchucklesit Inlet	375	53.34	0.12	1.73	1.70	1.72	1.72
53–39B			390	53.22		1.72	1.71	1.65	1.72
53–43A	30/7/53	Banfield Inlet	287	64.13	1.89	3.13	3.21	2.38	3.17
53–43B			292	62.26		2.94	2.90	2.82	2.92
53–44A	30/7/53	Banfield Inlet	256	69.93	2.61	3.81	3.75	3.54	3.78
53–44B			242	67.32		3.71	3.72	3.45	3.72
53–67A	7/8/53	Vernon Bay	213	52.33	0.48	1.71	1.63	1.63	1.67
53–67B			240	53.81		1.72	1.69	1.68	1.71
53–83A	14/8/53	Uchucklesit Inlet	178	57.63	0.45	2.04	2.06	2.01	2.05
53–83B			156	57.18		1.98	2.00	1.97	1.99
53–84A	14/8/53	Uchucklesit Inlet	425	58.20	0.16	2.14	2.20	2.15	2.17
53–84B			220	58.04		2.20	2.15	2.18	2.18
53–102A	25/8/53	Ucluelet Inlet	310	62.25	0.33	2.79	2.73	2.71	2.76
53–102B			318	62.58		2.93	2.81	2.89	2.87

Randomness of Selection of 100 Fish from the Sample for Weighing and Measuring

This was checked by weighing the remainder of the fish preserved as a unit (when there were more than 20 extra fish), calculating the mean weight of these fish, and comparing this average with a similar determination for the 100 fish selected. In 138 such comparisons, the sample weights were greater 85 times, the remainder weights greater 48 times, and the weights equal 5 times. The average difference in sample and remainder average weights was 2.7% (0.101/3.718) of the average weight for all samples. In 1952 this average difference was 0.1% (0.006/5.113), in 1953 it was 3.3% (0.090/2.700) and in 1954 it was 4.8% (0.184/3.788). Thus although the error involved here is slightly greater than that involved in the selection of a sample, and shows a slight bias toward larger fish, it is relatively small for most samples and may be considered insignificant. Indeed, the two sets of determinations of average weight, when compared by "*t*" tests, showed no significant differences (1952, $P > 0.9$; 1953, $P > 0.6$; 1954, $P > 0.3$; all years, $P > 0.6$. When, occasionally, the individual errors were high (up to 17%) some selection was unavoidably introduced because a considerable proportion of either the larger or smaller fish were so damaged while being captured that they could not be measured.

Accuracy of Average Weight Determination

Individual fish were weighed to the nearest 0.05 gram. This involves an error of 2% over the average weight range, but it can reach 10% in samples of smaller fish. Any consistent bias in recording weights approximately intermediate between two weight classes could thus have a significant effect on the sample average. To check for such errors, a comparison was made, for all samples of over 20 fish, between the average weight determined from the sums of the weights of the individual fish and the average weight determined by an immediately subsequent weighing of the entire sample. In 183 such comparisons, the average determined from the total of the individual weights was larger 108 times (59%), smaller 63 times (34%), and there was no difference 12 times (7%). The average excess of one determination over the other was 0.91% (0.034/3.718) of the average weight for all samples. In 1952 this average difference was 2.02% (0.103/5.113); in 1953, 0.26% (0.007/2.700); and in 1954, 0.11% (0.004/3.788). Thus, although there was a slight tendency for the average from the total weight to be larger than that for the sample weighed as a unit, this difference scarcely exceeded the accuracy limit of the initial measurements and was not significant. The two sets of determinations of average weight when compared by "*t*" tests showed no significant differences (1952, $P > 0.8$; 1953, $P > 0.9$; 1954, $P > 0.9$; all years, $P > 0.8$).

APPENDIX 3: RELATIONSHIP OF LENGTH GROUPS IN SAMPLES TO MAJOR SPAWNINGS

The analysis by probability plots of length-frequency distribution of juvenile herring showed the presence of more than one length group in most samples. If the description of these size groups is valid, the size differences must be related to some biological cause. The most obvious explanation is an age difference. If this is so, the number of size-groups should be related to the number of distinct spawnings within the locality. An investigation of this relationship is feasible only in relatively isolated localities where mixing with other sub-populations is negligible. The juvenile herring population in Departure Bay seems to satisfy this prerequisite.

Major herring spawnings in the Departure Bay vicinity over the period of 1950 to 1953 were compared with the length-groups in the juvenile samples (Hourston, 1956). In 1950 the major spawnings were on March 7–11, March 20–29 and April 4–9. Length-frequency analysis shows two size-groups consistently present, with one more in several samples. One sample indicated an additional size-group, perhaps comprising strays, or, more likely, being an unreal product such as occasionally arises in a graphic analysis of this nature. It would thus appear that one size-group was present for each major spawning. In 1951, major spawnings were on March 8–11, March 16–19 and March 26. In the juvenile stocks that year, two size-groups were persistently present and a third size-group was indicated in several samples. Here again the number of evident size-groups in the juvenile stocks corresponds with the number of major spawnings. Similarly, in 1952 there were three evident size-groups and three major spawnings (March 6, March 9 and March 15). In 1953 two persistent size-groups and an additional quite evident one were produced from three major spawnings (March 8, March 17–21 and April 8).

It would thus appear that these size-groups are due to the age differential resulting from spawnings at different times. This graphic analysis, therefore, probably detects real differences.

APPENDIX 4: AVERAGE JUVENILE HERRING POPULATION AND POPULATION RANGE IN BARKLEY SOUND DETERMINED FROM CONTRIBUTIONS OF THE 1942 TO 1951 YEAR-CLASSES TO THE POPULATION OF ADULT HERRING

The contribution of a year-class to the adult herring population is measured from the number of fish of that year-class which are caught during and prior to the year in which the majority of recruitment occurs, plus the number that spawn in that year, plus the number remaining immature. For the lower east coast of Vancouver Island it was estimated that 74.9%

of the fish are recruited to the spawning population at age 3–,[1] with 0.4, 7.5 and 17.2% recruitment at ages 1–, 2– and 4–, respectively (Tester, 1955). Thus, 82.8% of the stock is recruited by age 3–. Since the population on the west coast of Vancouver Island is similar in age composition to that on the lower east coast of Vancouver Island, these percentages should apply generally to the Barkley Sound herring. Thus the contribution of a year-class at the major recruitment age 3– would be:

$$C_3 + B_3 + C_2 s_{2-3} + C_1 s_{1-3} + \frac{C'_4 + B'_4}{s_{3-4}}$$

where C = catch at age indicated in the subscript

C'_4 = catch of fish vulnerable for the first time at age 4–

B_3 = spawners at age 3–

B'_4 = fish spawning for the first time at age 4–

s = fractional survival between the ages indicated in the subscript

Estimates of the new recruits at age 4–, ($C'_4 + B'_4$), are not available, but could be derived from the age 3– estimates by applying the recruitment rates given above. However, a more straightforward and probably equally accurate determination for the total strength of a year-class at age 3–, ignoring the minor effects of the fishery on 1st-year fish (less than 0.2%), would be approximated by:

$$N_3 = \frac{C_3 + B_3 + C_2 s_{2-3}}{R_3}$$

where $R_3 = 0.828$, the fraction of recruitment completed by age 3–, and $s_{2-3} = 0.748$. Estimates determined in this way were tabulated for the 10-year period represented by the 1942–52 year-classes, omitting the 1950 year-class because of the lack of a fishery in its recruitment year (Table C).

TABLE C. Estimation of the potential population of 3rd-year fish (N_3) resulting from the 1942–1952 year-classes, using the formula $N_3 = \frac{C_3 + B_3 + C_2 s_{2-3}}{R_3}$, where $R_3 = 0.828$ and $s_{2-3} = 0.748$.

Year-class	C_3	B_3	C_2	Potential N_3
1942	23.07	167.06	27.78	254.78
1943	151.63	62.78	20.82	277.82
1944	116.88	60.20	15.74	228.13
1945	145.50	41.84	8.45	237.57
1946	123.06	80.73	33.84	276.75
1947	182.04	97.52	12.31	348.83
1948[a]	63.60	25.99	15.22	121.97
1949	69.92	50.90	5.60	151.01
1951	187.61	69.30	0	310.28
1952	83.09	103.50	7.89	234.88
Average	114.64	76.28	16.41	244.20

[a] There was no fishery in 1952, when these fish would normally have become adult. For this year-class the estimate was obtained from catch plus spawning at age 4–, allowing for natural mortality of 38% (Fig. 16A; $q = i = 0.48$ and $m = a = 0.38$ where q and i are the instantaneous natural and total mortality rates and m and a are the annual natural and total mortality rates).

---

[1] "Age 3–" refers to fish in their third year of life, mostly taken between November and February; they have completed their third season of growth, but are not yet a full 3 years old, having been hatched in March or April.

Stevenson (1955c) used a natural mortality rate for British Columbia herring of 50% per year "in the absence of contradictory evidence" over the period from year 1 to recruitment during year 3 (he considered natural mortality rate to be constant over the life span of the metamorphosed fish). However, Tester (1955) has shown that natural mortality increases with age at least after recruitment, and, presumably, before recruitment also. In addition, on the basis of Stevenson's mortality rates, the average juvenile population over the period from 1942 to 1951 would have been 777 million with a low of 488 million (1948) and a high of 1,395 million (1947). But the 1953 and 1954 juvenile populations (640 million) would have been well below average under these circumstances, whereas reports on relative abundance indicate that they were above average. Thus Stevenson's natural mortality rates for this period are probably high.

An alternative estimate of the juvenile populations associated with the recruitments given above may be derived from Tester's (1955) estimates of instantaneous mortality between the first year and recruitment. The number of juveniles required to produce a given recruitment as age 3– fish is given by:

$$N_1 = \frac{N_3}{s_{1-3}} \tag{1}$$

where N_1 = number of 1st year fish
N_3 = number of 3rd year fish
s_{1-3} = survival from 1st year to 3rd year.

$$s_{1-3} = e^{-i_{1-2}-i_{2-3}} \tag{2}$$

where i_{1-2} = total instantaneous mortality from the 1st to the 2nd year
i_{2-3} = total instantaneous mortality from the 2nd to the 3rd year.

$$i = p+q \tag{3}$$

where p = instantaneous mortality from fishing
q = instantaneous mortality from natural causes.

Extrapolation of curves drawn by Tester (1955) gives values of 0.12 and 0.25 for q_{1-2} and q_{2-3} respectively for the herring population on the lower east coast of Vancouver Island. Tester states that, in general, estimates of natural mortality in Area 23 (Barkley Sound) would be similar. Although Tester's data came from recruited fish, which may behave differently in this respect, and although the trend could change in the early age range, the extrapolations do not appear grossly unreasonable from general considerations.

Over the period 1946–47 to 1953–54 the percentage in the catch of fish in their second year was approximately 0.0004.

Thus $i_{1-2} = q_{1-2} = 0.12$ (since p_{1-2} is negligible); and $i_{2-3} = q_{2-3} + p_{2-3}$. Now p_{2-3} is a function of μ_{2-3}, which is the rate of exploitation by the fishery during the second year of life, and of q_{2-3}, which is the natural mortality rate for the same period. Putting C_2 for catch in year 2:

$$\mu_{2-3} = \frac{C_2}{N_2} = \frac{C_2}{N_3/s_{2-3}}$$

$$\frac{C_2}{N_3} = (s_{2-3})\ (\mu_{2-3})$$

Putting total annual mortality equal to a:

$$\frac{C_2}{N_3} = (e^{-i_{2-3}}) \left(\frac{a}{i}\right)_{2-3} (p_{2-3})$$

Now $C_2 =$ average number of 2nd year fish in catch over the period
$= 16.41 \times 10^6$ for 1942–43 to 1951–52 in Barkley Sound
(from basic data)

$N_3 =$ average number of 3rd year fish in the population
(catch + potential spawners over the period)
$= 244.20 \times 10^6$ for 1942–43 to 1951–52 in Barkley Sound
(from basic data)

$q_2 = 0.25$ according to Tester (1955)

To obtain the C_2/N_3 ratio of 0.0672 when $q_2 = 0.25$, p_2 must be 0.12.
From (3), $i_{2-3} = 0.25 + 0.12 = 0.37$, and $i_{1-3} = 0.12 + 0.37 = 0.49$.
From (2), $s_{1-3} = 0.61$; from (1) $N_1 = 400$.

Similar data for the smallest and largest year-classes are shown below:

	Smallest year-class (1948)	Largest year-class (1947)
N_3	121.97×10^6	348.83×10^6
C_2	15.22×10^6	12.31×10^6
C_2/N_3	0.125	0.0353
q_{2-3}	0.25	0.25
p_{2-3}	0.27	0.06
i_{2-3}	0.52	0.31
i_{1-2}	0.12	0.12
i_{1-3}	0.64	0.43
s_{1-3}	0.53	0.65
N_1	230×10^6	537×10^6

Thus, using Tester's estimate of natural mortality the average annual recruitment from 1942–43 to 1951–52 would have been produced by a juvenile population of 400 million fish. The smallest year-class (1948) would have been produced by 230 million juveniles and the largest (1947) by 537 million juveniles.

The 1953 and 1954 year-classes were estimated at about 640 million fish in the juvenile stage. Although these year-classes may be above average in strength, consistent local reports on relative abundance of juveniles in 1947 indicate that the 1947 year-class was definitely larger. Since the estimates made at the juvenile stage in 1953 and 1954 are considered minimal, the juvenile population estimates made above from recruitment and natural mortality data are probably low. Indeed the estimate of q between the first and second year seems remarkably low (0.12). Tester has questioned the validity of applying his extrapolation to the unrecruited age groups.

Tester (1955) also gives estimates for q for Areas 23 and 24. Since the Area 23 fish make up over 90% of this stock (Stevenson *et al.*, 1952, and previous reports in this series), Tester's estimates should apply very well to Barkley Sound. Plotting these estimates (Fig. 16A), and following Tester's procedure, a line was drawn through the values representing age 5– to 6– and 6– to 7–. This line also went through the point representing age 4– to 5– but did not go through the point representing age 7– to 8–. However, the latter point was the least reliable

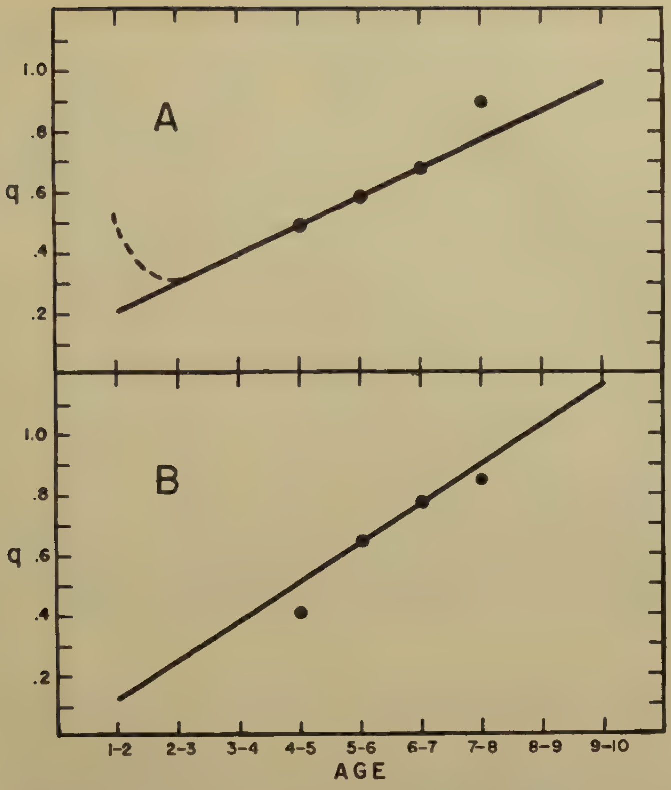

FIGURE 16. The relationship of instantaneous natural mortality (q) to age for each year in the life of the herring.
A. Areas 23 and 24 on the west coast of Vancouver Island.
B. Lower east coast of Vancouver Island.

(Tester, 1955). This line differs in slope from the general case for the lower east coast employed by Tester (Fig. 16B) and does not go through the origin. Employing the q values determined from this graph the above calculations of N_1 were repeated, as shown below:

	Average 1942–51	Smallest year-class (1948)	Largest year-class (1947)
N_3	244.20×10^6	121.97×10^6	348.83×10^6
C_2	16.41×10^6	15.22×10^6	12.31×10^6
C_2/N_3	0.0672	0.125	0.0353
q_{2-3}	0.29	0.29	0.29
p_{2-3}	0.12	0.30	0.06
i_{2-3}	0.41	0.59	0.35
i_{1-3}	0.20	0.20	0.20
i_{1-2}	0.61	0.79	0.55
s_{1-3}	0.54	0.45	0.58
N_1	452×10^6	271×10^6	601×10^6

Thus, using natural mortality data from Areas 23 and 24 only, the average annual recruitment from 1942–43 to 1951–52 would have been produced by a juvenile population of 452 million fish. The smallest year-class (1948) would have been produced by 271 million juveniles and the largest (1947) by 601 million juveniles. These estimates, although higher than those calculated above, still appear relatively low in comparison with the direct estimates for 1953 and 1954 (640 million). Again the extrapolation of the natural mortality curve may not be justified. On the other hand the correction factors applied to the scouting estimates may be high if marking mortality was appreciably higher than the negligible amount determined experimentally. In any event, the differences between the two determinations are small considering the assumptions involved in each method and the sources of error.

Alternatively, an estimate of natural mortality from the first to the third year might be made from the estimate of 1953–54 juveniles (640 million), the 1942–51 average age 3– population ($N_3 = 244$ million) and the average age 2– rate of fishing, $p_2 = 0.12$. A two-year decrease from 640 to 244 million means $s_{1\text{-}3} = 0.38$, hence $i_{1\text{-}3} = 0.96$, hence $q_{1\text{-}3} = 0.96 - 0.12 = 0.84$. This is a considerably higher figure for instantaneous natural mortality rate than the combined figure 0.49 ($= 0.29 + 0.20$) obtained from the linear extrapolation in Figure 16A. Thus q may really be approximately stable at about 0.4 from ages 1– to 4–; or, more likely perhaps, it may reach nadir in the interval $q_{2\text{-}3}$, and be higher again among the younger fish ($q_{1\text{-}2}$). A possible combination which adds up to $q_{1\text{-}3} = 0.84$ is indicated by the dotted line of Figure 16A: $q_{2\text{-}3} = 0.30$ and $q_{1\text{-}2} = 0.54$. From the biological point of view, at age 2– to 3– herring are large enough that many predators can no longer swallow them, and are fast enough to escape others that could; while relatively few of them are as yet involved with the dangerous excursions and physiological stresses which accompany reproduction.

Rhythmic Cell Division in Populations of *Gonyaulax polyedra*[*†‡]

BEATRICE M. SWEENEY and J. WOODLAND HASTINGS[§]
Division of Marine Biology, The Scripps Institution of Oceanography, La Jolla, California, and
Department of Biological Sciences, Northwestern University, Evanston, Illinois

SYNOPSIS. In cultures of the marine dinoflagellate *Gonyaulax polyedra* grown with alternating light and dark periods of 12 hours each, at least 85% of all cell divisions which occur in a day take place during a 5-hour period spanning the end of the dark period and the beginning of the light period. A very distinct maximum in the number of recently divided cells occurs at about the time the light period begins.

This diurnal periodicity in cell division is lost after 4 to 6 days in continuous bright light, but will persist for at least 14 days in continuous dim light. The period of approximately 24 hours under constant conditions is only slightly altered by varying light intensity and temperature, both of which factors are known to affect markedly the generation time. The time at which cell division occurs is therefore postulated to be controlled by some sort of rhythmic or clock mechanism.

Similarities between the cell division rhythm and the endogenous rhythm of luminescence in this organism are discussed. The occurrence of a glow, or steady light emission of low intensity, at about the time of cell division, is described, and it is suggested that this glow may result from cellular changes accompanying certain stages of cell division.

THE PHOTOSYNTHETIC marine dinoflagellate *Gonyaulax polyedra* is one of the many microorganisms which are responsible for the luminescence of the ocean. Its luminescence is usually observed only upon stimulation (by agitation of the water, for example), when the cells emit bright flashes of light (8). *G. polyedra* was isolated by one of us (B.M.S.) from a net sample taken off Scripps pier in 1952, and has been maintained in culture in the laboratory since that time. We have recently reported (7,23) that its luminescent response varies in a diurnal fashion, such that cultures stimulated at night emit considerably more light than cultures stimulated during the daytime. In the course of these studies we noted that undisturbed cultures emit a continuous dim luminescence during part of the night. This glow is so dim that it usually cannot be seen by the dark-adapted eye, and it seems altogether unrelated to the very bright flash-

---

[*] This research has been supported in part by grants from the National Science Foundation and the Graduate School of Northwestern University and by a grant from the Rockefeller Institute to the Scripps Institution of Oceanography.

[†] We are grateful to Mrs. Nao Belser for her assistance in carrying out these experiments.

[‡] Contribution from the Scripps Institution of Oceanography, University of California, New Series. NO. 1028

[§] Present address: Department of Chemistry, University of Illinois, Urbana.

Reproduced by Permission

Copyright 1958 by the Society of Protozoologists
Reprinted from THE JOURNAL OF PROTOZOOLOGY.
J. PROTOZOOL., 5(3), 217-224 (1958).

ing response. Upon investigation, it was found that cell division was taking place at approximately this time of night, and that in fact, it occurred very infrequently at other times of day.

Phased cell division of this sort has been previously demonstrated in several other dinoflagellates and it seems likely that the phenomenon is rather common in this group of organisms. Many years ago it was reported by Gough(6) and Jörgensen(11) that, in the sea, members of the dinoflagellate genus *Ceratium* divide only at night. This genus is most convenient for the detection of cell division because the theca, which is extended anteriorly and posteriorly into long horns, is split obliquely at division. Each daughter cell receives a half theca with its attendant horn or horns and regenerates the other half. Thus the horns are of unequal length in recently-divided cells until this regeneration is complete. Using this criterion for cell division, examinations were made of plankton collections taken at intervals throughout the day and night. Gough reported that recently-divided cells were not found during the day and were infrequent in samples collected before 1:00 A.M. At 3:30 A.M., however, 70% of the individuals possessed horns of unequal length. Subsequent samples contained diminishing numbers of recently-divided *C. fusus*. Jörgensen also found a maximum in the cell division of *C. tripos* but at a somewhat later time, between 3:00 and 7:00 A.M.

In other dinoflagellates, newly-divided cells are not so easily detectible in plankton samples. Furthermore, dinoflagellates were for many years counted among the more difficult organisms to maintain in culture. Consequently, these early observations were not extended in the ensuing years. More recently, however, a number of investigators have been able to culture dinoflagellates successfully (see 1, 2, 10, 18, 21, 22). In cultures of *Peridinium triquetrum* under natural illumination, Braarud and Pappas(2) were able to show that division took place only between 5:00 A.M. and 1:00 P.M., with a maximum between 9:00 A.M. and 10:00 A.M. On the other hand, Nozawa(15) found no variations in the frequency of mitotic figures in cultures of the colorless dinoflagellate *Oxyrrhis marina*. His experiments were carried out, however, with cultures grown in continuous darkness. All dinoflagellates which have been cultured may be grown in continuous illumination, so that it is clear that a dark period is not necessary for cell division to occur.

It seemed likely that the phased division in *G. polyedra* was of importance in connection with the general problem of diurnal rhythmicity (see 4,16), and that additional study might give valuable information concerning the mechanism of cellular rhythmicity. Moreover, cultures of *G. polyedra* or other dinoflagellates might provide excellent material for the study of the biochemistry and physiology of the mitotic cycle.

MATERIALS AND METHODS

For this investigation, unialgal cultures of *G. polyedra* were grown in Fernbach flasks at 20°C. with illumination provided by "cool white" fluorescent lamps. When alternating light and dark periods were required, these lamps were scheduled by means of an interval timer to be on for 12 hours and off for 12 hours during each 24-hour period (LD). The intensity of illumination could be reduced from a maximum of about 1400 foot candles by means of neutral density screens. The culture medium was composed of 75% filtered sea water, 2% soil extract(17), 2×10^{-3} M KNO_3, 2×10^{-4} M K_2HPO_4, 6×10^{-6} M $FeCl_3$, and 2.7×10^{-5} M ethylenediamine tetraacetic acid (EDTA) at pH 8.0-8.2. All distilled water used in these experiments was distilled a second time in a Pyrex glass still

Since recently-divided cells of *G. polyedra* remain attached, forming a pair for a short time after division, the occurrence of cell division was determined by counting pairs. The number of pairs present at any time in a population was determined by counts with living material, since pairs are more easily detected when the cells are motile than when they are fixed. A sample of the cell population was examined for pairs at appropriate time intervals.

Cell population determinations were made by counting cells in 0.2 ml. aliquots of appropriately diluted cell suspensions. Counts were made in triplicate, and usually agreed within 10%.

Measurements of light emission were made using a sensitive photomultiplier tube and automatic recording. It was possible to measure light intensity directly or to integrate the total light emission, as described previously(23).

RESULTS

Periodicity in LD cultures. If cultures of *G. polyedra* are kept under conditions of alternating light and dark periods of 12 hours each (LD), it may be demonstrated that, during the dark period, there is a high frequency of apparently spontaneous flashing. In addition, as mentioned earlier, a very dim glow occurs during the latter part of the dark period. These observations are made by taking an aliquot of the cell suspension and placing it in front of the phototube and recording the intensity of the luminescence emitted by the cells. Typical recordings of these phenomena are reproduced in Fig. 1. The maximum intensity of the glow occurs 10 to 11 hours following the time at which the cells are transferred from light to dark in LD cultures.

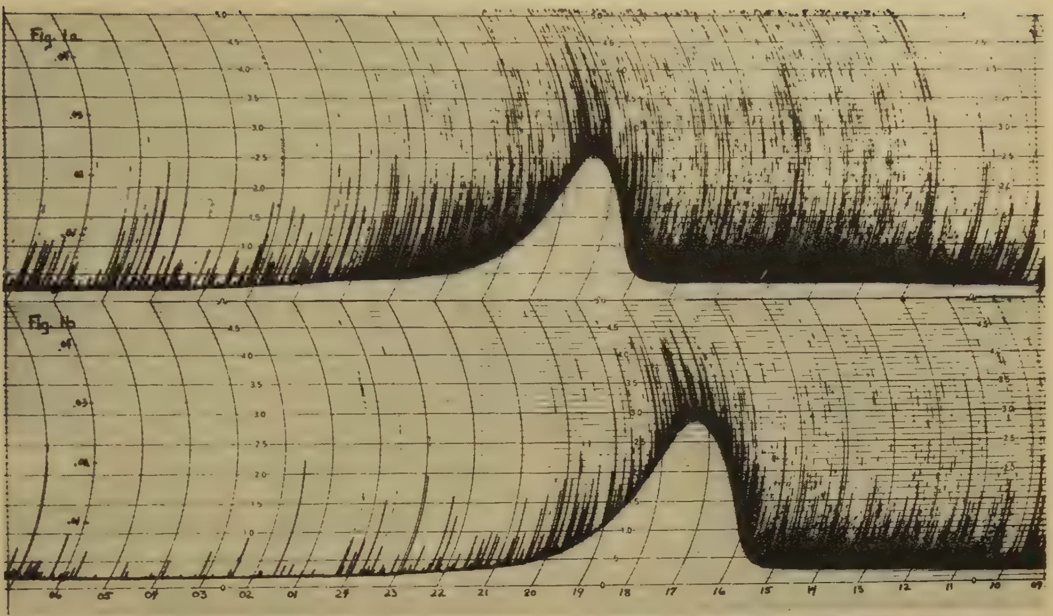

Fig. 1. Recordings of the apparently spontaneous flashing and the luminescent glow in a cell suspension of *G. polyedra* grown in LD with light of 1100 foot candles from 2100 to 0900. During the recording, cells were maintained at 25.0 ± 0.1°C. Ordinate: light intensity; abscissa: time of day. One vertical division equals one hour. Direction of record from right to left. Fig. 1a: cell suspension placed in darkness at 0900; Fig. 1b: cell suspension placed in darkness at 2400. Note that the time at which the maximum in the intensity of the glow occurs in b is changed by only two hours, although it was put in the dark nine hours earlier.

It may be noted that the flashes appear to be distinct from the continuous glow. Some or all of the cells are emitting light continuously and the flashes occur as essentially independent events. We do not know whether all or only some of the cells in the population are emitting a glow, but we think that only some of the cells are involved (see discussion). We have no information concerning whether flashing is associated with particular cells or all cells in the population.

Two observations suggested that the phenomenon of glowing was related to a rhythmic mechanism, and not strictly dependent upon the light and dark periods. First, when cultures were put in the dark before the end of the light period, the time at which the glow occurred was not greatly changed. One of several such experiments is illustrated in Fig. 1. Secondly, if cultures are left in darkness, a glow occurs again on the second and third days (see Fig. 6), even though no light period has intervened.

When microscopic observations were made upon LD cultures, it was found that there were large numbers of paired cells present at about the time the glow occurred, indicating that cell division was taking place at this time (Fig. 2). The maximum in the number of paired cells occurs one to two hours after the maximum in the glow intensity, or at about the end of the normal dark period. As many as 20% of the cells may be in the paired condition at this time, while at other times very few cells in the paired condition are found. The sequence of events is independent of the solar time of the light and dark periods (Table I).

If division occurs only during a short time just prior to the beginning of the light period, as counts of pairs

TABLE I. The time when a maximum in the number of dividing cells was observed in cultures of *G. polyedra* receiving 12 hours artificial light at different times of day. Temperature, 18-20°C.

Time of the light period (P.S.T.)	Light intensity in foot candles	Average generation time in days	Time (P.S.T.) when maximum number of pairs occurred
0800–2000	1200	—	0845
1100–2300	600	2.2	1115
		3.5	1115
		2.0	1115
		—	1100
		—	1030
	200	6.9	1100
		8.2	1020
1545–0345	600	2.9	1500
		2.5	1430
1800–0600	1400	1.8	1600–1700
2000–0800	800	—	1745

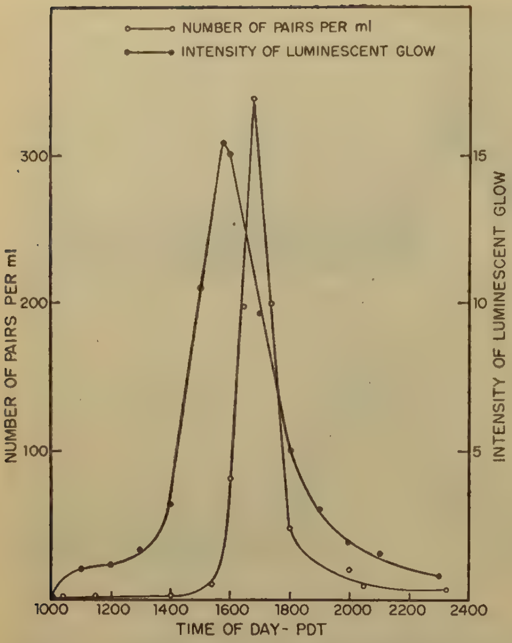

Fig. 2. The intensity of the luminescent glow (●) and the number of paired cells per ml. (○) at different times of day in *G. polyedra* grown in LD with light from 1900 to 0700.

indicate, then the increase in the cell population is not continuous. When cell counts were made at frequent intervals, a stepwise increase in the cell population was observed (Fig 3), one step occurring in each 24 hours at a time when cell division is predicted from counts of pairs. In these experiments pairs were observed only at the end of the dark period, corresponding to the time at which the sharp rise in the population took place.

From experiments in which cell counts as well as pair counts were made, it was possible to account for all cell divisions (calculated to have taken place from the measured increase in the cell population) by assuming that daughter cells remain attached, as a pair, for about 30 minutes.

Effect of constant conditions upon rhythm. It was next determined whether the observed periodicity in cell division was directly dependent on the periodic light changes in the environment or whether it would persist under constant environmental conditions. When cell populations grown under LD conditions were transferred to continuous bright light (1000 foot candles) it was found that the rhythmicity damped out over the course of several days. After 6 days, a completely random pair frequency was observed. The growth curve of cultures kept in continuous bright light for long periods should therefore, show no staircase effect. This was indeed found to be the case (Fig. 3) and, in these experiments also, the frequency of pairs was found to be independent of the time of day.

However, when cultures grown under LD conditions were transferred to continuous dim light (100 foot candles) at the beginning of a light period, a diurnal periodicity in cell division was found to persist for at least 14 days. The variation in the number of paired cells over the last few days of such an experiment is plotted in Fig. 4. It is clear that the rhythmicity in cell division will continue for a considerable length of time as long as the cultures are kept in dim light. It may be noted that, in the cultures kept in dim light for 14 days, the peaks are not so sharp as in LD cultures.

Cultures grown in LD conditions and transferred to darkness also show a continued rhythm in cell division. Two successive maxima in the number of paired cells have been observed, the time between the maxima being about 24 hours. Such experiments cannot be con-

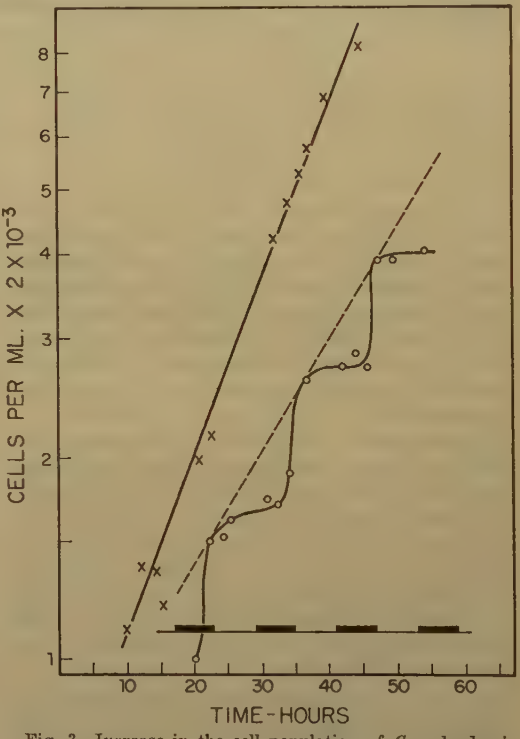

Fig. 3. Increase in the cell population of *G. polyedra* in continuous light (×), and in LD with light from 1800 to 0600 (○), the dark periods being indicated by black bars along the abscissa. Light intensity, 900 foot candles; temperature, 21.5° ± 1° C. Average generation time in continuous light, 1 day; in LD, 1.5 days.

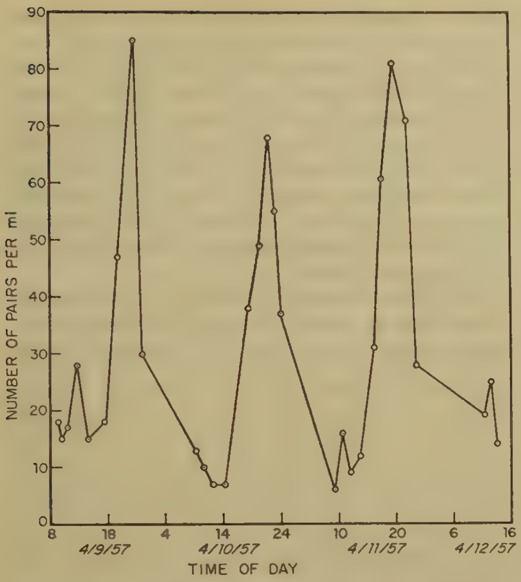

Fig. 4. The numbers of paired cells present in a cell suspension of *G. polyedra*, on the 12th, 13th and 14th day of continuous dim light (100 foot candles) at 19° C. *G. polyedra* was grown in LD with light from 1100 to 2300 and transferred to continuous dim light on 3/29/57 at 1100. The average generation time from 4/8/57 to 4/11/57 was 3.8 days.

tinued over a long time because *G. polyedra* is an obligate photoautotroph, and so does not continue to divide for long when kept in the dark. The persistence of the phasing of cell division in constant conditions (either light or dark) indicates, however, that the rhythmicity is not strictly dependent upon periodicity of the environment.

The natural period of the rhythm. In cells kept under LD conditions, the period of the rhythm in cell division, as measured by the time between maxima in the number of paired cells, is twenty-four hours. Under constant environmental conditions the period is approximately, but not exactly, 24 hours. In continuous dim light (100 foot candles) at 19°C. for example, the length of the period is 22.5 hours (Fig. 4). The duration of the period when no oscillations in the environment are present may be considered the "natural" period of the rhythmic process under investigation(16). The natural period of cell division varies with the temperature, being shorter at lower temperatures, as is the period of the rhythm in luminescence(9). In continuous light (100 foot candles), the length of the period of cell division was 23.9 hours at 18.5° and 25.4 hours at 25°C. (Fig. 5).

The dim luminescent glow referred to above also shows a natural period close to 24 hours, the length of which is similarly dependent on temperature. In Fig. 6, three recordings are reproduced which demonstrate the temperature dependence of the natural period of this rhythmically-occurring glow. It may be noted that the intensity of the glow is also temperature dependent, the magnitude being almost thirty times greater at 25° than at 18°C.

The generation time of the cell suspensions used for pair counts was determined from cell density measurements made at intervals during the course of experiments, both in LD conditions (Table I and Fig. 3) and in continuous dim light (Figs. 4 and 5). A wide variation in generation time was encountered, since a wide range of light intensities was employed. However, the average generation time was always greater than 24 hours in instances where there was phasing of cell division. There appears to be no relationship between the length of the period of the rhythm of cell division and the *average* generation time. It is evident, however, that the generation time of any given cell must be equal to an even multiple of the period of the rhythm when cell division is phased.

DISCUSSION

It is possible that the steady emission of light, or the glow, is related to cellular changes which occur during some stage or stages of cell division. The temporal relationships involved suggest this. Since a maximum in the number of paired cells present always occurs an hour or two following the maximum in the luminescence, one is led to suppose that cell division proper, or a certain stage of the process, is in fact accompanied by a steady light emission. In an organism such as the firefly or *G. polyedra*, where light emission occurs as a flash, only upon stimulation, the achievement of the dark condition is necessarily an active process. The reactants in the chemical reaction which gives rise to luminescence must be kept *apart* in order for the cell to remain dark. This "active dark" process may be related to membrane phenomena, similar to muscle and nerve, so that cell excitation results in the initiation of a reaction *via* changes in the properties of the membrane. It seems likely that cell division could involve changes which would result in a partial breakdown of the "active dark" process.

The rhythm in cell division in populations of *G. polyedra* shows marked similarities to the endogenous rhythm of luminescence previously described for this dinoflagellate(7,23). Both persist in continuous dim light, but are lost in continuous bright light. In darkness, both persist for only a few days, with a progressive reduction in amplitude. The length of the period of both the luminescent and the cell division rhythm is 24 hours in LD conditions. Under constant conditions, the length of the natural period has a similar relationship to temperature. The phase of both rhythms may be shifted so that it occurs at any time of day by appropriate changes in the timing of the light and dark periods. It seems likely that both rhythms are related to a basic metabolic rhythm of some sort, but additional experiments will be necessary to determine whether this is so.

Diurnal rhythms in cell division have been reported in a number of organisms other than dinoflagellates. For example, Stalfelt(20) found such a rhythm in *Pisum sedativum*, and Karsten(12) in *Spirogyra* and several desmids. In *Oedogonium cardiacum*, Bühnemann(3) describes a rhythm in mitosis which continues for a time after the cells are transferred to continuous light. Maxima in the number of mitotic figures occur approximately every 24 hours at a time corresponding to the middle of the dark period. Studies of the occurrence of mitotic figures in epidermal and hair follicle cells of litter-mate white mice(5) provide evidence that cell division in this animal shows a diurnal periodicity that persists in darkness but is obliterated in continuous light. However, the generation time of the cells in question was not determined in any of the cases cited above.

When cell division in a population is experimentally synchronized, as has been possible in a number of organisms(13,14,19), the length of the period of the cell

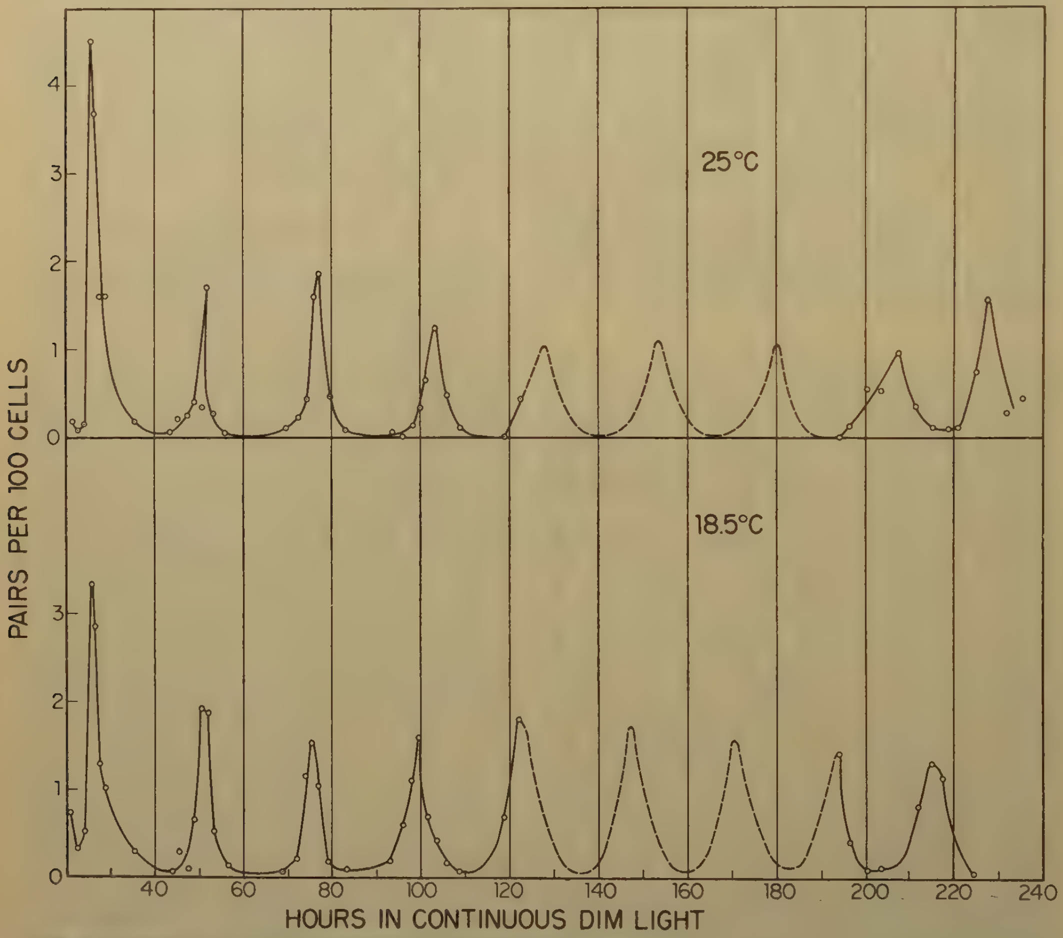

Fig. 5. The per cent of paired cells present in a cell suspension transferred from LD to continuous dim light (200 foot candles) at the beginning of a light period (zero time) at 18.5° C. (lower curve) and at 25° C. (upper curve). The average length of the period of cell division: 23.9 hours at 18.5° and 25.4 hours at 25° C. The average generation time: 4.2 days at 18.5° and 3.8 days at 25° C.

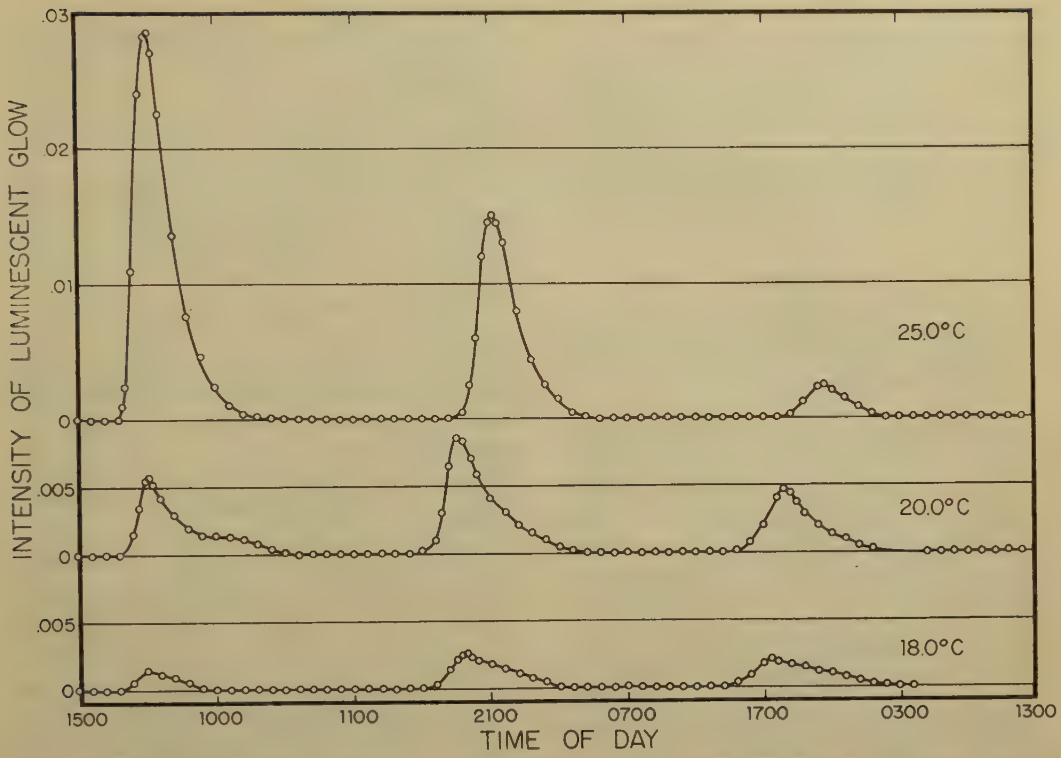

Fig. 6. The time course of the luminescent glow in *G. polyedra* at three different temperatures in darkness. Cell suspension grown in LD at 20° C. with light from 2100 to 0900 and placed in darkness at the designated temperature at 0900. Recordings from three aliquots measured on consecutive days in the sequence 18° - 25° - 20° C. Average of the glow rhythm: 22.9 hours at 18° C.; 23.3 hours at 20° C.; and 24.7 hours at 25° C.

division rhythm will be roughly determined by the generation time. The rhythm in the cell division of *Nitzschia palea* induced by a ten-day dark period(24) may well belong in this category, since the period is 10 to 12 hours and the generation time is of similar duration. However, unless the generation time of a given organism is one day, a diurnal rhythm could not arise from synchrony of cell division.

In *G. polyedra,* the diurnal rhythm persists in darkness, in dim light, and for about 4 days in bright light, at temperatures of 18° and 24°C. Under these conditions, the average generation time varies widely, and it is not possible that the rhythm is the result of a synchrony in cell division. It is evident from our data that the generation time in *G. polyedra,* when cell divisions are phased, is n times the period of the rhythm. Since divisions occur essentially at only one time of the day in LD cultures, a given cell must have a generation time of either 24 hours, or 48 hours, or a higher multiple of 24 hours. Moreover, in a population where the measured average generation time was, for example, 1.5 days, some of the cells must have had a generation time of 24 hours, while others had generation times of a higher multiple of 24 hours.

It therefore appears that the observed rhythm in cell division is controlled by a rhythmic mechanism not related directly to the mitotic cycle. In *G. polyedra,* rhythmic metabolic changes with approximately a 24 hour period are evident in the changes which take place in the luminescence(8,23). It is suggested as an hypothesis that the initiation of cell division takes place only at a certain phase of this metabolic rhythm. At this time, all cells which are sufficiently mature proceed to initiate division, as if in response to a signal. Other cells, which are not sufficiently mature, await the next occurrence of this determining phase.

The situation with respect to non-phased cultures, which have been grown in bright light, is not known. It might be that each cell retains the basic rhythm and divides only every n times 24 hours, but the individual cells are out of phase with one another. On the other hand, it may be that the generation time of each cell is accurately represented by the measured average generation time of the culture.

It might be possible to synchronize cultures of *G. polyedra* by experimental techniques. Thus far we have not been successful. In order to maintain synchronization it would clearly be necessary to adjust conditions of light and temperature so as to achieve an *average* generation time precisely equal to n times the period.

REFERENCES

1. Barker, H. A. (1935). The culture and physiology of the marine dinoflagellates. *Arch. Mikrobiol.*, **6**, 157-181.

2. Braarud, T. & Pappas, I. (1951). Experimental studies on the dinoflagellate *Peridinium triquetrum* (Ehrb.) Lebour. *Norske Vidensk.-Akad. Oslo. Avh. I. Mat.-Natury.* Kl. No. 2, 1-23.

3. Bühnemann, F. (1955). Das endodiurnale System der Oedogoniumzelle. IV. Die Wirkung verschiedener Spektralbereiche auf die Sporulations- und Mitoserhythmik. *Planta.*, **46**, 227-255.

4. Bünning, E. (1956). Endogene Aktivitatsrhythmen, in Ruhland, H., ***Encyclopedia of Plant Physiology,*** Vol. 3, General Physiology of the Plant Cell, Berlin, 878-907.

5. Carleton, A. (1934). A rhythmic periodicity in the mitotic division of animal cells. *J. Anat.*, **68**, 251-263.

6. Gough, L. H. (1905). Report on the plankton of the English Channel in 1903. *Mar. Biol. Assoc. U. K. International Fishery Investigation. First Report on Fishery and Hygrographical Investigations in the North Sea and Adjacent Waters (Southern Area).* 1902-1903. London, 325-377.

7. Hastings, J. W., Wiesner, M., Owens, J. & Sweeney, B. M. (1956). The rhythm of luminescence in a marine dinoflagellate. *Anat. Rec.*, **125**, 611.

8. Hastings, J. W. & Sweeney, B. M. (1957). The luminescent reaction in extracts of the marine dinoflagellate, *Gonyaulax polyedra. J. Cellular Comp. Physiol.*, **49**, 202-225.

9. Hastings, J. W. & Sweeney, B. M. (1957). On the mechanism of temperature independence in a biological clock. *Proc. Natl. Acad. Sci.*, **43**, 804-811.

10. Haxo, F. T. & Sweeney, B. M. (1955). Bioluminescence in *Gonyaulax polyedra,* in Johnson, F. H., ***The Luminescence of Biological Systems,*** A.A.A.S., Washington, D. C., 415-420.

11. Jörgensen, E. (1911). Die *Ceratien.* Eine kurze Monographie der Gattung *Ceratium* Shrank. *Internat. Rev. gesamt. Hydrobiol. und Hydrograph. Biolog. Supplement Ser. II,* 1-124.

12. Karsten, G. (1918). Über die Tagesperiode der Kern- und Zellteilungen. *Zeit. Bot.*, **1**, 1-20.

13. Lark, K. G. & Maale, O. (1954). The induction of cellular and nuclear division in *Salmonella typhimurium* by means of temperature shifts. *Biochem. et Biophys. Acta,* **15**, 345-356.

14. Nihei, T., Sasa, T., Miyachi, S., Suzuki, K. & Tamiya, H. (1954). Change of the photosynthetic activity of *Chlorella* cells during the course of their normal life cycle. *Arch. Mikrobiol.*, **21**, 155-164.

15. Nazawa, K. (1940). Problem of the diurnal rhythm in the cell division of the dinoflagellate, *Oxyrrhis marina. Annot. Zool. Jap.*, **19**, 170-174.

16. Pittendrigh, C. S. & Bruce, V. G. (1957). An oscillator model for biological clocks, in ***Rhythmic and Synthetic Processes in Growth*** (Ed., Dorothea Rudnick), p. 75-109. Princeton Univ. Press.

17. Pringsheim, E. G. (1946). *Pure Cultures of Algae.* Cambridge University Press, p. 119.

18. Provasoli, L., McLaughlin, J. J. A. & Pintner, I. J. (1954). Relative and limiting concentrations of major mineral constituents for the growth of algal flagellates. *Trans. N. Y. Acad. Sci. Ser. II,* **16**, 412-417.

19. Scherbaum, O. & Zeuthen, E. (1954). Induction of synchronous cell division in mass cultures of *Tetrahymena pyriformis. Exptl. Cell Res.*, **6**, 221-227.

20. Stalfelt, M. G. (1921). Studien über die Periodizität der Zellteilung und sich daran anschliessende Erscheinungen. *Kunst. Svenska Vetersk. Hand.*, **62**, 1-114.

21. Sweeney, B. M. (1951). Culture of the dinoflagellate *Gymnodinium* with soil extract. *Am. J. Bot.*, **38**, 669-677.

22. ——— (1954). *Gymnodinium splendens,* a marine dinoflagellate requiring vitamin B_{12}. *Am. J. Bot.*, **41**, 821-824.

23. Sweeney, B. M. & Hastings, J. W. (1957). Characteristics of the diurnal rhythm of luminescence in *Gonyaulax polyedra. J. Cellular Comp. Physiol.*, **49**, 115-128.

24. Von Denffer, D. (1948). Die planktische Massenkultur pennater Grunddiatomen. *Arch. Mikrobiol.*, **14**, 159-202.

Reprinted from Journal of the Optical Society of America, Vol. 48, No. 5, 354-357, May, 1958
Printed in U. S. A.

Nephelometer for the Measurement of Volume Scattering Function *in Situ**†

John E. Tyler and W. H. Richardson
Scripps Institution of Oceanography, University of California, La Jolla, California

(Received January 2, 1958)

A submarine nephelometer has been built for use in measuring the volume scattering function of natural waters. Theory and construction details of the optical system are given, including pertinent data for the photodetector used. The instrument is capable of measuring volume scattering function between angles of 20° and 170° in typical coastal waters. Results of preliminary tests with the instrument are given.

INTRODUCTION

Scattering in natural waters is the result of multiple reflections from organisms, gas bubbles, and detritus as well as of scattering by the molecules composing the hydrosol itself. It is commonly observed that the degree of scattering varies discontinuously with depth. This is true in waters having a high degree of biological activity and also in coastal waters where a major portion of the scattering agent may be detritus stirred up by wave action. The measurement of the scattering properties of natural waters presents some special problems that are not ordinarily encountered in the measurement of laboratory samples. Ocean and lake waters are balanced aquaria and are highly sensitive to environmental factors. Great changes can take place if these waters are bottled. Gas bubbles collect on the walls of the container, some species of plankton may die whereas others may undergo accelerated propagation, and detritus settles out or rises to the surface. In a matter of minutes the sample in the bottle may no longer represent the part of the ocean from which it was taken, and one would be hard put to justify the effort required to collect it. Thus the usual laboratory procedure of putting the sample into the instrument must be reversed.

Depth is an important parameter in biological oceanography, for example, and also in any program of physical measurements. Instrumentation must consequently meet the mechanical and optical requirements imposed by a type of operation which requires that the instrument be lowered into the hydrosol.

By definition the value of the volume scattering function[1] $\sigma(\theta)$ in the direction θ is

$$\sigma(\theta)=\frac{dJ(\theta)}{Hdv},$$

where $dJ(\theta)$ is an element of intensity in the direction θ, H is the irradiance on the volume, and dv is the element of sample volume. It is clear that in designing instrumentation for the measurement of volume-scattering function provision must be made to determine the sample volume (dv) and the irradiance input to the volume.

INSTRUMENT

In the instrument described here a well defined beam of light is used in conjunction with a Waldram[2] stop to irradiate uniformly a sample volume which is defined by the intersection of a beam of detectivity with the light beam. The beam of detectivity can be rotated around the center of the volume through an angle of about 180°. The details of the optical system are shown in Fig. 1. The projection beam is obtained by means of a uniformly-irradiated field stop which is imaged on the sample in such a way that its image is the same size as the exit pupil of the projection lens. The limiting rays are thus parallel to the axis of the system and can all be made perpendicular to the glass window of the watertight enclosure. Under these conditions the limiting rays will not be deviated if the index of refraction at the window is changed from 1.0 to 1.333.[3] The diagonal rays of the beam will, of course, be deviated inward if an increase in index of the medium occurs and a change in flux distribution within the beam will result, but the same total flux will be incident on the sample volume regardless of any change in the index of refraction. (Changes in attenuation by scattering or

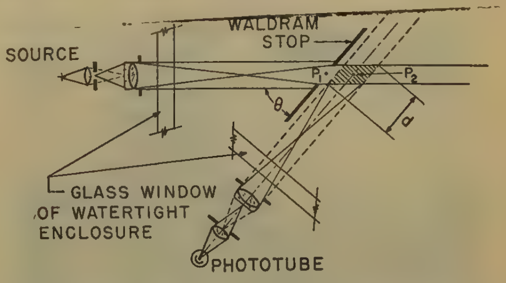

Fig. 1. Details of the optical system of the nephelometer. P_1 is the axis of rotation of the Waldram stop and P_2 is the axis of rotation of the scanning system. The sample volume is made independent of θ by the operation of the Waldram stop.

---

* Contribution from the Scripps Institution of Oceanography, University of California, (new series). 1029

† This work has been supported by the Bureau of Ships and by the Bureau of Aeronautics through Contract NObs-72092.

[1] For photometric symbols see, Committee on Colorimetry, J. Opt. Soc. Am. 34, 245–266 (1944).

[2] J. M. Waldram, Trans. Illum. Eng. Soc. (London) 10, 147–188 (1945); W. E. K. Middleton, *Vision through the Atmosphere* (University of Toronto Press, Toronto, 1952), pp. 201–202.

[3] This is an important feature since some of the calibration procedures are much more easily accomplished in air.

Reproduced by Permission

absorption are not under consideration at this point in the discussion.) This collimated light beam is ideally suited for use with a Waldram stop because of the uniform flux distribution across the beam at the image. Independent measurements at and near the image plane showed uniform flux distribution in the cross section of the beam for a considerable distance on both sides of the image. Thus changes in the position of the image along the axis owing to changes in index of refraction will be unimportant to the operation of the Waldram stop as well as to the proper irradiation of the volume.

The beam of detectivity is generated with the same type of optical system used for the light beam and is designed to intersect the light beam over the axis of rotation of the scanning system (see Fig. 1). The volume thus defined (about 3.2 cm^3) has a shape that depends on the angle of observation.

Uncertainties in the measured value of the scattering function will be present as a result of dimensional changes in the sample volume during the scanning cycle. In Fig. 1 the dimension d is minimum at $\theta=90°$. If the scanning arm moves in either direction from 90°, d increases and the uncertainty in the measurement of $\sigma(\theta)$ increases because of the fact that the flux from the nearest point of the volume and that from the farthest point of the volume are undergoing exponential attenuation over different path lengths and do not combine to give an average for the measurement. This effect would be much worse, of course, if the Waldram stop were not used.

CALIBRATION

The relative magnitude of the sample volume at each angle of observation is determined by means of a volume-calibrating attachment (see Fig. 2) which was developed by Mr. Benjamin S. Pritchard.[4] This device consists of a lead screw mounted parallel to the beam of detectivity and driven at constant speed by a synchronous motor. The lead screw in turn drives a small carriage carrying a white Lambert reflector through the light beam and consequently through the sample volume. At any position of the Lambert reflector the phototube signal will be proportional to the reflectance (or transmittance) of the reflector (R), the irradiance of the Lambert reflector (H), and a sectional area (A) through the volume at this position, i.e.,

$$\text{Reading}=kRAH, \tag{1}$$

where k represents the proportionality constant. By holding the light intensity constant, the reading (at each fixed angular setting) becomes proportional only to the area.

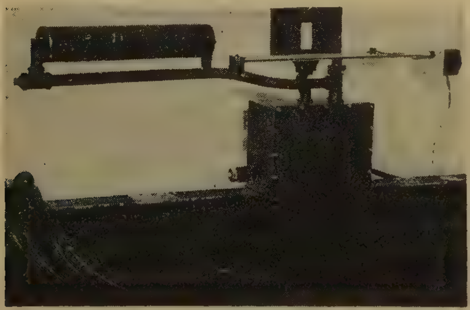

FIG. 2. Scanning system of nephelometer showing volume calibration attachment in place on the scanning arm. The light source is at the left (not shown).

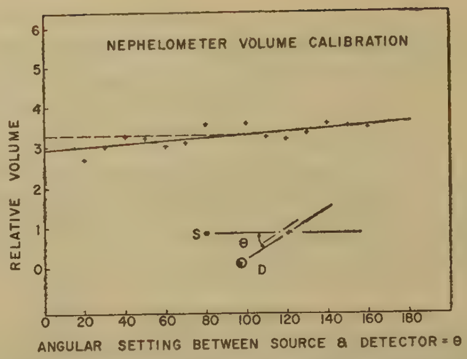

FIG. 3. Plot of sample volume *vs* angular setting of scanning arm. The variability is believed to be caused by systematic errors which do not have physical significance. For this paper volume corrections were based on the "best straight line" which is shown.

Recording the phototube output on a synchronous drive chart gives a plot of (kA) *vs* χ, the longitudinal dimension of the volume along the axis of detectivity, and the volume V will of course be

$$V=\int_{\chi_1}^{\chi_2} k_1 A dx, \tag{2}$$

where k_1 is the new proportionality constant.

The experimental limits of χ are quite well defined and no difficulty has been experienced in their practical determination.

Figure 3 is a plot of the relative volume *vs* the angle of observation. The absolute magnitude of the volume can be found easily from geometrical considerations when the beams intersect at 90°. The geometrical dimensions required for this computation were obtained by scanning the light beam with a photoelectric probe of small aperture and plotting flux *vs* transverse position. The beam of detectivity was similarly scanned with a light probe. The edges of these two beams were found to be well defined and the beams were uniform, respectively, in flux and sensitivity.[5]

---

[4] B. S. Pritchard and H. R. Blackwell, Final Report No. 2557-2-F, Vision Research Laboratories, July (1957); Engineering Research Institute, University of Michigan, Ann Arbor, Michigan.

[5] Nonuniform flux distribution in the light beam, or nonuniform sensitivity in the beam of detectivity could be very troublesome

(632)

The value of R (or T) called for by Eq. (1) can be determined by using the instrument as a goniophotometer. This involves removing the Waldram stop, positioning the Lambert plate at the center of rotation, and scanning through 180°. Since the flux incident on the plate is found by measuring the direct beam with the same optical system and the same phototube, instrumental factors cancel yielding true gonioreflectance or goniotransmittance values directly. The details of this procedure are given in the section entitled Theory.

The flux input to the volume which is needed for the evaluation of H in Eq. (3) can be determined for the immersed instrument by measuring the flux input in air, again using the instrument's own detection system, and correcting for the beam transmission of the water path between the source and the volume. The beam transmittance for this work was measured with a beam transmissometer having a light beam of the same optical design as the nephelometer.

CIRCUITRY

The phototube used in this instrument is an end-on multiplier phototube (Dumont No. 6291) selected for high sensitivity and low noise. Its characteristics are as follows:

Cathode sensitivity; 42 μa/lu measured with 210 v between the cathode and all other electrodes.
Gain; 2.18×10^6 at 138 v per stage plus 106 v between last dynode and anode.
Dark current; not greater than 0.2 μa at 1600 v.
Anode sensitivity; 92 amp/lu at 138 v per stage and 106 v between anode and last dynode.

The phototube signal goes to a logarithmic-type chassis, a development of the circuit described by Monroe Sweet,[6] and the output from the chassis goes to a strip-chart recorder. The circuit and recorder are designed to accommodate a change of five log cycles in light level. The circuit constants are adjusted to achieve a linear relationship between light input (in logarithmic units) and recorder-scale reading. Adjustments are made on a 4-meter photometer bench using a stable light source and 0.1 log-unit steps as determined by the inverse square law.

THEORY

As previously stated, the value of the scattering function at any angle is

$$\sigma(\theta)=\frac{dJ(\theta)}{Hdv}, \tag{3}$$

where $dJ(\theta)$ is the intensity of the scattered light in the direction θ, H is the irradiance on the volume, and dv the sample volume.

The value of $J(\theta)$ is the flux emitted by the sample volume (dp_1) per unit solid angle $d\omega$ or; referring to Fig. 4,

$$J(\theta)=\frac{dp_1}{d\omega}=\frac{CR_\theta e^{\alpha r_2}}{dA_1/r_2^2}. \tag{4}$$

Here the instrument reading R_θ at the angle θ is corrected for the attenuation suffered in traversing the water path r_2, and is shown directly proportional to the flux collected by the phototube through the coupling factor C.[7] dA_1 is the area of the collector; α is the beam attenuation coefficient.

The irradiance (H) on the volume is the flux input (dp_0) per unit area (dA_0). This measurement is made in air with the same phototube and optics used to measure $J(\theta)$ and must be corrected for beam spread. Thus:

$$H=\frac{dp_0}{dA_0}=\frac{CR_0e^{-\alpha r_1}}{dA_1}\times\frac{dA_2}{dA_0}, \tag{5}$$

where R_0 is the reading in air, coupled to the flux collected by the same coupling factor C, and corrected for the beam attenuation of the path r_1. This flux is collected on an area dA_2 and is corrected by the factor dA_2/dA_0 to obtain the irradiance input to the sample volume.

At $\theta=90°$ the sample volume $dv=dA_1x$ since the

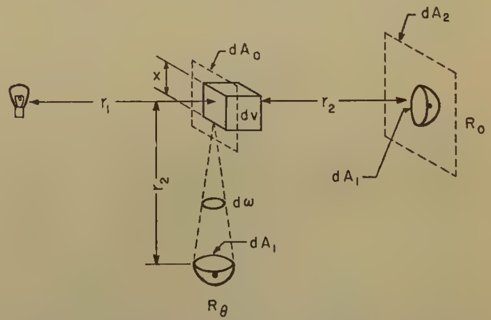

FIG. 4. The scanning arm, here represented as dA_1, is shown below the volume with its axis vertical (instead of horizontal as in previous figures).

---

in the determination of volume-scattering function since calibration procedures and computations are all based on uniform-flux and sensitivity distributions. The present instrument is not perfect in these respects but is tolerable.

[6] Monroe H. Sweet, J. Soc. Motion Picture and Television Engrs. 54, 35–62 (1950).

[7] The measuring head of optical instruments is here considered to be made up of a collector which is designed to accept light in accordance with some preconceived definition (e.g., radiance or irradiance), and a detector which may include the optical filter in the system. These components are joined by a "coupling" which must be designed to assure proper and constant sampling of the radiant flux for all lighting conditions that will be met in making measurements with the instrument. An important property of this coupling is its efficiency represented here by the symbol C.

beam of detectivity is parallel sided. Thus at 90°

$$\sigma(90°)=\frac{R_{90}}{R_0}\cdot e^{\alpha(r_1+r_2)}\left[\frac{r_2^2 dA_0}{dA_1 dA_2 \chi}\right]. \qquad (6)$$

Values of $\sigma(\theta)$ at other angles are obtained by means of the equation,

$$\frac{\sigma(90)}{R_{90}}\times R_\theta=\sigma(\theta). \qquad (7)$$

The value of the scattering function at any angle is seen to be directly proportional to the measured reading at each angle θ and inversely proportional to the beam transmittance of the path (r_1+r_2).

$$\sigma(\theta)=R_\theta e^{\alpha(r_1+r_2)}\left[\frac{r_2^2 dA_0}{dA_1 dA_2 \chi R_0}\right]. \qquad (8)$$

MEASUREMENTS

A series of measurements was made in a 1300-gallon light-tight tank using San Diego tap water (i.e., Colorado River water) filtered through a 2-μ sintered bronze thimble.[8] In order to assure the same water basis for the whole series, the scattering agent was successively added to the tank of water. The scattering agent used in these tests was a single sample of skim milk.

Because of the circuitry employed, the measurements were made in a dark tank. Measurements were made of the filtered water and after contamination with 100, 200, 400, 600, and 800 cc of skim milk. At each concentration the beam transmittance of the hydrosol was also measured. Equation (8) was then employed to obtain the relative values of the scattering function shown in Fig. 5.

COMMENTS

This underwater nephelometer was designed for use in typical coastal or bay water. It can be seen from Fig. 4 that, for the narrow-band filter used in this test, the instrument had insufficient sensitivity to detect the back scattering from the filtered San Diego tap water. At the other extreme, a degree of turbidity can be visualized which would render the instrument useless, for as turbidity increases the collimated light beam becomes excessively diffuse before reaching the sample volume, the effective size of the sample volume will be increased, and the problems of determining irradiance input as well as sample volume will be greatly increased. This problem and also the problem of mechanical interference between the light beam and the phototube housing seem to be inherent to this type of instrument.

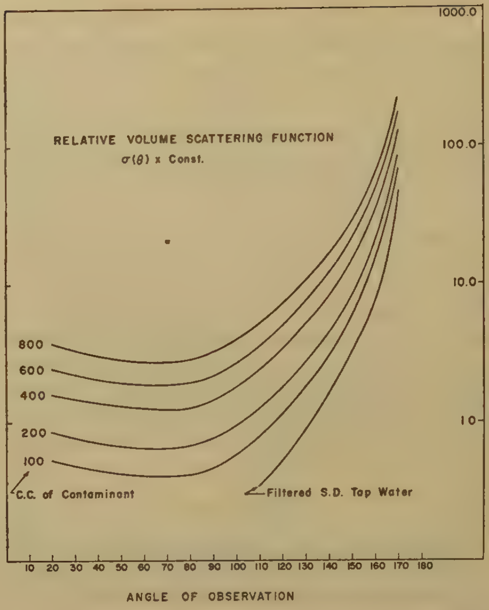

FIG. 5. These tests were run to study the operating characteristics of the instrument in water of high and low-scattering properties. For these tests it was unnecessary to evaluate the constant of Eq. (8) (in brackets). By evaluating this constant, this figure would give values of the volume scattering coefficient for this particular sample, for a 60-mμ spectral band centered at 480 mμ.

ACKNOWLEDGMENTS

The authors wish to acknowledge with thanks the guidance and constructive criticism of Dr. S. Q. Duntley, Director of the Visibility Laboratory, whose long-time interest in the optical properties of natural waters has made this work possible. They also wish to acknowledge the engineering assistance of Mr. R. W. Austin and Mr. Robert Howarth, who have provided the accurate and reliable circuitry for this instrument, and Mr. George Tate, Senior Electronics Technician, and Mr. Alden Hooton, Principal Laboratory Mechanician, whose skill and craftsmanship have resulted in a rugged, smooth-running, and trouble-free instrument.

---

[8] This device removes air from the water as well as particulate matter larger than 2 μ.

Reprinted from SCIENCE, October 24, 1958, Vol. 128, No. 3330, page 1003.

Ionium-Thorium Chronology in Deep-Sea Sediments of the Pacific

Abstract. The ratio of ionium to thorium varies exponentially with depths in deepsea sediments of the Pacific Ocean and gives rates of accumulation of the order of millimeters per thousand of years. Surface values of the ratio were not constant over the eastern Pacific Ocean. This observation may result from differences in thorium isotope concentrations in near bottom waters which furnish these isotopes to the sediments.

The method of ionium-thorium chronology (*1*) of deep-sea sediments is based on the simultaneous removal of ionium (Th^{230}, $t_{1/2} = 80,000$ years, a member of the U^{238} radioactive series) and thorium (Th^{232}, $t_{1/2} = 1.4 \times 10^{10}$ years) from the water to one or more of the mineral components of the deposits. The critical assumptions for the application of the method follow. (i) The Io/Th ratio has remained constant in the waters adjacent to the sediments over the time intervals involved. (ii) The chemical species of Io and Th in the sea water are the same, and these isotopes have identical distributions among them. (iii) The analyzed materials do not contain detrital materials, of continental or volcanic origin, with significant contributions of Io or Th. This method appears preferable to the previous method of radium chronology (*2*) inasmuch as the observed diffusion of radium from the decay site of its parent ionium can invalidate any age determinations (*3*).

Table 1. Ionium-thorium ratios in three cores from the Eastern Pacific Ocean (Capricorn 50BG—latitude 14° 55′N, longitude 124° 12′W, 4270 m; Chinook 11—latitude 49° 39.5′N, longitude 177° 39′W, 4850 m; Downwind 49HG—latitude 42° 02′S, longitude 98° 01′W, 4350 m). The ratios are given in terms of disintegrations of Io per disintegration of Th per unit time.

Depth interval in core (cm)	Io/Th ratios		
	Capricorn 50BG	Chinook 11	Downwind 49HG
0–4	30	16	35
4–8	23	18	26
8–12	16	11	19
12–16	9.0	10	5
16–20	8.4	7.0	2
20–24	6.1	6.2	
24–28	5.3	4.4	

The isotopes of Th were isolated from sediment samples by previously described methods (*4*) and subsequently plated on a 1-in. platinum disc. Preferential solution of the nondetrital matter was accomplished with hot, concentrated hydrochloric acid. The principal detrital minerals, quartz and feldspars, were insoluble and were discarded following centrifugation. The recovery of the Th isotopes from the samples was determined with UX$_1$ (Th^{234}), and yields varied between 50 and 98 percent. The plated Io and Th were readily differentiated and quantitatively assayed with an alpha-ray spectrometer, a Frisch screen-grid ion chamber being used as a detector. The dominant alpha energies of Io and Th are 4.6–4.7 and 3.98, respectively (*5*).

Preliminary analyses (*6*) of a number of Eastern Pacific deep-sea cores have emphasized three significant results. First of all, exponential decreases in the ratio with depth have been observed in 10 of the 12 cores analyzed. Two South Pacific cores had values of the ratio that were both low and essentially invariant with depth. Whether such results indicate a lack of deposition over the last few hundred thousand years or a loss or disturbance of the upper section of the core during the handling has as yet not been determined. Table 1 gives typical analyses on three cores collected by expeditions of the Scripps Institution of Oceanography.

Secondly, determinations of the recent rates of accumulation of these Eastern Pacific clays, made on the basis of these data and of the half-life of ionium, are remarkably uniform, with values for the Capricorn, Chinook, and Downwind cores of 1, 2, and 1 mm per 1000 years, respectively, in the upper 10 cm. A dramatic drop in the Io/Th ratio, corresponding to nearly 2 half-lives of ionium over a few centimeters' distance, is observed in the Downwind core. Such a change has been observed in but one other core, also from these southerly latitudes.

Finally, *the surface ratios* fall into two distinct groups: a set in the region between the Aleutian Islands and Hawaii with values averaging about 15 and a second group, in the region between longitude 120° and 140°W and latitude 40°N and 40°S, with a ratio varying around 35. The cores given in Table 1 are representative of such groups. The isotopes of lead show a similar distribution pattern (*7*).

These results can be interpreted on the basis of the assumption that the deep-oceanic water masses, which are in contact with the sediment surfaces, furnish these isotopes to the sediments. Hence, these two regions should have circulating, overlying water masses which possess values for the Io/Th ratio which are similar to those found in the surface layers of the sediment deposits. The distinctive isotopic composition of thorium in a given water mass probably reflects the weathering processes responsible for the introduction of thorium and uranium into the water mass and the inorganic and biochemical processes in the ocean that cause their removal.

EDWARD D. GOLDBERG
MINORU KOIDE
Scripps Institution of Oceanography, La Jolla, California

References and Notes

1. E. Picciotto and S. Wilgain, *Nature* 173, 632 (1954).
2. C. S. Piggot and W. D. Urry, *Am. J. Sci.* 239, 81 (1941).
3. G. Arrhenius and E. D. Goldberg, *Tellus* 7, 226 (1955); F. F. Koczy, *Nature* 178, 585 (1956).
4. E. D. Goldberg and E. Picciotto, *Science* 121, 613 (1955).
5. A description of the plating techniques and instrumentation is in preparation.
6. This report is a contribution from the Scripps Institution of Oceanography. This study was sponsored by the Office of Naval Research under contract with the University of California.
7. T. Chow and C. Patterson, personal communication.

18 June 1958

Contributions from the Scripps Institution of Oceanography, New Series, NO. 1030
Reproduced by Permission

(*Reprinted from Nature, Vol.* 182, *pp.* 1156–1158, *Oct.* 25, 1958)

Surface Concentrations of Manganese Nodules

MANGANESE nodules were investigated during the Downwind Expedition, a part of the International Geophysical Year programme of the Scripps Institution of Oceanography of the University of California. Attempts were made to collect bottom photographs, cores and dredge hauls in the same areas, to measure the distribution at the surface and in depth, and to obtain large samples for physical and chemical analysis.

Although nodules were sampled and photographed in various places along the expedition track between California, Tahiti and South America, the greatest concentration was found on the red clay bottom deeper than about 4 km. in the south-western Pacific Basin. Nodules had been discovered in the basin by the *Challenger* eighty-five years before. The two ships of the expedition followed the track of the *Challenger* and explored a narrow band about 2,700 km. long in a south-easterly direction from latitude 25° S. to 45° S. in the eastern part of the basin. Two bottom photographs, twenty-three gravity cores and two dredge hauls were obtained. Photographs (Fig. 1) indicate that about a quarter

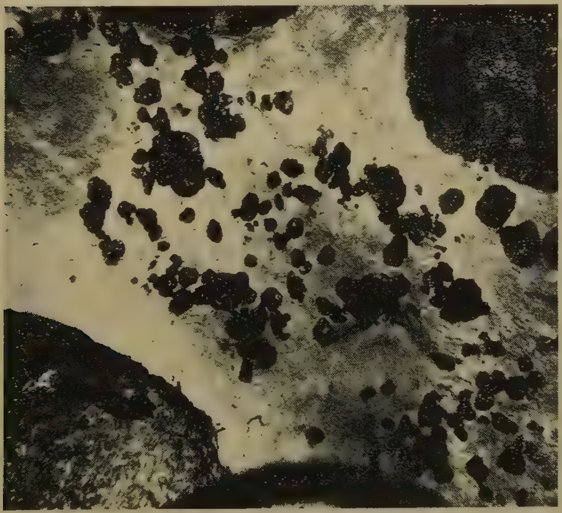

Fig. 1. Photo *DWP*–11. Area about 6 m.^{2}

(637)

Contributions from the Scripps Institution of Oceanography, New Series, No 1031

Reproduced by Permission

Table 1. DOWNWIND EXPEDITION BOTTOM PHOTO STATIONS SHOWING ABUNDANT MANGANESE NODULES

Station No.	Region	Latitude	Longitude	Depth in metres	Per cent of bottom covered	gm.cm.$^{-2}$
DWP-2	Baja Calif. Smt. Prov.	10° 25′ N.	130° 35′ W.	4,712	Abundant	
DWP-5	French Polynesia	18° 31′ S.	141° 23·5′ W.	4,080	Abundant	
DWP-8	French Polynesia	21° 37′ S.	147° 40′ W.	4,684	26	2½
DWP-10	South-western Pacific Basin	32° 08′ S.	140° 30′ W.	4,754	23	1
DWP-11	South-western Pacific Basin	42° 50′ S.	125° 32′ W.	4,560	46	4

to a half of the sea floor in this basin is covered with manganese nodules and that the weight per unit area is about 1–4 gm. cm.$^{-2}$ (Table 1). The surface concentration was determined by standard statistical procedures. Density of the nodules is about 2·0 gm. cm.$^{-3}$. The scale of the photographs is known, and the volume of the nodules can be estimated because the smaller nodules are roughly spherical and the lengths of their shadows give a scale for measuring the thickness of slab-shaped nodules. The sizes computed agree reasonably closely with the sizes dredged.

The group of cores gives less definite evidence of the fraction of the bottom covered with nodules in the south-western Pacific Basin but it provides a means of interpolation between the widely separated camera stations. Some twenty-three gravity cores contained samples as follows: six sediment but no nodules; four manganese oxide fragments in core nose; four small nodules only; nine sediment and nodules including eight with nodules at surface. Omitting one smaller core for uniformity, each of twenty-two cores has a cross-sectional area of 18 cm.^{2}. The four cores with manganese oxide fragments may be assumed to be hits on large nodules each with an area of 18 cm.^{2}. The thirteen cores with nodules alone or nodules and sediment have fifteen nodules at the surface with an average diameter of approximately 1 cm. These figures indicate one-fifth of the bottom is covered with nodules along the transverse. Consequently, the average coverage of nodules indicated by coring is about the same as the minimum shown on photographs. The average coverage from coring would be greater if four other coring attempts were counted as hits on large nodules. On each of these a ball-break indicated that the cores hit bottom, but no sample of any kind was obtained in the cores. However, nodules were indicated by black streaks and scratches not only on corers but on the camera and temperature probe. Similar streaks on equipment were observed in this area during the *Challenger* Expedition[1] and interpreted as indicating very abundant nodules.

Nodules are not limited to the surface of the sea bottom. Of fifteen cores that penetrated deeper than 11 cm., three contained nodules at depths of 8–11 cm. Of thirteen cores penetrating to 72 cm., six had nodules 48–72 cm. below the surface. No other nodules have been found in a maximum penetration of 140 cm. One core penetrated to approximately 47–50 cm. where a small nodule was lodged in the core catcher. This is the only core which ceased penetrating when it reached one of the nodule-rich zones. Consequently, there is no positive indication that large nodules (which would stop the corer) occur anywhere except at the surface. Moreover, some of the cores may have hit the bottom more than once, with the result that some nodules that appear to be buried in sediment were actually at the surface.

Manganese nodules are a potential resource so that an estimate of the amount in the south-western Pacific Basin may be of interest. The U.S.S. *Enterprise* took a latitudinal line of samples by sounding lead across the basin at about 50° S. Several records of 'black specks' and one 'black stone' may indicate manganese nodules or fragments. No other samples are available, and it is only an assumption that the concentration of nodules found along the Downwind track is characteristic of the whole basin. The basin deeper than 4 km. has an area of roughly 10^7 km.^{2}. If the concentration of nodules is uniform at 1 gm. cm.$^{-2}$, the total weight of the surface deposit is 10^{17} gm. Average chemical analyses of Pacific nodules suggest that iron and manganese are present in the deposit in amounts of 10^{16} gm., and cobalt, copper and nickel and rare earths each amount to 10^{15} gm.

Dredge hauls and cores show that nodules are distributed within perhaps 5×10^7 km.^{2} of the Pacific Basin, but little is known about the concentration per unit area. Photograph *DWP*-8 in French Polynesia indicates that nodules cover about a quarter of the surface, but the photograph is oblique and subject to greater errors of interpretation than photographs *DWP*-10 and -11 (Fig. 1). Similar concentrations are suggested by photographs in other areas, but the nodules are partially covered with sediment and only rough estimates are justified. Nevertheless, the scanty evidence available suggests that manganese nodules cover a considerable fraction of the deep sea floor in many parts of the Pacific Basin. This circumstance presents a puzzle, because the upward growth of nodules may be one or two orders of magnitude slower than commonly accepted average deposition rates of sediment in the deep sea[2].

H. W. MENARD

Scripps Institution of Oceanography,
University of California,
La Jolla, California.

C. J. SHIPEK

U.S. Navy Electronics Laboratory,
San Diego, California.

---

[1] Murray, J., and Renard, A. F., "Deep-sea Deposits". H.M.S. *Challenger*, Sci. Results, 362 (1891).

[2] Goldberg, E. D., and Arrhenius, G. O. S., *Geochim. et Cosmochim Acta*, 13, 198 (1958).

Printed in Great Britain by Fisher, Knight & Co., Ltd., St. Albans.

Reprinted from PACIFIC SCIENCE, *vol. XII, no. 4, Oct., 1958*

On Certain Thaliacea (Tunicata) from the Pacific Ocean, with Descriptions of Two New Species of Doliolids[1]

TAKASI TOKIOKA[2] and LEO BERNER[3]

THE MATERIAL upon which this paper is based has been taken from the extensive plankton collections available at the Scripps Institution of Oceanography. The samples examined were from three sources: the Shellback Expedition to the area off Central and South America in 1952, the Mid-Pacific Expedition to the Marshall Islands area in 1950, and from the routine Marine Life Research Program sampling off the west coast of the United States and Baja California, Mexico. The two expeditions were in part supported by grants from the Office of Naval Research. The Marine Life Research Program is the Scripps Institution's component of the California Cooperative Oceanic Fisheries Investigations, a project sponsored by the Marine Research Committee of California. The work has been further supported by a postdoctoral grant from the Rockefeller Foundation for the senior author.

Two new doliolids found in the plankton samples collected on the Shellback Expedition have already been described (Tokioka and Berner, 1957), and further examination of the samples has yielded two additional new doliolids from the same area.

In addition to the descriptions of the two new species, both of which belong to the genus *Doliolina*, additional notes are given on *Doliolina undulata* Tokioka and Berner 1957, *Doliopsoides horizoni* Tokioka and Berner 1957, *Doliolina intermedium* (Neumann) (1906), *Cyclosalpa strongylenteron* Berner 1955, and *Cyclosalpa bakeri* Ritter 1905.

Doliolina obscura new species
Fig. 1A–E

Many specimens of this species were found at Shellback stations 137, 142, 145, 155, 160, and 180. The species also occurs quite often in the samples collected by the Marine Life Research Program, although it is never numerous.

The gonozooids may be somewhat stumpy in outline; they are usually less than 5 mm. long and may range up to 4 mm. in body diameter. The test is of moderate thickness, is rather soft, and may be easily stripped from the body. When found with the test in place the specimens tend to be covered with detrital material from the sample.

Muscles I, VII, and VIII are narrower than muscles II-VI. Muscle VII is distinctly interrupted at the mid-ventral line. The sixth and seventh intermuscular zones, especially the latter, are narrower than the others.

The endostyle (*ed.*) is long, extending anteriorly at least to three-fourths of the second intermuscular zone and posteriorly to the anterior margin of muscle V. The anterior margin of the peripharyngeal band (*p.b.*) extends nearly to muscle I. The ciliated groove (*c.g.*) is situated in the middle of the second intermuscular zone. The dorsal ganglion (*d.g.*) is

---

[1] Contribution from Scripps Institution of Oceanography, New Series. Manuscript received April 24, 1957. No. 1032

[2] Present address: Seto Marine Biological Laboratory, Japan.

[3] Scripps Institution of Oceanography, University of California, La Jolla, California.

Reproduced by Permission

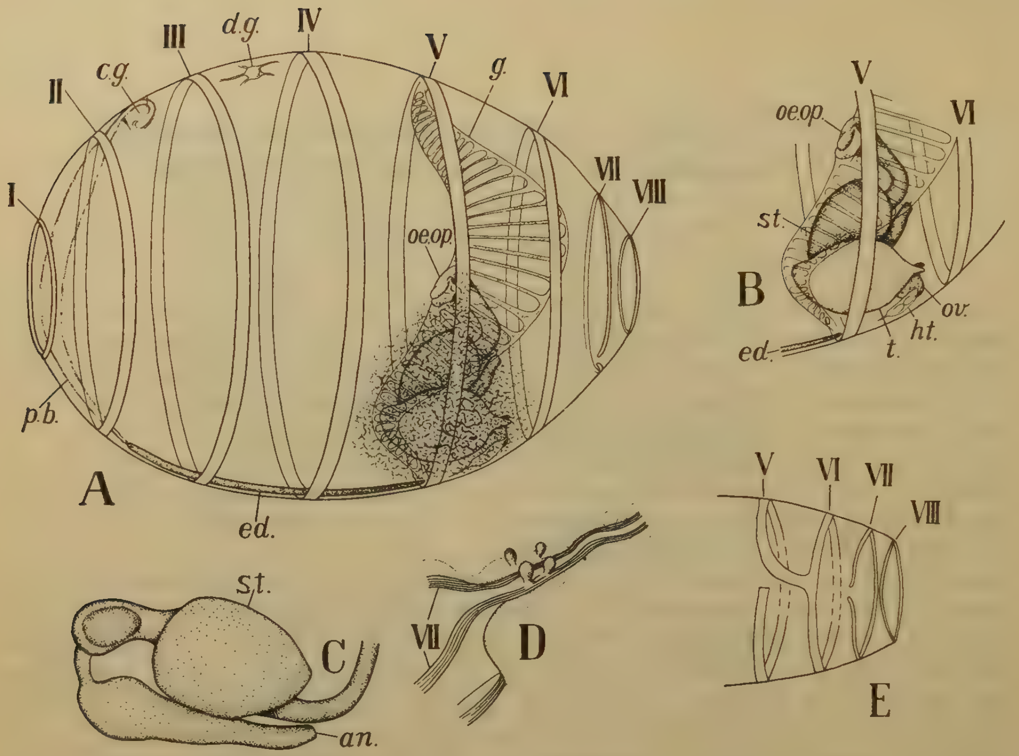

FIG. 1. *Doliolina obscura* n. sp. A, Animal from left side: a 5 mm. gonozooid. B, Alimentary organs and gonads from left side. C, Alimentary canal. D, Ventral protuberance, phorozooid. E, Aberrant form showing arrangement of muscles viewed ventrally.

Abbreviations: I-VIII, body muscles; *an.*, anus; *c.g.*, ciliated groove; *d.g.*, dorsal ganglion; *ed.*, endostyle; *g.*, gill septum; *ht.*, heart; *int.*, intestine; *oe.op.*, oesophageal opening; *ov.*, ovary; *pb.*, peripharyngeal band; *st.*, stomach; *t.*, testis; *v.d.*, vas deferens.

situated in the third intermuscular zone with its posterior edge at the center of the zone. The gill septum (*g.*) is sigmoid in shape extending from the dorsal to ventral position of muscle V, (Fig. 1*a*). At the lower flexure the anterior margin reaches slightly beyond the middle of the fourth intermuscular zone. At the upper flexure the posterior margin extends slightly beyond the posterior margin of muscle VI. The median crest of the gill septum is slightly displaced to the right side in the ventral half of its course, where the massive alimentary organs and gonads are situated. There are about 40 elongate stigmata.

The alimentary organs and gonads are surrounded by densely aggregated corpuscles which make it very difficult to examine the structure of the organs closely. These corpuscles are probably reddish orange when the animal is alive. Staining of the specimens with Rose Bengal makes it somewhat easier to study this portion of the body.

The oesophageal opening (*oe. op.*) is located near the center of the circle described by muscle V. The stomach (*st.*) is located on the sagittal plane of the body and is roughly oval in outline. The intestine forms a simple loop and ends with the anus (*an.*) at a position slightly behind the cardiac end of the stomach. The hind stomach is distinct and there is an obvious constriction between it and the following portions of the gut.

The ovary (*ov.*) is located near the middle of the fifth intermuscular zone or slightly posterior to it. The testis (*t.*) is a fusiform-shaped stumpy mass, oriented anteroposteriorly, and extending from the ovary to near the middle of the fourth intermuscular zone. The heart is located near the ovary.

The phorozooid is similar in appearance to the gonozooid, though the corpuscular aggregation over the area of the gut tends to be reduced in the phorozooid. Both the ventral ends of muscle VII extend into the ventral protuberance (Fig. 1D).

At a glance this new species closely resembles *D. mülleri* (Krohn 1852). It differs from the latter by having the ventral interruption of muscle VII and in the anterior-posterior position of the testis. In *D. mülleri* the testis is situated somewhat dorsoventrally and muscle VII forms a complete loop. The sigmoid curve of the gill resembles *D. sigmoides* Garstang 1933 (=*Doliolum krohni* Neumann 1906). The new species completely lacks the epidermal tentaclelike processes characteristic of *D. sigmoides*. Interrupted muscle VII is another differentiating characteristic. The new species differs from *D. undulata* in the shape of the stomach and in the shape and location of the testis. In addition, the aggregation of corpuscles around the alimentary organs and the gonads is unique. The species name comes from this aggregation which makes these organs obscure.

The specimens upon which this description is in part based are deposited in the U.S. National Museum under the following numbers:

HOLOTYPE: U.S.N.M. no. 11371, *Doliolina obscura*, gonozooid, 1 specimen from Shellback station 137 located at 13° 43.5′ S. 81° 08.5′ W.

PARATYPES: U.S.N.M. no. 11372, gonozooids, 10 specimens, *Doliolina obscura* from Shellback station 137.

From the MLR material one aberrant form was taken in which the fifth body muscle was interrupted and the left limb of that muscle extended back to connect with muscle VI. In other respects this specimen did not differ from the species. The muscle arrangement is shown in Figure 1E.

Doliolina separata new species

Fig. 2

A few specimens of this diminutive doliolid were found in the samples from Shellback stations 137, 145, and 180. Most of them were poorly preserved and immature, but three mature, fairly well-preserved specimens were found at station 137. The following description is based on these three specimens.

The specimens were 1.5, 1.7, and 1.7 mm. long. The body is somewhat elongate. The test is of moderate thickness and is easily stripped from the body. Under the microscope many minute cells can be observed on the surface of the test.

Body muscles I, VII, and VIII are very narrow. Muscle II is somewhat narrower than muscles III-VI. Muscle VII is clearly interrupted at the mid-ventral line. The first and seventh intermuscular zones are narrower than the others.

The endostyle (*ed.*) is very long, extending from the posterior margin of muscle II to near the anterior margin of muscle V. The anterior border of the peripharyngeal band (*p.b.*) closely approaches muscle I. The ciliated groove (*c.g.*) is situated approximately in the middle of the second intermuscular zone. The dorsal ganglion (*d.g.*) is located in the third intermuscular zone near the posterior margin of muscle III. The gill septum (*g.*) extends from muscle VI dorsally to muscle V ventrally, and bears 10 pairs of somewhat elongate stigmata.

The oesophageal opening is located at the center of the circle formed by muscle VI. The whole alimentary canal forms an S-shaped loop towards the anteroventral side, in the

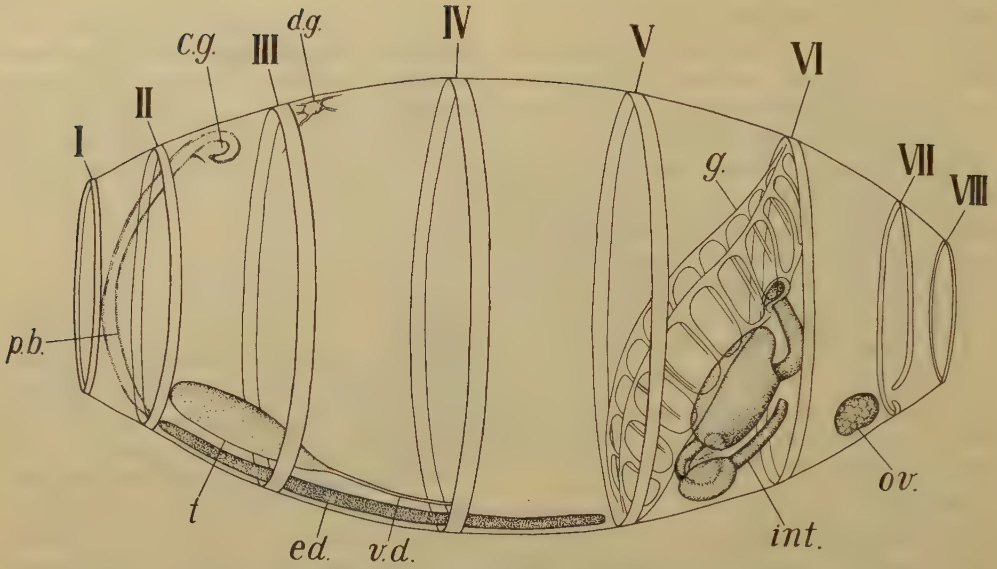

FIG. 2. *Doliolina separata* n. sp., a 1.7 mm. gonozooid from left side.

sagittal plane of the body. The stomach is roughly an elongate ellipse in outline with its cardiac portion prominently protruded. The anus opens near the cardiac end of the stomach. The anterior margin of the intestinal loop (*int.*) extends to near the posterior margin of muscle V. The mid-intestinal region is swollen in some specimens. Usually there is a small group of cells on each side of the intestinal loop, in some cases these groups may consist of two parts, one large and one small.

The ovary (*ov.*) is situated ventrally near the middle of the sixth intermuscular zone. The testis (*t.*) is a club-shaped organ extending from the posterior margin of muscle II to slightly beyond the posterior margin of muscle III. The vas deferens (*v.d.*) opens into the pharynx at the level of muscle IV.

The phorozooid is quite similar to the gonozooid. It lacks gonads and has a ventral protuberance, into which the ends of muscle VII project.

Doliolina separata n. sp. resembles *D. krohni* (Herdman 1888) and *D. indicum* (Neumann 1906) in that it has an obliquely stretched gill septum. The shape of the testis is somewhat reminiscent of *D. intermedium* (Neumann 1906). The ventral interruption of muscle VII and the peculiar arrangement of the gonads, in which the ovary and testis are widely separated from each other, is unique and this latter characteristic is the basis for the specific name here given.

The material upon which this description is in part based is deposited in the U.S. National Museum:

SYNTYPES: U.S.N.M. no. 11373, 2 specimens, Gonozooid, *Doliolina separata* from Shellback station 137.

ALLOTYPES: U.S.N.M. no. 11374, 4 specimens, Phorozooid, *Doliolina separata* from Shellback station 137.

Doliolina intermedia (Neumann 1906)
Fig. 3

Doliolum intermedium Neumann, 1906: 211–212.

Many specimens of *D. intermedium* have been found in the Shellback and the Mid-

(644)

Pacific material. They have an average length of about 10 mm. The test is very soft, of moderate thickness, and is easily stripped from the animal. All eight body muscles are complete. Muscles VII and VIII are very narrow and muscle VI is somewhat narrower than muscles I-V. The third intermuscular zone is the widest and the seventh is the narrowest.

The endostyle (*ed.*) extends anteriorly to beyond the second intermuscular zone and posteriorly to the middle of the fourth zone. The anterior margin of the peripharyngeal band (*p.b.*) approaches the posterior margin of muscle I. The ciliated groove (*c.g.*) is situated in the center of the second intermuscular zone. The dorsal ganglion (*d.g.*) is located in the third intermuscular zone near the posterior margin of muscle III. The gill septum (*g.*) attaches at muscle IV dorsally at the middle, or slightly beyond, the fourth intermuscular zone ventrally. It bears about 50 pairs of elongate stigmata.

The loop of the alimentary canal is situated vertically in the fifth intermuscular zone with the oesophageal opening (*oe. op.*) on the sagittal plane. The stomach is elongate and rectangular in outline with the anterior margin slightly convex. The hind-stomach is very distinct with an extreme constriction between it and the intestine. The anus is located near the cardiac end of the stomach.

The ovary (*ov.*) is situated just in front of muscle VII. The testis (*t.*) projects anteriorly along the left side of the endostyle with its anterior portion often curving dorsally along the posterior side of the peripharyngeal band.

Doliolina undulata Tokioka and Berner 1958
Fig. 4

Doliolina undulata Tokioka and Berner, Pacific Sci. 12(2):135–138.

Several more specimens of *D. undulata* have been found in the material from the Shellback Expedition. In some of these, most frequently small mature specimens, the testis is stretched obliquely between muscles V and VI with

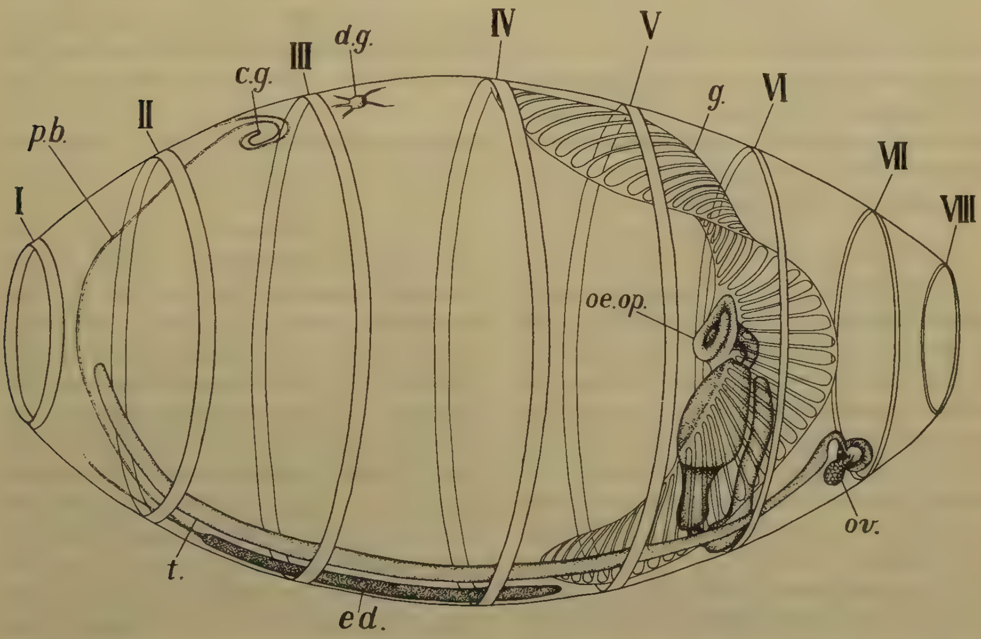

FIG. 3. *Doliolina intermedia* (Neumann) 1906, a 10 mm. gonozooid from left side.

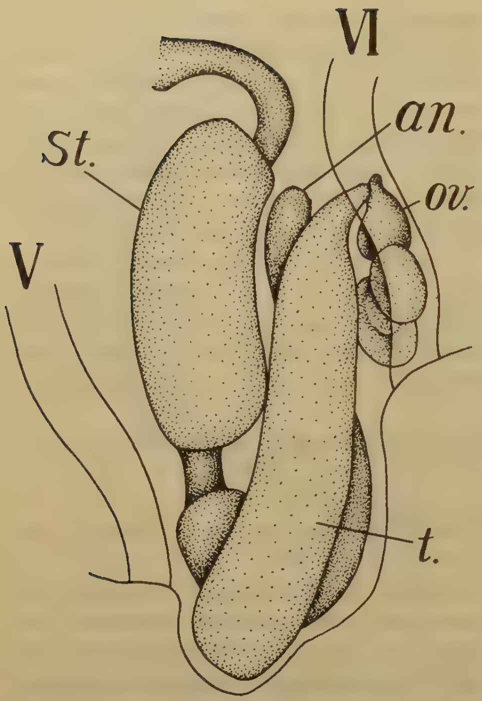

FIG. 4. *Doliolina undulata* Tokioka and Berner 1958, alimentary organs and gonads, from left side.

very little undulation. In these cases the ventral part of the body, just posterior to muscle V, is distended by the testis. The appearance of the testis and its relative position against the intestinal loop are fundamentally the same as in specimens with the undulating testis.

Subdivisions of the genus DOLIOLINA

With the descriptions of *D. undulata* Tokioka and Berner (1958) and here of *D. obscura* and *D. separata*, we find two types of muscle pattern within the genus *Doliolina*. These patterns, one in which all of the muscles form complete loops and one in which the seventh muscle is interrupted ventrally, distinctly divide the genus into two groups. On this basis we have established the following subdivision of the genus:

1) *Doliolina* perfecta: The muscle bands of this group all form complete bands. The following species are included: *indica* (Neumann 1906), *intermedia* (Neumann 1906), *resistible* (Neumann 1913), *mülleri* (Krohn 1852), *krohni* (Herdmann 1888), and *sigmoides* Garstang 1933.

2) *Doliolina* imperfecta: Within this group the seventh muscle band is always interrupted at the mid-ventral line. The species in this group are known only from the eastern Pacific Ocean, and include: *undulata* Tokioka and Berner 1958, *separata* n. sp., and *obscura* n. sp.

The shape and position of the gonad and the arrangement of the gill septum vary considerably within the two groups, and in some cases convergence of these features may be seen. We thus hesitate to treat them as subgenera of *Doliolina* but feel the problem may better be settled by more extensive collections and further critical examination of the respective species.

The discovery of three species of doliolids, in addition to the one previously known (*Dolioletta mirabilis*), in which a body muscle is interrupted gives support to the argument for the abandonment of the ordinal name Cyclomyaria for the doliolids, in favor of the name Doliolida. This change has been generally accepted since Garstang's review (1933).

Doliopsoides horizoni Tokioka and Berner 1958

Figs. 5A, B

Many additional specimens of *D. horizoni* have been found in the material from the Shellback Expedition. In some of these the alimentary organs are better preserved than in any of the previous specimens. Close examination of these organs reveals that the stomach is provided with several fingerlike protuberances. In one especially well-preserved specimen, four pairs of these protuberances were found on the ventral, posterior portion of the cardiac stomach and two pairs on the ventral, posterior portion of the pyloric stomach. The number of protuberances is not constant among the specimens.

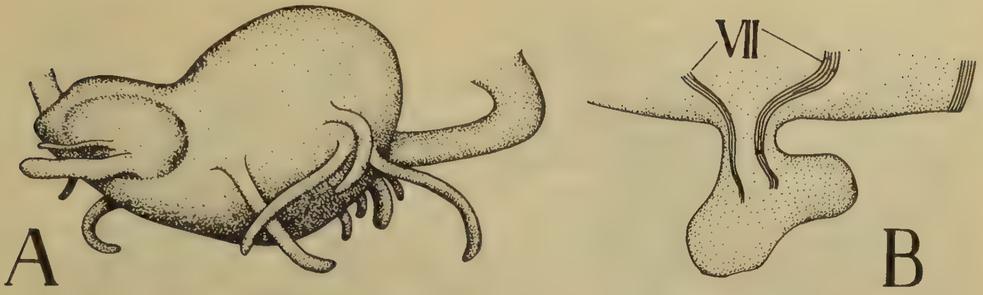

FIG. 5. A, *Doliopsoides horizoni* Tokioka and Berner 1958, stomach showing protuberances. B, *Doliopsoides horizoni*, ventral protuberance of phorozooid.

One individual of the phorozooid generation was found among the specimens. It has a short ventral protuberance into which both ends of muscle VII project.

COMPARISON OF ALIMENTARY REGION OF *Cyclosalpa strongylenteron* AND *C. bakeri*

In the examination of aggregate individuals of *Cyclosalpa strongylenteron* Berner 1955, some distinct asymmetries were found in the arrangement of the alimentary organs and gonads. These features differed somewhat between the dextral and sinistral individuals, although the musculature showed almost complete symmetry. The features of the alimentary organs and the gonads are compared with those of the aggregate form of *C. bakeri* Ritter 1905, whose visceral portion closely resembles that of *C. strongylenteron*.

In *Cyclosalpa strongylenteron* Berner 1955 (Figs. 6A, B, 7) the dextral individuals are those derived from the right side of the stolon when it is placed so that the stolo-individuals are situated dorsal side up, with the posterior end toward the right and with the proximal end of the stolon pointing away from the observer. The sinistral individuals are those derived from the left side of the stolon.

In the dextral individuals the intestinal loop is U-shaped. The anus (*an.*) opens on the left side at a level slightly anterior to the oesophageal opening (*oe. op.*). There is a large elongate blind sac or caecum (*l.c.*) attached to the ventral side of the lower branch of the loop, about one third of the way between the oesophageal opening and the posterior margin of the loop. The tip of the caecum reaches posteriorly nearly to the posterior margin of the gut loop but seldom beyond it. A small sac or protuberance (*r.c.*) is found on the left wall of the alimentary tract just dorsal to the base of the large caecum (Fig. 7). The duct of the circum-intestinal gland (*d.c.g.*) opens into the tip of this small sac, which could be considered merely a swelling of the proximal end of the duct. It is clear, however, that it is actually a projection of the alimentary tract. The swollen portion is stained reddish orange by Rose Bengal, like the alimentary tract, rather than purplish red like the duct. The relative positions of the small and large sacs indicate that they are the right and left caeca respectively.

The testis (*t.*) is about half the length of the left caecum and is situated on the right side of the ventral branch of the intestinal loop near its posterior margin. The vas deferens (*v.d.*) crosses the duct of the circum-intestinal gland on the left side and opens into the atrial cavity just in front of the point where the dorsal visceral muscles (*l.x.* and *r.x.*) from each side unite. These joined muscles project posteriorly into the center of the intestinal loop passing to the right of both the vas deferens and the duct of the circum-intestinal gland. The left visceral muscle (*l.x.'*) runs along the ventral side of the intestinal loop,

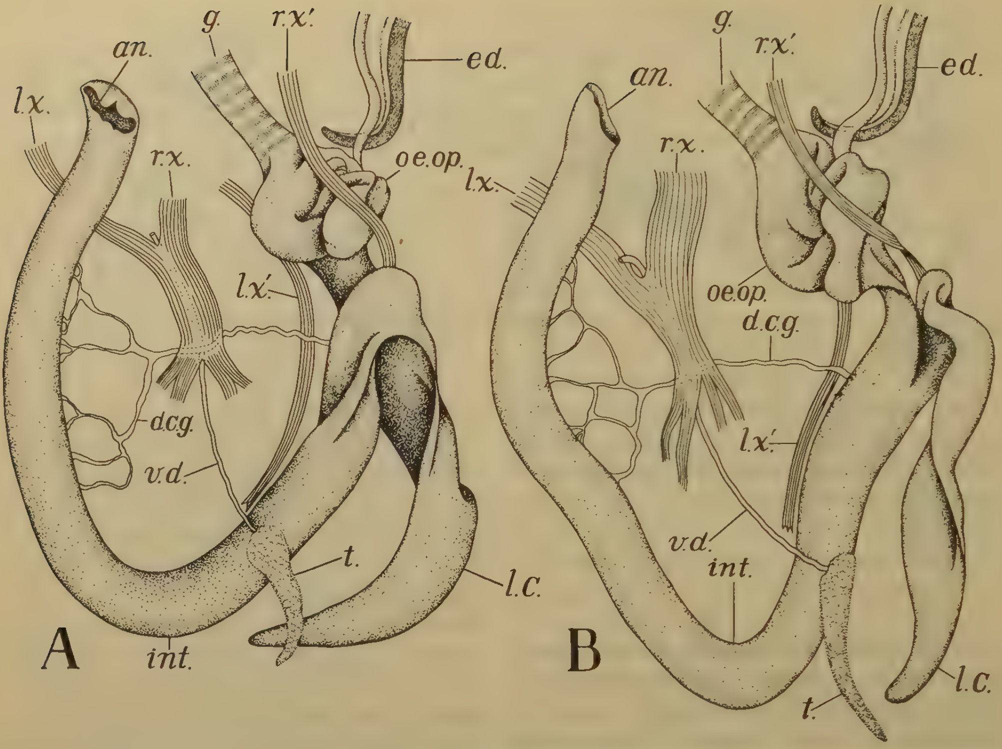

FIG. 6. A, *Cyclosalpa strongylenteron* Berner 1955, visceral region of the aggregate form, sinistral individual, from the right side. B, Same for dextral individual.

Abbreviations: *an.*, anus; *d.c.g.*, duct of the circum-intestinal gland; *ed.*, endostyle; *em.*, embryo; *g.*, gill; *ht.*, heart; *int.*, intestine; *l.c.*, left blind sac; *l.o.*, luminous organ; *l.x.*, left dorsal visceral muscle; *l.x'.*, left ventral visceral muscle; *oe.*, oesophagus; *r.c.*, right blind sac; *r.x.*, right dorsal visceral muscle; *r.x'.*, right ventral visceral muscle; *t.*, testis; *v.d.*, vas deferens.

crosses the duct of the circum-intestinal gland on the left side, and extends to near the base of the testis. The right visceral muscle (*r.x.'*) extends along the left side of the left caecum to a point near its posterobasal portion.

In the sinistral individuals the small right caecum is completely missing. The left caecum turns across the alimentary tract on the right side as shown in Figure 6A. The duct of the circum-intestinal gland opens at the base of the left caecum. Other structures are the same as in the dextral individuals.

The asymmetries found in the relation between the large (left) caecum and the small, or absent, right caecum, the arrangement of the testis, vas deferens, duct of the circum-intestinal gland and the visceral muscles, are all of a primary character. The twist of the left caecum, shown in the sinistral individuals, may be considered to have been brought about by enatiomorphism.

The structure of the intestinal loop of the aggregate form of *Cyclosalpa bakeri* Ritter 1905 (Fig. 8) closely resembles that of the aggregate form of *C. strongylenteron*. It is U-shaped, with the anus (*an.*) opening on the same level as the oesophageal opening (*oe. op.*). The right caecum is absent in both the dextral and the sinistral individuals. In the dextral individuals the left caecum (*l.c.*) is attached ven-

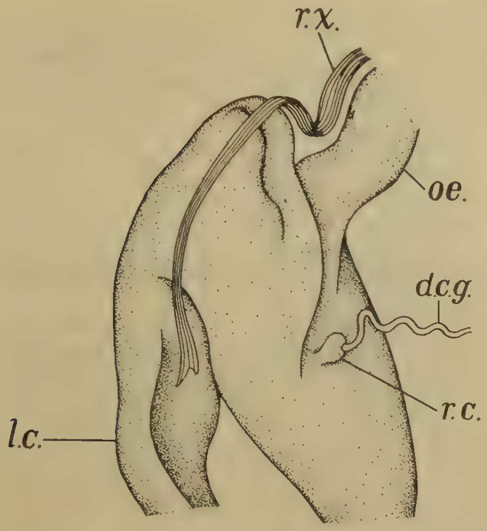

FIG. 7. *Cyclosalpa strongylenteron* Berner 1955, basal portion of left blind sac from left side.

trally about two thirds of the way down the lower branch of the intestinal loop. Its distal end reaches far beyond the posterior margin of the loop. In the sinistral individuals the caecum is twisted counterclockwise around the alimentary tract, as in the case of the sinistral individuals of *C. strongylenteron*. In the dextral individuals the duct of the circum-intestinal gland (*d.c.g.*) opens into the intestine on the left side at the level of the anterio-basal portion of the caecum. In the sinistral individuals it opens into the base of the caecum itself.

The testis (*t.*) is held completely within a posterior protuberance projecting from the posterior portion of the intestinal loop. It is considerably longer than in *C. strongylenteron*. The vas deferens runs across the right side of the intestine, crosses the duct of the circum-intestinal gland on the left side, and opens into the atrial cavity at a position far anterior to the anus.

The right visceral muscle (*r.x.*) runs down the right side of the intestinal loop to its posterior margin. The left visceral muscle (*l.x.*) projects deep into the posterior protuberance with the testis. In the dextral individuals the caecum is superficially placed in the median plane and asymmetry can be found only in the arrangement of the vas deferens and the difference in length of the visceral muscles. Such asymmetries are all of a primary nature.

If the structure of the visceral regions of the aggregate forms of *C. bakeri*, *C. strongylenteron*, and *C. virgula* are compared, we may be able to say to which *C. strongylenteron* is more closely related. On this basis it occupies an intermediate position between *C. virgula*, which has the small right caecum in both the dextral and sinistral individuals, and *C. bakeri*, in which the right caecum is lacking in both individuals. If, however, the musculature is phylogenetically more important than the structure of the visceral portion of the body, the above hypothesis is untenable.

During the examination of *C. bakeri* two

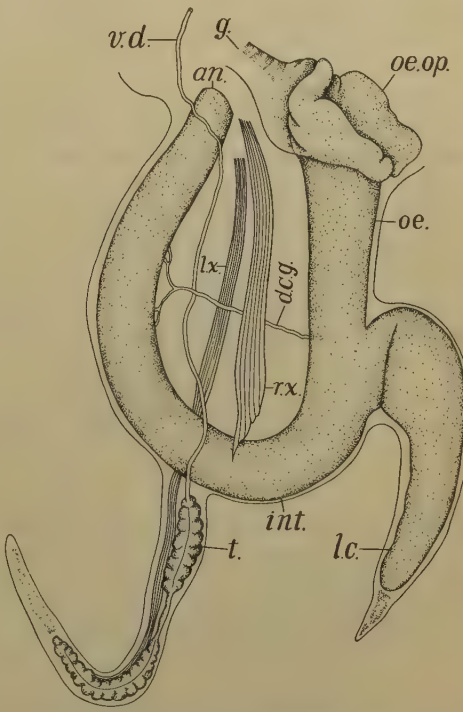

FIG. 8. *Cylosalpa bakeri* Ritter 1905, visceral portion of dextral individual, from right side.

individuals of the aggregate generation were found which appeared to have light organs (Fig. 9). The organs were situated midlaterally, one on each side of the body between muscles II and III. This is the first report of possible light organs in the aggregate generation of *C. bakeri*.

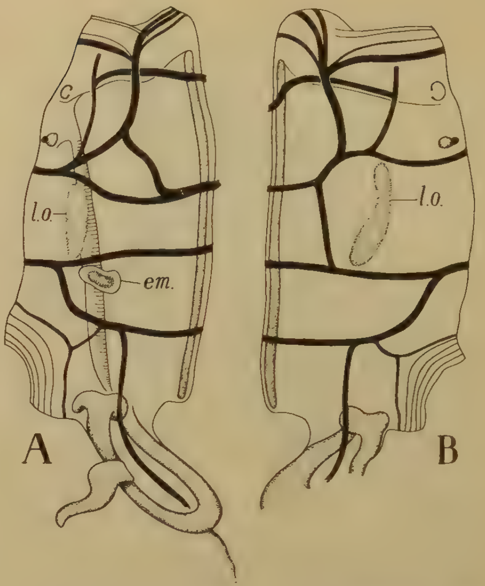

FIG. 9. *Cyclosalpa bakeri*, a 12 mm. aggregate form showing placement of luminous organ. A, from right side; B, from left side.

SUMMARY

Two new species in the genus *Doliolina*, *D. obscura* and *D. separata*, have been described. The genus *Doliolina* has been subdivided into two groups. The first is the *Doliolina* perfecta, in which all the muscle bands form complete loops, the second the *Doliolina* imperfecta, in which the seventh muscle band is interrupted ventrally.

The presence of fingerlike protuberances on the stomach of *Doliopsoides horizoni* have been described. Specimens of *Doliolina undulata* in which the undulations of the testis are much reduced are described. This straightening of the testis appears to be associated with early maturity.

Doliolina intermedium is reported from the central and tropical Pacific Ocean. The specimens differ from those previously described in having a slightly longer testis and in the nearness of the ovary to muscle VII.

The structure of the intestinal region of *C. strongylenteron* and *C. bakeri* are reviewed. On the basis of the structure of this region *C. strongylenteron* is placed in a position intermediate between *C. bakeri* and *C. virgula*.

The presence of what appear to be light organs in the aggregate generation of *C. bakeri* is noted.

REFERENCES

BERNER, L. D. 1955. Two new pelagic tunicates from the eastern Pacific Ocean. *Pacific Sci.* 9(2): 247–253.

GARSTANG, W. 1933. Report on the Tunicata. Part I, Doliolida. *Brit. Antarctic* (*Terra Nova*) *Exped. 1910*, *Brit. Mus. Nat. Hist.*, *Zool. Rpt.* 4 (6): 195–251.

HERDMAN, W. A. 1888. Report upon the Tunicata collected during the voyage of H.M.S. "Challenger," during the years 1873–76. III. Ascidiae Salpiformes, Thaliacea, etc. IN *The Voyage of H.M.S. Challenger, Zoology* 27 (77): 1–163.

KROHN, A. D. 1852. Über die Gattung *Doliolum* und ihre Arten. *Arch. Naturgesch.* 28: 53–65.

NEUMANN, G. 1906. *Doliolum.* IN *Wiss. Ergeb. Deutsch. Tiefsee-Exped.* 12 (2): 93–243.

RITTER, W. E. 1905. The pelagic Tunicata of the San Diego region. *Calif. Univ.*, *Pubs. Zool.* 2: 51–112.

TOKIOKA, T., and L. D. BERNER. 1958. Two new Doliolids from the eastern Pacific Ocean. *Pacific Sci.* 12(2):135–138.

PERSPECTIVES IN MARINE BIOLOGY

A. A. BUZZATI-TRAVERSO
Scripps Institution of Oceanography
University of California
La Jolla, California

This is not an attempt to summarize or synthesize the subject matter of either the papers presented at the symposium on Perspectives in Marine Biology or of the ensuing discussions. All contributions, whether of the official speakers or of other participants who took part in the discussion, are recorded in their entirety in this volume. They stand on their own merits, and any attempt on my part to condense the material contained in them would be utterly superfluous. What I would like to do in the following pages is something different and yet pertinent to the theme of the symposium: to present a digest of the ideas expressed by the participants during the sessions of the "idea groups" that were active during the symposium and the purpose of which was, indeed, to produce definite suggestions for the possibly forthcoming fields of development in marine biology.

The main feature of the meeting in La Jolla was that of having the subject matter of marine biology under the scrutiny of an heterogeneous group of biologists. Many of them had devoted most of their lives to the study of marine organisms and of their environment, but almost equal in number were biologists who have been primarily interested in basic problems of living matter, irrespective of whether they could be attacked by using organisms living on land or in the sea. What follows will probably reveal the inevitable bias deriving from the fact that I belong to the latter group. During the last few years, however, I have made a definite effort to become personally acquainted with the viewpoints of professional marine biologists of various countries. This experience will enable me, I hope, to give a not too one-sided picture of current perspectives in marine biology.

What is marine biology? This question was raised at the beginning of our symposium and remained throughout the meetings as the basic unofficial theme of many polite arguments. On the one hand, some said: "There is no real separation between the field of marine biology and general biology. The problems of the two are identical. The fascinating problems of general biology are the ones which are also fascinating in marine biology." On the other hand, others maintained that, though justifiable at the applied level, marine biology has no right of citizenship among the

Contributions from the Scripps Institution of Oceanography, New Series, No. 1033
Reproduced by Permission

branches of basic biological research: "The rapid advances that have been made in biology in recent years were attained not with reference to any particular habitat but to problems which became more sharply defined than they had ever been before. Is there then such a thing as terrestrial biology as contrasted to marine biology?"

It seems to me that the contrast between the opposite viewpoints is only formal, the debaters perhaps used the same words to indicate different thoughts, but I am sure that they were equally convinced that, without assuming there are basic problems of biology peculiar to the marine environment, several fundamental biological questions can be studied with the help of marine forms. There certainly is historical justification for the use of the term "marine biology." If our ancestors had not abandoned the sea and the human race were an ocean dweller, by this time there would be laboratories for "terrestrial biology" just below the lower limit of the tide and someone would be arguing about the validity of this term. The establishment of marine biological laboratories throughout the world has also certainly contributed to the diffusion of the term under discussion. Perhaps the unspoken difficulty lies in the fact that the term marine biology implies an inherent and clearly found difference at the biological level between organisms living in the sea and those living on land, and no such differences have been demonstrated. Until this happens, if it will, our term is wrong in that it anticipates a conclusion before it has been reached. One can speak of marine animals or marine plants as contrasted to animals and plants living on land, since the qualification refers to definite living objects; but the qualification is probably not warranted when used in reference to a field of human endeavor.

If we then take marine biology to mean the biological study of those organisms which live in the sea, we can accept this widely used shorthand designation and see that this study can be approached at two different levels. In the first place, one may wish to discover what the marine environment can offer to reach a better understanding of general biological problems. In the second place, one may wish to know what biological studies can be developed in order to understand the marine environment. The two approaches are not mutually exclusive, but neither are they necessarily complementary. For instance, whereas the study of plankton navigation may reveal something fundamental about the ability of living matter to perceive the plane of polarization of light, the understanding of prey-predator relationships in marine fishes may not add anything new to the theory of natural selection.

The latter approach emphasizes the marine part of the study: the former emphasizes the biological part. Our notion can thus be schematized as follows:

MARINE ORGANISMS
↗ ↖
Biological study Oceanographic study

Several ideas and several suggestive possibilities of development in the study of marine organisms have been brought forward, and I have attempted to classify them according to this scheme as follows.

Biological

1. Biochemical techniques and approaches should be applied wherever possible. Research on the comparative biochemistry of cold-blooded animals should be effectively encouraged and developed.

2. Studies on the speciation of marine organisms should be promoted.

3. Interesting aspects of comparative physiology as related to evolution could be analyzed by transplanting individuals belonging to a littoral species from one extreme of its distribution range to the other. In this way one may discover the limits of acclimation and how much of the phenotypic, morphological, and physiological differences are genotypic or environmental in origin.

4. Studies on the cytogenetics of marine animals should be encouraged. It would be particularly interesting to relate such data to life histories and ecological habits.

5. The study of the paleontology of marine organisms appears especially promising because it may furnish one particular parameter that is almost entirely unknown, namely the rate at which evolution is proceeding.

6. Systematics should be included in all marine biological programs. It is the basis on which the rest of biology builds.

7. It is now possible to establish a connection between the biogeography of the sea and the physiology of marine organisms. Such studies should be furthered by comparing biological cycles, metabolic and biochemical patterns, and genetic differences of the same species in different districts of their distribution.

8. The study of plankton populations may yield important data for the general theory of population dynamics. Laboratory experiments on such problems are likely to be very enlightening.

9. The problem of aging can be best studied on some marine animals. Sea anemones can be kept alive for eighty years and, perhaps, indefinitely. The cytological and physiological study of this phenomenon, accompanied by tissue culture, might reveal very important data related to this issue.

10. The study of the spectacular migrations of eels, salmon, and other fishes and of their causative agents ought to be studied more intensely than is done at present.

11. Among marine organisms, phenomena of phototaxis, phototropism, and cyclic rhythms are especially frequent. For this reason they appear to be very favorable material for investigating the molecular basis of these phenomena.

12. The succession of plant and animal populations in the ocean and the fact that they are immersed in a fluid medium renders the ocean especially suitable for analyzing the significance of antibiosis and symbiosis under natural conditions.

13. A very important problem is the study of micronutrients in the sea; the current condition of marine biology in this respect can be compared with that of physiology in 1900 before the discovery and elucidation of hormones and vitamins.

Oceanographic

1. What are the underlying physical and chemical differences between similar bodies of water which, by the use of present-day techniques, can be distinguished only by the different biological populations they support?

2. Ecological studies should be primarily quantitative. There should be a quantitative treatment of the ocean as a household. Most quantitative studies have not prepared balance sheets.

3. The mathematical approach should be emphasized in the study of populations of marine organisms.

4. There is a need in marine ecology for rapid assay methods, comparable to those developed for plant ecology.

(653)

5. Community studies in the field are not sufficient. It is necessary to develop investigations on experimental synecology.

6. There is an urgent need for gross information on the distribution and succession of populations. It should be possible to develop new tools for collecting such data.

7. Much greater emphasis than at present should be placed on the study of nannoplankton. Special devices should be developed for collecting and studying such minute organisms.

8. More effort should be placed on the laboratory study of plankton. Attempts to breed planktonic forms under laboratory conditions should be intensified in order to learn more about their nutritional requirements, physiology, behavior, and variation.

9. A coördinated quantitative mapping of level-bottom communities in relation to their temperature adaptation should be encouraged. Instead of attempting to have similar surveys carried out at different places with standardized equipment, well-qualified and well-equipped mobile teams, which would make surveys wherever necessary, should be used.

10. There is a great need for studies on diseases of marine organisms. They may well be responsible for the rise and fall of large populations in the ocean.

11. Studies on the physiology of coral reefs should be promoted.

12. There is a need for a phylogenetic, ecological, and physiological approach to the interrelations between fresh-water, marine, and brackish-water organisms.

13. Instead of fixing the collected organisms by the usual method, attempts should be made to freeze living animals and plants in glycerol and to study them in laboratory upon thawing. Using liquid air, such material might be preserved indefinitely.

14. Attempts should be made to collect some of the gigantic bathypelagic animals.

15. How could we utilize the potential productivity of the deep waters?

Clearly, of the thirteen suggested themes that stress the biological approach to the investigation of marine organisms, the first eight pertain to the great chapter of evolutionary studies. The recent bloom of work on land animals and plants in this area has been prompted by the acquisition of fundamental knowledge on the mechanism of inheritance. The problems concerning the transformation of organisms in the course of the earth's history that had remained quiescent for over thirty years (because it did not appear possible to add anything substantial to the picture drawn by the classical comparative morphologists and by the paleontologists) became the object of renewed interest and effort on the part of population geneticists. During the last twenty years a large quantity of evolutionary studies from the point of view of genetics has appeared and has undoubtedly contributed to an increasingly satisfactory interpretation of the great events of phylogenesis. Even the process of evolutionary change itself has been caught in the act in nature, and has been reproduced and analyzed under laboratory conditions. Any of the recent symposium volumes on evolution shows the great strides achieved in recent times, but also illustrates the fact that almost nothing has been done at this level with regard to marine organisms. Is this owing to the fact that animals and plants living in the ocean do not lend themselves to such type of investigations? I believe that this is not the case. In fact, in recent years some very interesting results have been obtained from the study of the population genetics of a few marine animals.

The genetics of marine organisms is in its infancy; more knowledge in this area is required if we wish to gain an understanding of evolutionary processes in the ocean. Let us consider the cytological aspect, in the first place in terms of chromosome morphology, taxonomy, and mechanics. As it has been shown by C. D. Darlington in his book The Evolution of Genetic Systems, the interrelationships between mating systems, chromosome numbers, and chiasma frequencies have played a great role in the evolution of plants. The available evidence on animals is much more limited since relatively very little is known about chromosome numbers and meiotic behavior in the numerous animal phyla that are only represented in the sea. For example, in the book by S. Makino (1951), Chromosome Numbers in Animals, we find data on chromosome numbers only for the following number of species: Porifera, 7; Coelenterata, 23; Nemertini, 7; Annelida, 72; Mollusca, 135; Molluscoidea, 7; Echinodermata, 29; Crustacea, 156; for a total of 426, some of which are terrestrial forms, as contrasted to 1,820 insects and 563 vertebrates, of which only 95 are fishes. Almost no knowledge is available on chiasma frequencies in marine forms. It would be of remarkable interest to collect information on the genetic systems of marine forms with respect to their life cycles and their being sessile or capable of movement. Such data would, at the same time, provide us with very precious information about the significance of chromosome numbers and forms in many phyla almost completely neglected from this viewpoint. That this area of study is promising and can be developed now is shown also by some recent investigations, such as those by Hans Staiger, who found that variability in chromosome numbers of some mollusks is correlated with their morphology and ecology.

The Mendelian genetics of marine organisms is also very little known. With the exception of few data on some crustaceans, such as Tisbe reticulata (Bocquet, 1951) and Sphaeroma serratum (Bocquet, Levi, and Teissier, 1951) and on the serpulid Pomatoceros triqueter (Føyn and Gjøen, 1954), the field is practically virgin. These studies suggest that more effort in this direction is likely to be rewarding, since one finds in the literature numerous examples of variability, probably of genetic nature. Thus, intraspecific variability has been described, for example, in tunicates (Ciona), in Anthozoa (Metridium), in Scyphozoa (Aurelia), in sponges (Triaxonida, Tetraxonida), in echinoderms (Astropecton, Strongylocentrotus, etc.), in cephalopods (Sepia), in other mollusks (oysters, Patella, Acmaea, Littorina), in crustaceans (Diastylis, Limnoria, Tigriopus, etc.), in fishes (herring, hake, Zoarces, perch, etc.). Another promising field for investigations is the study of endemic forms. According to Sven Ekman, the number of endemic forms is much larger in the North Pacific than in other parts of the oceans; it seems worthwhile to check the validity of this statement and, if found correct, to study which factors might be responsible for this phenomenon.

The genetic basis of morphisms has been widely analyzed in several animal species in recent years, and the phenomenon appears as very significant for microevolution. Many examples of polymorphic species have been described for marine animals, especially in shore forms (Huxley, 1955). The modern techniques of skin-diving and of underwater photography could be very profitably used for the collection of data and these could be later analyzed at the genetic level by means of experiments in the laboratory. The previously mentioned studies on Tisbe and Sphaeroma are good examples of how profitable such sort of investigation could be.

Finally, the genetic study of speciation appears to be very promising. We have a large number of marine invertebrates whose sessile nature makes it possible that in their speciation patterns more similar to that of terrestrial plants rather than animals have been followed. It is in fact conceivable that one may find in such groups ecogenotypes comparable to those described by Turesson, J. Clausen, and others for flowering plants. If this were the case, species might be distinguished from ecotypes by means of cytological study as well as by experimental breeding. On the other hand, there are on record several examples of north-south disjunctions among marine animals, and it would be very instructive to analyze the degree of differentiation reached by various polar forms, and to compare them with parallel cases of bipolarity in terrestrial plants. Furthermore, the recent work by Ernst Mayr (1954) on echinoderms indicates that speciation of littoral forms follows the pattern already known for terrestrial animals. Here and there geographic isolation appears as the determining factor in bringing about differentiation at the specific level. But this very mechanism cannot be at work in planktonic forms, which must have originated in absence of geographical barriers. As soon as planktonic animals will become available to the geneticist, he will have to attack experimentally this puzzling problem.

One more type of promising research is that of attempting a reexamination of the taxonomic position of species within genera, by means of collecting specimens over their distribution area, breeding them under laboratory conditions, and crossing strains of different geographic origin. Studies of this type, which are under way in our laboratory on a large collection of strains of copepods belonging to the genus _Tigriopus_, originating from all over the world, are already giving interesting results. It can be hoped that within a relatively short time it will be possible to revise this genus using genetic data as well as the more classic morphological and distributional ones.

Evolutionary problems in marine invertebrates could be approached also at the level of experimental population studies. At the present stage of our understanding of how natural selection operates on Mendelian populations there is a need for renewed emphasis on the kind of experiments and quantitative analysis opened by the classic work of Raymond Pearl. In principle, aquatic organisms appear better suited for such type of research than are insects like _Drosophila_ or _Tribolium_, since a more thorough control of the environmental variables can be achieved in a fluid medium. One of the important open questions in this area is that of the measurement of Darwinian fitness; it has been suggested that one possible approach to the assessment of this parameter is the measure of the metabolic efficiency of an organism, i.e., its ability to transform the available sources of energy into body weight (Buzzati-Traverso, 1955). This ability is undoubtedly partly determined by inheritance. Therefore one would accept that in a genetically heterogeneous population an increasing concentration of genes determining higher metabolic efficiency takes place under the action of natural selection. Since body weight and metabolic rates are also related to body size, one could attempt to analyze at the experimental level what causes the well-known clines in the dimensions of several species living at different latitudes. Moreover, this approach might contribute to an understanding of the trends toward larger size documented in several animal phyla. Under bacteria-free conditions a simple system of unicellular alga-small grazing crustacean could provide an ideal setup for such an experiment.

Another important problem of evolution that could be best studied using marine animals is that of the speed of evolutionary change. Only very indirect evidence is available at present on actual rates of evolution in various groups of organisms. This is probably due to the fact that organisms that have been most studied from the genetic viewpoint are not widely represented in the recent fossil record. If one could succeed in breeding animals whose immediate ancestors are well represented in the Pleistocene and in the Tertiary, the road would be open toward filling this gap in our current knowledge. Sea urchins and shore mollusks appear particularly promising in this respect. And by means of a similar experimental approach one might also collect some evidence bearing on the apparent slower pace of evolution in the marine environment, as contrasted to the terrestrial one. Furthermore, since recent experimental evidence indicates that mutation rates are somewhat influenced by environmental conditions, it certainly would be very interesting to test the lability of genetic systems of organisms living in a very stable environment such as the deep sea; bacteria may provide a suitable material for investigation of this sort.

We come now to the remaining five suggested themes that stress the biological approach to the study of marine organisms. They all are physiological in character; the last two appear to me to be of major significance. After the pioneering work of C. E. Lucas (1947), who stressed the significance of external metabolites for the distribution of planktonic plants and animals, an ever-increasing amount of evidence has been collected indicating that (1) extremely diluted organic and inorganic compounds are necessary in sea water for the survival and reproduction of ocean dwellers, (2) substances having antibiotic activity might be responsible for the survival of very delicate forms during the most critical periods of their life cycles, and (3) some external nutrilites are indeed present in samples of water. Since such essential substances have concentrations of only a few micrograms per liter, their detection, identification, and measurement encounter very great technical difficulties. As it is shown by some preliminary data collected in our laboratory by W. L. Belser, biochemical mutants of bacteria having a wide spectrum of nutritional requirements provide a suitable bioassay for such an investigation. Thus, mutants of Serratia marinorubrum that require biotin, uracil, and purine have allowed the identification of minute quantities of these organic compounds in samples taken from the Pacific off the shore of Costa Rica. Continuing in this direction it may become possible to explain the yet mysterious successions of phyto- and zoöplankton known to every marine biologist, and to make sense in chemical terms of the problems of ecology. It may perhaps turn out that the main difference between marine and terrestrial living forms lies in the requirement by the former of metabolites. The conquest of land on the part of animal and plants might thus have involved not only major changes in the mechanism of respiration but also in that of food uptake and metabolism.

Such investigations appear very significant also in that they represent a most stimulating link between the biological and the oceanographic set of problems in marine biology. If this type of chemical ecology will be developed, many difficulties of biological-oceanographic studies will have been overcome. In this area the greatest unknown quantities are those pertaining to the distribution of the biomass according to size and range of organisms. H. Kubitschek pointed out in the course of our discussions that "only estimates with unknown errors exist for this quantity, and that there is an urgent need for a rough measurement." He gave also a number of suggestions on how to tackle this problem. "Perhaps graded sieves could be used from plankton on down, grading by factors of ten, down to the millipore filter region. Perhaps it might be possible to develop automatic recording of fish, large and small, or of single plankton elements with single frame exposures such as is done with cosmic rays apparatus. Perhaps light intensity could be monitored by simple and inexpensive CdS cells into a go-no-go apparatus so that pictures would be taken only when intensity was appropriate; a focusing device would be needed to limit exposures to a fairly sharply defined range; the appearance of a fish at the focusing distance would trigger the camera. Perhaps an estimate of plankton distribution and concentration could be made by automatic camera anchored at a spot in the ocean, photographing the plankton in its neighborhood once or several times a day. A ship could pick up the exposed film, say, every six months. Spring mechanisms will easily allow 30 feet of film, i.e., on 16 mm. film about 1200 photographs. A sunlight-recharged battery could operate a simple pendulum actuator such as is used in shop-window displays, or a photocell could watch the hour hand of a self-winding watch. In this way one could partly overcome the current survey effort, both in distance and time, involved in the study of plankton distribution."

There undoubtedly is a need for a fresh and original approach in the development of new tools and gears for the collection and study of plankton and benthos at their various size ranges. Seven out of the fifteen suggested areas of study from the oceanographic viewpoint do indeed stress such a need.

In connection with such quantitative evaluation of the amount and type of living matter in the ocean, more theoretical and experimental studies on the dynamics of populations become now necessary. Several conclusions of the mathematical analysis of fishery problems should now be checked by means of laboratory experiments on artificial populations.

Furthermore, a very serious attempt should be made to obtain accurate physiological measurements aboard oceanographic vessels.

It seems to me that at the present stage of our knowledge we should concentrate our efforts on living marine organisms rather than on preserved ones. In a few words, let us have less descriptive and more experimental marine biology.

Both at the biological and at the oceanographic level there is no dearth of problems waiting to be solved, in the study of marine organisms. Let us only hope that, a few years from now, some of the topics we have outlined as perspectives may be described by somebody else or by ourselves as achievements in marine biology.

REFERENCES

Buzzati-Traverso, A. A.
1955. Evolutionary changes in components of fitness and other polygenic traits in Drosophila melanogaster populations. Heredity. 9:153-186.

Bocquet, C.
1951. Recherches sur Tisbe (= Idyaea) reticulata. Arch. de Zool. Exper. et Gén. 87:335-416.

Bocquet, C., C. Levi, and G. Teissier
1951. Recherches sur le polychromatisme de Sphaeroma serratum. Arch. de Zool. Exper. et Gén. 87:245-298.

Darlington, C. D.
1939. The evolution of genetic systems. (Cambridge Biological Studies.) Cambridge, Macmillan, 149 pp.

Føyn, B., and I. Gjøen
1954. Studies on the serpulid Pomatoceros triqueter L. II. The colour pattern of the branchial crown and its inheritance. Nytt Magasin for Zoologi. 2:(85-90).

Huxley, J.
1955. Morphism and evolution. Heredity. 9:1-52.

Lucas, C. E.
1947. The ecological effects of external metabolites. Biol. Rev. 22:270-295.

Makino, S.
1951. Chromosome numbers in animals. (American ed.) Ames, Iowa State College Press, 290 pp.

Mayr, E.
1954. Geographic speciation in tropical echinoids. Evol. 8:1-18.

GENETICS AND MARINE ALGAE

RALPH A. LEWIN
Scripps Institution of Oceanography
University of California
La Jolla, California

All photosynthetic plants that are not land plants (i.e., bryophytes or tracheophytes) are customarily lumped together in a heterogeneous assemblage of forms called "algae." But green algae, for instance, are physiologically, and probably phylogenetically, more closely related to land plants than they are to red or brown algae. Personally, I prefer to associate all green plants, ranging in level of organization from algae to mosses and vascular plants, into a comprehensive phylum, the Chlorophyta. Since virtually all studies in plant cytology and genetics have been confined to fungi or the Chlorophyta, it is reasonable to expect that some special problems and some unexpected novelties may emerge from a study of other phyla.

We have neglected these in the past, for several reasons. We are terrestrial animals, feeding ourselves and pasturing our flocks almost exclusively on members of the Chlorophyta. Fresh-water plankton and the soil microflora make but indirect impact on our lives. It is only along the seashores that we become aware of the variety and bulk of Rhodophyta and Phaeophyta, red and brown algae largely confined to coastal marine habitats. And few biologists have the ready access or the hardy disposition needed for year-round study of such plants. Much of our present knowledge of seaweed biology has thus a vacational flavor, deriving from short-term studies made during summer months. Genetics needs generations of experimental material grown under controlled conditions if it is to yield fruitful results, and it does not lend itself to dilettantism.

Furthermore, before we can breed plants, we must know how to grow them. But the marine environment is very different from our own, and our knowledge of the physiology of red or brown algae is woefully small when compared with that of the green plants. We have all grown at least one crop or blossom in our back gardens, with some idea of its requirements for soil drainage or fertilizer, light or shade; yet very few multicellular marine algae have been raised to maturity by anyone. In most of the attempts made in the past, temperature control was inadequate, illumination or CO_2 was insufficient, the requirements for essential mineral or organic nutrilites were poorly understood, weeds—usual-

Contributions from the Scripps Institution of Oceanography, New Series. No. 1034
Reproduced by Permission

ly diatoms—took over, growth ceased, and necrosis set in. These are not favorable circumstances for genetic studies.

Geneticists, who lean heavily on cytology, have special problems to contend with among the algae. Cytological studies of seaweeds have been scant and often unrewarding, perhaps largely because our routine techniques have been developed for the cells and tissues of land plants. The thalli of many red and brown algae have bulky intercellular matrices of acidic polysaccharides, which tend to "gum up" our standard fixation and staining methods.

These obstacles could undoubtedly be overcome, most of them by the use of knowledge already at hand, the rest by further experiment. But can we reasonably expect from studies of marine algal genetics any information that could not be obtained in other ways? I think so.

There is, first, the obvious impact of genetics on our understanding of algal taxonomy and life cycles. The specific limits in many genera are unclear, sometimes devolving on a single particular character, sometimes on a singularly particular taxonomist, and one wonders about the validity of species so defined. Many familiar genera of green algae (e.g., Cladophora and Caulerpa), browns (e.g., Ectocarpus and Fucus), and reds (e.g., Gigartina and Polysiphonia) contain difficult groups of this kind, species complexes that must ultimately yield to the attacks of modern experimental taxonomy. A few Fucus hybrids have already been raised to maturity (Parriaud, 1954), but their fertility has not been established. As we learn more about the genes controlling lobing or branching, hair formation or host range, we may expect the names of many so-called species of seaweed to be submerged in synonymy. When we extend our studies to genes controlling physiological factors, such as the limits of tolerance to desiccation, insolation, or osmotic pressures, we shall undoubtedly find that there are ecovars of marine algae, such as the dwarf salt-marsh fucoids, just as genetically determined as they are in angiosperms. And, if we are to take the term "genetics" in its broader sense, we may anticipate the disappearance even of genera, when different forms are found to constitute phases of the same life cycle. A number of examples of this sort have emerged already: Aglaozonia and Cutleria, Trailliella and Bonnemaisonia, Conchocelis and Porphyra, etc.

Incidentally, why do we so often find the diploid stages of such plants in regions, often at the northern limits of their range, where the haploid seems to be absent? Aglaozonia in Scotland, and Trailliella in the Baltic (if, in fact, T. intricata is diploid), are but two examples of this phenomenon. Are all these cases attributable to an absence of meiosis in the sporangia where we would normally expect it to occur? If there is no meiosis in the gametangia of the fucoid Halidrys siliquosa, as Elliot and Moss (1953) indicate, are the eggs invariably parthenogenetic? Is apomixis also the case in Gigartina stellata, in which tetrasporophytes are unknown? These are some of the questions for which the formal phycologist would like genetic answers.

Special problems of evolution, too, may arise when we consider marine algae. Sublittoral plants occupy an environment in which water supply is constant and temperatures range over only a few degrees, in contrast with land habitats. How might these differences be expected to affect the mechanisms of evolutionary change, the rates of mutation and recombination? We should also remember that marine algae do not carpet the ocean floor, but merely occupy favorable niches along its shallow margins. How would the processes of speciation and gene spread operate in organisms whose distribution is almost linear, extending in a winding interrupted strip thousands of kilometers in length, yet only a few meters wide? We know so little about the viability and range of dispersal of algal gametes and spores that we can barely speculate on these matters.

These are possible contributions of genetics to classical marine phycology. But what is more interesting, to me, is the reverse of the coin —what can marine algae offer to genetics? What plants suitable for genetic studies could we fish out of the sea, and what special advantages might they offer? Here abound fascinating possibilities, as yet almost untouched, for many seaweeds have genetic features that are not duplicated on land. As an example, in most Florideae there are four distinct kinds of plants in the life cycle: haploid males, haploid females, "parasitic" diploid carposporophytes, and diploid tetrasporophytes. In the great majority, the gametophytic haploid and tetraspore-bearing diploid thalli are vegetatively similar. The advantages of such a system to the geneticist are obvious. In the haploid we could directly observe the effects of recessive genes, and comparisons could be made with their manifestations in the homozygous diploids and in the heterozygotes. This might be excellent material for studies on the phenomena of dominance. Moreover, many genetic and morphogenetic problems arise when we consider thallus differentiation between the two dissimilar diplophases. And when we recall that as a rule the fertilized egg nucleus does not remain within its own cytoplasm but migrates into and through neighboring units to the auxiliary cell, we see that unusual opportunities are afforded for studies of maternal or cytoplasmic inheritance.

If we had suitable species to work with, then by using the methodology of biochemical genetics we might be able to tackle complex problems in physiology, too. Could we obtain color mutants, for example, by the use of mutagens on a red alga? What might they tell us about normal processes of phycobilin synthesis? How would they behave photosynthetically?

The problem of the recalcitrant zygospore would not arise in genetic studies of a marine alga. Terrestrial and fresh-water Chlorophyta are frequently confronted with drought, and many have developed resistant stages to withstand such periods of adversity. Most fresh-water green algae form thick-walled zygospores capable of—indeed, often obligately requiring—a prolonged resting period before undergoing meiosis and germinating. Many studies of algae in laboratory culture have had to be abandoned at this stage, since no means were known for inducing rapid maturation or regular germination of such spores. But the eternal oceans do not dry up, and the zygotes of marine algae do not form thick-walled spores. Instead, they germinate directly, usually giving rise to a diploid thallus, and meiosis is delayed until the production of sporangia. In this way, after one act of zygosis there follow many separate meioses, as in angiosperms.

Tetrad analysis, too, could be carried out in many marine algae. Among the Phaeophyta, tetrasporangia are produced only in the Dictyotales, where sex segregation was experimentally demonstrated, in Dictyota dichotoma, by Schreiber (1935). In the Rhodophyta, however, tetrasporangia are the rule, being borne on the free-living diploid plants in most Florideae, and on the ends of gonimoblast filaments in a few Nemalionales such as Liagora tetrasporifera. Since we may wish to separate the spores mechanically, it is of interest to compare the sizes of some algal and fungal meiosporangia (see fig. 1). In many red algae there is the additional possibility of locating the genes in relation to their centromeres by analysis of ordered tetrads. In some, e.g., Antithamnion cruciatum, the tetrasporangia are elongate and divide in cruciate fashion, first transversely, then longitudinally: in others they are zonate, the spores being arranged in linear order. Unless the spindles of the second meiotic division overlap, pairs of sister nuclei would be expected to occupy neighboring spores in the row. The zonate tetrasporangia of the European species, Cruoria pellita, are as much as 250μ long; but I suspect that the culture of this encrusting alga might present special difficulties.

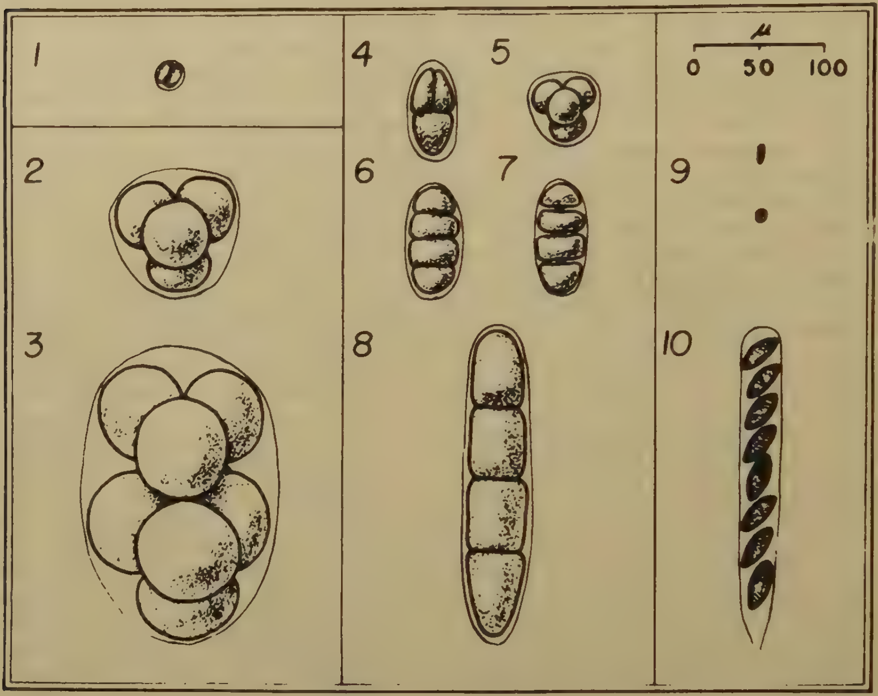

Fig. 1. Some algal and fungal meiosporangia, drawn to same scale. 1. Chlorophyta: Chlamydomonas zygospore germinating; 2. Phaeophyta: Dictyota tetrasporangium; 3. Phaeophyta: Fucus oögonium; 4. Rhodophyta: Antithamnion tetrasporangium; 5. Rhodophyta: Callithamnion tetrasporangium; 6. Rhodophyta: Agardhiella tetrasporangium; 7. Rhodophyta: Lithophyllum tetrasporangium; 8. Rhodophyta: Cruoria tetrasporangium; 9. Ascomycetales: Saccharomyces asci; 10. Ascomycetales: Neurospora ascus.

Since cultural difficulties will undoubtedly arise, the selection of suitable marine species for genetic studies should be made judiciously. We might bear in mind that the recent rapid progress in genetics has resulted largely from studies of organisms like Drosophila, Mus, and Crepis—pests or weeds that flourish around garbage dumps. To weight the balance in our favor, we should choose the algal equivalents of such forms—tolerant species without finicking dispositions, capable of withstanding a wide range of environmental conditions, euryhaline, eurythermal, and physiologically phlegmatic. We should pick them from among the algae that flourish in tide pools, subjected to rapid changes of pH, temperature, salinity, insolation, and contamination. We should look for them among the weeds that infest our marine aquaria, encrusting the glass or clogging the circulating system. Since we are impatient beings, we should select forms that invade and flourish in newly opened habitats and depend for their success on their capacities for initial and rapid colonization, rather than tough stalwarts that may owe their continued existence to ecological tenacity and dogged perseverance. Since we like to keep our laboratories at somewhat higher temperatures than those of the boreal oceans, we might also seek experimental species in the still and shallow waters of tropic seas. For preference, we should select forms that can be readily propagated vegetatively as well as sexually, so that we could have clonal material to work with. And, to conform with the dimensions of ordinary laboratory glassware, our selected algae should be ones of diminutive stature, capable of growth to maturity in tubes or small flasks. If they can tolerate the conditions at an air/agar interface, so much the better.

Now, what marine algae have presented themselves as potential candidates for the role of a photosynthetic Neurospora? Among the Chlorophyta, Ulva and Enteromorpha come at once to mind. They have, as a rule, alternation of isomorphic generations, and several species are bisexual. They are some of the first weeds to invade newly exposed surfaces along the shores, both on bared rocks and in pools, where they appear capable of withstanding remarkably high temperatures. Species of Enteromorpha are among the most euryhaline of littoral and estuarine algae. They mature fairly rapidly, often in a matter of weeks, and produce abundant gametes or zoöspores. The latter can be streaked out and will germinate on agar media, so the isolation of pure cultures—not only clonal but bacteria-free—presents few problems. Cladophora species,

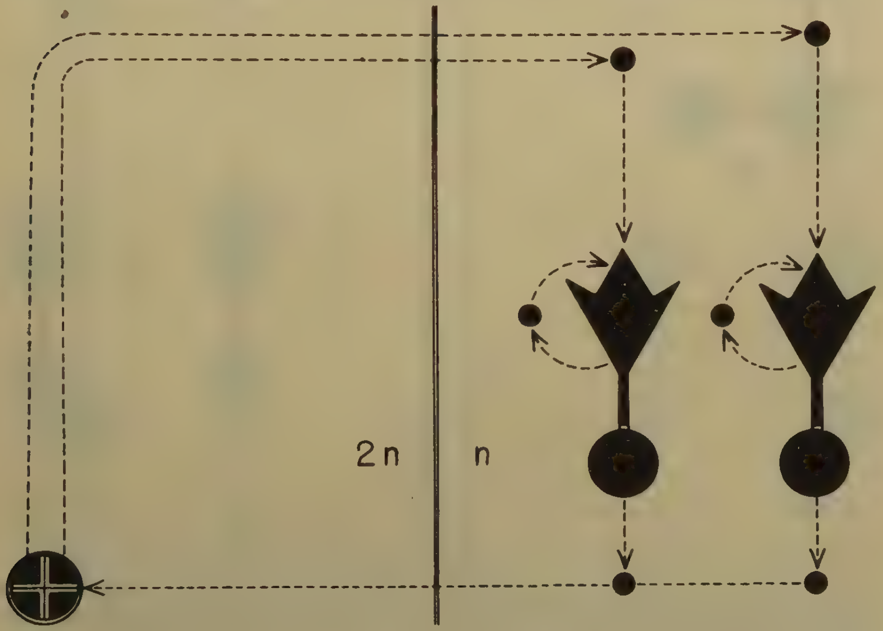

Fig. 2. Life cycle, haploid, except for the zygote, in which meiosis occurs. Typical of fresh-water green algae (e.g., Ulothrix).

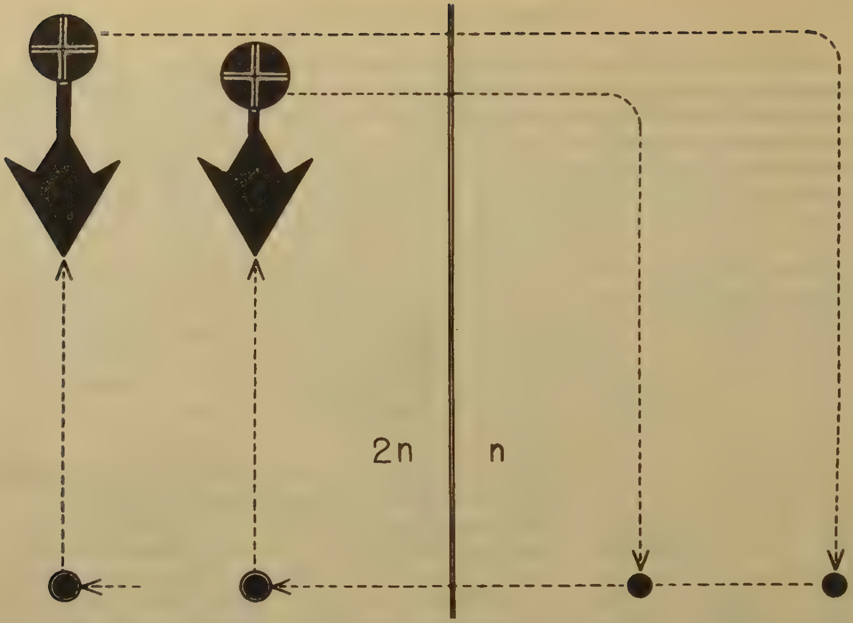

Fig. 3. Life cycle, diploid, except for the gametes. Typical of most animals, some brown algae (e.g., Fucus) and some green algae (e.g., Caulerpa).

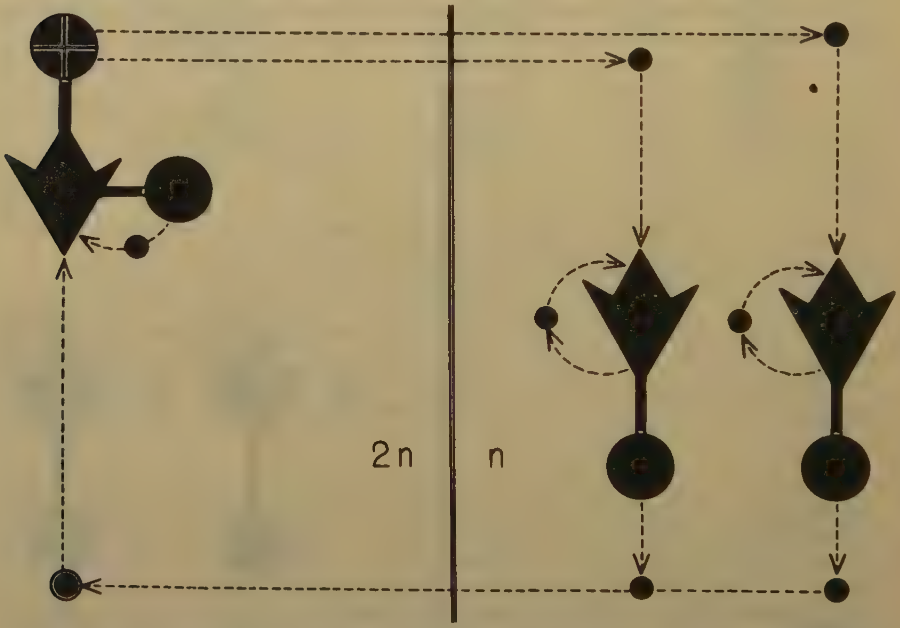

Fig. 4. Life cycle characterized by alternation of diploid and haploid generations, which may or may not be similar. Typical of land plants (Bryophyta and Tracheophyta), most brown algae (e.g., Ectocarpus, Cutleria) and marine green algae (e.g., Ulva, Cladophora).

(666)

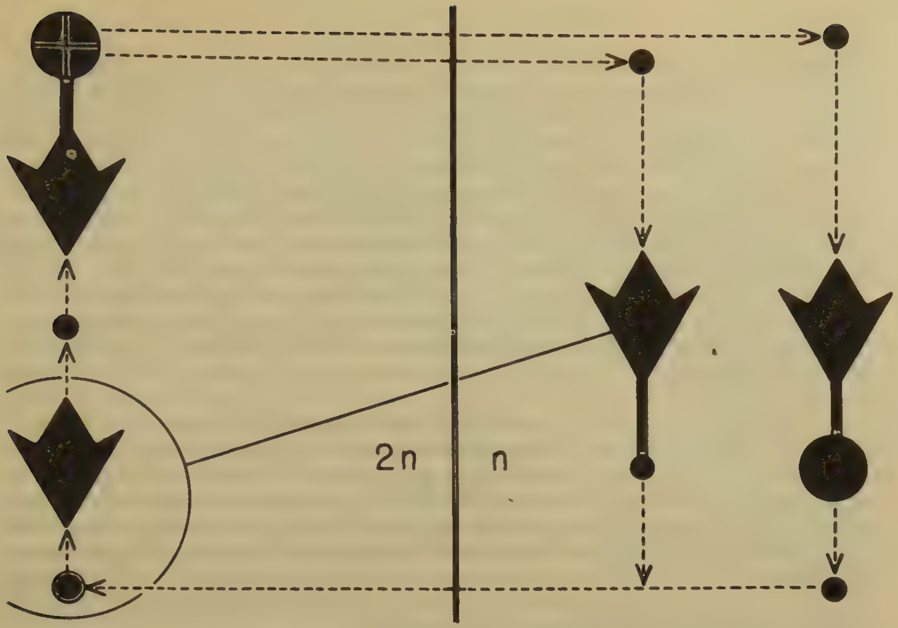

Fig. 5. Life cycle characterized by free-living haploid and diploid thalli, with an interposed diploid phase growing on the haploid gametophyte, and reproducing by carpospores, which give rise to tetrasporophytes. Typical of Florideae (e.g., Callithamnion).

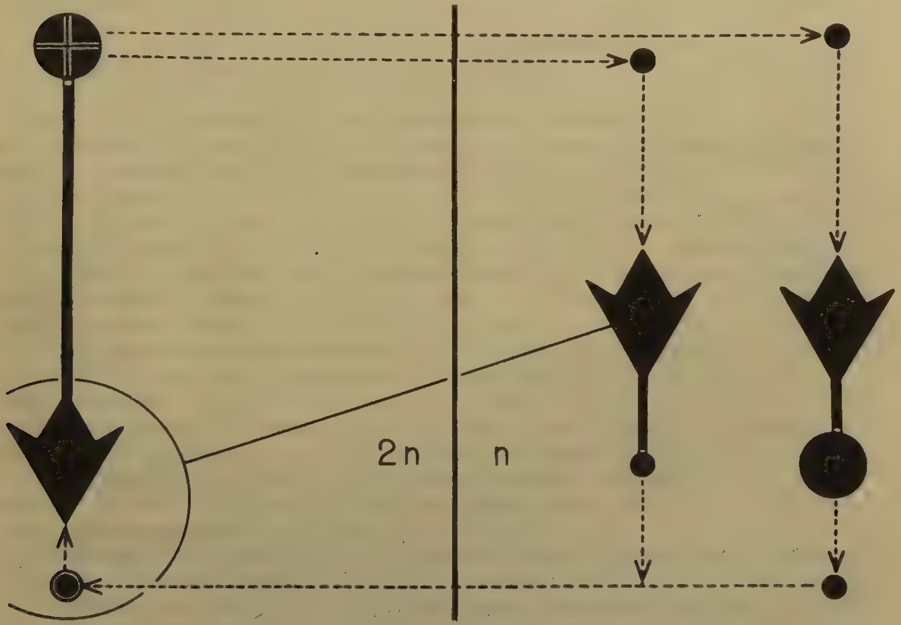

Fig. 6. Life cycle with diploid phase growing on the haploid gametophyte, and producing tetrasporangia directly. Some red algae of the Nemalionales (e.g., Liagora tetrasporifera).

too, might lend themselves to such studies. Føyn (1934) and Bliding (1944) have contributed considerably to our knowledge of these algae in culture, and their work should provide a sound basis for genetic investigations. *Urospora* is of special interest in that one species, *U. mirabilis*, is believed to have alternation of heteromorphic generations (Jorde, 1933). Hämmerling and his colleagues (1953) have obtained a wealth of valuable information from species of the subtropical genera *Acetabularia* and *Acicularia*, which in the vegetative condition are uninucleate diploids. *Batophora oerstedtii*, a related species common on the Florida Keys, grows well in crude laboratory culture, and might lend itself to similar studies. Dostál (1945) cultivated the coenocytic *Caulerpa prolifera* over prolonged periods, even within the borders of nonmaritime Czechoslovakia, but perhaps its growth would be too slow for an ambitious geneticist.

Turning now to the Phaeophyta, we find fewer forms of obvious promise. There have been several studies of *Ectocarpus siliculosus* (e.g., Papenfuss, 1935); and *E. parasiticus*, which can even be grown on agar, has been cultured through several asexual generations under bacteria-free conditions. This, then, might be one genus worth looking into, along with *Myrionema* and similar related forms. Neushul (unpublished) has recently achieved some success in the cultivation, not only of *Ectocarpus* species, but also of members of the Dictyotales, though none of the latter has yet been raised to maturity.

Among the Rhodophyta we encounter a wide range of algae which might submit to domestication. Recent work by Drew (1955) has suggested that *Porphyra* and *Bangia* may have more involved life cycles than we have hitherto believed; and at least one species of *Bangia* can be raised in test tubes. These related genera, ecologically the red counterparts of *Ulva* and *Enteromorpha*, likewise include species that are capable of rapid growth in springtime, and of surviving after being drenched by rain or baked crisp by the summer sun. Here, too, dioecious species can be found (e.g., *Porphyra lanceolata*), and low chromosome numbers ($n = 4$ in *P. linearis*: Magne, 1952) provide an additional advantageous feature. Some encrusting red algae like *Hildenbrandia prototypus* and *Lithophyllum* spp. commonly grow in marine aquaria; and the former, at least, is certainly tolerant of wide osmotic fluctuations in the water. However, in *Hildenbrandia* only tetrasporic plants are known, whereas in *Lithophyllum* the sporangia are frequently two-spored, and even tetraspores may be produced apomeiotically (Suneson, 1950). In the filamentous *Spermothamnion turneri*, Drew found evidence for two races, one exhibiting a regular alternation of haploid ($n = 30$) and diploid generations, the other with diploid gametophytes and tetraploid sporophytes. Sterile triploids are believed to result from interracial crossing (cf. Barber, 1947). In *Plumaria sericea*, a triploid race ($3n = 93$) appears to have overcome the immediate disadvantages of sexual sterility, and reproduces apomictically by so-called paraspores; indeed, at the northern fringes of its range this is the race most commonly encountered. Drew (1955) has also reported success in the cultivation of *Antithamnion spirographidis*, following the development of each stage of the life cycle in the laboratory. Hassinger-Huizinga (1952) was able to initiate genetic studies with the related alga *Callithamnion corymbosum* ($n = 30$), which she carried through several experimental generations and in which she demonstrated segregation of sex in the tetrasporangia. Occasional irregularities arose, such as bisexual plants, some of which could be attributed to the presence of one or two supernumerary chromosomes, but many details remain to be worked out. *Trailliella intricata*, which has been successfully cultured by Koch (1950), would certainly repay further study. So, too, would *Acrochaetium* and *Rhodochorton* species, which may grow like fine red grass on pilings and intertidal rocks. The existence of an aerial species (Rosenvinge, 1900) indicates that some of these forms might prove especially tolerant of laboratory conditions.

A recent report by Jones (1956) indicates that plants of *Gracilaria verrucosa* may arise from fused cellular masses derived from several tetraspores or carpospores. There is also now a suggestion that a similar situation may occur in the green siphonaceous alga *Codium fragile* (Arasaki *et al*., 1956). We have therefore to bear in mind the possibility that some of the thalli we find along the shore might even be chimaeral.

Lastly, we should not forget the diatoms, the pasture plants of the seas. They grow rapidly under favorable conditions, with one or two cell divisions per day. We have already in culture many centric and pennate species, most of the latter being bacteria-free clones that can be handled on agar slants as conveniently as yeasts. Recent studies by Stosch (1956) indicate that certain marine centric diatoms may be experimentally induced to reproduce sexually, which augurs well for genetic studies in this group of plants. The control of pore patterns in the lacy siliceous frustules of diatoms would seem a particularly fascinating field for genetic investigation.

In keeping with the title of the symposium, I have tried to make this contribution less of a review of past accomplishments than a preview, surveying briefly some present trends, and indicating, perhaps rashly, a few of the more promising paths ahead. I hope there will be intrepid adventurers to explore some of them.

REFERENCES

Arasaki, S., H. Tokuda, and K. Fujiyama
1956. The reproduction and morphogeny in *Codium fragile*. Bot. Mag. Tokyo. 69:39-44.

Barber, H. N.
1947. Genetics and algal life cycles. Austral. J. Sci. 9:217-218.

Bliding, C.
1944. Zur Systematik der schwedischen Enteromorphen. Bot. Notiser, pp. 331-356.

Dostál, R.
1945. Morphogenetic studies on *Caulerpa prolifera*. Bull. Internat. Acad. Tchèque Sci. 46(11):133-149.

Drew, K. M.
1955. Life histories in the algae. Biol. Rev. 30:343-390.

Elliot, E., and B. Moss
1953. Incidence of meiosis in the life-cycle of *Halidrys siliquosa* Lyngb. Nature. 171:357.

Føyn, B.
1934. Lebenszyklus, Cytologie und Sexualität der Chlorophycee *Cladophora suhriana* Kütz. Arch. Protistenk. 83:1-56. (Also *Ulva lactuca*, *ibid*.:154-177.)

Hämmerling, J.
1953. Nucleo-cytoplasmic relationships in the development of *Acetabularia*. Internat. Rev. Cytol. 2:475-498.

Hassinger-Huizinga, H.
1952. Generationswechsel und Geschlechtsbestimmung bei Callithamnion corymbosum (Sm.) Lyngb. Arch. Protistenk. 98:91-124.

Jones, W. E.
1956. Effect of spore coalescence on the early development of Gracilaria verrucosa (Hudson) Papenfuss. Nature. 178:426-427.

Jorde, I.
1933. Untersuchungen über den Lebenszyklus von Urospora Aresch. und Codiolum A. Braun. Nyt. Mag. Natürv. 73:1-19.

Koch, W.
1950. Entwicklungsgeschichtliche und physiologische Untersuchungen an Laboratoriumskulturen der Rotalge Trailliella intricata Batters. Arch. Mikrobiol. 14:635-660.

Magne, F.
1952. La structure du noyau et le cycle nucléaire chez le Porphyra linearis Grev. C.R. Acad. Sci., Paris. 234:986-988.

Papenfuss, G. F.
1935. Alternation of generations in Ectocarpus siliculosus. Bot. Gaz. 96:421-446.

Parriaud, H.
1954. Sur un hybride expérimental: Fucus vesiculosus L. x F. chalonii J. Feld. C.R. Acad. Sci., Paris. 238:832-834.

Rosenvinge, L. K.
1900. Note sur une floridée aérienne (Rhodochorton islandicum nov. sp.). Bot. Tidsskr. 23:61-81.

Schreiber, E.
1935. Über Kultur und Geschlechtsbestimmung von Dictyota dichotoma. Planta. 24:266-275.

Stosch, H. A. von
1956. Entwicklungsgeschichtliche Untersuchungen an zentrischen Diatomeen. II. Arch. Mikrobiol. 23:327-365.

Suneson, S.
1950. The cytology of the bispore formation in two species of Lithophyllum and the significance of the bispores in the Corallinaceae. Bot. Notiser, pp. 429-450.

DISCUSSION

L. R. Blinks

Would the multinucleate habit of many siphonaceous algae offer any advantage or disadvantage for genetic study?

R. A. Lewin

Yes, we might be able to take advantage of the siphonaceous habit. In forms lacking cross walls we could perhaps graft together thalli of unlike genotype, and study the physiological interactions of dissimilar nuclei in the cytoplasm of heterokaryons.

M. B. Allen

There seems to be a common tendency to equate "marine algae" with the large littoral forms and to exclude the phytoplankton from this category. However, the planktonic organisms may also provide interesting and valuable material for studies related to genetics. The plankton contains representatives of several groups of algae whose sexual mechanisms, if any, and evolutionary relationships are so far obscure. The chrysomonads may be mentioned as an example. Investigations of such organisms should be rewarding from the point of view of increasing our knowledge of reproductive mechanisms. These organisms also provide material par excellence for studies of biochemical evolution. The variety of patterns of photosynthetic pigments and products found in the different groups of algae affords an opportunity for carrying out with plant material the type of evolutionary study advocated by Professor Baldwin for animal forms. Such studies may provide clues to relationships among these little-understood organisms and may also increase our understanding of the processes of photosynthesis.

The technical point that planktonic algae are likely to be easier to handle in the laboratory than the large, attached algae might also be mentioned.

R. A. Lewin

I quite agree. However, in this paper I wished to emphasize those potentialities of marine algae which are not shared by fresh-water forms. Since most unicellular groups have fresh-water as well as marine representatives, and the former are usually somewhat easier to cultivate, I felt I should not discuss the unicellular algae at any length.

G. F. Papenfuss

There are a number of parasitic forms in the red algae and in the brown algae. In quite a large proportion of the red algal parasites and in one genus of brown algae the closest relative of the parasite is the host. The nature and origin of such behavior has been, hitherto, a matter of speculation. Genetic and biochemical studies may provide the explanation.

Many red algae have three generations, namely, haploid sexual plants, diploid carposporophytes, which are partly parasitic on the female plants, and free-living diploid tetrasporangial plants. In a number of instances, the sexual plants also form tetrasporangia. In the few instances of this kind that have been studied cytologically, it was observed that the nuclear divisions in the sporangia were irregular. Further cytological study of this condition is necessary, especially toward the elucidation of the possibility of the occurrence of polyploidy in these forms.

MARINE MICROÖRGANISMS: SOME GENERALIZATIONS CONCERNING THEIR IMPORTANCE TO MARINE LIFE

WILLIAM L. BELSER*
Scripps Institution of Oceanography
University of California
La Jolla, California

One aspect of marine biology which was briefly mentioned but never elaborated upon during the course of this symposium deserves further consideration. I refer to the study of marine microörganisms and the ways in which they are interrelated with all life in the sea. The importance of this segment of the marine population cannot be denied, and knowledge and utilization of these microörganisms present several interesting perspectives for marine biology.

It would be presumptuous of me to attempt a complete review here. For this reason I shall confine this discussion to a few generalizations concerning little-explored problems relating to microörganisms in the sea, and some speculation on the utilization of these microörganisms.

Inorganic relations.—The nutritional activities of autotrophic marine bacteria may seem, on the surface, to be primarily of academic interest. Considering the importance of the autotrophic metabolism of microörganisms in the biological economy of terrestrial forms, however, it might be wise to consider these reactions a little more carefully in the marine forms. Nitrate and nitrite reduction, sulfur oxidation, and carbon dioxide fixation by soil microörganisms play an important role in the productivity of the earth; but the integration of these and other reactions may be of little import to the green or blue-green algae, which are capable of carrying out these reductions themselves. Nevertheless, it is conceivable that there might be many organisms which are completely, or at least partially, dependent upon a source of reduced nitrogen, and which could be stimulated by bacteria that would reduce it. In this respect, even the above-mentioned green and blue-green algae can grow better, in fact preferentially use ammonium ions when they are available to them (Fogg, 1953). Similar arguments might also obtain for the importance of sulfur,

---

*Public Health Research Fellow of the National Cancer Institute.

Contributions from the Scripps Institution of Oceanography, New Series, No. 1035
Reproduced by Permission

CO_2, and trace element metabolism. Until we have learned more about the inorganic metabolism in the sea, and the role of microörganisms in that metabolism, it is difficult to arrive at any valid assessment of the importance of marine microörganisms in this scheme. Suffice it to say, here is an area of investigation that should be explored much more carefully.

Organic relations.—There are several facets to the organic relationship between bacteria and other plants and animals in the sea. One of these is the process of decay, whereby bacteria contribute greatly to the growth of other organisms by recycling organic materials and phosphate and nitrate in the food chain. Although there are undoubtedly large numbers of scavengers among the higher organisms, there can be little doubt that the bacteria play an important part in disposing of dead plants and animals, thus making available vital constituents to other living organisms.

On the opposite side of the metabolic fence, we have the anabolic activities of the bacteria. The synthesis of growth factors by bacteria is well known in terrestrial forms and in several instances in marine bacteria (Erickson et al., 1953). The possible role of such growth factors in phytoplankton growth has been considered by Provasoli (1958), Margalef (1958), and others. Most of this work has been confined to studies of vitamin synthesis and requirement, but with more refined techniques we might find a whole host of compounds synthesized by bacteria and utilized by plankton. This is a field that urgently requires more study, if the full picture of plankton succession is to be elucidated. One must also consider the possibility that bacteria could alter or modify compounds produced by one plankton organism to a form that could be utilized by another plankton organism in its succession. This type of intermediary action might be difficult to demonstrate, but certainly seems plausible.

Throughout all three of the metabolic patterns, which have been mentioned, only the possible utilization of bacterial metabolic by-products by higher organisms has been considered. One must bear in mind, however, the enormous direct contribution that these untold millions of bacteria make to the food chain, in their role as prey to the many marine predators. There must be many early larval stages which subsist largely on bacteria and other particles of similar size, not to mention the various protozoans that feed upon bacteria as well, and are in turn fed upon.

Another vaguely explored, but fascinating, line of investigation would be a study of symbiotic and/or commensal relationships between bacteria and other organisms. Gut flora of highly specialized feeding-type animals, for example, or loose commensal relationship between bacteria and algae, could prove academically exciting, and economically important. What a wonderful picture can be conjured up from one's imagination of the seeding of the Gulf of California or Puget Sound, with commensal alga and bacterium, with sufficient "primer" biochemicals to initiate a bloom. I find this a highly exciting perspective for marine biology, and one that is potentially of extreme importance.

Parasitism and disease.—Finally we come to the problem of disease. Bacterial diseases have been observed and described, as epizoötics or endemic infections among various animals. There is no denying the devastating effect such diseases could have upon a static population such as one finds in an oyster bed, where the filter-feeders themselves would concentrate the infective agents. But even among the fish, traveling in schools, or aggregating for spawning, disease could make terrible inroads. Better knowledge of such host-parasite interrelationships might permit a certain amount of control over loss of valuable resources in the future. Fresh-water fisheries are already being faced with myxobacterial epidemics, gill disease, ulcer disease, caused by a Hemophilus species, and many others. Some of these diseases respond to antibiotics, some to temperature variation, and others to a variety of chemical compounds. Increased knowledge of the bacteria responsible for these diseases has indicated which treatment to use for what disease, and in some cases has led to the development of new treatments.

One hopeful aspect of the problem of disease in marine animals is the possibility that they might be used for the control of pests, such as barnacles or teredos. If one could isolate organisms from diseased barnacles, for instance, and culture them in the lab, massive doses of the disease-producing organisms could be seeded into the areas where the pests are operating. By inducing such an endemic infection, it might be possible to bring the numbers of offenders down to a controllable level, saving millions of dollars each year.

Marine fungi have also been implicated as parasites in a number of marine plants and animals. Labyrinthula has been considered to be responsible for the decimation of eelgrass on the Atlantic coast, with disastrous effect upon the mollusk and other communities which inhabited the eelgrass beds. Another fungus parasitizes clam and oyster larvae, decreasing the productivity of these forms. The fragmentary state of our knowledge of the kinds, varieties, and numbers of marine fungi demands more extensive study of these interesting and highly important organisms.

Viruses, too, must be considered within the framework of parasitism and disease. To date, no disease attributable to a virus in a higher marine organism has come to my attention. Yet it would be odd, indeed, if they did not occur, and more diligent screening and refinement of present techniques should make it possible to demonstrate their presence. It is impossible to estimate the economic importance of viral disease until we learn more about their number, variety, pathogensis, and hosts. These studies are a challenging problem to all marine microbiologists, and deserve attention from them.

In summary, I wish to point out that the purpose of this paper is to emphasize the paucity of our knowledge of marine microörganisms, and the need for much more extensive work in this field. I intend no criticism of the excellent work already done, but wish to impress upon marine biologist and general microbiologist alike, the necessity for a concerted effort to understand the nutrition, synthesis, and habitats of the marine microörganisms in order that they may be properly related to the higher forms that have been studied so much more extensively. This is fundamental to our complete understanding of marine life, and in the future, to our intelligent and efficient utilization of the sea as a source of food.

REFERENCES

Erickson, L. E., and L. Lewis
1953. On the occurrence of vitamin B_{12}-factors in marine algae. Arkiv. för Kemi. 6(40):427-442.

Fogg, G. E.
1953. The metabolism of algae. London, Methuen and Co., Ltd., 149 pp.

Margalef, R.
1958. Temporal succession and spatial heterogeneity in phytoplankton. In Perspectives in marine biology, ed. A. A. Buzzati-Traverso. Berkeley and Los Angeles, Univ. of Calif. Press, 622 pp.

Provasoli, L.
1958. Growth factors in unicellular marine algae. Ibid.

282 *Experimental Cell Research* **15**, *282–299* (*1958*)

TROPISTIC RESPONSES OF ZYGOTES OF THE FUCACEAE TO POLARIZED LIGHT[1]

L. F. JAFFE

Scripps Institution of Oceanography, La Jolla, Calif., U.S.A.

Received December 10, 1957

In 1934, Castle [5] reported that a beam of vertically vibrating light[2] needed to be about 10 per cent more intense than an oppositely directed beam of horizontally vibrating light in order to nullify the latter's tendency to effect phototropic bending of an upright *Phycomyces* sporangiophore. This finding of *polarotropism*, an orientation of growth by the polarization of light, was unique; for previous claims [1, 22, 24] were and remain entirely unconvincing and unconfirmed. Castle interpreted the polarotropic response as arising from differential external reflection. This view now seems incorrect [17]; but so viewed the phenomenon revealed nothing and was not pursued.

Recently, I found a striking polarotropic response of *Fucus* zygotes [16]. Zygotes treated with plane polarized white light coming from both above and below tend to germinate horizontally and in the plane of vibration.

I have here tried to study whether or not the polarotropic response of the zygotes is a variant of their response to unpolarized light. For it might not be; the polarized irradiation might orient growth by directly aligning molecules—a hypothesis which invites examination despite the want of evidence for it.

MATERIALS AND METHODS

Obtaining zygotes.—Receptacles, or fertile fronds, of *Fucus furcatus* were collected at Carmel Point, Carmel, California; those of *Pelvetia fastigiata* at Reef Rock, La Jolla. They were treated and stored as described by Whitaker [33] and Jaffe [15], respectively. Three to six days after collection, the receptacles were transferred to a room held at 15 ± 3/4°C where all subsequent operations were carried out; these started immediately with a treatment used to stimulate gametangial liberation.

---

[1] Contribution from the Scripps Institution of Oceanography. The experimental work was done as a Postdoctoral Fellow in Marine Biology at the S.I.O. Instrumentation was carried out under a contract with the Bureau of Ships. Analysis of the data was carried out at the author's current address, Brandeis University, Waltham, Massachusetts, with the support of both Brandeis and the Office of Naval Research (Contract Nonr 1677 (02) NR 164–406).

[2] The direction of vibration here is that of the electric vector.

Contributions from the Scripps Institution of Oceanography, New Series, No. 1036
Reproduced by Permission

For *Fucus*, Whitaker's method [33] of simply immersing the stored receptacles in 15°C sea water sometimes failed in these experiments. For this reason, the following further expedient was resorted to: About one hour after immersion the receptacles were placed about two inches below a 20 watt white fluorescent lamp; marked shedding ensued one to three hours later. The treatment for *Pelvetia* has been described [15].

The receptacles of *Fucus* and of *Pelvetia* were discarded about 45 and 15 minutes respectively after shedding began. It was at about this time of discard that 50 per cent of the egg-bearing capsules were estimated to have broken down. This estimated time was taken as the "time of fertilization". Where illumination proved necessary in subsequent operations, only ruby lamps were employed.

The sexual products were allowed to remain in the dark for about 20 minutes after discard so as to complete the dissolution of the öogonial capsules and the fertilization of the eggs. The zygotes were then thoroughly washed with artificial sea water [16] and suspended in the same medium to form a "stock suspension".

Method for vertical illumination.—The central light source was a 500 watt projection lamp powered through a voltage stabilizer. Most of the infrared component was filtered out of the horizontally emanating light by immersing the lamp in the center of a 0.6 molar ferrous sulfate solution held in a glass cylinder; each horizontal beam traversed 37 mm of this filter before emerging. The filter was water-cooled during lamp operation and adequately protected against oxidation by a layer of mineral oil above it, 0.05 molar H_2SO_4 in it and a piece of brass at its bottom.

Horizontal beams from the central light source traversed windows in each of nine boxes; thence they were deflected downward by 45° prisms through appropriate filter trains so as finally to irradiate each of nine egg-bearing culture dishes with two 17 millimeter square patches of plane polarized approximately monochromatic light of known intensity. The filter train in each box consisted of the following components (starting with the one nearest the light source): (i) An over-all Wratten neutral filter (fine adjustment was provided by changing the distance between the light source and the optical box). (ii) An interference filter. The transmission peaks and half band widths used are listed in Table I. (iii) One or more cut-off filters. (iv) Two 17 mm square windows, one being covered by Wratten neutral filters, whose measured transmission was 10 per cent. (v) A Polaroid type H linear polarizing filter.

The intensities impinging on the eggs in each patch of light were measured by replacing the culture dishes with a suitably masked photronic cell whose output was read off a stabilized indicating amplifier. The light intensity measured as reaching a patch via the window *not* directly above it never exceeded 3 per cent of the total reaching it. The photometric setup was calibrated in relative energy terms by comparing its reaction with that of a thermopile (whose output was read off a galvanometer) to light beams of the same spectral composition used in treating the eggs. Tests using appropriate extra filters showed that the light beams used were free of infrared. The absolute energies used were determined by calibration with a Bureau of Standards lamp.

Method for horizontal illumination.—The light source for the lower intensities used was a 15 watt, 6 volt tungsten filament lamp. Its image was focused through 9 cm of 0.04 *M* $CuSO_4$ + 0.04 *M* HCl onto a 1 cm square of white paper. This then acted as a secondary source of white light free of infrared and of polarization. For doses of 10^{18} quanta/cm² or greater, the source was changed to a 30 watt sealed spot lamp

(679)

TABLE I. *Response of* Fucus *zygotes to monochromatic plane polarized light coming from above.*

The dose is expressed as quanta/cm². For all values of $V_2 > 44$ %, the per cent of outgrowths classified as up averaged 1.0 ± 0.8; for 12 % < $V_2 < 44$ %, per cent up = 3 ± 2 %; for $V_2 < 12$ %, per cent up = 8 ± 5 %.

Peak λ (mμ)	Half band width	Egg batch	% bipolar alignment, V_2, for dose of: 10^{18}	10^{17}	10^{16}	% twins for dose of: 10^{18}	10^{17}	10^{16}
398	14	a		55 ± 5	44 ± 6		23 ± 4	10 ± 3
		c		61 ± 4	31 ± 6		25 ± 4	16 ± 3
425	9	a		60 ± 4	61 ± 4		30 ± 4	14 ± 3
		c		64 ± 4	49 ± 4		31 ± 4	28 ± 3
436	9	a		71 ± 4	63 ± 4		26 ± 4	22 ± 4
		c		64 ± 4	59 ± 4		22 ± 3	20 ± 3
454	10	c		62 ± 4	57 ± 4		24 ± 4	14 ± 3
459	9	a	67 ± 4	61 ± 4		24 ± 5	46 ± 5	
		c		75 ± 3	60 ± 5		43 ± 4	19 ± 4
483	9	a	80 ± 3	68 ± 3		35 ± 5	36 ± 5	
		c		78 ± 3	61 ± 4		29 ± 4	22 ± 3
499	12	a	77 ± 3	73 ± 3		40 ± 6	35 ± 5	
		c		60 ± 4	42 ± 5		20 ± 3	10 ± 3
522	9	a	65 ± 4	30 ± 7		34 ± 5	8 ± 3	
		b	65 ± 4	37 ± 6		12 ± 3	8 ± 3	
		c	62 ± 4	25 ± 6		25 ± 4	14 ± 3	
546	8	a	12 ± 7	− 6 ± 7		4 ± 2	7 ± 2	
		c	21 ± 6			8 ± 2		
567	17	a	33 ± 6	17 ± 8		7 ± 3	6 ± 3	
		b	27 ± 7	8 ± 7		3	3	
579	4	b	− 11 ± 7	9 ± 7		0	2	
605	13	b	− 1 ± 7			2		
627	16	b	− 2 ± 7			0		
650	8	b	− 1 ± 7			0		
662	9	b	2 ± 8			0		
690	13	b	− 2 ± 7			2		
710	13	b	− 19 ± 6	− 5 ± 7		3	2	
Dark		a		0 ± 7			4 ± 2	
		b		− 9 ± 7			2	
		c		− 1 ± 6			14 ± 3	

(680)

without a depolarizing paper in its beam. The test eggs lay in horizontally placed rectangular chambers made of microslides. A beam from the source traversed a Polaroid H filter and/or a Wratten neutral filter where appropriate, descended upon one side of each chamber at about $5\frac{1}{2}°$ to the horizontal, and passed through a window so as to illuminate directly only the bottom of the chamber, whence it was totally reflected. Thus each egg was illuminated by two beams whose resultant direction was exactly horizontal. It is estimated that no more than 1 per cent of the "unpolarized" light used in some cases was polarized by reflection before striking the eggs. Light intensities were mainly regulated by changing the distance between the chamber and the source, and were measured using a photronic cell calibrated against a thermopile. On the basis of the emission spectrum of a 2780° K tungsten filament lamp [32] and a measurement of the filter's transmission spectrum, it is estimated that about $\frac{1}{5}$ of the radiant energy striking the eggs lay between 400 and 500 mμ, virtually all the rest lying in the longer wavelength visible.

Analyzing outgrowth directions.—Tenfold magnified shadowgraphs were made of all cultures four days after fertilization. The initial angles of rhizoidal outgrowth as projected in the horizontal plane, or plane of the shadowgraph, were then measured. For the experiments with vertical and equatorial illumination, this analysis was restricted to those embryos whose original centers lay more than 380 mμ or about five egg diameters from their nearest neighbors. In cases where an outgrowth had originated so close to the top of a zygote as to entirely hide its thickened origin, it was classified as "up".

RESULTS

Alignment within the plane perpendicular to the direction of illumination.—As previously reported [16] the polarotropic response was effected by illumination coming from both above and below. A subsequent exploratory experiment showed a similar response to illumination from above only. With this in mind, the effects of treating *Fucus* zygotes before germination with different wavelengths of polarized light coming from above only were investigated. One resultant distribution of outgrowth angles is plotted in Fig. 1 *a*.

To characterize the degree of bipolar alignment of each measured distribution, the parameter, V_2 was calculated [7]:

$$V_2 = \Sigma p \cos 2\theta,$$

where p = the percentage of all outgrowths whose projection in the horizontal plane originated at an angle θ to the vibration axis. (Outgrowths classified as up were omitted in the calulation of V_2.)

Note that for a distribution perfectly aligned in the vibration axis, $V_2 = +100$ per cent; for one perfectly aligned perpendicular to this axis, $V_2 = -100$ per cent; for a uniform distribution, $V_2 = 0$ per cent; for a random distribution, $V_2 = 0$ ± ~~70 × 7~~

10 7

per cent $\sqrt{N}$, where N is the total number of outgrowths not pointing up [27]. The "vector method", using V_2, extracts much more information from the data than one of simply dividing it into the two categories, $-45°$ to $+45°$ and $+45°$ to $+135°$. Theoretically, it would require the measurement of two to four times as many angles (as V_2 varies from 0 to 80 per cent) to attain the same accuracy with a two category method as with the vector method (see below). The theoretical variances of V_2, $\sigma(V_2)$, were read off a plot of $\sigma(V_2)$ vs. V_2 constructed for circular normal distributions. These have the form [13]:

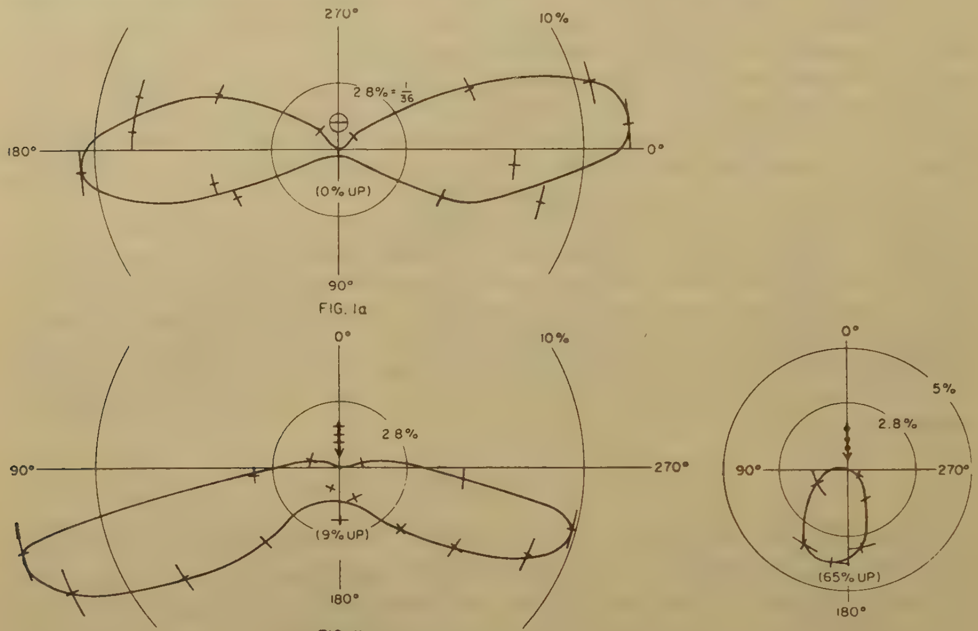

FIG. 1a

FIG. 1b

FIG. 1c

Fig. 1.—Illustrative distributions of outgrowth directions of *Fucaceae* eggs in response to treatment with plane polarized light. Per cent of all outgrowths per 10° interval plotted vs. angle. 1*a*—*Fucus* eggs treated with 10^{17} quanta of 483 mμ polarized light coming from above (egg batch c). 0°–180° axis marks plane of vibration. $V_2 = 78$ per cent; $\theta_2 = 0.5°$; $V_1 = 6$ per cent. 1*b*—*Pelvetia* eggs treated with white light horizontally polarized and coming horizontally in the direction of the arrow. 10^{17} quanta of the light lay between 400 and 500 mμ. 1*c*—Same as 1*b* except vertically polarized.

$$F(\theta) = \frac{e^{K \cos 2\theta}}{2\pi I_0(K)},$$

where K is a parameter characterizing the degree of alignment.[1] The graph was made using the following two characteristics of circular normal distributions, taken from

---

[1] $I_0(K)$, $I_1(K)$, and $I_2(K)$ are Bessel functions of the first kind of pure imaginary argument.

Gumbel *et al.* ([13], p. 139) and from Greenwood and Durand ([12], p. 236) respectively:

$$V_2 = I_1(K)/I_0(K)$$

$$\sigma(V_2) = \frac{1}{\sqrt{N}} \cdot \sqrt{\frac{1}{2} + \frac{I_2(K)}{2\,I_0(K)} - \left(\frac{I_1(K)}{I_0(K)}\right)^2}.$$

Evidence that the circular normal distribution is an adequate model is provided in Fig. 2. In order to reveal the shape of the empirical distributions, the largest possible sample was obtained as follows: Those eight distributions for which V_2 happened to lie between 60 and 62 per cent were pooled. Furthermore, each group of four symmetrical ten degree intervals (e.g. 0–10°, 170–80°, 180–90°, and 350–60°) were pooled. In Fig. 2, the histogram represents this empirical data and the smooth curve is taken from that circular normal distribution for which $V_2 = 61$ per cent.

The main result of this investigation appears in Fig. 3*a*, where the bipolar alignment parameters, V_2, are so arranged as to allow the drawing of an action spectrum. The doses employed in all the treatments whose results are listed across from a given dosage were equalized within about 10 per cent. Each dose was applied by means of a ten hour long constant intensity treatment starting two hours after fertilization. (Under comparable conditions, the first zygotes are reported to begin germination 10 to 14 hours after fertilization [34].) In Table I, these same data appear together with estimates of standard deviations and other accessory information.

Consideration of Fig. 3*a* and Table I indicates that a maximum of sensitivity of the eggs toward the growth aligning effect lies between 435 mμ and

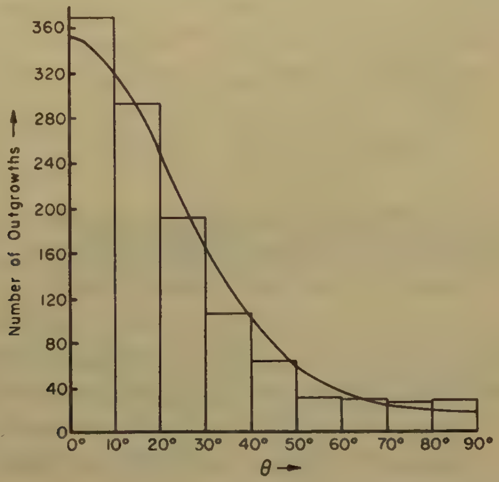

Fig. 2.—Exact shape of distributions of *Fucus* outgrowth directions in response to polarized light coming from above.

490 mμ. In this region the total dose required to produce 60 per cent orientation is 10^{16} quanta/cm² which is 4×10^4 ergs/cm² at 480 mμ. The sensitivity falls relatively slowly toward short wavelengths; at 400 mμ it is about 1/10 maximal. But it falls precipitously toward long wavelengths; at 522 mμ, it is about 1/100 maximal; at 546 and 560 mμ, no more than 1/1000 maximal; between 579 and 710 mμ, no more than 1/10,000 maximal.

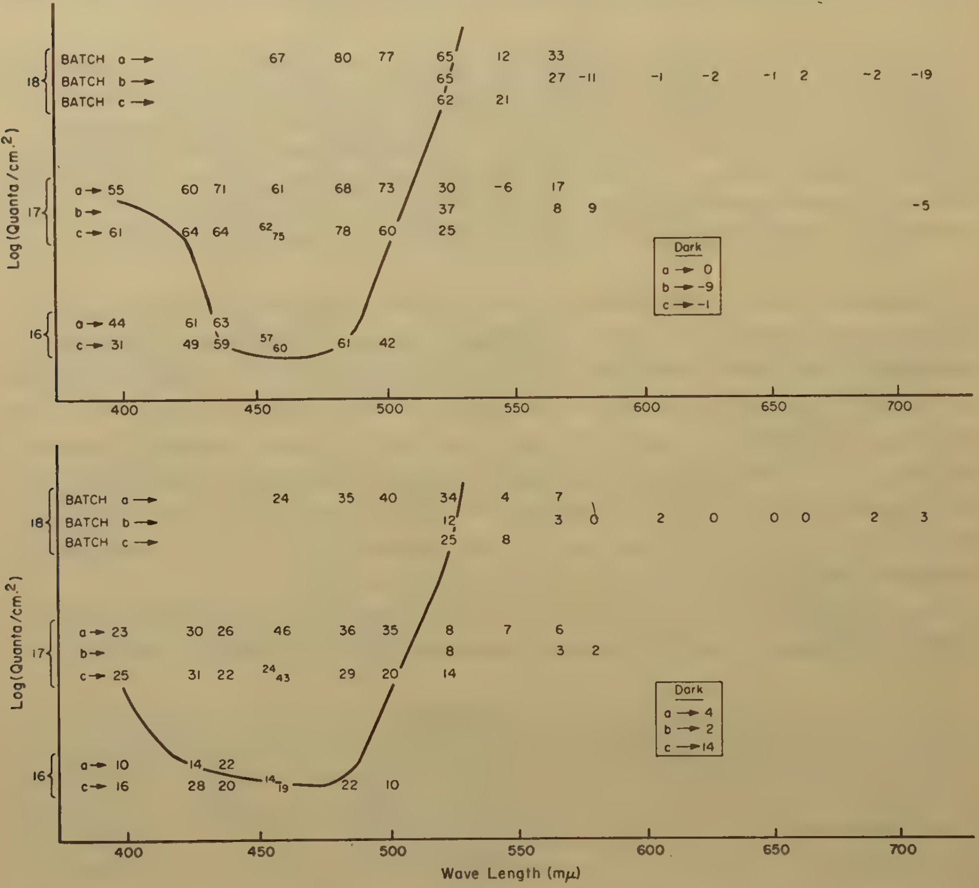

Fig. 3.—Wavelength dependence of response of *Fucus* eggs to plane polarized light coming from above. Fig. 3*a* (above): Alignment response, V_2. The curve is drawn through interpolated doses giving 60 per cent alignment. Fig. 3*b* (below): Twinning response. The curve is drawn through interpolated doses giving 25 per cent twinning.

It has been assumed that the central tendency of the outgrowths is exactly 0°. Analysis of the present data establishes this point with considerable preci-

TABLE II. *Evidence that outgrowth distributions lack any unipolar component.*

	Strong bipolar orientation ($V_2 = 60 - 80$ %)	Weak bipolar orientation ($V_2 = -20$ to $+20$ %)
Empirical $\sigma(V_1)$	7.0 %	5.9 %
Expected $\sigma(V_1)$	7.7 %[b]	6.9 %[a]
Empirical $\sigma(W_1)$	3.5 %	6.2 %
Expected $\sigma(W_1)$	3.5 %[c]	6.9 %[a]

[a] From Rayleigh distribution [27].
[b] Weighted average between Rayleigh and binomial distributions.
[c] For a mixture of independent Rayleigh and binomial distributions.

sion. The central tendency of each distribution was first characterized by the parameter:

$$\theta_2 = \tfrac{1}{2} \text{ arc tan } \left(\frac{\Sigma p \sin 2\theta}{\Sigma p \cos 2\theta}\right).$$

The results were then averaged for all 22 distributions which showed at least 60 per cent alignment, yielding the value, +0.30 ±2.8°.

Moreover, the above data concerns a tendency to grow out either in one direction or its opposite. In view of the symmetry of the known directive influences—light vibration plane, light direction, substratum plane, and residual group effects—it is to be expected that there will be an equal tendency to develop in any two opposite directions; this too is well confirmed by analysis. The requisite information was obtained by first calculating both components of the *unipolar* alignment vector for each distribution:

$$V_1 = \Sigma p \cos \theta, \qquad W_1 = \Sigma p \sin \theta.$$

Table II shows the good agreement between their empirical standard deviations from zero and their theoretical ones as estimated on the basis of random fluctuations.

Alignment within the plane containing the light direction.—Zygotes of *P. fastigiata* were illuminated with white light from one horizontal direction during the period from two to nine hours after fertilization. (Preliminary experiments showed that some zygotes first begin to germinate about 10 to 12 hours after fertilization under similar conditions.)

(685)

TABLE III. *Alignment of germination of* P. fastigiata *zygotes by unilateral unpolarized light.*

The dose given is of the estimated fraction of light lying below 500 mμ. 180° indicates germination directly away from the light; 0°, toward it. Outgrowths classified as "up" were not included in the totals. Temperature is 15°C except as noted.

	Dose (quanta/cm²)					
	0	10^{14}	10^{15}	10^{16}	10^{17}	10^{19}[b]
Light on (hrs. after fertiliz.)	[a]	2	2	2	2	1 ½
Light off (hrs. after fertiliz.)		9	9	9	9	3 ½
% of outgrowths: 0–90°	47±4	49±5	43±6	19±3	6±2	19±2
90–135°	31±4	29±5	39±6	54±4	43±4	28±3
135–180°	22±4	22±4	19±4	27±4	51±4	53±3
160–180°	11±3	6±2	7±3	10±3	20±3	

[a] Dark control.
[b] $T = 16°C$.

In this case, it is first necessary to consider the response to *un*polarized light. Consider Table III. Compare the dark control with the response to 10^{16} quanta/cm². It will be seen that the response to this intensity is *not* an aggregation of outgrowths in the vicinity of the rear pole, or 180°; rather, it is a tendency to accumulate outgrowths in the *subequatorial* zone between 90° and 135°. At 10^{15} quanta/cm², a weaker, but still significant subequatorial response is seen. However, at 10^{17} and 10^{19} quanta/cm², a rear pole response appears.

In Table IV, find the comparable responses of *F. furcatus* zygotes as reported by Whitaker and Lowrance [34]. 10^{16} quanta/cm² of unilateral unpolarized illumination yields a clear subequatorial response when applied between 9 and 16 hours after fertilization; however, earlier or more intense treatments yield a rear pole response.

The responses to horizontally directed polarized light may now be considered. Fig. 1 *b* shows an illustrative outgrowth distribution—that in response to a dose of *horizontally* vibrating light of which 10^{17} quanta/cm² lay between 400 and 500 mμ. Evidently these outgrowths are strongly concentrated around a subequatorial angle. Fig. 1 *c* shows another illustrative outgrowth distribution—that in response to the same dose of *vertically* vibrating light. Sixty-five per cent of these zygotes grew "up", the rest tending to

TABLE IV. *As Table III, for* F. furcatus.

(Data of Whitaker and Lowrance [34].)

Dose ...	10^{16}	10^{16}											10^{17}
Light on	[a]	5	6	7	8	9	10	11	12	13	14	15	2
Light off	[a]	6	7	8	9	10	11	12	13	14	15	16	27
0–90°	49 ± 3	38	15	2	5	8	8	10	15	14	23	31	0
90–135°	25 ± 2	28	36	46	52	68	72	66	62	66	62	52	8
135–180°	26 ± 2	34	49	52	43	24	20	24	23	20	15	17	92

[a] Averages of 14 observations of zygotes treated for one hour with 10^{16} quanta/cm^2 during the *insensitive* periods from 2–15 and 16–27 hours after fertilization. Their tabulated empirical variances appear to be good gages of those of the other figures.

develop directly away from the light. (A zygote cannot grow downward because of the hard substratum.)

Between 10^{15} quanta/cm^2, the lowest dose eliciting a non-random response, and 5×10^{19} quanta/cm^2, the highest dose tested, the responses did not differ qualitatively from the above illustrations. Hence, for the purpose of rapidly visualizing the response to plane polarized light over this range, Fig. 1*a*, 1*b*, and 1*c* may be considered as three orthogonal views of the same distribution. In brief, this distribution is shaped like a wing nut; the wings lie in the vibration plane and point at two symmetric subequatorial angles.

Now, to more precisely describe the responses to horizontally directed lights, both polarized and unpolarized, the distributions were characterized by two bipolar parameters: ϕ_2, a measure of central tendency, and L_2, a measure of the degree of orientation around ϕ_2.

$$\phi_2 = \tfrac{1}{2} \text{ arc tan } \left[\frac{\Sigma\,[p(\phi) + p(-\phi]\,\sin 2\,\phi}{\Sigma\,p(\phi)\,\cos 2\,\phi} \right],$$

$$L_2 = \sqrt{\Sigma\,[p(\phi) + p(-\phi)]\,\sin 2\,\phi]^2 + [\Sigma\,p(\phi)\,\cos 2\,\phi]^2}.$$

where $p(\phi)$ is the percentage of all outgrowths whose projection in the horizontal plane originated at an angle ϕ to the direction of illumination.

ϕ_2 and L_2 are parameters descriptive of behavior in the plane of the light direction corresponding to θ_2 and V_2 in the plane perpendicular to the light direction. For the distribution shown in Fig. 1*b*, $\phi_2 = 115°$ and $L_2 = 70$ per cent. These parameters furnish a somewhat misleading description of the

TABLE V. *Response of* Pelvetia *zygotes to unilateral white light.*

In the experiment using egg batch *A*, 140 to 290 eggs were counted per treatment; for batch *B*, 80 to 150. (Distributions characterized by ϕ values in parentheses are not significantly different from random ones.)

	Quanta/cm² (400–500 mμ)							
	0	10^{14}	10^{15}	10^{16}	10^{17}	10^{18}	5×10^{19}	0
Egg batch ...	*A*	*A*	*A*	*A*	*A*	*B*	*B*	*B*
Polarization:								
Horizontal								
ϕ_2	(102°)	(164°)	106°	111°	115°	117°	128°	(51°)
L_2	6	7	17	52	70	62	76	3
% Up	38	44	44	19	9	20	5	62
None								
ϕ_2	(102°)	95°	104°	122°	137°			
L_2	6	10	21	26	42			
% Up	38	44	45	43	34			
Vertical								
ϕ_2	(102°)	(78°)	125°	137°	152°	145°	169°	(51°)
L_2	6	3	10	16	21	9	31	3
% Up	38	44	47	60	65	85	65	62
ϕ_1	(150°)	(27°)	160°	186°	168°	185°	179°	(245°)
L_1^*	4	4	32	39	71	71	91	9

responses to vertically polarized light since these are unipolar. Hence these latter were likewise characterized by unipolar parameters:

$$\phi_1 = \text{arc tan}\left[\frac{\Sigma p \sin \phi}{\Sigma p \cos \phi}\right],$$

$$L_1^* = \frac{1}{1-p(u)} \sqrt{(\Sigma p \sin \phi)^2 + (\Sigma p \cos \phi)^2}.$$

Note that ϕ_1 and L_1^* are measures of the behavior only of those outgrowths not pointing "up". For the distribution shown in Fig. 1 *c*, $\phi_2 = 152°$, $\phi_1 = 168°$, $L_2 = 21$ per cent, and $L_1^* = 71$ per cent.

Now consider Table V in which these characterizations of the responses to horizontally directed light are presented.

Two main points can be extracted from it: (i) The polarized light response and the subequatorial response to *un*polarized light fade out over about the same intensity range. Fig. 4 shows this economically. In it there is plotted against intensity, a clear measure of the response to the *polarized* character of the light (the difference between L_2 for horizontally and for vertically vibrating light), and a comparable measure of the response to unpolarized light (the difference between L_2 for unpolarized light and the dark control). (ii) The shift with increasing dose of unpolarized light from a subequatorial to a rear pole response is paralleled by a slow drift toward higher angles of the polarotropic response: ϕ_2 increases 22° as the dose of horizontally vibrating light increases 5×10^4 times.

Alignment after equatorial illumination.—Fucus zygotes were treated from all directions in a plane with equal doses of unpolarized white light, one third of which lay below 500 mμ. They were exposed at 11°C from 2 to 24 hours after fertilization. In essence the technique was to support the zygotes at the center of a doughnut-shaped fluorescent lamp, with appropriate depolarizing neutral filters and hoop-shaped slits interposed between lamp and zygotes.

The zygotes so treated tended strongly to germinate perpendicular to the plane of illumination. Thus in two cases in which the total dose was about 10^{17} quanta/cm^2, V_2 was equal to 65 ± 9 per cent and 78 ± 7 per cent.

Twinning.—Many *Fucus* embryos developed an outgrowth originating from each of two separate, and usually opposite, regions of the zygote. Such embryos were classified as twins. The percentage of twins as a function of the wavelength and intensity of the polarized light used is presented in Fig. 3*b* and Table I. The action spectrum for this response is readily consistent with that for the alignment effect, but the data are more variable so that the wavelength of maximum effectiveness can be restricted only to the broader region between 410 and 500 mμ.

In this polarotropism study, the *Pelvetia* zygotes never developed two normal outgrowths, though rare embryos showed both a normal and a minute, abortive one. For some entirely obscure reason, in other experiments executed four years before, up to 15 per cent of cultures of *Pelvetia* zygotes sometimes developed into twins.

DISCUSSION

The hypothesis that the polarized irradiation orients growth by directly aligning molecules must be rejected. For two results support what is in any event a simpler assumption—that the orientation of the zygotes' growth by unpolarized and by polarized light are both variants of the general phenomenon of phototropism. First, the zygotes' polarotropic action spectrum (Fig. 3*a*) fits what is known of their tropistic response to unpolarized light

TABLE VI. *Comparison of wavelength dependence (in the visible) of polarotropism with phototropism.*

Phenomenon	Material	Most effective wavelengths	Sensitivity: yellow/peak	Authority
Phototropism	*Phycomyces* sporangiophore	400–460	$\leq 10^{-3}$	Castle, 1931 [4]
,,	*Coprinus* sporophore	400–465	$\leq 10^{-3}$	Boriss, 1934 [2]
,, (low threshold response)	*Avena* coleoptile	435–450, (465–480)[a]	$\leq 10^{-4}$[b]	Johnston, 1934 [18] Curry, 1957 [8] Shropshire, 1957 [29]
Phototropism	*Pilobolus* sporangiophore	430–490	$\leq 10^{-1}$	Bünning, 1937 [3]
Polarotropism	*Fucus* zygote	435–490	$\leq 10^{-4}$ to 10^{-3}	This paper

[a] Secondary peak.
[b] [31].

(it cuts off above 500 mμ for *Cystoseira* [25]), and to all other phototropic spectra (Table VI). Secondly, the polarotropic response and the subequatorial response to unpolarized light fade out over about the same intensity range (Fig. 4).

From a developmental viewpoint, the most revealing residuum is that the polarized light treatment can induce up to half the zygotes to grow into twins. For this implies that the polarity is not established through the rotation of

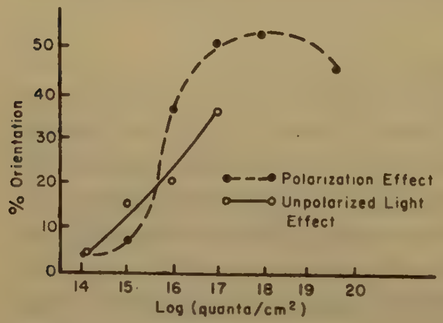

Fig. 4.—Phototropic response of *Pelvetia* eggs to horizontally directed white light.

some preformed asymmetric inclusion, such as the nucleus; it must arise in some more epigenetic manner.

It is also of interest to inquire further into the mechanism of the tropistic responses. First, let us consider the *subequatorial response* to unpolarized light. Whitaker and Lowrance interpreted both responses as caused by an influence directing growth toward the rear pole; the subequatorial accumulations supposedly resulted from a more intense reorientation of partially determined primordia from the anterior hemisphere to the subequatorial

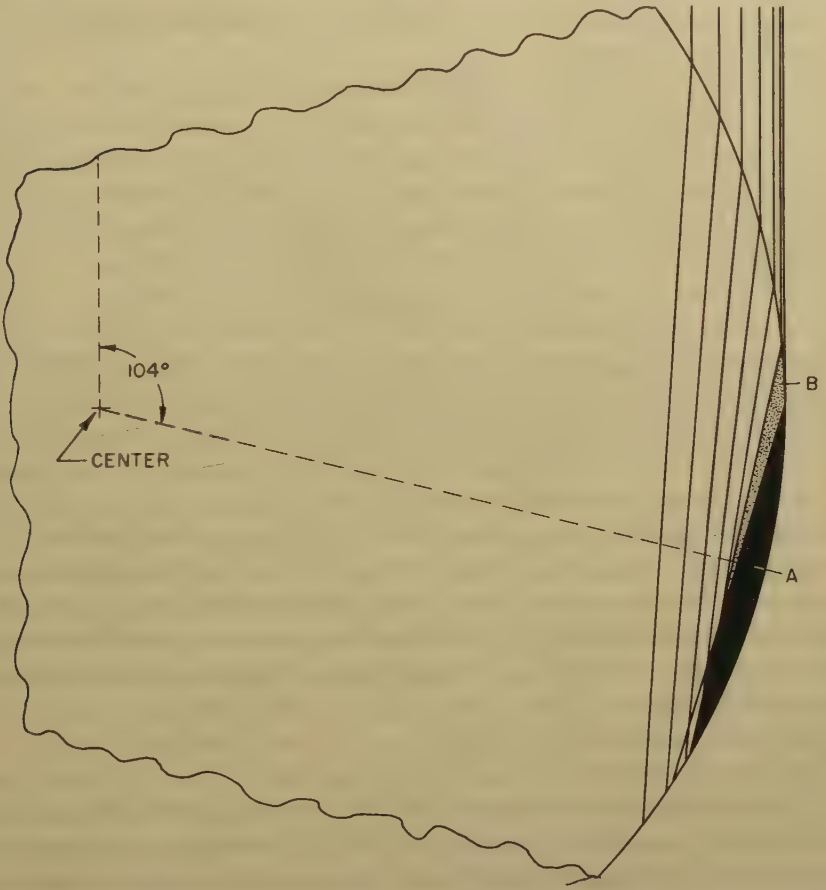

Fig. 5.—Model to show that a shallow subequatorial band in a unilaterally illuminated cell remains dark. Zone *A* is entirely by-passed, while zone *B* receives beams which have lost at least half their energy by external reflection. (Drawn for a spherical cell of refractive index, $n = 1.4$ immersed in a medium, such as sea water, for which $n = 1.34$).

zone than from the latter region to the rear pole. If this were true, then the concentrations of outgrowths arising near the rear pole would be substantially above the uniform level, even in the most extreme cases; but there, they are, if anything, below this level. (See Table III, 10^{15} and 10^{16} quanta/cm^2; Table IV, illumination started 13 to 15 hours after fertilization.) Hence the subequatorial response must be considered a consequence of a truly subequatorial directive influence.

I can conceive of only one general hypothesis to explain such an influence: Growth is directed toward the subequatorial zone because its peripheral portions are the darkest region of the cell. Consider Fig. 5. Only scattered light reaches the by-passed band (A) at the zone's periphery and under it is a second shallow band (B) heavily shaded by reflection losses. This analysis likewise explains several other facts: (i) Spores of the mosses, *Neckera complanata* and *Amblystegium serpens* grow out at "90°" to unilateral and presumably unpolarized light of low intensities [14]. (Heitz's report is undocumented so it may well be that the response is actually *sub*equatorial.) (ii) The zygotes of four species of *Fucus* [16, 19] as well as spores of *Equisetum* [26] germinate equatorially in response to *bi*lateral illumination. (iii) The zygotes of *F. furcatus* (these results) and the spores of *Equisetum* [26] both grow out at 90° to the light directions in response to equatorial illumination. It should be emphasized that this analysis requires that the effective photoreceptors be concentrated in a surface layer. For those rays which are diverted from the by-passed zone by the cell's lens action are concentrated just beneath the surface (Fig. 5). If photoreceptors were as abundant in this subsurface region as in the more peripheral shell, then it would be most difficult to understand how the net photochemical action in the subequatorial zone could be lower than at the rear pole.

It likewise seems almost inescapable that when the *rear pole response* occurs, the most posterior region of the cell becomes effectually the darkest, but the mechanism of this shift is obscure. Photoreceptor molecules deeper in the cell may come into play, a subtle chloroplast movement may change the pattern of scattering and absorption, or the cell may integrate the incoming information by centering its response at the unique center of the darkest hemisphere instead of some indeterminate point of the darkest ring.

Now consider the mechanism of the polarotropic response. It is a variant of the subequatorial one. Hence in some manner the photoreceptor molecules in those meridians of the subequatorial zone lying parallel to the vibration plane must receive least light, How? Since Fresnel reflection is least effective at the cell surfaces in these meridians, *differential external reflection* will cause a relatively greater illumination of the preferentially germinating regions and must be rejected as an explanation. Moreover, *differential internal reflection* cannot over-compensate for this effect because following its first internal reflection each ray has not only been weakened by its second reflection, by absorption and by scattering but traverses a region relatively far from the preferentially germinating one.

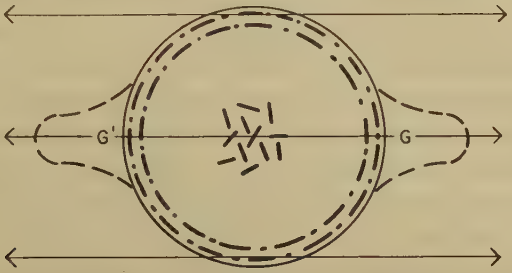

Fig. 6.—Model of egg to show that the photoreceptor molecules in the germinating regions (*G* and *G'*) will absorb least light if the photoreceptors are located near the cell surface and are periclinally oriented. Light enters perpendicular to plane of page, vibrating as shown by double-headed arrows. Dashes within egg represent the axes of maximum light absorption of photoreceptors; dots are photoreceptors lying perpendicular to plane of page; photoreceptors lying between polar and equatorial regions not indicated.

Two possibilities remain: (i) *Differential scattering:* Peripheral molecules in the meridian parallel to the vibration plane are open to substantially less light intracellularly scattered from rays vibrating perpendicular to the scattering plane than the corresponding molecules in the perpendicular meridian, and will therefore receive less scattered light. Moreover, since Latimer's recent studies [21] suggest that algal chloroplasts are remarkably effective scatterers, differential scattering cannot be lightly dismissed as too small an effect.

(ii) *Photoreceptor orientation:* This is the most attractive possibility, since the dichroic ratios of most dyes [20] are plainly large enough to explain the polarotropic response if these molecules were but oriented properly in the cell. Since the zygote looks and acts as though it were radially symmetrical, the only reference point for photoreceptor orientation is the cell surface. Hence these molecules, if they are oriented at all, must either tend to have their axes of maximum absorption arranged parallel to or perpendicular to the nearby cell surface. Examination of Fig. 6 shows that a parallel orientation is the requisite one. Acting together with the by-passing effect, it would cause the photoreceptor molecules in the germinating region to absorb the smallest fraction of the light passing through.

The one structure in which the arrangement of photoreceptor molecules is definitely known is the vertebrate rod. It is notable that this arrangement is analogous to that postulated above for the *Fucaceae* zygote. For the axes of maximum absorption in the rod lie in planes perpendicular to the rod and anisotropically within these planes [9, 28]; hence they lie periclinally, i.e. parallel to the nearby membranes [10, 30].

The only report of polarotropism, other than in the *Fucaceae* zygote, is that of Castle in the *Phycomyces* sporangiophore [5]. It is notable that this finding is most readily rationalized by invoking an arrangement of dichroic photoreceptors again analogous to that postulated for the *Fucaceae* zygote. Contrary to Castle's claim, differential reflection cannot explain the observation [17], while an alignment of photoreceptors in the direction of greatest wall strain can. In the case of the spherical *Fuceacae* zygotes this is simply the postulated periclinal one; in the case of the cylindrical sporangiophore, it is further restricted, being both periclinal and perpendicular to the cell's long axis [6].

Finally, it may be noted that the close-packed tubular membranes of the arthropod ommatidium are believed to define the region in which the photoreceptor molecules lie, and are so arranged that a periclinal arrangement of these photoreceptors could explain the capacity of the arthropod eye to detect the plane of vibration of light [11, 23, 35].

SUMMARY

The following picture is drawn from experiments on two members of the Fucaceae, *Fucus furcatus* and *Pelvetia fastigiata:*

1. In their "polarotropic" response to unidirectional illumination with plane polarized visible light, the zygotes tend to germinate in the plane of vibration, and "subequatorially" (from 90° to 135° away from the source). (Fig. 1.) Up to half the embryos so produced may be bipolar forms.

2. The tropistic response to similar unpolarized light is dual. Under some partially defined conditions it is subequatorial; under others, directly away from the source.

3. The polarotropic response and the subequatorial response to unpolarized light fade out over the same intensity range (Fig. 4).

4. The polarotropic action spectra (Fig. 3) belong to the phototropic group of spectra as found with other organisms (Table VI).

5. It is concluded that in all three tropistic responses to light, growth tends to occur where certain photoreceptor molecules absorb the least light.

6. It is suggested that under unpolarized illumination the subequatorial

(694)

and peripheral photoreceptors absorb least light primarily because they are by-passed by the cell's focusing action (Fig. 5), while under polarized illumination the subequatorial photoreceptors in the vibration plane absorb least light because they are periclinally oriented (Fig. 6).

I wish to thank Dr. Francis Haxo and Mr. James Snodgrass for the use of their equipment and facilities.

REFERENCES

1. Bhatnagar, S. S. and Lal, R. B., *Nature* **117**, 302 (1926).
2. Boriss, H., *Planta* **22**, 644 (1934).
3. Bünning, E., *Planta* **26**, 719 (1937).
4. Castle, E. S., *J. Gen. Physiol.* **14**, 701 (1931).
5. —— *ibid.* **17**, 751 (1934).
6. —— *J. Cellular Comp. Physiol.* **10**, 113 (1937).
7. Curray, J. R., *J. Geol.* **64**, 117 (1956).
8. Curry, G. M., Doctoral Thesis at Harvard University, Cambridge, 1957.
9. Denton, E. J., *Compt. rend.* **239**, 1315 (1954).
10. De Robertis, E., *J. Biophys. Biochem. Cytology* **2**, 319 (1956).
11. Goldsmith, T. H. and Philpott, D. E., *ibid.* **3**, 429 (1957).
12. Greenwood, J. A. and Durand, D., *Ann. Math. Statistics* **26**, 233 (1955).
13. Gumbel, E. J., Greenwood, J. A. and Durand, D., *J. Am. Statis. Assoc.* **48**, 131 (1953).
14. Heitz, E., *Verhandl. schweiz. naturforsch. Ges.* **120**, 168 (1940).
15. Jaffe, L., *Nature* **174**, 743 (1954).
16. —— *Science* **123**, 1081 (1956).
17. —— (in preparation).
18. Johnston, E. S., Smithsonian Misc. Collections **92**, 1 (1934).
19. Kniep, A., *Jahrb. wiss. Botan.* **44**, 635 (1907).
20. Land, E. H. and West, C. D., *in* Colloid Chemistry (ed. by J. Alexander), vol. **VI**, Reinhold, New York, 1946.
21. Latimer, P., *Plant Physiol.* **32**, Supplement, xvii (1957).
22. Macht, D. I., *J. Gen. Physiol.* **10**, 41 (1927).
23. Miller, W. H., *J. Biophys. Biochem. Cytology* **3**, 421 (1957).
24. Morrison, T. F., *Science* **61**, 392 (1925).
25. Mosebach, G., *Ber. deut. botan. Ges.* **56**, 210 (1938).
26. —— *Planta* **33**, 340 (1943).
27. Rayleigh, Lord (Strutt, J. W.), The Theory of Sound, 2nd Ed., 1894. Reprinted by Dover Publications, New York, 1945.
28. Schmidt, W. J., *Z. Zellforsch. u. mikroskop. Anat.* **22**, 485 (1934).
29. Shropshire, W., Read at Am. Inst. Biol. Sc. Meeting, Stanford, 1957.
30. Sjöstrand, F. S., *J. Cellular Comp. Physiol.* **42**, 15 (1953).
31. Sonne, C., *Strahlentherapie* **31**, 778 (1929).
32. Strong, J., Procedures in Experimental Physics, Prentice-Hall, Inc., New York, 1938.
33. Whitaker, D. M., *Biol. Bull.* **70**, 100 (1936).
34. Whitaker, D. M. and Lowrance, E. W., *J. Cellular Comp. Physiol.* **7**, 417 (1936).
35. Wolken, J. J., Capenos, J. and Turano, A., *J. Biophys. Biochem. Cytol.* **3**, 441 (1957).

(696)

BATHYTHERMOMETER Telemeters Ocean Data

By JAMES M. SNODGRASS

and

JOHN H. CAWLEY, Jr.

Special Development Division
Scripps Institute of Oceanography
University of California
La Jolla, California

Contributions from the Scripps Institution of Oceanography, New Series, No. 1037

Reproduced by Permission

Reprinted from ELECTRONICS, May 1, 1957
Copyrighted (all rights reserved) by McGraw-Hill Pub. Co., Inc.
330 W. 42nd St., New York 36, N. Y.

(697)

By JAMES M. SNODGRASS

and

JOHN H. CAWLEY, Jr.

Special Development Division
Scripps Institute of Oceanography
University of California
La Jolla, California

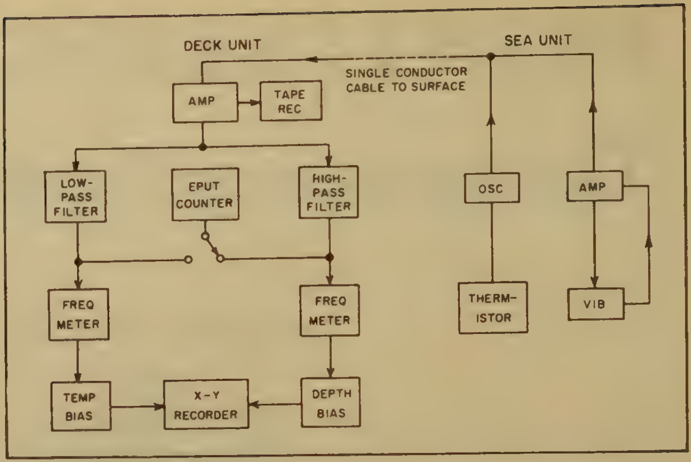

FIG. 1—Outputs of depth and temperature sensing systems are separated in high and low-pass filters for X-Y chart recorder

BATHYTHERMOMETER

SUMMARY —— Two-unit transistorized system lowered from ship gives plot of temperature against depth. Absolute accuracy in depth is better than ±0.25 percent and temperature sensitivity of 0.05 degree C can be obtained. Vibrating wire transducer and thermistor Wien-bridge oscillator provide depth and temperature data, respectively

OCEAN temperature as a function of depth provides valuable information for oceanographic studies. Previous methods of measurement by mechanical means provided an accuracy of ± 0.5 C and ± 5 ft in depth.

Resolution of the order of 1 ft in 1,000 in depth and 0.1 C in temperature are required in present-day oceanographic work. In addition, continuous profile recording is desirable. The system described here is one approach to this problem.

In the block diagram of Fig. 1, frequency variation of a thermistor Wien-bridge oscillator is used to measure temperature. Depth information is provided by monitoring the frequency change of a vibrating wire connected to a flexible diaphragm. Both signals are sent over a single conductor to the ship where they are separated by high-pass and low-pass filters for recording.

Depth Measurement

A Vibrotron is a vibrating-wire transducer in which a mechanical displacement is converted into a frequency change of a vibrating wire. The wire is connected at one end to a pressure-sensing diaphragm. A displacement of the diaphragm changes the tension in the wire thus changing the frequency of vibration. Frequency range of the unit used in this equipment is approximately 9,600 to 11,240 cps.

Electrically, the vibrating wire is similar to an electrically driven tuning fork. The wire is of nonmagnetic material and is placed in a fixed magnetic field at right angles to the axis of the wire. When the wire vibrates at its natural frequency, it becomes an a-c generator, generating a voltage that can be amplified by conventional means. If some of the amplified voltage is fed back to the ends of the wire in phase with the generated voltage, vibration is sustained.

An agc circuit is added to the amplifier to control the amplitude of vibration. The output frequency of the system is a pure sine wave, controlled by the axial displacement of the wire. The output frequency is thus nearly a linear function of the pressure applied to the pressure-sensing diaphragm.

Research ship equipped with boom for raising and lowering bathythermometer to measure temperature gradient of ocean water

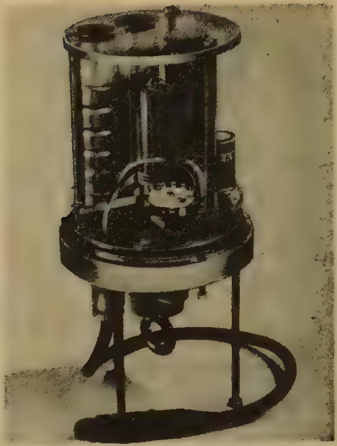

Depth sensing unit with cover removed to show vibrating-wire transducer (center)

Telemeters Ocean Data

Figure 2 illustrates the circuitry for the three-stage transistor amplifier used with the vibrating wire transducer. Because the vibrating wire and static wire impedances are relatively low, a step-up transformer is utilized. The grounded-emitter first stage is resistance-capacitance coupled to the grounded-emitter second stage, which in turn, is directly coupled to the grounded-collector output stage. A properly phased positive-feedback loop is fed from the low-impedance emitter of Q_3 to the center-tap of two resistances bridged across the primary of the input transformer.

An automatic-gain-control network is necessary to drive the Vibratron at constant amplitude. Because the relationship between amplitude and frequency of vibration is exponential, it is necessary to maintain the amplitude constant for a given stability. A voltage of between one and two millivolts measured across the vibrating wire is considered satisfactory.

Under the operating conditions chosen, gain of the first grounded-emitter stage is essentially dependent upon the value of r_e. If I_e is varied over a range of 75 to 20μa, the graph of Fig. 3A shows the variation in voltage gain of the first stage versus input voltage. The measured value of r_e at one milliampere for the type 202 transistor used is 33 ohms. The variation in the measured and computed values results in part from assumptions made in deriving the equation for voltage gain.

The graph of Fig. 3B plots output voltage as a function of input voltage for the three-stage amplifier. Also plotted is emitter current of the first stage as a function of input voltage. The overall result of the automatic gain control action is less than $\frac{1}{2}$-db change in output voltage for a 3-db change in the input voltage at values over one millivolt input.

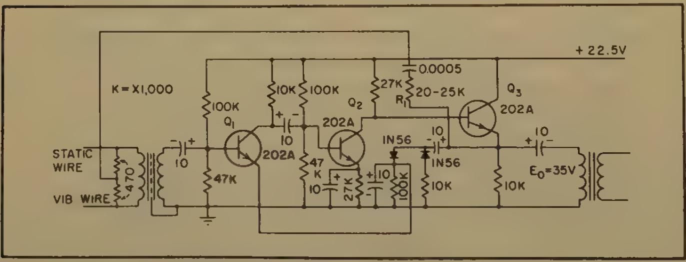

FIG. 2—Transistor amplifier for vibrating wire transducer uses agc to maintain output level at constant amplitude

Temperature Stability

The temperature stability of the amplifier is considered adequate for this application. Sea-water temperature generally is found in the range of 0 to 28 C. Bias stabilization is generally established by the large emitter resistors and the voltage dividers in the base circuits of the first two stages. The degree of temperature stability was measured in actual tests from 5 to 55 C. Fig. 3C shows the results of out-

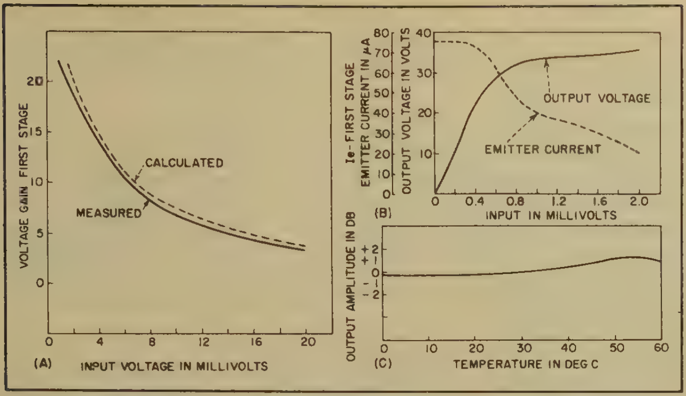

FIG. 3—First stage gain (A), output and agc response (B) and frequency response curve (C) for transistor amplifier used for depth measurement

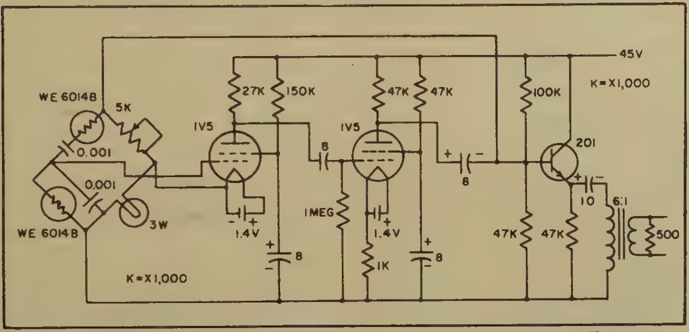

FIG. 4—Wien-bridge oscillator circuit used to measure water temperature. Units encapsulated in epoxy resin and sealed in pressure tight housing.

put voltage against temperature. Only minor distortion was noticed over this range.

The output voltage is approximately 0.5 volt when working into a loaded 500-ohm line.

Temperature Sensing Circuits

The temperature sensitive oscillator is of the Wien bridge type, with 6014A thermistors as resistive elements in the reactive arms of the bridge. This type oscillator was chosen because of its simplicity and dependable performance. Its one disadvantage is that separate filament batteries are necessary when using filament type tubes. The circuit is shown in Fig. 4.

The bridge balance and oscillator frequency is set by

$$R_1 = 2r$$

$$f_o = \frac{1.59 \times 10^1}{\sqrt{C^2R^2}}$$

where f_o = frequency of oscillation, R_1 = negative feedback resistor, r = lamp resistance, R = thermistor resistance and C = capacitance in each half of positive feedback arm.

The temperature coefficient of resistance for the thermistor chosen is −3.9 percent per deg C. Unfortunately, the resistance versus temperature characteristic is nonlinear as shown by the following equation:

$$R = R_o e \exp B[(1/T) - (1/T_o)]$$

where R_o is resistance at reference temperature in deg K, and B is a constant dependent on thermistor material.

When the resistance of the reactive arms is allowed to vary according to this relationship, the frequency-temperature graph of Fig. 5 is formed. An average sensitivity of about 40 cps per deg C is established.

Battery Supply

The tubes chosen use 40-ma filaments, making economic battery operation feasible. The grounded-collector transistor output stage serves to isolate the output circuit from the oscillator section. An output voltage of 0.5 volt is available when loaded by a 500-ohm line.

The temperature stability of this oscillator is satisfactory for this application. When properly adjusted, a frequency variation of one to two cps over an eight-hour period at constant temperature is normal.

Over a temperature range of 5 to 50 C, a frequency change of four to five cps was observed in laboratory tests.

Speed of response is important since the instrument is lowered and raised through the water at a rate of 2.5 feet per second. A thermal time constant of one second or less is necessary to resolve all the detail present. A step-function change in temperature will result in a frequency equilibrium within two seconds in sea water. This time has been cut to the order of one second on occasion by grinding down the glass surface of the thermistor beads.

Instrument Housings

Both the pressure sensitive transistor amplifier and the temperature sensitive oscillator are encapsulated in a silica-filled epoxy resin. Plug-in construction is used to simplify

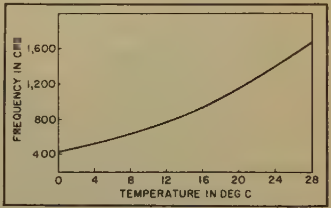

FIG. 5—Plot of oscillator frequency variation with temperature

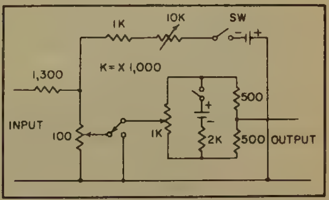

FIG. 6—Zero set circuit used with recorder. Variable resistor and potentiometer are helical type

maintenance and construction.

The instrument is divided into pressure and temperature units and individually housed so that they might be used separately if desired.

The cases are of 5 in. inside diameter, 0.312 in. stainless steel tube. The end plates are of 1-in. brass with O-ring pressure seals. Packing glands are used pass the instrument leads to the surface.

The two instrument housings are pressure tight and designed for a maximum pressure of 5,000 lb per sq in., with an adequate safety factor.

The outputs of the pressure and temperature units are coupled on one side to the instrument case and the other to a single-wire polyethylene-insulated cable. The cable is a 19-strand steel wire with a tensile strength of about 2,800 pounds. The polyethylene jacket brings the overall diameter of the cable to approximately 0.32 inch. The polyethylene jacket also performs the extremely important job of giving the cable buoyancy. This allows the cable to support much greater instrument loads at greater depths, since the cable itself is almost weightless in sea-water.

At the surface the signal is taken off the research vessel's winch via slip-rings. A sea return to the instrument is used with a zinc plate serving as the ground-return connection.

Surface Instrumentation

Surface instrumentation, as shown by the block diagram, consists of a broad-band amplifier capable of handling frequencies up to 15 kc. The frequencies are then separated by a high-pass and a low-pass filter and passed to a demodulator. The resulting d-c outputs are functions of pressure and temperature.

To make these parameters suitable for recording on an X-Y function plotter, a circuit to set zero bias and scale factor is a necessity. It is shown in Fig. 6. This zero offset method is used to set at center scale on the recorder the midrange of both the temperature and pressure functions.

Pressure signal is applied to the X-axis and temperature signal to the Y-axis. This makes it possible to roll the chart manually after each successive run, thus completing a family of bathythermometer curves.

The two channels are also recorded on magnetic tape. A dual channel recorder is used with the combined temperature and pressure information recorded on one channel and a constant 5,000-cps signal on the other. The advantages of this type data storage and playback are self-evident and work is being continued to perfect this phase of the instrumentation problem.

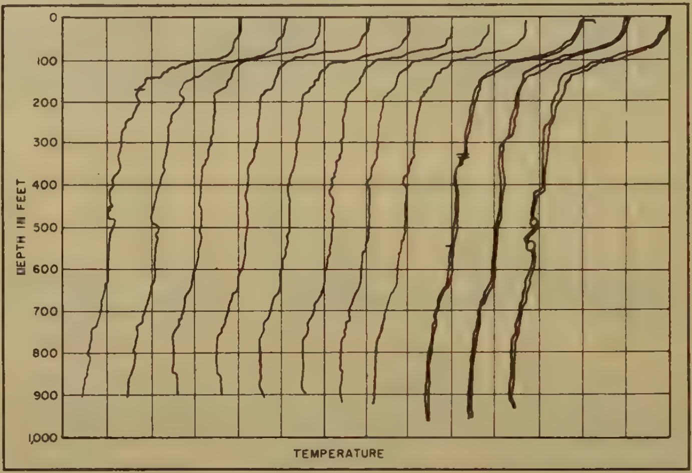

FIG. 7—Typical family of temperature-depth curves obtained with bathythermometer off the coast of San Diego, California

Test Results

This instrument has been used at sea with good results. Fig. 7 is a continuous bathythermometer plot taken at sea off San Diego, California. The research vessel was drifting very slowly. Over the narrow range covered, the temperature scale is nearly linear. Small positive and negative temperature gradients are readily apparent and possible sound channels are indicated.

The vibrating-wire transducer has an absolute resolution of approximately 0.003 inch at the 2.5 ft lowering rate generally used. The overall system is limited by the time constant of the frequency meter. The resulting resolution of the overall depth-measuring system is therefore of the order of 0.3 inch. Absolute accuracy in depth is better than ±0.25 percent or ±2.5 ft in 1,000.

The temperature sensitivity is approximately 40 cps per deg. C. When these parameters are converted to direct current and applied to the function plotter with a ten-inch chart width, a depth variation of ±2.5 ft per 1,000 can easily be read. If ten degrees of temperature are applied to ten inches of chart, a temperature variation of 0.050 deg C can be accurately plotted.

Reproduction of pressure and temperature plots takes place without significant hysteresis effects. This was checked while at sea, where surface temperature and pressure can be accurately measured.

This work was carried out at the Special Developments Division of the Scripps Institution of Oceanography and was supported by funds from the Office of Naval Research and the Bureau of Ships, United States Navy. The authors extend their gratitude to all who took part in this problem, and in particularly to G. T. Barlow and R. M. Blei for their help and assistance in the construction of the equipment.

THE CEYLONESE CYPRINID GENUS *EUSTIRA* GÜNTHER CONSIDERED A SYNONYM OF *DANIO* HAMILTON.—In discussing the classification of the danios, Myers (1953, Aquarium Jour., 24: 235–38) drew attention to numerous gaps that still remain to be filled before final word can be said as to their classification. Recently, while studying the nomenclatorial status of certain genera of Indian fishes, it was found that one of the Ceylonese genera ascribed to different positions in the system by various ichthyologists needed more scrutiny. The genus referred to is *Eustira*, described by Günther (1868, Cat. Fishes British Mus., 7: 331), to include a new cyprinid fish from Ceylon named by him *Eustira ceylonensis*. Günther placed *Eustira* under the group "Abramidina" of the family Cyprinidae and described it briefly as follows: Body oblong, much compressed, the entire abdominal edge being trenchent, scales of moderate size; lateral line abruptly bent downwards behind the pectoral fin; mouth obliquely directed upwards; barbels none. Dorsal fin of moderate length, without spines, opposite the anal; anal fin long, many rayed, caudal fin forked, pectorals elongate; ventrals well developed. Pseudobranchiae; gillrakers fine, lanceolate, rather widely set. Pharyngeal teeth 5.3.2–2.3.5, uncinate, not denticulated.

The fin rays and scale counts of *E. ceylonensis* were given by Günther as "D. 12. A. 17. V. 7. L. lat. 35. L. transv. 7–1/2/2," and the origin of the dorsal fin was noted as being slightly in advance of that of the anal fin. The species was also characterized as having pectoral fins shorter than the head, reaching only as far back as the pelvics.

Because of the slightly inadequate descriptions of the genus and the species, *Eustira* has been confused with *Chela* Hamilton, *Laubuca* Bleeker, and *Perilampus* Day (*nec* McClelland), by Day (1875–78, Fishes of India), Weber and de Beaufort (1916, Fishes of the Indo-Australian Archipelago, 3), Deraniyagala (1930, Eventognathi of Ceylon, and 1952, Coloured Atlas of Some Vertebrates from Ceylon, 1), Smith (1945, Bull. U. S. Nat. Mus., 188), and others. In fact, while recognizing *Eustira* as a subgenus of *Laubuca*, Weber and de Beaufort (1916, *op. cit.*, 48) remarked: "We do not think that the genus *Eustira* is generically distinct from *Laubuca*; we therefore give it only the value of a subgenus, containing *Eustira ceylonensis* Gthr. and our *Eustira maassi*." They distinguished the subgenus *Eustira* from *Laubuca s. str.*, by the downward curvature of the lateral line behind the pectorals, abrupt in *Eustira*, gentle in *Laubuca*.

While considering *E. ceylonensis* as a synonym of *Chela laubuca* Hamilton, Deraniyagala (1930, *op. cit.*) in a footnote commented on its doubtful similarity to species of *Danio*; but in his latest work on Ceylon fishes (Deraniyagala, 1952, *op. cit.*), he once again treated *E. ceylonensis* as a synonym of *Chela laubuca*.

In view of these conflicting views on the systematic position of *Eustira* and due to the fact that no additional material of the orthotype has been recognized from Ceylon since it was first described, a reexamination of the type material in the British Museum (Natural History) seemed desirable. Fur-

Contributions from the Scripps Institution of Oceanography, New Series, No. 1038
Reproduced by Permission

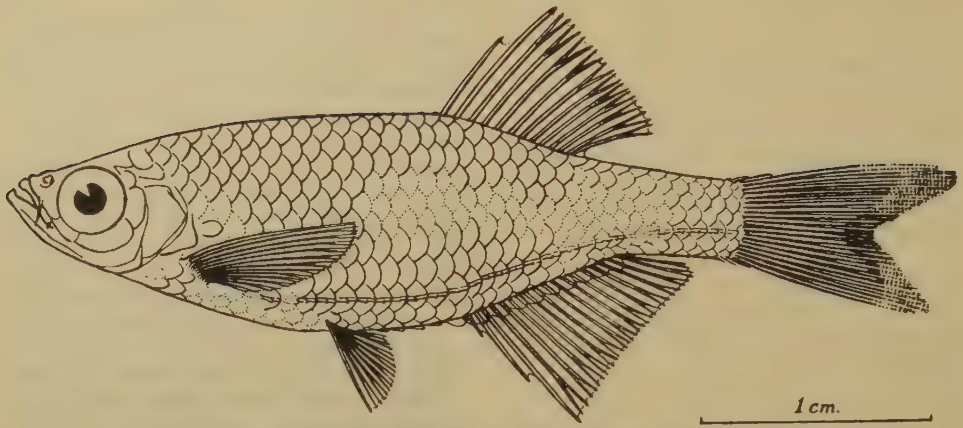

Fig. 1. *Danio malabaricus* (Jerdon) drawn from the holotype of *Eustira ceylonensis* Günther

thermore it was felt that this would help in clarifying certain discrepancies in the descriptions of the genus and species by Günther. The type series consists of six specimens cited as purchased from Mr. Cumming, from Ceylon.

While on a visit to England, the late Dr. S. L. Hora kindly examined for me the types of *E. ceylonensis* in the British Museum. In a letter dated September 23, 1953 he informed me that in "Günther's specimens the origin of D. is slightly in advance of A.; number of branched anal rays 15; scales transversely 8/1/2." No figure of *E. ceylonensis* has been published. This deficiency has now been remedied by an excellent figure of the type specimen (Fig. 1), sent to me by Dr. Ethelwynn Trewavas of the British Museum. The two pairs of rudimentary barbels, present in the specimens and shown in the drawing, escaped Günther's attention, for he characterized *Eustira* as being devoid of barbels. During my visit to the British Museum in July, 1955, I was able to reexamine once again the type material and to verify the points mentioned above. I now find that in the following important characters *Eustira* differs from *Chela* as the latter genus is defined at present (Silas, MS).

1. The dorsal fin originates ahead of the anal fin, rather than behind the front of that fin.
2. There are two pairs of barbels (none in *Chela*).
3. The pectoral fins are shorter than the head, instead of being elongate and much longer than the head.
4. The abdominal margin is rounded, rather than being keeled.

Eustira is obviously distinct from *Chela*, and its rounded abdominal margin separates it from all other cultrate genera of the subfamily Abramidinae. The combination of characters mentioned above places *Eustira* in the Rasborinae. In fact, *Eustira* fully agrees with the description of one of the well-known genera in this subfamily, namely *Danio* Hamilton. There is not a single character by which the two nominal genera can be said to differ. Hence I propose that *Eustira* be considered a synonym of *Danio*.

Only one species of *Danio*, namely *D. malabaricus* (Jerdon) is known at present from Ceylon, although the exact status of the Ceylonese form in relation to the typical form of the Cauvery drainage in southern India needs elucidation. The type specimen of *E. ceylonensis*, figured here, shows in addition to the two pairs of barbels, the following characters not noted by the original author: the pelvic fin has 8 rays (i, 7); the anal fin has 18 rays (iii, 15), the last ray divided to the base; the caudal fin has 19 rays. Taking all these data into consideration, there is not a single character by which *E. ceylonensis* can be separated from the Ceylonese form, or representative, of *Danio malabaricus*, to the synonymy of which it is here relegated.

The subgenus of *Laubuca* to which Weber and de Beaufort misadvisedly assigned the name *Eustira* is thus left without a valid name. The problem is under further study.

I wish to thank Dr. Carl L. Hubbs for going through the manuscript and Drs. Sunder Lal Hora and Ethelwynn Trewavas for the help rendered.—E. G. Silas, *Scripps Institution of Oceanography, La Jolla, California.*

(704)

(705)

EMBRYOLOGY AND EVOLUTION OF THE PELAGIC FISH EGG.—It has long been known that many species of marine fishes, and a few in fresh water, have free-floating pelagic eggs. The important role of floating eggs in ecology and distribution is well recognized, but the possible evolutionary history of this type of egg in the fishes has received little attention other than some rather desultory speculation. A recent paper by Shelbourne (1956, Journ. Mar. Biol. Assn. U. K., 35: 275–86) discussed certain characteristics of fish eggs and embryos from different ecological situations and suggested a new approach to the problem of the origin of the pelagic marine fish egg. The present note points out some exceptions to his characterization of the pelagic embryo, and offers some comments on the evolution and systematic interpretation of egg types in the fishes.

Shelbourne reviewed the contrasting characteristics of the three major ecological categories of fish eggs and embryos. Of these, freshwater demersal eggs and marine pelagic eggs differ most sharply. The former characteristically have denser yolk, the median finfolds of the embryo are low and thin, the integument is closely applied to the underlying tissue surfaces, and there is a more or less well developed circulation on the yolksac. Marine pelagic eggs, he stated, have a more dilute yolk, the embryo develops large inflated median finfolds with extensive fluid-filled subdermal spaces, and blood vessels do not develop on the yolksac. Characteristics of marine demersal eggs and their embryos fall variously between these two extremes.

Shelbourne postulated that, in order to achieve buoyancy, the yolk of the marine pelagic egg must be more highly diluted with fluid than is the yolk of a typical demersal egg. The yolk is utilized as embryonic development proceeds, but if the non-nutrient dilutent fluid were to be lost the egg would lose its buoyancy and sink. The fluid is retained by transferring it to subdermal spaces between the developing tissue layers over the yolksac and within the median finfolds that form along the body and tail. This retention of fluid results in great enlargement and inflation of the finfolds and of the covering over the yolksac and in a more or less conspicuous separation of the integument from the underlying tissues. He suggested that the open, fluid separation of the tissue layers in turn prevents formation of closed blood vessels in these regions during early stages, and that pelagic embryos thus do not have a vascular yolksac. The heart opens directly into an extensive subdermal sinus, and the free intercommunication of fluid through the subdermal spaces carries nutrient materials about and takes the place of the more usual closed-vessel circulation during early stages.

This interpretation of the embryonic basis of the pelagic egg was derived from Shelbourne's own embryological studies, supported by his extensive review of the literature on fish eggs and larvae. However, certain fishes he did not cite have pelagic eggs which do develop prominent blood vessels on the yolksac. These fishes, the allotriognaths and some of the synentognaths, are conspicuous exceptions to his key statement that the yolksac is not vascular in pelagic embryos. Examples described and figured in the literature include *Trachypterus taenia* (Lo Bianco, 1908, Mitth. Zool. Sta. Neapel, 19: 1–17), *Trachypterus cristatus* (Sanzo, 1918, R. Com. Talass. Ital., No. 65: 1–15), and *Lophotes cepedianus* (Sanzo, 1940, Mem. Com. Talass. Ital., No. 272: 1–6) among the allotriognaths; and *Oxyporhamphus micropterus* (as an "unidentified scomberesocid" in Delsman, 1924, Treubia, 5: 408–18) and *Scomberesox saurus* (Sanzo, 1940, Mem. Com. Talass. Ital., No. 276: 1–6) among the synentognaths. From materials studied at Scripps Institution I can confirm the occurrence of well-developed blood vessels on the yolksac in pelagic embryos of

ized studies by embryologists.—GRACE L. ORTON,
Scripps Institution of Oceanography, University of California, La Jolla, California.

Contributions from the Scripps Institution of Oceanography, New Series, No. 1039

Reproduced by Permission

Reprinted from the Geophysical Journal of the Royal Astronomical Society,
Vol. 1, *No.* 4, 1958

A Magnetic Survey off the West Coast of the United States between Latitudes 32° and 36° N, Longitudes 121° and 128° W

R. G. Mason

(Received 1958 July 30)

Summary

A total magnetic intensity map covering the area between latitudes 32° and 36° N and longitudes 121° and 128° W is presented. It shows a series of narrow anomalies of about 400 γ amplitude trending north–south for 300 miles over a substantially flat abyssal plain. Some possible interpretations are discussed. The anomalies arise at shallow depths beneath the ocean bottom and are consistent with the presence of relatively thin layers of magnetized material overlying a less magnetic crust; they could equally well arise from topography of the upper surface of a continuous magnetic basement for the most part concealed by an overlying blanket of sediments.

The anomalies are intersected by the Murray fracture zone, which interrupts their pattern in such a way as to suggest a right lateral displacement of about 84 nautical miles.

1. Introduction

Since the latter part of 1952 the Scripps Institution of Oceanography has been towing a total field magnetometer astern one or other of its research ships engaged in routine oceanographic investigations. With a few exceptions, as for example in the study of the Tonga Trench (Raitt, Fisher & Mason 1955), the results have been restricted to long and unrelated profiles obtained during passage of the ship. These have limited application since they give no indication of the lateral extent or direction of anomalous magnetic trends and therefore provide no basis for quantitative geological interpretation.

In August 1955 the opportunity arose to tow the magnetometer behind the U.S. Coast and Geodetic Survey Ship *Pioneer* engaged in making detailed hydrographic surveys with closely spaced and accurately surveyed lines. As a result an extensive area of the deep Pacific off the west coast of the United States (Figure 1) has now been mapped with the detail and accuracy generally associated with airborne magnetometer surveys over the land, and advantage can be taken of the techniques which have been developed for the interpretation of such surveys.

This paper deals with the practical aspects of the survey and discusses some possible interpretations consistent with present day speculation on the nature of the ocean floor. The work was supported by the U.S. Office of Naval Research.

Reproduced by Permission

2. The survey

A notable feature of the field operation was the complete coverage of the area with a regular grid of accurately surveyed lines, usually only five miles apart. The position of the ship was determined at approximately eight-mile intervals by means of a radio navigation system using ground wave propagation and fixed beacons on shore. The probable error of an observation varies with time of day and distance from the beacons but is of the order one-tenth of a mile. The ship's tracks were for the most part directed east–west, that is across the principal grain of the anomalous magnetic field, but sufficient lines were run in the north–south direction to eliminate any possibility of ambiguity in contouring.

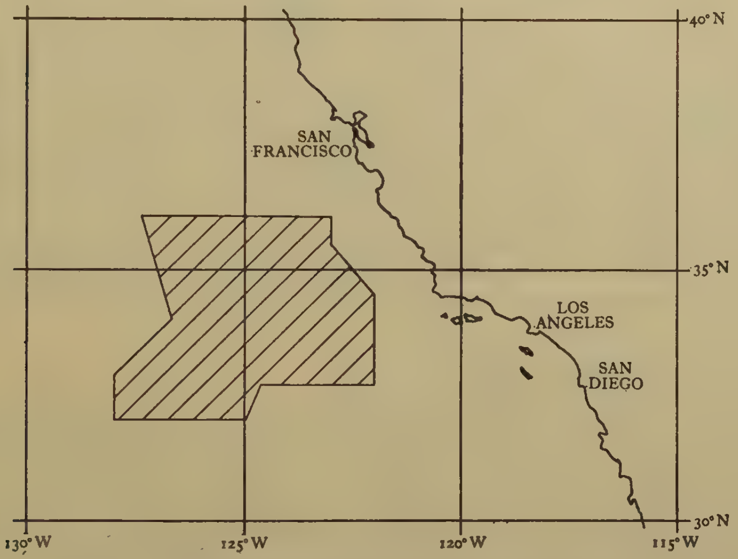

FIG. 1.—Map showing the area covered by the survey.

The magnetometer was an ASQ-3A MAD, originally designed for detection of submarines, modified for geophysical investigations according to plans developed by the U.S. Naval Ordnance Laboratory and further modified to improve its long term stability and render it suitable of use over long periods at sea. It is a gimbal mounted flux gate oriented in the direction of the Earth's magnetic field by two other flux gate elements which control orienting servo motors. The unit comprising the gimballed flux gates and associated motors was housed in a streamlined fish of plastic material which was connected to the electronic and recording equipment on the ship by a 500 ft electrical tow-cable. At that distance the effect of the ship on the measured field was negligible, ranging between about $\pm 5\,\gamma$, depending upon the ship's heading.

The magnetometer was calibrated ashore against a proton precession magnetometer at approximately monthly intervals. Its total drift over the period of the survey was $20\,\gamma$. Taking into account the principal sources of error, namely inherent drift, inaccurate adjustment, and the effect of the ship, the probable absolute error of a single observation is about $10\,\gamma$. With proper adjustment the relative error between any two points on the same line is negligible.

The magnetic map (Figure 2) was constructed by first plotting the measured field value, in 50 γ units, along the ship's track and contouring the result with an interval of 50 γ. The normal geographic change of the total magnetic intensity was determined by dividing the map into 20 mile squares, computing the mean field for each square and smoothing these values in both the north–south and east–west directions by a least squares process. A plot was then made of these smoothed values and this was subtracted from the original plot and the difference contoured with an interval of 50 γ.

No attempt was made to remove the usual time variations of the Earth's magnetic field from the data. However, records of the total field at Palo Alto, near San Francisco, were available for several periods of a few days around the time of the survey and these were found to agree closely with the corresponding records from Tucson, Arizona, magnetic observatory. Since Palo Alto is about 700 miles WNW of Tucson but less than 100 miles to the north of the area under investigation it may be concluded that Tucson records give a fair indication of time variations over the area of the survey. There were no magnetic storms during the course of the survey and the extreme range of the mean hourly values of the total field at Tucson was only 60 γ for the whole period. The mean daily range of the hourly values was 25 γ. These variations are small compared with the amplitudes of the principal anomalies and although they may introduce small errors in the pattern of the contours, particularly in the areas of shallow magnetic relief, they can have little effect on the positions and magnitudes of the more significant anomalies.

3. Preliminary interpretation

The magnetic data and the one relevant seismic section at that time available were sent to the Gravity Meter Exploration Company of Houston, Texas, for preliminary interpretation. On the basis of a number of depth estimates, using techniques which they describe as "such as might be devised putting into effect the principles outlined in GSA Memoir No. 47" (Vacquier & others 1951), they reach the general conclusion that the anomalies arise from relatively shallow structures. Referring in particular to the observed anomaly across the section marked A–A′ in Figure 2, which corresponds approximately to the location of the seismic section of Figure 3, their report states, in paraphrase:

> "In an attempt to determine the size and shape of the structures responsible for the anomalies a number of theoretical anomaly curves were computed. From Figure 2 it can be seen that a number of the more pronounced anomalies, particularly in the western part of the survey, are oriented north–south geographic. Figure 4 shows the computed anomaly for an east–west crossing of an infinite north–south block. The thickness of the block is 0·4 times the depth of burial, or approximately 2 km. The susceptibility value used is quite high, 0·0109 c.g.s. The asymmetry of the computed anomaly arises from the difference between the orientation of the block and the orientation of magnetic north. Superimposed on the computed anomaly is the measured anomaly across section A–A′. The agreement is striking. We feel that the anomalies are caused by magnetized material in the form of a relatively thin slab above the normal oceanic crust. This would correspond with the layer marked 'volcanics' on the seismic section.
>
> A point of interest is the high susceptibility value that is necessary for the theoretical curve to fit the observed data. It is high even for the basic igneous

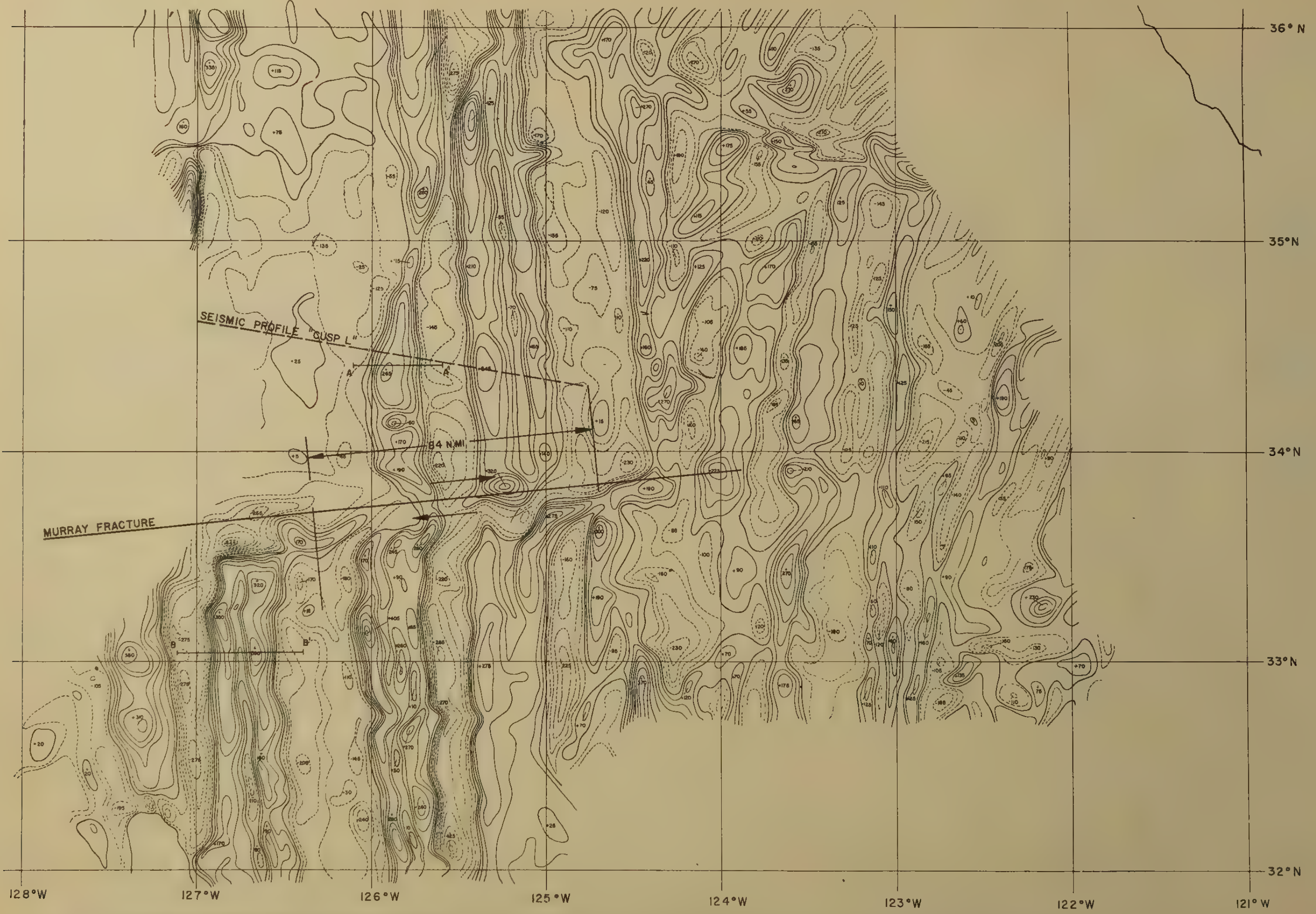
SEISMIC PROFILE "CUSP L"
MURRAY FRACTURE
84 N.MI.
A
A'
B
B'
36° N
35°N
34°N
33°N
32°N
128°W
127°W
126°W
125°W
124°W
123°W
122°W
121°W

FIG. 2.—Map of the total magnetic intensity after removal of the Earth's normal field. The contour interval is 50 γ. Lines A–A′ and B–B′ locate the magnetic profiles of Figures 4 and 6 respectively and the dashed line indicates the position of the seismic profile interpreted in Figure 3. A horizontal displacement of 84 nautical miles along the Murray fracture is indicated.

(714)

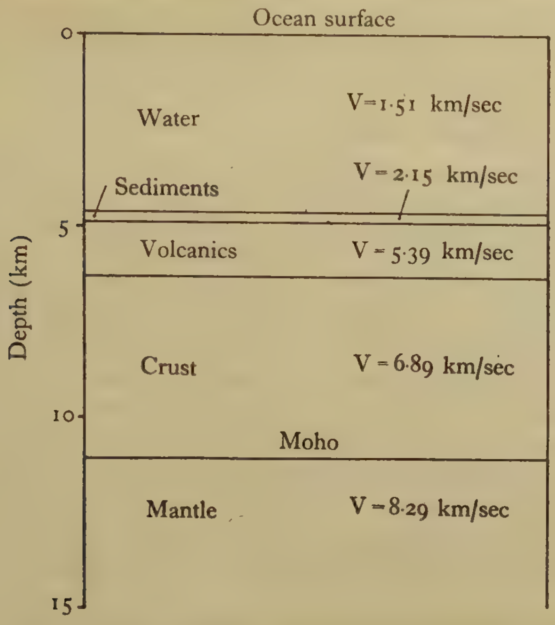
Ocean surface
Depth (km)
0
5
10
15
Water
V=1·51 km/sec
Sediments
V=2·15 km/sec
Volcanics
V=5·39 km/sec
Crust
V=6·89 km/sec
Moho
Mantle
V=8·29 km/sec

FIG. 3.—Interpretation of seismic refraction profile "Cusp L".

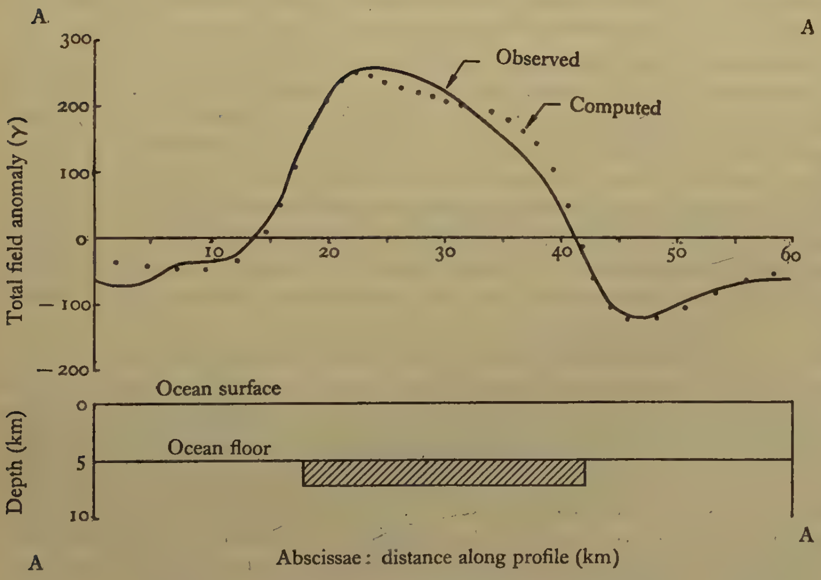

FIG. 4.—Two-dimensional interpretation of magnetic profile A–A′. The dots represent the anomaly which would be produced by an infinite north–south block, of susceptibility 0·0109, computed for a field of 50 000 γ dip 59°, declination 17° E.

materials that might be expected in this area. It is our opinion that such a high value may be indicative of appreciable remanent magnetization of the slabs obtained during cooling in the presence of the Earth's field."

4. Further two-dimensional solutions

The suggestion that the anomalies arise from lava flows is consistent with contemporary speculations on the nature of the ocean floor (Revelle & Raitt 1957). However, it is not necessarily the only possible explanation. The remarkable regularity of the more prominent anomalies throughout the several hundred miles of their length covered by the survey points to a relatively simple cause and encourages a more thorough investigation of possible two-dimensional solutions.

Referring again to magnetic profile A–A′, the solution is restricted in vertical extent by the floor of the ocean at about 4·6 km and, presumably, by the Mohorovičić discontinuity which, according to the seismic data, is here at a depth of about 11 km. It is further restricted in that physical considerations impose a maximum value on the depth of its upper boundary, as will be shown later. If certain simplifying assumptions are made about its shape and state of magnetization, then with a suitable choice of depth and susceptibility it is possible to derive a unique section, within the above limits of depth, which will fit the anomaly exactly.

Figure 5a shows one such section, derived on the basis of a uniformly magnetized single continuous section with a plane lower surface at a depth of 6·3 km, corresponding to the base of the "volcanics", and with induced and permanent magnetization in the direction of the present field equivalent to a susceptibility of 0·015. The derived upper surface, which is unique, extends at its highest point into the sedimentary layer. This and the sections discussed later were built up, by trial and error, of several hundred infinite rectangular strips each 0·5 km wide by 0·2 km thick. The observed curve was matched to within one or two γ.

Similar computations have been made for a plane upper surface. Figure 5b shows three such sections based respectively on equivalent susceptibilities of 0·015, 0·0075 and 0·005, the upper surface in each case lying at a depth of 5 km, corresponding to the base of the sediments. The first is contained almost entirely within the "volcanics" layer, the second extends well down into the crust and has steeper edges, the third is terminated by the Mohorovičić discontinuity. In general, for a fixed upper surface an increase in susceptibility leads to a thinner section of similar shape but more drawn out at the edges, a reduction makes the section thicker and its sides steeper. In theory there is no upper limit to the susceptibility, and corresponding thinness, of the section, but the depth limitation imposed by the Mohorovičić discontinuity leads to a lower limit of 0·005.

The result of increasing the depth of the upper surface is illustrated in Figure 5c. The sides become increasingly steeper until at a depth of 6·2 km, for a susceptibility of 0·015, the structure becomes an almost rectangular block with its lower surface at 7·8 km. This block is the deepest structure of susceptibility 0·015 that can be fitted to the anomaly, though it is possible to make the upper surface still deeper, and the lower surface correspondingly shallower, by increasing the susceptibility. The limiting case is an infinitely thin sheet, of infinite susceptibility, at a depth of 7·0 km.

In their report, the Gravity Meter Exploration Company draw attention to the fact that several of the north–south anomalies appear to have two maxima, with an intervening minimum, and suggest that the lines of minimum field have

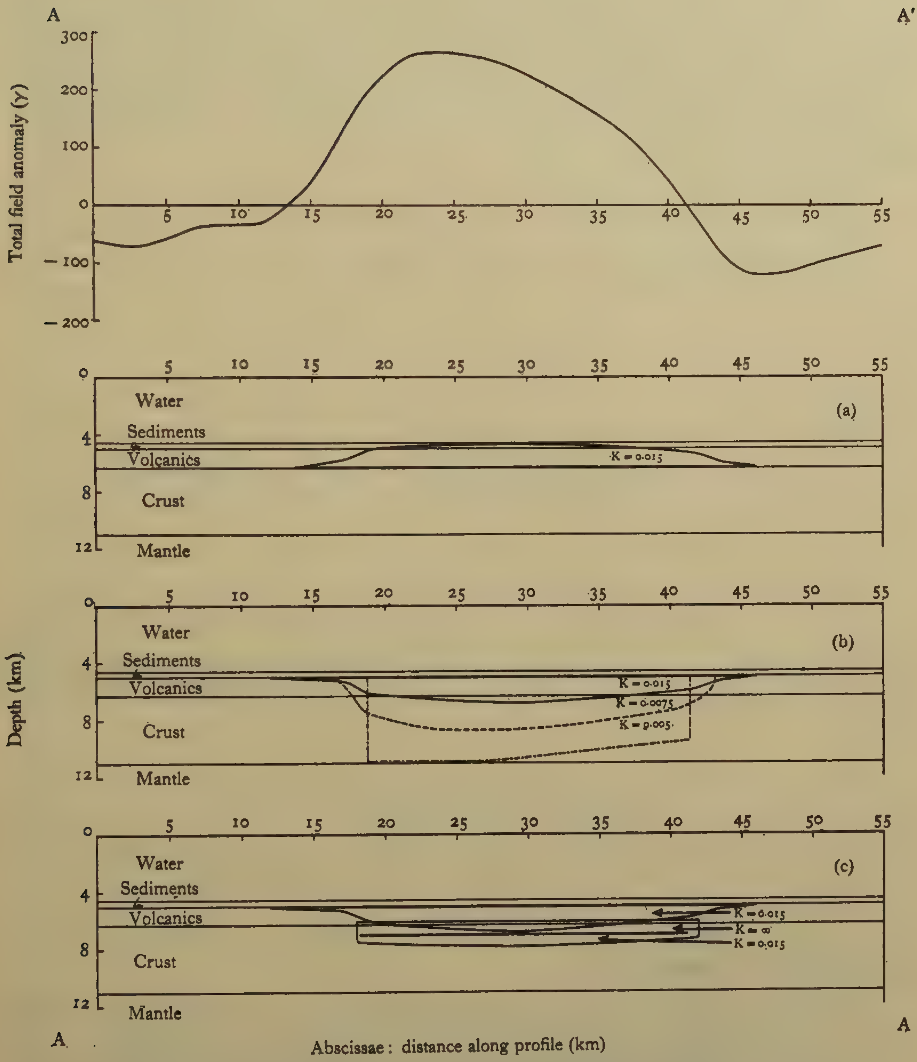

FIG. 5.—Two-dimensional interpretation of magnetic profile A–A′ for a field of 50 000 γ dip 59°, declination 17° E: (*a*) with plane lower surface at 6·3 km depth, (*b*) with plane upper surface at 5 km depth, for various susceptibilities, (*c*) showing the effect of varying the depth of the upper surface.

some structural significance. Figure 6 shows the magnetic profile along the line marked B–B′ in Figure 2, which crosses one such anomaly, together with a derived section based on the assumptions of a plane upper surface at a depth of 5 km and uniform magnetization equivalent to a susceptibility of 0·015 in the present direction of the Earth's magnetic field. In general this section responds to changes in depth and susceptibility in the same way as the sections of Figure 5, except that for greater depths the section breaks into two isolated parts. On the assumption of a depth of 11 km to the Mohorovičić discontinuity, the least possible susceptibility is 0·01.

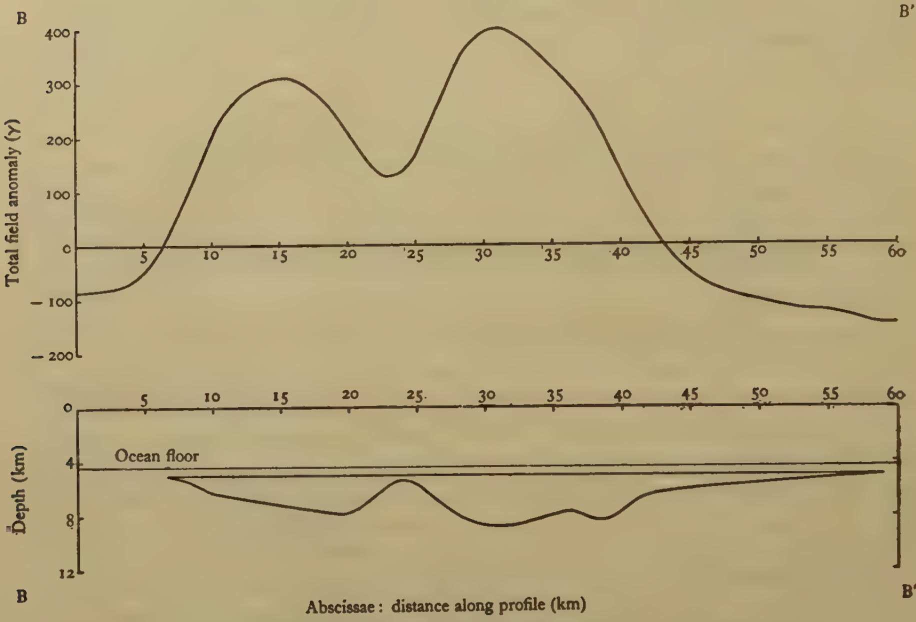

FIG. 6.—Two-dimensional interpretation of magnetic profile B–B′ for a field of 50 000 γ, dip 59°, declination 17° E, susceptibility 0·015.

5. Remanent magnetization

Attention was drawn earlier to the high susceptibility values needed to explain the observed anomalies. The preceding analysis shows that for section A–A′ the least possible susceptibility is 0·005, corresponding to the improbable case of a structure extending from the ocean bottom to the base of the crust. For the more plausible structures the susceptibility must be well in excess of 0·01, or higher than the known susceptibilities of any of the common rocks. This strongly suggests that the rocks involved here are basic igneous rocks, which are characterized not only by a high susceptibility but also by a high intensity of remanent magnetization, commonly several times greater than the intensity of induced magnetization in the Earth's field. Thus in the present case, where the Earth's field is 50 000 γ, an apparent susceptibility of 0·015 could be accounted for by a true susceptibility of 0·005 together with an intensity of remanent magnetization of 0·005 G in the direction of the Earth's field, both acceptable values for a basic igneous rock.

The interesting question arises as to whether, since the direction of remanent magnetization will correspond to the direction of the Earth's field at the time when the rocks were formed, in all probability different from the present direction, anything can be learned about the direction of magnetization that may throw light on the age of the formations. Two factors bear on the problem. Geological evidence (Menard 1955) points to a Cretaceous or early Tertiary age for the Murray fracture, and the magnetic structures are older than this since their pattern is interrupted by it. Palaeomagnetic measurements (see Runcorn 1956 for a summary of relevant information) suggest that since Jurassic times the direction of the Earth's magnetic field in North America has centred around that of a dipole field, with normal or reversed polarity, but that during earlier periods it was quite different.

Figure 7 shows four sections computed to test the effect of varying the horizontal direction of remanent magnetization. The susceptibility was taken to be 0·005 in all cases and the intensity of remanent magnetization 0·005 G dipping at an angle of 59°, the present dip, but in four different azimuths, namely 34° W, 0°, 17° E (the present magnetic declination) and 34° E respectively. Although the section corresponding to the present direction is perhaps the most symmetrical, there is no compelling reason for preferring one to the other or for rejecting any one. This lack of sensitivity to azimuth is a consequence of the fact that only the components of magnetization perpendicular to the strike, i.e. the vertical and the

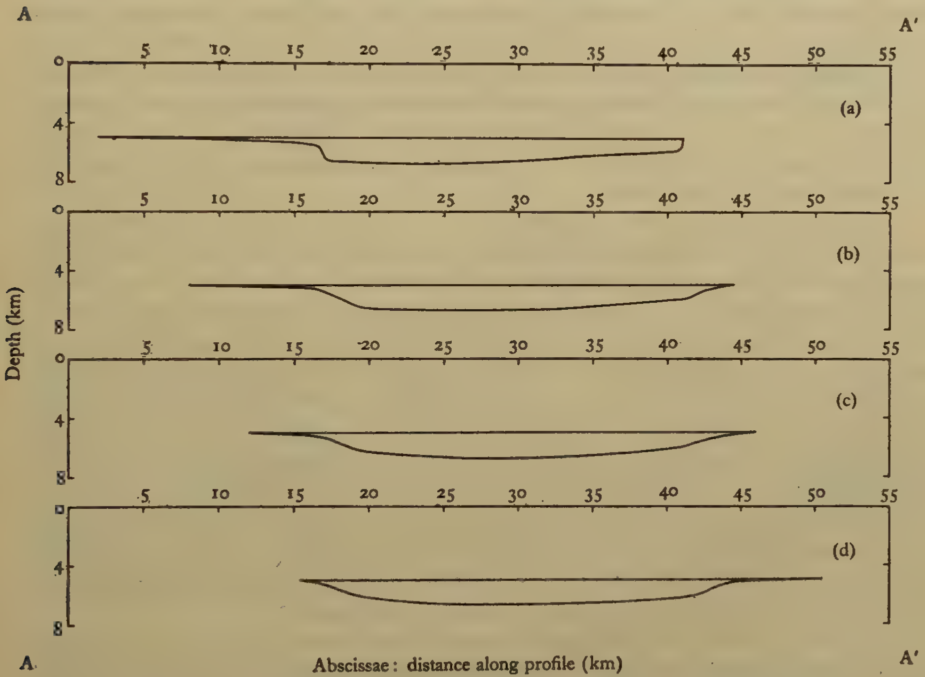

FIG. 7.—Two-dimensional interpretation of magnetic profile B–B′ for a field of 50 000 γ, dip 59°, declination 17° E, susceptibility 0·005 and intensity of remanent magnetization 0·005 G dipping at 59° in azimuths (*a*) 34° W, (*b*) 0°, (*c*) 17° E, (*d*) 34° E.

east–west, contribute to the anomaly, and for steep dips the former predominates. For a dip of 70° all computed sections would lie between the limiting sections of Figure 6, irrespective of azimuth. A more thorough investigation is beyond the scope of this paper. However, it seems clear that, since any remanent magnetization is required to augment rather than to oppose the present field, the vertical component must be substantially downwards and this makes any appreciable degree of reversed magnetization unlikely if the magnetic poles were anywhere near their present positions.

6. Conclusions

Although the discussion of the preceding sections was based upon a much simplified picture of the situation, there can be little doubt that the major positive anomalies are underlain by an excess, probably totalling at least 1 km in thickness, of a material highly magnetic by comparison with adjacent formations and almost certainly a basic igneous rock. Its upper surface is relatively shallow and probably lies in the "volcanics" layer of the seismic section, or at most no deeper than in the upper part of the crust. Its extent in depth is uncertain but it may be supposed to terminate at a depth no greater than the Mohorovičić discontinuity. Despite its thickness it shows little or no correlation with topography, as far as can be judged from the best available topographic maps, suggesting that it is either buried in consolidated sediments of relatively high seismic velocity or emplaced in less magnetic igneous rocks.

The most obvious and acceptable geological explanation is that the excess material represents lava flows which have spread out over the floor of the ocean, possibly filling pre-existing troughs, or depressions produced by the weight of the accumulating flows. This picture is consistent with the section of Figure 4a and the upper section of Figure 4b, which thin out at the edges in a manner characteristic of lava flows. Within the limits of the survey the major anomalies cover an area of about 50 000 sq km. In extent therefore, and in thickness, the flows would rank with the largest continental lava fields, such as the Columbia River basalts which cover an area of 120 000 sq km and in places reach thicknesses approaching 2 km. An alternative hypothesis, consistent with the section of Figure 4a, is that the excess material represents topography of the upper surface of the crust, itself supposedly the more magnetic layer, brought about by marginal faulting or by folding. In that case it must be presumed that the topography has for the most part been covered by a blanket of sediments.

Whatever their origin and form, the rock bodies which give rise to the north–south anomalies indicate lines of weakness in the ocean floor which were active prior to the formation of the Murray fracture zone. An offset of the pattern of the magnetic features as they cross it suggest a right lateral displacement of 84 nautical miles along the Murray fracture. This displacement, the north–south lineation of the anomalies and the right lateral displacement along the San Andreas fault, may well be related by a single structural hypothesis, possibly connected with a westerly movement of the North American continent relative to the floor of the Pacific.

This paper has been mainly concerned with the north–south anomalies because they are the most striking feature of the magnetic map and because the seismic section provides a framework for discussion which is lacking in the case of the NNE–SSW trending anomalies on the eastern portion of the map. It is hoped that further geophysical investigations, particularly seismic, planned on the basis of this map will help to throw more light on the complicated structural situation in this area and hence on the more general problem of the relationship between continent and ocean.

7. Acknowledgments

The work was performed while the author was a member of the staff of the Scripps Institution of Oceanography, on leave of absence from Imperial College, London. He gratefully acknowledges the co-operation of the U.S. Coast and Geodetic Survey in connection with the ship's operation and in providing records from Tucson Magnetic Observatory, the facilities for calibrating the magnetometer, and the Palo Alto records, generously made available by the Varian Associates of Palo Alto, California, and the interest taken in the results by Drs L. L. Nettleton and N. C. Steenland of the Gravity Meter Exploration Company of Houston, Texas. He is indebted to various of his colleagues at Scripps for their advice and encouragement, in particular to the Director, Dr Roger Revelle, to Drs H. W. Menard and Victor Vacquier for their advice on the geological and magnetic aspects of the work respectively, to Dr R. W. Raitt who supplied the seismic data and to Mr Arthur D. Raff, who was responsible for the engineering aspects of the project and supervised the field operation.

Imperial College of Science,
London, S.W.7.
1958 *July* 29.

References

Menard, H. W., 1955. *Bull. Geol. Soc. Amer.*, **66,** 1149–1198.

Raitt, R. W., Fisher, R. L. & Mason, R. G., 1955. *Geol. Soc. Amer. Spec. Paper* 62, 237–254.

Revelle, R. R. & Raitt, R. W., 1957. "Sediment Thickness of the Pacific Ocean Floor". Paper read at the 10th Annual Conference, Institute of Geophysics, U.C.L.A., Dec. 1957.

Runcorn, S. K., 1956. *Encycl. of Physics*, **47,** Geophys. I, 470–497.

Vacquier, V., Steenland, N. C., Henderson, R. G. & Zietz, I., 1951. *Geol. Soc. Amer. Mem.* 47.

Reprinted from
ANNUAL REVIEW OF NUCLEAR SCIENCE
Vol. 8, 1958

THE RADIOACTIVITY OF THE ATMOSPHERE AND HYDROSPHERE[1,2]

By Hans E. Suess[3]
Scripps Institution of Oceanography, La Jolla, California

Introduction

Radioactive nuclear species that occur on the surface of the earth can be grouped into three classes: (*a*) Extremely long-lived species that have survived from the time when the elements formed (primary radionuclides) and their daughter products (secondary radionuclides). (*b*) Radioactive nuclei that are currently formed in nature, primarily by cosmic-ray induced processes. (*c*) Man-made radioactive substances, such as those produced through the testing of atomic devices or in nuclear reactors.

Radioactive isotopes follow the geochemical behavior of their respective elements. They can be used as tracers in the study of geochemical processes. If their rates of radioactive decay are comparable with the rates of these processes, then the possibility exists of determining the rate of the geochemical processes through the measurement of radioactivities. The long-lived radioactive species of class (*a*) have proved extremely useful for geologic age measurements and the study of geologic processes of a time scale of millions of years. Phenomena occurring in the atmosphere and hydrosphere, such as mixing and chemical transfer, will occur with time scales rarely exceeding a few thousand years. For their study activities of relatively short half lives will be useful.

It appears now that both the hydrosphere and the atmosphere have to be treated as consisting of at least two parts, between which transfer and exchange of material is relatively slow. One may consider two atmospheric reservoirs: the stratosphere, containing about one-sixth of the atmosphere by weight, and the troposphere. The two marine reservoirs are: the so-called

---

[1] The survey of literature pertaining to this review was completed in April, 1958.

[2] The following abbreviations are used throughout the text: curie = c; disintegrations per minute = d/m; half-life = $T\frac{1}{2}$; millicurie = mc; microcurie = μc; micromicrocurie = μμc; mile = mi.; square centimeter of earth's surface = cm._e^2; sunshine unit = SU; tritium unit = TU.

The following conversion factors will be found useful: 1 c = 2.22×10^{12} d/m; 1μμc = 2.22 d/m; 1 mc/mi.^{2} = 0.0856 d/m per cm.^{2}; 1 μc/10^6 cu. ft. = 78.5 d/m per m^3; 1μμc/gal. (U.S.) = 0.59 d/m per liter; 1 megacurie distributed uniformly over the whole earth = 0.435 d/m cm._e^2; 1 TU (1 T atom per 10^{18} H atoms) = 6.6 d/m T per liter H_2O; 1 SU = 2.22 d/m Sr^{90} per gm. Ca.

[3] Contribution from the Scripps Institution of Oceanography, New Series. This paper represents in part results of research carried out by the University of California under contract with the Office of Naval Research and the Atomic Energy Commission.

Contributions from the Scripps Institution of Oceanography, New Series, No. 1041
Reproduced by Permission

mixed layer, i.e., water above the thermocline which represents about one-fortieth of the total ocean water, and deep ocean water.

For the study of mixing phenomena between these reservoirs, the discovery of cosmic-ray produced radioactivities has opened a wide field of new possibilities. The most important of these activities is undoubtedly carbon 14 found to occur in nature by Libby (1) in 1948. A few years later natural tritium was discovered by Libby (2) and co-workers and independently by Faltings & Harteck (3). The relatively large amounts of artificially produced tritium released during the past years into the atmosphere have now obscured the original natural tritum distribution. Fortunately, earlier measurements by Libby and co-workers (4, 5) answer most of the questions relative to natural tritum. Following the work of Libby, several investigators have now found a number of additional radioactive nuclear species currently produced by cosmic rays in nature. With respect to the cosmic-ray produced as well as to the artificially formed radioactive nuclei, two types of quantities are primarily of interest: (*a*) concentrations and (*b*) production and fallout rates. Concentrations of radioactivities are usually given as disintegrations per unit of time per amount or volume, or curies per amount or volume.

In general, it is necessary to use refined experimental techniques for measurements of low-level activities present in nature. A previous article by Anderson & Hayes (6) summarizes recent advances in these techniques. Libby's method of subtracting the μ-meson background by anticoincidence counting is generally applied for β-counting. Comparable sensitivities can be achieved for the measurement of γ-activities by use of scintillation counting techniques, preferably with multi-channel instruments.

The review article by Kohman & Saito (7) on radioactivity in geology and cosmology contains more general information on properties and occurrence of radionuclei in nature. The following paper can only give a brief account of the nature of geochemical, meteorological, and oceanographic problems involved in the interpretation of the distribution of radioactivity in the atmosphere and hydrosphere of our planet. It attempts to facilitate the selection of the original literature for further study.

PRIMARY RADIONUCLIDES AND THEIR DAUGHTERS

Table I lists the concentrations of the extremely long-lived nuclides in ordinary standard sea water (salinity, 3.5 per cent) according to the most recent measurements. This table does not include the radionuclides Sm^{147}, Lu^{176}, La^{138}, and Re^{187}. The concentrations of these elements are not well known. The relatively high solubility of uranium in sea water is due to carbonate complexing. The solubility of thorium appears to be much smaller.

The upper limit of the thorium concentration listed in Table I is based on two determinations of Pacific Ocean water by Sackett, Potratz & Goldberg (8). Radioactive tracer techniques using Th^{234} were employed. The uranium values given in Table I are those of Rona, Gilpatrick & Jeffrey (9) who employed a mass-spectroscopic isotope dilution technique, with U^{235}

(724)

TABLE I

Average Concentrations of Radioactive Elements in Sea Water

Element	Concentration		Isotope	$T_{\frac{1}{2}}$ 10^9y.	d/m liter	Reference
	g/g*	mol./liter				
Th	$<5\times10^{-11}$	$<2\times10^{-10}$	Th^{232}	13.9	$<0.01\alpha$	(8)
U	3.3×10^{-9}	1.5×10^{-8}	U^{235}	0.71	0.23α	
			U^{238}	4.51	5α	(9)
K	3.8×10^{-4}	1×10^{-2}	K^{40}	1.3	$470\beta+\gamma$	(7)
Rb	1.21×10^{-7}	1.35×10^{-6}	Rb^{87}	59	5.3β	(10)

* Grams of element per gram of sea water.

as spike. These authors obtained, for five samples from the Atlantic and the Gulf of Mexico and for one from the Pacific Ocean, values ranging from 3.19 to 3.45 μg./liter of sea water, with an average as given in Table I. The new rubidium value of Smales & Webster (10) was also determined by means of stable isotope dilution.

Table I does not contain the daughter products of uranium and thorium which behave in a rather complex way. The low solubility of thorium causes Th^{230} (ionium, half life 80,000 years) to precipitate with thorium in a time which is short compared to this half life. Urry (11) was the first to attempt to use the ionium concentration in deep-sea sediments for estimates of the rate of sedimentation. However, the ionium concentrations were derived by measuring its daughter radium and by assuming radiogenic equilibrium between ionium and radium. It was shown by Arrhenius & Goldberg (12) that, after deposition, radium migrates into certain minerals and, therefore, may not always remain in the layer of deposition. Radium also redissolves in part with the calcium and goes back into the deep ocean water. This fact was shown by Koczy (13) who found deep ocean water richer in radium than the ocean water in higher layers. Ionium dates of ocean sediments based on radium measurements will, therefore, frequently not be reliable. Such dates can only be accepted after a detailed study of various factors.

Direct measurements of the ionium concentration in sediments by assays of thorium and of its isotopic composition were first attempted by Picciotto & Wilgain (14). More recently, more extensive measurements have been made by Goldberg & Koide (15) leading to reliable values for deposition rates of sediments.

Blifford *et al.* (16) have recently carried out new measurements of atmospheric radon and thoron concentrations in different parts of the world. The radon concentration is about one order of magnitude higher over continental areas than over the oceans. It varies with the nature and condition of the soil. The concentration of thoron ($T\frac{1}{2} = 59$ sec) is about a factor of ten smaller than the concentration of radon. The results of Blifford *et al.*, agree with early measurements of Benndorf & Hess (17), but are lower than those reported by Israel (18). A few of Blifford's measurements are listed as examples in Table II. The values represent daily averages at approximately 1600 local time. A diurnal cycle in the radon concentration was found to exist at all locations. This observation agrees with previous findings of Wilkening (19). The causes of these effects have not yet been investigated in detail. Pronounced seasonal variations were observed also. Decay products from radon and thoron in rains have been studied by Damon & Kuroda (20). The concentration of radionuclides produced by spontaneous fission of U^{238} in the atmosphere and hydrosphere is today many orders of magnitude below the limits of detection because of the presence of much larger quantities of artificial fission products.

TABLE II

AVERAGE CONCENTRATION OF RADON AND THORON IN AIR FROM MEASUREMENTS BY BLIFFORD *et al.* (16) IN 1950 AND 1951

Place	d/m per meter³	
	Radon	Thoron
U.S.A.		
Washington, D. C.	100	4
Chicago, Ill.	50	5
West Coast	10	0.6
Puerto Rico	0.2	0.07
Pacific Islands	1.5	low
North Africa	17	5
Alaska	7	0.1

COSMIC-RAY PRODUCED RADIOACTIVITIES

The amount of radioactive particles produced by cosmic-ray events is proportional to the incoming cosmic-ray flux and shows the same dependence on geomagnetic latitude as does the cosmic-ray intensity. The difference in the production rate per $cm._e^2$ between geomagnetic equator and poles is approximately a factor of four (21). The average number of primary cosmic-ray particles that hit the earth is of the order of one per $cm.^2$ and per second. The possibility of secular variations in the cosmic-ray intensity resulting from changes in the magnetic field of the earth and the possible effects of such variations on the radiocarbon inventory have been discussed by Elsasser, Ney & Winckler (22). The number of nuclei of a certain nuclear species formed by cosmic rays can sometimes be estimated from star production rates in nuclear emulsions or from yields in high-energy experiments (23).

Carbon 14.—An account of the production and distribution of natural radiocarbon has been given in a previous article by Anderson (24) in 1953. The atomic C^{14} produced by (n, p) reaction on N^{14} is oxidized in the atmosphere to molecular CO_2. The possibility has been discussed by Harteck (25) that this oxidation is slow and that the C^{14} remains in the form of carbon monoxide for many years before the oxidation is completed. Experimental proof of such delay in the oxidation will be difficult to obtain because of the presence of man-made carbon monoxide in the atmosphere.

Since 1954 noticeable amounts of artificially produced C^{14} have been added to the atmosphere. The following applies to the situation before artificial C^{14} became significant:

TABLE III

Amount of Carbon in the Various Exchangeable Reservoirs (1) as Revised in (28)

Reservoir	Carbon content gm. per cm.,^{2}
Atmospheric CO_2	0.126
Terrestrial biosphere (living)	0.06
Humus	0.215
Marine biosphere	0.002
Dissolved organic matter in sea	0.533
Total inorganic carbon in sea	6.94
Total exchangeable carbon	7.88

Table III lists the so-called reservoirs into which C^{14} is distributed and the amounts of carbon present in each reservoir (1, 26, 27, 28). As a first approximation, one may assume that the distribution of C^{14} into these reservoirs will occur within a time which is short compared with the average life of C^{14}, i.e., 8000 years. If this assumption is made and if isotope fractionation effects are neglected, a constant C^{14}/C^{12} ratio is to be expected for all the different reservoirs. Actually, minor deviations (of the order of a few per cent) from a completely uniform C^{14}/C^{12} ratio occur for two reasons: (*a*) The equilibrium distribution is not quite uniform because of mass dependent terms in the thermodynamic constants for isotope exchange. (*b*) The exchange and transfer rate of CO_2 between the reservoirs is not infinitely fast compared with the average life of C^{14}.

For the carbonates of surface ocean water these two effects just happen to cancel each other almost completely. Marine beach shells show the same C^{14}/C^{12} ratio within one per cent as organic terrestrial plant material, if one corrects for effects from industrial fuel combustion (see below), although the C^{13}/C^{12} ratio is about 2.5 per cent higher in carbonate than in wood (29). This difference of 2.5 per cent in the C^{13}/C^{12} ratio corresponds to a difference of 5 per cent in the C^{14}/C^{12} ratio and shells should therefore show a specific C^{14} activity about five per cent higher than that of wood of the same age. Actually, no significant difference in the C^{14} activity of shells and wood is found, and therefore one may say that marine surface material has an apparent age of about 300 or 400 years. This fact can be used for estimating the residence time of CO_2 in the atmosphere before it becomes dissolved into the sea.

If one assumes that mixing within the ocean is fast compared with 400 years, or, in other words, that the average carbon in the ocean shows an apparent age of 300 to 400 years, then the residence time (τ_s) for the carbon in the ocean would be about 300 to 400 years and for the atmosphere (τ_a) about five to seven years. Slower mixing would make these residence times correspondingly larger. The residence time (τ) is defined as the amount of carbon in a reservoir divided by the amount transferred into other reservoirs or exchanged with the carbon of other reservoirs per year.

Values for τ_a can be obtained in an entirely different way by considering the effect of industrial fuel combustion on the specific C^{14} activity of carbon. Between the end of the nineteenth century and 1950, approximately 12 per cent of the CO_2 present in the atmosphere was added to the atmosphere. This was CO_2 derived from the combustion of fossil fuel, and was, therefore, free of C^{14}. If none of this CO_2 had been absorbed by the oceans, or had equilibrated its isotopic composition with other reservoirs, then the specific C^{14} activity of wood grown in 1950 should be about 12 per cent lower than that of wood grown before the beginning of the industrial revolution. Exchange with the carbon of the terrestrial biosphere could lower this effect by not more than a factor of two. The actual decrease in the specific activity of wood since the nineteenth century has been measured by Suess (30), Hayes, Anderson & Arnold (31), Williams (32), and Fergusson (33). A decrease has been observed by all authors and values have been obtained ranging up to four per cent. The high values, however, undoubtedly arise from local contamination of air masses near industrial centers. It seems now fairly well-established that the world-wide C^{14} depletion of atmospheric carbon dioxide in 1950 was about 1.75 per cent. Fergusson gives for this quantity 2.03 ± 0.15 per cent for 1954. The effect is the same within 0.5 per cent in both hemispheres. Fergusson (33), therefore, concludes that atmospheric mixing across the equator occurs within less than two years.

From these data the rate of uptake of CO_2 in the oceans can be calculated and a value of about seven years is obtained for the residence time τ_a of CO_2 in the atmosphere if fast mixing is assumed in both reservoirs. This value, however, is to be taken here as an upper limit, because slow mixing of the top layer of the oceans above the thermocline into deeper water masses would lead to a shorter residence time of CO_2 in the atmosphere. Revelle &

Suess (26) conclude from the empirical data available that the residence time of CO_2 in the atmosphere before it is dissolved in the sea, τ_a , must be of the order of ten years. It is at present hardly possible to give a more exact figure for τ_a, because the processes which have to be considered for a more accurate calculation seem to have rate constants of comparable orders of magnitude. In particular, the overturn time of the terrestrial biosphere and the mixing rate through the marine thermocline are presumably also of the order of magnitude of ten years and are not well-known.

Attempts to obtain a more accurate figure for τ_a from detailed calculations that include estimates on the rate of internal ocean mixing were made by Craig (28) and by Fergusson (33). Craig gives $\tau_a = 7 \pm 3$ years on the basis of a specific ocean model and independently by comparing the observed C^{14} activities with the estimated cosmic-ray production rate of C^{14}. Fergusson obtains $\tau_a = 2$ years, a result inconsistent with the lower limit derived from the apparent age of surface sea carbonate.

Over the past 50 years a decrease of the order of one per cent in the C^{14} activity of marine carbonates has been observed by Williams (32) and by Rafter (34). This small effect from industrial fuel burning on marine surface carbonate is of the expected magnitude.

Measurements at the Lamont Geological Observatory (35) show the existence in the Atlantic of deep water masses with an apparent C^{14} age of more than 1000 years relative to surface water. Fergusson & Rafter (36) obtained similar results for the South Pacific. More experimental results will be needed for a conclusive interpretation of the picture.

Tritium.—The concentration of the hydrogen isotope, tritium, in rains and surface waters is commonly given in tritium units; one tritium unit is the concentration corresponding to a T/H ratio of 10^{-18}. Surface ocean water and oceanic rain contain in general about one TU of natural tritium, whereas the tritium concentration in rain over continents, in rivers and lakes is of the order of several TU. Since about 1954 these amounts have been radically changed by the addition of artificial tritium into the atmosphere. Fortu-

TABLE IV

AVERAGE NATURAL TRITIUM CONCENTRATIONS (PRE-1954) ACCORDING TO LIBBY *et al.* (4, 5, 38)

Material	$T/H \times 10^{18}$
Ocean surface water	~1
Marine rains	~1
Chicago rains	7.8
Mississippi River (St. Louis)	6.0
Lake Michigan	1.6
French and Italian wines (corrected for T decay)	4
Antarctic snow	16

(729)

nately, a sufficiently large number of tritium measurements exist on samples collected prior to 1954 which give a fairly complete picture of the occurrence of natural tritium. Measurements of natural tritium are still possible by the application of Libby's idea of using vintage wines as a source of water of a known age from the time before artificial tritium contamination became important. Also Arctic and Antarctic ice contains a record of tritium concentrations from previous times.

As an air mass moves over a continent, its tritium content increases because of an addition of newly formed tritium to the atmosphere and lack of drainage into the ocean. In the evaluation of this effect, the steady-state conditions of the tritium in the water vapor of the air, in the ground water, in lakes, and in rivers have to be considered with respect to incoming and outgoing amounts across the continental boundaries.

A material-balance study of tritium in the water vapor over a continent gives the cosmic-ray production rate of tritium in the atmosphere. Earlier estimates (4, 5) seem to indicate a production rate $\overline{Q}=0.14$ T/cm.^{2} sec. in agreement with estimates from nuclear production cross sections and cosmic-ray intensities. However, Craig (37) has drawn attention to the fact that the results of Kaufman & Libby (4) and von Buttlar & Libby (5) can only be interpreted in a consistent way by assuming a considerably larger value of $\overline{Q}$. This conclusion follows from a more detailed discussion of meteorological data, as well as from the interpretation of tritium measurements of surface ocean water, with the assumption that mixing times are in agreement with the observed C^{14} distribution.

According to Begemann & Libby (38) a higher $\overline{Q}$ value is also in agreement with more recent observations of the behavior of artificial tritium on the North American continent. Their data on artificial tritium give residence times for tritium in various continental water bodies that can be used for calculating $\overline{Q}$ from the data on the distribution of natural tritium. Begemann and Libby conclude that about one tritium atom/cm.^{2} sec. must reach the surface of the earth. The discrepancy of such a $\overline{Q}$ value with the value $\overline{Q}<0.4$ derived from tritium production cross sections was taken by Feld (64) and by Craig (37) as an indication that tritium from the sun's surface might be accreted by the earth. If most of the tritium came from extraterrestrial sources, then an influx of about 1.7 T atoms/cm.^{2} sec. would have to be assumed, with about 1.2 atoms/cm.^{2} sec. reaching the earth's surface (37).

The earth's atmosphere contains about 0.5 p.p.m. (by volume) of molecular hydrogen. A very remarkable observation was made by Faltings & Harteck (3) who found that this free hydrogen contains over a thousand times more tritium than the water vapor in air. Harteck & Suess (39) found that the deuterium content of this hydrogen does not correspond to the equilibrium concentration but is approximately the same as in ordinary water. They concluded that the hydrogen must be produced photochemically in the upper atmosphere. Harteck (40) attempted to explain the high tritium concentration in the free H_2 by considering the individual steps in the oxidation mechanism of the cosmic-ray produced tritium atoms to water. However, if slow mixing of stratospheric and tropospheric air is assumed, with a residence time of stratospheric air comparable to the half life of tritium (see below), then it is possible to account for the high tritium concentration of the free atmospheric hydrogen by the simple assumption that it reflects conditions prevailing in the upper atmosphere, where the water vapor concentration is low and the HTO/H_2O ratio should, therefore, be very high.

Beryllium 7 and beryllium 10.—The natural occurrence of these isotopes was discovered by Arnold & Al-Sali (41) and Arnold (42), respectively, and their existence was confirmed by Peters and his collaborators (43, 44). Be^7 is present in measurable amounts in rains. It can, after chemical separation, be identified by its 0.479 Mev γ-radiation that occurs in 11 per cent of the disintegrations. Be^{10} was identified in pelagic sediments of extremely low rate of deposition, so that the extraction from one single sample contained the Be^{10} deposited during some 100,000 years.

A careful theoretical study of cross sections for the production of Be^7 by cosmic rays was made by Benioff (45). From a comparison of $\overline{Q}$ values thus obtained with the empirical ones given by Arnold, Benioff concludes that the Be^7 formed in the stratosphere does not contribute appreciably to the activity found in rains, and that the hold-up time in the stratosphere must be long compared with the Be^7 half life of 54 days. This agrees with observations on artificial fallout (see below). The washout time of Be^7 from the troposphere was found to be of the order of a few weeks, again in agreement with other evidence.

Other cosmic-ray produced radionuclides.—The data on other cosmic-ray produced activities discovered in rains are most incomplete. The values listed in Table V are based on a few measurements of a more or less preliminary nature. In most cases more work seems essential to establish conclusive evidence.

ARTIFICIALLY PRODUCED RADIOACTIVITIES

The man-made radionuclides introduced into the atmosphere and the oceans consist primarily of fission products of U^{235} and Pu^{239}. Hydrogen bombs produce tritium in amounts comparable to or larger than the total inventory of natural tritium on the surface of the earth. The radiocarbon concentration in the atmosphere has been increased noticeably over the past years. Other neutron-induced activities generated by nuclear bombs are relatively small but measurable (52). Finally, the presence of transuranium elements in H-bomb debris has been reported (53).

Fission products.—Our knowledge of the distribution of artificially produced fission products on the surface of the earth is to a large extent based on the work of Libby and co-workers. In particular, Sr^{90} determinations have been carried out at the University of Chicago under the name "Sunshine project" since 1950 (54).

Libby (55) distinguishes three types of fall-out from atomic weapons: (*a*)

TABLE V

APPROXIMATE AVERAGE CONCENTRATIONS AND PRODUCTION RATES OF COSMIC-RAY PRODUCED RADIOACTIVITIES

Isotope	$T_{\frac{1}{2}}$	d/m per liter rain	Atoms per cc. rain	$\bar{Q}$: atoms per minute per cm.²		Reference
				Total	Troposphere	
T	12.3y	5 to 100	50,000 to 10^6	100	60	(38)
Be^7	53d	10 to 60	2,000 to 6,000	6.3	1.3	(41, 43)
Be^{10}	2.7×10^6y	in deep sea sediments		3 to 6		(42, 44)
C^{14}	5570y	Spec. mod. carbon activity 14.7±0.5 d/m		150		(46)
Na^{22}	2.6y	~0.02	~40			(47)
P^{32}	14.5d	~1	~40			(48, 49)
P^{33}	25d	~0.5	~30			(49)
S^{35}	87d	~2	~400			(50)
Cl^{39}	55 min.	50	2.5			(51)

local fall-out, (*b*) tropospheric fall-out, and (*c*) stratospheric fall-out. The local fall-out is mainly caused by settling of large-sized particles and covers considerable areas near test sites. The second type is due to relatively small-sized particles that are not carried into the stratosphere but remain in the atmosphere until they settle out or are brought down by rains. This type of fall-out tends to remain in the same general latitude as the test site, but may circle the earth several times before it is precipitated. Practically all the tropospheric and stratospheric fall-out is brought down by rain (58).

The stratospheric fall-out amounts to about half or more of the total activity produced, depending on firing conditions. Libby finds that the average time this material stays in the stratosphere is of the order of 10 years. Only about 10 per cent of the stratospheric radioactivities descend per year into the tropopause, where they are washed out within a few weeks by rain. A theory of the mechanism of the precipitation of fall-out material by rain has been developed by Greenfield (56). The stratospheric fall-out is the part that produces world-wide effects. It is not well-known yet whether this fall-out is roughly uniform, or whether the downward mixing from the stratosphere is much more rapid at high latitudes or along the jet stream belt, as might be expected from meteorologic considerations discussed by Machta (57).

A general consequence of the slow mixing of the atmosphere through the tropopause is a piling up of certain activities produced or introduced in the stratosphere. According to Libby (58) the average concentration of Sr^{90} in stratospheric air per unit of mass is about two orders of magnitude higher than that in tropospheric air. Evidence from T and C^{14} data, and considerations by Benioff (45) regarding Be^7, also indicate such a situation. The slow mixing, however, is unexpected from the point of view of other meteorologic evidence and presents a new and serious meteorologic problem.

In general, no effects of chemical separation of solid fission products can be observed, so that their relative concentrations can be calculated fairly accurately from the respective fission yields and half lives, if the time of origin is known. In turn, observed ratios of amounts of fission products with different half lives allow the calculation of the age of the fall-out sample and the distinction between stratospheric and tropospheric fall-out. For such determinations the measured ratio of Sr^{89} (51d) to Sr^{90} (28y) or that of Ba^{140} (12.8d) to Sr^{90} is frequently used. Libby expects that further measurements of this type will answer the question of whether the relatively high fall-out along a belt between 35° and 55° north latitude is mainly due to tropospheric fall-out from tests conducted in this range of latitude, or to the increased rate of downward mixing from the stratosphere in higher latitude or along the path of the jet stream and the relatively high precipitation in this range of latitude (58). Libby estimates for December 1957 a total world-wide stratospheric fall-out of Sr^{90} of the order of 0.25 d/m per cm.^{2}. For certain latitudes the addition of tropospheric fall-out increases this number. The Sr^{90} fall-out reached maximum values around 45° north of the order of 2.5 d/m per cm.^{2}.

The amount of fission products in surface ocean water depends on the amount of fall-out that the particular location has received per unit of surface and on the rate of mixing of the surface ocean water into deeper layers. It is generally assumed that the ocean mixes fast down to the inversion layer, the so-called thermocline, which is at an average depth of about 75 meters. Additional information on the rates of mixing can be expected from further analyses. Sr^{90} determinations have so far given values ranging between 0.01 and 0.3 d/m per liter of sea water (54, 59). The situation in the oceans, however, is complicated by the uptake and enrichment of many elements by marine organisms (52).

Kr^{85} (10.4y) represents a special case among the fission products. As inert gas it remains in the atmosphere. The only data on Kr^{85} in air in the literature are those of de Vries (60) who found that a sample of krypton, collected in March 1955, showed an activity of 25,000 d/m per mole of krypton. This corresponds to about 1.1 d/m per cm.^{3} of krypton, or 1 d/m per one cubic meter of air. In 1957 the Kr^{85} activity in the atmosphere increased to at least three times this value (61). Nuclear weapons are not the only source of Kr^{85}

released into the atmosphere. It can be assumed that most of the Kr^{85} generated in nuclear reactors finds its way into the atmosphere.

Artificial tritium.—A few days after the Castle tests in Spring, 1954, the amount of tritium in rains in the United States reached levels close to 1000 tritium units. At that time it was possible to measure the tritium concentration in ordinary tap water without electrolytic enrichment. The measurements of Begemann & Libby (38) show that over the following weeks the tritium concentration leveled off corresponding to a decay curve with a period of about 40 days, somewhat longer than the period that would correspond to the residence time of water vapor in the troposphere. Rains in the southern hemisphere and Antarctic snow did not show any marked increase in the tritium concentration. Begemann & Libby (38) assume that most of the tritium produced by an H-bomb remains in the troposphere or is brought back from the stratosphere in the form of relatively large water droplets or more probably ice crystals that settle out much faster than the fine particles containing fission products.

Begemann and Libby estimate that an average of 10^9 tritium atoms (corresponding to 100 d/m of tritium) per $cm.^2$ have been deposited on the northern hemisphere as a consequence of the Castle test. No noticeable amount has crossed the equator. At least three more peaks in the tritium concentration of rains have been observed during the past years following the detonation of hydrogen bombs.

This artificial "tagging" of water is being used in the study of ground water inventories, continental water balance, mixing rates, and water circulation patterns (38).

Artificial radiocarbon. In 1956 Libby (55) anticipated an increase in atmospheric C^{14} from neutrons produced in atomic bomb testing. Such increase has now been observed by a number of investigators. Rafter & Fergusson (62) have measured the specific C^{14} activity of CO_2 in surface air of New Zealand, as well as of wood and ocean carbonates. They found an average increase from 1954 until 1957 of about 2.1 per cent per year. A slight indication for an increase before 1954 was present in some results obtained in the Washington Radiocarbon Laboratory (46) from tree ring measurements. Similar results on different materials have been found by de Vries in Holland (63), Munnich in Heidelberg, and Williams in Houston (64). The combined results show that the artificially produced C^{14} has by 1957 increased the C^{14} content of atmospheric CO_2 by about 10 per cent, and hence greatly overcompensated for the effect of the combustion of fossil fuels that since the end of the nineteenth century has led to a steady decrease in the specific C^{14} activity.

LITERATURE CITED

1. Libby, W. F., *Radiocarbon Dating* (University of Chicago Press, Chicago, Ill., 124 pp., 1952)
2. Grosse, A. V., Johnston, W. H., Wolfgang, R. L., and Libby, W. F., *Science*, **113**, 1 (1951)

(734)

3. Faltings, V., and Harteck, P., *Z. Naturforsch.*, **5a**, 438 (1950)
4. Kaufman, S., and Libby, W. F., *Phys. Rev.*, **93**, 1337 (1954)
5. Buttlar, H. von, and Libby, W. F., *J. Inorg. & Nuclear Chem.*, **1**, 75 (1955)
6. Anderson, E. C., and Hayes, F. N., *Ann. Rev. Nuclear Sci.*, **6**, 303 (1956)
7. Kohman, T. P., and Saito, N., *Ann. Rev. Nuclear Sci.*, **4**, 401 (1954)
8. Sackett, W. M., Potratz, H., and Goldberg, E., *Science* (In press)
9. Rona, E., Gilpatrick, L. O., and Jeffrey, L. M., *Trans. Am. Geophys. Union*, **37**, 697 (1956)
10. Smales, A. A., and Webster, R. K., *Geochim. et Cosmochim. Acta*, **11**, 139 (1957)
11. Urry, W. D., *Am. J. Sci.*, **240**, 426 (1942); *J. Marine Research* (*Sears Foundation*), **7**, 618 (1948)
12. Arrhenius, G., and Goldberg, G., *Tellus*, **7**, 226 (1955); Arrhenius, G., Bramlette, M. N., and Picciotto, E., *Nature*, **180**, 85 (1957)
13. Koczy, F. F., *Rept. Swed. Deep-Sea Expedition*, **10** (2) (In press, 1956)
14. Picciotto, E., and Wilgain, S., *Nature*, **173**, 632 (1954)
15. Goldberg, E., and Koide, M. (Unpublished data)
16. Blifford, I. H., Friedman, H., Lockhart, L. B., and Baus, R. A., *J. Atmospheric and Terrest. Phys.*, **9**, 1 (1956)
17. Von Benndorf, H., and Hess, V., in Müller-Pouillett, *Lehrb. d. Physik*, **5**, 519–662 (F. Vieweg, Braunschweig, Germany, 1928)
18. Israel, H., in *Compendium of Meteorology*, 155 (Malone, T. M., Ed., American Meteorological Society, Boston, Mass., 1334 pp., 1951)
19. Wilkening, M. H., *Nucleonics*, **10**, 6, 36 (1952)
20. Damon, P. E., and Kuroda, P. K., *Trans. Am. Geophys. Union*, **35**, 208 (1954)
21. Simpson, J. A., *Phys. Rev.*, **81**, 639, 895 (1951)
22. Elsasser, W., New, E. P., and Winckler, J. R., *Nature*, **178**, 1226 (1956)
23. Currie, L. A., Libby, W. F., and Wolfgang, R. L., *Phys. Rev.*, **101**, 1557 (1956); Fireman, E. L., *Phys. Rev.*, **97**, 1303 (1955); Soberman, R. K., *Phys. Rev.*, **102**, 1309 (1956)
24. Anderson, E. C., *Ann. Rev. Nuclear Sci.*, **2**, 63 (1953)
25. Harteck, P., *Proc. Nuclear Sci., Meeting* (Houston, Texas, in press, November, 1957)
26. Revelle, R., and Suess, H. E., *Tellus*, **9**, 18 (1957)
27. Arnold, J. R., and Anderson, E. C., *Tellus*, **9**, 28 (1957)
28. Craig, H., *Tellus*, **9**, 1 (1957)
29. Craig, H., *Geochim. et Cosmochim. Acta*, **3**, 53 (1953)
30. Suess, H. E., *Nuclear Processes in Geologic Setting*, 52 (Natl. Research Council, Washington, D. C., 1953); *Science*, **122**, 415 (1955)
31. Hayes, F. N., Anderson, E. C., and Arnold, J. R., *Proc. Intern. Conf. Peaceful Uses Atomic Energy, Geneva*, **14**, 188 (1955)
32. Williams, M. (Private communication)
33. Fergusson, G. J., *Proc. Roy. Soc.* (*London*), [A] **243**, 561 (1958)
34. Rafter, T. A., *New Zealand J. Sci. Technol.*, [B] **37**, 20 (1955); **18**, 871 (1957)
35. Broecker, W. S., Ewing, M., Gerard, R., Heezen, B. C., and Kulp, J. L., *J. Deep-Sea Research* (In press)
36. Fergusson, G. J., and Rafter, T. A. (Unpublished data)
37. Craig, H., *Phys. Rev.*, **105**, 1125 (1957); *Natl. Acad. Sci. Natl. Research Council Publ.*, **551**, Chap. 11 (1957)
38. Begemann, F., and Libby, W. F., *Geochim. et Cosmochim. Acta*, **12**, 277 (1957)

39. Harteck, P., and Suess, H. E., *Naturwissenschaften*, **36**, 218 (1949); Suess, H. E., *Trans. Am. Geophys. Union*, **34**, 343 (1953)
40. Harteck, P., *J. Chem. Phys.*, **22**, 1746 (1954)
41. Arnold, J. R., and Ali Al-Sali, H., *Science*, **121**, 451 (1955)
42. Arnold, J. R., *Science*, **124**, 584 (1956)
43. Thor, R., and Zutshi, P. K., *Tellus*, **10**, 99 (1958)
44. Goel, P. S., Kharkar, D. P., Lal, D., Narsappaya, N., Peters, B., and Yatirajam, V., *Deep-Sea Research*, **4**, 202 (1957)
45. Benioff, P. A., *Phys. Rev.*, **104**, 1122 (1956)
46. Suess, H. E., *Science*, **122**, 415 (1955)
47. Marquez, L., Costa, N. L., and Almeida, I. G., *Nuovo cimento*, **6**, 1292 (1957)
48. Marquez, L., and Costa, N. L., *Nuovo cimento*, **2**, 1038 (1955)
49. Lal, D., Narasappaya, N., and Zutshi, P. K., *Nuclear Phys.*, **3**, 69 (1957)
50. Goel, P. S., *Nature*, **178**, 1458 (1956)
51. Winsberg, L., *Geochim. et Cosmochim. Acta*, **9**, 183 (1956)
52. See for example: *Natl. Acad. Sci., Natl. Research Council, Publ.*, **551**, Chap. 11 (1957)
53. Fields, P. R., *et al.*, *Phys. Rev.*, **102**, 180 (1956)
54. Martell, E. A., "The Chicago Sunshine Method," *Atomic Energy Commission Unclassified Report, AECU*-3262 (1956)
55. Libby, W. F., *Science*, **123**, 657 (1956); *Proc. Natl. Acad. Sci. U. S.*, **42**, 365 (1956)
56. Greenfield, S. M., *J. Meteorol.*, **14**, 115 (1957)
57. Machta, L. (Unpublished data); Machta, L., List, R. J., and Hubert, L. F., *Science*, **124**, 474 (1956)
58. Libby, W. F., *U. S. Atomic Energy Commission Document* (Lausanne address before the Swiss Academy of Medical Sciences, March 27, 1958)
59. Sugihara, T. T. (Unpublished data)
60. Vries, H. de, *Appl. Sci. Research* [B], **5**, 387 (1956)
61. Oeschger, H., and Houtermans, F. G. (Personal communications)
62. Rafter, T. A., and Fergusson, G. J., *Science*, **126**, 557 (1957)
63. Vries, H. de, *Science*, **128**, 250 (1958)
64. Personal communications

(736)

BULLETIN OF THE AMERICAN ASSOCIATION OF PETROLEUM GEOLOGISTS
VOL. 42, NO. 11 (NOVEMBER, 1958), PP. 2567-2618, 30 FIGS.

SEDIMENTARY REFLECTIONS OF DEPOSITIONAL ENVIRONMENT IN SAN MIGUEL LAGOON, BAJA CALIFORNIA, MEXICO[1]

HARRIS B. STEWART, Jr.[2]
San Diego, California

ABSTRACT

The environment of deposition at San Miguel Lagoon is characterized by wide ranges in the measured factors. When the lagoon is isolated from the ocean, large fluctuations in bottom-water temperature with time mask any variations from place to place. Chlorinity, on the other hand, changes so slowly with time that areal variations are meaningful. Dissolved oxygen concentration and pH vary diurnally and areally, and these variations are used to delineate five aqueous environments within the lagoon.

Three different types of sediment within the lagoon are related to the following processes of transportation and deposition: wave processes, river processes, and slow deposition from quiet water. Analyses of sediments from other west coast lagoons show that these same processes may be inferred. Distribution of Foraminifera reflects the influence of the barrier in restricting water exchange with the ocean. Calcium carbonate values in the sediments are low (0.2–2.3 per cent), and the erratic distribution pattern results from variations in the sources, rate of dilution, and physico-chemical factors. In a lagoon where large amounts of organic material are contributed, low values for the organic carbon content of the sediments (0.36–5.60 mg./g.) are attributed to a high rate of decomposition. Higher organic carbon values are found in the finer-grained sediments.

The sediments reflect the overlying water in only those areas where they are genetically related to that water. In these areas lower calcium carbonate content was found in sediments underlying water with lower pH. Finer grain sizes are accompanied by less dissolved oxygen in the overlying water, and higher organic carbon content occurs with less dissolved oxygen and lower pH in the overlying water. Inferences are made from this study about the nature of ancient coastal lagoon deposits.

INTRODUCTION

This study was undertaken to investigate the relation of the sediments to the environment of deposition in a coastal lagoon. An attempt is made to evaluate the significant environmental factors and to determine to what extent the environment is reflected by the sediments. San Miguel Lagoon (Fig. 1), on the Pacific coast of Baja California, Mexico, was chosen for the major part of this study because it was accessible and largely undisturbed by man. Because the lagoon is less than a mile long and $\frac{1}{4}$ mile wide, the boundary conditions, sediment sources, and depositional processes could be observed in detail. Closely spaced samples permitted evaluations of environmental and sedimentary properties on a scale that would have been impractical in a larger area.

DESCRIPTION OF AREAS

San Miguel Lagoon (Fig. 2) is located behind a bay barrier built across the mouth of the valley of the Rio San Miguel. The region is one of generally high

---

[1] Contribution from the Scripps Institution of Oceanography, New Series. Manuscript received, July 12, 1957; revision, May 31, 1958.

[2] Present address: Coast and Geodetic Survey, Washington 25, D. C.

The field and laboratory work was done with equipment and facilities supplied by the Scripps Institution of Oceanography of the University of California. The writer is indebted to Fred B Phleger and Francis P. Shepard for many helpful suggestions. George S. Bien and Mary C. Barstow gave instruction and technical assistance in the chemical analyses and members of The Marine Foraminifera Laboratory assisted in identifying Foraminifera. Robert E. Hanson made the chlorinity determinations, and James R. Moriarty assisted in preparing many of the illustrations.

Contributions from the Scripps Institution of Oceanography, New Series, No. 1042

Reproduced by Permission

coastal relief and low rainfall. The bay barrier is a continuation of the sand beach lying below the sea cliffs north of the lagoon and extends across the mouth of the valley to a cliffed headland. The barrier averages 50 yards in width, and the interior is dotted with small sand hummocks or dunes averaging 6–8 feet high and up to 30 feet across. The barrier completely isolates the lagoon from the ocean during much of the year, and a narrow channel crosses the barrier at the southern end along the base of the cliffs when the lagoon is open.

The lagoon is bordered by marshes except at the bay barrier and along the cliffs at the southern end of the barrier. These border marshes are covered with a dense plant growth, primarily *Salicornia* and *Spartina*, and three narrow dead-end channels connect the interior of the marshes with the lagoon.

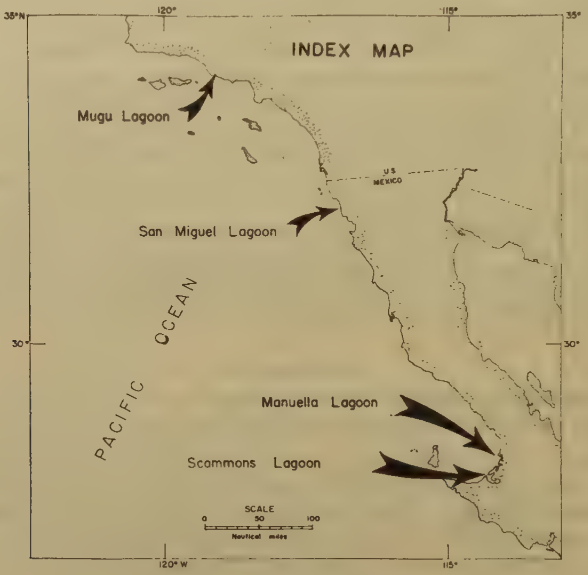

FIG. 1.—Location of areas studied.

The lagoon at highest water is less than 10 feet deep, and the greater part is less than 2 feet deep (Fig. 2). The inflowing stream flows throughout the year, but most of the year it is shallow and narrow, being supplied primarily by warm springs 10–20 miles inland. During the late fall and early winter hard rains often swell the stream to flood proportions, and a plume of brown sediment-laden water has been observed to extend as much as 2 miles seaward from the lagoon.

Scammons Lagoon (Fig. 3) and Manuella Lagoon lie approximately 300 miles south of San Diego on the west coast of Baja California (Fig. 1). These differ from

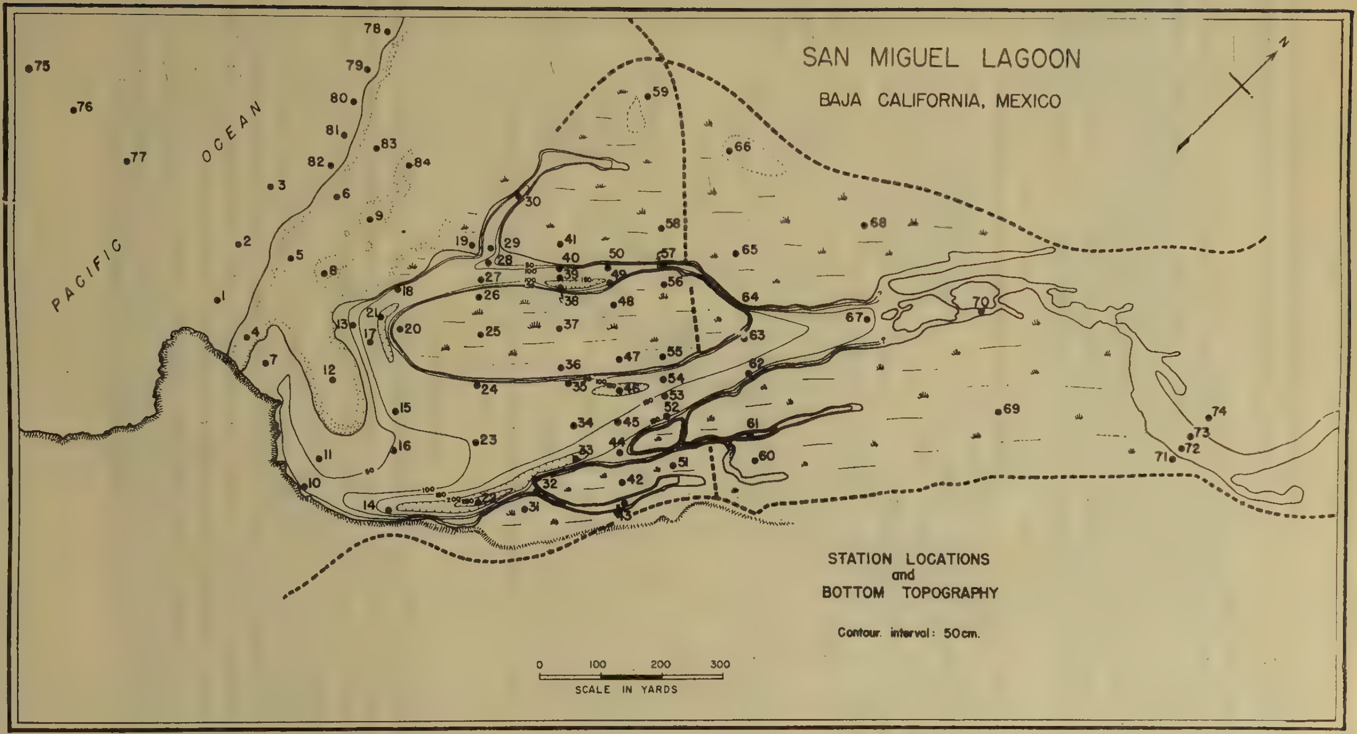
SAN MIGUEL LAGOON
BAJA CALIFORNIA, MEXICO
N
PACIFIC OCEAN
STATION LOCATIONS and BOTTOM TOPOGRAPHY
Contour interval: 50cm.
0
100
200
300
SCALE IN YARDS

FIG. 2.—Location of stations and bottom topography, San Miguel Lagoon, Baja California, Mexico.

San Miguel Lagoon in that they are located on a flat desert coast, have no entering rivers, are in constant connection with the ocean, and are in an area of large migrating sand dunes.

Mugu Lagoon (Fig. 1), near Port Hueneme, California, is at the southeastern edge of the Oxnard Plain. It is parallel with the coast, 4 miles long, and averages ¼ mile in width. Most of the year a narrow channel connecting the lagoon with the ocean is maintained by tidal action. Intermittent Calleguas Creek enters the lagoon from the north. It carries little sediment during most of the year, but during floods contributes large amounts of coarse material to the upper lagoon.

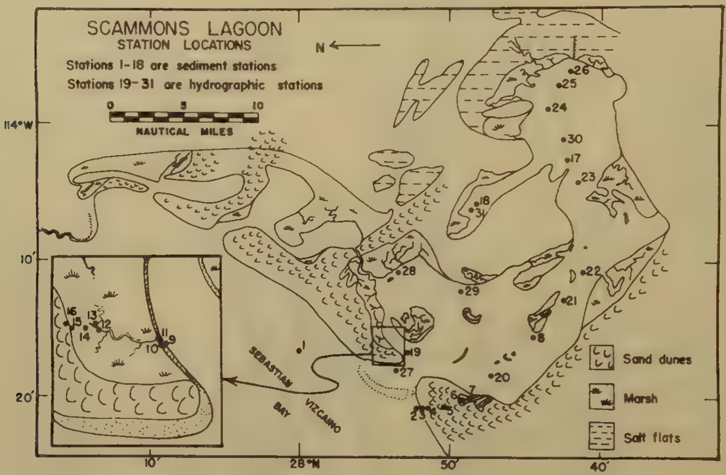
SCAMMONS LAGOON
STATION LOCATIONS
Stations 1-18 are sediment stations
Stations 19-31 are hydrographic stations
0
5
10
NAUTICAL MILES
N
114°W
10′
20′
10′
28°N
50′
40′
SEBASTIAN
VIZCAINO
BAY
1
2
3
4
5
6
7
8
9
10
11
12
13
14
15
16
17
18
19
20
21
22
23
24
25
26
27
28
29
30
31
Sand dunes
Marsh
Salt flats

FIG. 3.—Location of stations, Scammons Lagoon, Baja California, Mexico.

FIELD METHODS

The majority of the sediment samples seaward of the lagoons were collected from the R/V *E. W. Scripps* by using an orange-peel sampler modified to prevent washing of the sample *en route* to the surface (Phleger, 1952). Some were obtained by diving with an aqua-lung.

Samples of the beaches and dunes were collected by forcing a 2-ounce glass jar into the sand. The lagoon sediments were obtained by forcing a 4-foot length of 2-inch plastic tubing into the bottom, corking and retrieving it under water. Bottom-water samples were obtained at each sediment station in San Miguel Lagoon by lowering a water-sampling device (Stewart, 1956a) that recovered 500 ml. of water from one inch above the bottom. Numerous field trips were made to San Miguel Lagoon between April, 1953, and September, 1955.

LAGOON WATERS

TEMPERATURE

When the bay barrier is open, temperature variations from place to place within the lagoon can be attributed primarily to the influx of the colder ocean water which is warmed in the shallow lagoon and returned to the ocean on the ebb tide. Measurements made while the lagoon was in open connection with the ocean showed the water overlying the tidal sand flat near station 54 to have a temperature of 30°C., whereas the water flowing into the lagoon from the ocean was only 16.1°C. Similar temperature variations as a function of tidal action were reported from San Francisco Bay by Sumner *et al.* (1914).

When the lagoon is closed, however, the temperature variation with time is the result of the rapid heating and cooling of the shallow lagoon water. Figure 4 shows that during a 20-hour period the surface-water temperature at station 28 ranged from a high of 30°C. at 4:00 P.M. to 19.5°C. at 4:00 A.M. Bottom-water temperature variations paralleled those of the surface but were of lower magnitude. Bottom-water temperatures show no areal pattern but reflect the gradual warming of the water during each sampling day superimposed on a general cooling during the sampling period (Stewart, 1956a, Fig. 17).

The temperature measurements suggest the wide range of environmental variations encountered in a closed coastal lagoon. They further indicate that al-

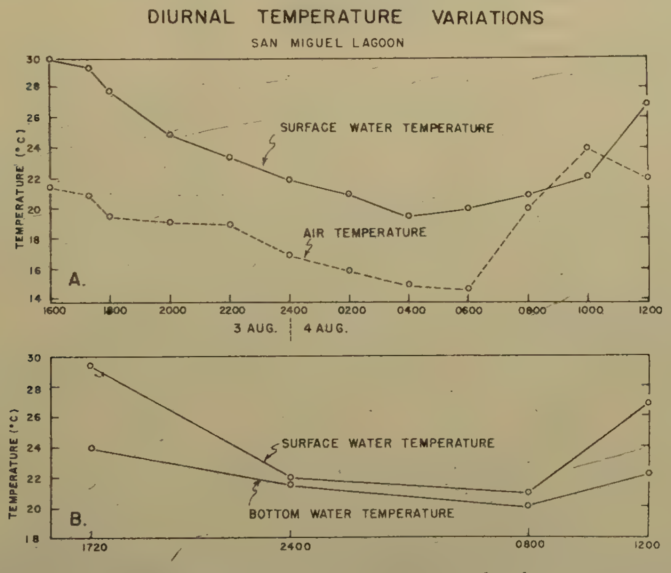

FIG. 4.—Diurnal temperature variations. A. Air temperature and surface-water temperature. B. Surface and bottom-water temperature.

though temperature may be an important environmental characteristic, the diurnal variation is so large that any variation from place to place is completely masked.

CHLORINITY

When the bay barrier was open, samples for chlorinity determination were obtained along a profile through the entrance and up the lagoon to discover the nature of the exchange of lagoon water with the ocean. Determinations were also made on the 44 bottom-water samples collected with the sediment cores when the lagoon was closed. These latter were made in order to determine the amount of dilution that had taken place in the 5 months that the lagoon had been separated from the ocean and to give values that would enable the chlorinity to be compared with other variables in the water and the sediments. Results are expressed as chlorinity rather than salinity, because in areas of high dilution (low salinity) the ions probably are not in a constant ratio, and the calculation of salinity from the chlorinity is not valid.

Locations of samples and the chlorinity distribution on both flood and ebb tides are shown in Figure 5. The extreme shallowness of the water should be noted: water depths ranged from less than 3 feet to only 4 inches. In this shallow channel the isochlors on a flood and an ebb tide form distinct patterns (Fig. 5). The strong vertical gradient and weak horizontal gradient at stations 7, 11, and 22 on the flood tide resemble the salt-wedge type of estuary, and the pattern is similar to that found at the mouth of the Mississippi River at Southwest Pass (Rhodes, 1950). The water at the four other stations in the profile is only slightly stratified, and the pattern reflects strong vertical mixing similar to that found in the James Estuary by Pritchard (1952). When the tide raises the water level in the ocean above the height of the lagoon sill, a salt-water wedge moves into the lower channel, and the fresher water flows out over it with only slight mixing. This strong vertical gradient becomes less pronounced with distance from the mouth because of mixing by waves moving up the channel and because of friction at the interface between the salt wedge and the low-chlorinity water above. Intense mixing and a larger proportion of river water at the shoaler stations farthest from the ocean are reflected by the almost complete lack of stratification and the lower chlorinities at the upper stations (Fig. 5a).

The vertical chlorinity distribution near the end of the ebb tide (Fig. 5b) is similar to that of a typical vertically mixed estuary such as the Severn Estuary described by Bassindale (1943). The almost vertical isochlors at the upper part of the channel and the chlorinity values considerably higher than the 0.34 °/₀₀ of the inflowing river water indicate that the water leaving the lagoon has been thoroughly mixed. Stations 16 and 22 have slightly higher chlorinities at the surface than at the bottom. This is to be expected in such thoroughly mixed water, and Bassindale (1943) reported that in the Severn Estuary 19 of the 72 pairs of surface and bottom observations showed slightly greater salinity at the surface.

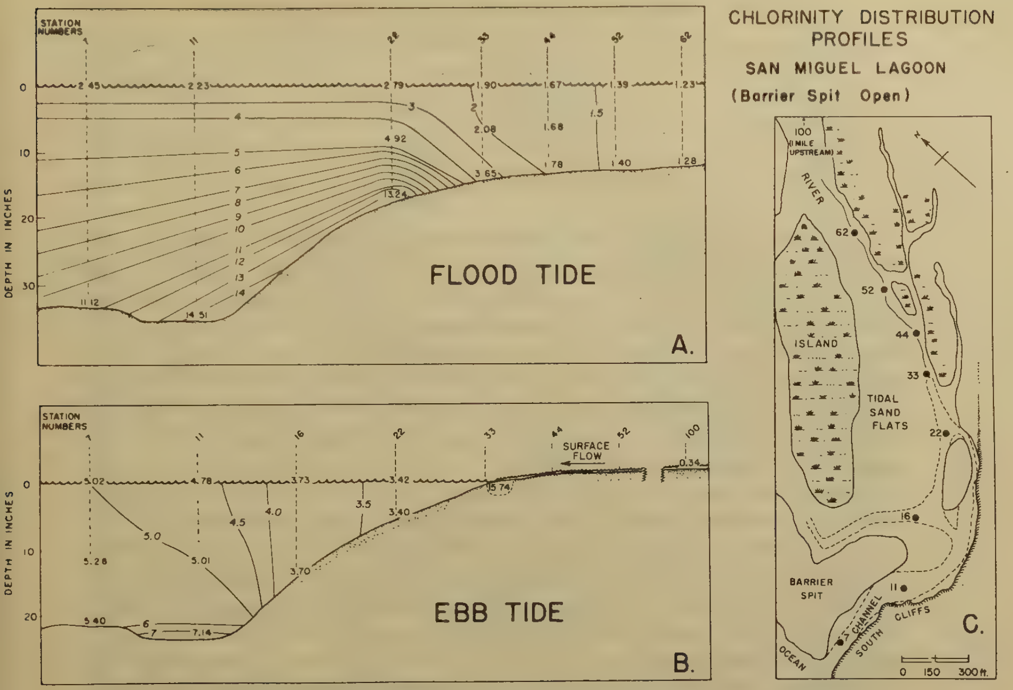

FIG. 5.—Chlorinity distribution profiles. A. Samples obtained on flooding tide. B. Samples obtained on ebbing tide. C. Location of samples.

Water that seeped into a hole dug at low tide in the tidal sand flat near station 33 had a chlorinity of 15.74 °/₀₀. This is the highest value found within the lagoon and is only slightly less than normal ocean chlorinity (18–19 °/₀₀). Undoubtedly chlorinities of this magnitude exist within the lagoon during tides higher than the 2.7-foot tide on which the flood-tide samples were obtained. This type of water is probably retained by the bottom sediments and not diluted to any extent during subsequent covering by waters of lower chlorinity, a phenomenon described by Reid (1930) and Alexander *et al.* (1932). Its ecologic significance in the distribution of burrowing organisms within an estuary is discussed by Reid (1932).

Two months after the bay barrier had isolated the lagoon from the ocean, chlorinity measurements were made at two stations within the lagoon, and these values are compared in Table I with values obtained 5 months after closing. During this period, inflowing river water raised the water level of the lagoon 6 cm., and dilution and mixing reduced the bottom-water chlorinity at these two stations an average of 3.32 °/₀₀.

TABLE I. COMPARISON OF CHLORINITY (°/₀₀) AT TWO STATIONS AFTER CHANNEL HAD BEEN CLOSED 2 MONTHS AND 5 MONTHS

Station	*Closed 2 Months*		*Closed 5 Months*
	Surface	*Bottom*	*Bottom*
10	1.77	4.76	0.87
14	1.80	3.62	0.86

The areal distribution of the bottom-water chlorinity 5 months after the channel had been closed is shown in Figure 6. The ocean samples show a normal ocean chlorinity of 18.5 °/₀₀, and the values within the lagoon range from 0.42 °/₀₀ to 1.24 °/₀₀. Chlorinity decreases with distance up the river, and the higher values are found at the deepest station in the lagoon (sta. 22), in the deeper parts of the north channel, and in the narrow dead-end marsh channels.

The decreasing chlorinity with distance up-river from the lagoon reflects dilution by the river water. No marked decrease with distance from the barrier is observed. This suggests that the water from washovers (high waves that crest the barrier and wash into the lagoon) which occurred prior to the time of sampling had been thoroughly mixed and lost its identity or else had flowed along the bottom to the deeper parts of the lagoon. A chlorinity of 2.22 °/₀₀ was obtained on the bottom only a few yards from the barrier where a large volume of salt water had washed over into the lagoon only 3½ hours before. Three days previously a chlorinity of 0.88 °/₀₀ had been measured at the same place. This indicates that the water from the washover did mix with the lagoon water to some extent, but the chlorinity suggests that this water did not remain near the barrier. Station 22 is the one with the deepest water and had the highest chlorinity value for the lower lagoon (1.04 °/₀₀), suggesting that this is the place where the washover water collects.

The three highest chlorinity values occur in the narrow, dead-end marsh channels with relatively high values found also in the deeper part of the north channel. The high chlorinities in the marsh channels are believed to reflect the chlorinity of water trapped there by the closing of the bay barrier and subsequently less diluted because of isolation from the rest of the lagoon. This mechanism also explains the higher chlorinities found in the deeper part of the north channel. This area is by-passed by the sluggish surface current from the river that flows south of the island, the channel is so narrow that wind waves are smaller than in the open lagoon, and the area is in part a closed basin.

DISSOLVED OXYGEN

Measurements of dissolved oxygen concentration in San Miguel Lagoon were made to ascertain (1) the magnitude of any diurnal variation, so that this factor might be taken into account when considering the areal variation among samples collected at different times of the day, (2) if an anaerobic environment exists in

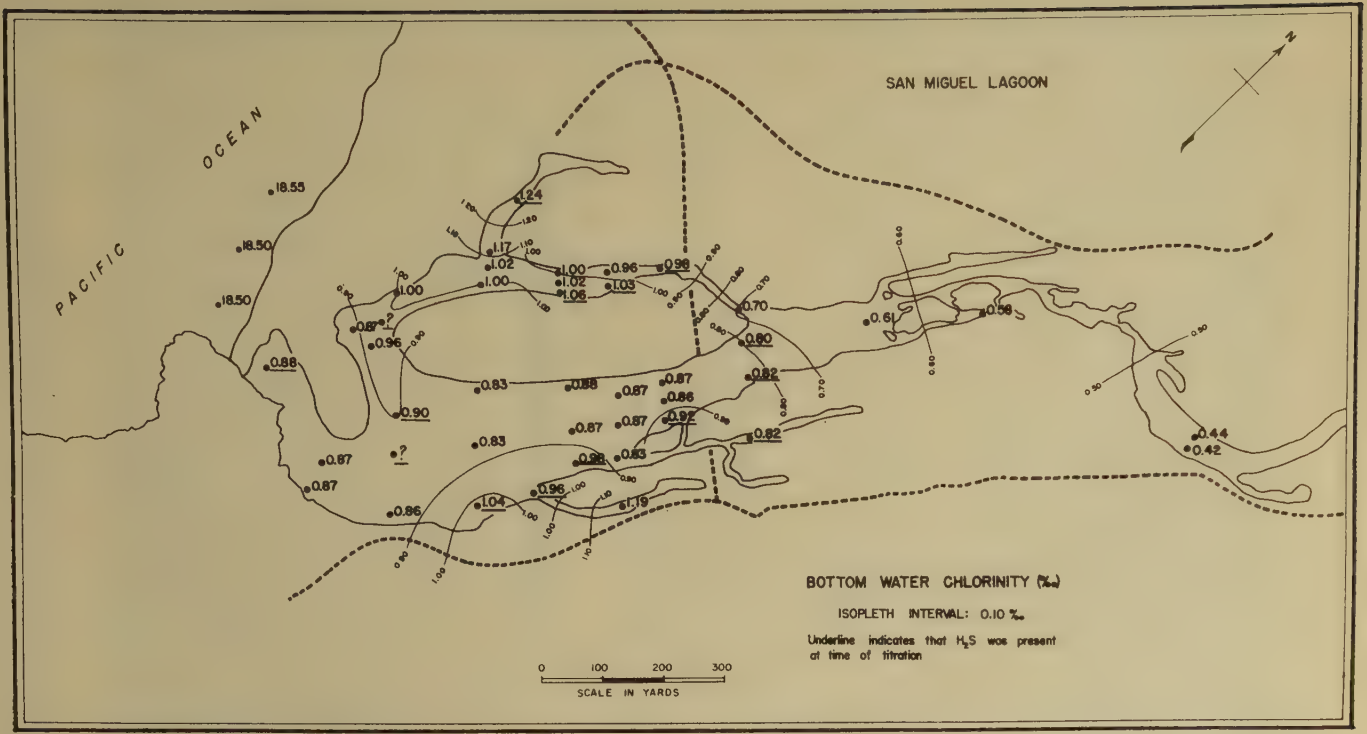
SAN MIGUEL LAGOON
N
PACIFIC
OCEAN
18.55
18.50
18.50
BOTTOM WATER CHLORINITY (‰)
ISOPLETH INTERVAL: 0.10 ‰
Underline indicates that H₂S was present at time of titration
0
100
200
300
SCALE IN YARDS
1.24
1.17
1.02
1.00
1.00
1.02
1.06
0.96
1.03
0.98
0.70
0.61
0.58
0.60
0.62
0.62
0.87
0.86
0.92
0.87
0.87
0.88
0.83
0.83
0.83
0.98
0.96
1.04
1.19
0.86
0.87
0.87
0.88
0.87
?
0.96
0.90
?
0.44
0.42

Fig. 6.—Areal distribution of bottom-water chlorinity 5 months after closing of bay barrier. Isopleth interval $0.10^\circ/_{oo}$. Underline indicates that H_2S was present at the time of titration.

the bottom water, and (3) whether dissolved oxygen concentration as an environmental factor has any effect on the underlying sediments.

Twelve surface-water samples for measurement of the diurnal variation in dissolved oxygen concentration were obtained at station 28 in the north channel. These samples were taken over a 20-hour period from 4:00 P.M. until noon of the following day. The dissolved oxygen concentration in these and the 44 bottom-water samples for the areal study was determined in the field by a modification of the Winkler method (Wooster, 1950).

Diurnal samples.—The diurnal variation in dissolved oxygen concentration is shown graphically in Figure 7 together with the air and water temperatures and the saturation concentrations. The surface dissolved oxygen concentration varied from 3.69 ml./L to 8.78 ml./L, or from 57 per cent saturated to more than 60 per cent supersaturated. A general decrease in the amount of dissolved oxygen is noted from 4:00 P.M. until 6:00 A.M. the following morning when the concentration began to rise. The variations in the oxygen concentration parallel variations in both the air and the water temperature. This can not be considered as cause and effect, since the solubility of oxygen in water is greater at lower temperatures, and the lower temperatures here accompany *lower* oxygen concentrations. It would be expected that the water temperature and the production of photosynthetic oxygen by the thick growth of widgeon grass (*Ruppia maritima*)

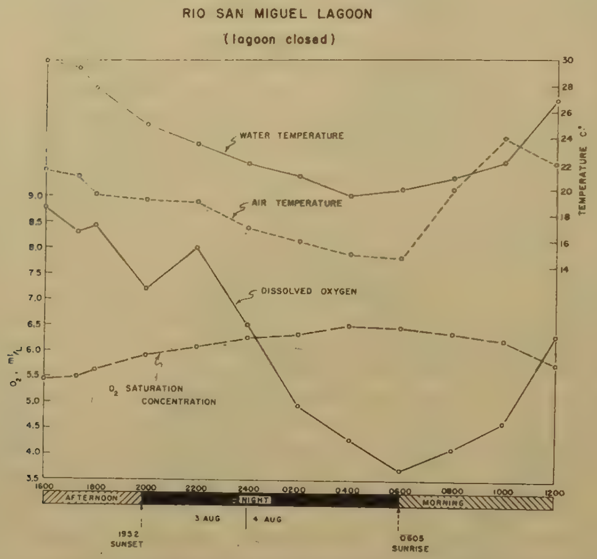

FIG. 7.—Diurnal variation in dissolved oxygen concentration in surface water at station 28, 1600 August 3 to 1200 August 4, 1953.

which chokes the north channel would both be related to the influx of solar energy. By using the times of sunrise and sunset as the limits of the time during which solar energy is supplied, and by using the variations in air temperature as an approximate index of the variations of this solar energy, the dependence of the oxygen concentration on solar energy may be seen (Fig. 7). Like the air temperature, the dissolved oxygen concentration attains its lowest value with the 6:00 A.M. sample and then rises steadily as the sunlight becomes available for photosynthesis with the resultant production of oxygen. The concentration continues to increase until the end of the sampling period at noon. The maximum oxygen value during the sampling period is at 4:00 P.M., and values then decrease with time as the amount of available solar energy decreases with the setting sun. Respiration (oxygen consumption) dominates during the night, reducing the oxygen concentration until sunrise, when the sunlight is again available for photosynthesis. A similar diurnal cycle was reported by Newcombe *et al.* (1939) for an arm of Chesapeake Bay and by Debyser (1955) for lagoons of the Ivory Coast. This diurnal variation must be borne in mind when considering the areal variation of dissolved oxygen concentration in samples collected at different times of the day.

Areal samples.—The areal distribution of dissolved oxygen in the bottom waters is shown in Figure 8. Measured concentrations range from 0 to 7.72 ml./L within the lagoon, and the three samples from the ocean range only from 5.03 ml./L to 5.14 ml./L. Only one of the 44 samples contained no measurable oxygen, two others contained less than 1 ml./L, and 11 contained less than 3 ml./L. Values increase with distance up-river from the lagoon, and the lowest values are in the north channel, in the narrow dead-end marsh channels, and in two small enclosed depressions (stations 21 and 22).

The dissolved oxygen values for these 44 bottom-water samples were plotted against the time of day at which each sample was obtained to see if a diurnal influence could be detected (Fig. 9a). When all the samples are considered, there appears to be little correlation between the time of day and the oxygen concentration. Thus, for the area as a whole, the variations in dissolved oxygen concentration with time apparently are masked by the larger variations from place to place.

The lower lagoon stations, however, cover a relatively large area where studies here described show the environmental conditions to be fairly uniform at any one time, and oxygen variations from place to place might therefore be expected to be at a minimum. If the water samples from this area are considered separately (Fig. 9b), the oxygen values appear to group along the line joining the values for the surface samples in the diurnal study at station 28. This indicates that diurnal variations in the dissolved oxygen concentration do occur in the bottom water and can be detected within areas having small areal variations. The three ocean samples show almost no variation in dissolved oxygen concentration areally or with time.

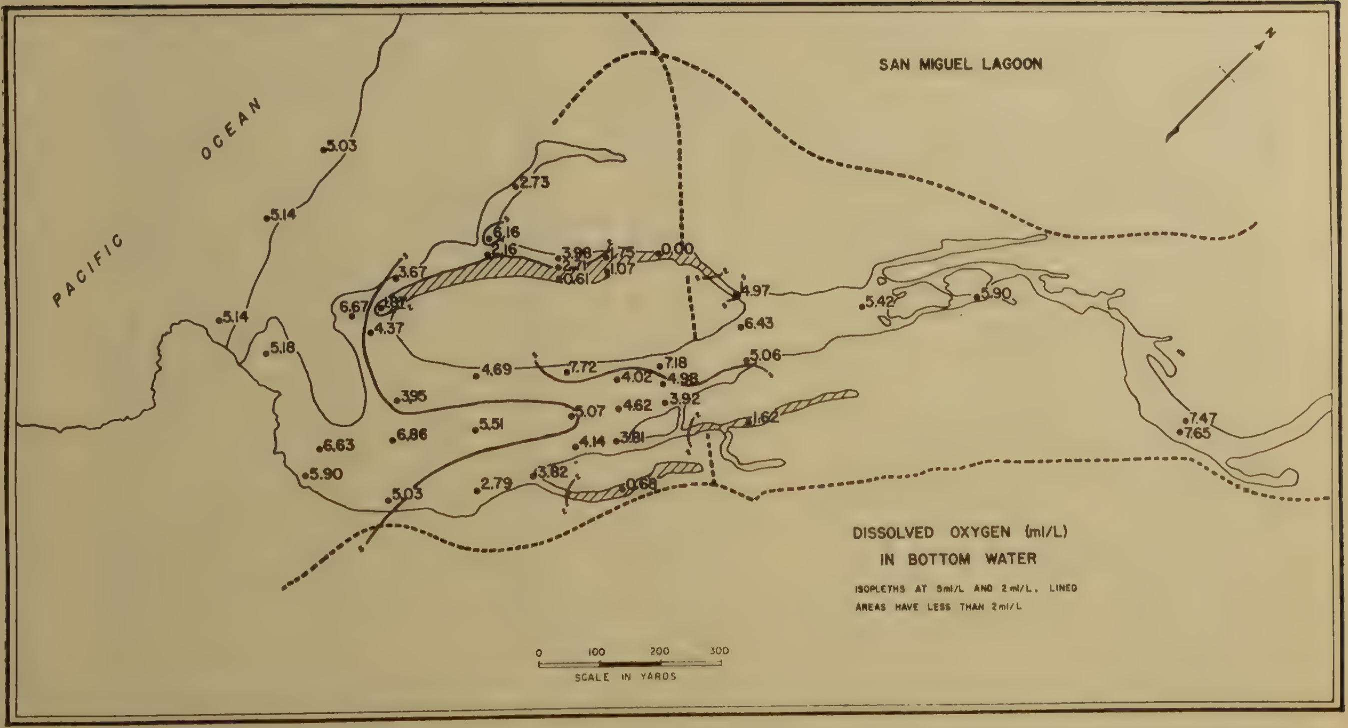
SAN MIGUEL LAGOON
N
PACIFIC
OCEAN
DISSOLVED OXYGEN (ml/L)
IN BOTTOM WATER
ISOPLETHS AT 5ml/L AND 2 ml/L. LINED
AREAS HAVE LESS THAN 2 ml/L
0
100
200
300
SCALE IN YARDS
5.03
5.14
5.14
5.18
2.73
6.16
2.16
3.98
2.71
0.61
1.75
1.07
0.00
4.97
6.43
5.42
5.90
3.67
6.67
2.81
4.37
4.69
7.72
7.18
4.02
4.98
5.06
3.95
5.07
4.62
3.92
1.62
5.51
6.86
6.63
5.90
4.14
3.81
3.82
0.68
2.79
5.03
7.47
7.65

FIG. 8.—Areal distribution of dissolved oxygen concentration in bottom water. Isopleths at 5 ml/L and 2 ml/L. Shaded areas have less than **2** ml/L.

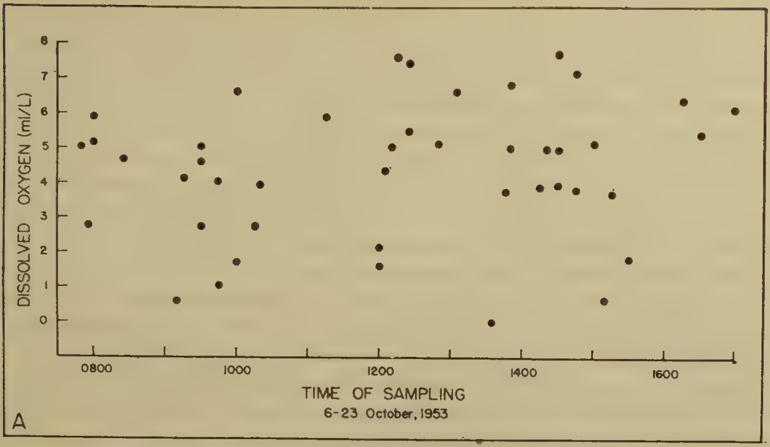

ALL STATIONS, SAN MIGUEL LAGOON

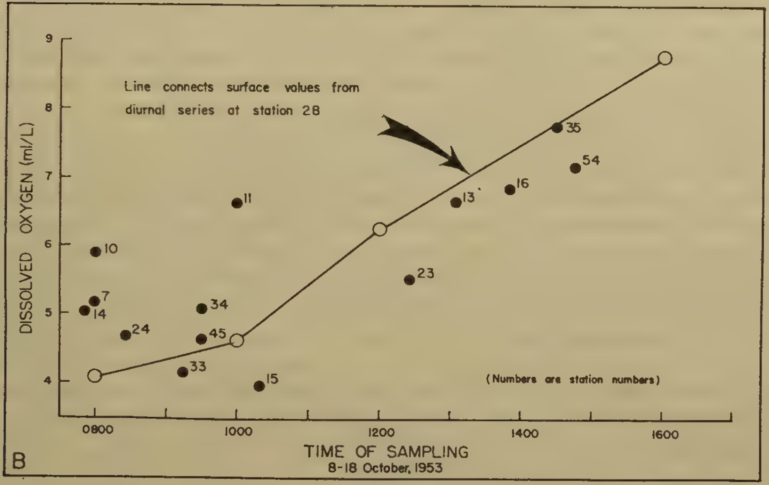

LOWER LAGOON STATIONS ONLY

FIG. 9.—Dissolved oxygen concentration in bottom water plotted against time of sampling. A. For all stations. B. For lower lagoon stations only.

Although the major part of the dissolved oxygen in the lagoon is contributed by the large submersed aquatic plants, some is contributed by green algae. Pads of green algae up to 4 inches across and covered with small bubbles were observed on the bottom near station 45. The same phenomenon has been reported from east coastal tidal flats by Nelson (1947). This was also noted at station 29 where a sediment core had a thin green algal mat resting on the surface of the sediment. The core was allowed to stand in the sun, and minute bubbles were observed breaking away from the mat and rising through the water standing above the sediment in the transparent core tube. Algae may account for the abnormally high oxygen value measured at station 29 (Fig. 8).

Anaerobic conditions at the time of sampling apparently existed only at station 57 in the north channel. The other north channel stations were low in oxygen, especially those in the deeper enclosed basin, as were the narrow dead-end marsh channels and the closed depressions at stations 21 and 22. This suggests that the lower oxygen values result at least in part from the impaired circulation previously mentioned. These low values are not a function of depth alone, for the narrow marsh channels, though low in oxygen, are relatively shallow.

The 5 ml./L isopleth (Fig. 8) follows almost exactly the edge of the areas of the thick submersed plant, *Ruppia maritima*. However, it is the *lower* oxygen values that are found where the plants are thickest. This is in part due to the fact that these oxygen values are for the bottom water rather than the surface water. Within these depressions and enclosed areas circulation is further restricted by the plants themselves, but more important is the observed growth pattern of these plants. *Ruppia maritima* commences growth from the dormant winter stage in June (Graves, 1908), and at that time in San Miguel Lagoon short submersed stems bearing green leaves were noted at numerous places on the bottom. As it grows, the slender stem becomes longer and more branched until it reaches the surface where a luxuriant growth of leaves is supported. At the time the water samples were collected, the leaves below the upper few feet were observed to be yellow in the areas where the plants were thickest. They were brown at greater depths, and the bottom few feet of the plants were bare gray-green stalks. This indicates that photosynthesis was taking place only in the upper layers and suggests that the thick upper parts of the plants effectively block sunlight from the lower parts. Thus as the plants grow thicker, less and less sunlight penetrates to the lower leaves which then die and are added to the accumulation of decomposing plant material on the bottom. The decomposition of this organic material would cause a continuous depletion of oxygen (Waksman and Hotchkiss, 1938; Richards and Redfield, 1954), further reducing the measurable oxygen in the bottom water.

pH

The pH was measured for each of the bottom-water samples from San Miguel Lagoon and for one sample from the river 4 miles above the lagoon. Measurements were made with a Beckman pH meter using glass and calomel electrodes. The instrument was standardized in the field each morning against a solution of known pH. Water for these determinations was drawn off as soon as the sample was brought ashore, the temperature was read, and the instrument corrected accordingly. These samples were apparently well buffered, for equilibrium was usually established within a very few seconds, and in only a few instances was there any noticeable drift.

The areal distribution of the bottom-water pH after the lagoon had been isolated for 5 months is shown in Figure 10. Values range from pH 7.2 to 10.1. Although the average pH value for the lagoon samples is 8.6, 37 per cent of the determinations gave values higher than pH 9, and the pH of 10.1 recorded from station 54 is more than one pH unit above any measurement known to the writer from a comparable environment.

The wide range of pH values measured within the lagoon must be the result of processes acting within the lagoon, because the river pH of 8.0 and the average of pH 8.1 for the three nearshore ocean samples indicate similar values for the only sources of water entering the lagoon.

These relatively high pH values are undoubtedly due to the high rate of photosynthesis within the lagoon. The increase in pH during the day resulting from the photosynthetic removal of carbon dioxide, and the decrease in pH during the night when carbon dioxide is added by respiration are well known phenomena in environments somewhat comparable with San Miguel Lagoon (Powers, 1920; Bruce, 1924; Carl, 1940; Debyser, 1949; Jaquet, 1949; and Stevenson, 1954). The pH of the 14 lower lagoon stations plotted against the hour at which each sample was taken (Fig. 11) shows that in the relatively uniform environment of the lower lagoon there is a general increase in pH with time during the day.

AQUEOUS ENVIRONMENTS

The variations in temperature, chlorinity, dissolved oxygen, and pH of the water samples obtained while San Miguel Lagoon was isolated from the ocean may be used to define separate water units within the lagoon. It has been shown that diurnal variations can be detected only within an area where the areal variation is small, and an area with little areal variation is essentially a uniform environment with respect to the measured properties. Thus diurnal variations may be used to delineate these relatively uniform aqueous environments in the following manner.

As has been shown, photosynthesis causes an increase in both the dissolved oxygen concentration and the pH during the day. A series of samples taken at the same station over a period of several hours during the day would ideally give a straight-line relation of increasing pH with increasing concentration of the dissolved oxygen, and the length of the line would be a function of the length of time over which the samples were obtained. A corollary of this is that samples taken from different stations within the same area during the same period would have pH and oxygen values that would also fall along this line, but the deviation would depend on how much these samples differed from those by which the original line was established. Thus it was reasoned that samples from any one environment would group along the line, indicative of the average conditions within that environment, and that the length of the line would depend on the time range

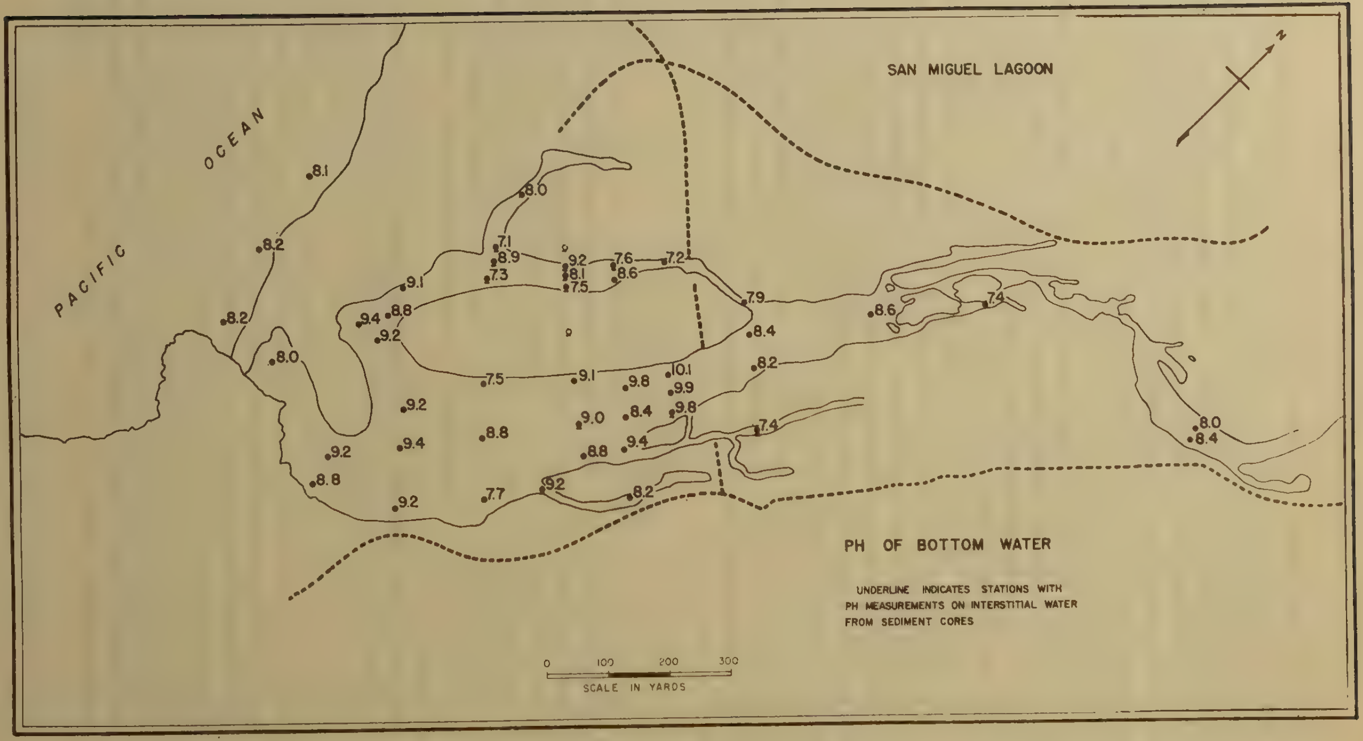
SAN MIGUEL LAGOON
N
PACIFIC OCEAN
PH OF BOTTOM WATER
UNDERLINE INDICATES STATIONS WITH PH MEASUREMENTS ON INTERSTITIAL WATER FROM SEDIMENT CORES
0 100 200 300
SCALE IN YARDS
8.1
8.2
8.2
8.0
8.0
7.1
8.9
7.3
9.1
9.4
8.8
9.2
9.2
7.6
7.2
8.1
8.6
7.5
7.9
8.4
8.6
7.4
8.2
7.5
9.1
9.8
10.1
9.9
9.8
9.2
9.4
8.8
9.0
8.4
8.8
9.4
7.4
9.2
8.8
9.2
7.7
9.2
8.2
8.0
8.4

Fig. 10—Areal distribution of pH of bottom water.

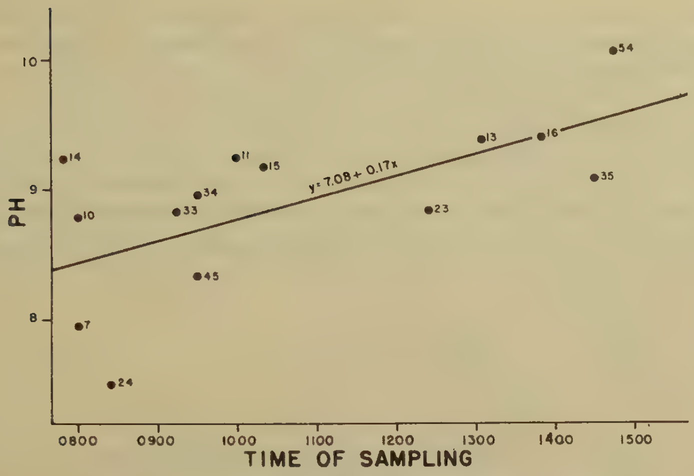

FIG. 11.—pH of bottom water plotted against time of sampling, lower lagoon stations only. Numbers are station numbers.

over which the samples were collected. When the pH is plotted against the dissolved oxygen concentration for all the samples and each point is numbered to identify the station, the following facts are apparent (Fig. 12).

1. There are five geographically distinct areas within which conditions are

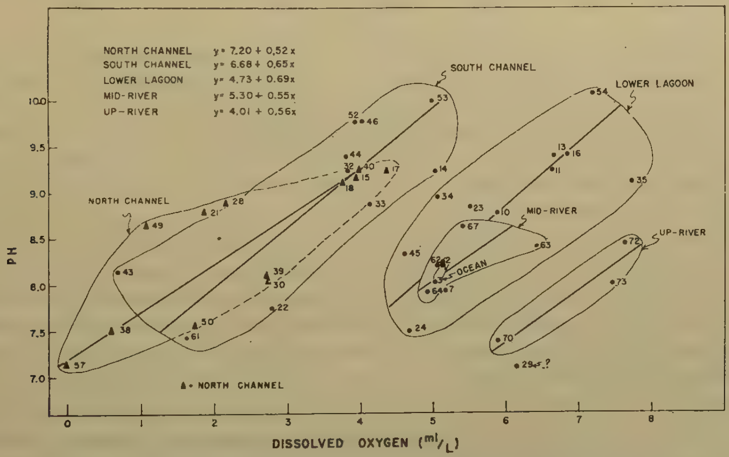

FIG. 12.—Bottom water pH plotted against dissolved oxygen concentration. Numbers are station numbers.

sufficiently uniform to cause the samples to group about a separate line. These areas are designated "up-river," "mid-river," "north channel," "south channel," and "lower lagoon."

2. All five lines are essentially parallel, indicating that in each area the rate of change of dissolved oxygen and pH is nearly the same.

3. With only two exceptions (stations 29 and 46), the samples within each group are from contiguous stations outlining separate geographic areas within which conditions are relatively uniform and are different from conditions in adjacent areas. The areal distribution of the stations within each group is shown in Figure 13.

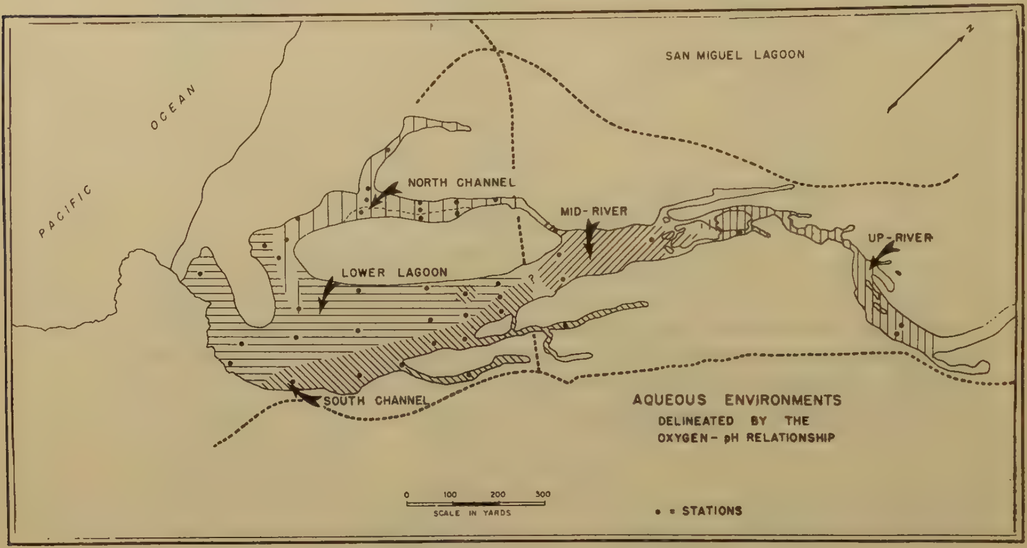
PACIFIC
OCEAN
SAN MIGUEL LAGOON
N
NORTH CHANNEL
MID-RIVER
UP-RIVER
LOWER LAGOON
SOUTH CHANNEL
AQUEOUS ENVIRONMENTS
DELINEATED BY THE
OXYGEN-pH RELATIONSHIP
0 100 200 300
SCALE IN YARDS
• = STATIONS

FIG. 13.—Areal distribution of aqueous environments delineated by oxygen-pH relationship shown in Figure 12.

4. The ocean samples (stations 1, 2, and 3) fall together, indicating little change in either oxygen or pH from place to place or with time.

5. All environments have similar pH ranges, and the displacement of the areas in the oxygen direction indicates that the dissolved oxygen is more important than the pH in defining these environments. If these environments were merely a function of the differences in the total amount of photosynthesis, the environments with the higher oxygen values would also have higher pH values, but this is not the case. The displacement of the areas in the oxygen direction is caused by variations in dissolved oxygen concentration due to some other factor or factors in addition to photosynthesis.

The observed values are the net effect of the various factors operating in each environment. Some of the possible causes for these separate aqueous environments may be indicated by considering the measured oxygen distribution as reflecting a dynamic equilibrium between oxygen production and utilization. The oxygen sources for these bottom waters are (1) photosynthesis during the day and (2) oxygen derived from the overlying waters where it was either produced by photosynthesis or absorbed from the atmosphere. Oxygen leaves the system by (1) plant and animal respiration, (2) oxidation of organic material, and (3) loss to the overlying water and the atmosphere.

The amount of oxygen put into the system may be considered to be in equilibrium with the amount lost since oxygen is not accumulating nor are the waters devoid of oxygen. The measured values, therefore, show the state of this equilibrium in the five different areas. If a notation is made of the per cent oxygen saturation at each station and isopleths drawn (Fig. 14), it is seen that in order to maintain this equilibrium, oxygen must be entering the system in the north channel, south channel, and mid-river areas, and leaving the system in parts of the lower lagoon and the up-river areas. In the north channel and to a less extent in the south channel, a strong vertical oxygen gradient must exist, for the low per cent saturation values are in areas of dense growth of *Ruppia* at the surface. Considerable organic material accumulates on the bottom in these areas, and its decomposition must utilize oxygen at a rate faster than it can be supplied from the overlying water, resulting in the low oxygen values measured. In the up-river area, on the other hand, the average of 103.6 per cent oxygen saturation suggests only that here oxygen production exceeds utilization, not that more oxygen is

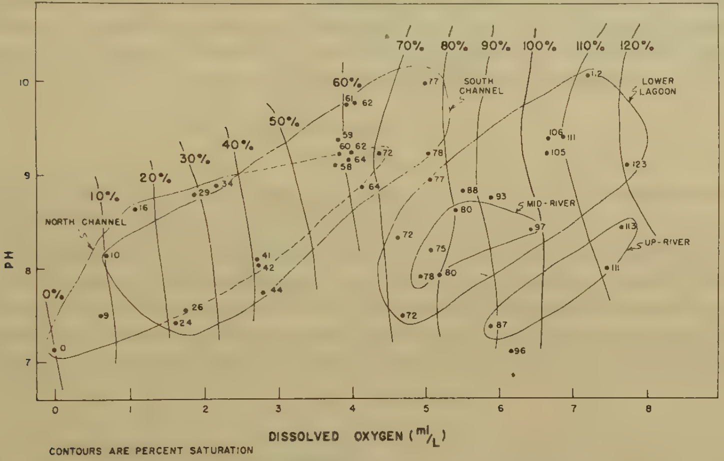

FIG. 14.—Oxygen-pH relation showing per cent saturation.

actually produced than in the areas with low values. This up-river area has clear water, clean sands, and no black muds suggestive of organic decomposition; therefore, utilization is low, measured values are high, and oxygen is being lost from the system. Thus the distinguishing feature of these separate aqueous environments is not the total oxygen production but rather the measurable oxygen that represents the balance between production and utilization in each area.

When the areal distribution of the chlorinity of the same samples (Fig. 6) is compared with the distribution of these aqueous environments (Fig. 13), it is seen that four of the five environments have unique chlorinity ranges: up-river, 0.42–0.58 $^{\circ}/_{\circ\circ}$; mid-river 0.61–0.82 $^{\circ}/_{\circ\circ}$; lower lagoon, 0.83–0.88 $^{\circ}/_{\circ\circ}$; and north channel 0.90–1.24 $^{\circ}/_{\circ\circ}$. This further suggests that these are indeed separate environments. In addition, the three stations with highest chlorinity (stations 29, 30, and 43) are all in narrow dead-end marsh channels, suggesting that these areas may constitute an additional aqueous environment.

LAGOON SEDIMENTS

GENERAL

The environmental factors previously discussed can not be measured directly in ancient sediments. Only by studying the modern sediments themselves and determining how the measurable sedimentary characteristics reflect their environment of deposition can any useful criteria be established for reconstructing the environment of deposition from similar ancient deposits. The characteristics used in the present study are particle-size distribution, coarse-fraction studies, occurrences of Foraminifera, calcium carbonate content, and organic carbon content.

PARTICLE-SIZE DISTRIBUTION

Size analyses were made on all samples from San Miguel, Scammons, Manuella, and Mugu lagoons to evaluate particle-size distribution as an environmental indicator. Samples were dried, split, and wet-sieved through a $\frac{1}{16}$-mm. sieve. If less than 5 per cent of the sample was finer than $\frac{1}{16}$ mm., the entire sample was analyzed by the Emery settling tube method (Emery, 1938). If 15 grams or more of the material finer than $\frac{1}{16}$ mm. were available, the hydrometer method was used employing a procedure modified from Day (1950), and if less than 15 grams, the analysis was by the pipette method (Krumbein and Pettijohn, 1938, p. 166). Most samples were well sorted and could be analyzed by one method; but if this was not possible, coarser and finer material were analyzed separately, and the cumulative frequency curves for each were combined as described by Inman (1953a, p. 22). Results are expressed in terms of phi measure (Inman, 1952) which serve as approximate graphic analogues of the moment measures of statistics.

The areal variation of the median diameter (Mdϕ) and of the phi deviation measure ($\sigma\phi$) of the samples from San Miguel Lagoon are given in Figure 15.

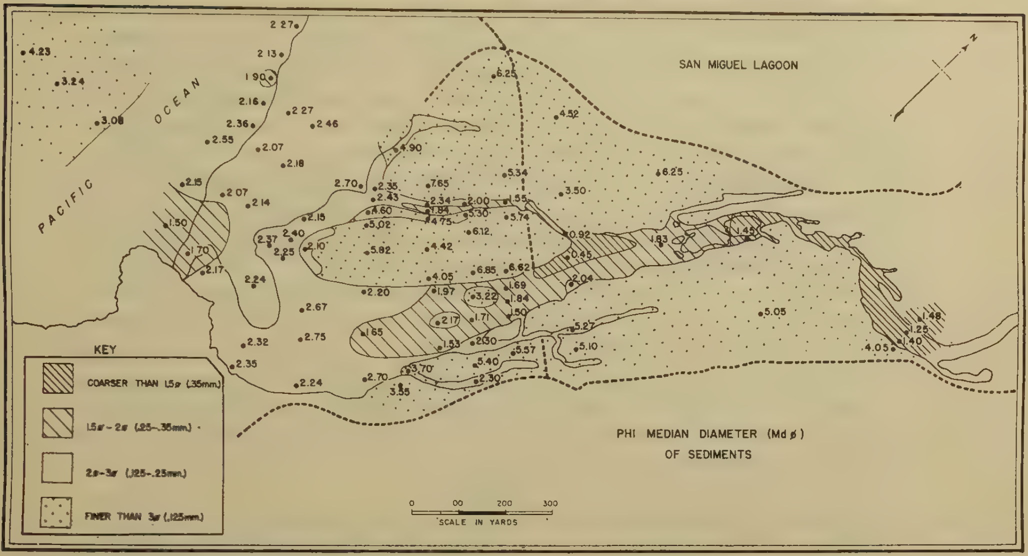
SAN MIGUEL LAGOON
PACIFIC OCEAN
N
KEY
COARSER THAN 1.5φ (.35mm.)
1.5φ - 2φ (.25-.35mm.)
2φ-3φ (.125-.25mm.)
FINER THAN 3φ (.125mm.)
PHI MEDIAN DIAMETER (Md φ) OF SEDIMENTS
0 100 200 300
SCALE IN YARDS
4.23
3.24
3.08
2.27
2.13
1.90
2.16
2.36
2.55
2.27
2.46
2.07
2.18
2.15
2.07
2.14
1.50
1.70
2.17
2.37
2.40
2.25
2.10
2.15
2.24
2.67
2.32
2.75
2.35
2.24
2.70
2.35
2.43
4.60
5.02
5.82
4.90
7.65
2.34
1.84
4.75
2.00
5.30
1.55
5.74
6.12
4.42
4.05
6.85
6.62
2.20
1.97
3.22
1.69
1.84
2.17
1.71
1.50
1.65
1.53
2.30
3.70
5.40
5.57
2.70
3.55
2.30
6.25
4.52
5.34
3.50
6.25
0.92
0.45
1.83
1.45
2.04
5.27
5.10
5.05
4.05
1.48
1.25
1.40

Fig. 15.—A. Areal distribution of phi median diameter (Mdϕ) of San Miguel Lagoon sediments.

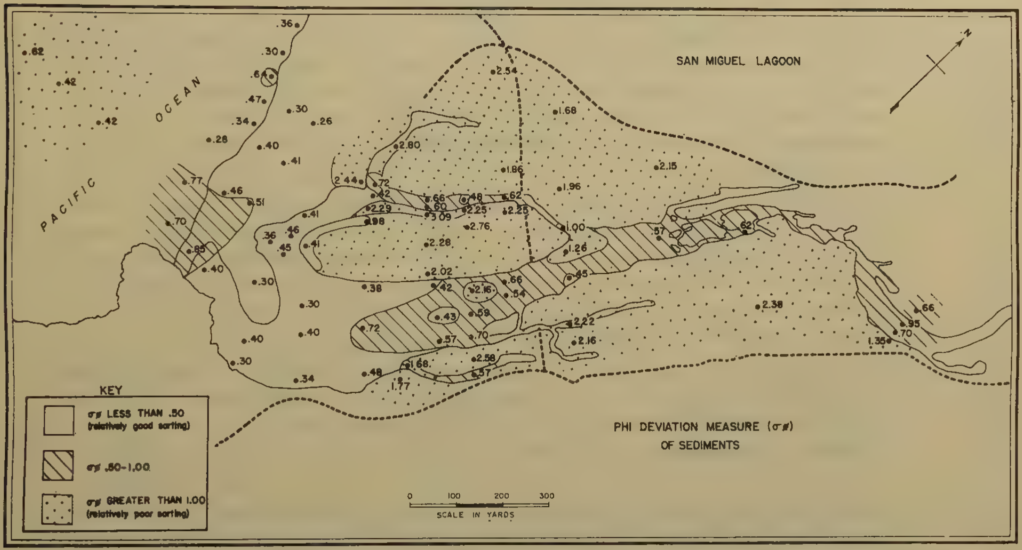
SAN MIGUEL LAGOON
PACIFIC OCEAN
N
KEY
σφ LESS THAN .50 (relatively good sorting)
σφ .50-1.00
σφ GREATER THAN 1.00 (relatively poor sorting)
PHI DEVIATION MEASURE (σφ) OF SEDIMENTS
0 100 200 300
SCALE IN YARDS
.62
.42
.42
.36
.30
.64
.47
.34
.28
.30
.26
.40
.41
.77
.46
.51
.70
.65
.40
.36
.46
.45
.41
.41
.30
.30
.40
.40
.30
.34
.48
2.44
.72
2.80
.42
2.29
.98
.66
.60
3.09
.48
2.25
.62
2.25
2.76
2.28
2.02
1.86
.38
.42
2.16
.66
.54
.59
.43
.72
.57
.70
1.68
2.58
.57
1.77
2.54
1.68
1.96
2.15
1.00
1.26
.45
.57
.62
2.22
2.16
2.38
1.35
.66
.95
.70

Fig. 15.—B. Areal distribution of phi deviation measure ($\sigma\phi$).

Values for the median diameter range from 0.45ϕ (0.73 mm.) to 7.65ϕ (0.005 mm.). To show the relation of the phi median diameter to the phi deviation measure and the phi skewness for these sediments, these parameters are plotted as the x, y, and z co-ordinates of a Cartesian coordinate system, and the points delineate solids in space. If these points are projected onto two planes, called a "size-distribution diagram," the sediments fit generally into three groups (Fig. 16). Group I comprises sediments from the lower lagoon, bay barrier, and ocean beach and has median diameters of 2–3ϕ (0.25 to 0.125 mm.). The sorting of these sediments ($\sigma\phi$) is the best of the three groups and values range from 0.28 to 0.48. Skewness values ($\alpha\phi$) are negative and range from -2.7 to -0.5. Group II consists of sediments in the river and upper lagoon with median diameters generally coarser than 2ϕ (0.25 mm.), sorting values range from 0.45 to 1.25, and skewness values from -0.47 to $+0.05$. Group III consists of all but one of the marsh samples plus some samples from narrow dead-end marsh channels and from the deeper part of the north channel. Median diameters are generally smaller (higher Mdϕ values) than in the other two groups and range from 2.5 to 6.5ϕ (0.176 to 0.011 mm.), and both the sorting values (1.0 to 3.1) and the skewness values ($+0.5$ to $+0.85$) are highest in this group.

The areal variation in median diameters (Fig. 15a) shows a pattern almost identical with that of the phi deviation measure (Fig. 15b). This substantiates the conclusions of Krumbein and Aberdeen (1937) and Hough (1942) that the same environmental factors influence both the size and the sorting of the sediments at any given place within a lagoon or bay. Within San Miguel Lagoon those "environmental factors" are believed to be the processes in operation there. Moreover, it is believed that the primary process that acted upon any sediment sample within this lagoon may be inferred with a fairly high degree of probability from the size characteristics of that sample alone. Figure 16 shows the median diameter (Mdϕ) plotted against the sorting ($\sigma\phi$) for all the samples from San Miguel Lagoon, and the location of each is indicated by the station number. From this it is readily apparent that Group II contains all of the samples from the river, Group III contains all but one of the marsh samples, and Group I contains all of the samples from the bay barrier and ocean beach with three significant exceptions discussed later. Other samples from the lagoon fall into one of these three groups. Figure 17 shows the areal distribution of the sediments in each group, and it is significant that the pattern is not random but that the 13 lagoon samples in the group containing all the river samples outline an area extending the area of the river samples well into the lagoon. Similarly, the 16 lagoon samples in the group containing most of the samples from the bay barrier delineate a sedimentary unit in the lagoon adjacent to the barrier.

From this it is concluded that the three groups based on the size, sorting, and skewness of the sediments are the direct result of the sedimentary processes operating on the barrier and in the lagoon. These processes are divided into three groups: (1) wave processes, consisting of the normal ocean processes shoreward

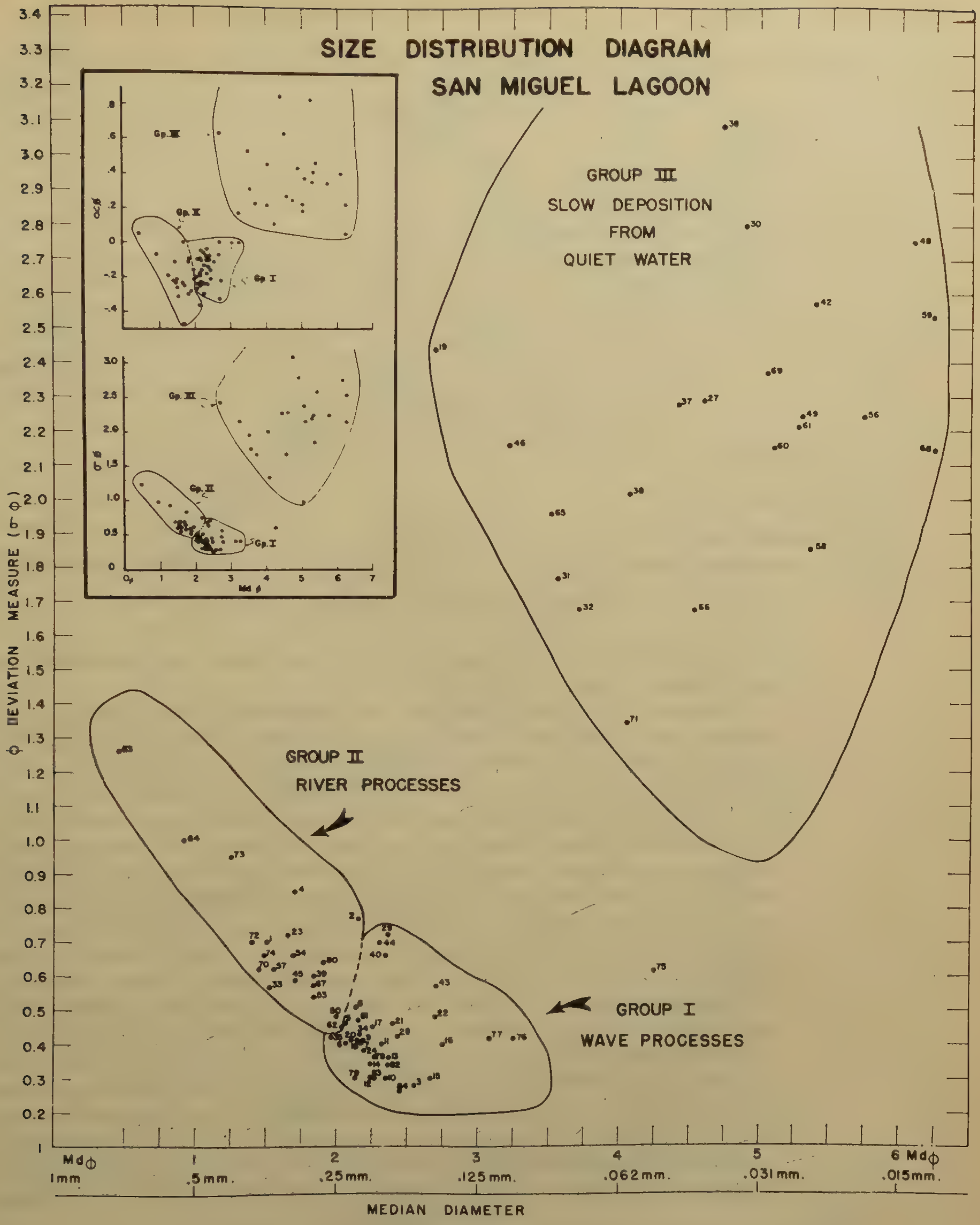

FIG. 16.—Size-distribution diagram, San Miguel Lagoon sediments. Numbers are station numbers.

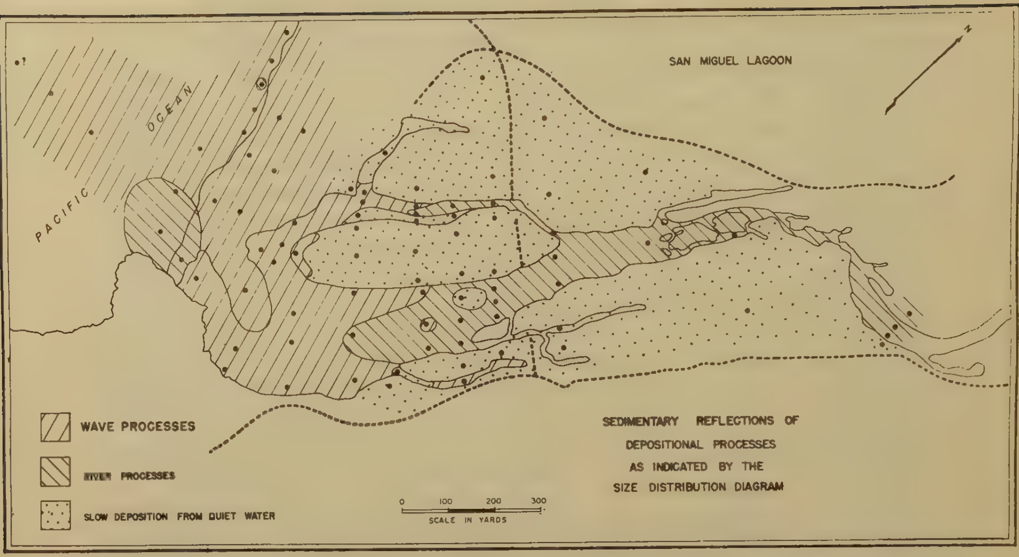
SAN MIGUEL LAGOON
N
PACIFIC
OCEAN
WAVE PROCESSES
RIVER PROCESSES
SLOW DEPOSITION FROM QUIET WATER
0 100 200 300
SCALE IN YARDS
SEDIMENTARY REFLECTIONS OF DEPOSITIONAL PROCESSES AS INDICATED BY THE SIZE DISTRIBUTION DIAGRAM

FIG. 17.—Areal distribution of sedimentary reflections of depositional processes delineated by size-distribution diagram.

of the surf zone, (2) river processes, primarily floods, and (3) slow deposition from quiet water.

Obviously all sediments from other areas which have been subjected to ocean processes will not fall within the size-distribution limits of those samples at San Miguel Lagoon. Cobble beaches are found in many parts of the world, and an outcrop of clay or mudstone along a beach, such as the Magothy clay outcrops on the New Jersey coast, may result in beach material predominantly within the clay size range. Sediments from such beaches would have size, sorting, and skewness values well outside the limits of those ascribed here to wave processes. It is felt, however, that this does not invalidate the interpretation, for the cobbles and the clays on such beaches do not yet reflect wave processes to an extent that obliterates the effect of the processes in action prior to their subjection to wave processes as they are here defined. Thus, if the cobbles were derived from a river or from the erosion of a conglomerate bed, the size-distribution characteristics are still those of river processes or whatever process originally determined the characteristics of the conglomerate bed. Such sediments subjected to wave processes for a sufficient length of time would eventually develop particle-size characteristics indicative of that process. Similarly, the clay beach reflects the processes of deposition of the source bed, and such material on the beach is merely in transit and when redeposited offshore will probably reflect the process of deposition from quiet water. Thus the land-derived material is subjected to various

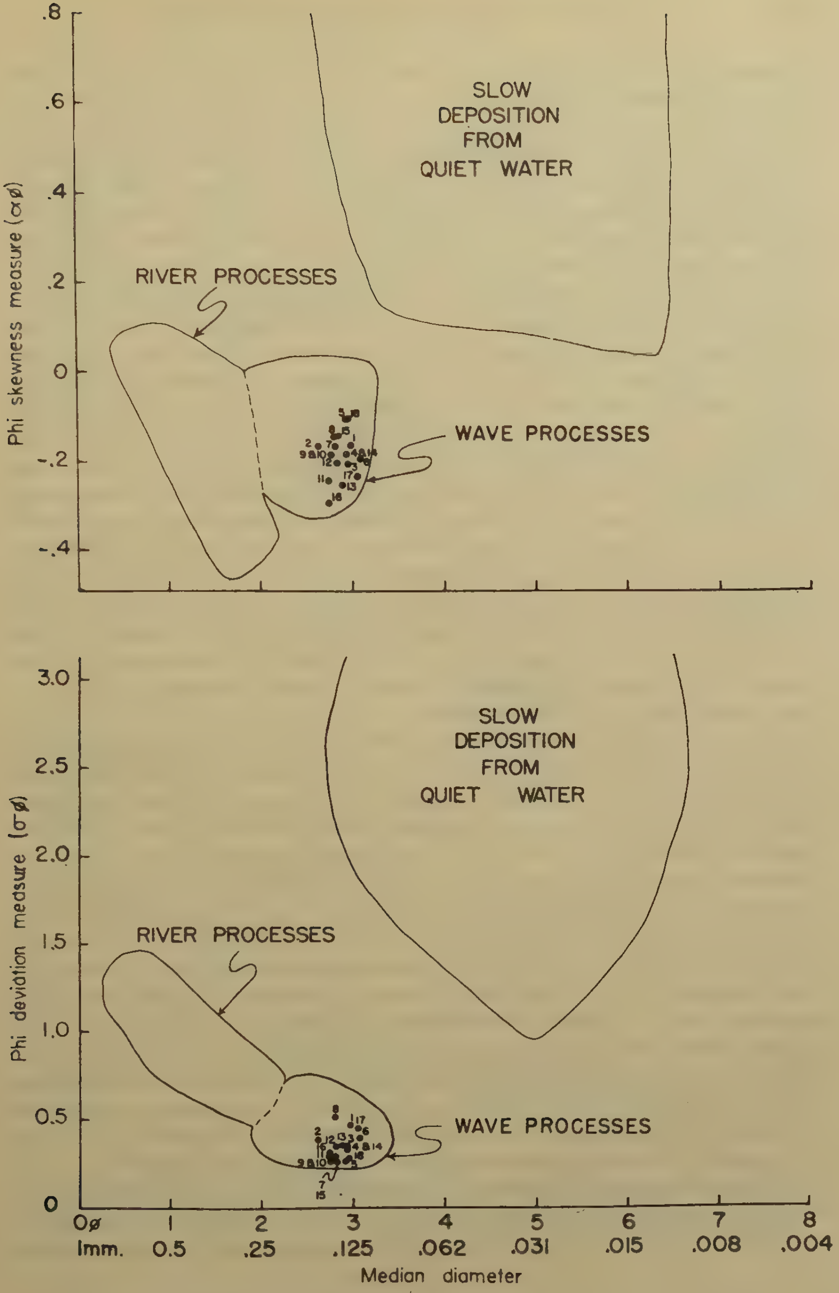

FIG. 18.—Size-distribution diagram, Scammons Lagoon. Numbers are station numbers.

processes of varying intensity, each of which attempts to alter the size-distribution characteristics of that sediment.

The relation of particle-size distribution to processes of transportation and deposition is complex. Significant advances in this field have been made by Inman (1949, 1953a), Griffiths (1951), Inman and Chamberlain (1956), Folk and Ward (1957), and Passega (1957). It has been shown (Inman, 1949; Griffiths, 1951; and others) that when the size distributions are considered for a large number of samples from the beach, nearshore, and offshore areas, the best sorting is in the size range of 2 to 3ϕ (0.25 to 0.125 mm.) and that the sorting is poorer in both coarser and finer sediments. This is also true for the San Miguel samples, but the variations found there are not continuous and therefore permit a distinction to be made between processes. In this connection it is notable that the ocean samples taken farthest from shore at Manuella Lagoon (sta. 21, Fig. 19), Mugu Lagoon (sta. 1, Fig. 20), and San Miguel Lagoon (sta. 75, Fig. 16), all have size and sorting values that place them between the areas here ascribed to wave processes and processes of slow deposition from quiet water. Thus, where a large set of samples extends from the beach out into a deep-water area of slow deposition, the entire range of values may be expected. At San Miguel Lagoon, however, the separation into ranges of values ascribed to each process is possible because this transition does not exist, and the processes are of sufficiently different intensity that the sediments subjected to each are easily recognized. The particle-size distribution of these sediments is discussed in terms of these processes because they obviously are genetically related to them, although the actual mechanical principles involved are unknown.

Sediments subjected to wave processes.—The sediments on the seaward side of the barrier (except those at stations 1, 2, and 4 discussed separately) have relatively uniform size, sorting, and skewness values, and it is believed that they have been subjected to the same processes. These values also fall within the range of values for samples from the foreshore and nearshore areas at La Jolla, California (Inman, 1953a), and a similar range is reported for 26 beach samples from Breton Island off the Mississippi Delta (Inman and Chamberlain, 1956, Fig. 11). These sediments at San Miguel Lagoon are therefore interpreted as having been subjected to processes of transportation and deposition, here termed wave processes. The processes involved along the southern California coast have been described fy LaFond (1939), Grant and Shepard (1939), Shepard and LaFond (1940), Grant (1943), and summarized by Inman (1953b). The lower lagoon sediments that fall within this group (Fig. 17) are therefore interpreted as having been subjected to the same wave processes and subsequently carried into the lagoon primarily by tidal currents operating when the channel was open, but also by wind action and by washovers when the channel was closed.

There is one marsh sample (sta. 20) with a position on the size-distribution diagram within the range of values ascribed to wave processes which at first appears anomalous. This station, however, is not a normal marsh environment but

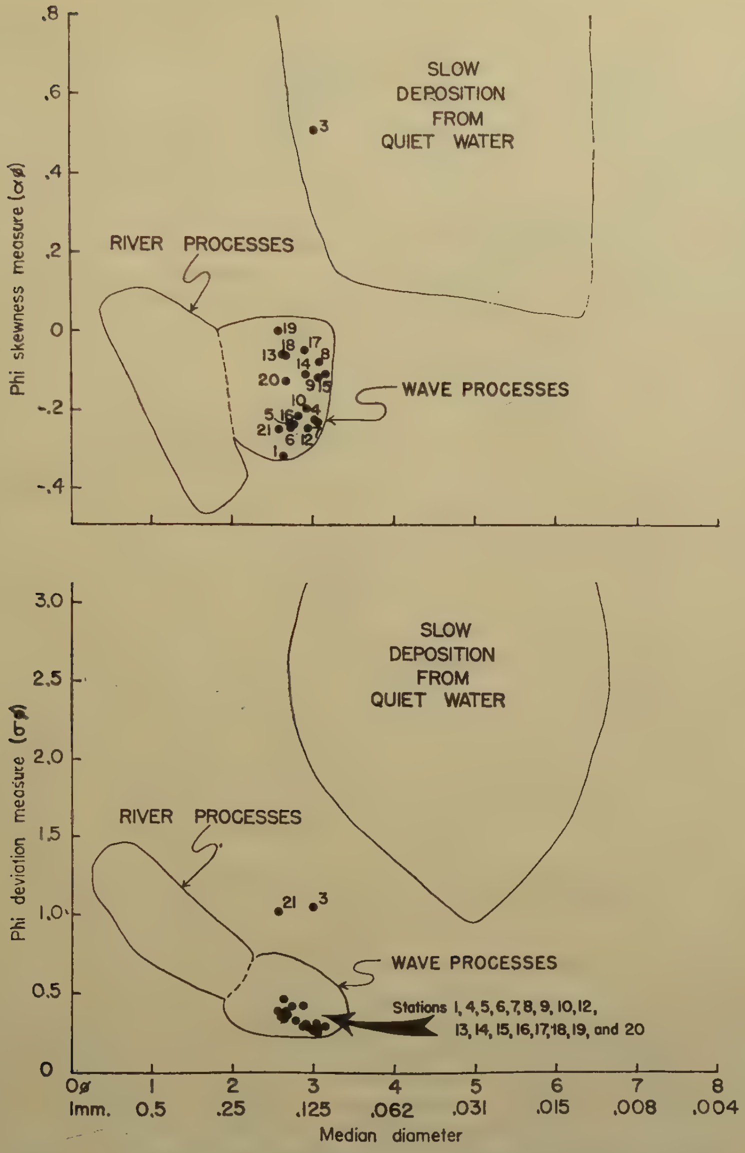

FIG. 19.—Size-distribution diagram, Manuella Lagoon. Numbers are station numbers.

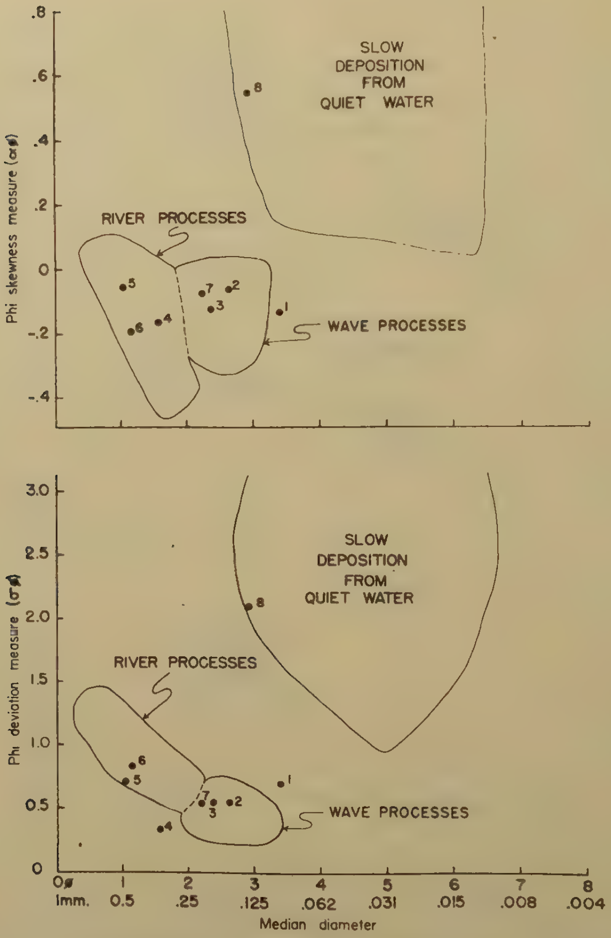

FIG. 20.—Size-distribution diagram, Mugu Lagoon. Numbers are station numbers.

is on an arcuate, levee-like topographic high that borders the seaward edge of the central island. Van Straaten (1951) described similar "levees" along the seaward edges of the marshes in the Dutch Wadden Sea, and Stevenson (1950) found "ridge-like natural levees" on the seaward edges of the marshes at Newport Bay, California. This feature at San Miguel Lagoon is undoubtedly a similar levee built at a time when beach sand was brought into the lagoon by waves that either overrode the barrier or entered a previous channel that crossed the barrier opposite the end of the island. Suspended material brought in by these waves was deposited as a natural levee when the velocity was reduced as the water spread over the island. The shape, location, and similarity to other sea-built levees indicate a seaward source for these sediments, and the occurrence there of sediments with particle-size distribution interpreted as resulting from wave processes lends weight to the accuracy of this interpretation.

Sediments subjected to river processes.—The samples in the river above the lagoon fall into one group on the particle-size distribution diagram (Fig. 16) and are interpreted as having been subjected to transportation and deposition by the river. The limits of the areal extent of the sediments within this group extend far into the lagoon, suggesting that these lagoon sediments also were brought in by the river during floods, or at least at a time when the transporting power of the river was greater than at the time of sampling. The concentration of the coarsest sediments in the lagoon at the up-river end of the island results from the sudden diminishing of the transporting power of the river in flood when the waters impinge against the upstream end of the island. Local residents informed the writer that when the Rio San Miguel is in flood there is a great "boil" at that end of the island, and that the torrent is split there with the greater part of the water flowing south of the island. This is indicated by the sediments south of the island being generally coarser and more poorly sorted than those north of it, and the area of sediments influenced by river processes is larger on the south side of the island (Fig. 17).

The isolated occurrence on the bay barrier of three samples (stations 1, 2, and 4) with the size-distribution characteristics of sediments subjected to river processes is significant. These three samples occur where the channel crossed the barrier when the lagoon was open, and they are interpreted as river sediments deposited when the transporting power of the river in flood was reduced where the river entered the ocean. Subsequent wave processes have been incapable of removing or modifying this coarser material, and it remains on the barrier as a lag sediment.

Sediments deposited from quiet water.—The sediments on the border marshes at San Miguel Lagoon are the fine-grained, poorly sorted sediments typical of marshes bordering bays and lagoons. Louderback (1939) found that the sediments on San Francisco Bay marshes are the finest-grained in the area, and similar sediments have been reported from marshes at Newport Bay, California (Stevenson, 1954), from marshes on Cape Cod, Massachusetts (Hough, 1942), from marshes in the British Isles (Richards, 1934), and in Holland (Van Straaten, 1954a). Sedimentation on the marshes at San Miguel Lagoon occurs periodically when rising lagoon waters inundate the marshes. Current action is diminished by the thick growth of plants, and the particles in suspension settle out of the quiet water.

Samples from three stations in narrow dead-end marsh channels (stations 30, 32, and 61) also fall within the area on the size-distribution diagram interpreted as reflecting deposition from quiet water. Also in this group are the samples from stations 27, 38, and 49 in the deeper part of the north channel and station 46 in a closed depression south of the island. These samples are from areas of thick aquatic plants (primarily *Ruppia* and *Chara*) that trap the finer sediments, and all are in depressions or protected arms where such sediments might be expected to escape removal by currents.

The validity of using the measures of the size, sorting, and skewness of a single sediment sample from a coastal lagoon as indicative of the processes to which it has been subjected was checked by obtaining samples from other coastal lagoons. These samples were similarly analyzed, the values plotted as size-distribution diagrams, and the areas of the San Miguel Lagoon values ascribed to each of the three processes were superimposed on these diagrams.

Scammons Lagoon.—Eighteen samples from the Scammons Lagoon area were collected from 22 fathoms seaward of the lagoon, ocean beach, dune, lagoon marsh, and upper lagoon 11 miles from the entrance (Fig. 3 shows locations). All samples fall within the limits of San Miguel Lagoon samples influenced by wave processes (Fig. 18).

Scammons Lagoon is at the edge of the Vizcaino Desert, and no river enters the lagoon. This explains the lack of sediments reflecting river processes and also the lack of abundant fine-grained material for typical marsh deposition. Strong onshore winds and tidal currents bring large amounts of sand into the lagoon, from a seaward direction, processes which would contribute sand which has been influenced by wave processes. Evidence from the foraminiferal assemblages at these stations (Stewart, 1956a) supports the contention that these sediments are derived from seaward.

Manuella Lagoon.—Samples were collected at Manuella Lagoon from one mile seaward of the barrier, from the foreshore, berm, and dune on the barrier spit, from the lagoon, a tidal sand flat, a tidal creek, and from the marshes. A similar size-distribution diagram was constructed for these sediments and the San Miguel Lagoon limits superimposed (Fig. 19). Eighteen of the 19 samples have values indicative of wave processes, and since the lagoon is just north of Scammons Lagoon, the explanation is the same as that offered for those sediments.

Mugu Lagoon.—Samples were obtained at Mugu Lagoon from various environments and a similar size-distribution diagram constructed (Fig. 20). The three offshore samples (stations 1, 2, and 3) have size characteristics indicative of wave processes, and the marsh sample (sta. 8) is indicative of slow deposition, processes typical of the environment where each was obtained. Sample 7, on the other hand, collected from a tidal sand flat within the lagoon far from the present channel entrance, reflects wave processes. Aerial photographs of the area flown six months earlier show that the channel at that time was east of its present location and that the area of this sample was part of a large delta built into the lagoon opposite that channel. Coarse-fraction analyses showed the sample to be most like that at station 16 in San Miguel Lagoon located on a similar delta.

Samples from stations 5 and 6 on the crest of the barrier spit reflect river processes, and sample 4 on the foreshore of the barrier is on the boundary between river and wave processes (Fig. 20). The presence of river sediments on the barrier to a height of 6 feet above the high-tide line was explained when investigation revealed that material dredged from the upper lagoon near the mouth of Calleguas Creek had been dumped along the length of the barrier spit to increase its height. Even though dredged and redeposited, these sediments retained the size-distribution characteristics of sediments deposited by river processes. Thus the sample at station 4 on the ocean foreshore of the barrier similarly reflects river processes, but the sorting has subsequently been improved by the action of wave processes.

COARSE-FRACTION STUDIES

Studies of the percentage of the various constituents in the fraction coarser than .062 mm. of the San Miguel sediments were made under the binocular microscope, with the technique of Shepard and Moore (1954). Constituents used in this study included shells, quartz, dark minerals, mica, rock fragments (including all other minerals not counted specifically), plant fragments, aggregates, Foraminifera, and ostracods. Seven sedimentary environments were delineated on the basis of these studies. Typical histograms are shown in Figure 21, and the average coarse-fraction composition for each environment is given in Table II. The areal distribution of these environments (Fig. 22) is very similar to that of the various areas delineated by the size-distribution diagrams (Fig. 17), further substantiating the validity of these techniques in sediment studies.

The differences between the interpretation of the sediments by these two methods are significant. Sample 20, for example, from the sea-built levee on the island reflects wave processes in its size-distribution, but coarse-fraction studies indicate a marsh environment. Similarly stations 1, 2, and 4 on the barrier reflect

TABLE II. AVERAGE COARSE FRACTION FOR ALL SAMPLES IN EACH ENVIRONMENT, SAN MIGUEL LAGOON

Environment	*Shells*	*Quartz*	*Dark Minerals*	*Rock Fragments*	*Mica*	*Plants*	*Aggregates*	*Other*	*Per Cent Total* <.062 mm.
Nearshore ocean	0.3	68.5	6.5	3.2	17.7	0.4	3.0	Forams 0.3	24.1
Ocean beach	—	74.6	10.0	12.9	2.3	—	—	—	0.2
Dune	—	66.5	21.9	11.4	0.2	—	—	—	0.2
Lagoon near ocean	—	79.9	10.1	5.3	3.4	0.1	0.4	Ostr. Shls. 0.6 0.2	0.5
River and Ign. near river	—	76.2	6.6	11.8	4.3	0.1	0.8	Ostrod. 0.2	1.0
Lagoon no spec. influence	0.4	62.8	8.4	2.4	20.6	1.3	3.9	Forams 0.2	41.4
Marsh	—	28.9	5.7	2.6	17.5	33.3	12.0	—	80.0

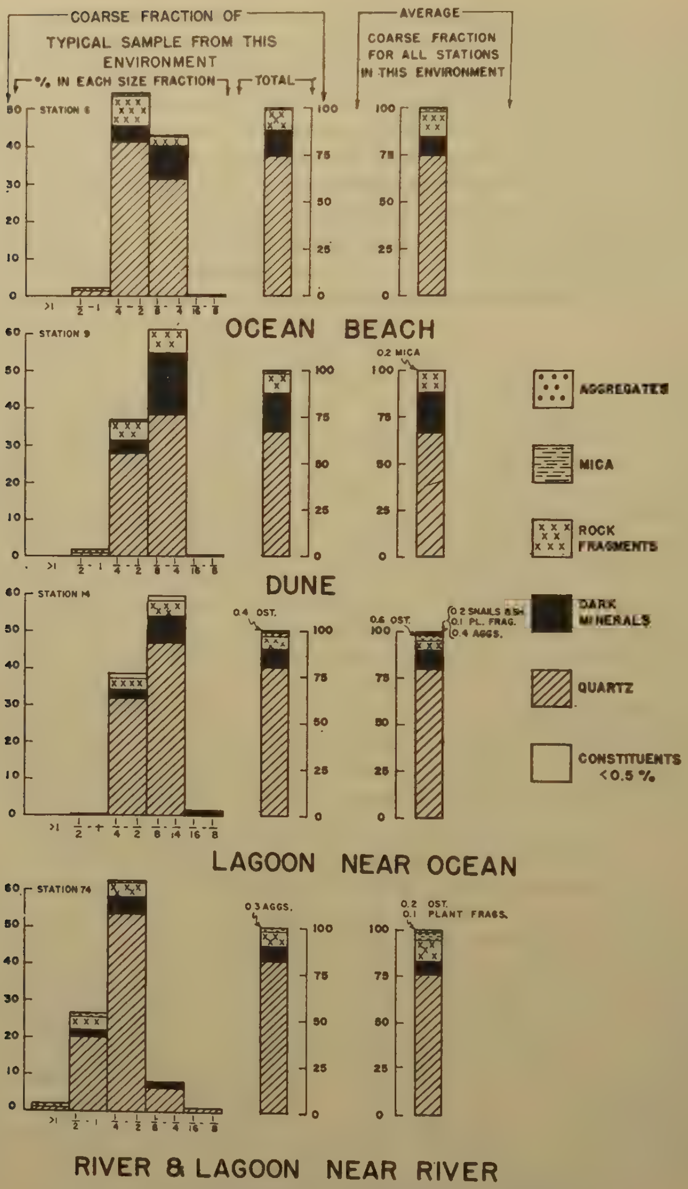

FIG. 21.—Coarse-fraction histograms of samples from "nearshore ocean," "marsh," and "lagoon no special influence" environments.

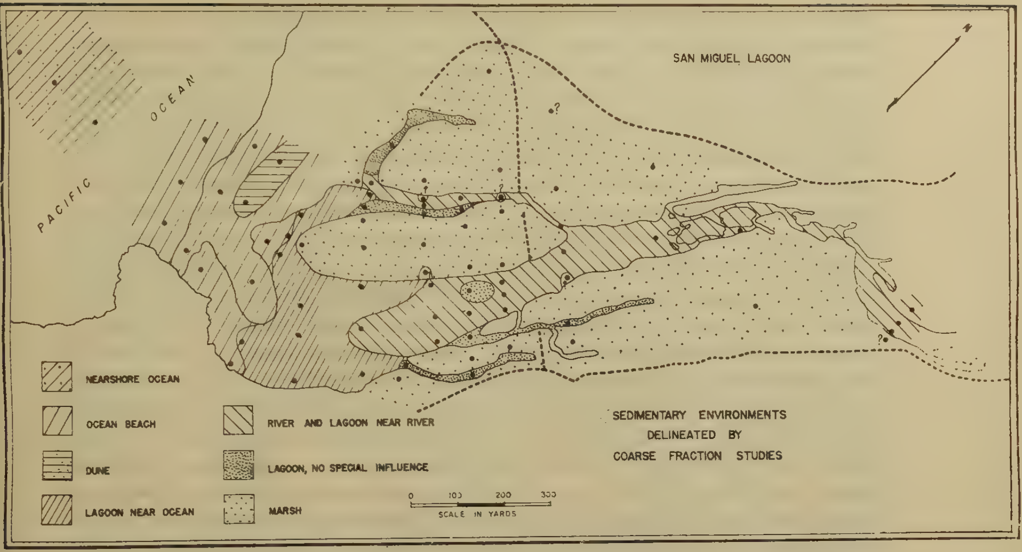
SAN MIGUEL LAGOON
PACIFIC
OCEAN
?
NEARSHORE OCEAN
OCEAN BEACH
DUNE
LAGOON NEAR OCEAN
RIVER AND LAGOON NEAR RIVER
LAGOON, NO SPECIAL INFLUENCE
MARSH
0 100 200 300
SCALE IN YARDS
SEDIMENTARY ENVIRONMENTS
DELINEATED BY
COARSE FRACTION STUDIES

FIG. 22.—Areal distribution of sedimentary environments delineated by coarse-fraction studies.

river processes in size distribution, but the coarse fraction shows an ocean beach environment. This suggests that the particle-size distribution is an indication of the process to which a sediment has been subjected, whereas the coarse-fraction studies indicate the environment where the sediment is deposited. Usually the process is part of the environment; hence this distinction is possible only at such stations as the above, where the process that acted upon the sediment is no longer active in the environment.

FORAMINIFERA

Since there were relatively few Foraminifera in the San Miguel Lagoon samples, they were concentrated in the size-fraction larger than 0.62 mm. by flotation with carbon tetrachloride. The floated material was composed of a concentration of Foraminifera, ostracods, small shell fragments, plant fibers, seeds, and some mica. Examination of the fraction finer than .062 mm. showed only a few juvenile forms, and their recovery and identification were not practicable.

Foraminifera were abundant in samples taken at depths of 20 and 40 fathoms seaward of San Miguel Lagoon but were generally rare in the lagoon sediments. Only at station 61 were they relatively abundant, and even there they comprise less than one per cent of the total sample. Of the 34 lagoon samples studied, 14 contained no Foraminifera, and 11 each yielded less than 10 specimens. Even though the number of species and specimens within the lagoon is small, the distribution appears significant.

Table III shows the occurrences of species in San Miguel Lagoon. The near-shore samples and those on the ocean beach contain a typical shallow-water marine assemblage. The lagoon fauna, however, presents no such clear-cut picture. "*Rotalia*" *beccarii* (Linné) vars. and *Elphidium* cf. *translucens* Natland comprise 92 per cent of the specimens from the Lagoon (Table III), have wide and similar distributions, and at the two stations with the highest populations are the only species present. Studies in three nearby areas show that these species live in comparable though less rigorous environments. Davies (1954) in a study of Mission Bay, an open coastal lagoon in southern California, found both species living in and restricted to shallow muddy areas of the back bay where the content of decaying organic matter is high. Walton (1955) reported "*Rotalia*" *beccarii* vars. only from the estero (coastal lagoon) and not from the adjacent Todos Santos Bay which is in open connection with the sea. He found the species living in the estero only at the station farthest from the open entrance to the bay. Although examination of Walton's material showed that his *Elphidium* sp. is not the same as the *E.* cf. *translucens* from San Miguel Lagoon, he did find *E.* sp. only in the estero. Arnal (1955) found "*Rotalia*" *beccarii* vars. (reported as *Streblus tepidus*) comprising 70–80 per cent of the specimens obtained from Playa del Rey Lagoon, a closed lagoon on the coast of Santa Monica Bay, California.

Numerous individuals of these two species from San Miguel Lagoon appear abnormal, having irregularly shaped chambers at the apertural end. Comparable abnormalities were reported by Arnal (1955) from closed Playa del Rey Lagoon for specimens of "*Rotalia*" *beccarii* vars. Le Calvez and Le Calvez (1951) reported that closed lagoons on the French coast having large environmental fluctuations also contain abnormal specimens. Because of the wide and similar dis-

TABLE III. OCCURRENCES OF FORAMINIFERA IN ACTUAL NUMBER OF SPECIMENS PER SAMPLE OF UNIFORM SIZE, SAN MIGUEL LAGOON

Station	7	13	14	16	22	23	25	27	28	29	30	32	33	35	36	37	38	39	40	41	42	43	45	46	49	50	51	53	54	57	58	61	67	72	Total
Total population	1	0	2	2	26	5	0	22	1	10	107	90	3	0	0	0	54	0	0	0	0	4	1	18	53	0	1	3	6	0	0	190	0	0	600
Globigerina bulloides					1																								1						2
G. sp.					5	1																													6
Buliminella elegantissima					1							1																							2
Cassidulina subglobosa					1																														1
C. tortuosa					1																														1
Cibicides fletcheri	1			1	6							1																1							10
Discorbis companulata					2																														2
D. sp.					1																														1
Elphidium cf. translucens					3	2		2		6	40	14					11							2	8			1	5			120			214
E. sp.													1												1										2
Entosolenia squamosa												1																							1
Haplophragmoides tenuum					1																														1
Jadammina polystoma																							1				1								2
Robulus sp.					1																														1
"Rotalia" beccarii vars.	1					2		18	1	4	67	73	1				43							16	44							70			340
"R" lomaensis			2	1	3																														6
Trochammina inflata								2					1									4						1							8

tributions of these two species in San Miguel Lagoon, because of their abundance in other west coast lagoons, and because of the occasional abnormalities found only in the lagoon samples and only in these two species, they are believed to be the only species that are adapted to the wide range of environmental conditions in this lagoon.

In the Gulf of Mexico both *Elphidium* spp. and "*Rotalia*" *beccarii* vars. are open-gulf species that may have migrated into the lagoons, have found the environment suitable, and have become two of the dominant elements of the lagoon microfauna (Phleger, 1954). This suggests that these forms, now found on the Baja California coast only in the lagoons, once may have lived in the open ocean. After migration into the lagoons and adaptation to that environment, the ocean forms were somehow eliminated, leaving only the lagoonal representatives. This mechanism of migration and adaptation to a restricted environment with the subsequent elimination of the parent stock offers a possible explanation for the discontinuous distribution of certain species found only in similar but non-interconnected environments. The common occurrence of *Trochammina inflata* (Montagu) in many of the world's marshes, but its absence in the intervening oceans, is an example.

Since *Trochammina inflata* (Montagu) and *Jadammina polystoma* Bartenstein and Brand are common marsh species (Phleger and Walton, 1950; Parker, Phleger, and Peirson, 1953; Walton 1955), it is interesting that the marsh areas of San Miguel Lagoon contain so few individuals of these species. Walton (1955) found an average of 31 *Trochammina inflata* and 13 *Jadammina polystoma* in samples of comparable size at each of his 13 stations on the estero marsh, only 20 miles south of San Miguel Lagoon. Samples from 7 stations on the border marshes and island marsh at San Miguel Lagoon were examined, and only one specimen of *Jadammina polystoma* was found. Eight specimens of *Trochammina inflata* and one additional specimen of *Jadammina polystoma* were found in the samples from the lagoon and the marsh channels, but the marshes themselves are essentially barren. Even ostracods, common in most of the lagoon samples, were not found in the marsh.

The probable explanation for this is that these are not normal salt marshes which are wet at each high tide. When the San Miguel barrier is first open, there is a large exchange of water between the lagoon and the ocean with each tidal cycle and the marshes are wet from beneath. As the barrier increases in height, there is a decrease in the volume of the tidal prism, and less water is available to the marshes. At the same time, the surface water is becoming less saline due to continued dilution by inflowing river water. By the time the water level is high enough to inundate the marshes, the barrier has closed completely and the lagoon water is nearly fresh. The conditions in this marsh are those of a typical salt marsh during only a small portion of the lagoon cycle. The marshes are dry for part of the cycle; and when they are flooded for any length of time, the water is almost fresh.

Isolated specimens of *Cibicides fletcheri* Galloway and Wissler and of "*Rotalia*" *lomaensis* Bandy were found in the lower lagoon. Both species are normal open-ocean forms and undoubtedly represent marine forms washed into the lagoon, either through the channel when it was open or across the barrier by washovers after the channel had closed. Their occurrence in the lower lagoon is considered as resulting from mixing at the boundary between the two environments.

The assemblage at station 22 in the lower lagoon is distinctive. As shown in Table III, 12 of the 17 species found in the lagoon occur at this station, and 6 are found exclusively there. Eighty-eight per cent of the specimens at station 22 are shallow open-ocean forms, and only one of the 12 species (*Elphidium* cf. *translucens*) can be regarded as a normal lagoon form. In addition to the Foraminifera, numerous sponge spicules and two specimens of the marine diatom *Coscinodiscus* were found at this station.

This primarily marine assemblage supports the hypothesis advanced previously from the chlorinity and depth data that sea water entering the lagoon as washovers flows along the bottom and collects in the region of station 22. If open-ocean Foraminifera are carried along with the water, it must move over the bottom as a unit with only slight mixing. When it arrives in the deepest part of the lagoon, the Foraminifera settle to the bottom. Slow dilution by the overlying lower-chlorinity water reduces the chlorinity of the water in the depression, so that when the next high tide washes over the barrier the sea water will have a higher density than the water from the previous washover and will flow to the bottom of the depression. In this manner Foraminifera from successive washovers can be deposited in one small area.

CALCIUM CARBONATE

Determinations of the calcium carbonate content were made on 58 sediment samples. Analysis was by the manometric method with techniques developed by George Bien of the Scripps Institution. A known weight of sediment is digested in dilute hydrochloric acid, and the volume of gas evolved is measured, corrected to standard temperature and pressure, and converted to per cent carbonate as calcium carbonate per gram of sample. Triplicate analyses were run on each sample. At least two of these values agreed for 69 per cent of the samples and this was the value accepted. For the others, if the discrepancy was less than 0.1 per cent the three values were averaged; otherwise, additional determinations were made.

Areal distribution of per cent calcium carbonate per gram of sample is shown in Figure 23. Values range from 0.16 per cent to 2.28 per cent with the average less than one per cent. Values increase with distance up-river from the lagoon, and decrease along the ocean beach with distance from the position of the former channel. The calcium carbonate occurs in the sediments as shells of snails, the tests of Foraminifera and ostracods, fragments of calcareous algae (rare), and small fragments of unknown origin incorporated in white aggregates of fibrous organic material.

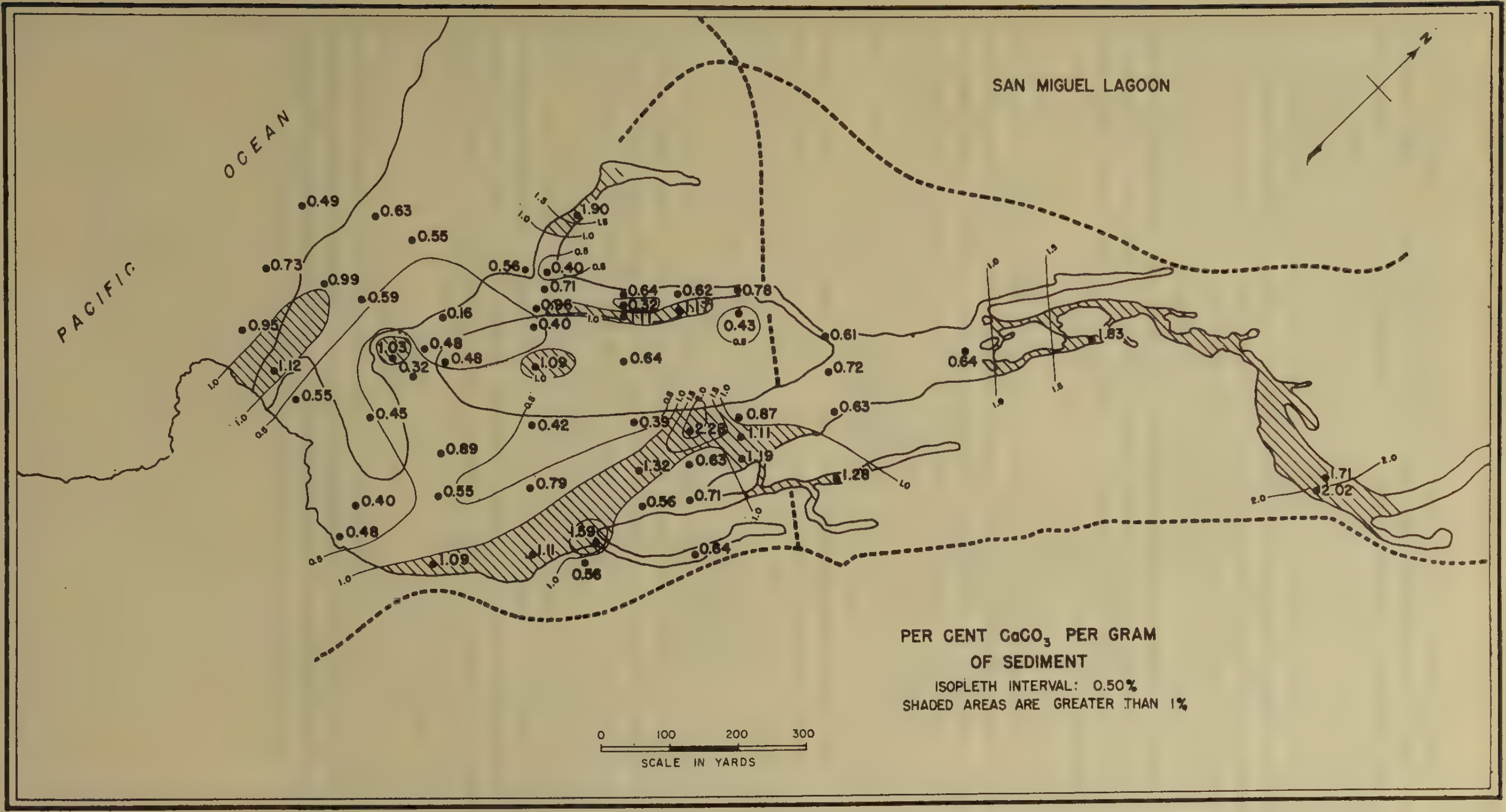
SAN MIGUEL LAGOON
N
PACIFIC OCEAN
PER CENT CaCO$_3$ PER GRAM OF SEDIMENT
ISOPLETH INTERVAL: 0.50%
SHADED AREAS ARE GREATER THAN 1%
0
100
200
300
SCALE IN YARDS
0.49
0.63
0.55
0.73
0.99
0.59
0.95
1.12
0.55
0.16
0.48
0.48
1.03
0.32
0.45
0.89
0.40
0.48
0.55
0.56
0.40
0.71
0.96
0.40
1.90
0.64
0.32
1.11
0.62
1.13
0.78
0.43
1.09
0.64
0.42
0.79
0.39
2.28
0.87
1.11
1.32
0.63
1.19
0.56
0.71
1.59
1.11
1.09
0.56
0.64
0.61
0.72
0.63
1.28
0.64
1.83
1.71
2.02

FIG. 23.—Areal distribution of per cent calcium carbonate per gram of sediment. Isopleth interval 0.50 per cent. Shaded areas are greater than 1 per cent.

The calcium carbonate content of these sediments is low compared with the 5–20 per cent for samples from Barataria Bay, Louisiana (Caldwell, 1940), or for San Antonio Bay and other bays along the central Texas coast where average values of about 20 per cent were reported by Shepard and Moore (1955, Fig. 41). Trask (1932), however, reported values of 0–2 per cent as typical of sediments from brackish environments. Stevenson (1954) reported that the sediments of Newport Bay, California, rarely contain more than two per cent of calcium carbonate, and Debyser (1955) found an average of only 1.04 per cent for samples from the Abidjan lagoons on the Ivory Coast of Africa.

The amount of calcium carbonate in any sediment is dependent on (1) the sources, (2) the amount of clastic material diluting it, and (3) the physico-chemical factors acting upon it during transportation and during and after deposition. Within San Miguel Lagoon these three factors vary within wide limits areally and with time, resulting in the somewhat erratic pattern of the calcium carbonate distribution shown in Figure 23.

The increase of calcium carbonate with distance up-river suggests the river as one source. At station 72 with the second highest per cent of calcium carbonate the material occurred as small fragments of indeterminate origin. This river source is also suggested by the decrease in calcium carbonate along the ocean beach away from the point where the channel crossed the bay barrier. This parallels variations in the coarse-fraction constituents that are also interpreted (Stewart, 1956a) as indicative of a river source for these sediments.

Although not abundant within the lagoon, shells and tests of organisms constitute a source for some of the calcium carbonate. The six stations with the largest populations of Foraminifera (stations 22, 30, 32, 38, 49, and 61) all had more than one per cent calcium carbonate per gram, suggesting that the tests of these organisms may be an important source of calcium carbonate.

The association in coastal lagoons of higher calcium carbonate with finer sediments, reported by Caldwell (1940) and Shepard and Moore (1955, p. 1520), is not generally true for San Miguel Lagoon, because the river source of calcium carbonate is also the source of the coarsest sediments. Although the fine-grained sediments do have relatively high calcium carbonate values, so do the coarser-grained up-river samples. The ocean beach samples, on the other hand, show a definite *decrease* in calcium carbonate with decreasing size, due to the fact that both parameters are dependent on distance from the river source. Most samples, however, indicate no relation between calcium carbonate content and sediment size.

ORGANIC CARBON

Determinations of the organic carbon content of the San Miguel Lagoon sediments were made by using a modification of the Krogh method (Krogh and Keys, 1934). The carbonate is removed with phosphoric acid, and the remaining carbon in a weighed sample is converted with concentrated sulphuric acid to carbon dioxide, passed in a stream of oxygen through a combustion tube, and collected in a trap of barium hydroxide. The carbon dioxide given off is measured by back-titrating the remaining barium hydroxide with hydrochloric acid using phenolphthaline as an indicator. Duplicate analyses were made and averaged, and the results are presented as mg./g. of organic carbon.

Because of faulty apparatus, 59 of the 74 determinations were invalidated, and this study is based on the remaining 15 samples. The areal distribution of the organic carbon in San Miguel Lagoon is shown in Figure 24. Values range from 0.36 mg./g. to 5.60 mg./g., and the highest values are found in the narrow dead-end marsh channels and the deeper parts of the north channel.

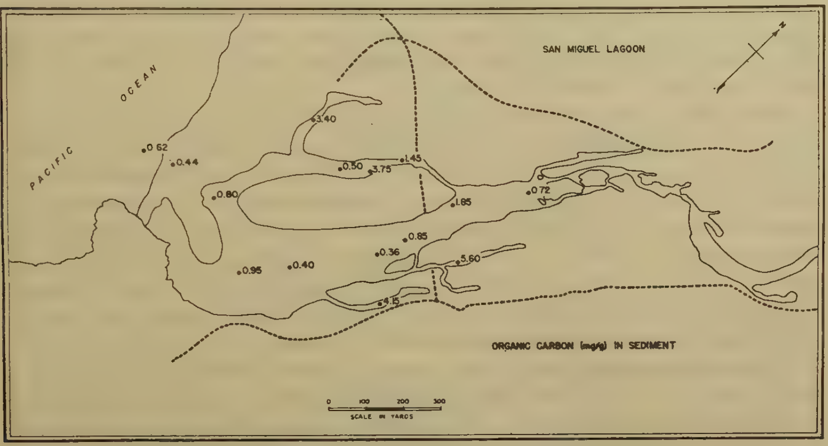

FIG. 24.—Areal distribution of organic carbon in mg/g of sediment.

The samples from the narrow dead-end marsh channels and the deeper parts of the north channel are predominantly black muds smelling strongly of hydrogen sulphide, conditions suggesting high organic content. However, the average content of organic matter in these black sediments is less than one per cent, using the factor of 1.8 suggested by Trask (1939) for estimating the total organic content from the carbon content. Comparable low values for the organic content of black sediments have been reported by several workers. Corcoran (personal communication) found only 1.27 per cent organic matter (0.7 per cent organic carbon) in black sediments from Mission Bay, California, smelling strongly of hydrogen sulphide. Trask (1932, p. 158) found that in Salina Guaranao, a closed coastal lagoon on the coast of the Gulf of Venezuela, a "black jelly-like substance" covering the bottom contained less than 3 per cent organic material (reported as a nitrogen content of 16 parts per 10,000). Sudry (1910) found that the black hydrogen-sulphide muds of the Thau Lagoon near Cette in southern France contained "total carbon" of only 2–3 per cent.

In San Miguel Lagoon there is a large amount of organic material available for inclusion in the sediments. The thick growth of *Ruppia maritima* and other aquatic plants has been mentioned. When these plants die in the fall, large amounts accumulate on the bottom and along the sides of the lagoon. The filamentous blue-green alga *Anabaena* forms floating "islands" up to 5 feet across when the lagoon is closed, and in June, 1953, *Anabaena* covered the entire surface of one of the narrow dead-end marsh channels. Plankton tows show the lagoon to be rich in copepods and cladocerans, with many insect larvae, ostracods, and small planorbid snails. In addition, strictly marine forms washed over the bay barrier and into the lagoon soon die and are added to the lagoon sediments. In August, 1953, many dead and decomposing fish, primarily top smelt (*Artherinops affinis*) and shiner perch (*Cymatogaster aggregata*), both strictly marine forms, were found in the lagoon, and marine doliolids were found in the plankton tows following a period of high-tide washovers.

Measurements of the dissolved carbohydrate in the waters of this lagoon were made by G. J. Lewis of the Scripps Institution while the lagoon was in open connection with the ocean. His values (Lewis and Rakestraw, 1955) show that the concentration of dissolved carbohydrate in the lagoon water increases from a normal ocean value of 0.3 mg./L at the entrance to 0.9 mg./L at a distance of 100 yards from the entrance. At the time of his sampling, the lagoon waters were renewed with each tidal cycle, and the observed increase of 0.6 mg./L over normal sea water values must have taken place in less than 12 hours, reflecting relatively high concentrations of organic material in the lagoon.

Bacterial decomposition of the abundant organic material may proceed at such a fast rate that little measurable organic material is present in the sediment at any one time. Moberg *et al.* (1937) showed that the size of the bacterial population in sediments parallels the organic content, and ZoBell (1946, pp. 136–49) described the processes whereby bacteria may accomplish the complete decomposition of organic matter.

In the more aerated parts of the lagoon, the organic matter probably is rapidly oxidized. The areas deficient in oxygen have already been shown to be areas of large oxygen production but with attendant high utilization, probably in oxidation of the organic material (Waksman and Hotchkiss, 1938). Low oxygen concentrations tend to inhibit bacterial decomposition of organic material (ZoBell, 1946, p. 95), but anaerobic decomposition continues under these reducing conditions with the attendant formation of hydrogen sulphide (Waksman, 1941), which would further reduce the oxygen in the overlying water.

Formation of hydrogen sulphide in these sediments was demonstrated in a core containing 2 feet of sediment and 2 feet of the overlying water. The water was poured off and replaced by fresh water. The core was then shaken gently, and a strong odor was noted. A measurement of the hydrogen sulphide in this water by Sayed El Wardani, formerly of the Scripps Institution, gave a value of 8 ml. /L, showing a high concentration of hydrogen sulphide in the sediments. For comparison, an average of 9.14 ml./L of hydrogen sulphide was reported for the water of stagnant Norwegian fjords (Fleming and Revelle, 1939). Hydrogen sulphide from organic decomposition and from sulphate reduction may escape into the overlying water but is in part fixed in the sediment as the black metallic sulphides.

The finer-grained sediments in the lagoon have generally higher organic content (Fig. 25). The same relation has been reported from the Mississippi Delta (Krumbein, 1939), from the California basins (Revelle and Shepard, 1939; Emery and Rittenberg, 1952), from the Texas bays (Shepard and Moore, 1955, p. 1519), from the Dutch Wadden Sea (Van Straaten, 1954b), and elsewhere (see Trask, 1932, p. 76). In San Miguel Lagoon the higher organic carbon content with finer grain size may be in part due to the relative rates of deposition of these two constituents. The deeper parts of the north channel and the narrow dead-end marsh channels are areas of slow deposition of fine-size particles, as opposed to the more rapid deposition elsewhere in the lagoon. The organic matter, on the other hand, accumulates more rapidly in these same areas. Material carried into the stagnant depressions is no longer affected by bottom currents and remains there. These are also areas of abundant growing aquatic plants that contribute additional organic material.

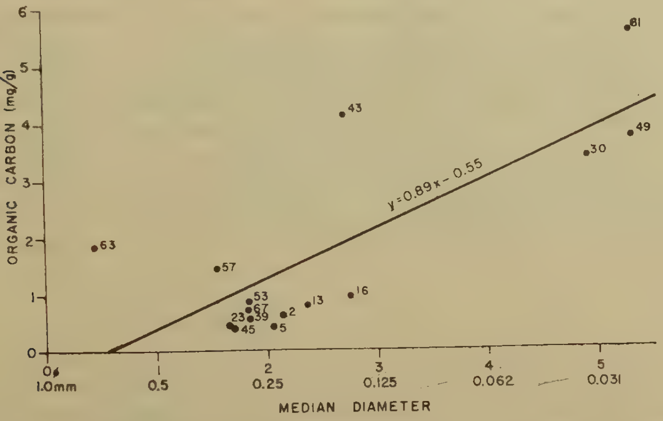

FIG. 25.—Mg/g organic carbon plotted against median diameter (Mdϕ) of sediment.

From the foregoing discussion, it is apparent that the preservation of organic material in lagoon sediments depends on (1) the rate of accumulation of the organic matter, (2) the rate of decomposition, (3) the rate of dilution by clastics, and (4) the rapidity of burial. In San Miguel Lagoon the rate of accumulation is high and dilution by clastics relatively low, but the rate of decomposition is also high, and rapid burial occurs only rarely, so the degree of preservation is low.

Various combinations of these factors could result in no organic material being preserved or in extremely large amounts being preserved, and all gradations between these two extremes.

RELATIONSHIP OF SEDIMENTS TO OVERLYING WATER

Calcium carbonate and pH.—When the per cent calcium carbonate per gram of sample is plotted against the pH of the overlying water (Fig. 26), the sediments underlying the up-river and mid-river aqueous environments and those in the deeper parts of the north channel show decreasing calcium carbonate with decreasing pH in the overlying water. Although each of these water units has essentially the same range of pH (7.3–8.6), the ranges of the per cent calcium carbonate in the underlying sediments are distinct. Values in sediments underlying the mid-river aqueous environment range from 0.61 to 0.72, in the deeper part of the north channel from 0.96 to 1.71, and the sediments under the up-river aqueous environment from 1.71 to 2.02 per cent calcium carbonate. Decreasing calcium carbonate with lower pH (Fig. 26) and the occurrence of discrete ranges of calcium carbonate values in sediments underlying separate water units are both sedimentary reflections of the overlying water. There is no apparent correlation between calcium carbonate and the pH of the water in the north channel, south channel, and lower lagoon aqueous environments.

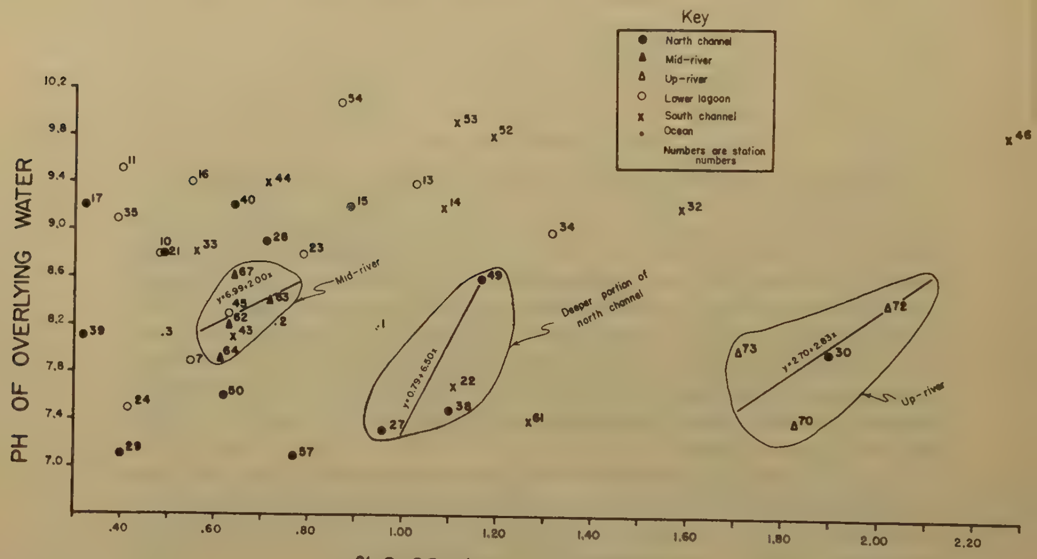

FIG. 26.—Per cent calcium carbonate per gram of sediment plotted against pH of overlying water. Symbols identify aqueous environment.

Grain size and dissolved oxygen.—There is generally less oxygen in waters overlying the finer sediments (Figs. 8 and 15a). The lower oxygen values probably are related to higher content of organic material, which has been shown to increase with decreasing grain size (Fig. 25). When this relation is considered within the framework of the separate aqueous environments (Fig. 27), however, less oxygen over finer sediments is found only in the mid-river and up-river areas and in the deeper part of the north channel, narrow dead-end marsh channels (stations 30, 32, and 61), and in the closed depression at station 46. As with the calcium carbonate-pH relation, the north channel, south channel, and lower lagoon do not show this correlation between the sediments and the overlying water.

Organic carbon and dissolved oxygen.—Figure 28a shows a trend of less oxygen in bottom waters overlying sediments with higher organic carbon content. This may be related to the increased use of oxygen during the decomposition in areas where organic material is more abundant. It may in part be related to reduced photosynthesis beneath the thick cover of aquatic plants.

Organic carbon and pH.—Figure 28b shows lower pH in the water overlying sediments with more organic carbon. This may reflect the accumulation of organic acids and carbon dioxide during organic decomposition in areas where organic material accumulates. The parallel of less oxygen with lower pH (Fig. 28a and b) suggests that this may also reflect reduced photosynthesis beneath the plants.

Sedimentary processes and aqueous environments.—The reason for the lack of correlation between sediments and the overlying bottom water in the north channel, south channel, and lower lagoon areas and the apparently good correlation elsewhere is apparent when the aqueous environments are compared with the sedimentary reflections of the depositional processes revealed by the size-distribution diagram. Figure 29 shows the size-distribution diagram for the San Migual Lagoon sediments, and a symbol at each station represents the aqueous environment of the overlying water. Both the up-river and mid-river environments overlie sediments reflecting only river processes. Sediments in the deeper part of the north channel, in narrow dead-end marsh channels, and at station 46 all reflect slow deposition from quiet water. The waters of the north channel, south channel, and lower lagoon, on the other hand, show no apparent correlation to the process of deposition of the underlying sediments.

The explanation is that only at the up-river, mid-river, and slow deposition stations were the sediments deposited from the water overlying them at the time the samples were collected, and hence these are the only stations at which the sediment properties are correlative with properties in the overlying water. The sediments at the lower lagoon stations were derived from seaward and deposited by tidal action when the barrier was open and thus are not genetically related to the water above them, which was sampled when the barrier was closed. Similarly, the sediments in the south channel and in the north channel (other than the

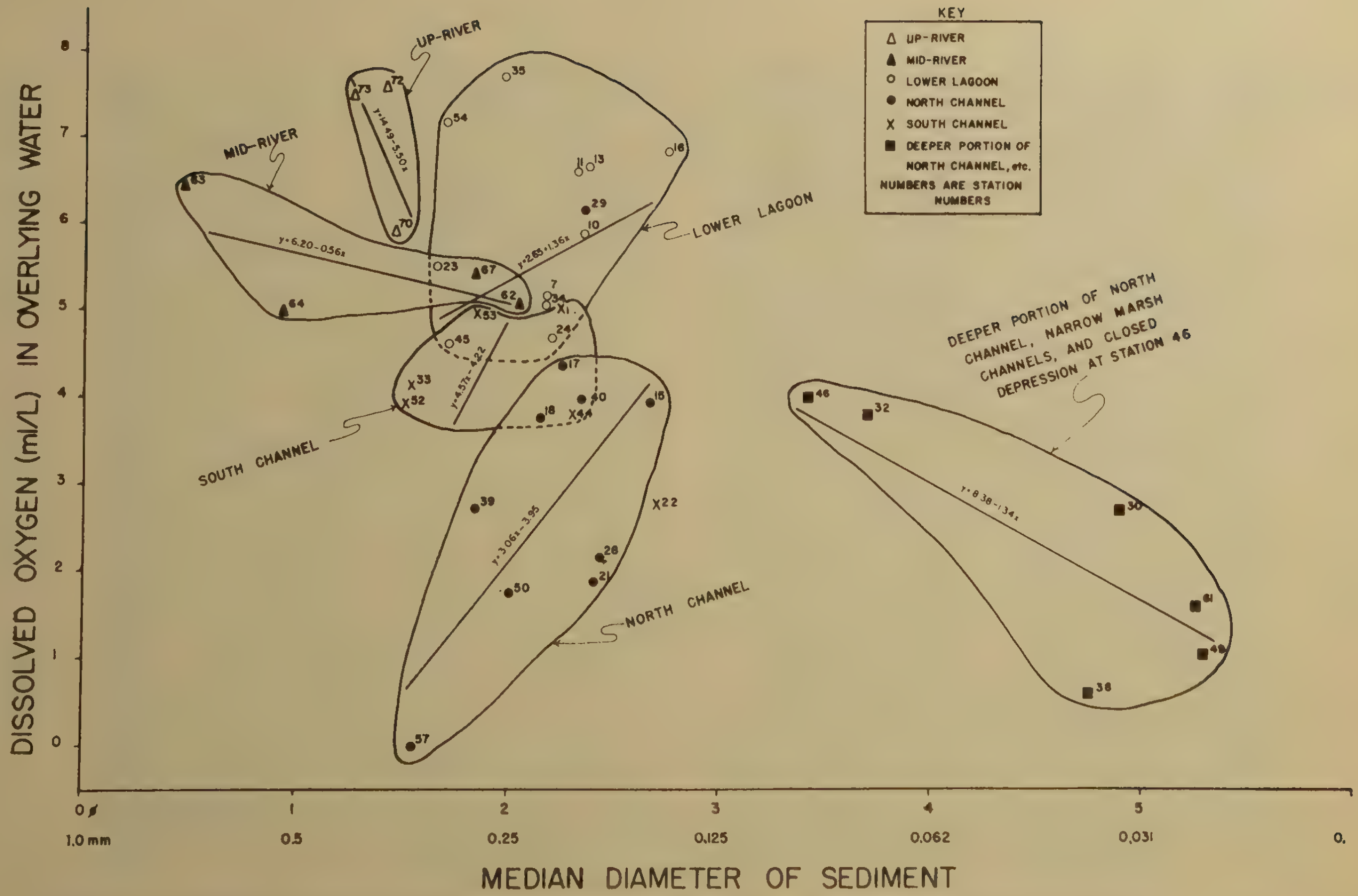

Fig. 27.—Median diameter of sediment (Mdϕ) plotted against dissolved oxygen concentration in overlying water. Symbols identify aqueous environments.

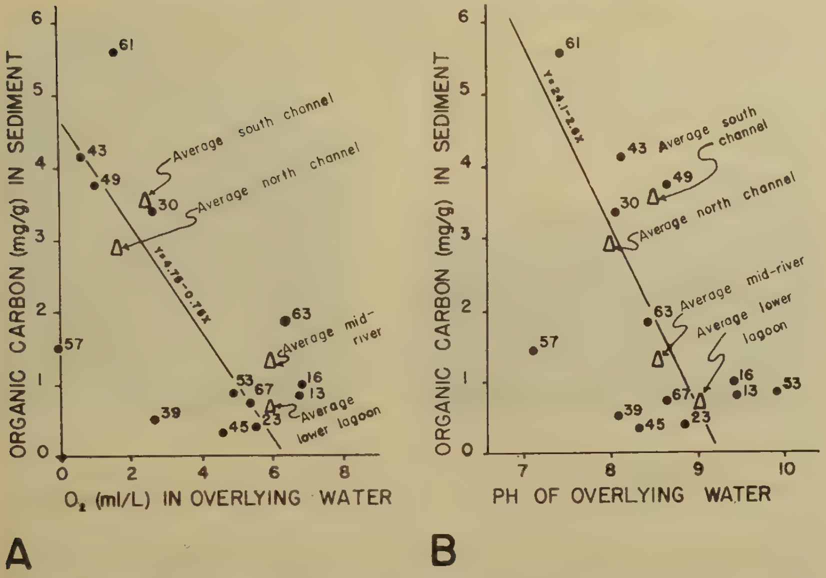

FIG. 28.—Organic carbon in mg/g of sediment plotted (A) against dissolved oxygen concentration in overlying water, and (B) against pH of overlying water.

deeper parts) have been shown (Fig. 17) to have been deposited by river processes. These are areas that receive river sediments in volume only during floods and are well seaward of the area influenced by the reduced river flow at the time of sampling. Consequently, these river-derived sediments seaward of the up-river and mid-river areas do not reflect the water overlying them at a time of reduced river discharge.

From these relationships it appears that if a sediment has been deposited from the type of water overlying it at the time samples of the sediment and of the overlying water are collected, there are recognizable sedimentary reflections of that overlying water. Conversely, if the sediment is not genetically related to the water overlying it at the time of sampling, there is little or no sedimentary reflection of that overlying water.

WIND ACTION AS SOURCE FOR LAGOON SEDIMENTS

At Scammons Lagoon active sand dunes on the barrier spit are migrating onto the lagoon marshes in response to the prevailing northwest winds (Fig. 30a). Similar dunes are moving into the northern arm of Manuella Lagoon. A tidal scarp 12–18 inches high is cut at the base of the dune on each rising tide, and the sand is spread to form a subaqueous fan below the dune. The upper layers of this

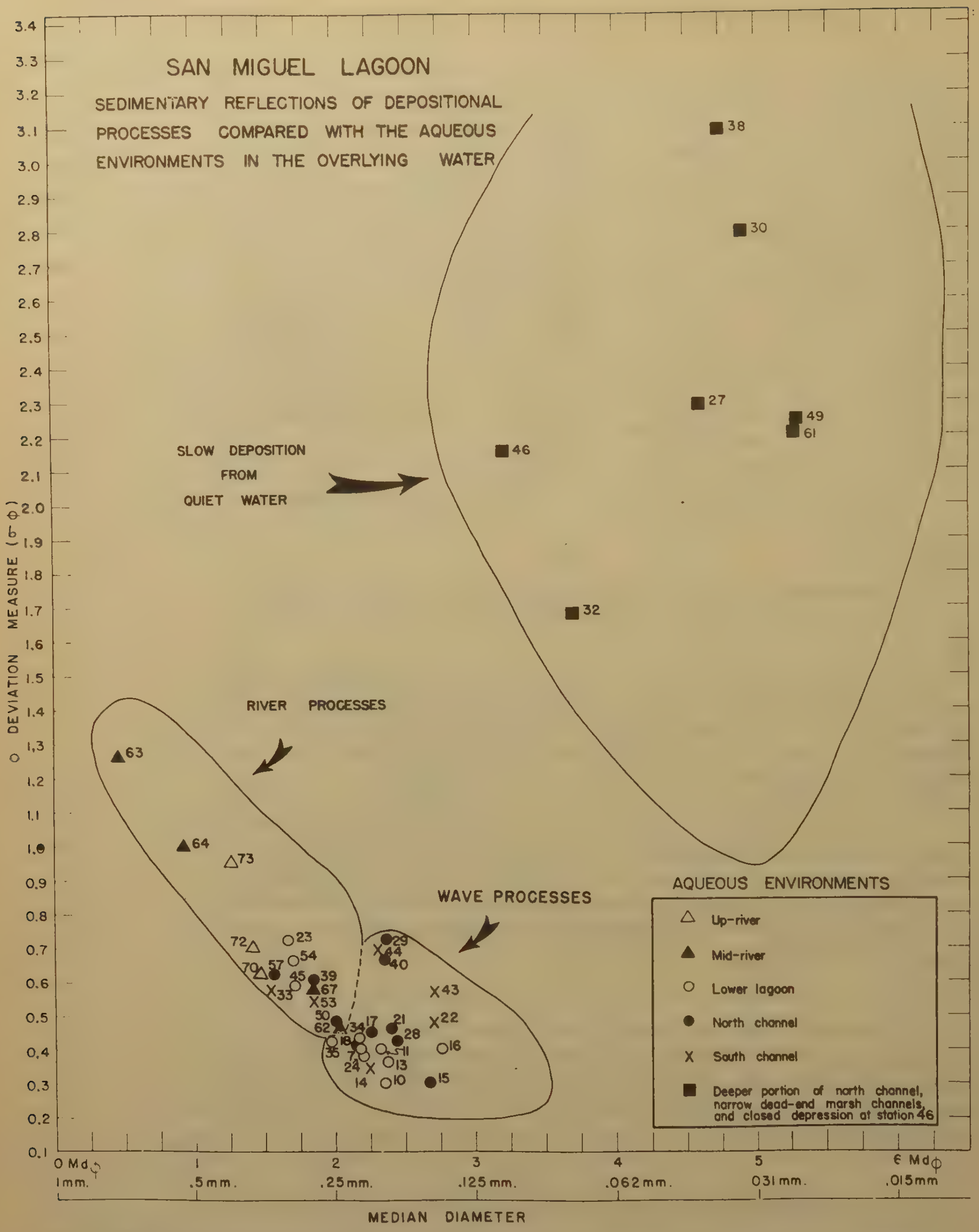

FIG. 29.—Sedimentary reflections of depositional processes compared with aqueous environments in overlying water.

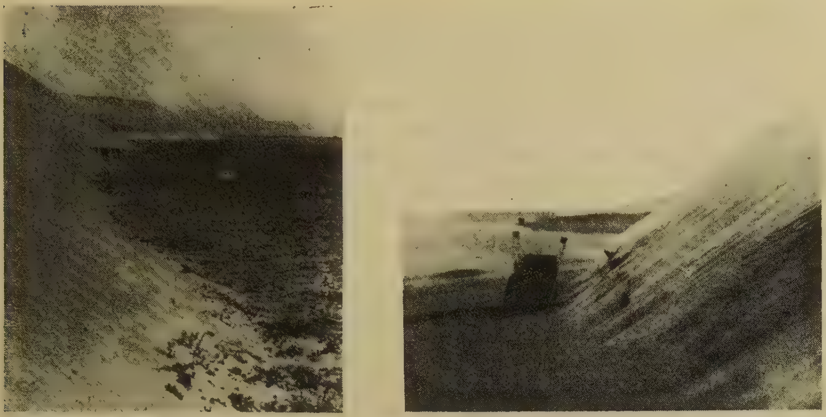

Fig. 30 A Fig. 30 B

FIG. 30.—Migration of dunes into coastal lagoons. (Left), Dunes at Scammons Lagoon encroaching on lagoon marsh at station 6. (Right), Dunes at Manuella Lagoon migrating into north arm of lagoon at station 7.

fan within the tidal range are gently dipping, and lagoonward the fan slopes steeply to the bottom in 14 feet of water. As the tide recedes, slumping on the face of the dune forms a series of small steeply dipping spurs along the face of the tidal scarp (Fig. 30b). The subsequent high tide spreads the sand from these spurs over the fan and forms a new scarp at the dune base. This process results in shoaling and prograding of the subaqueous fan so that it is eventually overridden by the subaerial part of the dune.

Eolian transportation of sand into coastal lagoons has been described from Barataria Bay, Louisiana, by Krumbein and Aberdeen (1937), for French coastal lagoons by Rivière (1952), and from the African coast by Guilcher and Nicolas (1954).

GEOLOGICAL INFERENCES

From the present study, certain inferences may be made about the nature of coastal lagoon deposits that might be preserved in the geologic record. Bass *et al.* (1937), Nanz (1954), and others have shown that the paleogeographical location and the shape of deposits can be utilized in reconstructing the environment of deposition. The location of coastal lagoon deposits would be in the region of transition from marine to continental sediments, and the shape would depend on the shape of the original lagoon and the effects of subsequent erosion. However, material deposited in a lagoon by an entering river would most probably have a trend at right angles to the regional depositional trend related to the coastline. If any of the adjacent marine sediments are preserved, it may be possible to use the particle-size distribution characteristics of these sediments to delineate the extent of ocean-derived material within the lagoon deposit. Some of this material may be present as a large sand body at the seaward end of the deposit, representing a lagoon delta at the inner end of the channel through the barrier. Highly contorted sediments may be found in these sediments (Stewart, 1956b).

Marsh deposits, if present, most likely occur along the landward borders of the lagoon deposit, but the pattern may also include marsh deposits along the inner edge of the barrier and as isolated islands within the lagoon sediments. Such deposits will generally be fine-grained material containing abundant plant fragments. Marsh deposits on the barrier may be overlain by cross-bedded sandstones reflecting the lagoonward migration of dunes.

Marked horizontal and vertical lithologic variations are typical of coastal lagoon deposits, and lithologic changes would be most pronounced at the seaward and landward edges. At their seaward edge, lagoon deposits would be expected to interfinger with sands originally deposited as a barrier, lagoon delta, washover fan, or dunes, or the deposit may have been truncated by marine erosion and be overlain unconformably by nearshore marine sediments. In a landward direction, lagoon sediments would be expected to interfinger with alluvial or deltaic deposits with increasing amounts of this continental material at greater distances from the barrier.

Within the coastal lagoon deposit, lithologic variations would reflect the lateral shifting of the aqueous environments with time and would include irregular lenses and interbeds of sandstone and shale. Ocean-derived material would be preserved as well sorted medium-grained sandstones and would be thicker at the seaward edge of the deposit.

Sediments deposited in lagoons with relatively high hinterlands would contain large volumes of coarse poorly sorted river detritus thickening in a direction away from the barrier. Coarser material would be found at locations of abruptly reduced velocity such as the upper end of islands. Coarse river material may also be found on the barrier where it was deposited when the river velocity was reduced on entering the sea, and nearshore processes were of insufficient duration or intensity to modify or remove it.

The distribution of fine-grained material in a lagoon deposit would depend on the entering volume and the size of the lagoon. Some would have settled slowly from quiet water in protected parts of the lagoon, and some would have collected in closed depressions when the channel through the barrier was closed. These factors would result in a discontinuous distribution within the sandstone of small bodies of shale, many of them black.

The preservation of organic material in lagoon deposits depends on (1) rate of accumulation of organic material, (2) rate of decomposition, (3) rate of dilution by clastics, and (4) rapidity of burial. Organic material would be more abundant in fine than in coarse sediments, and if not modified would be found as lenses or layers of black shale. Such black shales would suggest that the overlying water at the time of deposition was low in dissolved oxygen, a condition found in restricted arms and closed depressions. The lagoon studied has a high rate of accumulation of organic material primarily because of the high mortality rate related to environmental changes brought about by the alternate opening and closing of the barrier. Similar environmental changes with attendant mass mortalities undoubtedly took place in ancient lagoons, and if the rate of decomposition was slower than in the lagoon studied, it is conceivable that large amounts of organic material might have been buried. Thus coastal lagoons offer a mechanism for the accumulation of vast amounts of organic material, and the deposits of such lagoons may be important source beds for petroleum. The associated sand bodies similarly are potential reservoirs.

The presence of marine fossils in ancient sediments does not necessarily mean that the deposit in which they are found is also marine. Lagoonal sediments may contain fossils of marine organisms that were washed in over the barrier and unable to survive in that environment. Fresh-water forms that lived there during periods of reduced salinity while the barrier sealed the lagoon from the ocean may have been killed by the return to marine conditions following a rupture of the barrier. Marine forms that became established while the channel was open may have been killed by the lowered salinity after the channel was sealed off.

The alternation between typical marine and fresh-water forms vertically through the section might mistakenly be interpreted as reflecting alternating transgressions and regressions of the sea in response to successive glacial periods or pulsating tectonic activity, whereas all that is indicated is alternate opening and closing of a lagoon barrier.

The marine sediments just seaward of any coastal lagoon deposit would be expected to have a normal nearshore marine assemblage of Foraminifera. When the channel was closed, the change in aqueous environments would have been an abrupt change at the barrier, and under these conditions the lateral faunal change would also be abrupt. Some marine forms would be expected in the sediments, having been introduced with water brought in as washovers. Marine assemblages at depositional lows in the section may result from the collection there of washover water that flowed along the bottom to the deepest part of the lagoon. There may be typical lagoonal Foraminifera in addition to the marine forms, species that apparently could survive the wide range of environmental factors encountered in coastal lagoons. The presence of aberrant or abnormal individuals of these species is a possible additional reflection of the rigors of the lagoon environment.

Typical marsh species of Foraminifera may also occur in lagoon deposits, having been washed in from the adjacent marshes. The absence of these forms in apparent marsh deposits, however, does not necessarily invalidate the postulated marsh origin for these sediments. Marshes inundated only at highest water when the channel is closed may have no marsh forms, for the lagoon waters at these times may be so diluted by river water that typical marsh species can not survive on these low-salinity marshes.

Thus ancient lagoon deposits would be expected to contain any or all of the following: (1) beds with a mixed assemblage of fresh- or brackish-water and marine fossils, (2) sections containing predominantly marine fossils, possibly overlain by (3) a thin bed of abundant remains of marine forms indicative of a mass mortality, (4) beds of dominantly fresh-water forms with some marine forms especially near the barrier. These might be overlain by (5) a concentration of these forms reflecting another mass mortality when the barrier ruptured, and (6) some brackish-water forms that may persist through the section.

REFERENCES

Alexander, W. B., Southgate, B., and Bassindale, R., 1932, "The Salinity of the Water Retained by the Muddy Foreshore of an Estuary," *Jour. Marine Biol. Assoc.*, Vol. 18, pp. 297–98.

Arnal, R. E., 1955, "Some Occurrences of Abnormal Foraminifera," *Compass of Sigma Gamma Epsilon*, Vol. 32, No. 3, pp. 185–94.

Bass, N. W., Leatherock, C., Dillard, W. R., and Kennedy, L. E., 1937, "Origin and Distribution of Bartlesville and Burbank Shoestring Oil Sands in Parts of Oklahoma and Kansas," *Bull. Amer. Assoc. Petrol. Geol.*, Vol. 21, No. 1, pp. 30–66.

Bassindale, R., 1943, "Studies on the Biology of the Bristol Channel XI. The Physical Environment and Intertidal Fauna of the Southern Shores of the Bristol Channel and Severn Estuary," *Jour. Ecology*, Vol. 31, No. 1, pp. 1–29.

Bruce, J. R., 1924, "Seasonal and Tidal pH Variations in the Water of Port Erin Bay," *Univ. Liverpool, Oceanog. Dept., 38th Ann. Rept.*, pp. 35–39.

Caldwell, L. T., 1940, "Areal Variations of Calcium Carbonate and Heavy Minerals in Barataria Bay Sediments, Louisiana," *Jour. Sed. Petrology*, Vol. 10, No. 2, pp. 58–64.

Carl, G. C., 1940, "Some Ecological Conditions in a Brackish Lagoon," *Ecology*, Vol. 21, No. 1, pp. 65–74.

Davies, J. W., 1954, "Distribution of Recent Benthonic Foraminifera in Eastern Mission Bay," *Scripps Inst. Oceanog., Univ. California, Marine Foram. Lab.*, ms.

Day, P. R., 1950, "Physical Basis of Particle Size Analysis by the Hydrometer Method," *Soil Sci.*, Vol. 70, No. 5, pp. 363–74.

Debyser, Jacques, 1949, "Le pH de la pellicule superficielle d'une vase fluvio-marine," *Acad. Sci. Paris, Comptes Rendus*, Vol. 234, pp. 864–66.

———, 1955, "Étude sedimentologique du system lagunaire d'Abidjan (Côte d'Ivoire)," *Rev. Inst. Français du Pétrole et Ann. des Combustibles Liquides*, Vol. 10, No. 5, pp. 319–34.

Emery, K. O., 1938, "Rapid Method of Mechanical Analysis of Sands," *Jour. Sed. Petrology*, Vol. 8, No. 3, pp. 105–11.

———, and Rittenberg, S. C., 1952, "Early Diagenesis of California Basin Sediments in Relation to Origin of Oil," *Bull. Amer. Assoc. Petrol. Geol.*, Vol. 36, No. 5, pp. 735–806.

Fleming, R. H., and Revelle, R. R., 1939, "Physical Processes in the Ocean," *Recent Marine Sediments*, Amer. Assoc. Petrol. Geol., pp. 48–141.

Folk, R. L., and Ward, M. C., 1957, "Brazos River Bar: Study of the Significance of Grain Size Parameters," *Jour. Sed. Petrology*, Vol. 27, No. 1, pp. 3–26.

Grant, U. S., IV, 1943, "Waves as a Sand-Transporting Agent," *Amer. Jour. Sci.*, 5th Ser., Vol. 241, No. 2, pp. 117–23.

———, and Shepard, F. P., 1939, "Shallow-Water Sediment-Shifting Processes along the Southern California Coast," *Proc. 6th Pacific Sci. Conf.*, Vol. 2, pp. 801–5.

Graves, A. H., 1908, "The Morphology of *Ruppia Maritima*," *Trans. Connecticut Acad. Arts and Sci.*, Vol. 14, pp. 59–170.

Griffiths, J. C., 1951, "Size versus Sorting in Some Caribbean Sediments," *Jour. Geology*, Vol. 59, No. 3, pp. 211–43.

Guilcher, André, and Nicolas, J. P., 1954, "Observations sur la langue de Barbarie et les bras du Senigal aux environs de Saint Louis," *Comité Central d'Océanog. et d'Étude des Côtes, Bull. d'Information*, Vol. 6, pp. 227–42.

Hough, J. L., 1942, "Sediments of Cape Cod, Massachusetts," *Jour. Sed. Petrology*, Vol. 12, No. 1, pp. 10–30.

Inman, D. L., 1949, "Sorting of Sediments in the Light of Fluid Mechanics," *ibid.*, Vol. 19, No. 2, pp. 51–70.

———, 1952, "Measures for Describing the Size Distribution of Sediments," *ibid.*, Vol. 22, No. 3, pp. 125–45.

(786)

———, 1953a, "Areal and Seasonal Variations in Beach and Nearshore Sediments at La Jolla, California," *Beach Erosion Board Tech. Memo. 39.*

———, 1953b, "Beach and Nearshore Processes along the Southern California Coast," *Scripps Inst. Oceanog., Univ. California Submarine Geol. Rept. 27.*

———, and Chamberlain, T. K., 1956, "Particle-Size Distribution in Nearshore Sediments," in "Finding Ancient Shorelines," *Soc. Econ. Paleon. and Mineralogists Spec. Pub. 3*, pp. 106–27.

Jacquet, J., 1949, "Recherches écologique sur le littoral de la Manche," *Encyclopedie Biogéographique et Ecologique,* Paul Lecheralier, ed.

Krogh, A., and Keys, A., 1934, "Methods for the Determination of Dissolved Organic Carbon and Nitrogen in Sea Water," *Biol. Bull.*, Vol. 7, No. 1, pp. 132–44.

Krumbein, W. C., 1939, "Tidal Lagoon Sediments on the Mississippi Delta," *Recent Marine Sediments*, Amer. Assoc. Petrol. Geol., pp. 178–94.

———, and Aberdeen, E., 1937, "The Sediments of Barataria Bay," *Jour. Sed. Petrology*, Vol. 7, No. 1, pp. 3–17.

———, and Pettijohn, F. J., 1938, *Manual of Sedimentary Petrology*. 549 pp. D. Appleton-Century Company, New York.

LaFond, E. C., 1939, "Sand Movement near the Beach in Relation to Tides and Waves," *Proc. 6th Pacific Sci. Conf.*, Vol. 2, pp. 795–99.

Le Calvez, J., and Le Calvez, Y., 1951, "Contribution a l'Étude des Foraminifères des eaux saumâtres. I. Étangs de Canet et de Salses," *Vie et Milieu*, Tome 2, fasc. 2, pp. 237–54.

Lewis, G. J., III, and Rakestraw, N. W., 1955, "Carbohydrate in Sea Water," *Jour. Marine Res.*, Vol. 14, No. 3, pp. 253–58.

Louderback, G. D., 1939, "San Francisco Bay Sediments," *Proc. 6th Pacific Sci. Conf.*, Vol. 2, pp. 783–93.

Moberg, E. C., Fleming, R. H., Heusner, K., and Revelle, R. R., 1937, "The Organic Nitrogen Content of Marine Sediments Off the West Coast of North America," *Assoc. Oceanog. Phys. Proces-Verbaux*, No. 2, p. 154. (Also paper No. 39, *Scripps Inst. Oceanog., Univ. California Contribs. 1937.*)

Nanz, R. H., 1954, "Genesis of Oligocene Sandstone Reservoir, Seeligson Field, Jim Wells and Kleberg Counties, Texas," *Bull. Amer. Assoc. Petrol. Geol.*, Vol. 38, No. 1, pp. 96–117.

Nelson, T. C., 1947, "Some Contributions from the Land in Determining Conditions of Life in the Sea," *Ecological Monographs*, Vol. 17, No. 3, pp. 337–46.

Newcombe, C. L., Horne, W. A., and Shepard, B. B., 1939, "Studies on the Physics and Chemistry of Estuarine Waters in Chesapeake Bay," *Jour. Marine Res.*, Vol. 2, No. 2, pp. 87–116.

Parker, F. L., Phleger, F. B, and Peirson, J. F., 1953, "Ecology of Foraminifera from San Antonio Bay and Environs, Southwest Texas," *Cushman Found. Foram. Res. Spec. Pub. 2.* 75 pp.

Passega, R., 1957, "Texture as Characteristic of Clastic Deposition," *Bull. Amer. Assoc. Petrol. Geol.*, Vol. 41, No. 9, pp. 1952–84.

Phleger, F. B, 1952, "Foraminifera Ecology off Portsmouth, New Hampshire," *Bull. Mus. Comp. Zool.*, Vol. 16, No. 8, pp. 318–90.

———, 1954, "Ecology of Foraminifera and Associated Micro-organisms from Mississippi Sound and Environs," *Bull. Amer. Assoc. Petrol. Geol.*, Vol. 38, No. 4, pp. 584–647.

———, and Walton, W. R., 1950, "Ecology of Marsh and Bay Foraminifera, Barnstable, Massachusetts," *Amer. Jour. Sci.*, 5th Ser., Vol. 248, No. 4, pp. 274–94.

Powers, E. B., 1920, "The Variations of the Condition of Seawater Especially the Hydrogen Ion Concentration and Its Relation to Marine Organisms," *Pub. Puget Sound Marine Sta.*, Vol. 2, pp. 369–85.

Pritchard, D. W., 1952, "Salinity Distribution and Circulation in the Chesapeake Bay Estuarine System," *Jour. Marine Res.*, Vol. 11, No. 2, pp. 106–23.

Reid, D. M., 1930, "Salinity Interchange between Salt Water in Sand and Overflowing Fresh Water at Low Tide," *Jour. Marine Biol. Assoc.*, New Ser., Vol. 16, No. 2, pp. 609–14.

———, 1932, "Salinity Interchange between Salt Water in Sand and Overflowing Fresh Water at Low Tide, II," *ibid.*, Vol. 18, No. 1, pp. 229–306.

Revelle, R. R., and Shepard, F. P., 1939, "Sediments off the California Coast," *Recent Marine Sediments*, Amer. Assoc. Petrol. Geol., pp. 245–82.

Rhodes, R. F., 1950, "Effect of Salinity on Current Velocities," *Comm. on Tidal Hydraulics, Corps of Engineers, U. S. Army, Rept. 1*, pp. 41–100.

Richards, F. A., and Redfield, A. C., 1954, "A Correlation between the Oxygen Content of Sea Water and the Organic Content of Marine Sediments," *Deep-Sea Res.*, Vol. 1, No. 4, pp. 279–81.

Richards, F. T., 1934, "The Salt Marshes of the Dovey Estuary. IV. The Rate of Vertical Accretion, Horizontal Extension, and Scarp Erosion," *Annals of Botany*, Vol. 48, pp. 225–60.

Rivière, André, 1952, "Étude de sedimentologie littorale du Laboratoire de Géologie du S.P.C.N. à Paris," *Rev. Gén. Hydraulique*, An. 18, No. 67, pp. 10–13.

SHEPARD, F. P., AND MOORE, D. G., 1954, "Sedimentary Environments Differentiated by Coarse-Fraction Studies," *Bull. Amer. Assoc. Petrol. Geol.*, Vol. 38, No. 8, pp. 1792–1802.

———, AND ———, 1955, "Central Texas Coast Sedimentation: Characteristics of Sedimentary Environment, Recent History and Diagenesis," *ibid.*, Vol. 39, No. 8, pp. 1463–1593.

STEVENSON, R. E., 1950, "The Origin of Salt Marshes at Newport Bay, California," *Univ. Southern California, Dept. Geol. Rept.*

———, 1954, "The Marshlands of Newport Bay, California," *ibid.*, unpublished thesis.

STEWART, H. B., JR., 1956a, "Sediments and the Environment of Deposition in a Coastal Lagoon," *Scripps Inst. Oceanog., Univ. California*, unpublished thesis.

———, 1956b, "Contorted Sediments in a Modern Coastal Lagoon Explained by Laboratory Experiments," *Bull. Amer. Assoc. Petrol. Geol.*, Vol. 40, No. 1, pp. 153–61.

SUDRY, LOUIS, 1910, "L'étang de Thau," *Annales l'Inst. Océanog.*, Tome 1, Fasc. 10. 208 pp.

SUMNER, F. B., LOUDERBACK, G. D., SCHMITT, W. L., AND JOHNSON, E. C., 1914, "A Report upon the Physical Conditions in San Francisco Bay," *Univ. California Pub. in Zoology*, Vol. 14. 198 pp.

TRASK, P. D., 1932, *Origin and Environment of Source Sediments of Petroleum.* 323 pp. Gulf Publishing Company, Houston, Texas.

———, 1939, "Organic Content of Recent Marine Sediments," *Recent Marine Sediments*, Amer. Assoc. Petrol. Geol., pp. 428–53.

VAN STRAATEN, L. M. J. U., 1951, "Texture and Genesis of Dutch Wadden Sea Sediments," *Proc. 3d Internat. Congr. Sedimentology*, Groningen, Netherlands, pp. 225–44.

———, 1954a, "Sedimentology of Recent Tidal Flat Deposits and the Psammites du Condroz (Devonian)," *Geologie en Meinbouw*, New Ser., 19 Jaargang, pp. 25–47.

———, 1954b, "Composition and Structure of Recent Marine Sediments in the Netherlands," *Leidse Geol. Medelingen*, Deel 19, pp. 1–110.

WAKSMAN, S. A., 1941, "Aquatic Bacteria in Relation to the Cycle of Organic Matter in Lakes," *Symposium on Hydrology*, pp. 86–105. Univ. Wisconsin Press.

———, AND HOTCHKISS, MARGARET, 1938, "On the Oxidation of Organic Matter in Marine Sediments by Bacteria," *Jour. Marine Res.*, Vol. 1, No. 2, pp. 101–18.

WALTON, W. R., 1955, "Ecology of Living Benthonic Foraminifera, Todos Santos Bay, Baja California," *Jour. Paleon.*, Vol. 29, No. 6, pp. 952–1018.

WOOSTER, W. S., 1950, "Methods in Chemical Oceanography," *Scripps Inst. Oceanog., Univ. California Tech. Rept.* (November 25). 24 pp. mimeo.

ZOBELL, C. E., 1946, *Marine Microbiology.* 240 pp. Chronica Botanica Company, Waltham, Massachusetts.

Dikellorhynchus and *Kanazawaichthys:* Nominal Fish Genera Interpreted as Based on Prejuveniles of *Malacanthus* and *Antennarius,* Respectively[1]

Carl L. Hubbs

Like a considerable number of early-named nominal fish genera, two of recent introduction obviously represent what may be termed, for each, the prejuvenile stage of a well-known genus. This generalized term is proposed to cover a diversity of more or less strikingly—often bizarrely—modified pelagic life-history stages, of various marine fishes, that are not appropriately termed either postlarval or juvenile. Examples include the querimana stage of mugilids, and the similar early, pelagic stages, with iridescent blue or green upper parts and bright silvery lower parts, of many diverse genera (Hubbs, 1941: 184); also such highly modified, structurally specialized types as the acronurus stage of acanthurids, the tholichthys stage of chaetodontids, and the rhynchichthys stage of holocentrids. Such stages, taking the names of nominal, synonymized genera, are commonly characterized by strong spines, bony plates, or peculiar body form. Characteristically, prejuveniles metamorphose very rapidly into the juveniles, which are much more like the adult. For this reason, transitional specimens are seldom encountered.

The two recently named genera referred to above are *Dikellorhynchus* Smith (1956) and *Kanazawaichthys* Schultz (1957: 62). Anticipating the following discussion, it may be stated that *Dikellorhynchus incredibilis* Smith was based on the prejuvenile of a species of *Malacanthus,* presumably *M. hoedtii* Bleeker, and that *Kanazawaichthys scutatus* was based on the prejuvenile of *Antennarius radiosus* Garman.

The Dikellorhynchus Prejuvenile of *Malacanthus*

As Smith pointed out, the 70-mm. specimen on which he based the name *Dikellorhynchus incredibilis* agrees essentially with the species he called *Malacanthus hoedtii* Bleeker, "except for the ridged and spinose head, the peculiar [transverse, anchor-like, bony] rostral projection and the prominently keeled scales." He definitely anticipated what seems to me to be the logical conclusion, that *D. incredibilis* was based on the prejuvenile of some species of *Malacanthus.* Final proof of this view will need await a demonstration of the metamorphosis, which in all probability will prove to be very brief.

Like the analagous prejuveniles of other marine fishes, the dikellorhynchus stage of *Malacanthus* is probably an inhabitant of the open-sea, surface-pelagic habitat, and presumably transforms when it comes into contact with reef water. This view contrasts with Smith's tentative inference expressed in his statement that "the large eye and the nature of the head might indicate that" it "lives at some depth possibly in the 'Berycid' zone." The unique specimen was found on the beach on the east coast of South Africa, "after an onset of cold water in January 1955." The locality is south of the reported range of the genus, but such young stages of tropical fishes are frequently carried by currents far poleward, where they may suc-

---

[1] Contributions from the Scripps Institution of Oceanography, New Series No. 1043

Reproduced by Permission

cumb to unaccustomed cold. Such movements seem to have become unusually common in very recent years, particularly, of course, in the summer.

While this paper was in press, there appeared, by coincidence, the description of a supposedly new species of *"Dikellorhynchus,"* namely *D. tropidolepis* Berry (1958). This nominal species was based on 18 specimens, about 45 to 60 mm. in standard length, from the stomachs of two dolphinfish, *Coryphaena hippurus* Linnaeus, captured in the Western North Atlantic. Three of these had previously been recorded, and I believe correctly identified, as *Malacanthus plumieri* (Bloch), by Anderson, Gehringer, and Cohen (1956: 54). In reference to the relationship of *Dikellorhynchus* to *Malacanthus* Berry considered four suppositions, namely that the known specimens of *Dikellorhynchus* represent: (1) species characterized [as adults] by the spinose head and scales, (2) larvae of species undescribed as adults, (3) aberrant growth stages of species of *Malacanthus,* and (4) protracted larval stages of those species. I add and adhere to a fifth hypothesis, that they represent the normal pelagic prejuveniles of species of *Malacanthus.* They are no more bizarrely specialized than the prejuveniles of various tropical fishes. This fifth hypothesis is supported by the facts: (1) that *D. incredibilis* differs from *M. hoedtii* of the same ocean only in the characters interpretable as prejuvenile; (2) that *D. tropidolepis* differs from the sympatric *M. plumieri* in the same fashion; (3) that *D. tropidolepis,* as Berry specifies, differs from *D. incredibilis* in the very characters by which *M. plumieri* differs from *M. hoedtii*; and (4) that no specimens of *"Dikellorhynchus"* have been secured among the very extensive collections of recent years in the surface waters of the eastern Pacific, where *Malacanthus* does not occur. The occurrence of the dikellorhynchus stage of *M. plumieri* in the stomachs of dolphinfish, along with other organisms of pelagic habit, verifies my theory that this prejuvenile type is pelagic.

THE KANAZAWAICHTHYS PREJUVENILE OF *Antennarius*

Kanazawaichthys scutatus was proposed by Schultz (1957: 62–64, pl. 14, A), as a new genus and species, on the basis of four small specimens (15.8 to 29.5 mm. in standard length) from the Gulf of Mexico; three were "probably picked up in a dipnet near surface" and one was "taken from stomach of yellowfin tuna."

The genus *Kanazawaichthys* was differentiated "from all other genera in the family by having two pairs of bony plates on the head. The largest pair covers all the dorsoposterior part of the head behind and above the orbits. A small plate is below each eye. Otherwise the genus has the characters of *Antennarius."* Schultz indicated the close agreement of *"Kanazawaichthys scutatus"* with certain species of *Antennarius* in characters that he showed to be of diagnostic value in the taxonomy of the antennariids. The closest agreement was stated to be with the species that he classed in the subgenus *Fowlerichthys,* particularly with *Antennarius radiosus* Garman of the same general region.

The types of *Kanazawaichthys scutatus* differ further from transformed specimens of *Antennarius radiosus* in having the body more compressed and, in side view, more wedge-shaped, and in the plainer coloration (lacking the ocelli, the reticulations, and the bars on the fins of the adult).

Since I first saw the type specimens, prior to the description, I have felt convinced that the differential characters of *Kanazawaichthys scutatus* are ontogenetic and that the nominal genus and species merely represent the prejuvenile stages of some species of *Antennarius.* The fact that the type series overlaps in size some ordinary juveniles (of the related species, *A. ocellatus*) has seemed immaterial, though Schultz (personal communication) relied on this circumstance in retaining the nominal genus and species. In this connection it should be recalled that related species, such as *A. radiosus* and *A. ocellatus,* commonly differ in the size at metamorphosis; that within some species size of transformation varies widely, as the metamorphosis seems to be triggered by shore conditions, whenever they happen to be encountered; and that some fishes shrink in length during metamorphosis.

Schultz, however, did recognize the possibility that his nominal new genus and species represents a life-history stage of a known species. He stated, on page 63: "I suspect this species is pelagic and that these thickened bony plates act as a floating mechanism. Consideration was given to the possibility that this species might represent the young stage of some known species of frogfish and that at a later stage these plates might be lost."

I am very grateful to Leonard P. Schultz for this information and for his permission to incorporate his new findings and conclusion in this paper. I am also indebted to Royal D. Suttkus, for privileges and suggestions.

Confirmation of the hypothesis that *Kanazawaichthys scutatus* Schultz is a stage in the development, and therefore a synonym, of *Antennarius radiosus* Garman was recently secured when, in company with Schultz, I examined, with the kind permission of Royal D. Suttkus, the series of *A. radiosus* in the fish collection of Tulane University. By rare good fortune one of the thirteen lots, which comprise in all thirty specimens, illustrates nicely the transformation of the prejuvenile (Kanazawaichthys) into the ordinary juvenile. This series (TU 6222) of four specimens was collected by Suttkus and Edwin B. Joseph on February 15, 1953 at the northeast end of Grand Isle, Louisiana. It was obtained with a 150′ bag seine from over a sand bottom in a maximum depth of 3.5 feet; moderate breakers prevented seining in deeper water and produced a turbid condition. On the previous day, Grand Isle had been subjected to strong winds and five inches of rain.

Table I

Pectoral-ray Counts (Both Sides) in Two Species of *Antennarius*

The counts by Schultz are taken from his 1957 paper (p. 54); those by Hubbs are from specimens, in the Tulane collection, from the Gulf of Mexico.

	Pectoral Rays			
	11	12	13	14
Antennarius radiosus				
Counts by Schultz	..	..	99	5
Counts by Hubbs	..	4	51	5
Antennarius ocellatus				
Counts by Schultz	3	26	3	..
Counts by Hubbs	..	3	1	..

All other specimens in the Tulane collection are larger, and were trawled by the Oregon.

Series TU 6222 shows not only the fact and type of metamorphosis, but also illustrates variation in size at transformation (or, possibly, shrinkage in length during the process). This lot comprises the following specimens:

Specimen A, judged to be about one-third the way through metamorphosis, is 23.5 mm. in standard length.

Specimen B, judged to be about two-thirds the way through metamorphosis, is 22.5 mm. long.

Specimens C and D, already transformed, are 23.0 and 27.5 mm. long.

Since the types of *K. scutatus* measured 15.8 to 29.5 mm. in standard length, there must be notable variation in size of transformation, or considerable shrinkage during the process (for fishes with this type of development the second alternative seems the less plausible).

Specimen A, in early transformation, conspicuously retains the large turgid (but now only moderately hard) mass between the orbit and the interspace between the third dorsal spine and the origin of the second dorsal, and a trace of the hard swelling on the cheek. It approaches the type figure of *K. scutatus* in the cuneiform outline of the body and is less rotund than the transformed specimens. It is almost uniformly very pale yellowish in preservative, and shows only a faint rudiment of the basidorsal ocellus. The radial formula, counting, as Schultz obviously did not, the last two elements of the dorsal and anal fin as one ray, is: D_2 12, A 7, P_1 13–13; the first five dorsal soft-rays are so weakly branched as to appear simple except under high power; all anal rays are clearly branched. These fin characters are those of *A. radiosus.*

Specimen B, in later transformation, has the postorbital swellings much deflated, though still clearly apparent, and the cheek swellings scarcely perceptible. The body form is more turgid, but still less gibbous than in the transformed specimens. The general color tone is darker than in specimen A. Dark reticulations are beginning to show on the back, and the blotch representing the developing basidorsal ocellus is more conspicuous. The dorsal and anal soft-rays number 12 and 7, respectively, and the pectoral rays number 12 on each side (see discussion below).

Specimens C and D are typical juveniles of *A. radiosus,* with form and color definitely approaching that of the adult. The radial formula in each is the same as in specimen A.

None of the four specimens shows more than the barest trace of filaments on the esca of the illicium and in none are any pectoral rays branched.

It seems clear that all four specimens represent *Antennarius radiosus,* despite the fact that specimen B has 12 pectoral rays on each side—the modal number for *A. ocel-*

TABLE II

FREQUENCY DISTRIBUTION OF CONDITION OF BONY PLATES AND OF BASIDORSAL OCELLUS IN SMALL SPECIMENS OF *Antennarius radiosus*

Determination by Leonard P. Schultz from specimens in the United States National Museum.

	Bony Plates on Head			Basidorsal Ocellus		
Standard Length, mm.	Superficially Apparent	Covered by normal Skin, Visible on Dissection	Not Apparent	Lacking	Trace	Definitely Developed
16	1	2	..	1	2	..
17	..	2	..	..	2	..
18	1	1	..	..	1	1
19	..	..	..	..	..	..
20	..	3	..	..	1	2
21	..	1	1	..	1	1
22	..	3	1	..	2	2
23	..	3	2	..	..	5
24	..	1	..	..	1	..
25	..	..	..	..	..	..
26	..	..	..	..	..	..
27	..	..	..	..	..	..
28	..	..	..	..	..	..
29	1	..	2	..	..	3
30	1	..	1	..	1	1
31	..	..	1	..	..	1
32	..	..	2	..	..	2

latus, not represented in the 104 counts given by Schultz (1957: 54) for *A. radiosus*. But among the 26 larger specimens of *radiosus* in the Tulane collection I find two with 12 pectoral rays on one side and 13 on the other. In number of pectoral rays the two species seem to overlap somewhat more extensively than Schultz showed (Table I).

Since this paper was written Leonard P. Schultz has confirmed the present interpretation by a re-examination of the specimens of *Antennarius radiosus* of appropriate sizes in the United States National Museum. His findings are presented, with his kind permission, in Table II.

LITERATURE CITED

ANDERSON, WILLIAM W., JACK W. GEHRINGER, AND EDWARD COHEN. 1956. Physical oceanographic, biological, and chemical data/South Atlantic Coast of the United States/*Theodore N. Gill* Cruise 2. *U. S. Fish and Wildlife Serv., Spec. Sci. Rept., Fish No. 198: 1–270, figs. 1–20.*

BERRY, FREDERICK H. 1958. A new species of fish from the Western North Atlantic, *Dikellorhynchus tropidolepis* and *Malacanthus*. *Copeia*, 1958 (2): 116–125, figs. 1–13.

HUBBS, CARL L. 1941. The relation of hydrological conditions to speciation in fishes. In: *A Symposium on Hydrobiology, University of Wisconsin Press, Madison: 182–195.*

SCHULTZ, LEONARD P. 1957. The frogfishes of the family Antennariidae. *Proc. U. S. Nat. Mus., 107: 47–105, figs. 1–8, pls. 1–14.*

SMITH, J. L. B. 1956. An extraordinary fish from South Africa. *Ann. and Mag. Nat. Hist., (12) 9 (97): 54–57, pl. 1.*

SCRIPPS INSTITUTION OF OCEANOGRAPHY, UNIVERSITY OF CALIFORNIA, LA JOLLA, CALIFORNIA.

(794)

Notropis saladonis, a New Cyprinid Fish Endemic in the Río Salado of Northeastern México[1]

Carl L. Hubbs and Clark Hubbs

THE small minnow described below adds one more element of northern affinity to the predominantly Nearctic fauna of northeastern México. It was discovered during a review of the extensive material that Luciano Val Guerra collected in June 1951, during his fish-faunal survey of the Río Salado System (Guerra's material, as well as his M.A. thesis, "Ichthyological Survey of the Río Salado, México," is deposited in The University of Texas). Two additional series were subsequently located in collections made by Seth Eugene Meek and by E. G. Marsh, Jr. (deposited, respectively, in the Chicago Natural History Museum and the University of Michigan Museum of Zoology). For the opportunity of studying and reporting on this ichthyological discovery we are grateful to the collectors of the material and to the curators of the museums in which the specimens are stored.

Counts and measurements have been made in accordance with the criteria set forth by Hubbs and Lagler (1947: 8–15, figs. 2–5).

The Salado Shiner

Notropis saladonis, *sp. nov.*

Fig. 1, Maps 1–2

Material.—The 101 type specimens range in standard length from 15 to 38 mm. and are from 11 localities, all along the course of the Río Salado and one of its two main headwaters, Río Sabinas de Coahuila, in the Río Grande drainage basin of the states of Nuevo León and Coahuila, México (Map 1). The material is deposited in several museums, as follows: Chicago Natural History Museum (CNHM), Escuela Nacional de Ciencias Biológicas de México (ENCB), Natural History Museum of Stanford University (SU), (The University of) Texas Natural History Collection (TNHC), University of Michigan Museum of Zoology (UMMZ), and the United States National Museum (USNM).

The holotype, UMMZ 173132, an adult male 32 mm. in standard length, was collected by Luciano Val Guerra in Río Salado, 1 mile west of Manuel Martinez Parela and 10 miles south of Anahuac, Nuevo León, on June 11, 1951. The location is No. 7 on Map 2.

The paratypes are from 11 collecting stations, which are numbered in sequence upstream, on Map 2, and in the following list:

(1) Río Salado, 2 miles south of La Gloria, Nuevo León: collected by Guerra on June 8, 1951 (6 adults, 21–28 mm. in standard length, SU 50173).

(2) Río Salado, 2 miles northeast of the bridge on the Pan-American (Laredo-Monterrey) Highway: collected by Guerra on June 9, 1951 (11 adults, 22–29 mm., CNHM 62160).

(3) Río Salado, on the González Hacienda, 25 miles by road north-northeast of La Gloria, Nuevo León: collected by Guerra on June 9, 1951 (31 specimens, 16–32 mm., ENCB—–).

(4) Río Salado, on the González Hacienda, 1.5 miles southeast of the water pump, Nuevo León: collected by Guerra on June 9, 1951 (12 specimens, 17–31 mm., USNM 175276).

(5) Río Salado, on the González Hacienda, 3 miles south-southeast of the water pump, Nuevo León: collected by Guerra on June

---

[1] Contributions from the Scripps Institution of Oceanography, New Series, and from The University of Texas.

Contributions from the Scripps Institution of Oceanography, New Series, No. 1044
Reproduced by Permission

9, 1951 (16 specimens, 15–33 mm., TNHC 1680).

(6) Río Salado, 4 miles east of the Anahuac Road at Ejido Nuevo Camarón, Nuevo León: collected by Guerra on June 10, 1951 (2 adults, 28–29 mm., TNHC 5563).

(7) Río Salado, at the holotype locality (6 adults, 27–30 mm., UMMZ 173133).

(8) Río Salado, at the railroad town of Rodrigues, Nuevo León: collected by Seth Eugene Meek in 1906 or 1907 (7 adults, 29–38 mm., CNHM 62169).

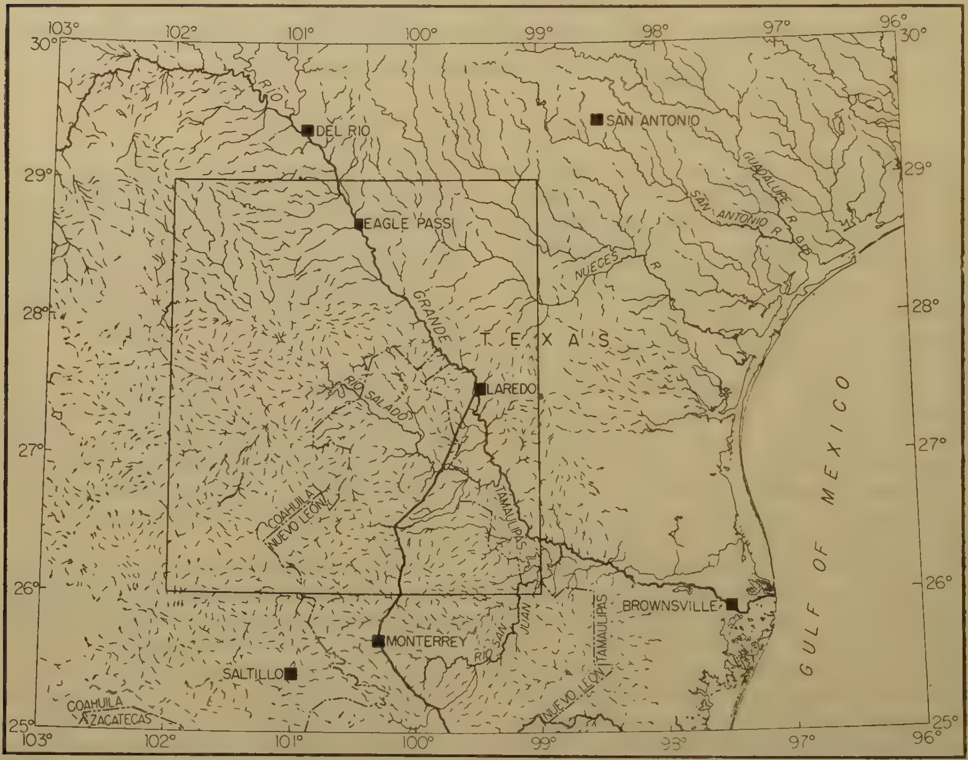
103°
102°
101°
100°
99°
98°
97°
96°
30°
29°
28°
27°
26°
25°
RIO
DEL RIO
SAN ANTONIO
EAGLE PASS
GUADALUPE R
SAN ANTONIO R
NUECES R
GRANDE
T E X A S
LAREDO
RIO SALADO
COAHUILA
NUEVO LEON
TAMAULIPAS
GULF OF MEXICO
SAN JUAN RIO
MONTERREY
BROWNSVILLE
NUEVO LEON
TAMAULIPAS
SALTILLO
COAHUILA
ZACATECAS

Map. 1. Stream drainages of northern México, showing relations of the Río Salado system. The base for Maps 1 and 2 is the World Aeronautical Chart, sheets 469, 470, 521, and 522 (as revised, 1951–1952).

(9) Río Sabinas de Coahuila, at Rancho de los Borregos, Juárez, Coahuila: collected by E. G. March, Jr., at his Station X, on April 7, 1939 (5 adults, 24–29 mm., UMMZ 130349).

(10) Río Sabinas de Coahuila, at Presita, Coahuila: collected by Guerra on June 15, 1951 (2 specimens, each 25 mm. long, UMMZ 173134).

(11) Río Sabinas de Coahuila, 2 miles southwest of San Felipe, Coahuila: collected by Guerra on June 15, 1951 (1 adult, 28 mm., TNHC 1722).

The specimens from locality 8 were found in resorting a series of *Notropis braytoni* Jordan and Evermann, catalogued as CNHM 5573, from "Roderigues, Nuevo León, México, S. E. Meek." In his report on the collection from Rodrigues, Meek (1908: 155) failed to record this series, but there seems to be no reason to doubt the provenance of the material.

Notes on Nomenclature.—The name *saladonis* is formed, by analogy with the Latin, as the genitive of Salado. Pending a solution of the problem, we herein follow precedent, which runs counter to the classical rules and to the International Code of Zoological Nomenclature, in treating *Notropis* as masculine and therefore giving the specific names the masculine endings. The name *saladonis*, however, is not subject to change on account of the gender of the generic name.

DIAGNOSIS

Notropis saladonis may be distinguished from each of the multitudinous species of *Notropis*, as this complex is currently constituted, by a distinctive combination of characters. It is a small species (maximum standard length, 38 mm.), with delicate texture, very thin scales, and slender fin rays. The principal anal rays number 8, rarely 7. The pharyngeal teeth number 4–4 (rarely 3 in one row). The scales are relatively large: usually 32 along the lateral line, 20 to 24 in greatest body circumference, and 11 to 16 before dorsal (10 to 13 rows). The anterior lateral line scales are weakly elevated; those in contact with the shoulder girdle, often markedly so. Very few and only the anteriormost have exposed fields as much as twice as high as long. The posterior borders of the lateral line scales are not emarginate. The lateral line is moderately decurved, rising to contact the lateral band behind the dorsal fin. The infraorbital canal is complete, or, rarely, narrowly interrupted. The body is moderately deep and rather strongly compressed: the width is less than half the depth. The head is rather deep:

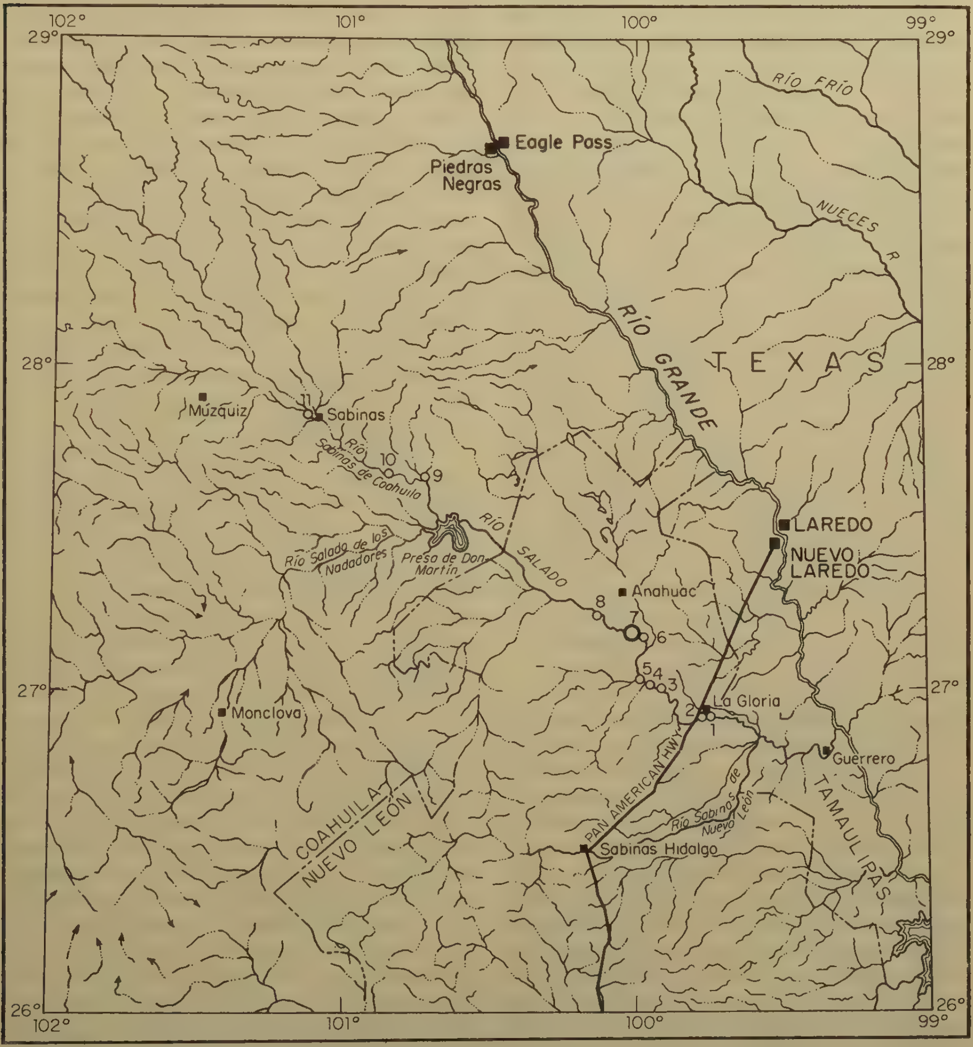
102°
101°
100°
99°
29°
28°
27°
26°
Río Frío
Eagle Pass
Piedras Negras
Nueces R.
Río Grande
TEXAS
Múzquiz
Sabinas
Río Sabinas de Coahuila
10
9
Río Salado de los Nadadores
Presa de Don Martín
Río Salado
LAREDO
NUEVO LAREDO
Anahuac
8
7
6
5
4
3
2
1
La Gloria
Guerrero
Monclova
Pan American Hwy.
Río Sabinas de Nuevo León
Sabinas Hidalgo
COAHUILA
NUEVO LEÓN
TAMAULIPAS

Map. 2. Río Salado, with record stations for the types of *Notropis saladonis*, numbered as listed in the text. The type-locality is No. 7.

its depth steps 1.3 to 1.4 in its length, and is about one-third greater than its width.

The general color tone is very pale, though the rather large and distinctly separated melanophores give the dorsum and the lateral band a diagnostically speckled appearance. The lateral band in consequence is not very conspicuous or discrete, and it is barely represented on the side of the snout. The basicaudal spot lies on the fin behind a clear area just beyond the hypural crease. The spot is small, wedge-shaped, and produced by only a few rather isolated macromelanophores. There is no marked massing of pigment before the dorsal origin or before the rudimentary caudal rays above or below, little intensification along the dorsal base, and almost none along the anal base. Behind the dorsal fin the middorsal streak is weak or absent. Pigmentation about the lateral line pores is inconspicuous. There is no pigment, or only a bare trace, along the ventral edge of the caudal peduncle, or about the anus.

The nuptial tubercles are confined on the head to the dorsal surface, where they are rather small and scattered. They become reduced on the snout, and do not reach the mouth. The tubercles on the pectoral rays are in one row basally, branching to about three irregular rows on each ray, with about four tubercles in each file per segment.

Comparisons and Relationships

From the assemblage of species now referred to as *Notropis* it is difficult to select those that seem most closely related to *N. saladonis*. It bears some points of resemblance to many species, but differs from each in many respects.

In the distinctive speckling of the dorsum and lateral band, *N. saladonis* remotely recalls *N. chihuahua* Woolman, with which it has many other characters in common. But in that species some of the isolated melanophores are very much larger, constituting giant macromelanophores. *N. chihuahua* also has a slenderer but thicker body, with the width more than half the depth. It also usually has smaller scales, about 34 to 37 in lateral-line, and 29 to 32 in body circumference. *N. chihuahua* has the lateral line only slightly decurved, and the anterior lateral line scales are not elevated. It has a definite dark wedge in front of the dorsal origin. The anal rays in *N. chihuahua* number 7 or 8 in about equal frequency (not consistently 7 as indicated in print). *N. chihuahua* occupies the basin of the Río Conchos, another tributary of the Río Grande in México, and certain small tributaries of the Río Grande in western Texas, but has not been taken in the basins of the Río Salado or Río San Juan.

In a number of respects, including body shape and color pattern, *N. saladonis* is rather similar to *N. braytoni* Jordan and Evermann, but that species is larger and coarser, usually has 7 anal rays and 15 or 16 pectoral rays, normally has a small but well-developed tooth in the lesser row on the pharyngeal, has the scales usually smaller (33 to 39 in lateral line, 24 to 28 in body circumference, nearly always 13 around caudal peduncle, 14 to 22 before dorsal), has the dorsal melanophores in contact, producing a cross-hatched appearance on the dorsum and a more solid lateral band, has a well-developed streak between dorsal and caudal fins, and has the nuptial tubercles more evenly distributed over the top of the head. *N. braytoni* occurs in the basins of the main tributaries of the Río Grande in México, namely the Río San Juan, the the Río Salado, and the Río Conchos (*N. robustus* Meek is a synonym), in the Río Grande proper, and in some of the tributaries of the Río Grande in Texas, including the Río Pecos. Sympatry in the Río Salado System indicates the full specific distinction of *N. saladonis* and *N. braytoni*.

N. saladonis also has much in common with *N. stramineus* (Cope)—the species heretofore generally called *N. deliciosus* (see Suttkus, Copeia, 1958, No. 4: 307–18)—but that species differs in its larger size and more solid build; and in having with rare exceptions 7 anal rays; and a more elongate and less compressed body, with the width more than half the depth; a much more pronounced middorsal stripe, with marked concentrations of pigment before the dorsal orgin and the caudal base; strong spots of pigment bounding the lateral line pores above and below; and finer and more widely distributed nuptial tubercles. *N. stramineus* as different subspecies, ranges from southern Canada to northeastern México, and shares the Río Salado System with *N. saladonis*.

There are points of resemblance also between *N. saladonis* and *N. ornatus* (Girard) but that species is very thick and chubby, with much the form of *Pimephales promelas* Rafinesque. Like that species, it is characterized, for a *Notropis*, by extreme

(798)

sexual dimorphism in form and color. It has unusually strong nuptial tubercles over the top of the head and over the snout. *N. ornatus* inhabits the Río Conchos division of Río Grande drainage basin and drainages with supposedly derived faunas to the west and south thereof.

N. saladonis has been compared also with the several species, in part undescribed, that inhabit the east-coast streams of México south of the Río Grande, and has been found to differ adequately from all of them. No other endemic Mexican species are close.

Perhaps the closest affinities of *N. saladonis* lie with *N. volucellus* (Cope) and *N. buchanani* Meek. A discussion of its possible kinship with those species involves a consideration of their relationship to one another. The senior author long regarded *buchanani* as a subspecies of *volucellus* (see Hubbs and Greene, 1928: 377–9). This view was followed by Trautman (1931) in his description of the big-river subspecies, *N. v. wickliffi*. More recently, however, thanks to a critical study by W. Ralph Taylor, it has developed that *buchanani* is a fully distinct species. Diagnostic characters have been stated by Bailey (1951: 222–3; 1956: 363) and by Trautman (1957: 93, 380–7, figs. 91–3). A study of the Méxican and Texas representatives of the combined group has convinced the authors of the validity of the specific separation. A further difference lies in the nuptial tubercles, which in *N. buchanani* we find to be confined on the head to the dorsal surface, whereas in *N. volucellus* they cover the snout and occur on the mandible and cheek. Furthermore, the dermal sense organs, as viewed under moderate magnification, are much more conspicuous in *N. buchanani* than in *N. volucellus* (presumably as an adaptation to living in more turbid waters). The supposed partial intergradation between *buchanani* and *volucellus* is not confirmed.

In many respects *N. saladonis* closely resembles *N. buchanani* and it agrees with that species in some of the features by which it is differentiated from *N. volucellus*. The compression of the body is one such character. So also is the enlargement and isolation of the melanophores, which is particularly notable in the far-southwestern populations of *N. buchanani* (see paragraph below). *N. saladonis* and *N. buchanani* further and distinctively agree in their very small size, fragile appearance, extremely pale general color, slender fin rays, similar meristic counts, and the restriction of the nuptial tubercles of the head to the dorsal surface. However, *N. saladonis* is clearly distinct from *N. buchanani*. *Notropis buchanani* differs from the Salado endemic in the almost invariable lack and at most incomplete development of the infraorbital canal, in having the anterior lateral line scales typically 3 to 5 times as high as long on the exposed fields, and in having the posterior border of these scales emarginate by the pores. The sense organs on the head, particularly on the cheek, are especially obvious, and a vertical row of sensory papillae is conspicuous under moderate magnification along the base of the exposed surface of the lateral-line scales. The nuptial tubercles on the top of the head are more enlarged (in relative size). The fins are all more elevated, more acute, and more falcate (the pelvic fin typically far overlaps the front of the anal base). The mouth is somewhat more oblique (at least in the Mexican representatives), rising to level with the bottom of the pupil. Pigment is massed to form a wedge in front of the dorsal fin and before the rudimentary caudal rays above and below, and there is more pigment along the bases of the dorsal and anal fins. In the better-pigmented specimens there is a greater tendency toward the black bordering of the lateral-line pores. One or two rows of black specks or dashes are more or less completely developed along the lower border of the caudal peduncle, and the peritroct is more or less blackened.

The better-pigmented specimens of *buchanani*, from the San Juan and Salado river systems in México, and from the Bosque River at Caldwell Crossing, near China Springs, McLennon County, Texas (UMMZ 92112), have very conspicuous giant melanophores, a rather definite dark lateral band, and the pigment in general unusually well-developed for this species. Other specimens from Mexico are very pale, but their paleness is due in part at least to the adherence of the melanophores to the lost scales. Subspeciation within *N. buchanani* may well be demonstrated, but will not affect the specific separation of *N. saladonis*. The two species live together in the Río Salado System and remain distinct. The collection from the Río Sabinas de Coahuila at Rancho de los Borregos, locality 9 in the list of specimens on page 298, includes, in addition to the 5 adults of *N. saladonis*, 38 specimens of *N. buchanani* and 1 hybrid between the two species. But within the North American cypinids such sporadic hybridization is not interpretable as evidence for conspecificity, nor even for close relationship (Hubbs, 1955: 7–10, figs. 2–3). From northeastern México *N. buchanani* ranges northward to the upper Mississippi and Ohio rivers.

N. saladonis also closely resembles *N. volucellus* (Cope), as that species is now constituted, and the two may be genetically akin. Points of resemblance include the tooth formula, the same ray counts, and the similar scale counts. The slight elevation of anteriormost lateral line scales approaches a diagnostic feature of *N. volucellus*. In size and texture the Salado shiner also approaches the mimic shiner. But there are many valid and consistent differences that hold not only in general, but also when *N. saladonis* is compared with the race of *N. volucellus,* namely *N. v. nocomis* (Jordan and Gilbert), that occurs nearest to the Río Salado. The contrasting characters of *N. volucellus* (all subspecies considered) are as follows: The size is larger, with the maximum standard length at any locality consistently greater than 40 mm., and the texture is less delicate. The scales are slightly more numerous, 33 to 38, in the lateral line. The anterior lateral-line scales are distinctly more elevated, having exposed fields about 2 to 4 times as high as long (varying with the subspecies); and the posterior borders of these elevated scales are more or less strongly emarginate beside the pores. The lateral line is little decurved anteriorly, and is either in contact with the lateral band throughout its length or is narrowly separated anteriorly, with a junction below the middle of the dorsal-fin base. The body is more terete, definitely thicker (the greatest width is more than half the greatest depth). The head is rather slender and is thicker (the depth steps 1.4 to 1.6 in the length and is only about one-fourth greater than the head width); and the interorbital and internarial areas are only slightly convex. The upper lip is usually somewhat overhung by the snout and usually rises only to about level with the lower border of the orbit. The general color tone is darker (least so in *N. v. wickliffi*), and the small melanophores are usually in contact, to give a more even, less-speckled shade. Pigment is more or less notably massed to form wedges in front of the dorsal origin and just before the rudimentary caudal rays, above and below; and is also concentrated, more or less, near the middle of the bases of the dorsal and anal fins; the middorsal stripe is more evident, even behind the dorsal fin. Pigment is more concentrated at the upper and lower borders of the lateral-line pores. There is a fairly strong, essentially biserial streak along the lower border of the caudal peduncle, and the peritroct is considerably blackened (except, perhaps, in *N. v. wickliffi*), though the pigment may be deep-lying and externally inconspicuous. The nuptial tubercles are moderately strong and extend completely over the snout, with no reduction, or even with some strengthening; some occur on the outer side of each mandible and others on the cheeks, with some strengthening ventrally. Sensory papillae are apparent (though not so strongly as in *N. buchanani*) in a vertical row along the base of the exposed field of each of the anterior lateral-line scales. *N. volucellus* ranges from southern Canada to the Guadalupe River system in central Texas, and has not been taken in or very close to México. Trautman (1957: 381, map 91) erred in extending the range into México (he did express doubt as to the status and distributional limits of the southwestern representatives).

In the possibly natural group comprising the species *saladonis, buchanani,* and *volucellus,* it will be seen, from the discussions just given, that the characters are often and variously paired, in the three comparisons between these forms.

DESCRIPTION

Size and Texture.—This is a very small species, not known to exceed 38 mm. in standard length (see pp. 297–8); and it is of very delicate skin texture.

Body Form.—The body is moderately deep (for proportions, see Table II)—on the average somewhat deeper in females than in males. The dorsal and ventral contours are almost equally and almost symmetrically curved. The form is more compressed than in most shiners of this general type: the greatest width is definitely less than half the maximum depth. The dorsal contour is highest and is slightly angulated at the origin of the dorsal fin. The predorsal contour is weakly arched to the occiput. The dorsal and anal bases are somewhat oblique. The contours of the caudal peduncle converge gently in nearly straight lines, to a point barely in advance of the anteriormost

(800)

caudal rays. The preanal contour is rather evenly curved forward to the isthmus, in a weak curve in the young and in males and in a broad curve in females. The lowest point of the contour is about three-fourths of the distance between pectoral base and pelvic base. Various body proportions are given in Table II.

Head Form.—In side view the head is roughly triangular, with the rostral angle narrowly rounded and with the axis a little below the middle. In top view the short muzzle is broadly U-shaped. The dorsal contour is broadly arched from tip of snout to above front of orbit, thence weakly arched to occiput. The ventral contour is gently and evenly curved. The head is relatively deep: the greatest depth, from the occiput to the isthmus, is about one-third greater than the maximum width of the head and steps 1.3 to 1.4 times into the head length (including the opercular membrane). The flattish sides of the head are subvertical. In the anterior view the interorbital and internarial regions are moderately convex, more so than in most similar species (this character shows in the figure of the female, but not in that of the male, because the head of the male, as figured, is twisted out of plane). The center of the eye is distinctly nearer to the tip of the snout than to the opercular margin. The eye is longer than the snout, and its length somewhat exceeds the bony interorbital width.

Mouth.—The mouth is moderately oblique. The premaxillary rises in a gentle curve to approximately level with the midpoint between the lower margins of pupil and orbit. The front of the upper lip is about even with the front of the snout and is never markedly overhung. The lower lip is definitely included. The upper jaw reaches variably to any point between the verticals from the anterior margins of the eye and of the pupil. Its length averages more than that of the snout but less than that of the orbit (Table II). Viewed from below the gape is U-shaped, with the separated rami either parallel or divergent. The isthmus is narrow. Various head proportions are given in Table II.

Pharyngeal Arch and *Teeth.*—The tooth-bearing lower pharyngeal arch is J-shaped. The tip of the short upper arm is pointed anteriorly. The lower arm abruptly narrows and straightens between the second and the third tooth, and again widens just above the bluntly pointed tip. The margin is abruptly angulated where the arch begins to narrow. The teeth are confined to the main row and normally number 4 on each side. In 39 specimens the formula is 4–4 in 36 and 4–3 in 3. The individual teeth are 2.5 to 4.0 times as long as broad. The hooked tips overhang the weakly-developed, entire grinding surfaces. There is no space for a tooth to develop in the lesser row. The equally long upper two teeth are longer than the lower two, and have narrower bases and more strongly hooked tips.

TABLE I

MERISTIC COUNTS ON TYPES OF *Notropis saladonis*
In the frequency column the count on the holotype is italicized.

Fin rays	Mean	Frequencies
Dorsal	7.99	7 (1), *8* (90)
Anal	7.84	7 (14), *8* (74)
Pelvic	7.84	7 (15), *8* (82)
Pectoral	14.11	13 (9), *14* (63), 15 (20)
Caudal	18.90	14 (1) . . . 18 (1), *19* (58), 20 (1)
Scale counts		
Lateral line	32.03	31 (9), *32* (46), 33 (9), 34 (1)
Above lateral line	4.98	4 (3), *5* (44), 6 (2)
Below lateral line	3.26	*3* (61), 4 (21)
Lateral line to pelvic	3.19	*3* (58), 4 (14)
Body circumference	23.09	20 (1) . . . *22* (26), 23 (10), 24 (23), 25 (35) . . . 27 (1)
Circumference, above	11.00	9 (1), 10 (2), *11* (41), 12 (2), 13 (1)
Circumference, below	11.66	*9* (9), 10 (12), 11 (39), 12 (5), 13 (1)
Caudal peduncle	12.02	*12* (51), 13 (1)
C. peduncle, above	5.00	*5* (52)
C. peduncle, below	5.02	*5* (55), 6 (1)
Scales before dorsal	13.20	11 (3), 12 (17), 13 (11), *14* (17), 15 (7), 16 (1)
Rows before dorsal	11.92	11 (17), *12* (33), 13 (12)

Intestine.—The intestine retains the simple compressed S-shape characteristic of the species still retained in *Notropis.*

Scales.—Over most of the body the squamation is complete and rather regular (for counts, see Table I). The squamation of the breast is variably reduced: the region from between the pectoral fins to the isthmus may be scaleless, provided with scattered scales, or completely scaled. The scales in the predorsal region are often somewhat irregular in arrangement and are slightly reduced in size. Everywhere the scales are extremely thin and delicate. On the sides of the body the exposed fields slightly approach a diamond shape, with the vertical axis somewhat greater than the longitudinal. Posteriorly the lateral-line scales are scarcely modified in shape, but toward the head they are weakly elevated (though less so than in *N. volucellus*): except on the two scales in contact with the shoulder girdle, and occasionally one or two immediately following, the exposed fields remain less than twice as high as long. All scales, including those of the lateral line anteriorly, have the posterior border rounded, without marked emargination. On each scale the radii on the posterior field span about one-third of the scale margin. The number of radii varies with the size of the scale; 6 to 8 extend from near the focus.

Table II

Proportional Measurements of Adult Types of *Notropis saladonis*

All proportions are expressed in thousandths of the standard length. Only larger specimens were measured. Not more than 5 of either sex were measured from a given locality.

		Males			Females		
	Holotype	Mean	Range	Number	Mean	Range	Number
Standard length	32.1	28.0	26.1–32.1	18	29.1	27.6–33.4	22
Body depth	271	267	247–282	18	285	266–306	22
Caudal peduncle depth	128	125	120–134	18	120	108–124	22
Caudal peduncle length	246	226	206–246	18	218	207–232	22
Head length	277	280	272–291	18	282	269–293	22
Head depth	187	199	187–212	18	200	192–206	22
Head width	156	148	142–156	18	148	138–156	22
Snout length	81	80	73–85	18	78	70–89	22
Orbit length	93	99	89–105	18	99	87–105	22
Upper jaw length	87	88	80–93	18	89	81–100	22
Suborbital width	31	31	25–36	18	30	26–35	22
Least bony interorbital	81	79	73–90	18	76	71–84	22
Predorsal length	520	519	505–547	18	520	494–546	22
Length of depressed dorsal fin	252	259	240–268	13	251	237–264	14
Pectoral fin length	221	216	204–230	16	205	195–237	17
Dorsal origin to lateral line	190	176	167–190	17	175	158–192	19
Pelvic insertion to lateral line	97	99	89–115	17	116	89–132	16
Width of upper lip	12	11	7–14	18	11	7–14	21
Overall width of mouth, including lips	69	70	63–79	18	69	64–78	22

Lateral Line.—The lateral line of the body is complete. Anteriorly it is moderately curved, almost following the ventral profile. For this reason it curves below the lateral band from above the end of the pectoral base to behind the dorsal fin, striking the band again at some point above the anal base. On the urosome it is essentially straight and gradually ascends to the middle of the band. The supratemporal canal is either short, with one terminal pore, or is of moderate length, with a terminal and a median pore. The supraorbital canal extends from just behind the posterior orbital rim to the anterior nostril. Its second pore is on a side canal. The infraorbital canal generally appears complete; it is complete in 9 of 10 specimens minutely examined, and in all 10 extends to below the anterior nostril. The one specimen with the canal incomplete has a short break on each side—on the posterior rim of the orbit on the left side, and at the bend near the dorsal margin of the orbit on the right. The complete preoperculomandibular canal extends from above the middle of the gape to about the level of the ventral rim of the orbit.

Sensory Papillae.—The sensory papillae on the cheek and other parts of the head are inconspicuous under ordinary magnifications of the wide-field microscope, and we fail to detect the papillae that form a vertical row along the base of the exposed field of the anterior lateral-line scales in certain species, notably *N. volucellus.* There is no trace of a barbel.

Nuptial Tubercles.—Breeding males (and, occasionally, to a very slight degree, large females) develop nuptial tubercles on the head and on the pectoral fin. Those on the head are confined to the dorsal surface and become scarce to absent over the heart-shaped parietal blotch, and become weak on the snout. They do not reach the mouth and are lacking on the mandible, cheeks, and opercular regions. Those on the top of the head are relatively small and are scattered. As usual, nuptial tubercles are developed on the upper surface of the second to the seventh or eighth pectoral ray (but not on the other fins). The individual organs are rather small, and are pointed but not definitely hooked. On each ray they start near the base in a single file, which soon branches. Near the middle of the tuberculate area the tubercles tend to form 3 irregular rows, with about 4 organs in each file per segment of ray.

Fins.—The fragile, slender-rayed, round-tipped, nonfalcate fins are of moderate size, and, for shiners of this type, of rather usual location (for measurements of dorsal and pectoral, and for predorsal and postanal lengths, see Table II). The dorsal originates slightly in advance of the pelvic. Its depressed length is about half the predorsal length in males, usually somewhat less in females. The anal originates behind the end of the dorsal base. Its depressed length approximates the length of the dorsal fin to the tip of the last ray. When the dorsal and anal fins are elevated, the distal borders are almost straight; when these fins are depressed, the anterior rays extend beyond the posterior rays. The caudal fin is strongly forked: the shortest middle ray is less than half as long as the longer lobe. The posterior margins of the pectoral and pelvic are straight to gently rounded. The pectoral does not reach the pelvic, and the pelvic usually does not reach the anal origin, and never extends far beyond. Ray counts are tallied in Table I.

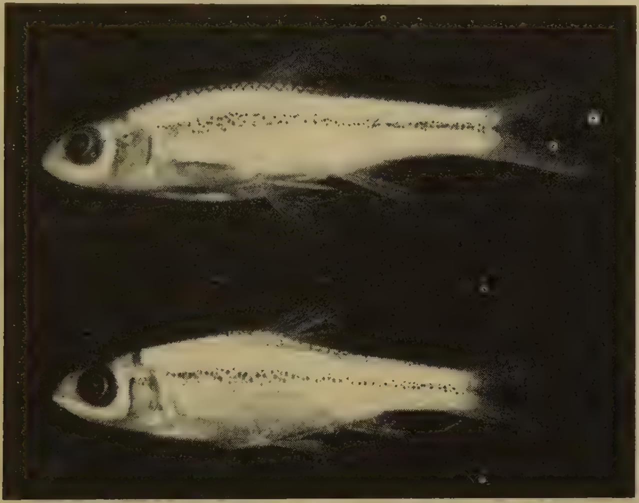

Fig. 1. Type specimens of *Notropis saladonis.* Above, holotype; below, female paratype from same collection.

Coloration.—In preservatives, the adult males and females look essentially alike. Neither show any evidence of bright colors, and it is assumed that this is one of the pale and weakly colored shiners, in life as well as in preservation. The specimens are distinctively and rather finely speckled, with no marked sexual dimorphism in the details of pigmentation (Fig. 1). The speckling is largely confined to the dorsum and to the lateral band, between which there is an irregular stripe about twice as wide as the band, with the pigment much reduced in intensity anteriorly and almost totally obsolete posteriorly. Below the band there is almost no pigment. On the anterior part of the trunk a few fine specks may lie between the band and the lateral line and a few very fine specks may develop along

(803)

the decurved part of the lateral line, just above and below the pores, or even just below the anterior part of the sensory line. Otherwise the lower sides are devoid of melanophores. The speckling is most prominent along the lateral band, which is narrower than the pupil posteriorly and rather diffuse on the trunk. The stripe is composed of large individual melanophores that seldom contact, and appear discrete to the unaided eye. The stripe ends at or just before the hypural crease, beyond which a pale area precedes the small basicaudal spot, which tends to be irregularly wedge-shaped and is constituted by only a few of the large discrete melanophores. The inner caudal rays have dark dashes along either edge, but these are hardly apparent without magnification. Anteriorly the lateral band is represented across the opercle by a few melanophores behind the upper preopercular margin. In a few specimens some melanophores are scattered on the upper cheek. Usually there is a faint row on the extreme lower edge of the orbit, and commonly a few specks on the sides of the snout, but never in a definite band around the muzzle. In some specimens a few melanophores occur on the lips, and usually an inconspicuous patch of pigment crosses the tip of the chin, but otherwise the ventral part of the head is unpigmented.

The dorsal pigmentation consists of a row of fine melanophores bordering each scale pocket, with color cells occasionally more or less enlarged to give the dorsum as well as the lateral band a speckled appearance. On the trunk this pigment pattern is continued, faintly, on the light stripe above the lateral band. The dark pigment is not particularly concentrated in a wedge in the front of the dorsal origin or in front of the rudimentary caudal rays, either above or below, nor just behind the occiput. The middorsal streak anterior to the dorsal fin consists of a faint median and a pair of lateral rows of scattered melanophores. There is some pigment, but not a pronounced dash, along the middle of the dorsal fin base. A few melanophores may flank the posterior dorsal rays, but behind the fin the middorsal streak is either absent, or consists of a pair of faint rows of scattered melanophores, which become more distinct posteriorly. The dorsal fin, like the caudal, but unlike the other fins, has fine dashed lines along the edges of the rays.

Small and inconspicuous melanophores are usually scattered along the anal-fin base, and in a few specimens a few minute scattered specks, at most, represent the stripe that is developed in most species along the lower border of the caudal peduncle. Otherwise the ventral regions are devoid of pigment.

The heart-shaped parietal blotch is uniformly darkened. Deep-lying pigment in the interorbital region is overlain by scattered melanophores, which extend onto the snout between the nostrils.

The peritoneum has scattered melanophores.

Distribution and Ecology

Notropis saladonis is apparently endemic to the Río Salado System (Map 1) and is the only species that we have found to be confined to this system. One other, *Notropis rutilus* (Girard), seems to be confined to Río Salado and Río San Juan divisions of the Río Grande System; it is a member of the *N. proserpinus* (Girard) complex, which consists of several allopatric representatives. That *N. saladonis* is restricted to the Río Salado System seems highly probable, for since 1930 the fish fauna of northeastern México has been under scrutiny (Hubbs and Gordon, MS) and numerous collections have been obtained and studied from the Río Grande proper, from its three tributary systems of consequence in México (those of the ríos San Juan, Salado, and Conchos), and from the tributaries of the Río Grande in Texas, New Mexico, and Colorado.

Within the Río Salado System the species is characteristic of, and, so far as now known, is restricted to, the main course of the river plus its upstream continuation, Río Sabinas de Coahuila (Map 2). The considerable number of collections and of specimens indicate that the species is definitely characteristic of this stream. It has not appeared in the collections from the lower tributary, Río Sabinas de Nuevo León, nor from the upper tributary, Río Salado de los Nadadores. In recent years, as in 1951, when Luciano Val Guerra conducted an extensive ichthyological survey in the drainage basin, the other tributaries have been almost entirely dry, and the main stream has been much reduced in flow. The fish fauna, however, including as it does such species as *Cycleptus elongatus* (LeSueur) and *Pylodictis olivaris* (Rafinesque) is suggestive of the biota of a fairly large stream. The appearance of *N. saladonis* suggests an inhabitant of rather

(804)

large, slow, and silty streams, and its form indicates mid-water swimming habits. According to the collection records, this species lives in waters with little vegetation, in turbid to clear waters flowing slowly over bedrock that is covered by mud and sandy silt. It appears to avoid clear spring-fed headwaters.

Reproduction

The collections taken from June 8 to 15 contain nuptial males and gravid females, and the specimens collected on April 7 were approaching full maturity. Three of the June collections also contain young fish, and in view of the very small size of the species it is assumed that they were young-of-the-year. Two June females, 23 and 24 mm. long, are not ripe. From these observations it is inferred that this shiner reproduces in spring and early summer.

Both sexes spawn at a small size. Nuptial males are 19 to 34 mm. in standard length; mature females, 21 to 38 mm. long. In the collections of April, 1939, and of June, 1951, the maximum sizes of males and females are 32 and 33 mm., respectively, whereas in the series of 7 taken in 1906 or 1907, the male is 34 mm. long and the 6 females are 29 to 38 mm. long. Possibly the decreased stream flow has led to a further dwarfing of the species. In the 3 series from the Río Sabinas de Coahuila the largest specimen is only 29 mm. long. The 18 males measured for Table II averaged 28 mm.; the 22 females, 29 mm. There seems to be little sexual dimorphism, even in size.

Literature Cited

Bailey, Reeve M. 1951. A check-list of the fishes of Iowa, with keys for identification. *In* James R. Harlan and Everett B. Speaker, *Iowa Fish and Fishing,* State of Iowa (Des Moines): *185–238, figs. 2–9 + 25 unnumbered figs.*

———. 1956. A revised list of the fishes of Iowa, with keys for identification. *In* James R. Harlan and Everett B. Speaker, *Iowa Fish and Fishing, 3rd ed.,* State of Iowa (Des Moines): *325–77, figs. 1–10 + 25 unnumbered figs.*

Hubbs, Carl L. 1955. Hybridization between fish species in nature. *Syst. Zool., 4: 1–20, figs. 1–8.*

——— and C. Willard Greene. 1928. Further notes on the fishes of the Great Lakes and tributary waters. *Pap. Mich. Acad. Sci., Arts and Letters, 8, 1927: 371–92.*

——— and Karl F. Lagler. 1947. Fishes of the Great Lakes Region. *Cranbrook Inst. Sci., Bull. 26: i–xi, 1–186, figs. 1–251 + 38 unnumbered figs., 1 map, 26 col. pls.* (also 1949 printing; revised edition in press).

Meek, Seth Eugene. 1908. Notes on fresh-water fishes from Mexico and Central America. *Field Columbian Mus. Publ. No. 124 (Zool. Ser., Vol. 7, No. 5), "Oct. 1907": 133–57.*

Trautman, Milton B. 1931. *Notropis volucellus wickliffi,* a new subspecies of cyprinid fish from the Ohio and upper Mississippi rivers. *Ohio Jour. Sci., 31: 468–74, fig. 1.*

———. 1957. *The fishes of Ohio*/with illustrated keys, Ohio State University Press (Columbus): i–xvii, 1–683, figs. 1–172 + 38 unnumbered figs., maps I–XI + 1–172, col. pls. 1–7.

University of California, La Jolla, California, and The University of Texas, Austin. Texas.

(805)

(806)

1958 No. 3 COPEIA August 28

Ogcocephalus darwini, a New Batfish Endemic at the Galápagos Islands[1]

Carl L. Hubbs

ONE HUNDRED years ago the epochal theory of evolution was announced by Darwin and by Wallace. Among the phenomena that led each to the conclusion that species are naturally derived, the phenomenon of endemism on islands was particularly indicative. Ever since, the analysis of endemism has played an important role in the development and clarification of evolutionary concepts. In view of the centennial celebrations honoring the memory of Darwin and Wallace, and in view of the circumstance that Darwin's most significant observations on insular endemism were made at the Galápagos Islands (Archipiélego de Colón), it seems appropriate to associate Darwin's name with another Galápagos endemic, a new batfish that I have had under study for some years.

Ogcocephalus darwini, sp. nov.

Pl. I, Fig. 1; Pl. II, Fig. 1; Pl. III, Fig. 1; Pl. IV, Figs. 1–2; Pl. V

Ogcocephalus [species].—Lundy, 1956: 468–9, 4 Figs. (popular account of capture, appearance, and habits of specimen SIO 56–60).

The only published account of this species, except for a number of newspaper stories (none carrying a specific name), is that of Lundy.

RELATIONSHIPS

This new fish is a member of the cosmotropical family Ogcocephalidae (the batfishes), which is one of the terminal groups of the highly modified order Pediculati (Lophiiformes). Within this family it is referable to the Ogcocephalinae (Jordan and Evermann, 1898: 2736), which seems to take its place among the growing list of fish groups recognized as characteristic of the warm waters of the New World, both Atlantic and Pacific. Whether the group deserves subfamily rank, and whether any Old World genera such as *Malthopsis* Alcock are referable to this group, are problems in need of consideration. With two exceptions, the hitherto-known American ogcocephalines are members of the West Indian fauna, and all of the Atlantic forms are referred to the type genus *Ogcocephalus* Fischer (spelling often emended to *Oncocephalus*).

The new species is obviously distinct from any of the Atlantic forms, as described by Jordan and Evermann (1898: 2736–2738; 1900: 3313, pl. 392), by de Miranda Ribeiro (1915: 1–4 [pagination separate for each family; would be pp. 645–8 if serially numbered, not including introductory matter or plates], 1 pl.), and by Hildebrand (in Longley and Hildebrand, 1940: 283–5, fig. 28; 1941: 311–315, pl. 33, fig. 2). It is quite different in coloration and has 14 to 16 pectoral rays, rather than 11 or 13.

Ogcocephalus darwini is obviously not closely related to either of the two previously known Pacific American ogcocephalines, but may be regarded as an insular derivative, or relict representative, of *O. porrectus* Garman. It is quite unlike *Zalieutes elater* (Jordan and Gilbert) in its less expanded disk, strongly projecting snout, more numerous pectoral rays, smaller tubercles, very different coloration, etc. (see Kumada, 1937: 62, pl. 102). Whether the generic separation of *elater* from *Ogcocephalus* will be continued is very dubious, but is a proper subject for critical consideration, such as Margaret G. Bradbury at Stanford University will afford in her revision of the group. *Z. elater* is generally recorded as ranging from México to Panamá, but it occurs as far north as off Pt. Conception, California, where two specimens were caught in halibut nets in January, 1945 (Irwin, 1945). One of these is here figured (Pl. IV, Fig. 3). Other specimens have been taken in southern California.

The obvious geminate of *Ogcocephalus darwini* is *O. porrectus*, described by Garman (1889: 86–8) from Albatross Station 3368, south of the Gulf of Panamá, in the vicinity of Cabo Corrientes, Colombia, at Lat. 05° 32′ 45″ N., Long. 86° 54′ 30″ W. on a rocky bottom at a depth of 66 fathoms, where the water temperature was 58.4° F. (surface water temperature, 82°). The 4 syntypes, 49, 56, 115.5, and 147 mm. in standard length, in the

---

[1] Contributions from the Scripps Institution of Oceanography, New Series No. 1045

Reproduced by Permission

Museum of Comparative Zoology, Harvard University, were taken in a small beam-trawl on February 28, 1891 (I have selected the 147-mm. specimen, shown on Plates I–III, as lectoholotype). No other specimens seem to have been obtained and the only subsequent listings of the species appear to be that of Fowler (1944: 527), as *Oncocephalus porrectus,* and that of Lundy (1956: 469), who gave the locality as "the depths of Panama Bay." All specimens in the United States National Museum from the Pacific identified as *Ogcocephalus* proved on examination in 1956 to be referable rather to the Halieutinae.

In a number of respects, in addition to the approximated ranges, *O. darwini* discloses relationship with *O. porrectus.* The pectoral rays are relatively numerous (14 to 16 in *darwini,* 14 in *porrectus*). The general proportions, body build, head physiognomy, and snout production are rather similar. The pattern of the bony tubercles is virtually identical. The double-striped pattern of *darwini* could be derived from the pattern of *porrectus* by intensification and fusion of the humeral spot and the anterior part of the rather faint stripes along the sides of the urosome; or, the stripes of *darwini* could have become disrupted and modified to produce the pattern of *porrectus.* Whether *darwini* is an insular derivative of *porrectus* or is the relict of a type ancestral to *porrectus,* or to both species, is not apparent.

In numerous minor respects, *O. darwini* differs from *porrectus* (Table I, Fig. 1, Pls. I–III). The tabulated comparison constitutes a diagnosis of the new species. Most of the differences lie in morphometry and in texture, in which respects *porrectus,* with the specific differences overshadowing the ontogenetic (see plates), accentuates and retains juvenile features. This is a point of evolutionary interest, because it is commonly the insular representatives that emphasize juvenile features. The juvenility of *porrectus* may be related to its rather deep-water habitat.

TABLE I

COMPARISON OF THE TWO RELATED PACIFIC SPECIES OF *Ogcocephalus*

Based on a direct comparison of types. The capital letters refer to graphs in Figure 1.

Character	*O. darwini*	*O. porrectus*
Tubercles at comparable sizes	Much smaller, flatter, less spinous; each much broader than high	Much larger, more elevated, more spinous; each much higher than broad
Sculpture below	Very fine	Rather coarse
Main dark color marks	Pair of dark stripes, on posterior half of disk and backward, very much longer than snout	Pair of blotches, near middle of disk, about as long as snout
Other dark markings on disk and tail	Hardly a trace of markings other than the main stripes	Irregular striping and blotching on side of tail; weak blotches on disk
General color tone	Dark	Light
Proportional size of disk region at comparable sizes (C, G, H)	Smaller	Larger
Body and peduncle at comparable sizes (A, B)	Deeper	Slenderer
Shape of disk and snout	More rounded at sides and tip	More sharply triangular
Snout (D, E)	Less elevated, and shorter	More elevated, and longer
Distance between pelvic axils (F)	Greater	Less
Body behind pectoral expansion (I)	Much wider	Slenderer
Average length of fins (Table II)	Greater	Less
Dorsal rays[1] (Table III)	3, seldom 2 or 4	2 or 3
Pectoral rays (Table III)	14 to 16, usually 15	14

[1] Counting last two elements as one ray.

DATA ON TYPE SPECIMENS

The holotype, in Scripps Institution of Oceanography, of the University of California, La Jolla (No. H51–214), an adult 135

(808)

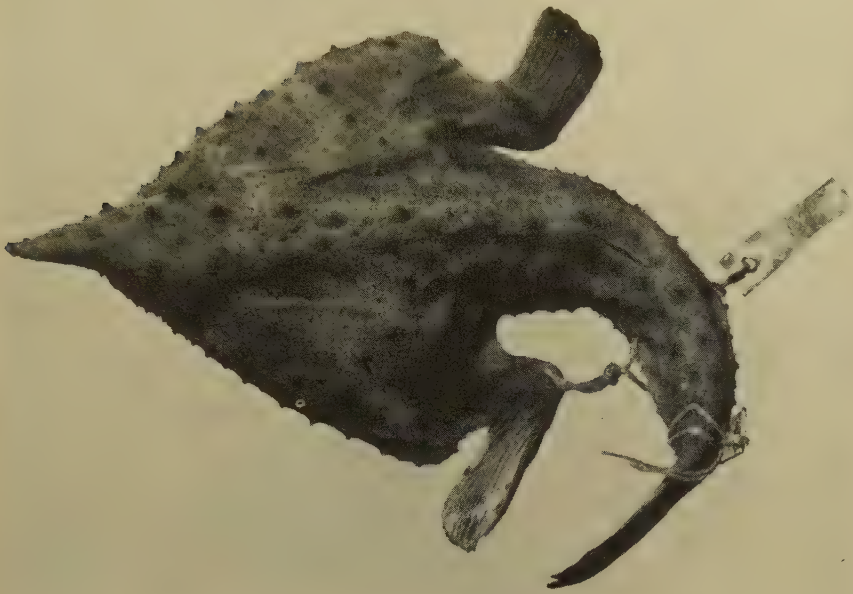

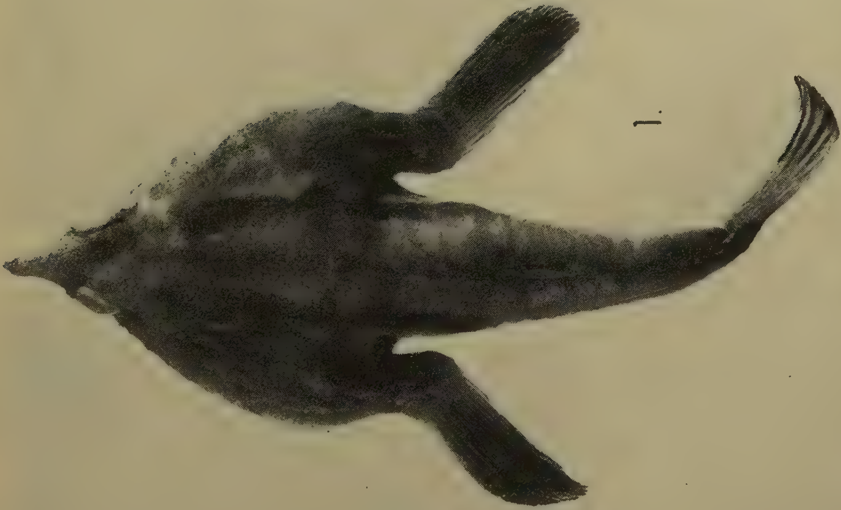

1.

Plate. I. Holotypes of *Ogcocephalus darwini* (Fig. 1) and of *O. porrectus* (Fig. 2) in dorsal view. Standard lengths respectively 135 and 147 mm. For Plates I–III the photographs of *O. darwini* were taken by James E. Ruppert of Scripps Institution of Oceanography, University of California, La Jolla; those of *O. porrectus*, by Frank White of Harvard University.

PLATE I

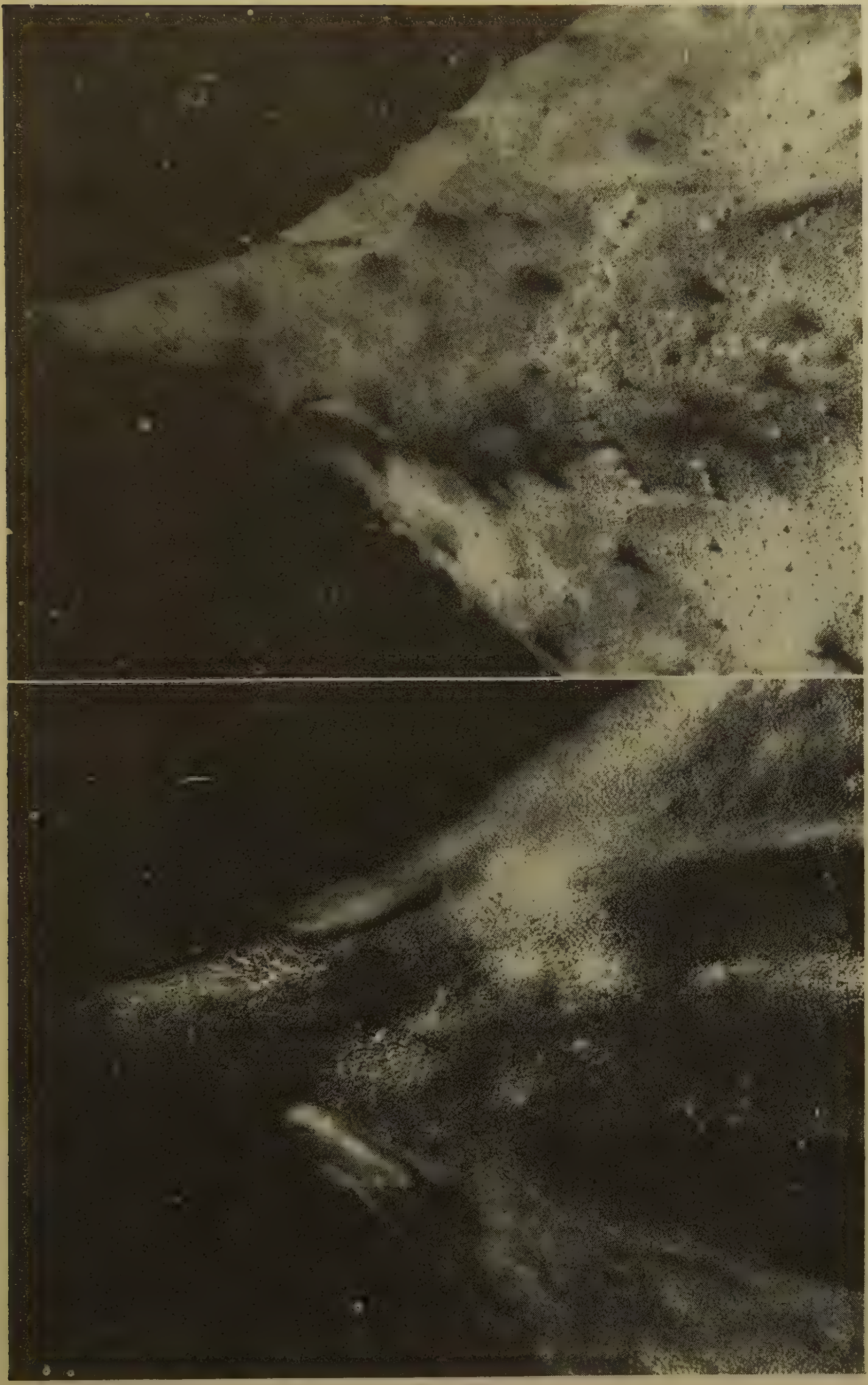

Plate II. Holotypes of *Ogcocephalus darwini* (Fig. 1) and of *O. porrectus* (Fig. 2). Dorsal views of anterior parts, magnified.

PLATE II

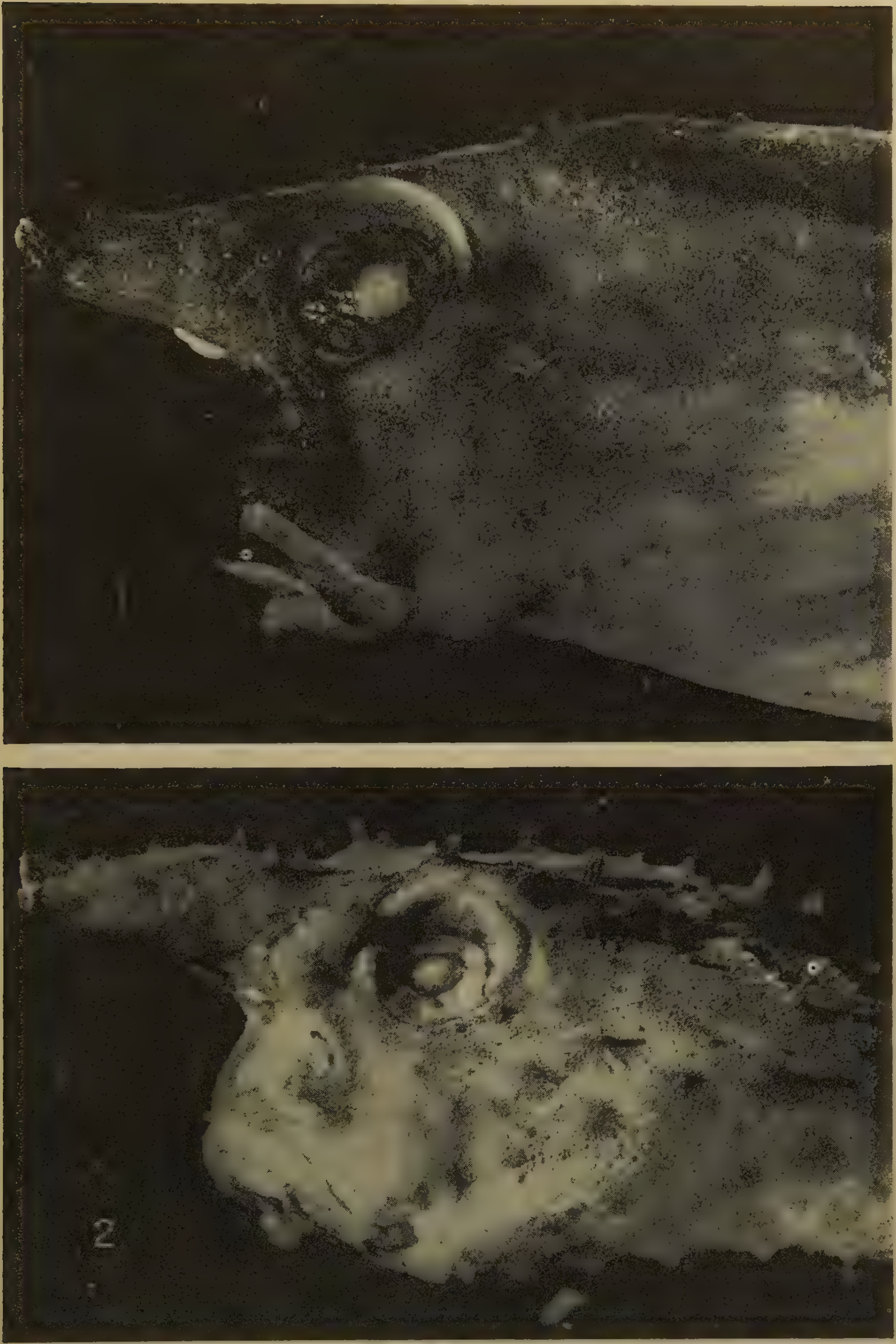

Plate III. Holotypes of *Ogcocephalus darwini* (Fig. 1) and of *O. porrectus* (Fig. 2). Lateral and very slightly anterior views of head region.

PLATE III

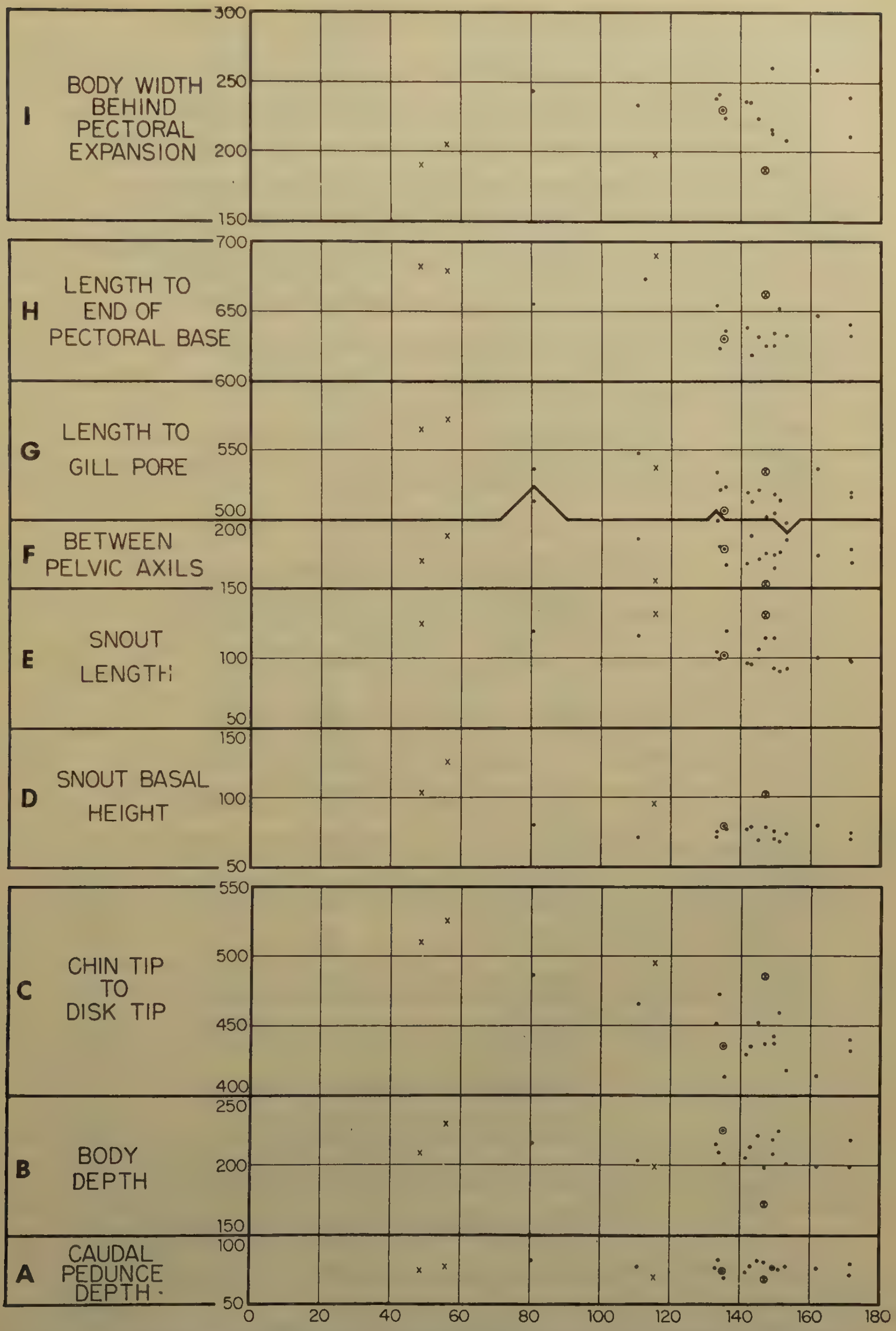

Fig. 1. Distinctive proportional measurements of the types of *Ogcocephalus darwini* (dots) and of *O. porrectus* (crosses). Symbols for the holotypes are encircled. Data from Table II.

(815)

TABLE II

PROPORTIONAL MEASUREMENTS OF THE TWO RELATED PACIFIC SPECIES OF *Ogcocephalus*

The measurements are expressed in thousandths of the standard length, those for the *O. darwini* types in italics and those for the *O. porrectus* types in boldface; in sequence of standard length. The capital letters in parenthesis designate characters graphed in Figure 1. P_1 = pectoral fin.

Standard length, mm.	To center of anus	To end P_1 base (H)	Length to gill pore (G)	Chin tip to disk tip (C)	D origin to C base	A origin to C base	Caudal fin length	Pectoral fin length	Pelvic fin length	Between pelvic axils (F)	Body depth (B)[1]	C peduncle depth (A)[1]	Width behind P_1 fins (I)[1]	Between gill pores	Gill pore to elbow	Disk width (expanded)[1]	Snout plus orbit	Snout length (E)	Snout depth (middle)[1]	Snout depth (base) (D)[1]	Snout width (base)[1]	Skull prominence width[1]	Interorbital width	Cornea length	Cornea to preorbital	Cornea to nostril	Upper jaw length	Mouth width (overall)	Supraorbital rim to angle of mandible[1]
48.7	**616**	**682**	**565**	**510**	**316**	**172**	**275**	**211**	**170**	**170**	**208**	**74**	**190**	**270**	**131**	**615**	**209**	**125**	**25**	**103**	**79**	**149**	**64**	**79**	**70**	**31**	**98**	**121**	**198**
56	**670**	**679**	**572**	**525**	**343**	**163**	**260**	**232**	**192**	**188**	**230**	**77**	**205**	**320**	**126**	**613**	**211**	**126**	**27**	**125**	**81**	**155**	**65**	**78**	**70**	**26**	**94**	**130**	**200**
80.6	*654*	*655*	*536*	*486*	*343*	*176*	*293*	*256*	*191*	*213*	*215*	*81*	*243*	*305*	*133*	*556*	*208*	*119*	*40*	*80*	*77*	*144*	*67*	*65*	*65*	*29*	*89*	*115*	*189*
110.6	*649*	*673*	*548*	*465*	*343*	*167*	*293*	*288*	*190*	*181*	*203*	*77*	*233*	*281*	*156*	*495*	*192*	*116*	*41*	*71*	*74*	*149*	*61*	*57*	*61*	*35*	*98*	*129*	*173*
115.5[2]	**628**	**690**	**537**	**495**	**345**	**177**	**235**	**267**	**177**	**156**	**199**	**69**	**198**	**289**	**165**	**550**	**194**	**132**	**42**	**95**	**78**	**127**	**59**	**55**	**71**	**27**	**93**	**118**	**192**
133	*631*	*654*	*534*	*451*	*340*	*169*	*247*	*283*	*180*	*199*	*215*	*76*	*238*	*308*	*143*	*567*	*185*	*104*	*36*	*71*	*71*	*134*	*59*	*66*	*66*	*26*	*88*	*116*	*180*
133.8	*611*	*623*	*521*	*472*	*347*	*180*	*236*	*256*	*174*	*180*	*209*	*82*	*241*	*296*	*132*	*573*	*180*	*99*	*45*	*75*	*82*	*134*	*64*	*66*	*68*	*28*	*87*	*117*	*181*
135[3]	*624*	*630*	*506*	*435*	*346*	*167*	*285*	*285*	*206*	*178*	*225*	*74*	*230*	*289*	*141*	*523*	*187*	*102*	*39*	*79*	*76*	*147*	*65*	*65*	*64*	*27*	*88*	*113*	*184*
135.6	*625*	*636*	*523*	*413*	*368*	*191*	*251*	*273*	*179*	*167*	*201*	*69*	*224*	*288*	*121*	*533*	*202*	*119*	*46*	*77*	*79*	*131*	*64*	*66*	*61*	*21*	*85*	*115*	*170*
141.7[4]	*627*	*638*	*519*	*429*	*332*	*158*	*245*	*246*	*168*	*168*	*205*	*73*	*236*	*279*	*138*	*481*	*189*	*96*	*39*	*77*	*82*	*139*	*70*	*74*	*59*	*18*	*87*	*111*	*190*
143	*621*	*619*	*512*	*435*	*328*	*183*	*274*	*267*	*189*	*187*	*213*	*78*	*236*	*302*	*120*	*557*	*193*	*95*	*36*	*78*	*73*	*122*	*67*	*66*	*60*	*26*	*87*	*114*	*179*
145[5]	*568*	*631*	*521*	*452*	*335*	*166*	*247*	...	*172*	*171*	*221*	*81*	...	*290*	...	*433*	*188*	*106*	*35*	*69*	*52*	*145*	*61*	*67*	*56*	..	*86*	*107*	*180*
147[3]	**636**	**662**	**534**	**485**	**341**	**167**	**241**	**230**	**149**	**153**	**172**	**68**	**187**	**269**	**146**	**544**	**199**	**131**	**48**	**102**	**76**	**121**	**62**	**54**	**64**	**28**	**90**	**116**	**166**
147.1	*599*	*625*	*501*	*437*	*345*	*181*	*235*	*226*	*159*	*175*	*198*	*80*	*224*	*250*	*124*	*486*	*195*	*114*	*43*	*78*	*79*	*137*	*67*	*63*	*69*	*22*	*87*	*114*	*176*
149.3	*631*	*625*	*504*	*442*	*346*	*158*	*238*	*220*	*177*	*174*	*218*	*76*	*216*	*303*	*143*	*538*	*182*	*97*	*33*	*70*	*64*	*127*	*57*	*71*	*58*	*21*	*89*	*114*	*175*
149.5	*625*	*634*	*518*	*437*	*324*	*175*	*269*	*266*	*195*	*165*	*208*	*76*	*213*	*250*	*144*	*473*	*199*	*114*	*44*	*75*	*74*	*174*	*65*	*64*	*58*	*25*	*84*	*114*	*175*
151	*642*	*652*	*513*	*459*	*329*	*157*	*260*	*255*	*168*	*176*	*224*	*75*	*260*	*302*	*136*	*540*	*172*	*90*	*31*	*68*	*71*	*124*	*58*	*59*	*68*	*28*	*91*	*116*	*187*
153	*620*	*632*	*497*	*418*	*316*	*133*	*248*	*275*	*188*	*185*	*201*	*77*	*208*	*292*	*145*	*523*	*176*	*92*	*37*	*73*	*77*	*159*	*62*	*65*	*59*	*25*	*88*	*117*	*175*
162	*638*	*647*	*536*	*414*	*323*	*157*	*244*	*233*	*158*	*173*	*199*	*76*	*259*	*295*	*123*	*523*	*185*	*100*	*39*	*89*	*70*	*128*	*60*	*65*	*60*	*23*	*84*	*103*	*177*
171.3	*629*	*640*	*516*	*440*	*343*	*193*	*229*	*246*	*160*	*178*	*199*	*71*	*211*	*290*	*134*	*470*	*179*	*98*	*36*	*69*	*72*	*125*	*65*	*55*	*60*	*23*	*79*	*109*	*159*
171.4	*602*	*632*	*519*	*432*	*354*	*151*	*267*	*254*	*187*	*169*	*218*	*79*	*239*	*295*	*136*	*558*	*185*	*97*	*39*	*74*	*78*	*156*	*62*	*64*	*61*	*25*	*88*	*122*	*181*

---

[1] Excluding major tubercles.

[2] 1.5 mm. added to replace missing spine.

[3] Holotype.

[4] Specimen considerably shrunken, but proportions scarcely altered.

[5] Specimen dried, but proportions listed, except disk width, little modified.

mm. in standard length, shown on plates I–V, was collected by Robert Devine, Navigator of the Tuna Clipper Chicken o' the Sea, on April 25, 1951 at Caleta Tagus (Tagus Cove), on Isla Isabela (Albemarle Island), Galápagos Islands (Archipiélago de Colón). This cove is located approximately at Lat. 00° 16.0′ S., Long. 91° 22.5′ W., as read from H. O. Chart 1798 (October, 1946). The collector reported that the specimen was taken at midnight by dip-net under light. The proportional measurements of the holotype are indicated in Table II and the ray counts (Table III) are all modal.

All other specimens examined are designated as paratypes, as they are all from the Galápagos Islands and are consistent in essential characters. The data follow, in sequence of the Collection Numbers as listed in the records of the Fish Collection at the Scripps Institution of Oceanography (for purpose of the record, borrowed specimens are included in the Scripps listing). The standard lengths are those obtained when the measurements were recently made for Table II.

TABLE III

FIN-RAY COUNTS IN TWO RELATED PACIFIC SPECIES OF *Ogcocephalus*

The last two elements in the dorsal and anal fins are counted as one ray.

Species	Dorsal Rays			Anal Rays		Unbranched C Rays			Branched C Rays			Total C Rays	Pectoral Rays			Pelvic Rays
	2	3	4	2	3	1	2	3	6	7	8	9	14	15	16	I, 5
darwini	1	15	1	1	16	1	14	2	2	14	1	17	7	25	2	34
porrectus	2	2		..	4	..	4		..	4	..	4	8	..	..	8

H50–18.—Received from Peoples Cannery of San Diego; collected by Bob Grove of the Tuna Clipper West Coast about January 1, 1950, at Punta Moreno, Isla Isabela, which is approximately at Lat. 00° 41′ S., Long. 91° 20′ W. It was taken in a "Galápagos bait-net" (see below, under Range and Habitat), while seining for "herring" in shallow water near shore. Length 135.6 mm.

H50–19.—Collected by John Furuya on the Tuna Clipper Sun Padre and received from him on February 17, 1950, when the ship returned to San Diego; taken in Bahía Elizabeth on the west side of Isla Isabela, in a Galápagos bait-net near shore in shallow water. The collection comprised three adult specimens which were studied and photographed. One was returned to the collector in 1951. The other two have been misplaced.

H50–132.—Collected by Jack Buchanan on the Tuna Clipper Sun Queen during the last week of April, 1950, in Bahía Elizabeth, Isla Isabela, in a Galápagos bait-net at a depth of about 3 fathoms. Length 151 mm.

H51–51.—Collected by Ernest Silva on the Tuna Clipper Bernadette in January or February, 1950, just outside Caleta Webb (Webb Cove) on Isla Isabela, which is at Lat. 00° 48′ S., Long. 91° 26′ W. It was found tangled in a Galápagos bait-net, near the bottom, and was preserved in rubbing alcohol. Illustrated on Plate IV, Figure 1. Length 80.6 mm.

H53–196.—Collected by "Mits" Hosaka on the Tuna Clipper Sun Traveler in late October, 1953, at Punta Mangle on Isla Fernandina (Narborough Island), which is approximately at Lat. 00° 27.0′ S., Long. 91° 23.0′ W. It was captured in a Galápagos bait-net at a depth of 2 fathoms, 50 yards offshore. Length 171.4 mm.

SIO 54–175.—Collected by Herman Hawkins on the Tuna Clipper Liberty Bell in June or July, 1954, at Caleta Tagus, Isla Isabela, which is at Lat. 00° 16.0′ S., Long. 91° 22.3′ W. The method of collection was not stated. This specimen was preserved in rubbing alcohol. Length 133 mm.

SIO 54–199.—Collected by Jay Plummer late in October, 1954, at Bahía Elizabeth, the nearshore position of which is roughly centered at Lat. 00° 36′ N., Long. 91° 06′ W. Length 162 mm.

SIO 55–16.—Collected by Lars Sunde, Chief Engineer of the Tuna Clipper Cape Falcon about January 1, 1955, at Punta Mareno, Isla Isabela (see H50–18 for position). It was taken in a Galápagos bait-net close to the beach in a depth not over 5 fathoms. Length 153 mm.

SIO 56–60.—Collected by M. M. Cardozo on the Tuna Clipper Mary E. Petrick in March or early April, 1956, on Isla Isabela. It was picked by hand from a Galápagos bait-net, near the bottom, by Mr. Cardozo while diving to tend the net. The net was set near shore at a depth of about 2.5 to 3.0 fathoms. The capture of this specimen has been described by Lundy (1956). It was preserved in rubbing alcohol. Length 149.5 mm.

SIO 57–20.—Collected September 15, 1950, at Bahía Banks, Isla Isabela (near the north end of the west shore, which is at approximately Lat. 00° 01′ S., Long. 91° 29′ W.); received in the University of Washington Fish Collection from Walter J. Eyerdam. Specimen considerably shrunken. Length 141.7 mm.

SIO 57–22 (Stanford University No. 17112).—Collected by William B. Morrel on the Tuna Clipper Santa Helena, on July 16, 1951, at the Galápagos Islands (exact location not recorded). The collector stated that he took the specimen by dip-net under light (Anita B. Daugherty, personal communication). Length 133.8 mm.

SIO 57–23 (Stanford University No. 14977).—Collected by William L. Luttrell, Engineer on the Purse Seiner SANTA HELENA (later converted to a Tuna Clipper bait-boat), about October or November, 1948, at Bahía Banks (see SIO 57–20), Isla Isabela. The specimen was caught in a tuna-net (purse-seine), of a type that was not fishing deeper than about 42 fathoms. It was first reported to have been taken near the surface where the depth is at least several hundred fathoms, but the collector recently told Anita B. Daugherty that the original information may have been incorrect, as the bottom is very irregular and drops off very abruptly. He now thinks it possible that the batfish was picked off the bottom. Length 171.3 mm.

SIO 57–24 (Stanford University No. 16901).—Collected by fishermen in 1948 aboard the Purse Seiner COLUMBIA at the Galápagos Islands, probably at Bahía Banks (see SIO 57–20). The net used was fishing for tuna to a depth of 20–25 fathoms at most, over "fairly deep" water. The crew reported to Anita B. Daugherty that on this trip they picked up about a dozen batfish while purse-seining for tuna. They brought back two specimens, dried, and gave the one here listed to Miss Daugherty. Length 145 mm. (slight allowance made for shrinkage).

SIO 57–111 (in collection of California State Polytechnic College).—Collected by fishermen on a tuna clipper on December 24, 1949, in Caleta Webb (Webb Cove), Isla Isabela (see H51–51 for position). It was taken in a Galápagos bait-net. The specimen was originally preserved in rubbing alcohol. Length 110.6 mm.

SIO 57–166.—Collected at the Galápagos Islands some years ago by fishermen on a tuna boat; probably brought in by William L. Luttrell, Engineer on the Purse Seiner SANTA HELENA (further data lost); received from Anita B. Daugherty of the California State Fisheries Laboratory. Length 149.3 mm.

SIO 57–167 (in collection of Allan Hancock Foundation, University of Southern California).—Dredged on December 13, 1934, on the Allan Hancock Pacific Expedition 1935, Galápagos Islands, at Station 345-35, between Daphne and Seymour islands at Lat. 00° 24′ 50″ S., Long. 90° 21′ 40″ W., at a depth of 30 fathoms. It was kept alive until January 2, 1935, and was obviously preserved in formalin. Length 147.1 mm.

SIO 58–39.—Collected by Joe Freer on the Tuna Clipper CHICKEN O' THE SEA in the latter part of 1954, on either the west side of Isla Isabela (Albemarle Island) or east side of Isla Fernandina (Narborough Island). Length 143 mm.

All specimens, except as indicated above, were brought to San Diego or San Pedro frozen, then preserved briefly in formalin. The specimens kept at Scripps Institution are in 40% isopropyl alcohol and are less shrunken than those in other collections, which are in ethyl alcohol.

RANGE AND HABITAT

All known specimens were taken about the Galápagos Islands, to which the species is apparently confined. It takes its place among the numerous endemics of these islands.

(818)

Most of the records are from the west shore of Isla Isabela (Albemarle Island), probably because this is an area where the American tuna fishermen commonly fish and "make bait." One specimen came from the east shore of Isla Fernandina (Narborough Island), facing Isabela. It is possible that the species is commonest in the region between islas Isabela and Fernandina, where conditions are affected by the Humboldt (Perú) Current and by upwelling. One specimen was dredged between Daphne and Seymour islands, north of Isla Santa Cruz or Chávez (Indefatigable Island).

Most of the known specimens were taken in "Galápagos bait-nets," which are hauled near shore over rough rocky bottom, with the aid of a diver to free the lead-line when snagged (these nets are hauled to obtain live bait to be used as chum in the operation of the bait-boats of the tuna-clipper fleet of San Diego). Some of the specimens, however, are reported to have been dip-netted under light or to have been taken in the nets of the purse-seine fleet (of San Pedro). It is therefore highly probable that some individuals move toward the surface, even out over deep water where very close to shore, as in Bahía Banks (Banks Bay) near the north end of Isla Isabela. We are finding that a considerable number of fishes seemingly adapted to bottom existence more or less regularly move toward the surface, especially at night.

METHODS OF COUNTING AND MEASURING

Since the batfishes are so peculiar, the methods here used in counting and measuring need specification. The vertebrae, counted by X-ray, include the hypural. The rays in the fins are often readily counted by noting the free tips, by sighting the body of the rays directly or by transmitted light, by feeling the separation by a sharp instrument, or by X-ray; but often, in any fin, the rays may be so obscured as to require partial dissection for a secure count. The last two elements in the dorsal and in the anal fin are enumerated as one ray, in line with the only single, simple criterion. The gills were counted by dissection in one paratype.

The standard length is measured by pressing the point of the dividers or calipers backward against a superficial swelling over the expanded bases of the middle caudal rays (Pl. IV, Fig. 2). The same method determines the end point for the distance from the origin of the dorsal and of the anal fin to

Plate IV

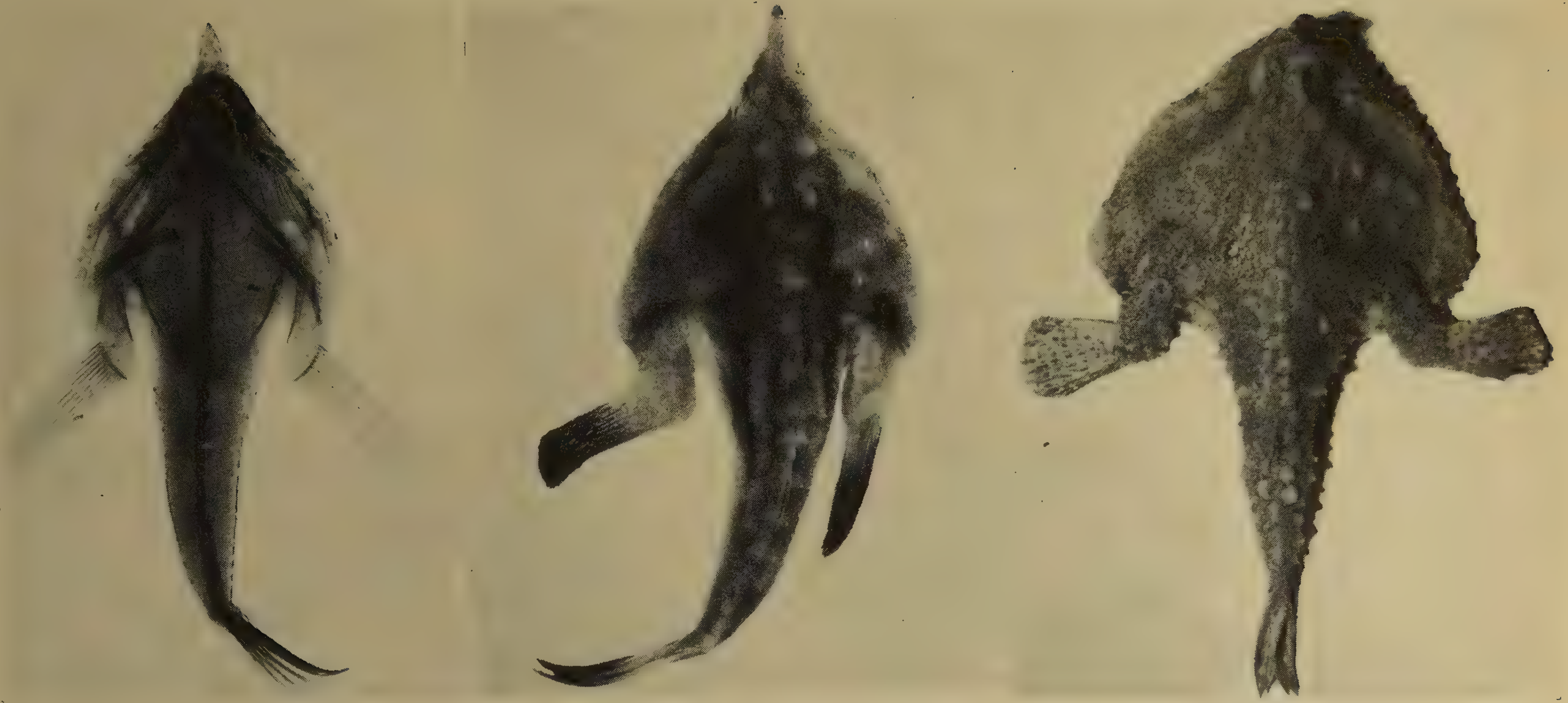

Plate IV. Pacific Species of Ogcocephalinae.

Fig. 1. *Ogcocephalus darwini,* smallest paratype (H51–51), 80.6 mm. in standard length. Photograph by Scripps Institution of Oceanography.
Fig. 2. *Ogcocephalus darwini,* X-ray photograph of holotype, by Nobuo Egami, to show skeletal features. Print by Scripps Institution of Oceanography.
Fig. 3. *Zalieutes elater,* from off Pt. Conception, California. Photograph furnished by Margaret C. Irwin, when with the Santa Barbara Museum of Natural History.

the caudal base. The origin of the dorsal and of the anal fin is the front base of the first ray, which may bear some fine prickles like those of the general integument (a hard sloping edge precedes the base of the first anal ray). Unless otherwise stated, the initial point of all measurements is the extreme tip of the snout, including the terminal spine or spines. In other measurements the major tubercles are excluded. In measuring "chin tip to disk tip" the end point is the rear of the last major tubercle near the outer angle of the disk (the underlying bony terminus is not precisely detectable). "Caudal fin length" is measured from the caudal base, determined as indicated above, to the extreme tip of a median ray. "Pectoral fin length" is from the posterior end of the base (near the "elbow") to the farthest tip. "Pelvic fin length" is from the middle of the base (determined as for the caudal fin) to the farthest tip. "Between pelvic axils" is taken across the hidden bases when the fins are spread apart. "Width behind P_1 [pectoral] fins" is taken where the body margin reaches a maximum curvature near the solid part of the urosome, behind the disk (a good measurement, though somewhat subjective).

Measurements involving the gill pore are to the nearest free margin of the pore. "Disk width (expanded)" varies greatly with preservation and with force used in expansion. Snout and orbit measurements are from the bony rim. "Skull prominence width" is taken where the prominence is widest, to points of greatest concavity on each side. "Interorbital width" is measured with points pressed tight. "Cornea" is that portion of the eye covering that is free of prickles. "Upper jaw length" is to the concealed rear tip.

DESCRIPTION

BODY FORM.—When fully expanded the disk approximates an equilateral triangle, with the width about equal to the length of either side. When the disk is contracted, with the pectoral peduncle appressed against the side of the body, the width is approximately two-thirds the length of either side. Anteriorly, the contour of each side is rather strongly concave, due to the projection of the long snout, whereas posteriorly each side is somewhat convex, more so than in *O. porrectus*. Behind the gill pore a broadly U-shaped indentation largely separates the pectoral peduncle from the sides of the trunk. The occipital region is rather markedly elevated into a somewhat dome-shaped prominence. The front of the head is also much elevated, so that in anterior view the region of the eyes and mouth is rather rectangular, about half again as high as wide. The trunk and tail region behind the disk is relatively thick, but also elongated. The width is about one-third greater than the depth. The outer-ventral edge is moderately ridged from the pectoral axil to the caudal base just below the end of the lateral line, and the intervening ventral surface is rather flat. The sides are subvertical and moderately convex, with a slight groove along the lateral line. Anteriorly, the dorsal surface is strongly arched and somewhat keeled, but posteriorly is quite flat. In lateral view the contours are considerably constricted along the caudal peduncle. Otherwise the contours taper rather evenly toward the caudal fin.

HEAD FORM.—The subconical snout projects beyond the orbit a distance about equal to that between the orbit and the occiput. The direction is essentially horizontal, but is variable, as are also the length and the contours of the snout. In general, the snout is about as high as wide. The nostrils are near the outer edge of the fleshy area over the premaxillary spines. The slitlike posterior nostrils lie close to the downward-curved bony rostral ridge that ends above the middle of the mouth. The smaller, nearly round anterior nostril is bordered by a slight fleshy rim. The spacious orbit is much larger than the clear, oblique cornea. The rest of the eye surface is covered by a fine shagreen. The eye is directed outward and slightly downward. The interorbital space is somewhat depressed as a shallow cavity, which is obliterated above the front of the orbit where the projecting snout takes shape. The width of the broad and flat suborbital region approximates the length of the cornea.

ILLICIUM.—The illicium (Pl. V) fits snugly into the anterior angle of a deep and rather acutely subtriangular fossa, the membrane of which is largely devoid of prickles where in contact with the head of the illicium, and also on its subvertical posterior wall. When the illicium is at rest, the short thick stem fills the deep, oblique part of the cavity, and ends ventrally in the esca, comprising a median whitish fleshy lobe and, on either side, a more prominent rounded lobe. These lateral lobes diverge backward, and are jointly separated from the broadly triangular and flatter anterior lobe by a thick and short neck. In anteroventral view the esca is approximately as long as the pupil.

Mouth.—As seen from below, the mouth is approximately semicircular. The lower jaw is included, and the upper lip is essentially in line with the subvertical front of the head below the base of the snout. The front of the mouth is distant from the illicium about the length of the cornea. The concealed extreme tip of the upper jaw lies on a vertical passing between pupil and rear of orbit. The gape in side view is very slightly oblique.

Teeth.—The fine, needle-like teeth form villiform bands on the jaws, vomer, palatine, and tongue. The weakly curved and rather broad premaxillary band is obliquely truncated laterally. The narrower mandibular band is somewhat more curved and tapers to a point laterally. The vomerine patch is larger than the pupil. It is broadest close to its convex anterior edge and tapers considerably to its squarely truncated rear. Each palatine patch is much smaller. Most of the broad upper surface of the tongue is covered by a flat dentate area, which is incompletely divided by a lengthwise groove.

Sensory line.—Just behind the vertical through the anus, over a space about equal to that of the eye, the lateral line takes an abrupt descent. Posteriorly, the lateral line runs a little below the middle of the side. In the holotype, the pores in the lateral line number 29—28, counting from a double pore at the origin of the horizontal line just behind the eye to the pore at the caudal base. Each pore is protected by a pair of spiny points that arch so as to nearly meet above and below, as described by Garman for *O. porrectus.* Similar structures appear along the infraorbital canal, which is angulated downward to near the corner of the mouth, and also appear along the preoperculomandibular line, which runs just below the edge of the disk and then forward around the chin, where the spiny protections for the pores are especially prominent. At the tip of the chin, in advance of the main series, two strongly protected pores form a supplementary crosswise series. Behind the mouth are two separated, protected pores, derived respectively from the infraorbital and the preoperculomandibular series. There are other pores of this type along the rostral fold, above the upper lip anteriorly. The pores of the supraorbital series are indistinct, except for three or four that are subvertically aligned just in advance of the orbit. A transverse commissure crosses the midline just in advance of the occiput. No fleshy filaments are apparent.

Shagreen and tubercles.—Except about the illicium, on the fossa of the gill pore, and on the lips, the external surfaces of the head and body are covered by a very fine prickly shagreen. This velvety surface extends rather uniformly out over most of the pelvic fin, and to a variable extent over the anal and dorsal. There is also a covering over most of the surface of each pectoral and caudal ray, where the rays are exposed when folded together.

The tubercles, unlike those of *O. porrectus,* have a very low central point, that is often hardly evident. The total height of each tubercle is very much less than the diameter. The tubercles are covered by spiny points like those on the intervening integument. Though somewhat smaller and very much flatter and less elevated and spinous, the tubercles follow essentially the same pattern as in *O. porrectus.* In advance of the eye, medially, there is a rather prominent and sharp tubercle at the very edge of the orbit, and, a little downward and forward, a poorly developed one. Along the upper and posterior edge of the orbit are two tubercles. In the occipital region four large bucklers form a rectangular pattern, with two in advance of the occiput and two just behind. Between these and the dorsal fin there are a number of bucklers, with a few quite large ones along the midline (these are somewhat paired transversely not far behind the occiput), and there is a strong pair at the front of the dorsal fin. The series is doubled along and immediately behind the dorsal fin, but tends to become single on top of the caudal peduncle. Strong tubercles, more or less biserial, arm the hard edge of the disk. Between these and the dorsal series a number of other tubercles are rather widely scattered. Smaller ones occur along the cheek and snout. A double row flanks the lateral line posteriorly, with a strong tendency toward the alignment of a pair opposite each pore. On the upper part of the tail region, a few others of variable size are scattered between the dorsal and the lateral-line series.

Gill structures and other internal characters.—The gill pores are oblique slits only about as long as the pupil. Dissection of a paratype discloses 2½ gills, as in other species of the genus. There is no gas-bladder, and no pyloric caeca. The vagus

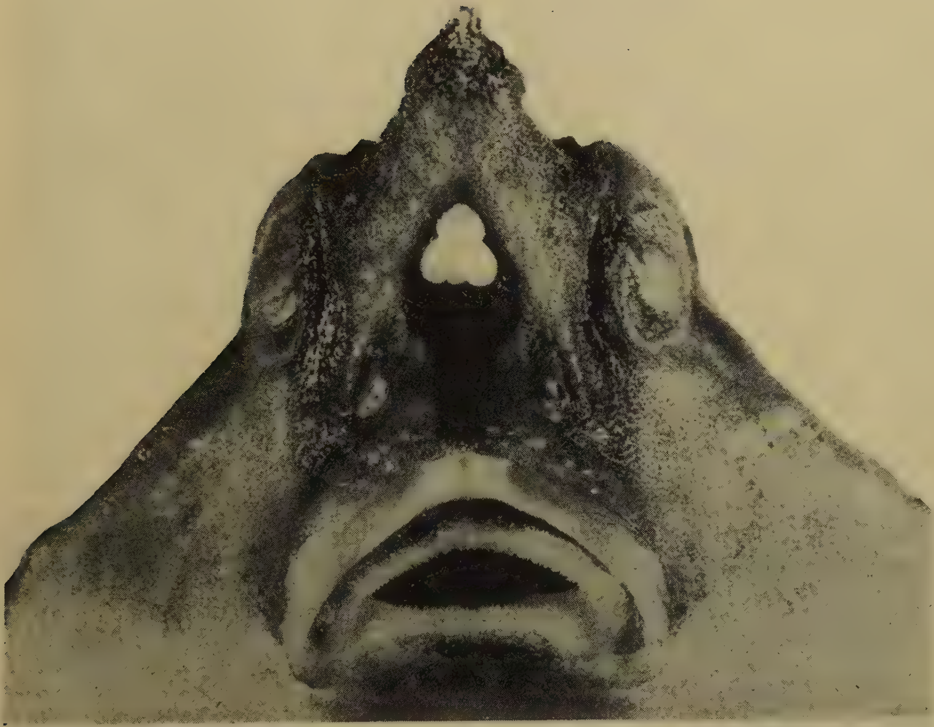

Plate V. Holotype of *Ogcocephalus darwini*. Anteroventral view, to show illicium and adjacent region. Photograph by Scripps Institution of Oceanography.

PLATE V

nerve extends perpendicular to the axis of the skull.

Other internal characters are shown by X-ray photographs (that of the holotype is reproduced as Plate IV, figure 2). The branchiostegal rays in each specimen number 4 + 2, all about equally robust. The upper-posterior 4 are very closely approximated basally, where inserted on the epihyal; the lower-anterior 2, on the ceratohyal, are well separated from the upper 4 and from one another. The postclavicle is very long and slender. The main otolith (the sagitta) is rather large and asymmetrically oval (Pl. IV, Fig. 2). The two other otoliths are minute.

The vertebrae number 19 in fourteen specimens and 20 in three (including the holotype). The first vertebra is nearly fused to the basioccipital, with sutures barely apparent, except, weakly, at the condyles, and is about three times as broad as long; its lines of ossification converge backward from the condyles. The second vertebra is about as long as it is broad on its anterior suture, which is much more prominent than those that follow in the trunk region and is definitely broader than its posterior suture. The next three vertebrae are definitely the longest, more than twice as long as broad. The next two or three become sharply and progressively reduced in length, and the sutures become stronger, to approach those of the much less rigidly conjoined posterior vertebrae. The next several vertebrae are nearly square. Those more posterior become about two-thirds as broad as long. The length remains nearly uniform. The hypural plate (included as usual in the vertebral count) is much elongated.

Fins.—The dorsal and anal fins are narrow lappets. The depressed length of the dorsal is about equal to the length of the snout and approximates two-thirds the length of the anal fin, which reaches approximately to the lower end of the caudal base. The dorsal originates about an eye length behind the anus, and the anal is inserted about halfway between the dorsal origin and the caudal base. Medially the margin of the caudal fin is rounded, and there is a slight tendency toward a rounded production of the upper and lower corners. The pectoral is broad and rounded. The almost cordlike pelvics, which originate about midway between the front of the mouth and the anus, extend outward from the flat ventral surface approximately to the edge of the expanded disk. Outward, the pelvics are broadened and obliquely truncated, with a pointed outer-posterior tip.

Coloration.—In preservative the colors are drab. The ground color is purplish gray above and whitish below, with some darkening about the chin. The one really conspicuous feature is the pair of stripes. These are not noticeably light-centered. The stripe of each side begins about the length of the cornea behind the orbit, and is rather broad, rounded, and somewhat intensified anteriorly. It continues backward along the lateral line, usually with some weakening and narrowing obliquely above the gill pore. There is some intensification along the lateral line back to about the front of the dorsal fin. In some specimens the band extends backward more or less behind the dorsal fin, either continuously or interruptedly. Behind the head there is a very slight darkening along the middorsal ridge anteriorly, with some broadening and intensification about the dorsal. Usually, especially in smaller specimens, the ground color becomes distinctly lighter just within the dark band on each side. The snout is considerably darkened, especially in larger specimens, and the front of the face back to below the lowest point of the orbit is definitely darkened. Usually there is also a dark blotch behind the posteriormost part of the eye. In the smaller specimens, another dark band, which is separated by a light bar from the other dark markings just described, extends from the eye to near the corner of the mouth. The smallest specimen also shows some radial markings on the eye.

The pectoral and caudal fins are considerably darkened outward, particularly on the sooty membranes. The dorsal fin is dusky, but the anal is pale, with some dark toward its tip. The pectorals are dark both below and above, but the pelvics are whitish. In the youngest specimen, the outer two-thirds of the dorsal and caudal are nearly jet black, as is the outer half of the anal, except on the front edge.

Life colors.—When received, several of the specimens varied from pink to deep red on the lower surface, and some showed red in the two dark dorsal stripes. The fresh colors were most vividly retained in specimen H 53–196, which on receipt was described as follows: upper parts, purplish gray; rather blue-gray on tubercles, and in an irregular blotch near middle of each side of disk; the two dark streaks, reddish brown; underparts, bright rose-red, becoming white or whitish on the lower (but not the upper) surface of the pelvics, on the outer tip of the anal, and, weakly, on the lower border of the caudal, also on the esca (but not the red stem) of the illicium; pectoral rays, pink-gray, encroached by the widening, blackish interradial streaks; the fin becoming almost solidly blackish inside the narrow red outer border.

Food.—Several of the X-ray photographs display food items, comprising, among the definitely recognizable animals, small mollusks, mostly snails, and small crabs.

Acknowledgments

As usual, I stand in debt to many. For the gift or loan of specimens of the new species, and for data regarding them, I am grateful to the fishermen mentioned in the list of specimens; and to Anita B. Daugherty, California Department of Fish and Game; Margaret H. Storey and Margaret G. Bradbury, Stanford University; Albert W. C. T. Herre, University of Washington; J. H. Applegate, California State Polytechnic College; W. E. Lundy, Panama Canal Natural History Society; and the Allan Hancock Foundation of the University of Southern California. Anita B. Daugherty, Margaret G. Bradbury, Albert W. C. T. Herre, and John Treadwell Nichols (of the American Museum of Natural History) have all relinquished to me the privilege of first describing the new species. William C. Schroeder of the Museum of Comparative Zoology made the types of *O. porrectus* available, arranged for photographs, and took some supplementary measurements. Leonard P. Schultz opened the collections of the United States National Museum. Nobuo Egami kindly took X-ray photographs of all available specimens. Margaret M. Irwin, when connected with the Santa Barbara Musum of Natural History, made available data on specimens of *Zalieutes elater* and provided a photograph (Pl. IV, Fig. 3).

Literature Cited

de Miranda Ribeiro, Alipio. 1915. Fauna Brasiliense—Peixes. V [Eleutherobranchios Aspidophoros] Physoclisti. *Arch. Mus. Nac. Rio de Janeiro, 17: 764 pp.* (separately numbered by taxonomically arranged families), pls. and figs. (unnumbered).

Fowler, Henry W. 1944. Results of the Fifth George Vanderbilt Expedition (1941) (Bahamas, Caribbean Sea, Panama, Galápagos Archipelago and Mexican Pacific islands). *Acad. Nat. Sci. Phila., Monogr. 6: 57–529, figs. 1–268.*

Garman, S. 1899. Reports of an exploration off the west coasts of Mexico, Central and South America, and off the Galapagos Islands, in charge of Alexander Agassiz, by the U. S. Fish Commission Steamer "Albatross," during 1891, Lieut. Commander Z. L. Tanner, commanding. XXVI. The fishes. *Mem. Mus. Comp. Zool. Harvard Coll., 24: 1–431, pls. 1–88, A–N.*

I[rwin], M[argaret] C. 1945. Batfish, *Santa Barbara Mus. Nat. Hist., Mus. Leaflet, 20: 39–45, 1 fig.*

Jordan, David Starr, and Barton Warren Evermann. 1898. Fishes of North and Middle America ... Part III. *Bull. U. S. Nat. Mus., 47 (3): i-xxiv,* 2183a-3136.

Kumada, Tosio (editor; text by Yosio Hiyama). 1937. Marine fishes of the Pacific Coast of Mexico. *Nissan Fisheries Inst. & Co., Odawara, Japan: 1–75, pls. 1–102.*

Longley, William H., and Samuel F. Hildebrand. 1940. *Carnegie Inst. Wash. Publ. 517: 223–285, figs. 1–28, pl. 1.*

——— ———. 1941. Systematic catalogue of the fishes of Tortugas, Florida with observations on color, habits, and local distribution. *Ibid., 535: i-xiii, 1–331, pls. 1–34.*

Lundy, William E. 1956. Galápagos produces the "Thing." *Natural History, 65: 468–9, 4 figs.*

Scripps Institution of Oceanography, University of California, La Jolla, California.

(826)

Black Swan in Kelp off Southern California.—About midday on May 24, Earle G. Cunnison and I flushed an adult Black Swan (*Chenopis atrata*) as we approached the kelp bed off Torrey Pines, San Diego, California. At the time we were in a small boat about 300 yards off shore. The swan rose about 75 yards ahead of us, flew westward, then circled southward, remaining over the sea at a height of less than 50 yards. Grinnell and Miller (Pac. Coast Avif. No. 27, 1944:559) reported that the Black

Swan is "sometimes seen out of captivity on lowland bodies of water in company of wild waterfowl." The bird we saw was alone.

In its native Australia the Black Swan is most abundant in fresh water, but at times it is common on salt water, particularly in lagoons and on tidal flats. It generally avoids open, rough water, moving as the wind changes to feed in the lee of a bank or point (Mathews, The Birds of Australia, 4, pt. 1, 1914–1915:12–22, pl. 200). The habitat where the bird reported here was observed therefore seems unusual. Inquiry at the San Diego Zoological Garden and from a local bird fancier who keeps Black Swans has failed to indicate that any birds of this species have been lost recently.—JAMES R. STEWART, *Scripps Institution of Oceanography, University of California, La Jolla, California, June 13, 1957.*

Contributions from the Scripps Institution of Oceanography, New Series, No. 1046

Reproduced by Permission

(829)

(830)

Thermocline Topography, Zooplankton Standing Crop, and Mechanisms of Fertilization in the Eastern Tropical Pacific

By

Wilhelm Brandhorst

Inter-American Tropical Tuna Commission, Scripps Institution of Oceanography*,
La Jolla, California

Introduction

A fishery will be successful only if a concentration of fish can be found in a restricted area. Nevertheless, it is very difficult to determine the factors which lead to such aggregation (cf. Fleming and Laevastu, 1956). In regions of higher latitude, the feeding habits, migration, and reproductive cycle of fish are closely connected with the seasonal changes of meteorological and hydrographical conditions. Though the latter are complex and variable in time and space, a number of investigators have found good correlations between commercial catches and such factors as temperature, nutrient content, and precipitation (see Dietrich and Kalle, 1957, pp. 230–33; Tait, 1952; Sverdrup, Johnson, and Fleming, 1955, p. 762). Frequently these factors govern the phytoplankton production which is responsible for a rich food supply in certain areas, causing fish aggregation. Sometimes, however, in inshore waters where strong gradients exist and observation points are closely spaced, it is possible to show a direct dependence of fish behaviour (e.g., spawning, migration) upon salinity and temperature (Brandhorst, 1955; 1956).

It has been shown in the central Pacific, that tunas occur most frequently in the upwelling region along the equator with relatively high plankton standing crop (Cromwell, 1953; King and Demond, 1953; Sette, 1955). The purpose of this study is to point out the centres of high zooplankton standing crop in the eastern tropical Pacific, some of which are good tuna fishing areas; and to suggest how these rich crops can be accounted for by hydrographic factors.

---

* Contribution from the Scripps Institution of Oceanography, New Series, No. 1047

Reproduced by Permission

Thermocline depth and zooplankton distribution

In most regions in low latitudes a strong thermocline is found throughout the year. One result of this stratification is that the replenishment of nutrients from below to the upper lighted zone is impeded. Only by processes which change the structure of, or reduce the depth of the thermocline can nutrients in offshore waters be made available for plant production. Nutrients may be brought to the surface by upwelling; in areas where this occurs the thermocline is weakened. Nutrients may also be introduced into the surface layer where a thermocline sometimes "outcrops", or is sufficiently near the surface to allow mixing of nutrient-rich water into the shallow surface layer. Conditions are also favourable if the compensation depth for phytoplankton photosynthesis is located below the top of the thermocline; then a photosynthetically productive zone may exist in water, richer in nutrients, in and below the thermocline.

Over large areas in the eastern tropical Pacific, the thermocline is found at relatively shallow depths (c. 20–50 m), and therefore nutrients are likely to be readily available for plant production. According to STEEMANN NIELSEN (1955) production in the tropical oceans is limited mainly by the nutrient supply. Variations in transparency of the water may also effect the available radiation and, hence, the depth of compensation and the production rate. In most regions, however, this factor seems to be less important than the available supply of nutrients. HENTSCHEL and WATTENBERG (1930) were able to correlate directly plankton and phosphate data from the South Atlantic Ocean. In the eastern tropical Pacific there are not enough phosphate data available to make such a study. However, if the supply of nutrients can be related to the thermocline depth, as outlined above, it should be profitable to examine the relationship between the thermocline topography and the distribution of plankton.

The thermocline topography is deduced from bathythermograph (BT) observations taken by naval ships and research vessels of different countries and institutions since 1944. From these data, filed on cards in the BT Section of the Scripps Institution of the University of California, the depth of the top of the thermocline was obtained. This is defined as the transition point on the temperature-depth trace that divides the water column into an upper mixed (almost isothermal) layer and a lower thermocline layer. In most cases this depth was easily determined, but sometimes its identification was difficult due to a weak temperature gradient or to the presence of two or three "small" thermoclines. Such examples were carefully examined, and a depth chosen which agreed with records from adjacent stations. If more than one observation per degree square was made on the same day, the values obtained were averaged. Final averages of thermocline depth were computed, in collaboration with Mr. CROMWELL, for each season for areas of one-degree squares.

Most of the available zooplankton data were obtained in the autumn season. Consequently the corresponding chart of thermocline depth (Fig. 1) is based only upon observations between October and December. The number of days in which one or more BT observations were taken within each degree square is also shown. Contour lines joining points with equal thermocline depths have been drawn at intervals of either 10 m (for depths of 0–50 m) or of 20 m (for greater depths). Areas for which there are insufficient data are indicated by broken contour lines.

The most direct comparison between organic production and nutrient supply

(833)

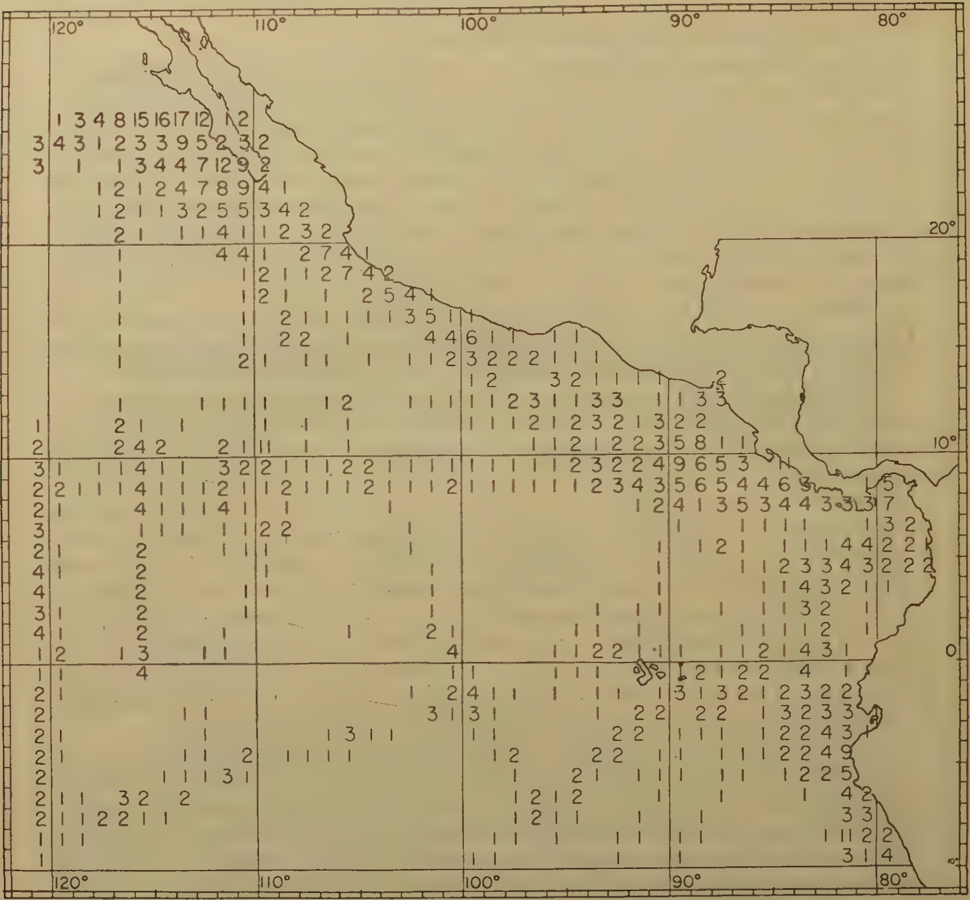

Figure 1 a.

Figure 1 a and b. Mean thermocline depth (m) over the eastern tropical Pacific from bathythermograph observations during October – December in the years 1944 to 1956. The number of observations per degree square is indicated in Figure 1 a.

(as related to thermocline depth) would require measurements *in situ* of photosynthetic production. Only a few such measurements have been made (HOLMES, SCHAEFER, and SHIMADA, 1957; KING, AUSTIN, and DOTY, 1957). In the eastern tropical Pacific, however, there exists a general correlation among production *in situ*, chlorophyll, and zooplankton standing crop as shown by HOLMES, *et al.* (1957, Figs. 12 and 14) and HOLMES (1958). Consequently the zooplankton volume was taken as the index of biological productivity; values were obtained from the routine observations of several expeditions using the oblique net tow. The hauls were made with a one-metre (mouth diameter) plankton net from approximately 300 metres depth up to the surface. Description of the method employed is given in HOLMES, *et al.* (1957, p. 132).

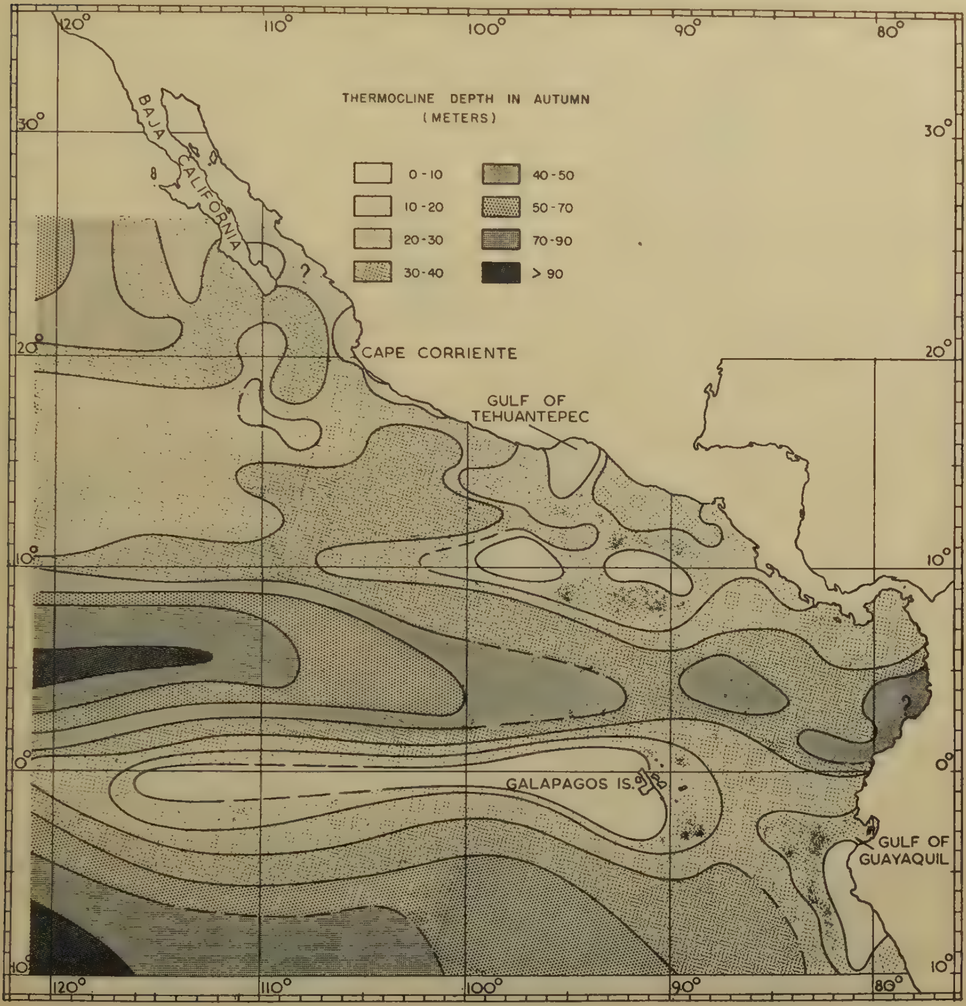
THERMOCLINE DEPTH IN AUTUMN
(METERS)
0 - 10
10 - 20
20 - 30
30 - 40
40 - 50
50 - 70
70 - 90
> 90
BAJA CALIFORNIA
CAPE CORRIENTE
GULF OF TEHUANTEPEC
GALAPAGOS IS.
GULF OF GUAYAQUIL
120°
110°
100°
90°
80°
30°
20°
10°
0°
10°

Figure 1 b.

Zooplankton and oceanographical data published in the following reports were used in this study: –

Wooster (1952a); Eastropic Data Report, Scripps Institution of Oceanography (1956); Holmes (1957); King, *et al.* (1957); Wooster and Cromwell, in press; and unpublished plankton data from MLR Cruise 5612, by courtesy of Dr. Elbert H. Ahlstrom, US Fish and Wildlife Service, La Jolla, California.

The zooplankton values (Fig. 2) are given in cubic centimetres of wet plankton (displacement volume) per 1000 cubic metres of water strained, excluding organisms larger than 5 cm³. The number of observations in each degree square

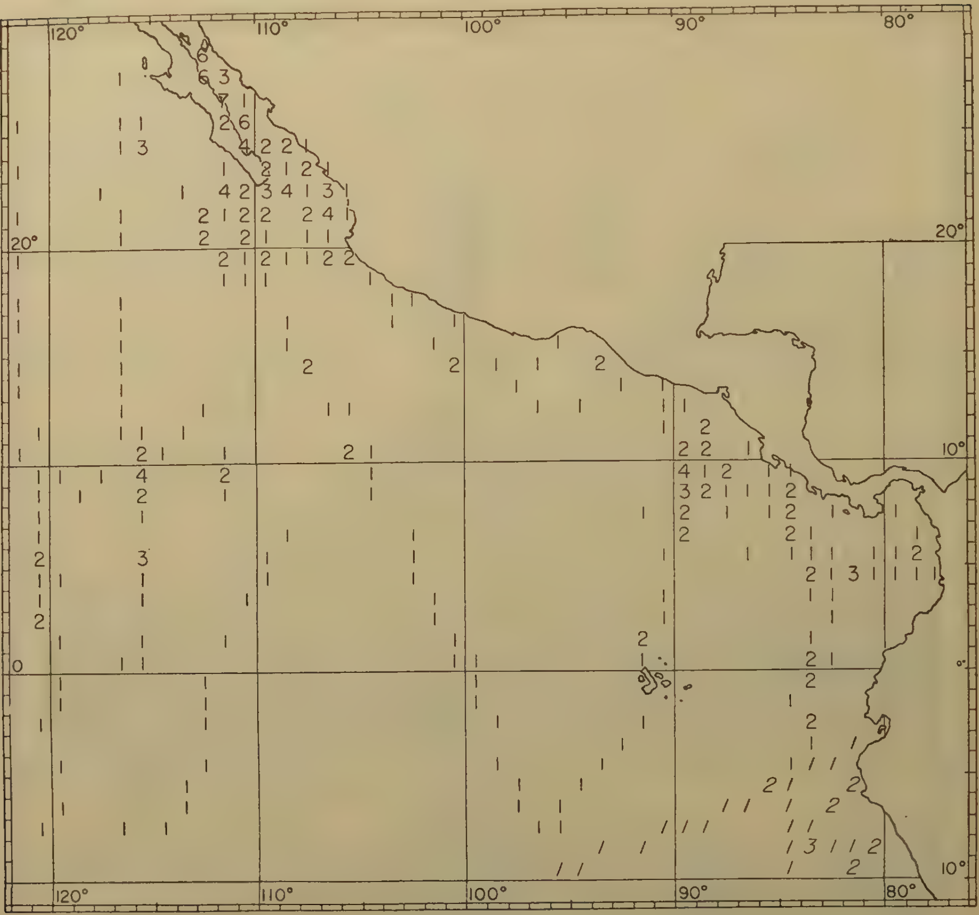

Figure 2 a.

Figure 2 a and b. Mean zooplankton standing crop in wet displacement volume per 1000 cubic m strained, minus the organisms larger than 5 cm³. From observations obtained on "Eastropic", "MLR 5612", and "Scope" Cruises, during October – December in the years 1955 and 1956. In Figure 2 a the number of net tows per degree square is indicated, with earlier summer values from "Shellback" Expedition (1952) given in italics.

is also indicated. Since no net tows have been taken in the area off Peru during autumn, some summer data for this area from the "Shellback" Expedition (WOOSTER, 1952a) are incorporated in the autumn chart (numbers in italics).

The main features of the zooplankton distribution correspond roughly with those of the thermocline topography in Figure 1. An area with a high standing crop of zooplankton is generally also a region with a shallow thermocline depth. Some examples follow: –

(a). In the upwelling zone along the equator between 115° W Long. and the Galapagos Islands, the zooplankton standing crop is between 100 and 200 cc/1000 m³.

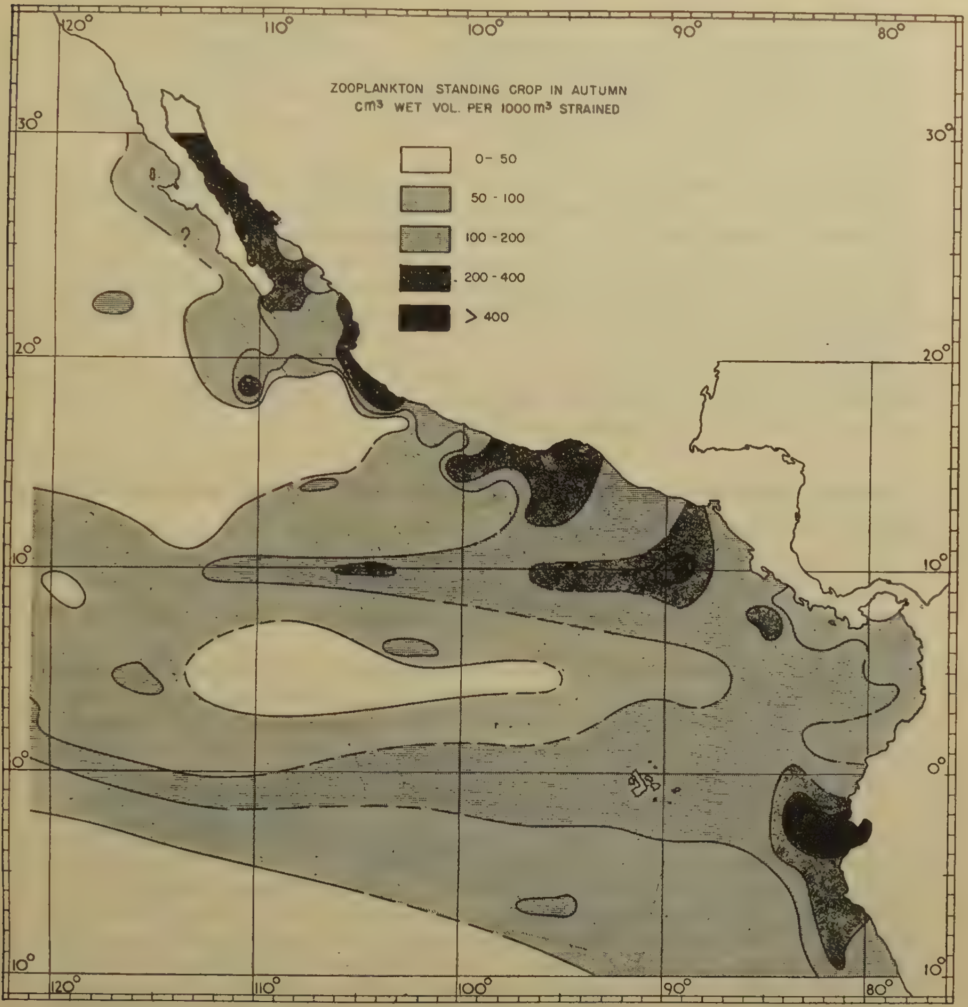
ZOOPLANKTON STANDING CROP IN AUTUMN
cm³ WET VOL. PER 1000 m³ STRAINED
0 - 50
50 - 100
100 - 200
200 - 400
> 400
120°
110°
100°
90°
80°
30°
20°
10°
0°
10°
?

Figure 2 b.

(b). The values for the Central American Ridge, along 10° N Lat., described by Wooster and Cromwell (in press), are as high as those along the equator. In its eastern part, however, they are higher, 200 to 400 cc/1000 m³, and in the region of the shallowest thermocline — the so-called "dome" — more than 400 cc/1000 m³ were sporadically measured.

(c). A very fertile region around the Gulf of Guayaquil, with over 500 cc/1000 m³, is characterized by a shallow thermocline depth of less than 10 m.

(d). The Gulf of Tehuantepec, a shoal area in the thermocline topography, is associated with a high standing crop of 200–400 cc/1000 m³.

(e). Extremely rich plankton catches with more than 500 cc/1000 m³ have been obtained in a small region around Cape Corriente at the Mexican coast, with a thermocline depth less than 10 m.

(f). Values with more than 400 cc/1000 m^3 were found in some inner parts of the Gulf of California. Few BT data were obtained here (see inset chart), and do not allow an interpretation.

(g). An isolated area with a zooplankton standing crop of more than 200 cc/1000 m^3 is located south of Baja California, at about 18°N, where the thermocline is somewhat less than 20 m.

Poor areas correspond in general with a deeper thermocline depth. At the deep trough in thermocline topography along 5°N Lat., associated with the Equatorial Counter Current, low zooplankton values (about 50–100 cc/1000 m^3 or less) were measured. South of the equator there is a region with a standing crop of less than 50 cc/1000 m^3 while the thermocline depth is more than 70 m. On the contrary, a barren offshore area between 12°N and 19°N coincides with a rather shallow thermocline.

Since there are vast areas without biological data, the zooplankton distribution given in Figure 2 cannot be regarded as final. Further collections will be necessary to confirm the apparent relationship.

Fertilizing mechanisms and special hydrographic features associated with high zooplankton standing crop

In addition to indicating the uppermost depth at which nutrients are readily available, the thermocline depth is also related to the prevailing current system, since the mass distribution is rather closely represented by the temperature field.

The moderately high standing crop along the equator is sustained by upwelling. Although this process is well explained for the central part of the Pacific by CROMWELL (1953), it might be useful to illustrate and describe the somewhat different situation in the eastern part by a cross section obtained on the "Eastropic" Expedition (Fig. 3).

In the central Pacific the cool surface water in the upwelling region is imbedded in warm water to the north and south, while the thermocline is situated at about 150–200 m. In the eastern Pacific the South Equatorial Current, which is an offshore extension of the Peru Current, carries cool and phosphate-rich water, and obscures a corresponding strong transition of properties south of the equator. Here the thermocline lies in about 30 m and from this depth the isopleths of thermosteric anomaly [δ_T] (MONTGOMERY and WOOSTER, 1954) from 340 to 500 cl/ton rise sharply, intersecting the surface between the equator and one degree south. One evidence of upwelling, the upsloping of isopleths, is more pronounced in the represented section than in those of CROMWELL (1953, 1954) and AUSTIN (1954) from the central part of the ocean. The phosphate content of the surface in the vicinity of the equator, however, is in both areas similar, ranging from 0·7–1·2 μg-at/l of PO_4-P and indicating favourable conditions for phytoplankton.

The series of sections shown in Figure 3 further demonstrates the conformity between the average condition in the autumn, obtained from several years of BT observations (Fig. 1), and a condition found during two weeks in the autumn of 1955. The thermocline trough at 5°N and the Central American Ridge at 10°N are well pronounced. At the latter, the thermocline might lie above the compensation depth, enabling plant life to exist in the thermocline layer (HOLMES, *et al.*, 1957, Fig. 5.)

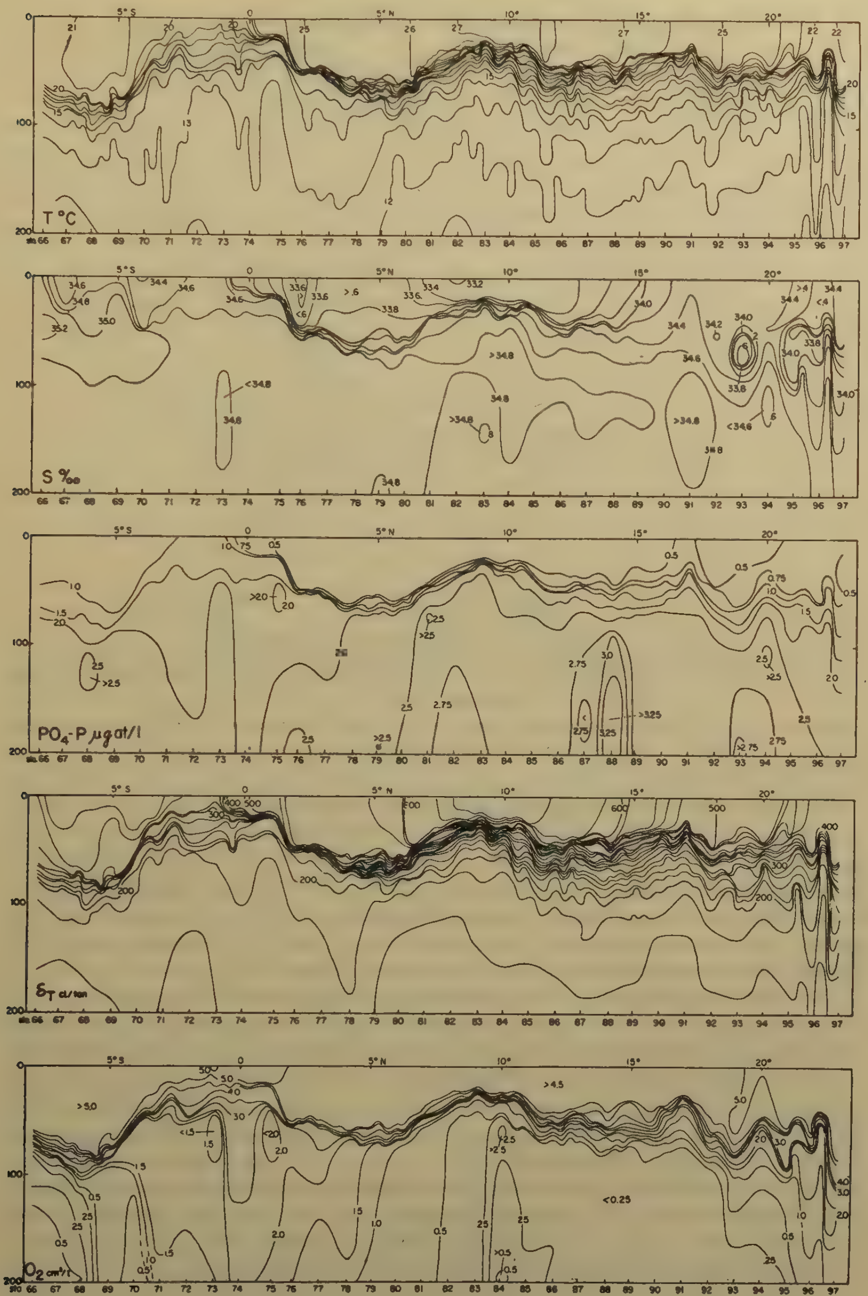

Figure 3. Cross sections showing the distribution of temperature, salinity, inorganic phosphate, thermosteric anomaly, and oxygen during the period 1.–15. December 1955 on "Eastropic" Expedition. Station positions are given in Figure 11.

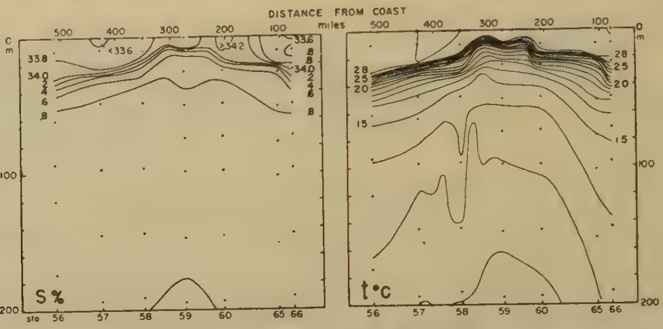

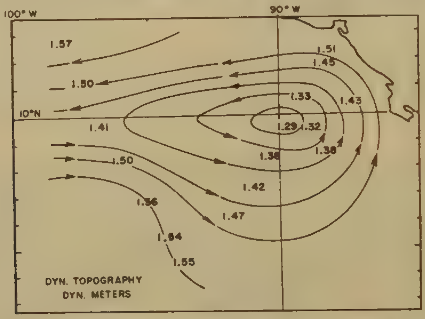

Figure 4a (upper). Cross sections showing the distribution of salinity and temperature during the period 24. May – 4. June 1952 on "Shuttle" Expedition (after WOOSTER and CROMWELL, in press).

Figure 4b (lower). Dynamic topography in dynamic metres over 1000 m during the "Shuttle" Expedition. Station positions are given in Figure 11.

Of further interest is the high surface phosphate at about 17°N (station 91), corresponding with an upsloping of δ_T and salinity isopleths. This feature might be associated with a transition further west (at 124° W) described by WOOSTER and CROMWELL (in press). Net tows carried out on "Eastropic" at this particular station did not yield a high volume of plankton. On other cruises, however, greater catches were obtained in the region at about 17° N, where a shallow thermocline is indicated in the average autumn chart (Fig. 1.)

The "dome", a region of very shallow thermocline off the west coast of Costa Rica was described by WOOSTER and CROMWELL (in press) as associated with the north edge of the Equatorial Counter Current and a northward flowing coastal current inshore. Their "Shellback" and "Shuttle" sections show the thermocline at a depth of about 10 m or less in approximately 9° N Lat. and 89°W Long. In a "Shuttle" section, here reproduced in Figure 4a, salinity values characteristic of the thermocline layer can be found at the surface in the vicinity of this particular feature (station 60). High phosphate concentrations were always encountered here at the surface. The explanation, however, that stirring by wind causes this surface enrichment does not seem to be very satisfactory since the doldrums are centered around this region.

Average charts of surface temperature by SCHOTT (1935, Tables 20–23) indicate cooler water during winter where his current charts (Tables 29 and 30) show a sharp change in the direction of the Counter Current from east

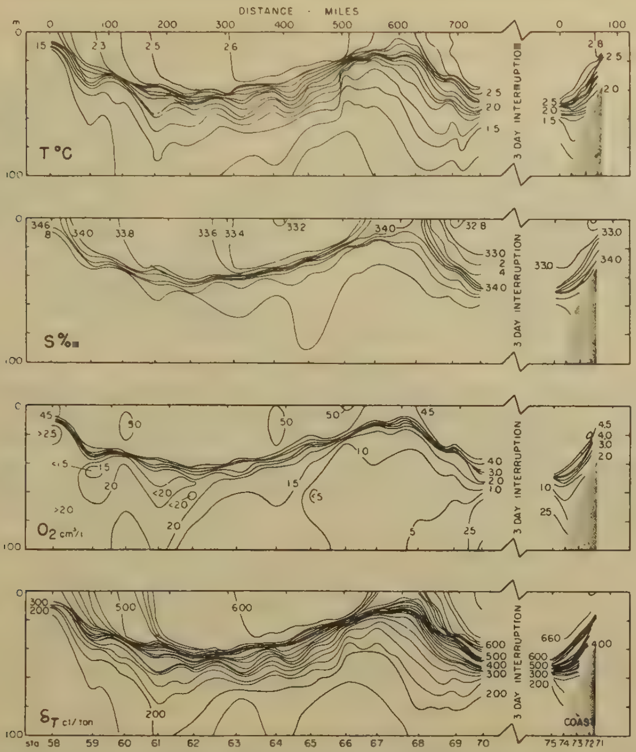

Figure 5. Cross section showing the distribution of temperature, salinity, oxygen, and thermosteric anomaly taken between 28. November and 5. December 1955 on "Eastropic" Expedition. Station positions are given in Figure 11.

toward the north-west, forming partly the westbound North Equatorial Current and partly the northward-flowing coastal current. This suggests an explanation in connexion with the current system.

Changes in the dynamics of this system, e. g., variations in the current velocity of the westbound North Equatorial Current, the eastbound Counter Current or the northbound coastal current require a corresponding alteration of the mass distribution. As the "shear" increases, the slope of the thermocline will also increase with a possible effect of raising the thermocline up to the surface. Such an intersection of the thermocline with the surface, which brings up cool, nutrient-rich water of high salinities, was encountered during the "Eastropic" Expedition.

It can be seen clearly from the sections presented in Figure 5 that the surface layer is very thin and shows properties different from those of the surface layer in adjacent areas. Nutrients become available for plant growth (Fig. 6b), resulting in high zooplankton standing crops of more than 200 (sometimes over 400) cc/1000 m³ (Fig. 2). For demonstration of the flow pattern centered around the "dome", the dynamic topography over 1000 m was computed and drawn both for early summer (May, 1952) and late autumn (Nov.-Dec., 1955) using

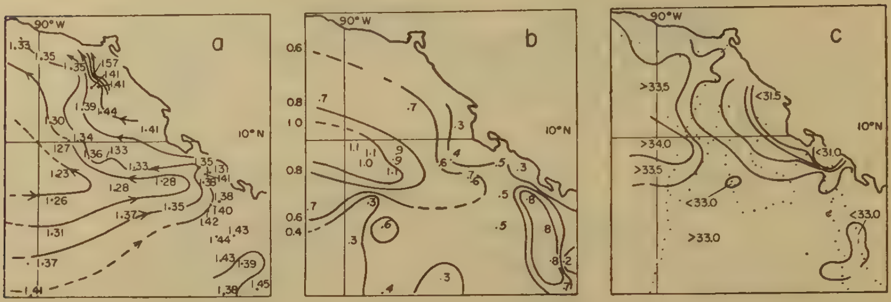
a
b
c
90° W
10° N
1.33
1.35
1.57
1.41
1.39
1.44
1.30
1.34
1.27
1.36
1.33
1.23
1.28
1.26
1.35
1.37
1.31
1.38
1.40
1.42
1.43
1.45
1.41
0.6
0.8
1.0
0.4
.7
1.1
.9
.3
.6
.5
.8
.2
>33.5
<31.5
>34.0
<31.0
<33.0
>33.0

Figure 6. Charts of: –

(a) Dynamic topography in dynamic metres over 1000 m. Stations occupied from 3. November – 7. December 1955 on "Eastropic" Expedition at "dome".
(b) Surface phosphate concentrations, measured in autumn and summer during 1953 to 1956; summer values are in italics.
(c) Surface salinities taken between 3. November – 7. December 1955 on "Eastropic" Expedition.

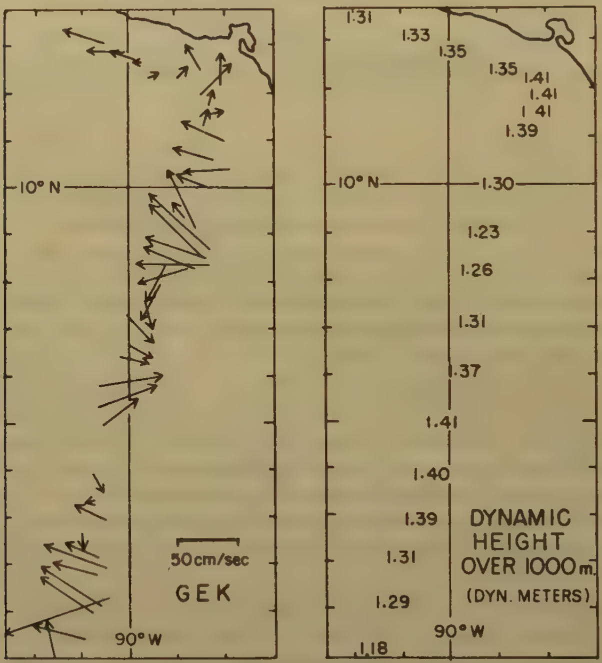
10° N
50 cm/sec
GEK
90° W
1.31
1.33
1.35
1.35
1.41
1.41
1.41
1.39
10° N
1.30
1.23
1.26
1.31
1.37
1.41
1.40
1.39
1.31
1.29
1.18
DYNAMIC HEIGHT OVER 1000 m.
(DYN. METERS)
90° W

Figure 7. GEK measurements and dynamic height over the Central American Dome. Stations occupied between 28. November and 5. December 1955 on "Eastropic" Expedition (see Figure 11).

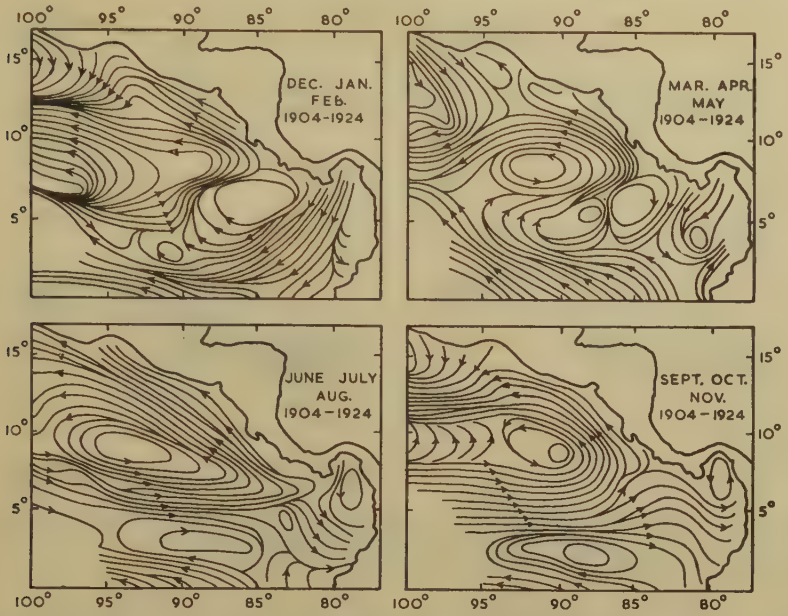

Figure 8. Seasonal variations in the surface currents in the Central American region (after FLEMING, 1940).

data obtained on the "Shuttle" (Fig. 4b) and "Eastropic" Expeditions (Fig. 6a). Both charts show the "dome" present at almost the same location, and Figure 6a reveals that the "dome" can spread out toward the coast of Costa Rica. Unfortunately we have no "Eastropic" data from near this location further west than 90° W, and it is not possible to locate the exact centre. Geomagnetic electrokinetograph (GEK) observations made simultaneously on this profile and the computed dynamic heights do not agree completely as to the position of the "dome" centre (Fig. 7).

A good picture of the seasonal variations of the positions of the "dome" is given by CROMWELL (in press) in his seasonal charts of thermocline topography, and implied by FLEMING (1940) in his streamline charts of the surface current, based on the US Hydrographic Office Pilot Charts (Fig. 8). The δ_T section (Fig. 5) also indicates a south-east-flowing current close inshore along the Costa Rican coast, occupying a shallow depth of less than 100 m. Dynamic heights for these inshore stations were not computed for Figure 6a.

The above mentioned temperature charts of SCHOTT (1935) suggest that "outcropping" might be accentuated during winter in this area, which has an average surface temperature of 2° C less than the surroundings at that season. It is also true that the sections during December (Fig. 5) show "outcropping", those of May (Fig. 4a) merely a higher salinity value at the surface, the temperature difference having been eliminated, probably by solar heating. Two summer sections (WOOSTER and CROMWELL, profiles XIa-d, XVa-h, in press) show only an elevated thermocline. At all three times, however, with or without

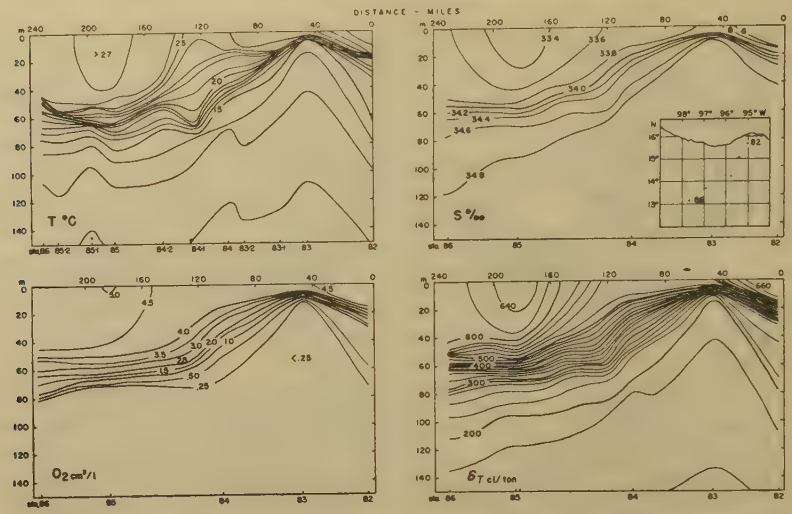

Figure 9. Cross section showing temperature, salinity, oxygen, and thermosteric anomaly in the Gulf of Tehuantepec during the period 9. December to 10. December 1955 on "Eastropic" Expedition. (See Figure 11 for station positions).

"outcropping", high nutrient content at the surface was found, suggesting the possibility of other mechanisms involved in the enrichment process which supports the high production in this area. A study of this phenomenon is being published by CROMWELL (in press).

CROMWELL (1956) suggested that the high standing crop in the Gulf of Tehuantepec is a result of strong mixing by the northerly winds (US Weather Bureau, 1938). These winds are produced by anticyclones to the northward, which blow through the low and narrow Tehuantepec Pass, and sometimes reach gale force in winter. They might cause strong mixing, associated with upwelling.

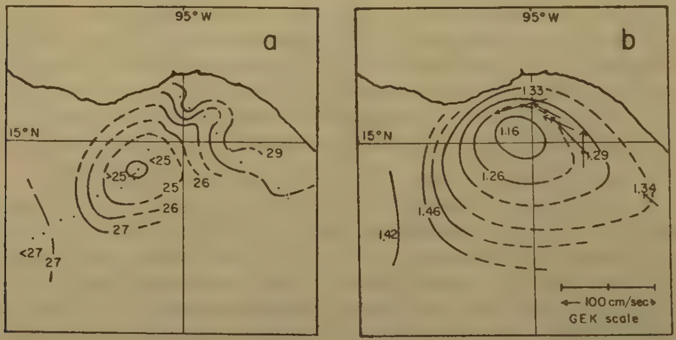

Figure 10. Charts of: – (a) Surface temperature.
(b) Dynamic topography in dynamic metres over 1000 m with few incorporated geomagnetic electrokinetograph measurements. Values obtained during the period 8. December – 11. December 1955 in the Gulf of Tehuantepec on "Eastropic" Expedition.

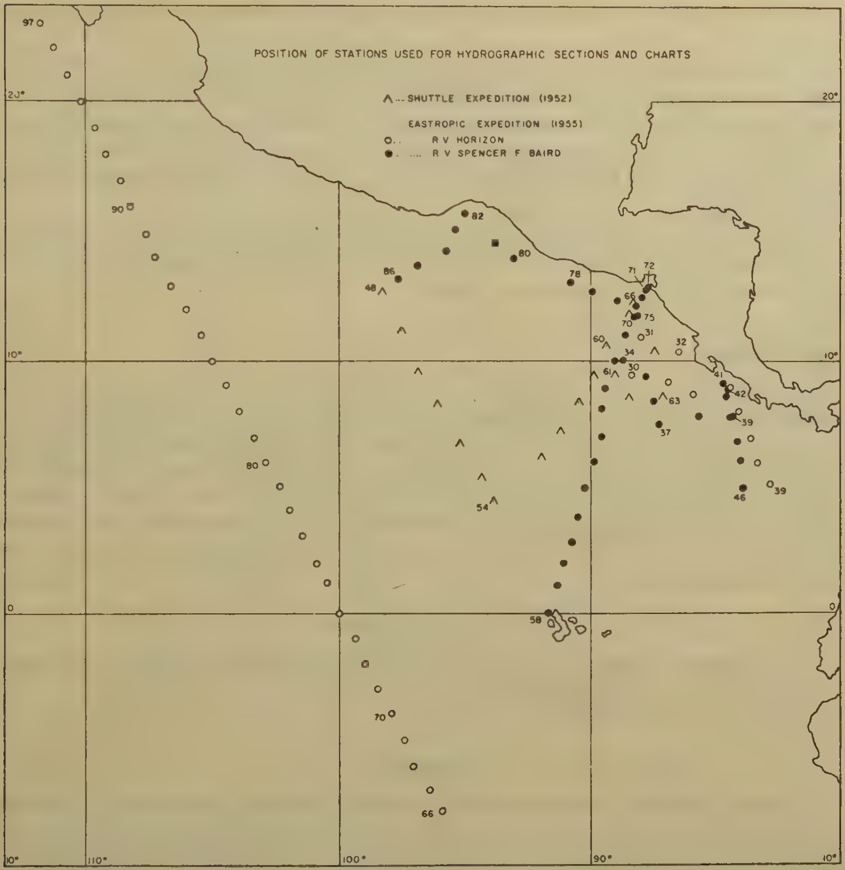
POSITION OF STATIONS USED FOR HYDROGRAPHIC SECTIONS AND CHARTS
Λ -- SHUTTLE EXPEDITION (1952)
EASTROPIC EXPEDITION (1955)
○ .. R V HORIZON
● . .... R V SPENCER F BAIRD
20°
10°
0
10°
110°
100°
90°
97
90
80
70
66
82
80
86
48
78
71
72
66
75
70
31
60
34
32
30
61
41
42
63
39
37
46
39
54
58

Figure 11. Position of stations used for hydrographic sections and charts.

On the "Eastropic" Expedition a profile through the gulf was completed during strong winds with speeds up to 40 knots. Hydrographic features were found which were very similar to those of the Central American Dome. According to the cross sections presented here (Fig. 9), the centre is located about 70 miles from the coast (station 83). In all sections, here, most isopleths rise very sharply to a depth of 10 m or intersect the surface. Some 150 miles south-west of the centre and 20 miles north-eastward, high oxygen concentrations and temperatures, and lower salinities are found at the surface. The BT station No. 84–1 shows an indication of mixing. Figures 10a and 10b illustrate the surface temperature and the dynamic topography. They incorporate a few GEK measurements which were obtained at the beginning of the storm. From the figures it can be deduced that this "dome" is associated with strong current, circling counter-clockwise in the gulf. It is remarkable that the cool surface water does not coincide with the centre of the dome. This might be due to the strong wind with the possible effect of shifting the cool water southward, but a similar feature is also found over the Central American Dome without stronger winds. SCHOTT's charts (1935, Plates 20 and 24) and the Hydrographic Office

Publications Nos. 570 and 577 also indicate cooler water in this region during the winter.

The fertile region around the Gulf of Guayaquil, by the coasts of north Peru and Ecuador, corresponds to an area with a strong transition between warm equatorial water and the cool upwelling water of the Peru Current. This area is described by several investigators, including SCHOTT (1931); GUNTHER (1936); SCHWEIGGER (1943, 1949); WOOSTER (1952a, 1952b); and WOOSTER and CROMWELL (in press).

The productive regions along the Mexican coast around Cape Corriente, and the inner parts of the Gulf of California, cannot be explained since no BT data are available for the season involved.

Tuna abundance

The results of catch statistics (SHIMADA, 1958; GRIFFITHS, unpublished manuscript) indicate the geographical distribution of the yellowfin tuna abundance, measured both by total landings and by catch-per-standardized-day's fishing. Some of the main areas of high zooplankton standing crop appear as regions of good fishing (e.g., the Central American and Tehuantepec "domes", Gulf of Guyaquil, Galapagos Islands), at least during part of the year. There are too few data to link seasonal fluctuation of zooplankton with those of tuna abundance.

Acknowledgment

I am indebted to Drs. J. F. TALLING, M. B. SCHAEFER, and Mr. Townsend CROMWELL for helpful criticisms of the manuscript.

Summary

1. One of the most important factors influencing aggregation of pelagic fish in tropical waters is the food supply, based ultimately on the production of phytoplankton. Since there is a strong thermocline throughout the year and no seasonal turnover of the water column in large areas of the tropics, the availability of nutrients to the plants is dependent largely upon the depth of the thermocline.

2. A chart of the thermocline topography during the autumn, based on bathythermograph observations, is compared with a chart showing zooplankton distribution. There is an inverse relationship between the depth of the thermocline and the size of the standing crop of zooplankton, which also appears to be related, at least in some regions, to the abundance of tuna.

3. Additional fertilizing mechanisms in certain areas of high standing crop are described by means of cross sections and charts which show dynamic topography and the surface distribution of temperature, salinity, and phosphate.

References

AUSTIN, T., 1954. "Mid-Pacific oceanography III, transequatorial waters". US Fish & Wildl. Serv., Spec. sci. Rep.-Fish., 131.

BRANDHORST, W., 1955. "Hydrographie des Nord-Ostsee-Kanals". Kieler Meeresf., **11**: 174–87.

BRANDHORST, W., 1956. "Über Laichen und Aufwuchs des Frühjahrsherings im Nord-Ostsee-Kanal". Kieler Meeresf., **12**: 186–99.

CROMWELL, T., 1953. "Circulation in a meridional plane in the central equatorial Pacific". J. Mar. Res., **12**: 196–213.

CROMWELL, T., 1954. "Mid-Pacific oceanography II, transequatorial waters". US Fish & Wildl. Serv., Spec. sci. Rep.-Fish., 131.

CROMWELL, T., 1956. "Eastropic Expedition". Pacific Fisherm., **54** (8): 25–29.

CROMWELL, T., (in press). "Thermocline topography, horizontal currents and – ridging – in the eastern tropical Pacific". (Pap. Ninth Pacif. Sci. Congr. Bangkok, 1957).

DIETRICH, G. & KALLE, K., 1957. "Allgemeine Meereskunde". 492 pp. Gebrüder Borntraeger, Berlin-Nikolassee.

EASTROPIC Expedition, (unpubl.) "Data collected by Scripps Institution vessels on Eastropic Expedition (Sept.-Dec. 1955)". Univ. Calif., Scripps Inst. Oceanogr., Ref. 56–28, 156 pp.

FLEMING, R. H., 1940. "A contribution to the oceanography of the central American region". Proc. Sixth Pacif. Sci. Congr. California, **3**: 167–75.

FLEMING, R. H., & LAEVASTU, T., 1956. "The influence of hydrographic conditions on the behavior of fish". FAO Fish. Bull., **9**: 181–96.

GRIFFITHS, R. C., (unpubl. MS.)

GUNTHER, E. R., 1936. "A report on oceanographical investigations in the Peru coastal current". Discovery Rep., **13**: 107–276.

HARVEY, H. W., 1955. "The chemistry and fertility of sea waters". 221 pp. Cambridge Univ. Press.

HENTSCHEL, E., & WATTENBERG, H., 1930. "Plankton und Phosphat in der Oberflächenschicht des südatlantischen Ozeans". Ann. Hydrogr. Berl., **58**: 273–77.

HOLMES, R. W., 1958. "Surface chlorophyll 'A', surface primary production, and zooplankton volumes in the eastern Pacific Ocean". Rapp. Cons. int. Explor. Mer, **144**: 109–16.

HOLMES, R. W., SCHAEFER, M. B., & SHIMADA, B. M., 1957. "Primary production, chlorophyll A and zooplankton volumes in the eastern tropical Pacific Ocean". Bull. int. Amer. Trop. Tuna Comm., **2**: 129–69.

HOLMES, R. W., ed., (unpubl.) "Physical, chemical and biological observations in the eastern tropical Pacific, Nov.-Dec. 1956". Rep. Scripps Inst. Oceanogr.

KING, J. E., & DEMOND, J., 1953. "Zooplankton abundance in the Central Pacific". US Fish & Wildl. Serv., Fish. Bull., **54**: 111–44.

KING, J. E., AUSTIN, T., & DOTY, M. S., 1957. "Preliminary report on expedition EASTROPIC". US Fish & Wildl. Serv., Spec. sci. Rep.-Fish., 201.

MONTGOMERY, R. B., & WOOSTER, W. S., 1954. "Thermosteric anomaly and the analyses of serial oceanographic data". Deep-Sea Res., **2**: 63–70.

SCHOTT, G., 1931. "Der Perustrom und seine nördlichen Nachbargebiete in normaler und anormaler Ausbildung". Ann. Hydrogr. Berl., **59**: 161–69 and 200–13.

SCHOTT, G., 1935. "Geographie des Indischen und Stillen Ozeans". 413 pp. Verlag C. Boysen, Hamburg.

SCHWEIGGER, E., 1943. "Pesquería y Oceanografía del Perú". 356 pp. Compañía Administr. del Guano, Lima.

SCHWEIGGER, E., 1949. "Der Perustrom nach zwölfjährigen Beobachtungen". Z. Erdk., **3**.

SETTE, O. E., 1955. "Consideration of mid-ocean fish production as related to oceanic circulatory systems". J. Mar. Res., **14**: 398–414.

SHIMADA, B. M., 1958. "Geographical distribution of the annual catches of yellowfin and skipjack tuna from the eastern tropical Pacific Ocean from vessel logbook records, 1952–1955". Bull. int. Amer. Trop. Tuna Comm., **2**: 289–363.

STEEMANN NIELSEN, E., 1955. "Production of organic matter in the oceans". J. Mar. Res., **14**: 374–86.

SVERDRUP, H. U., JOHNSON, M. W., & FLEMING, R. H., 1955. "The Oceans, their Physics, Chemistry and General Biology". 1060 pp., Prentice-Hall, New York.

TAIT, J. B., 1952. "Hydrography in relation to fisheries". 106 pp. Edward Arnold, London.

US Navy Electronics Laboratory. "'Shuttle' Expedition 1952." Manuscript data file Scripps Instn. Oceanogr. To be published in Oceanic Observ. Pacif., Univ. Calif. Press.

US Navy Hydrographic Office, 1947. "Atlas of Surface Current, Northern Pacific Ocean". Publ. No. 570, US Navy, Washington.

US Navy Hydrographic Office, 1950. "Atlas of Pilot Charts, Pacific and Indian Ocean". Publ. No. 577, US Navy, Washington.

US Weather Bureau, 1938. "Atlas of Climatic Charts of the Ocean". Publ. No. 1247, US Dept. Agric., Washington.

WOOSTER, W. S., 1952a. "'Shellback' Expedition, 17 May to 27 August 1952". Scripps Inst. Oceanogr., unpubl. Rep., Ref. 52–63.

WOOSTER, W. S., 1952b. "Exploración Oceanográfica del Pacífico Ecuatorial-Oriental". Bull. Soc. Geogr. Lima, **6**: 79–82.

WOOSTER, W. S., & CROMWELL, T., (in press). "An oceanographic description of the eastern tropical Pacific". Bull. Scripps Inst. Oceanogr.

(848)

PROCEEDINGS
OF THE
CALIFORNIA ACADEMY OF SCIENCES
FOURTH SERIES
Vol. XXIX, No. 8, pp. 273–313, 1 map, 3 plates July 10, 1958

A NEW FISH, *CHAETODON FALCIFER*, FROM GUADALUPE ISLAND, BAJA CALIFORNIA, WITH NOTES ON RELATED SPECIES[1]

BY

CARL L. HUBBS and ANDREAS B. RECHNITZER
Scripps Institution of Oceanography

CONTENTS

Page
Introduction 274
A New Species from Guadalupe Island 275
  Chaetodon falcifer, Hubbs and Rechnitzer, new species 275
    Type Specimen 275
    Collecting Notes and Habitat Data 275
    Distribution 278
    Distinctions 279
    Relationships 282
    Diagnosis 285
    Description of Fins 285
    Scales and Lateral Line 286
    Body and Head Characters 288
    Osteological Features 289
    Coloration 291
    Measurements 294
    Derivation of Name 294

---

[1] Contributions from the Scripps Institution of Oceanography, New Series. No. 1048

Reproduced by Permission

(849)

CONTENTS—Cont.

Distinctive Characters and Relationships of the Three Other Eastern Pacific Chaetodontines .... Page 295
Chaetodon humeralis Günther 295
Heniochus nigrirostris (Gill) 296
Forcipiger longirostris (Broussonet) 299
Taxonomic Notes on Atlantic Relatives of *Chaetodon falcifer* 300
Chaetodon aya Jordan 300
Chaetodon marcellae Poll 304
Prognathodes aculeatus (Poey) 304
Systematic and Zoogeographical Conclusions 307
Literature Cited 309

INTRODUCTION

Isla Guadalupe, an oceanic island rising from deep water off Baja California, about 225 nautical miles south and slightly west of San Diego, and separated by 133 miles from the nearest other land (Isla San Gerónimo), is proving to be characterized by a high incidence of endemism in its littoral marine as well as in its terrestrial biota. The marine endemics include a considerable number of littoral fishes. A few of these, including two gobiesocids discovered by the senior author and recently described by Briggs (1955: 79–80 and 100–101, figs. 5, 95, and 100), have been proposed as full species. Others remain to be named, either as species or subspecies (the problem is currently under study by the senior author and Eric Godwin Silas). Of the apparently endemic species perhaps the most strikingly distinctive is the butterflyfish described in this paper.

Except as noted, the systematic methods, especially of counting and measuring, are those proposed by Hubbs and Lagler (1952). Angles were measured as proposed by Hubbs (1946).

We are indebted to a number of colleagues for assistance in the examination of material, for data, and for suggestions in the presentation. In particular, we acknowledge such help from Leonard P. Schultz of the United States National Museum, who verified our conclusions regarding the value of the lateral-line character and the placement of the species *nigrirostris,* who made material in the National Museum freely available, and who had two photographs prepared. We are similarly grateful to Loren P. Woods of the Chicago Natural History Museum, who, like Schultz, provided much information on the lateral-line characteristics of many species and offered valued suggestions regarding the taxonomy of the group, which he has extensively studied. Woods also loaned us specimens of *Chaetodon aya.* We express appreciation also to Boyd W. Walker, our colleague at the Uni-

(850)

versity of California at Los Angeles, who has made available extensive material of the previously known eastern Pacific chaetodontines and has otherwise been of help and encouragement in the preparation of the paper. Robert L. Wisner made the X-ray photograph reproduced as plate I, figure 2. Max Poll of the Koninklijk Museum van Belgisch-Kongo has allowed the reproduction of the type figure of *Chaetodon marcellae.* W. I. Follett and Lillian Dempster of the California Academy of Sciences have assisted generously in the processing of the manuscript.

A NEW SPECIES FROM GUADALUPE ISLAND

Chaetodon falcifer Hubbs and Rechnitzer, new species.
(Plate I.)

Type Specimen

A large adult, 138 mm. in standard length, collected at a depth of 100 feet on the east shore of Guadalupe Island, off Baja California, México, on November 16, 1954; Cat. No. 20734, Department of Fishes, California Academy of Sciences.

Collecting Notes and Habitat Data

The only known specimen of this species (pl. I, fig. 1) was speared by Rechnitzer during a deep-poisoning operation on November 16, 1954, supplemented with detonation of Primacord on November 17, in a cove on the generally calm eastern shore of the volcanic island, about 0.5 mile north of Morro Sur (South Bluff), at 28° 53′ 24″ N. Lat., 118° 15′ 00″ W. Long. (as measured on Hydrographic Office Chart 1688 (1956); on the older chart, 1681, the island was misplaced 1.5 mile to westward and 0.6 mile to southward). Rechnitzer swam down with aqualung equipment to try to collect a bright orange-yellow fish (a pomacentrid?) that he had seen while applying the derris-root paste at a depth of about 20 feet. Failing to relocate that specimen in the clouded water, he went lower, to the rocky bottom at a depth of about 100 feet, where, about a foot off the bottom, under a slight ledge at the base of the vertical underwater cliff, he saw, in the extremely clear water, and speared, the magnificent butterflyfish we are describing.

Where the fish was obtained, plants, other than encrusting coralline algae, were few and scattered. In shallower water there was much attached *Sargassum* and other algae and some eelgrass *(Zostera).* The temperature was recorded by one of the divers as 65° F. from top to bottom. In addition to rock there was some sand and gravel on the level bottom, which was about 100 feet deep. The vertical rock wall was penetrated by deep recesses and vertical crevices, which provided excellent cover for reef fishes.

Bearing in mind the favorable habitats at this station and the large

(851)

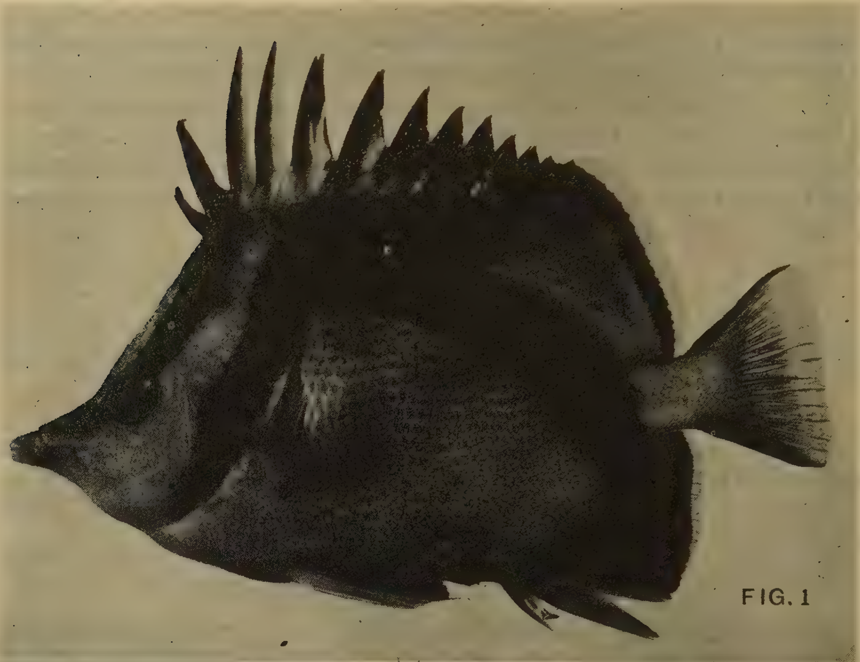

FIG. 1

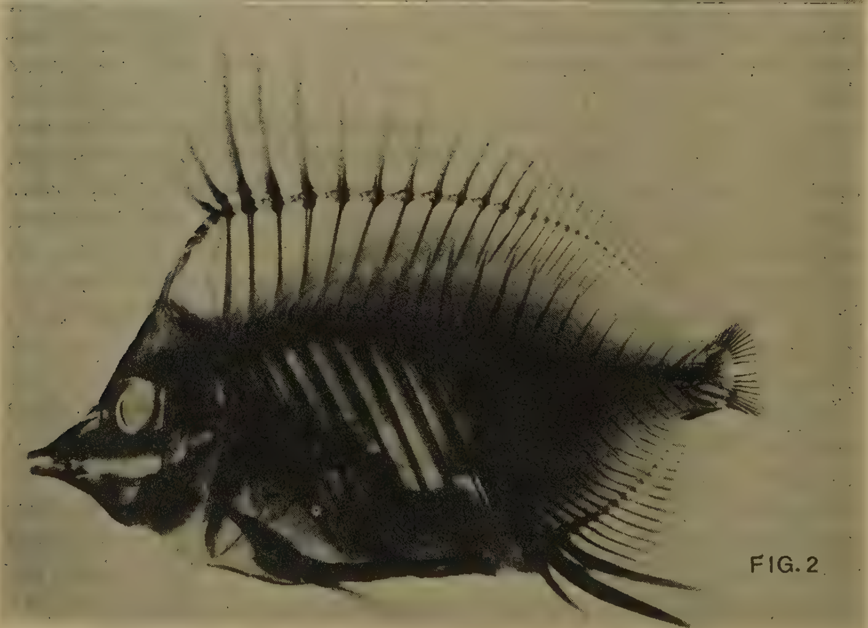

FIG. 2

party of collectors (thirteen, including six with aqualungs), it is not surprising that a considerable proportion of the depauperate littoral fish fauna of Guadalupe was taken with the *Chaetodon*. The thirty-three species listed below were included in the collection and are therefore to be listed as approximate associates of the butterflyfish. Species only observed are marked with an asterisk. Endemics are marked with a dagger.

- Sternoptychidae
  - *Vinciguerria lucetiae* Garman
- Exocoetidae
  - **Cypselurus californicus* (Cooper)
- Apogonidae
  - *Apogon guadalupensis*† (Osburn and Nichols)
- Serranidae
  - *Paralabrax clathratus* (Girard)
- Atherinidae
  - *Atherinopsis californiensis* subsp.†
  - *Atherinops affinis guadalupae*† Hubbs
- Carangidae
  - **Seriola dorsalis* (Gill)
  - *Trachurus symmetricus* (Ayres)
- Branchiostegidae
  - *Caulolatilus princeps anomalus* (Cooper)
- Embiotocidae
  - *Embiotoca* sp., possibly differentiated
  - *Damalichthys* sp.†
  - *Brachyistius aletes*† (Tarp)
- Pomacentridae
  - *Chromis punctipinnis* (Cooper), somewhat differentiated
  - *Azurina hirundo*† (Jordan and McGregor)
  - *Hypsypops* sp.†
- Labridae
  - *Bodianus diplotaenia* (Gill)
  - *Pimelometopon pulchrum* (Ayres)
  - *Halichoeres semicinctus* (Ayres)
  - *Oxyjulis californica* (Günther), possibly differentiated
- Girellidae
  - *Girella nigricans* (Ayres)
- Scorpididae
  - *Medialuna californiensis* (Steindachner)
- Scorpaenidae
  - *Scorpaena guttata guadalupae* Fowler (occurs also in Gulf of California)
  - *Scorpaenodes xyris* (Jordan and Gilbert), possibly differentiated
- Cottidae
  - *Artedius creaseri* (Hubbs), possibly differentiated
- Gobiidae
  - *Lythrypnus zebra* (Gilbert), possibly differentiated
  - *Lythrypnus dalli* (Gilbert), possibly differentiated
- Clinidae
  - *Alloclinus holderi* (Lauderbach)
  - *Heterostichus rostratus guadalupensis*† Hubbs
  - *Gibbonsia elegans erroli*† Hubbs
  - *Gibbonsia norae* Hubbs, also on San Benito Islands
- Tripterygiidae
  - *Enneapterygius* sp., not endemic
- Brotulidae
  - *Eutyx diagrammus* Heller and Snodgrass, also on Galápagos Islands
- Balistidae
  - *Xanthichthys lineopunctatus* (Hollard)

PLATE I

Figure 1. Holotype of *Chaetodon falcifer*, 138 mm. in standard length, from Guadalupe Island, México. Photo by Scripps Institution.

Figure 2. X-ray photograph, by Robert L. Wisner, of holotype of *Chaetodon falcifer*. Print by Scripps Institution.

The collecting at this station (SIO 54–219) was a joint operation of two parties, largely from the Scripps Institution of Oceanography, led, respectively, by the junior author on the Institution's Research Ship *Paolina T*, and by the senior author on the Research Ship *Orca*, of the J. W. Sefton Foundation. Thanks are due to all members of the dual expedition, especially to Joseph W. Sefton, Jr., who, often and graciously, made the *Orca* available for biological explorations.

DISTRIBUTION

It is possible, indeed highly probable, that this apparently deep-water *Chaetodon* is much commoner about Guadalupe Island than the collecting of only one specimen would indicate. However, no other specimen has been seen, despite the fact that, of late, the island has been subjected not only to rather intensive collecting but also to a considerable amount of aqualung diving by several experienced and observant divers, including Conrad Limbaugh. During the expedition of November, 1954, six divers with self-contained underwater breathing apparatus were under water much of the time during seven consecutive days. The center of abundance of the species may well be deeper than 100 feet (as seems to be true of the related Atlantic species); or, it may occur chiefly on the western shore of the island, where the surf is usually strong and where collecting below tidal limits has been very limited.

It is also possible, though we think rather improbable, that the species occurs farther south, either along the mainland or on the Revillagigedo Islands. It has not been included among the chaetodontids taken during the extensive collecting in those areas in recent years, particularly by parties working under or for Boyd W. Walker of the University of California at Los Angeles and John E. Fitch of the California Department of Fish and Game. A considerable amount of more or less deep-water poisoning has been included in those operations. For these reasons, *Chaetodon falcifer* may be listed, provisionally at least, among the endemic fishes of Guadalupe Island. The interpretation of *C. falcifer* as a relative of the deep-water Atlantic species, *C. aya* and *C. marcellae,* weakens but hardly destroys the indication of endemicity.

Even though endemic, *Chaetodon falcifer* is to be included among the tropical elements in the intermixed warm-temperate and tropical fish fauna of Isla Guadalupe. In the eastern Pacific it probably represents the northern limit in the present distribution of the tropical family Chaetodontidae. The qualification "present" is used because, about one hundred years ago, when the fauna of southern California was distinctly more tropical than at present (Hubbs, 1948), *Chaetodon humeralis* Günther seems to have occurred at

(854)

San Diego. We are informed by Leonard P. Schultz that two specimens of that species in the United States National Museum are recorded as having been collected by Lt. Trowbridge at San Diego, California. The low catalog number (3170) indicates that the specimens were in fact entered in the collection nearly 100 years ago. Lt. W. P. Trowbridge was one of the most effective of the West Coast collectors on the Pacific Railroad Surveys. Somehow the species escaped inclusion in Girard's reports on the fishes collected by these surveys. Presumably the specimens came to light after the bulk of the collections had been studied and cataloged, for the number is higher than those recorded for the species reported by Girard. In this connection it may be noted that Girard (1858: 338) referred to other specimens from San Diego that had become "mislaid in the moving of the Smithsonian collections from one end of the building to another a few months since." Some slight doubt regarding the validity of the San Diego record can not be dispelled, but we believe that *C. humeralis* is to be added to the list of tropical fishes that occurred at San Diego during the warm period a century ago.

Distinctions

Chaetodon falcifer is not closely related to any of the three chaetodontines already known from the eastern Pacific. It does not belong in the same subgenus as *C. humeralis* Günther (1860: 19–20; 1869: 419, pl. 65, fig. 3), which is the only one of the three that we retain in the genus *Chaetodon.* It agrees with that species, as well as with the two others, in the high spinous dorsal with deeply incised interspinal membranes, but it has a much sharper and more produced snout and very much smaller scales, and the scale rows on the middle of the trunk are subhorizontal and those above the lateral line are parallel with the lateral line (instead of being strongly oblique in each area). Furthermore, the coloration is strikingly different, and there are numerous trenchant distinctions in the bony and scaly structures of the head, and in the squamation of the caudal fin (see pp. 295–296).

The Guadalupe species differs even more significantly, we believe, from the other eastern Pacific form currently referred to *Chaetodon,* namely *C. nigrirostris* (Gill). In that species, as is indicated later (pp. 296–299), the lateral line continues to the caudal base: a character that seems to call for its placement in another genus. Provisionally, we refer it to the genus *Heniochus. Chaetodon falcifer* and *Heniochus nigrirostris* differ in many other respects, as in coloration, in the squamation of the head, in the characters of the gape and lips, etc. The differences can be appreciated by comparing the following description of *C. falcifer* with the descriptive notes on *H. nigrirostris* (pp. 296–297).

When compared with *Forcipiger longirostris* (Broussonet), *C. falcifer* is seen to differ not only in the much less extremely produced beak, but also in the lateral-line character, in which *Forcipiger* and *Heniochus* agree, and in many features of coloration.

Inasmuch as some Indo-Pacific fishes, including one of the three eastern Pacific chaetodontines, have hurdled the broad barrier between the central Pacific islands and the New World (Ekman, 1953; Myers, 1941, and others) to become established in the Panamaic fauna, *C. falcifer* has been compared with descriptions and figures of the multitudinous Indo-Pacific species of the Chaetodontinae. In this comparison numerous treatises have been consulted, including Bloch (1796), Cuvier (in Cuvier and Valenciennes, 1831), Günther (1860), Bleeker (1876a–1878), Jordan and Fowler (1902), Jordan and Evermann (1905), Jordan and Seale (1906), Kendall and Goldsborough (1911), Ahl (1923), Herre and Montalban (1927), Fowler (1928, and supplements), Fowler and Bean (1929), Weber and de Beaufort (1936), and Munro (1955). Also checked were species listed in the *Zoological Record* as having been published since the appearance of Ahl's monograph in 1923. Nothing corresponding closely with *C. falcifer* has come to light. It is concluded, therefore, that this species is not a stray from the present Indo-Pacific fauna.

On comparing *C. falcifer* with the Atlantic species of the genus, we find marked differences, but many characters shared with *C. aya* Jordan of the western Atlantic and *C. marcellae* Poll of the eastern tropical Atlantic (see pp. 300–304). There are consistent differences in the color marks. In the Pacific species the preocular part of the first band runs almost horizontally along the upper part of the side of the snout, rather than obliquely across the front part of the cheek just behind the mouth, and the posterior mark has a scythelike form with an anterior arm extending down to the opercular region, rather than being confined to a simple bar running obliquely downward and backward across the body from near the middle of the spinous dorsal (in *C. aya*), or subvertically downward from the end of the first dorsal (in *C. marcellae*). Furthermore, the scales are much finer in *C. falcifer* than in the Atlantic species, and there are many other, minor differences. A careful comparison of the type of *C. falcifer* with the 17 available specimens of *C. aya* discloses the numerous differences outlined in table 1. *Chaetodon falcifer* apparently differs from *C. marcellae* in most of the characters that distinguish it from *C. aya.*

(856)

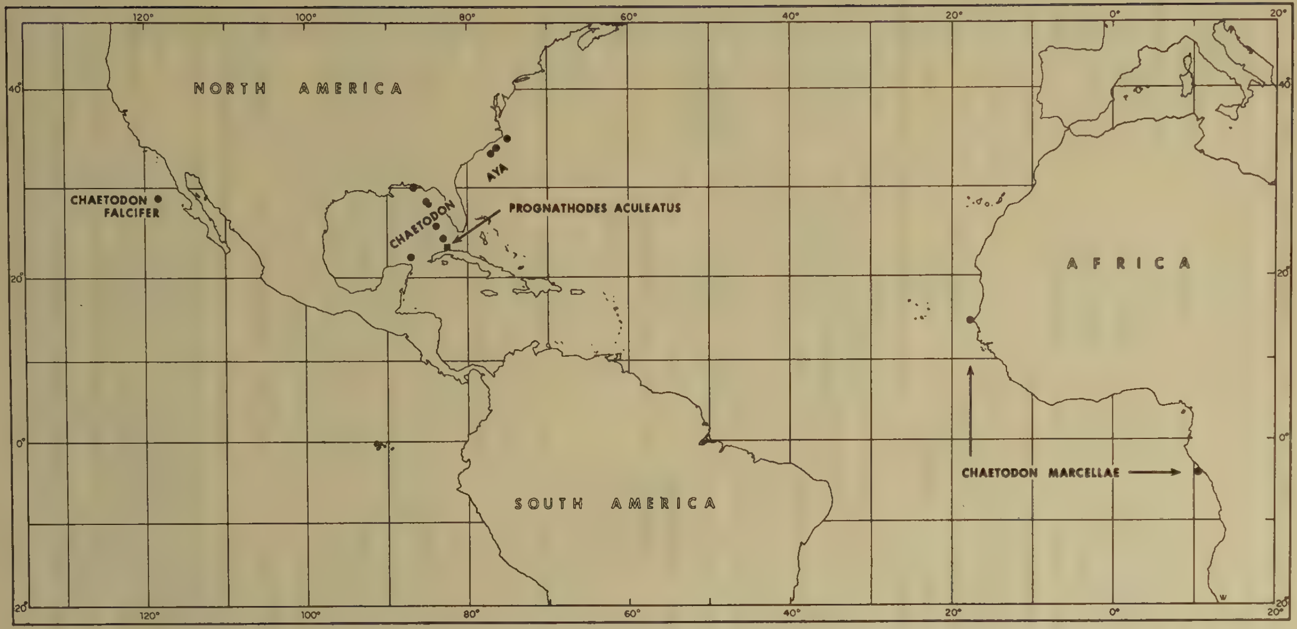
120°
100°
80°
60°
40°
20°
0°
20°
40°
20°
0°
20°
NORTH AMERICA
SOUTH AMERICA
AFRICA
CHAETODON FALCIFER
CHAETODON
AYA
PROGNATHODES ACULEATUS
CHAETODON MARCELLAE

Map 1. Known record stations for *Chaetodon falcifer* and allied species. The record station for one specimen (C.N.H.M. 64369) was received too late for inclusion, but essentially coincides with the northernmost station plotted.

Table 1. Comparison of *Chaetodon falcifer* with *C. aya*

	Chaetodon falcifer	*Chaetodon aya*
Dorsal soft-rays	21	17 to 19
Anal soft-rays	16	14 to 16, usually 15
Pectoral rays	15	13 to 15, usually 14
Scale rows, straight line[1]	51 to 53	32 to 38
Scales in first row above lateral line[2]	64 to 66	27 to 36
Pores in lateral line[3]	44 to 46	23 to 32
Scales from dorsal fin to lateral line[4]	15	9 to 12
Scales from anal fin to lateral line[4]	26	17 to 21
Scales around caudal peduncle[5]	30	20 to 26
Lateral line ends:	Close to end of soft dorsal	Below front part of soft dorsal[6]
Main marking on body[7]	Scythe-shaped, with extension onto opercles	Oblique band, extending onto spinous dorsal
Band below eye extending:	Along side of snout	To just back of upper jaw
Dorsal and anal fins	With much black, and a definite light border	Almost clear, except on extension of bars; no definite light edge
Upper and lower borders of caudal fin	Largely blackish	Not blackened
Angle, body axis and margin of soft dorsal[8]	72°	75° to 87°
Maximum known size	138 mm.	98.5 mm.

RELATIONSHIPS

We have not been able to allocate *C. falcifer* with complete assurance in any of the named subdivisions of *Chaetodon*, as these have been characterized in various published revisions (subsequent authors have based their groupings, though not their nomenclature, largely on the subgeneric divisions proposed or accepted by Bleeker from 1876 to 1878).

When checked with Ahl's monographic revision of 1923, *falcifer* is seen to agree essentially with subgenus *Chaetodon,* and not with the subgenera *Gonochaetodon* and *Megaprotodon,* which Weber and de Beaufort (1936) later recognized as genera. When compared with the three divisions of "Gruppe" rank into which Ahl split the subgenus *Chaetodon,* respectively with two, four, and three further subdivisions of "Sektion" rank, *falcifer* is excluded from group 1 by reason of the body form and from group 3 by having the median trunk scales little enlarged, with well-rounded margins and with the subhorizontal alignment retained; also in having more than 45 scale rows crossing the median line of the body. This leaves "Gruppe II," from sections D to F of which *falcifer* is excluded by the subhorizontal scale rows. From "Sektion C, *Chaetodon* s. str. = *Tetragonoptrus* Bleeker," as briefly diagnosed by Ahl (p. 80), *falcifer* is not obviously excluded, but it has smaller scales than any of the species as counted by Ahl, except the very different "*Chaetodon Sanctae Helenae* Günther." In fact, the scales are rather too high for his generic diagnosis (p. 7): Ahl characterized the genus *Chaetodon* as having about 30 to 50 scales in "L. lat." (defined on p. 6 as the number "vom oberen Ansatz des Kiemendeckels" to the caudal flexure). Ahl thus contrasted *Chaetodon* with *Hemitaurichthys, Microcanthus,* and *Vinculum,* each of which was indicated as having 60 or more (60–90) scale rows. Those three genera all have the lateral line of the primitive *Heniochus* type, and one of them, *Microcanthus,* has been shown by Fraser-Brunner (1946) to have been wrongly classed in Chaetodontidae.

---

[1] Rows crossing a straight line from scapular process behind upper end of gill opening to caudal flexure; for this and for all other paired series, both sides were counted on all specimens.

[2] Including all scales that impinge above on a lateral-line scale.

[3] Including occasional unpored scales definitely in the lateral-line series.

[4] From edge of sheath at side of first spine in an oblique row to but not including the lateral line.

[5] Scales in not quite overlapping position around narrowest part of peduncle.

[6] Ending rarely, on one side only, on vertical passing slightly before visible front of soft dorsal or a little behind middle of soft-dorsal base.

[7] When considering colorational characters, compare plate I, figure 1 with plate II, figure 1 and plate III, figure 1.

[8] Angle between body axis (from front of snout to middle of caudal base) and a symmetrical tangent to the rounded margin of the soft dorsal fin.

Chaetodon falcifer differs more trenchantly from any of the species placed by Ahl in his section *Chaetodon* in having a much longer, more produced, more pointed snout, in this respect definitely approaching *Forcipiger* and *Chelmon.* It agrees fully with none of the subdivisions of *Chaetodon,* including the segregated genera *Gonochaetodon, Megaprotodon,* and *Anisochaetodon,* as diagnosed by Weber and de Beaufort (1936). Further studies may call for its recognition as a member of a new subgenus, or possibly genus (presumably to include also the Atlantic species, discussed below).

Several characters that *Chaetodon falcifer* shares with *Heniochus nigrirostris* and *Forcipiger longirostris* (Broussonet), which is regarded as including *F. flavissimus* Jordan and McGregor, suggest the remote possibility of a relationship with one or both of those species; close enough, if verified, to run counter to the classification we have adopted.

Chaetodon falcifer agrees with *H. nigrirostris* in the size of the scales, in which respect *C. falcifer* contrasts with almost all species currently left in *Chaetodon.* It also agrees with that species, though not so exclusively, in the orientation of the scale rows. In the form of the spinous dorsal the two species are similar, having strong and high spines with very deeply incised membranes; but in *C. falcifer* the third and fourth spines are subequal, whereas in *H. nigrirostris* the fourth spine is definitely the longest, as it is (to a greater degree) in the other species referred to *Heniochus* (furthermore, in the apparently closely related Atlantic species, *C. aya,* the third spine is definitely the highest). There are also some resemblances (as well as sharp differences) in the color pattern, for both species lack the suborbital bar characteristic of most species of *Chaetodon* and have the nuchal bar continued forward on the snout (though with interruptions in *H. nigrirostris*). The posterior dark crescent in *H. nigrirostris* suggests the posterior part of the scythelike mark of *C. falcifer,* though it is farther back and farther up.

Chaetodon falcifer approaches *Forcipiger longirostris* in the sharpness and production of the snout and in the reduced size of the scales. In both species the dorsal spines are high and the interspinal membranes are deeply incised. In both, the nuchal band is continued through the eye to and along the upper part of the snout. In some of these characters all three species under discussion show resemblances. At present, however, we interpret each of these resemblances as the result of convergent evolution. Numerous differences between all the forms may be noted by comparing the following description of *C. falcifer* with the descriptive notes of the three other Pacific species (pp. 295–300).

As already suggested (p. 00), *C. falcifer* seems to find its closest relatives in two Atlantic species, *C. aya* of the western Atlantic and *C. marcellae* of west Africa, which are treated in more detail on pages 300–304. The distinctive resemblances (compare figures) include the sharpness and production of the muzzle (a character that is carried to a farther extreme in *Prognathodes aculeatus* of the West Indian fauna); the very high, strong, and greatly excised dorsal and anal spines; the rather regular and little modified alignment of the scale rows; the rectangular form of the body behind the head; the more or less forward dislocation of the subocular bar (carried to an extreme in *C. falcifer*); a dark bar along the top of the head anteriorly; the presence and intensity of the blackish bar from eye to front of dorsal; the extension of the posterior bar to an abrupt end on the scale-covered base of the anal fin, etc. These resemblances seem to outweigh the sharp differences between *C. falcifer* and *C. aya* that are outlined in table 1, and that also apply largely to *C. marcellae.*

The close relationship between *C. falcifer, C. aya,* and *C. marcellae* is further suggested by their distinctively deep-water habitats. The type of *C. falcifer,* as indicated earlier, was collected at a depth of 100 feet. All specimens of *C. aya* and *C. marcellae,* so far as recorded, were taken at

(860)

even greater depths. The type of *C. aya* was from the stomach of a red snapper from Snapper Banks off Pensacola, Florida, where the depths fished at that time were reported by the collector, in his survey of the fisheries grounds (Stearns, 1887), to be 20 to 50 fathoms. Another specimen was trawled off North Carolina (Nichols and Firth, 1939: 87) at a reported position where the coast chart (1110) indicates the depth as approximately 150 fathoms (considerable error either in distance or direction would not fix the trawling spot at a depth of less than 100 fathoms)! Hildebrand (in Longley and Hildebrand, 1941: 150–151) reported the capture of seven specimens near Tortugas, Florida, at two stations, at depths of 39 and 40 fathoms, respectively, and added, "apparently not entering shallow shore waters." The additional known specimens of *C. aya* (see pp. 302–303) have been taken at depths recorded as 24, 25 to 30, 25 to 75, 37, 40 to 45, 62, and 75 fathoms.

DIAGNOSIS

Outstanding characters of *Chaetodon falcifer* are the very long and sharply produced snout, in which respect it definitely approaches *Forcipiger;* the rather small scales, intermediate in size between those on most species of *Chaetodon* and those typical of the species of *Heniochus* and related genera; the lack of a suborbital bar and the extension of the nuchal band, as in *Forcipiger,* through the eye to and along the snout; and the peculiar scythe-shaped blackish mark on the body. Less distinctive, but serving to separate the species from many others in *Chaetodon* (and segregated genera) are the dorsal and anal fin formulas, respectively XIII, 21 and III, 16; the high and strong dorsal and anal spines, with deeply incised membranes; the alignment of the scale rows, which are subhorizontal below the lateral line and parallel with that line above it; the rounded margins and only moderate enlargement of the median trunk scales; the rather rectangular body form; the low mouth; and the alignment of the inner jaw teeth anteriorly in twelve rather even cross rows.

DESCRIPTION OF FINS

DORSAL FIN. The dorsal rays number XIII, 21. The base of the spinous dorsal measures 1.6 in the soft-dorsal base. The dorsal spines are very strong and high anteriorly. The subequal third and fourth spines are the highest. Each, as measured from the edge of the scaly sheath, is as long as the soft-dorsal base. The interspinal membranes are deeply incised, very deeply anteriorly. The least width of the membrane at the front of the two longest spines is less than one-sixth the height of the spine. The soft dorsal has a weakly rounded margin, with the median part nearly straight and forming an angle of 72° between its tangent and the axis of the body; the margin along the first three or four rays is nearly horizontal; that along the last few rays is rounded and is directed downward and slightly forward. None of the dorsal soft-rays are produced.

Anal fin. The rays number III, 16. The spines are very strong. The second is very notably strengthened and considerably elongated, though when depressed it just reaches the tip of the third spine. The free front edge of the second spine is as long as the base of the soft anal. The interspinal membranes are very deeply incised. The membrane at the front of the second spine is one-sixth the length of the front edge of that spine. The margin of the soft anal is nearly straight and nearly vertical medially, and is moderately curved forward along the anteriormost and posteriormost rays.

Other fins. The caudal has a weakly convex border, with the upper angle rather pointed, though not produced, and the lower angle more broadly rounded. The very slightly falcate pectoral, which reaches to above the anus, is about one eye's length shorter than the head. The first pelvic soft-ray ends in a free filament, which is more than half as long as the orbit and reaches to between the genital papilla and the origin of the anal fin. The length of the pelvic equals that of snout plus orbit. Principal caudal rays, $9 + 8 = 17$; pectoral rays 15 on each side, or, more precisely, distinguishing unbranched and branched rays respectively on left and right sides, ii, 12, i—ii, 11, ii.

Scales and Lateral Line

Scale number and size. The scales are relatively small and numerous. Along a straight line from the upper end of the gill opening to the caudal flexure we enumerate 51—53 transverse rows (counting both sides) behind the scapular process, and 4 rows on the process; there are 3 additional rows of scales, smooth and well embedded, on the concealed part of the shoulder girdle. Along the first row above the lateral line, beginning behind the scapular process and enumerating all scales that definitely impinge above on a lateral-line scale, we count 64—66 scales. From the edge of the scaly sheath beside the first spine, in an oblique row to but not including the lateral line, we count on each side 15 scales below the dorsal and 26 above the anal. There are about 30 rows, not including scales that overlap on the exposed field, around the narrowest part of the caudal peduncle. The scales become markedly reduced in size on the thick scaly area over the basal part of the soft-dorsal fin. The scales also become very small on the

(862)

nape, occiput, opercles, and muzzle. They are somewhat but not notably enlarged on the side of the trunk forward to the pectoral fins, but these larger scales grade evenly into the others.

Scale form, seriation, and disposition. The scales are regular in outline, with evenly rounded margins, even where moderately enlarged. Below the lateral line the scale rows are approximately horizontal, with a slight upward flexure posteriorly that increases to about 18° on the fleshy area over the anal base. Some rows are arched upward a little where the scales are most enlarged. Toward the pelvic fins the rows become irregular. Above the lateral line the rows are essentially parallel with this line and are similarly curved, on the body proper, but become irregular, and peripherally assume an oblique orientation, on the thick scaly fin bases, especially on the second dorsal.

Where, on and about the head, the scales become greatly reduced in size, the rows become very irregular or hardly apparent. Very small rough scales are developed on the posterior part of the premaxillary, especially in files along the fine rugose ridges. A narrow band of ctenoid scales crosses the top of the premaxillaries just in front of the rostral groove (this character will likely prove variable, as it is in *C. aya*). The exposed part of the maxillary, behind the anterior grooved area, is evenly covered with small ctenoid scales. Fine ctenoid scales cover the mandibles forward to a little beyond the end of the gape. There is only a small scaleless area around the anterior nostril and below the posterior nostril. This scaleless strip extends backward to the orbit below the anterior prolongation of the upper bony orbital rim. A very narrow and irregular scaleless groove, seemingly distinctive among the American Pacific species of the subfamily, but which will probably prove variable, as it is in *C. aya,* extends forward from in front of the anterior nostril to the row of scales bordering the rostral edge. A small triangular scaleless area (which will probably prove variable, as it is in other species) extends upward and backward from the upper bony orbital rim. At the apex, the width of this scaleless area is only about one-fifth that of the orbit. The fleshy upper orbital rim, largely concealed by the bony rim, bears some scales, mostly small and smooth (probably also a variable character, or one affected by loss of scales).

The scaleless margin of the soft dorsal is about one-third as wide as the orbit; that of the soft anal, about one-fourth the orbit. In each fin the outer part of the interradial membranes is more or less scaleless for an additional distance about equal to the width of the totally scaleless margin. Anteriorly, these scaleless grooves are more extensive. Along the thickened base of each alternate dorsal spine and along one side of the third anal spine an acute triangle of scales runs well out on the spine. Except on a basal band about two-thirds as wide as the orbit, and near the upper and lower margins, the caudal fin is very weakly scaled. The scales on the branching rays are very small, delicate, and difficult to see. Beyond the scaly base single or double files of scales extend only a very short distance outward on each interradial membrane, scarcely at all on the membranes between the innermost rays. (It is possible that ctenoid scales may have covered more of the caudal in life.)

LATERAL LINE. The lateral line forms an almost even arc backward to its end about five tiny scale rows before and above the end of the dorsal base. The pores behind the scapular process number 44–46. The small lateral-line scales are more isolated from one another than in *C. aya.* On the midsides in advance of the vertical from the end of the lateral line, on the right side only, are two pored scales in series (not included in the count).

BODY AND HEAD CHARACTERS

BODY FORM. Behind the head, the body, including the fleshy scaled fin bases, is virtually square. The vertical depth from the edge of the dorsal scale sheath to near the pelvic insertion steps 1.75 in the standard length. The edge of the thick scaly covering of the dorsal fin is approximately straight and horizontal from the second dorsal spine to the extreme front part of the soft dorsal. The ventral contour is similarly almost straight and horizontal from a little in front of the pelvic insertion to the extreme anterior part of the soft anal. From the dorsal origin to the concavity of the snout the profile is almost straight (very slightly sigmoid) and forms an angle of 52° with the body axis and an angle of 83° with the chord of the anteroventral contour behind the muzzle. The scaly bases of the soft-dorsal and soft-anal fins appear very steep in external view, though the actual structural bases as measured on the X-ray photograph (plate I, figure 2) describe an angle of only 81°.

SNOUT AND MUZZLE. The snout is notably produced, narrowed, and sharpened. Its dorsal profile forms an angle of 150° with the profile between the snout and the dorsal fin. The angle of the muzzle is about 40° in lateral view and 29° in dorsal aspect (each measurement excluding the abruptly rounded tip.) The greatest width in front of the eye steps 1.8 in the length of the snout. Since the snout is a little longer than the postorbital, the center of the eye is slightly behind the middle of the length of the head, which, including the opercular membrane, steps 2.8 in the standard length.

MOUTH AND JAWS. The front of the low and subhorizontal gape lies definitely below the lower border of the orbit. The lower border of the upper jaw forms an angle of 21° with the body axis. The gape is not quite half the length of the upper jaw, which enters the head length 3.5 times. The anterior parts of the jaws are expanded forward to accentuate the beaklike form of the snout. The midline length of the upper lip is actually more than half the length of the orbit. Above and behind a deep fissure the lips are sculptured by parallel grooves and more or less crenate ridges. The fissure is about three-fourths as long as the orbit. It starts, in side view, near the middle of the anterior premaxillary expansion and extends to approximately the middle of the length of the posterior maxillary dilation, near its lower border. There is no vertical groove on the maxillary. The margin of the upper lip is somewhat pendant, especially on the sides opposite a slight anterior lobation of the lower lip. The front of the gape is narrowly and evenly rounded transversely, with no marked irregularity on either lip.

Teeth. The teeth of the jaws extend to the end of the gape. Those of the outer row are slightly enlarged. The very fine inner teeth are definitely aligned in each jaw in twelve nearly straight transverse rows across the semispherical tip of the beak. Posteriorly the inner teeth are less regularly arranged and form a narrower band. The midline length of each anterior tooth patch measures 3.5 in the orbit. The vomer is edentulous.

Gill rakers. The rakers, including rudiments, number 5 + 11 on the outer arch. Those of the upper limb are soft. The longest, near the middle of the lower limb, barely reach the second raker below.

Bony margins. The preorbital border is finely denticulate, especially at the squarish anterolateral corner. The preopercular denticulations, mostly very fine, are somewhat enlarged and directed backward at the rounded angle, above which the nearly vertical margin is rather strongly concave and below which the somewhat oblique edge is weakly concave. The exposed border of the scapular process is also denticulate.

The upper border of the orbit is roughened by several series of minute denticulations. In the scaleless area, extending upward and backward from the upper orbital rim, the fine spinulation continues for a short distance and then becomes transformed into larger points and very short ridges, rendering the whole exposed area rough (perhaps more so than in other specimens). The bony orbital rim is scarcely expanded in the prefrontal region. It is extended downward and forward about halfway to the posterior nostril, departing here from the margin of the orbit and lying above the scaleless area behind the nostrils (this character will probably vary widely, as it does in other species). The bony orbital margin is extended down the posterior edge, to continue below the orbit and up to near the middle of the front edge. Around the lower half of the orbit the more or less trenchant bony rim is armed in the type specimen with a row of fine serrulations, in places backed by other, minute points.

Osteological Features

Vertebrae and hypurals. Many of the bony structures can be made out on an X-ray photograph (plate I, figure 2). The vertebrae number 10 + 14 (including the hypural plate). The first two are reduced in size. The caudal rays impinge on eleven hypural elements, six above and five below, of which 3 + 3 comprise the hypurals proper, arising from the lower edge of the upturned axis. The hypurals support all seventeen principal caudal rays except the lowermost two, which arise, respectively, just above and on the more posterior of the two hypural-like interhemals of the twenty-third vertebra. On the six hypurals the principal rays originate according to the following formula, counting downward: 3 + 4 + 2 = 9; 1 + 4 + 1 = 6. The four upper procurrent rays arise from the two loose epurals, and a minute blob of ray tissue lies beyond the tip of the neural element of the last vertebra. The three lower procurrent rays arise from the two hemal elements connected with the last normal centrum. Only the posteriormost procurrent ray, above and below, is segmented.

Vertebral spines and interspinals. The interneurals of the last two dorsal spines arise on either side of the definitely longer neural spine of the twelfth vertebra. This neural spine is sagittally expanded toward the base, thus contrasting with the spines that follow. From the twelfth to the eighth the neural spines remain nearly at right angles to the vertebral column, increase in thickness, and become shorter, finally to reach only halfway to the base of the dorsal spines. From the seventh to the third the neural spines become oblique and still shorter. The first two become more erect and the first is the smallest. The interneurals increase in strength forward from that of the last dorsal spine to that of the second spine, which interneural is directed slightly forward to fit between the first two neural spines close to the vertebrae. The interneural of the first dorsal spine comprises a flat shaft that impinges on the following interneural and that bears, at its upper end, a strong thornlike process directed forward and downward. The two rodlike interneurals that arise on either side of the tip of the first neural spine have, at the top, nearly fused, forward-directed, thornlike processes, which, together with the larger process just mentioned, form a bridge, hidden beneath the sharp anterodorsal rim of the body, between the first dorsal spine and the very strong, high, and sharply elevated supraoccipital spine. The hemal spine of the first caudal vertebra is considerably expanded where it lies behind the very strong spinelike interhemal of the second anal spine. That interhemal reaches slightly more than halfway to the central line of the vertebral column.

Skull. Above the orbital rim and the base of the first vertebra, the skull in side view forms approximately an equilateral triangle, with the apex, at the base of the supraoccipital spine, located above the isthmus a distance equal to that from the tip of the snout to the posterior margin of the shoulder girdle. In side view the premaxillaries and dentaries are very slender. The least dorsoventral dimension of the premaxillaries, near the rear of the anterior dental expansion, is only 0.1 the antorbital length of the skull.

Coloration

(Plate I, figure 1)

Scythe-shaped mark. The outstanding colorational feature of this species is the scythelike mark on the sides of the head and body. In life this mark was deep brown-purple, almost jet-black. After over a year in 40% isopropyl alcohol, following initial preservation in formalin, this color, like many of the others, is little changed. The short "handle" of the "scythe" begins abruptly at the upper-posterior part of the interopercle, beneath and behind the preopercular angle. The "handle" continues upward and slightly backward to cover the subopercles and the opercle behind the upper bony process. There are dusky dapplings on the adjoining branchiostegal membrane. Continuing its steep course, at an angle of 62° with the axis of the body, the mark crosses the opercular membrane and attains a position astride the lateral line. Along the middle third of its anterior section, where it is slightly arched backward, the mark is about as wide as the orbit. The front edge of the band is weakly arched forward dorsally and extends to a rounded angle, somewhat greater than a right angle. The angle of the axis is about 80°. The apex is separated from the edge of the scaly sheath near the front of the fifth dorsal spine by an interval about two-thirds as wide as the orbit. The lower-posterior border of the anterior section of the mark follows throughout most of its length a nearly straight course, a little steeper than the anterodorsal contour of the body. Dorsally the ventral border arches rather abruptly backward, to reach its apex below the posterior exposed base of the fifth dorsal spine, in the third scale row below the lateral line. From the apex the lower border is gently curved to the acute end of the "scythe" on the sixth anal soft-ray. The upper border continues backward and slightly downward, nearly straight, to descend below the lateral line at a point nearly in line with the last spine of the normally expanded dorsal fin; that is, at a point about midway between the apex of the mark and the end of the dorsal base. From this point the upper edge of the "scythe" arches backward and then downward to the lower-posterior end. On the fleshy base of the anal fin the posterior edge of the mark is nearly straight and nearly vertical. The mark is separated from the end of the dorsal base by a distance two-thirds the length of the orbit; from the caudal flexure, by one orbital length; and from the end of the anal base, by about one-fourth the orbit. The width of the band, measured either downward and backward from the anterior apex, or at the greatest width posteriorly, steps 2.4 in the head length. The least width between those points, not far behind the apex, is 3.3 in the head.

Band through eye, and adjacent color. Another prominent and conspicuous mark is the band, rather rich-brown in life and sooty blackish in preservative, that extends from the base of the first two or three dorsal spines downward and slightly forward to the upper rim of the orbit. With decreased intensity, though still conspicuous, it cuts obliquely across the eye and then continues, much less steeply and with a weak downward curvature, well above the mouth, toward but not quite to the rostral fold; except near the eye, the lower border is horizontal. The narrow light area in front of the band was somewhat yellow in life. Above and behind the eye there was considerable yellow both before and behind the band. On the head above the eye the mark is blackest, with a further intensification along either edge. Farther upward and backward the anterior edge remains sharp, along the narrow light V on the predorsal contour. Posteriorly, the upper part of the band fades gradually into a pale color, with (in preservative at least) silvery specks at the scale bases. These specks extend to the "scythe." The greatest width of the stripe, where well defined, is about three-fourths that of the orbit.

Middorsal stripe on head. A third stripe, about one-third as wide as the orbit, dusky-centered and blackish-edged, extends from above the middle of the eye to the premaxillary groove. It is continued forward, on the top of the broad premaxillary expansion, as a solid blackish bar about one-fourth to one-sixth as wide as the orbit.

Side of head. In advance of the "scythe" the sides of the head in life reflected rather strong blue glints, which were strongest on the opercles. The very edge of the orbit, posteriorly and ventrally, is light (bright yellow in life). Since the ocular bar is extended forward on the side of the snout there is no trace of a suborbital bar, and since the anterior part of the "scythe," representing the second bar of many species, extends across the opercles, there are no markings about the pectoral base. In the field notes no evidence was recorded of definite light margins on the main dark bars, such as are evident on specimens of *C. aya* preserved in alcohol.

Above and behind the "scythe." Above and behind the "scythe," down to the level of the upper edge of the caudal peduncle, and extending over the thickened scaly base of the dorsal fin, the color in life was purplish-gray over a yellowish base. The purplish-gray remains in the alcohol-preserved specimen. In this area there are faint dusky specks at the scale bases. Where it is exposed along the upper edge of and behind the "scythe,"

the lateral line in life was iridescent silvery on the specialized scales, and in alcohol the line remains light. In life the caudal peduncle was yellow-brown, becoming almost clear yellow ventrally. In alcohol the peduncle is lightened, especially on the lower surface.

BELOW THE "SCYTHE." Below the black mark the sides were brightened in life by silvery-violet reflections. In this area there were rather indistinct purplish-gray streaks along the middle of the scale rows. Anteriorly, this color became almost solid on the scales, except for a creamy anterior border. The purplish-gray streaks remain in alcohol, and silvery flecks are generally interspersed between the streaks.

VENTRAL SURFACE AND LOWER FINS. In life the ventral surface was lemon. This color extended onto the pelvic and anal fins and became intensified on the membranes behind the spines. Otherwise these fins were dusky olive-yellow, shading outward to blackish-brown at the margin of the pelvic soft-rays (excluding the pale filament) and just within the margin of the soft part of the anal fin. In alcohol the anal spines are pale gray, but the soft anal becomes almost solid black on the sharp outer edge of the dark area. The clear margin becomes pinched out at the first anal soft-ray. Along the upper, posterior part of the fin the abruptly clear margin is about one-sixth as wide as the orbit. The pelvic in alcohol remains blackish toward the posterior margin, leaving the spine, the front of the first soft-ray, and the filament pale gray. The pectoral was essentially clear in life. In alcohol its upper margin is slightly darkened and the rays are set off by fine purplish edges.

CAUDAL FIN. In life this fin had some purplish-gray on the rays. In alcohol the fin is slightly dusky, with a blackish upper and lower border, and there are blackish edges along the rays near the middle third of their length.

DORSAL FIN. In life the spines of this fin were purple-black and the median interspinal membranes were blotched with yellow and purplish-gray. The outer part of the fin from the seventh spine backward was sooty with some purple, and with some yellow showing through. The soft dorsal was purplish-gray over pale yellow basally, then light yellowish in an irregular, subvertical band, which was followed by a blackish-purple band inside the almost clear, slightly purple-gray margin. In alcohol the blackish color remains. It is more or less solid on the exposed parts of the spines, except for a lighter basal streak from the third to the tenth spines. The first two membranes are almost solidly blackish. The third to sixth membranes are light, with blackish dappling. Except on the pale basal streak the following membranes, where exposed, are blackish, especially behind the spines. The blackish area on the outer-posterior part of the spinous dorsal is continued backward, and then downward on the soft dorsal, as a submarginal blackish band, which becomes narrower and intensified toward the end of the fin. On the anterior third of the soft dorsal the band is about as wide as the orbit and fades into the purplish base of the fin, but on the posterior two-thirds of the fin the blackish and purplish areas are separated by the remnants of the subvertical yellowish band. Throughout the fin the dark streak is abruptly separated from the margin by the clear light area, which, except toward the ends, is about one-third as wide as the orbit. Thus, the soft dorsal and the soft anal are very similarly colored.

Measurements

Proportions of parts computed as thousandths of the standard length (138 mm.). Greatest body depth (from near pelvic insertion vertically to top of scaly sheath), 554; least depth of caudal peduncle, 104; length of peduncle from end of anal base to caudal flexure on midline, 86. Predorsal length, 425; prepelvic length, 433; caudal flexure to anal origin, 397; thence to pelvic insertion, 317; thence to isthmus, 223. Length of head to edge of opercular membrane, 354. Widths of head: at widest point, 130; at muzzle, across front of orbits, 81; across maxillaries, 70; opposite front of rostral groove, 45. Length of upper jaw, 103; midline length of upper lip, 46. From anterior nostril to rostral groove, 69. Length of orbit (between free rims), 79. Least distance from free rim of orbit: to front of upper lip (length of snout), 147; to rostral fold (preorbital width), 97; to suborbital margin, behind mouth (suborbital width), 70; to other orbit (least fleshy interorbital width, anteriorly), 75; to farthest point on margin of opercular membrane (postorbital), 141; to preopercular angle, 119; to ventral contour of head, 109; to dorsal origin, 246. Length of dorsal spines (along middle of side above edge of scaly sheath, disregarding scaly extensions along front of alternate spines): first, 96; second, 178; third and fourth, 280 each; fifth, 246; sixth, 225; seventh, 193; eighth, 168; ninth, 137; tenth, 120; eleventh, 100; twelfth, 85; thirteenth, 67. Length of anal spines, similarly measured from scaly sheath: first, 93; second, 198; third, 165. Other fin measurements: length of anal base, 310; length of middle caudal rays, 180; length of pectoral from upper axil, 266; width across pectoral base, 81; length of pelvic spine along front, 226; length of pelvic fin, including filament, 293.

Derivation of Name

The species name *falcifer* is the Latin word signifying scythe-bearer, in allusion to the diagnostic scythe-shaped color mark. We treat it as a noun and it is therefore not declinable.

DISTINCTIVE CHARACTERS AND RELATIONSHIPS OF THE THREE OTHER EASTERN PACIFIC CHAETODONTINES

An examination of the three other chaetodontines of the eastern Pacific, made in the University of California at Los Angeles by courtesy of Boyd W. Walker, has disclosed a considerable number of distinctive characters in the structure of the head and in the squamation of the head and caudal fin. Sharp differences between all four species are apparent in most of these characters. Some of these specific differences may well prove useful in the definition of species groups and subgenera, perhaps even of genera. Since we have no present opportunity to test the wider application of these features in the classification of the group, we offer only the following descriptive remarks, accompanied by inferences as to the relationships of the three species.

Chaetodon humeralis Günther.

The series of specimens (W 51–20) studied in most detail was taken by Boyd W. Walker and party on January 25, 1951, on the shoreward side of Isla Venado, near Mazatlán, Sinaloa, México, but others were examined to verify the consistency of the characters.

Mouth and gape. As seen from above, the mouth is rather evenly arched and shows only a trace of lateral knobs.

Lips. The upper lip is divided laterally by a prominent lengthwise groove, behind which the skin is broken into rather fine but sharp folds and creases. The main lengthwise groove is continued backward and downward as a deep fissure, behind which the surface is scaly and before which it is smooth, except for an irregular subvertical groove seen only in this species.

Teeth in jaws. In each jaw there are about 8 cross rows of fine teeth behind the somewhat enlarged outer row. In the lower jaw the rows are broadly curved.

Bony margins. The preopercle and the lower preorbital margin are finely denticulate. The bony orbital rim is weakly denticulate at the very edge only. There is no rough exposed bony area above the orbit.

Squamation about orbit and muzzle. There is no scaleless area above the orbit. In fact, the narrow fleshy band along the upper part of the orbit is fully exposed and is closely covered with hard ctenoid scales. These scales expand the flattish interorbital area a little on each side. The scaleless fossa about the nostrils is very small. The snout is well scaled forward to the rostral groove except for a small area on each side about a slight knob at the front of each preorbital. The lower edge of the preorbital is nearly concealed by scales. The posterior exposed lobe of the maxillary is covered with strongly ctenoid scales.

Squamation of caudal fin. The caudal is covered by ctenoid scales over more than three-fourths of its length, leaving a naked margin somewhat wider than that on the soft parts of the dorsal and anal. The basal band of body-type scales is broader than in the other species. The small though rough scales are in strips centered along the interradial membranes, but these strips contain several scale rows, and they are so wide that there intervenes between each pair only a narrow, more or less closed groove along the unbranched part of each ray out beyond the thickly scaled basal area of the fin.

Relationships. This, the only previously described species from the eastern Pacific to be retained in *Chaetodon,* seems fully distinct from its nearest congenors in the Indo-Pacific and West Indian faunas. No attempt has been made to seek its nearest apparent relatives.

Heniochus nigrirostris (Gill).

The specimen (W 52–258) examined in most detail was collected in Bahía San Lucas, Baja California, by Murray A. Newman and John E. Fitch, on December 1, 1952. Other examples were checked to verify the characters.

Mouth and gape. The front of the gape is almost straight and transverse, with an almost lobular angle on either side of each jaw.

Lips. In this species the lips are only weakly grooved in advance of, and above, about three moderate oblique fissures in the premaxillary region. There is no main longitudinal groove and no vertical groove on the maxillary, the exposed face of which is moderately rugose.

Teeth in jaws. The inner teeth are in only about 6 transverse rows in the front part of each jaw. In the lower jaw the arrangement is less regular than in the upper jaw and the rows are less transverse, because of the close approximation of the mandibles.

Bony margins. The preopercle and the lower margin of the preorbital vary from nearly smooth to finely and regularly denticulate. The lower border of the orbit is finely denticulate with tiny uniserial teeth. On the upper orbital border the bony points are more numerous and are pluriserial. This rough and exposed bony margin continues into a triangular expansion above and inward from the middle of the orbit. On the nearly naked, slightly fleshy area on each side of the interorbital, inward from and in front of the rugose area, there is evident a branching pattern of lateral-line canals. In the prefrontal region, the upper orbital margin is produced as a slight flange, with somewhat strengthened denticulations.

SQUAMATION ABOUT ORBIT AND MUZZLE. The fleshy upper orbital rim is scaleless in this species. Under the prefrontal flange just mentioned this dermal band bears several finely papillate dermal ridges. The rugose bony area within and above the bony orbital rim is nearly all scaleless, as is a fleshy area in advance thereof. The scales on the top of the head become obsolete between the nostrils, with few extending slightly farther forward. There is a wide, almost wholly scaleless fossa about the nostrils, continuous with the naked front of the muzzle. There appear to be no scales on the maxillary.

SQUAMATION OF CAUDAL FIN. The body-type scales form a rather narrow basal band on the caudal, with extensions toward the upper and lower margins of the fin. Over most of the rest of the fin the scales (bearing moderate ctenii) extend much less than halfway to the rear margin; they are in single series overlying the subbasal part of the interradial membranes, leaving the intervening rays largely free of scales.

GENERIC POSITION. As can be seen from the figures of *nigrirostris* published by Jordan and Evermann (1900: 3283, pl. 248, fig. 620), by Gilbert and Starks (1904: 148–149, pl. 24, fig. 47), and by Schultz (1951: 486, fig. 94), and as can be determined from Hildebrand's key and descriptions (Meek and Hildebrand, 1928: 766–770), *nigrirostris* differs sharply from other species referred to *Chaetodon* (including *C. falcifer*) in having the lateral line extended to the middle of the base of the caudal fin, instead of ending at the axil of the soft dorsal fin or at some point high on the fish anterior to and approximately in line with the axil. This distinction in posterior termination and position of the lateral line was used by Herre and Montalban (1927: 13–14), justifiably we think, as a primary character in the generic analysis of the family. Weber and de Beaufort (1936: 15–16) also utilized the character in their generic analysis of the Chaetodontinae (but, in this respect, inadvertently misplaced *Heniochus* in their key). The same or similar lateral-line characters have been employed in recent analyses of the genera of the subfamily Pomacanthinae (Fraser-Brunner, 1933; Smith, 1955).

For these reasons we think that *nigrirostris* is misplaced in the genus *Chaetodon*. It does not, however, fit perfectly into any of the genera as defined by Herre and Montalban, or by such other revisers as Günther (1860: 2), Bleeker (1878: 22–72, and preceding papers), Jordan and Evermann (1898: 1673; 1905: 362), Ahl (1927: 7), Weber and de Beaufort (1936: 14–16), and Woods (in Schultz, 1953: 566–575).

The species *nigrirostris* would fit into *Heniochus* quite well if the fourth dorsal spine were more produced or if the orbital or nuchal spines were developed (the apparent predorsal spine in Schultz's 1951 figure 94 is a printer's artifact, as can be seen by checking this figure with another, from the same drawing, published by Jordan and Evermann). But since *Heniochus* is characterized either by having the fourth dorsal spine more or less prolonged or by having hornlike processes on either the orbit or the nape, or both, *nigrirostris* may be interpreted as having been derived from the common ancestor of this assemblage, as thus heterogeneously diagnosed, for it, as the inferred ancestor presumably did, lacks the specialized processes and has the fourth dorsal spine only slightly produced (less so than in any species currently referred to *Heniochus*). Pending further studies, we suggest that *nigrirostris* be referred to *Heniochus,* and thus be named *Heniochus nigrirostris* (Gill). It might also be referred to *Hemitaurichthys,* though it differs from the species of that genus, as currently distinguished (as by Weber and de Beaufort, 1936: 15, 24–25), in having the fourth dorsal spine rather than the middle ones highest, the scales less reduced in size, and the body outline less elliptical. These are relatively minor characters. Until more trenchant differences are encountered, some doubt will pertain to the separation of *Hemitaurichthys* from *Heniochus.*

We feel considerable reserve in the reference of *nigrirostris* to *Heniochus,* because the current classification of the chaetodontines is so unsatisfactory. Furthermore, Loren P. Woods, who has studied the family extensively, has suggested (in letter) that the contrasting lateral-line characters on which we have relied may tend to intergrade. But on checking his notes on this character, for 39 species that he placed in *Chaetodon,* it appears that he found the lateral line proper incomplete and ending far above the axis of the body in all, with the tubes ending at some point under the posterior half of the soft dorsal (or, under the middle part of the second dorsal in *C. triangulum,* which is referred to *Gonochaetodon* by Weber and de Beaufort, and in *C. auriga*). In two species he found, in addition, some lateral-line structures in a separate series on the midside of the caudal peduncle (as is also true of some pomacanthines). In *C. auriga* Forskål he observed a few "pored scales" but no tubes on the peduncle, and in *C. miliaris* Quoy and Gaimard he located on the peduncle a double row of pitted scales. In the same two species we find only some neuromast pits (in part short-linear in *C. miliaris*) in the axial scale row on the peduncle and on a few scales running upward and forward, but not nearly connecting with the lateral line proper. We have found similar neuromast pits in some specimens of *C. aya,* which may also have other pits on the first scale row above the lateral line and, scatteringly, elsewhere on the body. The type of *C. falcifer* has, on the right side only, two misplaced tubes and pores on the midside before the vertical from the end of the lateral line. We do not regard such irregularities as of any great taxonomic significance.

Furthermore, Leonard P. Schultz, after examining for us a long range of species in the United States National Museum, concurs in our interpretation of the generic significance of the lateral-line character and in the provisional reference of *nigrirostris* to *Heniochus*. Examination of many published figures seems to confirm the significance of the lateral-line distinction. Certain apparent exceptions to the lateral-line character appearing on the plates in Bleeker's "Atlas" (1878) become resolved when it is seen that the names and figures were inadvertently transposed on plate 375 for *Coradion melanopus* and *Megaprotodon strigangulus* and on plate 376 for *Tetragonoptrus (Linophora) Rafflesii* and *Coradion chrysozonus*.

Forcipiger longirostris (Broussonet).

The specimens studied were one (W 55–161) taken at Isla Clarion of the Revillagigedo group by Richard H. Rosenblatt and Raymond M. Gilmore on May 7, 1955, and two (W 53–351) from Isla Socorro, of the same group, taken by Bayard H. Brattstrom on November 18, 1953.

Mouth and gape. The very peculiar mouth of this species has been duly described. In top view it is very narrow and rounded.

Lips. There are no prominent grooves or ridges on either the premaxillary or the maxillary region.

Teeth and jaws. The inner teeth in the front part of the beak are arranged in about 20 to 25 cross rows in the upper jaw and in 25 or more rows in the lower jaw.

Bony margins. The preopercular edge varies from strictly entire to incipiently denticulate. The lower border of the preorbital is smooth anteriorly, slightly to moderately denticulate posteriorly. The lower border of the suborbitals is either free (with smooth edge) or bound down. The upper and lower anterior corners of the preorbital are produced in bony lobes. When and where naked, the surface of the preorbital is more or less strongly sculptured, somewhat like the skull above each orbit. In that region, to a varying degree, the skull bones are exposed in a crescentic area, with definite bony ridges in a very complicated pattern, largely lengthwise anteriorly and dorsally, largely scroll-like posteriorly and ventrally. The actual bony rim is rough but hardly denticulate.

Squamation about orbit and muzzle. The scaleless area above the orbital rim varies considerably, but near the rim is probably always naked. On the preorbital the scales may be cycloid and confined to an anterodorsal patch, or may be ctenoid over almost the whole bone. There is a large scaleless narial fossa and most of the top of the snout anterior to the nostrils is naked; but here also the completeness of the squamation varies. The top of the beak just before the rostral fold may be either naked, like the rest of the beak, or may bear a variable patch of smooth scales. The narrow fleshy band along the upper orbital rim is scaleless, and in some specimens is concealed beneath the bony rim.

SQUAMATION OF CAUDAL FIN. The squamation of the tail fin is essentially as in *H. nigrirostris,* with a narrow basal band of ordinary overlapping scales and irregular uniserial rows extending out on the membranes, but ending short of the middle of the rays over most of the fin.

RELATIONSHIPS. It seems highly probable that *Forcipiger* was derived from a *Heniochus*-like ancestor with a primitive lateral line. Its chief modification seems to be the beaklike muzzle, which is presumably an adaptation for the procurement of food in small recesses, on the coral reefs that are spectacularly overgrazed. The interpretation of *Prognathodes* as convergent in the beaklike structure (see following section) lessens the apparent taxonomic value of the character and discounts any probable direct relationship between *Forcipiger* and such species of *Chaetodon* as *C. falcifer* and *C. aya.*

TAXONOMIC NOTES ON ATLANTIC RELATIVES OF *CHAETODON FALCIFER*

Following are the synonymies, records, and taxonomic notes for the three little-known Atlantic species that we regard as rather close relatives of *Chaetodon falcifer.*

Chaetodon aya Jordan.

(Plate II, figure 1; Plate III, figure 1.)

Chaetodon aya JORDAN, 1886: 225 (original description; distinguished by coloration; Snapper Banks, near Pensacola, Florida). EIGENMANN and HORNING, 1887: 5, 8, 18 (comparison and diagnosis, based on type; northern Gulf Coast of Florida; Pensacola). JORDAN and EVERMANN, 1898: 1673, 1676–1677 (comparisons; description; rather deep water; Gulf of Mexico). AHL, 1923: 122–123 (after Jordan and Evermann; placed in section *Chaetodontops*, misspelled *Chaedontops* on p. 111). BREDER, 1929: 215, 217 (comparisons; Gulf of Mexico; chiefly in rather deep water; "may represent the young of some other species").

PLATE II

Figure 1. *Chaetodon aya* Jordan, from half-grown specimen (C.N.H.M. 45564) 65 mm. long, trawled off northern Florida at a depth of 25–30 fathoms. The dark margins on the soft dorsal and anal fins and the dark bar on the caudal are photographic artifacts. Photo by Scripps Institution.

Figure 2. Holotype of *Chaetodon marcellae* Poll, reproduced, by permission, from Poll (1950: fig. 1).

(876)

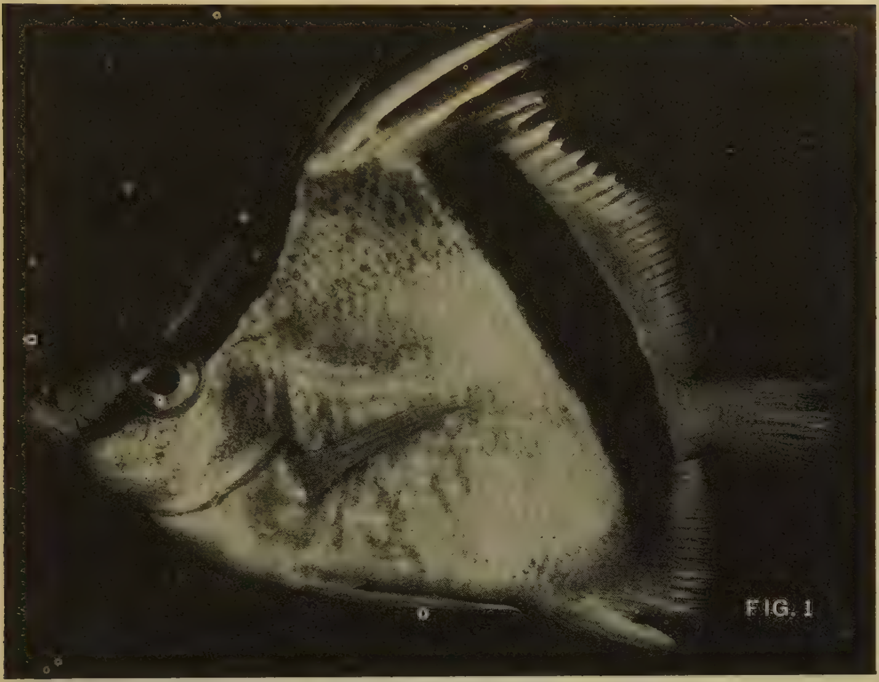

FIG. 1

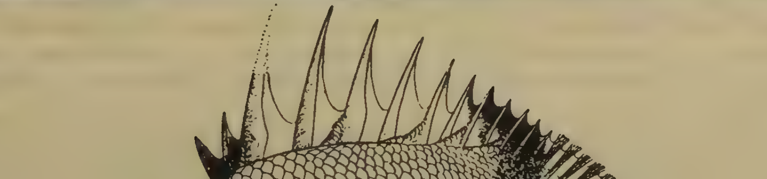

FIG. 2

Nichols and Firth, 1939: 87–88 (off North Carolina; faunal relationships; description). Hildebrand, in Longley and Hildebrand, 1941: 150–151 (Tortugas, Florida; depth distribution; color; counts and proportions; except smallest specimen, which is *C. ocellatus*).

Increased collecting in deeper water has yielded a moderate amount of material of this species, which was long known only from the holotype. Following are data on the material in the United States National Museum and the Chicago Natural History Museum. No specimens were located in the Museum of Comparative Zoology, in the Academy of Natural Sciences of Philadelphia, or in the University of Michigan Museum of Zoology. The only other specimen known is the one reported by Nichols and Firth.

U.S.N.M. 37747 (1 half-grown, 28.7 mm. in standard length, slightly over 1¼ inches to end of broken caudal): near Pensacola, Florida, Silas Stearns.—This is obviously the holotype.

U.S.N.M. 37862 (1 subadult, 63 mm. long): "W. Coast of Florida, Str. *Albatross*, 1885."—This specimen has not been mentioned in the literature. It is much too large to be the holotype.

U.S.N.M. 116850 (7 specimens, half-grown to adult, 32–82 mm.): south of Tortugas, Florida.—These are the specimens collected by William H. Longley and reported by Hildebrand (in Longley and Hildebrand, 1941: 150) as having been taken at two stations: the two largest, 70–82 mm. long, now tied together with tin tag number 12, from 39 fathoms; the five smallest, 32–69 mm. long, from 40 fathoms. These series correspond with Longley's total-length measurements of 90–102 and 41–85 mm., respectively. The eighth specimen, 27 mm. in total length, 22 mm. to caudal, which Hildebrand reported as obviously representing a third collection of the species, for which no data could be found in Longley's notes, proves to be a typical young example of *Chaetodon ocellatus*. It has been recataloged as U.S.N.M. 164519.

U.S.N.M. 131893 (1 adult, 81 mm. long): Gulf of Mexico, at *Albatross* Sta. 2365, just north of the tip of Yucatán Peninsula, at 22° 18′ 00″ N. Lat., 87° 04′ 00″ W. Long., depth 24 fathoms, bottom of white rock and coral, January 30, 1885.

U.S.N.M. 151980 (1 adult, 98.5 mm. long): Long Bay, South Carolina, trawled by the *Albatross III* on cruise 31-C, Sta. 3, tow 5 (No. 14593), from 33° 35.5′ N. Lat., 76° 53.5′ W. Long., to 33° 36′ N., 76° 51′ W., depth 40–45 fathoms, February 10, 1950.—This specimen is shown on plate III, figure 1.

U.S.N.M. 152023 (1 adult, 82 mm. long): off Carolina Beach, North Carolina, trawled by the *Albatross III* on cruise 31-A, Sta. 2, tow 2 (No. 14506), from 34° 05′ N. Lat., 76° 21′ W. Long., to 34° 01′ N., 76° 18′ W., depth 25–75 fathoms, January 19, 1950.

C.N.H.M. 45564 (2 subadults, 63–65 mm. long): Gulf of Mexico, off northern Florida, trawled by the *Oregon* at Sta. 727–728, 28° 44′ N. Lat., 85° 01′ W. Long., depth 25–30 fathoms, December 16, 1952.—One of these specimens is shown on plate II, figure 1.

C.N.H.M. 46566 (1 adult, 77 mm. long): Gulf of Mexico, off southern Florida, trawled by the *Oregon* at Sta. 33, 25° 55′ N. Lat., 83° 53′ W. Long., depth 62 fathoms, June 24, 1950.

C.N.H.M. 59898 (1 adult, 81.5 mm. long): Gulf of Mexico, off northern Florida, trawled by the *Oregon* at Sta. 916, 28° 23′ N. Lat., 84° 49′ W. Long., depth 37 fathoms, October 3, 1953.

C.N.H.M. 64369 (1 adult, 75.5 mm. long): off North Carolina, trawled by the *Combat* at Sta. C-384, 35° 54′ N. Lat., 75° 25′ W. Long., depth 75 fathoms, June 17, 1957.

Counts were made on all specimens examined, on both sides for bilateral structures. The variation found in scale counts is indicated in table 1. Following is the observed variation in ray counts, with number of specimens in parentheses: dorsal spines 13 (16), 14 (1); dorsal soft-rays, 17 (2), 18 (8), 19 (7); anal spines, 3 (17); anal soft-rays, 14 (2), 15 (14), 16 (1); principal caudal rays, 16 (1, with fourth ray from bottom more widely forked than usual). 17 (16); pectoral rays, not distinguishing unbranched and branched rays, 13—13 (1), 14—14 (10), 14—? (1), 14—15 (3), ?—15 (1); 15—15 (1); pelvic rays, I, 5—I, 5 (17).

Checking in sequence the description of *C. falcifer,* we noted the following characters on the specimens of *C. aya* listed above. The outermost pelvic soft-ray is produced into a short filament, about as in *C. falcifer.* In some specimens a few neuromast pits were observed on the scales of the midlateral row on the caudal peduncle, and on a few scales near the base of the peduncle, in a row extending upward and slightly forward. Other scales, scattered, bear such pits. Some of the scales in the row impinging above on the lateral line bear pits in some individuals. The scales across the top of the premaxillaries in front of the rostral fold vary from none to a band covering about half the exposed width of the premaxillaries. The groove from the nostrils to the rostral fold is variously scaled over. Variable also is the degree of scalelessness and of bony tuberculation on the small triangular area above and behind the bony orbital rim. The length of the gape varies from considerably less than half to a little more than half the length of the upper jaw. The bony ridge between the upper orbital border and the posterior nostril may be detached or scarcely developed, but may also extend nearly to the nostril. In most specimens the narrow fleshy upper orbital rim, more or less protruding from the bony rim, is devoid of scales, perhaps as the result of loss, because in some examples this margin bears spiny scales. In some individuals this fleshy rim is scarcely apparent. Especially in the fish preserved in alcohol, and therefore retaining guanin, the rear border or even both edges of the band above the eye and both borders of the posterior bar are abruptly margined by a light streak. In the squamation of the caudal fin *C. aya* may differ from *C. falcifer,* but the loss of scales on this fin is difficult to appraise. In a few specimens strongly ctenoid scales cover most of the caudal fin, except along the posterior margin, but in general such scales are confined to the basal part of the fin and the scales that may have been lost have not left any conspicuous pockets. Except as noted above or in table 1, and except for internal characters and detailed measurements that were not taken, the description of *C. falcifer* applies quite well to *C. aya.*

Chaetodon marcellae Poll.

(Plate II, figure 2.)

Chaetodon (Oxychaetodon) marcellae POLL, 1950 (November): 2–7, fig. 1 (original description; comparisons; 25 miles southwest of Pointe de Banda, west Africa, at 3° 57.5′ S. Lat., 10° 36.5′ E. Long.).

Chaetodon altipinnis CADENAT, "1950" (but on rear cover is indication of publication in 1951, as follows: "dépôt légal 1951, 1er trimestre, no 236"): 239, 307, 315, 318, fig. 174 (original diagnosis; Sénégal).

This interesting species was described almost simultaneously by Poll and by Cadenat. Poll has advised us that his publication actually did appear in 1950. It is obviously a very close relative of the western-Atlantic *Chaetodon aya.* In fact, the only really sharp difference that is apparent on comparing Poll's description and figure with *C. aya* lies in the position of the posterior dark bar, which originates near the end instead of near the middle of the soft dorsal and is nearly vertical instead of rather strongly oblique (compare plate II, figure 1 and plate III, figure 1, with plate II, figure 2). This is obviously an adequate distinction.

Poll referred *marcellae* to the Indo-Pacific subgenus *Oxychaetodon,* but the agreement is not close. He failed to appreciate the intimate relationship with *C. aya,* which until now has not been figured, and which Ahl referred to the subgenus *Chaetodontops.*

Chaetodon marcellae, like *C. aya* and *C. falcifer,* is obviously a relatively deep-water species. The type was taken far offshore at a depth of 85 meters, on a bottom of sandy brown mud.

This species may be included among the not inconsiderable number of essentially New World types that has become established in tropical west Africa (p. 308).

Prognathodes aculeatus (Poey).

(Plate III, figure 2.)

Chelmon aculeatus POEY, 1860 (July): 202–203 (original description; rare; Cuba).

Prognathodes aculeatus POEY, 1868: 354 (reference; characters). EIGENMANN and HORNING, 1887: 2–3 (diagnosis; relations; after Günther and Poey). JORDAN and EVERMANN, 1898: 1671 (description; synonymy; after Günther and Poey). AHL, 1923: 11 (synonomy; relations; description; West Indies; Havana, Cuba).

Prognathodus aculeatus BLEEKER, 1876a: 303, 1876b: 315, and 1877: 32, 34 (characters; genus; synonymy).

Chelmo pelta GÜNTHER, 1860 (September): 38 (original description; locality uncertain).

As the synonymy indicates, this species was originally associated with *Chelmon.* Ever since the genus *Prognathodes* was based on this species by Gill (1862: 238), it has been regarded as a close relative of the Indo-Pacific genera *Chelmon, Chelmonops,* and *Forcipiger,* obviously on the basis of the beaklike modification of the muzzle in all four genera. But those three genera have the lateral line of the *Heniochus* type (continuous to the caudal base), whereas in *Prognathodes aculeatus* the lateral line ends, as in *Chaetodon aya,* under the anterior part of the soft-dorsal fin, only about one scale row from the structural base of the rays. Since we regard the lateral-line character as of prime taxonomic significance, we interpret *Chelmon, Chelmonops,* and *Forcipiger* as modifications of a primitive member of the *Heniochus* series, and *Prognathodes* as only a parallel modification of *Chaetodon.*

In fact, *Prognathodes aculeatus* appears to have arisen from *Chaetodon aya* or from a very similar, related species. This view was anticipated by Hildebrand in his estimate of *C. aya* as being rather intermediate between more ordinary species of *Chaetodon* and *Prognathodes.* The many points of resemblance between *Prognathodes aculeatus* and *Chaetodon aya* can hardly be fortuitous. In its beaklike modification *P. aculeatus* merely exaggerates the characters of *C. aya.* In squamation, body form, extremely strong and greatly excised fin spines, and other respects, the two species are remarkably alike (see plate II). Even the fin formula is approximately the same (the type of *P. aculeatus* has XIII, 19 dorsal, III, 15 anal, 17 caudal, 14—14 pectoral, and I, 5 — I, 5 pelvic rays. Each species has finely denticulate bones around the orbit and has the muzzle well scaled forward to the rostral edge, with a more or less scaleless groove from nostril to the rostral fold, and the chin well scaled almost to its front. Each has the preopercular and scapular edges finely denticulate. In each the lateral line ends under the anterior part of the soft dorsal, as is noted above. The dark band through the eye is very similar.

Although the two forms are so much alike, there can be no doubt that *P. aculeatus* is at least specifically distinct from *C. aya.* It differs from *C. aya* not only in the much more modified beak, as described below, but also in other respects. For instance, the posterior dark bar is apparently lacking, and the caudal peduncle is slenderer (least depth is less instead of more than one-fourth the length of the head).

In view of the definite approach to *Prognathodes* of some species of *Chaetodon,* notably *C. falcifer, C. aya,* and *C. marcellae,* some ichthyologists may not wish to retain *Prognathodes* as a distinct genus. The only known differences lie in the beak structure. The jaws are slenderer and more produced. The upper lip instead of covering much of the premaxillaries is confined to the extreme edge, leaving nearly all of the exposed premaxillary

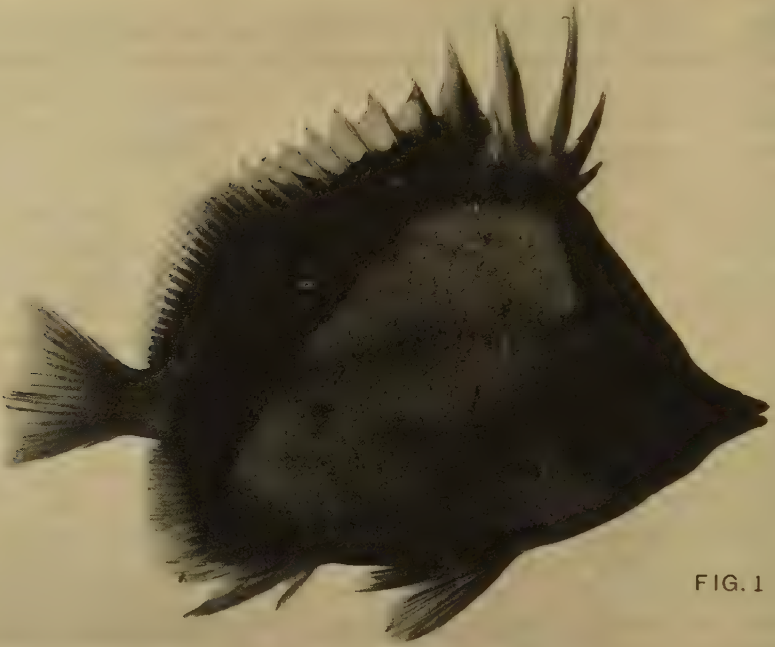

FIG. 1

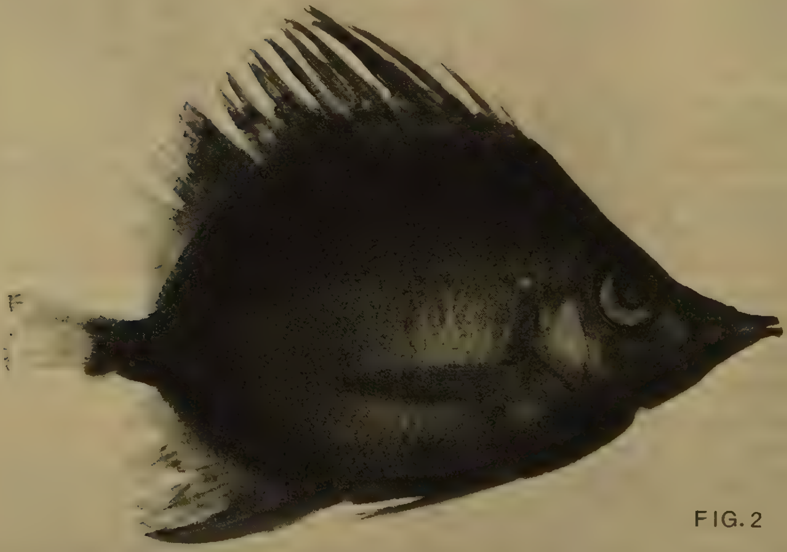

FIG. 2

(882)

surface smooth, bony, and scaleless, rather than rough, fleshy, and more or less scaled. Pending a more general study of the whole group, we suggest that *Prognathodes* be retained as a monotypic genus.

The only specimen of *P. aculeatus* that we have located is U.S.N.M. 4716. It is labelled as from "Cuba, Prof. F. Poey," and it bears Felipe Poey's original number 56. Although it seems slightly smaller than the specimen described by Poey (61 mm. in standard length, 73 mm. to the somewhat broken tip of the caudal, rather than 80 mm.) it is regarded as the holotype of *Chelmon aculeatus* Poey, and has been so designated in the National Museum records (Poey's measurement may have been rounded out to 80 mm. and the specimen may have shrunk slightly since he measured it; restored, the total length would probably slightly exceed 75 mm.). The specimen was entered as *Prognathodes pelta* and is no doubt the one Gill examined when he described the genus, designating *P. pelta* as the type species. It is shown as plate III, figure 2.

SYSTEMATIC AND ZOOGEOGRAPHICAL CONCLUSIONS

Chaetodon falcifer is described as a strikingly distinct new species of butterflyfish from rather deep water at Guadalupe Island, an oceanic island in the Pacific Ocean well off the coast of Baja California. It is regarded as probably an endemic species, in an island fauna marked by a high incidence of endemism. It is, however, a deep-water form, which may have escaped attention elsewhere.

Whether endemic or not on Guadalupe Island, *C. falcifer* ranks as one of the tropical elements in the mixed tropical and temperate fauna of this island. Currently, it is probably the northernmost representative of the Chaetodontidae in the eastern Pacific. There are apparently reliable indications, however, that *Chaetodon humeralis* ranged north to San Diego during the warm period approximately one hundred years ago.

The closest relatives of *C. falcifer* appear, on the basis of similar morphology and of the distinctively deep-water habitat, to be two Atlantic species, *C. aya* of the western North Atlantic and *C. marcellae* of tropical west Africa. The West Indian *Prognathodes aculeatus* appears to be a derivative of *C. aya* (or of a closely related species), differing in the more extreme modification of the beak. These circumstances illustrate two zoogeographical

---

PLATE III

Figure 1. ***Chaetodon aya*** **Jordan, from adult (U.S.N.M. 151980) 98.5 mm. long, trawled off Long Bay, South Carolina, at a depth of 40–45 fathoms. Photo by United States National Museum.**

Figure 2. Holotype of ***Chelmon aculeatus*** **Poey =** ***Prognathodes aculeatus*** **(Poey), a specimen (U.S.N.M. 4716) 61 mm. in standard length. Photo by United States National Museum.**

tendencies that are being increasingly indicated by critical taxonomic studies; namely, (1) the tendency for New World fishes to possess a marked independence and integrity, indicative of lines of evolution essentially distinct from those of related Old World types, and (2) the tendency for New World types to be sparingly but definitely represented in the fauna of tropical west Africa.

In the classification of the Chaetodontidae far too much emphasis has been placed on the beaklike modification, such as is exhibited to a moderate degree by the species *C. falcifer, C. aya,* and *C. marcellae,* and, much more strikingly, by *Prognathodes aculeatus.* Thus, *P. aculeatus* has been consistently associated with the recognized genera *Chelmon, Chelmonops,* and *Forcipiger* because of the similar beakline feature, but those genera have a more primitive and more complete lateral line and appear to have stemmed from the *Heniochus* group, whereas *Prognathodes* is rather clearly a derivative of *Chaetodon.* Genera in several other families of coral-reef fishes, for example, *Lo* among the Siganidae and *Gomphosus* among the Labridae, have developed a similar beak, which seems to be a modification for plucking food out of generally inaccessible crevices, on the notably overgrazed coral reefs. This is one of many examples among fishes of a nutritional character that has been overemphasized in taxonomy, but which is much subject to parallel and convergent evolution.

It seems rather clear that the beak was independently evolved in the chaetodontines with an incomplete lateral line and in those with a complete line. The species *Chaetodon falcifer, C. aya, C. marcellae,* and *Prognathodes aculeatus* probably constitute one such phyletic line, but other species of *Chaetodon* with an incipient beak, such as those referred to subgenus *Oxychaetodon,* are likely of separate origin. Of the beaked chaetodontines with a complete lateral line, we see no assurance that *Chelmon, Chelmonops,* and *Forcipiger* represent a single natural group. Certainly Bleeker, Ahl, Jordan, and other students have erred in classing together all chaetodontids with a beak.

The lateral-line character appears to be of greater significance as an index of phylogeny in the group. On the basis of its simpler, more complete and more primitive lateral line, the eastern Pacific species *Chaetodon nigrirostris* is referred to the *Heniochus* series, tentatively to the genus *Heniochus. Heniochus nigrirostris* and *Forcipiger longirostris* are the only New World members of this series, and in the western hemisphere they are confined to the Pacific. They presumably represent, respectively, relatively old and new migrants, from the vast Indo-Pacific fauna, that have crossed the east-Pacific barrier. The Chaetodontinae as a whole are chiefly Indo-Pacific.

On these interpretations the high specialization of most species of *Heni-*

(884)

ochus and of *Chelmon, Chelmonops,* and *Forcipiger* is coupled with a basically primitive feature in lateral-line structure. This view is consistent with the increasingly evident generalization that specialized and primitive characters tend to be combined.

Various anatomical details will apparently prove of value in the much-needed generic revision of the family. Some characters of this sort are pointed out for the four species of chaetodontines now known from the eastern Pacific.

The lateral-line distinctions are repeated in the Pomacanthinae, and it is conceivable that they may be of greater phylogenetic significance than the enlarged head spines recognized as diagnostic of that subfamily. The primary divergence in the family may have involved the lateral-line character, and each division may have developed one or more enlarged head spines. If this view should prevail, the Pomacanthinae would appear to be a polyphyletic group, presumably not worthy of subfamily recognition. We see no justification for the elevation of the group to family rank (Pomacanthidae), as proposed by Smith (1955), even though we assume it to be a natural assemblage.

Obviously there has been independent and convergent evolution either in the head-spine or lateral-line characters. On available evidence a decision as to which character is of more primary significance seems arbitrary. Such a situation is often encountered when taxonomic evidence in ichthyology is viewed afresh and critically.

LITERATURE CITED

AHL, ERNST

1923. Zur Kenntnis der Knochenfischfamilie Chaetodontidae, insbesondere der Unterfamilie Chaetodontinae. *Archiv für Naturgeschichte,* Abt. A, 89 (5):1–205, pls. 1–3.

BLEEKER, PIETER

1876a. Systema percarum revisum. Pars II. *Archives Néerlandaises des Sciences exactes et naturelles,* sér. B, Sciences naturelles, 11:289–340.

1876b. Notice sur les genres et sur les espèces des Chétodontoïdes de la sous-famille des Taurichthyiformes. *Verslagen en Mededeelingen der Koninklijke Akademie van Wetenschappen, Amsterdam, Afdeeling Natuurkunde,* ser. 2, 10(3):308–320.

1877. Révision des espèces insulindiennes de la famille des Chétodontoïdes. *Verhandelingen der Koninklijke Akademie van Wetenschappen, Amsterdam, Afdeeling Natuurkunde,* 17:1–174.

1878. Atlas ichthyologique des Indes Orientales Néerlandaises. Vol. 9:1–80, pls. 355–420. Fréderic Muller, Amsterdam.

BLOCH, MARC ÉLIÉSER

1796. Ichthyologie ou histoire naturelle des Poissons. Part, 4: 969–1291; part 6:pls. 109–216. Berlin.

BREDER, CHARLES M., JR.

1929. Field book of marine fishes of the Atlantic coast from Labrador to Texas. i–xxxvii, 1–332, many figs. G. P. Putnam's Sons, New York and London.

BRIGGS, JOHN C.

1955. A monograph of the clingfishes (order Xenopterygii). *Stanford Ichthyological Bulletin*, 6:i–iv, 1–224, figs. 1–114, maps 1–15.

CADENAT, J.

"1950" (1951). Poissons de mer du Sénégal. Initiations africaines, III. 1–345, figs. 1–241. Institut français d'Afrique Noir, Dakar.

CUVIER and VALENCIENNES

1831. Histoire naturelle des Poissons. Vol. 7:i–xxix + 5 + 1–531, pls. 170–208. Paris.

EIGENMANN, CARL H., and JENNIE E. HORNING

1887. A review of the Chaetodontidae of North America. *Annals of the New York Academy of Sciences*, 4(7–8):1–18.

EKMAN, SVEN

1953. Zoogeography of the sea. i–xiv, 1–417, figs. 1–121. Sidgwick and Jackson, Limited, London.

FOWLER, HENRY W.

1928. The fishes of Oceania. *Memoirs of the Bernice P. Bishop Museum*, 10: i–iii, 1–540, figs. 1–82, pls. 1–49.

FOWLER, HENRY W., and BARTON A. BEAN

1929. The fishes of the series Capriformes, Ephippiformes, and Squamipennes, collected by the United States Bureau of Fisheries Steamer "Albatross," chiefly in Philippine seas and adjacent waters. *United States National Museum, Bulletin* 100, Vol. 8:i–xi, 1–352, figs. 1–25.

FRASER-BRUNNER, A.

1933. A revision of the chaetodont fishes of the subfamily Pomacanthinae. *Proceedings of the Zoological Society of London*, 1933:543–599, figs. 1–29, pl. 1.

1945. On the systematic position of a fish, *Microcanthus strigatus* (C. & V.). *Annals and Magazine of Natural History*, ser. 11, 12(91):462–468, figs. 1–3.

GILBERT, CHARLES H., and EDWIN C. STARKS

1904. The fishes of Panama Bay. *Memoirs of the California Academy of Sciences*, 4:1–304, pls. 1–33.

(886)

GILL, THEODORE

1862. Remarks on the relations of the genera and other groups of Cuban fishes. *Proceedings of the Academy of Natural Sciences of Philadelphia*, [vol. 14] 1862(5):235–242.

GIRARD, CHARLES

1858. Fishes. General report upon the zoology of the several Pacific railroad routes. Part 4:i–xiv, 1–400, 21 pls. *In* Reports of explorations and surveys . . . for a railroad from the Mississippi River to the Pacific Ocean, vol. 10. U. S. Senate Ex. Doc. no. 78, 33d Congress, 2d Session, Washington.

GÜNTHER, ALBERT

1860. Catalogue of the acanthopterygian fishes in the collection of the British Museum. Squamipinnes, Cirrhitidae, Triglidae, Trachinidae, Sciaenidae, Polynemidae, Sphyraenidae, Trichiuridae, Scombridae, Carangidae, Xiphiidae. Vol. 2:i–xxi, 1–548, 1 fig. London.

1868. An account of the fishes of the states of Central America, based on collections made by Capt. J. M. Dow, F. Godman, Esq., and O. Salvin, Esq. *Transactions of the Zoological Society of London*, 6(7):377–494, pls. 63–87.

HERRE, ALBERT W., and HERACLIO R. MONTALBAN

1927. The Philippine butterfly fishes and their allies. *The Philippine Journal of Science*, 34(1):1–113, pls. 1–24.

HUBBS, CARL L.

1946. An arm protractor for the precise measurement of angles in systematic ichthyology. *Copeia*, 1946 (2):79–80, fig. 1.

1948. Changes in the fish fauna of western North America correlated with changes in ocean temperatures. *Journal of Marine Research*, 7(3): 459–482, figs. 1–6.

HUBBS, CARL L., and KARL F. LAGLER

1952. Fishes of the Great Lakes region. *Cranbrook Institute of Science, Bulletin* 26:i–xi, 1–186, figs. 1–251 + 38, 26 col. pls., 1 map.

JORDAN, DAVID S.

1886. Notes on some fishes collected at Pensacola by Mr. Silas Stearns, with descriptions of one new species *(Chaetodon aya)*. *Proceedings of the United States National Museum*, 9:225–229.

JORDAN, DAVID STARR, and BARTON WARREN EVERMANN

1898. The fishes of North and Middle America: a descriptive catalogue of the species of fish-like vertebrates found in the waters of North America, north of the Isthmus of Panama. *United States National Museum, Bulletin* 47(2):i–xxx, 1241–2183, 1 fig.

1900. The fishes of North and Middle America. . . . *United States National Museum, Bulletin* 47(4):i–ci, 3137–3313, pls. 1–392.

JORDAN, DAVID STARR, and BARTON WARREN EVERMANN—Cont.

1905. The shore fishes of the Hawaiian Islands, with a general account of the fish fauna. *Bulletin of the United States Fish Commission*, for 1903, 23 (1): i–xxviii, 1–574, figs. 1–229, pls. 1–65, col. pls. 1–73.

JORDAN, DAVID STARR, and HENRY W. FOWLER

1902. A review of the Chaetodontidae and related families of fishes found in the waters of Japan. *Proceedings of the United States National Museum*, 25:513–563, figs. 1–6.

JORDAN, DAVID STARR, and ALVIN SEALE

1906. The fishes of Samoa. Description of the species found in the archipelago, with a provisional check-list of the fishes of Oceania. *Bulletin of the [United States] Bureau of Fisheries*, [for] 1905, 25:173–455, figs. 1–111, pls. 33–37, col. pls. 38–53.

KENDALL, WILLIAM C., and EDMUND L. GOLDSBOROUGH

1911. Reports on the scientific results of the expedition to the tropical Pacific, in charge of Alexander Agassiz, by the U. S. Fish Commission Steamer "Albatross," from August, 1899, to March, 1900, Commander Jefferson S. Moser, U.S.N., commanding. XIII. The shore fishes. *Memoirs of the Museum of Comparative Zoölogy at Harvard College*, 26:241–344, pls. 1–7.

LONGLEY, WILLIAM H., and SAMUEL F. HILDEBRAND

1941. Systematic catalogue of the fishes of Tortugas, Florida, with observations on color, habits, and local distribution. *Carnegie Institution of Washington Publication* 535, *Papers from the Tortugas Laboratory*, 34: i–xiii, 1–331, pls. 1–34.

MEEK, SETH E., and SAMUEL F. HILDEBRAND

1928. The marine fishes of Panama. *Field Museum of Natural History, Publication* 249, Zool. ser., 15(3): xxv–xxxi, 709–1045, pls. 72–102.

MUNRO, IAN S. R.

1955. The marine and fresh water fishes of Ceylon, i–xvi, 1–351, figs. 1–19, pls. 1–56. Department of External Affairs, Canberra.

MYERS, GEORGE S.

1941. The fish fauna of the Pacific Ocean, with especial reference to zoögeographical regions and distribution as they affect the international aspects of the fisheries. *Proceedings of the Sixth Pacific Science Congress of the Pacific Science Association Held at the University of California, Berkeley, Stanford University, and San Francisco, July 24th to August 12th, 1939*, 3, "1940":201–210.

NICHOLS, J. T., and F. E. FIRTH

1939. Rare fishes off the Atlantic coast, including a new grammicolepid. *Proceedings of the Biological Society of Washington*, 52:85–88, fig. 1.

POEY, FELIPE

1860. Memorias sobre la historia natural de la isla de Cuba, acompañadas de sumarios latinos y extractos en francés. Vol. 2(3):97–336, pls. 10–12, 14, Habana.

(888)

POEY, FELIPE—Cont.

1868. Synopsis piscium cubensium. Repertorio fisico-natural de la isla de Cuba, 2:279–484 (reprinted, in same year, with same pagination and with added title, Catálogo razonado de los peces de la isla de Cuba).

POLL, MAX

1950. Description de deux Poissons percomorphes nouveaux des eaux cotières de l'Atlantique Sud (1948–1949). *Institut royal des Sciences naturelles de Belgique, Bulletin* 26(49):1–14, figs. 1–2.

SCHULTZ, LEONARD P.

1951. *Chaetodon tinkeri*, a new species of butterflyfish (Chaetodontidae) from the Hawaiian Islands. *Proceedings of the United States National Museum*, 101:485–488, fig. 94, pl. 15.

SMITH, J. L. B.

1955. The fishes of the family Pomacanthidae in the western Indian Ocean. *Annals and Magazine of Natural History*, ser. 12, 8(89):377–384, pls. 4–5.

STEARNS, SILAS

1887. The fishing-grounds of the Gulf of Mexico belonging to the United States. 55–58, charts 16–17. *In* Fisheries and Fishery Industries of the United States, by George Brown Goode and associates. Sect. 3. United States Commission of Fish and Fisheries, Washington.

WEBER, MAX, and L. F. DE BEAUFORT

1936. The fishes of the Indo-Australian Archipelago. Perciformes (continued). Families: Chaetodontidae, Toxotidae, Monodactylidae, Pempheridae, Kyphosidae, Lutjanidae, Lobotidae, Sparidae, Nandidae, Sciaenidae, Malacanthidae, Cepolidae. Vol. 7:i–xvi, 1–607, figs. 1–106. E. J. Brill, Leiden.

WOODS, LOREN P.

1953. Subfamily Chaetodontinae. 566–596, pls. 49–58. *In* Fishes of the Marshall and Marianas islands: Asymmetrontidae through Siganidae, by Leonard P. Schultz and collaborators, *United States National Museum, Bulletin* 202, vol. 1.

SOME OBSERVATIONS ON CARDIAC AUTOMATISM IN CERTAIN ANIMALS*

By DAVID JENSEN‡

(From the Division of Marine Biology, The Scripps Institution of Oceanography, University of California, La Jolla)

(Received for publication, May 12, 1958)

ABSTRACT

Certain aspects of the acetylcholine hypothesis of cardiac automaticity have been tested *in vitro* with spontaneously beating cardiac tissue from rabbits, rats, clams, and hagfish. The beat of atria from rabbits and rats may be depressed or excited by acetylcholine, depending upon the state of the tissue. Proguanil and cocaine inhibition of the beat in the rat may be antagonized by acetylcholine so that reversal of the depression occurs. The action of acetylcholine on the hearts of clams was found to be strictly inhibitory. Proguanil and cocaine, in contrast to their action on mammalian atria, exert a stimulatory effect on the heart of the molluscs studied. In fact, cocaine stimulated these hearts when they were inhibited by acetylcholine.

Studies on the non-innervated hagfish heart revealed that this tissue is completely insensitive to the action of acetylcholine. Extracts prepared from beating hearts of this species will accelerate hypodynamic hearts of the hagfish as well as of the mussel. An extract of the neurogenic lobster heart was without effect on the hagfish heart. Proguanil was likewise ineffective in concentrations which produced inhibition and excitation in rat and clam hearts respectively.

It was concluded that acetylcholine does not play a role in the myogenic automatism of all species, and that another mechanism is responsible is suggested on the basis of results obtained in the hagfish hearts.

INTRODUCTION

Cardiac automaticity is a prime example of the spontaneous rhythmic contractility exhibited by many tissues throughout the animal kingdom. The type of pacemaker responsible for this activity is generally considered to be in one of two categories: neurogenic or myogenic, depending upon the source of the

---

* This study was supported jointly by the Los Angeles County Heart Association and the Riverside County Heart Association; the author is happy to acknowledge their magnanimous contributions to this project, as well as that of Mr. E. M. Stolaroff who made a generous gift to the Los Angeles County Heart Association for partial support of this work.

‡ Established Investigator, Riverside County Heart Association.

J. Gen. Physiol., 1958, Vol. 42, No. 2

Contributions from the Scripps Institution of Oceanography, New Series, No. 1049

Reproduced by Permission

impulse driving the contractile machinery. The classic experiments on the origin of the heart beat in the ganglionic tissue of *Limulus polyphemus* (Carlson, 1904 *a*) may be cited to illustrate neurogenic automatism, whereas the early chick embryo heart illustrates a non-innervated yet spontaneously contractile organ (Patten, 1949). In the latter case, the myocardial elements may be considered chemoreceptors as well as effectors, and thus are individually sensitive to the effects of locally produced metabolites.

Little is known about the detailed mechanism of stimulus production in myogenic tissues. Although a number of workers suggested that acetylcholine might play a role in this process, none was able to demonstrate an excitatory as well as an inhibitory action of this compound in mammalian tissues. It remained for Burn and his colleagues at the University of Oxford to investigate this problem systematically. During a study of the pharmacological properties of the antimalarial proguanil (paludrine), Burn and Vane (1949) noted that under the influence of this compound, acetylcholine inhibition of the spontaneous beat of isolated rabbit auricles was gradually changed to a stimulatory action. Next, in order to eliminate the effect of any drug on the heart, auricles were allowed to beat *in vitro* until they became quiescent (Bülbring and Burn, 1949). In 63 per cent of the experiments it was possible to restart the auricular beat with acetylcholine. In addition, studies on the choline acetylase system indicated that enzyme activity, hence acetylcholine synthesis, was directly related to mechanical activity. Observations on the ciliary movement in frog esophageal membrane, rabbit trachea, and gill plates of *Mytilus edulis* (Kordik, Bülbring, and Burn, 1952; Bülbring, Burn, and Shelley, 1953) also led to the conclusion that acetylcholine produced locally in the tissue was responsible for initiating the rhythmic activity. These and other studies resulted in the hypothesis that acetylcholine is a local hormone, and that the spontaneous activity of the tissue is dependent upon the balance between a rhythmic synthesis by choline acetylase and destruction by cholinesterase of the compound (Burn, 1953; Burn and Kottegoda, 1953; Bülbring, Kottegoda, and Shelley, 1954).

In view of the fundamental importance of this hypothesis, it was considered worthwhile to confirm some of these observations, and to extend these studies to several other species. The present report deals with experiments conducted upon the isolated myocardial tissue of rabbits, rats, clams, and hagfish. Clams (*Venus mercenaria*) were chosen because of the myogenicity of the beat (Krijgsman and Divaris, 1955) and the extreme sensitivity to acetylcholine exhibited by their hearts (Welch and Taub, 1948). Hagfish (*Polistotrema stouti*) were of great interest, especially as the systemic heart of the adult is extrinsically non-innervated and has no intrinsic ganglionic tissue (Greene, 1902; Carlson, 1904 *b*; Augustinsson *et al.*, 1956). Since this is the only chordate known which exhibits this condition as an adult, these primitive fish afford a unique opportunity for investigation of myogenic automaticity in an organ sufficiently large to permit gross experimentation.

General Methods

All studies were performed on spontaneously beating isolated heart preparations. A double-walled glass cylinder served as the heart chamber; water circulating from a constant temperature bath through the outer jacket kept the medium surrounding the heart at ± 0.1°C. during any study. The hearts were washed with fresh medium of appropriate temperature through an inlet located in the bottom of the cylinder. A constant volume of 10.0 ml. was maintained, and the medium was gassed from the bottom of the chamber.

The rate and isotonic force of the heart beat were recorded continuously by means of a Statham strain gage coupled to an Esterline-Angus recording milliameter.

If a study extended over a period of several days, fresh medium was prepared daily. Sterile technique was not employed. However, in the mammalian experiments inclusion of small amounts of penicillin, or tetracycline hydrochloride (Pfizer) in the solution was found to be helpful in combating bacterial action. No effects on the heart beat were noted when these compounds were included.

Drugs were made up as concentrated stock solutions immediately before use and were equilibrated to the temperature of the bath before addition. Prior to adding any compound to the chamber, an equivalent volume of fluid was withdrawn; concentrations given are after dilution. Throughout these studies the concentrations of the drugs are expressed on a weight:volume basis; thus 1 mg./10 ml. = $1:10^4$ (or 1:10,000). The weights employed were of the salts.

The following compounds were employed; their sources are also indicated: acetylcholine iodide, Eastman Organic Chemicals, Rochester, New York; cocaine hydrochloride, New York Quinine and Chemical Works, Inc., New York; ergonovine maleate, Mann Research Laboratories, New York; lysolecithins (50 per cent α'-monooleyl L-α-glycerylphosphoryl choline and 50 per cent β-monooleyl L-α-glycerylphosphoryl choline), Dr. Erich Baer, University of Toronto; proguanil hydrochloride (paludrine: *l*-(*p*-chlorophenyl)-4-isopropylbiguanide hydrochloride), Ayerst Laboratories Inc., New York; serotonin creatinine sulfate, Abbott Laboratories, Chicago.

This report deals with experiments carried out on a total of 104 individual heart preparations. Whenever feasible, several studies were carried out on the same heart; thus the experimental and control observations were recorded on the same preparation.

RESULTS

The hearts employed for these studies were obtained from seven species which embraced two animal phyla: Chordata and Mollusca.

Mammalia

(*a*) *Rabbit Experiments.*—Young adult male New Zealand white rabbits were used for these studies; the average body weight was 3.5 kg.

The atria were prepared for recording by the method of Bülbring, Kottegoda, and Shelley (1954), and then placed in the equilibrated chamber containing Locke's solution. The gas used in all experiments was 95 per cent O_2–5 per cent CO_2, and the pH of the medium was 7.4. Excellent spontaneous beat of the isolated auricles was obtained in all cases reported here, and this could be maintained for from 24 to 48 hours. Thirteen rabbits were used.

The purpose of these experiments was to determine whether or not acetylcholine would stimulate as well as inhibit the heart beat. The preparations were allowed to become hypodynamic spontaneously *in vitro* without addition of drugs or any other agents.

In eight out of thirteen preparations (62 per cent) a clear-cut stimulatory response to acetylcholine was observed. Of the twenty-eight positive responses recorded, this effect ranged from regularization of the beat, increases in rate and/or force, to restarting of completely quiescent preparations. An example of the latter case is illustrated in Fig. 1. Twenty-four and one-half hours after the atria were placed in the bath they had been at a standstill for several hours. Addition of acetylcholine, 1:10^6, to the bath caused resumption of the beat after about 1 minute. Approximately 5 minutes after the contractions started the acetylcholine was washed out and the beat stopped. Alternate treatment of this preparation with acetylcholine (1:10^7 to 1:10^5) and washing with fresh medium enabled the heart to be started and stopped six more times. In one case it was restarted (after an interval of 1½ hours) by acetylcholine, 1:10^6, and it beat steadily for 2 hours, only to stop again when the acetylcholine was removed. During this interval, further additions of acetylcholine (to a final concentration of 3:10^6) did not significantly alter either the rate or force of the beat.

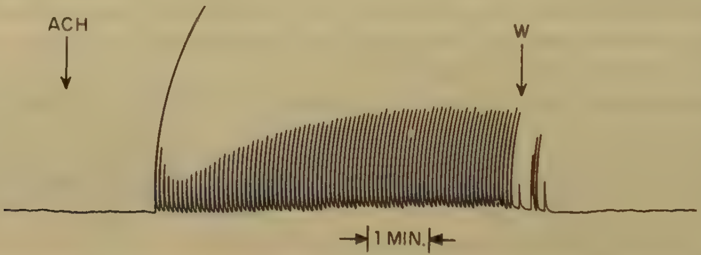

FIG. 1. Stimulatory effect of ACH, 1:10^6, on spontaneously hypodynamic rabbit atria. (The following abbreviations are used in the figures: ACH = acetylcholine; C = cocaine; P = proguanil; HHE = hagfish heart extract; W = wash.)

It is worth noting that in freshly extirpated atria, acetylcholine, 1:10^7 to 1:10^5, exerted only an inhibitory effect on rate and force; later, in the same preparation an identical dose of the compound was ineffective or only slightly so, while still later the effect was changed to a positive response.

The temperature at which these studies were carried out (20°C.) apparently

(894)

influenced the results only insofar as maintenance of the integrity of the auricles was concerned; that is, when the auricles were allowed to beat continuously at 28°C., their survival as evidenced by a later positive response to acetylcholine administration was less likely. In contrast, when the temperature of the medium was lowered, say to 20°C., for at least half of the time during which they were beating *in vitro*, positive results were much more likely.

These results are in good agreement with those reported earlier (Bülbring and Burn, 1949).

(*b*) *Rat Experiments.*—Adult male rats (350 to 400 gm.) of the Long-Evans strain were used for these studies. The atria were prepared for recording as in the rabbit experiments, except that Tyrode's solution pH 7.5 (Holtz and Westermann, 1955) was used for the medium.

Auricular preparations from twenty animals were employed. In addition to spontaneous hypodynamia (nine experiments), proguanil hydrochloride (nine experiments) and cocaine hydrochloride (two experiments) were used to limit the contractility of the atria.

In the spontaneously hypodynamic preparations acetylcholine stimulation was observed in five of the nine atria (55 per cent). With the same concentration of acetylcholine, the effect ranged, as in the rabbit, from initial inhibition, to no effect, to a definite increase in rate and force as the experiment progressed. The concentrations of acetylcholine studied ranged from $1:10^7$ to $1:10^5$. Again it was noted that maintenance of the preparations for long periods at about 28°C. apparently exerted a deleterious effect on their continued survival and it was found that a temperature of 20°C. was most effective.

In the experiments using proguanil, it was found when this compound in a concentration of $1:10^4$ was allowed to act on the beating auricles from 1 to 2 hours, that the contractions would cease. (Normally under these conditions the preparations would beat with undiminished vigor for about 4 hours.) In six of the nine preparations studied (67 per cent), it was possible to restart the auricles after periods of quiescence ranging from 15 minutes to 1 hour by the addition of acetylcholine, $1:10^7$ to $1:10^5$ (twelve observations).

In two experiments, using fresh auricular preparations, it was found that cocaine would inhibit and acetylcholine would restart the beat. This is illustrated in Fig. 2. Approximately 30 minutes after the experiment was started, addition of acetylcholine, $1:10^6$, produced a 50 per cent reduction in the force of the beat. After washing out the acetylcholine and allowing sufficient time for recovery (15 minutes), cocaine hydrochloride, $1:10^4$, was added. Two and one quarter minutes later, the heart came to a complete standstill, and remained quiescent for 45 minutes at which time acetylcholine, $2:10^6$, was added. Within 30 seconds, resumption of the beat occurred, and a second addition of acetylcholine, $2:10^6$, 3 minutes after contractions began produced no further effect. Fifteen minutes later, cocaine and acetylcholine were both washed out, and the beat continued. These observations were repeated eight more times on this heart and it was also noted that after the beat was restored, acetylcholine, 1:10^6, would inhibit the beat once again, in a manner similar to the observation recorded in Fig. 2 A.

These results were confirmed in a second atrial preparation.

Pelecypoda

Since the spontaneously beating hearts of certain marine molluscs, notably the quahog (*Venus mercenaria*), are extraordinarily sensitive to inhibition by very low doses of acetylcholine (Welch and Taub, 1948), it appeared of interest to test this compound for excitatory activity on hypodynamic clam hearts.

For these studies, twenty-five heart preparations from *V. mercenaria*, two from the Pismo clam (*Tivela stultorum*), and one from a gaper clam (*Schizothaerus nuttalli*) were used.

The hearts were prepared for recording by the method of Welch and Taub (1948). Survival *in vitro* of from 1 to 3 days was obtained by placing the isolated hearts in sea water buffered to pH 7.6, aerated with 95 per cent O_2–5 per cent CO_2, and maintained at 16°C.

As in the rat auricles, paludrine, 1:10^4, was used in seven experiments in an attempt to render the spontaneously beating ventricles hypodynamic. In marked contrast to the rat however, it was found in all cases that this compound actually stimulated the rate and force of these preparations. In fact, proguanil would induce a regular beat in an almost quiescent heart. This observation is illustrated in Fig. 3 in which a weakly beating preparation was markedly stimulated by the addition of 1 mg. of proguanil to the bath. In view of this finding, proguanil was useless as an agent for limiting the spontaneous activity of these hearts.

On twenty spontaneously hypodynamic clam hearts, acetylcholine (1:10^{11} to 1:10^6) was completely ineffective in producing or stimulating a beat (thirty-eight observations). The threshold for inhibition in a fresh heart was about 1:10^{10} in *Venus*, and about 5:10^9 in *Tivela* and *Schizothaerus*. In all species studied, cocaine (1:10^3, 5:10^3) and ergonovine maleate (1:10^5, 1:10^6) were markedly stimulatory.

Fig. 4 illustrates a marked inhibition by acetylcholine, 1:10^8, on an isolated ventricle of *T. stultorum*. While the ventricle was inhibited by this compound, addition of cocaine hydrochloride (1:10^4) in the presence of the acetylcholine induced a sharp stimulation of the force of the beat with a concomitant slight diminution of rate. These results are in diametric opposition to those obtained in the rat auricle where cocaine inhibited and acetylcholine restarted the beat.

Cyclostomata

In view of the contrast between the results obtained with acetylcholine on mammalian and molluscan hearts, it was considered of interest to test the effect

(896)

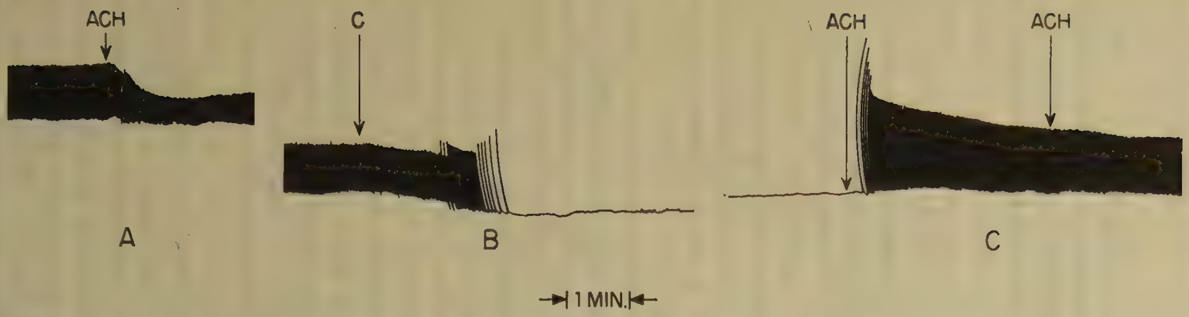

FIG. 2. Effects of ACH and C on spontaneously beating rat atria. A, inhibition produced by ACH, 1:10⁶. B, after wash and 15 minutes' recovery, C, 1:10⁴, induced cessation of the beat. C, 45 minutes later (no wash), ACH, 2:10⁶, stimulated the preparation; a second addition of ACH, 2:10⁶, after 3.5 minutes had no effect.

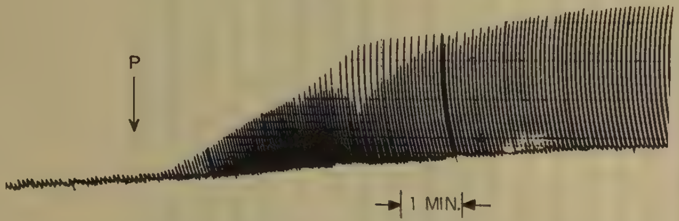

FIG. 3. Stimulatory effect of P, 1:10⁴, on the isolated heart of the quahog clam, *Venus mercenaria*.

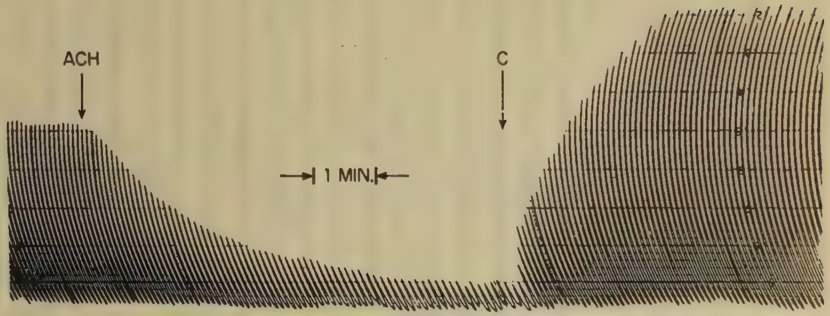

FIG. 4. Inhibition by ACH, 1:10⁸, and stimulation by C, 1:10⁴, in an isolated heart of the Pismo clam, *Tivela stultorum*.

of this compound on hypodynamic contractile tissue known to be aneural. Survey of the literature revealed that the systemic heart of a primitive marine chordate, the hagfish, lacked extrinsic or intrinsic innervation (Greene, 1902; Carlson, 1904 *b*; Augustinsson *et al.*, 1956), and thus was admirably suited for this investigation.

The California hagfish, *Polistotrema stouti*, was used. As 15°C. is the approximate environmental temperature of these animals, it was chosen for the experiments. Average size of the animals was about 35 cm., body weight 45 gm.

Although the hagfish possesses three hearts, only the systemic organ was employed in this investigation. The preparation consisted of the joined auricle and ventricle.

The isolated hearts would beat spontaneously for 1 to 3 days in any of several media: whole sea water, sea water diluted one-third by distilled water, or the artificial sea water of Lyman and Fleming (1940). Later, an artificial medium was devised empirically which contained: NaCl, 20.0 gm.; $MgCl_2 \cdot 6H_2O$, 5.0 gm.; $CaCl_2$ (anhydrous), 2.25 gm.; KCl, 0.70 gm., made up to 1 liter with distilled water. This solution could be diluted to 75 per cent of full strength without exerting any noticeable effect on the rate or force of the heart beat. The pH of the various media tested ranged from 6 to 8, but no differences in the beat were noted. Air was used to gas the medium.

In all, forty-three heart preparations were used for these studies. Acetyl choline ($1:10^6$ to $1:10^2$) exerted no effect on the rate or force of the spontaneous heart beat in over fifty observations. This lack of effect had previously been noted, but only to a concentration of $1:10^6$ (Östlund, 1954). This is illustrated in Fig. 5. Six hours after the start of this experiment, 100 mg. of acetylcholine were added to the bath ($1:10^2$) and the beat continued unchanged for 15 minutes. After the compound was removed by washing, the beat continued with the same rate and force as before. Similarly, when the beat slowed as the length of time the heart was isolated increased, acetylcholine failed completely to exert any effect. Finally, systemic hearts which had ceased beating spontaneously were completely unaffected by the addition of acetylcholine to the bath, although ten out of twelve hearts studied in this way responded to electrical stimulation by a sharp contraction, indicating that the contractile mechanism was still capable of response.

Proguanil ($1:10^4$) did not affect the spontaneous heart beat in several preparations. Cocaine was ineffective also, until the concentration of $8:10^4$ was reached, at which point atrioventricular block occurred, each chamber beating independently of the other. This was readily reversed by washing.

In view of certain recent studies on a digitalis-like effect of certain lysolecithins in the frog heart (Titus, Weiss, and Hajdu, 1956; Hajdu, Weiss, and Titus, 1957), it was of interest to determine whether this material would influence the heart beat of the hagfish. In six experiments a preparation of mixed

(898)

synthetic α- and β-lysolecithins was homogenized in the medium to form a colloidal suspension and was added to the chamber at a final concentration of $1:10^4$. Neither stimulation nor depression was observed on fresh or partially hypodynamic hearts.

Serotonin creatinine sulfate was tested in concentrations of $1:10^7$ to $1:10^5$; no effect was observed in any experiment.

The hagfish heart appeared quite refractory to the drugs studied: nothing that had been tested appeared to influence the rate, hence pacemaker activity, of the heart beat. Several reports in the literature on myogenic automaticity in different species (Arvanitaki and Cardot, 1933; Hykes and Hykesova, 1932) prompted the author to attempt stimulation of a partially hypodynamic hagfish heart with extracts prepared from cardiac tissue of living hagfish. The preliminary results of these studies are considered to be of sufficient importance to warrent their inclusion here.

The systemic hearts from a number of fish were dissected free of blood vessels, connective tissue, etc., rinsed quickly in distilled water, blotted, and while still beating frozen quickly in a vial chilled by dry ice. (The average hagfish systemic heart weighs roughly 125 mg.) The pooled hearts from a number of animals were kept frozen at −10°C. until used. Tissue stored in this manner for up to 2 months did not lose its efficacy.

The extract was prepared by placing a sufficient mass of tissue in a glass homogenizing tube so that after addition of a proper volume of medium each milliliter of the resulting homogenate represented about 300 mg. of fresh muscle (wet weight). The hearts were homogenized by hand with a teflon pestle while ice cold; mild centrifugation was then employed to remove large particles and connective tissue. The resulting clear pinkish supernate was used for the experiments.

The pH of the extract approximated that of the medium and before addition to the test heart, the extract was brought to the temperature of the bath.

Repeatedly, it was found that the extract had no effect on either rate or force of freshly isolated hagfish hearts beating at a frequency of 12 to 20 times per minute. In eight preparations however, whose rate had slowed markedly but whose force of contraction was still strong, addition of 2 or 3 ml. of the extract produced a slight but definite increase in the rate but not in the force of the beat after a latent period varying from 2 to 8 minutes. This increase was maintained until the material was removed by washing and then the earlier rhythm was resumed. Fig. 6 illustrates this finding. The initial heart rate was 14/minute. Twenty-six hours after the beginning of the experiment, the spontaneous rate had slowed to 3/minute and the pattern of the beat was irregular although the force was strong. Addition of 2.0 ml. of the extract induced a doubling of the rate to 6/minute about 3 minutes later which was maintained for 20 minutes. Fifteen minutes after washing, the rate was again 3/minute.

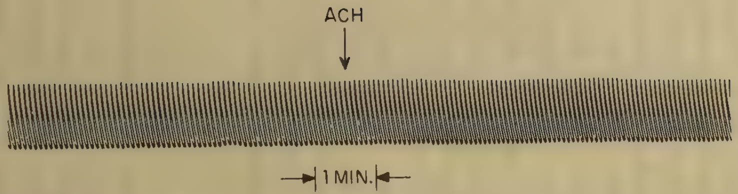

FIG. 5. Lack of response to ACH, 1:10², by the isolated spontaneously beating heart of the California hagfish, *Polistotrema stouti.*

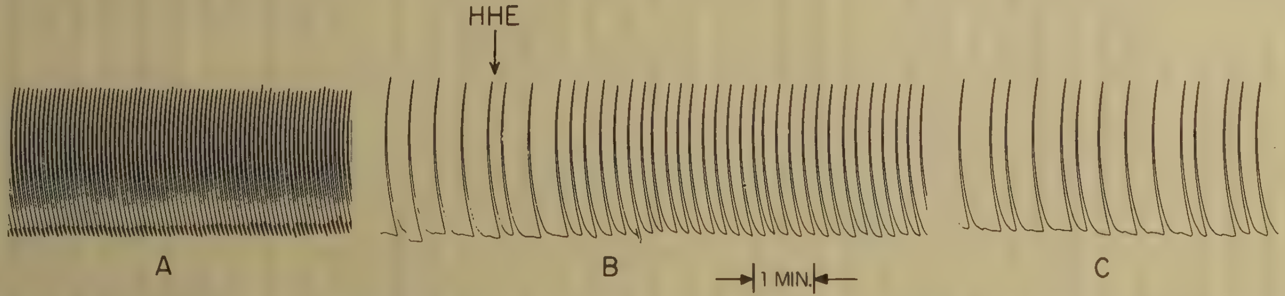

FIG. 6. Effect of HHE on the isolated spontaneously beating heart of the California hagfish, *Polistotrema stouti.* A, control record, start of experiment. B, 26 hours later; addition of 2.0 ml. of HHE produced doubling of the rate which was maintained for 20 minutes until the extract was removed by washing. C, 15 minutes after washing.

This result was obtained five more times in this preparation and repeatedly confirmed in the other experiments. In no case to date, however, would the extract restart a completely quiescent heart. It merely accelerated or regularized the beat of hearts which had slowed spontaneously.

Results obtained from heating the extract in boiling water for 5 minutes have been inconclusive to date. In one study acceleration occurred after heating; in two others the results were negative. This point requires further investigation.

An extract was prepared by the method already described from several neurogenic hearts of the spiny lobster, *Panulirus interruptus*. The results of these studies on three hypodynamic hagfish hearts were completely negative; the pattern and rate of the beat remained unchanged by addition of the extract of this tissue.

The hagfish heart extract was also tested on a fresh but non-beating heart of the mussel, *Mytilus californianus*, maintained as described under "Mollusca" (see Fig. 7). Acetylcholine, 1:10^6, 1:10^5, and 5:10^5, failed to induce a spontaneous beat in this preparation; however, addition of 2.0 ml. of the extract induced a slow (4/minute) but regular beat 4 minutes after addition of the material to the bath. Washing 15 minutes later resulted in immediate cessation of the beat. This observation was repeated five times on this heart and it was found that acetylcholine, 1:10^6, would inhibit the beat which was induced by the hagfish heart extract. Therefore, this effect is apparently not specific for the one species.

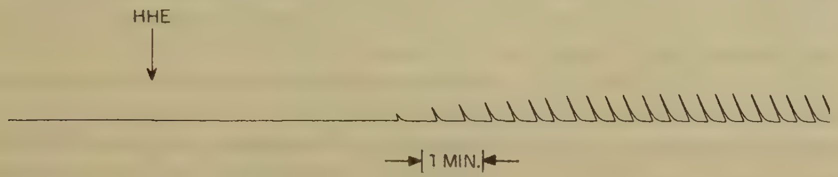

FIG. 7. Stimulatory effect of 2.0 ml. of HHE on a non-beating heart of the California mussel, *Mytilus californianus*.

DISCUSSION AND CONCLUSIONS

The gradual decrease of rhythmic activity which occurs in an isolated heart may be considered to represent a type of heart failure, produced under relatively well controlled environmental conditions. The fact that acetylcholine is capable of stimulating certain mammalian myocardial tissue suffering this type of failure is most interesting, but does not necessarily imply that this compound has a role in automaticity. Demonstration of a stimulatory effect has not as yet been achieved in the range of physiological temperatures and this factor may prove to be of the utmost importance in this regard. A possible explanation of the role of acetylcholine in mammalian cardiac automatism rests on experiments reported by Marshall and Vaughan Williams (1956). These workers found that cooling spontaneously beating rabbit atria below 20°C. would result in cessation of the contractions; however, even after there was no detectible mechanical activity, it was possible to find small non-propagated localized pacemaker potentials in the vicinity of the sinus node in nineteen of twenty-five experiments. Addition of acetylcholine to the heart at this point resulted in propagated action potentials and mechanical contraction once more. Thus, acetylcholine was considered to have restored the link between pacemaker and contractile activity which was broken by cooling. Additional evidence favoring this idea was published recently by Burn and Rand (1957). Using the isolated rabbit atrium–vagus nerve preparation of McEwen (1956), these workers demonstrated that as the temperature was lowered, vagal stimulation produced only inhibition. However, when the temperature reached the point at which contractions ceased (about 15°C.) vagal stimulation now produced contractions. Thus the excitatory and inhibitory actions of acetylcholine may be mediated through the sinoauricular node, rather than in a general fashion directly upon the myocardium as a whole.

The marked contrast among species in their response to the agents investigated in the present study is most interesting. Proguanil and cocaine inhibition of the mammalian tissue and subsequent acetylcholine stimulation are evidence of antagonism between these compounds. The fact that proguanil is capable of stimulating molluscan cardiac tissue is most surprising, and it indicates, at least superficially, basic differences in the organization of the different tissues. Further evidence for this view rests on the observation that acetylcholine was only inhibitory in the clam hearts studied, yet the fact that cocaine would stimulate in the presence of acetylcholine inhibition is again in direct contrast to the experiments on the rat heart. Especially interesting are the studies on the aneural hagfish heart. Since no organized, localized, innervated pacemaker is apparent in the myocardium of this species, nervous intervention is precluded in the interpretation of the effects of drugs. These hearts, whether fresh or hypodynamic, are completely insensitive to acetylcholine; in this regard they closely resemble other myogenic hearts such as *Fundulus* (Armstrong, 1935), chick (Markowitz, 1931), and *Limulus* (Prosser, 1942) embryos prior to innervation as well as adult *Anopheles* (Jones, 1956), *Artemia* and *Eubranchipus* (Prosser, 1942). Apparently innervation and acetylcholine sensitivity are linked; if this be so, then it is quite difficult to visualize how acetylcholine can mediate automaticity in non-innervated structures, and it is concluded that this compound does not assume a role in the rhythmic activity of such tissues.

The evidence presented indicates the presence in the hagfish heart of a substance (or substances) capable of stimulating the rate, hence pacemaker function. Acetylcholine may be ruled out. Catecholamines (adrenalin and noradrenalin), although present in the hagfish heart in relatively high concentrations, exert no influence on its normal activity (Östlund, 1954). Serotonin was likewise ineffective, as were lysolecithins. Further investigations on the nature of the cardiac active material present in the hearts of this species are being conducted at present.

In conclusion, it is felt that the rhythmic activity of myogenic tissues does not depend upon an acetylcholine-cholinesterase mechanism, but rather upon another biochemical process which may act upon and within the cell membranes themselves, perhaps through changes in permeability and ionic transport.

The author is deeply grateful to Dr. William G. Clark and Dr. Samuel A. Weisman, Physiology and Pharmacology Section, Veterans Administration Center, Los Angeles, for providing laboratory facilities for some of these studies, as well as for their unfailing interest and cooperation.

Special thanks are due to Professor Carl L. Hubbs of this institution for providing collecting facilities for the hagfish, laboratory space, and the benefit of many helpful discussions; as well as to Dr. Paul R. Saunders, Dr. Arthur L. Kelly, and Dr. Denis L. Fox for their critical review of the manuscript.

Thanks are also due to Professor Erich Baer of Toronto for a generous gift of mixed lysolecithins and the Ayerst-McKenna Co. of New York for the proguanil hydrochloride.

LITERATURE CITED

Armstrong, P. B., 1935, The role of the nerves in the action of acetylcholine on the embryonic heart, *J. Physiol.*, **84,** 20.

Arvanitaki, A., and Cardot, H., 1933, Action d'extraits tissulaires et cellulaires sur l'activité du coeur *d'Helix pisana*, *Compt. rend. Soc. biol.*, **112,** 465.

Augustinsson, K.-B., Fänge, R., Johnels, A., and Östlund, E., 1956, Histological, physiological and biochemical studies on the heart of two cyclostomes, hagfish, (*Myxine*) and lamprey (*Lampreta*), *J. Physiol.*, **131,** 257.

Bülbring, E., and Burn, J. H., 1949, Action of acetylcholine on rabbit auricles in relation to acetylcholine synthesis, *J. Physiol.*, **108,** 508.

Bülbring, E., Burn, J. H., and Shelley, H. J., 1953, Acetylcholine and ciliary movement in the gill plates of *Mytilus edulis*, *Proc. Roy. Soc. London*, *Series* B, **141,** 445.

Bülbring, E., Kottegoda, S. R., and Shelley, H., 1954, Cholinesterase activity in the auricles of the rabbit heart and their sensitivity to eserine, *J. Physiol.*, **123,** 204.

Burn, J. H., 1953, Acetylcholine and the heart beat, *Lancet*, 1161.

Burn, J. H., and Kottegoda, S. R., 1953, Action of eserine on the auricles of the rabbit heart, *J. Physiol.*, **121,** 360.

Burn, J. H., and Rand, M. J., 1957, Excitation and inhibition of rabbit atria by the vagus nerves, *J. Physiol.*, **8,** 172.

Burn, J. H., and Vane, J. R., 1949, The relation between the motor and inhibitor actions of acetylcholine, *J. Physiol.*, **108,** 104.

Carlson, A. J., 1904 *a*, The nervous origin of the heart-beat in *Limulus*, and the nervous nature of co-ordination or conduction in the heart, *Am. J. Physiol.*, **12,** 67.

Carlson, A. J., 1904 *b*, Contributions to the physiology of the California hagfish, (*Bdellostoma dombeyi*), *Z. allg. Physiol.*, **4,** 259.

Greene, C. W., 1902, Contributions to the physiology of the California hagfish, *Polistotrema stouti*, II. The absence of regulative nerves for the systemic heart, *Am. J. Physiol.*, **6,** 318.

Hajdu, S., Weiss, H., and Titus, E., 1957, The isolation of a cardiac active principle from mammalian tissue, *J. Pharmacol. and Exp. Therap.*, **120,** 99.

Holtz, P., and Westermann, E., 1955, Versuche mit Acetyl-, Propionyl-, und Butyrylcholin am isolierten Herzvorhofpräparat, *Arch. exp. Path. u. Pharmakol.*, **225,** 421.

Hykes, O. V., and Hykesova, D. E., 1932, Influence de l'extrait de coeur d'escargot sur le coeur de la larve du moucheron, *Compt. rend. Soc. biol.*, **110,** 391.

Jones, J. C., 1956, Effects of drugs on *Anopheles* heart rates, *J. Exp. Zool.*, **133,** 573.

Kordik, P., Bülbring, E., and Burn, J. H., 1952, Ciliary movement and acetylcholine, *Brit. J. Pharmacol. and Chemotherapy*, **7,** 67.

Krijgsman, B. J., and Divaris, G. A., 1955, Contractile and pacemaker mechanisms of the heart of molluscs, *Biol. Rev.*, **30,** 1.

Leusen, I., Demeester, G., and de Witte, J., 1955, Influence de l'acetyl-digitoxine-alpha sur le muscle papillaire du chat, *Arch. internat. pharmacod. et thérap.* **102,** 153.

Lyman, J., and Fleming, R. H., 1940, Composition of sea water, *J. Marine Research*, **3,** 134.

Markowitz, C., 1931, Response of explanted embryonic cardiac tissue to epinephrine and acetylcholine, *Am. J. Physiol.*, **97,** 271.

Marshall, J. M., and Vaughan Williams, E. M., 1956, Pacemaker potentials. The excitation of isolated rabbit auricles by acetylcholine at low temperatures, *J. Physiol.*, **131,** 186.

McEwen, L. M., 1956, The effect on the isolated rabbit heart of vagal stimulation and its modification by cocaine, hexamethonium and ouabain, *J. Physiol.*, **131,** 678.

Östlund, E., 1954, The distribution of catechol amines in lower animals and their effect on the heart, *Acta Physiol. Scand.*, **31,** suppl. 112, 1.

Patten, B. M., 1949, Initiation and early changes in the character of the heart beat in vertebrate embryos, *Physiol. Rev.*, **29,** 31.

Prosser, C. L., 1942, An analysis of the action of acetylcholine on hearts, particularly in arthropods, *Biol. Bull.*, **83,** 145.

Titus, E., Weiss, H., and Hajdu, S., 1956, Isolation of a cardiac-active principle from mammalian tissues, *Science*, **124,** 1205.

Welch, J. H., and Taub, R., 1948, The action of choline and related compounds on the heart of *Venus mercenaria*, *Biol. Bull.*, **95,** 346.

(904)

Extracts from

Zoogeography

A SYMPOSIUM PRESENTED ON AUGUST 26-27, 1957,
AT THE STANFORD UNIVERSITY JOINT MEETING OF
THE AMERICAN INSTITUTE OF BIOLOGICAL SCIENCES
AND THE PACIFIC DIVISION OF THE AMERICAN
ASSOCIATION FOR THE ADVANCEMENT OF SCIENCE

AND

A SYMPOSIUM PRESENTED ON DECEMBER 28, 1957,
AT THE INDIANAPOLIS MEETING OF THE AMERICAN
ASSOCIATION FOR THE ADVANCEMENT OF SCIENCE

Edited by
CARL L. HUBBS

Publication No. 51 of the
AMERICAN ASSOCIATION FOR THE ADVANCEMENT OF SCIENCE
WASHINGTON, D. C. 1958

Contributions from the Scripps Institution of Oceanography, New Series, No. 1050
Reproduced by Permission

© 1958
The American Association for the
Advancement of Science

Library of Congress Catalog
Card Number 59-59993

Printed in the United States of America
The Horn-Shafer Company
Baltimore, Maryland

(906)

This volume is dedicated

to the memory of

two great zoogeographers,

CHARLES DARWIN AND
ALFRED RUSSEL WALLACE

◆

Whose observations and reflections on the distribution of animals provided much of the evidence that led them, just one hundred years ago, to propose to the world the epochal concept of Organic Evolution, which unshackled the minds of men and helped inaugurate the Age of Science.

(908)

Preface

As science expands and fragments, reviews and syntheses of broad areas become increasingly useful and necessary. Among the more effective means of review and synthesis are the symposia that are being held in increasing numbers at scientific meetings. Two such symposia, in 1957, encompassed the field of zoogeography, with due attention to the underlying data of geomorphology, paleoclimatology, paleontology, and physiology. The fifteen papers that have become available from these two symposia comprise a notable and rather comprehensive, though somewhat diverse contribution to zoogeography and to its background sciences. The extent of the contribution is greatly enhanced by the publication of these assembled papers as one of the symposium volumes of The American Association for the Advancement of Science.

The first of these two symposia (Part I) was held under the prime auspices of the Pacific Section of The Society of Systematic Zoology, as a feature of the joint meeting of the American Institute of Biological Sciences and the Pacific Division of the American Association for the Advancement of Sciences, at Stanford University, in August, 1957. The symposium, bearing the ample title "The Origins and Affinities of the Land and Freshwater Fauna of Western North America," was abundantly cosponsored by the American Society of Ichthyologists and Herpetologists (Western Division), American Society of Zoologists, California Academy of Sciences, Pacific Coast Entomological Society, Society for the Study of Evolution, and Western Society of Naturalists. The fourteen papers ran through well-attended morning and afternoon sessions on August 26 and 27, plus a final panel discussion that nearly filled a spacious hall on the evening of the second day. The large and attentive audiences demonstrated the liveliness of the subject. Audience contribution was so spirited at the panel discussion that I had difficulty in closing the session at a reasonable hour.

It was my pleasure and privilege to act as general chairman of this symposium. In conducting the sessions I was ably joined by the late Karl P. Schmidt, as one of the last of his many generous acts, and by George F. Edmunds, Jr. Panel members William H. Burt, Alden H. Miller, Robert W. Pennak, Herbert H. Ross, and Dr. Schmidt helped enliven the informal discussion.

Gratitude is expressed to the fifteen participants, all of whom made notable contributions. Most of the contributors made an extensive and thorough analysis of their chosen subjects, and some treated their topics in exhaustive and carefully documented style.

Credit for the success of this symposium goes to the symposium committee, all of the University of California, Los Angeles: John N. Belkin, chairman, Donald Heyneman, and Marietta Voge. These zoologists were the prime actors in the conception of the idea, in lining up the able speakers, in arranging and managing the sessions, and, as not the least difficult task, in extracting manuscripts from thirteen of the participants. They also helped in processing the manuscripts. I am sure that the officers of the meetings, the speakers, the audiences, and, now, the scientific public, join me in expressing hearty thanks to these tireless and self-effacing workers.

The second symposium (Part II), which is herein represented by three of the six papers, was a feature of the American Association for the Advancement of Science meeting at Indianapolis, and was held on December 28, 1957. It was entitled "Geographic Distribution of Contemporary Organisms," and constituted Part I of the general symposium, "Some Unsolved Problems in Biology, 1957." This was a joint program of AAAS sections F (Zoological Sciences) and G (Botanical Sciences), and was extensively cosponsored, by the Society of Systematic Zoology, Ecological Society of America, Genetics Society of America, American Society of Naturalists, and Botanical Society of America. The program was arranged by Harold H. Plough, of Amherst College, as Secretary of Section F, ably assisted by Ernst Mayr of Harvard University and E. Raymond Hall of the University of Kansas. Dr. Hall presided at the symposium and contributes the introductory remarks.

We of the Pacific Section of the Society of Systematic Zoology welcome the privilege of combining the papers resulting from our symposium with the three submitted from the Indianapolis symposium. As editor of the combined symposia, I want to express the feeling that they very nicely complement the contributions from the first symposium.

CARL L. HUBBS

Scripps Institution of Oceanography,
University of California,
La Jolla
October 1958

(910)

General Conclusions

Carl L. Hubbs
Scripps Institution of Oceanography, University of California, La Jolla

The fourteen papers from the symposium on *The Origins and Affinities of the Land and Freshwater Fauna of Western North America*, plus the three richly supplementing contributions from the symposium on *Geographic Distribution of Contemporary Organisms*, constitute a vast storehouse of information on zoogeography, on companion fields, and on various sciences that provide the background that is necessary for a full understanding of zoogeography. The seventeen contributions deal not only with the actual distribution of many but of course not all groups of land and freshwater animals, along with some aspects of phytogeography, but also with various biogeographical topics, and with the background material. Most of the contributors deal largely with western North America, but a few cover all of North America, and one even straddles the whole New World.

The contributions are diverse not only in respect to the groups of organisms, the areas covered, and the topics stressed, but also in the angle of approach, in the length and completeness of review, in the amount of original material, in the thoroughness (or lack) of documentation, and in the abundance, paucity, or lack of illustrations. The separate articles vary from abstracts (two) and mere thoughtful commentaries, on some phase of the general subject, to long, scholarly studies that give us, for the first time, the summary of a distinguished author's long-continued and intensive research.

The whole volume has both the strength and the weakness that goes with diversity. It is strong in the variety of viewpoints and specialties, in the high competence of each invited participant in some aspect of zoogeography or in one of the basically related sciences, and in the potential synthesis that is favored by the close association of the diverse contributions. It is weak in the fragmentation of the subject, due to the increasing specialization of scientists, in the lack of attention to some groups and topics (an unavoidable defect in the age of specialization), and in the limited detail and documentation in some of the papers.

The diversity of treatment calls at the outset for an organized indication (Table I) of the coverage of the various papers, in terms of geographic, evolutionary, systematic, and background considerations.

The individual papers are referred to in the table (and in the following text) by number as given in the Contents. In the table, degree of emphasis (in the papers as printed) is roughly approximated by the type: roman for least emphasis, *italics*, for more thorough treatment, and **boldface** for most exhaustive coverage.

The emphasis on background considerations and on evolutionary and systematic correlatives, brought to focus in the table, is a strong indication of a healthy rebound from the course of overspecialization. The trend toward interdisciplinary research is exemplified in several of the contributions, and is perhaps best illustrated, as well as stated, in Martin's contribution (15) on Pleistocene ecology. The same happy trend is glowingly evident in several of the other papers, notably, for example, those by MacGinitie (2) and by Blair (17).

The overall treatment further indicates a shift from the classical, purely descriptive biogeography to a kinetic approach, which is more concerned with processes and explanations than with the classification of the earth into a hierarchy of biogeographical regions. Attention is focused on floral and faunal elements of diverse origin, which may be mixed in any one area, and on the past and present dispersions of these biotic elements. This concept of biotic elements, which was advanced particularly by Ernst Mayr (followed herein by Parkes, 16), penetrates into the limited regional classifications of faunas in these symposia. Linsley (13), for example, maps the same area of the central California coast as a diluted part of both the Vancouveran and Californian faunas, and Rehn (12) apportions the western North American orthopteran fauna according to regions of origin.

Past and continuing shifts in biota receive considerable attention, in line with the more kinetic approach that is fortunately coming into vogue. The background for such biotic dispersals is elucidated in several of the papers, notably by King's (1) sweep through the grand history of changes in the face of the earth over western North America, by MacGinitie's (2) analysis of climatic trends and fluctuations in this region since Cretaceous time, and by the excellent reviews by Martin (15) and by Blair (17) on the dramatic events of the Pleistocene and their consequences.

Some new, refined approaches in biogeographical analysis are emphasized. One of these is the quantitative reconstruction of past vertebrate biocoenoses through the study of all identifiable material obtained by soil washing—a truly revolutionary (and long overdue) development, as D. E. Savage (4) indicates. Another major refinement is the more precise and penetrating systematic analysis, such as is indicated in most of the reports, notably those by Peabody and J. M. Savage (8), R. R. Miller (9), and Parkes (16). Another circumstance favoring sound biogeographical conclusions is the life-long devoted specialization on single groups, throughout their range, that is obvious in the contributions by several of the authors, notably A. H. Miller (6), R. R. Miller (9), and the entomologists: Ross (11), Rehn (12), Linsley (13), and Hovanitz (14). Radiocarbon dating becomes a tool of research in biogeography, as in other areas (Martin, 15). Quantitative studies, including pollen analysis, are helping to displace inference with data. And, most effective of all as a lead toward a fuller understanding of the events and processes in biogeography is the recourse to interdisciplinary and multidisciplinary approaches.

The fabric of this symposium has been woven of threads that vary so much in color, size, and strength as to make it difficult to pick out these threads to reweave a simple review and conclusion. On some basic lines, however, there is sufficient consensus to permit some generalization.

One initial thought that seems justified is that biogeography is still a propitious field of inquiry. Certainly, many of the defects of the past are attributable to excessive inference on the basis of inadequate data. Through more intensive research, sharpened by new techniques and enriched by interdisciplinary approach, sound data are certain to result, and broader and more reliable interpretations are bound to develop. Through the symposium there is to be found much justification for this optimism.

A notable feature of the whole series of papers is that there is hardly a mention of the transoceanic land bridges that biogeographers not long ago threw around with abandon. King (1) assures us that geologists hold to the theory of the essential permanence of the ocean basins, and the biologists seem to have proceeded on this assumption. The verified intercontinental connections across the Isthmus of Panama and especially across the Bering Strait region are duly treated. The intimate relationships between the Palearctic and Nearctic faunas are pointed out by Parkes (16) and other authors, and are rightly assumed to indicate a past continuity, but, as Burt (5), Rehn (12), and Hovanitz (14) point out with admirable reserve, there is, as yet, usually little basis for postulating the region of origin and the direction of dispersal. In some groups there may have been a complex interchange.

In general, it is admitted, or apparently assumed, that the reconstruction of the past history of a group, whether of origin or dispersal, cannot ordinarily be postulated with assurance on the sole basis of the present distributional pattern. Considerable variance in reserve or reliance, however, is displayed in such reconstructions. Bartholomew (3) and Burt (5) go so far as to say there are no separate "origins," because there has been a continuum of life, but are they not playing with semantics? In terms of given natural groups or stages of evolution there is an origin, in both time and space.

The criteria of center of origin, or of differentiation, as some would prefer to say, are definitely discussed by only two of the authors, D. E. Savage (4) and Burt (5). Savage's criteria are the more impressive because they emphasize the fossil record. His first criterion of area of origin is the region from which the oldest fossil is known. This is fine for groups with a well-known fossil record, but for groups with few known fossils may, as Parkes (16) notes, be even more treacherous than criteria based on present distributions. Savage's second criterion is an earlier record of progenitors (the sort of evidence that puts man's origin securely in the Old World)—again good, if the data are adequate. His third criterion is the area of greatest taxonomic diversity. This criterion may usually hold, but certainly not always. It seems not to apply, for example, to the origin of the catostomid fishes, which are almost restricted to North America, but which R. R. Miller (9) and I believe, on scanty but pertinent distributional and fossil evidence, to have originated in Asia, though they seem to have undergone most of their differentiation in North America. Savage argues wisely that phyletic age, relict occurrence, and vagility must be taken into account, but he doesn't indicate just how. Other frequently expounded criteria are just mentioned, along with Mathew's hypothesis that primitive forms are peripheral.

Savage sharply criticizes the location of the major center of origin in the Old World tropics, on the basis of the evidence that the present Holarctica is temperate to boreal. As both he and MacGinitie (2) point out, the northern lands were subtropical through much of Cenozoic time. Obviously, much of evolutionary history is still hidden in a fog of ignorance. The task of the historians of life has barely begun. And until we know the past, we cannot fully understand the present nor guess the future.

Several of the authors hold to the view long championed by Chaney and by Axelrod, and here expounded by MacGinitie (2), that world climate became progressively more arid and cooler through Tertiary time, while increased relief and other factors caused greater local diversity. It seems that there was a general northward shift in the climatic zones. All this caused a great translocation of the geo-floras, and, presumably, of the accompanying animal communities. Some zoologists, for example Peabody and J. M. Savage (8), have been bold enough to reconstruct origins and dispersals of certain animals on the basis of the history of the geofloras with which they infer these animals were associated. Are they treading on firm ground or on quicksand?

It seems to be the general consensus that the vast uniformity of life that characterized the early Cenozoic, in both space and time, gradually changed to diversity throughout Tertiary time, in a grand crescendo that reached ecstatic proportions in the Pleistocene. Martin (15) and Blair (17) have compiled impressive evidence favoring the view, which seems to me to be well justified, that the Ice Ages were periods of intense cold, during which climatic belts were displaced far southward (and far downward on the mountains), and during which even the tropics were very considerably cooled. During the Wisconsin period the temperate biota of eastern North America seems to have been forced into refugia in Florida and Mexico (Blair, 17), while in the West (Miller, 9) there was extensive extermination of the freshwater fauna in the north and a vast development of lakes in the Great Basin and southward.

Table I. Index to Subject Coverage in Symposia on Zoogeography

Numbers in parenthesis refer to the separate papers by the stated authors. Degree of emphasis is roughly approximated by type—roman for least emphasis, *italics* for more thorough treatment, **boldface** for most exhaustive coverage.

Geographical Considerations

- CRITERIA (on Centers of Origin or Differentiation): **D. E. Savage (4),** *Burt (5)*, Rehn (12), Hovanitz (14), Parkes (16)
- EFFECTS OF MAN
  - Of Primitive Man: *Martin (15)*
  - Of Modern Man: Pennak (10)
- AREAS TREATED BIOGEOGRAPHICALLY
  - Entire New World: **Hovanitz (14)**
  - Nearctica: *D. E. Savage (4)*, *Martin (15)*, *Parkes (16)*, R. R. Miller (9), Linsley (13)
  - Southeastern United States: *Blair (17)*
  - Western North America: **King (1), MacGinitie (2), D. E. Savage (4), Burt (5), Peabody and J. M. Savage (8), R. R. Miller, (9), Rehn (12),** *Pennak (10)*, *Ross (11)*, *Linsley (13)*

Background Considerations

- PHYSIOLOGICAL BACKGROUND: *Bartholomew (3)*, Hovanitz (14)
- GEOLOGICAL BACKGROUND
  - General: **King (1),** MacGinitie (2), Peabody and J. M. Savage (8)
  - Hydrographic History: **R. R. Miller (9),** *King (1)*
  - Pleistocene Events: **Martin (15),** *King (1)*, MacGinitie (2), Blair (17)
  - Physiographic Relations: **King (1), Peabody and J. M. Savage (8),** *R. R. Miller (9)*, *MacGinitie (2)*, *Hovanitz (14)*, Blair (17)
- PALEONTOLOGICAL BACKGROUND
  - Plantes: **MacGinitie (2),** Linsley (13), Martin (15), Blair (17)
  - Insecta: *Linsley (13)*, Ross (11), Rehn (12), Martin (15)
  - Pisces: **R. R. Miller (9),** Blair (17)

Evolutionary and Systematic Considerations

- PHYLOGENIES: *D. E. Savage (4)*, Burt (5), R. R. Miller (9), Ross (11)
- EVOLUTIONARY RATES: *Martin (15)*, D. E. Savage (4), Ross (11)
- SPECIATION: *Peabody and J. M. Savage (8)*, A. H. Miller (6), Pennak (10), Hovanitz (14), Martin (15), Parkes (16), Blair (17)
- GROUPS TREATED BIOGEOGRAPHICALLY
  - Plantes: **MacGinitie (2),** *Martin (15)*, Linsley (13), Blair (17)
  - Invertebrata: *Pennak (10)*
  - Insecta
    - Dermaptera and Orthoptera: **Rehn (12)**
    - Northern and Montane Insects: **Ross (11)**
    - Cerambycidae: **Linsley (13)**

TABLE I. Index to Subject Coverage in Symposia on Zoogeography —Continued

Geographical Considerations	*Background Considerations*	*Evolutionary and Systematic Considerations*
Relations with Asia: **Burt (5), Parkes (16),** *MacGinitie (2), D. E. Savage (4),* A. H. Miller (6), R. R. Miller (9), Ross (11), Rehn (12), Linsley (13), Hovanitz (14) Relations with South America: **Hovanitz (14),** *D. E. Savage (4), Burt (5),* R. R. Miller (9), Linsley (13), Blair (17) Relations of Eastern to Western North America: *Blair (17), Pennak (10),* Burt (5), A. H. Miller (6), R. R. Miller (9), Ross (11), Linsley (13), Hovanitz (14), Martin (15)	Amphibia and Reptilia: *Peabody and J. M. Savage (8)* Aves: Parkes (16) Mammalia: **D. E. Savage (4),** *Martin (15), Blair (17)* PALEOCLIMATOLOGICAL BACKGROUND Cretaceous: *MacGinitie (2)* Tertiary: **MacGinitie (2),** King (1), Peabody and J. M. Savage (8), Linsley (13), Blair (17) Pleistocene: **Martin (15), Blair (17),** *MacGinitie (2),* King (1), Stebbins (7), Hovanitz (14) PALEOECOLOGICAL BACKGROUND: **MacGinitie (2), Blair (17),** *Martin (15),* D. E. Savage (4), Burt (5) ECOLOGICAL BACKGROUND: **Martin (15),** *Pennak (10), Linsley (13), Hovanitz (14), Blair (17),* R. R. Miller (9), Ross (11)	Lepidoptera: **Hovanitz (14)** Pisces: **R. R. Miller (9),** Blair (17) Amphibia and Reptilia: *Peabody and J. M. Savage (8),* Stebbins (7), Martin (15), Blair (17) Aves: **Parkes (16),** A. H. Miller (6) Mammalia: **D. E. Savage (4), Burt (5),** *Martin (15),* Blair (17) Man: *Martin (15)*

Despite the evidence of extreme climatic change at the close of Wisconsin time and during the Postpleistocene millenia, Martin (15) holds to the view that the extinction of the large Pleistocene mammals is attributable not to climatic change, but to man. I favor the theory of a combination of factors.

After the recurrent restoration of humidity in the Pleistocene, the trend toward aridity seems to have continued in the West. The deserts seem to have marched northward and to have spread out like a vast desiccating fan toward the Pacific Coast and onto the Great Plains. This trend is just mentioned in the abstract by Stebbins (7), and it is considered, but I believe probably set too far back in Cenozoic time, by Peabody and J. M. Savage (8). Desiccation is plausibly held by R. R. Miller (9) and by Pennak (10) to have been largely responsible for the impoverished freshwater fauna of the West and for the high incidence of local endemism. A. H. Miller (6) attributes the high ratio of endemism among the birds of the Californian fauna to the isolation of this fauna by deserts.

In some groups, as the Orthoptera (Rehn, 12) and Reptilia, in contrast, the intensification and spread of the Sonoran region seems to have been a potent evolutionary stimulus.

Redispersals following the vast displacements of the Pleistocene are held to have induced some very interesting speciational situations. Blair (17) postulates the genetic responses, during Recent sympatry, of cognates that had been isolated in the Floridan and Mexican refugia. Hovanitz (14) similarly treats the consequences of cohabitation of butterflies previously segregated by the Wisconsin ice sheet. One pair, he states, has, by hybridization, thus produced a third species.

Geologically recent topographic changes are held to have conditioned other significant speciational events. Hovanitz (14) attributes the high incidence of endemism of butterflies in the Andes to the new environments suddenly furnished by the rapid uplift of the Cordillera, and he regards this type of response as of general significance. Peabody and Savage (8) explain speciational relations among amphibians and reptiles in California on the basis of the establishment of a Coast Range Corridor. They cite evidence that the Sierra Nevada and Coast Ranges were long separated on the south by a marine barrier, so that the forms on the two ranges became subspecifically differentiated, though intergrading where their ranges converged in the north. They postulate that when the corridor became established the cognates met, but, because of the degree of separation, remained distinct in cohabitation, behaving here as full species at the respective ends of an otherwise specific continuum (in other words, forming "open circles").

In a slightly Chauvanistic vein, these authors close their paper with this exultation: "We may confidently reaffirm and echo A. B. Howell's assertion of thirty years ago that the fauna of the Pacific Coast is of unusual interest and presents many fascinating problems. Californians have a land-bridge laboratory in their own back yard!" But, as is suggested by the references just made to Hovanitz and to Blair, similarly fascinating situations exist outside the Golden West. Zoogeographical gold is where you find it!

(920)

SOME EFFECTS OF PRESSURE ON A PHENYLGLYCOSIDASE* **

LESLIE RALPH BERGER

Scripps Institution of Oceanography, University of California, La Jolla, Calif. (U.S.A.)

A relatively small increase or decrease in pressure may be reflected by a relatively large change in a biological or biochemical activity of an organism. For example, the relative viscosity of the protoplasm of the *Amoeba* decreases by 50 % with a change of only 100 atmospheres[1]; the intensity of luminescence at 35° of *Photobacterium phosphoreum* increases over 30 % by an increase in pressure of less than 70 atmospheres[2].

Although many studies have been made on the effects of pressure and temperature on enzyme systems, bioluminescence, the luciferin–luciferase system in particular has received concentrated attention. The results of these investigations have done much to correlate on a molecular level many previously unexplained empirical observations.

The purpose of this work is to show the behavior of a phenylglycoside–glycosidase system under various conditions of pressure and temperature and to interpret from the data in so far as is possible the factors which influence this system.

MATERIALS AND METHODS

The enzyme used in this study is produced by a strain of *Streptomyces griseus*. It is elaborated into the culture filtrate when the organism is grown on a mineral salts solution and chitin. The resolution, properties, and function of this enzyme in the decomposition of chitin were reported by BERGER AND REYNOLDS[3]. Although this enzyme preparation contained small amounts of two chitinases, they do not interfere with the hydrolysis of the substrate. This substrate, the phenylglycoside phenyl-β-D-2-acetamido-2-deoxyglucopyranoside, was synthesized from glucosamine-HCl and phenol by the procedures described previously[3].

Kinetic experiments were made at enzyme saturation. Fig. 1 shows the effect of the substrate concentration on the rate of reaction of a concentrated solution of the enzyme at 35° and ambient pressure. In all experiments reported subsequently, a dilution of this enzyme solution was used; the substrate concentration was 0.01 *M*. The effect of products on the rate of reaction was also tested. Addition of 30 mg/ml and 50 %-saturated solution of N-acetylglucosamine to the reactants neither inhibited the rate of reaction nor increased the rate at which the reaction dropped off with time.

The apparatus used for raising and maintaining fluid samples at increased hydrostatic pressure was described in detail by ZOBELL AND OPPENHEIMER[4]. It consists of a pressure cylinder completely filled with water connected to a hand-operated hydraulic pump with 50% aqueous glycerol as the hydraulic fluid. The pressure cylinders were incubated in a large water bath. Temperatures were adjusted to ± 0.05° of the desired value; the bath maintained itself at ± 0.015° of the set temperature as determined by a continuously recording instrument.

Measurements of the hydrolysis of the substrate under varying conditions of pressure and temperature were made as follows. Separate solutions of the glycoside and the enzyme in 0.02 *M*

---

* Contribution from Scripps Institution of Oceanography, New Series.

** This paper represents results of research done by the University of California under contract with the Office of Naval Research. Reproduction in whole or in part is permitted for any purpose of the United States Government.

Contributions from the Scripps Institution of Oceanography, New Series, No. 1052

Reproduced by Permission

phosphate buffer, pH 6.3, were chilled to below 5°, mixed, placed into small test tubes with a capacity of about 3 ml. At 5° the enzymic hydrolysis is not measurable over a period of 24 h.

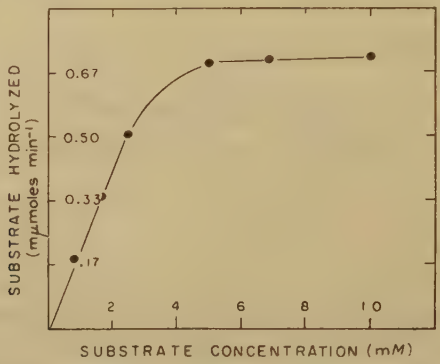

Fig. 1. Effect of substrate concentration on the rate of reaction of the phenylglycosidase. Different concentrations of the substrate were mixed with a constant amount of enzyme and incubated at 35°. At intervals, aliquots were analyzed for the amount of phenol liberated by the reaction.

The tubes were closed with No. 000 rubber stoppers, and kept in an ice bath until used. They were then dropped into the pressure cylinders previously equilibrated in the water bath. The cylinders were closed, pumped to pressure and replaced in the water bath. Less than 1 min is required for the entire operation. After suitable incubation, the pressure was released, the tubes were removed, and 1 ml of their contents was pipetted into each of two 20-ml test tubes chilled in ice. When a series of incubations had been completed, the 1-ml aliquots were analyzed for the amount of phenol freed by the modified method of FOLIN AND CIOCALTEU[5] described previously[3].

Measurements of the inactivation of the enzyme in the presence of substrate were made by extending the procedure described above. After removing the tubes from the pressure cylinders, the contents of each was divided into two portions. One portion was analyzed for phenol without further treatment; the other was placed in a 35° water bath at ambient pressure and incubated for an additional period of time prior to analysis for phenol. The rate at which the substrate was hydrolyzed in this second incubation compared to that of control solutions is a direct measure of the inactivation during the initial treatment.

These methods were modified somewhat for determining enzyme inactivation in the absence of substrate. The rate of the enzymic hydrolysis after treatment at various conditions of pressure and temperature was measured as follows. The enzyme alone was placed into tubes in the pressure cylinders, incubated, and removed as described above. The substrate was added, and the mixture was incubated at ambient pressure at 35° for varying periods of time prior to the assay for phenol. The rate of hydrolysis by the treated enzyme compared to that of the untreated enzyme is a measure of the inactivation.

RESULTS AND DISCUSSION

Hydrolysis of the substrate by the glycosidase was measured at 1, 250, 500, and 1000 atmospheres at 5° intervals from 20° to 50°. The results are shown in Fig. 2. At the lower temperatures, especially, but also as high as 45°, increased pressure decreases the rate of enzymic hydrolysis. Increased pressure also prevents the progressive decrease in hydrolytic activity, thus more substrate is hydrolyzed at higher pressures and temperatures after 10 to 15 min.

Graphic estimation of the 0-time slopes of the curves in Fig. 2 gave values of maximum velocity, *k*, for the reaction under each set of conditions. Because of sizable amounts of enzymic inactivation before the first measurement, it is probable that the estimates at higher temperatures are biased too low. Fig. 3 is a plot of ln *k* against

References p. 528.

the reciprocal of absolute temperature. From the straight portions of these curves, *Δ H* in calories per mole was calculated using one form of the Arrhenius Equation. The values of *Δ H* are summarized in Table I. In the temperature range studied, *Δ H* is approximately equal to the activation energy of the reaction.

TABLE I

Δ H VALUES FOR THE HYDROLYSIS OF THE PHENYLGLYCOSIDE AT DIFFERENT PRESSURES

Pressure (atm.)	*1*	*250*	*500*	*1,000*
Estimated slope (from Fig. 3)	—7,500	—11,700	—13,000	—10,400
Δ H (cal/mole)	—3,780	— 5,890	— 6,540	— 5,230

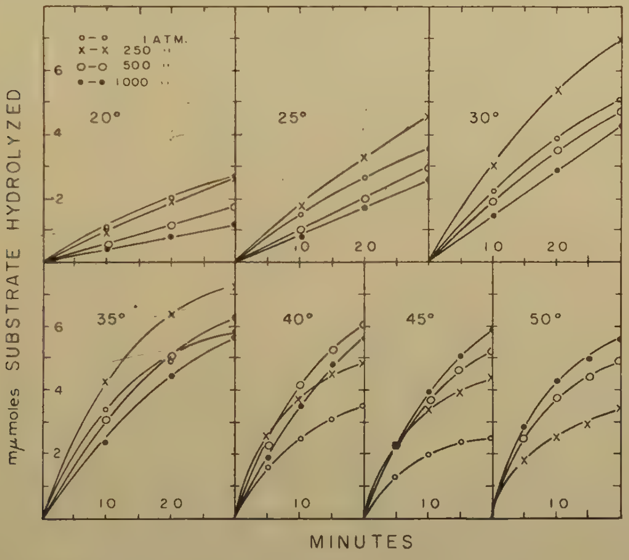

Fig. 2. Effect of temperature and pressure on the hydrolysis of the phenylglycoside by the glycosidase. Chilled solutions of the enzyme and substrate in 0.02 *M* phosphate buffer at pH 6.3 were mixed, placed into small test tubes, and stoppered. The tubes were placed into cylinders previously equilibrated at the desired temperatures and pumped to the required pressures. At intervals, the cylinders were decompressed, and the contents of the tubes were analyzed for the phenol liberated by the reaction.

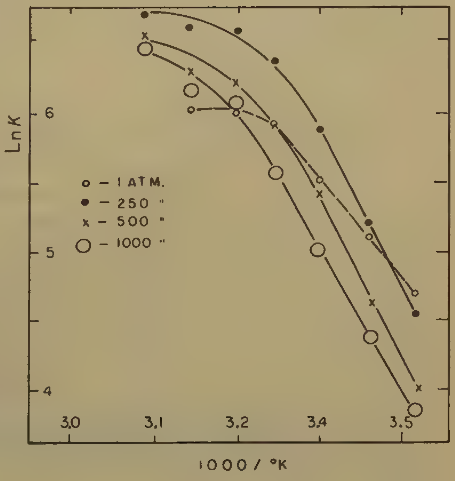

Fig. 3. Plot of the initial rates of reaction of the glycosidase on the phenylglycoside against absolute temperature^{-1} at different pressures. The initial rates of reaction were estimated graphically from the data plotted as in Fig. 3.

By plotting ln k against the pressure (Fig. 4) a curve is obtained for each temperature, the slope of which is a function of the change in molecular volume for the transition state. The volume changes are presented in Table II. The magnitude of the changes (+ 20.4 to + 32.2 ml per mole) is consistent with values observed for several other enzyme systems[6].

The effect of pressure on thermal inactivation of the enzyme system was studied in two ways. The enzyme was subjected to various pressures and temperatures in the absence of substrate (Fig. 5) and in the presence of substrate (Fig. 6). In the absence of the substrate, increased pressure accelerated the inactivation of the enzyme. This suggests that a net negative volume change occurs in the inactivation. In the presence of the substrate, however, increased pressure retarded enzymic inactivation indicating

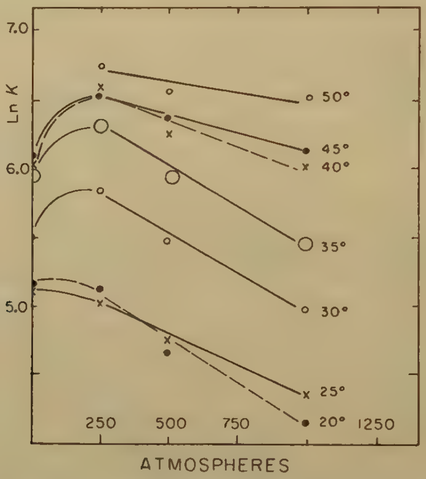

Fig. 4. Plot of the initial rates of reaction of the phenylglycosidase against pressure. Initial rates of reaction were estimated graphically from the data as plotted in Fig. 3. The slopes of the straight portions of the curves were determined by the method of least squares for the data above 1 atmosphere. Molecular volume changes for the transition state at each temperature, ΔV, were determined from the relationship $d \ln k = -\Delta V/RT\, dP$ where $R = 82.07$ ml atm mole^{-1} deg^{-1}, T = abs. temperature.

TABLE II

MOLECULAR VOLUME CHANGE OF THE TRANSITIONAL STATE DURING HYDROLYSIS OF THE PHENYLGLYCOSIDE

Temperature (°C)	*Estimated slope**	*Volume change (ml/mole)*
20	+ 0.00133	+ 32.2
25	+ 0.00113	+ 27.6
30	+ 0.00115	+ 28.6
35	+ 0.00111	+ 28.2
40	+ 0.00080	+ 20.5
45	+ 0.00082	+ 21.4
50	+ 0.00077	+ 20.4

* Slopes were estimated by the method of least squares for the data (Fig. 4) above 1 atmosphere. Molecular volume change, ΔV, was calculated from the relationship $d \ln k = -\Delta V/RT\, dP$.

References p. 528.

a positive volume change for this reaction. At ambient pressure, in the presence of the substrate, the inactivation shows apparent first order kinetics; this is not evident at higher pressures. These observations suggest that the mechanism of inactivation even at ambient pressure is probably not a single process.

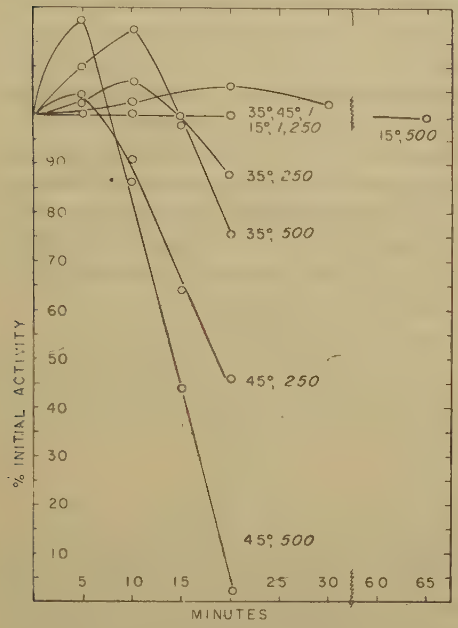

Fig. 5. Inactivation of the phenylglycosidase by heat at different pressures in the absence of substrate. The enzyme solution was pressurized at different temperatures. After increasing time intervals, the solutions were mixed substrate and incubated at ambient pressure at 35°. Aliquots were removed periodically and analyzed for phenol liberated by the reaction. Results are presented as the % of the activity of the control enzyme solution. Italicized numbers refer to pressure in atmospheres.

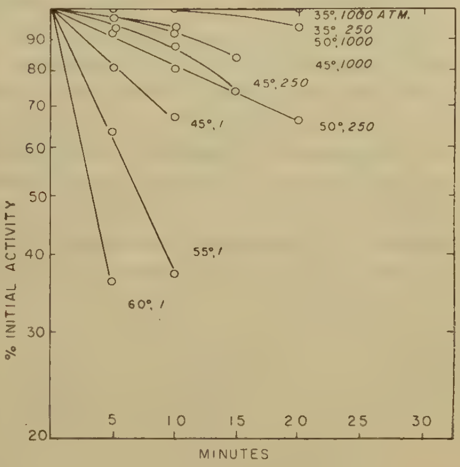

Fig. 6. Inactivation of the phenylglycosidase by heat at different pressures in the presence of substrate. Tubes containing enzyme and substrate were mixed, incubated at various temperatures and pressures as described under Fig. 3. At intervals, one series of replicate tubes was analyzed for the amount of hydrolysis which occured in the pressure cylinders. The second series of replicate tubes were reincubated at 35° at ambient pressure for an additional period of time prior to analysis for phenol. The activity of the enzyme during the second incubation is plotted against the length of the initial treatment and is expressed as the % of the activity of the untreated enzyme (second incubation only).

Increased activity was repeatedly observed when the enzyme was pressurized for short periods of time. Preliminary experiments failed to demonstrate return to the initial activity.

The thermal inactivation of the glycosidase in the presence of the glycoside results in structural changes in the native protein which differ from those caused by inactivation in the absence of the glycoside. Because increased pressure inhibits both enzymic activity and thermal inactivation in the presence of substrate, it is possible that it is the activated enzyme–substrate complex which is denatured at elevated temperatures. The acceleration of inactivation by pressure in the absence of substrate is contrary to most previous reports for protein denaturation. A decrease in molecular volume is generally the result of increased ionization or dehydration. Both of these factors are believed to initiate the denaturation of proteins under certain conditions;

References p. 528.

the final result, however, is a structural rearrangement of the protein resulting in a net volume increase.

One clue to the magnitude of the molecular changes occurring in the inactivation of the phenylglycosidase by heat is revealed in estimates of the energies of inactivation. Rough values of +650 calories per mole in the presence of substrate and +400 calories per mole in its absence were calculated. Such low energies, of course, are not comparable to those for the denaturation of proteins which are often 3 magnitudes greater. However, these values do indicate that only small changes in structure may be required to completely inactivate a specific enzyme.

An interesting example of reversible and irreversible inactivation may be seen in the findings of MORITA AND ZOBELL[7] regarding the effect of pressure on the succinic acid dehydrogenase of *E. coli*. Part of their data is replotted in Fig. 7. Inhibition of the enzyme system at 200 and 600 atm. appears nearly to reverse itself 20 min after the substrate and hydrogen donor were added. In samples previously pressurized at 1000 atm., the inactivation is essentially irreversible. Further analysis of this data (Fig. 7-*insert*) indicates a mole volume change of +50.5 ml per mole for both types of inactivation, estimated from the initial rates of methylene blue reduction.

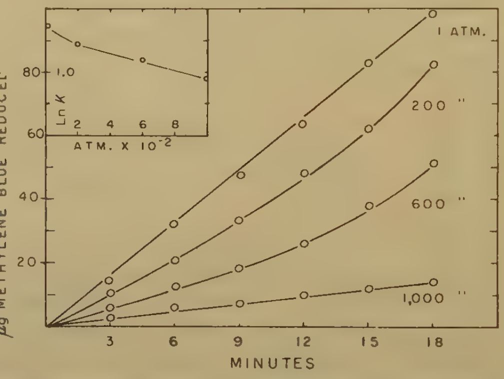

Fig. 7. *Large figure*: (Replotted from MORITA AND ZOBELL, *J. Bacteriol.*, 71 (1956) 668). Micrograms of methylene blue reduced with succinic acid as the hydrogen donor at 30° after different periods of time by 2 mg of lyophilized (9-day) cells of *E. coli* which 30 min previously had been subjected to various pressures for 4 h at 30°. *Insert*: Plot of initial rate of reaction (estimated from large figure) against pressure. Molecular volume change was calculated to be +50.5 ml per mole.

The glycosidase studies were made in phosphate buffer. One may argue that changes in the activity of the enzyme at increased pressure are due to shifts in the pH of the medium. The dissociation of $H_2PO_4^-$ is accompanied by an unusually large molecular volume change: about 24 ml per mole[8]. Starting at the pK of the dissociation, with an increase of 1000 atmospheres the pH change was calculated to be —0.37 units. The effect of pH on the activity of the glycosidase was studied by[3]. A decrease of 0.5 pH units at pH 6.3 changed the activity less than 5 %. Whether this value is increased significantly by increased pressure has not been determined.

CURL AND JANSEN[9] showed that the inactivation of pepsin increases with pressure around the pH of maximum stability. JOHNSON *et al.*[10] found that the luminescence of *P. phosphoreum* decreases with decreased acidity and that this reduction in light intensity is not reversible with the release of pressure.

References p. 528.

Irreversible denaturation of an enzyme system by heat is often preceded by a reversible inactivation. For example the luciferin activity of *Cypridina* decreased 55 % at 48° compared to room temperature. By lowering the temperature to ambient, 85 % of the original activity was recovered[11].

If irreversible and reversible denaturations overlap over a considerable range of temperature, and if there is a difference in their energies of inactivation, then graphic analysis of the magnitude of these factors is not clearcut. Implicitly assumed in such analyses is that the inactivation processes are the result of a single event or mechanism, and indeed this is often the case. But since any number of events occurring simultaneously can cause the inactivation of a highly complex enzyme, the interpretation of kinetic data is simple only when some particular event predominates. Conversely, finding, for example, apparent first-order kinetics for an inactivation process (as was found in part of this study) may lead one erroneously to conclude that the process is simple.

The introduction of pressure as an additional variable further complicates the interpretation of what specifically happens to an enzyme molecule when it is activated or inactivated under a given set of conditions. It is evident, therefore, that to correlate more closely the specific effects of pressure and/or temperature with particular properties of the glycosidase system will require further study.

SUMMARY

The rate of hydrolysis of a phenylglycoside by a glycosidase has been studied over the range 20° to 50° at pressures from ambient to 1000 atmospheres. Increased pressure inhibits both the rate of hydrolysis and the rate of thermal denaturation. However, when substrate is absent, thermal inactivation of the enzyme is accelerated by increased pressure. Some thermodynamic characteristics of the system are presented.*

REFERENCES

[1] D. E. S. Brown and D. A. Marsland, *J. Cell. Comp. Physiol.*, 8 (1936) 159.
[2] D. E. Brown, F. H. Johnson and D. A. Marsland, *J. Cell Comp. Physiol.*, 20 (1942) 151.
[3] L. R. Berger and D. M. Reynolds, *Biochim. Biophys. Acta*, 29 (1958) 522.
[4] C. E. ZoBell and C. H. Oppenheimer, *J. Bacteriol.*, 60 (1950) 771.
[5] O. Folin and V. Ciocalteu, *J. Biol. Chem.*, 73 (1927) 627.
[6] K. J. Laidler, *Arch. Biochem. Biophys.*, 30 (1951) 226.
[7] R. Y. Morita and C. E. ZoBell, *J. Bacteriol.*, 71 (1956) 668.
[8] K. Linderstrøm-Lang and C. F. Jacobsen, *Compt. rend. trav. lab. Carlsberg, Ser. chim.*, 24 (1941) 1.
[9] A. L. Curl and E. F. Jansen, *J. Biol. Chem.*, 185 (1950) 713.
[10] F. H. Johnson, H. Eyring, R. Steblay, H. Chaplin, C. Huber and G. Gherardi, *J. Gen. Physiol.*, 28 (1945) 463.
[11] A. M. Chase, *J. Gen. Physiol.*, 33 (1950) 535.

Received April 5th, 1958

---

* The author is indebted to Dr. Allen G. Marr for his valuable criticisms and suggestions during the course of this study.

(928)

Printed in The Netherlands

XVth International Congress of Zoology, Sect. III, Paper 46

NATURAL HISTORY OF THE GRAY WHALE

C. L. Hubbs

Scripps Institute of Oceanography, La Jolla, California

Eschrichtius gibbosus (= *E. glaucus* = *Rhachianectes glaucus*), one of the most distinctive of the larger cetaceans, is the sole representative of the Eschrichtiidae (= Rhachianectidae). It retains some primitive features, such as simple head form and relatively numerous hairs, and shares characters with Balaenidae and Balaenopteridae. It is confined to the North Pacific and the adjacent Arctic and barely transgresses the Tropic of Cancer. It occurred in Europe in Pleistocene and prehistoric Recent times and in the western Atlantic until early whaling. Occasional sightings of whales during winter suggest the remote possibility that a few survive in the Atlantic.

The residual population is thought to comprise two stocks, one summering in Okhotsk Sea and migrating down the west coast of the Sea of Japan to breed in the bays of southern Korea; the other summering in the western part of Bering Sea and the adjacent Arctic, and migrating down western North America to breed in the lagoons of Mexico. The migratory behavior on the two sides of the Pacific is strikingly similar.

The eastern population seems to strike across the open North Pacific to reach the western United States in the fall; then down the coast, singly or in gams of 2 to 13 or more that may be associated in "waves", very close to shore, navigating from point to point, with some dispersions between, but rounding the points very close to the reef or kelp beds. The course is generally rather straight, and the cruising speed is 2 to 12, generally 3 to 6 miles per hour. They do very little feeding on the southward run. Migration continues on moonlit but not on moonless nights.

The time of migration is remarkably constant. In consistency with early whaling data, the censuses at San Diego since 1946 indicate few stragglers prior to early December, a build up until about Christmas, then the peak movement throughout January and through one to three weeks of February. In February the last southward and first northward migrants pass. The northward movement continues through March and April, occasionally until early May. Strays have been recorded from late spring until early fall.

On the northward journey the Grays move less consistently close to shore and the cows with calves seem to take a more offshore path. They seem to feed at times. They hold to the coast farther northward, along Washington and the west coast of Vancouver Island, before striking across the open sea. The northward migrants are thin from prolonged abstinence.

Contributions from the Scripps Institution of Oceanography, New Series, No. 1053
Reproduced by Permission

San Diego Bay in the southernmost part of California has been abandoned as the northernmost breeding ground, perhaps because sea temperatures have cooled during the past century, perhaps because of human activity. More than 90% of the American population breeds in shallow lagoons of Mexico, between 28° and 24° N. Lat., in an area complementary to breeding grounds of finbacks and humpbacks.

Nearly all the calves are born singly in the shallow muddy lagoons. They nurse underwater as the cow floats. Generally the calf swims close by the mother, but as it grows wanders some. During disturbances the calf stays close and may even be lifted on the cow's flipper (local testimony indicates that this is the defense behavior when killer whales attack). The calves are powerful swimmers; when photographed from a helicopter they threw a strong bow-wave. One kept up with three adults for about three miles when chased at 15 to 20 miles per hour, but at the end was so exhausted that it lay on its side at the surface. It had been so pressed that it surfaced only half as often as adults, though ordinarily calves breathe twice as often.

Copulation has been observed in the lagoons and during the northward migration. One bull was seen by Huey to mate near a lagoon entrance with two cows, each with a calf. Tiny embryos have been found in northward migrants on both sides of the Pacific, whereas, according to Andrews, almost all cows on the southward trip carry young nearly ready for birth. The gestation period therefore seems to be about one year. The same evidence is consistent with the hypothesis that the gray whale females bear young each year, but is inconsistent with the finding that other large whales do not ordinarily breed every year. Scammon assumed a two-year cycle, because the few females he took with small embryos were in better condition than those he assumed had just foaled. Perhaps the resting females do not migrate far enough to have entered the southern whaling grounds. Or the Gray Whale in this respect, as in others, may be unlike the balaenopterids. The rather rapid recoveries of the depleted populations favor the hypothesis of an annual cycle.

The Gray Whale displays some peculiarities in behavior. In normal cruising the members of a gam tend to surface simultaneously, spouting a few times in rather rapid succession (with a vertical, rather mushroom-like, weakly doubled spout of moderate height), just showing the back, then sounding with, usually, a full show of flukes, to advance well below the surface for about three to twelve minutes. In the lagoons movements are less regular, and often show as mud trails from the air, as the whales move in shallow water. They occasionally become stranded and unlike other whales are not killed as a result. Gray Whales apparently sense obstructions and killer whales at a considerable distance, and as an escape reaction may exhale deep below the surface and merely expose the blowholes to inhale. They often zigzag when closely approached. When wounded or pestered repeatedly they show signs of violent anger and will then, only, attack boats. Observed reactions suggest acute hearing. Recent recordings suggest a capacity to produce sounds, but earlier efforts to record sounds were negative.

Gray Whales are extremely subject to attachment of species-specific barnacles and amphipods, which produce conspicuous whitish patches either of the parasites or of scars. Algae, even kelp, may grow on the skin. Several strandings in California in 1958 suggest a possible disease. Killer whales are potent enemies.

The primeval population on the American west coast has been variously estimated as 10,000 to 40,000 or more. Early slaughter (in the mid-1850's), especially of females in the lagoons, soon brought the population to threatened and assumed extirpation, certainly to economic extinction. With whaling nearly eliminated, the population increased enough to support a small fishery in the 1920's and 1930's. Extirpation was again approached, and, incorrectly, assumed. During the past twenty years of protection by international agreement the eastern-Pacific stock has recuperated. Shore census of migrants at San Diego begun by me in 1956 and recently made by Dr. Raymond M. Gilmore and the National Park Service (which conducts a very popular whale watch at the Cabrillo National Monument) has indicated an increase, with recent counts between 1,000 and 2,000. An annual air survey of the lagoon area since 1952, by Gifford C. Ewing with me, Gilmore and others, has yielded counts of Gray Whales as high as 1,261 on a single trip (as many as 742 in one day), with vast concentrations in and near Scammons and San Ignacio lagoons. Making due allowance for whales not observable on each type of census, the current population may be estimated as 3,000 ± 1,000.

There are suggestions that the population rise is levelling off. When such stabilization can be verified, limited harvesting regulated by continued census and research may be indicated. The evidence from whaling records and from current observations that the males remain largely outside the lagoons, in heavy concentration, whereas the calving females stay largely inside, and indications of polygamy, suggest the possibility of harvesting surplus males, after the fashion so effectively followed in the harvest of fur seals.

(932)

526. 1

REMARKS CONCERNING THE PRESENT POSITION OF THE POLE

by

WALTER H. MUNK

Scripps Institution of Oceanography, La Jolla, Calif.*

Abstract

The distribution of continents and oceans largely determines the inertia of the Earth's crust. The axis about which the moment of inertia is a maximum pierces the surface 400 miles southwest of Hawaii. This is the position the north pole would eventually occupy provided (1) the equatorial bulge is not »frozen» but will adopt (in a time of order τ) the shape appropriate to diurnal rotation, (2) oceans and continents are isostatically balanced, (3) the distribution of ocean and continents remains fixed relative to one another, and (4) no other comparative asymmetries in the distribution of matter exists. The rate of polar migration depends on τ. BONDI and GOLD have interpreted the damping of the 14-month wobble in terms of plastic flow in the Earth's mantle, and obtain $\tau = 10$ years. If this value were applicable, then under the foregoing assumptions the travel time of the pole to Hawaii is 100,000 years, a rate of travel 1000 times the upper limits given by astronomical measurements during the last sixty years and by paleomagnetic evidence over the last 10 million years. For earlier times the paleomagnetic evidence indicates a direction opposite to that derived here. This leaves some questions to be answered.

---

* Contribution from the Scripps Institution of Oceanography, New Series. No. 1054

14 — *Geophysica 6:3*

Reproduced by Permission

Introduction

The usual starting point of any discussion on polar wandering is to presume the Earth to be in equilibrium until suddenly disturbed by some implausible rearrangement of matter. The ensuing motion of the pole is then computed for an Earth made of material that can be modeled by appropriate combinations of springs and dashpots. Finally, the computed polar path is found to be in agreement with a bewildering array of paleoclimatic, and more recently paleomagnetic, evidence.

It may be pertinent to inquire whether for any prevailing Earth model the *present* distribution of matter is consistent with the *present* position of the pole. For example, as a consequence of GOLD's [4] model the pole ought to be south of Hawaii. There are ways out of this dilemma, as always, and these may provide some significant geophysical restraints.

The starting point of GOLD's theory is that the dimensions of the equatorial bulge are those appropriate to an equivalent rotating fluid. This suggests that the bulge adjusts itself to diurnal rotation no matter what the orientation of the axis of rotation may be. If the bulge does not offer any long term stability in the position of the pole, what does? The first thing that comes to mind is the distribution of continents and oceans. Compared to the equatorial bulge these are tiny markings on the surface, still they might be the determining factor if the continental distribution is permanent and the bulge appropriately plastic. A rapidly spinning rubber ball would orient itself relative to the rotational axis in accordance with tiny surface markings.

Principal axes of the crust

The problem then is to determine the principal axes of the Earth's crust, neglecting the equatorial eccentricity. If the continents formed a ring around the globe, then obviously one principal axis would be at right angles to this ring, and the continents would be on top of the equatorial bulge. The actual distribution is too complicated to obtain an answer by inspection, but we might guess that the pole should be in the Pacific. This turns out to be a good guess.

Let x,y,z be associated with the present geographic coordinates: x is drawn from the Earth's center through the equator at the meridian of Greenwich, y intersects the equator 90° east of Greenwich, and z is through the north pole. Moments A,B,C and products D,E,F of inertia are then given by

(934)

$$A = \Sigma m(y^2+z^2) \ \ etc.; \qquad D=\Sigma myz \ \ etc.$$

To evaluate $A, B, \ldots F$ it is convenient to switch to the spherical coordinates r, Θ, Φ, where Θ is the colatitude and Φ the east longitude. Now suppose that the variation of density with depth is uniform for all continents, to be designated by $\varrho'(r)$, similarly $\varrho(r)$ refers to oceanic sections. The excess of continental over oceanic inertia equals

$$\begin{aligned} A&=\int\!\!\int\!\!\int(\varrho'-\varrho)r^4(\sin^2\Theta\sin^2\Phi+\cos^2\Theta)\sin\Theta\, dr\, d\Theta\, d\Phi=Ia \\ I&=\int(\varrho'-\varrho)\, r^4\, dr, \qquad a=\int\!\!\int(\sin^2\Theta\sin^2\Phi+\cos^2\Theta)\sin\Theta\, d\Theta\, d\Phi \end{aligned} \tag{1}$$

with a evaluated over continental parts of the Earth. Similarly $B=I\,b$, $\ldots F=I\,f$. We may visualize $A \ldots F$ as the inertia of continental veneers glued on the surface of a sphere.

The problem is to find the principal axis x', y', z', i.e., the axis for which the products of inertia

$$D'=\Sigma m\, y'\, z' \ \text{etc}.$$

vanish. The direction cosines of the x', y', z'-system relative to the x, y, z-system are defined by the scheme

	x	y	z
x'	α_1	β_1	γ_1
y'	α_2	β_2	γ_2
z'	α_3	β_3	γ_3

The solution is

$$\alpha_i \sim e(b-\lambda_i)+df, \quad \beta_i \sim d(a-\lambda_i)+ef, \quad \gamma_i \sim (a-\lambda_i)(b-\lambda_i)-f^2$$

with the proportionality factor determined by $\alpha_i^2+\beta_i^2+\gamma_i^2=1$. The three principal moments of inertia are $A'=I\,a'$, $B'=I\,b'$, $C'=I\,c'$, where $\lambda=a'$, $\lambda=b'$, $\lambda=c'$, are the three roots of the cubic equation

$$\begin{vmatrix} \lambda-a & f & e \\ f & \lambda-b & d \\ e & d & \lambda-c \end{vmatrix} =0$$

The moment of inertia about *any* axis with direction cosines $\alpha_1, \alpha_2, \alpha_3$ relative to the principal axes, is $I\,q$, where

$$q(\alpha_1,\alpha_2,\alpha_3)=a'\alpha_1^2+b'\alpha_2^2+c'\alpha_3^2. \tag{2}$$

The results of numerical calculations are given in Table 1. REVELLE and I have previously evaluated the necessary integrals over all oceans using 10° × 10° grids, and the continental values in column (1) were found by subtraction. Recent seismic work has shown that the dividing line between continental and oceanic structure corresponds roughly to the 1000 fathoms depth contour rather than the coastline. The values in the second column refer to these enlarged continents. After my calculation had been completed, my attention was drawn to the work of MILANKOVITCH [10], which contains values for a 20°×20° grid bounded at the coastline. Milankovitch's values are in column (3). I think his values for a,b,c are too large. The quantity $(a+b+c)/8\pi$ designates the fraction of the Earth's surface covered by continents. His values give 0.41. The accepted ratio is 0.29.

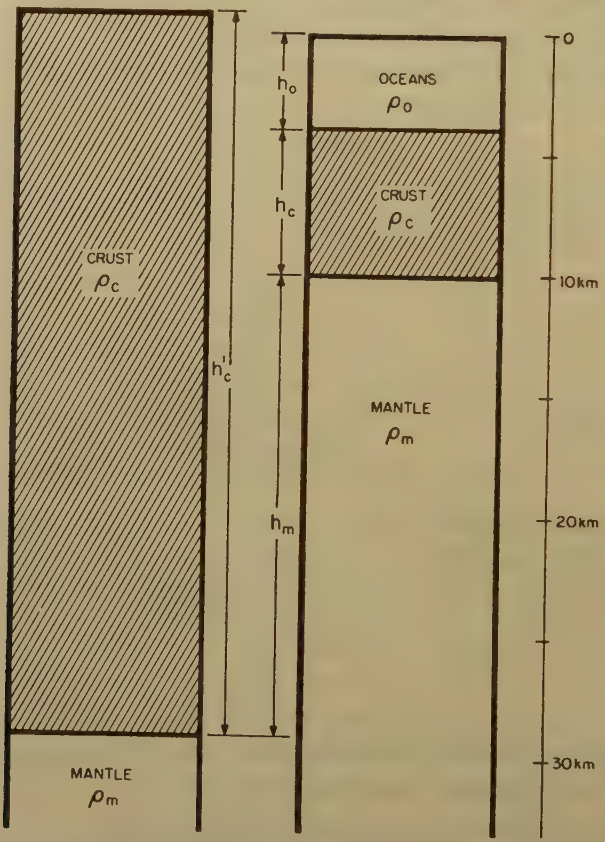

Fig. 1. Standard continental and oceanic sections. The continental section consists of crust material of density $\varrho_c=2.75$ g cm^{-3} and thickness $h'_c=30$ km. The oceanic section consists of ocean ($\varrho_o=1.025$ g cm^{-3}, $h_o=4$ km), crust ($\varrho_c=2.75$ g cm^{-3}, $h_c=6$ km). The density of the mantle is $\varrho_m=3.25$ g cm^{-3}, and $h_m=19.1$ km.

(936)

In all events there is an over-all agreement between the three calculations. The axis of maximum moment of inertia has a pole near Hawaii, and the axis of minimum moment has one near Archangel not too far from the actual pole. The results could hardly be in lesser accord with the present position of the pole.

Milankovitch did not attempt to evaluate the integral I. On the basis of available seismic and gravity work it is now possible to do so. Worzel and Shurbet [14] have proposed standard continental and oceanic sections. I have used a slightly simplified model (Fig. 1) by omitting the sediment layer. Continents and oceans are in isostatic equilibrium.

$$\varrho_c h'_c = \varrho_w h_o + \varrho_c h_c + \varrho_m h_m \,. \tag{3}$$

The elevation of continents above sea level turns out to be

$$z = h'_c - (h_o + h_c + h_m) = 0.9 \text{ km} \tag{4}$$

which is an acceptable value.

Table 1. Moments and products of inertia, $a, b, \ldots, e$, the three principal moments a', b', c', and their northern hemisphere poles for continents bounded by the coast line, the 1000 fathom line, and according to the calculation by Milankovitch and Haubrich.

	coast line	1000 fathoms	Milankovitch	Haubrich
a	2.757	3.473	3.700	4.553
b	2.571	3.137	3.442	3.924
c	2.234	2.692	3.038	3.665
d	0.202	0.192	0.191	0.412
e	0.172	0.161	0.240	0.199
f	0.0725	−0.090	−0.002	−0.056
a'	2.809	3.547	3.790	4.569
Θ	75°	76°	70°	86°
	176°	199°	192°	178°
b'	2.665	3.152	3.491	4.252
Θ	66°	76°	76°	124°
	273°	293°	287°	73°
c'	2.088	2.603	2.899	3.321
Θ	29°	20°	24°	36°
	56°	66°	49°	69°

The evaluation of I (equation 1) involves third order approximations. First order terms cancel because the crust is thin compared to the radius of the Earth; second order terms cancel because of isostacy. Details are cumbersome and uninteresting. The result is

$$\begin{aligned} I &= 2r_0^3(\varrho_c h'^2_c - \varrho_m h_m^2 - \varrho_c h_c^2 - \varrho_o h_o^2 - 2\,\varrho_c h_c h_m - 2\,\varrho_o h_o h_m - 2\,\varrho_o h_o h_c) \\ &= 1.78 \times 10^{39}\ \text{g cm}^2. \end{aligned} \tag{5}$$

where r_0 is the Earth's radius.

Figure 2 shows the moment of inertia of continents (the q-topography, Eq. 2) about any pole, in units of I. The topography has a maximum,

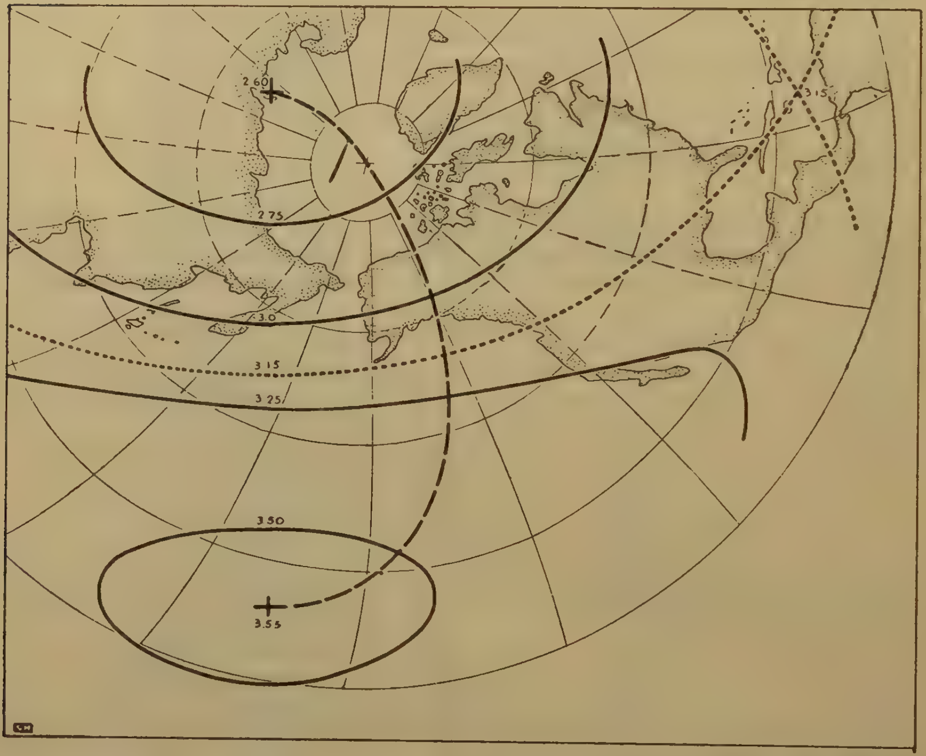

Fig. 2. Inertia of continents. The base chart is in polar coordinates with respect to the principal pole c' (near Archangel). Colatitudes Θ with respect to c' are equally spaced circles (not shown), with the equator ($\Theta = 90°$) through the Hawaii and West Indies poles. The light lines are co-ordinates relative to the present pole. The heavy lines give relative moment of inertia of the crust, q, about any axis; thus $q = 2.70$ about the present axis. The line through the present pole at right angles to the q-topography represents the probable path of polar wandering.

(938)

a', at the Hawaii pole, a minimum, c', at the Archangel pole, and a saddle point at the West Indies (value b'). For comparison, we have the following principal moments of inertia:

Earth	I_e	$=0.8\times10^{45}$ g cm^2
Equatorial bulge	I_b	$=3.0\times10^{42}$ g cm^2
Continents (isostatically balanced)	$a'I$	$=0.6\times10^{40}$ g cm^2

The calculations of Haubrich

After reading a rough draft of this manuscript, Mr. Richard Haubrich felt the need of treating the more general case of variable continents. He has permitted me to report his results here. Haubrich adapted the model of Worzel and Shurbet [14], including the layer of oceanic sediments. When the continental elevation is at sea level ($z=0$) the density and thickness of the continental crust are 2.84 g cm^{-3} and 32.8 km respectively.

For an Airy-type compensation he solved equations (3) and (4) for h'_c and h_m as functions of continental elevation z, and evaluated $I(z)$ from (5):

z in km	0	.2	.5	1	2	4
I in 10^4 g cm^2	.19	.21	.25	.30	.43	.75

For a Pratt-type compensation h_o, h_c and h_m are fixed, and h'_c is determined from equation (4). The right side of equation (3) is now written $\varrho'_c h'_c$ instead of $\varrho_c h'_c$, and ϱ'_c is evaluated:

z in km	0	.2	.5	1	2	4
ϱ'_c in g cm^{-3}	2.84	2.82	2.80	2.76	2.68	2.52

For $z=0$ the models are identical; for $z=1$ km the Pratt-type compensation gives $I=.46\times10^{40}$ g cm^2 compared to $.30\times10^{40}$ for the Airy-type compensation, and 0.18×10^{40} from my calculations with $z=0.9$ km. Some of the discrepancy between Haubrich's and my calculations arises from the difference in the model; still the discrepancy is larger than I had suspected.

The tensor of inertia is evaluated from integrals such as

$$A=\iint I(\Theta,\Phi)(\sin^2\Theta\sin^2\Phi+\cos^2\Theta)\sin\Theta\, d\Theta d\Phi$$

taken over continental parts of the Earth. $I(\Theta,\Phi)$ is the value of I for a mean elevation $z(\Theta,\Phi)$ of a 10°×10° square. It is no longer possible to factor A into a product of two integrals, $A=Ia$ as in the case of uniform continents (Eq. 2).

HAUBRICH's results for the Airy-type compensation are included in Table 1. The pole of maximum inertia is still in the central Pacific, but 10° further south than I found. The pole of minimum inertia is displaced towards the Himalaya complex in accordance with the larger moment of intertia accorded to high-lying regions. For a Pratt-type compensation the discrepancy between the uniform and non-uniform continent models would be larger still.

Further remarks concerning principal axes

The differences in the computed positions of the axes for various models give some indication of the limits placed by our present knowledge of the crust. Seismic evidence has not made a clear-cut decision between the two basic types of compensation. The shallow Moho under the Colorado and Mexican plateaus favors a Pratt-type compensation; the root beneath the Appalachians speaks for an Airy-type compensation. No allowance has been made in any of the models for the large shoal areas of the oceans (subcontinents) whose structure is intermediate between that of oceans and continents.

The following two examples serve to bring out explicitly the role played by major features. An icecap (density $\varrho_i=0.9$ g cm^{-3}, thickness $h_i=3$ km) covers Greenland. As a result of the ice load the crust is pushed downward into the mantle. Assuming Airy-type compensation, the products of inertia are

$$D_i=I'd_i,\ E_i=I'e_i, \text{ where}$$

$$I'=\varrho_i h_i a^4 \iota,\quad \iota=4\frac{h'_c}{a}\left(1-\frac{\varrho_c}{\varrho_m}\right)+2h_i\left(1-\frac{\varrho_i}{\varrho_m}\right)=0.003$$

with ι designating the isostatic factor. For Greenland bounded at the coastline $d_i=-0.010$, $e_i=0.011$. The resultant products of inertia are $D_i=-1.33\times10^{34}$ g cm^2, $E_i=1.47\times10^{34}$ g cm^2, compared to $D=Id=3.4\times10^{38}$ g cm^2, $E=2.9\times10^{38}$ g cm^2 for all continents. Clearly the inertia of the Greenland icecap is negligible, and no reasonable icecap can balance the torque exerted by continents. The Himalaya complex raises 3×10^{22}g of matter above normal continental height, and the Andes about 1×10^{22}g. The Alps are negligible. The products of inertia of the incremental masses, assumed isostatically compensated, are 1.3×10^{37}g cm^2 and 0.4×10^{37}g cm^2 respectively. These values are sufficiently large compared to the products of inertia of the crust to account for the order of difference between HAUBRICH's calculation and mine (Table 1); still the over-all result as portrayed in Fig. 2 is substantially correct, the contour interval being of the order 10^{39}g cm^2.

GOLD has pointed out that a polar ocean provides a polar trap. If the pole were to move towards shore, additional ice is deposited there which would eventually drive the pole offshore. He suggests that the Arctic Ocean may account for the apparent stability of the pole over the last few million years. The foregoing calculations indicate that the effect of an icecap is relatively small.

The path of polar wandering

BURGERS [2] and INGLIS [6] have treated the dynamics of polar wandering for an elasto-viscous Earth: this corresponds to a spring and dashpot in series (Maxwell body; SCHEIDEGGER, [12]) so that for disturbances of short period the elastic properties dominate, whereas under prolonged stress the body yields like a fluid. For a sudden upheaval in the crust (say) the solution consists of oscillatory terms that are damped like $e^{-t/\tau}$, together with the velocity components

$$\dot{l} = -\frac{r_o}{\tau}\frac{E}{C-A}, \qquad \dot{m} = -\frac{r_o}{\tau}\frac{D}{C-A} \tag{6}$$

of the pole's wandering toward Greenwich, and 90° East of Greenwich, respectively. The moment of inertia of the equatorial bulge is $C-A$ and large compared to $B-A$. The principal pole of the Earth (not the crust) is at

$$l_p = -r_o E/(C-A), \qquad m_p = -r_o D/(C-A)$$

with respect to the coordinate system used to compute the inertial tensor. As the pole of rotation wanders, the position of the equatorial bulge changes with respect to the original coordinate system, and this affects the products of inertia D and E, and hence the position of the principal pole. Polar wandering continues until the principal axes of the Earth coincide once more with those of the crust. The reader is referred to BURGERS and INGLIS for a mathematical treatment, and to GOLD who anticipated these results by qualitative reasoning.

The derivation of (6) is based on the principle of conservation of angular momentum. Products of inertia D,E are associated with the difference in the inertia of equivalent continental and oceanic areas. In the case of isostatic compensation the difference is of second order; it arises only because continents are a bit further from the axis of rotation than oceans. It is instructive to point out that one can adopt an alternate point of view, which is to start with the difference in centrifugal force exerted on equivalent continental and oceanic areas. In the case of isostacy this again depends on a second order effect: the centrifugal force on continents is somewhat larger, these being further removed from the axis of rotation. This second order force is known as the Polfluchkraft of Eötvös. It has become so involved in speculations concerning continental drift, that it seems appropriate to emphasize that it enters here in a more subtle way. There is no need for this force to shift continents relative to one another, nor to slip the crust over the rest of the Earth; rather there is a torque on the Earth as a whole which will alter its orientation relative to the axis of rotation until the torque vanishes. This final position corresponds once more to rotation about the principal axis of the crust.

Polar wandering can be visualized as a slow wave-like propagation of the equatorial bulge with respect to the Earth, much like a tidal bulge. From the point of view of an observer in space the bulge remains fixed relative to the ecliptic plane, and the Earth slowly turns under it. This is not a *slippage* of the crust over the mantle as suggested by many authors. Slippage would require that the thickness of a viscous boundary layer be small compared to the Earth's radius, whereas just the reverse is true.[1]

Milankovitch reasoned that the pole must slide »downhill» toward the pole of maximum inertia, that is, along a line normal to the q-topography. This seems reasonable enough, yet I do not find it an obvious result. A derivation of the path, starting with (6), is given in the Appendix. It turns out that a path along the orthogonal is an adequate approximation provided the damping time τ is long compared to the period of free nutation. The observed ratio is 8:1.

The equation of the path is simple in terms of the geographical coodinates with respect to the principal continental axis: Let Θ' be colatitude south of the Archangel pole, and Φ' longitude east of the Hawaii pole. Eq. (2) can be written

---

[1] For a viscosity $\nu = 10^{20}$ cm^2 sec^{-1} and a period T of only 10 years, the thickness of the layer is $\sqrt{\nu T/\pi} = 10^{14}$ cm $= 10^5$ times the Earth's radius.

(942)

$$\sin^2\Theta'(k-\sin^2\Phi')=(q-c')/(a'-b')\,, \qquad k=(a'-c')/(a'-b')\,.$$

The family of lines at right angles to the q-contours is then

$$\tan\Theta' \cos\Phi' \tan^k\Phi' = \text{constant}\,, \tag{7}$$

an equation given by MILANKOVITCH. The orthogonal line through the present pole is drawn in Figure 2.

The direction of polar wandering

The computed direction of polar wandering is toward the principal pole near Hawaii. On the basis of paleoclimatic evidence which he considered as »unzweideutig», MILANKOVITCH drew the arrow along his orthogonal (which does not differ too much from the orthogonal in Figure 2) pointing *away* from the Pacific. JARDETSKY [7] seems to have gone along with this interpretation. Recent paleomagnetic evidence also indicates wandering away from the Pacific, but the evidence is far from *unzweideutig*, I think, and the time scales of the climatic and magnetic evidence do not agree at all well. The interpretation of Milankovitch and Jardetzky implies a reverse polarity, or a negative value of the integral I. This means that the inertia of continents is *less* than that of oceans in contradiction with the present isostatic model. On this basis GUTENBERG ([5], p. 203) has criticized Milankovitch's paper.

However the suggestion of a reverse polarity desires further consideration. In the isostatic model the inertia of the crust depends on the second order term resulting from the slightly larger radial distance of continents than oceans. Suppose that isostatic balance does not hold precisely, but that there is a slight erosion of continental matter and sedimentation on the ocean floor which is not compensated. This represents a first order effect which might reverse the sign of I. This is an intriguing possibility. It would place the pole of maximum inertia at Archangel, where it is a relatively small distance from the actual pole (though HAUBRICH's calculation places it further south); whereas for the isostatic model the pole is about as far removed from the principal pole as it can be.

For the isostatic model $I=1.78\times10^{39}$g cm². How much material would have to be eroded from continents and deposited on the sea floor to make $I=0$, presuming the erosion process to be uncompensated? The oceans occupy 2.5 times the area occupied by continents. For $\varrho_c\Delta h$ g cm^{-2} removed from continents, 0.4 $\varrho_c\Delta h$ g cm^{-2} are deposited as sediments, and I is diminished by $1.4\,\varrho_c \Delta h\, r_0^4$. Uncompensated erosion by $\Delta h = 28$ meters will make $I = 0$. Hence if the elevation of continents above sea level by 900 meters represents an isostatic elevation of 930 together with an uncompensated lowering by 30 meters, the sign of I would indeed be negative.

What do these models imply with regard to gravity anomalies? The simplest procedure is to take continents as elevated strips on an infinite plane. First take the absurd example of complete lack of compensation. If the oceans are condensed from a density ϱ_o to ϱ_c, sea level is lowered by $h_o(1 - \varrho_o/\varrho_c) = 2.5$ km, and the elevation of continents above the condensed sea is $\Delta h = 0.9 + 2.5 = 3.4$ km. The gravity anomaly over the central portion of the continent is

$$\Delta g = 2\pi\, G\, \varrho_c \Delta h = 0.392 \text{ cm sec}^{-2},$$

where G is the gravitational constant. For the compensated model the gravity anomaly is found by an extension of the formula given by Jeffreys ([8], p. 175). The strip extends from $\xi = -L$ to $\xi = +L$. Jeffreys has shown that Δg is remarkably uniform except near the continental edges, and we might as well restrict ourselves to the center, $\xi = 0$. Writing $\Delta\varrho = \varrho'(\zeta) - \varrho(\zeta)$ for the excess of continental over oceanic density at depth ζ, we have

$$\begin{aligned} \Delta g &= 4G \textstyle\int\int \Delta\varrho \sin \varkappa L\, e^{-\varkappa L} \varkappa^{-1}\, d\varkappa\, d\zeta\,, \\ &= 4G \textstyle\int \Delta\varrho \cot^{-1}(\zeta/L)\, d\zeta\,, \\ &= 2\pi G \textstyle\int \Delta\varrho\, d\zeta - \dfrac{4G}{L} \textstyle\int \Delta\varrho\, d\zeta\,. \end{aligned}$$

Δg gives the excess of free-air gravity anomalies on continents over that on oceans. In the case of isostasy, only the second term remains. For the model in Figure 1 and for $2L = 6000$ km this gives $\Delta g = +0.8$ mgals. In the case of an uncompensated lowering of continents by $\Delta h = 4.8$ meters, the positive anomaly is annulled. Uncompensated erosion by 28 meters gives $\Delta g = -4.5$ mgals. There may be some concern about the thin plate model of continents, but it can be shown that little is changed by allowing for the spherical shape. The calculations are given by Jeffreys ([8], 5.06) and need not be repeated here. The results are sommarized in Table 3.

If gravity anomalies on continents were consistently higher, or lower than over oceans, then the question of whether I is positive or negative could be decided. Unfortunately relatively large local anomalies make it impossible to make this decision. Certainly the assumption of no compensation is wildly wrong, but it is impossible to tell whether compensation is by 100% or 99%, and this is what we need to know. JEFFREYS ([8], p. 175) gives the following average values of free-air anomalies: Continents 0°—60° East, $+8.4 \pm 3.6$ mgals; Atlantic Ocean $+6.4 \pm 4.7$; North and South America, -1.6 ± 5.7; these averages do not suggest that the oceans have consistently lower anomalies than the continents.

There is a fair chance that this problem can be resolved from the observed orbit of the IGY satellites.

The following hypothetical train of events may serve to illustrate the present considerations. Suppose that initially continents and oceans are compensated. The inertia of the continents exceeds that of the oceans (I is positive) and the pole is south of Hawaii. The free-air gravity anomaly over continents is about $+1$ mgal. Subsequently erosion takes place, and the continents lose mass, the sea bottom gains mass. The erosion is too rapid for isostatic compensation to be effective or perhaps the stresses involved are below some critical values required for the initiation of compensating currents in the mantle. As a result, the excess inertia of the continents dwindles, and by the time the continents have been eroded by 30 meters and the sedimentary blanket thickened by something like 15 meters, the inertia per unit area is the same for continents and oceans. Subsequent erosion reverses the polarity of the principal axis and the pole of rotation moves rapidly towards the present position. At the time of reversal the gravity anomaly over continents is about -5 mgals. Further erosion will stabilize the pole in its new position. Uncompensated erosion by an additional 30 meters would assure that the pole remain essentially in its present position without being materially affected by icecaps and mountain formations.

Table 3. Horizontal pressure difference in the mantle between continents and oceans, free air gravity anomalies on continents and products of inertia of continents for various models

	ΔP dynes cm^{-2}	Δg milligals	I g cm^2
(1) No compensation	92×10^7	392	154×10^{39}
(2) Isostasy	0	0.8	1.78×10^{39}
(3) No gravity anomalies	-0.2×10^7	0	1.48×10^{39}
(4) No continental torque	-1.1×10^7	-4.5	0

At the end of the erosional epoch, the isostatic state is again approached, and the pole switches back to Hawaii.

The gravity data are not unfavorable to this hypothesis, but there is some difficulty in reconciling the required departures from isostasy with fluidity indicated by the damping of the wobble. A surface load leads to an adjustment in the shape of the Earth. This involves local deformation (high order spherical harmonics) as well as global deformation (low order harmonics). The local adjustments take place relatively slowly, the global adjustments occur rapidly. The products of inertia involve deformations of order 2, and so does the equatorial bulge. Hence the time constant of isostatic adjustment of the inertia terms turns out to be the same as the time constant τ of polar wandering: 10 years according to BONDI and GOLD (see next section). In the case of a uniform sedimentation it follows that the departure from isostasy is due to sediments deposited in 10 years. This is of the order 5 cm, and not 15 meters as required. There is still the possibility that the uncompensated load is maintained until some critical stress is exceeded. The elasto-viscous model is then wrong. BONDI and GOLD's theory of the damping of the wobble becomes doubtful, for certainly the stresses involved are then far below the critical value.

But even if the Earth can maintain sufficient anisostasy to reverse I, one would expect polar wandering towards Archangel at a rate of a few tens of meters per year, unless by chance I is very near zero. This is still too fast. To say that the distance between the present pole and Archangel is too small to be significant is to imply that the values of d and e in Table 1 do not differ significantly from zero. I think they do.

The rate of polar wandering

The observed damping time of the 14-month nutation (Chandler wobble) has been estimated by RUDNICK [11] as 10 years and by WALKER and Young [13] as 10 to 30 years. BONDI and GOLD [1] have presented arguments as to why the damping must be due to dissipation in the Earth's mantle; if so, then according to the elasto-viscous model the damping time and the time constant τ of polar wandering are one and the same, and accordingly the rate of polar wandering can be computed for a given disturbance from equation (6). Using the value $\tau=10$ years it is embarrassingly simple to turn the Earth around. The Himalayas alone could do it in a 100 million years, and so could reasonable climatic fluctuation in sea level. Even winds would have a non-negligible effect.

Numerical values appropriate to the 1000 fathom uniform continents give a movement by 100 meters per year toward Vancouver. Astronomical observations place an upper limit of 5 meters during the last 50 years. The rate would slowly increase, being largest when the pole is in the Gulf of Alaska, midway between the two principal poles; from then on polar wandering diminishes. The actual rate can be found from equations (7) and (10). The time required to travel most of the way to the Hawaii pole is of the order (Appendix, Eq. 10)

$$\frac{I_b}{(a'-b')I}\,\tau$$

or 100,000 years. Paleomagnetic evidence places an upper limit of about 10° latitude during the last ten million years. In both instances the limits are 1/1000 the derived values.

Inhomogeneities in the mantle

The calculations so far have been made under the assumption that the distribution of continents and oceans are the features most likely to be responsible for the position of the pole.

Irregularities in the distribution of matter in the *mantle* could be an important factor. Jeffreys ([8], p. 177) has compiled a free-air anomaly chart for the world. These anomalies represent departures from the *normal gravity*, which contains terms in $\cos^2\Theta$ and $\cos^2 2\Theta$. There are large areas for which gravity observations are lacking, and when these become available the coefficient of $\cos^2\Theta$ and $\cos^2 2\Theta$ in the formula for normal gravity will be altered. This means that the plotted free-air pattern is subject to uncertainty not only in regions where observations are lacking, but in other regions as well.

The first thing one notices from Jeffreys's chart is that the free-air gravity anomalies bear no obvious resemblance to the continental structure. If the continental structure were badly out of isostatic adjustment, then there would be such a resemblance. The least forced interpretation is that the continental structure is nearly in isostatic adjustment (though small but important departures of the kind discussed in the previous section can by no means be ruled out), and that the observed gravity anomalies have their source in the mantle. They might be an indication of bubbles of heavy and light material supported by viscous forces in convection currents. The pressure along the bottom of a boiling pot of porridge is not constant, nor is the gravity along the surface. The observation that the pole is not now moving quickly implies then that the distribution in the mantle has been essentially stationary for at least 100,000 years.

The observed gravity pattern does not provide a unique solution concerning the depth of the mass anomalies. Assume that they occur at one fixed distance r_1 from the Earth's center, and let σ_2 designate that part of the density anomaly per unit area that can be represented by spherical harmonics of degree two. These are the only terms in the density distribution that contribute to the products of inertia. Thus

$$D = \iiint r^4 \varrho(r) \sin^2\Theta \cos\Theta \sin\Phi \, dr \, d\Theta \, d\Phi = r_1^4 \sigma_2$$

where

$$\sigma_2 = \iint \sigma(\Theta,\Phi) \sin^2\Theta \cos\Theta \sin\Phi \, d\Theta \, d\Phi \, .$$

Define

$$g_2 = \iint g(\Theta,\Phi) \sin^2\Theta \cos\Theta \sin\Phi \, d\Theta \, d\Phi$$

and similarly g_2' by replacing $\sin\Phi$ with $\cos\Phi$. The free-airanomalies at the surface due to σ_2 are (JEFFREYS, [8], p. 171)

$$g_2 = \frac{12\pi G}{5} \left(\frac{r_1}{r_0}\right)^3 \sigma_2$$

and we can express D in terms of g_2. It is convenient to introduce the Earth's moment of inertia, $I_e = \frac{1}{3} M a^2$, its mass $M = \frac{4}{3}\pi \varrho_e a^3$ and the mean gravity at the surface, $\bar{g} = \frac{4}{3}\pi G r_0 \varrho_e$. Then

$$D = \frac{5}{4\pi} I_e \frac{r_1}{r_0} \frac{g_2}{\bar{g}}, \qquad E = \frac{5}{4\pi} I_e \frac{r_1}{r_0} \frac{g_2'}{\bar{g}}$$

Harmonic analysis of Jeffreys's chart gives

$$g_2 = -0.41 \text{ mgals}, \qquad g_2' = 2.10 \text{ mgals}$$

so that

$$D = -1.4(r_1/r_0)10^{38} \text{ g cm}^2, \qquad E = 6.9(r_1/r_0)10^{38} \text{ g cm}^2$$

compared to

$$D = 3.4 \times 10^{38} \text{ g cm}^2 \qquad E = 2.9 \times 10^{38} \text{ g cm}^2$$

(948)

for the isostatically compensated crust. The ratio r_1/r_0 varies from 1/2 at the bottom of the mantle to 1 at the top. The first thing to notice is that the products of inertia of the mantle, as inferred from free-air gravity anomalies, are of the same order as those of the crust; the second thing is that they are not properly distributed in longitude to balance those of the crust. It will be recalled that the isostatic balanced continents tend to move the pole toward Vancouver. What is required for balance are gravity anomalies with the extreme values of the second degree harmonic distributed as follows:

	130°W	50°E
Northern Hemisphere	+5 mgals	−5 mgals
Southern Hemisphere	−5 mgals	+5 mgals

Such distribution cannot be ruled out on the basis of our present knowledge of gravity.

It should be pointed out that, according to the present hypothesis, it is not accidental that the inertial terms in the mantle should be of equal magnitude to those in the crust. Suppose for the moment those in the mantle were much larger. Then the pole would rapidly adjust so as to reduce their magnitude, and in the final position only a small residue would be left, just large enough to balance the crust.

If this explanation of the present position of the pole is the correct one, then there are three sets of principal axes, that of the crust, that of the mantle, and the combined set. The combined set then presumably coincides with the true axis. Crust and mantle would twist relative to one another, until eventually the axes of crust and mantle coincide with each other and with the axis of rotation. The twisting motion might be from 1000 to 10,000 times slower than polar wandering. First of all the shear is larger because only a thin outer shell is involved, and secondly the viscosity of the outer mantle may be larger than the average viscosity of the Earth.

Discussion

For an elasto-viscous Earth with isostatically compensated continents and oceans the stable position of the pole is near Hawaii; if it were elsewhere it would reach Hawaii probably in 100,000 years. The following alternatives might account for the fact that the pole is not near Hawaii. (1) The equatorial bulge is frozen. The pole then remains practically where it is regardless of the distribution of continents and oceans; Bondi and Gold's treatment of the damping of the Chandler wobble is not correct, and the problem remains to be solved. (2) The bulge is fluid, and the pole is determined by the distribution of continents. These are not balanced isostatically, but more than 30 meters have been eroded from continents and deposited on the sea floor without compensation. This scheme would place the stable pole much nearer the observed position (but I think still too far away). There is no conflict with observed gravity values, but it is difficult to assign sufficient fluidity to account for the damping of the Chandler wobble and yet achieve the required degree of anisostacy to reverse the polarity of the principal axes. (3) There are mass anomalies in the mantle which together with the distribution of land and sea determine the axis of rotation. The associated gravity anomalies would be of the same order as those observed, but the required pattern is quite different from the one drawn by Jeffreys. (4) I favor a still different alternative: the Earth is anelastic in the sense that it behaves as an elastic solid for short-period disturbances, and, given sufficient time, will adopt a shape appropriate to an equivalent rotating fluid. This much it has in common with the elasto-viscous model; but there are any number of laws which have such an asymptotic behavior without requiring that the time constant of nutational damping be identified with the time constant of polar wandering. Scheidegger [12], for example, suggests that for time intervals of hours to 15,000 years the Earth behaves as a »Kelvin body» (spring and dashpot in series) with a »viscosity» of 10^{17} cm^2 sec^{-1}, whereas for time intervals larger than 15,000 years it behaves as a »Bingham body» (finite yield strength) with viscosity of 2×10^{21} cm^2 sec^{-1}. For a 10 years damping time then the pole requires $10^5 \times (2 \times 10^{21}/10^{17}) = 2 \times 10^9$ years to migrate to Hawaii; there is no discrepancy with astronomic and paleo-magnetic observation, in fact there is no polar wandering in the usual sense. — In all events some very serious doubts concerning the elasto-viscous model have been raised by Carl Eckart during a symposium at the Massachusetts Institute of Technology in September 1956, and these have their roots in the distinction between »deformation» and »strain» (Eckart, [3]). More recently Knopoff and MacDonald (in press) have proved that no possible combination of springs and dashpots can adequately portray the damping of seismic waves. It appears that the extrapolation from nutational damping to polar wandering is on shaky ground. Our dilemma is resolved if the time

(950)

constant of polar wandering is increased by a factor 10^3 over what was used in this paper; if the factor is larger than 10^5 there can be no polar wandering.

Appendix

At time 0 the pole of rotation is at

$$x=0, \qquad y=0, \qquad z=r_0 .$$

$$x'=\gamma_1 r_0 , \qquad y'=\gamma_2 r_0 , \qquad z'=\gamma_3 r_0$$

in terms of present coordinates and principal axes respectively. After a time δt the pole is at

$$x=\delta x, \qquad y=\delta y , \qquad z=r_0 ,$$

and

$$x'=\gamma_1 r_0+\alpha_1 \delta x+\beta_1 \delta y ,$$

with similar expressions for y', z'. The direction cosines of the new axis are of the form $\gamma_1+\delta\gamma_1$, so that

$$x'=(\gamma_1+\delta\gamma_1) r_0 .$$

Hence

$$\alpha_1 \delta x+\beta_1 \delta y=r_0 \delta\gamma_1$$
$$\alpha_2 \delta x+\beta_2 \delta y=r_0 \delta\gamma_2$$
$$\alpha_3 \delta x+\beta_3 \delta y=r_0 \delta\gamma_3$$

We shall need to express the products of inertia in terms of the principal system

$$\begin{aligned} D&=\sum m y z=\sum m(\beta_1 x'+\beta_2 y'+\beta_3 z')(\gamma_1 x'+\gamma_2 y'+\gamma_3 z') \\ &=\sum m \beta_1\gamma_1 x'^2+\sum m \beta_2\gamma_2 y'^2+\sum m \beta_3\gamma_3 z'^2 \\ &=\tfrac{1}{2}[\beta_1\gamma_1(B'+C'-A')+\beta_2\gamma_2(C'+A'-B')+\beta_3\gamma_3(A'+B'-C')] \\ &=\beta_1\gamma_1 (C'-A')+\beta_2\gamma_2 (C'-B') . \end{aligned} \tag{9a}$$

Similarly

$$E=\alpha_1\beta_1 (C'-A')+\alpha_2\gamma_2 (C'-B') \tag{9b}$$

Combining (6) (8) and (9) and setting $K=I/(C_0-A_0)$ gives

$$\frac{\delta\gamma_1}{\delta t}=-\frac{K\alpha_1}{\tau}e-\frac{K\beta_1}{\tau}d$$

$$= -\frac{K}{\tau}\left[\gamma_1\left(\alpha_1^2+\beta_1^2\right)(c'-a')+\gamma_2(\alpha_1\,\alpha_2+\beta_1\,\beta_2)(c'-b')\right]$$

$$= -\frac{K}{\tau}\left[\gamma_1\left(1-\gamma_1^2\right)(c'-a')-\gamma_2(\gamma_1\cdot\gamma_2)\,(c'-b')\right]$$

$$\frac{\delta\, ln\, \gamma_1}{\delta t} = \frac{K}{\tau}\left[\left(\gamma_1^2-1\right)(c'-a')+\gamma_2^2(c'-b')\right]$$

Similarly

$$\frac{\delta\, ln\, \gamma_2}{\delta t} = \frac{K}{\tau}\left[\gamma_1^2\,(c'-a')+\left(\gamma_2^2-1\right)(c'-b')\right]$$

$$\frac{\delta\, ln\, \gamma_3}{\delta t} = \frac{K}{\tau}\left[\gamma_1^2\,(c'-a')+\gamma_2^2\,(c'-b')\right]$$

and

$$\frac{\delta}{\delta t}(ln\,\gamma_2 - ln\,\gamma_1) = \frac{K}{\tau}\left[(c'-a')-(c'-b')\right] = -\frac{K}{\tau}(a'-b')\,. \qquad (10)$$

But $\gamma_2/\gamma_1 = \tan \Phi'$, so that

$$\tan \Phi' = \tan \Phi_0'\, e^{-K(a'-b')t/\tau} \qquad (11)$$

where Φ_0' designates the east longitude of the pole (referred to principal axes) at the present time, $t=0$. From the last two equations

$$\frac{\delta}{\delta t}\, ln\, (\gamma_3/\gamma_2) = \frac{K}{\tau}(c'-b')$$

Dividing by (10) yields

$$\frac{\delta\, ln\, (\gamma_3/\gamma_2)}{\delta\, ln\, (\gamma_2/\gamma_1)} = \frac{b'-c'}{a'-b'} = k-1$$

which reduces to equation (7) in the text.

Acknowledgements. I am indebted to Sam Hinton for Fig. 2. This work was made possible by support from the National Science Foundation.

(952)

REFERENCES

1. Bondi, H. and T. Gold, 1955: On the damping of the free nutation of the earth, *Mon. Not. Roy. Ast. Soc.*, **115**, 41—46.
2. Burgers, J. M., 1955: Rotational motion of a sphere subject to visco-elastic deformation, *Proc. Konikl. Ned. Akad. Wetenshap. B*, **58**, 219—237.
3. Eckart, C., 1948: The theory of elasticity and anelasticity, *Phys. Rev.*, **73**, 373—382.
4. Gold, T., 1955: Instability of the Earth's axis of rotation, *Nature*, **175**, 526—534.
5. Gutenberg, B., 1951: *Internal constitution of the Earth*, 2nd Ed., Dover.
6. Inglis, David R., 1957: Shifting of the Earth's axis of rotation, *Rev. of Mod. Physics*, **29**, 9—19.
7. Jardetzky, W., 1949: On the rotation of the Earth during its evolution, *Trans. Amer. Geophys. Union*, **30**, 797—817.
8. Jeffreys, Sir Harold, 1952: *The Earth*, Cambridge Press.
9. Knopoff, L. and G. MacDonald: The attenuation of small amplitude stress waves in solids, *Rev. of Mod. Physics*, (in press).
10. Milankovitch, M., 1934: Der Mechanismus der Polverlagerungen und die daraus sich ergebenden Polbahnkurven, *Gerlands Beitr. z. Geoph.*, **42**, 70—97.
11. Rudnick, P., 1956: The spectrum of the variation in latitude, *Trans. Amer. Geophys. Union*, **37**, 137—142.
12. Scheidegger, A. E., 1957: Rheology of the Earth, *Canadian J. of Physics*, **35**, 383—397.
13. Walker, A. M. and A. Young, 1957: Further results on the analysis of the variation of latitude, *Mon. Not. Roy. Astr. Soc.*, **117**, 119—141.
14. Worzel, J. L. and G. L. Shurbet, 1955: Gravity interpretations from standard oceanic and continental section, *Geol. Soc. Amer. Spec. Paper* **62**, 87—100.

FURTHER NOTES ON SOME APPENDICULARIANS FROM THE EASTERN PACIFIC[1][2]

Takasi TOKIOKA

Seto Marine Biological Laboratory, Sirahama

With 10 Text-figures

This is the second taxonomic note on appendicularians collected by and stored in the laboratory of the Scripps Institution of Oceanography. After the manuscript of my paper, "Two new appendicularians from the Eastern Pacific, with notes on the morphology of *Fritillaria aequatorialis* and *Tectillaria fertilis*" (Tokioka, 1957) had been sent to the editor of the Transactions of the American Microscopical Society, the examination of the plankton samples collected by Shellback and Equapac Expeditions was continued for three months. During this time, I found a few more perfectly preserved specimens of *Fritillaria taeniogona* Tokioka and some sexually mature individuals of the form described under the name of *Fritillaria aequatorialis* Lohmann in the paper mentioned above. Critical studies of these specimens made it clear that the former were related to the genus *Tectillaria* more closely than to the genus *Fritillaria*. The latter group differs distinctly from *Fritillaria aequatorialis* Lohmann not only in the form of the tail, but also in the structure of the gonad, thus they belong to a new species, for which the name "*pacifica*" is proposed. In addition, the results of the detailed examination of *Fritillaria aberrans* Lohmann and *Fritillaria magna* Lohmann, both described rather insufficiently to this date, and short notes on *Folia gracilis* Lohmann and *Megalocercus abyssorum* Chun are given here. Among the morphological characteristics of *Fritillaria aberrans* and *Fritillaria magna* Lohmann, it is most interesting that a circular muscle-like band is found in the anterior part of the pharynx, previously no muscular band has ever been observed on the trunk of any of the appendicularians.

Before going further, I wish to express my hearty thanks to members of the staff who granted me the fovour of having a seat at Scripps Institution of Oceanography for a year, and especially to Prof. Martin W. Johnson for his kindness in providing facilities.

---

1) Contribution from Scripps Institution of Oceanography, New Series. No. 1055

2) Contributions from the Seto Marine Biological Laboratory, No. 316.

Publ. Seto Mar. Biol. Lab., VII (1), 1958. (Article 1)

Reproduced by Permission

1. *Megalocercus abyssorum* CHUN, 1888

(Fig. 1)

CHUN, C. (1888): Die pelagische Tierwelt in grösseren Meerestiefen und ihre Beziehungen zu der Oberflächenfauna. Bibliotheca Zoologica, I (1), pp. 40–42.

SEELIGER, O. (1893–1911): BRONN's Klassen und Ordnungen des Tier-Reichs, III Supplement Tunicata I abt., pp. 138–139, Taf. I figs. 3–5.

LOHMANN, H. und BÜCKMANN, AD. (1926): Ergebn. Deutsch. Südpolar-Exped., Bd. 18 (Zool. Bd. 10).

LOHMANN, H. (1933–34): KÜKENTHAL u. KRUMBACH-Handbuch d. Zoologie, Bd. V, Zweite Hälfte Tunicata, p. 186, Figs. 64–3 and 149.

BERNARD, M. F. (1954): Bull. Société d'Hist. Nat. Afrique d. Nord, Tom. 45, pp. 344–347, 2 figs.

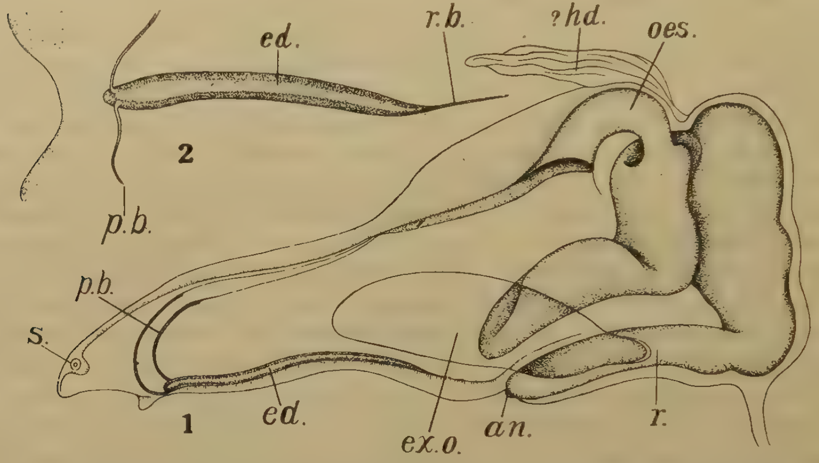

Fig. 1. *Megalocercus abyssorum* CHUN. 1—Left side of the 1.6 mm long trunk from MP–10. 2—Endostyle of the same specimen, dorsal side. *an.*···anus, *ed.*···endostyle, *ex.o.*··· gill opening, *?hd.*···?hood, *oes.*···oesophagus, *p.b.*···peripharyngeal band, *r.*···rectum, *r.b.*···retropharyngeal band, *s.*···statocyst.

Two specimens found in the examined samples, and belonging to the genus *Megalocercus*, differ distinctly from *M. huxleyi* (RITTER) which is distributed very widely and commonly in the Pacific. They each have a strangely shaped left stomach-lobe with a striking elongate blind caecum at the antero-ventral angle, which projects forward along the dorsal side of the rectum (*r.*) as far as its distal end, reaching approximately the level of the anus (*an.*). The endostyle (*ed.*) is elongate and very slender; the gill openings (*ex.o.*) are very large and devoid of ciliated spiracles. The smaller of the two specimens has a hood-like appendage (?*hd.*) attached dorsally near the junction between the small right stomach-lobe and the rather voluminous intestine. It is not clear whether this is a natural structure or a piece of torn epidermis. The existence of a blind caecum at the antero-ventral edge of the left stomach-lobe in these two specimens is so remarkable that they can't be considered as malformed individuals of *M. huxleyi.* It is much more natural to regard them as *M. abyssorum* CHUN. Both specimens are immature. The tail fin is quite wide and devoid of any gland cells. Measurements of these specimens are:

Specimen	Length of trunk	Length of tail	Locality	Haul depth
No. 1	1.6 mm	5.2 mm	Midpac 10 4°41.1′N 140°06.0′W	ca. 80 fathoms
No. 2	3.6 mm	14 mm	Shellback 145 ca. 12°S ca. 85°W	ca. 400 m – 0

M. abyssorum has only been reported from the waters around Italy and the Bay of Algeria. This is the first report of the species from other than the Mediterranean Sea.

2. *Folia gracilis* LOHMANN, 1892

(Fig. 2)

LOHMANN, H. (1892): Vorbericht über die Appendicularien der Plankton-Expedition. Ergebn. Plankton-Exped., Bd. I, A, p. 147, Fig. 33.

Folia aethiopica—LOHMANN, H. (1892): ibid, Fig. 29.

LOHMANN H. (1896): Ergebn. Plankton-Exped., Bd. II, E c, pp. 81–83, Pl. XIX.

Folia gracilis—LOHMANN, H. and BÜCKMANN, AD. (1926): Ergebn. Deutsch. Südpolar-Exped., Bd. 18 (Zool. Bd. 10).

LOHMANN, H. (1931): Deutsch. Tiefsee-Exped., Bd. XXI, Hft. 1.

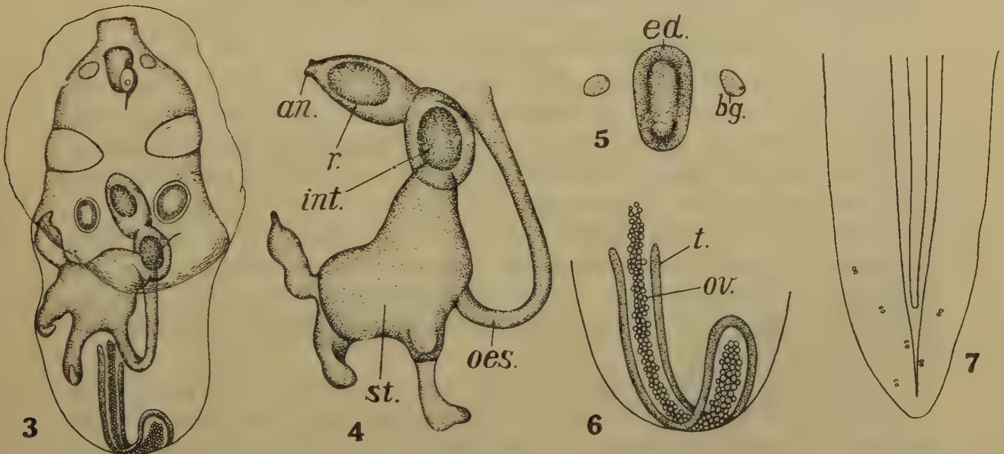

Fig. 2. *Folia gracilis* LOHMANN. 3—Dorsal side of the trunk, ×127. 4—Dorsal side of the alimentary canal, enlarged. 5—Endostyle and buccal glands. 6—Dorsal sight of the gonad, enlarged. 7 Distal half of the tail. *an.*···anus, *bg.*···buccal gland, *ed.*···endostyle, *int.*···intestine, *oes.*···oesophagus, *ov.*···ovary, *r.*···rectum, *st.*···stomach, *t.*···testis.

This species is already known from the Central Pacific, having been found in the plankton samples collected by Friedlich DAHL (1896–97) near the Bismarck-Archipelago (LOHMANN, 1931). I found a single small specimen in the sample taken at the Shellback station 142 (ca. 15°S×ca. 85°W, ca. 400 m—0). The trunk is 477 μ in length and the tail is 1625 μ long. The general structure of the trunk of the present specimen conforms well with that given by LOHMANN (1896), although there are some slight differences between LOHMANN's specimens and mine. The first is the existence of three remarkable glandular protuberances on the stomach of the Shellback specimen. The second is in the shape of the testis, which in the present specimen, is a thin string-like gland, situated on the mid-line of the posterior trunk and arranged as is shown in 6 of Fig. 2. The last is in the existence of several minute gland cells in the poterior part of the tail fin of the Shellback specimen. The posterior end of the chorda is a considerable distance from the posterior end of the musculature. The width of the chorda/the width of the musculature is 0.30–0.31 near the middle of the tail. All these differences are probably due to the condition of preservation or the degree of maturity. They don't appear to be valid as specific or racial characteristics differentiating the Shellback specimen from LOHMANN's specimens.

3. *Fritillaria aberrans* LOHMANN, 1896

(Figs. 3–5)

LOHMANN, H. (1896): Die Appendicularien der Plankton-Expedition. Ergebn. Plankton-Exped., Bd. II, E c, pp. 36–37, Taf. V figs. 5 and 6.

Fritillaria magna—LOHMANN, H. (1896): ibid, pp. 37–39, Taf. V figs. 4, 7–9.

Fritillaria aberrans+*Fritillaria magna*—LOHMANN, H. (1933): KÜKENTHAL and KRUMBACH-Handb. d. Zool., Bd. V, Zweite Hälfte Tunicata, Lief. 2, pp. 138–139, Fig. 126.

It seems to be necessary first to review the descriptions of *Fritillaria aberrans* LOHMANN and *Fritillaria magna* LOHMANN and to discuss the differences between these two species on the basis of previous data. The original discriptions were made from four specimens caught by the Plankton-Expedition, two of *F. magna* and two, in a very imperfect state of preservation, of *F. aberrans*. Subsequently, their names have appeared in some of the lists of appendicularians collected by various expeditions. No further morphological description has been given except for that of the tail musculature, which appeared in "Handbuch der Zoologie" (1933). Thus, the morphological details of these species are only rather imperfectly known. In the following table they are compared.

The differences between the two species may be summarized into four points: (1) the structure of the alimentary organs, (2) the appearance of the bottom wall of the pharynx between the spiracles, (3) the absence of "Nesselzellen"-like elements on the oikoplast-epithelium in *F. aberrans* and (4) the number and arrangement of muscle bands in the tail musculature.

I have found 49 specimens of a form of *Fritillaria*, which is referable to both

	F. aberrans	*F. magna*
Trunk	Exact shape unknown, genital portion is missing in all specimens studied. Hood is present. 1000–1390 μ long excluding the posterior genital portion.	Elongate, at least in the individual with developed testis. Genital portion long; posterior end rounded. Hood well developed and terminating anteriorly in an obtuse end. Up to 5 mm in length.
Pharynx	Endostyle as in *F. magna.* Spiracles very long. A small sac-formed glandular organ present on the outer side of each spiracle? Bottom of pharynx between the spirables is walled with two series of cells with distinct nuclei.	Endostyle is situated nearly in front of the oikoplast-epithelium and curled strongly to the dorsal side; its anterior terminal portion is much broader than the rest. Spiracles very long. A small elongate sac-formed glandular organ is present on the outer side of each spiracle, approximately at the middle of spiracles.
Oesophagus		Short, but thick.
Stomach and Intestine	Large stomach is situated on the left and intestine and rectum on the right side. A number of spherical protruded cells are found on the stomach. A glandular appendage, a squashed bladdery vesicle, on each side of the intestine.	Large stomach occupies the whole dorsal side of the mass of the alimentary organs and is provided with a number of large spherical protruded cells in the younger specimen, but with a number of bundles of finger-shaped protuberances in the older individual. A cell group on each side of the intestine, consists of 3–4 cells, of which one is thickly walled and with somewhat brighter contents.
Gonad		Testis large and elliptical in shape. Ovary unknown.
Oikoplast-epithelium	"Das Fehlen der Nesselzellen ähnlichen Elemente des Integuments."	Consisting of many small follicular cells as in *F. fraudax.*
Small gland cells		Two pairs of gland cells on the dorsal side of the genital portion.
Tail	Musculature consists of 10–14 muscle bands which are each distinctly discernible, but not separated from one another.	Musculature of a medium width and consisting of 5–10 wide muscle bands which are 23–58 μ in breadth and slightly separated from one another. Fin is wide and ends posteriorly in a single pointed terminal.

of the species under discussion. Two were from Equapac samples, 2 form Midpac samples and 45 in the Shellback samples; the Shellback and Equapac samples were taken by oblique hauls generally between 400 m depth and the surface, the Midpac samples were from 400–600 m depth to the surface (MP–3 600–500 m, MP–7 220 fathoms). Many specimens were imperfectly preserved, but some retained portions of the body which were perfectly preserved. The following description of the form is synthesized:

Trunk: Elongate as in *F. haplostoma* FOL. The anterior portion of the trunk, in front of the stomach, is considerably longer than the posterior portion, behind the stomach, in immature individuals (65 : 42 in an individual from MP–3). The two portions are nearly equal in individuals with mature gonads (21 : 19 in a mature individual). Generally the trunk is broadest at attachment of the hood and narrowest just posterior to the stomach, the width/the length of the trunk varies from 0.26 to 0.8 in a 6.2 mm long individual from MP–3. A distinct hood is present; the shape of the upper lip is similar to that of *F. haplostoma*. The tip of the upper lip generally protrudes from the hood and is usually obtusely pointed, although it may be sharply acute as in an individual from MP–3, or rounded as in some specimens from the Shellback and Equapac samples. Sometimes the hood may be long enough to cover the whole upper lip. The posterior margin of the trunk is generally truncated, or rarely, narrowed and forming a pointed end. It is not certain whether such appearance is natural. The oiloplast-epithelium seems to cover the dorsal side of the distal half of the anterior portion of the trunk. A pair of very elongate spiracles are situated wholly beneath this epithelium. The endostyle is short and strongly curved upwards. A pair of large roundish gland cells are found behind the endostyle approximately at the level of the anterior end of the spiracles. A pair of minute gland cells are situated slightly posterior to the above-mentioned pair. A gland cell of medium size is located on the outer side and at about the middle of each spiracle.

The most remarkable characteristic is the existence of a muscle-like structure encircling the pharynx at about the center of the posterior half of the endostyle. The structure is rather delicate, but distinctly discernible by staining the specimens with Rose Bengal. Frequently it is found broken. At first, I thought it might be the peripharyngeal band, but its location clearly differs from that of the peripharyngeal band and moreover it faintly shows a structure which may be expressed as fibrous. I am inclined to consider this structure as a primitive circular muscle. So far as I am aware, there is no certain record of the existence of any muscle on the trunk of appendicularians, except for a fibrous structure found at the heart. In the late 19th century it was supposed that the epithelium of *Megalocercus abyssorum* was a kind of musculature (CHUN, 1888), but this was nothing but the misidentification of the imperfectly preserved oikoplast-epithelium as musculature. This may thus be the first time the existence of body musculature has been found in appendicularians with any considerable certainty. It is very desirable that more perfectly preserved specimens

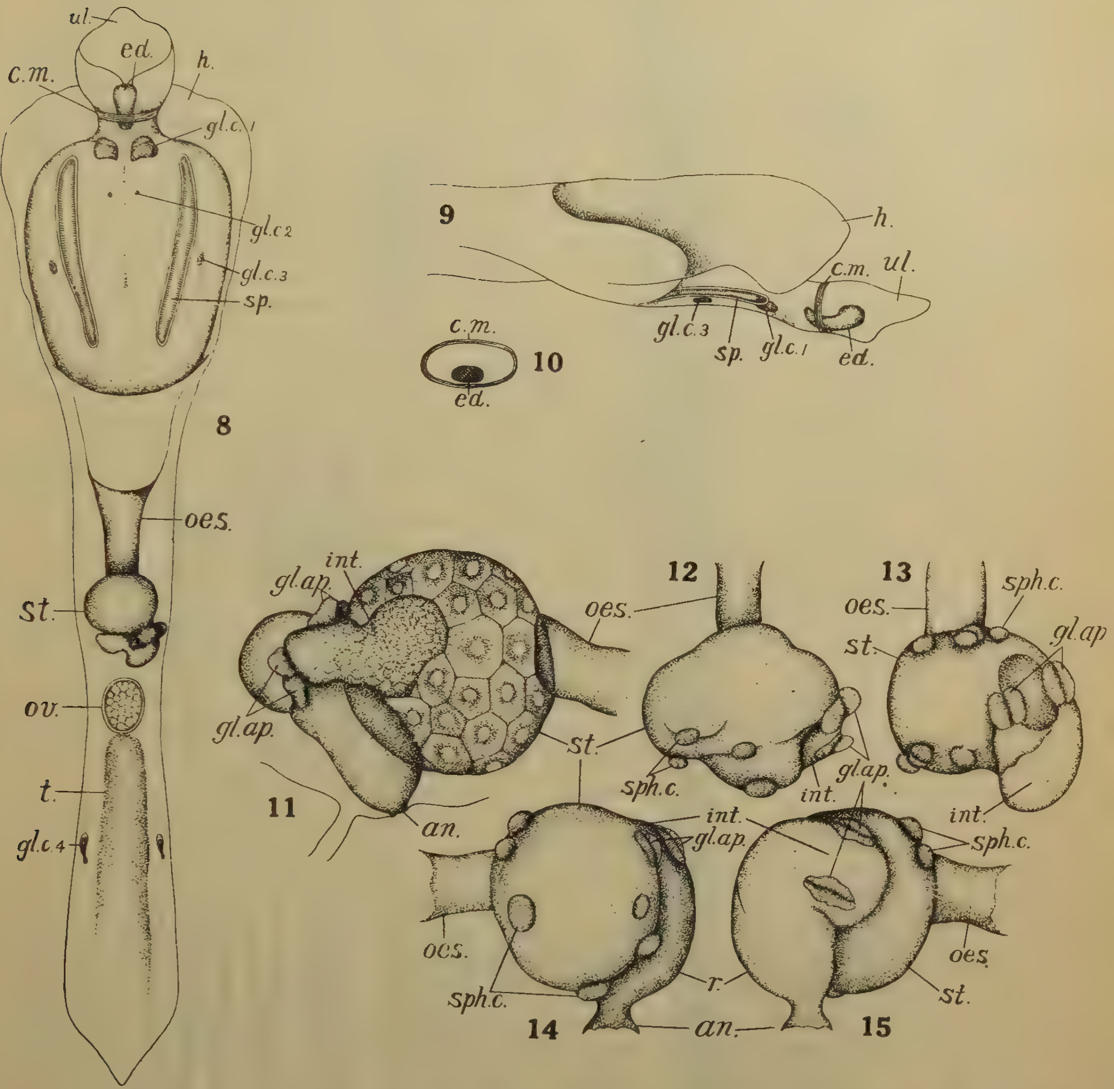
ul.
ed.
h.
c.m.
gl.c.1
gl.c.2
gl.c.3
sp.
8
oes.
st.
ov.
t.
gl.c.4
9
h.
c.m.
ul.
gl.c.3
sp.
gl.c.1
ed.
c.m.
10
ed.
int.
gl.ap.
gl.ap.
11
an.
oes.
st.
12
oes.
sph.c.
int.
gl.ap.
13
oes.
st.
sph.c.
gl.ap
int.
int.
gl.ap.
sph.c.
oes.
sph.c.
r.
an.
oes.
st.
14
15

Fig. 3. *Fritillaria aberrans* LOHMANN. **8** Ventral side of the trunk. **9** Pharyngeal portion, right side. **10**–Schematic representation of the section through the circular muscle. **11** Alimentary organ of an individual from MP 3, right side. **12** Alimentary organ of other specimen, dorsal side. **13**—ditto, dorsal side. **14**–ditto, left side. **15**—Right side of the same alimentary organ. ***an.***···anus, ***c.m.***···circular muscle, ***ed.***···endostyle, ***gl.ap.***···glandular appendage, ***gl.c.*** 1–4···small gland cells, ***h.***···hood, ***int.***···intestine, ***oes.***···oesophagus, ***ov.***···ovary, ***r.***···rectum, ***sp.***··· spiracle, ***sph.c.***···spherical cells projecting out from the stomach wall, ***st.***···stomach, ***t.***···testis, ***ul.***···upper lip.

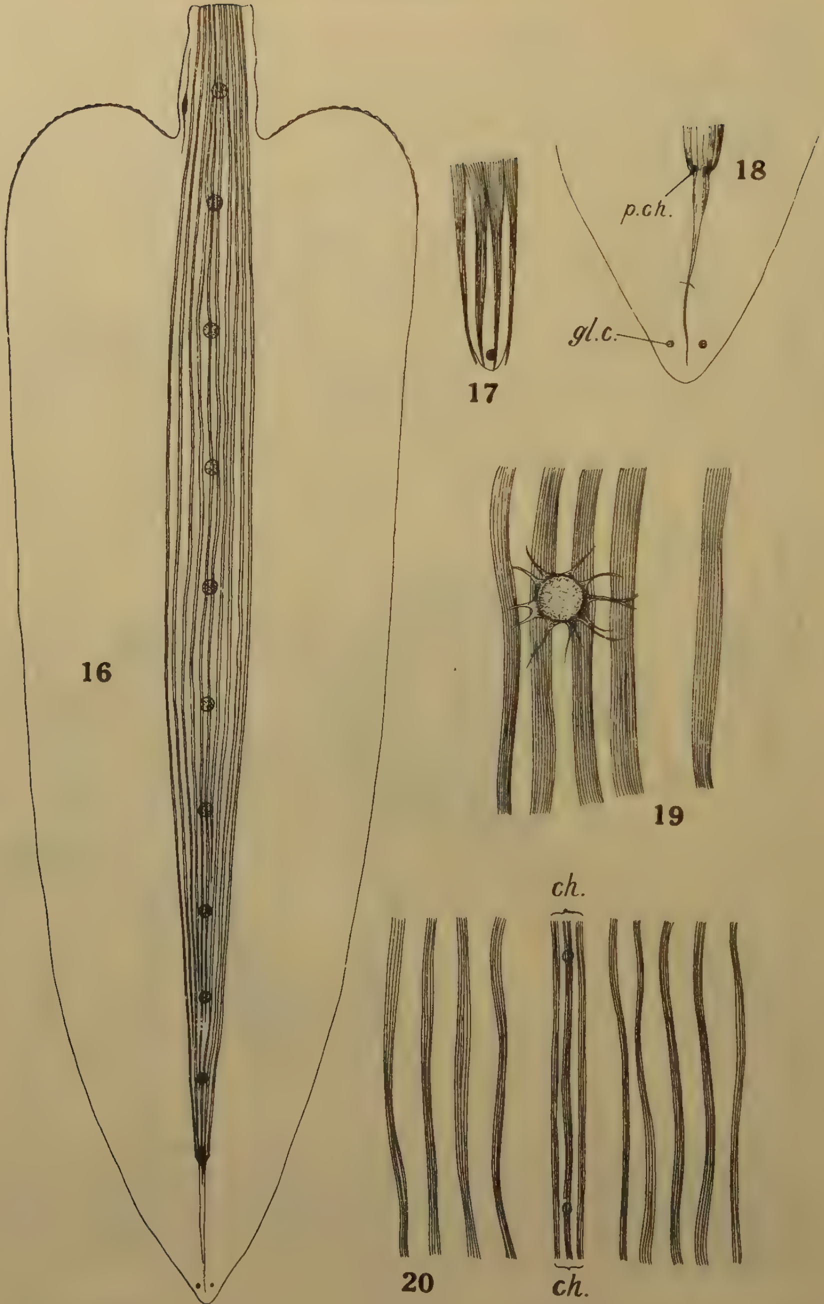

Fig. 4. ***Fritillaria aberrans*** Lohmann. **16**—Tail of an individual from MP-3, ×ca. 15. **17**—Posterior end of the tail musculature, magnified. **18**—Extension of a fine muscle band beyond the posterior end of the tail musculature, magnified. **19**—A part of the tail musculature, showing a chordal nucleus, ×127. **20**—Ditto, less magnified. ***ch.***···chorda, ***gl.c.***···gland cell, ***p.ch.***···posterior end of chorda.

be carefully examined to confirm this structure, for the existence of circular musculature in the appendicularians may allude to the possibility of the existence of a certain direct relationship between this animal group and Thaliacea.

The oesophagus is thick, the stomach is spherical in shape with the intestine and rectum situated on its right posterior side. The relative positions of these organs is considerably variable, depending on the state of the preservation. Usually there are several (2–3 to 6–7) protruded spherical cells over the stomach surface. In some rare cases, however, none of these cells are found on the stomach, and its surface is nearly smooth. The stomach, in an individual from MP–3, was 520 μ in diameter. Generally a pair of glandular appendages are found on the intestine as in *F. haplostoma*. They are usually squashed, or flattened so strongly that in some specimens they can hardly be detected. In many cases, the appendages are deeply depressed along their axes parallel to the intestine, leaving both sides highly elevated, so that they look as if they each consist of two lamine. In two of the specimens examined, each glandular appendage appears to consist of two cells. It is not clear, however, whether they really consist of two cells or a single cell which is strongly folded into two swollen laminae. More critical examination of perfectly preserved specimens is necessary before a definite description of the structure of the glandular appendage can be given.

Gonads were found in a single individual from MP–3. The ovary was an oval mass located just behind the stomach and the testis seems to form an elongate mass as in *F. haplostoma*. An elongate gland cell is present on each side of the testis near its middle (*gl. c.* 4).

Measurements of representative specimens are:

Source	Length of trunk	Length of tail	C/M×100
SB - 112	3.3 mm	8.5 mm	43.3
SB - 112	2.6 mm (anterior portion)	8.1 mm	
SB - 180	4.9 mm	8.5 mm	
MP - 3	6.2 mm	12.5 mm	

Tail: The largest tail was 13 mm in length. The musculature is of moderate width and consists of 10–12 (most frequently 10) muscle bands on one surface, in the present material. Generally speaking, the muscle bands touch one another in younger specimens, while they are separated from one another in fully grown individuals. Near the posterior end the musculature consists of 4 muscle bands on one surface and terminates just at the posterior end of the chorda. In some specimens, however, these four muscle bands extended posteriorly beyond the distal end of the chorda, and unite into two thin bands which then fuse into a single fine band. The width of the chorda/the width of the musculature is rather large (2/3 in an individual from MP–3) in younger specimens, but it decreases remarkably in fully grown individuals, in which the muscle bands are widely separated. The ratio is only 1/7–1/9 in an individual from SB–115. The chorda is covered on each surface by 3–4 muscle bands and provided with 11 roundish chordal nuclei in a specimen from MP–3. The fin is rather wide, ending posteriorly in a single acute tip as in *F. haplostoma*. The margin along the shoulder-like antero-lateral angles is ciliated. Only a small pair of gland cells, near the posterior end, is observed on the surface of the fin. The 12.5 mm long tail, of an individual from MP–3, is broadest at the level of the shoulder-like antero-lateral angles (width/length=0.32). The musculature is widest (780 μ) slightly anterior to the middle of the fin.

The above-mentioned form appears to resemble both *F. aberrans* and *F. magna*. It most likely combines these two species into a single one. The first of the four differences between *aberrans* and *magna*, the differences found in the structure of the alimentary organs, is rather variable in the present form. Lohmann's *magna* has 3–4 cells instead of the single glandular appendage of intestine as in *aberrans*. It is, however, very possible that one of these 3–4 cells, which is thickly walled and with somewhat clear contents, may represent the glandular appendage and other 2–3 cells belong to the spherical protruded cells which are found scattered over the stomach surface. The fact that Lohmann's original specimens of these two species, especially of *aberrans*, were in a very unsatisfactory condition, seems to decrease considerably the validity of the above-mentioned distinction. The second and the third of the differences are evidently due to the state of preservation. The last of the four differences, the number and arrangement of muscle bands of tail musculature, are quite continuous between *aberrans* and *magna*. It appears that they vary with age,

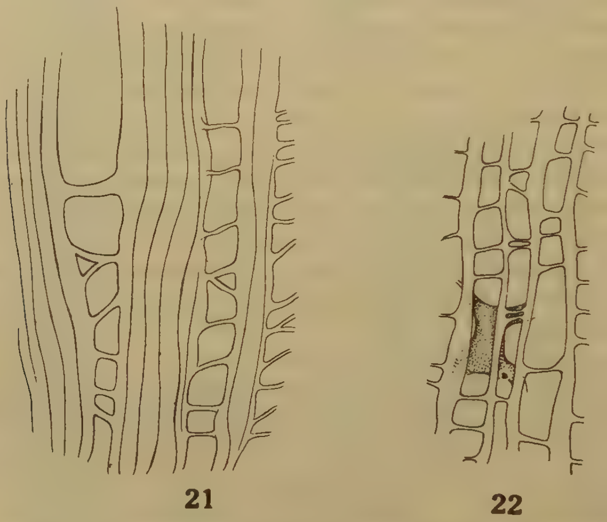

Fig. 5. *Fritillaria fraudax* Lohmann. **21–22**—Parts of the tail musculature of an old, fully grown individual, magnified.

condition of preservation and even individually. The liberation of respective muscle bands is not confined to this "Formenkreis", but also it can be seen in other species. A part of the tail musculature of an old fully grown individual of *F. fraudax* LOHMANN, from SB–60, is shown as an example (Fig. 5).

Throughout above-mentioned discussions, I am inclined to believe that *F. aberrans* and *F. magna* are identical, and the name *F. aberrans* should be reserved according to the law of the page priority.

4. *Fritillaria pacifica* n. sp.

(Figs. 6–9)

Fritillaria aequatorialis—TOKIOKA, T. (1957): Two new appendicularians from the Eastern Pacific, with notes on the morphology of *Fritillaria aequatorialis* and *Tectillaria fertilis*. Trans. American Microscop. Soc., Vol. LXXVI, No. 4, pp. 364–365, Figs. 3C, 4 D–E.

Forty-one specimens in all have been examined, 26 from Equapac material and 15 from Shellback material. When I described the morphology of the tail of this form (TOKIOKA, 1957), I had no specimens with any trace of gonads. The identification was made on the most perfectly preserved specimen from SB–10, which is shown here in Fig. 6. The trunk was 1510 μ in length and somewhat elongate in outline. The genital portion (empty in this specimen), posterior to the alimentary organ, was about half as long as the anterior portion in front of the stomach, which was much more spacious than the genital part. The mouth closely resembles that of *Fritillaria fraudax* LOHMANN (Fig. 9) and is wholly covered by the hood. The oikoplast-epithelium consists of two pairs of elongate elliptical cell groups and is bordered by six large cells along the posterior margin. The endostyle is very markedly curved. The spiracles are rather large and elliptical in outline. The ciliated dorsal lamina can be traced to near the mid point between the posterior end of the endostyle and the oesophageal opening where it becomes quite obscure.

The oesophagus is very long and the stomach is comparatively small, oval in outline and rather smooth walled. The intestine and rectum are situated at the right posterior side of the stomach. There are a pair of distinct roundish glandular appendages on the intestine as found in many species belonging to the subgenus *Eurycercus*. Two additional thin wing-shaped horizontally placed glandular appendages are located at the posterior end of the intestine. In some specimens, a few small spherical cells project from the general contour of the intestine. The wing-shaped glandular appendages consist of a ventral appendage located on the median line of the trunk and a dorsal one slightly displaced to the left. In some mature specimens, the appendages are found detached from the surface of the alimentary organ. The heart is very prominent and somewhat displaced to the left side of the ventro-median line.

The above-mentioned features of the trunk, especially the relative smallness of

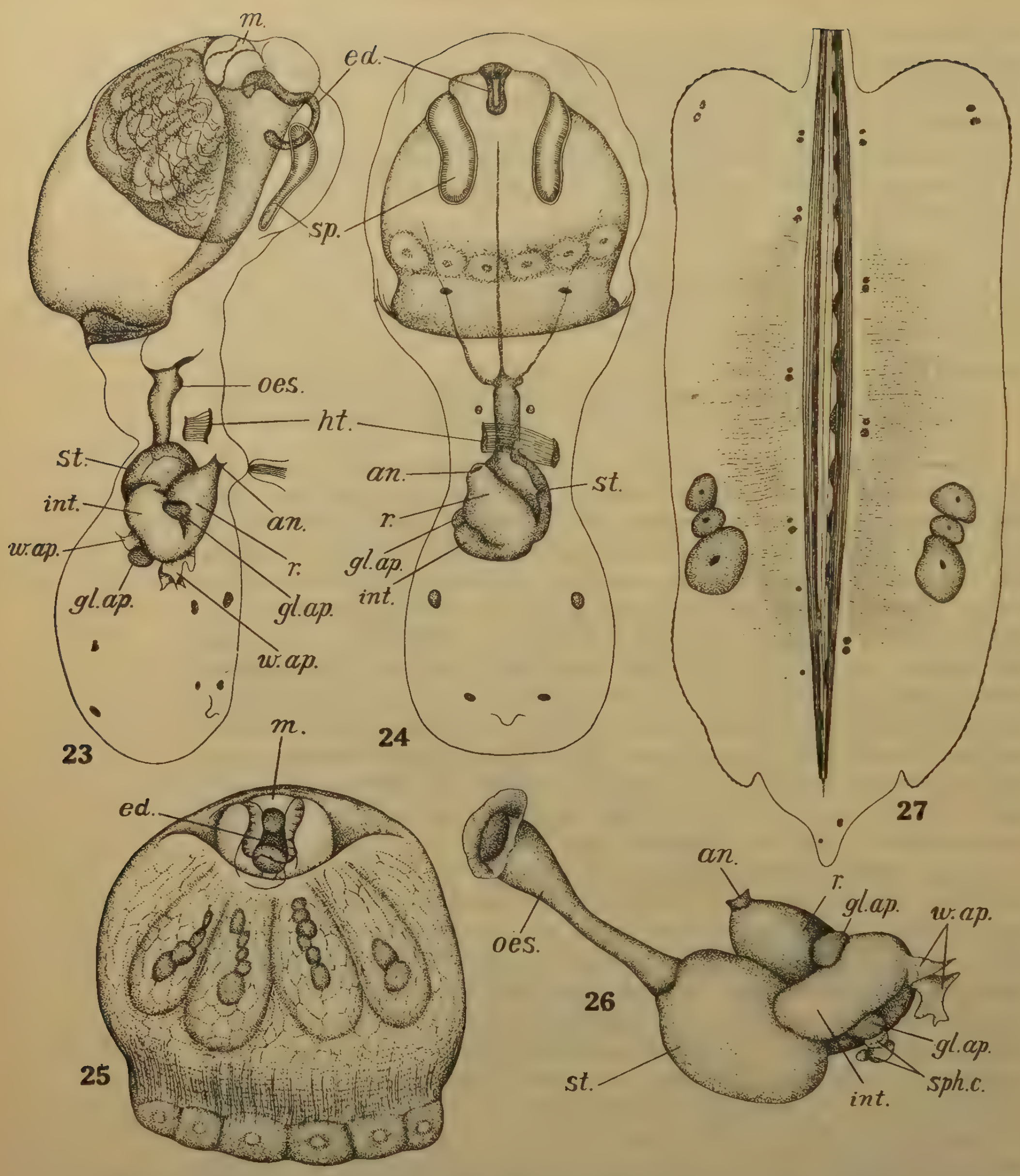
m.
ed.
sp.
oes.
ht.
st.
int.
an.
r.
w.ap.
gl.ap.
gl.ap.
w.ap.
23
ed.
sp.
an.
st.
r.
gl.ap.
int.
24
27
m.
ed.
25
an.
r.
gl.ap.
w.ap.
oes.
26
gl.ap.
sph.c.
st.
int.

Fig. 6. *Fritillaria pacifica* n. sp. **23**—Right side of the trunk. **24**—Ventral side of the trunk. **25**—Oikoplast-epithelium, dorsal side. **26**—Alimentary organ, dorsal. **27**—Tail. *an.*···anus, *ed.*···endostyle, *gl.ap.*···glandular appendage, *ht.*···heart, *int.*···intestine, *m.*···mouth, *oes.*···oesophagus, *r.*···rectum, *sp.*···spiracle, *sph.c.*···spherical cell projecting out from the stomach surface, *st.*···stomach, *w.ap.*···wing-shaped membranous glandular appendage.

the genital portion, compared with the spacious pharyngeal part and the general appearance of the alimentary organ, resemble so closely those of *Fritillaria aequatorialis* Lohmann, described and figured in 1896, that I dared to identify my specimen as *F. aequatorialis.* This was in spite of the distinct difference in the structure of the tail for I thought Lohmann's description of the tail of *F. aequatorialis* might have been made on some imperfectly preserved specimens. Later, however, I found a single specimen with fully mature gonad in the sample from SB-55 (Fig. 7). The gonad of this specimen consisted of the string-formed ovary and a somewhat membraneous testis, whose lateral sides were curled upwards. This structure of the testis apparently differs from that of *F. aequatorialis* which has "ein eiförmiger, voluminöser Hoden, mit seiner Längsachse schräg von vorn unten nach hinten und oben gerichtet".

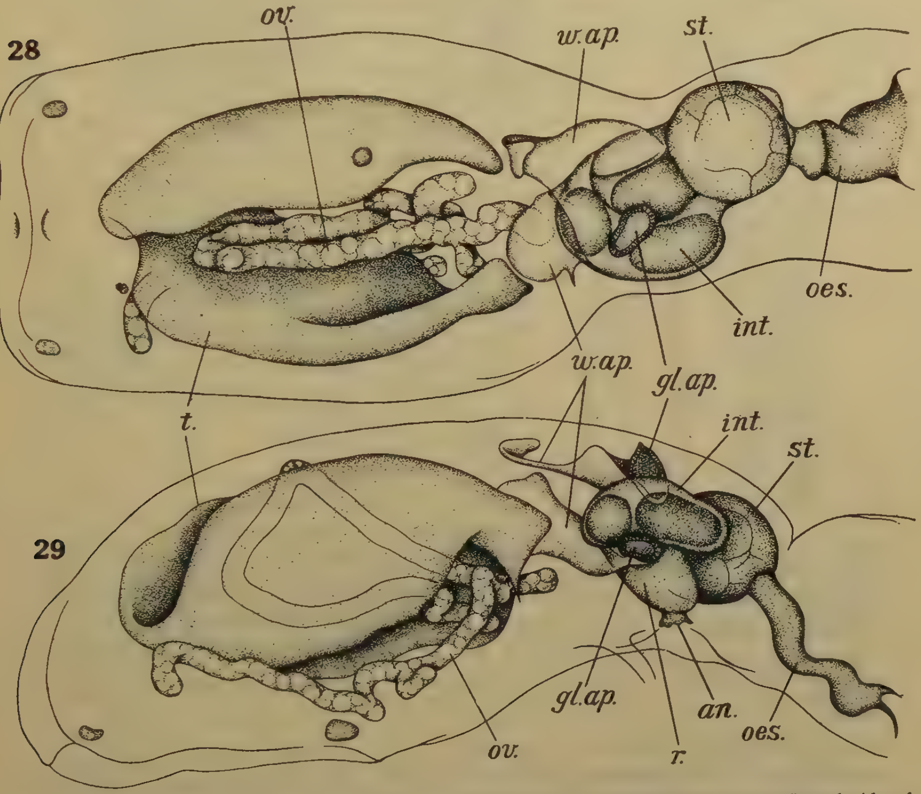

Fig. 7. *Fritillaria pacifica* n. sp., an individual with fully matured gonad, SB-55. 28—Dorsal side of the posterior half of the trunk. 29—Right side of the same portion. *an.*···anus, *gl.ap.*···glandular appendage, *int.*···intestine, *oes.*···oesophagus, *ov.*···ovary, *r.*···rectum, *st.*···stomach, *t.*···testis, *w.sp.*···wing-shaped membranous glandular appendage.

The ovary of *F. aequatorialis* is also string-shaped as indicated in the original description—"Ihn (the testis) umgeben rechts und links in der Form eines Gürtels je 1 wurmförmigen Ovarialstrang, der bei älteren Thieren Rosenkranz-ähnliche Einschnürungen in Eifächer zeigt". The ovary and the testis were arranged so complicatedly or rather irregularly in the specimen from SB-55, I could find no definite difference between the gonads of respective forms until specimens with gonads in various stages of development were found in samples of the Equapac Expedition. By examining these specimens in detail, it is definitely established that the structure of the gonad of the present questionable form differs distinctly from that of *F. aequatorialis.* The structure of the gonad is shown in Fig. 8.

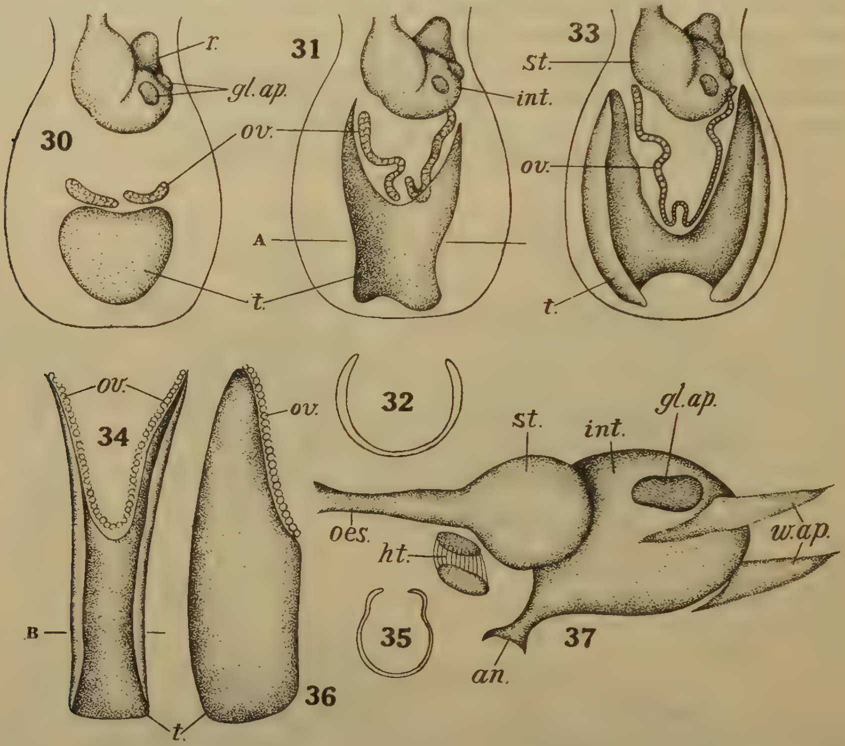

Fig. 8. ***Fritillaria pacifica*** n. sp., gonads and alimentary organ shown somewhat schematically. **30, 31, 33**—Three stages of the successive development of the gonad. **32**—Transverse section through the line A of the testis shown in **31**. **34**—Gonad of an individual from SB-137, dorsal. **35**—Transverse section through the line B of the testis shown in **34**. **36**—Left side of the same testis. **37**—Left side of the alimentary organ, shown somewhat schematically. *an.*···anus, *gl.ap.*···glandular appendage, *ht.*···heart, *int.*···intestine, *oes.*···oesophagus, *ov.*···ovary, *r.*···rectum, *st.*···stomach, *t.*···testis, *w.ap.*···wing-shaped membranous glandular appendage.

In earlier stages, the testis forms a semicircular disc placed horizontally with a convex posterior margin and a truncate anterior edge. The ovaries are represented by two sausage-shaped pieces situated along the anterior margin of the testis. The lateral sides of the testis extend gradually towards the anterior and dorsal side, thus finally it grows up to a laminary mass curled up to the dorsal side along the lateral margins. Its anterior margin is remarkably concave. The ovaries of both sides become longer along the concave anterior margin of the testis and are usually found united in fully mature gonads.

It is clear that the specimens treated here represent a new species distinctly differentiated from any known species of *Fritillaria*. The specific name "*pacifica*" is proposed here for this new species, whose most striking characteristics are the unique shape of the tail and the structure of the gonad.

Finally a short note is given on the distribution of small gland cells throughout the trunk (Fig. 9). There is a small cell on each side of the mouth; two pairs of cells are found in the pharyngeal portion, one near the level of the anterior end of the spiracles and the other at the level near the posterior end of the oiloplast-epithelium. There is a small cell on each side of the oesophagus near its anterior margin, and a single cell near the right dorsal side of the cardiac end of the stomach. Three pairs of cells are found in the genital portion, two on the dorsal side and one along the posterior margin of the trunk. Some of these small gland cells often may be missing.

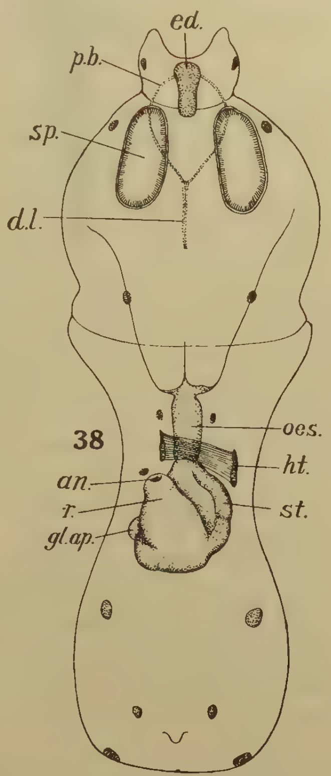

Fig. 9 (38). *Fritillaria pacifica* n. sp. Distribution of small gland cells on the trunk, ventral. *an.*···anus, *d.l.*···dorsal lamina, *ed.*···endostyle, *gl.ap.*···glandular appendage, *ht.*···heart, *oes.*···oesophagus, *p.b.*···peripharyngeal band, *r.*···rectum, *sp.*···spiracle, *st.*···stomach.

Measurements:

Source	Length of trunk	Width of trunk	Length of tail	Width of tail
EQP-H 17	1192 μ		1950 μ	870 μ
EQP-H 17	1340 μ		2170 μ	910 μ
EQP-H 17	1340 μ		2170 μ	975 μ
SB 10	1510 μ	540 μ	2275 μ	870 μ
SB 55	1730 μ			

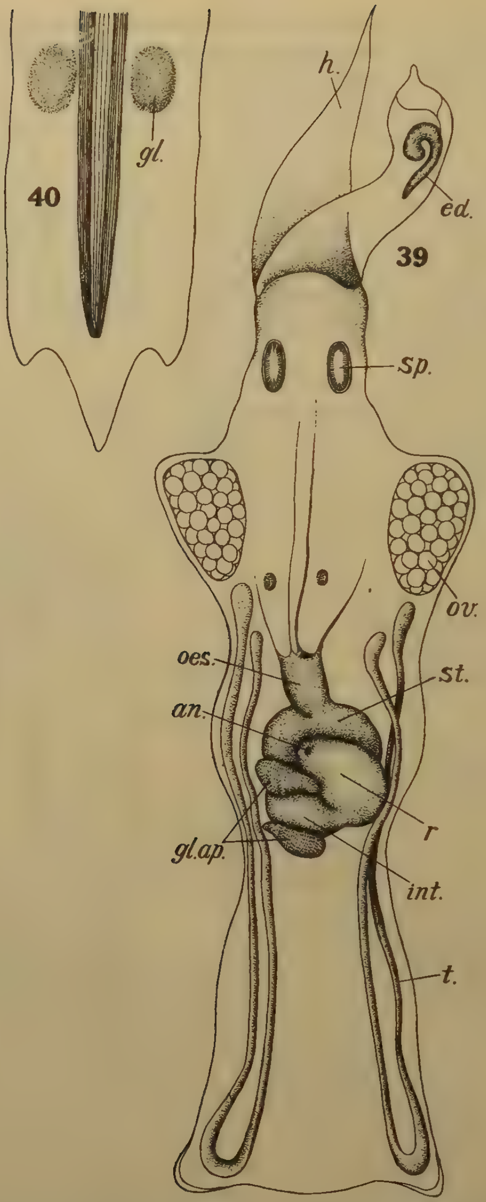
40
gl.
h.
ed.
39
sp.
ov.
oes.
st.
an.
r
gl.ap.
int.
t.

Fig. 10. *Tectillaria taeniogona* (TOKIOKA). **39**—Ventral side of the trunk. **40**—Distal half of the tail. *an.*···anus, *ed.*···endostyle, *gl.*···glandular tissue, *gl.ap.*···glandular appendage, *h.*···hood, *int.*···intestine, *oes.*···oesophagus, *ov.*—ovary, *r.*···rectum, *sp.*···spiracle, *st.*···stomach, *t.*···testis.

Mature specimens of *F. aequatorialis* from the Plankton Expendition are 600–700 μ in trunk length, much smaller than *F. pacifica.*

5. *Tectillaria taeniogona* (TOKIOKA), 1957

(Fig. 10)

Fritillaria taeniogona—TOKIOKA, T. (1957): Two new appendicularians from the Eastern Pacific, with notes on the morphology of *Fritillaria aequatorialis* and *Tectillaria fertilis.* Trans. American Microscop. Soc., Vol. LXXVI, No. 4, pp. 363-364, Figs. 3A and B.

A comparatively well preserved specimen was found in the plankton sample from SB–187. The shape of the mouth part resembles somewhat that of *F. haplostoma,* the upper lip being obtusely pointed at the anterior end. Spiracles are comparatively small and elliptical in outline. A pair of small gland cells are present on the pharyngeal wall at the level slightly in front of the anterior end of the oesophagus. The intestine and rectum are situated on the right or right posterior side of the stomach. A very distinct pair of glandular appendages are found on the intestine. They are stained purplish red by Rose Bengal, while the intestinal wall is stained red orange by the same dye. A pair of ovaries are found near the middle of the area between the spiracles and the oesophagus.

The posterior end of the tail fin is pointed and there is a pair of subterminal notches near the distal end, somewhat posterior to the termination of the tail musculature. A vague glandular tissue, roughly round in outline, is faintly observed on each side of the tail musculature, approximately a quarter of the way from the distal end of the tail. Although the exact structure of the oiloplast-epithelium is not yet known for the present species, the above-mentioned structures of both trunk and tail make it reasonable that the present specimen should belong to the genus *Tectillaria* rather than to *Fritillaria.* The genus *Tectillaria* thus acquires here its second member.

LITERATURE

BERNARD, M. F. (1954): Capture de *Megalocercus abyssorum* CHUN (Oikopleuridae) dans la baie d'Alger. Bull. Soc. Hist. Nat. Afrique d. Nord, Tom. 45, pp. 344-347, 2 Figs.

CHUN, C. (1888): Die pelagische Thierwelt in grösseren Meerestiefen und ihre Beziehungen zu der Oberflächenfauna. Bibliotheca Zoologica. Stuttgart. Bd. I, part 1, pp. 1-66, pls. 1-V.

LOHMANN, H. (1896): Die Appendicularien der Plankton-Expedition. Ergebn. Plankton-Expedition, Bd. II, Ec, 148, pp., 24 pls.

LOHMANN. H. (1931): Die Appendicularien. Wiss. Ergebn. Deutsch. Tiefsee-Exped. 1898-99, Bd. 21, part 1.

LOHMANN, H. (1933-34): Appendicularia in: KÜKENTHAL u. KRUNBACH, Handb. d. Zool., Bd. 5 (2), Liefs. 1-3, pp. 3-192.

LOHMANN, H. and BÜCKMANN, AD. (1926): Die Appendicularien der Deutschen Südpolar-Expedition 1901 bis 1903. Ergebn. Deutsch. Südpol.-Exped., Bd. 18 (Zool. Bd. 10), pp. 63-231.

TOKIOKA, T. (1957): Two new appendicularians from the Eastern Pacific, with notes on the morphology of *Fritillaria aequatorialis* and *Tectillaria fertilis.* Trans. American Microscop. Soc., Vol. LXXVI, No. 4, pp. 359-365, Figs. 1-4.

(972)

REVUE SUISSE DE ZOOLOGIE
Tome 65, nº 33 — Juillet 1958

Mitgeteilt an der Generalversammlung der Schweizerischen Zoologischen Gesellschaft in Zürich den 8. und 9. März 1958

Nº 33. **Adriano A. Buzzati-Traverso.** — Genetische Probleme der marinen Biologie. (Mit 3 Textabbildungen.)

(Scripps Institution of Oceanography, La Jolla, Calif. und Istituto di Genetica dell'Università di Pavia.)

Wenn wir die Daten, die wir über die Genetik der Landtiere und Landpflanzen besitzen, mit denen vergleichen, die über die Genetik der marinen Organismen zur Verfügung stehen, so fällt auf, dass unsere Kenntnis über die Genetik der Landtiere unvergleichlich grösser ist.

In der vorliegenden Publikation sollen nun die folgenden Probleme der Genetik mariner Tiere zur Sprache kommen:

1. Formal-genetische Untersuchungen an marinen Tieren,
2. Geschlechtsbestimmung und Chromosomenstruktur,
3. Artbildung und Evolution,
4. Analyse marin-ökologischer Systeme mit Hilfe genetisch-bakteriologischer Methoden.

Dabei ist es nicht möglich, alle Ergebnisse von Untersuchungen nur unter einer der vier Rubriken zu besprechen, da einige Probleme zu mehr als einer dieser Rubriken Bezug haben werden.

1. *Formal-genetische Untersuchungen an marinen Tieren*

Die formale oder mendelsche Analyse ist dadurch sehr erschwert, dass sich die marinen Tiere nur mit grosser Mühe kultivieren lassen. Die wünschenswerten Eigenschaften eines guten genetischen Objektes, nämlich kurzer Lebenszyklus, Widerstandsfähigkeit und einfache und leicht kontrollierbare Kulturbedingungen, sind leider bei den marinen Tieren selten zu finden, da viele, insbesondere die Invertebraten, oft ein pelagisches Larvenstadium haben. Besonders für dieses pelagische Larvenstadium sind die Kulturbedingungen nicht leicht zu reproduzieren. Aus diesem Grunde hat sich das Interesse in diesem Gebiete entweder auf kleine Organismen mit

Contributions from the Scripps Institution of Oceanography, New Series, No. 1056
Reproduced by Permission

einfachem Lebenszyklus oder auf solche Organismen konzentriert, deren ökonomische Bedeutung einen grösseren Einsatz von Personal und Mitteln ermöglichte.

Die formal-genetischen Untersuchungen von Bocquet (1951) an Crustaceen stellen einige sehr interessante Beispiele dar. Er konnte in den natürlichen Populationen des Copepoden *Tisbe*, der Gruppe Harpacticidae, siebenFormen auf Grund ihrer Pigmentmuster unterscheiden und diese sieben Formen einer entsprechenden Anzahl Genen zuordnen. Diese Gene folgen den mendelschen Gesetzen und gehören höchstwahrscheinlich einem System multipler oder eng gekoppelter Gene an. Später konnten Battaglia und Pulze (1957) nachweisen, dass die natürlichen Populationen dieser Art in den Lagunen von Venedig vier Formen enthalten, die mit vier Formen Bocquet's identisch sind, und dass es sich hier, wie wir später sehen werden, um einen balancierten Polymorphismus handelt, der auf der höheren Vitalität der Heterozygoten beruht. Für den Isopoden *Sphaeroma serratum* konnten Bocquet und L. Teissier (1951) nachweisen, dass die fünf markantesten Farbformen ebenfalls auf einem System von Allelen beruhen. Über einen weiteren Fall von mendelscher Vererbung bei dem Serpuliden *Pomatoceros triqueter* berichteten Føyn und Gjøen in 1954.

In unserem Laboratorium in Kalifornien konnten wir am Copepoden *Tigriopus californicus* (Abb. 1), einem Harpacticoiden, Fälle quantitativer Vererbung beobachten, die von einem polygenischen System abhängen. Auf der Suche nach einem Tier, das sich für ausgedehnte Untersuchungen über die Probleme der Populationsgenetik und Rassenbildung sowohl in der Natur als auch im Laboratorium eignen würde, fanden wir in diesem Copepoden ein geeignetes Objekt. *Tigriopus* ist sehr widerstandsfähig und besitzt eine schnelle Generationenfolge. Er kann leicht unter Laboratoriumsbedingungen kultiviert werden, ausserdem erträgt er weite Schwankungen der Temperatur, der Salinität, des pH und des Sauerstoffgehaltes. Er ist sehr fertil, und eine Generation wächst in zwei Wochen heran. *Tigriopus* ist ein Cosmopolit und ist in den Gezeitentümpeln und Spritzwassern fast aller Oceane zu finden. Normalerweise füttern wir *Tigriopus* mit *Platymonas*, einer einzelligen Alge. Bei einem Vergleich von Stämmen, die von verschiedenen Lokalitäten der nordamerikanischen Küste des Stillen Oceans stammen, konnte ich ziemliche Unterschiede in der durchschnittlichen Eizahl im Eisack beobachten. Da die Anzahl der Eier eines Individuums von grosser Wichtigkeit für dessen Fortpflanzungseignung ist, schien es von Interesse zu untersuchen, ob und wie dieses Merkmal vererbbar wäre. Dr. A. Ar-rushdi setzte darum ein Experiment an, das entscheiden sollte, ob die beobachtete Variabilität durch die Umwelt oder genetisch bestimmt ist. Eine vorläufige Ausarbeitung der Daten ergibt eine 12%ige Vererbbarkeit dieses Charakters. Dieses Ergebnis schien weitere Untersuchungen über dieses Merkmal zu rechtfertigen. Herr Jim Lance des La Jolla Laboratoriums ist im Augenblick damit beschäftigt, die Anzahl der vitalen Eier von circa 5400 Weibchen zu bestimmen. Diese Analyse ist wichtig, denn sie soll uns etwas über den Einfluss

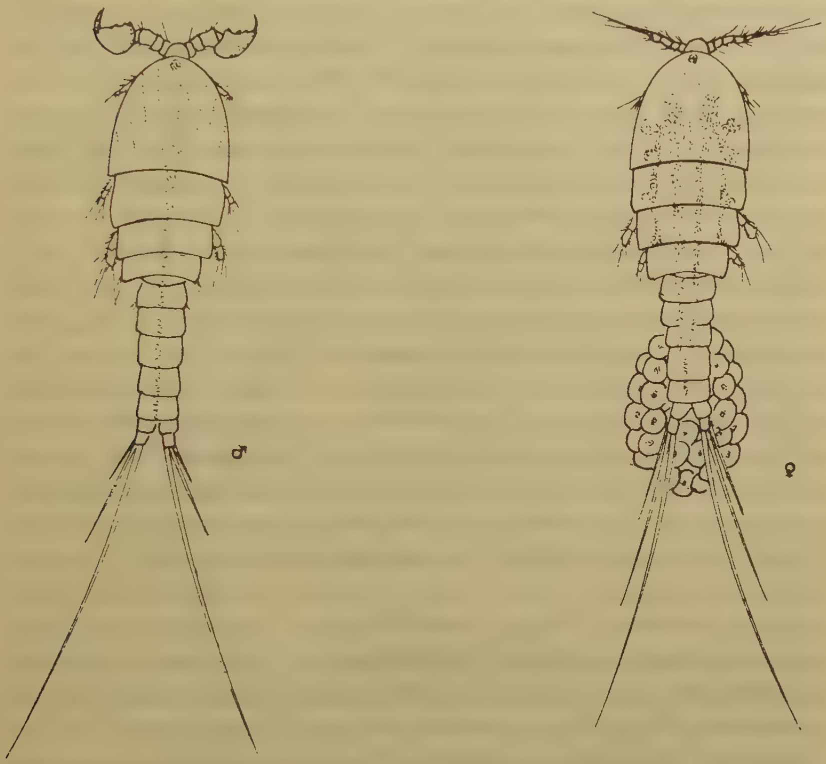

Abb. 1.
Tigriopus. californicus

dieses Merkmals auf die Dynamik der Populationen aussagen, die diskontinuierlich von Kanada bis Mexiko verbreitet sind. Leider war es bis jetzt trotz systematischer Suche nicht möglich, morphologische Mutationen zu finden, die für eine mendelsche Analyse brauchbar wären.

In diesem Zusammenhang möchte ich erwähnen, dass es möglich ist, die Alge *Platymonas*, die als Nahrung für *Tigriopus* dient, in bakterienfreier Kultur zu halten. Mit Hilfe von Antibiotica und der Technik der serialen Verdünnung ist es gelungen, auch *Tigriopus* bakterienfrei aufzuziehen. Aber obwohl es gelang, etwa 100 Individuen bakterienfrei durch zwei Generationen zu züchten, scheint es doch, als ob biochemische Faktoren einen negativen Einfluss auf die Geschlechtsreife ausübten. Immerhin wird es mit Hilfe der bakterienfreien Kulturen möglich sein, genetisch-physiologische Aspekte an diesem Copepoden zu studieren.

Auf dem Gebiet der physiologischen Genetik verdienen die Arbeiten von LOOSANOFF (1954; LOOSANOFF und NOMEJKO, 1951) an Tafelaustern ein besonderes Interesse. LOOSANOFF entwickelte eine geniale Technik, mit deren Hilfe es ihm gelang, die Auster *Crassostrea virginica* über mehrere Generationen im Laboratorium zu züchten, und weiterhin war es ihm möglich, mehrere Temperatur-Rassen dieser Auster unter Laboratoriumsbedingungen zu untersuchen.

An Austern aus Florida, South Carolina, Virginia, New Jersey and New England wurde der Einfluss der Temperatur auf die Maturität der Spermatozoa und Eier untersucht. Zwei Kriteria wurden zur Beurteilung der Geschlechtsreife herangezogen.

Erstens wurde der Zeitraum in Tagen bestimmt, der von den Austern bei einer bestimmten Temperatur benötigt wurde, um reife Eier oder aktive Spermien zu bilden.

Zweitens wurde der Zeitraum der Anpassungsperiode an eine bestimmte Temperatur festgestellt, der nötig war, um die Austern zur Abgabe von Eiern oder Spermien zu veranlassen.

LOOSANOFF konnte beobachten, dass 50% der Austern von Long Island Sound, wenn sie bei 21°, 24° oder 27° gezüchtet wurden, nach 15, 8 beziehungsweise 5,5 Tagen reife Gameten enthielten. Die entsprechende Versuchsgruppe der New-Jersey-Austern erreichte dieses Stadium erst nach 55, 32, beziehungsweise 22,5 Tagen. Ein weiterer Unterschied zwischen den Austern von Long Island

Sound und den New-Jersey-Austern bestand darin, dass, wenn beide bei einer Temperatur von 21° C gehalten wurden, 50% der Long Island Sound-Austern schon nach 18 Tagen reife Eier oder aktive Spermien abgaben, während das gleiche Phänomen bei den New Jersey-Austern erst nach 78 Tagen beobachtet werden konnte. Für diese Temperaturreaktionen und auch andere Reaktionen konnte nachgewiesen werden, dass sie in den verschiedenen Rassen genetisch determiniert sind. Weiterhin gelang es LOOSANOFF, für *Grosalpinx cinerea*, einem parasitischen Gastropoden, der Löcher durch die Austernmuschel bohrt, ähnliche Temperatur-Rassen nachzuweisen.

Da es LOOSANOFF und DAVIS (1950) und IMAI und HATANAKA (1949) gelang, Salzwasser-Pelecypodenlarven durch die Metamorphose zu züchten, ist es nun möglich, Hybridationen bei Muscheln durchzuführen. So wurde zum Beispiel *Venus mercenaria* mit *V. campechiensis* und *V. notata* gekreuzt. Auch von japanischen Wissenschaftern wurden verschiedene Kreuzungsexperimente durchgeführt. Y. MATSUI (1958) untersuchte verschiedene Variationen der Perlenbildung der Auster *Pinctada martensii* nach physiologischen und biochemischen Gesichtspunkten. Es scheint, als ob auch diese Variationen genetisch bedingt sind.

Eine grosse Anzahl von interspezifischen Varietäten wahrscheinlich genetischer Natur sind für marine Organismen beschrieben worden, und es ist bestimmt der Mühe wert, diese einer genetischen Analyse zu unterwerfen. In diesem Zusammenhang möchte ich auf einige Beispiele hinweisen. In dieser Hinsicht sind zum Beispiel *Ciona* unter den Tunicaten, *Metridium* unter den Anthozoa, *Aurelia* unter den Scyphozoa interessant. Unter den Schwämmen wären *Triaxonida* und *Tetraxonida* von Interesse, unter den Echinodermen *Astropecten*, *Strongylocentrotus* etc., unter den Cephalopoden *Sepia*, unter den Mollusken *Patella*, *Acmaea* und *Littorina*, unter den Crustaceen *Diastylis*, *Limnoria* und ähnliche Gattungen. Weiter sind unter den Fischen z. B. Hering, Lachs und *Zoarces* bestimmt interessante Objekte. Auch das Studium der endemischen Formen dürfte interessante Resultate ergeben. Nach Sven EKMAN (1953) sollen die endemischen Formen im Nordpazifik viel zahlreicher sein als in den anderen Oceanen. Es würde sich lohnen, diese Angaben zu überprüfen und, falls sie bestätigt werden — was sehr wahrscheinlich ist —, die für dieses

Phänomen verantwortlichen Faktoren einem intensiven Studium zu unterwerfen.

2. *Geschlechtsbestimmung und Chromosomenstruktur*

Untersuchungen über den Mechanismus der Geschlechtsbestimmung der marinen Tiere gehören heute schon zur klassischen Literatur, um nur z. B. an die berühmten Studien des Schweizer Zoologen Fritz Baltzer an *Bonellia viridis* zu erinnern. Hier sollen nun zwei divergierende Theorien über das unterschiedliche Verhalten der *Bonellia*-Larven diskutiert werden. Witschi, Hartmann, Morgan und Herbst basieren ihre Theorie auf der totalen Homogenität aller individuellen Genotypen und schreiben die individuellen Unterschiede einzig und allein dem Einfluss der Umweltfaktoren zu. Einer anderen Meinung sind Baltzer, Goldschmidt und Seiler. Im Gegensatz zu den vorigen Autoren nehmen sie an, dass die Populationen genetisch heterogen sind, und dass das Geschlecht durch ein Zusammenwirken von genetischen und Umwelt-Faktoren bestimmt wird. Ich habe diese verschiedenen Auffassungen hier erwähnt, weil in den letzten Jahren eine grosse Anzahl von Daten über verschiedene andere marine Formen bekannt geworden sind, die sehr zu Gunsten der Auffassungen von Baltzer, Goldschmidt und Seiler sprechen. In diesem Zusammenhang seien die sehr ausführlichen Arbeiten von Montalenti (1941) erwähnt über Hermaphroditismus und Gonochorismus bei *Anilocra physodes*, einer cymothoiden Crustacee und die Arbeiten von Bacci (1947, 1949, 1951, 1955) an *Patella coerulea* des Genus *Fissurella*, an dem Echinodermen *Asterina gibbosa* und an diversen Polychaeten. Ein interessanter Fall ist zum Beispiel *Patella coerulea. Patella* wurde lange Zeit für ein typisches Beispiel eines Gonochoristen gehalten, das heisst ein Tier mit kleinen Männchen und grossen Weibchen. 1927 sprach J. H. Orton die Vermutung aus, dass es sich hier um einen proterandrischen Hermaphroditen handle. Nach intensiven statistischen und histologischen Untersuchungen konnte Bacci nachweisen, dass dies tatsächlich der Fall war. Alle Individuen sind anfänglich funktionelle Männchen. Später konnte bei den meisten eine Geschlechtsumstimmung beobachtet werden, und die meisten Individuen werden weiblich. Die Übergangsphase, während derer männliche und weibliche Keimzellen in den Gonaden zu finden sind, ist so kurz, dass sie wohl von der Mehrzahl der Autoren übersehen worden war. BACCI's intensive Untersuchungen brachten zwei sehr interessante Tatsachen zu Tage. Erstens zeigten etwa 8% der Individuen keine Geschlechtsumstimmung. Es handelte sich um kleine Weibchen, die nicht durch eine vorherige männliche Phase gegangen waren, oder um grosse Männchen, die sich anscheinend nicht in Weibchen transformierten. Diese kleinen Weibchen und grossen Männchen wurden „primäre" Männchen und „primäre" Weibchen genannt. Zweitens konnte BACCI beobachten, dass die einzelnen Individuen einer Population die Geschlechtsumstimmung zur gleichen Zeit, d.h. wahrscheinlich im gleichen Alter durchmachen. Einige durchlaufen eine sehr kurze männliche Phase, andere eine etwas längere und wieder andere eine noch längere männliche Phase.

Auf Grund dieser und ähnlicher Ergebnisse, die an den oben genannten Objekten gewonnen wurden, entwickelten MONTALENTI und BACCI (1951) für diese Organismen eine Theorie der Geschlechtsbestimmung, die auf einem polygenen System basiert. Die Frequenz der Faktoren dieser polygenen Systeme kann in den diversen Populationen verschieden sein, und daraus ergeben sich unterschiedliche Frequenzen der einzelnen Geschlechtsformen. Individuen, die eine höhere Anzahl dominanter, männlicher Faktoren besitzen, durchlaufen eine lange männliche und eine kurze weibliche Phase. Genotypen mit wenig dominanten und vielen rezessiven Faktoren durchlaufen eine kurze männliche und eine lange weibliche Phase. Individuen mit ungefähr gleicher Anzahl männlicher dominanter und weiblicher rezessiver Faktoren besitzen etwa gleichlange weibliche und männliche Phasen. Im Jahr 1955 konnte BACCI die Gültigkeit dieser Theorie am Polychaeten *Ophryotrocha puerilis*, einem proterandrischen Hermaphroditen, überprüfen. BACCI führte einige Selektionsexperimente an einigen Stämmen von Neapel und von Plymouth durch, um zu sehen, ob man den Zeitpunkt der Geschlechtsumstimmung beeinflussen könne. Diese Experimente, die sich über einen Zeitraum von vier Generationen erstreckten, waren erfolgreich bei Selektion in der einen wie in der anderen Richtung. Eine Geschlechtsumstimmung tritt bei den neapolitanischen Exemplaren bei einer Länge von ungefähr 18 setigeren Segmenten ein, dagegen bei den Exemplaren aus Plymouth bei ungefähr 20 Segmenten. BACCI konnte nun durch Selektion erreichen, dass in der 4. Generation einige Individuen auftraten, die bei einer Länge von 11 bis 12 Segmenten Oocyten aufwiesen. Diese Tiere besassen praktisch keine männliche Phase und machten anscheinend keine Geschlechtsumstimmung durch. Sie sind deshalb als reine Weibchen zu bezeichnen. Durch Selektion in der anderen Richtung war es möglich, Individuen mit sehr langer männlicher Phase zu züchten. Einige erreichten eine Länge bis zu 26 Segmenten und starben, ohne Oocyten hervorgebracht zu haben. Diese Tiere können als reine Männchen bezeichnet werden. Diese Experimente zeigen also, dass es mit Hilfe von Selektion möglich ist, in relativ wenigen Generationen reine Männchen und reine Weibchen aus einer unbalancierten hermaphroditischen Form zu erhalten. Somit stützen sie die Hypothese, dass die Variabilität der sexuellen Phasen in einer Population proterandrischer Hermaphroditen des unbalancierten Typs auf genetischer Heterogenität beruht.

Auch in Organismen, die weder Hermaphroditen sind noch intersexuelle Phasen haben, könnte es möglich sein, dass die Geschlechtsbestimmung auf polygenischen Systemen beruht. Für diese Deutungsmöglichkeit konnte Dr. A. AR-RUSHDI aus unserem Laboratorium in Kalifornien einige Daten beitragen. Nach Angaben von TAKEDA (1947) sollte die Geschlechtsbestimmung des Copepoden *Tigriopus japonicus* phänotypisch sein. Dr. AR-RUSHDI versuchte diese Ergebnisse an der kalifornischen Art *Tigriopus californicus* zu reproduzieren. Er konnte in diesem Fall feststellen, dass bei *Tigriopus californicus* die Geschlechtsbestimmung genotypisch ist und dass wir es hier mit einer polygenischen Geschlechtsbestimmung zu tun haben. Untersuchungen über das Geschlechtsverhältnis bei der Nachkommenschaft individueller Eisäcke ergab starke Abweichungen vom 1:1-Verhältnis. Bei einer Gruppe von 80 Weibchen konnte beobachtet werden, dass 75% der Nachkommen männlich waren. Manchmal traten sogar Familien von mehr als 60 Mitgliedern auf, die nur aus Männchen bestanden. Um dieses Phänomen zu analysieren, wurde ein ausgedehntes Selektionsexperiment angesetzt, in dem getrennt zu Gunsten der Männchen und zu Gunsten der Weibchen selektioniert wurde. Obwohl die Daten noch nicht ganz ausgewertet worden sind, können wir jetzt schon sagen, dass es möglich ist, das Geschlechtsverhältnis mit Hilfe der Selektion so weit zu verschieben, dass wir Nachkommenschaften von 80% Weibchen oder auch nur 0,5%

(980)

Weibchen erhalten. Cytologische Untersuchungen ergaben, dass *Tigriopus* bei beiden Geschlechtern 12 Chromosomenpaare besitzt. Die Chromosomen lassen sich morphologisch nicht voneinander unterscheiden. Die Existenz von Geschlechtschromosomen ist sehr unwahrscheinlich. Chiasmata konnten nur bei den Männchen beobachtet werden. Auf Grund dieser Beobachtungen scheint es sehr wahrscheinlich, dass bei *Tigriopus* der Mechanismus der Geschlechtsbestimmung durch ein System von Polygenen kontrolliert wird. Die Anzahl der männchen- und weibchenbestimmenden Gene kann durch Selektion verschoben werden. Die Erblichkeit dieses Merkmals scheint sehr stark zu sein. Mit diesen Resultaten als Grundlage scheint es jetzt möglich, eine Analyse der Selektionsfaktoren durchzuführen, die die unter natürlichen Bedingungen beobachteten Abweichungen vom 1 : 1-Geschlechtsverhältnis in den Gezeitentümpeln verursachen. Zu diesem Zweck hat mein Mitarbeiter LANCE Untersuchungen repräsentativer Proben reifer Eisäcke aus den Gezeitentümpeln angesetzt. Er lässt die Eier im Laboratorium ausschlüpfen und dann an den reifen *Tigriopus*-Individuen das Geschlechtsverhältnis bestimmen. Die Proben werden monatlich den Gezeitentümpeln entnommen und die vorläufigen Resultate lassen vermuten, dass während einer Jahresperiode ziemliche Schwankungen im Geschlechtsverhältnis erfolgen.

Weitere Untersuchungen über die Cytologie dieses Organismus haben gezeigt, dass in der Meiose ein sehr interessanter Mechanismus der Chromosomenassoziation vorkommt. Ich möchte auch noch erwähnen, dass es wahrscheinlich ist, dass die durchgeführten Kälteschocks Polyploidie induziert haben. Die Resultate können aber erst nach weiteren Untersuchungen als definitiv betrachtet werden. Dieses Beispiel einer cytologischen, genetischen und Selektions-Untersuchung an ein- und demselben Objekt haben gezeigt, wie lohnend eine Analyse dieser Phänomene bei einem marinen Organismus sein kann.

In diesem Zusammenhang möchte ich die Aufmerksamkeit auf das Studium der Chromosomenzahl und-mechanik lenken. Während wir über eine ziemlich weite Kenntnis der Chromosomenzahlen und -morphologie der Landtiere und höheren Pflanzen verfügen, ist unsere Kenntnis der Chromosomenverhältnisse der marinen Tiere noch sehr beschränkt. In der Tabelle I ist verzeichnet, was bis 1951 in dieser Hinsicht bekannt war. Diese Tabelle ist einer Übersicht von S. MAKINO entnommen. Die meisten der vorhandenen Daten stammen ausserdem aus der Zeit vor dem ersten Weltkriege, aus einer Zeit also, die die heutige Perfektion der cytologischen Technik noch nicht kannte. Von wenigen Ausnahmen abgesehen stehen zum Beispiel fast keine Daten über die Chiasmahäufigkeit bei marinen Organismen zur Verfügung. Wenn man sich dann die sehr anregende Verallgemeinerung von D. C. DARLINGTON vor Augen hält, die dieser Autor in seinem Buch „The Evolution of Genetic Systems“ in bezug auf die Beziehungen zwischen Chromosomenzahl, Chiasmafrequenz, Paarungssystemen, Lebenszyklus und Variabilität entwickelte, so erscheint es sehr lohnend, eine Übersicht über die Chromosomenzahlen und Chiasmafrequenzen insbesondere derjenigen Gruppen von marinen Tieren zu gewinnen, deren Lebenszyklus näher mit dem der Blütenpflanzen als mit dem der höheren Tiere verwandt ist.

TABELLE 1.

Anzahl der Arten von marinen Invertebraten, deren Chromosomenzahl bekannt ist
(nach MAKINO, 1951)

Porifera	7
Coelenterata	15
Plathelminthes	37
Nemertini	7
Annelida	31
Mollusca	44
Molluscoidea	6
Echinodermata	29
	176
Land-Invertebraten	2.578

In seiner Analyse legt DARLINGTON dar, dass im Laufe der Evolution die natürliche Selektion in den verschiedenen Pflanzentypen ein Optimum der genetischen Rekombination hervorgebracht hat, und zwar indem sie die Chromosomenzahlen und die Chiasmafrequenzen jeweils einem bestimmten Paarungssystem angepasst hat. Bekanntlich gibt es unter den marinen Tieren viele sesshafte Formen, die über freischwimmende Gameten oder Larvenstadien verfügen, und daher im Lebenszyklus mehr den höheren Pflanzen als den Tieren mit autonomer Bewegungsmöglichkeit ähneln. Es wäre bestimmt von grösstem Interesse, den Chromosomenmechanismus dieser Phyla zu untersuchen und die Ergebnisse mit den besser bekannten Phyla der Landtiere zu vergleichen. In diesem Zusammenhang sei auf die Überlegungen hingewiesen, die BARIGOZZI (1958) kürzlich über die Bedeutung der sesshaften Stadien im Lebenszyklus in bezug auf die Populationsgenetik entwickelt hat.

Mit diesen Ausführungen ist kein vollständiger Überblick über die Arbeiten über Geschlechtsbestimmung und Chromosomenstruktur der marinen Tiere gegeben, sondern es sind hier nur einige Gebiete erwähnt, die besonders versprechend und anregend erscheinen.

3. *Artbildung und Evolution*

Durch die schnelle und intensive Entwicklung des Gebietes der Populationsgenetik und der modernen Systematik ist eine grosse Anzahl von Daten über die Variabilität natürlicher Populationen, über die Bedeutung des Mechanismus des Polymorphismus, über die Probleme der interspezifischen Hybridation und über die Verhältnisse zwischen Systematik, Phylogenie und Genetik bekannt geworden. Auch hier wieder ist die Kenntnis der marinen Formen im Verhältnis zu der der Landformen sehr gering. Trotzdem können wir annehmen, dass hier die gleichen Mechanismen am Werk sind, die die modernen Autoren für die anderen Organismengruppen erarbeitet haben. Es würde zu lange dauern, einen Überblick über alle existierenden Daten dieses Gebietes zu geben, denn es würde eine Neubewertung einer grossen Anzahl von Daten aus der zoologischen Literatur erfordern. Julian HUXLEY betonte (1955), dass Polymorphismus bei sehr vielen marinen Tieren zu beobachten ist. Zum Beispiel gibt es verschiedene Farbtypen bei der Seeanemone *Metridium senile*, die unterschiedliche Lichtempfindlichkeiten besitzen und in der Lage sind, sich an die verschiedenen Lichtbedingungen im Atlantik anzupassen. In Neu-Seeland dagegen sind die Arten von *Metridium* monomorph, d. h., sie sind weiss und leben in Zonen sehr geringer Lichtintensitäten. In ähnlicher Weise hat sich anscheinend *Tealis* adaptiert, aber hier haben wir es mit einem Phänomen zu tun, das HUXLEY cryptischen Polymorphismus nennt. Die verschiedenen Farbtypen vertreten nämlich verschiedene Hintergründe. Die Beschreibung ähnlicher Fälle von Polymorphismus findet man bei vielen Mollusken, bei Crustaceen wie Copepoden, Isopoden und Decapoden, bei Echinodermen wie den Seesternen

Marthasterias glacialis, *Henricia sanguinolenta*, *Solaster pappus* und dem Schlangenstern *Ophiothrix fragilis*, bei Ascidien wie *Botryllus schlosseri* und bei Schwämmen wie *Halicondria panicea* und *Hymeniacidion sanguinea.*

Die grosse Bedeutung der Interpretation des Polymorphismus auf genetischen Grundlagen kann an der Untersuchung des Schweizer Zoologen H. STAIGER (1954) demonstriert werden. STAIGER entdeckte höchst interessante Zusammenhänge zwischen Morphologie und Cytologie des Prosobranchiers *Thais lapillus.*

Für diese Art ist eine grosse Variabilität der Erscheinungsform (Grösse, Form, Skulptur, Färbung und Zeichnung der Schale) kennzeichnend. Diese Variabilität konnte von einigen Verfassern in Beziehung zu Verschiedenheiten des Habitats und der entsprechenden ökologischen Bedingungen gesetzt werden. H. STAIGER stellte nun fest, dass innerhalb der Art *Thais lapillus* ein Polymorphismus in bezug auf die Chromosomenzahl besteht. Zwei extreme numerische Formen (untersucht in der Region von Roscoff, Bretagne) weisen die Haploidzahlen 13 und 18 auf. Verschiedene Populationen zeigen verschiedene Grade der Heterogenität der Chromosomen. Heterogene Populationen besitzen in verschiedenem Masse eine inter-individuelle Variation der numerischen Konstitutionen und dementsprechend eine mittlere Haploidzahl zwischen den Grenzen 13 und 18. Gesamtheterogenität wie numerischer Typ stehen eindeutig in Beziehung zu ökologischen Faktoren des Habitats (Abb. 2). Der Typ mit 13 Chromosomen bewohnt die nahrungsreichen aber exponierten Lokalitäten der Gezeitenregion, die durch starke Wellenbewegung ausgezeichnet sind. Der Typ mit 18 Chromosomen dagegen besiedelt die vor Wellenbewegung geschützten Orte, und zwar vorwiegend die relativ nahrungsarme Zone der Braunalgen *Ascophyllum nodosum.* Die reinsten (homogenen) Populationen befinden sich an Lokalitäten mit extremen Habitatsbedingungen; Orte mit intermediären Habitatsbedingungen werden von chromosomal intermediären (heterogenen) Populationen bewohnt. Parallel zum ökologischen Gradienten der Gezeitenzone verläuft also ein chromosomaler Gradient.

Die Zahl der Chromosomen steht in so engem Verhältnis zur Morphologie der Muschelschale, dass Dr. STAIGER in der Lage ist, an Hand der Muschelschale die Chromosomenzahl vorauszusagen. Dieses Beispiel zeigt, wie wichtig es ist, die genetische Grundlage der morphologischen Merkmale zu studieren, auch wenn diese so eng mit den Umweltbedingungen korreliert sind wie in diesem Falle.

Dr. Staiger hatte gehofft, an der Küste des Stillen Oceans ähnliche Phänomene bei den Prosobranchier-Arten *Th. emarginata*, *Th. lamellosa*, *Th. canaliculata*, *Th. lima* derselben Gattung zu finden. Diese vier Arten gehören zu demselben Subgenus *Nucella* (oder *Polytropa*), zu dem auch die atlantische Art *Th. lapillus* gehört. Die morphologischen und ökologischen Differenzierungen entsprechen den interspezifischen, die bei der atlantischen Art mit dem Chromosomendimorphismus in Zusammenhang stehen. Es stellte sich aber leider heraus, dass alle vier Thais-Arten der nordpazifischen Küste haploid 35 Chromosomen besitzen. Bei Populationen der San Juan Islands von Habitaten unterschiedlicher Expositionsgrade konnte weder numerischer noch struktureller Chromosomendimorphismus beobachtet werden. Inzwischen hat man jetzt auch erkannt, dass die Chromosomenverhältnisse der

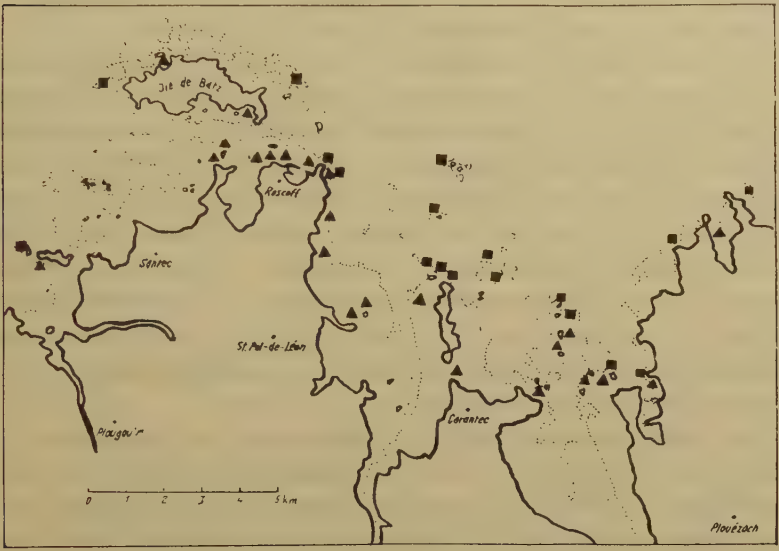

Abb. 2.

Verbreitung der Typen mit 13 Chromosomen (Vierecke) und mit 18 Chromosomen (Dreiecke) bei *Thais lapillus* an der Küste der Bretagne (nach Staiger, 1954).

Art *Thais lapillus* eine grosse Ausnahme sowohl in der Ordnung *Neogastrepoda* als auch im Genus *Thais* darstellen.

Die haploide Chromosomenzahl von 35 scheint für diese Gruppe die Grundzahl zu sein. Dieselbe Chromosomenzahl war schon früher bei zwei europäischen Arten der Familie *Muricidae* (zu der auch die Gattung *Thais* gehört) bei 3 Arten der *Buccinidae* und mehreren Mitgliedern anderer Familien gefunden worden. *Thais lapillus* scheint also die einzige Ausnahme zu sein.

Während seines Aufenthaltes in Kalifornien untersuchte Dr. Staiger eine Art der Isopoden aus der Familie der *Janiridae*. Da diese Art eine geringe Zahl relativ grosser Chromosomen besitzt schien sie für ähnliche Untersuchungen sehr geeignet zu sein. Eine ganze Reihe ökologisch differenzierter Arten der Genera *Janiropsis* und *Jaeropsis* waren für die Gezeitenzone der Küste des Stillen Oceans bekannt. Für eine Art *(Janiropsis kincaidi)* des Stillen Oceans war die Chromosomenzahl bekannt. *J. kincaidi* besitzt haploid 6 Chromosomen. Die atlantische Art *J. breviremis* hat 5 Chromosomen und somit die bis jetzt niedrigste Zahl, die bei Isopoden bekannt geworden ist.

Alle diese Arbeiten wurden unternommen, um Arten mit geeigneten Chromosomen zu finden, an denen eine Analyse der Variationssysteme durchgeführt werden könnte. Leider sind bis jetzt noch keine entsprechenden Arten entdeckt worden. Eine ausführliche Übersicht über die Chromosomenzahlen der Gattung *Thais*, einschliesslich der südlicheren Arten aus dem Golf von Kalifornien und verwandter Genera *(Acanthia*, *Ocenebra)*, würde uns bestimmte Einblicke in die chromosomale Artbildung der Ordnung *Neogastropoda* geben. Die Gattung *Janiridae* aus der Familie der Isopoden ist höchstwahrscheinlich für ähnliche Untersuchungen geeignet.

Ein weiteres Beispiel, das uns zeigt, wie wichtig es ist, natürlich auftretenden Polymorphismus einer genetischen Analyse zu unterwerfen, geben die Arbeiten von Dr. Battaglia an der Universität Padua. Wie schon oben erwähnt, kommt *Tisbe reticulata* in den Lagunen von Venedig in den vier Hauptphänotypen *maculata*, *violacea*, *trifasciata* und *punctata* vor. Dr. Battaglia konnte nun zeigen, dass die Manifestation des Farbmusters durch eine Serie von mindestens drei Allelen desselben Locus, von denen zwei Allele dominant über einem dritten rezessiven sind, bedingt ist.

Die zwei Allele, die dominant über das dritte rezessive Allel sind, zeigen keine Dominanz, wenn sie zusammen auftreten, indem die Heterozygoten phänotypisch zu unterscheiden sind. Kreuzungen zwischen den verschiedenen Genotypen haben ergeben, dass die Heterozygoten vitaler als beide Homozygoten sind. Aus der Tabelle II kann man sehen, dass die Vitalität der Heterozygoten auch unter verschiedenen Umweltbedingungen viel höher ist als die der Homozygoten. Durch die Arbeit von BATTAGLIA wurde somit zum ersten Male an Hand von Laboratoriumsexperimenten in natürlichen Populationen ein positiver Selektionswert für die polymorphen Konditionen eines marinen Organismus nachgewiesen. Es ist daher wahrscheinlich, dass dieses Phänomen, das in den Landorganismen weit verbreitet ist, auch bei den marinen Formen eine wichtige Rolle spielt.

TABELLE 2.

F_2 der Kreuzung „maculata“ × „violacea“
I, II, III = verschiedene Kreuzungsbedingungen
(nach BATTAGLIA und PULZE, 1957)

Kreuzung	Phaenotyp				Total	χ^2 F.g., 2
		„viol.“	„viol.-macul.“	„macul.“		
„macul.“ × „viol.“ I (39)	Beob.	248	820	223	1.291 ♂♂ und ♀♀	95,3 P < 0,001
	Erw.	322,75	645,5	322,75		
	Untersch.	– 74,75	+ 174,5	– 99,75		
„macul.“ × „viol.“ II (48)	Beob.	290	881	325	1.496 ♂♂ und ♀♀	48,91 P < 0,001
	Erw.	374	748	374		
	Untersch.	– 84	+ 133	– 49		
„macul.“ × „viol.“ III (53)	Beob.	873	1.955	888	3,716 ♂♂ und ♀♀	10,248 P = 0,001—0,01
	Erw.	929	1.858	929		
	Untersch.	– 56	+ 97	– 41		

A. J. KOHN (1958) hat erst kürzlich eine Zusammenfassung veröffentlicht, in der er zeigte, dass bei den marinen Tieren die Artbildung einem ähnlichen Schema folgt wie bei Landtieren. Ich will nicht wiederholen, was schon so hervorragend durch Kohn dargestellt worden ist. Durch seine Untersuchungen über die geographische Artbildung konnte Ernst Mayr (1954) zeigen, dass auch für die marinen Formen dieser Prozess durch genetische Variabilität und Isolation erklärt werden kann. An Hand eines Studiums über die Artbildung bei der Gastropoden-Gattung *Acmaea* konnte Test (1946) die Bedeutung der sympatrischen Artbildung für diese Form nachweisen. Diese klassischen Modelle der Artbildung, d. h. allopatrische und sympatrische, scheinen aber nicht auszureichen, um die taxonomische Diskontinuität des Zooplanktons zu beschreiben, da im Meer anscheinend keine Isolationsmechanismen vorhanden sind. Diese besondere Situation im Meer, d. h. des marinen ökologischen Systems, kann vielleicht durch einen folgenden eigenartigen Mechanismus erklärt werden.

Nehmen wir an, zu einem Zeitpunkt t_a existiere eine Population einer planktonischen Art in einer Zone A des Meeres, und von dieser Zone A führe eine Strömung in eine andere Zone B. Die Individuen der Population A werden durch die Strömung nach der Zone B transportiert. Nehmen wir weiter an, dass in der Zone B andere hydrographische Bedingungen als in A herrschen. Zu einem Zeitpunkt t_1 können wir dann erwarten, dass die Population in der Zone B sich aus den Individuen der Population der Zone A zusammensetzt, die sich an die anderen hydrographischen Bedingungen der Zone B anpassen konnten. Die anpassungsfähigen Individuen bilden dann die Population B. Obwohl nun die Population B weiterhin Individuen der Population A empfängt, werden nur diejenigen Genkombinationen überleben, die sich an die Umweltbedingungen in B anpassen können. Vor einigen Jahren konnte ich bei *Drosophila* ein ähnliches System im Laboratorium studieren. Unterwirft man eine Population über einen bestimmten Zeitraum hinweg einer natürlichen Selektion, so werden gewisse Gene, die sich nicht an diese Umweltbedingungen anpassen können, eliminiert. Wenn man jetzt diese Gene erneut in die Population einführt, so werden sie schneller als zuvor eliminiert (Buzzati-Traverso, 1955). Es ist sehr wahrscheinlich, dass dieser sehr elementare genetische Isolationsmechanismus im Ocean durch physikalische Eigenschaften der Umwelt hervorgerufen werden kann, z. B. durch eine Meeresströmung, die lange Zeit ihre Richtung nicht ändert. Wenn dieser elementare Mechanismus für eine Zeit funktioniert hat und die Population B einen gewissen Grad der Divergenz von der ursprünglichen Population A erreicht, können kompliziertere Isolationsmechanismen auftreten, die dann der Population B ermöglichen, sich zu einer eigenen Art zu entwickeln, die sich nicht mehr mit der ursprünglichen Art A kreuzen lässt.

Nun möchte ich an Hand einiger Daten, die wir im Augenblick bei der Gattung *Tigriopus* sammeln, zeigen, dass man die Untersuchungen über Evolution und Systematik mit modernen Methoden auch an marinen Formen durchführen kann. Die Gattung *Tigriopus* ist an den Küsten aller Oceane zu finden. Da an der kalifornischen Form intensive Untersuchungen durchgeführt werden sollten, schien es angebracht, erst einmal ihre taxonomische Stellung in bezug auf die beiden anderen beschriebenen Formen zu bestimmen. Zu diesem Zweck wurde *T. californicus* morphologisch verglichen mit der europäischen Form *T. brevicornis* und der orientalischen Form *T. japonicus* und Kreuzungen zwischen den drei Formen durchgeführt.

Die Untersuchungen wurden erstens eingeleitet, um bessere Angaben über die Morphologie der Arten zu besitzen, zweitens um den Variationstypus und die Variationsbreite bei den einzelnen Arten zu bestimmen, drittens um neue Daten über die Verbreitung der Formen zu erhalten, viertens um durch interspezifische Hybridisation die Gültigkeit der beschriebenen Arten zu bestätigen und fünftens um zu sehen, ob diese Gattung sich für ein Studium der Artbildung eignen würde.

Aus den bis jetzt durchgeführten Untersuchungen hat sich ergeben, dass die drei Arten zu Recht bestehen, da sie sich morphologisch und genetisch von einander unterscheiden. Weiter wurde eine grosse Anzahl reziproker Kreuzungen mit den vorhandenen Stämmen durchgeführt. Wie aus der Karte (Abb. 3) zu ersehen ist, besitzen wir Stämme aus Asien, Europa und Amerika.

Kreuzungsversuche zwischen Individuen aus Split und Dröbak waren ohne Erfolg. Die 29 reziproken Kreuzungsversuche zwischen den Stämmen aus Split und denen aus Millport ergaben Larven nur bei zwei Kreuzungen, nämlich

Kreuzung No. 2 (S × M): 58 Larven aus 8 partiell fertilen Eisäcken,
Kreuzung No. 5 (S × M): 48 Larven aus 5 partiell fertilen Eisäcken.

80% der Larven aus diesen beiden Kreuzungen starben im 1. Naupliusstadium ab, und vom Rest überlebten nur vier im 4. Naupliusstadium. Wenn man dagegen Stämme aus Split mit denen von Livorno kreuzt, so sind die Kreuzungen völlig fertil, d. h. die

Stämme gehören einer mediterranen Form an. Ähnliche Resultate hat Bozic (1953) mit Stämmen aus Villefranche und Roscoff erhalten. Die mediterrane Form stellt höchstwahrscheinlich eine neue Art dar, die sich aber bis jetzt morphologisch noch nicht eindeutig von den anderen Arten abgrenzen lässt. Weitere Kreuzungen mit Individuen von anderen Lokalitäten der europäischen Küste werden zeigen, ob eine Diskontinuität zwischen diesen beiden Formen wirklich besteht.

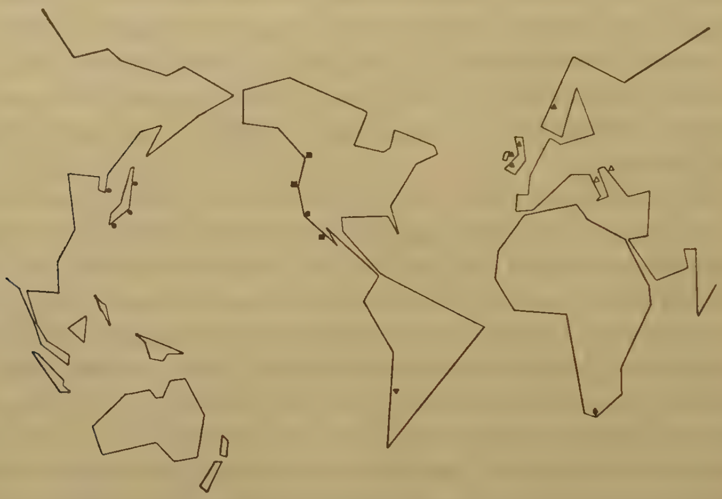

Abb. 3.

Geographische Verbreitung der kultivierten Stämme der Gattung *Tigriopus*.

Vor nicht langer Zeit bekamen wir zwei Formen aus Chile und aus Südafrika. Diese beiden Formen unterscheiden sich morphologisch von den bekannten Arten und lassen sich auch nicht mit ihnen kreuzen. Höchstwahrscheinlich haben wir es hier mit zwei neuen Arten zu tun. In Kürze hoffen wir, Material aus dem Gebiet Neu-Seeland-Tasmanien, aus den Küstengebieten Argentiniens, der Osterinseln, der Galapagos-Inseln, Französisch West-Afrikas, Algeriens, des Libanons, Indiens, der USSR, Frankreichs und Portugals zu erhalten. Weiter hoffen wir, Material von den Clipperton- und Cocos-Inseln, aus Panama und der Nordost-Küste der Vereinigten Staaten zu bekommen.

Im Fall *Tigriopus* haben wir versucht, die Systematik der Gattung von den verschiedenen Gesichtspunkten der Morphologie, der Genetik, der Cytologie und der geographischen Verbreitung her aufzubauen. Der Erfolg, den man durch einen solchen breiten Angriff eines Problemes erreichen kann, ist durch die ausführliche systematische Beschreibung der Gattung *Drosophila* belegt. Zweifellos ist die Gattung *Drosophila* taxonomisch die bestbekannte Gattung, über die wir zur Zeit verfügen. Dieser Stand unserer Kenntnis konnte nur erreicht werden, weil es möglich war, eine grosse Anzahl der Arten im Laboratorium zu züchten und so nach verschiedenen Gesichtspunkten zu untersuchen. Unsere Erfahrungen mit *Tigriopus* machen es sehr wahrscheinlich, dass in einigen Jahren *Tigriopus* ein ähnlich gut untersuchtes Beispiel eines marinen Objektes darstellen wird. In Anbetracht der grossen Zahl der Probleme, die z. B. im Gebiet der Systematik der Crustaceen noch auf eine Lösung warten, scheint ein Versuch, *Tigriopus* einem intensiven Studium von verschiedenen Gesichtspunkten her zu unterwerfen, sehr vielversprechend und lohnend.

4. *Analyse marin-ökologischer Systeme mit Hilfe genetisch-bakteriologischer Methoden*

Der Pionierarbeit von C. E. Lucas (1947), in der er die Bedeutung der externen Nährstoffe für die Verbreitung des Zoo- und Phytoplanktons hervorhob, folgten eine ganze Anzahl Arbeiten, deren Ergebnisse man folgendermassen zusammenfassen kann:

1. Organische und anorganische Stoffe müssen in sehr grosser Verdünnung im Ocean vorhanden sein, um die Vermehrung und Existenz der marinen Organismen zu gewährleisten. 2. Antibiotische Substanzen sind notwendig, um sehr delikaten Formen zu gestatten, die kritischen Phasen ihres Lebenszyklus zu überstehen. 3. Externe Nährstoffe (metabolische Stoffe) sind tatsächlich im Meerwasser nachgewiesen worden. Da diese Substanzen im Meerwasser in nur sehr geringen Konzentrationen anzutreffen sind, bereitet ihr quantitativer und qualitativer Nachweis grosse technische Schwierigkeiten.

Bekanntlich reagieren biochemische Mutanten der Bakterien spezifisch auf sehr geringe Konzentrationen von Nährstoffen. Es erschien also angebracht zu prüfen, ob diese Mutanten sich für biologische Nachweise verwenden lassen.

Von dieser Idee ausgehend, versuchte Dr. W. B. **Belser**, Mutanten zu induzieren, die sich für einen solchen biologischen Nachweis eignen würden. Versuche, *Escherichia coli*, von der schon diverse Mutanten bekannt waren, dem hohen Salzgehalt des Meerwassers anzupassen, erwiesen sich als unpraktisch und zu zeitraubend. So wurden also eine ganze Anzahl anderer Bakterien auf geeignete Charakteristika untersucht und von diesen *Serratia marinorubrum* als am besten geeignetes Objekt ausgewählt. *S. marinorubrum* wächst gut auf einem anorganischen Medium, dem als einzige Kohlenstoffquelle Glycerol zugegeben wird.

Ausserdem kann *S. marinorubrum* Salzgehalte von Süsswasserkonzentrationen bis zur 3-fachen Meerwasserkonzentration tolerieren. Somit ist die Anwendungsmöglichkeit von *S. marinorubrum* nicht nur auf Meerwasser beschränkt, sondern sie kann auch bei der Analyse von Seen, Flüssen und Brackwasser verwendet werden.

Die Bakterien wurden in der logarithmischen Wachstumsphase mit ultraviolettem Licht bestrahlt und nach der Incubation auf induzierte Mutanten getestet. Der Mutationstest wurde mit Minimalmedium und der Technik der verzögerten Anreicherung durchgeführt. Die resultierenden Mutanten wurden isoliert und auf ihren spezifischen Nährstoffbedarf hin untersucht.

Ebenfalls wurde die optimale Grenzkonzentration und die untere Sensibilitätsgrenze jeder Mutante bestimmt. Weiter wurde untersucht, ob sich die einzelnen Mutanten für einen quantitativen Nachweis eignen würden. Zur Zeit verfügt Dr. **Belser** über 8 Mutanten, von denen 6 für Biotin, Uracil, Isoleucin, Adenin, Histidin beziehungsweise Methionin spezifisch sind. Eine 7. Mutante reagiert auf Pepton, aber bis jetzt konnte noch keine Substanz gefunden werden, für welche diese Mutante spezifisch ist. Die 8. Mutante reagiert auf alle vier Purinbasen oder deren Riboside.

In einem Vorexperiment wurde die Brauchbarkeit dieser Mutanten für Tests in natürlichem Meerwasser geprüft. 29 Meerwasserproben wurden Dr. **Belser** von Mitgliedern der SCOPE Expedition des US Fish- and Wildlife Service zur Verfügung gestellt. Diese Proben wurden entlang der Küste von La Jolla bis Costa Rica aus verschiedenen Tiefen und von der Oberfläche des Meeres mit Nansenflaschen entnommen.

(992)

Die nächste Tabelle (III) soll eine Idee geben, welche Daten man von einer solchen Technik erwarten kann.

TABELLE 3.

Organische Wuchsstoffe im Seewasser, determiniert durch Bakterien (nach W. B. BELSER, unveröff.)

Tiefe in Meter	Sterilitätskontrolle	Biotin	Uracil	Purin
10	0	0	0	0
25	0	0	0,08	0,4
50	0	0	0,08	0
75	0	0,02	0	0

Die Bestimmung der Konzentration ist visuell und daher können die Werte nur approximativ bestimmt werden, aber ihre Grössenordnung ist zweifellos richtig. Eine Überschlagsrechnung, die auf den durchschnittlichen Werten für Gesamtkohlenstoff der pelagischen küstennahen Gewässer basiert ist, ergibt, dass 5—10% des Gesamtkohlenstoffs durch diese Substanzen repräsentiert sind (mittl. Gesamtkohlenstoffgehalt in dieser Gegend 1—5 mg/l). Eigentlich hätten die Werte um einen Faktor von 10 höher sein müssen, denn die Proben wurden den küstennahen Gewässern entnommen, d. h. Gebieten, die eine hohe Produktivität und somit einen hohen Gesamtkohlenstoffwert besitzen.

Ausserdem wurde eine direkte Korrelation zwischen Wuchsstoffen und Phytoplanktonkonzentration, und eine reziproke Korrelation zwischen Wuchsstoffen und Bakterienzahl beobachtet. Die bisherigen Resultate sind noch zu sporadisch, um eine Erklärung dieser Phänomene geben zu können, aber sie zeigen, in welcher Richtung weitere Untersuchungen unternommen werden sollten.

Zusammenfassend können wir sagen, dass dieser biologische Nachweis seine Berechtigung hat, zumindest in qualitativer Hinsicht. Weitere Experimente sind nötig um zu entscheiden, ob sich diese Methode auch für quantitativen Nachweis ausarbeiten lässt. Für den Meeresbiologen sind diese Ergebnisse besonders interessant, denn sie zeigen, dass Meerwasser nicht so uniform ist, wie meistens angenommen wird. Es variiert ziemlich, wie hier zum Beispiel für die Wuchsstoffe gezeigt wurde.

In diesem Zusammenhang möchte ich auf die mysteriösen Sukzessionen der Phyto- und Zooplanktonpopulationen hinweisen, die jedem Meeresbiologen bekannt sind. Vielleicht wird es bald möglich sein, diese ökologischen Phänomene auf chemische Faktoren des Meerwassers zurückzuführen. Es ist auch sehr wohl möglich, dass der Hauptunterschied zwischen dem Wasser- und Landlebewesen im Bedarf dieser Wuchsstoffe liegt. Die Eroberung des Landes durch die Pflanzen und Tiere hätte dann nicht nur Veränderungen in Atmungsmechanismus hervorgebracht, sondern auch den Mechanismus der Nahrungsaufnahme und des Stoffwechsels verändert.

LITERATURVERZEICHNIS

Bacci, G. 1947. *L'inversione del sesso e il ciclo stagionale della gonade in Patella cerulea.* Pubbl. Staz. Zool. Napoli 21: 183-217.

— 1949. *Osservazioni statistiche sulla determinazione dei sessi in Patella cerulea.* Pubbl. Staz. Zool. Napoli 22: 26.

— 1951. *On two sexual races of Asterisma gibbosa.* Experientia 7: 31-33.

— 1955. *La variabilità dei genotipi sessuali negli animali ermafroditi.* Pubbl. Staz. Zool. Napoli 26: 110-137.

Barigozzi, C. 1958. *Genetic systems in sessile and semisessile animals.* Symp. Perspectives in Marine Biology, ed. by A. A. Buzzati-Traverso (im Druck).

Battaglia, B. und Pulze, E. 1957. *Polimorfismo e superiorità degli eterzigoti nel copepode Tisbe reticulata.* Boll. Zool. 24: 1-7.

Bocquet, C. 1951. *Recherches sur Tisbe (Ydyea) reticulata n. sp.* Arch. de Zool. Exp. et Gen. 87: 335-416.

— Levi, C. und Teissier, G. 1951. *Recherches sur le polychromatisme de Sphaeroma servatum.* Arch. de Zool. Exper. et Gen. 87: 245-298.

Bozic, B. M. 1953. *Essais d'hybridation entre deux formes rapportées jusqu'ici à l'espèce Tigriopus fulvus Fisher (Copepodes Harpacticoides).* C. r. Acad. Science 237: 1568.

Buzzati-Traverso, A. A. 1955. *Evolutionary changes in components of fitness and other polygenic traits in Drosophila melanogaster populations.* Heredity 9: 153-186.

— 1958. *Perspectives in marine biology.* Symp. Perspectives in Marine Biology ed. by A. A. Buzzati-Traverso (im Druck).

(994

Darlington, C. D. 1939. *The evolution of genetic system.* Cambridge. McMillan, 149 pp.

Ekman, S. 1953. *Zoogeography of the sea.* London, Sidgwick und Jackson Ltd. 417 pp.

Føyn, B. und Gjøen, I. 1954. *Studies on the serpulid Pomatoceros triqueter L.* II. *The color pattern of the branchial crown and its inheritance.* Nytt Magazin Zool. 2: 85-90.

Huxley, J. S. 1955. *Morphisme and evolution.* Heredity 9: 1-52.

Kohn, A. J. 1958. *The process of speciation.* Symp. Perspectives in Marine Biology, ed. by A. A. Buzzati-Traverso (im Druck).

Imai, T. und Hatamaka, M. 1949. *On the artificial propagation of japanese oyster, Ostrea gigas Thum. by non colored naked flagellates.* Bull. Ist. Agric. Res. Tohoku Univ. 1: 33-46.

Loosanoff, V. L. 1954. *New advances in the study of bivalve larvae.* Amer. Scient. 42: 607-624.

— 1958. *Challenging problems in shellfish biology.* Symp. Perspectives in Marine Biology, ed. by A. A. Buzzati-Traverso (im Druck).

— und Davis, H. C. 1950. *Conditioning V. mercenaria for spawing in winter and breeding its larvae in the laboratory.* Biol. Bull. 98: 60-65.

— und Nomejko, C. C. 1951. *Existence of physiologically different races of oyster Crassostrea virginica.* Biol. Bull. 101: 151-156.

Lucas, C. E. 1947. *The ecological effect of external metabolites.* Biol. Rev. 22: 270-295.

Makino, S. 1951. *Chromosome numbers in animals.* Ames, Iowa State College Press. 290 pp.

Mayr, E. 1954. *Geographic speciation in tropical echinoids.* Evol. 8: 1-18.

Matsui, Y. 1958. *On the relation between formation of pearls and environments of pearl culture ground in the sea, and the problem of hybridization in the genus Pinctada.* Symp. Perspectives in Marine Biology, ed. by A. A. Buzzati-Traverso (im Druck).

Montalenti, G. 1941. *Note sulla sistematica e la biologia di alcuni Cimotoidi del golfo di Napoli.* Arch. Ocean. e Limnol. 5: 25.

— 1958. *Perspectives of research on sex problem in marine animals.* Symp. Perspectives in Marine Biology, ed. by A. A. Buzzati-Traverso (im Druck).

— und Bacci, G. 1951. *Osservazioni e ipotesi sulla determinazione del sesso negli ermafroditi.* Scientia Genet. 4: 5.

Orton, J. H. 1927. *Observations and experiments on sex changes in the european oyster (O. edulis).* J. Mar. Biol. Assoc. 14: 967.

STAIGER, H. 1954. *Der Chromosomendimorphismus beim Prosobranchier Purpura lapillus in Beziehung zur Ökologie der Art.* Chromosoma 6: 419-478.

TAKEDA. 1950. *Experimental studies on the effect of external agencies on the sexuality of a marine Copepod.* Physiol. Zool. 23: 288.

TEST, A. R. 1946. *Speciation in limpets of the genus Acmaea.* Contr. Lab. Vert. Biol. Univ. Michigan 31: 1-24.

ESTUDIO PRESENTADO POR ESCRITO

Contribución de la Scripps Institution of Oceanography

1.—INTRODUCCIÓN.

A través de varios años, la Scripps Institution of Oceanography de la Universidad de California se ha empeñado en el estudio de las aguas marinas de ambas Californias. Las investigaciones han tocado la biología, la química, la geología submarina y la hidrografía de la región estudiada.

Ultimamente, la mayor parte del esfuerzo ha sido llevado a cabo por la California Cooperative Oceanic Fisheries Investigation (CCOFI), grupo que está compuesto por la California Academy of Sciences, Hopkins Marine Station, Division of Fish and Game del Estado de California, South Pacific Fishery Investigations del U.S. Fish and Wildlife Service, y la Scripps Institution. Este programa de investigaciones nació en 1949, y actualmente está siendo continuado. Además, otras muchas investigaciones de menor magnitud han sido realizadas. El programa de CCOFI y los otros estudios, en lo que atañen a la región de la Baja California, serán discutidos a continuación.

El programa de CCOFI fue emprendido primordialmente para estudiar la pesquería de la sardina, que entonces se encontraba en estado decadente por la aparente continua disminución de la población. Desde que principió, ha llegado a incluir el estudio de otras especies de peces de importancia comercial. Se efectúan viajes al mar mensualmente, recorriendo la red de estaciones exhibida en la figura 1. De dos a cuatro barcos participan en estos viajes mensuales, los cuales han sido efectuados, casi sin interrupción, desde el mes de marzo de 1949. En cada estación hidrográfica se efectúa un arrastre de red (ver figura 2) para capturar una muestra de la vida microscópica del mar, y se baja una serie de botellas (17 por lo general) para obtener muestras de agua de distintas profundidades hasta 600

Contributions from the Scripps Institution of Oceanography, New Series, No. 1057
Reproduced by Permission

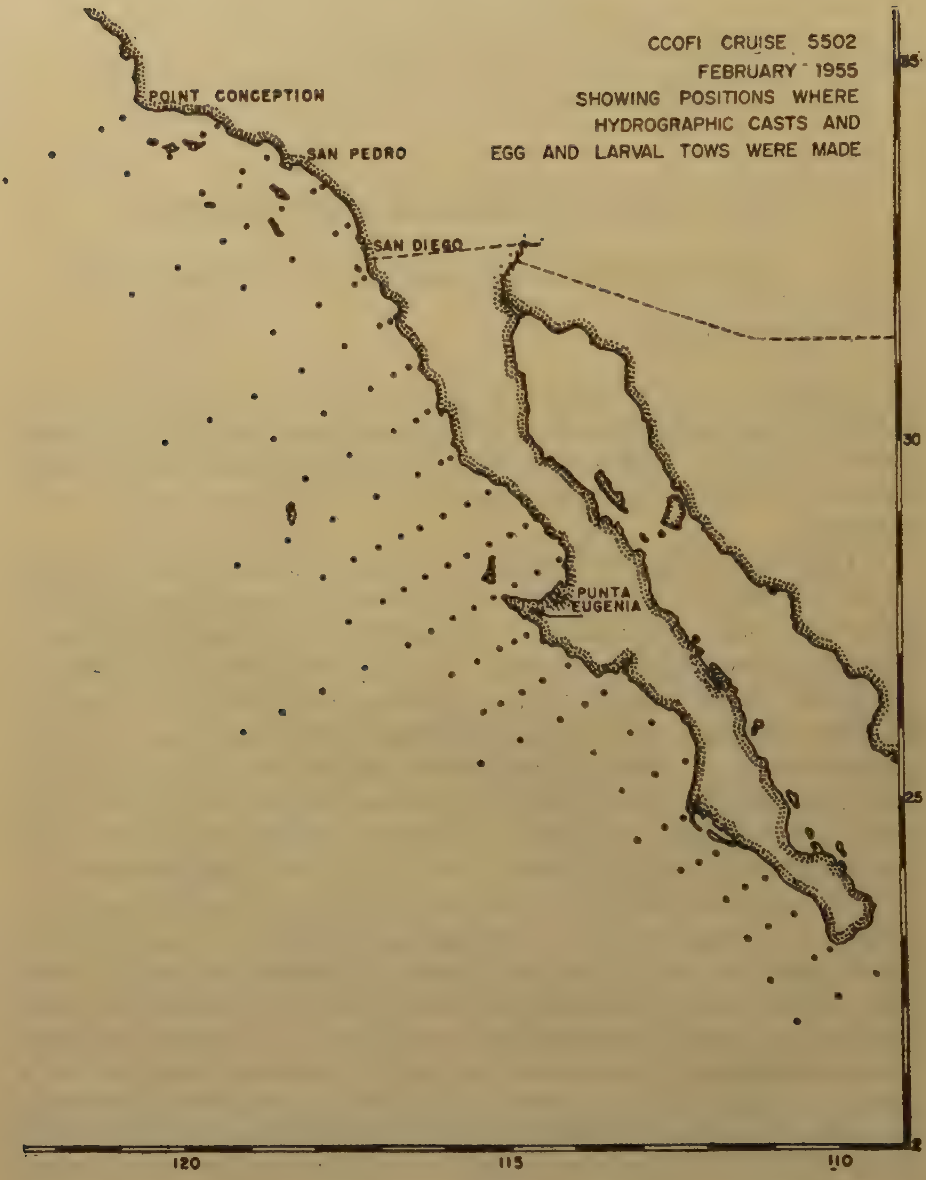
CCOFI CRUISE 5502
FEBRUARY 1955
SHOWING POSITIONS WHERE
HYDROGRAPHIC CASTS AND
EGG AND LARVAL TOWS WERE MADE
POINT CONCEPTION
SAN PEDRO
SAN DIEGO
PUNTA
EUGENIA
35
30
25
120
115
110

FIG. 1.—*Estudios Oceanográficos.*

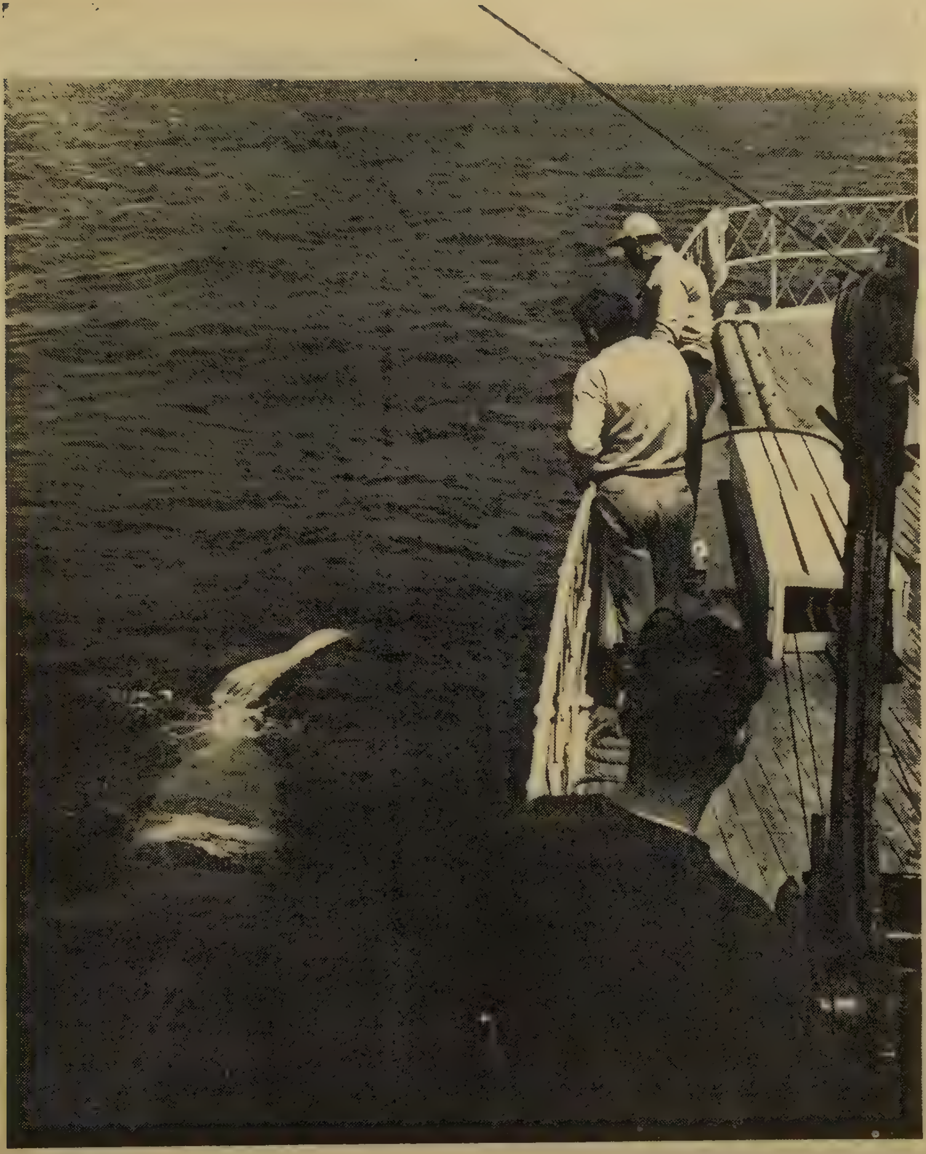

Fig. 2.—*Estudios Oceanográficos.*

metros, y también para medir la temperatura a esas profundidades mediante termómetros que acompañan a cada botella. Las muestras son analizadas posteriormente para determinar el contenido de oxígeno y la salinidad del agua. Sabiendo la temperatura y salinidad se puede calcular la densidad del agua, luego la profundidad a que se encuentra cada superficie isobárica, y la altura dinámica (dynamic height). Haciendo ciertas suposiciones, la altura dinámica nos da el conocimiento de la velocidad de la corriente. Mediciones de la corriente también se hacen con el "Geomagnetic Electrokinetograph", que registra la potencial eléctrica inducida en el agua como consecuencia de su movimiento por el campo magnético de la tierra, y de la cual puede calcularse la velocidad.

La temperatura superficial se registra continuamente a bordo del barco por medio del termógrafo. Entre las estaciones hidrográficas (que se separan una de otra por unos 60 km.) se efectúan tres o cuatro bajadas del "bathythermograph", obteniendo así gráficas continuas de la temperatura, en función de la profundidad, hasta 250 metros.

Se abandonan botellas flotantes desde todas las estaciones visitadas, que tienen dentro tarjetas pidiendo que el que las encuentre las devuelva a la Scripps Institution, anotando la localidad y fecha en que fueron halladas. Muchas de estas tarjetas han sido devueltas por los habitantes de Baja California que viven cerca de la costa, y de las Islas Cedros, Guadalupe y San Benito.

Además de estos viajes mensuales, a veces se efectúan viajes para estudios especiales. Se han hecho varios de tales viajes a la Bahía Sebastián Vizcaíno, que es una región de sumo interés desde los puntos de vista de la hidrografía y la biología. Debido a su poco fondo y al lento intercambio de agua con el océano, tiene los caracteres muy distintos de las aguas más alejadas de la costa.

2.—DESCRIPCIÓN DE LAS AGUAS OCEÁNICAS

2.—*La Hidrografía.*—Los trabajos de la CCOFI han ensanchado considerablemente los conocimientos de la hidrografía de las aguas contiguas a la Baja California. Los estudios en la Bahía Sebastián Vizcaíno, han expuesto a la luz una población de sardina en que el desove ocurre durante todo el año, y unas investigaciones especiales han tenido buen éxito en explicar el ambiente que posibilita este fenómeno. Mediciones directas de la corriente frente a la costa han indicado algunos de los fenómenos transitorios que deben ser considerados antes que uno pueda evaluar correctamente las observaciones

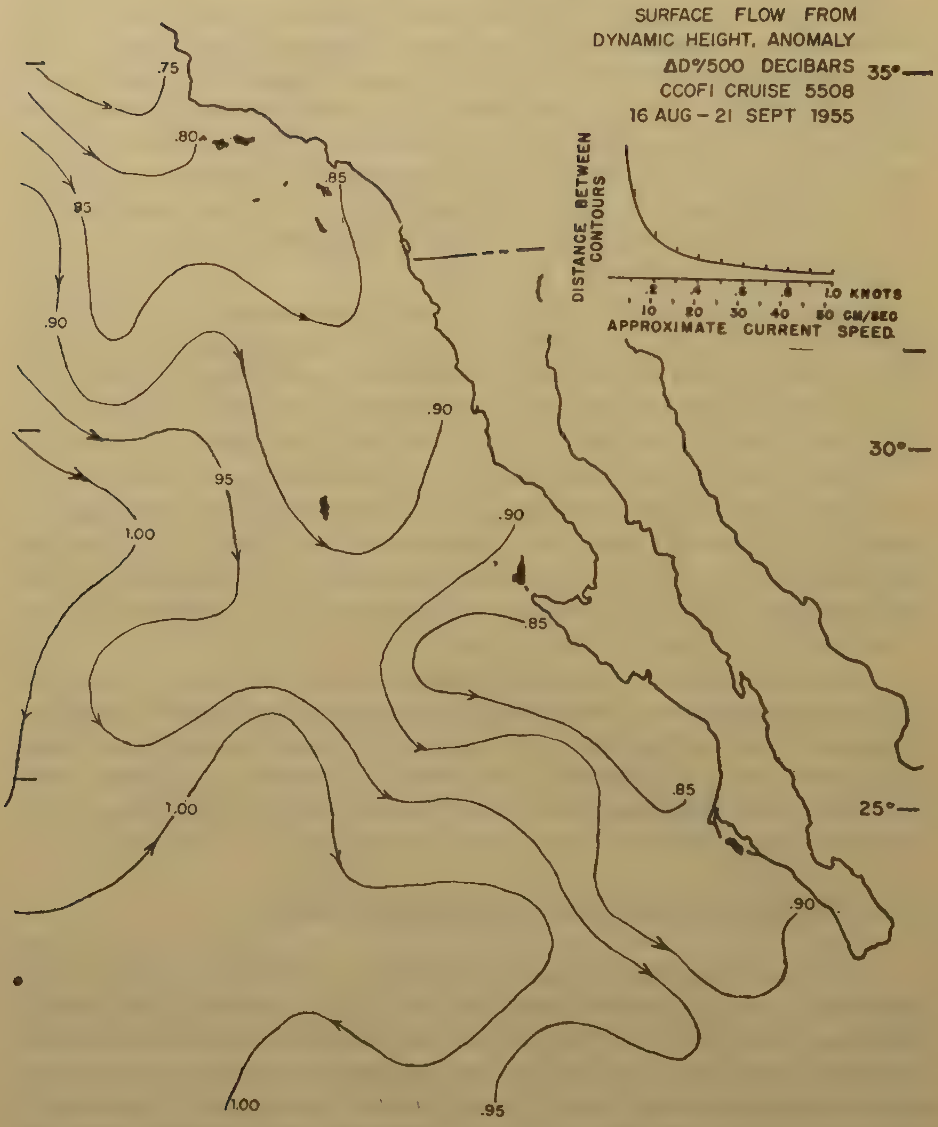
SURFACE FLOW FROM
DYNAMIC HEIGHT, ANOMALY
ΔD°/500 DECIBARS
CCOFI CRUISE 5508
16 AUG – 21 SEPT 1955
DISTANCE BETWEEN CONTOURS
.2
.4
.6
.8
1.0 KNOTS
10
20
30
40
50 CM/SEC
APPROXIMATE CURRENT SPEED
35°
30°
25°
.75
.80
.85
85
.90
.90
.90
95
1.00
.85
1.00
.85
.90
1.00
.95

FIG. 3.—*Estudios Oceanográficos.*

hechas mensualmente. Termógrafos han facilitado la investigación del afloramiento. No vamos a entrar detalladamente en estos pormenores, pero sí vamos a tratar algunas de las consideraciones generales de la hidrografía de las aguas océanicas.

Todos los datos hidrográficos originales van a publicarse próximamente en una serie de tomos que se llamará "Oceanographic Observations of the Pacific".

La mayor parte del agua frente a la costa de Baja California forma parte del gran circuito del Pacífico Norte, y está en movimiento hacia el Sur (Sverdrup, 1941a, 1941b). Ha llegado después de haber atravesado la parte septentrional (entre 40° y 50° N.) del Océano Pacífico, donde sufriría un enfriamiento y una dilución por la gran precipitación que hay en esa región. Al alcanzar la costa de Norteamérica, se desvía hacia el sureste y sigue lentamente en sentido paralelo a la costa, siendo interrumpido su progreso de vez en cuando por unos vórtices cerca de la costa. Algunos de estos vórtices son pequeños y transitorios, y otros son grandes y permanentes como él que casi siempre se encuentra frente a la costa entre 30° y 35° N. (Ver figura 3; Sverdrup, 1946; Sverdrup y Fleming, 1941). En esta región el agua es transportada al norte hasta Punta Concepción o aún más lejos, y en su lento movimiento su temperatura y salinidad son incrementadas por medio de la radiación solar y la evaporación, hasta que alcanzan valores mucho mayores que los de las aguas de alta mar (Ver figura 4 y 5). Otro vórtice, cuyo tamaño es de la mitad de éste, se encuentra en varias posiciones, dependiendo de la época en que se observe entre las islas Guadalupe y Cedros. Aunque no existe una explicación completa de estos vórtices, se cree que una razón primordial de su existencia es la geometría de la línea costera en que las puntas sobresalientes de Concepción y Eugenia desempeñan un papel importante.

El transporte total en los 1,500 metros superiores en una faja que se extiende hasta 700 kilómetros de la costa probablemente no excede de unos 10.000,000 metros cúbicos por segundo (Sverdrup *et. al,* 1946). Parte de esta agua continúa en su progreso al Sur, exhibiendo las mismas características de baja temperatura y salinidad en relación con el agua más alejada de la costa, hasta llegar casi al extremo de la península de Baja California. En este lugar, entre Punta Eugenia y Cabo San Lucas, el agua choca con el agua tibia y salina que tiene las mismas características, debajo de los 400 metros de profundidad, que el agua del Pacífico Ecuatorial, y se produce una gradiente fuerte de temperatura y salinidad. La dirección del flujo

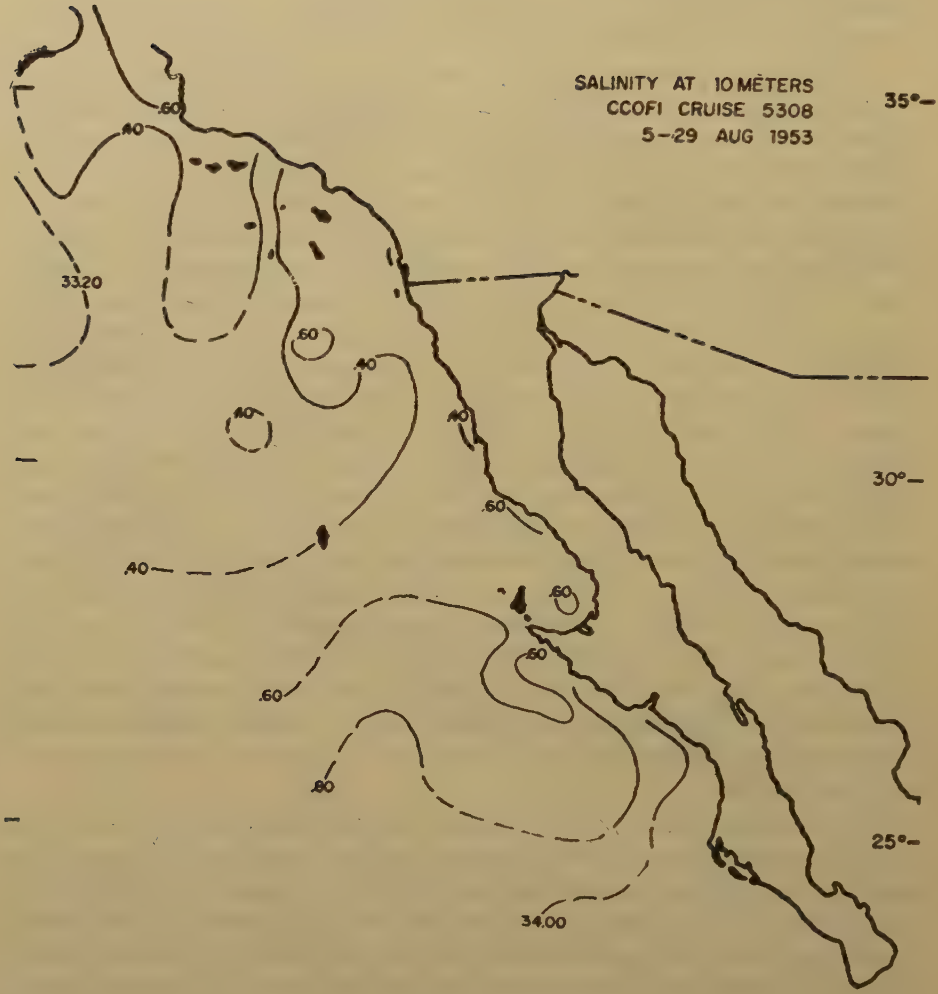
SALINITY AT 10 METERS
CCOFI CRUISE 5308
5-29 AUG 1953
35°
30°
25°
.60
.40
33.20
.60
.40
.40
.40
.60
.40
.60
.60
.60
.80
34.00

FIG. 4.—*Estudios Oceanográficos.*

(1004)

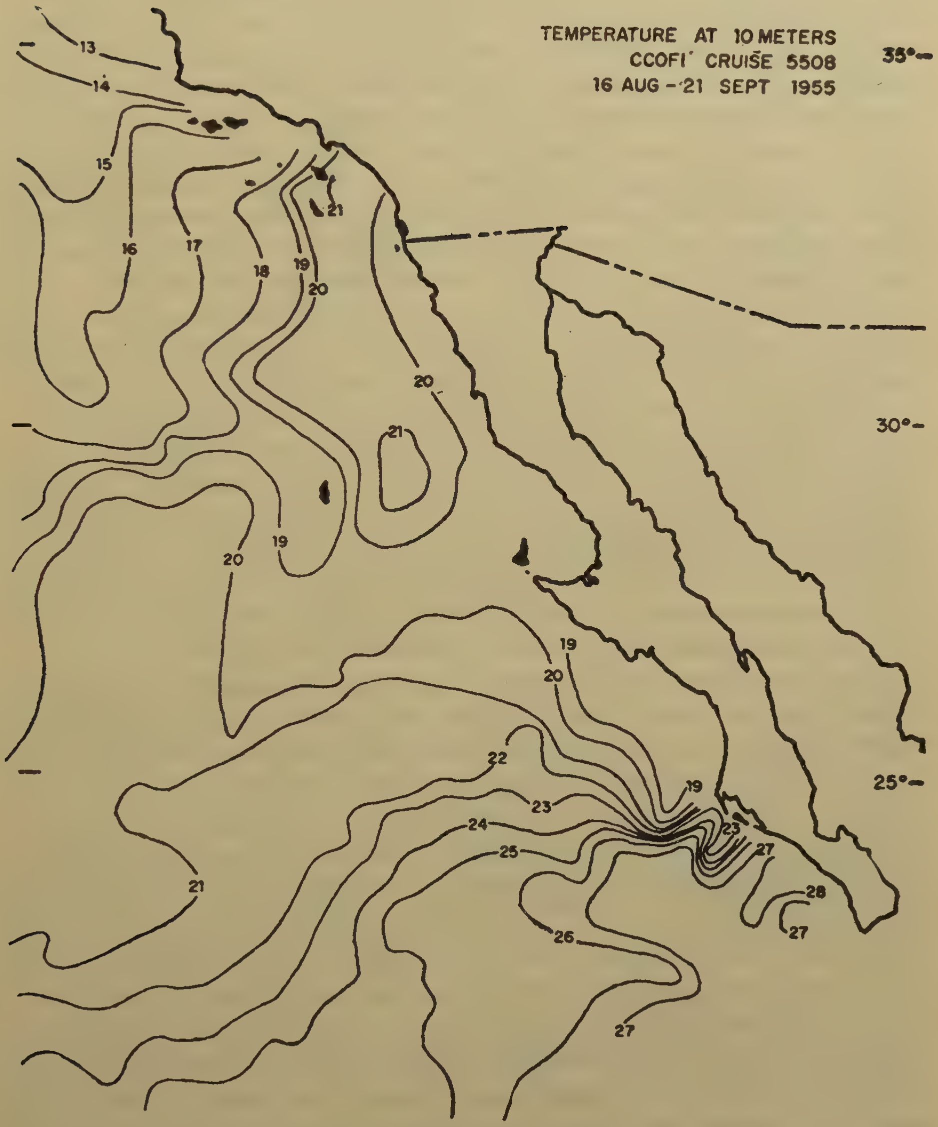
TEMPERATURE AT 10 METERS
CCOFI CRUISE 5508
16 AUG - 21 SEPT 1955
35°
30°
25°
13
14
15
16
17
18
19
20
21
20
21
19
20
21
19
20
22
23
24
25
19
23
27
28
27
26
27

Fig. 5.—*Estudios Oceanográficos.*

superficial en ambas masas de agua parece ser hacia el Sur, siendo más lenta la velocidad de la masa meridional de agua tibia.

El calentamiento del agua de la Corriente Californiana y la evaporación superficial a lo largo de su progreso al Sur, tienen el efecto de aumentar la salinidad en la capa superficial mezclada (entre la superficie y el "thermocline"). Inmediatamente debajo del "thermocline", a una profundidad de 60 a 100 metros, se encuentra una capa cuya salinidad es menor que la de las capas de arriba o de abajo, y puede considerarse como una de las características propias del agua de la Corriente Californiana, que la distingue de la que se encuentra inmediatamente al oeste y que también tiene una capa de salinidad mínima, pero que se encuentra a una profundidad mayor.

Se han hecho varias mediciones directas de la velocidad de las corrientes superficiales. Entre ellas se cuenta la campaña de CCOFI realizada en mayo de 1952, teniendo como objeto el de medir la corriente al Sur de Punta Eugenia. En esta ocasión, se suspendió una draga de corrientes debajo de un flotador, y se dejó libre para flotar a la deriva por cinco días, permaneciendo el barco junto a él para ir observando su posición. Este aparato fue lanzado al mar a unos 30 km., al oeste de la Bahía de Tortuga. Siguió una derrota directamente hacia el Sur, con una velocidad de medio nudo. Esto indicó que el agua inmediatamente al norte de la más tibia y salina de las cercanías del extremo de la península, se alejaba de la costa.

Otra característica prominente que tiene la costa de Baja California que mira al Océano Pacífico, es el afloramiento (Sverdrup, 1937) que ocurre en varias épocas del año, que consiste en el movimiento hacia la superficie de las aguas más profundas y, por lo tanto, más frías y ricas en sales nutritivas. Es un fenómeno de suma importancia en cuanto a la productividad fito-planctónica, puesto que ésta ocurre solamente si hay bastante concentración de sales nutritivas, y sólo también en las capas superiores iluminadas. Se ha observado el afloramiento por toda la costa occidental de Baja California, pero hay ciertos lugares y épocas del año en que es más probable que ocurra. Los sitios donde más frecuentemente se observa el afloramiento son las regiones inmediatamente al sur de Punta Concepción y al Sur de la Bahía de la Magdalena. Ambas regiones tienen su mayor actividad durante los primeros meses del año, aunque el afloramiento puede ocurrir también en otros meses. Asimismo, el afloramiento ocurre por el costado Sur de Punta Eugenia. A la altura de Cabo Colnett hay afloramiento frecuente, y el agua de baja temperatura

(1006)

y alta salinidad proveniente de este origen es llevada luego a las cercanías de la Bahía Sebastián Vizcaíno, o bien, adentro de la misma.

Se ha notado una variación considerable en la intensidad y cantidad del afloramiento. El año de 1955 se destacó entre todos, desde 1949 hasta ahora, por el afloramiento extremadamente intensivo que ocurrió a todo lo largo de la costa en Punta Eugenia, hasta el extremo Sur de la península. Fue tan intenso y perduró por tanto tiempo que la temperatura de las aguas superiores frente a esta costa disminuyó considerablemente, en ciertos lugares hasta cinco grados menos que los que suelen registrarse en años "normales". El descenso medio de la temperatura durante los primeros cinco meses de 1955, fue de uno y medio a dos grados en estas regiones. Esta situación perduró desde enero hasta junio de 1955, pero el segundo semestre del año 1955 se asemejaba más a los otros años. Enero de 1956 exhibió temperaturas normales y poco afloramiento, pero en febrero parece haberse reanudado este fenómeno de manera comparable con 1955.

Hay evidencias de una contracorriente sumergida en la costa de Baja California. Sverdrup sugiere ésto por razón de la analogía que existe entre esta región y la Corriente Peruana, e investigaciones ulteriores han sustentado esta hipótesis. Es difícil estimar la velocidad de esta corriente sumergida y su transporte total al norte, y no está claro en cuál sitio existe su límite norte.

3.—*La Biología.*—Primero, vamos a considerar la distribución de la vida fito-planctónica, o la vida vegetal del mar que constituyen los grandes números de plantas microscópicas, puesto que ella representa el primer eslabón en la cadena alimenticia entre las sales nutritivas y las formas superiores de vida, los peces, etc. La distribución, fluctuaciones estacionales y productividad de fito-plancton frente a la costa occidental de la Baja California nunca han sido investigadas detalladamente. Empero, se obtuvieron bastantes datos e información mediante los varios cruceros y expediciones de CCOFI para poder formarse una impresión general en cuanto al tamaño y productividad de la población fito-planctónica.

El área entre 20°N. y 30°N. al oeste de la Isla Guadalupe, es la región más pobre en fito-plancton conocida hasta la fecha. Los valores medios del contenido de clorofila "a" se aproxima a 0.1 mg. por metro cúbico, mientras que la productividad media de las aguas superficiales, medida por el método de Carbono-14 es de 0.35 mg. de carbono por metro cúbico por día. No se han realizado observaciones en esta área pelágica durante todas las estaciones del año, pero se cree que los valores dados arriba fluctúan muy poco.

Las aguas contiguas a la costa son distintas a las de la región de alta mar por su mayor riqueza y variabilidad, especialmente en las regiones de afloramiento donde se encuentran grandes concentraciones de fito-plancton (y donde se puede suponer que la productividad es alta), durante el tiempo en que las aguas profundas con sus sales nutritivas son elevadas a la zona iluminada. Cualesquiera fluctuaciones en la intensidad del afloramiento darán lugar a fluctuaciones posteriores en el fito-plancton. Esta región es rica aún cuando no ocurre el afloramiento. En junio de 1955, el contenido de clorofila "a" en cinco puntos cerca de la costa tenían el valor medio de 0.59 mg. por metro cúbico.

En la Bahía Sebastián Vizcaíno la fluctuación estacional en la población de fito-plancton ha sido estudiada. Se observaron florecimientos de diátomos en marzo de 1955, en cada una de las seis estaciones ocupadas, y también en octubre del mismo año, en la mayoría de las estaciones. El número de células de diátomos por litro excedía frecuentemente del 2×10^7 durante el máximo primaveral, y del 8×10^6 durante el florecimiento de octubre. Estos valores indican una población formidable de diátomos. "Naked Flagellates" fueron abundantes durante la mayor parte del año, siendo el valor típico de 9×10^6 células por litro.

Los dinoflagelados y coccolithophorales estuvieron en su apogeo a mediados del verano de 1955, pero nunca abundaron tanto como los diátomos.

En resumen, en las aguas contiguas a la costa occidental de la Baja California, hay una población rica y algo variable de fito-plancton, y en las aguas más alejadas de la costa se encuentra una región estéril.

La vida zooplanctónica, compuesta en su mayor parte por animales microscópicos, es la que se alimenta directa o indirectamente del fito-plancton, y puede considerarse como el segundo eslabón de la cadena alimenticia. Se han realizado varios estudios sobre algunas especies del zooplancton, pero no vamos a discutir los resultados aquí. En general, se puede suponer que las regiones ricas en fito-plancton lo son también en zooplancton, pero tratándose de problemas transitorios hay que tener presente que la población de fito-plancton debe estar presente en el agua antes de que pueda crecer una de zooplancton, lo que ocasionaría una demora en el ciclo del crecimiento del zooplancton relativo al de fito-plancton.

En cuanto a los peces de importancia económica, el United States Fish and Wildlife Service ha obtenido considerable información sobre la distribución y la abundancia de sus huevos y larvas. Se ha averiguado que la sardina *(Sardinops caerulea)* tiene dos áreas principales de desove, una de ellas en las cercanías de la Bahía Sebastián Vizcaíno y la otra frente a la costa en las cercanías de la línea divisoria entre Baja California y Alta California (Ahltrom, 1954b). Parece haber intercambio de peces individuales entre estas dos áreas. Esto es sustentado por el hecho de que durante los años de 1952 y 1953, la mayor parte de la población de sardina (95% o más) se encontraba en al región Sur de desove, pero en 1954 y 1955 hubo un desplazamiento notable hacia el norte, con este resultado: de un tercio a la mitad del desove ocurrió en la región norte en las últimas dos temporadas (ver figura 6). Es probable que este cambio haya resultado de la baja temperatura en las estaciones de invierno y primavera que se registró en los últimos dos años en las aguas frente a la costa Sur de la Alta California respecto a los años anteriores. La mayor parte del desove de la sardina ocurre durante los meses de febrero hasta junio, pero también ocurre durante todo el año, si bien en menor grado, en la región de la Bahía Sebastián Vizcaíno. Durante la temporada normal el desove ocurre a temperaturas entre 13.5° y 17.0°. El desove que ocurre fuera de la temporada normal en la Bahía Sebastián Vizcaíno tiene lugar a temperaturas considerablemente mayores, 17° a 22°, y puede representar el desove de una población separada.

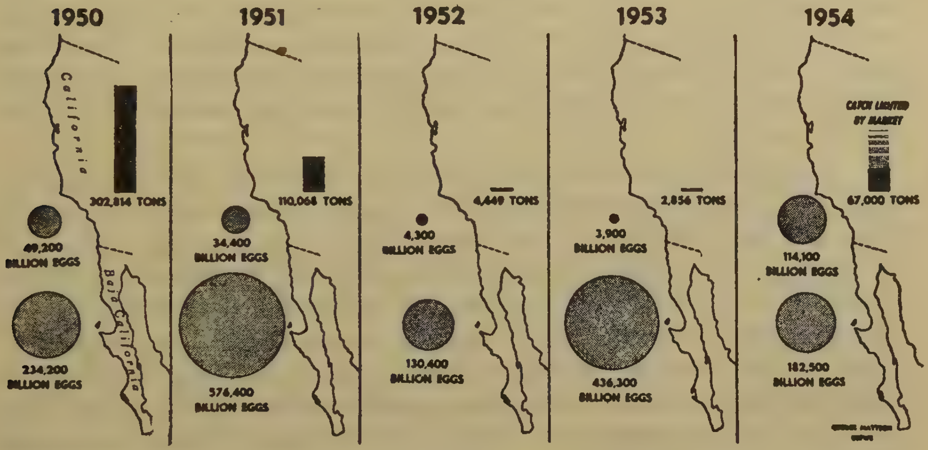
1950
1951
1952
1953
1954
California
Baja California
302,814 TONS
49,200 BILLION EGGS
234,200 BILLION EGGS
110,068 TONS
34,400 BILLION EGGS
576,400 BILLION EGGS
4,449 TONS
4,300 BILLION EGGS
130,400 BILLION EGGS
2,856 TONS
3,900 BILLION EGGS
436,300 BILLION EGGS
CATCH LIMITED BY MARKET
67,000 TONS
114,100 BILLION EGGS
182,500 BILLION EGGS

FIG. 6.—*Estudios Oceanográficos.*

El personal del U. S. Fish and Wildlife Service ha ido muestreando la pesca comercial de la sardina a través de algún tiempo en el puerto de Ensenada, gracias a la grata cooperación de la industria empacadora de pescado de esa población. Asímismo, se obtiene información importante sobre la composición por edades y tallas de la población de sardina en las aguas de Baja California y Alta California. Se publican anualmente los resultados de estos estudios (Felin *et al*, 1953, 1954). La gran cooperación y cortesía otorgadas a los científicos norteamericanos posibilitando los estudios de este género son sumamente agradecidas.

Se ha obtenido información sobre otras muchas especies de peces que tienen huevos y larvas pelágicos. La anchoa *(Engraulis mordax)*, que está distribuída extensamente desde Columbia Británica al Golfo de California, desova intensivamente a partir de Punta Concepción hacia el Sur (Ahlstrom, 1954a). Se ha notado un marcado aumento en la población de la anchoa durante el tiempo a través del cual se han ido realizando las rutinarias investigaciones oceanográficas-biológicas, y la población parece estar actualmente en buenas condiciones.

La caballa (*Trachurus symmetricus*) desova en las regiones pelágicas. La mayor abundancia de los huevos y larvas de este pescado se encuentran de 80 a 400 kilómetros a partir de la costa, y su centro de distribución se halla frente a la costa Sur de la Alta Califronia y a la costa Norte de la Baja California (Ahlstrom y Ball, 1954). También la merluza *(Merluccius productus)* desova en las regiones pelágicas y tiene una distribución extensiva y considerable abundancia. La temporada de desove en ambas especies es restringida. Las larvas de la merluza se capturan en abundancia solamente durante un período de tres meses, de febrero a abril, mientras que las de la caballa son capturadas durante los meses de marzo a julio (Ahlstrom y Counts, 1955). Por el contrario, los huevos y larvas de la anchoa son capturados durante todo el año, pero el desove de la anchoa tiene su apogeo durante los meses primaverales.

4.—BAHÍA SEBASTIÁN VIZCAÍNO

Esta región ha sido estudiada intensamente por su importancia respecto a la sardina. Es uno de los pocos lugares donde el desove de estos peces ocurre durante todo el año. Es posible que muchas de las sardinas pescadas y consumidas en los Estados Unidos hayan provenido de desoves frente a la costa de la Baja California en esta Bahía Sebastián Vizcaíno.

Se efectuaron viajes especiales a esta región en agosto y septiembre de 1952, y en septiembre de 1953, para estudiar la distribución de las varias propiedades del agua, concentración de huevos y larvas de sardina, otro plancton, y para estudiar la circulación de la bahía. Mediciones con el GEK ((geomagnetic electrokinetograph") y estudios con botellas flotantes fueron efectuados a fin de determinar las corrientes. Los resultados de algunos de estos estudios se muestran en las Figuras 7 y 8. La descripción de las aguas de la Bahía Sebastián Vizcaíno dada a continuación, está basada en los viajes rutinarios de CCOFI y también en los tres viajes especiales ya mencionados.

Parece que las aguas encontradas en la superficie de la bahía tienen por lo menos seis orígenes distintos. Debajo de la capa superficial se encuentra una capa gruesa cuya temperatura es casi uniforme, y cuya salinidad aumenta rápidamente con la profundidad. El agua de la Corriente Californiana entra en la bahía periódicamente formando manchas de agua de baja temperatura y salinidad. Esto puede ocurrir con rapidez, bajando la salinidad de toda la bahía por medio de la mezcla a través de un plazo tan corto como un mes. El agua proveniente del afloramiento se encuentra frecuentemente a la altura de Punta Canoas y de Punta Eugenia y es la más fría de la bahía. La región de Punta Canoas es la más importante, puesto que el agua proveniente del afloramiento que se origina allí es inmediatamente disponible a la bahía. Este afloramiento en las cercanías de Punta Canoas puede tender a estorbar la entrada del agua oceánica en la bahía. El agua de este origen es fría y salina y tiene efectos importantes en la bahía, especialmente el de bajar la temperatura durante los meses de verano.

El agua de la bahía se mantiene circulando, casi permanentemente, en la forma de un gran circuito que da vueltas en el sentido de las manecillas de un reloj, el centro del cual se encuentra al este de la Isla Cedro. Esta circulación se extiende a una profundidad de aproximadamente 60 metros, y tiene de 50 a 65 km. de diametro. Este es le origen del "agua central". Un brusco "thermocline" sube a la superficie, se reconoce como un "front". El agua central del circuito tiene la temperatura relativamente alta, pero su salinidad varía considerablemente durante el año. El agua de las lagunas costaneras influye en la inmediatamente contigua a la costa en la región sureste de la bahía, y puede ser el origen del agua que se encuentra en las capas inferiores del centro de la bahía. El agua superficial oceánica, encontrándose fuera de la bahía, al suroeste, es generalmente tibia y

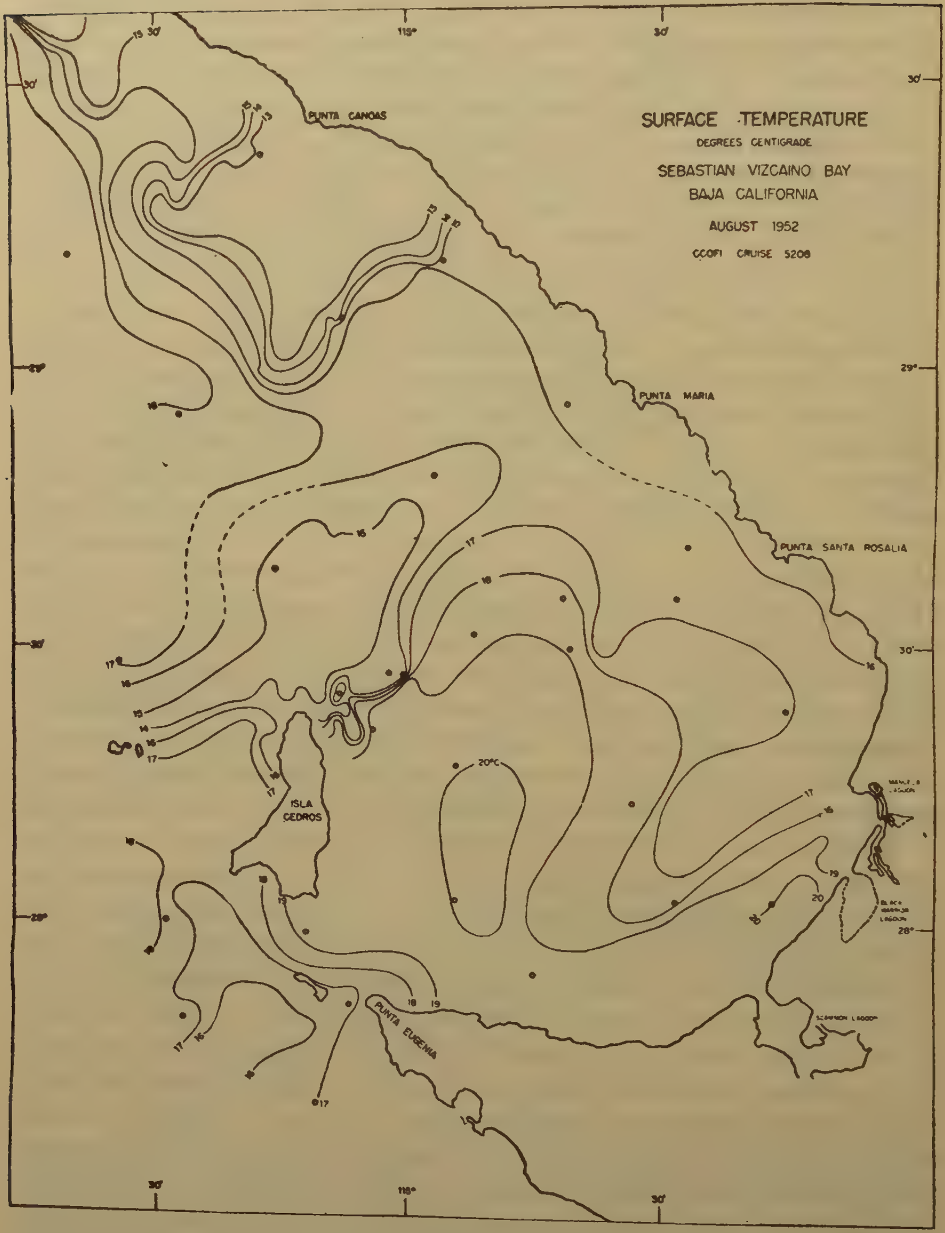
SURFACE TEMPERATURE
DEGREES CENTIGRADE
SEBASTIAN VIZCAINO BAY
BAJA CALIFORNIA
AUGUST 1952
CCOFI CRUISE 5208
PUNTA CANOAS
PUNTA MARIA
PUNTA SANTA ROSALIA
ISLA CEDROS
PUNTA EUGENIA
SCAMMON LAGOON
20°C
115°
30'
29°
28°

Fig. 7.—*Estudios Oceanográficos.*

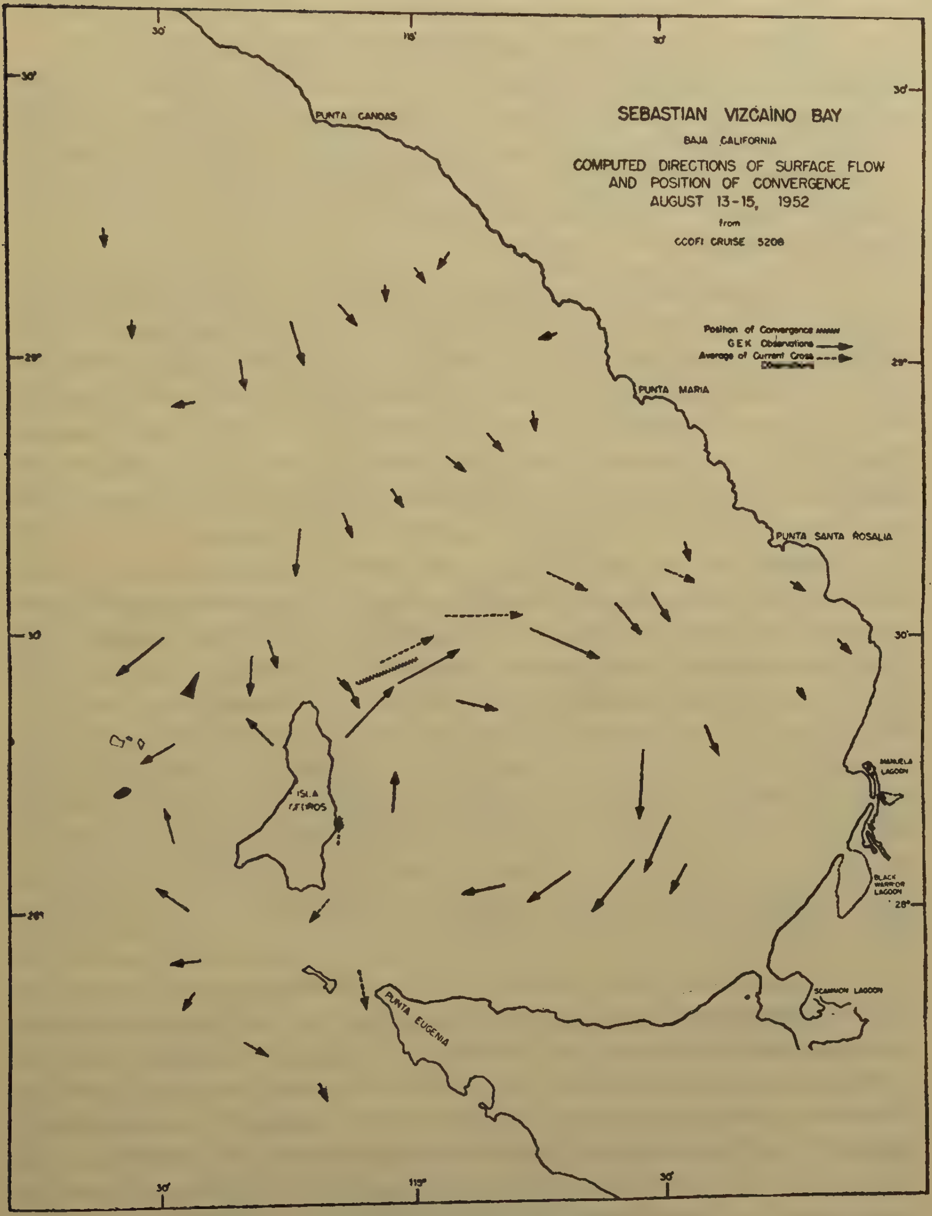
SEBASTIAN VIZCAINO BAY
BAJA CALIFORNIA
COMPUTED DIRECTIONS OF SURFACE FLOW
AND POSITION OF CONVERGENCE
AUGUST 13-15, 1952
from
CCOFI CRUISE 5208
Position of Convergence
GEK Observations
Average of Current Cross
[redacted]
PUNTA CANOAS
PUNTA MARIA
PUNTA SANTA ROSALIA
MANUELA LAGOON
BLACK WARRIOR LAGOON
SCAMMON LAGOON
ISLA CEDROS
PUNTA EUGENIA
30'
115°
30'
30'
29°
30'
28°

FIG. 8.—*Estudios Oceanográficos.*

salina, y hay evidencia de que esta agua entra en la bahía después que termina el afloramiento en el otoño.

Durante el viaje de agosto de 1952, el afloramiento estaba ocurriendo en las regiones de Punta Canoas y Punta Eugenia. El agua de baja salinidad de la Corriente Californiana se encontraba a la entrada de la bahía, y la del centro de la bahía tenía las propiedades características del "agua central". Como consecuencia, existía un marcado "front" al noroeste de la Isla Cedros, y el agua de la bahía estaba más fría que la oceánica.

En el siguiente mes (septiembre de 1952), el afloramiento había cesado en ambas regiones, dando lugar a un notable calentamiento de la bahía. El agua de baja salinidad de la Corriente Californiana había invadido la mayor parte de la bahía, disminuyendo así la salinidad. El circuito central se había desplazado al norte, y sus aguas superficiales se habían extendido eliminando casi los "front" superficiales. En general, toda el agua de la bahía se encontraba más homogénea.

Durante el viaje de septiembre de 1953, se encontró que el estado de la bahía era notablemente semejante al del viaje de septiembre del año anterior, pero sobresalían tres importantes diferencias, a saber: (1) El circuito central se encontraba desplazado a la región suroeste de la bahía, (2) el agua oceánica de alta salinidad parecía entrar en la bahía al norte de la Isla Cedros, y (3) el agua de alta temperatura y salinidad de las lagunas costaneras se evidenciaba con más claridad a lo largo de las costas sur y sureste. El agua de la bahía ya se había diluído con el agua de la Corriente Californiana para entonces, de modo que este viaje nos ilustra la manera en que la temperatura y salinidad son incrementadas durante los meses de otoño, si falta el afloramiento.

La superficie de la bahía sufre un incremento de temperatura de 5 a 7 grados en las regiones de afloramiento a fines de verano, y un descenso de salinidad en la misma época. La salinidad vuelve a aumentar en el otoño antes de que descienda la temperatura. Este descenso comienza durante los meses de noviembre y diciembre y continúa hasta fines de la primavera o principios del verano, cuando se registran las temperaturas más bajas. Los resultados de los viajes de agosto y septiembre nos han dado alguna idea de cómo ocurre esta variación, y cómo está intercalada con el movimiento y disponibilidad de las varias masas de agua.

5.—EL GOLFO DE CALIFORNIA

Se llevaron a cabo dos cruceros al Golfo de California, el primero en 1939 y el segundo en 1940, para investigar la hidrografía, batimetría, sedimentos, la biología y la química de la región (Anderson, 1950; Durhan, 1950; Gilbert y Allen, 1943; Natland, 1950; Revelle, 1950; Shepard, 1950; Sverdrup, 1939, 1940b, 1940c). La figura 9 muestra una carta batimétrica de las aguas de ambos lados de la península de Baja California, la cual es una versión modificada de una preparada por el doctor F. P. Shepard basada primordialmente en los sondeos hechos durante esos dos cruceros. Este año (1956) se efectuó un viaje a la región en el mes de febrero, y se proyecta otro que habrá de llevarse a cabo en abril. La discusión que se da a continuación se basa en su mayor parte en los resultados de los cruceros mencionados.

Primero, consideremos el ambiente en que está situado el golfo. Este parece ser de una complicada estructura, que se caracteriza por una serie de cuencas producidas por una falla (ver figura 9). Algunas de estas cuencas alcanzan una profundidad mayor de 3,500 metros. Hay la falta casi completa del zócalo continental, excepto en el norte en las cercanías del delta (ahora inactivo) del Río Colorado, donde hay una vasta área de agua con profundidad menor de 200 metros. Al oeste, la sierra de Baja California se eleva bruscamente de la costa excepto en la región de la cabecera del golfo, donde la sierra se encuentra más tierra adentro. Por la costa oriental hay una faja de llanuras de 40 a 80 kilómetros de ancho que separa la sierra de la costa. Osorio-Tafall (1943) da una descripción más detallada sobre la fisiografía del golfo.

Se encuentran numerosos esteros y lagunas costaneras a lo largo de la costa oriental del golfo. Las lagunas que están situadas en la región norte reciben muy poca agua dulce proveniente de la precipitación sobre el continente. Su desarrollo está relacionado con las mareas, cuya amplitud es grande en esta región. Más al sur, desde Guaymas a Mazatlán, hay una serie continua de estas lagunas costaneras que reciben grandes cantidades de agua dulce proveniente de las lluvias de esta región.

El golfo mismo está situado en una región árida en donde la evaporación excede al efecto conjunto de la precipitación y del aporte de los ríos. El clima árido se debe a dos factores: el carácter general de la circulación atmosférica alrededor del centro de baja presión sobre México, y la sierra alta y continua de la península de Baja

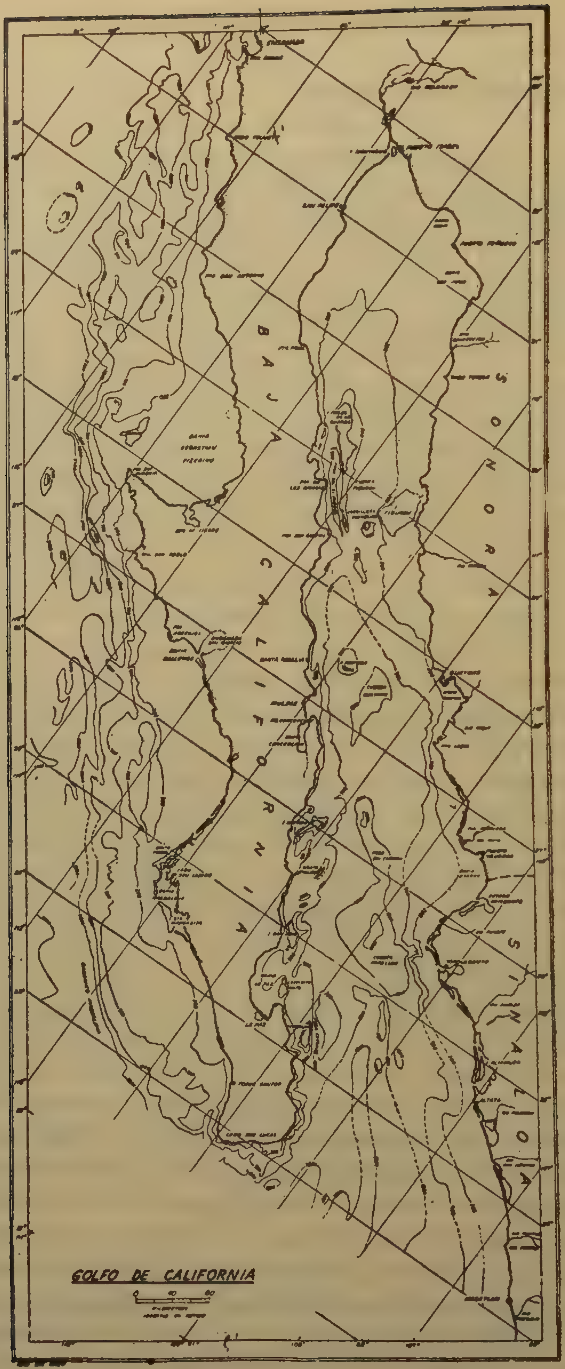
BAJA CALIFORNIA
SONORA
SINALOA
GOLFO DE CALIFORNIA
0 40 80

FIG. 9.—*Estudios Oceanográficos.*

California, la cual previene que el Océano Pacífico ejerza su influencia sobre la región. Por lo tanto, se puede decir que la mayor parte del golfo es controlada por un clima de tipo continental.

Durante el invierno y la primavera, cuando la baja presión se encuentra el este o al sureste, los vientos extremadamente secos del desierto soplan del norte. En el verano, la baja presión está situada sobre la región norte de Sonora y, por consiguiente, masas de aire húmedo que se han originado sobre el océano son introducidas en el golfo. El principio de la temporada de las lluvias coincide con la posición más norte de la baja presión. La precipitación es muy escasa en la parte norte del golfo y algo mayor en el sur. Como consecuencia de la rápida evaporación y la escasa precipitación y contribuciones de los ríos, casi tres metros de agua se pierden anualmente en la atmósfera. Esta pérdida de agua hace incrementar la salinidad del golfo y, por lo tanto, estimular la advección de agua del océano contiguo.

La salinidad cerca de la costa, pero lejos de las bahías y lagunas de poca profundidad varía entre 35.0 partes por mil en la entrada y 35.5 partes por mil en el norte (en marzo). La salinidad en las bahías y lagunas puede exceder este valor, y en algunos sitios la evaporación es tan intensa que la sal se precipita dejando extensivas salinas.

La penetración de agua del Océano Pacífico en el golfo ocurre a profundidades medianas, o sea de 500 a 800 metros. Esta agua oceánica se caracteriza por un mínimo de salinidad (34.5 34.6 partes por mil) y una temperatura de 6 a 8 grados. Después de entrar en el golfo, sigue hacia el norte hasta llegar a la latitud de 29° N., donde encuentra una cordillera submarina o dintel (ver figura 9) situado transversalmente en el golfo entre las Islas Angel de la Guarda y Tiburón. Este dintel se encuentra a 200 metros debajo de la superficie y tiene gran importancia porque impide el intercambio del agua entre las cuencas norte y sur debajo de esta profundidad. La masa de agua que se encuentra al sur de este dintel tiene caracteres muy distintos al agua del norte, siendo solamente una continuación del agua oceánica un poco modificada por la evaporación que incrementa su salinidad. En cambio, el agua que se encuentra al norte del dintel de Tiburón es de origen puramente local, habiéndose formado por medio de la evaporación y el enfriamiento superficiales y el hundimiento posterior. Esto es ampliamente comprobado por la alta temperatura y el alto contenido de oxígeno que muestran las capas inferiores del agua. No existe una temperatura menor de 11° en ninguna parte al norte del dintel de Tiburón.

Durante el invierno y la primavera predominan los vientos fuertes del norte que impulsan el agua hacia afuera del golfo. Esta pérdida de agua en el océano, debida a los vientos, es diez veces mayor que la debida a la evaporación en estas estaciones. Para compensar la pérdida, se requiere una efusión al golfo en las capas inferiores de 350,000 metros cúbicos por segundo. En el verano, cuando predominan los vientos del sur, el golfo tiene poca influencia sobre las aguas del océano.

En el lugar donde el agua del golfo choca con la de la corriente californiana o con las aguas norecuatoriales, las propiedades del agua varían bruscamente de una posición a otra, dando lugar a lo que podemos llamar un "front". En la región del golfo, es conocida la existencia de dos "fronts'. El más prominente de éstos se encuentra en las cercanías de Cabo San Lucas, y se llama "San Lucas Front". Representa la frontera entre el agua de alta salinidad y alta temperatura del golfo y el agua de baja salinidad y baja temperatura de la corriente californiana. El otro suele encontrarse a la altura de Cabo Corrientes y consiste en un cambio brusco de salinidad entre el agua del golfo y la norecuatorial. Además, existe un 'front" entre las corrientes californiana y norecuatorial. Así pues, las cercanías de la entrada al golfo representan una región de transición entre tres masas distintas de agua.

Ahora, consideremos la distribución de las diversas propiedades del agua en el golfo, y la manera en que el viento y la topografía submarina influyen en esta distribución. Entre las propiedades de interés se cuentan la temperatura, salinidad, contenido de oxígeno, fosfatos y silicatos, puesto que todas son de suma importancia en el estudio de la productividad del golfo. Los factores que influyen en la distribución de estas propiedades son múltiples y complejos. La actividad biológica tiene influencia sobre la distribución de oxígeno y sales nutritivas; el exceso de evaporación determina la salinidad; y la absorción de calor determina la temperatura. También tienen que tomarse en cuenta los efectos modificadores de los vientes y corrientes que transportan las aguas superficiales de un sitio a otro. La mezcla de agua debida a las mareas se tiene que tomar en cuenta en la región de la cabecera del golfo, y cerca de la línea costanera. Por lo tanto, no puede esperarse que la distribución de propiedades se atenga a una regla sencilla. De todas maneras, puede ser posible pronosticar con cierto grado de precisión el estado general que existe en cualquier región del golfo, en cualquier estación del año, utilizando las observaciones del viento (fuerza y dirección). temperaturas del aire y del agua, humedad, etc.

Conociendo la distribución de temperatura y salinidad, se puede calcular la *estabilidad,* que tiene gran importancia sobre la fecundidad de cualquier región que se considere. Si la estabilidad es alta, como lo es en verano y otoño en el golfo debido a la alta temperatura del agua superficial, las sales nutritivas de las capas superiores del mar se agotan porque no pueden ser renovadas desde profundidades mayores. Como consecuencia de esto, la productividad es baja durante estas estaciones, y el agua tiene el aspecto azul y transparente.

En otoño, el enfriamiento de las capas superficiales y la fuerza del viento han aumentado a tal punto que acaban con el "thermocline" (rápido descenso de temperatura con la profundidad), permitiendo que las sales nutritivas del agua de las capas inferiores asciendan a enriquecer el agua superficial por medio de la mezcla. De esta manera, las aguas superiores del golfo permanecen enriquecidas durante el invierno, dando lugar a un "florecimiento" de fito-plancton tan pronto llegan las más intensivas radiaciones y calentamientos solares de primavera. Así, las estaciones de invierno y primavera son las más productivas en el golfo. El "florecimiento" puede llegar a tal intensidad que el agua se decolora.

El afloramiento es otro proceso por medio del cual las sales nutritivas pueden ser acarreadas de las profundidades a la superficie. Las regiones de afloramiento pueden pronosticarse por las direcciones del viento y de la línea costanera. El afloramiento ha de esperarse a sotavento de las prominencias de tierra, y a menor grado frente a la costa si la tierra se encuentra al lado izquierdo de la dirección del viento (en el hemisferio norte). En el caso de un viento del norte en el golfo, es probable que el afloramínto ocurra al sur de la Isla Tiburón, en la Bahía de Guaymas, en Bahía Yavaros, y en la Bahía de Topolobampo. El agua que proviene del afloramiento puede reconocerse por su salinidad y temperatura menores en comparación con el agua superficial. Con vientos del sur, la costa oriental de Baja California es región de afloramiento, pero, por el hecho de que predominan los vientos del norte en el golfo, la costa de Sonora y Sinaloa es generalmente la más fecunda.

Las corrientes superficiales las podemos estimar por la fuerza del viento. La velocidad media del viento en el golfo es baja y, por lo tanto, las corrientes no debidas a las mareas son generalmente débiles, de 5 a 20 centímetros por segundo. El espesor de la capa superficial mezclada por el viento varía entre 40 y 80 metros solamente, pero a veces hay ventarrones que mezclan el agua hasta 200 metros de profundidad. En muchos sitios, la mezcla producida por las mareas es de mayor importancia que la producida por el viento, especialmente en los estrechos angostos, donde se han observado corrientes de la marea con velocidad hasta de siete nudos.

El contenido de oxígeno en función de profundidad exhibe un mínimo entre 300 y 500 metros, y el contenido de fosfatos un máximo entre 500 y 800 metros. En ambos casos, la profundidad del mínimo o máximo aumenta hacia el interior del golfo. El contenido de silicatos en función de profundidad no exibe ningún máximo ni mínimo, y su concentración puede ser casi constante en los 50 y 100 mts. superiores. El contenido de sales nutritivas utilizadas por las plantas microscópicas aumenta hacia el interior del golfo en la capa superior; pero debajo de 400 metros este incremento no es tan marcado. La más alta concentración de fosfatos varía entre 0.9 y 1.1 ug-at/L, mientras la más alta concentración de silicatos es de 160 ug-at/L, ocurriendo contigua al fondo sobre los sedimentos silíceos. En cuanto al contenido de oxígeno, valores menores que el correspondiente a la saturación son generalmente encontrados durante las estaciones calurosas y especialmente en la parte sur del golfo. Valores mayores de saturación (hasta 50%) ocurren frecuentemente durante la primavera, al norte del dintel de Tiburón, cuando la producción de fito-plancton es alta.

A veces se obverva una diferencia notable entre las aguas orientales y occidentales del golfo. Los que hayan volado sobre el golfo habrán notado frecuentemente una transición brusca entre el agua verde y azul. Como regla general, el agua verde es rica en plancton, y la azul tiene muy poco o nada. El afloramiento a lo largo de las costas puede dar lugar al aspecto distinto del agua de los dos lados del golfo.

Muchas de las conclusiones expresadas aquí son basadas en pocos datos obtenidos hace más de quince años por medio de métodos antiguos, y muchos de los valores citados tendrán que ser modificados al efectuarse más estudios sobre la región. Se espera que, en el futuro, un mayor esfuerzo se dirija hacia la investigación de los muchos aspectos interesantes del Golfo de California, beneficiando así a toda la República Mexicana.

6.—ESTUDIOS ESPECIALES.

Estudios sobre bahías y lagunas costaneras.—Se han llevado a cabo investigaciones sobre los sedimentos y las relaciones con su ambiente físico-químico en varias bahías y lagunas. En el año 1952, en el curso de ocho viajes a la región, 250 muestras de sedimentos fueron colectadas en la Bahía Todos Santos y regiones contiguas, y 33 en el Estero de Punta Banda. Los foraminíferos bentónicos vivos y muertos fueron analizados para determinar las relaciones que existen entre ellos y el agua que se encuentra encima (Walton, 1955).

La laguna San Miguel (a la altura del kilómetro 62 de la carretera Tijuana-Ensenada) fue escogida como ejemplo típico de varias de tales lagunas costaneras, y fué objeto de un estudio intensivo (Stewart, 1956). Muestras del sedimento del fondo fueron estudiadas en cuanto al tamaño de los granos, contenido de material orgánico, carbonato cálcico, organismos microscópicos, y las variaciones de estas propiedades en relación con las de su ambiente acuático en la laguna. Se emprendió este estudio para establecer bases para el reconocimiento de sedimentos antiguos depositados bajo las mismas condiciones que se encuentran en el record geológico. Otros estudios semejantes fueron conducidos en las lagunas Ojo de Liebre (Scammon) y Manuela.

Las lagunas costaneras en el lado oriental de la península han sido estudiadas muy poco. Se han hecho reconocimientos aéreos de estas lagunas, y muestras de los sedimentos de algunas de ellas han sido estudiadas.

Estudio de faunas antiguas y contemporáneas, y su relación con el ambiente.—La división de Marine Vertebrates de la Scripps Institution ha hecho varias investigaciones en la Baja California desde el año 1945. Estas investigaciones han abarcado la península entera con sus islas y aguas vecinas, pero han sido más intensivas a lo largo de la costa occidental, desde la frontera con Estados Unidos hasta la laguna San Ignacio.

Al principio, el estudio costero abarcó la distribución de los peces y otras formas de la vida marina. De pronto se observó que los peces que vivían en el agua fría característica de la costa central de la Alta California también habitaban la costa noroeste de la península. Esta observación condujo a un estudio, que actualmente está siendo continuado, sobre la temperatura del mar contiguo a la costa (Hubbs, 1948). En general, el agua costanera de la región noroeste de Baja California es más fría que la de la costa sur de Alta California, un hecho ampliamente atestiguado por el carácter de la fauna y flora marinas. Al costado sur de las puntas y prominencias, donde la línea costanera sigue la dirección noroeste-sureste, los vientos predominantes producen el afloramiento que ocasiona el enfriamiento (y el enriquecimiento) de las aguas superficiales. Al costado norte de estas puntas y en las inmediaciones de la costa, las aguas superficiales se estancan y se ponen tibias. En ciertos lugares, la diferencia de temperatura de un lado a otro de una punta es sumamente grande. Por ejemplo, la diferencia de temperatura entre los dos lados de Punta Banda, separados por una distancia solamente de tres kilómetros, ha llegado a ser de 12° C.

Durante el estudio y las observaciones sobre la temperatura, se hizo el descubrimiento de que los montones de desperdicios (middens) dejados por los aborígenes contenían restos de una especie norteña de almeja que ya no existe en Baja California. Este hecho sugiere que en el pasado había un clima más frío. Se emprendió una investigación para determinar las temperaturas habidas durante las épocas pasadas, por medio de un análisis de isotopos. Como resultado de este estudio se ha averiguado que existió un período caluroso hace 300 años, uno frío hace de 600 a 1,100 años y otros calurosos hace 2,500 y 4,000 años. Se van acumulando datos de otras épocas, algunas aún más antiguas.

La distribución de los peces está siendo estudiada a lo largo de toda la costa occidental de la Baja California y de sus islas vecinas. Las distinciones entre los peces de la Isla Guadalupe, que es la más lejana de la tierra, y de las demás regiones, se estudian con particular interés. Los peces de esta isla han estado aislados durante tanto tiempo que muestran marcadas diferencias en comparación con los peces de la península. El doctor Carl Hubbs, de la Scripps Institution, fue el primero en hacer este descubrimiento durante el crucero del yate "Zaca", de Errol Flynn, en 1946.

A partir del año 1947 han sido efectuadas repetidas investigaciones sobre la ballena gris (*Eschrichtius glaucus*). El incremento espectacular en el tamaño de este cetáceo ha sido observado con gran interés, y sus hábitos migratorios y reproductivos han sido estudiados, especialmente dentro de las grandes lagunas costaneras donde estas ballenas entran durante la época de cría. Escenas de las hembras con sus ballenatos, filmadas en la laguna San Ignacio, están incluídas en la película "Cruise of the Zaca". Gilmore (1955) da una discusión y fotografías de las ballenas dentro de la laguna Ojo de Liebre (Seammon).

También se han hecho investigaciones sobre el gran aumento en la población del elefante marino (*Mirounga angustirostris*), en las islas frente a la costa occidental de Baja California (Bartholomew, 1952). Este incremento lo posibilitaron las leyes protectoras que restringen la caza. En el año 1954, el doctor Hubbs redescubrió la foca

Fina de Guadalupe (*Arcto cephalus Townsendi*), que en un tiempo fue de importancia económica y que se creía extinta. Se está estudiando el pequeño núcleo existente, y gestiones internacionales están siendo llevadas a cabo con la esperanza de asegurar la protección adecuada para que esta especie aumente en número. Lograr un incremento suficiente de la población de esta especie y de los otros mamíferos marinos, puede conducir a la restauración de un recurso de gran valor.

Se han realizado investigaciones sobre la hidrografía y fauna, presentes y pasadas, de la región del delta del Río Colorado. Se ha verificado la existencia de una gran laguna antigua en la cuenca de la Laguna Salada (Hubbs y Miller, 1948). Se ha dado atención a otros muchos aspectos de la historia fisiográfica, y a las faunas presentes y pasadas de la Baja California, que es una de las más prometedoras de todas las regiones para las investigaciones científicas.

RECONOCIMIENTO.

Varios investigadores contribuyeron a este informe con los resultados de sus estudios en la región de Baja California, y en general puede decirse que los autores sólo desempeñamos el papel de redactores, al recopilar estos diversos trabajos. Expresamos nuestro agradecimiento al doctor Elbert Ahlstrom del U.S. Fish and Wildlife Service, por el material sobre los peces de las aguas oceánicas; al señor Robert Holmes, por el material sobre el fito-plancton; el doctor Carl Hubbs, por el material sobre las faunas antiguas y contemporáneas y la relación con su ambiente; al doctor Fred Phleger, por el material sobre la geografía de la región del Golfo de California; al señor Gunnar Roden, por el material sobre las aguas del Golfo de California; al señor Harris Stewart, por el material sobre las lagunas costaneras; y al señor Jhon Wyllie, por el material sobre la Bahía Sebastián Vizcaíno. Además, le debemos las gracias a la señorita Augusta Barandiarán, de la Comisión Interamericana del Atún Tropical, por su valiosa ayuda en la preparación de este manuscrito.

BIBLIOGRAFIA

Ahlstrom, Elbert H.—Pilchard eggs and larvae and other fish larvae, Pacific
1952 Coast, 1950. U.S. Fish and Wildl. Serv., Spec. Sci. Rept.: Fisheries, No. 80, pp 1-58.

Ahlstrom, Elbert H.—Pilchard eggs and larvae and other fish larvae, Pacific
1953 Coast, 1951. U.S. Fish and Wildl. Serv., Spec. Sci. Rept.: Fisheries, No. 102, pp. 1-55.

Ahlstrom, Elbert H.—Pacific sardine (Pilchard). Eggs and larvae and other
1954a fish larvae. Pacific Coast, 1952. U.S. Fish and Wildl. Serv., Spec. Sci. Rept.: Fisheries, No. 123, pp. 1-76.

Ahlstrom, Elbert H.—Distribution and abundance of eggs and larval popula-
1954b tions of the Pacific Sardine. U.S. Fish and Wildl. Serv., Fish. Bull., 56(93), pp. 84-140.

Ahlstrom, Elbert H., and others.—The sardine in its environment. A popular
1950 account of the Objectives of the Pacific Coast Sardine Research Program. Pan-American Fisherman, Dec. 1950, pp. 15.

Ahlstrom, Elbert H., and *Orville P. Ball.*—A description of the eggs and larvae
1954 of the jack mackerel (*Trachurus symmetricus*), and a discussion of the distribution and abundance of jack mackerel larvae off western North America during 1950 and 1951 U.S. Fish and Wildl. Serv., Fish. Bull 56 (97), pp. 209-245.

Ahlstrom, E. H., and *R. C. Counts.*—Eggs and larvae of the Pacific hake *Mer-*
1955 *luccius productus.* U.S. Fish and Wildl. Serv., Fish Bull. 56(99), pp. 295-329.

Ahlstrom, E. H., and *D. Kramer.*—Pacific sardine (pilchard) eggs and larvae
1955 and other fish larvae, Pacific Coast, 1953. U.S. Fish and Wildl. Serv., Spec. Sci. Rept.: Fisheries No. 155, 74 pp.

Allen, W. E.—Observations on surface distribution of marine diatoms of
1923 Lower California in 1921. Proc. Calif. Acad. Sc. XII., pp. 437-442.

Allen, W. E.—Plankton Diatoms of the Gulf of California obtained by the
1937 Allan Hancock expedition in 1936. The Allan Hancock Pacific. Expeditions, III, pp. 47-59. Univ. South. Calif. Press. Los Angeles, Calif.

Allen, W. E.—The Tempelton Crocker Expedition to the Gulf of Calif.
1938 in 1935. The Phytoplankton. Trans. Amer. Micr. Soc. XLVII, pp. 328-335.

Anderson, C. A.—1940 E. W. Scripps Cruise to the Gulf of California. Part
1950 I, Geology of Islands and Neighboring Land Areas. Geol. Soc. of Amer. Memoir 43, pp. 1-50.

Anderson, E. R.—The exchange of energy between a body of water and the
1953 atmosphere with application in evaporation. Univ. of Calif., Scripps Inst. of Oceanogr., La Jolla, Calif. Dissertation.

Anderson, F. M., and *G. D. Hanna.*—Cretaceous geology of Lower Califor-
1935 nia. Calif. Acad. Sci., Pr. 4th Serv., v. 23, pp. 1-34.

Barnhart, Percy S., and *Carl L. Hubbs.*—*Pontinus Vaughani* a new scorpaenid
1948 fish from Baja California. Bull. Scripps Inst. Oceanogr., Univ. Calif. 5(5), pp. 371-390, fig. 1.

Bartholomew, Geo. A., Jr.—Reproductive and social behavior of the northern
1952 elephant seal Univ. Calif., Publ. Zool., 47(15), pp. 369-472, figs. 1-2, pls. 38-57.

Bartholomew, Geo. A., and *Carl L. Hubbs.*—Winter population of pinnipeds
1952 about Guadalupe Island, San Benito and Cedros Islands, Baja California. Jour. Mammalogy, 33(2), pp. 160-171, figs. 1-3, pls. 1-2.

Beal, C. H.—Reconnaissance of the geology and oil possibilities of Baja Ca-
1948 lifornia, Mexico. Geol. Soc. America, Mem. 31, 138 pp., 11 pls.

California Dept. of Natural Resources.—Bibliography of Marine geology and
1955 oceanography, Calif. Coast Special Report 44, Div. of Mines.

Clark, Frances N., and John C. Marr.—Population Dynamics of the Pacific
1955 Sardine. Progress Report Calif. Coop. Oceanic Fish. Invest., 1 July 1953 to 31 March 1955, pp. 11-48.

Cromwell, Townsend, and *Joseph L. Reid, Jr.*—Observations of oceanic fronts
1956 on hypothesis concerning the maintenance of frontal layers. In press.

Cupp, Easter E., and *W. E. Allen.*—Plankton diatoms of the Gulf of Cfa.
1938 obtained by Allan Hancock Pacific Expedition in 1937. The Hancock Pacific Expedition, III, pp. 61-99. Univ. South. Calif. Press.

Durhan, J. Wyatt.—1940 *E. W. Scripps* cruise to the Gulf of Calif. Part II.
1950 Megascopic paleontology and marine stratigraphy. Geol. Soc. America, Mem. 43, 216 pp.

Felin, Frances E.—Population heterogeneity in Pacific pilchard U.S. Fish
1954 and Wildl. Serv., Fish. Bull. 54(86), pp. 201-225.

Felin, Frances E., John Mac Gregor, Anita E. Daugherty and Daniel J. Miller.
1953 —Age and length composition of the sardine catch off the Pacific Coast of the United States and Mexico in 1952-1953. Calif. Fish and Game 39(3), pp. 409-417.

Felin, Frances E., J. S. Mac Gregor, Anita E. Daugherty and Daniel J. Miller.
1954 —Age and length composition of the sardine catch off the Pacific Coast of the United States and Mexico in 1953-1954. Calif. Fish and Game, 40(4), pp. 423-431.

Felin, Frances E., J. S. Mac Gregor, A. E. Daugherty and D. J. Miller.—Age
1955 and length composition of the sardine catch off the Pacific Coast of the United States and Mexico in 1954-1955. Calif. Fish and Game 41(4), pp. 285-293.

Flores, T.—Carta geológica de la Baja California, Cartas geológicas y mi-
1931 neras de la República Mexicana, No. 1, Inst. Geol. México.

Gilbert, J. Y., and *W. E. Allen.*—The Phytoplankton of the Gulf of Califor-
1943 nia obtained by the E. W. Scripps in 1939 and 1940. Jour. Mar. Research 5(2), pp. 89-110.

Gilmore, Raymond M.—Calving of California gray whales. Pacific Disco-
1954 very, Berkeley, 7(3), pp. 13-15, 30 illus. May-June.

Gilmore, Raymond M.—The return of the gray whale. Scientific American,
1955 N. Y., 192(1), pp. 62-67, 7 illus. January.

Howard, C. S.—Composition of the Colorado River. Lake Mead Comprehen-
1954 sive. Survey, 1948-1949. v. 11, p. 165. U.S. Dept. of the Interior. Geol. Survey.

Hubbs, Carl L.—Changes in the fish fauna of western North America corre-
1948 lated with changes in ocean temperatures. Jour. Mar. Research, 7(3), pp. 459-482, figs. 1-6.

Hubbs, Carl L.—Probable record of the beaked whale, *Ziphius cavirostris,* in
1951 Baja California. Jour. Mammalogy, 32(3), pp. 365-366.

Hubbs, Carl L.—Establishment of a forage fish, the red shiner (*Notropis*
1954 *Lutrensis*), in the lower Colorado River system. Calif. Fish and Game, 40(3) pp. 287-294, figs. 1-3.

Hubbs, Carl L.—Black Scoters reported from Baja California. The Condor, 1955 57(2), pp. 121-122.

Hubbs, Carl L., and *J. L. McHugh.*—Pacific sharpnose shak (*Scoliodon Longurio*) in California and Baja California. Calif. Fish and Game, 36 1950 (1), 1950, pp. 7-11, figs. 3-4.

Hubbs, Carl L., and *Robert R. Miller.*—The Great Basin with emphasis on 1948 Glacial and Postglacial Times. II. The Zoological evidence: Correlation Between fish distribution and hydrographic history in the desert basins of western United States. Bull. Univ. Utah, 38(20) (Biol. Sci., 10(7)), pp. 18-166, figs. 10-29.

Jacobs, W. C.—The energy exchange between the sea and atmosphere and 1951 some of its consequences. Univ. of Calif. Press. Berkeley and Los Angeles, 122 pp.

Johnston, I. M.—Expedition of the California Academy of Sciences to the 1924 Gulf in 1921. Proc. Calif. Acad. Scien. XII, pp. 951-1218. San Francisco, Calif.

Johnson, Martin W.—The Correlation of water movements and dispersal of 1939 pelagic larval stages of certain littoral animals, especially the san crab, *Emerita*. Jour. Mar. Research, v. 2, pp. 236-245.

Lindgren, W.—Notes on the geology of Baja California, Mexico. Calif. Acad. 1888 Sci., Pr. 2nd ser., v. 1, pp. 173-196.

Marr, John C.—Sardine Spawning Surveys. Pan-American Fisherman, 10(3), 1955 pp. 14-15.

McEwen, George F.—Rate of upwelling in the region of San Diego computed 1934 from serial temperatures. Fifth Pacific Sci. Cong., Canada, 1933, Proc., v. 3, p. 1763.

Miller, Robert Rush, and *Carl L. Hubbs.*—An erroneous record of the Cali-1954 fornia Killifish, *Fundulus parvipinnis*, from Cabo San Lucas, Baja California. Copeia, 1954, No. 3, pp. 234-235.

Munk, Walter H.—Internal Waves in the Gulf of California. Sears Found., 1941 Jour. Mar. Research, v. 4, pp. 81-91.

Natland, M. L.—1940 E. W. Scripps cruise to the Gulf of California. Part 1950 IV. Deport on the Pleistocene and Pliocene Foraminifera, Geol. Soc. America, Mem. 43, 55 pp.

Nelson, E. W.—Lower California and its natural resources. Nat. Acad. Sci., 1921 Mem. 16(1), 194 pp.

Osorio Tafall, B. F.—El Mar de Cortés y la productividad fitoplanctónica de
1943 sus aguas. Anal. Esc. Nac. Cienc. Biol., III, pp. 73-118.

Osorio Tafall, B. F.—La expedición del M. N. Gracioso por aguas del extremo
1944 noroeste mexicano. Anal. Esc. Nac. Cienc. Biol., III, pp. 331-360.

Pattullo, J., W. H. Munk, R. Revelle, and E. Strong.—The seasonal oscillation
1955 in sea level. Jour. Mar. Research, v. 14, pp. 88-156.

Reid, Joseph L. Jr.—Observations of Internal Tide in October 1950. In press.
1956

Revelle, R.—Sediments of the Gulf of California. Geol. Soc. Amer. Bull. 50,
1939 pp. 170-171.

Rovelle, R.—1940 E. W. Scripps expedition to the Gulf of California. Part
1950 V, Sedimentation and Oceanography. Geol. Soc. Amer. Mem. 43.

Roden, G. I.—The Gulf of California survey on the present state of knowledge.
1956 To be published shortly.

Schott, W.—Geographie des Indischen und Stillen Ozeans. C. Boysen, Hamburg,
1935 pp. 280.

Servicio Meteorológico Mexicano.—Boletín Anual, 1936-1943, Tacubaya, D.F.

Shepard, Francis P.—1940 E. W. Scripps cruise to the Gulf of California.
1950 Par III. Submarine topography of the Gulf of California. Geol. Soc. America, Mem. 43, 32 pp.

Smithsonian Institute.—Smithsonian Meteorological tables, Washington.
1951

South Pacific Fishery Investigations.—Zooplankton volumes off the Pacific
1952 Coast, 1951. U.S. Fish and Wildl. Serv., Spec. Sci. Rept.: Fisheries, No. 73, pp. 1-37.

South Pacific Fishery Investigations.—Zooplankton volumes off the Pacific
1953 Coast, 1952. U.S. Fish and Wildl. Serv., Spec. Sci. Rept.: Fisheries, N. 100, pp. 1-41.

South Pacific Fishery Investigations.—Zooplankton volumes off the Pacific
1954a Coast, 1949-50. U.S. Fish. and Wildl. Serv., Spec. Sci. Rept.: Fisheries, No. 125, pp. 1-54.

South Pacific Fishery Investigations.—Zooplankton volumes off the Pacific
1954b Coast, 1953. U.S. Fish and Wildl. Serv., Spec. Sci. Rept.: Fisheries, No. 132, pp. 1-38.

Staff of the South Pacific Fishery Investigations.—Zooplankton volumes off
1955 the Pacific Coast, 1954. U.S. Fish and Wildl. Serv., Spec. Sci. Rept.: Fisheries, N. 161, pp. 1-35.

Stewart, Harris B. Jr.—Sediments and the environment of deposition in a
1956a coastal lagoon. Unpublished phD. thesis, Univer. of Calif., Scripps Ints. Oceanog.

Stewart, Harris B., Jr.—Contorted sediments in a modern coastal lagoon ex-
1956b plained by laboratory experiments. Amer. Assoc. Petroleum Geologists Bull. 40(1), pp. 153-161.

Sverdrup, H. U.—On the process of upwelling. Jour. Mar. Research, 1(2),
1937 pp. 155-164.

Sverdrup, H. U.—Cruises of the E. W. Scripps in 1939. Science Monthly,
1939 Oct. 1939, pp. 389-392.

Sverdrup, H. U.—Research within physical oceanography and submarine geo-
1940a logy at the Scripps Institution of Oceanography during April 1940 to April 1941. Trans. Am. Geoph. Soc., pp. 490-495.

Sverdrup, H. U.—The Gulf of California. Ass. Ocean. Phys. Proces Verbaux,
1940b 3, pp. 170-171.

Everdrup, H. U.—The Gulf of California: Preliminary discussions of the E.
1940c U. cruise in February and March 1939. Proc. Sixth. Pac. III Cong. Scripps. pp. 161-166.

Sverdrup, H. U.—Water masses and currents of the North Pacific Ocean.
1941a Science, May 9, 1941, 93 (2419), p. 436.

Sverdrup, H. U.—An anlysis of the Ocean Currents off the American West
1941b Coast between 40°N and 40°S.

Sverdrup, H. U.—Oceanic Observations of the Scripps Institution in 1939 (da-
1943 ta). Univ. Calif. Press. Berkeley and Los Angeles.

Sverdrup, H. U., and *W. E. Allen.*—Distribution of diatoms in relation to the
1939 character of water mases and currents off southern California. Jour. mar. Research, v. 2, pp. 131-144.

Sverdrup, H. U., and *R. H. Fleming.*—The waters off the coast of southern
1941 California, March to July, 1937. Scripps Inst. Oceanogr., Bull. 4 (10), pp. 261-378.

Sverdrup, H. U., Martin W. Johnson and Richard H. Fleming.—The Oceans,
1946 their physics, chemistry and general biology. Prentice-Hall, Inc. 1087 pp.

Tanner, Z. L.—Report on investigations of the U.S. Fish Commision Steamer
1888 *Albatross*, for the year ending June 30, 1889. U.S. Commision of Fish and Fisheries Commissioners Report 1888, pp. 395-512.

Thorade, H.—Uber die Kalifornische Meeresstromung. Anal. Hydrogr. und
1909 Marit. Meteor., v. 37, pp. 17-34 and 63-76.

Townsend, C. H.—United States Fish Commission Steamer *Albatross* Dredging
1901 and other records. U.S. Fish Commission Report 1900, pp. 387-562.

U.S. Coast And Geodetic Survey.—Surface water temperatures at tide stations.
1951 Spec. Publ. No. 280.

U.S. Coast and Geodetic Survey.—Density of sea water at tide stations. Spec.
1954 Publ. No. 281.

U.S. Coast and Geodetic Survey.—Tide Tables. West Coast South and North
1956 America. Publ. No. 781.

U.S. Hydrographic Office.—Sailing Directions. West coast of Mexico and
1951 Central America Publ. No. 84. Chart Nos. 619, 620, 621, 622, 638, 639, 640, 800, 849, 850, 938, 1024, 1335, 1664, 1666, 1667, 2087, 2103, 2130, 2181, 2193, 5388.

U.S. Weather Bureau.—Climatological data, National Summary. Vols. 1, 2, 3.
1950

University of California Press.—Oceanographic Observations of the Pacific, 1949. In Press. (Observations for subsequent years to be published also.)

University of California, Scripps Institution of Oceanography, 1949-1952.—Physical and chemical data reports of the MLR program; cruises 1-23, 34, 35 and 36.

Walton, William R.—Ecology of living benthonic Foraminifera, Todos Santos
1955 Bay, Baja California. Journ. Paleo. 29(6), pp. 952-1018.

Yoshida, K.—An Example of Variations in Oceanic Circulation in response
1955 to the Variations in Wind Field. Jour. of the Oceanographical Society of Japan, 11(3), October 1955, pp. 1-6.

Reprinted from Biological Bulletin, Vol. 115, No. 3, pp. 440–458, December, 1958
Printed in U. S. A.

A PERSISTENT DIURNAL RHYTHM OF LUMINESCENCE IN GONYAULAX POLYEDRA

J. WOODLAND HASTINGS AND BEATRICE M. SWEENEY

*Division of Biochemitsry, Noyes Laboratory of Chemistry, University of Illinois,
Urbana, Illinois, and Division of Marine Biology, The Scripps Institution
of Oceanography, La Jolla, California*

A PERSISTENT DIURNAL RHYTHM OF LUMINESCENCE IN GONYAULAX POLYEDRA[1]

J. WOODLAND HASTINGS AND BEATRICE M. SWEENEY

Division of Biochemistry, Noyes Laboratory of Chemistry, University of Illinois, Urbana, Illinois, and Division of Marine Biology, The Scripps Institution of Oceanography, La Jolla, California

The photosynthetic marine dinoflagellate, *Gonyaulax polyedra,* emits a brief flash of light (duration, about 90 milliseconds) when stimulated by agitation. It is one of the many organisms responsible for the luminescent display sometimes observed in the ocean at night when the water is disturbed (see Harvey, 1952). Previous studies with this organism (Haxo and Sweeney, 1955; Sweeney and Hastings, 1957a) have shown that the luminescent response to stimulation varies rhythmically in a diurnal fashion. Cultures grown in natural illumination, or in artificial lights with alternating light and dark periods of 12 hours each (= LD), display a much greater luminescence during the dark period (Fig. 2).

When LD cultures are transferred to a dark chamber, the rhythm continues but its amplitude decreases progressively. By action spectra studies, it has been found (Sweeney, Haxo and Hastings, unpublished data) that this decrease in amplitude arises from the need for light in the organic nutrition of *Gonyaulax,* via photosynthesis. This finding prompted the search for constant environmental conditions under which the endogenous rhythm would persist, without the loss of amplitude which occurs in continuous darkness.

The possibility of maintaining the cells heterotrophically was explored, but the consistently negative results obtained indicated that *Gonyaulax* is an obligate photo-auxotroph. Continuous bright light inhibits the rhythmic fluctuations in luminescence, and it has not been possible to separate, by using light of different colors, the photosynthetic requirements for light from the inhibitory action of light on rhythmicity. It has been found, however, that if LD cultures are placed in a continuous dim light, the rhythm of luminescence persists without loss of amplitude. It has thus been possible to investigate in some detail the nature of this endogenous rhythm.

MATERIALS AND METHODS

G. polyedra has been maintained in a modified sea water medium described previously (Sweeney and Hastings, 1957a). The growth rate is dependent upon light, temperature, and the concentrations of mineral nutrients. The maximum growth rate which we have measured is one division per day, but under the condi-

---

[1] This research has been supported in part by grants from The National Science Foundation, the Graduate Schools of Northwestern University and the University of Illinois, and the Marine Life Research Program of the California Cooperative Oceanic Fisheries Investigation. Part of the research was carried out at Northwestern University, Evanston, Illinois. Contribution from the Scripps Institution of Oceanography, new series. No. 1059

Reproduced by Permission

tions used in the experiments to be described the rates were always less than this. The illumination was provided by "cool white" fluorescent lamps, the intensity being measured in foot-candles with a Weston illumination meter.

The experimental procedure was as follows: stock cultures were maintained in Fernbach flasks containing 1500 ml. of medium. In preparation for an experiment, 2-ml. aliquots from these cultures were pipetted into each of several hundred test tubes at cell densities between 2000 and 7500 cells per ml. All tubes were then subjected to the appropriate conditions of light and temperature. To measure the luminescence at any given time, two tubes were removed, assayed, and then discarded. The cells were stimulated to luminesce by bubbling air through the cell suspension, and the resulting phototube current was accumulated on a capacitor. Luminescence is expressed in terms of the total amount of light emitted during one minute of stimulation, at the end of which time essentially all luminescence has ceased. Additional details of the light measurement procedure may be found elsewhere (Sweeney and Hastings, 1957a).

RESULTS

Demonstration of the persistent rhythm. A persistent rhythm of luminescence may be observed if cells which have been kept for a time under LD conditions are transferred to continuous dim light (about 100 foot-candles). A typical example of the persistent rhythm under conditions of constant light and constant temperature is shown in Figure 5. In similar experiments, we have continued measurements for as long as 14 days; the rhythmic pattern continues undamped during this time. At the light intensity used in such experiments there was little growth.

The natural period of the rhythm. The period of the rhythm is measured by the time between successive maxima in luminescence. When the cells are subjected to alternating light and dark periods on a daily (24-hour) schedule, the period of the rhythm is 24 hours (Fig. 2). Under conditions of constant illumination, however, the rhythmic changes have a period which is close to, but not necessarily exactly 24 hours. Pittendrigh and Bruce (1957) have referred to this as the *natural period,* or the innate period of an endogenous rhythm when light and temperature are held constant.

The natural period in *Gonyaulax* is a function of at least two environmental factors, light intensity and temperature. The effect of light intensity upon the period is illustrated in Figure 1. Cells were placed in continuous light at three different intensities, and it is evident that the natural period was shorter at higher intensities. These experiments also illustrate the light intensity dependence of the inhibitory effect of continuous illumination upon the rhythm. At the two higher light intensities the amplitude of the rhythm was progressively damped, while at the lowest light intensity no marked damping of the amplitude of the rhythm was evident.

The effect of temperature upon the natural period is not large but, contrary to expectation, the period becomes longer rather than shorter as the temperature is raised (Hastings and Sweeney, 1957b). At 16° C. the period was found to be 22.8 hours while at 26.7° C. it was 26.5 hours. A Q_{10} of less than 1.0 is unusual, and the results were interpreted as evidence for a compensation mechanism which functions to keep the period approximately temperature-independent.

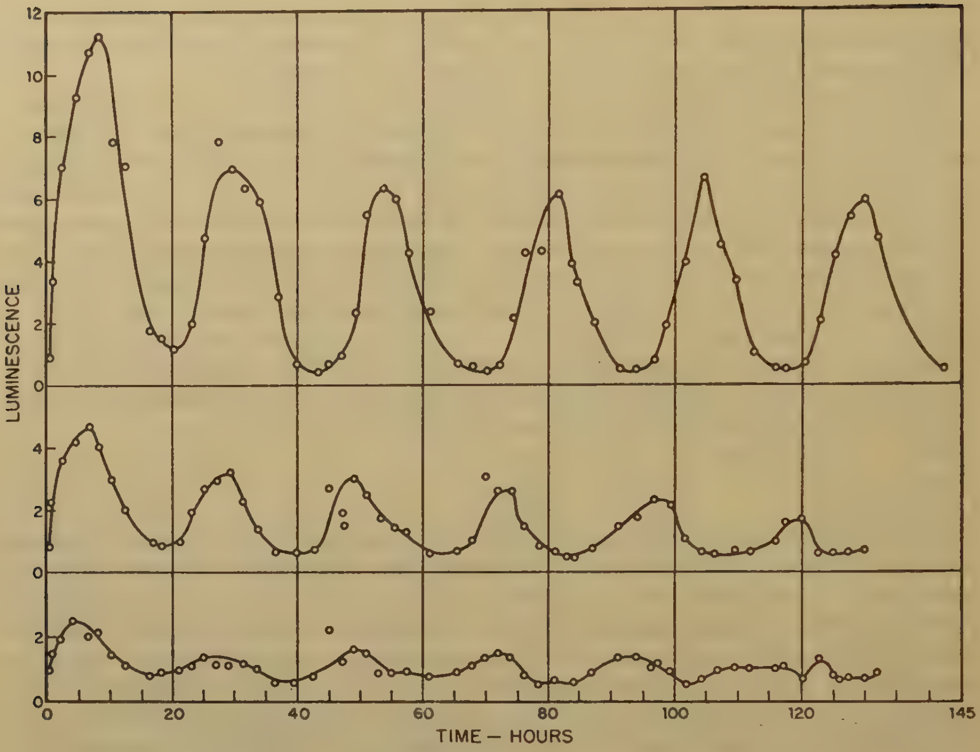

FIGURE 1. The effect of light intensity upon the natural period at constant temperature (21° C.). The cells were grown in LD conditions (800 foot-candles during the light period). The beginning of the experiment, shown on the graph as 0 time, fell at the end of a normal light period. At this time, some cells were placed in the dark, and others in light of 120 foot-candles (upper curve), 380 foot-candles (middle) and 680 foot-candles (bottom). The average periods were as follows: 680 foot-candles, 22.0 hours; 380 foot-candles, 22.8 hours; 120 foot-candles, 24.5 hours; dark, 24.5 hours (not shown on graph; one period measured).

In view of the relatively small temperature effect, the period of this rhythm may be characterized as essentially temperature-independent.

The endogenous nature of the diurnal rhythm. The persistence of the rhythm of luminescence under conditions of constant temperature and light intensity indicates that the mechanism of the rhythmicity is endogenous. Several other experiments serve to support this conclusion.

Figure 2 illustrates one of many experiments in which the phase of the rhythm was shifted by changing the time at which the light and dark periods occurred. In such experiments the phase (*i.e.*, the solar time at which the maximum in luminescence occurs) may be shifted so that it will bear any desired relationship to the solar day. In cultures which are subsequently transferred to constant conditions of dim light or darkness, the phase of the persistent rhythm is related to the previous light and dark program rather than to solar time, or any other factor. Changes in the phase of the endogenous rhythm have not been observed when light and temperatures were held constant.

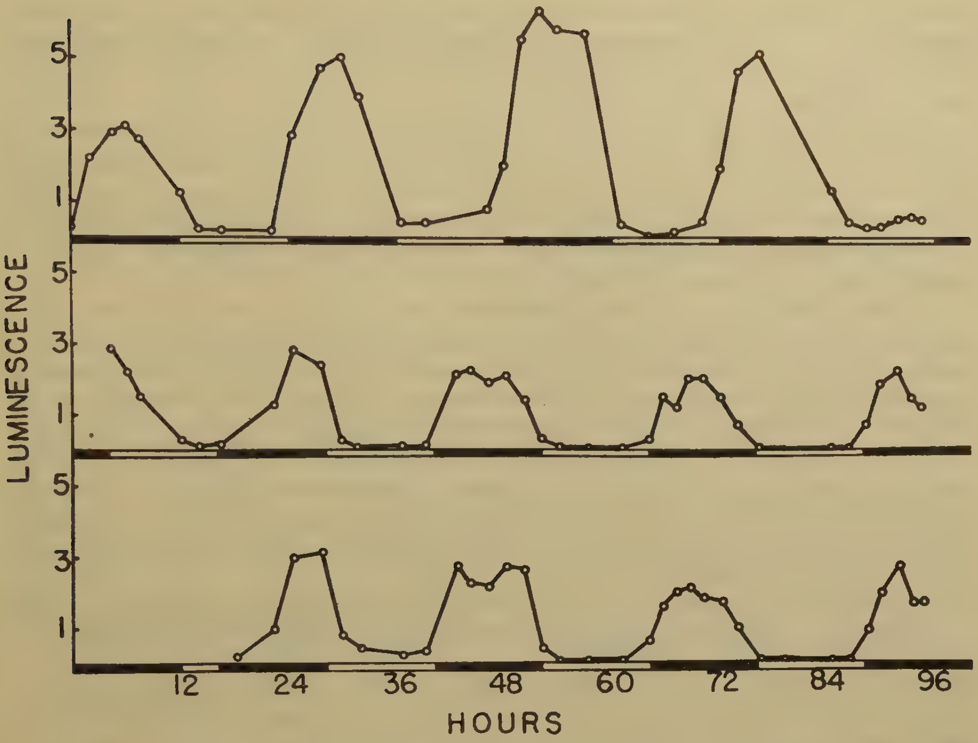

FIGURE 2. This experiment illustrates the effect of changing the solar time at which the light and dark periods occur. The upper curve shows the pattern of luminescence changes in an LD culture which had been on the schedule indicated for some time. The black bars on the time axis indicate dark periods. The lower two graphs illustrate the effect of imposing upon cultures (which were previously on the schedule shown in the top graph) an LD schedule in which the light and dark periods were at a different time of day. The new schedules were started at zero hours on the graph. Temperature, about 26° C. Light intensities used, about 250 foot-candles.

A series of experiments has been carried out from which it is evident that pre-treatment with diurnal light and dark periods (*i.e.*, one dark plus one light period equals 24 hours) is not necessary in order to demonstrate an endogenous rhythm. That is to say, there is no evidence that a "learning" or "memory" process is involved. For example, cells have been exposed to "non-diurnal" light and dark periods which together add up to greater or less than 24 hours, followed by conditions of either constant light or constant dark. An experiment of this sort is shown in Figure 3. In this experiment, cells were exposed to alternating light and dark periods of 7 hours each for about 100 hours. During this period the luminescence changes were quite evidently governed by these light and dark periods so that there was a maximum in luminescence every 14 hours. At the end of this treatment, some cells were placed in constant dim light and others in darkness. In both cases a diurnal rhythm with a period of approximately 24 hours was evident. The 14-hour cycle had not been "learned," even though it had been possible to entrain the luminescence rhythm to the 14-hour cycle. A difference between those placed in darkness and those in dim light was that the amplitude of the rhythm in darkness progressively decreased as a result of the lack of light (see introduction).

Similar experiments have been carried out in which the alternating light and dark periods were 6 hours each, 8 hours each, and 16 hours each, giving cycles of 12, 16 and 32 hours, respectively. The results were similar to those shown in Figure 3. After about 100 hours of such a non-diurnal light-dark cycle the cells were placed in constant dim light and a rhythm of luminescence having a period close to 24 hours was evident.

Another series of experiments has shown that it is not necessary to pre-treat the cells with any sort of alternating light and dark periods in order to demonstrate endogenous diurnal rhythmicity. As mentioned previously, if cells are grown in continuous bright light (*ca.* 800–1500 foot-candles) there is no detectible rhythmicity. Cells maintained in this way for several months, or for as long as several years, have been found to exhibit a diurnal rhythmicity when they are placed in darkness (Haxo and Sweeney, 1955; Sweeney and Hastings, 1957a). The phase of the rhythm which is initiated when the cells are moved from bright light to darkness is independent of the solar time, and related only to the time at which the light-to-dark transition is made.

A similar result was obtained when cells which had been grown in bright light for almost one year were merely transferred to dim light. This experiment is

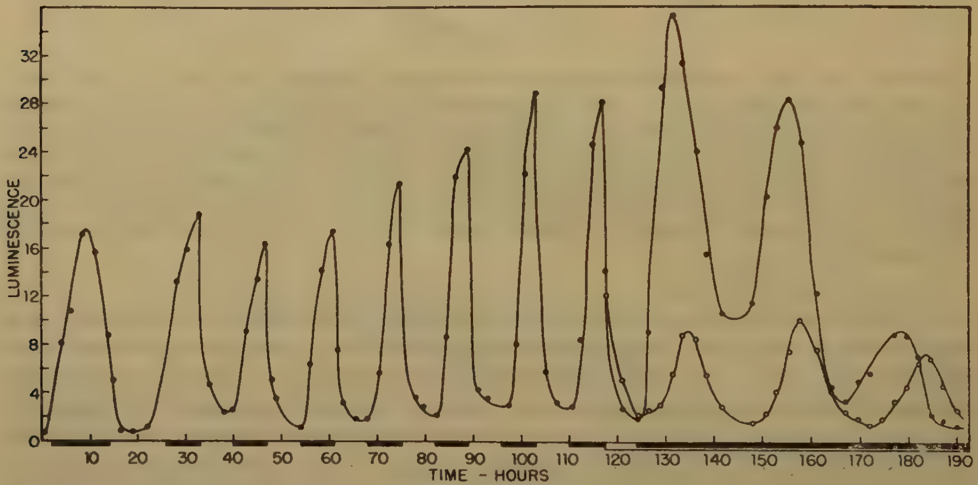

FIGURE 3. This illustrates the entrainment of the luminescence rhythm to a 14-hour cycle and the manifestation of an endogenous diurnal rhythm when the cells are placed in constant conditions subsequent to the treatment. Dark periods are indicated by black bars on the time axis. The cells were on an LD schedule previous to the time when the 14-hour cycle was started (at 26 hours). Light intensity throughout the 14-hour cycling was 800 foot-candles. At 117 hours some aliquots were removed from the dark and placed in constant light at 230 foot-candles. The luminescence changes in these cultures are shown by the circles. From 124 hours on, the other aliquots were left in the dark and the luminescence changes are plotted with solid dots. Temperature, 21° C.

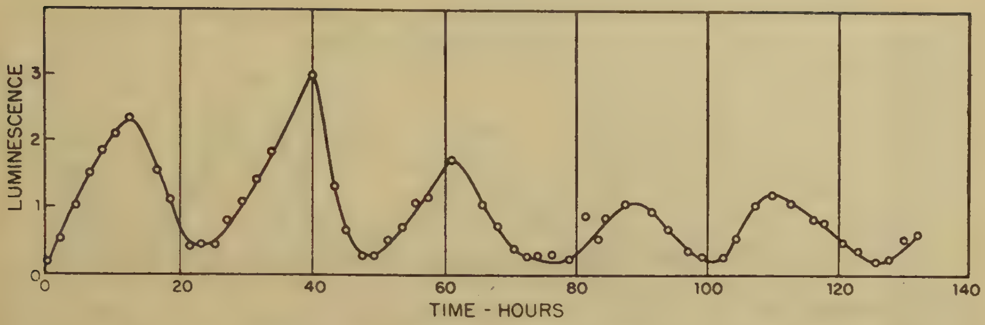

FIGURE 4. The initiation of an endogenous diurnal rhythm of luminescence by means of a one-step change in illumination. Cultures which had been grown in bright light for one year were moved from bright light (800 foot-candles) to dim light (90 foot-candles) at the time indicated on the graph as 0 hours. Luminescence measurements were made approximately every two hours thereafter. Temperature, 21.0° C. Average period, 24.5 hours.

illustrated in Figure 4. It differs from the previously mentioned experiment (in which cultures were moved from bright light to darkness) in that the amplitude does not decrease with time, since light is available for the nutrition of the cells. The precise phase relationship to the time of transfer from bright light is somewhat different, but here also it is not related to solar time.

Phase shift by light perturbation. It is clear from Figure 2 that the phase of the rhythm may readily be shifted by an appropriate manipulation of the light and dark periods to which the cells are exposed. It is not necessary, however, to expose the cells to a new light-dark cycle in order to reset the phase of the rhythm. A single exposure to a different light intensity can result in a stable phase shift. Pittendrigh and Bruce (1957) have discussed the significance of phase resetting of biological rhythms by single light perturbations. If rhythmicity results from an innate oscillatory mechanism characterized by its own natural period, and the phase (but not the period) is determined by the sequence of light and darkness, then it is to be expected that non-repeated light changes should suffice to change the phase. The perturbation therefore need not contain any information concerning period.

The experiment shown in Figure 4 illustrates phase setting by a single step-type light perturbation. The phase of the previously aperiodic cells was determined by the time at which the light intensity was changed. The shifting of phase in already rhythmic cultures is evident in the experiments shown in Figure 3. The entrainment of the rhythm to a 14-hour cycle may be explained by assuming that each transition, either from darkness to light or from light to darkness, serves to shift the phase, so that repetitive phase resetting occurs.

A phase shift in the *Gonyaulax* rhythm by single light perturbations has also been demonstrated in other ways. Figure 5 illustrates a shift in the phase of rhythmic cells which were given a single exposure to either bright light or darkness. The phase shift which results in such experiments has been found to be stable since, in experiments where measurements were continued for an additional 48 hours, the phase difference between the controls and the treated cells remained unchanged.

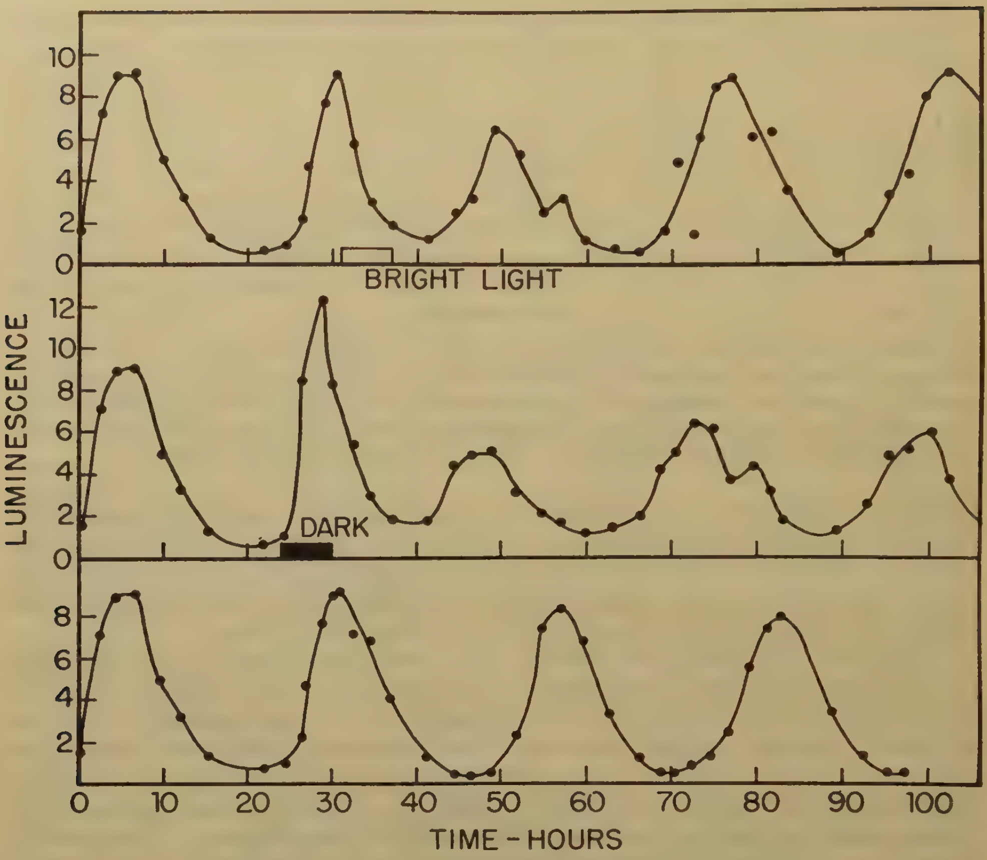

FIGURE 5. This experiment illustrates a phase shift in the rhythm following changes in light intensity. Cells previously kept under LD conditions were placed at constant temperature (23.5° C.) and constant light intensity (100 foot-candles) at the end of a 12-hour dark period. Two days later (zero time on the graph) measurements of luminescence were begun and the endogenous rhythm was apparent. Some cultures (upper curve) were transferred to bright light (1400 foot-candles) for a period of 6 hours and then returned to the previous condition (100 foot-candles). Other cultures (middle curve) were transferred to darkness for 6 hours and returned to dim light at 200 foot-candles. The time at which treatment was given is indicated by bars on the time axis. In both cases a marked phase shift in the rhythm is evident. The control (lower curve) was left in dim light all the while. Average period in control: 25.7 hours.

Figure 6 shows another technique which has been used in the study of phase shifting by single perturbations. Rhythmic cells were placed in the dark and, at a later time, received an exposure to light. Although the amplitude of the rhythm decreases over the next few days, the times at which maxima in luminescence occur are evident, so that the phase may be determined. The number of hours by which the phase is shifted would be expected to be some function of both the magnitude of the perturbation, and the time in the old cycle at which it is administered. The technique of interrupting darkness by light has been used to investigate these parameters.

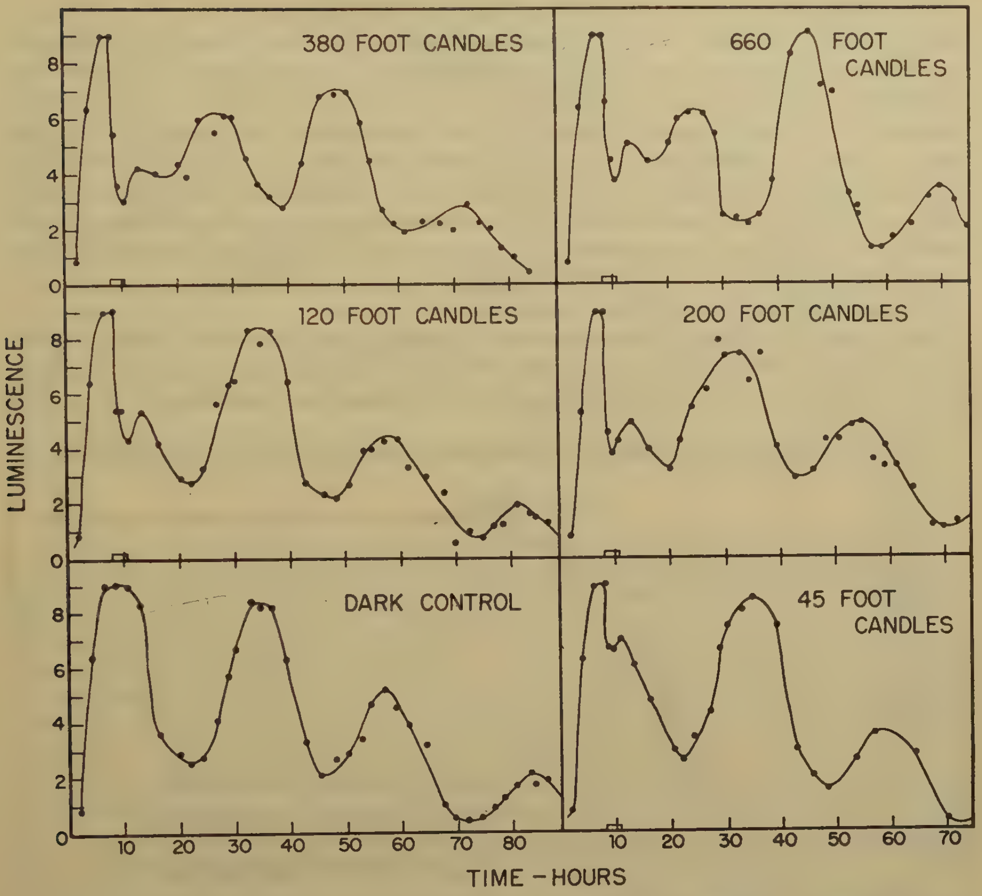

Figure 6. This illustrates phase shifting in a rhythmic culture by a single 2½-hour exposure to light, and the effect of intensity upon the magnitude of the phase shift. Prior to the time shown on the graph, all cultures were in LD conditions, and "two hours" on the time axis was the end of the last 12-hour light period. All cultures were put in the dark at that time and the control was left in the dark thereafter. The remaining cells were exposed to a 2½-hour illumination beginning 6 hours after the light-to-dark transition (indicated by the rectangle on the time axis). Following this 2½-hour illumination they were returned to darkness for the remaining time. The intensities used are shown in the figure. A 2½-hour exposure to 1400 foot-candles (not plotted) was found to be no more effective than the exposure to 660 foot-candles (Fig. 7). Temperature during experiment, 21° C.

The effect of varying the light intensity was determined in experiments such as the one shown in Figure 6. The amount of phase shift was found to increase with increasing light intensities, up to a "saturation" value of about 800 foot-candles. This relationship is illustrated in Figure 7, and the stability of the resetting is shown by plotting on the same graph the phase shift measured at each of the subsequent cycles. Several experiments of this sort have been carried out and the same type of relationship has been observed. The quantitative values obtained in separate experiments were somewhat different, however, and the reason for this variation has not been determined.

The magnitude of the perturbation may also be changed by varying the duration of light exposure. In an experiment similar to that shown in Figure 6, the duration instead of the intensity was varied. All exposures (at 800 foot-candles) were started simultaneously, six hours after the cells were placed in darkness. A longer exposure to such a light perturbation was found to be more effective than a shorter exposure. The amount of phase shift was found to be proportional to the duration of the exposure, up to a maximum phase shift of about 11½ hours, which was achieved with 2½ hours exposure. The relationship between phase shift and duration might be expected to be different, depending upon the time in the old cycle at which the perturbations were given, as discussed below. This aspect has not been studied, however.

The effect of varying the time in the cycle at which the perturbation is given has been studied by again using a procedure similar to that used in the experiments shown in Figure 6. Cells grown in LD conditions were transferred to a dark

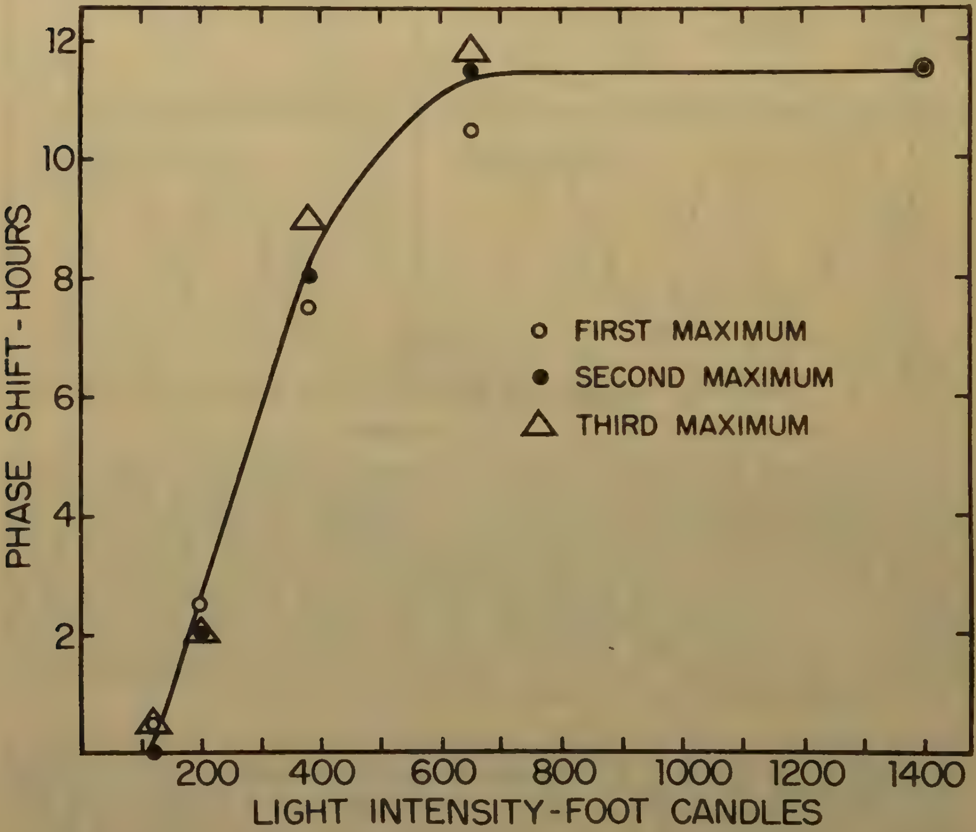

Figure 7. The relationship between the intensity of a single 2½-hour light perturbation and the number of hours by which the phase is shifted. Data taken from the experiments shown in Figure 6. Different symbols, as marked on the graph, give the phase difference between the control and the experimentals, measured at each of the three maxima in luminescence subsequent to the perturbation.

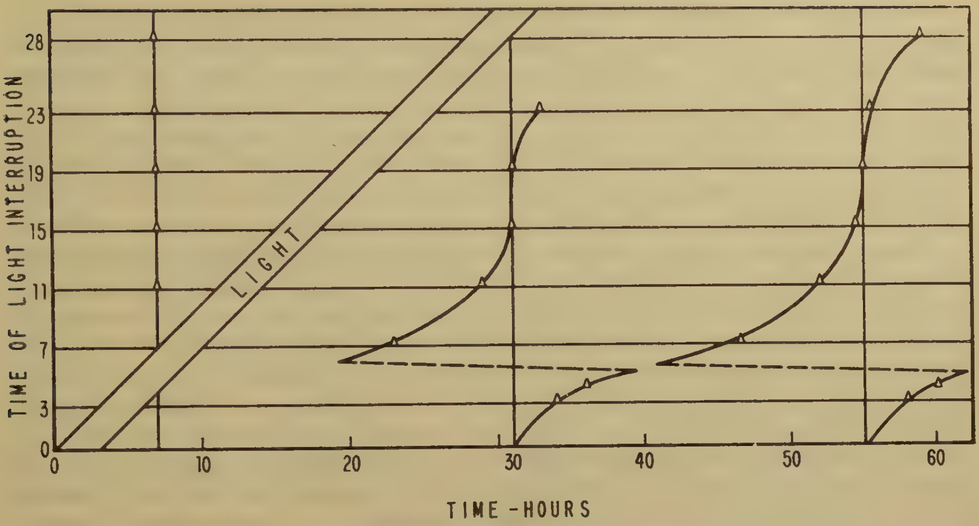

FIGURE 8. The effect of light perturbations (1400 foot-candles for 3 hours) given at different times during the cycle, upon the phase of the endogenous rhythm. Cells which had been kept under LD conditions were placed in the dark at zero time on the graph, which was the end of a 12-hour light period. The times at which the maxima in luminescence occurred in the control, which remained in the dark all the while, are indicated by vertical lines. In the experimentals, a triangular symbol shows a time at which a maximum in luminescence occurred, and thus represents phase. The experiments were carried out in a way similar to those illustrated in Figure 6. Each horizontal line represents a different experiment. For example, the line at 11 hours on the ordinate was an experiment in which a maximum in luminescence occurred at 7 hours. A light perturbation was begun at 11 hours and terminated at 14 hours. Maxima in luminescence occurred subsequently at 29½ hours and 52½ hours. The other experiments are represented in a similar way. The relationship between the time in the cycle at which the light perturbation was administered and the number of hours by which the phase was changed may be better visualized by rotating the figure by 90°.

chamber at the end of a light period. At regular time intervals thereafter, some of the cells were removed and exposed for three hours to light at an intensity of 1400 foot-candles, and then returned to darkness. Times at which exposures to light were made were selected so that the experiment served to scan somewhat more than a full 24-hour cycle. A control received no exposure to light, and the times at which maxima in luminescence occurred in this control are indicated by the vertical lines in Figure 8.

The results of the experiments are summarized in Figure 8. First of all, it may be noted that the new phase, following a light perturbation, was not directly related to the time at which the light perturbation was administered. That is, the maxima in luminescence did not occur at a fixed time interval following the light treatment. If that had been the case, the symbols indicating phase would fall along a line at 45°, parallel to the lines representing the times at which light exposures occurred. This latter type of result was obtained in experiments mentioned previously (Figure 4, for example) where a rhythm was initiated in an arrhythmic culture, and the phase was determined only by the time at which the light intensity was changed.

Secondly, it is apparent that the sensitivity to light perturbations was greater during the first 12 hours (Fig. 8) than during the second 12 hours of the cycle. During the first 12 hours a rather pronounced phase shift resulted, whereas during the second 12 hours there was little or no phase shift. In other longer term experiments it has been found that this variation in sensitivity continues in a rhythmic way. It may therefore be stated that, in general, the cells are maximally sensitive to a light perturbation at a time when luminescence is near maximum, and that this sensitivity declines to a minimum at a time when luminescence is minimum.

Finally, however, it may be noted from Figure 8 that a light exposure given before the maximum in luminescence results in a phase delay, so that the time between the light perturbation and the subsequent maximum in luminescence is greater than 24 hours. On the other hand, a light exposure given after the maximum in luminescence results in a phase advance, such that the next maximum in luminescence occurs in less than 24 hours. This difference is illustrated by the light perturbations which start at three hours and at seven hours in Figure 8.

Perturbation by mechanical stimulation. It is of interest to consider the nature of the cellular component or components which, being modified as a result of the light perturbation, result in the observed phase shift. If perturbation by means other than light also resulted in a change in the components of the rhythmic mechanism, then a phase shift would be similarly expected. It seemed possible that mechanical stimulation might be effective in this regard. Consequently, a perturbation experiment was carried out, in which air was bubbled through the cell suspensions instead of exposing the cells to light (Fig. 9). No phase shift occurred; the cells which had been stimulated retained the same phase as the unstimulated controls.

The experiment also shows that it is possible to modify the concentrations of compounds which are involved in the luminescence rhythm without having any effect upon the phase of the rhythmic mechanism itself. It was found previously (Hastings and Sweeney, 1957a) that the rhythm of luminescence involves a daily variation in the amount of extractable components of the luminescent system (luciferin and luciferase). Mechanical stimulation causes the luminescent reaction to occur, so that one would suppose that the concentrations of components in the luminescent system (and other biochemical systems coupled to it) might be changed. In fact, the apparent effect of stimulation is similar to the effect of light; the luminescence decreases to a low level in both cases. But since no phase shift occurred following stimulation, it does not seem likely that the luminescent system could be directly involved in the basic rhythmic mechanism, although it is clearly coupled to such a mechanism. Moreover, it is evident that there is no feedback from the luminescent system to the system controlling the phase of the rhythm. From previous evidence we had suggested that the luminescent system might itself constitute an autonomous chemical oscillation (Hastings and Sweeney, 1957b). The results described above, however, favor a hypothesis which proposes a basic mechanism of cellular rhythmicity to which various physiological and biochemical processes, such as luminescence or cell division (Sweeney and Hastings, 1957b; 1958), could be coupled.

Cellular interaction. Since all the experiments which have been described are carried out with large cell populations (4000–15,000 cells per tube), the ques-

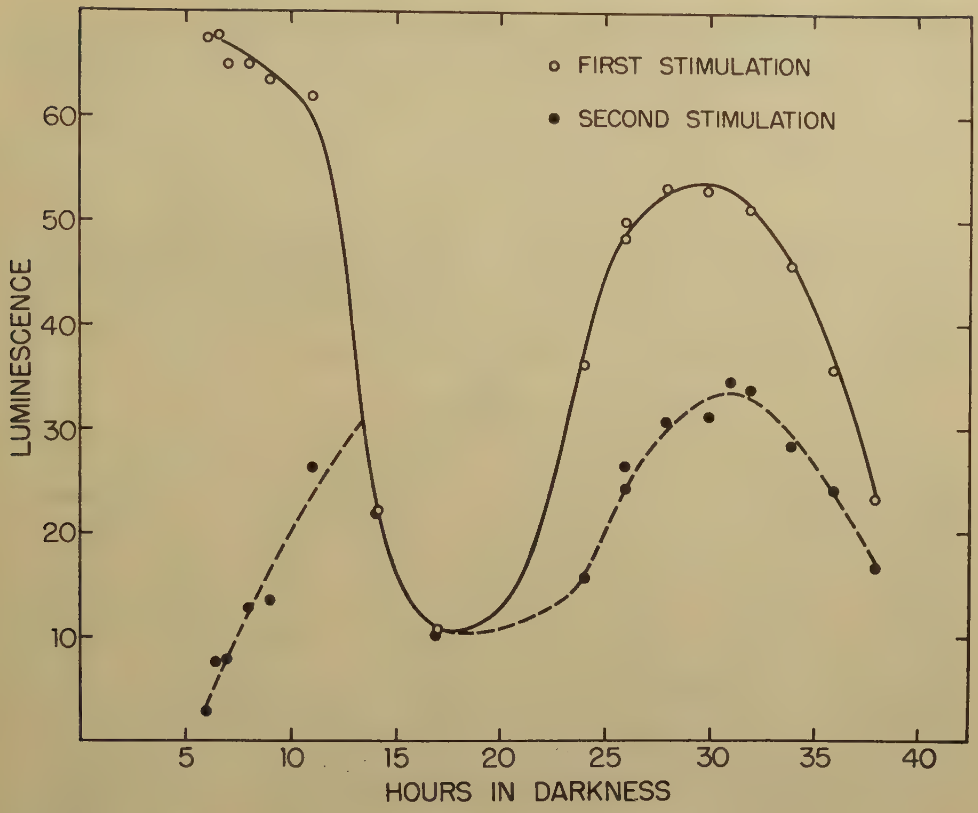

Figure 9. The effect of perturbation by mechanical stimulation upon the phase of the rhythm. Previous to the time shown, all cultures were in LD conditions, and zero time on the graph was the end of a light period. At this time all aliquots were placed in the dark. Six hours later a large number of aliquots were stimulated by bubbling air, but were not exposed to light. The luminescence changes of both these and the controls were determined through the subsequent maximum in luminescence. No significant change in the phase of the stimulated cultures was observed.

tion arises as to whether or not some cellular interaction might occur. Since the rhythmic mechanism involves fluctuations in the concentrations of chemical components within the cells, it is conceivable that certain diffusible compounds might escape into the medium, and that their concentrations might also fluctuate in a diurnal fashion. The importance of such a phenomenon would be evident if the supposed compound or compounds could function, as in a feedback mechanism, for stabilizing the frequency and/or phase of the rhythm. It is also possible that some other phenomenon, such as cellular motility, could be involved in such a feedback mechanism. This latter possibility seems unlikely, however, in view of the fact that mechanical stimulation, with its attendant violent motion and disturbance of cellular motility, did not result in a phase change.

An experiment in which this question was investigated is illustrated in Figure 10. Two cultures were maintained under LD conditions for several weeks with their phases different by 5 hours. Samples were pipetted from each culture and moved to constant dim light at the end of a dark period. After each had been under constant conditions for several days (their phases still being different by

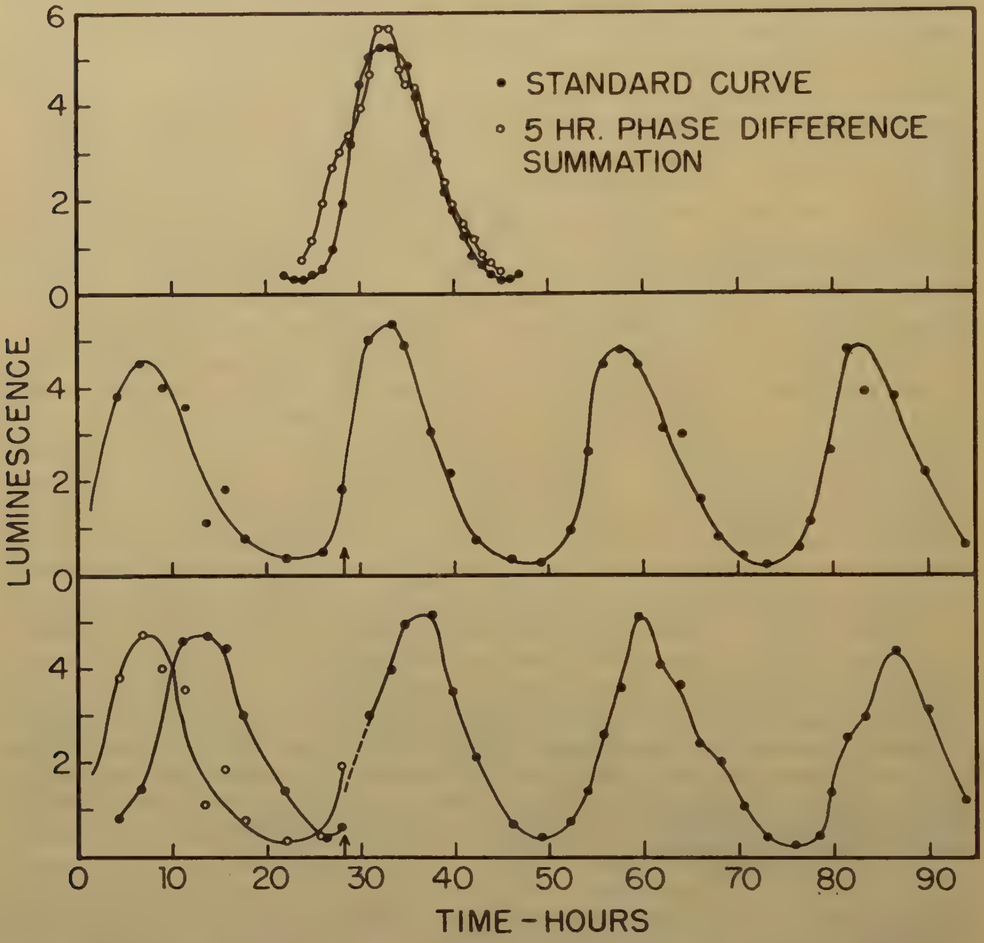

Figure 10. The effect of mixing two rhythmic cultures which were out of phase with one another. Cultures which had been in constant dim light for several days, having a 5-hour phase difference as shown (bottom curves), were mixed at the time indicated by the arrow. The rhythm continued, with a phase having its maximum at a time precisely halfway between the maxima of the two original cultures. The middle curve shows the result of mixing cultures having the same phase, done at the time indicated by the arrow. No change of phase was observed. The upper graph shows the result which would be theoretically expected upon mixing two cultures 5 hours out of phase, on the assumption that no interaction was involved. Two "standard" luminescence curves, which were measured from a culture which had not been mixed, were summated with a 5-hour phase difference. For purposes of comparison, the resultant curve is plotted on the graph along with the original standard curve, the latter having been displaced by 2½ hours on the time axis and normalized to the calculated curve. It may be seen that the shape of the calculated curve does not differ greatly from that of the original "standard" luminescence curve.

5 hours), the cultures were mixed in equal proportions, and the luminescence changes in the mixed cultures were measured.

If two typical curves showing the luminescence rhythm are summated, the phase of the two curves being different by five hours (75°), the resultant curve differs only slightly in shape from the original curves (Fig. 10, top). The maximum of the resultant curve lies precisely midway between the maxima of the two original curves.

In the actual mixing experiment, the maximum in luminescence of the mixed cultures occurred halfway between the maxima of the two separate unmixed cultures. Moreover, the shape of the curve from the mixed cultures was very similar to that which was obtained when the measured luminescence of the separate cultures was summated. The mixing experiment therefore indicates that no cellular interaction was involved.

Discussion

The subject of persistent endogenous rhythms has been recently reviewed by Harker (1958), Pittendrigh and Bruce (1957), and Bünning (1956). These reviewers, as well as other authors, have taken the view that the property of rhythmicity may be a nearly universal feature of organisms. This view is derived, largely, from the observation that endogenous rhythms are extremely widespread, having been reported from a large variety of both plants and animals. Furthermore, Pittendrigh and Bruce develop the generalization that most, if not all organisms can measure time; that they possess clocks. They consider that the basic mechanism evolved early, and that it has been retained in the course of evolution as a part of the adaptive organization of all organisms. Their use of the word "clock" refers to the basic mechanism involved in cellular rhythmicity, and the essential properties of this mechanism are considered to be similar in different organisms.

Pittendrigh and Bruce (1957) thus distinguish between the clock as the basic mechanism, and the persistent rhythms which are presumed to be controlled by the clock. Other authors (Brown, Hines, Webb and Fingerman, 1950; Stephens, 1957a; Harker, 1958) have similarly concluded that an overt persistent rhythm may be distinguished from an underlying mechanism, and our studies with *Gonyaulax* give support to this thesis. For example, since it was found that concentrations of compounds taking part in the luminescent reaction could be changed without shifting the phase of the rhythm, it is probable that the luminescence rhythm does not in itself constitute the basic mechanism. Furthermore, we have recently reported a persistent rhythm of cell division in *Gonyaulax* (Sweeney and Hastings, 1957b). The luminescence rhythm and the cell division rhythm have essentially identical properties. Moreover, we have not been able to demonstrate a phase shift in one rhythm which is not accompanied by a similar phase shift in the other rhythm. These findings give additional support to the hypothesis that one basic mechanism controls both rhythms.

The identity and physico-chemical nature of the presumed basic clock mechanism in persistent rhythms remains undefined. But if the properties of this basic mechanism in *Gonyaulax* may be deduced from the rhythm of luminescence, then it is evident that the mechanism possesses essential clock-like properties; the period is not greatly affected by environmental factors, but the phase is labile to resetting by the appropriate external changes. We may note, in addition, that light emission in *Gonyaulax* is clocked so that it is maximal during the night phase, when it is visible; and without environmental inhibition, luminescence is minimal during the day phase. However, since the possible utility of the light emission is not known, the functional significance of clocked luminescence is not apparent.

Many of the characteristics of the rhythm of luminescence which we have described are similar to the characteristics of persistent rhythms in a variety of other organisms, ranging from other unicellular forms to mammals. The comparisons outlined below do not pretend to be complete, but they serve to illustrate the point. The remarkable similarities found support the view of Pittendrigh and Bruce (1957), that the basic mechanism involved in rhythmicity is the same in all organisms.

Practically all the persistent diurnal rhythms described have natural periods which are close to but different from 24 hours. This includes rhythms in *Drosophila* (Pittendrigh, 1954), *Uca* (Webb, Brown and Sandeen, 1954), *Oedogonium* (Bühnemann, 1955a), *Euglena* (Bruce and Pittendrigh, 1956), and many others. The natural period may range, in different organisms, from about 21 to 27 hours. In fact, significant differences in the natural periods in different individual mice are well documented (Pittendrigh and Bruce, 1957).

Studies of rhythms in a variety of organisms, including the bee (Wahl, 1932), *Uca* (Brown and Webb, 1948), *Avena* (Ball and Dyke, 1954), *Drosophila* (Pittendrigh, 1954), and *Euglena* (Bruce and Pittendrigh, 1956), have shown that in each case the period is nearly the same at temperatures which differ by 15° C., or more. It is interesting to note that the effect of temperature upon the period of the *Gonyaulax* rhythm is similar to that reported by Bühnemann (1955b) for the rhythm of sporulation in *Oedogonium,* in that the apparent Q_{10} for both is less than 1.0. Two cases may therefore be interpreted as the result of an over-compensation in the mechanism responsible for temperature independence (Hastings and Sweeney, 1957b).

Only a few experiments have been specifically designed to detect the effect of different light intensities upon the natural period of persistent rhythms. In those cases which have been reported (see Harker, 1958), the natural period has been found to change no more than an hour or two under different light intensities.

The entrainment of rhythms to periods different from 24 hours has been reported in several organisms, including *Euglena* (Bruce and Pittendrigh, 1956) and *Oedogonium* (Bühnemann, 1955a). In these and other cases, as in *Gonyaulax*, the rhythms return to the characteristic natural period when the organisms are returned to constant conditions.

On the other hand, several experiments have been reported in which rhythmic organisms still continue to show a 24-hour rhythm while being subjected to light-dark cycles which differ from 24 hours. For example, Webb (1950) found that the period of the *Uca* rhythm was not changed while the organisms were subjected to light (95 foot-candles) and dark periods of 16 hours each, and Tribukait (1954) found that entrainment to an imposed light-dark cycle occurred in the mouse only so long as the imposed cycles did not differ greatly from the natural period.

Studies with *Gonyaulax* suggest a possible reason for the lack of apparent entrainment in experiments such as those cited above: the light intensities used may not have been sufficiently bright. In *Gonyaulax,* the luminescence rhythm may be entrained to periods which differ greatly from the natural period. Our interpretation of this entrainment is that repetitive phase resetting results in a period corresponding to the imposed schedule. The importance of light intensity as a parameter in phase shifting by single light perturbations has been documented in experiments with *Gonyaulax.* That it is equally important in entrainment has been shown in an experiment with *Gonyaulax* described elsewhere (Hastings and Sweeney, 1958), in which it was found that entrainment occurred at a light intensity of 800 foot-candles, but not at 200 foot-candles.

Entrainment of rhythms to imposed cycles which are only slightly longer or shorter than the natural period has been discussed by Pittendrigh and Bruce (1957). Their interpretation suggests that the mechanism may be different from that involved in entrainment to cycles differing greatly from the natural period.

The role of 24-hour light-dark cycles in establishing the phase of diurnal rhythms has long been recognized, and experiments with many organisms have demonstrated that, as in *Gonyaulax,* the phase shifts in response to a new light-dark cycle which is out of phase with solar night and day. The fact that the light intensity used in such experiments is of importance has been shown by Brown, Fingerman and Hines (1954).

That non-repeated light perturbations are capable of establishing or changing the phase of a persistent rhythm has been stated as an important generalization only in recent years (Pittendrigh and Bruce, 1957), although some previous studies (Kalmus, 1940; Webb, 1950) do provide examples of the phenomenon. The phenomenon provides another analogy between the characteristics of persistent rhythms and the known properties of physical oscillators. It is well known that a single disturbance or perturbation applied to an oscillating system will quite generally shift its phase without any modification to the period, and the behavior of a simple pendulum is a good example. Pittendrigh and Bruce (1957) have found phase shifts following single light perturbations in persistent rhythms of *Euglena* and *Drosophila,* and the rhythm in *Gonyaulax* provides another example of the phenomenon.

Detailed studies on the effect of the duration and intensity of single perturbations have not yet been reported in other organisms, but it appears that the nature of the phase shift in *Gonyaulax* may differ in one respect from that reported for *Drosophila* (Pittendrigh and Bruce, 1957). Following a single light perturbation in *Drosophila* there may occur "transients," so that the phase is not reset immediately but comes to its stable position only after several cycles. In *Gonyaulax,* on the other hand, phase has been found to be reset immediately. The reason for this difference is not known, but it may be related to the relative complexity of the organisms involved.

With respect to the phenomenon of phase shifting, Bruce and Pittendrigh (1957) have discussed whether the resetting signal is the step-up in light intensity (dawn) or the step-down in light intensity (dusk). Several experiments with *Gonyaulax* have adequately illustrated that the phase is labile to both, so that neither event may be said to be the timing cue to the exclusion of the other. For example, the experiments shown in Figure 3 illustrate both a light-to-dark transition followed by constant darkness, and a dark-to-light transition followed by constant light. In both cases, the last transition resulted in a phase shift.

The action spectrum for shifting the phase of the luminescence rhythm by a single light perturbation shows relatively sharp maxima in effectiveness at 475 mμ and 650 mμ (Hastings and Sweeney, unpublished). The red maximum, in particular, suggests that chlorophyll acts as a photosensitizer for phase shifting. Since the effects of single light perturbations are essentially the same in plants and animals, we may conclude that in *Gonyaulax* the photosensitizers involved in phase determination are not a part of the basic mechanism of rhythmicity. In animals, also, the photoreceptor pigments of the eye are not a part of the basic mechanism, although they function in phase determination by light. Whitaker (1940) reported that blinded mice possess a natural period of about 24 hours in their activity rhythm, but that the rhythm could not be entrained by 24-hour light-dark cycles to correspond with solar night and day, as in normal mice.

It is known that temperature changes (Pittendrigh, 1954; Stephens, 1957a), and perhaps certain other factors (Harker, 1958) may also serve to establish or reset phase. There is no report, however, that mechanical disturbances can be effective in other organisms in this regard.

The possibility that individuals in a population may entrain each other was suggested by Pittendrigh and Bruce (1957). However, Stephens (1957b) was unable to demonstrate any significant phase modification in individual fiddler crabs when they were placed together with crabs possessing a different phase. A similar result was found in the present studies with *Gonyaulax.*

It is of interest to note that the shape of the luminescence curve obtained in experiments where *Gonyaulax* cultures possessing different phases were mixed is not greatly different from that for the unmixed cultures. Indeed, as already pointed out, this is the expected result of adding two luminescence curves which are five hours out of phase with one another. Thus, a population composed of cells having at least two different phases is difficult to distinguish from the usual experimental populations, in which we have assumed that all cells possess the same phase. This experiment serves to caution us. In a biological rhythm having a sinusoidal shape, measurements from populations may not accurately represent the behavior of individual cells.

We do not know how the luminescence of the individual *Gonyaulax* cell at different times in the cycle compares with that measured in a population. The question is an important one, and there are several possibilities which, in the absence of any relevant data, need not be discussed here. This problem is being investigated utilizing measurements of the rhythm of cell division, where the performance of an individual cell may be repeatedly and relatively easily scored.

Although several suggestions have been made concerning the physico-chemical nature of the basic mechanism involved in persistent diurnal rhythmicity (Pittendrigh and Bruce, 1957; Hastings and Sweeney, 1958), none has received any substantial support. It is hoped that information concerning the extent and kind of biochemical changes associated with the rhythms will be of value in understanding this basic problem. Studies of this nature are in progress with *Gonyaulax.*

SUMMARY

1. The characteristics of a persistent diurnal rhythm of luminescence in the dinoflagellate *Gonyaulax polyedra* are described.

2. The light emission upon stimulation, from cultures which are kept in alternating light and dark periods of 12 hours each (= LD), is 40 to 60 times greater during the dark period than during the light period. If LD cultures are placed in continuous dim light (100 foot-candles) a diurnal rhythm of luminescence persists. If LD cultures are placed in continuous bright light (> 1500 foot-candles) the rhythm is damped, and no fluctuations occur in the amount of light emitted.

3. The occurrence of rhythmicity is not dependent upon prior exposure to LD conditions. Cultures which have been grown in bright light for as long as one year show a diurnal rhythm when placed in constant dim light or darkness. Cultures kept in alternating light and dark cycles which are greater or less than 24 hours similarly show a diurnal rhythm when returned to constant dim light or darkness. "Training" or "memory" is therefore not involved.

4. The rhythm can be entrained by light-dark cycles which are different from 24 hours. The period of the luminescence rhythm corresponds to light-dark cycles which have periods ranging between 12 and 32 hours.

5. The period of the rhythm is always close to 24 hours when the cells are kept under constant conditions, but it varies slightly depending upon the temperature and light intensity.

6. The phase of the rhythm under constant conditions is related to the time at which the previous light and dark periods occurred. Moreover, the phase may be shifted by interposing a non-repeated exposure to a different light intensity. The number of hours by which the phase is shifted in such an experiment is dependent upon the intensity and duration of the light treatment, and the time in the cycle when it is administered.

7. Exhaustive mechanical stimulation does not alter the phase of the rhythm.

8. When cultures having different phases were mixed, no evidence was found which would indicate that there was any interaction between them.

9. The evidence presented indicates that the diurnal rhythmicity is the consequence of a basic oscillatory mechanism which is inherent to the cell.

LITERATURE CITED

BALL, N. G., AND I. J. DYKE, 1954. An endogenous 24-hour rhythm in the growth rate of the *Avena* coleoptile. *J. Exp. Bot.*, **5**: 421–433.

BROWN, F. A., JR., AND H. M. WEBB, 1948. The temperature relations of an endogenous daily rhythmicity in the fiddler crab, *Uca*. *Physiol. Zoöl.*, **21**: 371–381.

BROWN, F. A., JR., M. N. HINES, H. M. WEBB AND M. FINGERMAN, 1950. Effects of constant illumination upon the magnitude of the diurnal rhythm of *Uca*. *Anat. Rec.*, **108**: 604.

BROWN, F. A., JR., M. FINGERMAN AND M. N. HINES, 1954. A study of the mechanism involved in shifting of the phases of the endogenous daily rhythm by light stimuli. *Biol. Bull.*, **106**: 308–317.

BRUCE, V. G., AND C. S. PITTENDRIGH, 1956. Temperature independence in a unicellular "clock." *Proc. Nat. Acad. Sci.*, **42**: 676–682.

BRUCE, V. G., AND C. S. PITTENDRIGH, 1957. Endogenous rhythms in insects and microorganisms. *Amer. Nat.*, **91**: 179–195.

BÜHNEMANN, F., 1955a. Die rhythmische Sporenbildung von *Oedogonium cardiacum* Wittr. *Biol. Zentralbl.*, **74**: 1–54.

BÜHNEMANN, F., 1955b. Das endodiurnale System der *Oedogonium*-Zelle. III. Über den Temperatureinfluss. *Zeitschr. Naturforschg.*, **10b**: 305–310.

Bünning, E., 1956. Endogenous rhythms in plants. *Ann. Rev. Plant Physiol.*, **7**: 71–90.

Harker, Janet E., 1958. Diurnal rhythms in the animal kingdom. *Biol. Rev.*, **33**: 1–52.

Harvey, E. N., 1952. Bioluminescence. Academic Press, New York, New York.

Hastings, J. W., and B. M. Sweeney, 1957a. The luminescent reaction in extracts of the marine dinoflagellate *Gonyaulax polyedra*. *J. Cell. Comp. Physiol.*, **49**: 209–226.

Hastings, J. W., and B. M. Sweeney, 1957b. On the mechanism of temperature independence in a biological clock. *Proc. Nat. Acad. Sci.*, **43**: 804–811.

Hastings, J. W., and B. M. Sweeney, 1958. The *Gonyaulax* clock. *In:* Photoperiodism and related phenomena in plants and animals (Ed., Alice P. Withrow), A.A.A.S. Press, Washington, D. C. (in press).

Haxo, F. T., and B. M. Sweeney, 1955. Bioluminescence in *Gonyaulax polyedra*. *In:* The luminescence of biological systems, pp. 415–420 (Ed., F. H. Johnson), A.A.A.S. Press, Washington, D. C.

Kalmus, H., 1940. Diurnal rhythms in the axolotl larva and in *Drosophila*. *Nature*, **145**: 72–73.

Pittendrigh, C. S., 1954. On temperature independence in the clock-system controlling emergence time in *Drosophila*. *Proc. Nat. Acad Sci.*, **40**: 1018–1029.

Pittendrigh, C. S., and V. G. Bruce, 1957. An oscillator model for biological clocks. *In:* Rhythmic and synthetic processes in growth, pp. 75–109 (Ed., Dorothea Rudnick), Princeton University Press.

Stephens, G. C., 1957a. Influence of temperature fluctuations on the diurnal melanophore rhythm of the fiddler crab, *Uca*. *Physiol. Zoöl.*, **30**: 55–69.

Stephens, G. C., 1957b. Twenty-four hour cycles in marine organisms. *Amer. Nat.*, **91**: 135–151.

Sweeney, B. M., and J. W. Hastings, 1957a. Characteristics of the diurnal rhythm of luminescence in *Gonyaulax polyedra*. *J. Cell. Comp. Physiol.*, **49**: 115–128.

Sweeney, B. M., and J. W. Hastings, 1957b. A persistent rhythm of cell division in populations of *Gonyaulax polyedra*. *Plant Physiol.*, **32**: XXV (Suppl.)

Sweeney, B. M., and J. W. Hastings, 1958. Rhythmic cell division in populations of *Gonyaulax polyedra*. *J. Protozoology*, **5**: 217–224.

Tribukait, B., 1954. Aktivitatsperiodik der Maus im kunstlich verkurtzen Tag. *Naturwiss.*, **41**: 92–93.

Wahl, O., 1932. Neue Untersuchungen über das Zeitgedachtnis der Bienen. *Zeitschr. vergl. Physiol.*, **16**: 529–589.

Webb, H. M., 1950. Diurnal variations of response to light in the fiddler crab, *Uca*. *Physiol. Zoöl.*, **23**: 316–337.

Webb, H. M., F. A. Brown, Jr. and M. I. Sandeen, 1954. A modification in the frequency of the persistent daily rhythm of the fiddler crab. *Anat. Rec.*, **120**: 796.

Whitaker, W. L., 1940. Some effects of artificial illumination on reproduction in the white-footed mouse, *Peromyscus leucopus noveboracensis*. *J. Exp. Zool.*, **83**: 33–60.

(1052)

Reprinted from Biological Bulletin, Vol. 115, No. 2, pp. 227–238, October, 1958
Printed in U. S. A.

ON THE EVOLUTION OF HEMOGLOBIN. RESPIRATORY PROPERTIES OF THE HEMOGLOBIN OF THE CALIFORNIA HAGFISH, POLISTOTREMA STOUTI[1]

CLYDE MANWELL

Scripps Institution of Oceanography of the University of California, La Jolla, California

The Cyclostomata, which is composed of the hagfishes (Myxinoidia) and the lampreys (Petromyzontia), is considered on morphological (Young, 1950) and biochemical (Florkin, 1949; Wald, 1952) evidence to be the most primitive group of living craniate vertebrates. Whereas the molecular weight of vascular hemoglobin of all known non-cyclostome vertebrates corresponds to four oxygen-combining units (hemes) per molecule, the hemoglobin of both hagfishes and lampreys consists of but a single heme per molecule (Svedberg, 1933; Lenhert, Lowe and Carlson, 1956). With regard to amino acid composition, cyclostome hemoglobin appears to be intermediate between vertebrate and invertebrate hemoglobins (Florkin, 1949).

The oxygen equilibrium of hemoglobin solutions prepared from the blood of the sea lamprey, *Petromyzon marinus*, has been recently studied (Wald and Riggs, 1951). This hemoglobin possesses a hyperbolic oxygen dissociation curve (as would be expected on the basis of the above-mentioned molecular weight), a low oxygen affinity, and an extremely large Bohr effect. Wald (1952) has claimed that the evolution of hemoglobin has proceeded in three stages (p. 366): "(1) the heme enzymes of cellular respiration [cytochrome oxidase being considered as the phylogenetic precursor of hemoglobin (Wald and Allen, 1957)]; (2) cell and tissue hemoglobins concerned primarily with oxygen storage; and, (3) circulatory hemoglobins, concerned with the transport of oxygen from the lungs, gills, and skin to the internal tissues." Wald emphasizes that in this progression the three main biochemical aspects of the combination of hemoglobin with oxygen are altered: (1) the oxygen dissociation curve changes from hyperbolic to sigmoid—*i.e.*, heme-heme interaction develops; (2) the affinity for oxygen decreases—*i.e.*, the oxygen molecule is held less tightly to the heme; and (3) the oxygen affinity becomes a function of pH—*i.e.*, a Bohr effect is developed.

In view of these facts concerning the cyclostomes, and Wald's (1952) theory on the evolution of hemoglobin, it is of interest to evaluate the oxygen equilibrium of the hemoglobin of the California hagfish, which is perhaps an even more primitive vertebrate than the lamprey.

The author wishes to thank Denis L. Fox and the other members of the Division of Marine Biology for their assistance in and discussion of these studies,

---

[1] Contribution from the Scripps Institution of Oceanography. New Series. no. ~~1062~~ 1059

and David Jensen for provision of hagfish and for assistance in bleeding of specimens.

MATERIALS AND METHODS

Blood was obtained from 30 specimens of the California hagfish, *Polistotrema stouti* (Lockington), formerly called *Bdellostoma* or *Eptatretus stouti.* The blood was collected by placing capillary tubes adjacent to the severed ends of blood vessels; no anticoagulant was necessary, for the blood of this animal has little clotting ability. The blood was occasionally contaminated with a trace of the ubiquitous slime; this was easily removed by diluting the blood with isotonic phosphate-buffered saline and filtering through glass wool. In several cases blood from a single animal provided enough hemoglobin for a single oxygen equilibrium determination. However, the hemoglobin concentration is low (3–4%), and usually less than 1 cc. of blood is available from each animal; therefore, blood from several animals was often pooled. Erythrocytes were either (1) washed once in 15 cc. of isotonic saline and used immediately for determination of the oxygen equilibrium of dilute erythrocyte suspensions (equivalent to whole blood), or (2) washed two more times and then hemolyzed. Distilled water hemolysis did not give satisfactory results; up to 80% of the hemoglobin remained inside the cell. Therefore, a trace of powdered saponin was added to a suspension of one volume of cells to two volumes of distilled water. Several hours later the hemoglobin solution was separated as a supernatant by centrifugation, diluted with an equal volume of potassium phosphate buffer ($\Gamma/2 = 0.4$) of the desired pH, and then filtered through Whatman No. 5 paper. Such a hemoglobin solution is stable for days, although (except where specifically indicated) it was used immediately for oxygen equilibrium measurements. Preparation of hemoglobin was at 0–1° C., except for centrifugation at 8–12° C.

Oxygen equilibria were evaluated as in previous studies (Manwell, 1958a, 1958b). Erythrocytes were suspended in 9 parts isotonic sodium chloride (0.54 *M*) to 1 part potassium phosphate buffer of desired pH. To eliminate rapid settling of cells during spectrophotometric determination of oxyhemoglobin, and to reduce light-scattering effects, many erythrocyte suspensions were diluted 3 : 1 with Karo (a mixture of sugars, dextrins, and soluble starch, which has a high refractive index and thus effects a partial clarification of the cell suspension). Erythrocytes could be stored for a week in such a medium without hemolysis, although this undesirable effect took place to a slight extent in a few experiments involving prolonged equilibration. Therefore, some experiments were performed on cells simply suspended in buffered saline to which a trace of powdered bovine serum albumin was added to increase cell stability; in these instances absolutely no hemolysis was observed during or for a day after equilibrium measurements, although there was greater fluctuation in spectrophotometric readings due to settling of cells and rouleaux.

Most experiments were performed at 18° C., slightly above the upper limit of the physiological temperature range of the hagfish. However, in connection with a determination of the heat of oxygenation of this hemoglobin some studies were made at 11° C., well within the normal temperature range, and at 29–30° C.

(1054)

RESULTS

Instead of presenting all data in the form of the usual "oxygen dissociation curve," the linear transformation based on the Hill approximation,

$$y = 100 \frac{(p/p_{50})^n}{1 + (p/p_{50})^n},$$

is used in Figures 1 and 3 (Lemberg and Legge, 1949). The variables y and p are the per cent oxyhemoglobin and the partial pressure of oxygen, respectively.

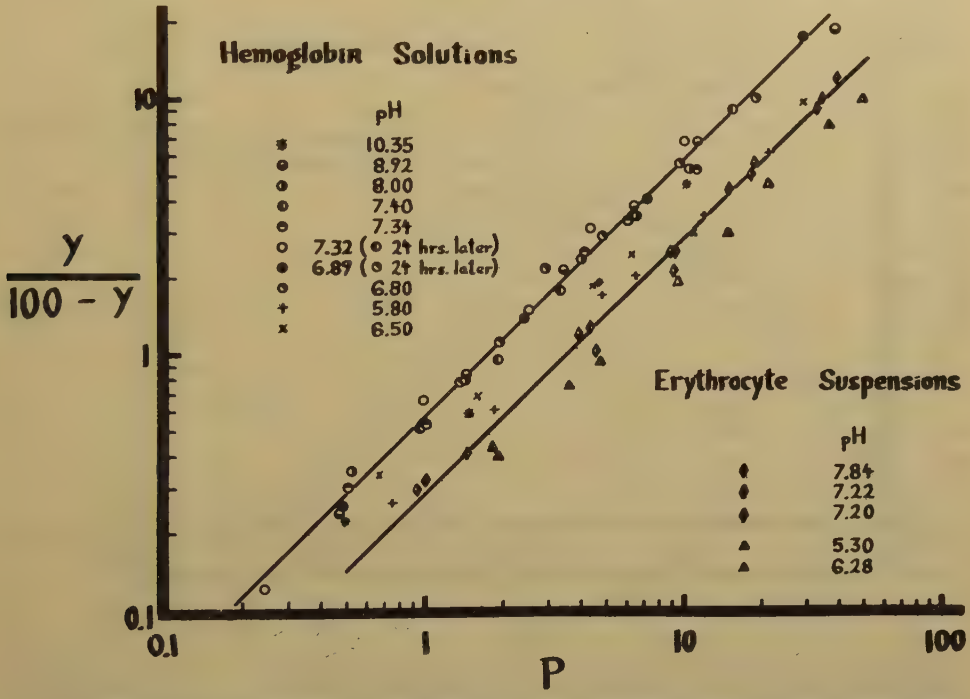

FIGURE 1. Oxygen equilibrium of hemoglobin of the California hagfish, *Polistotrema stouti*. Three to four per cent hemoglobin solutions in potassium phosphate buffer; final ionic strength = 0.2. Erythrocyte suspensions in isotonic phosphate-buffered saline with Karo added as explained in text. Temperature = 18° C. The solid lines are drawn arbitrarily with a slope (n) = 1.00 and a p_{50} corresponding to approximately physiological pH's.

That value of p for which y equals 50% is the p_{50}. The "sigmoid coefficient," n, is a measure of the heme-heme interactions. Hence, p_{50} is an inverse measure of the oxygen affinity, and n determines the shape of the oxygen dissociation curve. If the slope of the transformation, log $[y/(100 - y)]$ as a function of log p, is one, then the hemes are totally independent—*i.e.*, there is no heme-heme interaction. As can be seen from Figures 1 and 3, where the solid lines are drawn with a slope of 1.00, this is true of hagfish hemoglobin inside and outside the erythrocyte, and at high and low temperatures.

Between pH 6.7 and 9.0 hagfish hemoglobin in solution shows no detectable Bohr effect. Outside that pH range a significant decrease in oxygen affinity occurs; however, this effect appears to be a prelude to more drastic changes (methemoglobin formation and decrease in solubility), which become apparent several hours after equilibrium measurements. This is in contrast to the solutions at intermediate pH which are stable for days and display identical oxygen equilibria when re-analyzed one or two days after the original measurements (see Figure 1). No Bohr effect was observed for erythrocyte suspensions at pH's above neutrality; however, paralleling the behavior of hemoglobin in solution, a slight oxygen affinity decrease occurs at acid pH's. The effect was shown not only by the partially clarified suspensions (Fig. 1), but also when no Karo was present (Fig. 2). In contrast to hemoglobin solutions such acidic erythrocyte suspensions were stable, possibly because of the presence of cellular reducing systems able to reduce any methemoglobin. The observed decrease in oxygen affinity could represent a very small Bohr effect; however, until it is shown that the decrease in oxygen affinity is *rapid* and *entirely reversible*, the possibility of slight denaturative changes in the protein cannot be overlooked, especially in view of the results obtained for hemoglobin solutions.

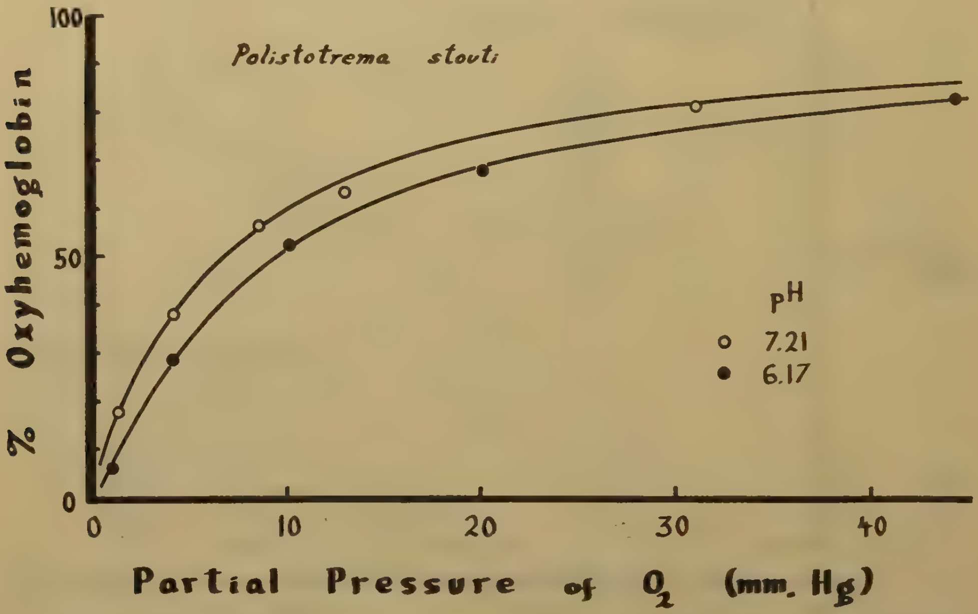

FIGURE 2. Oxygen dissociation curves of erythrocyte suspensions of the California hagfish, *Polistotrema stouti*, at two different pH's, showing the possible very slight Bohr effect. Erythrocytes in phosphate-buffered saline; no Karo present. Temperature = 20–21° C.

The presence of CO_2 specifically decreases the oxygen affinity, in addition to its effect resulting from the increase in acidity, for hemoglobin of the horse (Margaria and Milla, 1955) and the teleost *Sebastodes ruberrimus* (Manwell, unpublished data). That CO_2 does not cause any special Bohr effect for hagfish hemoglobin is shown in Figure 3.

Because the possible Bohr effect of hagfish hemoglobin is so small and occurs at almost one pH unit below the normal pH of hagfish blood (7.5–7.7; Prosser *et al*, 1950; David Jensen, personal communication), it is reasonable to assume that it is of no physiological significance, especially as CO_2 does not have any specific effect.

Knowledge of the heat of oxygenation (ΔH°) of hagfish hemoglobin enables one to predict the position of the oxygen equilibrium at any particular physiological temperature. In addition, absence of a Bohr effect facilitates the evaluation of ΔH°, for corrections representing the effects of ionizations of heme-linked groups do not need to be applied. Using data presented in Figure 3, a value of ΔH° = −9.3 kcal. (one atmosphere of dissolved oxygen gas at the standard state) was obtained as in a previous study (Manwell, 1958a). This value of ΔH° is similar to those observed for hemoglobin of sheep (− 8.2 kcal.; Paul and Roughton, 1951), the holothurian *Cucumaria miniata* (− 8.4 kcal.; Manwell, 1958f), and adult and fetal spiny dogfish, *Squalus suckleyi* (− 8.7 to − 9.5 kcal.; Manwell, 1958d). This group of values for the heat of oxygenation of various hemoglobins is not

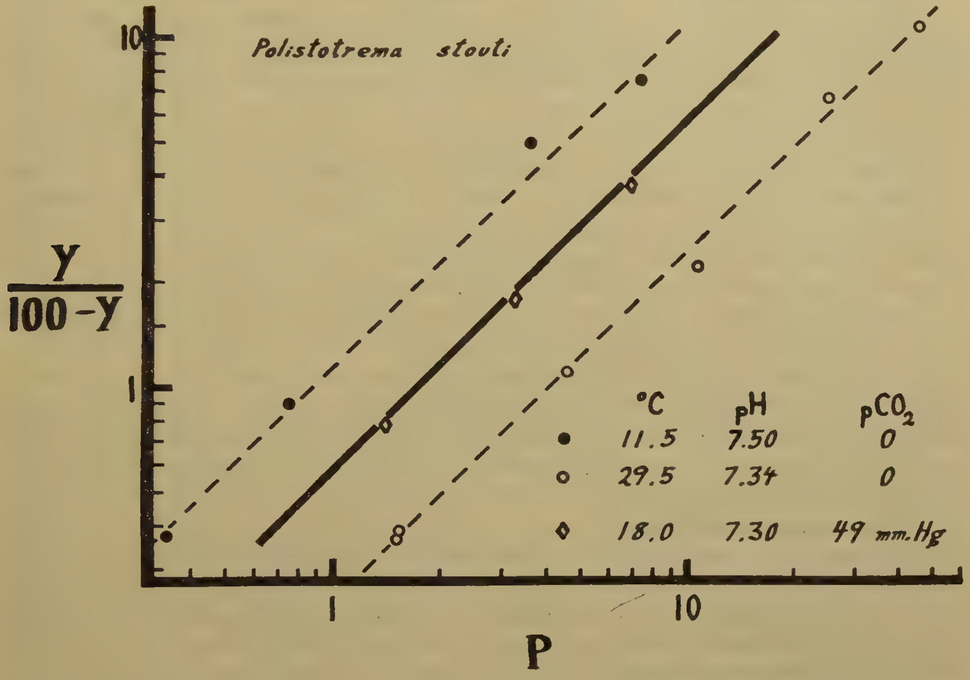

FIGURE 3. Oxygen equilibria under a variety of conditions of hemoglobin solutions prepared from the blood of the California hagfish, *Polistotrema stouti.* Dashed lines are drawn to approximate the oxygen equilibrium at 11.5 and 29.5° C. The solid line is drawn on the basis of data presented in Figure 1 in order to facilitate the comparison of hemoglobin solutions in the presence and in the virtual absence of CO_2.

characterized by the extensive variation seen in older data (reviewed by Paul and Roughton, 1951); theoretical considerations imply that there be relatively little variation in these values for a particular respiratory pigment, although significant differences occur between hemoglobin, hemocyanin, and hemerythrin (Klotz and Klotz, 1955; see, also, Manwell, 1958a).

DISCUSSION

Biochemical and Physiological

Hagfish hemoglobin has a hyperbolic oxygen dissociation curve. Beyond that point, however, resemblance to sea lamprey hemoglobin (Wald and Riggs, 1951) ceases. Hagfish hemoglobin lacks a Bohr effect over a pH range well in excess of pH's to be expected in living hagfish. The hagfish is, accordingly, the first adult vertebrate whose blood is known to lack a Bohr effect. In addition, the oxygen affinity of hagfish blood is very high—at physiological conditions as high, if not higher than that of any known vertebrate blood; the p_{50} is 2–4 mm. Hg[2] over the temperature range of 5–15° C. By way of comparison, p_{50} for human blood is 26 mm. Hg at pH $= 7.3$–7.4 and a temperature of 37° C. (Prosser *et al.*, 1950). *Arenicola* hemoglobin has an especially high oxygen affinity, $p_{50} = 2$–2.5 mm. Hg at 20° C. (Allen and Wyman, 1952); yet, by virtue of its extremely sigmoid oxygen dissociation curve ($n = 6$) *Arenicola* hemoglobin appears to be more suitable for oxygen transport than hagfish hemoglobin.

The comparison between hemoglobin solutions and erythrocyte suspensions prepared from the blood of the hagfish indicates that no specific interaction occurs between the hemes of adjacent hemoglobin molecules inside the cell. Hence, these data are consistent with—but do not necessarily establish—the idea that the molecular weight of hagfish hemoglobin *in situ* corresponds to but one heme per molecule—*i.e.*, approximately 17,000–18,000.

Comparison of the results with the introduction to this study shows that hagfish hemoglobin possesses all three of the features of the oxygenation reaction considered to be primitive by Wald (1952). However, the properties of hagfish hemoglobin, considered to be characteristic of *storage* hemoglobin by Wald, are displayed by a vascular hemoglobin, which one might accordingly assume to be involved in oxygen *transport*.

Living hagfish have been examined in an attempt to see whether there may be a significant difference in the color of blood entering and leaving the tissues and the gills, a condition which would indicate participation of the hemoglobin in oxygen transport. Unanesthetized hagfish were pinned at the extreme caudal and cranial ends (but not unnaturally stretched out) to a board immersed in oxygenated sea water at 10–12° C. The animals struggled violently until both ends were pinned down; they then remained quiescent for the duration of the experiment. A median ventral incision was made in the vicinity of the liver and the heart, care being taken to avoid cutting any blood vessels. The slime secretions were periodically removed. When slime production ceased, blood in the dorsal aorta (leaving the gills) and in various veins (leaving the tissues) was compared visually with "reduced" and oxygenated standards in hagfish blood vessels. Blood in the veins appeared to be almost de-oxygenated; blood in the arteries was approximately 50% oxygenated. This condition did not change over several hours of continuous observation. By reference to the oxygen dissociation curves, it can be seen that the internal oxygen tensions were extremely low, although the hemoglobin was functional in oxygen transport. An improved physiological experimental approach would be highly desirable; however, the hagfish—considering its small size, its surprisingly violent activity when handled, and its copious slime-producing abilities—is not an especially suitable form in which to determine arterial-venous oxygen concentrations.

---

[2] This approximate range of p_{50} for hagfish blood at physiological temperatures has been calculated (Manwell, 1958a) on the basis of the p_{50} for erythrocyte suspensions at 18° C. (see Fig. 1) and the heat of oxygenation ($\Delta H°$) of hagfish hemoglobin in solution.

Wald (1952) comments (p. 367): "The business of a circulatory hemoglobin, having combined with oxygen at the body surface, is to release it in the tissues *at high tensions. . . .*" (Italics are those of Wald.) Clearly, hagfish hemoglobin is biochemically unable to function in such a way; and, the observations made on living specimens tend to strengthen the idea of oxygen transport at *low* internal oxygen tensions in *Polistotrema stouti.* Redmond (1955) has found extensive evidence for oxygen transport at low internal oxygen tensions in several decapod crustaceans. Several studies indicate that such a condition also exists in some but not all annelids (reviewed by Eliassen, 1953; see also, Jones, 1954; Eliassen, 1955; Manwell, 1958e). Adult spiny dogfish, *Squalus suckleyi,* have a hemoglobin with a hyperbolic oxygen dissociation curve inside and outside the erythrocyte (Manwell, 1958d); yet, polarographically determined oxygen tensions of blood leaving the heart were never above 5 mm. Hg in 15 resting dogfish. Very low venous oxygen tensions have been observed in some teleosts—but not the mackerel (Black, 1951). Especially interesting in this regard is the marked *suppression* of heme-heme interaction by the erythrocytes of some teleosts and a species of holocephalian (Manwell, unpublished data); although n for clingfish *Gobiesox* hemoglobin in solution is 2.5–2.6 and thus approaches values of n for mammalian hemoglobins (2.6–3.0), inside the red blood cell the oxygen equilibrium of *Gobiesox* hemoglobin is almost devoid of heme-heme interaction ($n = 1.2$–1.4); this trend is exactly the opposite of what would be expected were the sigmoid oxygen dissociation curve always so vital for oxygen transport.

Under conditions where the tissues tolerate—or require—low oxygen tensions the properties usually associated with a transport hemoglobin would be of little selective advantage. In addition, if a large diffusion gradient were necessary to account for movement of sufficient oxygen across the epithelium of the gills or skin, then such properties as low oxygen affinity and large Bohr effect would prevent loading of the respiratory pigment with sufficient oxygen in the organ of external respiration. ("Sufficient" does not imply *complete* saturation; see Redmond, 1955.) Partial use of anaerobic metabolism could free tissues from dependence on large internal oxygen tension gradients. At the same time as such a rigorous dependence on oxygen were reduced, however, so would the metabolic efficiency decline (aerobic metabolism yielding several times more energy per unit weight of substrate than anaerobic metabolism). Consequently, one might expect large, very active animals (*e.g.*, cephalopods, some fishes, birds, and mammals) to have evolved increasing dependence on the more efficient aerobic metabolic pathways—and at the same time oxygen transport at high internal oxygen tensions. In such cases the sigmoid oxygen dissociation curve, the low oxygen affinity, and the large Bohr effect would be of the greatest selective advantage in increasing the efficiency of the respiratory pigment. It is well known that squid hemocyanin, mammalian and avian hemoglobins, and mackerel and trout hemoglobins possess all of these characteristics (reviewed by Florkin, 1949; Prosser *et al.*, 1950).

Phylogenetic

In terms of Wald's (1952) previously mentioned theory on the origin and evolution of hemoglobin one might be tempted to infer that the primitive hagfish has retained in a hemoglobin used in oxygen transport all three oxygenation properties to be expected of hemoglobin in an earlier stage of evolution—that represented by an oxygen storage hemoglobin. However, some or all of the properties of hagfish hemoglobin may represent specialization to a particular mode of life far different from that of known fossil Agnatha. The hagfishes are, in spite of some primitive characteristics, well-adapted, biologically successful animals. Over several types of ocean bottom in temperate seas the hagfishes are among the dominant scavengers—or parasites—feeding on dead and dying fishes; they are often present in such numbers as to restrict or prevent several types of fishing operations (Young, 1950). Certain characteristics of the hagfish, such as the rasping tongue, complete absence of scales and bone, and the habit of feeding on teleost fishes, are not properties of fossil Agnatha (Ostracoderms). These features must have evolved independently of other aspects of early vertebrate phylogeny. The differences in the properties of sea lamprey (Wald and Riggs, 1951) and hagfish hemoglobin may be correlated with the well-known ecological observation: the hagfish enters, often in large numbers, the body of its prey and thus is often exposed to low O_2 and high CO_2 tensions; the lamprey remains attached to the surface of its host, thereby having well-oxygenated water of low carbon dioxide tension available for its respiration at all times. In addition, so far as is known, the hagfish does not make any sustained active movement comparable to the anadromous migration of the sea lamprey.

Several other objections to Wald's (1952) theory in its present form can be raised:

(1) Cytochrome oxidase has been considered the phylogenetic precursor of hemoglobin because: (a) it combines reversibly with CO and reacts with O_2; and, (b) beef heart cytochrome oxidase has an extremely high oxygen affinity, no Bohr effect, and an almost hyperbolic equilibrium curve with CO—all properties that a "primitive" hemoglobin ought to possess (Wald and Allen, 1957). Unfortunately, neither the prosthetic group (Paul, 1951; Stotz, Morrison and Marinetti, 1956) nor the protein moiety (Lemberg and Legge, 1949) of this respiratory enzyme (or enzyme complex) resembles the corresponding parts of hemoglobin as closely as might be desired. Cytochrome *c* would be a better, although not entirely satisfactory, hemoglobin phylogenetic precursor. At least its prosthetic group is the same as that of hemoglobin, although linked to the protein differently; and, its protein moiety is readily water-soluble, although of lower molecular weight (one heme per 13,000–15,000) and higher isoelectric point (pI = 10) (Paleus, 1955) than any known hemoglobin. When the heme of cytochrome *c* is not completely protected by coordination of the iron with the imidazole groups of two

histidine residues, the enzyme combines with CO and is oxidized by O_2 (Lemberg and Legge, 1949; Theorell, 1956). Bartsch and Kamen (1958) isolated a bacterial heme protein—originally called a "pseudohemoglobin"—which resembles cytochrome *c* in many respects, although its isoelectric point (pI = 5) is comparable to that of invertebrate and cyclostome hemoglobins (Prosser *et al.*, 1950) and it is readily oxidized by O^2 and combines reversibly with CO. The carbon monoxide reaction of this bacterial heme protein is *not* invariant to pH change—in contrast to cytochrome oxidase (Wald and Allen, 1957). In support of *some* connection between the syntheses of cytochrome and hemoglobin is the finding of Ycas (1956) that aerobically grown yeast in the presence of antimycin produces less cytochrome *a* and more hemoglobin than controls; however, as Ycas suggests, this relation may be explained by assuming that the heme of hemoglobin is a precursor to the modified heme of cytochrome *a*. At present there is so little comparative biochemical information on the cytochromes and other heme-containing enzymes that one cannot rule out the possibility that the proteins of various hemoglobins have arisen from apoenzymes of quite unrelated biocatalysts; certainly, the protoheme prosthetic group is always phylogenetically available. Several proteins besides globin will combine with heme, although none are yet known that will enable this heme to combine reversibly with molecular oxygen (Lemberg and Legge, 1949).

(2) Wald (1952) states (p. 369): "The hemoglobins that have arisen so sporadically among invertebrates of various orders are all storage hemoglobins." However, oxygen transport by hemoglobin occurs in several annelids (Johnson, 1942; Eliassen, 1955; reviewed by Eliassen, 1953; Manwell, 1958e), the brine shrimp *Artemia* (Gilchrist, 1954), and even such small arthropods as daphnids (Hoshi, 1957). As the experiments of Redmond (1955) show, the presence of a respiratory pigment in the blood of invertebrates in low concentration does not rule out significant oxygen transport by that pigment. Coelomic hemoglobins, such as those of *Urechis* (Redfield and Florkin, 1931) and *Cucumaria miniata* (Manwell, 1958f), are usually assumed to function in oxygen storage; however, the movement of coelomic fluid, either by muscular contraction or cilia, presents the possibility of oxygen transport by the coelomic hemoglobin from cloacal diverticula (*Urechis*) or respiratory trees (*Cucumaria*) to tissues in or adjacent to the coelom.

(3) That a hyperbolic oxygen dissociation curve, high oxygen affinity, and no Bohr effect should represent primitive conditions (Wald, 1952) requires comment. The properties of the oxygen equilibrium of the vertebrate storage hemoglobin (myoglobin) rest on studies of crude extracts or purified preparations prepared from the muscles of five species of mammals (reviewed by Lemberg and Legge, 1949; see also, Rossi-Fanelli and Antonini, 1958). As Lemberg and Legge point out, the oxygen equilibrium of myoglobin *in situ* in the muscle remains to be evaluated. The findings, that n could be as high as 1.6 for oxygen equilibria of extractions of *Cryptochiton* myoglobin (Manwell, 1958c) and that n could be as high as 2.8 in the reaction of horse metmyoglobin with various ligands (Kiese and Kaeske, 1942), indicate that heme-heme interactions can exist under certain conditions in tissue hemoglobins. One would expect tissue hemoglobins to have a high oxygen affinity because of limitations on the intracellular oxygen tensions imposed by the combination of passive diffusion of oxygen and aerobic cellular

metabolism. In the case of *Cryptochiton* even when the oxygen dissociation curve of the radular myoglobin is sigmoid, it lies far to the left of the corresponding curve for the vascular hemocyanin; hence, the presence of heme-heme interactions in the myoglobin does not interfere with the functional oxygen transfer system (Manwell, 1958c). Interactions between oxygen-affine centers have evolved in all four major classes of respiratory pigments (hemoglobin, hemocyanin, chlorocruorin, and hemerythrin); Bohr effects are found in all these classes except hemerythrin (reviewed by Prosser *et al.*, 1950).[3]

There is reason to believe that heme-heme interactions and the Bohr effect are not necessarily specialized acquisitions restricted to respiratory pigments in an advanced state of evolution but are expressions of very basic properties found in many unrelated proteins. The frequently observed variation of enzyme kinetics as a function of pH often involves interaction between proton-affine centers on the protein moiety and the active center (Alberty, 1956). Heme-heme interaction, likewise, has its parallel in the interaction between centers having similar reactivities in proteins possessing two or more such sites per molecule. Such interactions occur in the binding of dyes and ions to some multivalent proteins (Klotz, 1954) and in the kinetics of some enzymes (Botts and Morales, 1953).

Finally, the ease with which certain reagents (various mercurials, formaldehyde, and glutathione) will remove the heme-heme interactions, partially restore those interactions, greatly increase the oxygen affinity, and/or modify the Bohr effect (Guthe, 1954; Riggs and Wolbach, 1956) implies that these properties are not invariant for a particular hemoglobin molecule. In addition, the differences in the oxygen equilibrium of some hemoglobins inside and outside the red blood cell (Root, Irving and Black, 1939; Manwell, unpublished data) indicate also that a considerable lability exists with regard to the properties of the oxygen equilibrium.

It seems reasonable to assume that the phylogenetic order of first appearances was: heme-containing respiratory enzymes, tissue hemoglobins, vascular hemoglobins. However, the present discussion indicates the difficulty of knowing (a) if a certain set of characteristics of the oxygen-hemoglobin equilibrium—*e.g.*, high oxygen affinity, no heme-heme interactions, and no Bohr effect—is basically primitive, and (b) if any particular component of the cytochrome system or any other heme-containing enzyme is evolutionally the forerunner of hemoglobin.

SUMMARY

1. Oxygen equilibria of hagfish hemoglobin inside and outside the red blood cell have been obtained under a variety of conditions. The oxygen affinity of the hemoglobin in the erythrocyte suspensions is high ($p_{50} = 3$–4 mm. Hg at 18°), although it is even higher in hemoglobin solutions ($p_{50} = 1.8$ mm. Hg at 18° C.). There is no interaction between hemes ($n = 1.00$) and virtually no Bohr effect. The effect of temperature on the oxygen equilibrium of hagfish hemoglobin is

---

[3] Absence of the Bohr effect has been confirmed for various sipunculid coelomic hemerythrins (Manwell, 1958a, and unpublished studies on *Dendrostomum zostericolum* and *Siphonosoma ingens*); however, the coelomic hemerythrin of the brachiopod *Lingula*, a form that is morphologically essentially unchanged since the Cambrian period, has a Bohr effect that is two-thirds the magnitude of that observed for human adult hemoglobin (Manwell, 1958, unpublished experiments)!

similar to that observed in recent experiments on other hemoglobins ($\Delta H^\circ = -9.3$ kcal. for hagfish hemoglobin).

2. Several aspects of Wald's (1952; see, also, Wald and Allen, 1957) theories on the evolution and function of hemoglobin are criticized in view of these data on hagfish hemoglobin and on the basis of information in the literature. It is concluded that: (1) At present there is no reason to favor cytochrome oxidase as *the* phylogenetic precursor of hemoglobin. (2) Many invertebrate hemoglobins function in oxygen transport. (3) If the internal oxygen tensions are sufficiently low, a respiratory pigment participating in oxygen transport does not need to possess a low oxygen affinity, a sigmoid oxygen dissociation curve, and a marked Bohr effect. (4) It is impossible to say if a particular set of properties of the oxygen equilibrium is basically "primitive." (5) Physiological conclusions on hemoglobin should be made upon studies of the pigment *in the natural condition—i.e.*, myoglobin in the muscle, or intracellular vascular hemoglobin in the erythrocyte.

LITERATURE CITED

Alberty, R. A., 1956. Kinetic effects of the ionization of groups in the enzyme molecule. *J. Cell. Comp. Physiol.*, **47**, Sup. 1: 245–281.

Allen, D. W., and J. Wyman, 1952. The oxygen equilibrium of hemerythrin of *Arenicola cristata*. *J. Cell. Comp. Physiol.*, **39**: 383–389.

Bartsch, R. G., and M. D. Kamen, 1958. On the new heme protein of facultative photoheterotrophs. *J. Biol. Chem.*, **230**: 41–63.

Black, E. C., 1951. Respiration in fishes. *Univ. Toronto Studies Biol. No. 59*: 91–111.

Botts, J., and M. Morales, 1953. Analytical description of the effects of modifiers and of enzyme multivalency upon the steady state catalyzed reaction rate. *Trans. Faraday Soc.*, **49**: 1–12.

Eliassen, E., 1953. The physiology of the vascular system of invertebrates. I. A monography on the blood pigments. *Univ. Bergen Arbok, Naturvit. rekke*, **11**: 1–65.

Eliassen, E., 1955. The oxygen supply during ebb of *Arenicola marina* in the Danish Waddensea. *Univ. Bergen Arbok, Naturvit. rekke*, **12**: 1–9.

Florkin, M., 1949. Biochemical Evolution. Edited and translated by S. Morgulis. Academic Press, New York.

Gilchrist, B. M., 1954. Haemoglobin in *Artemia*. *Proc. Roy. Soc. London, Ser. B*, **143**: 136–146.

Guthe, K. F., 1954. The effect of formaldehyde on the oxygen equilibrium of hemoglobin. *J. Gen. Physiol.*, **37**: 775–780.

Hoshi, T., 1957. Studies on physiology and ecology of plankton. XIII. Haemoglobin and its role in the respiration of the daphnid, *Simocephalus vetulus*. *Sci. Rep. Tohoku Univ., 4th Ser. (Biology)*, **23**: 35–58.

Johnson, M. L., 1942. The respiratory function of the haemoglobin of the earthworm. *J. Exp. Biol.*, **18**: 266–277.

Jones, J. D., 1954. Observations on the respiratory physiology and on the haemoglobin of the polychaete genus *Nephthys*, with special reference to *N. hombergii* (Aud. et M.-Edw.). *J. Exp. Biol.*, **32**: 110–125.

Kiese, M., and H. Kaeske, 1942. Verbindungen des Muskelhämoglobins. *Biochem. Zeitschr.*, **312**: 121–149.

Klotz, I., 1954. Protein interactions. *In:* The Proteins, H. Neurath and K. Bailey, eds. Academic Press, New York, Vol. 1, Part A, 727–806.

Klotz, I., and T. A. Klotz, 1955. Oxygen-carrying proteins: a comparison of the oxygenation reaction in hemocyanin and hemerythrin with that in hemoglobin. *Science*, **121**: 477–480.

Lemberg, R., and J. W. Legge, 1949. Hematin Compounds and Bile Pigments. Interscience Publishers, Inc., New York.

LENHERT, P. G., W. E. LOWE AND F. D. CARLSON, 1956. The molecular weight of hemoglobin from *Petromyzon marinus*. *Biol. Bull.*, **111**: 293–294.

MANWELL, C., 1958a. Oxygen equilibrium of *Phascolosoma agassizii* hemerythrin. *Science*, **127**: 592–593.

MANWELL, C., 1958b. Respiratory properties of the hemoglobin of two species of diving birds. *Science*, **127**: 705–706.

MANWELL, C., 1958c. Oxygen equilibrium of myoglobin and hemocyanin from the amphineuran mollusc *Cryptochiton stelleri*. *J. Cell. Comp. Physiol.*, in press.

MANWELL, C., 1958d. A "Fetal-Maternal Shift" in the ovoviviparous spiny dogfish *Squalus suckleyi*. *Physiol. Zoöl.*, in press.

MANWELL, C., 1958e. Alkaline denaturation and oxygen equilibrium of annelid hemoglobins. *J. Cell. Comp. Physiol.*, in press.

MANWELL, C., 1958f. Oxygen equilibrium of *Cucumaria miniata* hemoglobin and the absence of the Bohr effect. *J. Cell. Comp. Physiol.*, in press.

MARGARIA, R., AND E. MILLA, 1955. Effetti acidificanti dell'ossigenazione dell'Hb in condizioni fisiologiche. *Boll. Soc. ital. biol. sper.*, **31**: 1250–1253.

PALEUS, S., 1955. Studies on cytochrome *c*. *Svensk. Kem. Tidskr.*, **67**: 273–290.

PAUL, K. G., 1951. The iron-containing enzymes. A. Cytochromes. *In:* The Enzymes, J. B. Sumner and K. Myrback, eds. Academic Press, New York, Vol. 2, Part 1: 357–396.

PAUL, W., AND F. J. W. ROUGHTON, 1951. The equilibrium between oxygen and sheep haemoglobin at very low percentage saturations. *J. Physiol.*, **113**: 23–35.

PROSSER, C. L., D. W. BISHOP, F. A. BROWN, JR., T. L. JAHN AND V. J. WULFF, 1950. Comparative Animal Physiology. Saunders, Philadelphia.

REDFIELD, A. C., AND M. FLORKIN, 1931. The respiratory function of the blood of *Urechis caupo*. *Biol. Bull.*, **61**: 185–210.

REDMOND, J. R., 1955. The respiratory function of hemocyanin in crustacea. *J. Cell. Comp. Physiol.*, **46**: 209–247.

RIGGS, A. F., AND R. A. WOLBACH, 1956. Sulfhydryl groups and the structure of hemoglobin. *J. Gen. Physiol.*, **39**: 585–605.

ROOT, R. W., L. IRVING AND E. C. BLACK, 1939. The effect of hemolysis on the combination of oxygen with the blood of some marine fishes. *J. Cell. Comp. Physiol.*, **13**: 303–313.

ROSSI-FANELLI, A., AND E. ANTONINI, 1958. Reversible splitting of human myoglobin. Physicochemical properties and oxygen equilibrium of reconstituted proto- and deutero-myoglobin. *Arch. Biochem. Biophys.*, **72**: 243–244.

STOTZ, E. H., M. MORRISON AND G. MARINETTI, 1956. Components of the cytochrome system. *In:* Enzymes: Units of Biological Structure and Function, O. H. Gaebler, ed. Academic Press, New York, 401–416.

SVEDBERG, T., 1933. Sedimentation constants, molecular weights, and isoelectric points of the respiratory proteins. *J. Biol. Chem.*, **103**: 311–325.

THEORELL, H., 1956. Nature and mode of action of oxidizing enzymes. *Science*, **124**: 467–470.

WALD, G., 1952. Biochemical evolution. *In:* Modern Trends in Physiology and Biochemistry, E. S. G. Barron, ed. Academic Press, New York, 337–376.

WALD, G., AND D. W. ALLEN, 1957. The equilibrium between cytochrome oxidase and carbon monoxide. *J. Gen. Physiol.*, **40**: 593–608.

WALD, G., AND A. RIGGS, 1951. The hemoglobin of the sea lamprey, *Petromyzon marinus*. *J. Gen. Physiol.*, **35**: 45–53.

YCAS, M., 1956. Formation of Hb and the cytochromes by yeast in the presence of antimycin "A." *Exp. Cell. Res.* **11**: 1–6.

YOUNG, J. Z., 1950. Life of the Vertebrates. Oxford University Press.

(1064)

Reprinted from *Printed in U.S.A.*
THE PHYSICS OF FLUIDS VOLUME 1, NUMBER 6 NOVEMBER-DECEMBER, 1958

Surface Wake of a Submerged Sphere*

CARL ECKART
Scripps Institution of Oceanography, University of California, La Jolla, California
(Received August 13, 1958)

The problem of a sphere moving in an infinite homogeneous incompressible liquid has been discussed by many writers. The corresponding problem for a semi-infinite liquid with a free surface has not been treated earlier.

It is shown that the surface wake of such a submerged sphere is approximately the same as that which would be caused by a traveling pressure disturbance in the atmosphere above the free surface. This is, essentially, a consequence of the Bernoulli theorem.

If the motion is sufficiently slow, the surface reacts to this equivalent pressure as a barometer (equilibrium theory). For more rapid motions, dynamic effects reduce the response of the surface, but leave a wake in the region already traversed by the sphere. The calculation of this wake involves the usual distinction between incoming and outgoing waves, which is introduced in the Fourier transform of the solution. The resulting integrals are evaluated by Kelvin's approximate method of stationary phase.

1. INTRODUCTION

THE problem of a sphere moving in a homogeneous incompressible liquid has been solved, but under strongly simplifying assumptions.[1] The results obtained in this way may be formulated as follows. Let the sphere, of radius a, move along the x axis with the constant velocity S, and let the velocity of the fluid at the point x, y, z be

$$\mathbf{u} = -\nabla\phi. \tag{1}$$

Then

$$\begin{aligned}\phi &= \tfrac{1}{2}Sa^3(x - St)/r^3\\ &= \tfrac{1}{2}a^3\,\frac{\partial}{\partial t}\left(\frac{1}{r}\right),\end{aligned} \tag{2}$$

where r is the distance from x, y, z to the momentary center of the sphere,

$$r^2 = (x - St)^2 + y^2 + z^2. \tag{3}$$

This result rests on three major assumptions:

I. There is no free surface or other boundary to the fluid;

II. A steady state has been reached without
  A. creating vorticity;
  B. creating turbulence.

Consequently, Eqs. (1), (2), (3) do not represent the facts. For example, the sphere experiences no drag force, and leaves no wake.

The first point can be established by calculating the pressure:

$$\begin{aligned}p &= \rho\,\partial\phi/\partial t\\ &= \tfrac{1}{2}\rho S^2a^3[3(x - St)^2 - r^2]/r^5.\end{aligned} \tag{4}$$

When any component of this pressure is integrated over the surface of the sphere, the result is zero.

The second point follows at once from the fact that $\mathbf{u}$ approaches zero very rapidly with distance from the sphere—inversely as the cube of this distance.

Consequently, it becomes necessary to consider

---

* Contribution No. 387 from Scripps Institution of Oceanography.

[1] H. Lamb, *Hydrodynamics* (Dover Publications, New York, 1945), p. 123.

Contributions from the Scripps Institution of Oceanography, New Series, No. 1060
Reproduced by Permission

how the three simplifying assumptions can be eliminated. This is particularly important in the case of I since the surface expression of the wake is of interest. The other assumptions will not be considered here.

2. SURFACE EFFECTS: EQUILIBRIUM THEORY

The linearized equations for a homogeneous incompressible fluid, with its free undisturbed surfaces at $z = 0$ and of infinite depth, can be reduced to

$$\rho(\partial\mathbf{u}/\partial t) = -\nabla p, \tag{5}$$

$$\nabla^2 p = 0, \tag{6}$$

$$\frac{\partial^2 p}{\partial t^2} + g\frac{\partial p}{\partial z} = 0 \quad \text{at} \quad z = 0, \tag{7}$$

$$p = 0 \quad \text{at} \quad z = -\infty. \tag{8}$$

If there is a rigid sphere, moving with velocity S along the line $z = -D$, $y = 0$, an additional condition must be satisfied,

$$\mathbf{n}\cdot\mathbf{u} = S\mathbf{i}\cdot\mathbf{n}, \tag{9}$$

on the surface of the sphere, where $\mathbf{n}$ is the unit normal to the surface, and $\mathbf{i}$ the direction of motion.

Equations (1), (2), and (4) do not satisfy Eq. (7), but do satisfy the others. Set

$$p = p_0 + p_1, \tag{10}$$

where p_0 is given by the last line of Eq. (4). Then p_1 must satisfy the equations

$$\nabla^2 p_1 = 0, \tag{11}$$

$$\frac{\partial^2 p_1}{\partial t^2} + g\frac{\partial p_1}{\partial z} = -\left\{\frac{\partial^2 p_0}{\partial t^2} + g\frac{\partial p_0}{\partial z}\right\} \quad \text{at} \quad z = 0, \tag{12}$$

$$p_1 = 0 \quad \text{at} \quad z = -\infty. \tag{13}$$

It must also satisfy an equation like Eq. (9), but this will be ignored. This is justifiable, to a first approximation, if the sphere is not too close to the surface—$a/D \ll 1$. Successively better approximations can be obtained, if necessary by Riemann's alternating procedure.[2]

If, instead of being caused by the moving sphere, p_1 were caused by an atmospheric pressure disturbance, A, Eq. (12) would be replaced by

$$\frac{\partial^2 p_1}{\partial t^2} + g\frac{\partial p_1}{\partial z} = \frac{\partial^2 A}{\partial t^2} \quad \text{at} \quad z = 0. \tag{14}$$

Equations (12) and (14) may therefore be combined to calculate an equivalent atmospheric pressure that would cause the same wake as the sphere. This is readily found to be

$$A = -\tfrac{1}{2}\rho a^3\left\{S^2\,\frac{3(x - St)^2 - R^2}{R^5} - g\,\frac{D}{R^3}\right\}, \tag{15}$$

where

$$R^2 = (x - St)^2 + y^2 + D^2. \tag{16}$$

At the epicenter of the moving sphere, $x = st$, and $R = D$; therefore

$$A_e = \frac{1}{2}\left(\frac{a}{D}\right)^3[\rho S^2 + \rho g D]. \tag{17}$$

At any point, the surface displacement will almost certainly not be greater than

$$A_e/\rho g = \frac{1}{2}\left(\frac{a}{D}\right)^3[S^2/g + D], \tag{18}$$

which yields a high estimate of the order of magnitude of the surface displacement. Table I gives numerical values of the two terms of Eq. (18), for a sphere of 10-meter radius. The displacements listed may be compared to the "equilibrium tidal heights"; they ignore dynamic effects, and are likely to be serious overestimates for the larger values of S and smaller values of D. In particular, the dynamic theory will show that the two terms of Eq. (15) make approximately the same contribution to the wake.

TABLE I. $a = 10$ meters.

S, m/sec	D, meters	$\frac{1}{2}(a/D)^3\,S^2/g$ meters	$\frac{1}{2}\,a^3/D^2$ meters
0.5	50	10^{-4}	0.20
5.0		0.01	
25.0		0.25	
0.5	100	1.25×10^{-5}	0.05
5.0		1.25×10^{-3}	
25.0		3.1×10^{-2}	
0.5	200	1.6×10^{-6}	0.0125
5.0		1.6×10^{-4}	
25.0		4.0×10^{-3}	

3. SURFACE EFFECTS: DYNAMIC THEORY

In Sec. 2, the dynamic theory of the surface effects has been reduced to the theory of a traveling atmospheric pressure disturbance. This is somewhat similar to the idea of the "Bernoulli effect." The pressure disturbance problem has been treated by various writers. The present status of the literature is fairly well represented by Lamb,[1] (p. 464 *et seq.*); Havelock,[3] (pp. 42–46); Eckart[4]; and Stoker.[5]

---

[2] P. Frank and R. von Mises, *Die Differential-und Integralgleichungen der Mechanik und Physik* (Vieweg, Braunschweig, 1935), Vol. 2, p. 642.

(1066)

A somewhat more complete treatment of the steady-state problem will be attempted here; consequently all variables depend only on $x - st$, y, and z; without loss of generality, one may set $t = 0$. Equations (11), (13), and (14) may then be written (the subscript on p_1 being omitted)

$$\nabla^2 p = 0, \tag{19}$$

$$\frac{\partial^2 p}{\partial x^2} + \kappa \frac{\partial p}{\partial z} = \frac{\partial^2 A}{\partial x^2} \tag{20}$$

$$\kappa = g/S^2, \tag{21}$$

$$p = 0 \quad \text{at} \quad z = -\infty. \tag{22}$$

It will be supposed that the equivalent atmospheric pressure has been expressed as a Fourier integral:

$$A(x, y) = \Re \iint' B(\alpha, \beta) e^{i(\alpha x + \beta y)} \, d\alpha \, d\beta, \tag{23}$$

the symbol $\Re$ indicating that the real part of the integral is equal to A, and the accent, that the range of integration is

$$0 \leq \alpha \leq \infty,$$

$$-\infty \leq \beta \leq \infty.$$

In order to write out the general solution for p an auxiliary variable of integration, σ, is needed, whose range is

$$0 \leq \sigma \leq \infty.$$

This is the condition for outgoing waves, analogous to the Sommerfeld radiation condition; if σ were given the range $-\infty \rightarrow 0$, incoming waves would be obtained. Then the solution is

$$p = \Re \iiint' (-i\alpha^2 B) \exp [i(\alpha x + \beta y) + kz + i\sigma(\alpha^2 - \kappa k)] \, d\alpha \, d\beta \, d\sigma, \tag{24}$$

where

$$k = (\alpha^2 + \beta^2)^{\frac{1}{2}} \geq 0.$$

The integral is conditionally convergent, and the integration over σ must be performed last. That Eq. (25) satisfies Eqs. (19) and (22) follows from an inspection of the integrand. When Eq. (24) is substituted into the left side of Eq. (20), the integral becomes convergent; it becomes possible to perform the integration over σ first, and to show that the two sides of Eq. (20) are identical. The surface displacement, h, can be calculated from Eq. (24) as

$$\rho g h = \Re \iiint' (-i\alpha^2 B) \exp \{i[\alpha x + \beta y + \sigma(\alpha^2 - \kappa k)]\} \, d\alpha \, d\beta \, d\sigma, \tag{25}$$

and only this integral will be treated.

The practical solution of our problem thus required two calculations:

1. the determination of B from Eq. (15);
2. the evaluation of the integral in Eq. (25).

The first calculation is given in Appendix I and yields the result

$$B = (a^3/2\pi k) e^{-kD} (\rho S^2 \alpha^2 + \rho g k). \tag{26}$$

It is necessary to discuss the second calculation in more detail, otherwise the reader will not understand the result. Equation (25) may be written

$$\rho g h = \Re \iiint' (-i\alpha^2 B) e^{iP} \, d\alpha \, d\beta \, d\sigma, \tag{27}$$

where the phase is

$$P = \alpha x + \beta y + \sigma(\alpha^2 - \kappa k). \tag{28}$$

The introduction of polar coordinates

$$\begin{aligned} x &= -r \cos \phi, & y &= r \sin \phi, \\ \alpha &= k \cos \theta, & \beta &= k \sin \theta, \end{aligned} \tag{29}$$

(note the minus sign and that $-\pi/2 \leq \theta \leq \pi/2$) converts Eq. (29) into

$$P = -kr \cos (\theta + \phi) + \sigma(k^2 \cos^2 \theta - \kappa k). \tag{30}$$

An approximation to h can be obtained by using Kelvin's method of stationary phase,[1,3,5,6] which is essentially a generalization of the Fraunhofer-Cornu method of solving diffraction problems. The idea is that in those parts of the range of integration where P changes rapidly, the values of the integrand average out and make no contribution to the value of the integral. This is determined only by the values of B and P at or near the points where the derivatives of P vanish. These are the points of stationary phase.

In the present case, they are determined by solving the equations

$$\partial P/\partial \sigma = k^2 \cos^2 \theta - \kappa k = 0, \tag{31}$$

---

[3] J. H. Havelock, *The Propagation of Disturbances in Dispersive Media.* (Cambridge University Press, New York, 1914).

[4] C. Eckart, J. Appl. Phys. **24**, 1485 (1953).

[5] J. J. Stoker, *Water Waves* (Interscience Publishers, Inc., New York, 1957) Chap. 8.

[6] C. Eckart, Revs. Modern Phys. **20**, 399 (1948).

$$\partial P/\partial k = -r\cos(\theta+\phi) + \sigma(2k\cos^2\theta - \kappa) = 0, \tag{32}$$

$$\partial P/\partial\theta = kr\sin(\theta+\phi) - \sigma k^2\sin 2\theta = 0, \tag{33}$$

for σ, k, θ as functions of κ, r, ϕ. Equation (32) yields

$$k = \kappa/\cos^2\theta; \tag{34}$$

Eq. (33) yields

$$\sigma = r\cos(\theta+\phi)/\kappa; \tag{35}$$

and then Eq. (34) becomes

$$\tan(\theta+\phi) = 2\tan\theta. \tag{36}$$

Equation (36) shows that θ is a function of ϕ only, so that the required solution has been found implicitly. A kinematic derivation of Eq. (36) is given in reference 3.

Equation (36) has no solution for $|\phi| > 19°28'$; consequently $h = 0$ (to the present approximation) outside this sector, which lies astern of the moving object because of the minus sign in Eq. (29).

When $|\phi| \leq 19°28'$, Eq. (36) has two solutions, for one of which $|\theta| > 35°16'$; for the other $|\theta|$ is less than this value. It will be found that these two roots correspond to the two wave trains that are so obvious when one looks at a well-developed surface wake, and which are sometimes called the bow and stern wakes. The numerical solution of Eq. (36) is facilitated by the first two columns of Table II. The two roots of Eq. (36) will be called θ_1 and θ_2, $(\theta_1 \leq \theta_2)$, and will be used as parameters in all that follows. For future reference, it may be noted that $\theta = 35°16'$ is the root of

$$3\cos^2\theta - 2 = 0. \tag{37}$$

TABLE II.

Eq. (36)		Eq. (35)	Eq. (38)	
θ_i	ϕ_i	k_i/κ	$-P_i/\kappa r$	$-\kappa r/P_i$
0°	0°00′	1.0000	1.0000	1.0000
10°	9°25′	1.0326	0.9739	1.0268
20°	16°3′	1.1325	0.9156	1.0922
30°	19°6′	1.3333	0.8729	1.1456
34°	19°27′	1.4552	0.8666	1.1539
35°16′	19°28′	1.5000	0.8664	1.1542
36°	19°27′	1.5279	0.8662	1.1545
40°	19°12′	1.7042	0.8725	1.1461
50°	17°14′	2.4201	0.9366	1.0677
60°	13°54′	4.0000	1.1092	0.9016
70°	9°41′	8.5470	1.5308	0.65333
80°	4°58′	33.2256	2.9136	0.3432
90°	0°00′	∞	∞	0.0000

Using Eqs. (34), (35), and (36), the stationary values of the phase are found to be

$$P_i = -\kappa r\cos(\theta_i+\phi)/\cos^2\theta_i; \tag{38}$$

this is tabulated, in nondimensional form, in columns 4 and 5 of Table II.

The remainder of the calculation consists in (1) treating $\alpha^2 B$ as a constant near each of the points stationary phase; (2) expanding P by Taylor's theorem and neglecting terms higher than second degree; (3) evaluating the resulting integrals, which can be reduced to the Cornu spiral type. The result of the calculation is that

$$(h/a) = (\pi a/r)^{\frac{1}{2}}\{h_1 f_1\cos(P_1 - \pi/4) - h_2 f_2\sin(P_2 - \pi/4)\}, \tag{39}$$

where

$$h_i = (ga/S^2)^{\frac{3}{2}}\exp(-gD/S^2\cos^2\theta_i), \tag{40}$$

and

$$f_i = \{\cos(\theta_i+\phi)\,|2 - 3\cos^2\theta_i|\}^{-\frac{1}{2}}. \tag{41}$$

The dependence of the amplitude on r, which is now the distance from the epicenter, is entirely contained in the first factor, $(\pi a/r)^{\frac{1}{2}}$. The approximations used restrict the validity of Eq. (39) to values of κr that are considerably greater than unity.

The dependence on speed is entirely contained in the factors h_i, which vanish both for $S = 0$ and $S = \infty$. They achieve their maxima for the speeds

$$S_i = (2gD/3)^{\frac{1}{2}}/\cos\theta_i. \tag{42}$$

These maxima are

$$\begin{aligned}(h_i)_{\max} &= (ga/eS_i^{\,2})^{\frac{3}{2}} \\ &= (3a/2eD)^{\frac{3}{2}}\cos^3\theta_i.\end{aligned} \tag{43}$$

The speeds given by Eq. (42) are generally very high, so that the exponential in Eq. (40) will usually reduce h_i to values considerably below these maxima.

The factors f_i depend only on the bearing of the epicenter and become infinite when $\phi = \pm 19°28'$, showing that the present approximation is valid only in the interior of the wake. Here, these factors are of the order of magnitude unity. It is probable that a more exact calculation would show that they do not exceed this general magnitude at any point, but have a maximum (perhaps equal to 2 or 3) at points just inside the wake boundaries, and drop rapidly to zero when $|\phi| > 19°28'$.

The two terms of Eq. (39) represent the bow and stern wakes. (This terminology is convenient, even though it may not be dynamically accurate in all

(1068)

respects.) The sine and cosine factors are responsible for the characteristic appearance of a well-developed surface wake, but do not affect the general magnitude of the disturbance, which is determined primarily by the amplitude factors. Because of the many factors determining it, this magnitude is not easily tabulated, but it is usually found to be considerably less than the values given in Table I.

APPENDIX TO SEC. 3. CALCULATION OF B

It is known that

$$1/R = \iint (1/2\pi k)e^{-kD+i(\alpha x+\beta y)}\,d\alpha\,d\beta, \qquad \text{(A-1)}$$

where

$$R = (x^2 + y^2 + D^2)^{\frac{1}{2}}, \quad k = (\alpha^2 + \beta^2)^{\frac{1}{2}},$$

and the integration over both α and β extends from $-\infty$ to $+\infty$. Consequently

$$1/R = \Re \iint{}' (1/\pi k)e^{-kD+i(\alpha x+\beta y)}\,d\alpha\,d\beta. \qquad \text{(A-2)}$$

Differentiation with respect to D yields

$$D/R^3 = \Re(1/\pi) \iint{}' e^{-kD+i(\alpha x+\beta y)}\,d\alpha\,d\beta. \qquad \text{(A-3)}$$

Differentiating twice with respect to x yields

$$(R^2 - 3x^2)/R^5 = \Re \iint{}' (\alpha^2/\pi k)e^{-kD+i(\alpha x+\beta y)}\,d\alpha\,d\beta. \qquad \text{(A-4)}$$

Substitution into Eq. (15) and comparison with Eq. (23) then yields

$$B = (\rho a^3/2\pi)[(S\alpha^2/k) + g]e^{-kD}. \qquad \text{(A-5)}$$

(1070)

SPECTRAL ANALYSIS OF A SEA-SURFACE TEMPERATURE AND ATMOSPHERIC PRESSURE RECORD OFF SOUTHERN CALIFORNIA[1]

By

GUNNAR I. RODEN

ABSTRACT

Sea-surface temperature and atmospheric pressure records during the past 40 years indicate that an inverse relation exists between the temperature at La Jolla, California, and the pressure difference at Lat. 30N, Long. 110–130W. A spectral analysis of these records is made and the energy density, autocorrelation, coherence and phase relations are investigated.

Introduction. During the last 40 years, records have been made of the temperature of the sea surface at the end of Scripps Pier, La Jolla, California. These records, if plotted against time, show seasonal as well as nonseasonal variations. These nonseasonal variations are not understood at the present time, though in many cases it has been possible to relate them to large scale changes in the atmospheric circulation (Roden and Reid, MS.). In order to eliminate seasonal variations of temperature and wind, anomalies are used in the present investigation. The term "anomaly," here defined as the monthly mean minus the mean monthly mean, has been applied to all points of the record. The wind anomaly is expressed in the form of a pressure difference anomaly, taken between Long. 110W to 130W at Lat. 30N (U. S. Weather Bureau, 1917–1956). The variation of the pressure difference and temperature anomalies with time is shown in Fig. 1. A positive pressure difference anomaly means an increased geostrophic wind from the north. It is seen that anomalies of considerable magnitude exist and that there appears to be an inverse relation between the pressure difference and temperature. The latter is consistent with the idea that north wind gives upwelling and advection of cold water. Some of the anomalies seem to be persistent over a long time. It is the purpose of this paper to subject these records to spectral analysis and to investigate whether the impressions gained visually are substantiated.

Spectral Analysis. The method used is that developed by Tukey (1949) and further described by Munk, Snodgrass and Tucker (MS.); it involves the auto- and cross-correlations, from which the energy

---

[1] Contribution from the Scripps Institution of Oceanography, New Series. No 1061

Reproduced by Permission

Reprint from SEARS FOUND. MAR. RES.

(1072)

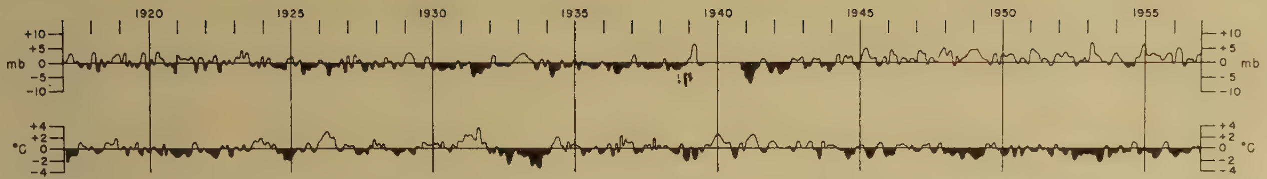

FIGURE 1. (top) Pressure difference anomaly at Lat. 30N between Long. 110W–130W; (bottom) Temperature anomaly, LaJolla Pier.

densities, coherence and phase relationships can be obtained. A definition of these quantities is given in the last mentioned paper and no recourse into the theory will therefore be attempted here. In the present case the analysis of the anomaly records was carried out by a Remington 1103 digital computer at the Convair plant in San Diego, California, for $n = 480$ (number of serial values) and $m = 62$ (number of spectral lines). The results are shown in Figs. 2 and 3. The energy spectrum of the pressure difference anomaly (Fig. 2a) shows that most of the energy is contained in the low frequency part of the spectrum, *viz.*, between zero and 1.6 cycles per year. The total energy amounts to 4.62(mb)^2. The peak at about one cycle per year is quite pronounced; however, it is an artificial feature due to the incomplete elimination of the annual term and therefore it is of no significance. The high frequency part of the spectrum contains relatively little energy

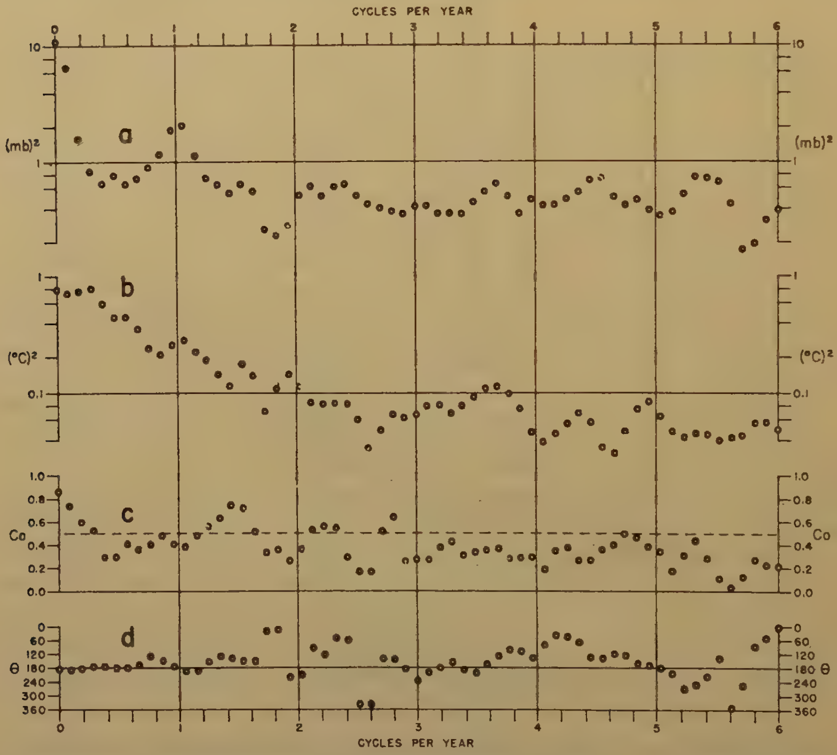

FIGURE 2. *a*, Energy spectrum of pressure difference anomaly; *b*, Energy spectrum of temperature anomaly; *c*, Coherence between pressure difference and temperature anomaly; *d*, Phase lead of pressure difference anomaly over temperature anomaly.

(1074)

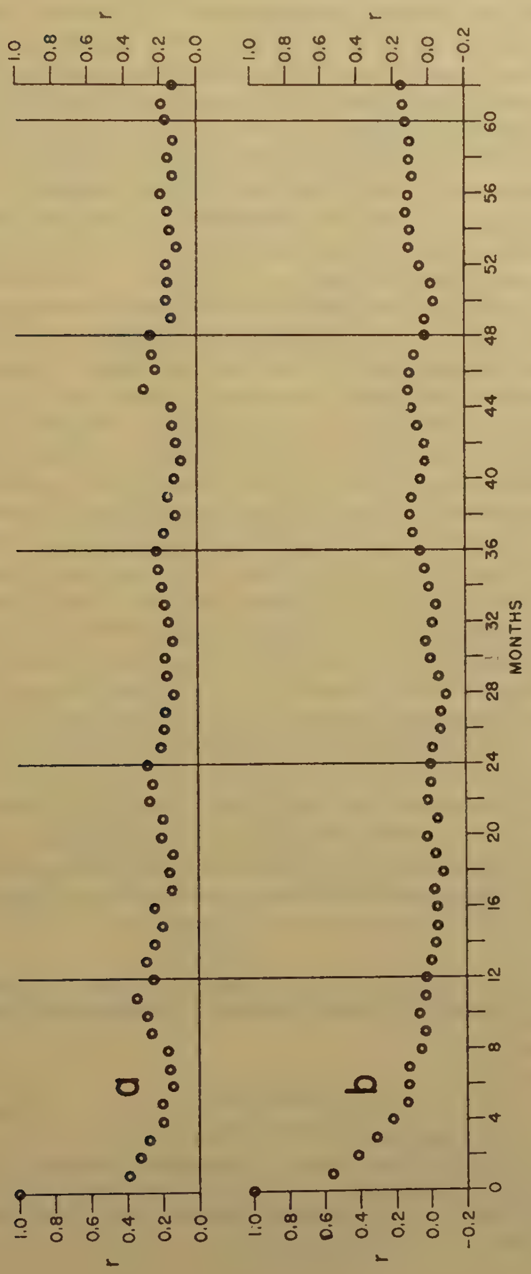

FIGURE 3. *a*, Autocorrelation of pressure anomaly; *b*, Autocorrelation of temperature anomaly.

and its features are probably insignificant. The energy spectrum of the temperature anomaly (Fig. 2b) is similar to the pressure difference anomaly in that the largest part of the energy is contained in the low frequency part of the spectrum. The total energy is 0.87 (°C)^2. The coherence between the pressure difference and temperature anomalies is shown in Fig. 2c. The 95% confidence limit (for discussion, consult Munk, Snodgrass and Tucker, MS.) lies at 0.51 (dashed line). From this it is seen that the coherence is significant for low frequencies only. Prominent peaks occur at approximately 1.5, 2.3 and 2.8 cycles per year, but their meaning is not readily understood. The phase (Fig. 2d) represents the phase lead of the pressure difference anomaly over the temperature anomaly. The outstanding feature is the 180 degree phase difference, indicating that an inverse relation exists between both. This confirms the visual impression shown in Fig. 1. The inverse relationship is particularly pronounced for frequencies between 0 and 1.7, and again between 2.6 and 3.4 cycles per year. The autocorrelation of the pressure and temperature anomalies is shown in Figs. 3a and 3b, respectively. The 95% confidence limits lie at $r = \pm 0.1$. The interesting feature is that the autocorrelation of the pressure anomaly remains positive for more than 62 months and that the function decreases very little with time after the sharp drop during the first month. The autocorrelation of the temperature anomaly reaches the 95% confidence limit after six months. The slight increase of function with time at the end of the record is probably insignificant.

Summing up the spectral analysis of the records has yielded the following results: a) there exists an inverse relation between the anomalies of temperature at La Jolla Pier and the pressure difference (*i.e.*, the northerly wind component) at Lat. 30N, Long. 110–130W; b) the coherence between pressure difference and temperature anomalies is better for low frequencies (long periods) than for high frequencies (short periods); c) the pressure difference anomalies are persistent over a longer time than are the temperature anomalies.

Acknowledgment. The author is indebted to Walter H. Munk, Gordon W. Groves and Gaylord Miller for valuable discussion and suggestions.

REFERENCES

MUNK, W. H., F. E. SNODGRASS AND M. J. TUCKER
Spectra of low frequency ocean waves. (Unpublished manuscript).
RODEN, G. I., AND J. L. REID, JR.
On a relation between atmospheric pressure and sea surface temperatures in the North Pacific Ocean. (Unpublished manuscript).

(1076)

Tukey, G. W.
1949. A sampling theory of power spectrum estimates. Symp. Appl. Autocorrelation Analysis of Phys. Probl. ONR. Woods Hole, Mass. pp. 47–62.
U. S. Weather Bureau
1917–1956. Monthly mean sea level pressure for the northern hemisphere. Published monthly by the Extended Forecasting Section of the U. S. Weather Bureau, Washington, D. C.

(1077)

(1078)

(1079)

COMPARISON OF LIGHT DISTRIBUTION ABOVE AND BELOW WATER[1]

By

JOHN E. TYLER

Scripps Institution of Oceanography, University of California
La Jolla, California

ABSTRACT

Recent measurements of natural light distribution in homogeneous lake water have revealed interesting and heretofore unrecorded optical effects in the near-surface layers. These effects are graphically described and explained.

From 1935 to 1945, studies of the angular distribution of natural light underwater revealed many interesting features of the underwater light field (1, 2, 4, 5, 7, 8). Concurrently, instrumentation in this field advanced with the development of the "shadowing-screen" photometer, described by Pettersson (1) and by Johnson and Liljequist (2), and of the Gershun (3) tube photometer, which directly limited the solid angle of acceptance. However, the work was performed at depths below five meters, and the instruments were limited to a low resolving power (15 to 20°). Consequently, no information was obtained on the distribution of light in the near-surface layers.

It is clear that, from a point just below the calm surface of a large body of water, the directional distribution of natural light overhead will be a compressed version of the scene above the surface. This is in keeping with Snell's law of refraction. As the depth of observation is increased, the light field will change from this complex structure; image detail will be lost and the shape of the radiance distribution solid will become smooth; with increasing depth the brightest spot in the field will move toward the zenith and the shape of the radiance distribution solid will become more symmetrical around the vertical axis. Finally, at some unknown depth, the radiance distribution solid becomes substantially fixed in shape.

Because of the exponential nature of the attenuation of light in water, these changes in light distribution will take place most rapidly in the surface layers. Thus the upper layers are at once the most interesting, the most complex, and the most difficult to explore.

---

[1] Contribution from Scripps Institution of Oceanography, University of California, New Series. This work has been supported by the Bureau of Ships and by the Bureau of Aeronautics under Contract NObs-72092.

Reprint from SEARS FOUND. JOURN. MAR. RES.

Contributions from the Scripps Institution of Oceanography, New Series, No. 1062

Reproduced by Permission

(1080)

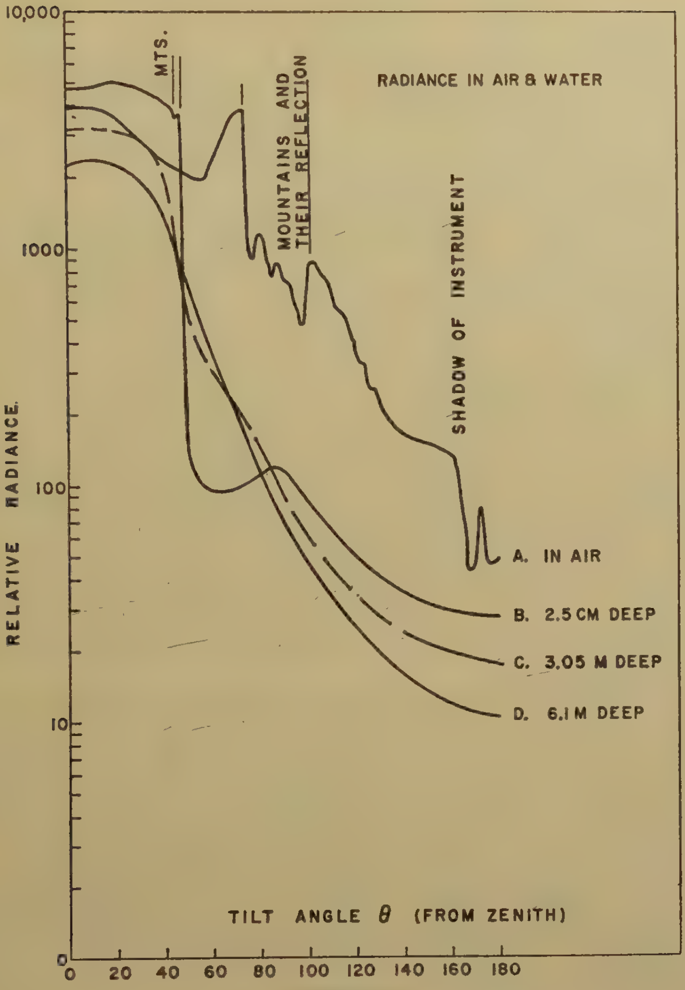

Figure 1

During recent field work at Lake Pend Oreille, Idaho, details of some of the optical effects that occur in these upper layers were explored with an underwater photometer having a resolving power of 6.6°; this underwater photometer was first described in 1955 (6). Measurements of the radiance distribution in a single vertical plane were made on an overcast day,[2] first in air and then from different depths beneath the surface. The fully corrected data are shown in Fig. 1.

---

[2] The sun was not visible. Its position was approximately 45° west of the instrument heading and at an altitude of 61.0°.

Curve A shows results of observations taken in air. From $\theta = 0°$ to $\theta = 74°$ the curve reports the radiance of the overcast sky; at $\theta = 74°$ the dark mountainous skyline is recorded, and this is followed by detail representing patches of dark rock or snow. From $\theta = 90°$ to $\theta = 102°$ the reflection of the mountains is recorded and this is then followed by reflection of the sky disturbed by slight wave action. At 162° the instrument's own shadow image is recorded.

Curve B shows the radiance distribution in the same direction as that in curve A but from a depth of 2.5 cm below the water surface. In the zenith direction, B shows higher radiance than A because the space light contributed by 2.5 cm of water is greater than the absorption of this same path. (It is also possible that some change took place in the zenith overcast during the short time interval between curves A and B.) Optical compression of the sky tends to keep the radiance at a high level for the first 40°. The skyline itself is very much compressed and can no longer be resolved, but the edge of the Snell circle of light appears sharp and distinct at 48°. Beyond 48° the instrument measures the radiance of the short path to the surface plus a longer reflected path that looks down into the water at an angle equal to $(180° - \theta)$. This accounts for the changes in slope of the curve between 48 and 88°. Beyond 88° the path radiance is due entirely to space light from one direction only, which decreases steadily as the tilt angle increases to 180°.

Curve C shows the radiance distribution in the same direction as curves A and B but from a depth of 3.05 m. Some detail can still be observed. The steep slope between 40 and 48° is the remaining radiance change at the edge of the Snell circle of light. The dark band at 60° exhibited in B is nearly obscured by space light; in C, between 50 and 80°, it can just be seen together with its brighter rim.

Curve D shows the radiance distribution in the same direction as the other curves but from a depth of 6.1 m. At this depth all fine detail is lost, leaving only the gross changes in radiance between zenith and nadir settings.

Between 90 and 180° the underwater curves for various depths can be approximately predicted from the equation

$$N_D = N_0 \, e^{-CD},$$

where N_D is the radiance at depth D, N_0 is the radiance at depth 0 and $C = f(\theta)$. Below 6.1 m the coefficient C tends to become independent of θ, approaching an asymptotic value which is characteristic of the hydrosol.

(1082)

REFERENCES

(1) PETTERSSON, HANS
1938. Measurements of the angular distribution of submarine light. Rapp. Cons. Explor. Mer, *108* (2): 9.

(2) JOHNSON N. G. AND G. LILJEQUIST
1938. On the angular distributions of submarine daylight and on the total submarine illumination. Svenska hydrogr.-biol. Komm. Skr., Hydrogr. *14:* 3.

(3) GERSHUN, A. (Translated by PARRY MOON)
1939. The Light-Field. J. Math. Phys., *18:* 51–151.

(4) POOLE, H. N.
1945. The angular distribution of submarine daylight in deep water. Sci. Proc. R. Dublin Soc., *24* (4): 29–42.

(5) WHITNEY, L. V.
1941. The angular distribution of characteristic diffuse light in natural waters. J. mar. Res., *4* (2): 122–131; J. opt. Soc. Amer., *31:* 714–722.

(6) DUNTLEY, S. Q., *et al.*
1955. An underwater photometer. J. opt. Soc. Amer., *45:* 904(A).

(7) TAKENOUTI, YOSITADA
1940. Angular distribution of submarine solar radiations and the effect of altitude of the sun upon the vertical extinctions coefficient. Bull. Jap. Soc. sci. Fish., *8:* 213–219.

(8) JERLOV, N. G. (JOHNSON)
1951. Optical studies of ocean waters. Reports of the Swedish Deep-sea Expedition, 1947–1948. *3*, Physics and Chemistry #1: 1–59.